Water Mediated Interaction between Phospholipid and Saccharide in Aqueous Solution and Frozen State

Keiko TANAKA,*[,a] Tokuji TAKEDA,[a] and Koichiro MIYAJIMA[b]

Osaka Municipal Technical Research Institute,[a] Joto-ku, Osaka 536, Japan and Faculty of Pharmaceutical Sciences, Kyoto University,[b] Sakyo-ku, Kyoto 606, Japan. *Received February 18, 1991*

The heating thermograms of differential scanning calorimetry (DSC) on the binary and three component systems, saccharide/water, dipalmitoylphosphatidylcholine (DPPC)/water and saccharide/DPPC/water, were investigated at various compositions from −120 °C to 40 °C. Maltose and glucose were used as saccharides. The thermograms of the saccharide/DPPC/water system were very similar to those of the saccharide/water system. The average amount of unfreezable water per molecule in the ternary system was found to be simply an arithmetic average of those of the binary systems. The solid–liquid state diagram of saccharide and water in the DPPC/saccharide/water system was analyzed. Based on these results, no direct interaction between the saccharide molecules and DPPC molecules in the frozen state was concluded. The saccharides were found to raise the gel–liquid–crystalline phase transition temperatures of the hydrated multilamellar of DPPC, and its mechanism was proposed to be a water-mediated interaction.

Keywords differential scanning calorimetry; saccharide; dipalmitoylphosphatidylcholine (DPPC); unfreezable water; phase transition; hydrogen-bonding; frozen state

Introduction

Recently, lipid vesicles constructed from bilayers of phospholipid molecules, so-called "liposomes," have been extensively studied as a potential drug carrier in the pharmaceutical field. In this connection, freezing[1,2] and freeze-drying[3,4] of liposomes have been attempted with the addition of stabilizers such as saccharides and polyalcohols. Many studies[2,5,6] have revealed the stabilizing mechanisms of saccharides. In the freezing state, two damage mechanisms of liposomes should be considered, *i.e.*, the mechanical breaking of the membrane caused by ice crystal formation, and the fusion of liposomes. In the saccharide solution, liposomes are covered with a concentrated solution or glass of the mixture of the saccharide and the unfreezable water in the freezing state, and it prevents liposomes from penetration by ice crystal and from fusion.[2] In the freeze-drying process, liposomes are exposed to a highly desiccated environment after the freezing. The damage of liposomes has been ascribed to both their fusion and the passing of the gel–liquid–crystalline transition during the rehydration process of the freeze-dried liposomes. This damage can be inhibited by the saccharide layer covering the liposomes by hydrogen-bonding with the phosphate groups of phospholipids in the dry state.[4,6] Such hydrogen-bonding was also found in the freeze-dried mixture of a water soluble protein and a saccharide,[7] and was reported to play an important role in the stabilization of the protein during freeze-drying.[7,8]

Although the formation of hydrogen-bonding is a well-accepted fact, it is still not clear when this bonding forms during the freeze-drying process. In the present study, differential scanning calorimetry (DSC) heating thermograms of saccharide/water, dipalmitoylphosphatidylcholine (DPPC)/water and saccharide/DPPC water system were investigated from −120 °C to 40 °C with maltose and glucose as saccharides. The temperatures of the melting of ice and the glass transition and quantity of unfreezable water per molecule (N) of the ternary system were compared with those of the binary systems. The effect of saccharides on the gel–liquid–crystalline phase transition temperature of hydrated multilamellar of DPPC was also investigated. Based on these results, we showed that there is no hydrogen-bonding formation between saccharides and DPPC both in the solution state and in the freezing state.

Experimental

Materials DPPC was supplied from Nihon Seica Co., Ltd., and its purity was more than 99%. The DPPC was desiccated at 95 °C and at 0.1 Torr on P_2O_5 for 6 h before use. The residual water content of the dry DPPC was assumed to be less than 1%, as it showed no endothermic transition peak below 90 °C.[9] Glucose and maltose were obtained from Wako Chemical Co., Ltd. Glucose was desiccated at 90 °C and at 0.1 Torr on P_2O_5 for 6 h, and maltose·H_2O was desiccated at room temperature and at 0.1 Torr on P_2O_5 for 2—3 d before use. A molecule of the hydration water of maltose·H_2O is known not to evaporate by this desiccation process.[10] The mixtures of DPPC and saccharide were prepared by dissolving the appropriate amount of dry DPPC and dry saccharide in methanol–benzene (8:2) solution, and evaporating the solvent at 60 °C and at 0.1 Torr for 1 h. The mixtures were then desiccated at room temperature and at 0.1 Torr on P_2O_5 for 2—3 d.

DSC Studies DSC thermograms were obtained by using a high sensitivity Seiko calorimeter (TC-100). Dry lipids, dry saccharides and dry mixtures were directly weighed in an aluminum or silver sample holder, respectively, except for the saccharide/water system of the saccharide weight percentage below 50%. The required amounts of water were added to the holders by a micro-syringe. After the sample holders were hermetrically closed, they were equilibrated at 95 °C for about 6 h. No water was lost during this procedure. The measurements were performed at a heating rate of 5 °C/min from −120 °C to 40 °C after they were cooled to −120 °C at a cooling rate of about 10 °C/min. For experimental convenience, only heating thermograms were obtained. The heat absorbed was determined from the area under the peaks using the heat of melting ice as a standard. For measurement of the transition temperatures of hydrated DPPC, dry DPPC was directly weighed in silver sample holders. The required amounts of aqueous saccharide solution of various concentrations were added by micro-syringe. After being hermetrically sealed, they were equilibrated at 55 °C for longer than 2 h. The measurements were performed at 0.5 °C/min from 10 °C to 70 °C. Repeated heating runs produced the same thermal behavior.

Results

Saccharide/Water System The DSC heating thermograms of saccharide/water systems are obtained by changing the weight percentage of the saccharide. Figure 1 shows those of a maltose/water system and they represent several patterns depending on the maltose weight percentage (W_{mal}). At W_{mal} below about 10%, only an endothermic peak due to the melting of an ice crystal appeared: there is no peak due to the melting of the eutectic mixture. At W_{mal} above about 10%, a small step in the base line

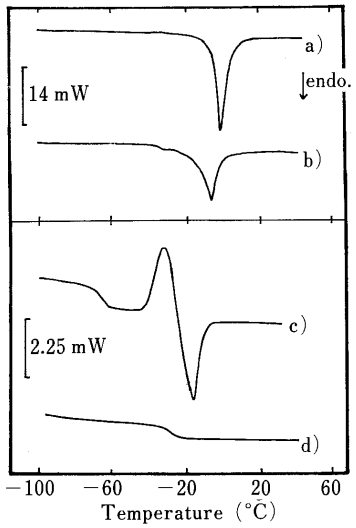

Fig. 1. DSC Heating Thermograms of the Maltose/Water System
Weight percentage of maltose, a) 19%; b) 48%; c) 67%; d) 87%.

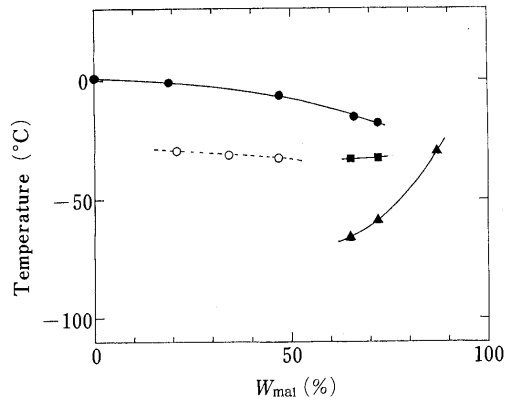

Fig. 2. The Solid–Liquid State Diagram of the Maltose/Water System
●, the peak temperature of melting of ice, (T_m); ■, the peak temperature of recrystallization, (T_r); ▲, the glass transition temperature, (T_g); ○, T_g' indicated in this test.

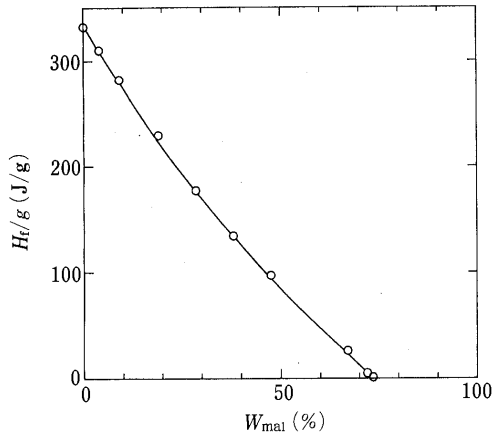

Fig. 3. The Relationship between the Heat of Melting of Ice per Gram of the Maltose/Water System (H_f/g) and the Weight Percentage of Maltose (W_{mal})

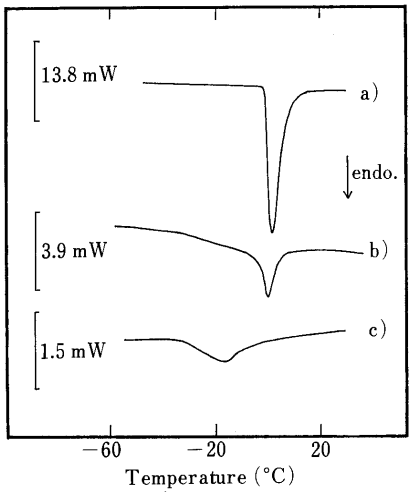

Fig. 4. DSC Heating Thermograms of the DPPC/Water System
Weight percentage of DPPC, a) 20%; b) 80%; c) 86%.

is detected near the starting temperature of melting. This may be due to the glass transition of the mixture of maltose and unfreezable water in the presence of ice crystal. In the range of 60% to 70%, glass transition is clearly observed, followed by recrystallization and melting of ice crystals. At W_{mal} above about 70%, only glass transition is exhibited. Based on the thermal data in Fig. 1, the solid–liquid state diagram can be obtained as shown in Fig. 2. T_m and T_r represent the peak temperatures of endothermic and exothermic peaks, respectively. T_g shows the glass transition temperature. $T_{g'}$ corresponds to the temperature shown as a small step in Fig. 1b. The glucose/water system shows results similar to the maltose/water system. Franks[11] reported the thermal data of the glucose/water system and combined them with other literature data in a solid–liquid state diagram.[12] Our results of the glucose/water system show good agreement with theirs, except for two points: transition temperatures are slightly different, and the two minor endothermic peaks detected by Franks *et al.*[11] are not found in our data. These are probably due to differences in experimental conditions for thermal analysis. In Fig. 3, the relationship between the heat of melting per gram of the maltose/water system (H_f/g) and W_{mal} is represented. It shows a nonlinear relationship, and the amount of unfreezable water per maltose molecule can be calculated from the composition at which H_f/g becomes zero. The values for glucose and maltose are 4.5 ± 0.4 and 6.7 ± 0.3, respectively. They agreed fairly well with those from DSC by other workers.[13]

DPPC/Water System The DSC heating thermograms of DPPC/water systems are investigated at various weight percentages of DPPC (W_{DPPC}) as shown in Fig. 4. They show good agreement with the thermograms reported by Grabielle *et al.*[14] As they analyzed in detail, at W_{DPPC} below 80%, the T_m hardly change and are around 0 °C. When the W_{DPPC} is above 80%, the T_m begin to drop abruptly. No endothermic peak due to the melting of ice crystal is observed at W_{DPPC} above 87%. The quantity of unfreezable water can be calculated as 5.3 ± 0.5 molecules per molecule of DPPC.

The hydration properties of phospholipids have been already investigated by calorimetric mesurements,[14] the adsorption isotherm method,[15] nuclear magnetic resonance (NMR)[16] and X-ray studies.[17] These studies have demonstrated the presence of several types of water with properties differing from the bulk state in the phospholipid/water system. Water molecules adjacent to the phosphate groups were most strongly bound with highly restricted

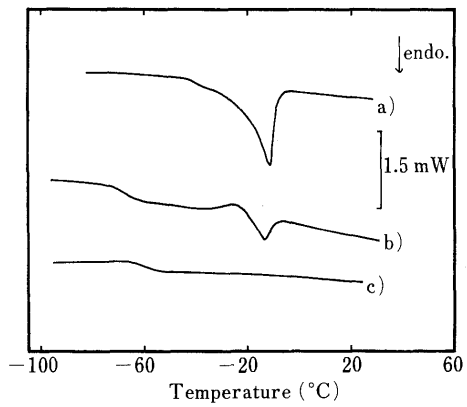

Fig. 5. DSC Heating Thermograms of the Maltose/DPPC/Water System at the Molar Ratio of Maltose to DPPC at Unity

Weight percentage of the mixture of maltose and DPPC (W_{mix}), a) 74.9%; b) 81.0%; c) 82.7%.

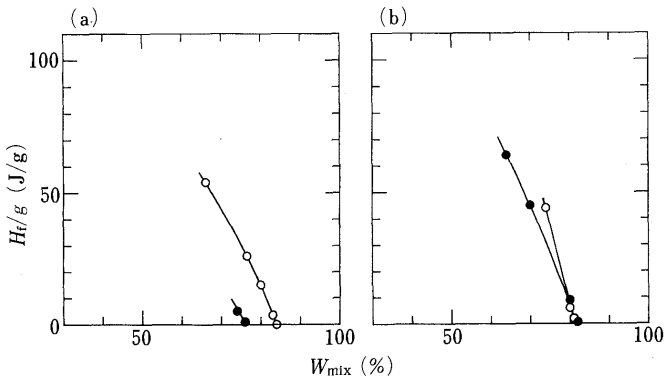

Fig. 6a. The Relationships between H_f/g and W_{mix} of the Glucose/DPPC/Water System

The molar ratio of glucose and DPPC, ○, 1:1; ●, 4:1.

Fig. 6b. The Relationships between H_f/g and W_{mix} of the Maltose/DPPC/Water System

The molar ratio of maltose and DPPC, ○, 1:1; ●, 7:3.

motion, and their amount was 4—6 molecules per molecule of phospholipid. In all probability, about 5 molecules of unfreezable water obtained in our experiment are assigned to this strongly bound water around the phosphate groups.

Saccharide/DPPC/Water System Figure 5 shows the DSC heating thermograms of the maltose/DPPC/water system at various weight percentages of the mixture of maltose and DPPC (W_{mix}). The molar ratio of maltose to DPPC is kept constant at unity. They produce thermograms similar to the maltose/water system (Fig. 1), suggesting that maltose molecules are fully hydrated. DSC heating thermograms are also investigated at various molar ratios of maltose or glucose to DPPC. These results give the relations between H_f/g and W_{mix}, and are obtained as shown in Fig. 6. The average quantities of unfreezable water (N) are calculated and shown in Fig. 7 as a relationship between N and the molar fraction of a saccharide (X). N are found to be linearly related to X in both systems. This result indicates that the average values of N for the saccharide/DPPC/water system are simply arithmetic averages of those for the saccharide/water and DPPC/water systems. It is suggested that there is no hydrogen-bonding formation between the phosphate group of DPPC and the –OH group of a saccharide. Hydrogen-bonding sites of

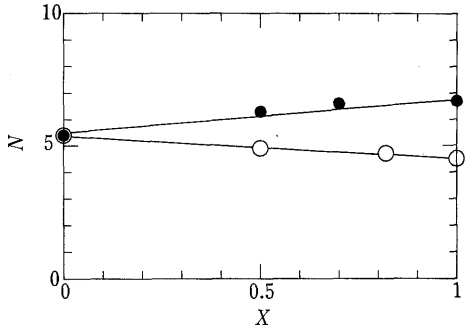

Fig. 7. The Relationships between N and the Molar Fraction of Saccharide (X)

○, Glucose; ●, maltose. N: the average amount of unfreezable water.

TABLE I. Values of T_m, T_g, f_m and f_g at Various W_{mix} for Each Saccharide/DPPC/Water System

	Mole ratio	W_{mix} (%)	T_m (°C)	T_g (°C)	f_m	f_g
Glu : DPPC	1 : 1	65.4	−5.4	ND	5.5	ND
		80.7	−17.3	−85.8	4.6	5.3
		82.2	−20.8	−83.9	4.6	5.3
	4 : 1	73.8	−18.9	−83.7	4.3	4.6
		75.0	−20.5	−82.2	4.3	4.6
Mal : DPPC	1 : 1	74.9	−10.4	ND	5.6	ND
		81.0	−13.7	−67.2	4.6	5.0
		82.7	ND	−60.9	ND	5.0
	7 : 3	53.1	−4.3	ND	5.6	ND
		69.8	−11.3	ND	6.1	ND

ND = not determined.

the DPPC molecule for water molecules and saccharide molecules are considered to be same, *i.e.*, the phosphate groups of DPPC.[6] If there were direct interaction between DPPC and the saccharide, the N *vs.* X plot should deviate from a linear relationship.

Further evidence for the absence of direct bonding between saccharides and DPPC can be obtained from analysis of the transition temperature, T_m and T_g: assuming that there is no direct interaction between DPPC and saccharide, the liquid–solid phase diagram of saccharide and water in the DPPC/saccharide/water system must be identical to the diagram of the saccharide/water system. The weight percentage of saccharides comparable to the binary system (W'_s) can be represented by equation (1) by taking the hydration water of DPPC into account,

$$W'_s = 100\, W_s/(W_s + W_h - f M_{H_2O} W_D/M_D) \qquad (1)$$

where W_s, W_h and W_D are the weight percentages of saccharide, water and DPPC in the saccharide/DPPC/water system, respectively. M_{H_2O} and M_D are molecular weights of water and DPPC. The f is the hydration number of water molecules per a molecule of DPPC. The values of W'_s are obtained from the binary diagram for each experimental value of T_m or T_g in the ternary system, and f values are calculated by Eq. 1. The f_m and f_g correspond to T_m and T_g, respectively. The values are summarized in Table I. As shown in Table I, the average value of f is about 5, and it shows good agreement with the quantity of water which can form hydrogen-bonding with the phosphate group of DPPC as mentioned above. The result well confirms the

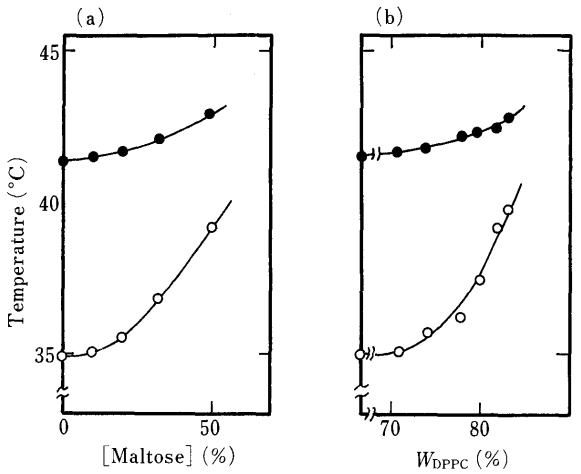

Fig. 8a. The Relationships between the Transition Temperatures and the Maltose Concentration

●, T_c; ○, T_p.

Fig. 8b. The Relationships between the Transition Temperatures and W_{DPPC}

●, T_c; ○, T_p.

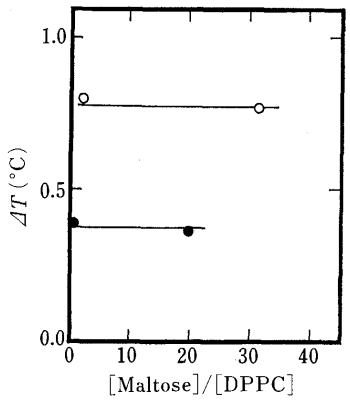

Fig. 9. The Relationship between the Increment of T_c, ΔT, and [Maltose]/[DPPC] at Two Maltose Concentrations

●, 20%; ○, 32%.

validity of the assumption that there is no hydrogen-bonding formation between the phosphate groups of DPPC and a saccharide molecule during the freezing state. They interact most probably through hydrogen bonded water molecules.

Effect of Saccharides on the Transition Temperature of Hydrated DPPC DSC heating thermograms of the hydrated multilamellas of DPPC in a maltose or glucose aqueous solution are investigated at various saccharide and DPPC concentrations. Figure 8a shows the transition temperatures of DPPC, *i.e.*, the main transition temperature of $P'_\beta \rightleftharpoons L_\alpha$ (T_c) and the pre-transition temperature of $L'_\beta \rightleftharpoons P'_\beta$ (T_p) as a function of the maltose concentration, [maltose], at the DPPC concentration, [DPPC], of 1%. Both T_c and T_p rise with the maltose concentration, and at a maltose concentration of 50%, T_c and T_p are 1.5 °C and 4 °C higher than in the absence of maltose, respectively. Enthalpy change, ΔH, of each transition does not depend on [maltose]. The relationships between the transition temperatures and the glucose concentration are similar to those for maltose. The increment of T_C, ΔT, is shown in Fig. 9 as a function of the ratio of [maltose] to [DPPC], [maltose]/[DPPC], at [maltose] of 20% and 32%. These results show that ΔT is not dependent on [maltose]/[DPPC] but on [maltose].

Some saccharides are known to increase the phase transition temperatures of the hydrated multilamellas of DPPC.[5,6,18] Strauss *et al.*[5] found such increases in a sucrose aqueous solution, and attributed their origin to a direct interaction between the sucrose molecule and DPPC molecule. If the increase were caused by such direct interaction as they mentioned, ΔT should depend not only on [maltose] but also on [maltose]/[DPPC]. Our results show that ΔT scarcely depends on [maltose]/[DPPC]. Therefore, no direct interaction may exist between the maltose molecule and the DPPC molecule in the presence of bulk water in this system. The next question is, "Why the transition temperatures of the hydrated multilamellar of DPPC increase with the saccharide concentration?" It is reported that T_c and T_p in the DPPC/water system increase by decreasing the weight percentage of water, W_{H_2O}, below 25%, because the distance between the bimolecular membrane of DPPC becomes shorter and the ordering degree of the water increases; in other words, the hydration state of the head group of DPPC changes.[19,20] In Fig. 8b, the relationships between T_c or T_p and W_{DPPC} for the DPPC/water system are represented from the data published by Grabielle *et al.*[19] The increasing behavior of the transition temperatures in Fig. 8a is very similar to that in Fig. 8b. The reason for the increase observed in our results can be ascribed to the change in the hydration state of the head groups of DPPC, that is, the water mediated interaction.

Discussion

Although it is well established that the formation of hydrogen-bonding between a saccharide and phospholipid molecules is indispensable for the stabilization of liposomes during freeze-drying, it is not clear at which stage this bonding forms during the freeze-drying process. Strauss *et al.*[5] showed that the stabilization ability of sucrose was abolished by the addition of Europium (Eu^{3+}), which forms an ionic linkage, and also that sucrose increased the transition temperatures of hydrated multilamellar vesicles. From these results they suggested that the direct interaction between saccharides and phospholipids occur in the presence of bulk water. On the contrary, Crowe *et al.*[6] and Rudolph *et al.*[20] proposed that the interaction likely occurred during freezing when the phospholipids and saccharides were concentrated well beyond their bulk concentration. They mentioned that the increase of the transition temperature of hydrated multilamellar by the addition of saccharides was due to an osmotic dehydration of the polar head groups, because they could not detect a T_c-elevating effect on unilamellar vesicles. They showed that "Eu^{3+}-induced" fusion during the freeze-thawing of a liposome suspension was reduced relative to an increasing saccharide concentration. From this result they suggested that there was competition for bond-formation for the head group of DPPC between the saccharide and the Eu^{3+} in a freezing state.[21]

Our results show that amount of strongly bound water of the phosphate groups of DPPC is not changed by the addition of saccharides in a freezing state. And the elevation of T_c or T_p of hydrated DPPC by the addition of a saccharide

is ascribed to a water mediated interaction. From these results, the formation of hydrogen-bonding most likely occurs after the removal of a large amount of water from the system during freeze-drying. Based on our interpretation, we suspect that the reduction of "Eu^{3+}-induced" fusion of liposomes by the addition of saccharides observed by Anchordoguy *et al.*[21] is due.to the high viscosity of the system. Becuase the fusion follows the collision of liposomes, the degree of the fusion is greatly affected by the viscosity near the liposome. In a frozen state, the surface of the liposome is covered with a concentrated aqueous or glassy saccharide layer, whose viscosity is very high. In such situations, Eu^{3+}-induced fusion is most probably prevented by an increase in saccharide concentration.

In conclusion, we found that there is no direct interaction between the saccharide and phospholipid molecules in the aqueous solution state or in the frozen state.

References

1) E. M. G. Van Bommel and D. J. A. Crommelin, *Int. J. Pharm.*, **22**, 299 (1984).
2) K. Miyajima, K. Tomita, and M. Nakagaki, *Chem. Pharm. Bull.*, **34**, 2689 (1986).
3) S. Abu-Zsid, M. Morii, and N. Takeguchi, *Maku*, **9**, 43 (1984).
4) L. M. Crowe, J. H. Crowe, A. S. Rudolph, C. Womersly, and L. Appel, *Arch. Biochem. Biophys.*, **242**, 240 (1985).
5) G. Strauss, P. Schurtenberger, and H. Hauser, *Biochim. Biophys. Acta*, **858**, 169 (1986).
6) J. H. Crowe, L. M. Crowe, J. F. Carpenter, A. S. Rudolph, C. A. Wistrom, B. J. Spargo, and T. J. Anchordoguy, *Biochim. Biophys. Acta*, **947**, 367 (1988).
7) J. F. Carpenter and J. H. Crowe, *Biochemistry*, **28**, 3916 (1989).
8) K. Tanaka, T. Takeda, and K. Miyajima, *Chem. Pharm. Bull.*, **39**, 1091 (1991).
9) D. Chapman, R. M. Willian, and B. D. Ladbrooke, *Chem. Phys. Lipids*, **1**, 445 (1967).
10) F. Shahidi, P. G. Farrell, and L. T. Edward, *J. Solution Chem.*, **5**, 807 (1976).
11) F. Franks, "Water-A Comprehensive Treatise," Vol. 7, ed. by F. Franks, Plenum Press, New York and London, 1982, p. 299.
12) B. Luyet and D. H. Rasmussen, *Biodynamica*, **10**, 167 (1968).
13) S. Bociek and F. Franks, *J. Chem. Soc., Faraday Trans. 1*, **75**, 262 (1979).
14) C. Grabielle-Madelmont and R. J. Perron, *J. Colloid Interface Sci.*, **95**, 483 (1983).
15) D. A. Wilknson, H. J. Morowitz, and J. H. Prestegard, *Biophys. J.*, **20**, 169 (1977).
16) Y. Tricot and W. Niederberger, *Biophys. Chem.*, **9**, 195 (1979).
17) A. Tardieu, V. Luzzati, and F. C. Reman, *J. Mol. Biol.*, **75**, 711 (1973).
18) B. Z. Chowdhry, G. Lipka, and J. M. Sturtevant, *Biophys. J.*, **46**, 419 (1984).
19) C. Grabielle-Madelmont and R. Perron, *J. Colloid Interface Sci.*, **95**, 471 (1983).
20) A. S. Rudolph, J. H. Crowe, and L. M. Crowe, *Arch. Biochem. Biophys.*, **245**, 134 (1986).
21) T. J. Anchordoguy, A. S. Rudolph, J. F. Carpenter, and J. H. Crowe, *Cryobiology*, **24**, 324 (1987).

The Photocycloaddition Reactions of Uridine and Related Compounds with 2,3-Dimethyl-2-butene

Ichiro ISHIKAWA,[a] Tsuneo ITOH,[a,1)] Hiroaki TAKAYANAGI,[a] Jun-ichi OSHIMA,[a] Norio KAWAHARA,[b] Yoshihisa MIZUNO,[a] and Haruo OGURA*,[a]

School of Pharmaceutical Sciences, Kitasato University,[a] 5–9–1, Shirokane, Minato-ku, Tokyo 108, Japan and Hokkaido Institute of Pharmaceutical Sciences,[b] 7–1, Katsuraoka-cho, Otaru-shi, Hokkaido 047–02, Japan. *Received November 13, 1990*

The photochemical reactions of uracil and 5-fluorouracil derivatives with simple alkenes have been investigated. Photocycloaddition of uracil or 5-fluorouracil derivatives and 2,3-dimethyl-2-butene in acetone gave an enantiomeric mixture of cross cycloadducts (4, 7) in moderate yields. Under similar conditions, diastereomers of 4-substituted 7,7,8,8-tetramethyl-*cis*-2,4-diazabicyclo[4.2.0]octane-3,5-dione nucleosides (14—17) were formed from uridine or 5-fluorouridine derivatives in good yields. The structures and stereochemistry of these cycloadducts of the nucleoside series were elucidated on the basis of the proton nuclear magnetic resonance spectra and X-ray crystallographic analysis.

Keywords ribonucleoside; photocycloaddition; X-ray crystallographic analysis; 2,4-diazabicyclo[4.2.0]octane; Vorbrüggen ribosylation; ^{1}H-NMR

Photochemical cycloaddition reactions between nucleobases, *viz.*, uracil derivatives, and simple olefins have been extensively investigated.[2,3)] Many workers[4)] have also studied the photodimerizations of pyrimidine nucleosides. However, the photoadditions between nucleosides and simple alkenes have received little attention except for the work of Charlton and Lai,[5)] who have prepared the 2,3-dimethyl-2-butene adducts of uridine derivatives. We considered that these photocyclizations might provide a route to a variety of bicyclic pyrimidine nucleosides, and it was anticipated that these adducts might be useful for biological studies. They might also serve as useful intermediates for syntheses of naturally occurring nucleobases of nucleosides.[6)] Earlier studies by Swenton *et al.*[2)] on the reaction of 1,3-dimethyluracil or 5-fluoro-1,3-dimethyluracil with isobutene showed that cycloadditions of this type take place in a stereoselective way. That means that the cyclization of a symmetrical olefin, *viz.*, 2,3-dimethyl-2-butene, and uracil (**2b** or **6c**) may give rise to a relatively uncomplicated mixture from which each product could be easily fractionated. Thus, we carried out the acetone-sensitized cycloaddition of 1,3-dialkyluracils and symmetrical olefins. In the present paper we describe the outcome of the above-mentioned reactions including the structural elucidation of products.

Photoaddition was performed in acetone at room temperature by the use of a 400 W high-pressure mercury lamp fitted with a Pyrex filter.

The acetone-sensitized cycloaddition of 1,3-dimethyluracil (**2b**) and 2,3-dimethyl-2-butene (**3**) proceeded smoothly, leading to the formation of the cycloadduct (**4b**) in 76% yield. The similar photocycloaddition of 1,3-diethyluracil (**2d**) also proceeded to give the adduct (**4d**) in 56% yield.

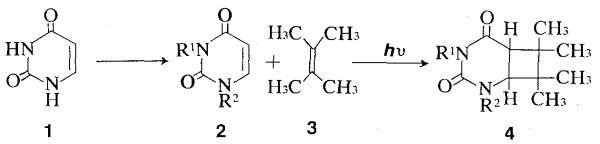

1 2 3 4

a : R^1=H, R^2=CH_3
b : R^1=R^2=CH_3
c : R^1=H, R^2=CH_2CH_3
d : R^1=R^2=CH_2CH_3
e : R^1=H, R^2=$CH_2C_6H_5$
f : R^1=R^2=$CH_2C_6H_5$

Chart 1

The structures of these products (*cf.* **4b** and **4d**) were elucidated by spectral [mass spectra (MS) and nuclear magnetic resonance (NMR)] as well as elemental analyses. NMR data for both adducts are consistent with cyclobutane structures; for example, in the ^{1}H-NMR spectrum of **4b**, signals at δ 5.71 and 7.15 due to the 5,6-vinyl protons in **2b** are absent, while new signals appeared at δ 2.9 and 3.6 ppm. In addition, the splitting pattern of **4d** is characteristic of the cyclobutane ring. The signals appeared as a pair of doublets and those due to hydrogens of four methyl groups appeared as four separate singlets (δ 0.93, 0.97, 1.12, and 1.23). These compounds (**4b**, **d**) showed differentiation-inducing and growth-inhibitory activities towards HL-60 cells.[7)]

This finding of differentiation-inducing activity of the cyclobutane ring system prompted us to prepare 2,4-diazabicyclo[4.2.0]octane-3,5-dione derivatives and nucleosides thereof.

Alkylation of uracil (**1**) or 5-fluorouracil (**5**) with alkyl halide (MeI or EtI) in dry acetone gave 1-alkyl- or 3-alkyluracils or 1,3-dialkyluracils (**2**, **6**) in moderate yields. Aralkylation of **1** and **5** with benzyl chloride [K_2CO_3 in dimethylsulfoxide (DMSO)] afforded 1-benzyluracil (**2e**) and 1-benzyl-5-fluorouracil (**6f**) in 57% and 62% yields, respectively. 1,3-Dibenzyluracil (**2f**) and 1,3-dibenzyl-5-fluorouracil (**6g**) were obtained in 79% and 72% yields from the reaction of **1** and **5**, respectively, with benzyl chloride using 60% NaH in *N*,*N*-dimethylformamide (DMF). The structures of the products were confirmed by spectral (MS, NMR, and ultraviolet (UV)) as well as elemental analyses. The acetone-sensitized photocycloaddition of **2** and **6** with **3** afforded **4** and **7**, respectively, in excellent yields. The

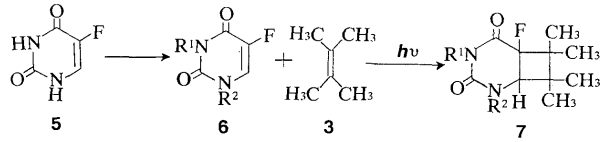

5 6 3 7

a : R^1=H, R^2=CH_3
b : R^1=CH_3, R^2=H
c : R^1=R^2=CH_3
d : R^1=H, R^2=CH_2CH_3
e : R^1=R^2=CH_2CH_3
f : R^1=H, R^2=$CH_2C_6H_5$
g : R^1=R^2=$CH_2C_6H_5$

Chart 2

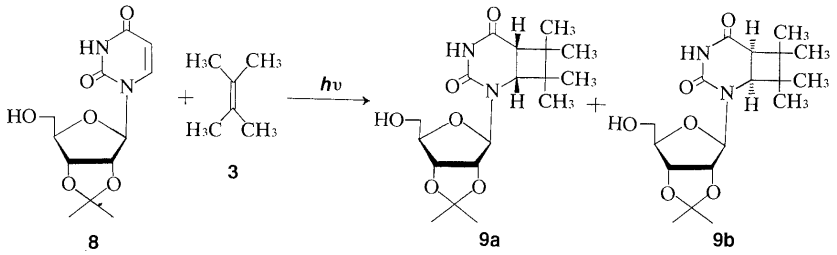

Chart 3

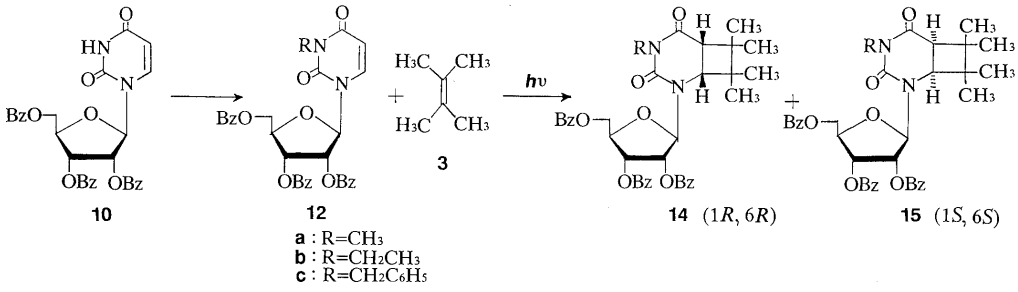

Chart 4

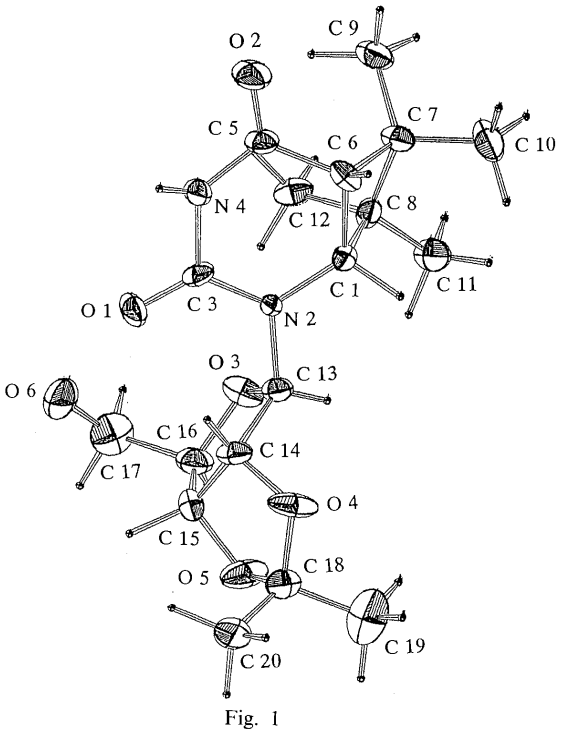

Fig. 1

structures of **4** and **7** were established on the basis of MS and NMR, and elemental analyses (Charts 1 and 2). Analogously, the photocycloaddition between **8** and **3** afforded two adducts (**9a** and **b**) in the ratio of 9 : 1 (54% and 6% isolated yields). The MS and NMR data of these compounds are consistent with the assigned cycloadduct structures (**9a** and **9b**). The structure of **9a** including the stereochemistry was definitively established by means of an X-ray crystal structure analysis. A perspective drawing of **9a** is shown in Fig. 1 on the basis of the absolute configuration of D-ribose. The absolute configurations at C-1 and C-6 were both assigned as *R*. Taking the above results into consideration, we anticipate that the second adduct (**9b**) has the 1*S*, 6*S* configuration.

Ribosylation of **1** and **5** were performed according to the general procedure (Vorbrüggen procedure)[8,9] to give **10** and **11**. 3-Alkyl-2′,3′,5′-tri-*O*-benzoyluridines (**12**, **13**) were obtained in good yields on treatment of **10** or **11** with various alkyl halides. In addition, the photocycloadducts **14**—**17** were obtaine from **11**, **12**, and **13** with **3**. Compounds **14a**, **15a** and **16a**, **17a** were isolated by preparative thin-layer chromatography (TLC) developed with $CHCl_3$–EtOH (10 : 1). The configurations of these compounds (**14a**, **15a** and **16a**, **17a**) were confirmed by NMR; the NMR data of **14a** and **16a** were quite similar to the NMR data of **9a**, and those of **15a** and **17a** are similar to those of **9b**. Photoaddition involving the uridine derivatives (**12b**, **c** and **13b**, **c**) afforded two major products, which could not be separated. However, it was found by means of NMR that the reaction mixture consists of two major products. The configurations as well as structures of these compounds

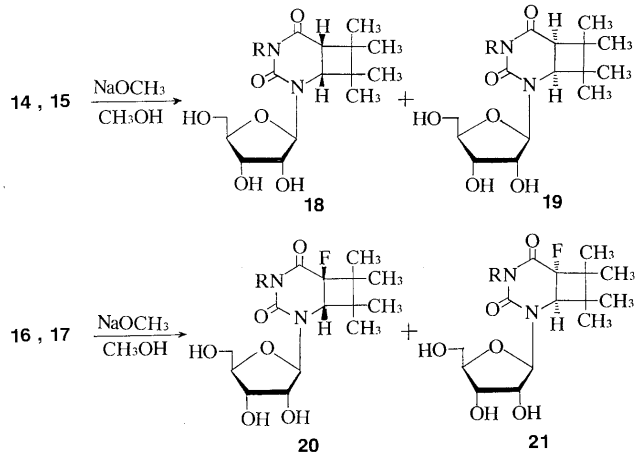

Chart 5

TABLE I. Product Distribution in Cycloaddition

Products	Yield (%)	Ratio of diastereomers *endo* : *exo*[11]
9a, **9b**	60	9 : 1[a]
14a, **15a**	64	1.2 : 1[a]
14b, **15b**	91	3 : 2[b]
14c, **15c**	93	3 : 2[b]
16a, **17a**	92	5 : 2[a]
16b, **17b**	99	5 : 2[b]
16c, **17c**	96	3 : 1[b]
16d, **17d**	92	3 : 1[b]

a) The ratio was determined from the isolated yields. *b*) The ratio was estimated from the NMR spectra.

(**14b**, **c**, **15b**, **c** and **16b—d**, **17b—d**) were determined by NMR as described above, and the ratios of the respective products were determined on the basis of the integration of anomeric proton signal in the ^{1}H-NMR spectra. Finally, 7,7,8,8-tetramethyl-2-(*β*-D-ribofuranosyl)-*cis*-2,4-diazabicyclo[4.2.0]octane-3,5-diones (**18—21**) were prepared in excellent yields by treating **14—17** with sodium methoxide in MeOH at 50—60 °C.

It is worth noting that some of the products (**4b**, **d**, **6b**, **d**, **e**, **g**, and **9a**) exhibit differentiation-inducing and growth-inhibitory activities towards HL-60 cells.[7,10]

The results may be summarized as follows. i) 2,4-Diazabicyclo[4.2.0]octane-3,5-diones were prepared from the uracil derivatives by acetone-sensitized irradiation. ii) Diastereomeric 2,4-diazabicyclo[4.2.0]octane-3,5-dione nucleosides were prepared from uridine derivatives in an analogous way, and these diastereomeric nucleosides were isolated by preparative TLC. iii) The structure and stereochemistry of 2,4-diazabicyclo[4.2.0]octane-3,5-dione nucleosides were confirmed by ^{1}H-NMR and X-ray crystallographic analyses. iv) Some of the products (**4b**, **d**, **6b**, **d**, **e**, **g**, and **9a**) showed differentiation-inducing and growth-inhibitory activities towards HL-60 cells.[7,10]

Finally, some interesting observations in the present studies are worthy of comment. Of the pair of diastereomers produced by the addition reactions, the "*endo*"-adduct is predominant as compared with the "*exo*"-adduct[11] (see Table I). This outcome of the cycloaddition may be explained by the relative rates of competing reactions, by analogy with another cycloaddition, *viz.*, the Diels–Alder reaction, where the "*endo*"-addition takes place faster. Namely, under our reaction conditions (kinetically controlled conditions), the "endo"-addition occurs faster, so the "*endo*"-cycloadduct is the major product. Elucidation of the exact mode of the reaction will require further studies. Nevertheless, it is interesting that the ratio of the "endo" adduct and the "*exo*"-adduct has something to do with the nature of the protecting groups in the sugar portion. The predominance of the "*endo*"-product with 2′,3′-*O*-isopropylideneuridine is very marked. A similar propensity associated with a reaction involving 2′,3′-*O*-isopropylideneuridine has been reported quite often, *e.g.*, in the 5-hydroxymethylation of 2′,3′-*O*-isopropylideneuridine.[12]

Experimental

General Melting points were determined in a capillary tube and are uncorrected. MS were recorded on a JEOL D-100 instrument. ^{1}H-NMR spectra were recorded on a Varian EM-390 NMR spectrometer or Varian VXR-300 spectrometer with Me_4Si (TMS) as an internal standard in $CDCl_3$ or in DMSO-d_6. Microanalyses were performed by the staff of the Microanalytical Laboratory of this school. The cell dimensions and diffraction intensities were measured on a Rigaku four-circle diffractometer, using graphite-monochromated Cu K_α radiation. Column chromatography was performed on Wakogel C-200. TLC was performed on Kieselgel 60 GF_{254} (20 cm × 20, Merck) and spots were detected under UV light. Unless otherwise stated, the solvents were removed in a rotary evaporator coupled to a water aspirator (*ca.* 20 mmHg).

Reaction of Uracil (1) with Methyl Iodide A mixture of uracil (**1**, 2.24 g, 20 mmol), methyl iodide (4.26 g, 30 mmol) and potassium carbonate (1.38 g, 10 mmol) in dry acetone (40 ml) was stirred at 60—70 °C for 24 h in a sealed steel tube. The resulting solution was filtered to remove potassium carbonate and the unreacted uracil (1.15 g), and the filtrate was concentrated *in vacuo*. The residue in $CHCl_3$ was chromatography over silica gel and eluted with $CHCl_3$ to give **2a** and **2b**.

1-Methyluracil (2a) Recrystallization of **2a** from $CHCl_3$–EtOH (1 : 1) afforded 212 mg (17%) as white needles, mp 232—233 °C (lit.[13] mp 233—234 °C. MS *m/z*: 126 (M^+). ^{1}H-NMR (DMSO-d_6) δ: 3.21 (3H, s, NCH_3), 5.46 (1H, d, 5-H, J=7.8 Hz), 7.58 (1H, d, 6-H, J=7.8 Hz), 11.12 (1H, br, NH). UV λ_{max}^{EtOH} nm (log ε): 263 (3.87). UV $\lambda_{max}^{1\ N\ NaOH-EtOH\ (1:10)}$ nm (log ε): 263 (3.65). *Anal.* Calcd for $C_5H_6N_2O_2$: C, 47.62; H, 4.80; N, 22.22. Found: C, 47.54; H, 4.85; N, 22.06.

1,3-Dimethyluracil (2b) This compound was recrystallized from $CHCl_3$ to give 415 mg (30%) as white needles, mp 123—125 °C (lit.[13] mp 125 °C). MS *m/z*: 140 (M^+). ^{1}H-NMR ($CDCl_3$) δ: 3.33, 3.40 (3H each, s, NCH_3), 5.71 (1H, d, 5-H, J=7.8 Hz), 7.15 (1H, d, 6-H, J=7.8 Hz).

Reaction of 1 with Ethyl Iodide A mixture of **1** (1.12 g, 10 mmol), ethyl iodide (2.34 g, 15 mmol) and potassium carbonate (0.69 g, 5 mmol) was added to dry acetone (20 ml). The resulting mixture was worked up according to the procedure described above for **2a** to give **2c** (120 mg, 22%) as white crystals, **2d** (215 mg, 23%) as a colorless oil, and unreacted uracil (682 mg) as a white powder.

1-Ethyluracil (2c) This compound had mp 145—146 °C (lit.[13] mp 145—146 °C). MS *m/z*: 140 (M^+). ^{1}H-NMR (DMSO-d_6) δ: 1.16 (3H, t, $CH_2\underline{CH}_3$, J=7.2 Hz), 3.69 (2H, q, $\underline{CH}_2CH_3$, J=7.2 Hz), 5.50 (1H, d, 5-H, J=7.8 Hz), 7.67 (1H, d, 6-H, J=7.8 Hz), 11.13 (1H, br, NH). UV λ_{max}^{EtOH} nm (log ε): 263 (3.96). UV $\lambda_{max}^{1\ N\ NaOH-EtOH\ (1:10)}$ nm (log ε): 263 (3.81). *Anal.* Calcd for $C_6H_8N_2O_2$: C, 51.42; H, 5.75; N, 19.99. Found: C, 51.19; H, 5.97; N, 19.81.

1,3-Diethyluracil (2d) This compound was obtained as oil (lit.[14] mp 14—15 °C). MS *m/z*: 168 (M^+). ^{1}H-NMR ($CDCl_3$) δ: 1.21, 1.30 (3H each, t, $CH_2\underline{CH}_3$, J=7.2 Hz), 3.80, 3.99 (2H each, q, $\underline{CH}_2CH_3$, J=7.2 Hz), 5.69 (1H, d, 5-H, J=8.0 Hz), 7.15 (1H, d, 6-H, J=8.0 Hz). *Anal.* Calcd for $C_8H_{12}N_2O_2$: C, 57.13; H, 7.19; N, 16.66. Found: C, 57.02; H, 7.24; N, 16.40.

1-Benzyluracil (2e) A mixture of **1** (1.12 g, 10 mmol), benzyl chloride (1.89 g, 15 mmol), and potassium carbonate (0.69 g 5 mmol) in DMSO (20 ml) was stirred at 60—70 °C for 1h. A 4% aqueous solution of NaOH (20 ml) was added to the hot reaction solution. The mixture was extracted with benzene (20 ml × 3), and the aqueous phase was adjusted to pH 2—3 with concentrated HCl. On standing in a refrigerator, crystals precipitated was collected by filtration, and washed with water. The crude product was purified by recrystallization from MeOH to give **2e** (1.15 g, 57%) as white

needles, mp 171—173 °C (lit.[15] mp 173 °C). MS *m/z*: 202 (M^+). ^{1}H-NMR (DMSO-d_6) δ: 4.85 (2H, s, $C\underline{H}_2C_6H_5$), 5.53 (1H, d, 5-H, J=7.8 Hz), 7.70 (1H, d, 6-H, J=7.8 Hz), 7.18—7.35 (5H, m, $CH_2C_6\underline{H}_5$), 11.23 (1H, br, NH). UV λ_{max}^{EtOH} nm (log ε): 261 (3.84). UV $\lambda_{max}^{1\,N\,NaOH-EtOH\,(1:10)}$ nm (log ε): 261 (3.70). *Anal.* Calcd for $C_{11}H_{10}N_2O_2$: C, 65.33; H, 4.98; N, 13.86. Found: C, 65.21; H, 5.04; N, 13.65.

1,3-Dibenzyluracil (2f) A solution of **1** (2.24 g, 20 mmol) in DMF (40 ml) was treated with 60% NaH (1.60 g, 40 mmol), and the resulting mixture was stirred at 40—50 °C for 1 h. After the evolution of hydrogen gas ceased, benzyl chloride (3.78 g, 30 mmol) was added to the reaction mixture, and the whole was stirred at 50—60 °C for 2 h. A 4% aqueous solution of NaOH (20 ml) was added to the resultant reaction solution, which was then extracted with AcOEt (30 ml × 3). The combined extracts were dried (Na_2SO_4), and concentrated *in vacuo* to dryness. The residue was recrystallized from $CHCl_3$–hexane (1 : 1) to give **2f** (4.62 g, 79%) as colorless prisms, mp 71—72 °C. MS *m/z*: 292 (M^+). ^{1}H-NMR ($CDCl_3$) δ: 4.87, 5.11 (2H each, s, $C\underline{H}_2C_6H_5 \times 2$), 5.68 (1H, d, 5-H, J=7.8 Hz), 7.06 (1H, d, 6-H, J=5.4 Hz), 7.16—7.57 (10H, m, $CH_2C_6\underline{H}_5 \times 2$). *Anal.* Calcd for $C_{18}H_{16}N_2O_2$: C, 73.95; H, 5.52; N, 9.58. Found: C, 73.70; H, 5.64; N, 9.31.

Reaction of 5-Fluorouracil (5) with Methyl Iodide A mixture of 5-fluorouracil (**5**, 1.30 g, 10 mmol), methyl iodide (2.13 g, 15 mmol), and potassium carbonate (0.69 g, 5 mmol) in dry acetone (20 ml) was stirred at 60—70 °C for 24 h. The resulting solution was filtered, and the filtrate was concentrated *in vacuo*. The resulting residue was taken up in a small volume of $CHCl_3$, and fractionated by silica gel column chromatography with $CHCl_3$ to give **6a**, **b**, and **6c**.

5-Fluoro-1-methyluracil (6a) This compound was recrystallized from acetone–EtOH (1 : 1) yield, 777 mg (27%, pale yellow needles), mp 255—257 °C (lit.[16] mp 257—260 °C). MS *m/z*: 144 (M^+). ^{1}H-NMR (DMSO-d_6) δ: 3.23 (3H, s, NCH_3), 7.98 (1H, d, 6-H, J=6.0 Hz), 11.60 (1H, br, NH). UV λ_{max}^{EtOH} nm (log ε): 271 (3.96). UV $\lambda_{max}^{1\,N\,NaOH-EtOH\,(1:10)}$ nm (log ε): 269 (3.79). *Anal.* Calcd for $C_5H_5FN_2O_2$: C, 41.67; H, 3.47; N, 19.44. Found: C, 41.40; H, 3.43; N, 19.20.

5-Fluoro-3-methyluracil (6b) This compound was recrystallized from acetone–EtOH (1 : 1) to give 355 mg (12%) as white needles, mp 170—171 °C. MS *m/z*: 144 (M^+). ^{1}H-NMR (DMSO-d_6) δ: 3.21 (3H, s, NCH_3), 7.76 (1H, d, 6-H, J=5.7 Hz), 11.02 (1H, br, NH). UV λ_{max}^{EtOH} nm (log ε): 263 (3.81). UV $\lambda_{max}^{1\,N\,NaOH-EtOH\,(1:10)}$ nm (log ε): 293 (3.96). *Anal.* Calcd for $C_5H_5FN_2O_2$: C, 41.67; H, 3.47; N, 19.44. Found: C, 41.42; H, 3.52; N, 19.24.

5-Fluoro-1,3-dimethyluracil (6c) Recrystallization of **7c** from $CHCl_3$–hexane (1 : 1) gave 550 mg (17%) as white needles, mp 128—129 °C (lit.[17] mp 128—130 °C). MS *m/z*: 158 (M^+). ^{1}H-NMR ($CDCl_3$) δ: 3.36, 3.38 (3H each, s, NCH_3), 7.30 (1H, d, 6-H, J=5.4 Hz). *Anal.* Calcd for $C_6H_7FN_2O_2$: C, 45.57; H, 4.43; N, 17.72. Found: C, 45.79; H, 4.56; N, 17.47.

Reaction of 5 with Ethyl Iodide A mixture of **5** (1.30 g, 10 mmol), ethyl iodide (2.34 g, 15 mmol), and potassium carbonate (0.69 g, 5 mmol) was added to dry acetone (20 ml). The mixture was treated as described above to give **6d** (553 mg, 35%) and **6e** (409 mg, 22%), each as white needles.

1-Ethyl-5-fluorouracil (6d) This compound showed mp 183—184 °C. MS *m/z*: 158 (M^+). ^{1}H-NMR (DMSO-d_6) δ: 1.15 (3H, t, $CH_2C\underline{H}_3$, J=7.2 Hz), 3.64 (2H, q, $C\underline{H}_2CH_3$, J=7.2 Hz), 8.07 (1H, d, 6-H, J=6.3 Hz), 11.67 (1H, br, NH). UV λ_{max}^{EtOH} nm (log ε): 270 (3.79). UV $\lambda_{max}^{1\,N\,NaOH-EtOH\,(1:10)}$ nm (log ε): 270 (3.69). *Anal.* Calcd for $C_6H_7FN_2O_2$: C, 45.57; H, 4.43; N, 17.72. Found: C, 45.58; H, 4.46; N, 17.62.

1,3-Diethyl-5-fluorouracil (6e) This compound showed mp 66—68 °C. MS *m/z*: 186 (M^+). ^{1}H-NMR ($CDCl_3$) δ: 1.20, 1.29 (3H each, t, $CH_2C\underline{H}_3$, J=7.2 Hz), 3.77, 4.00 (2H each, q, $C\underline{H}_2CH_3$, J=7.2 Hz), 7.23 (1H, d, 6-H, J=5.7 Hz). *Anal.* Calcd for $C_8H_{11}FN_2O_2$: C, 51.61; H, 5.91; N, 15.05. Found: C, 51.50; H, 6.15; N, 14.99.

1-Benzyl-5-fluorouracil (6f) A mixture of **5** (6.50 g, 50 mmol), benzyl chloride (9.53 g, 75 mmol), and potassium carbonate (3.45 g, 25 mmol) in DMSO (100 ml) was treated according to the procedure described above for **2e** to give **6f** (6.80 g, 62%) as white needles, mp 170—171 °C (lit.[18] mp 173—174 °C). MS *m/z*: 220 (M^+). ^{1}H-NMR (DMSO-d_6) δ: 4.89 (2H, s, $C\underline{H}_2C_6H_5$), 7.18 (1H, d, 6-H, J=5.4 Hz), 7.26—7.43 (5H, m, $CH_2C_6\underline{H}_5$), 9.10 (1H, br, NH). UV λ_{max}^{EtOH} nm (log ε): 271 (3.98). UV $\lambda_{max}^{1\,N\,NaOH-EtOH\,(1:10)}$ nm (log ε): 269 (3.57). *Anal.* Calcd for $C_{11}H_9FN_2O_2$: C, 60.00; H, 4.09; N, 12.73. Found: C, 60.22; H, 4.30; N, 12.51.

1,3-Dibenzyl-5-fluorouracil (6g) Compound **5** (1.30 g, 10 mmol) was dissolved in DMF (20 ml), and 60% NaH (1.20 g, 30 mmol) was added to the resulting solution. The mixture was treated according to the procedure described above for **2f** to give **6g** (2.22 g, 72%) as white needles, mp 148—149 °C. MS *m/z*: 310 (M^+). ^{1}H-NMR ($CDCl_3$) δ: 4.35 (2H, s, $C\underline{H}_2C_6H_5$), 4.88, 5.15 (1H each, s, $C\underline{H}_2C_6H_5$), 7.15 (1H, d, 6-H, J=5.4 Hz), 7.20—7.57 (10H, m, $CH_2C_6\underline{H}_5 \times 2$). *Anal.* Calcd for $C_{18}H_{15}FN_2O_2$: C, 69.68; H, 4.84; N, 9.03. Found: C, 69.57; H, 4.88; N, 9.28.

General Procedure for the Synthesis of 3-Alkyl-2′,3′,5′-tri-*O*-benzoyluridines (12a—c) A mixture of 2′,3′,5′-tri-*O*-benzoyluridine (**10**, 5 mmol)[8] and 60% NaH (5 mmol) in DMF (50 ml) was stirred at 60 °C for 1 h. Alkyl halide (7.5 mmol) was added, and the mixture was stirred at 60—70 °C for 10 h. Water (50 ml) was added to the solution, and the mixture was extracted with $CHCl_3$ (30 ml × 3). The combined extracts were dried (Na_2SO_4), and then the filtrate was concentrated *in vacuo*. The residue was taken up in a small volume of $CHCl_3$, and subjected to column chromatography on silica gel with $CHCl_3$–EtOH (20 : 1). The fraction containing the desired product was collected and concentrated, and the residue was recrystallized from an appropriate solvent; yields, melting points, and MS data are listed in Table II.

2′,3′,5′,-Tri-*O*-benzoyl-3-methyluridine (12a) ^{1}H-NMR ($CDCl_3$) δ: 3.30 (3H, s, NCH_3), 4.50—4.88 (3H, m, 4′-H, 5′-H), 5.65 (1H, d, 5-H, J=7.8 Hz), 5.77 (1H, dd, 2′-H, J=4.8, 6.0 Hz), 5.90 (1H, dd, 3′-H, J=4.2, 6.0 Hz), 6.22 (1H, d, 1′-H, J=4.8 Hz), 7.33 (1H, d, 6-H, J=7.8 Hz), 7.24—7.65, 7.83—8.21 (15H, m, $C_6H_5 \times 3$). *Anal.* Calcd for $C_{31}H_{26}N_2O_9$: C, 65.26; H, 4.59; N, 4.91. Found: C, 65.12; H, 4.75; N, 4.79.

2′,3′,5′-Tri-*O*-benzoyl-3-ethyluridine (12b) ^{1}H-NMR ($CDCl_3$) δ: 1.17 (3H, t, $CH_2C\underline{H}_3$, J=7.2 Hz), 3.95 (2H, q, $C\underline{H}_2CH_3$, J=7.2 Hz), 4.54—4.90 (3H, m, 4′-H, 5′-H), 5.62 (1H, d, 5-H, J=8.2 Hz), 5.76 (1H, dd, 2′-H, J=4.8, 6.0 Hz), 5.90 (1H, dd, 3′-H, J=4.2, 6.0 Hz), 6.28 (1H, d, 1′-H, J=4.8 Hz), 7.34 (1H, d, 6-H, J=8.2 Hz), 7.25—7.68, 7.86—8.20 (15H, m, $C_6H_5 \times 3$). *Anal.* Calcd for $C_{32}H_{28}N_2O_9$: C, 65.75; H, 4.83; N, 4.79. Found: C, 65.64; H, 4.87; N, 4.68.

2′,3′,5′-Tri-*O*-benzoyl-3-bezyluridine (12c) ^{1}H-NMR ($CDCl_3$) δ: 4.52—4.90 (3H, m, 4′-H, 5′-H), 5.03, 5.06 (1H each, s, $C\underline{H}_2C_6H_5$), 5.65

TABLE II. Reactions of **10**, **11** with Alkylating Agents

Starting material	Alkylating agent	60% NaH	K_2CO_3	Solvent	Product		
					Yield (%)	mp[a] (°C)	MS (*m/z*)
10 2.78 g, 5 mmol	MeI 1.07 g, 7.5 mmol	0.20 g, 5 mmol	—	DMF	40	57—60	570
10 2.78 g, 5 mmol	EtI 1.17 g, 7.5 mmol	0.20 g, 5 mmol	—	DMF	59	75—76	584
10 2.78 g, 5 mmol	BnCl 0.95 g, 7.5 mmol	0.20 g, 5 mmol	—	DMF	55	76—78	646
11 2.87 g, 5 mmol	MeI 1.07 g, 7.5 mmol	—	345 mg, 2.5 mmol	Acetone	57	88—89	588
11 5.74 g, 10 mmol	EtI 2.34 g, 15 mmol	—	0.69 g, 5 mmol	Acetone	55	72—73	602
11 5.74 g, 10 mmol	BnCl 1.91 g, 15 mmol	—	0.69 g, 5 mmol	Acetone	54	77—78	664

a) Recrystallized from $CHCl_3$–hexane (1 : 1).

TABLE III. Photocycloaddition Reactions of **2** or **6** with **3** in Acetone at Room Temperature

Starting material	Product			*Anal.* Calcd (%)			Found (%)		
	Yield (%)	mp[a] (°C)	MS (*m/z*)	C	H	N	C	H	N
2a	77	154—156	210	62.83	8.63	13.32	62.79	8.81	13.15
2b	76	69—70	224	64.25	8.99	12.49	64.18	9.05	12.37
2c	68	183—184	224	64.25	8.99	12.49	64.16	9.15	12.36
2d	56	Oil	252	66.63	9.59	11.10	66.38	9.47	11.09
2e	89	144—145	286	71.30	7.74	9.78	71.41	7.90	9.95
2f	73	Oil	376	76.56	7.50	7.44	76.51	7.66	7.31
6a	56	130—131	228	57.89	7.46	12.28	57.63	7.44	12.08
6b	99	123—124	228	57.89	7.46	12.28	58.01	7.04	12.10
6c	93	136—137	242	59.50	7.85	11.57	59.77	7.67	11.39
6d	41	Oil	242	59.50	7.85	11.57	59.60	7.79	11.32
6e	81	Oil	270	62.22	8.52	10.37	62.18	8.79	10.60
6f	99	159—160	304	67.11	6.91	9.21	67.37	7.19	9.28
6g	93	98—100	394	73.10	6.85	7.11	72.98	7.03	6.92

a) Recrystallized from $CHCl_3$–hexane (1 : 1).

(1H, d, 5-H, J=8.4 Hz), 5.70 (1H, t, 2′-H, J=5.4 Hz), 5.90 (1H dd, 3′-H, J=4.2, 5.4 Hz), 6.33 (1H, d, 1′-H, J=5.4 Hz), 7.18—7.63, 7.80—8.18 (21H, m, C_6H_5×4, 6-H). *Anal.* Calcd for $C_{37}H_{30}N_2O_9$: C, 68.72; H, 4.68; N, 4.33. Found: C, 68.75; H, 4.81; N, 4.17.

General Procedure for the Synthesis of 3-Alkyl-2′,3′,5′-tri-*O*-benzoyl-5-fluorouridines (13a—c) A mixture of 2′,3′,5′-tri-*O*-benzoyl-5-fluorouridine (**11**)[9], alkyl halide and potassium carbonate in dry acetone was stirred at 60—70 °C for 7 h, then filtered, and the filtrate was concentrated. The residue was taken up in a small volume of $CHCl_3$, and subjected to column chromatography on silica gel, with $CHCl_3$–EtOH (20 : 1). The crude product was recrystallized from an appropriate solvent; yields, melting points, and MS data are listed in Table II.

2′,3′,5′-Tri-*O*-benzoyl-5-fluoro-3-methyluridine (13a) ^{1}H-NMR ($CDCl_3$) δ: 3.30 (3H, s, NCH_3), 4.58—4.80 (3H, m, 4′-H, 5′-H), 5.63—5.93 (2H, m, 2′-H, 3′-H), 6.27 (1H, d, 1′-H, J=5.4 Hz), 7.24—7.70, 7.85—8.20 (16H, m, C_6H_5×3, 6-H). *Anal.* Calcd for $C_{31}H_{25}FN_2O_9$: C, 63.27; H, 4.25; N, 4.76. Found: C, 63.56; H, 4.40; N, 4.68.

2′,3′,5′-Tri-*O*-benzoyl-3-ethyl-5-fluorouridine (13b) ^{1}H-NMR ($CDCl_3$) δ: 1.14 (3H, t, $CH_2C\underline{H}_3$, J=7.2 Hz), 3.96 (2H, q, $C\underline{H}_2CH_3$, J=7.2 Hz), 4.60—4.83 (3H, m, 4′-H, 5′-H), 5.63—5.97 (2H, m, 2′-H, 3′-H), 6.33 (1H, d, 1′-H, J=5.4 Hz), 7.20—7.73, 7.87—8.22 (16 H, m, C_6H_5×3, 6-H). *Anal.* Calcd for $C_{32}H_{27}FN_2O_9$: C, 63,79; H, 4.49; N, 4.65. Found: C, 63.57; H, 4.56; N. 4.51.

2′,3′,5′-Tri-*O*-benzoyl-3-benzyl-5-fluorouridine (13c) ^{1}H-NMR ($CDCl_3$) δ: 4.63—4.80 (3H, m, 4′-H, 5′-H), 5.08 (2H, s, $C\underline{H}_2C_6H_5$), 5.53—5.95 (2H, m, 2′-H, 3′-H), 6.40 (1H, d, 1′-H, J=5.4 Hz), 7.17—7.67, 7.75—8.20 (21H, m, C_6H_5×4, 6-H). *Anal.* Calcd for $C_{37}H_{29}FN_2O_9$: C, 66.87; H, 4.37; N, 4.22. Found: C, 66.74; H, 4.42; N, 4.12.

General Procedure for Photocycloaddition of 2 or 6 to 2,3-Dimethyl-2-butene (3) A solution of **2** or **6** (2 mmol) and 2,3-dimethyl-2-butene (**3**, 1.68 g, 20 mmol) in dry acetone (600 ml) was irradiated with a 400 W high-pressure mercury lamp through a Pyrex filter under a nitrogen atmosphere for 72 h. After evaporation of the solvent, the residue was subjected to column chromatography on silica gel with $CHCl_3$–EtOH (10 : 1). A fraction containing the product was collected and evaporated to dryness, and the residue was recrystallized from an appropriate solvent to give an analytical sample of **4** or **7**; yields, melting points, MS data, and combustion values are listed in Table III.

2,7,7,8,8-Pentamethyl-*cis*-2,4-diazabicyclo[4.2.0]octane-3,5-dione (4a) ^{1}H-NMR ($CDCl_3$) δ: 1.00, 1.03, 1.12, 1.27 (3H each, s, CCH_3), 2.96 (3H, s, NCH_3), 2.94 (1H, d, 6-H, J=10.2 Hz), 3.65 (1H, d, 1-H, J=10.2 Hz), 8.08 (1H, br, NH).

2,4,7,7,8,8-Hexamethyl-*cis*-2,4-diazabicyclo[4.2.0]octane-3,5-dione (4b) ^{1}H-NMR ($CDCl_3$) δ: 0.93, 0.97, 1.12, 1.23 (3H each, s, CCH_3), 2.93, 3.20 (3H each, s, NCH_3), 2.98 (1H, d, 6-H, J=9.6 Hz), 3.58 (1H, d, 1-H, J=9.6 Hz).

2-Ethyl-7,7,8,8-tetramethyl-*cis*-2,4-diazabicyclo[4.2.0]octane-3,5-dione (4c) ^{1}H-NMR ($CDCl_3$) δ: 0.99, 1.02, 1.09, 1.24 (3H each, s, CCH_3), 1.09 (3H, t, $CH_2C\underline{H}_3$, J=7.2 Hz), 2.90, 3.77 (1H each, m, $C\underline{H}_2CH_3$), 2.88 (1H, d, 6-H, J=10.2 Hz), 3.76 (1H, d, 1-H, J=10.2 Hz), 8.37 (1H, br, NH).

2,4-Diethyl-7,7,8,8-tetramethyl-*cis*-2,4-diazabicyclo[4.2.0]octane-3,5-dione (4d) ^{1}H-NMR ($CDCl_3$) δ: 0.93, 0.96, 1.09, 1.25 (3H each, s, CCH_3), 1.15, 1.21 (3H each, t, $CH_2C\underline{H}_3$, J=7.0 Hz), 2.93 (1H, d, 6-H, J=10.2 Hz), 3.67 (1H, d, 1-H, J=10.2 Hz), 2.71—3.10 (1H, m, $C\underline{H}_2CH_3$), 3.63—4.05 (1H, m, $C\underline{H}_2CH_3$), 3.88 (2H, q, $C\underline{H}_2CH_3$, J=7.0 Hz).

2-Benzyl-7,7,8,8-tetramethyl-*cis*-2,4-diazabicyclo[4.2.0]octane-3,5-dione (4e) ^{1}H-NMR ($CDCl_3$) δ: 0.84, 0.86, 0.89, 1.11 (3H each, s, CCH_3), 2.82 (1H, d, 6-H, J=9.6 Hz), 3.71 (1H, d, 1-H, J=9.6 Hz), 4.01, 4.87 (1H, each, d, $C\underline{H}_2C_6H_5$, J=15.0 Hz), 7.22—7.43 (5H, m, $CH_2C_6\underline{H}_5$), 10.12 (1H, br, NH).

2,4-Dibenzyl-7,7,8,8-tetramethyl-*cis*-2,4-diazabicyclo[4.2.0]octane-3,5-dione (4f) ^{1}H-NMR ($CDCl_3$) δ: 0.79, 0.88, 0.96, 1.15 (3H each, s, CCH_3), 2.85 (1H, d, 6-H, J=10.0 Hz), 3.60 (1H, d, 1-H, J=10.0 Hz), 3.84, 5.22 (1H each, d, $C\underline{H}_2C_6H_5$, J=15.0 Hz), 5.06 (2H, s, $C\underline{H}_2C_6H_5$), 7.20—7.57 (10H, m, $CH_2C_6\underline{H}_5$×2).

6-Fluoro-2,7,7,8,8-pentamethyl-*cis*-2,4-diazabicyclo[4.2.0]octane-3,5-dione (7a) ^{1}H-NMR ($CDCl_3$) δ: 0.92, 1.05, 1.18, 1.18 (3H each, s, CCH_3), 2.99 (3H, s, NCH_3), 3.73 (1H, d, 1-H, J=22.8 Hz), 8.22 (1H, br, NH).

6-Fluoro-4,7,7,8,8-pentamethyl-*cis*-2,4-diazabicyclo[4.2.0]octane-3,5-dione (7b) ^{1}H-NMR ($CDCl_3$) δ: 0.87, 1.01, 1.12 (3H each, s, CCH_3), 1.20 (3H, d, CCH_3, J=3.9 Hz), 3.21 (3H, s, NCH_3), 3.83 (1H, d, 1-H, J=22.8 Hz), 7.00 (1H, br, NH).

6-Fluoro-2,4,7,7,8,8-hexamethyl-*cis*-2,4-diazabicyclo[4.2.0]octane-3,5-dione (7c) ^{1}H-NNR ($CDCl_3$) δ: 0.82, 0.99, 1.18 (3H each, s, CCH_3), 1.21 (3H, d, CCH_3, J=4.2 Hz), 3.00, 3.22 (3H each, s, NCH_3), 3.78 (1H, d, 1-H, J=22.8 Hz).

2-Ethyl-6-fluoro-7,7,8,8-tetramethyl-*cis*-2,4-diazabicyclo[4.2.0]octane-3,5-dione (7d) ^{1}H-NMR ($CDCl_3$) δ: 0.82, 1.00, 1.14, 1.18 (3H each, s, CCH_3), 1.14 (3H, t, $CH_2C\underline{H}_3$, J=7.2 Hz), 3.75 (1H, d, 1-H, J=22.8 Hz), 3.91 (2H, q, $C\underline{H}_2CH_3$, J=7.2 Hz), 8.43 (1H, br, NH).

2,4-Diethyl-6-fluoro-7,7,8,8-tetramethyl-*cis*-2,4-diazabicyclo[4.2.0]-octane-3,5-dione (7e) ^{1}H-NMR ($CDCl_3$) δ: 0.82, 1.01, 1.18 (3H, each, s, CCH_3), 1.25 (3H, d, CCH_3, J=3.9 Hz), 1.15 (3H, m, $CH_2C\underline{H}_3$), 1.23 (3H, t, $CH_2C\underline{H}_3$, J=7.2 Hz), 3.07, 3.68 (1H each, m, $C\underline{H}_2CH_3$), 3.72 (1H, d, 1-H, J=22.8 Hz), 3.92 (2H, q, $C\underline{H}_2CH_3$, J=7.2 Hz).

2-Benzyl-6-fluoro-7,7,8,8-tetramethyl-*cis*-2,4-diazabicyclo[4.2.0]octane-3,5-dione (7f) ^{1}H-NMR ($CDCl_3$) δ: 0.88, 0.95, 1.02, 1.10 (3H each, s, CCH_3), 3.72 (1H, d, 1-H, J=22.8 Hz), 4.13, 4.99 (1H each, d, $C\underline{H}_2C_6H_5$, J=15.0 Hz), 7.18—7.47 (5H, m, $CH_2C_6\underline{H}_5$), 8.47 (1H, br, NH).

2,4-Dibenzyl-6-fluoro-7,7,8,8-tetramethyl-*cis*-2,4-diazabicyclo[4.2.0]-octane-3,5-dione (7g) ^{1}H-NMR ($CDCl_3$) δ: 0.58, 0.87, 0.91 (3H each, s, CCH_3), 1.11 (3H, d, CCH_3, J=3.9 Hz), 3.68 (1H, d, 1-H, J=22.8 Hz), 4.11, 5.01 (1H each, d, $C\underline{H}_2C_6H_5$, J=14.4 Hz), 5.09 (2H, s, $C\underline{H}_2C_6H_5$), 7.15—7.56 (10H, m, $CH_2C_6\underline{H}_5$×2).

Photoaddition of 2′,3′-*O*-Isopropylideneuridine (8) to 3 A solution of 2′,3′-*O*-isopropylideneuridine (**8**, 1.50 g, 5.28 mmol) and **3** (4.40 g, 52.8 mmol) in dry acetone (600 ml) was irradiated with a 400 W high-pressure mercury lamp through an Pyrex filter under nitrogen atmosphere for 48 h. After evaporation of the solvent, the residue was subjected to preparative TLC (precoated TLC plates, Silica gel 60F-254, Merck) with $CHCl_3$ to give **9a** (1.05 g, 54%) as colorless needles (mp 218—219 °C from $CHCl_3$) and **9b** (117 mg, 6%) as a colorless syrup. The ratio of **9a** and **9b** was 9 : 1 as determined from the isolated yields.

TABLE IV. Atomic Coordinates (10^4) with Their Standard Deviations in Parentheses and Equivalent Isotropic Temperature Factors

Atom	x	y	z	B_{eq}	Atom	x	y	z	B_{eq}
O1	−1874 (6)	9738 (3)	8811 (10)	5.0	C8	−116 (9)	8549 (4)	4876 (12)	3.1
O2	−3757 (7)	8319 (3)	5917 (12)	5.7	C9	−1494 (10)	7627 (4)	4603 (17)	4.5
O3	818 (5)	9741 (2)	7560 (10)	3.9	C10	−997 (12)	8165 (5)	1816 (17)	6.0
O4	−269 (7)	10861 (3)	5099 (10)	5.1	C11	1130 (10)	8571 (4)	3999 (18)	5.1
O5	1306 (7)	11050 (3)	6960 (11)	5.7	C12	46 (9)	8367 (4)	6851 (15)	4.0
O6	−101 (9)	10046 (4)	11266 (10)	6.6	C13	−39 (8)	9914 (3)	6188 (14)	3.2
N2	−1024 (6)	9478 (3)	6105 (9)	2.2	C14	−428 (8)	10510 (4)	6615 (15)	3.6
N4	−2747 (7)	9023 (3)	7266 (11)	3.5	C15	515 (11)	10708 (4)	8017 (14)	4.3
C1	−938 (8)	9082 (3)	4673 (12)	2.7	C16	1223 (9)	10206 (4)	8633 (16)	4.4
C3	−1860 (8)	9445 (4)	7443 (14)	3.1	C17	1061 (13)	10047 (5)	10651 (18)	6.2
C5	−2926 (8)	8652 (4)	5878 (15)	3.5	C18	597 (9)	11283 (4)	5517 (14)	3.9
C6	−2067 (8)	8710 (3)	4296 (13)	3.0	C19	1419 (14)	11342 (7)	3878 (22)	8.2
C7	−1176 (8)	8204 (4)	3851 (15)	3.4	C20	−29 (14)	11830 (4)	6037 (19)	6.5

TABLE V. Bond Lengths (Å) with Their Standard Deviations in Parentheses

O1–C3	1.225 (12)	C5–C6	1.499 (13)
O2–C5	1.202 (11)	C6–C1	1.538 (12)
O3–C13	1.434 (11)	C6–C7	1.582 (12)
O3–C16	1.429 (12)	C7–C8	1.604 (13)
O4–C14	1.405 (12)	C7–C9	1.521 (13)
O4–C18	1.411 (12)	C7–C10	1.514 (16)
O5–C15	1.417 (13)	C8–C11	1.502 (15)
O5–C18	1.425 (12)	C8–C12	1.528 (13)
O6–C17	1.342 (16)	C13–C14	1.514 (12)
N2–C1	1.418 (10)	C14–C15	1.529 (14)
N2–C3	1.342 (11)	C15–C16	1.492 (14)
N2–C13	1.493 (10)	C16–C17	1.544 (17)
N4–C3	1.399 (11)	C18–C19	1.508 (18)
N4–C5	1.365 (12)	C18–C20	1.518 (15)
C1–C8	1.559 (12)		

TABLE VI. Bond Angles (°) with Their Standard Deviations in Parentheses

C3–N2–C1	123.4 (6)	C19–C18–C20	112.8 (10)
C3–N4–C5	129.2 (8)	O1–C3–N4	118.4 (8)
C13–N2–C1	116.5 (6)	O1–C3–N2	125.4 (8)
C13–N2–C3	119.8 (6)	N4–C3–N2	116.2 (8)
C13–O3–C16	111.5 (6)	O2–C5–N4	121.0 (9)
C14–O4–C18	109.4 (7)	O2–C5–C6	123.2 (9)
C15–O5–C18	107.8 (7)	N4–C5–C6	115.7 (7)
O3–C13–N2	107.2 (6)	C5–C6–C1	114.2 (7)
O3–C13–C14	107.7 (7)	C5–C6–C7	118.2 (7)
N2–C13–C14	117.3 (7)	C1–C6–C7	89.3 (6)
O4–C14–C13	110.9 (8)	N2–C1–C6	117.7 (7)
O4–C14–C15	105.7 (7)	N2–C1–C8	120.5 (7)
C13–C14–C15	103.9 (7)	C6–C1–C8	90.4 (6)
O5–C15–C14	102.3 (7)	C1–C8–C7	87.7 (6)
O5–C15–C16	108.3 (8)	C1–C8–C11	116.6 (7)
C14–C15–C16	107.7 (8)	C1–C8–C12	112.8 (7)
O3–C16–C15	107.0 (8)	C7–C8–C11	117.6 (8)
O3–C16–C17	107.9 (8)	C7–C8–C12	112.7 (7)
C15–C16–C17	115.4 (9)	C11–C8–C12	108.4 (8)
O6–C17–C16	115.7 (10)	C6–C7–C8	87.2 (6)
O4–C18–O5	104.3 (7)	C6–C7–C10	109.3 (8)
O4–C18–C19	106.8 (9)	C6–C7–C9	118.3 (8)
O4–C18–C20	111.5 (8)	C8–C7–C10	113.9 (8)
O5–C18–C19	108.3 (9)	C8–C7–C9	117.0 (8)
O5–C18–C20	112.8 (8)	C10–C7–C9	109.6 (8)

(1*R*,6*R*)-2-(2,3-*O*-Isopropylidene-β-D-ribofuranosyl)-7,7,8,8-tetramethyl-*cis*-2,4-diazabicyclo[4.2.0]octane-3,5-dione (9a) mp 218—219 °C. MS *m/z*: 368 (M^+). ^{1}H-NMR ($CDCl_3$, 300 MHz) δ: 1.00, 1.07, 1.08, 1.23 (3H each, s, CCH_3), 1.33, 1.53 (3H each, s, isopropylidene), 2.93 (1H, d, 6-H, J=10.0 Hz), 2.95 (1H, br, 5′-OH), 3.68—3.86 (2H, m, 5′-H), 3.87 (1H, d, 1-H, J=10.0 Hz), 4.17 (1H, dd, 4′-H, J=3.3, 6.3 Hz), 4.82 (1H, d, 1′-H, J=3.0 Hz), 4.97 (1H, dd, 3′-H, J=3.3, 6.6 Hz), 5.09 (1H, dd, 2′-H, J=3.0, 6.6 Hz), 8.14 (1H, br, NH). *Anal.* Calcd for $C_{18}H_{28}N_2O_6$: C, 58.68; H, 7.66; N, 7.60. Found: C, 58.59; H, 7.82; N, 7.53.

(1*S*,6*S*)-2-(2,3-*O*-Isopropylidene-β-D-ribofuranosyl)-7,7,8,8-tetramethyl-*cis*-2,4-diazabicyclo[4.2.0]octane-3,5-dione (9b) MS *m/z*: 368 (M^+). ^{1}H-NMR ($CDCl_3$, 300 MHz) δ: 1.03, 1.04, 1.08, 1.24 (3H each, s, CCH_3), 1.35, 1.52 (3H each, s, isopropylidene), 2.98 (1H, d, 6-H, J=10.0 Hz), 3.20 (1H, br, 5′-OH), 3.71—3.95 (2H, m, 5′-H), 3.86 (1H, d, 1-H, J=10.0 Hz), 4.16 (1H, dd, 4′-H, J=3.3, 6.3 Hz), 4.80 (1H, d, 1′-H, J=4.0 Hz), 4.95 (1H, dd, 3′-H, J=3.3, 6.3 Hz), 5.27 (1H, dd, 2′-H, J=4.0, 6.3 Hz), 7.44 (1H, br, NH). *Anal.* Calcd for $C_{18}H_{28}N_2O_6$: C, 58.68; H, 7.66; N, 7.60. Found: C, 58.42; H, 7.90; N, 7.37.

X-Ray Crystallographic Analysis of 9a A crystal of **9a** with the dimensions of 0.3 × 0.4 × 0.4 mm^3 was used for the analysis. The cell dimensions and diffraction intensities were measured on a Rigaku four-circle diffractometer, using graphite-monochromated Cu K_α radiation (λ = 1.5479 Å).

Crystal Data: $C_{18}H_{28}N_2O_6$, orthorhombic, space group $P2_12_12_1$, a=10.871(2) Å, b=23.802(5) Å, c=7.365(1) Å, V=1905.7 Å^3, Z=4, D_c=1.284 g·cm^{-3}. One thousand four hundred and eighty three independent reflections in the range of $2\theta < 150°$ were collected by the use of the 2θ–ω scan mode with a scanning rate of 8° (2θ) min^{-1}. A total of 1375 independent reflections with $|F_O| > 3\sigma(|F_O|)$ were obtained and corrected for Lorentz and polarization factors but not for absorption. The structure was elucidated by a direct method using MULTAN.[19] The E-map of the phase set with the highest figure of merit showed the skeleton of the molecule, whose structure was refined by a block-diagonal least squares method with anisotropic temperature factors. A difference Fourier synthesis was then calculated and the positions of all hydrogen atoms except those of methyl groups were found. The positions of the 15 hydrogen atoms in methyl groups were calculated and inculded in the final stage of refinement. The atomic scattering factors were those given by the International Tables for X-Ray Crystallography.[20] The final R value was 8.9%, where $R = \sum||F_O| - |F_C||/\sum|F_C|$.

The final atomic parameters are listed in Table IV. Bond lengths and angles are shown in Tables V and VI. No abnormal lengths or angles were found in the structure.

General Procedure for the Photoaddition of 11—13 to 3 A solution of one of **11—13** (2 mmol) and **3** (1.68 g, 20 mmol) in dry acetone (600 ml) was irradiated with a 400 W high-pressure mercury lamp through a Pyrex filter under a nitrogen atmosphere for 72 h. After evaporation of the solvent, the residue was subjected to column chromatography on silica gel with $CHCl_3$–EtOH (10 : 1), and the products were recrystallized from appropriate solvents; yields, melting points, MS data, and combustion values are listed in Table VII.

(1*R*,6*R*)-4,7,7,8,8-Pentamethyl-2-(2,3,5-tri-*O*-benzoyl-β-D-ribofuranosyl)-*cis*-2,4-diazabicyclo[4.2.0]octane-3,5-dione (14a) and (1*S*,6*S*)-4,7,7,8,8-Pentamethyl-2-(2,3,5-tri-*O*-benzoyl-β-D-ribofuranosyl)-*cis*-2,4-diazabicyclo[4.2.0]octane-3,5-dione (15a) The ratio of **14a** and **15a** was 1.2 : 1 as determined from the isolated yields.

14a: ^{1}H-NMR ($CDCl_3$, 300 MHz) δ: 0.89, 0.91, 0.93, 1.01 (3H each, s, CCH_3), 2.93 (1H, d, 6-H, J=10.2 Hz, 3.17 (3H, s, NCH_3), 3.94 (1H, d, 1-H, J=10.2 Hz), 4.53—4.77 (3H, m, 4′-H, 5′-H), 5.86 (1H, t, 2′-H, J=6.0 Hz), 5.89 (1H, dd, 3′-H, J=4.0, 6.0 Hz), 6.21 (1H, d, 1′-H,

TABLE VII. Photocycloaddition Reactions of **11**—**13** with **3** in Acetone at Room Temperature

Starting material	Product	Product			*Anal.* Calcd (%)			Found (%)		
		Yield (%)	mp (°C)	MS (*m/z*)	C	H	N	C	H	N
12a	**14a**	35	140—141[a]	654	67.87	5.85	4.28	67.61	6.03	4.07
	15a	29	71—73[a]	654	67.87	5.85	4.28	67.79	5.98	4.11
12b	**14b, 15b**	91	Foam	668	68.25	6.03	4.19	68.15	6.16	3.99
12c	**14c, 15c**	93	Foam	730	70.67	5.79	3.83	70.53	5.91	3.65
11	**16a**	66	116—118[a]	658	65.65	5.32	4.26	65.37	5.52	4.20
	17a	26	88—90[a]	658	65.65	5.32	4.26	65.43	5.41	4.08
13a	**16b, 17b**	99	Foam	672	66.07	5.51	4.17	65.87	5.72	3.90
13b	**16c, 17c**	96	Foam	686	66.46	5.72	4.07	66.25	5.86	3.95
13c	**16d, 17d**	92	Foam	748	68.97	5.51	3.74	68.81	5.73	3.49

a) Recrystallized from benzene–hexane (1 : 1).

TABLE VIII. Debenzoylations of **14**—**17** with NaOMe

Starting material	Product			*Anal.* Calcd (%)			Found (%)		
	Yield (%)	mp (°C)	MS (*m/z*)	C	H	N	C	H	N
14a	90	123—124[a]	342	56.12	7.65	8.18	55.88	7.85	8.11
15a	92	Foam	342	56.12	7.65	8.18	56.07	7.72	8.09
14b, 15b	91	Foam	356	57.29	7.92	7.86	57.00	8.19	7.65
14c, 15c	96	Foam	418	63.14	7.23	6.69	63.36	7.43	6.42
16a	61	127—128[a]	346	52.01	6.69	8.08	51.92	6.77	7.98
17a	69	121—122[a]	346	52.01	6.69	8.08	51.89	6.81	8.02
16b, 17b	75	Foam	360	53.32	6.99	7.77	53.10	7.18	7.56
16c, 17c	90	Foam	374	54.53	7.26	7.48	54.43	7.39	7.45
16d, 17d	78	Foam	436	60.53	6.69	6.41	60.43	6.53	6.13

a) Recrystallized from EtOH.

J=6.0 Hz), 7.31—7.63, 7.92—8.15 (15H, m, $C_6\underline{H}_5\times3$).

15a: ^{1}H-NMR ($CDCl_3$, 300 MHz) δ: 0.91, 0.92, 0.96, 1.10 (3H each, s, CCH_3), 2.95 (1H, d, 6-H, J=10.2 Hz), 3.19 (3H, s, NCH_3), 3.89 (1H, d, 1-H, J=10.2 Hz), 4.50—4.89 (3H, m, 4′-H, 5′-H), 5.56 (1H, dd, 2′-H, J=5.0, 6.0 Hz), 5.87 (1H, d, 1′-H, J=5.0 Hz), 5.98 (1H, t, 3′-H, J=6.0 Hz), 7.26—7.60, 7.87—8.14 (15H, m, $C_6\underline{H}_5\times3$).

(1*R*,6*R*)-4-Ethyl-7,7,8,8-tetramethyl-2-(2,3,5-tri-*O*-benzoyl-β-D-ribofuranosyl)-*cis*-2,4-diazabicyclo[4.2.0]octane-3,5-dione (14b) and (1*S*,6*S*)-4-Ethyl-7,7,8,8-tetramethyl-2-(2,3,5-tri-*O*-benzoyl-β-D-ribofuranosyl)-*cis*-2,4-diazabicyclo[4.2.0]octane-3,5-dione (15b) The ratio of **14b** and **15b** was 3 : 2 as determined from the ^{1}H-NMR spectra.

14b: ^{1}H-NMR ($CDCl_3$, 300 MHz) δ: 0.88, 0.91, 0.93, 0.98 (3H each, s, CCH_3), 1.10 (3H, t, $CH_2C\underline{H}_3$, J=7.0 Hz), 2.91 (1H, d, 6-H, J=10.2 Hz), 3.85 (2H, q, $C\underline{H}_2CH_3$, J=7.0 Hz), 3.92 (1H, d, 1-H, J=10.2 Hz), 4.53—4.77 (3H, m, 4′-H, 5′-H), 5.84 (1H, t, 2′-H, J=6.0 Hz), 5.89 (1H, dd, 3′-H, J=4.0, 6.0 Hz), 6.25 (1H, d, 1′-H, J=6.0 Hz), 7.30—7.61, 7.85—8.13 (15H, m, $C_6\underline{H}_5\times3$).

15b: ^{1}H-NMR ($CDCl_3$, 300 MHz) δ: 0.92, 0.93, 0.95, 1.09 (3H each, s, CCH_3), 1.14 (3H, t, $CH_2C\underline{H}_3$, J=7.0 Hz), 2.93 (1H, d, 6-H, J=10.2 Hz), 3.82—3.94 (2H, m, $C\underline{H}_2CH_3$), 3.88 (1H, d, 1-H, J=10.2 Hz), 4.51—4.89 (3H, m, 4′-H, 5′-H), 5.55 (1H, dd, 2′-H, J=5.3, 6.0 Hz), 5.90 (1H, d, 1′-H, J=5.3 Hz), 5.98 (1H, t, 3′-H, J=6.0 Hz), 7.28—7.60, 7.88—8.15 (15H, m, $C_6\underline{H}_5\times3$).

(1*R*,6*R*)-4-Benzyl-7,7,8,8-tetramethyl-2-(2,3,5-tri-*O*-benzoyl-β-D-ribofuranosyl)-*cis*-2,4-diazabicyclo[4.2.0]octane-3,5-dione (14c) and (1*S*,6*S*)-4-Benzyl-7,7,8,8-tetramethyl-2-(2,3,5-tri-*O*-benzoyl-β-D-ribofuranosyl)-*cis*-2,4-diazabicyclo[4.2.0]octane-3,5-dione (15c) The ratio of **14c** and **15c** was 3 : 2 as determined from the ^{1}H-NMR spectra.

14c: ^{1}H-NMR ($CDCl_3$, 300 MHz) δ: 0.80, 0.86, 0.87, 0.94 (3H each, s, CCH_3), 2.93 (1H, d, 6-H, J=9.8 Hz), 3.93 (1H, d, 1-H, J=9.8 Hz), 4.53—4.76 (3H, m, 4′-H, 5′-H), 5.01 (2H, br, $C\underline{H}_2C_6H_5$), 5.80 (1H, t, 2′-H, J=6.5 Hz), 5.86 (1H, dd, 3′-H, J=3.0, 6.5 Hz), 6.37 (1H, d, 1′-H, J=6.5 Hz), 7.20—7.62, 7.88—8.15 (20H, m, $C_6\underline{H}_5\times4$).

15c: ^{1}H-NMR ($CDCl_3$, 300 MHz) δ: 0.84, 0.88, 0.92, 1.06 (3H each, s, CCH_3), 2.95 (1H, d, 6-H, J=9.8 Hz), 3.90 (1H, d, 1-H, J=9.8 Hz), 4.50—4.88 (3H, m, 4′-H, 5′-H), 4.96 (2H, br, $C\underline{H}_2C_6H_5$), 5.50 (1H, t, 2′-H, J=5.5 Hz), 5.96 (1H, d, 1′-H, J=5.5 Hz), 5.98 (1H, t, 3′-H, J=5.5 Hz), 7.20—7.62, 7.88—8.15 (20H, m, $C_6\underline{H}_5\times4$).

(1*S*,6*S*)-6-Fluoro-7,7,8,8-tetramethyl-2-(2,3,5-tri-*O*-benzoyl-β-D-ribofuranosyl)-*cis*-2,4-diazabicyclo[4.2.0]octane-3,5-dione (16a) and (1*R*,6*R*)-6-Fluoro-7,7,8,8-tetramethyl-2-(2,3,5-tri-*O*-benzoyl-β-D-ribofuranosyl)-*cis*-2,4-diazabicyclo[4.2.0]octane-3,5-dione (17a) The ratio of **16a** and **17a** was 5 : 2 as determined from the isolated yields.

16a: ^{1}H-NMR ($CDCl_3$, 300 MHz) δ: 0.96, 0.96, 0.98 (3H each, s, CCH_3), 0.89 (3H, d, CCH_3, J=4.0 Hz), 4.06 (1H, d, 1-H, J=21.0 Hz), 4.57—4.75 (3H, m, 4′-H, 5′-H), 5.70 (1H, dd, 2′-H, J=6.5, 7.5 Hz), 5.83 (1H, dd, 3′-H, J=3.0, 6.5 Hz), 6.42 (1H, d, 1′-H, J=7.5 Hz), 7.32—7.64, 7.93—8.16 (15H, m, $C_6\underline{H}_5\times3$), 7.78 (1H, br, NH).

17a: ^{1}H-NMR ($CDCl_3$, 300 MHz) δ: 0.94, 1.02, 1.09 (3H each, s, CCH_3), 1.08 (3H, d, CCH_3, J=4.0 Hz), 4.05 (1H, d, 1-H, J=21.0 Hz), 4.54—4.90 (3H, m, 4′-H, 5′-H), 5.58 (1H, dd, 2′-H, J=5.5, 6.0 Hz), 5.89 (1H, d, 1′-H, J=5.5 Hz), 5.92 (1H, dd, 3′-H, J=6.0, 8.0 Hz), 7.28—7.60, 7.84—8.13 (15H, m, $C_6\underline{H}_5\times3$), 7.81 (1H, br, NH).

(1*S*,6*S*)-6-Fluoro-4,7,7,8,8-pentamethyl-2-(2,3,5-tri-*O*-benzoyl-β-D-ribofuranosyl)-*cis*-2,4-diazabicyclo[4.2.0]octane-3,5-dione (16b) and (1*R*,6*R*)-6-Fluoro-4,7,7,8,8-pentamethyl-2-(2,3,5-tri-*O*-benzoyl-β-D-ribofuranosyl)-*cis*-2,4-diazabicyclo[4.2.0]octane-3,5-dione (17b) The ratio of **16b** and **17b** was 5 : 2 as determined from the ^{1}H-NMR spectra.

16b: ^{1}H-NMR ($CDCl_3$, 300 MHz) δ: 0.86, 0.93, 0.96 (3H each, s, CCH_3), 0.91 (3H, d, CCH_3, J=4.0 Hz), 3.20 (3H, s, NCH_3), 4.03 (1H, d, 1-H, J=21.5 Hz), 4.56—4.75 (3H, m, 4′-H, 5′-H), 5.74 (1H, dd, 2′-H, J=6.5, 7.0 Hz), 5.85 (1H, dd, 3′-H, J=3.0, 7.0 Hz), 6.37 (1H, d, 1′-H, J=6.5 Hz), 7.33—7.64, 7.94—8.17 (15H, m, $C_6\underline{H}_5\times3$).

17b: ^{1}H-NMR ($CDCl_3$, 300 MHz) δ: 0.83, 0.97 (3H each, s, CCH_3), 1.08, 1.10 (3H each, d, CCH_3, J=4.0 Hz), 3.21 (3H, s, NCH_3), 3.98 (1H, d, 1-H, J=22.0 Hz), 4.53—4.88 (3H, m, 4′-H, 5′-H), 5.65 (1H, dd, 2′-H, J=5.0, 6.0 Hz), 5.81 (1H, d, 1′-H, J=5.0 Hz), 5.98 (1H, t, 3′-H, J=6.0 Hz), 7.27—7.60, 7.84—8.16 (15H, m, $C_6H_5\times3$).

(1*S*,6*S*)-4-Ethyl-6-fluoro-7,7,8,8-tetramethyl-2-(2,3,5-tri-*O*-benzoyl-β-D-ribofuranosyl)-*cis*-2,4-diazabicyclo[4.2.0]octane-3,5-dione (16c) and (1*R*,6*R*)-4-Ethyl-6-fluoro-7,7,8,8-tetramethyl-2-(2,3,5-tri-*O*-benzoyl-β-D-ribofuranosyl)-*cis*-2,4-diazabicyclo[4.2.0]octane-3,5-dione (17c) The ratio of **16c** and **17c** was 3 : 1 as determined from the ^{1}H-NMR spectra.

16c: ^{1}H-NMR ($CDCl_3$, 300 MHz) δ: 0.87, 0.94, 0.96 (3H each, s, CCH_3), 0.90 (3H, d, CCH_3, J=4.0 Hz), 1.15 (3H, t, $CH_2C\underline{H}_3$, J=7.0 Hz), 3.89 (2H, q, $C\underline{H}_2CH_3$, J=7.0 Hz), 4.01 (1H, d, 1-H, J=22.0 Hz), 4.57—4.75

(3H, m, 4′-H, 5′-H), 5.72 (1H, dd, 2′-H, J=6.0, 7.0 Hz), 5.85 (1H, dd, 3′-H, J=3.0, 6.0 Hz), 6.39 (1H, d, 1′-H, J=7.0 Hz), 7.33—7.63, 7.94—8.16 (15H, m, $C_6H_5 \times 3$).

17c: ^{1}H-NMR ($CDCl_3$, 300 MHz) δ: 0.85, 0.97 (3H each, s, CCH_3), 1.08, 1.10 (3H, d, CCH_3, J=4.0 Hz), 1.15 (3H, t, $CH_2C\underline{H}_3$, J=7.0 Hz), 3.86—3.94 (2H, m, $C\underline{H}_2CH_3$), 3.96 (1H, d, 1-H, J=22.0 Hz), 4.53—4.88 (3H, m, 4′-H, 5′-H), 5.64 (1H, dd, 2′-H, J=4.5, 6.0 Hz), 5.83 (1H, d, 1′-H, J=4.5 Hz), 5.98 (1H, t, 3′-H, J=6.0 Hz), 7.26—7.60, 7.82—8.12 (15H, m, $C_6H_5 \times 3$).

(1*S*,6*S*)-4-Benzyl-6-fluoro-7,7,8,8-tetramethyl-2-(2,3,5-tri-*O*-benzoyl-β-D-ribofuranosyl)-*cis*-2,4-diazabicyclo[4.2.0]octane-3,5-dione (16d) and (1*R*,6*R*)-4-Benzyl-6-fluoro-7,7,8,8-tetramethyl-2-(2,3,5-tri-*O*-benzoyl-β-D-ribofuranosyl)-*cis*-2,4-diazabicyclo[4.2.0]octane-3,5-dione (17d) The ratio of **16d** and **17d** was 3 : 1 as determined from the ^{1}H-NMR spectra.

16d: ^{1}H-NMR ($CDCl_3$, 300 MHz) δ: 0.63, 0.81, 0.90 (3H each, s, CCH_3), 0.85 (3H, d, CCH_3, J=4.0 Hz), 4.00 (1H, d, 1-H, J=21.5 Hz), 4.57—4.74 (3H, m, 4′-H, 5′-H), 5.01 (2H, br s, $C\underline{H}_2C_6H_5$), 5.71 (1H, dd, 2′-H, J=6.5, 7.0 Hz), 5.84 (1H, dd, 3′-H, J=3.0, 6.5 Hz), 6.47 (1H, d, 1′-H, J=7.0 Hz), 7.18—7.62, 7.84—8.16 (20H, m, $C_6\underline{H}_5 \times 4$).

17d: ^{1}H-NMR ($CDCl_3$, 300 MHz) δ: 0.63, 1.03, 1.32 (3H each, s, CCH_3), 1.04 (3H, d, CCH_3, J=4.0 Hz), 3.98 (1H, d, 1-H, J=21.5 Hz), 4.52—4.88 (3H, m, 4′-H, 5′-H), 4.98 (2H, br s, $C\underline{H}_2C_6H_5$), 5.59 (1H, dd, 2′-H, J=5.0, 6.0 Hz), 5.92 (1H, d, 1′-H, J=5.0 Hz), 5.96 (1H, t, 3′-H, J=6.0 Hz), 7.20—7.61, 7.84—8.15 (20H, m, $C_6\underline{H}_5 \times 4$).

General Procedure for the Debenzoylation of 14—17 A solution of one of **14—17** (2 mmol) in anhydrous MeOH (24 ml) was treated with 1 N NaOMe in MeOH (0.46 ml) and then heated at 50—60 °C for 3 h. The reaction mixture was neutralized carefully with Dowex 50 (H^+-form) resin to pH 6.0. The resin was removed by filtration and washed well with MeOH. The filtrates and washings were combined and evaporated *in vacuo*. The residue was subjected to column chromatography on silica gel with $CHCl_3$–MeOH (5 : 1). The eluate was evaporated *in vacuo*, and the residue was recrystallized from an appropriate solvent; yields, melting points, MS data, and combustion values are listed in Table VIII.

(1*R*,6*R*)-4,7,7,8,8-Pentamethyl-2-(β-D-ribofuranosyl)-*cis*-2,4-diazabicyclo[4.2.0]octane-3,5-dione (18a) ^{1}H-NMR [DMSO-d_6 (added D_2O)] δ: 0.80, 0.84, 0.94, 1.19 (3H each, s, CCH_3), 2.93 (1H, d, 6-H, J=10.0 Hz), 3.04 (3H, s, NCH_3), 3.45—3.71 (3H, m, 4′-H, 5′-H), 3.82 (1H, br t, 3′-H, J=5.0 Hz), 3.97 (1H, br t, 2′-H, J=6.5 Hz), 4.00 (1H, d, 1-H, J=10.0 Hz), 5.56 (1H, d, 1′-H, J=6.5 Hz).

(1*S*,6*S*)-4,7,7,8,8-Pentamethyl-2-(β-D-ribofuranosyl)-*cis*-2,4-diazabicyclo[4.2.0]octane-3,5-dione (19a) ^{1}H-NMR [DMSO-d_6 (added D_2O)] δ: 0.85, 0.88, 0.99, 1.19 (3H each, s, CCH_3), 2.89 (1H, d, 6-H, J=10.0 Hz), 3.04 (3H, s, NCH_3), 3.46—3.72 (3H, m, 4′-H, 5′-H), 3.79 (1H, dd, 2′-H, J=5.5, 7.5 Hz), 3.89 (1H, dd, 3′-H, J=2.0, 5.5 Hz), 4.23 (1H, d, 1-H, J=10.0 Hz), 5.74 (1H, d, 1′-H, J=7.5 Hz).

(1*R*,6*R*)-4-Ethyl-7,7,8,8-tetramethyl-2-(β-D-ribofuranosyl)-*cis*-2,4-diazabicyclo[4.2.0]octane-3,5-dione (18b) and (1*S*,6*S*)-4-Ethyl-7,7,8,8-tetramethyl-2-(β-D-ribofuranosyl)-*cis*-2,4-diazabicyclo[4.2.0]octane-3,5-dione (19b) 18b: ^{1}H-NMR [DMSO-d_6 (added D_2O)] δ: 0.84, 0.86, 0.93, 1.19 (3H each, s, CCH_3), 1.13 (3H, t, $CH_2C\underline{H}_3$, J=7.0 Hz), 2.92 (1H, d, 6-H, J=10.0 Hz), 3.45—3.71 (3H, m, 4′-H, 5′-H), 3.74 (2H, q, $C\underline{H}_2CH_3$, J=7.0 Hz), 3.82 (1H, dd, 3′-H, J=4.0, 6.0 Hz), 3.97 (1H, t, 2′-H, J=6.0 Hz), 3.99 (1H, d, 1-H, J=10.0 Hz), 5.57 (1H, d, 1′-H, J=6.0 Hz).

19b: ^{1}H-NMR [DMSO-d_6 (added D_2O)] δ: 0.81, 0.89, 0.99, 1.19 (3H each, s, CCH_3), 1.02 (3H, t, $CH_2C\underline{H}_3$, J=7.0 Hz), 2.88 (1H, d, 6-H, J=10.0 Hz), 3.45—3.71 (3H, m, 4′-H, 5′-H), 3.75 (2H, q, $C\underline{H}_2CH_3$, J=7.0 Hz), 3.79 (1H, dd, 2′-H, J=5.0, 7.5 Hz), 3.89 (1H, dd, 3′-H, J=2.0, 5.0 Hz), 4.21 (1H, d, 1-H, J=10.0 Hz), 5.77 (1H, d, 1′-H, J=7.5 Hz).

(1*R*,6*R*)-4-Benzyl-7,7,8,8-tetramethyl-2-(β-D-ribofuranosyl)-*cis*-2,4-diazabicyclo[4.2.0]octane-3,5-dione (18c) and (1*S*,6*S*)-4-Benzyl-7,7,8,8-tetramethyl-2-(β-D-ribofuranosyl)-*cis*-2,4-diazabicyclo[4.2.0]octane-3,5-dione (19c) 18c: ^{1}H-NMR [DMSO-d_6 (added D_2O)] δ: 0.68. 0.77, 0.92, 1.18 (3H each, s, CCH_3), 2.98 (1H, d, 6-H, J=10.0 Hz), 3.42—3.72 (3H, m, 4′-H, 5′-H), 3.81 (1H, dd, 3′-H, J=4.0, 6.0 Hz), 3.98 (1H, t, 2′-H, J=6.0 Hz), 4.03 (1H, d, 1-H, J=10.0 Hz), 4.89 (2H, s, $C\underline{H}_2C_6H_5$), 5.57 (1H, d, 1′-H, J=6.0 Hz), 7.20—7.33 (5H, m, $C_6\underline{H}_5$).

19c: ^{1}H-NMR [DMSO-d_6 (added D_2O)] δ: 0.78, 0.82, 0.98, 1.18 (3H each, s, CCH_3), 2.96 (1H, d, 6-H, J=10.0 Hz), 3.42—3.72 (3H, m, 4′-H, 5′-H), 3.78 (1H, dd, 2′-H, J=5.0, 7.5 Hz), 3.90 (1H, dd, 3′-H, J=2.0, 5.0 Hz), 4.26 (1H, d, 1-H, J=10.0 Hz), 4.89 (2H, s, $C\underline{H}_2C_6H_5$), 5.78 (1H, d, 1′-H, J=7.5 Hz), 7.20—7.33 (5H, m, $C_6\underline{H}_5$).

(1*S*,6*S*)-6-Fluoro-7,7,8,8-tetramethyl-2-(β-D-ribofuranosyl)-*cis*-2,4-diazabicyclo[4.2.0]octane-3,5-dione (20a) ^{1}H-NMR [DMSO-d_6 (added D_2O)] δ: 0.81, 0.91, 1.05 (3H each, s, CCH_3), 1.14 (3H, d, CCH_3, J=3.6 Hz), 3.39—3.75 (3H, m, 4′-H, 5′-H), 3.83 (1H, dd, 3′-H, J=3.0, 6.0 Hz), 3.92 (1H, dd, 2′-H, J=6.0, 6.5 Hz), 4.23 (1H, d, 1-H, J=22.4 Hz), 5.56 (1H, d, 1′-H, J=6.5 Hz).

(1*R*,6*R*)-6-Fluoro-7,7,8,8-tetramethyl-2-(β-D-ribofuranosyl)-*cis*-2,4-diazabicyclo[4.2.0]octane-3,5-dione (21a) ^{1}H-NMR [DMSO-d_6 (added D_2O)] δ: 0.89, 0.93, 1.10 (3H each, s, CCH_3), 1.13 (3H, d, CCH_3, J=3.2 Hz), 3.47—3.75 (3H, m, 4′-H, 5′-H), 3.80 (1H, dd, 2′-H, J=5.0, 7.5 Hz), 3.90 (1H, dd, 3′-H, J=2.0, 5.0 Hz), 4.47 (1H, d, 1-H, J=22.4 Hz), 5.72 (1H, d, 1′-H, J=7.5 Hz).

(1*S*,6*S*)-6-Fluoro-4,7,7,8,8-pentamethyl-2-(β-D-ribofuranosyl)-*cis*-2,4-diazabicyclo[4.2.0]octane-3,5-dione (20b) and (1*R*,6*R*)-6-Fluoro-4,7,7,8,8-pentamethyl-2-(β-D-ribofuranosyl)-*cis*-2,4-diazabicyclo[4.2.0]octane-3,5-dione (21b) 20b: ^{1}H-NMR [DMSO-d_6 (added D_2O)] δ: 0.73, 0.88, 1.05 (3H each, s, CCH_3), 1.15 (3H, d, CCH_3, J=3.3 Hz), 3.10 (3H, s, NCH_3), 3.25—3.77 (3H, m, 4′-H, 5′-H), 3.80—4.00 (2H, m, 2′-H, 3′-H), 4.34 (1H, d, 1-H, J=22.4 Hz), 5.62 (1H, d, 1′-H, J=6.5 Hz),

21b: ^{1}H-NMR [DMSO-d_6 (added D_2O)] δ: 0.82, 0.91, 1.10 (3H each, s, CCH_3), 0.93 (3H, d, CCH_3, J=3.0 Hz), 3.16 (3H, s, NCH_3), 3.25—3.77 (3H, m, 4′-H, 5′-H), 3.80—4.00 (2H, m, 2′-H, 3′-H), 4.52 (1H, d, 1-H, J=22.4 Hz), 5.76 (1H, d, 1′-H, J=7.0 Hz).

(1*S*,6*S*)-4-Ethyl-6-fluoro-7,7,8,8-tetramethyl-2-(β-D-ribofuranosyl)-*cis*-2,4-diazabicyclo[4.2.0]octane-3,5-dione (20c) and (1*R*,6*R*)-4-Ethyl-6-fluoro-7,7,8,8-tetramethyl-2-(β-D-ribofuranosyl)-*cis*-2,4-diazabicyclo[4.2.0]-octane-3,5-dione (21c) 20c: ^{1}H-NMR [DMSO-d_6 (added D_2O)] δ: 0.75, 0.89, 1.05 (3H each, s, CCH_3), 1.16 (3H, d, CCH_3, J=3.5 Hz), 1.17 (3H, t, $CH_2C\underline{H}_3$, J=7.0 Hz), 3.48—3.55 (2H, m, 5′-H), 3.69—3.82 (1H, m, 4′-H), 3.83—3.98 (2H, m, 2′-H, 3′-H), 4.03 (2H, q, $C\underline{H}_2CH_3$, J=7.0 Hz), 4.32 (1H, d, 1-H, J=22.4 Hz), 5.62 (1H, d, 1′-H, J=6.5 Hz).

21c: ^{1}H-NMR [DMSO-d_6 (added D_2O)] δ: 0.83, 0.92, 1.08 (3H each, s, CCH_3), 1.10 (3H, d, CCH_3, J=2.5 Hz), 1.15 (3H, t, $CH_2C\underline{H}_3$, J=7.0 Hz), 3.48—3.55 (2H, m, 5′-H), 3.67—3.82 (3H, m, 4′-H, $C\underline{H}_2CH_3$), 3.82—3.95 (2H, m, 2′-H, 3′-H), 4.50 (1H, d, 1-H, J=22.4 Hz), 5.78 (1H, d, 1′-H, J=7.5 Hz).

(1*S*,6*S*)-4-Benzyl-6-fluoro-7,7,8,8-tetramethyl-2-(β-D-ribofuranosyl)-*cis*-2,4-diazabicyclo[4.2.0]octane-3,5-dione (20d) and (1*R*,6*R*)-4-Benzyl-6-fluoro-7,7,8,8-tetramethyl-2-(β-D-ribofuranosyl)-*cis*-2,4-diazabicyclo-[4.2.0]octane-3,5-dione (21d) 20d: ^{1}H-NMR [DMSO-d_6 (added D_2O)] δ: 0.57, 0.79, 1.02 (3H each, s, CCH_3), 1.14 (3H, d, CCH_3, J=3.5 Hz), 3.46—3.56 (2H, m, 5′-H), 3.70—3.77 (1H, m, 4′-H), 3.82—3.99 (2H, m, 2′-H, 3′-H), 4.35 (1H, d, 1-H, J=23.0 Hz), 4.93 (2H, br s, $C\underline{H}_2C_6H_5$), 5.62 (1H, d, 1′-H, J=6.5 Hz), 7.21—7.98 (5H, m, $C_6\underline{H}_5$).

21d: ^{1}H-NMR [DMSO-d_6 (added D_2O)] δ: 0.67, 0.86, 1.08 (3H each, s, CCH_3), 0.95 (3H, d, CCH_3, J=3.0 Hz), 3.46—3.56 (2H, m, 5′-H), 3.70—3.77 (1H, m, 4′-H), 3.82—3.99 (2H, m, 2′-H, 3′-H), 4.54 (1H, d, 1-H, J=23.0 Hz), 4.98 (2H, br s, $C\underline{H}_2C_6H_5$), 5.89 (1H, d, 1′-H, J=7.5 Hz), 7.21—7.98 (5H, m, $C_6\underline{H}_5$).

Acknowledgement We are grateful to Mrs. H. Hatano, Mrs. A. Nakatani, Miss A. Nakagawa, Mrs. C. Sakabe, and Mrs. N. Satoh, School of Pharmaceutical Sciences, Kitasato University, for microanalyses and spectral measurements. This work was supported in part by Grants-in-Aid for Cancer Research (No. 61010096, No. 62010033 and No. 63010031) from the Ministry of Education, Science and Culture, Japan, and a Grant-in-Aid for Scientific Research (project-4) from the School of Pharmaceutical Sciences, Kitasato University, Japan.

References and Notes

1) The late Assistant Professor T. Itoh prepared this manuscript a few days before his untimely death on January 14th, 1990. The present co-workers gratefully acknowledge their in debtedness to his inspiration, enthusiasm, and leadership.
2) *a*) A. Wexler and J. S. Swenton, *J. Am. Chem. Soc.*, **98**, 1602 (1976); *b*) A. J. Wexler, J. A. Hyatt, P. W. Raynolds, C. Cottrell, and J. S. Swenton, *ibid.*, **100**, 512 (1978); *c*) T. G. Savino, L. K. Chenard, and J. S. Swenton, *Tetrahedron Lett.*, **24**, 4055 (1983); *d*) A. J. Wexler, R. J. Balchunis, and J. S. Swenton, *J. Org. Chem.*, **49**, 2733 (1984); *e*) V. V. Kaminski, A. J. Wexler, R. J. Balchunia, and J. S. Swenton, *ibid.*, **49**, 2738 (1984).
3) C. Kaneko and N. Shimomura, *Tetrahedron Lett.*, **23**, 2571 (1982).
4) A. A. Lamola, *Pure Appl. Chem.*, **34**, 281 (1973).
5) J. L. Charlton and H. K. Lai, *Can. J. Chem.*, **54**, 1445 (1976).
6) S. J. Farrow, C. R. Jones, D. L. Severace, R. M. Deibel, W. M. Baird, and H. A. Morrison, *J. Org. Chem.*, **55**, 275 (1990).
7) Y. Honma, T. Ikuta, T. Kasukabe, M. Hozumi, T. Itoh, and H. Ogura, *Anticancer Research*, **8**, 695 (1988).

8) a) U. Niedballa and H. Vorbrüggen, *J. Org. Chem.*, **39**, 3664 (1974); *b*) H. Vorbrüggen, K. Krolikiewicz, and B. Bennua, *Chem. Ber.*, **114**, 1234 (1981).
9) M. Saneyoshi, M. Inomata, and F. Fukuoka, *Chem. Pharm. Bull.*, **26**, 2990 (1978).
10) M. Hozumi, T. Itoh, Y. Honma, N. Kawahara, I. Ishikawa, and H. Ogura, Eur. Patent Appl. EP 299413 [*Chem. Abstr.*, **110**, 231659 (1989)].
11) "*endo*"-adduct refers to the diastereoisomer bearing two hydrogen atoms or florine and hydrogen atoms at positions 1 and 6 above the plane of the uracil ring. "*exo*"-adduct refers to the other diastereoisomer.
12) *a*) R. E. Cline, R. M. Fink, and K. Fink, *J. Am. Chem. Soc.*, **81**, 2521 (1959); *b*) K. H. Scheit, *Chem. Ber.*, **99**, 3884 (1966).
13) K. Yamauchi and M. Kinoshita, *J. Chem. Soc., Perkin Trans. 1*, **1973**, 391.
14) G. E. Hilbert and T. B. Johnson, *J. Am. Chem. Soc.*, **52**, 2001 (1930).
15) C. C. Cheng and L. R. Lewis, *J. Heterocycl. Chem.*, **1**, 260 (1964).
16) M. J. Robins and S. R. Naik, *J. Am. Chem. Soc.*, **93**, 5277 (1971).
17) M. Fikus, K. L. Wierzchowski, and D. Shugar, *Biochem. Biophys. Res. Commun.*, **16**, 478 (1964).
18) B. R. Baker and G. D. F. Jackson, *J. Pharm. Sci.*, **54**, 1758 (1965).
19) P. Main, S. E. Hull, L. L. Lessinger, G. Germain, J. P. DeClercq, and M. M. Woolfson, "MULTAN 78," a system of computer programs for the automatic solution of crystal structures from X-ray diffraction data, Univs. of York, England, and Louvain, Belgium (1978).
20) "International Tables for X-Ray Crystallography," Vol. 4, Kynoch Press, Birmingham, 1974, p. 71.

Chem. Pharm. Bull. **39**(8) 1931—1938 (1991)

Synthetic Studies of Carbapenem and Penem Antibiotics. I. Facile Synthesis of a Key Intermediate: 4-Acetoxy-3-(1-hydroxyethyl)-2-azetidinone

Makoto SUNAGAWA, Haruki MATSUMURA, Masao ENOMOTO, Takaaki INOUE, and Akira SASAKI*

Research Laboratories, Sumitomo Pharmaceuticals Co. Ltd., 3-1-98 Kasugade-naka, Konohana-ku, Osaka 554, Japan. *Received November 28, 1990*

A highly efficient synthesis of (3*R*,4*R*)-4-acetoxy-3-[(*R*)-1-hydroxyethyl]-2-azetidinone, which is a key intermediate for the synthesis of carbapenem and penem antibiotics, was accomplished. It was found that oxymercuration-reduction of easily obtainable 4-alkyloxycarbonyl-1-(di-*p*-anisylmethyl)-3-ethenyl-2-azetidinone could be employed as a key stereoselective reaction. The chiral starting material was obtained by optical resolution or asymmetric (2+2) cycloaddition. The desired product was afforded in four steps, that is, oxymercuration-reduction, oxidative decarboxylation, protection of the hydroxy group and removal of the N-protecting group.

Keywords penem; carbapenem; (*R*)-1-hydroxyethyl group; (3*R*,4*R*)-4-acetoxy-3-[(*R*)-1-hydroxyethyl]-2-azetidinone; (2+2) cycloaddition; oxymercuration-reduction; oxidative decarboxylation

Carbapenem and penem antibiotics **1** possess potent antibacterial activities as well as broad spectra of action. Therefore, much attention has been focused on synthetic studies of these compounds. In those studies, the (3*R*,4*R*)-4-acetoxy-3-[(*R*)-1-hydroxyethyl]-2-azetidinone derivative **2** has been widely utilized as a versatile intermediate. Many methods for synthesizing **2** have been reported[1] (Fig. 1). For the purpose of total synthesis of **1**, we initiated studies on the synthesis of **2** by new methodology. We describe here a facile synthesis of **2**.

Synthetic Design We designed the synthetic strategy shown in Chart 1. We selected the 3-ethenyl-2-azetidinone **3** as the starting material, because **3** can be easily obtained by (2+2) cycloaddition reaction of crotonyl chloride and Schiff base.[2] The key point of this synthetic route was how to obtain a high stereoselectivity in the conversion of the ethenyl group to a 1-hydroxyethyl group. We presumed that this might be achieved by using the oxymercuration-reduction method, which is well known to proceed according to the Markownikoff rule. We considered that the side of the olefin attacked by mercuric acetate would be controlled simply by the steric hindrance of the substituent on C-4 and the desired *threo* isomer could be obtained as the major product.

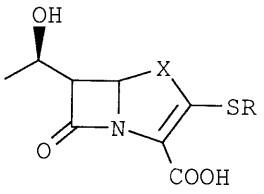

1
X=CH_2, CH–Me, S

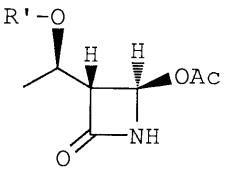

2
R': protecting group

Fig. 1

Concerning the acetoxy group on C-4, we expected that conversion of the ester group on C-4 to an acetoxy group could be achieved by alkaline hydrolysis followed by oxidative decarboxylation with lead tetraacetate.

Preparation of 3 To study the stereoselectivity of the oxymercuration reaction, the 3-ethenyl-2-azetidinone **3** in racemic form was prepared as follows. The (2+2) cycloaddition reaction of crotonyl chloride and the Schiff base **6a**, prepared from di-*p*-anisylmethylamine (DAM-NH_2) **4** and *n*-butyl glyoxylate **5a**, was carried out in the presence of triethylamine in toluene to afford the *n*-butyl ester **3a** in 94% yield. The stereochemistry of **3a** was assigned as 3,4-*cis* on the basis of the coupling constant between H-3 and H-4 in the proton magnetic resonance (^{1}H-NMR) spectrum ($J_{3,4}$=5.8 Hz). The alkaline hydrolysis of the *cis*-isomer **3a** in aqueous tetrahydrofuran (THF) and methanol (MeOH) afforded the thermodynamically more stable *trans*-carboxylic acid **3b** ($J_{3,4}$=1.3 Hz) in 85% yield. To identify the epimerization site, alkaline hydrolysis was performed in CD_3OD and D_2O (5:1). It was found that the epimerization took place at C-3, because the signal of H-3 disappeared while the H-4 signal remained in the ^{1}H-NMR spectrum.[3] Compounds **3c**—**e** were obtained as follows. Compound **3b** was treated with *p*-methoxybenzyl chloride and triethylamine in dimethylformamide (DMF) to give the *p*-methoxybenzyl ester **3c** in 95% yield. Reduction of **3a** with lithium borohydride in THF gave the alcohol

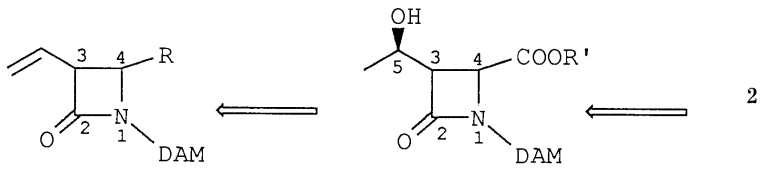

3 2

DAM= $CH\left(-\bigcirc-OMe\right)_2$

Chart 1

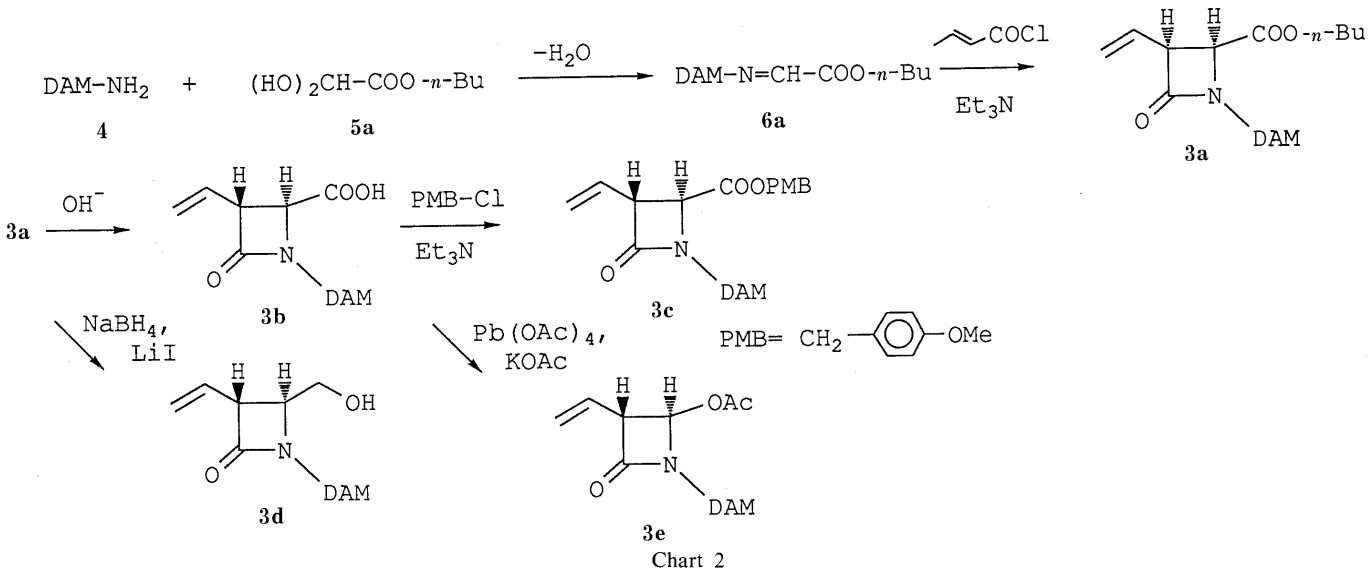

Chart 2

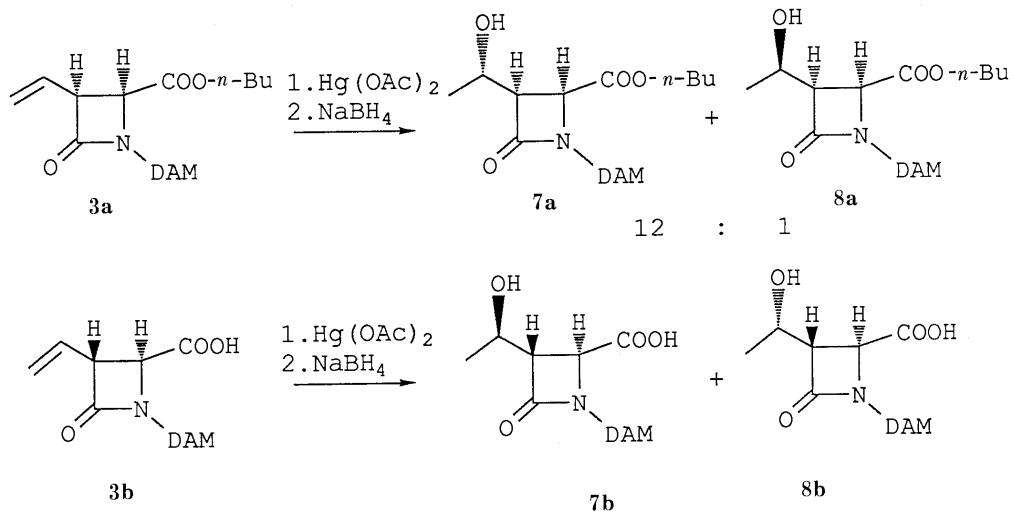

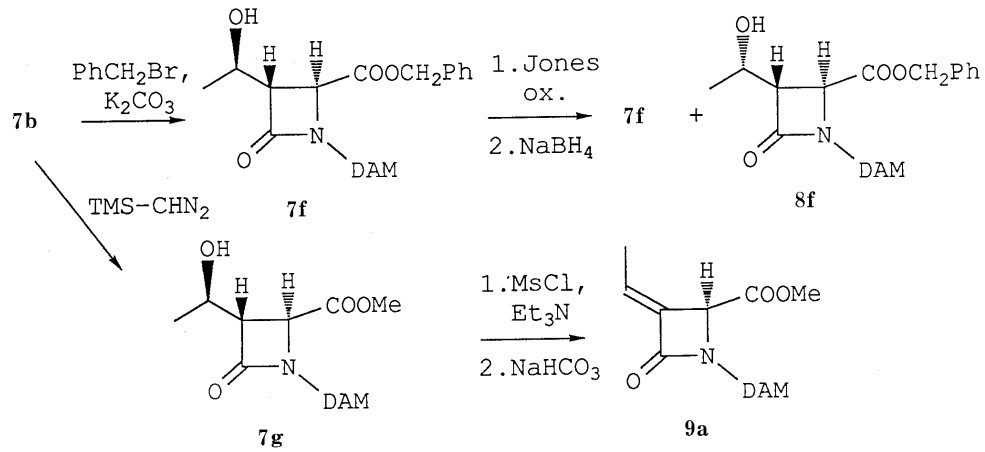

Chart 3

3d in 88% yield. The conversion of the carboxy group in **3b** to an acetoxy group was carried out with lead tetraacetate in the presence of potassium acetate in DMF to afford the acetate **3e** in a good yield[1b,4] (Chart 2).

Oxymercuration-Reduction Reaction of 3 The oxymercuration-reduction of the ethenyl group was investigated using β-lactams (**3a**—**e**) as shown in Charts 3 and 4. The treatment of **3a** with mercuric acetate in aqueous THF followed by reaction with sodium borohydride in the presence of alkali afforded 3-(1-hydroxyethyl)-2-azetidinone as a mixture of two isomers, **7a** and **8a**, in 85% yield. The ratio of **7a** and **8a** was determined to be 12:1 based on the integration of the H-3 signal in the ^{1}H-NMR. The major product **7a** was determined to be the 3,5-*threo* isomer based on the coupling constant between H-3 and H-5 in the ^{1}H-NMR ($J_{3,5}$=9.6 Hz in $CDCl_3$).[1e] Oxymercuration-reduction of the 3,4-*trans*-β-lactam **3b**, giving the diastereomeric products **7b** and **8b**, was performed in a similar manner to that of **3a**. The yield was 86% and the ratio of **7b** and **8b** determined by high performance liquid chromatography (HPLC) analysis was 80:1. In order to confirm that **8b** was the epimer of **7b** at C-5, the following transformation was examined. Esterification of **7b** with benzyl bromide and potassium carbonate in acetone gave **7f**, which was oxidized with Jones reagent and then reduced with sodium borohydride to give a 1:1 mixture of **7f** and **8f**. Compound **8f** could be separated from the mixture by preparative thin layer chromatography (preparative TLC) and converted into the corresponding carboxylic acid **8b** by hydrogenolysis. The minor product of the oxymercuration-reduction procedure was identified as **8b** derived from **7b** by HPLC analysis. Finally, the configurations of the 1-hydroxyethyl side chain in **7b** and **8b** were determined on the basis of the results of dehydration to the 3,5-ene derivatives.[5] After esterification of **7b** with trimethylsilyldiazomethane (TMS-CHN_2), the resultant methyl ester **7g** was mesylated and then treated with sodium bicarbonate in MeOH to afford **9a** exclusively in 67% yield. On the other hand, the same treatment of the methyl ester **8g** derived from **8b** gave a mixture of **9b** (47%) and **9a** (9%). Assignments by ^{1}H-NMR for the pair of ene lactams **9a** and **9b** were based on the anisotropic deshielding effect of the β-lactam carbonyl on the vinyl methyl group and the vinyl proton. The vinyl methyl group of **9a** appeared at δ 1.74, at higher field than that of **9b**, which appeared at δ 2.03. The vinyl proton of **9a** appeared at δ 6.26, at lower field than that of **9b**, which appeared at δ 5.74. Presuming *trans* coplanar elimination of methanesulfonic acid, it is concluded that the configuration of the 1-hydroxyethyl side chain of **7b** is 3,5-*threo* and that of **8b** is 3,5-*erythro* (Chart 3).

The oxymercuration-reduction of **3c**, **3d** and **3e** showed similar stereoselectivity to that of **3b** and afforded **7c** (90%), **7d** (85%) and **7e** (88%), respectively. The stereochemistry of **7c** and **7e** was determined by comparison with authentic samples derived from **7b** (Chart 4).

As described above, it was found that the conversion of the ethenyl group to a 1-hydroxyethyl group can be achieved highly stereoselectively, and the stereoselectivity was better in the case of *trans*-**3** (**3b**—**e**) than *cis*-**3** (**3a**). These results could not be completely explained by our presumption; that is, we considered that the conformation of the vinyl group

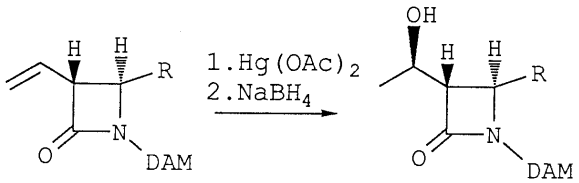

3c—e **7c—e**

c: R=COOPMB, **d**: R=CH_2OH, **e**: R=OAc

Chart 4

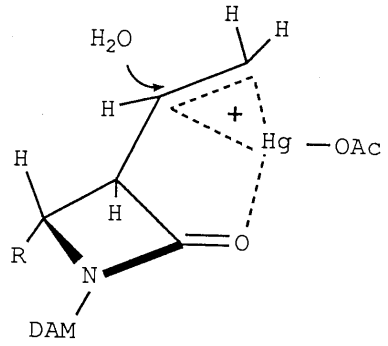

Fig. 2

was arranged so as to avoid the steric hindrance of the substituent on C-4. Mercuric acetate attacked from the less hindered side of the olefin, then a water molecule attacked from the opposite side and the subsequent reduction gave the *threo* isomer. If only the steric hindrance of the substituent at C-4 fixes the conformation of the vinyl group, the stereoselectivity would be higher in the case of *cis*-**3** (**3a**) than *trans*-**3** (**3b**—**e**). To explain the difference, other factors influencing the stereoselectivity should be considered. The extremely high stereoselectivity in the case of *trans*-**3** (**3b**—**e**) could probably be explained by postulating that in addition to the steric hindrance of the substituent (hydrogen atom) on C-4, mercuric acetate plays a role by coordinating with the carbonyl group of the β-lactam as well as the vinyl group[2c] (Fig. 2). The decrease of the stereoselectivity in the case of *cis*-**3** (**3a**) could be explained by the additional participation of the interaction between mercuric acetate and the carbonyl group of the ester group on C-4.

Preparation of Optically Active 3b With the aim of synthesizing optically pure **2**, the preparation of optically active **3b** was attempted by two methods, optical resolution and asymmetric (2+2) cycloaddition reaction. The optical resolution of **3b** was examined as follows. Compound **3b** was treated with oxalyl chloride and then with *l*-menthol in the presence of *N*,*N*-dimethylaminopyridine and triethylamine to afford a diastereomeric mixture of *l*-menthyl esters **10a** and **10b** (1:1, determined by HPLC: Lichrosorb SI-60, 1.5% iso-propanol in *n*-hexane). The recrystallization of the mixture from MeOH gave crystalline (3*R*,4*S*)-*l*-menthyl ester **10a** in an optically pure form (mp 114—115 °C, $[\alpha]_D^{22}$ +20.2° (*c*=0.26, $CHCl_3$)). The alkaline hydrolysis of **10a** with sodium hydroxide gave the corresponding acid (+)-**3b** ($[\alpha]_D^{22}$ +63.3° (*c*=0.12, $CHCl_3$)), which was converted into the methyl ester **11** using TMS-CHN_2.

Asymmetric (2+2) cycloaddition reactions using chiral Schiff bases were investigated as shown in Chart 6. This approach was found to be effective for the preparation of

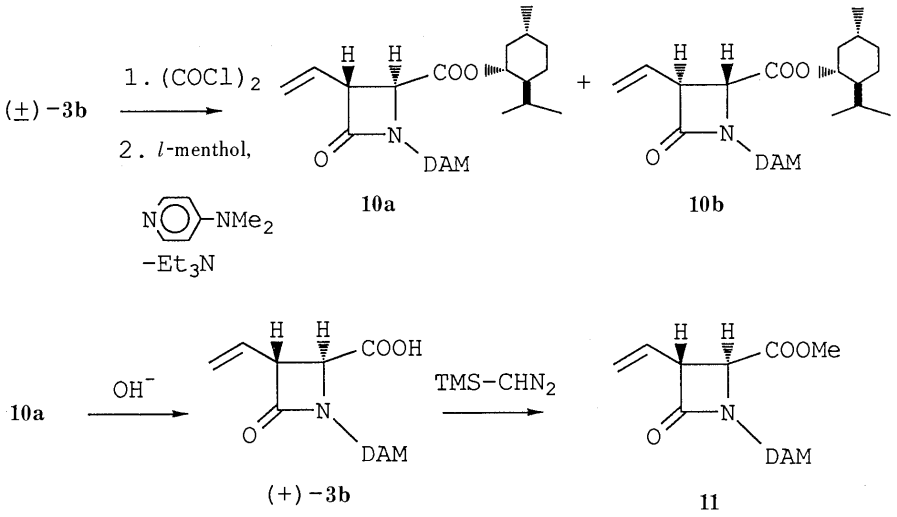

Chart 5

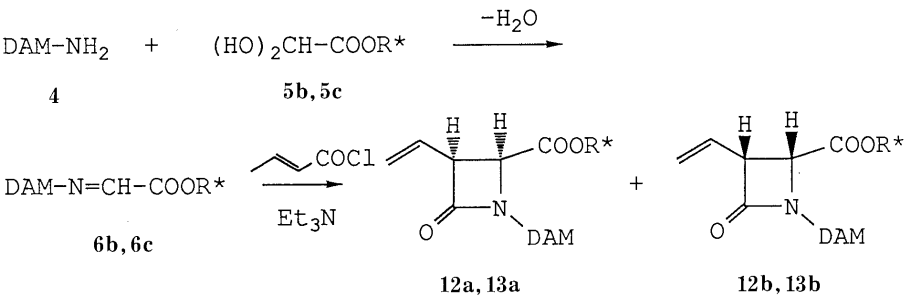

5b, 6b, 12a, 12b : R* = *l*-menthyl, 12a : 12b = 1 : 2

5c, 6c, 13a, 13b : R* = *d*-menthyl, 13a : 13b = 2 : 1

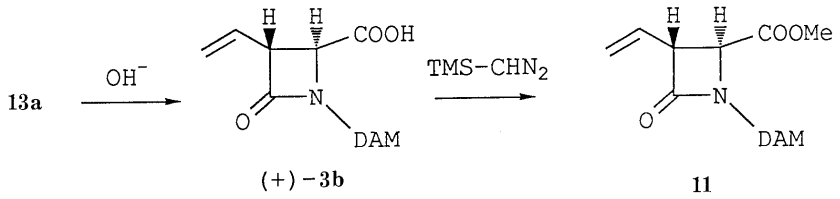

Chart 6

optically active **3b**.

First, a preliminary study was carried out using *l*-menthyl glyoxylate **5b**[6] and it was found that the undesired (3*R*,4*R*) isomer was the major product. That is, the Schiff base **6b**, prepared from DAM-NH_2 **4** and **5b**, was treated with crotonyl chloride to afford a mixture of **12a** and **12b** in the ratio of 1 : 2 (by HPLC analysis: Lichrosorb SI-60, 1.0% iso-propanol in *n*-hexane) in 92% yield. The structures of **12a** and **12b** were confirmed by derivatizing the mixture of **12a** and **12b** (2 : 5) to a mixture of **10a** and **10b** (**10a** : **10b** = 2 : 5.2, by HPLC analysis) by alkaline hydrolysis and esterification with *l*-menthol. Therefore, the *d*-menthyl moiety was selected as the chiral auxiliary in the asymmetric synthesis. A mixture of *d*-menthyl esters **13a** and **13b** was obtained in 82% yield using *d*-methyl glyoxylate **5c** in a similar manner to that described above. The ratio of **13a** and **13b** was 2 : 1 by HPLC analysis. Pure **13a** was obtained by recrystallization from MeOH. Then alkaline hydrolysis of **13a** gave the desired (+)-**3b**. The treatment of (+)-**3b** with TMS-CHN_2 gave the methyl ester **11**, which was identical with that obtained from **10a**.

Preparation of 2 Optically active (+)-**3b** was converted into the (*R*)-1-hydroxyethyl derivative (+)-**7b** (86%) by the treatment of (+)-**3b** with mercuric acetate and then with sodium borohydride. Transformation of (+)-**7b** into 4-acetoxy-3-(1-hydroxyethyl)-2-azetidinones **2** could be achieved through three reactions, that is, 1) oxidative decarboxylation to give an acetoxy group,[1b,4] 2) protection of the hydroxy group and 3) deprotection of the N-protecting group, di-*p*-anisylmethyl (DAM).[7] These reactions could be carried out in any sequence. Among the practical routes, the route from (+)-**7b** *via* (+)-**7e** seemed

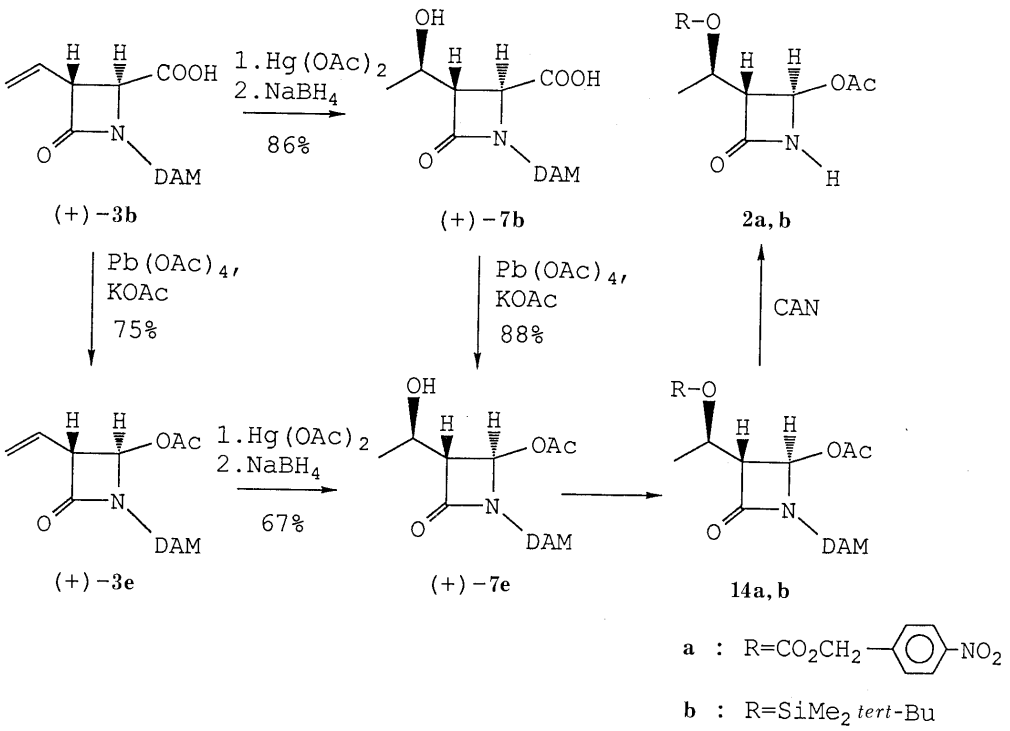

Chart 7

to be preferable because it gave the best overall yield. Thus, oxidative decarboxylation of (+)-**7b** to the acetate (+)-**7e** was accomplished by treatment with lead tetraacetate in a mixture of DMF and toluene in the presence of potassium acetate in 88% yield. The protection of the hydroxy group of (+)-**7e** with *p*-nitrobenzyl chloroformate in the presence of *N*,*N*-dimethylaminopyridine afforded **14a** in 90% yield and with *tert*-butyldimethylsilyl chloride in the presence of imidazole afforded **14b** in 86% yield. Subsequently the DAM group of **14a** and **14b** was oxidatively removed with cerium(IV) ammonium nitrate (CAN) in acetonitrile (MeCN) and water (9 : 1) to furnish the key intermediate **2a** ($[\alpha]_D^{22}$ +36.6° (c=0.09, $CHCl_3$)) in 94% yield and **2b** (mp 100—102 °C, $[\alpha]_D^{26}$ +48.2° (c=1.01, $CHCl_3$))[1a,c,d] in 68% yield, respectively.

The synthetic route from (+)-**3b** by way of (+)-**3e** and (+)-**7e** was also examined but the overall yield was less than that of the above route.

Conclusion

In summary, we have succeeded in establishing an effective method to synthesize **2**, which serves as a useful intermediate for the preparation of penem and carbapenem antibiotics. Taking into account the high stereoselectivity in the oxymercuration-reduction procedure and the use of easily obtainable 3-ethenyl-2-azetidinone as a starting material, the overall process is one of the most practical routes so far developed for preparing **2**.

Experimental

Melting points were measured using a Thomas-Hoover capillary melting point apparatus and were not corrected. Infrared (IR) spectral measurements were carried out with a Hitachi 260-10 infrared spectrometer. ^{1}H-NMR spectra were measured with a JEOL FX-90Q (90 MHz) and GX-270 (270 MHz) spectrometers. Chemical shift values are expressed as ppm downfield from tetramethylsilane used as an internal standard (δ-values). Mass spectra (MS) were taken with a Hitachi M-80B mass spectrometer. Measurements of optical rotation were performed with a JASCO DIP-181 digital polarimeter. Silica gel 60 (70—230 mesh, E. Merck) was used as an adsorbent for column chromatography. Preparative TLC was performed on Silica gel 60 F_{254} TLC plates (E. Merck).

Preparation of 3-Ethenyl-2-azetidinone (3) (3*RS*,4*RS*)-4-*n*-Butoxycarbonyl-1-(di-*p*-anisylmethyl)-3-ethenyl-2-azetidinone (**3a**): A mixture of di-*p*-anisylmethylamine (10.0 g, 41.2 mmol) and *n*-butylglyoxylate monohydrate (7.3 g, 49.3 mmol) in toluene (600 ml) was dehydrated azeotropically under reflux to give a solution of the Schiff base **6a**. After addition of triethylamine (Et_3N) (6.2 g, 61.3 mmol), a solution of crotonyl chloride (5.1 g, 49.5 mmol) in toluene (25 ml) was added dropwise at 70 °C over 1 h, followed by stirring for 2 h at the same temperature. The reaction mixture was cooled to 10 °C and washed successively with 2 N HCl, 5% aqueous $NaHCO_3$ and brine. The organic layer was dried over Na_2SO_4 and concentrated *in vacuo*. The residue was purified by column chromatography on silica gel to give **3a** as a viscous oil (16.5 g, 94%). IR (neat): 1762, 1735 (sh), 1605 cm^{-1}. ^{1}H-NMR ($CDCl_3$) δ: 0.89 (3H, t, J=7.3 Hz), 1.27 (2H, m), 1.46 (2H, m), 3.78 (3H, s), 3.80 (3H, s), 3.97 (1H, d, J=5.8 Hz), 4.00 (2H, m), 4.14 (1H, d, J=5.8 Hz), 5.27—5.43 (2H, m), 5.69—5.82 (1H, m), 5.80 (1H, s), 6.81—6.90 (4H, m), 7.15 (2H, d, J=8.8 Hz), 7.29 (2H, d, J=8.8 Hz). MS (EI) m/z: 423 (M^+).

(3*RS*,4*SR*)-4-Carboxy-1-(di-*p*-anisylmethyl)-3-ethenyl-2-azetidinone (**3b**): A 1 N NaOH solution (42 ml) was added to a solution of **3a** (16.9 g, 40 mmol) in THF (600 ml) and MeOH (500 ml) at room temperature, and the mixture was stirred for 2 h. After neutralization with 2 N HCl (22 ml), the reaction mixture was reduced to a quarter of the original volume *in vacuo*. The residue was diluted with 1 N NaOH (42 ml) and brine (450 ml), and washed with toluene (200 ml × 2). The alkaline aqueous layer was acidified with 2 N HCl (47 ml) and extracted with toluene (400 ml × 2). The extract was washed with brine, dried over Na_2SO_4 and concentrated *in vacuo* to give **3b** as a viscous oil (12.5 g, 85%). IR ($CHCl_3$): 1753, 1612 cm^{-1}. ^{1}H-NMR ($CDCl_3$) δ: 3.79 (3H, s), 3.84 (3H, s), 3.85 (1H, d, J=1.3 Hz), 5.30—5.43 (2H, m), 5.80—5.99 (1H, m), 5.84 (1H, s), 6.82—6.86 (4H, m), 7.15 (2H, d, J=8.6 Hz), 7.23 (2H, d, J=8.2 Hz). *Anal.* Calcd for $C_{21}H_{21}NO_5 \cdot H_2O$: C, 65.44; H, 6.02; N, 3.63. Found: C, 65.30; H, 5.57; N, 3.60.

(3*RS*,4*SR*)-1-(Di-*p*-anisylmethyl)-3-ethenyl-4-*p*-methoxybenzyloxycarbonyl-2-azetidinone (**3c**): Et_3N (3.30 g, 33.0 mmol) and *p*-methoxybenzyl chloride (5.12 g, 33.0 mmol) were added to a solution of **3b** (10.0 g, 27.0 mmol) in DMF (50 ml). The reaction mixture was stirred for 20 h at 70 °C, diluted with AcOEt, and washed successively with water, 2 N HCl, and aqueous $NaHCO_3$. The organic layer was dried over Na_2SO_4 and concentrated *in vacuo*. The residue was purified by column chromatography

on silica gel to give **3c** as a viscous oil (12.5 g, 95%). IR (neat): 1762, 1740 (sh) cm^{-1}. ^{1}H-NMR ($CDCl_3$) δ: 3.77 (3H, s), 3.78 (3H, s), 3.81 (3H, s), 3.7—3.9 (2H, m), 4.88 (2H, m), 5.2—5.45 (2H, m), 5.75—6.00 (1H, m), 5.85 (1H, s), 6.80 (2H, d, J=8.9 Hz), 6.83 (2H, d, J=8.9 Hz), 6.86 (2H, d, J=8.9 Hz), 7.08 (2H, d, J=8.9 Hz), 7.16 (2H, d, J=8.9 Hz), 7.20 (2H, d, J=8.9 Hz). MS (FD) m/z: 487 (M^+).

(3*RS*,4*RS*)-1-(Di-*p*-anisylmethyl)-3-ethenyl-4-hydroxymethyl-2-azetidinone (**3d**): LiI (317 mg, 2.36 mmol) and $NaBH_4$ (90 mg, 2.36 mmol) were added in portions to a solution of **3a** (500 mg, 1.18 mmol) in THF (8 ml). The mixture was refluxed for 4 h, concentrated *in vacuo*, and diluted with AcOEt and brine. The organic layer was dried over Na_2SO_4, and concentrated *in vacuo*. The residue was purified by column chromatography on silica gel to give **3d** as a viscous oil (367 mg, 88.0%). IR (neat): 3420 (br), 1728 cm^{-1}. ^{1}H-NMR ($CDCl_3$) δ: 3.48 (2H, m), 3.63 (1H, m), 3.71 (1H, m), 3.81 (3H, s), 3.82 (3H, s), 5.1—6.0 (3H, m), 6.02 (1H, s), 6.88 (2H, d, J=8.9 Hz), 6.90 (2H, d, J=8.9 Hz), 7.22 (4H, d, J=8.6 Hz). MS (FD) m/z: 353 (M^+).

(3*RS*,4*RS*)-4-Acetoxy-1-(di-*p*-anisylmethyl)-3-ethenyl-2-azetidinone (**3e**): Lead tetraacetate (2.17 g, 4.90 mmol) was added in portions to a solution of **3b** (1.50 g, 4.10 mmol) and AcOK (0.80 g, 8.2 mmol) in DMF (7.5 ml) with stirring at room temperature. After being stirred for 1 h, the reaction mixture was diluted with water and AcOEt. The organic layer was washed with water, dried over Na_2SO_4 and concentrated *in vacuo*. The residue was purified by column chromatography on silica gel to give **3e** as a viscous oil (1.17 g, 75%). IR ($CHCl_3$): 1760, 1735 (sh) cm^{-1}. ^{1}H-NMR ($CDCl_3$) δ: 1.90 (3H, s), 3.79 (6H, s), 5.0—5.7 (3H, m), 5.74 (1H, d, J=1.4 Hz), 5.91 (1H, s), 6.7—7.4 (8H, m). MS (FD) m/z: 381 (M^+).

Oxymercuration-Reduction of 3 (Preparation of 7) (3*SR*,4*SR*)-4-*n*-Butoxycarbonyl-1-(di-*p*-anisylmethyl)-3-[(*RS*)-1-hydroxyethyl]-2-azetidinone (**7a** and **8a**): A mixture of **3a** (4.2 g, 10 mmol) and mercuric acetate (3.2 g, 10 mmol) in THF (10 ml) and water (4 ml) was stirred at 25 °C for 1 h. After addition of 1 N NaOH (9 ml) at 0 °C, a solution of $NaBH_4$ (0.4 g) in 1 N NaOH (2 ml) was added dropwise at the same temperature and the whole was stirred for 20 min. The reaction mixture was neutralized with 1 N HCl, diluted with Et_2O and filtered over Celite to remove insoluble materials. The organic layer was washed successively with 10% aqueous $NaHCO_3$ and brine, dried over Na_2SO_4 and concentrated *in vacuo*. The residue was purified by column chromatography on silica gel to give a mixture of **7a** and **8a** (12 : 1) as a viscous oil (3.75 g, 85%). IR (neat): 3470 (br), 1740 (br), 1720 (sh), 1607 cm^{-1}. ^{1}H-NMR ($CDCl_3$) δ: 0.89 (3H, t, J=7.3 Hz), 1.2—1.4 (2H, m), 1.38 (3H, d, J=5.9 Hz), 1.4—1.6 (2H, m), 2.02 (1H, d, J=4.3 Hz), 3.20 (1H × 1/13, m), 3.39 (1H × 12/13, dd, J=5.6, 9.6 Hz), 3.78 (3H, s), 3.80 (3H, s), 4.01 (2H, m), 4.12 (1H × 12/13, d, J=5.6 Hz), 5.77 (1H × 12/13, s), 5.86 (1H × 1/13, s), 6.84 (2H, d, J=8.6 Hz), 6.87 (2H, d, J=8.6 Hz), 7.13 (2H, d, J=8.6 Hz), 7.26 (2H, d, J=8.6 Hz). MS (EI) m/z: 441 (M^+).

Compounds **7b—e** were obtained a similar manner to that described for **7a**.

(3*SR*,4*SR*)-4-Carboxy-1-(di-*p*-anisylmethyl)-3-[(*RS*)-1-hydroxyethyl]-2-azetidinone (**7b**): Amorphous powder (86% yield). It contained a small amount of the 3,5-*erythro* isomer **8b** (**7b** : **8b** > 80 : 1 by HPLC). IR (Nujol): 3250, 1750, 1723 cm^{-1}. ^{1}H-NMR ($CDCl_3$) δ: 1.28 (3H, d, J=6.6 Hz), 3.23 (1H, m), 3.76 (3H, s), 3.77 (3H, s), 4.16 (1H, d, J=2.6 Hz), 5.83 (1H, s), 6.83 (2H, d, J=8.9 Hz), 6.84 (2H, d, J=8.9 Hz), 7.18—7.26 (4H, m).

(3*SR*,4*SR*)-1-(Di-*p*-anisylmethyl)-3-[(*RS*)-1-hydroxyethyl]-4-*p*-methoxybenzyloxycarbonyl-2-azetidinone (**7c**): Viscous oil (90% yield). IR ($CHCl_3$): 3400, 1740 cm^{-1}. ^{1}H-NMR ($CDCl_3$) δ: 1.17 (3H, d, J=6.0 Hz), 3.13 (1H, dd, J=2.2, 3.4 Hz), 3.73 (3H, s), 3.76 (3H, s), 3.84 (3H, s), 4.12 (1H, d, J=2.2 Hz), 4.88 (2H, s), 5.82 (1H, s), 6.66—7.50 (12H, m). MS (FD) m/z: 505 (M^+).

(3*SR*,4*SR*)-1-(Di-*p*-anisylmethyl)-3-[(*RS*)-1-hydroxyethyl]-4-hydroxymethyl-2-azetidinone (**7d**): Viscous oil (85% yield). IR ($CHCl_3$): 3425, 1732 cm^{-1}. ^{1}H-NMR ($CDCl_3$) δ: 1.18 (3H, d, J=6.0 Hz), 3.33 (4H, m), 3.75 (6H, s), 5.87 (1H, s), 6.60—7.40 (8H, m). MS (FD) m/z: 371 (M^+).

(3*RS*,4*RS*)-4-Acetoxy-1-(di-*p*-anisylmethyl)-3-[(*RS*)-1-hydroxyethyl]-2-azetidinone (**7e**): Viscous oil (67% yield). IR ($CHCl_3$): 1752 cm^{-1}. ^{1}H-NMR ($CDCl_3$) δ: 1.30 (3H, d, J=6.27 Hz), 3.11 (1H, dd, J=0.7 Hz, 6.6 Hz), 3.79 (3H, s), 3.80 (3H, s), 4.10 (1H, m), 5.80 (1H, d, J=0.7 Hz), 5.93 (1H, s), 6.86 (2H, d, J=8.9 Hz), 6.87 (2H, d, J=8.9 Hz), 7.15 (2H, d, J=8.6 Hz), 7.23 (2H, d, J=8.6 Hz). MS (FD) m/z: 399 (M^+).

Determination of Stereochemistry in 7b and 8b (3*SR*,4*SR*)-4-Benzyloxycarbonyl-1-(di-*p*-anisylmethyl)-3-[(*RS*)-1-hydroxyethyl]-2-azetidinone (**7f**): K_2CO_3 (5.52 g, 40 mmol) was added to a solution of **7b** (7.7 g, 20 mmol) and benzyl bromide (4.1 g, 24 mmol) in acetone (100 ml). After being refluxed for 2.5 h, the reaction mixture was cooled and filtered. The filtrate was concentrated *in vacuo* and the residue was dissolved in AcOEt. This solution was washed with brine, dried over $MgSO_4$ and concentrated *in vacuo*. The residue was crystallized from hexane to give **7f** (9.47 g, quantitative yield). IR (KBr): 3424, 1741 cm^{-1}. ^{1}H-NMR ($CDCl_3$) δ: 1.24 (3H, d, J=6.3 Hz), 3.21 (1H, dd, J=2.3, 3.3 Hz), 3.76 (3H, m), 3.77 (3H, m), 4.14 (1H, d, J=2.3 Hz), 4.28 (1H, m), 4.96 (2H, s), 5.84 (1H, s), 6.79 (2H, d, J=8.9 Hz), 6.82 (2H, d, J=8.9 Hz), 7.1—7.4 (9H, m). *Anal.* Calcd for $C_{28}H_{29}NO_6$: C, 70.72; H, 6.15; N, 2.95. Found: C, 70.47; H, 6.13; N, 2.95.

(3*SR*,4*SR*)-4-Benzyloxycarbonyl-1-(di-*p*-anisylmethyl)-3-[(*SR*)-1-hydroxyethyl]-2-azetidinone (**8f**): a) Jones reagent (1.5 g) was added to a solution of **7f** (950 mg, 2.0 mmol) in acetone (15 ml) at 0 °C. The reaction mixture was stirred for 1 h at 0 °C, diluted with AcOEt and washed with brine. The organic layer was dried over $MgSO_4$ and concentrated *in vacuo* to give the corresponding ketone (950 mg, quantitative yield). This was used for the next treatment without purification. IR (Nujol): 1762, 1739, 1719 cm^{-1}. ^{1}H-NMR ($CDCl_3$) δ: 2.28 (3H, s), 3.73 (6H, s), 4.19 (1H, d, J=2 Hz), 4.45 (1H, d, J=2 Hz), 4.87 (2H, s), 5.80 (1H, s), 6.50—7.4 (13H, m).

b) A solution of $NaBH_4$ (76 mg, 2.0 mmol) in water (2 ml) was added to a solution of the crude ketone in iso-propanol (30 ml) at 0 °C. The mixture was warmed to room temperature, diluted with $CHCl_3$ and washed with brine. The organic layer was dried over $MgSO_4$ and concentrated *in vacuo* to give a mixture of **7f** and **8f** (1.01 g). The crude mixture (45 mg) was purified by preparative TLC (benzene–Et_2O (1 : 1)) to give **8f** as a viscous oil (15.6 mg). IR (neat): 3470, 1742 cm^{-1}. ^{1}H-NMR ($CDCl_3$) δ: 1.34 (3H, d, J=6.3 Hz), 3.20 (1H, dd, J=2.3, 5.3 Hz), 3.76 (3H, s), 3.78 (3H, s), 3.94 (1H, d, J=2.3 Hz), 4.09 (1H, m), 4.96 (2H, m), 5.84 (1H, s), 6.7—6.9 (4H, m), 7.1—7.4 (9H, m). MS (FD) m/z: 475 (M^+).

(3*SR*,4*SR*)-4-Carboxy-1-(di-*p*-anisylmethyl)-3-[(*SR*)-1-hydroxyethyl]-2-azetidinone (**8b**): A solution of **8f** (15 mg, 0.32 mmol) in AcOEt (5 ml) containing 10 mg of 10% Pd–C was stirred at room temperature for 3.5 h under a hydrogen atmosphere. After filtration, the filtrate was concentrated *in vacuo* to give **8b** as a viscous oil (12 mg, quantitative yield). IR (neat): 3360, 1738, 1718 (sh), 1700 (sh) cm^{-1}. ^{1}H-NMR ($CDCl_3$) δ: 1.31 (3H, d, J=6.6 Hz), 3.24 (1H, dd, J=2.3, 5.6 Hz), 3.77 (3H, s), 3.78 (3H, s), 3.90 (1H, d, J=2.3 Hz), 4.12 (1H, m), 5.79 (1H, s), 6.77 (2H, d, J=8.9 Hz), 6.79 (2H, d, J=8.9 Hz), 7.19 (2H, d, J=8.6 Hz), 7.24 (2H, d, J=8.6 Hz). MS (FD) m/z: 385 (M^+).

(3*SR*,4*SR*)-1-(Di-*p*-anisylmethyl)-3-[(*RS*)-1-hydroxyethyl]-4-methoxycarbonyl-2-azetidinone (**7g**): A 10% solution of trimethylsilyldiazomethane (TMS-CHN_2) in hexane (0.6 mmol) was added to a solution of **7b** (77 mg, 0.2 mmol) in MeOH (1 ml). The mixture was stirred for 1 h and concentrated *in vacuo*. The residue was purified by preparative TLC (toluene–AcOEt (1 : 1)) to give **7g** (80 mg, quantitative yield). IR (neat): 3430 (br), 1750 (sh), 1738, 1602, 1504 cm^{-1}. ^{1}H-NMR ($CDCl_3$) δ: 1.26 (3H, d, J=6.6 Hz), 3.21 (1H, dd, J=2.3, 4.0 Hz), 3.52 (3H, s), 3.78 (3H, s), 3.79 (3H, s), 4.14 (1H, d, J=2.3 Hz), 4.28 (1H, m), 5.87 (1H, s), 6.75—6.95 (4H, m), 7.05—7.35 (4H, m). *Anal.* Calcd for $C_{22}H_{25}NO_6$: C, 66.15; H, 6.31; N, 3.51. Found: C, 66.24; H, 6.39; N, 3.51.

(3*SR*,4*SR*)-1-(Di-*p*-anisylmethyl)-3-[(*SR*)-1-hydroxyethyl]-4-methoxycarbonyl-2-azetidinone (**8g**): Treatment of **8b** (15 mg, 0.039 mmol), prepared from **7b**, as described above gave **8g** (12.5 mg, 80%). IR (neat): 3450 (br), 1750 (sh), 1738 cm^{-1}. ^{1}H-NMR ($CDCl_3$) δ: 1.36 (3H, d, J=6.6 Hz), 3.21 (1H, dd, J=2.3, 5.3 Hz), 3.54 (3H, s), 3.79 (3H, s), 3.80 (3H, s), 3.94 (1H, d, J=2.3 Hz), 4.11 (1H, m), 5.86 (1H, s), 6.75—6.95 (4H, m), 7.10—7.40 (4H, m). MS (FD) m/z: 399 (M^+).

1-(Di-*p*-anisylmethyl)-(*E*)-3-ethylidene-4*SR*-methoxycarbonyl-2-azetidinone (**9a**): A solution of MsCl (17 mg, 0.15 mmol) in CH_2Cl_2 (0.5 ml) was added to a solution of **7g** (40 mg, 0.1 mmol) and Et_3N (20 mg, 0.2 mmol) in CH_2Cl_2 (1.5 ml) at 0 °C. The mixture was stirred for 30 min, quenched with dilute HCl and extracted with CH_2Cl_2. The organic layer was washed successively with aqueous $NaHCO_3$ and brine, dried over $MgSO_4$ and concentrated *in vacuo* to give the corresponding mesylate. A solution of the mesylate in MeOH (0.8 ml) was treated with $NaHCO_3$ (8 mg, 0.1 mmol) and the mixture was refluxed for 30 min, then concentrated *in vacuo*. The residue was purified by preparative TLC (toluene–AcOEt (2 : 1)) to give **9a** as a viscous oil (12.2 mg, 67%). IR (neat): 1756, 1608, 1510 cm^{-1}. ^{1}H-NMR ($CDCl_3$) δ: 1.74 (3H, dd, J=0.7, 7.3 Hz), 3.55 (3H, s), 3.79 (3H, s), 3.80 (3H, s), 4.48 (1H, dd, J=0.7, 1.7 Hz), 5.95 (1H, s), 6.26 (1H, dq, J=1.7, 7.3 Hz), 6.85 (2H, d, J=8.5 Hz), 6.86 (2H, d, J=8.5 Hz), 7.13 (2H, d, J=8.5 Hz), 7.24 (2H, d, J=8.5 Hz). MS (EI) m/z: 381 (M^+).

1-(Di-*p*-anisylmethyl)-(*Z*)-3-ethylidene-4*SR*-methoxycarbonyl-2-azetidinone (**9b**): Treatment of **8f** (7.8 mg, 0.02 mmol), prepared from **8b**, as described above gave **9b** (3.6 mg, 47%) and **9a** (0.7 mg, 9%) as viscous

oils. **9b**: IR (neat): 1750 cm^{-1}. ^{1}H-NMR ($CDCl_3$) δ: 2.03 (3H, dd, J=1.0, 7.3 Hz), 3.59 (3H, s), 3.79 (3H, s), 3.80 (3H, s), 4.34 (1H, m), 5.74 (1H, dq, J=1.3 Hz, 7.3 Hz), 5.90 (1H, s), 6.85 (2H, d, J=8.7 Hz), 6.87 (2H, d, J=8.7 Hz), 7.16 (2H, d, J=8.7 Hz), 7.26 (2H, d, J=8.7 Hz). MS (EI) m/z: 381 (M^+).

Preparation of Optically Active 3b. Method A: Optical Resolution (3*R*,4*S*)-1-(Di-*p*-anisylmethyl)-3-ethenyl-4-(*l*-menthyloxycarbonyl)-2-azetidinone (**10a**): A solution of oxalyl chloride (4.82 g, 38 mmol) in CH_2Cl_2 (10 ml) was added dropwise over 20 min to a solution of (±)-**3b** (11.66 g, 31.8 mmol) in CH_2Cl_2 (80 ml) containing DMF (1.2 g) at room temperature, followed by stirring for 1.5 h. The resulting acid chloride solution was added dropwise to a mixture of *l*-menthol (6.96 g, 44.6 mmol), Et_3N (8.58 g, 85 mmol) and *N*,*N*-dimethylaminopyridine (0.516 g, 4.2 mmol) in CH_2Cl_2 (10 ml) at 0 °C and the whole was stirred at the same temperature for 2 h. The reaction mixture was diluted with toluene (200 ml) and washed with brine. The organic layer was washed successively with 2 N HCl, 10% aqueous $NaHCO_3$ and brine, dried over Na_2SO_4 and concentrated *in vacuo*. The residue was crystallized from MeOH to give a mixture of two diastereomers of *l*-menthyl ester (**10a** and **10b**, **10a** : **10b** = *ca.* 1 : 1) as a crystalline material (11.7 g, 73%). mp 96—97 °C. IR ($CHCl_3$): 1760, 1740 (sh) cm^{-1}. ^{1}H-NMR ($CDCl_3$) δ: 0.67 (3H × 1/2, d, J=6.9 Hz), 0.71 (3H × 1/2, d, J=6.9 Hz), 0.83 (3H × 1/2, d, J=6.9 Hz), 0.85 (3H × 1/2, d, J=6.9 Hz), 0.88 (3H, d, J=6.6 Hz), 0.89 (3H, d, J=6.6 Hz), 0.6—1.9 (9H, m), 3.78 (3H, s), 3.79 (3H, s), 4.62 (1H, m), 5.2—5.5 (2H, m), 5.83 (1H × 1/2, s), 5.84 (1H × 1/2, s), 5.8—6.0 (1H, m), 6.84 (2H, d, J=8.6 Hz), 6.87 (2H, d, J=8.6 Hz), 7.13 (2H × 1/2, d, J=8.6 Hz), 7.14 (2H × 1/2, d, J=8.6 Hz), 7.28 (2H, d, J=8.6 Hz).

Seed crystals of **10a** could be obtained by fractional recrystallization of the mixture from MeOH. The mixture (11.7 g) was dissolved in MeOH (480 ml) under heating at 60 °C, and the MeOH solution was gradually cooled to 20 °C. After seeding of (+)-*l*-menthyl ester (4 mg), the mixture was further cooled to 0 °C over 2 h and stirred at 0 °C overnight. The resulting precipitate was collected by filtration to give the *l*-menthyl ester (**10a** and **10b**, **10a** : **10b** = 4.5 : 1), which was purified by recrystallization from MeOH to give optically pure **10a** (2.15 g, 18%). **10a**: mp 114—115 °C. $[\alpha]_D^{22}$ +20.2° (c=0.26, $CHCl_3$). IR (Nujol): 1765, 1722 cm^{-1}. ^{1}H-NMR ($CDCl_3$) δ: 0.67 (3H, d, J=6.9 Hz), 0.85 (3H, d, J=7.3 Hz), 0.88 (3H, d, J=6.6 Hz), 0.7—1.8 (9H, m), 3.79 (3H, s), 3.79 (3H, s), 4.62 (1H, m), 5.2—5.4 (2H, m), 5.83 (1H, s), 5.8—6.0 (1H, m), 6.84 (2H, d, J=8.9 Hz), 6.86 (2H, d, J=8.6 Hz), 7.13 (2H, d, J=8.3 Hz), 7.28 (2H, d, J=8.3 Hz). *Anal.* Calcd for $C_{31}H_{39}NO_5$: C, 73.63; H, 7.77; N, 2.77. Found: C, 73.37; H, 7.76; N, 2.73.

(3*R*,4*S*)-4-Carboxy-1-(di-*p*-anisylmethyl)-3-ethenyl-2-azetidinone ((+)-**3b**): Treatment of **10a** with 1 N NaOH as described for the formation of racemic **3b** gave the acid (+)-**3b** (74%). $[\alpha]_D^{22}$ +63.3° (c=0.12, $CHCl_3$). The IR and ^{1}H-NMR spectral data were identical with those of racemic **3b**.

(3*R*,4*S*)-4-Methoxycarbonyl-1-(di-*p*-anisylmethyl)-3-ethenyl-2-azetidinone (**11**): A solution of (+)-**3b** (73 mg, 0.2 mmol), prepared from **10a**, in MeOH (3 ml) was treated with 10% TMS-CHN_2 in hexane (0.4 mmol). The mixture was stirred at room temperature for 1 h and concentrated *in vacuo*. The residue was purified by preparative TLC (5 : 1) to give **11** (55 mg, 72%). mp 102—103 °C. $[\alpha]_D^{24}$ +39° (c=0.37, $CHCl_3$). IR (neat): 1758 cm^{-1}. ^{1}H-NMR ($CDCl_3$) δ: 3.53 (3H, s), 3.80 (3H, s), 3.80 (3H, s), 3.86 (1H, d, J=2.3 Hz), 5.25—5.45 (2H, m), 5.80—6.00 (1H, m), 5.89 (1H, s), 6.80—6.90 (4H, m), 7.14 (2H, d, J=8.6 Hz), 7.21 (2H, d, J=8.6 Hz). *Anal.* Calcd for $C_{22}H_{23}NO_5$: C, 69.27; H, 6.08; N, 3.67. Found: C, 69.00; H, 6.08; N, 3.69.

Method B: Asymmetric Synthesis (3*S*,4*S*)-1-(Di-*p*-anisylmethyl)-3-ethenyl-4-(*d*-menthyloxycarbonyl)-2-azetidinone (**13a**): A mixture of di-*p*-anisylmethylamine (243 mg, 1.00 mmol) and *d*-menthylglyoxylate monohydrate (230 mg, 1.00 mmol) in toluene (24 ml) was dehydrated azeotropically under reflux to give a toluene solution of the Schiff base. After addition of Et_3N (151 mg, 1.5 mmol), a solution of crotonyl chloride (126 mg, 1.2 mmol) in toluene (2 ml) was added dropwise at 70 °C over 20 min, followed by stirring for 3 h at the same temperature. The reaction mixture was diluted with toluene and washed successively with brine, 1 N HCl, brine, 5% aqueous $NaHCO_3$ and brine. The organic layer was dried over Na_2SO_4 and concentrated *in vacuo*. The residue was purified by column chromatography on silica gel to give a mixture of **13a** and **13b** (414 mg, 82%). The ratio of **13a** and **13b** was as determined 2 : 1 by HPLC analysis and from the ^{1}H-NMR spectrum. ^{1}H-NMR ($CDCl_3$) δ: 0.64 (3H × 2/3, d, J=6.6 Hz), 0.66 (3H × 1/3, d, J=6.9 Hz), 0.79 (3H × 2/3, d, J=7.3 Hz), 0.83 (3H × 1/3, d, J=7.3 Hz), 0.89 (3H, d, J=6.6 Hz), 3.78 (3H, s), 3.79 (3H × 2/3, s), 3.80 (3H × 1/3, s), 4.02 (1H, m), 4.08 (1H × 1/3, d, J=5.9 Hz), 4.09 (1H × 2/3, d, J=5.9 Hz), 4.59 (1H, m), 5.2—5.5 (2H, m), 5.7—5.8 (1H, m), 5.82 (1H, s), 6.80—6.95 (4H, m), 7.1—7.4 (4H, m). Recrystallization of the mixture from MeOH gave optically pure **13a**, mp 162—163 °C, $[\alpha]_D^{25}$ +5.8° (c=0.21, $CHCl_3$). IR (KBr): 1774, 1732 cm^{-1}. ^{1}H-NMR ($CDCl_3$) δ: 0.64 (3H, d, J=6.9 Hz), 0.79 (3H, d, J=6.9 Hz), 0.89 (3H, d, J=6.6 Hz), 3.78 (3H, s), 3.79 (3H, s), 4.02 (1H, m), 4.09 (1H, d, J=5.9 Hz), 4.57 (1H, m), 5.25—5.45 (2H, m), 5.70—5.81 (1H, m), 5.82 (1H, s), 6.80—6.95 (4H, m), 7.13 (2H, d, J=8.6 Hz), 7.33 (2H, d, J=8.3 Hz). *Anal.* Calcd for $C_{31}H_{39}NO_5 \cdot 1/4H_2O$: C, 72.98; H, 7.80; N, 2.75. Found: C, 73.13; H, 7.73; N, 2.72.

(3*R*,4*S*)-4-Carboxy-1-(di-*p*-anisylmethyl)-3-ethenyl-2-azetidinone ((+)-**3b**): Treatment of **13a** with 1 N NaOH as described for the formation of racemic **3b** gave the acid (+)-**3b** (88%), $[\alpha]_D^{21}$ +58.0° (c=1.28, $CHCl_3$). The IR and ^{1}H-NMR spectral data were identical with those of racemic **3b**.

(3*R*,4*S*)-1-(Di-*p*-anisylmethyl)-3-ethenyl-4-methoxycarbonyl-2-azetidinone (**11**): Treatment of (+)-**3b** prepared from **13a** (64 mg, 0.18 mmol) as described above gave **11** (49 mg, 74%), $[\alpha]_D^{22}$ +39° (c=0.99, $CHCl_3$). The IR and ^{1}H-NMR spectral data were identical with those of **11** derived from **10a**.

Preparation of 2 (3*S*,4*S*)-4-Carboxy-1-(di-*p*-anisylmethyl)-3-[(*R*)-1-hydroxyethyl]-2-azetidinone ((+)-**7b**): Treatment of (+)-**3b** with mercuric acetate and then $NaBH_4$ as described for the formation of racemic **7b** gave (+)-**7b** (86%), which was recrystallized from CH_2Cl_2 to give pure (+)-**7b**, mp 86—88 °C, $[\alpha]_D^{27}$ +11.0° (c=0.21, $CHCl_3$). *Anal.* Calcd for $C_{21}H_{23}NO_6$: C, 65.44; H, 6.02; N, 3.63. Found: C, 65.27; H, 6.04; N, 3.61. The IR and ^{1}H-NMR spectral data were identical with those of racemic **7b**.

(3*R*,4*R*)-4-Acetoxy-1-(di-*p*-anisylmethyl)-3-ethenyl-2-azetidinone ((+)-**3e**): Treatment of (+)-**3b** with lead tetraacetate as described for the formation of racemic **3e** gave (+)-**3e** (75%), $[\alpha]_D^{25}$ +79.0° (c=0.158, $CHCl_3$). The IR and ^{1}H-NMR spectral data were identical with those of racemic **3e**.

(3*R*,4*R*)-4-Acetoxy-1-(di-*p*-anisylmethyl)-3-[(*R*)-1-hydroxyethyl]-2-azetidinone ((+)-**7e**): Method A: Lead tetraacetate (2.7 g, 6.0 mmol) was added portionwise to a mixture of (+)-**7b** (2.0 g, 5.2 mmol) and AcOK (0.5 g, 5.1 mmol) in DMF (20 ml) and toluene (20 ml). The slurry was immersed in an oil-bath at 40 °C and stirred for 1 h. After decomposition of the residual lead tetraacetate with ethylene glycol, the reaction mixture was diluted with toluene and filtered over Celite. The organic layer was washed successively with brine, 10% aqueous $NaHCO_3$ and brine, dried over Na_2SO_4 and concentrated *in vacuo*. The residue was purified by column chromatography on silica gel to give (+)-**7e** (1.83 g, 88%).

Method B: Treatment of (+)-**3e** with mercuric acetate and then $NaBH_4$ as described for the formation of racemic **7e** gave (+)-**7e** (67%), $[\alpha]_D^{22}$ +26.0° (c=0.04, $CHCl_3$). The IR and ^{1}H-NMR spectral data were identical with those of racemic **7e**.

(3*R*,4*R*)-4-Acetoxy-1-(di-*p*-anisylmethyl)-3-[(*R*)-1-*p*-nitrobenzyloxycarbonyloxyethyl]-2-azetidinone (**14a**): A solution of *p*-nitrobenzyl chloroformate (2.94 g, 13.6 mmol) in CH_2Cl_2 (6.4 ml) was added dropwise to a mixture of (+)-**7e** (3.02 g, 7.6 mmol) and *N*,*N*-dimethylaminopyridine (1.86 g, 15.2 mmol) in CH_2Cl_2 (46 ml) at 0 °C, followed by stirring for 2 h. The mixture was quenched with dilute HCl and diluted with AcOEt. The organic layer was washed with brine, dried over Na_2SO_4 and concentrated *in vacuo*. The residue was purified by column chromatography on silica gel to give **14a** (3.90 g, 90%), $[\alpha]_D^{22}$ +40.5° (c=0.38, $CHCl_3$). IR (neat): 1770 (sh), 1740, 1610 cm^{-1}. ^{1}H-NMR ($CDCl_3$) δ: 1.44 (3H, d, J=6.3 Hz), 1.87 (3H, s), 3.27 (1H, dd, J=1.0, 5.6 Hz), 3.75 (3H, s), 3.77 (3H, s), 5.15 (1H, m), 5.25 (2H, s), 5.89 (1H, s), 6.11 (1H, d, J=1.0 Hz), 6.79 (2H, d, J=8.9 Hz), 6.82 (2H, d, J=8.6 Hz), 7.15 (2H, d, J=8.6 Hz), 7.20 (2H, d, J=8.3 Hz), 7.55 (2H, d, J=8.9 Hz), 8.25 (2H, d, J=8.9 Hz). *Anal.* Calcd for $C_{30}H_{30}N_2O_{10}$: C, 62.28; H, 5.23; N, 4.84. Found: C, 62.19; H, 5.39; N, 4.70.

(3*R*,4*R*)-4-Acetoxy-3-[(*R*)-1-*p*-nitrobenzyloxycarbonyloxyethyl]-2-azetidinone (**2a**): A solution of ceric (IV) ammonium nitrate (CAN) (12.8 g, 23.4 mmol) in water (8 ml) was added in portions to a solution of **14a** (5.76 g, 9.95 mmol) in MeCH (72 ml) at room temperature over 1 h. After being stirred for 0.5 h, the mixture was diluted with toluene and washed with 10% aqueous $NaHCO_3$ and brine. The organic layer was dried over Na_2SO_4 and concentrated *in vacuo*. The residue was purified by column chromatography on silica gel to give **2a** as a viscous oil (2.26 g, 94%), $[\alpha]_D^{22}$ +36.6° (c=0.09, $CHCl_3$). IR (neat): 3300, 1774, 1745, 1602 cm^{-1}. ^{1}H-NMR ($CDCl_3$) δ: 1.47 (3H, d, J=6.3 Hz), 2.11 (3H, s), 3.38 (1H, dd, J=1.3, 6.3 Hz), 5.16 (1H, m), 5.26 (2H, s), 5.86 (1H, d, J=1.3 Hz), 6.53 (1H, s), 7.55 (2H, d, J=8.9 Hz), 8.24 (2H, d, J=8.9 Hz). MS (FD) m/z: 353 ($M+1$)$^+$. *Anal.* Calcd for $C_{15}H_{16}N_2O_8$: C, 51.14; H, 4.58; N, 7.95. Found: C, 51.54; H, 4.86; N, 8.04.

(3*R*,4*R*)-4-Acetoxy-1-(di-*p*-anisylmethyl)-3-[(*R*)-1-(*tert*-butyldimethylsilyloxy)ethyl]-2-azetidinone (**14b**): Imidazole (143 mg, 2.10 mmol) and *tert*-butyldimethylsilyl chloride (316 mg, 2.10 mmol) were added to a solution of (+)-**7e** (399 mg, 1.00 mmol) in DMF (1.9 ml). After being stirred for 2 h, the reaction mixture was diluted with water and benzene. The organic layer was washed with water, dried over Na_2SO_4 and concentrated *in vacuo*. The residue was purified by column chromatography on silica gel to give **14b** as a viscous oil (440 mg, 86%), $[\alpha]_D^{27}$ +23.8° (c=0.505, $CHCl_3$). IR (neat): 1765, 1750 (sh), 1607 cm^{-1}. ^{1}H-NMR ($CDCl_3$) δ: 0.05 (3H, s), 0.82 (9H, s), 1.22 (3H, d, J=6.3 Hz), 1.84 (3H, s), 3.11 (1H, dd, J=1.0, 3.6 Hz), 3.79 (3H, s), 3.79 (3H, s), 4.17 (1H, m), 5.89 (1H, s), 6.17 (1H, d, J=1.0 Hz), 6.84 (2H, d, J=8.9 Hz), 6.85 (2H, d, J=8.9 Hz), 7.18 (2H, d, J=8.9 Hz), 7.23 (2H, d, J=8.9 Hz). MS (FD) m/z: 513 (M^+).

(3*R*,4*R*)-4-Acetoxy-3-[(*R*)-1-(*tert*-butyldimethylsilyloxy)ethyl]-2-azetidinone (**2b**): Treatment of **14b** (514 mg, 1.00 mmol) with CAN as described for the preparation of **2a** gave **2b** (196 mg, 68%), mp 100—102 °C (lit.[1a] mp 104 °C, lit.[1c] mp 101—103 °C, lit.[1d] mp 107—108 °C), $[\alpha]_D^{26}$ +48.2° (c=1.01, $CHCl_3$) (lit.[1c] $[\alpha]_D^{25}$ +47.9° (c=1.00, $CHCl_3$), lit.[1d] $[\alpha]_D$ +50.0° (c=0.41, $CHCl_3$)). IR (Nujol): 1776, 1740 cm^{-1}. ^{1}H-NMR ($CDCl_3$) δ: 0.06 (3H, s), 0.07 (3H, s), 0.87 (9H, s), 1.25 (3H, d, J=6.3 Hz), 2.11 (3H, s), 3.19 (1H, dd, J=1.3, 3.3 Hz), 4.23 (1H, m), 5.84 (1H, d, J=1.3 Hz), 6.49 (1H, s).

References and Notes

1) Other synthetic routes to 4-acetoxy-3-[(*R*)-1-hydroxyethyl]-2-azetidinones: *a*) K. Hirai, Y. Iwano, and K. Fujimoto, *Heterocycles*, **17**, 201 (1982); *b*) P. J. Reider and E. J. J. Grabowski, *Tetrahedron Lett.*, **1982**, 2293; *c*) M. Shiozaki, N. Ishida, H. Maruyama, and T. Hiraoka, *Tetrahedron*, **39**, 2399 (1983); *d*) W. J. Leanza, F. DiNinno, D. A. Muthard, R. R. Wilkening, K. J. Wildonger, R. W. Ratcliff, and B. G. Christensen, *ibid.*, **39**, 2505 (1983); *e*) M. Shiozaki, N. Ishida, T. Hiraoka, and H. Maruyama, *ibid.*, **40**, 1795 (1984); *f*) T. Chiba and T. Nakai, *Chem. Lett.*, **1985**, 651; *g*) T. Chiba, M. Nagatsuma, and T. Nakai, *ibid.*, **1985**, 1343; *h*) T. Ohashi, K. Kan, I. Sada, A. Miyama, and K. Watanabe, Eur. Patent Appl. 167154 (1986) [*Chem. Abstr.*, **105**, 97248*j* (1986)]; *i*) M. Mori, K. Kagechika, K. Tohjima, and M. Shibasaki, *Tetrahedron Lett.*, **1988**, 1409; *j*) S. Murahashi, T. Naota, T. Kawabara, T. Saito, H. Kumobayashi, and S. Akutagawa, *J. Am. Chem. Soc.*, **112**, 7820 (1990).

2) *a*) A. K. Bose, G. Spiegelman, and M. S. Manhas, *Tetrahedron Lett.*, **1971**, 3167; *b*) R. Zamboni and G. Just, *Can. J. Chem.*, **57**, 1945 (1979); *c*) A. K. Bose, L. Krishnan, D. R. Wagele, and M. S. Manhas, *Tetrahedron Lett.*, **1986**, 5955.

3) A solution of **3a** (12 mg, 0.028 mmol) in CD_3OD (0.5 ml) and D_2O (0.1 ml) was treated with NaOH (1.1 mg, 0.028 mmol) at room temperature, and the mixture was allowed to stand for 3 h, then the ^{1}H-NMR spectrum was measured. ^{1}H-NMR ($CD_3OD:D_2O$=5:1) δ: 3.72 (1H, s, H-4), 3.78 (3H, s), 3.80 (3H, s), 5.2—5.45 (2H, m), 5.76 (1H, s), 5.8—6.1 (1H, m), 6.87 (2H, d, J=8.6 Hz), 6.91 (2H, d, J=8.6 Hz), 7.24 (2H, d, J=8.9 Hz), 7.30 (2H, d, J=8.9 Hz). Compound **3b** (8.3 mg, 0.023 mmol) was also treated in the same manner as described above and the ^{1}H-NMR spectrum of the sodium salt of **3b** was measured. ^{1}H-NMR ($CD_3OD:D_2O$=5:1) δ: 3.65 (1H, m, H-3), 3.73 (1H, d, J=2.3 Hz, H-4), 3.79 (3H, s), 3.80 (3H, s), 5.2—5.45 (2H, m), 5.76 (1H, s), 5.9—6.1 (1H, m), 6.87 (2H, d, J=8.9 Hz), 6.91 (2H, d, J=8.9 Hz), 7.24 (2H, d, J=8.6 Hz), 7.30 (2H, d, J=8.6 Hz).

4) M. Sunagawa, H. Matsumura, T. Inoue, and M. Enomoto, Eur. Patent 0070204 (1987) [*Chem. Abstr.*, **99**, 105049*v* (1983)]. A part of our work was described in this patent.

5) A. Bouffard, D. B. R. Johnston, and B. G. Christensen, *J. Org. Chem.*, **45**, 1130 (1980).

6) J. Jurczak and A. Zamojski, *Roczniki Chemii Ann. Soc. Chim. Polonorum*, **44**, 2257 (1970).

7) M. Sunagawa, H. Matsumura, T. Inoue, and T. Hirohashi, U.S. Patent 4536334 (1985) [*Chem. Abstr.*, **94**, 192112*y* (1981)].

Cycloaddition in Synthesis of Sulfonamide Derivatives. IV.[1] One-Pot Synthesis of 3-Dimethylamino-4,1,2-benzoxathiazine 1,1-Dioxides, 3-Methoxy-4-methyl-1,2,4-benzothiadiazine 1,1-Dioxide and 3-Dimethylamino-1,4,2-benzodithiazine 1,1-Dioxides

Tsuneo IWAKAWA,* Hiroto TAMURA, Akira MURABAYASHI and Yoshio HAYASE

Aburahi Laboratories, Shionogi Research Laboratories, Shionogi & Co., Ltd., Koka-cho, Shiga 520–34, Japan. *Received December 27, 1990*

A novel, one-pot synthesis of 3-dimethylamino-4,1,2-benzoxathiazine 1,1-dioxides (7), 3-methoxy-4-methyl-1,2,4-benzothiadiazine 1,1-dioxide (9) and 3-dimethylamino-1,4,2-benzodithiazine 1,1-dioxides (11) is described. The procedure in the case of 7 involves [2+2] cycloaddition reaction of chlorosulfonyl isocyanate (CSI) with thiocarbamates with subsequent loss of carbonyl sulfide, followed by cyclization of the resulting *N*-chlorosulfonyl isothioureas under Friedel–Crafts conditions. Synthesis of 9 was achieved similarly. Also, by using dithiocarbamates instead of thiocarbamates, the 1,4,2-benzodithiazines 11 were synthesized.

Keywords [2+2] cycloaddition; chlorosulfonyl isocyanate; dithiocarbamate; thiocarbamate; Friedel–Crafts cyclization; 3-dimethylamino-4,1,2-benzoxathiazine 1,1-dioxide; 3-methoxy-4-methyl-1,2,4-benzothiadiazine 1,1-dioxide; 3-dimethylamino-1,4,2-benzodithiazine 1,1-dioxide

In a previous paper of this series, we reported the synthesis of *N*-(*C*-amino-alkylthiomethylene)benzenesulfonamides (A)[2] and *N*-arylsulfonylethoxyalamides (B)[3] by means of a novel [2+2] cycloaddition reaction of benzenesulfonyl isocyanate with dithiocarbamate and ethyl oxamate, respectively. In the course of our study on the preparation of heterocyclic compounds which bear the sulfonamide moiety, we developed a one-pot synthesis of 3-alkylthio-4*H*-1,2,4-benzothiadiazine 1,1-dioxide (C) which involves [2+2] cycloaddition reaction of chlorosulfonyl isocyanate (CSI) with dithiocarbamate as a key step.[1]

To explore further the utility of the [2+2] cycloaddition reaction of sulfonyl isocyanate in organic synthesis, we became interested in the synthesis of the title compounds, which have been comparatively little explored. In the present paper, we describe a new and facile synthesis of the title compounds, which is superior in simplicity and/or yield to the procedures used thus far.

Reaction of *p*-Toluenesulfonyl Isocyanate (TSI) with Carbamate, Thiocarbamate, Urea and Thiourea Derivatives To accomplish our aim, we first investigated the generality of the [2+2] cycloaddition reaction of sulfonyl isocyanate. Four compounds **1**—**4** were used as model compounds (Chart 2). The conditions and results of this reaction of TSI with **1**—**4** are summarized in Table I.

The reaction of **3** with TSI did not proceed under reflux in toluene for 3 h, resulting in quantitative recovery of **3**. The reaction of **4** with TSI gave similar results. However, interestingly, **1** and **2** under the same reaction conditions gave the corresponding **5** and **6**, in each case as a single stereoisomer, in 80% and 78% yields, respectively. When **1** and **2** were treated with TSI at room temperature for 24 h, the corresponding **5** and **6** were obtained in 65% and 70% yields, respectively. The structures of **5** and **6** were confirmed by elemental analyses and examination of the infrared (IR) absorption and proton nuclear magnetic resonance (^{1}H-NMR) spectra (see Experimental). These findings encouraged us to try to prepare the title compounds.

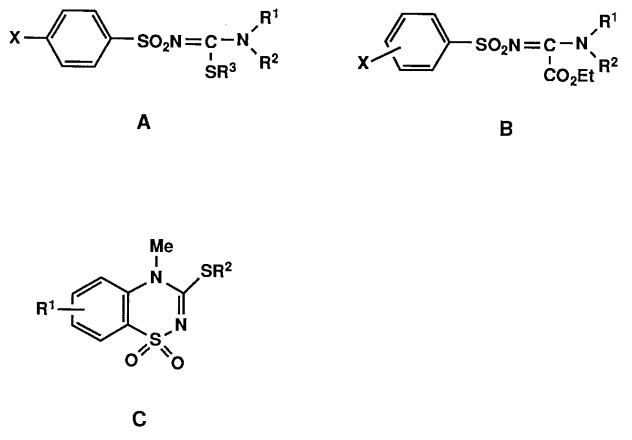

Chart 1

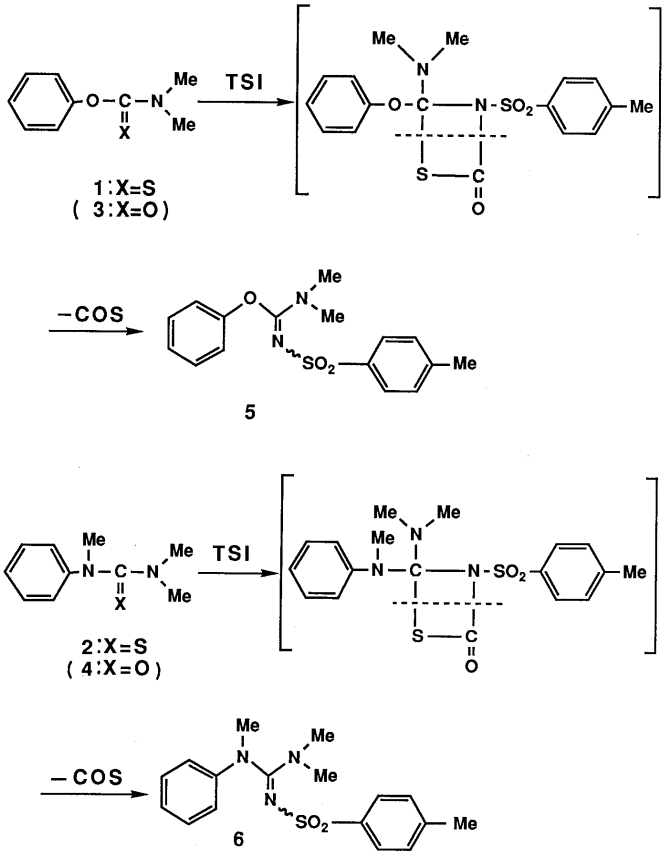

Chart 2

TABLE I. Reaction of TSI with **1**—**4**

S.M.	Reaction conditions	Product	Yield (%)
1	Reflux, 3 h	**5**	80
1	r.t., 24 h	**5**	65
2	Reflux, 3 h	**6**	78
2	r.t., 24 h	**6**	70
3	Reflux, 3 h	**5**	0
4	Reflux, 3 h	**6**	Trace

TSI = *p*-toluenesulfonyl isocyanate. S.M. = starting material. r.t. = room temperature.

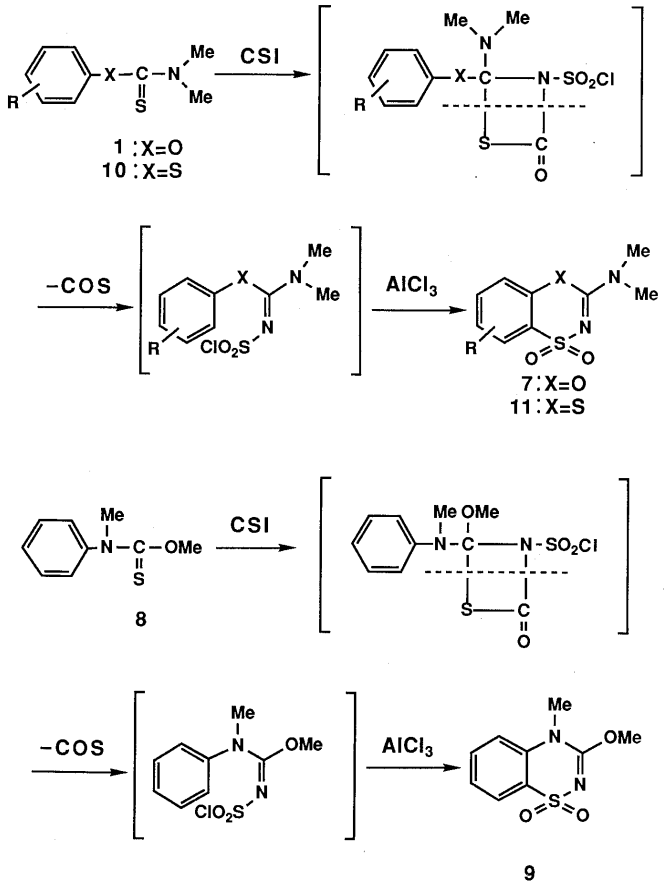

Chart 3

Numerous studies have been done on the [2+2] cycloaddition reaction of sylfonyl isocyanate,[4] but there has been no previous report of a [2+2] cycloaddition reaction of sulfonyl isocyanate with thiocarbamate or thiourea.

Synthesis of 3-Dimethylamino-4,1,2-benzoxathiazine 1,1-Dioxides (7) Literature survey yielded only one method for the preparation of **7**.[5] However, this procedure, involving the reaction of 2-hydroxyphenylsulfonylureas with phosphorus oxychloride, requires multiple steps and uncommon starting materials. Moreover, the yields are low. To overcome these problems, we investigated an alternative method for the preparation of **7**. As starting materials, *O*-phenyl *N*,*N*-dimethylthiocarbamates (**1a**—**e**) were easily prepared by the standard method (Tables II and IV).[6] Compound **1a** was treated with CSI in dry CH_2Cl_2 under stirring at room temperature for 30 min, then the solvent was replaced with dry CH_3NO_2, and the mixture was treated with $AlCl_3$ at room temperature for 2 h, giving **7a** in 76% yield. The other compounds (**7b**—**e**) were similarly obtained in 30—68% yields (Tables III and V).

Synthesis of 3-Methoxy-4-methyl-1,2,4-benzothiadiazine 1,1-Dioxide (9) To examine the scope of the above method, we applied it to the synthesis of **9**. The starting material, *O*-methyl *N*-methyl-*N*-phenylthiocarbamate (**8**), was prepared by a previously reported method.[7] Use of **8**, instead of **1**, afforded the desired compound **9** in 75% yield, by the same procedure as that described for the preparation of **7**.

TABLE II. *O*-Phenyl *N*,*N*-Dimethylthiocarbamates (**1a**—**e**)

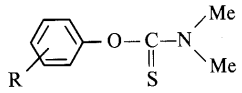

	R	mp (°C)	Formula	*Anal.* (%) Calcd (Found)		
				C	H	N
1a	H	Oil	$C_9H_{11}NOS$	59.64 (59.53	6.12 6.10	7.73 7.71)
1b	2-Me	Oil	$C_{10}H_{13}NOS$	61.50 (61.38	6.71 6.78	7.17 7.22)
1c	4-Me	91—92	$C_{10}H_{13}NOS$	61.50 (61.46	6.71 6.70	7.17 7.09)
1d	2-Cl	Oil	$C_9H_{10}ClNOS$	50.12 (49.94	4.67 4.72	6.49 6.59)
1e	4-Cl	51—53	$C_9H_{10}ClNOS$	50.12 (49.95	4.67 4.65	6.49 6.54)

TABLE III. 3-Dimethylamino-4,1,2-benzoxathiazine 1,1-Dioxides(**7a**—**e**)

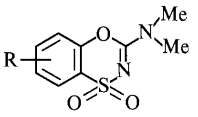

	R	Yield (%)	mp (°C)	Formula	*Anal.* (%) Calcd (Found)		
					C	H	N
7a	H	76	248—250	$C_9H_{10}N_2O_3S$	47.78 (47.40	4.46 4.46	12.38 12.23)
7b	5-Me	30	227—229	$C_{10}H_{12}N_2O_3S$	49.99 (50.31	5.03 5.04	11.66 11.74)
7c	7-Me	57	240—241	$C_{10}H_{12}N_2O_3S$	49.99 (49.95	5.03 4.96	11.66 11.61)
7d	5-Cl	50	239—240	$C_9H_9ClN_2O_3S$	41.47 (41.17	3.48 3.50	10.75 10.65)
7e	7-Cl	68	204—206	$C_9H_9ClN_2O_3S$	41.47 (41.31	3.48 3.48	10.75 10.75)

TABLE IV. Spectral Data for *O*-Phenyl *N*,*N*-Dimethylthiocarbamates (**1a**—**e**)

	IR $\nu_{max}^{CHCl_3}$ cm^{-1} (ν-N···C···S)	^{1}H-NMR ($CDCl_3$) δ (ppm)
1a	1495	3.35 (3H, s), 3.46 (3H, s), 7.04—7.08 (2H, m), 7.22—7.28 (1H, m), 7.36—7.42 (2H, m)
1b	1495	2.20 (3H, s), 3.37 (3H, s), 3.47 (3H, s), 6.99 (1H, d, J=8 Hz), 7.13—7.26 (3H, m)
1c	1500	2.36 (3H, s), 3.34 (3H, s), 3.46 (3H, s), 6.94 (2H, d, J=8 Hz), 7.18 (2H, d, J=8 Hz)
1d	1490	3.39 (3H, s), 3.47 (3H, s), 7.14—7.23 (2H, m), 7.30 (1H, ddd, J=8, 8, 2 Hz), 7.43 (1H, dd, J=8, 2 Hz)
1e	1490	3.34 (3H, s), 3.45 (3H, s), 7.01 (2H, d, J=9 Hz), 7.34 (2H, d, J=9 Hz)

Thus, [2+2] cycloaddition of CSI with **8** with subsequent loss of carbonylsulfide is followed by Friedel–Crafts cyclization of the resulting *N*-chlorosulfonyl isothiourea (Chart 3).

Attempted Synthesis of 3-Dimethylamino-4-methyl-1,2,4-benzothiadiazine 1,1-Dioxide (12) We next turned our attention to the conversion of *N,N*-dimethyl-*N'*-methyl-*N'*-phenylthiourea (**2**) to the corresponding **12** by means of a reaction analogous to those shown in Chart 3. However, the desired product could not be obtained, probably due to the lability of the intermediate 1-methyl-1-phenyl-3,3-dimethyl-2-chlorosulfonylguanidine under the reaction conditions employed.

Synthesis of 3-Dimethylamino-1,4,2-benzodithiazine 1,1-Dioxides (11) In general, **11** have been prepared by cyclization of 2-halogenobenzenesulfonamides with CS_2 followed by alkylation and subsequent treatment of the reaction products with dimethylamine.[8] However, this method is not entirely satisfactory because of the complicated procedure. Moreover, the preparation of the starting 2-halogenobenzenesulfonamide derivatives is somewhat troublesome.[9] Therefore, we became interested in finding a new and facile method for the synthesis of **11**. In a previous paper,[1] we reported the synthesis of C and here tried applying the method to the synthsis of **11**.

As shown in Chart 3, a similar reaction occurred and the desired compounds (**11a—f**) were obtained when we used the corresponding *S*-phenyl *N,N*-dimethyldithiocarbamates (**10a—f**) (Tables VI and VIII) as the starting material instead of the *S*-alkyl *N*-methyl-*N*-phenyldithiocarbamates. The results are summarized in Tables VII and IX. When **10f** was used as the starting material, no 8-methyl

Table V. Spectral Data for 3-Dimethylamino-4,1,2-benzoxathiazine 1,1-Dioxides (**7a—e**)

	IR $\nu_{max}^{CHCl_3}$ cm^{-1}	^{1}H-NMR ($CDCl_3$) δ (ppm)
7a	1160, 1170, 1275, 1635	3.19 (3H, s), 3.22 (3H, s), 7.20 (1H, d, J=8 Hz), 7.40 (1H, dd, J=8, 8 Hz), 7.57 (1H, ddd, J=8, 8, 2 Hz), 7.92 (1H, dd, J=8, 2 Hz)
7b	1155, 1310, 1610, 1635	2.39 (3H, s), 3.20 (3H, s), 3.23 (3H, s), 7.28 (1H, dd, J=8, 8 Hz), 7.41 (1H, d, J=8 Hz), 7.75 (1H, d, J=8 Hz)
7c	1160, 1280, 1310, 1640	2.41 (3H, s), 3.18 (3H, s), 3.20 (3H, s), 7.09 (1H, d, J=9 Hz), 7.35 (1H, dd, J=9, 2 Hz), 7.72 (1H, d, J=2 Hz)
7d	1360, 1375, 1320, 1640	3.21 (3H, s), 3.30 (3H, s), 7.35 (1H, dd, J=8, 8 Hz), 7.62 (1H, dd, J=8, 2 Hz), 7.83 (1H, dd, J=8, 2 Hz)
7e	1170, 1265, 1320, 1640	3.19 (3H, s), 3.21 (3H, s), 7.17 (1H, d, J=9 Hz), 7.52 (1H, dd, J=9, 3 Hz), 7.88 (1H, d, J=3 Hz)

Table VI. *S*-Phenyl *N,N*-Dimethyldithiocarbamates (**10a—f**)

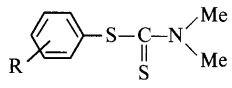

	R	mp (°C)	Formula	*Anal.* (%) Calcd (Found)		
				C	H	N
10a	H	90—91	$C_9H_{11}NS_2$	54.78 (54.62	5.62 5.56	7.10 7.04)
10b	2-Me	78—80	$C_{10}H_{13}NS_2$	56.83 (56.74	6.20 6.20	6.63 6.76)
10c	4-Me	110—112	$C_{10}H_{13}NS_2$	56.83 (56.77	6.20 6.11	6.63 6.68)
10d	2-Cl	100—101	$C_9H_{10}ClNS_2$	46.64 (46.38	4.35 4.37	6.04 6.18)
10e	4-Cl	96—97	$C_9H_{10}ClNS_2$	46.64 (46.56	4.35 4.38	6.04 6.15)
10f	3-Me	Oil	$C_{10}H_{13}NS_2$	56.83 (56.49	6.20 6.39	6.63 6.81)

Table VII. 3-Dimethylamino-1,4,2-benzodithiazine 1,1-Dioxides(**11a—f**)

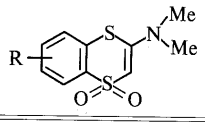

	R	Yield (%)	mp (°C)	Formula	*Anal.* (%) Calcd (Found)		
					C	H	N
11a	H	43	152—154	$C_9H_{10}N_2O_2S_2$	44.61 (44.43	4.16 4.13	11.56 11.54)
11b	5-Me	15	202—203	$C_{10}H_{12}N_2O_2S_2$	46.85 (46.77	4.72 4.69	10.93 10.99)
11c	7-Me	36	196—197	$C_{10}H_{12}N_2O_2S_2$	46.85 (46.70	4.72 4.68	10.93 10.75)
11d	5-Cl	11	139—141	$C_9H_9ClN_2O_2S_2$	39.05 (39.10	3.28 3.39	10.12 10.00)
11e	7-Cl	12	158—161	$C_9H_9ClN_2O_2S_2$	39.05 (38.70	3.28 3.42	10.12 10.24)
11f	6-Me	18	249—250	$C_{10}H_{12}N_2O_2S_2$	46.85 (46.72	4.72 4.74	10.93 10.85)

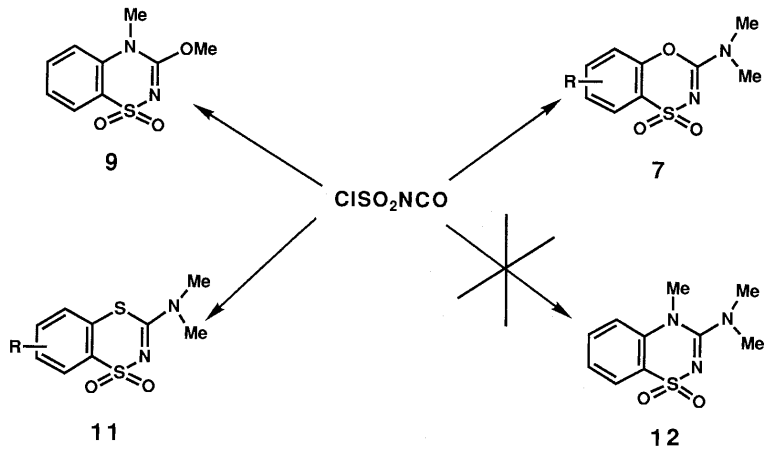

Chart 4

TABLE VIII. Spectral Data for *S*-Phenyl *N*,*N*-Dimethyldithiocarbamates (**10a—f**)

	IR $\nu_{max}^{CHCl_3}$ cm^{-1} (ν-N···C···S)	^{1}H-NMR ($CDCl_3$) δ (ppm)
10a	1500	3.50 (3H, s), 3.56 (3H, s), 7.30—7.60 (5H, m)
10b	1500	2.41 (3H, s), 3.52 (3H, s), 3.56 (3H, s), 7.23—7.44 (4H, m)
10c	1490	2.40 (3H, s), 3.50 (3H, s), 3.56 (3H, s), 7.26 (2H, d, J=7.8 Hz), 7.35 (2H, d, J=7.8 Hz)
10d	1495	3.53 (3H, s), 3.55 (3H, s), 7.31—7.57 (4H, m)
10e	1495	3.50 (3H, s), 3.55 (3H, s), 7.40 (4H, s)
10f	1500	2.39 (3H, s), 3.50 (3H, s), 3.56 (3H, s) 7.26—7.35 (4H, m)

TABLE IX. Spectral Data for 3-Dimethylamino-1,4,2-benzodithiazine 1,1-Dioxides (**11a—f**)

	IR $\nu_{max}^{CHCl_3}$ cm^{-1}	^{1}H-NMR ($CDCl_3$) δ (ppm)
11a	860, 1165, 1315, 1565, 1575	3.30 (3H, s), 3.33 (3H, s), 7.41—7.58 (3H, m), 8.12—8.18 (1H, m)
11b	860, 955, 1135, 1310, 1565	2.46 (3H, s), 3.34 (6H, s), 7.38—7.48 (2H, m), 8.05 (1H, dd, J=6.8, 2.0 Hz)
11c	860, 955, 1155, 1315, 1570	2.44 (3H, s), 3.29 (3H, s), 3.33 (3H, s), 7.33 (2H, s), 7.98 (1H, s)
11d	860, 950, 1165, 1315, 1570	3.36 (6H, s), 7.50 (1H, dd, J=7.8, 6.8 Hz), 7.61 (1H, d, J=6.8 Hz), 8.10 (1H, d, J=7.8 Hz)
11e	855, 950, 1160, 1310, 1560	3.30 (3H, s), 3.35 (3H, s), 7.39 (1H, d, J=8.8 Hz), 7.50 (1H, dd, J=8.8, 2.0 Hz), 8.15 (1H, d, J=2.0 Hz)
11f	860, 1115, 1165, 1315, 1565	2.43 (3H, s), 3.29 (3H, s), 3.31 (3H, s), 7.24 (1H, s), 7.33 (1H, d, J=7.8 Hz), 8.03 (1H, d, J=7.8 Hz)

congener was obtained, probably because of the steric hindrance of the methyl group.

Biological Results Some 1,4,2-benzodithiazine 1,1-dioxide derivatives have been reported to show fungicidal activity.[8] Thus, fungicidal activity testing of **11a—e** was carried out. From the viewpoint of molecular modification based on the concept of bioisosterism,[10] we also tested the fungicidal activity of **7a—e**, which can be viewed as bioisosteres of **11**. Contrary to our expectation, none of the compounds tested showed significant activity.

Conclusion We have newly developed practical and convenient synthetic methods for the title compounds by utilizing the novel [2+2] cycloaddition reaction of CSI with thiocarbamate or dithiocarbamate derivatives. Since CSI is commercially available and the starting thiocarbamate or dithiocarbamate derivatives are easy to prepare, the present method should be useful for the synthesis of heterocyclic compounds which bear the sulfonamide moiety.

Experimental

All melting points were determined on a Yanagimoto micro melting point apparatus and are uncorrected. IR spectra were recorded with a Hitachi 260-10 spectrometer. ^{1}H-NMR spectra were determined with a JEOL JNM-PMX 60 or JEOL JNM-GSX 270 spectrometer, and δ values are quoted relative to tetramethylsilane. The following abbreviations are used: s=singlet, d=doublet, t=triplet, q=quartet, m=multiplet, br=broad, dd=double doublet, ddd=double double doublet.

General Procedure for Preparation of Thiocarbamates (1a—e) NaH (60%, 64 mmol) was added in portions to a solution of phenol (53 mmol) in dry dimethylformamide (DMF) (50 ml) with stirring below 15 °C. Then, the reaction mixture was stirred at room temperature for 1 h, and dimethylthiocarbamoyl chloride (53 mmol) was added at 0 °C. After further stirring for 2 h at room temperature, the mixture was poured onto ice and extracted with ether. The ethereal solution was washed with brine, then dried over Na_2SO_4. The solvent was removed under reduced pressure and the residue was purified by silica gel chromatography (hexane–CH_2Cl_2, 2:1).

***N*,*N*-Dimethyl-*N'*-methyl-*N'*-phenylthiourea (2)** *N*-Methylaniline (18.7 mmol) and Et_3N (18.7 mmol) were added to a solution of dimethylthiocarbamoyl chloride (18.7 mmol) in toluene. Then the toluene solution was refluxed for 18 h and treated with water. The mixture was extracted with AcOEt. The organic layer was washed with brine, then dried over Na_2SO_4. The solution was concentrated under reduced pressure and the residue was subjected to column chromatography on silica gel with hexane–CH_2Cl_2 (2:3) as an eluent to give **2** (2.9 g, 81% yield). Oil. IR $\nu_{max}^{CHCl_3}$ cm^{-1}: 1495, 1385, 1340, 1325, 1100. ^{1}H-NMR ($CDCl_3$) δ: 3.01 (6H, s), 3.54 (3H, s), 7.03 (2H, d, J=8 Hz), 7.12 (1H, dd, J=8, 8 Hz), 7.34 (2H, dd, J=8, 8 Hz). *Anal.* Calcd for $C_{10}H_{14}N_2S$: C, 61.82; H, 7.26; N, 14.42. Found: C, 61.81; H, 7.26; N, 14.57.

***O*-Phenyl-*N*,*N'*-dimethylcarbamate (3)** NaH (60%, 24.3 mmol) was added to a solution of phenol (18.7 mmol) in DMF, and the mixture was stirred for 15 min at room temperature. Then dimethylcarbamoyl chloride (18.7 mmol) was added and the whole mixture was stirred for 30 min at room temperature and treated with ice. The mixture was extracted with ether. The organic layer was washed with brine, then dried over Na_2SO_4. The solution was concentrated under reduced pressure and the residue was chromatographed on silica gel with hexane–CH_2Cl_2 (1:1) as an eluent to give **3** (2.3 g, 74% yield). Oil. IR $\nu_{max}^{CHCl_3}$ cm^{-1}: 1710, 1490, 1390, 1170. ^{1}H-NMR ($CDCl_3$) δ: 3.00 (3H, s), 3.09 (3H, s), 7.11 (2H, d, J=8, 8 Hz), 7.18 (1H, dd, J=8, 8 Hz), 7.35 (2H, dd, J=8, 8 Hz). *Anal.* Calcd for $C_9H_{11}NO_2$: C, 65.44; H, 6.71; N, 8.48. Found: C, 65.41; H, 6.81; N, 8.48.

***N*,*N*-Dimethyl-*N'*-methyl-*N'*-phenylurea (4)** The same procedure as described for the preparation of 2 was employed. Yield 95%. Oil. IR $\nu_{max}^{CHCl_3}$ cm^{-1}: 1630, 1595, 1490, 1380, 1130. ^{1}H-NMR ($CDCl_3$) δ: 2.69 (6H, s), 3.22 (3H, s), 7.02—7.13 (3H, m), 7.32 (2H, dd, J=8, 8 Hz). *Anal.* Calcd for $C_{10}H_{14}N_2O$: C, 67.39; H, 7.92; N, 15.72. Found: C, 67.00; H, 7.93; N, 15.38.

1,1-Dimethyl-2-phenyl-3-toluenesulfonylisourea (5) mp 80—82 °C. IR $\nu_{max}^{CHCl_3}$ cm^{-1}: 1610, 1440, 1150, 1095. ^{1}H-NMR ($CDCl_3$) δ: 2.34 (3H, s), 3.05 (6H, br s), 6.87 (2H, d, J=8 Hz), 7.05—7.15 (3H, m), 7.26 (2H, dd, J=8, 8 Hz), 7.63 (2H, d, J=8 Hz). *Anal.* Calcd for $C_{16}H_{18}N_2O_3S$: C, 60.36; H, 5.70; N, 8.80. Found: C, 60.25; H, 5.68; N, 8.91.

1,1-Dimethyl-3-phenyl-2-toluenesulfonylguanidine (6) mp 120—121 °C. IR $\nu_{max}^{CHCl_3}$ cm^{-1}: 1555, 1490, 1395, 1145, 1085. ^{1}H-NMR ($CDCl_3$) δ: 2.39 (3H, s), 2.79 (6H, s), 3.31 (3H, s), 6.95 (2H, d, J=9 Hz), 7.09 (1H, dd, J=8, 8 Hz), 7.23 (2H, d, J=8 Hz), 7.31 (2H, dd, J=8, 8 Hz), 7.82 (2H, d, J=9 Hz). *Anal.* Calcd for $C_{17}H_{21}N_3O_2S$: C, 61.61; H, 6.39; N, 12.68. Found: C, 61.32; H, 6.20; N, 12.43.

General Procedure for Preparation of 3-Dimethylamino-4,1,2-benzoxathiazine 1,1-Dioxides (7a—e) Chlorosulfonyl isocyanate (7.2 mmol) was added dropwise to an ice-cooled solution of thiocarbamate (5.5 mmol) in CH_2Cl_2. The mixture was stirred at room temperature for 30 min. After removal of the solvent, the residue was dissolved in nitromethane (10 ml), then anhydrous aluminum chloride (8.3 mmol) was added. The reaction mixture was stirred at room temperature for 2 h, cooled, diluted with water and extracted with CH_2Cl_2. The extract was washed with brine, then dried. The solvent was removed under reduced pressure and the residue was crystallized from CH_2ClCH_2Cl.

***O*-Methyl *N*-Methyl-*N*-phenylthiocarbamate (8)** NaOMe (28%, 8.7 mmol) was added to a solution of thiophosgene (13 mmol) in dry tetrahydrofuran (THF) (10 ml) in portions with stirring below −45 °C. Then, the reaction mixture was stirred at −45 °C for 10 min, and *N*-methylaniline (8.7 mmol) was added at −45 °C. The mixture was stirred for 30 min below 0 °C, poured into water and extracted with CH_2Cl_2. The organic layer was dried over Na_2SO_4. The solvent was removed under reduced pressure and the residue was subjected to column chromatography on silica gel silica gel with hexane–CH_2Cl_2 (3:1) as an eluent to give **8** (200 mg, 13% yield). Oil. IR $\nu_{max}^{CHCl_3}$ cm^{-1}: 1500, 1480, 1450, 1390, 1295. ^{1}H-NMR ($CDCl_3$) δ: 3.61 (3H, br s), 3.95 (3H, br s), 7.05—7.52 (5H, m). *Anal.* Calcd for $C_9H_{11}NOS$: C, 59.64; H, 6.12; N, 7.73. Found: C, 59.79; H, 6.18; N, 7.76.

3-Methoxy-4-methyl-1,2,4-benzothiadiazine 1,1-Dioxide (9) Chlorosulfonyl isocyanate (1.3 mmol) was added dropwise to an ice-cooled solution of the thiocarbamate (**8**) (0.9 mmol) in dry CH_2Cl_2 (4 ml). The mixture was stirred at room temperature for 40 min. After removal of the solvent, the residue was dissolved in nitromethane (4 ml), then anhydrous

aluminum chloride (1.1 mmol) was added. The reaction mixture was stirred at room temperature for 12 h, diluted with water and extracted with CH_2Cl_2. The extract was washed with brine, then dried. The solvent was removed under reduced pressure and the residue was subjected to column chromatography on silica gel with hexane–AcOEt (2 : 1) as an eluent to give **9** (150 mg, 75% yield). mp 202—204 °C (lit[11] mp 200—202 °C). IR $\nu_{max}^{CHCl_3}$ cm^{-1}: 1615, 1460, 1385, 1310, 1170. ^{1}H-NMR ($CDCl_3$) δ:3.55 (3H, s), 4.08 (3H, s), 7.26 (1H, d, J=8 Hz), 7.41 (1H, dd, J=8, 8 Hz), 7.64 (1H, dd, J=8, 8 Hz), 8.01 (1H, d, J=8 Hz). *Anal.* Calcd for $C_9H_{10}N_2O_3S$: C, 47.78; H, 4.46; N, 12.38. Found: C, 47. 64; H, 4.43; N, 12.34.

General Procedure for Preparation of Dithiocarbamates (10a—f) A mixture of a thiophenol (36.3 mmol), dimethylthiocarbamoyl chloride (48.5 mmol), potassium *tert*-butoxide (43.7 mmol) and DMF (40 ml) was stirred at room temperature for 20 min and then at 90 °C for 30 min. The reaction mixture was diluted with water and extracted with ether. The ethereal solution was washed with saturated brine, then dried. The solvent was removed under reduced pressure and the residue was purified by silica gel chromatography (hexane : CH_2Cl_2 = 2 : 1), followed by recrystallization (hexane–AcOEt).

General Procedure for Preparation of 3-(*N*,*N*-Dimethylamino)-1,4,2-benzodithiazine 1,1-Dioxides (11a—f) Chlorosulfonyl isocyanate (6.1 mmol) was added dropwise to a solution of dithiocarbamate (5.1 mmol) in toluene (10 mmol). The mixture was stirred at 100 °C for 20 min. After removal of the solvent, the residue was dissolved in nitromethane (10 ml), then anhydrous aluminum chloride (5.6 mmol) was added all at once. The reaction mixture was stirred at 100 °C for 20 min, cooled, diluted with water and extracted with CH_2Cl_2.

The extract was washed with saturated brine, then dried. The solvent was removed under reduced pressure and the residue was purified by silica gel chromatography (CH_2Cl_2 : AcOEt = 9 : 1).

Acknowledgement We wish to express our thanks to Dr. Yoshiyuki Hayashi, Director of the Aburahi Laboratories of Shionogi & Co., Ltd., for his encouragement and permission to publish this work.

References and Notes

1) Part III: T. Iwakawa, H. Tamura and Y. Hayase, *Chem. Pharm. Bull.*, **38**, 1075 (1990).
2) Part I: T. Iwakawa, H. Tamura, T. Sato and Y. Hayase, *Chem. Pharm. Bull.*, **36**, 4755 (1988).
3) Part II: H. Tamura, T. Iwakawa and Y. Hayase, *Chem. Pharm. Bull.*, **38**, 1069 (1990).
4) C. King, *J. Org. Chem.*, **25**, 352 (1960); G. Kresze and R. Albrecht, *Angew. Chem.*, **74**, 781 (1962); R. Albrecht, G. Kresze and B. Mlakar, *Chem. Ber.*, **97**, 483 (1964); H. Ulrich, B. Tucker and A. A. R. Sayigh, *Angew. Chem., Int. Ed. Engl.*, **7**, 291 (1968); E. Schaumann, E. Kausch and J. P. Imbert, *Chem. Ber.*, **111**, 1475 (1978); D. Ndhar and A. Kbag, *Indian J. Chem.*, **22B**, 627 (1983); M. Baillarge and F. L. Goffic, *Synth. Commun.*, **17**, 1603 (1987); K. R. Rao, Y. V. D. Nageswar, T. N. Srinivasan and P. B. Sattur, *ibid.*, **18**, 877 (1988).
5) S. Suzue and T. Irikura, *Chem. Pharm. Bull.*, **16**, 806 (1968).
6) H. Tilles, *J. Am. Chem. Soc.*, **81**, 714 (1959).
7) M. A. Martinez and J. C. Vega, *Synthesis*, **1986**, 760.
8) N. Wada, M. Nezu, M. Hirata and K. Motojima, Japan. Patent Kokai 62-190178 (1978) [*Chem. Abstr.*, **108**, 167508*g* (1988)].
9) A. Marei, M. M. A. El-Sukkary, F. I. El-Dib and O. H. El-Sayed, *Hung. J. Ind. Chem.*, **9**, 427 (1981); Y. Muramoto and H. Asakura, *Nippon Kagaku Kaishi*, **1975**, 1070.
10) C. W. Thornber, *Chem. Soc. Rev.*, **1979**, 563.
11) M. Di Bella and A. Albasini, *Farmaco Ed. Sci.*, **21**, 631 (1966) [*Chem. Abstr.*, **66**, 28749*n* (1967)].

Chem. Pharm. Bull. **39**(8) 1944—1948 (1991) Vol. 39, No. 8

Degradation of Some Phthalideisoquinolines with Ethyl Chloroformate-Stereochemical Aspects

Dong-Ung LEE,*[,a] Kinuko IWASA,[b] Miyoko KAMIGAUCHI,[b] Narao TAKAO,[b] and Wolfgang WIEGREBE[c]

College of Natural Science, Dongguk University,[a] Kyongju, Kyongbuk 780–714, Korea, Kobe Women's College of Pharmacy,[b] Kobe 658, Japan, and Faculty of Chemistry and Pharmacy, University of Regensburg,[c] D-8400 Regensburg, Germany. *Received January 18, 1991*

Treatment of phthalideisoquinolines such as α- (1) and β-narcotine (2) as well as β- (3) and α-hydrastine (4) with ethyl chloroformate (ECF) at room temperature afforded, *via* the chloro-carbamates, the corresponding diastereomeric carbinols with high stereoselectivity. Instrumental analyses of each diastereomeric pair indicate that the major isomers derived from α- and β-narcotine as well as from α- and β-hydrastine are enantiomers of each other. The absolute configuration of the major carbinol 6a from α-narcotine (1) was determined by X-ray analysis. The probable difference between the reaction course of α- and β-narcotine is discussed. On the other hand, treatment of α-narcotine with ECF under reflux furnished *Z*-(8) and *E*-(9) enol lactones, while only the *Z*-isomer 12 could be isolated from the degradation of β-hydrastine (3) even at room temperature.

Keywords α-narcotine; β-narcotine; α-hydrastine; β-hydrastine; ethyl chloroformate; diastereoselectivity; enantiomer; diastereomeric carbinol; enol lactone; X-ray analysis; absolute configuration

Phthalideisoquinolines such as (−)-α-narcotine (**1**), (−)-β-narcotine (**2**), (−)-β-hydrastine (**3**), and (−)-α-hydrastine (**4**) possess two asymmetric centers: at C-1 of the tetrahydroisoquinoline nucleus and at C-9 of the γ-lactone ring (Charts 1 and 4). The ring cleavage of one or both cyclic systems in the above phthalideisoquinolines has been accomplished by various methods, *e.g.* Hofmann degradation,[1,2] or using benzyl bromide,[3] *m*-chloroperoxybenzoic acid,[4] or phenyl chloroformates,[5,6] to furnish the corresponding enol lactones (stilbenes) or keto acids. Some of these ring-cleaved phthalideisoquinolines are known to be present in nature as secophthalideisoquinolines.[7] This paper deals with the reactions of α- and β-narcotine as well as α- and β-hydrastine with ethyl chloroformate (ECF).

A. Degradation of α- and β-Narcotine with Ethyl Chloroformate When (−)-α-narcotine (**1**) was treated with ECF at room temperature, the chloro-carbamate **5** was obtained as a colorless crystalline material, which, however, could not be completely purified (Chart 1). Benzyl chlorides

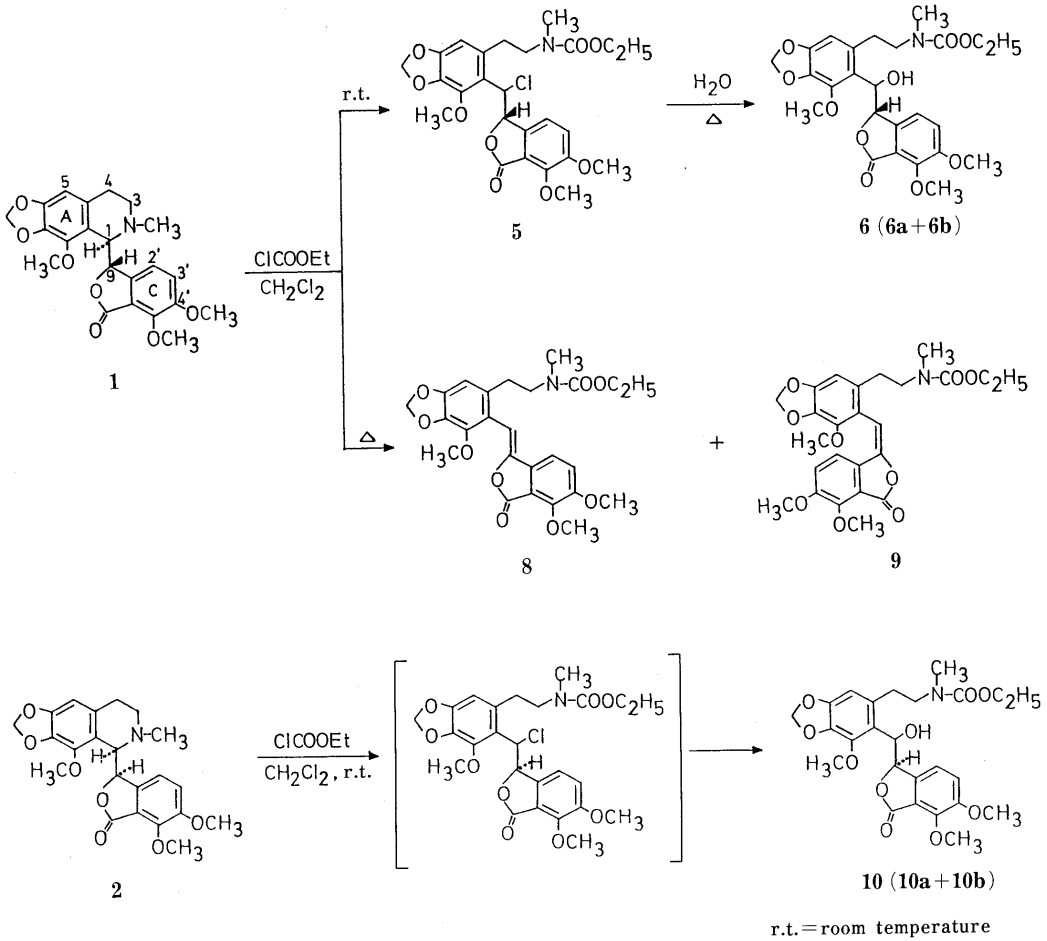

Chart 1

similar to **5** are generally known to be unstable, although a species of this type could be isolated by using special reaction conditions and work-up techniques.[8] Compound **5** was found to be contaminated with a small amount of **6a**, the main diastereomer of the carbinol **6**, as indicated by the doublet of H-3′ at 7.04 ppm, though its field disorption (FD)- and chemical ionization-mass spectrum (CI-MS) did not show peaks due to **6**. On account of the lability of the chloro-carbamate **5** (see below), we can not obtain data indicating the stereochemistry at C-1 of **5**. With the exception of the signals due to the carbinols **6a** and **6b**, (H-3′ at $\delta = 7.54$ ppm), there are no signals in the proton-nuclear magnetic resonance (^{1}H-NMR) spectrum of **5** pointing to the presence of a diastereomer. Nevertheless, the questions of the absolute configuration and stereochemical purity of **5** remain open. The same holds true for the chloro-carbamate **13** obtained from β-hydrastine **3** (see below).

When we tried to purify the chloro-carbamate **5** by column chromatography, a mixture of **5** and carbinol **6** (1 : 1) was obtained. Besides **6a**, the diastereomeric carbinol **6b** was formed in a trace amount (H-3′-doublet at $\delta = 7.54$ ppm). These assignments were established by spiking the mixtures with authentic compounds.

The crude chloro-carbamate **5** containing a small amount of **6a** was refluxed with water to yield **6a** and in a ratio of approximately 13 : 1 (^{1}H-NMR). This means that the conversion of α-narcotine (**1**) with ECF into the carbinol **6** *via* the chloro-carbamate **5** is highly stereoselective; therefore **6a** (major diastereomer) could be separated by chromatographic methods, showing an optical activity of $[\alpha]_D$ −44°.

On the other hand, when (−)-β-narcotine (**2**) was converted into the corresponding carbinol **10** under the conditions used for α-narcotine (**1**), the diastereomer ratio was approximately 5 : 1 for **10a** and **10b** (Chart 1). Furthermore, the optical activity of **10a** exhibits an opposite value ($[\alpha]_D$ +44°) to that of **6a** ($[\alpha]_D$ −44°), though its ^{1}H-NMR and other instrumental data are identical with those of **6a**, indicating that **6a** and **10a** are enantiomers of each other. These results point toward different stereochemical courses in the degradation of α- and β-narcotine with ECF, because the absolute configurations of α- and β-narcotine are known to be 1*R*,9*S* and 1*R*,9*R* respectively,[9,10] that is, the stereochemistry at C-1 in both narcotine diastereomers is the same.

The absolute configuration of **6a** was established by X-ray analysis. The crystal structure is presented in Fig. 1.

This X-ray determination indicates that the conformation of **6a** is *threo*. Therefore, the absolute configuration of **6a** is 1*S*,9*S*, because the absolute configuration of α-narcotine (**1**) is 1*R*,9*S* and the 9*S* configuration is not affected during the reaction. This result apparently proves an inversion in the overall two-step process **1**→**5**→**6a**. Because **6a** from α-narcotine (**1**) and **10a** from β-narcotine (**2**) are enantiomers of each other, the absolute configuration of **10a** corresponds to 1*R*,9*R*, which is identical with that of the starting material, β-narcotine. This fact indicates that the overall reaction includes a retention of configuration.

As already stated (see above) we cannot determine the absolute configuration of the chloro-carbamate **5**. Therefore, we cannot make definite statements concerning the reaction mechanism: a carbenium ion intermediate, substituted by Cl^- or water (with deprotonation), controlled by the non-affected center of chirality at C-9 (asymmetric induction) may produce the chloro-carbamate **5** and the carbinol **6**.

The high diastereoselectivity in the two-step reactions of α-narcotine (**1**) and β-narcotine (**2**) to give the carbinols **6** and **10**, respectively, points at least towards a partition of S_N2 reactions. This also holds true for the reactions of α- and β-hydrastine, **4** and **3**, resectively (see below).

Having ascertained the structure and stereochemistry of the carbinol **6a** and, therefore, of its enantiomer **10a**, we

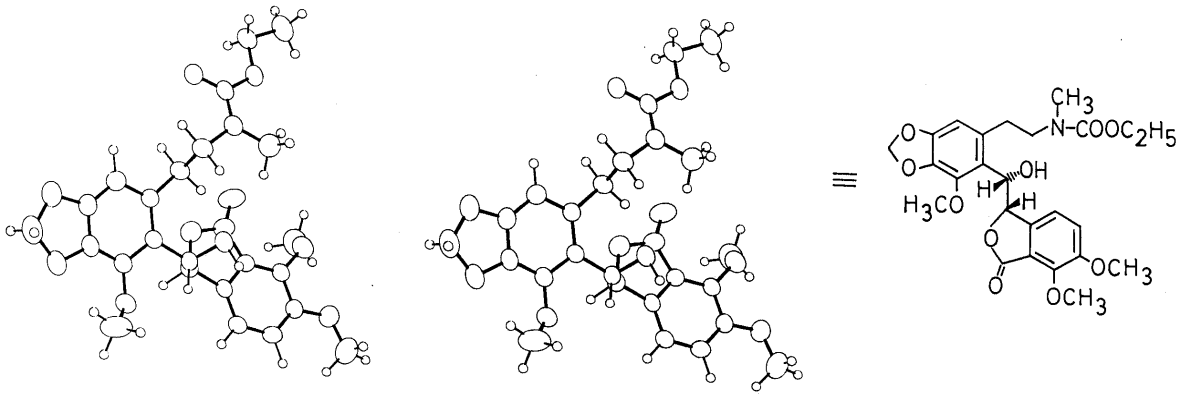

Fig. 1. Stereoscopic View of (1*S*,9*S*)-**6a**

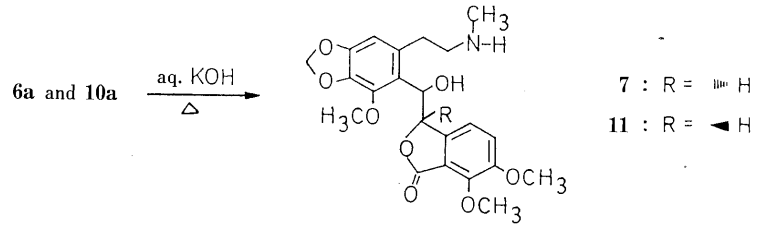

Chart 2

hydrolyzed **6a** and **10a** to the corresponding enantiomeric amines **7** and **11**. When α-narcotine (**1**) was treated with ECF under reflux, not at room temperature, two isomers *Z*-(**8**, 70%), which is thermodynamically more stable, and *E*-lactone (**9**, 4%) were produced (Chart 1). The stereochemistry of **8** and **9** could easily be confirmed by comparison with that of similar *E*/*Z*-isomers whose configurations have been established by nuclear magnetic resonance (NMR)[2] or by X-ray analysis.[5] Shamma and coworkers[2] did not obtain any enol lactone, but obtained the keto acid narceine (**16**) from mild Hofmann degradation (basic conditions) of α-narcotine. They suggested that hydrolysis of an intermediate enol lactone (CH_3 instead of $COOC_2H_5$ in **8**) must occur with great ease. This may, in our case, explain why an analogous keto acid was not formed in our ethyl chloroformate degradation (non-basic conditions) either at room temperature or under reflux conditions (*vide supra*).

The reason why α-narcotine does not form *E*/*Z*-isomers at room temperature may be the steric effect of its C-8 methoxy group, which prevents an anti-periplanar arrangement suitable for easy HCl elimination. In addition, the carbon-13 nuclear magnetic resonance (^{13}C-NMR) spectrum (Table II) of *E*-isomer **9** is contaminated with signals of the *Z*-isomer **8**, this may result from partial isomerization under the measuring conditions (50 °C for 5 h in $CDCl_3$).

Photoisomerization, as is usual in similar stilbenes,[11] was excluded. Moreover, oily **9** crystallized even upon grinding without any contact with solvent, being converted into crystalline **8**. The chemical shifts for H-2′ and H-3′ of the *Z*- (**8**) and *E*-isomer (**9**) are apparently different from each other (Table I). The H-2′ an H-3′ doublets (J=8 Hz) of the *E*-isomer **9** appear more upfield (δ=6.66 and 7.07 ppm) than those of the *Z*-isomer **8** (δ=7.49 and 7.28 ppm), since H-2′ and H-3′ in the *E*-isomer **9** are closer to the shielding zone of the aromatic ring A than the same protons in the *Z*-isomer **8**. The mass spectra of the enol lactones **8** and **9** are not identical. The fragment peaks at m/z=278, 250 and 206, respectively, in the spectrum of the *E*-isomer **9** are not found in that of the *Z*-isomer **8**. For this fragmentation, a direct bond cleavage at the aromatic ring after two 1,5-H-shifts may be suggested (Chart 3) (for fission of the double bond after electron impact in similar stilbenes, see ref. 12).

B. Degradation of α- and β-Hydrastine with Ethyl Chloroformate Degradation of (−)-β-hydrastine (**3**) and (−)-α-hydrastine (**4**) with ECF is somewhat different from that of α-narcotine (**1**) under the same conditions. When β-hydrastine (**3**) was treated with ECF at room temperature as described for **1** to **6**, the product mixture consists of three components on thin layer chromatography (TLC) (Chart 4).

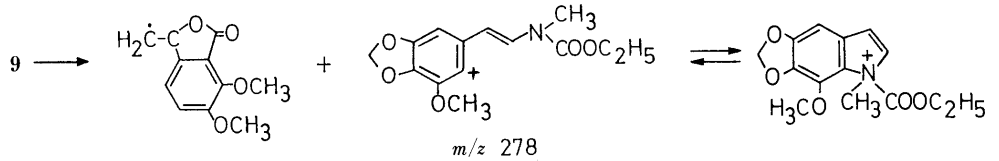

Chart 3

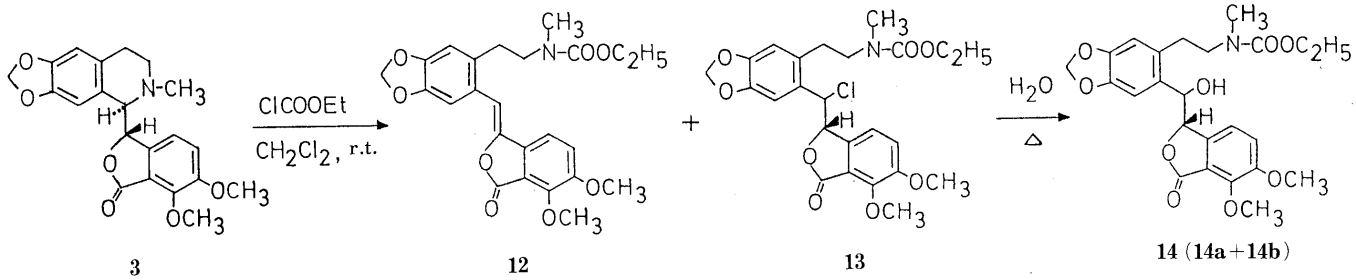

3 **12** **13** **14 (14a+14b)**

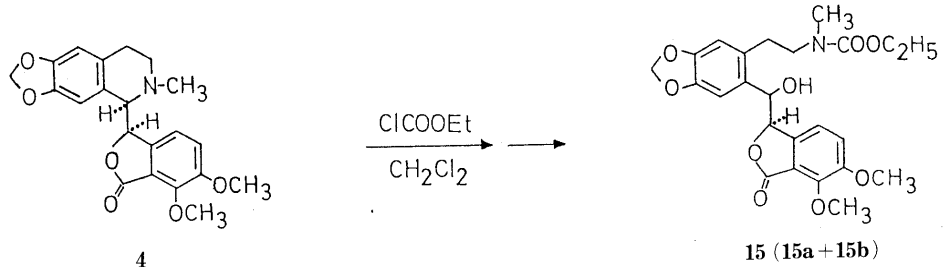

4 **15 (15a+15b)**

Chart 4

TABLE I. ^{1}H-NMR Chemical Shifts for Carbinols and Enol Lactones[a]

	8	9	6a, 10a	7, 11[b]	10b	12	14b, 15b	14a, 15a
$-CH_2-C\underline{H}_3$	1.15[c]	1.22[c]	1.23[c]	—	1.22[c]	1.22[c]	1.11[c]	1.18[c]
$N-CH_3$	2.76	2.78	2.79	2.27	2.82	2.89	2.86	2.79
$-CH_2-$	2.79[c]	2.72[c]	2.44—2.72[d]	2.54—2.67[d]	2.57—2.88[d]	2.94[c]	2.61—2.80[d]	2.58[c]
$-CH_2-N$	3.39[c]	3.30[c]	2.88—3.40[d]	2.94—3.15[d]	3.22—3.46[d]	3.43[c]	3.15—3.40[d]	3.27[c]
$-C\underline{H}_2-CH_3$	3.98[e]	4.10[e]	4.12[e]	—	4.06—4.24[f]	4.16[e]	4.00[e]	4.08[e]
$3\times OCH_3$	3.94	3.88	3.85	3.87	3.96	3.97	3.92	3.86
	4.14	4.14	4.04	4.01	4.12	4.18	4.09	4.06
	4.01	3.89	4.08	4.11	4.18	—	—	—
$-OCH_2O-$	5.93	6.01	6.02, 6.04[g]	5.97	5.96, 5.98[g]	6.00	5.97	5.98
H-1	6.36	6.44	4.82[h]	5.15[i]	4.74[j]	6.66[h]	4.96[i]	5.05[j]
H-9	—	—	5.86[i]	5.72[i]	5.70[i]	—	5.44[i]	5.48[i]
H-5	6.48	6.57	6.43	6.45	6.41	6.72	6.64	6.66
H-2′	7.49[i]	6.66[i]	6.36[h]	6.51[i]	7.25[i,k]	7.77[h,k]	7.23[h,k]	6.43[h]
H-3′	7.28[i]	7.07[i]	7.04[i]	7.07[i]	7.51[i,k]	7.32[i]	7.22[h,k]	7.06[i]
H-8	—	—	—	—	—	7.73[h,k]	7.07	7.04

a) At 200 MHz, 50 °C, $CDCl_3$, δ = ppm. Some chemical shifts were assigned by using 2D-NMR (COSY and HETCOR). *b*) Chemical shifts for OH and NH protons of **11**: 3.24 ppm (OH + NH, br, recorded at 25 °C). *c*) Triplet, J = 7.0 Hz. *d*) Multiplet. *e*) Quartet, J = 7.0 Hz. *f*) Hidden in OCH_3 protons. *g*) AB, J = 1.3—1.5 Hz. *h*) Broad singlet. *i*) Doublet, J = 8.0 Hz. *j*) Triplet, J = 7.0 Hz; doublet (J = 8.0 Hz) after D_2O exchange. *k*) Assignments may be reversed.

TABLE II. ^{13}C-NMR Chemical Shifts for CH Carbons for Carbinols and Enol Lactones

	6a	8	9	10b	12	14a	14b
C-1	73.4	99.6	103.1	72.7	101.6	72.2	71.1
C-5	105.3	104.1	104.1	105.3	110.4	108.0	107.4
C-8	—	—	—	—	110.0	110.0	110.1
C-9	82.5	—	—	80.3	—	83.0	81.4
C-2′	117.8	115.2	118.2[a]	118.3[a]	115.4	118.0[a]	118.9[a]
C-3′	119.3	120.3	119.7[a]	119.9[a]	120.6	119.4[a]	119.6[a]

a) Assignments may be reversed.

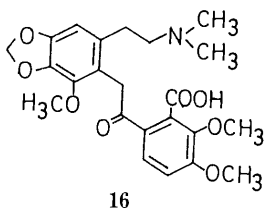

16

a) The upper fluorescent component shows characteristic absorptions with high intensity and long wavelength in its ultraviolet (UV) spectrum: λ_{max} nm ($\log\varepsilon$) = 227 (4.27), 240 (sh), 307 (4.09), 378 (4.22). It follows that this compound must have the *Z* geometry, which is identical with that of natural *N*-methylhydrastine [CH_3 instead of $COOC_2H_5$ in **12**, λ_{max} nm ($\log\varepsilon$) = 228 (4.33), 240 (sh, 4.22), 301 (4.09), 380 (4.23)], so confirming the structure of the enol lactone **12**. Enol lactones (*E*/*Z*-isomers) were derived from *β*-hydrastine (**3**) by various methods; among them, the mild Hofmann degradation of **3** affords both *Z*- and *E*-enol lactones.[2] However, other authors[5] using phenyl chloroformate under reflux did not mention the *E*-isomer. We also could not isolate the *E*-isomer from ethyl chloroformate degradation of **3**, but obtained the *Z*-isomer only. b) The main fraction on TLC was separated and identified as a chloro-carbamate **13** (see Experimental). c) The minor component on TLC was found to be the carbinol **14**. The above crude reaction mixture containing **12**, **13**, and **14** was heated with water to yield the corresponding diastereomeric carbinols **14a** and **14b** in a ratio of approximately 3 : 1. This is very different from the ratio of 13 : 1 for **6a** and **6b** derived from *α*-narcotine (**1**). Considering the same absolute configurations (1*R*,9*S*) of *α*-narcotine (**1**) and *β*-hydrastine (**3**), this drastic difference in stereoselectivity may stem from the C-8 methoxy group in *α*-narcotine, which is absent in *β*-hydrastine. Whaley and Meadow[13] reported that the action of ECF upon hydrastine under Schotten–Baumann conditions afforded meconine and *N*-carbethoxyhydrastinine. Similarly, meconine and *N*-carbethoxycotarnine were formed from narcotine.[13] Finally, the conversion of *α*-hydrastine (**4**) afforded **15a** and **15b** in a ratio of approximately 2 : 1. This result is also significantly different from the ratio of 5 : 1 for **10a** and **10b** derived from *β*-narcotine, whose absolute configuration is identical with that of *α*-hydrastine.[9] Several instrumental analyses also proved **14a** and **15a** as well as **14b** and **15b** to be enantiomers of each other.

Experimental

Melting points were taken on a Kofler hot stage apparatus, and are uncorrected. Infrared (IR) spectra were recorded on an EPI-G2 (Hitachi) spectrophotometer. ^{1}H- and ^{13}C-NMR spectra were obtained on Varian XL-200 (200 MHz) and VXR-500S (500 MHz) spectrometers in $CDCl_3$ solution with tetramethylsilane (TMS) as an internal standard. Mass spectra were determined on a Hitachi M80 instrument at 75 eV. The chemical ionization mass spectra were obtained by using isobutane as the ionizing gas. Optical rotations were measured using a DIP-SL (Jasco) polarimeter. Circular dichroism (CD) and UV spectra were determined on a Jasco ORD/UV-5 spectrometer. Microanalyses were performed by the Microanalytical Laboratory in Kobe Women's College of Pharmacy, Japan. TLC and preparative TLC were done on Silicagel 60F-254 glass plates.

(−)-3-{[2-(*β*-*N*-Ethoxycarbonyl-*N*-methylaminoethyl)-6-methoxy-4,5-methylenedioxyphenyl]chloromethyl}-6,7-dimethoxy-1(3*H*)-isobenzofuranone (5) *α*-Narcotine (**1**), (0.41 g, 1 mmol) in anhydrous dichloromethane (2 ml) was stirred with fresh ECF (0.4 ml, 4 mmol) at room temperature for 5 h. Thorough removal of the solvent and the excess ECF gave **5** as a colorless crystalline material, which was not further purified. $[\alpha]_D^{25}$ −26° ($CHCl_3$). IR (Nujol): 1700, 1765 (CO) cm^{-1}. ^{1}H-NMR (signals of **6** are omitted, 200 MHz at 50 °C) δ: 1.26 (t, J = 7.0 Hz, 3H, $-CH_2-C\underline{H}_3$), 2.32—3.38 (m, 4H, $-CH_2-$), 2.76 and 2.80 (2 × s, 3H, $-NCH_3$), 3.84, 4.10 and 4.12 (3 × s, 9H, $-OCH_3$), 4.14 (q, J = 7.0 Hz, 2H, $-C\underline{H}_2-CH_3$), 5.02 (br s, 1H, –CH–Cl), 6.02, 6.06 (AB, J = 1.3 Hz, 2H, $-OCH_2O-$), 6.14 (d, J = 8.0 Hz, 1H, –CH–O–), 6.34 (d, J = 8.0 Hz, 1H,

aromatic), 6.44 (s, 1H, aromatic), 6.96 (d, J=8.0 Hz, 1H, aromatic). MS m/z (relative intensity, %): 382 (69), 338 (29), 328 (21), 310 (26), 292 (29), 236 (30), 220 (100), 193 (27), 179 (22), 116 (60). FD-MS m/z: 521 ($M^+\cdot$), 485 (M−HCl). CI-MS m/z: 522 (M+1).

(−)-3-{[2-(β-*N*-Ethoxycarbonyl-*N*-methylaminoethyl)-6-methoxy-4,5-methylenedioxyphenyl]hydroxymethyl}-6,7-dimethoxy-1(3*H*)-isobenzofuranone (6a and 10b) and (+)-(10a) α-Narcotine (**1**) or β-narcotine (**2**)[10] (4.13 g, 0.01 mol) was dissolved in dichloromethane (10 ml) and stirred with ECF (4 ml, 0.04 mol) at room temperature for 5 h. The solvent and the excess ECF were thoroughly removed to give the crude products, which were refluxed with water for 5 h, then cooled reaction mixture was extracted with dichloromethane. Removal of the solvent gave the diastereomeric carbinol **6** or **10**, respectively. Preparative TLC with chloroform–ether (1 : 1) provided **6a** from **1**, and **10a** and **10b** from **2**. Compound **6b** could not be obtained in a sufficient amount for analyses. **6a**: mp 98—99 °C, $[\alpha]_D^{25}$ −44° (c=1.0, $CHCl_3$). *Anal.* Calcd for $C_{25}H_{29}NO_{10}$: C, 59.62; H, 5.80; N, 2.78. Found: C, 59.54; H, 5.72; N, 2.90. IR (Nujol): 1670 and 1760 (CO), 3350 (OH) cm^{-1}. UV λ_{max} nm (log ε): 212 (4.62), 292 (sh), 309 (3.49). CD (c=0.001, methanol) Δε (nm): −1.43 (310), +0.17 (283), −1.14 (260), +1.26 (249), −13.16 (230). MS m/z (relative intensity, %): 486 ($M^+\cdot$ −OH, 0.4), 310 (81), 282 (11), 236 (100), 220 (8), 207 (65), 206 (34), 194 (24), 193 (30), 179 (82), 165 (14), 116 (62). CI-MS m/z: 486 ($M^+\cdot$ −OH). ^{1}H- and ^{13}C-NMR: see Tables I and II. Crystal data: $C_{25}H_{29}NO_{10}$; M_r=503.51; crystal system, monoclinic; space group, $P2_1$; cell constants, a=8.377 Å, b=10.707 Å, c=14.349 Å, β=101.85; V=1259.57 Å^3; Z=2; D_x=1.328 g·cm^{-3}; D_m=1.316 g·cm^{-3}; $F(000)$=532; λ=1.5405 Å.

10a: mp 98—99 °C, $[\alpha]_D^{25}$ +44° (c=0.5, $CHCl_3$). *Anal.* Calcd as above. Found: C, 59.37; H, 5.80; N, 2.72. Other instrumental data are identical with those of **6a**. **10b**: mp 133—134 °C, $[\alpha]_D^{25}$ −18° (c=0.5, $CHCl_3$). *Anal.* Calcd as above. Found: C, 59.35; H, 5.90; N, 2.86. IR (Nujol): 1705, 1780 (CO), 3400 (OH) cm^{-1}. UV λ_{max} nm (log ε): 225 (4.26), 290 (3.33), 311 (3.44). MS m/z (relative intensity, %): 486 ($M^+\cdot$ −OH, 0.2), 310 (31), 282 (5), 236 (55), 220 (4), 207 (40), 206 (69), 194 (25), 193 (14), 179 (42), 165 (25), 116 (100). ^{1}H- and ^{13}C-NMR: see Tables I and II.

(*Z*)-3-[2-(β-*N*-Ethoxycarbonyl-*N*-methylaminoethyl)-6-methoxy-4,5-methylenedioxybenzylidenyl]-6,7-dimethoxy-1(3*H*)-isobenzofuranone (8) and (*E*)-(9) α-Narcotine (**1**) (4.13 g, 0.01 mol) in dichloromethane (10 ml) was treated with ECF (4 ml, 0.04 mol) under reflux for 4 h. The solvent and the excess ECF were thoroughly removed by evaporation *in vacuo*, then the crude product was separated by column chromatography with chloroform–ether (4 : 1) to furnish **8** (pale yellow crystals, second fraction, major) and 9 (yellow oil, 200 mg, first fraction, minor). Attempts to crystallize the oily **9** resulted in its easy conversion to **8**. **8**: mp 168—169 °C (ether). *Anal.* Calcd for $C_{25}H_{27}NO_9$: C, 61.87; H, 5.56; N, 2.89. Found: C, 61.75; H, 5.62; N, 2.85. IR (Nujol): 1705, 1775 (CO) cm^{-1}. UV λ_{max} nm (log ε): 222 (4.54), 285 (4.17), 355 (4.20). MS m/z (relative intensity, %): 485 ($M^+\cdot$, 12), 383 (24), 382 (100), 369 (12), 292 (17), 218 (14), 193 (34), 116 (90). ^{1}H- and ^{13}C-NMR: see Tables I and II. **9**: yellow oil. IR (neat): 1680, 1765 (CO) cm^{-1}. UV λ_{max} nm (log ε): 216 (4.76), 280 (sh), 348 (4.16). MS m/z (relative intensity, %): 485 ($M^+\cdot$, 9), 383 (24), 382 (100), 369 (12), 292 (18), 279 (15), 278 (81), 250 (20), 218 (16), 206 (11), 193 (42), 116 (92). ^{1}H- and ^{13}C-NMR: see Tables I and II.

(−)-3-{[2-(β-*N*-Methylaminoethyl)-6-methoxy-4,5-methylenedioxyphenyl]hydroxymethyl}-6,7-dimethoxy-1(3*H*)-isobenzofuranone (7) and (+)-(11) Compound **6a** or **10a** (0.2 g, 0.4 mmol), was dissolved in ethanol (20 ml) and refluxed with 50% aqueous KOH (10 ml) for 12 h. The reaction mixture was diluted with water and neutralized with 2 N HCl, then extracted with chloroform. After removal of the solvent, the crude oily product was purified by preparative TLC with methanol to provide **7** or **11**, respectively. **7**: $[\alpha]_D^{25}$ −27° (c=0.38, $CHCl_3$). IR (neat): 1620, 1760 (CO), 2700—3050 (NH), 3500 (br, OH) cm^{-1}. MS m/z (relative intensity, %): 431 ($M^+\cdot$, 4), 238 (100), 207 (74). CI-MS m/z: 432 (M+1). ^{1}H-NMR: see Table I. **11**: $[\alpha]_D^{25}$ +24° (c=0.5, $CHCl_3$). IR, MS, and ^{1}H-NMR spectrum are identical with those of **7**.

(*Z*)-3-[2-(β-*N*-Ethoxycarbonyl-*N*-methylaminoethyl)-4,5-methylenedioxybenzylidenyl]-6,7-dimethoxy-1(3*H*)-isobenzofuranone (12) and 3-{[2-(β-*N*-Ethoxycarbonyl-*N*-methylaminoethyl)-4,5-methylenedioxyphenyl]-chloromethyl}-6,7-dimethoxy-1(3*H*)-isobenzofuranone (13) Treatment of β-hydrastine (**3**) with ECF as described for **1** to **5** yielded **12** and **13**, which were separated by preparative TLC with benzene–ether (4 : 1).

12: yellow needles, mp 144 °C (ether). *Anal.* Calcd for $C_{24}H_{25}NO_8$: C, 63.30; H, 5.54; N, 3.08. Found: C, 63.44; H, 5.46; N, 2.98. IR (Nujol): 1680, 1775 (CO) cm^{-1}. UV λ_{max} nm (log ε): 227 (4.27), 240 (sh), 307 (4.09), 378 (4.22). MS m/z (relative intensity, %): 455 ($M^+\cdot$, 44), 353 (16), 352 (66), 339 (27), 311 (18), 262 (10), 193 (23), 116 (100). ^{1}H- and ^{13}C-NMR: see Tables I and II. **13**: IR (neat): 1680, 1760 (CO) cm^{-1}. ^{1}H-NMR (200 MHz at 50 °C) δ: 1.28 (t, J=7.0 Hz, 3H, $-CH_2-\underline{CH}_3$), 2.60—3.40 (m, 4H, $-CH_2-$), 2.87 (s, 3H, $-NCH_3$), 3.93 and 4.09 (2×s, 6H, $-OCH_3$), 4.18 (q, J=7.0 Hz, 2H, $-\underline{CH}_2-CH_3$), 5.20—5.70 (br d, 2H, –OCH–, –CH–Cl), 5.99 (s, 2H, $-OCH_2O-$), 6.64—7.20 (m, 4H, aromatic).

(−)-3-{[2-(β-*N*-Ethoxycarbonyl-*N*-methylaminoethyl)-4,5-methylenedioxyphenyl]hydroxymethyl}-6,7-dimethoxy-1(3*H*)-isobenzofuranone (14a and 15a) and (+)-(14b and 15b) Compounds **14a**, **14b**, **15a** and **15b** were obtained from the corresponding β-hydrastine (**3**) or α-hydrastine (**4**)[14] by the procedure described for **1** to **6a**. Purification was achieved by preparative TLC with benzene–ether (4 : 1).

14a: mp 135—136 °C (ether). $[\alpha]_D^{25}$ −9° (c=0.5, $CHCl_3$). *Anal.* Calcd for $C_{24}H_{27}NO_9$: C, 60.87; H, 5.74; N, 2.96. Found: C, 60.61; H, 5.79; N, 2.91. IR (Nujol): 1690, 1760 (CO), 3400 (OH) cm^{-1}. UV λ_{max} nm (log ε): 211 (4.67), 235 (sh), 295 (3.89), 310 (sh). MS m/z (relative intensity, %): 456 ($M^+\cdot$ −OH, 1), 280 (61), 206 (100), 194 (35), 177 (60), 149 (26), 116 (40). CI-MS m/z: 474 (M+1). ^{1}H- and ^{13}C-NMR: see Tables I and II. **14b**: $[\alpha]_D^{25}$ +8° (c=0.5, $CHCl_3$). IR (neat): 1670, 1760 (CO), 3400 (br, OH) cm^{-1}. UV λ_{max} nm (log ε): 216 (4.84), 235 (sh), 295 (4.38), 310 (sh). EI- and CI-MS are identical with those of **14a**. ^{1}H- and ^{13}C-NMR: see Tables I and II. **15a**: mp 135—136 °C (ether). $[\alpha]_D^{25}$ +9° (c=0.5, $CHCl_3$). *Anal.* Calcd as above. Found: C, 60.60; H, 5.72; N, 3.08. Other instrumental data are identical with those of **14a**. **15b**: $[\alpha]_D^{25}$ −8° (c=0.5, $CHCl_3$). Other instrumental data are identical with those of **14b**.

Acknowledgement We thank Prof. T. Ishida, Osaka College of Pharmacy, Japan, for X-ray analysis.

References

1) M. Freund and G. B. Frankforter, *Justus Liebigs Ann. Chem.*, **277**, 20 (1893).
2) G. Blasko, V. Elango, B. Sener, A. J. Freyer, and M. Shamma, *J. Org. Chem.*, **47**, 880 (1982).
3) W. Klötzer, S. Teitel, and A. Brossi, *Monatsh. Chem.*, **103**, 1210 (1972).
4) K. Iwasa, M. Kamigauchi, M. Sugiura, and N. Takao, *J. Nat. Prod.*, **50**, 1083 (1987).
5) W. Klötzer, S. Teitel, and A. Brossi, *Helv. Chim. Acta*, **55**, 2228 (1972).
6) H. L. Holland, M. Curcumelli-Rodostamo, and D. B. Maclean, *Can. J. Chem.*, **54**, 1472 (1976).
7) G. Blasko, D. J. Gula, and M. Shamma, *J. Nat. Prod.*, **45**, 105 (1982).
8) D. U. Lee and W. Wiegrebe, *Arch. Pharm.* (Weinheim, Ger.), **319**, 694 (1986).
9) K. Bláha, J. Hrbek Jun, J. Kovář, L. Pijewska, and F. Šantavý, *Coll. Czech. Chem. Commun.*, **29**, 2328 (1964).
10) A. R. Battersby and H. Spencer, *J. Chem. Soc.*, **1965**, 1087.
11) S. von Angerer, E. Eibler, D. U. Lee, and W. Wiegrebe, *Sci. Pharm.*, **57**, 1 (1989); A. R. Battersby and B. J. T. Harper, *J. Chem. Soc.*, **1962**, 3526.
12) K. K. Mayer, S. Prior, and W. Wiegrebe, *Monatsh. Chem.*, **117**, 533 (1986).
13) W. M. Whaley and M. Meadow, *J. Org. Chem.*, **19**, 666 (1954).
14) M. A. Marshall, F. L. Pyman, and R. Robinson, *J. Chem. Soc.*, **1934**, 1315.

Preparation of New Nitrogen-Bridged Heterocycles. XXVI.[1] Crystal Structures of Thieno[3,2-*a*]- and Thieno[2,3-*b*]indolizine Derivatives

Akikazu KAKEHI,*[,a] Suketaka ITO,[a] Tosio SAKURAI,[b] and Kunio URUSHIDO[b]

Department of Chemistry and Material Engineering, Faculty of Engineering, Shinshu University,[a] Wakasato, Nagano 380, Japan and Department of Chemistry, Faculty of Education, Shinshu University,[b] Nishinagano, Nagano 380, Japan. *Received January 21, 1991*

Single crystal X-ray analyses of thieno[3,2-*a*]- and thieno[2,3-*b*]indolizine derivatives were carried out and their structures were definitively established. The tricyclic ring systems in both molecules were nearly planar and their deviations from the least-squares planes were less than 6.26°. The structural factors for their indolizine moieties were very similar to those for known aromatic indolizines, but those for the thiophene rings were somewhat different. The deviation from co-planarity and the deformation of the thiophene ring in thieno[3,2-*a*]indolizine were greater than those in thieno[2,3-*b*]indolizine.

Keywords thieno[3,2-*a*]indolizine; thieno[2,3-*b*]indolizine; indolizine; fused indolizine; fused thiophene; X-ray analysis

Recently, we reported simple and convenient methods for the preparations of several thieno[3,2-*a*]- and thieno[2,3-*b*]indolizine derivatives by alkaline treatment of the corresponding polyfunctionalized indolizine derivatives.[2] Since the syntheses were accomplished by reliable intramolecular addition or condensation processes at the final stage, there is little doubt that the products have the expected structures. However, it is still valuable to confirm their structures because they have new fused heterocyclic ring systems, and the structural information obtained by chemical and physical means is limited. In this paper we wish to report the results of X-ray single crystal analyses of thieno[3,2-*a*]- and thieno[2,3-*b*]indolizine derivatives.

Results and Discussion

A single crystal (approximately $0.6 \times 0.5 \times 0.8$ mm) of ethyl 3-amino-2-benzoyl-4,6-dimethylthieno[3,2-*a*]indolizine-9-carboxylate (**1**) and a single crystal ($0.4 \times 0.4 \times 1.0$ mm) of ethyl 3,7-dimethyl-2-(*p*-methylbenzoyl)thieno[2,3-*b*]indolizine-9-carboxylate (**2**), prepared according to the procedure described in our previous paper,[2c] were used for the unit cell determinations and the data collections of a Rigaku AFC5S four-circle diffractometer, with graphite-monochromated Mo$K\alpha$ radiation ($\lambda = 0.71069$ Å). Both crystals were triclinic, space group $P\bar{1}$, $Z=2$ with $a = 10.728(3)$ Å, $b = 12.070(2)$ Å, $c = 7.810(3)$ Å; $\alpha = 100.22(2)°$, $\beta = 106.34(2)°$, $\gamma = 95.56(2)°$; $V = 943.4(5)$ Å^3, and $D_{calc} = 1.381$ g/cm^3 for **1**, and space group $P\bar{1}$, $Z=2$, with $a = 10.548(1)$ Å, $b = 12.637(2)$ Å, $c = 7.458(1)$ Å; $\alpha = 97.27(1)°$, $\beta = 101.03(1)°$, $\gamma = 81.45(1)°$, $V = 960.0(2)$ Å, and $D_{calc} = 1.354$ g/cm^3 for **2**.

The structures were solved by the direct method (MITHRIL),[3] and the non-hydrogen atoms were refined anisotropically. The hydrogen atoms were included in the structure factor calculation in idealized positions. The final *R*-factors after the full-matrix least-squares refinements were 0.052 for 2376 observed reflections for **1** and 0.050 for 3157 observed reflections for **2**. The positional and thermal parameters with their standard deviations for compounds **1** and **2** are listed in Tables I and II. The bond distances and angles for non-hydrogen atoms and ORTEP drawings[4] of the structures are shown in Tables III and IV and Figs. 1 and 2, respectively.

The bond distances and angles for the indolizine moiety in compounds **1** and **2** are very similar to those for 1-acetoxy-2,3- and 3-acetoxy-1,2-diphenylindolizine reported by Wadsworth and his co-workers.[5] The proton nuclear magnetic resonance (^{1}H-NMR) spectral data for the indolizine ring protons and the methyl protons of **1**[2c] and **2** are in good agreement with those of known fully aromatic

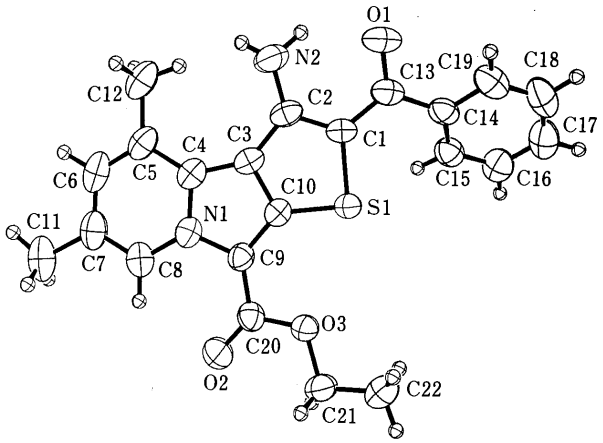

Fig. 1. ORTEP Drawing of Thieno[3,2-*a*]indolizine **1** Showing the Atom Labeling Scheme and 50% Probability Thermal Ellipsoids

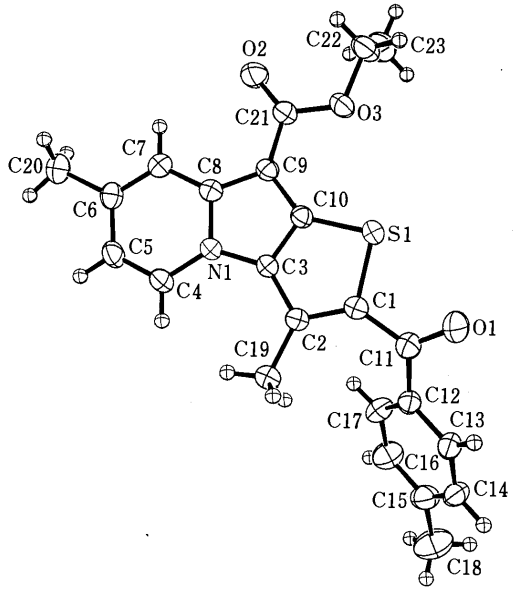

Fig. 2. ORTEP Drawing of Thieno[2,3-*b*]indolizine **2** Showing the Atom Labeling Scheme and 50% Probability Thermal Ellipsoids

TABLE I. Positional ($\times 10^4$) and Thermal Parameters (Å^2) of Thieno[3,2-*a*]indolizine (**1**) for Non-hydrogen Atoms with Their Standard Deviations in Parentheses

Atom[a]	*x*	*y*	*z*	B_{eq}
S1	3214 (1)	2331.3 (8)	9110 (1)	3.68 (3)
O1	−3 (3)	3795 (3)	8248 (5)	6.4 (1)
O2	7789 (3)	2574 (2)	12031 (4)	5.7 (1)
O3	5962 (2)	1649 (2)	9823 (3)	4.2 (1)
N1	6232 (3)	4419 (2)	12685 (4)	3.7 (1)
N2	2057 (3)	5242 (3)	10608 (5)	5.4 (1)
C1	2079 (4)	3297 (3)	9280 (5)	3.9 (1)
C2	2699 (4)	4352 (3)	10417 (5)	3.8 (1)
C3	4072 (4)	4354 (3)	11288 (5)	3.4 (1)
C4	5201 (4)	5049 (3)	12609 (5)	3.6 (1)
C5	5469 (4)	6114 (3)	13844 (5)	4.2 (2)
C6	6715 (5)	6466 (3)	15027 (6)	5.1 (2)
C7	7748 (5)	5837 (4)	15035 (5)	4.9 (2)
C8	7482 (4)	4817 (3)	13866 (5)	4.5 (2)
C9	5801 (4)	3361 (3)	11458 (5)	3.5 (1)
C10	4470 (4)	3328 (3)	10633 (5)	3.3 (1)
C11	9101 (5)	6286 (4)	16326 (6)	6.6 (2)
C12	4418 (5)	6846 (3)	13886 (6)	5.8 (2)
C13	695 (4)	3025 (3)	8358 (6)	4.4 (2)
C14	23 (4)	1828 (4)	7501 (5)	4.1 (1)
C15	373 (4)	898 (4)	8240 (5)	4.5 (2)
C16	−314 (4)	−184 (4)	7444 (6)	5.3 (2)
C17	−1375 (5)	−344 (4)	5884 (7)	5.9 (2)
C18	−1750 (4)	570 (5)	5153 (6)	6.1 (2)
C19	−1067 (4)	1659 (4)	5964 (6)	5.2 (2)
C20	6641 (4)	2532 (3)	11191 (5)	3.7 (1)
C21	6694 (4)	762 (4)	9327 (6)	5.0 (2)
C22	5803 (5)	−82 (4)	7759 (6)	5.8 (2)

a) See Fig. 1 for the numberings of **1**.

TABLE II. Positional ($\times 10^4$) and Thermal Parameters (Å^2) of Thieno[2,3-*b*]indolizine (**2**) for Non-hydrogen Atoms with Their Standard Deviations in Parentheses

Atom[a]	*x*	*y*	*z*	B_{eq}
S1	7010.3 (6)	3749.8 (5)	7713 (1)	2.69 (3)
O1	5792 (2)	1923 (2)	8215 (4)	5.2 (1)
O2	8736 (2)	6831 (2)	6356 (3)	3.9 (1)
O3	6957 (2)	6045 (1)	6445 (3)	3.03 (8)
N1	10653 (2)	3798 (2)	8213 (3)	2.24 (8)
C1	7802 (2)	2575 (2)	8681 (4)	2.6 (1)
C2	9146 (2)	2480 (2)	8899 (3)	2.4 (1)
C3	9494 (2)	3401 (2)	8301 (3)	2.3 (1)
C4	11929 (3)	3358 (2)	8668 (4)	2.8 (1)
C5	12892 (2)	3907 (2)	8481 (4)	3.1 (1)
C6	12621 (2)	4933 (2)	7807 (4)	2.7 (1)
C7	11347 (2)	5366 (2)	7372 (3)	2.5 (1)
C8	10336 (2)	4817 (2)	7575 (3)	2.3 (1)
C9	8965 (2)	5069 (2)	7255 (3)	2.3 (1)
C10	8472 (2)	4169 (2)	7690 (3)	2.3 (1)
C11	6812 (3)	1890 (2)	9096 (4)	3.1 (1)
C12	7284 (3)	1233 (2)	10686 (4)	2.9 (1)
C13	6663 (3)	325 (2)	10669 (4)	3.4 (1)
C14	6863 (3)	−220 (2)	12218 (5)	3.8 (1)
C15	7662 (3)	121 (2)	13818 (5)	4.0 (1)
C16	8281 (3)	1017 (3)	13831 (4)	4.2 (1)
C17	8104 (3)	1555 (2)	12273 (4)	3.5 (1)
C18	7841 (5)	−451 (3)	15538 (6)	6.4 (2)
C19	10097 (3)	1538 (2)	9526 (4)	3.4 (1)
C20	13714 (3)	5515 (3)	7550 (4)	3.6 (1)
C21	8256 (2)	6069 (2)	6655 (4)	2.6 (1)
C22	6110 (3)	6982 (2)	5770 (4)	3.6 (1)
C23	5806 (3)	7802 (3)	7296 (5)	4.6 (2)

a) See Fig. 2 for the numberings of **2**.

TABLE III. Bond Distances (Å) and Angles (°) of Thieno[3,2-*a*]indolizine (**1**) for Non-hydrogen Atoms with Their Standard Deviations in Parentheses

Bond distance (Å)			
S1–C1	1.780 (4)	C5–C6	1.370 (6)
S1–C10	1.719 (4)	C5–C12	1.502 (6)
O1–C13	1.249 (4)	C6–C7	1.402 (6)
O2–C20	1.213 (4)	C7–C8	1.348 (5)
O3–C20	1.347 (4)	C7–C11	1.499 (6)
O3–C21	1.450 (4)	C9–C10	1.385 (5)
N1–C4	1.395 (4)	C9–C20	1.437 (5)
N1–C8	1.378 (5)	C13–C14	1.496 (5)
N1–C9	1.402 (4)	C14–C15	1.387 (5)
N2–C2	1.340 (4)	C14–C19	1.389 (5)
C1–C2	1.398 (5)	C15–C16	1.379 (6)
C1–C13	1.432 (5)	C16–C17	1.382 (6)
C2–C3	1.438 (5)	C17–C18	1.373 (7)
C3–C4	1.424 (5)	C18–C19	1.387 (6)
C3–C10	1.407 (5)	C21–C22	1.470 (6)
C4–C5	1.414 (5)		
Bond angle (°)			
C1–S1–C10	90.1 (2)	C8–C7–C11	121.4 (5)
C20–O3–C21	116.4 (3)	N1–C8–C7	120.6 (4)
C4–N1–C8	122.4 (3)	N1–C9–C10	105.8 (3)
C4–N1–C9	110.8 (3)	N1–C9–C20	124.0 (3)
C8–N1–C9	126.8 (3)	C10–C9–C20	130.1 (3)
S1–C1–C2	112.0 (3)	S1–C10–C3	114.2 (3)
S1–C1–C13	124.0 (3)	S1–C10–C9	135.5 (3)
C2–C1–C13	124.0 (3)	C3–C10–C9	110.2 (3)
N2–C2–C1	122.3 (4)	O1–C13–C1	120.4 (4)
N2–C2–C3	125.6 (4)	O1–C13–C14	117.2 (4)
C1–C2–C3	112.1 (3)	C1–C13–C14	122.3 (3)
C2–C3–C4	141.8 (3)	C13–C14–C15	123.4 (4)
C2–C3–C10	111.2 (3)	C13–C14–C19	117.8 (4)
C4–C3–C10	107.0 (3)	C15–C14–C19	118.7 (4)
N1–C4–C3	106.2 (3)	C14–C15–C16	121.3 (4)
N1–C4–C5	117.4 (3)	C15–C16–C17	119.4 (4)
C3–C4–C5	136.3 (4)	C16–C17–C18	120.1 (4)
C4–C5–C6	118.4 (4)	C17–C18–C19	120.5 (4)
C4–C5–C12	121.3 (4)	C14–C19–C18	120.0 (4)
C6–C5–C12	120.2 (4)	O2–C20–O3	122.7 (4)
C5–C6–C7	123.2 (4)	O2–C20–C9	127.5 (4)
C6–C7–C8	118.0 (4)	O3–C20–C9	109.8 (3)
C6–C7–C11	120.6 (4)	O3–C21–C22	107.9 (3)

indolizine derivatives.[6] However, there are significant differences in the dihedral angles between the two least-squares planes of the indolizine ring. The dihedral angles between the pyridine and the pyrrole rings are 3.22° in **1** and 0.59° in **2**, and the indolizine ring of the latter is almost planar. On the other hand, the geometries of the thiophene rings in these molecules are considerably different from those of the parent thiophene[7] and benzo[*b*]thiophene derivatives.[8] First, there are large differences between the two sulfur–carbon (S–C) bond distances, and, second, the ring systems are not planar. The lengths of the S–C bonds (S1–C10) attached directly to the indolizine rings are 1.719 and 1.707 Å in **1** and **2**, respectively, and they are nearly the same as that (1.714 Å) of the parent thiophene[7] but are shorter than those (average 1.744 Å) of benzo[*b*]thiophenes.[8] This suggests that the S–C bonds have marked double-bond character due to the aromatic resonance structures, as expected in the parent thiophene.[7] On the other hand, the other S–C bonds (S1–C1, 1.780 Å in **1** and 1.759 Å in **2**) are longer than those of benzo[*b*]thiophenes,[8] and this is indicative of some reduction of the contribution of aromatic resonance structures at these bonds. The

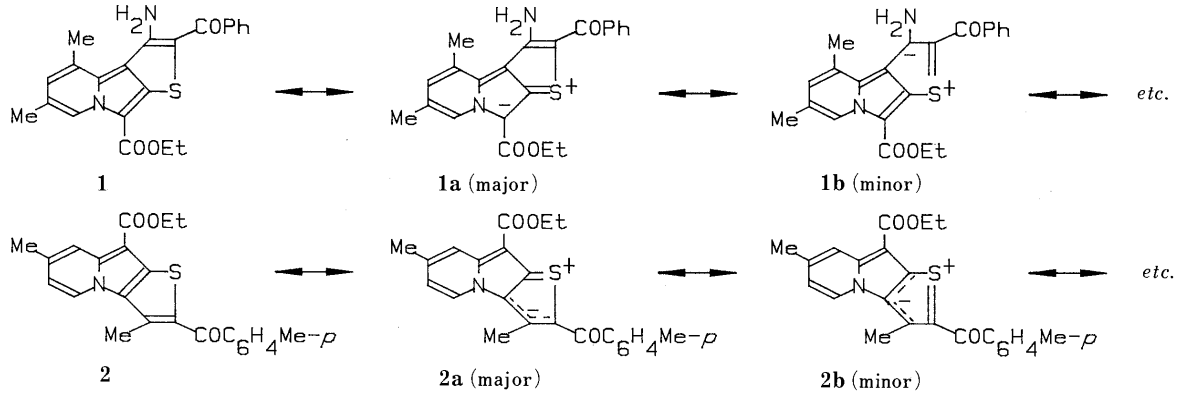

Fig. 3. Probable Resonance Structures for Thieno[3,2-*a*]- and Thieno[2,3-*b*]indolizines

TABLE IV. Bond Distances (Å) and Angles (°) of Thieno[2,3-*b*]-indolizine (**2**) for Non-hydrogen Atoms with Their Standard Deviations in Parentheses

Bond distance (Å)			
S1–C1	1.759 (3)	C6–C7	1.367 (4)
S1–C10	1.707 (3)	C6–C20	1.510 (4)
O1–C11	1.235 (3)	C7–C8	1.396 (3)
O2–C21	1.216 (3)	C8–C9	1.414 (3)
O3–C21	1.357 (3)	C9–C10	1.415 (3)
O3–C22	1.453 (3)	C9–C21	1.445 (3)
N1–C3	1.404 (3)	C11–C12	1.492 (4)
N1–C4	1.374 (3)	C12–C13	1.401 (4)
N1–C8	1.401 (3)	C12–C17	1.381 (4)
C1–C2	1.384 (3)	C13–C14	1.385 (4)
C1–C11	1.465 (4)	C14–C15	1.383 (5)
C2–C3	1.418 (3)	C15–C16	1.387 (4)
C2–C19	1.500 (4)	C15–C18	1.518 (5)
C3–C10	1.388 (3)	C16–C17	1.389 (4)
C4–C5	1.349 (4)	C22–C23	1.489 (5)
C5–C6	1.419 (4)		
Bond angle (°)			
C1–S1–C10	90.9 (1)	C8–C9–C10	106.0 (2)
C21–O3–C22	116.9 (2)	C8–C9–C21	125.3 (2)
C3–N1–C4	130.6 (2)	C10–C9–C21	128.7 (2)
C3–N1–C8	108.5 (2)	S1–C10–C3	110.7 (2)
C4–N1–C8	120.9 (2)	S1–C10–C9	139.4 (2)
S1–C1–C2	113.5 (2)	C3–C10–C9	109.9 (2)
S1–C1–C11	113.8 (2)	O1–C11–C1	119.6 (3)
C2–C1–C11	132.6 (2)	O1–C11–C12	118.8 (3)
C1–C2–C3	108.6 (2)	C1–C11–C12	121.3 (2)
C1–C2–C19	126.9 (2)	C11–C12–C13	119.1 (3)
C3–C2–C19	124.4 (2)	C11–C12–C17	122.2 (2)
N1–C3–C2	136.7 (2)	C13–C12–C17	118.2 (3)
N1–C3–C10	107.2 (2)	C12–C13–C14	120.3 (3)
C2–C3–C10	116.1 (2)	C13–C14–C15	121.3 (3)
N1–C4–C5	119.7 (2)	C14–C15–C16	118.4 (3)
C4–C5–C6	121.6 (2)	C14–C15–C18	121.3 (3)
C5–C6–C7	118.1 (2)	C16–C15–C18	120.4 (3)
C5–C6–C20	120.6 (2)	C15–C16–C17	120.7 (3)
C7–C6–C20	121.3 (3)	C12–C17–C16	121.1 (3)
C6–C7–C8	121.3 (2)	O2–C21–O3	123.6 (2)
N1–C8–C7	118.4 (2)	O2–C21–C9	125.8 (2)
N1–C8–C9	108.4 (2)	O3–C21–C9	110.6 (2)
C7–C8–C9	133.2 (2)	O3–C22–C23	111.8 (2)

least-squares plane of the thiophene ring intersect with those of the pyrrole and pyridine rings at 3.06 and 6.26° in **1** and at 2.99 and 2.41° in **2**, respectively, and, in particular, the deformation of the tricyclic ring system is greater in **1** than in **2**. These facts suggest that the major contributors to the resonance structures of the thieno[3,2-*a*]indolizine (**1**) and thieno[2,3-*b*]indolizine (**2**) are **1a** and **2a**, respectively, and the contributions of structures such as **1b** and **2b** are not so large (see Fig. 3).

Experimental

Melting points were measured with a Yanagimoto micromelting point apparatus and are uncorrected. The microanalyses were carried out on a Perkin-Elmer 240 elemental analyzer. The ^{1}H-NMR spectra were determined with a Varian EM360A spectrometer in deuteriochloroform with tetramethylsilane as an internal standard and the chemical shifts are expressed in δ values. The infrared (IR) spectra were taken with a Hitachi 260-10 infrared spectrophotometer.

Preparation of Thienoindolizines Ethyl 3-amino-2-benzoyl-4,6-dimethylthieno[3,2-*a*]indolizine-9-carboxylate (**1**) was prepared according to our recent paper,[2c] and a single crystal was grown from ethanol as a yellow needle. mp 204—205 °C (lit.[2c] 203—204 °C). On the other hand, ethyl 3,7-dimethyl-2-(*p*-methylbenzoyl)thieno[2,3-*b*]indolizine-9-carboxylate (**2**) was prepared freshly in 59% yield by the reaction of 3-acetyl-2-mercapto-7-methylindolizine-1-carboxylate with *p*-methylphenacyl bromide in the presence of alkali,[2c] since a suitable single crystal could not be obtained by the recrystallization of known derivatives.[2] A single crystal of **2** was grown from ethanol as yellow prism. mp 189—190 °C. IR ν(KBr): 1673 (CO), 1587, 1281, 1230, 1058 cm^{-1}. ^{1}H-NMR ($CDCl_3$) δ: 1.37 (3H, t, J=7.0 Hz, $OCH_2\underline{CH_3}$), 2.42 (6H, s, 7-Me, tolyl-Me), 2.79 (3H, s, 3-Me), 4.33 (2H, q, J=7.0 Hz, $O\underline{CH_2}CH_3$), 6.62 (1H, dd, J=7.0, 2.0 Hz, 6-H), 7.1—8.0 (4H, m, phenyl-H), 8.13 (1H, br s, 8-H), 8.49 (1H, d, J=7.0 Hz, 5-H). *Anal.* Calcd for $C_{23}H_{21}NO_3S$: C, 70.56; H, 5.41; N, 3.58. Found: C, 70.33; H, 5.47; N, 3.75.

Acknowledgement This work was supported in part by a Grant-in-Aid for Scientific Research (No. 02453085) from the Ministry of Education, Science and Culture.

References

1) For part XXV of this series, see A. Kakehi, S. Ito, T. Fujii, T. Sakurai, K. Urushido, S. Hatanaka, T. Mabuchi, and S. Matsushita, *Bull. Chem. Soc. Jpn.*, **63**, 3571 (1990).
2) *a*) A. Kakehi, S. Ito, S. Matsumoto, and Y. Morimoto, *Chem. Lett.*, **1987**, 2043; *b*) A. Kakehi, S. Ito, T. Fujii, Y. Morimoto, S. Matsumoto, and M. Shiohara, *Bull. Chem. Soc. Jpn.*, **62**, 119 (1989); *c*) A. Kakehi, S. Ito, N. Yamada, and K. Yamaguchi, *Chem. Pharm. Bull.*, **38**, 1527 (1990).
3) C. J. Gilmore, *J. Appl. Cryst.*, **17**, 42 (1984).
4) C. K. Johnson, "ORTEPII, Report ORNL-5138," Oak Redge National Laboratory, Oak Ridge, Tennessee, 1976.
5) D. H. Wadsworth, S. L. Bender, D. L. Smith, H. R. Luss, and C. H. Weidner, *J. Org. Chem.*, **51**, 4639 (1986).
6) F. W. Kröck and F. Kröhnke, *Chem. Ber.*, **102**, 659, 669 (1969); T. Sasaki, K. Kanematsu, A. Kakehi, and G. Ito, *Tetrahedron*, **28**, 4947 (1972); Y. Tamura, Y. Sumida, and M. Ikeda, *J. Chem. Soc., Perkin. Trans. 1*, **1973**, 2091; A. Kakehi and S. Ito, *Bull. Chem. Soc. Jpn.*, **47**, 938 (1974); J. Alvarez-Builla, M. G. Quintanilla, C. Abril, and M. T. Gandasegui, *J. Chem. Research*, (*S*), **1984**, 202.
7) W. R. Harshbarger and S. H. Bauer, *Acta Crystallogr., Sect. B*, **26**, 1010 (1970).
8) G. Argay and A. Kalman, *Cryst. Struct. Commun.*, **2**, 19 (1973); J. H. C. Hogg and H. H. Sutherland, *Acta Crystallogr., Sect. B*, **30**, 2058 (1974).

Linear Correlation of the Solvolysis Rates of Xanthates with the Grunwald–Winstein *Y* Values

Kazunobu HARANO, Hideo KIYONAGA, Chiaki YOKOTE and Takuzo HISANO*

Faculty of Pharmaceutical Sciences, Kumamoto University, 5–1 Oe-honmachi, Kumamoto 862, Japan. *Received January 30, 1991*

O-Cinnamyl and O-(2-methylthioethyl) S-methyl dithiocarbonates (xanthates) underwent thione–thiol rearrangement to the dithiol esters in various solvents. The reactions followed first-order kinetics and the rates were affected by change of the solvent polarity. Plots of the rate constants against the *Y* values showed good linear relationships. The rate constants may be used as a new empirical parameter of solvent polarity in place of *Y* values. Modified intermediate neglect of differential overlap (MINDO/3) calculations indicate that allylic xanthates undergo [3,3]-sigmatropic rearrangement *via* a polarizable transition state.

Keywords xanthate; thione–thiol rearrangement; solvent effect; allylic rearrangement; solvent polarity parameter; *Y* value; MINDO/3

In the previous paper,[1a] it was reported that solvolysis of *O*-(1-cyclopropylethyl) *S*-methyl dithiocarbonate (xanthate) (Ia) in various solvents results in thione–thiol rearrangement to give the corresponding dithiol ester, *S*-(1-cyclopropylethyl) *S*-methyl dithiocarbonate (IIa), and plots of the rate constants in protic solvents *vs.* Grunwald–Winstein *Y* values[2a] showed linear relationships, suggesting that the solvolysis rate constants of xanthates may be used as an empirical solvent polarity parameter for correlating the solvent ionizing power and the rate of reactions.

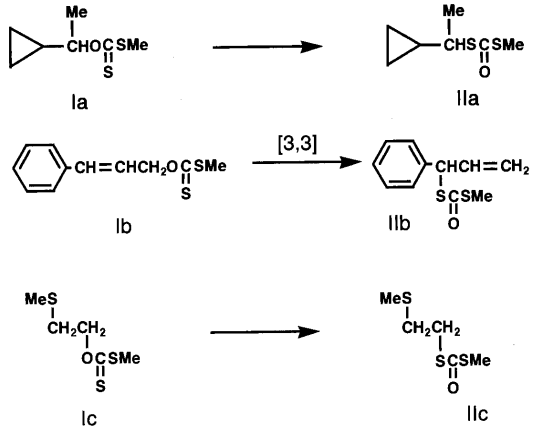

Chart 1

TABLE I. First-Order Rate Constants for Solvolyses of Ib, c in Various Solvents at 60 °C

Solvent	$k \times 10^5$ (s^{-1})		E_T value (kcal/mol)	*Y* value
	Ib	Ic		
Glycol	—	13.6	56.3	
MeOH	64.2	1.98	55.5	−1.090
80% EtOH	132.0	4.52	53.6	0.000
EtOH	29.8	0.792	51.9	−2.033
AcOH	42.8	1.01	51.9	−1.639
n-PrOH	20.6	0.320	50.7	
n-BuOH	23.2	0.603	50.2	
iso-PrOH	15.0	0.428	48.6	
iso-AmOH	15.7	0.306	47.0	
DMSO	77.5	—	45.0	
Sulfolane	74.7	4.18	44.0	
tert-BuOH	13.2	0.225	43.9	−3.260
DMF	64.9	4.05	43.8	
TMU	18.8	—	41.0	
Anisole	7.18	—	37.2	

However, *O*-(1-cyclopropylethyl) *S*-methyl xanthate (Ia) has some disadvantages as a substrate; it is a garlicky oil; it shows a large dependence of the reaction rate on solvent polarity, being inert in nonpolar solvents; it is not isolable in the pure state. So, we looked for better substrates.

In this paper, we present an excellent linear correlation between the rates of [3,3]-sigmatropic rearrangement[3] of *O*-cinnamyl *S*-methyl xanthate (Ib) and the *Y* values, and we also compare the data with those for *O*-(2-methylthioethyl) *S*-methyl xanthate (Ic),[4] which undergoes thione–thiol rearrangement *via* an episulfonium intermediate.

Results

Solvolysis of *O*-Cinnamyl *S*-Methyl Xanthate (Ib) and *O*-(2-Methylthioethyl) *S*-Methyl Xanthate (Ic) in Various Solvents The pure xanthates were synthesized according to a procedure developed in this laboratory. Compound Ib was isolated in crystalline form and was found to be stable in a refrigerator for several months. Compound Ic was purified by chromatography on silica gel, and was isolated

TABLE II. Activation Parameters for Solvolyses of Ib, c

Solvent	E_a (kcal/mol)		$\Delta S^{\neq}$ (e.u.)	
	Ib	Ic	Ib	Ic
EtOH	23.2	26.6	−7.2	−3.5
DMF	22.0	23.3	−8.5	−10.5
DMSO	18.5	—[a]	−18.7	—[a]
o-ClC_6H_4OH	17.8	20.6	−19.0	−18.1
p-ClC_6H_4OH	—[b]	21.1	—[b]	−11.5

a) A side reaction occurred with DMSO. *b*) The rate is too rapid to be measured even at room temperature.

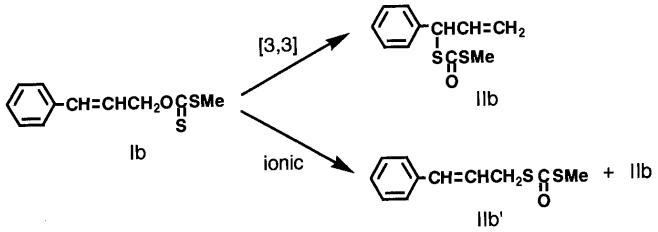

Chart 2

as an oil.

The reaction rates were determined in various solvents by measuring the decrease of the C=S chromophore. The absorption data were automatically collected and analyzed by using a non-weighted least-squares program. In all cases, good first-order rate plots were obtained. The results are summarized in Table I. The activation parameters calculated from the data are presented in Table II.

The proton nuclear magnetic resonance (^{1}H-NMR) spectra of the solvolysis products of Ib showed the presence of a mixture of isomeric dithiol esters, *S*-(1-phenylallyl) (IIb) and *S*-cinnamyl *S*-methyl dithiocarbonate (IIb'). The amounts of IIb' were as follows: *ca.* 35.8% in phenol; 10.3% in 80% aqueous ethanol; and 4% in ethanol.

Solvolysis of *O*-(2-methylthioethyl) *S*-methyl xanthate (Ic) also caused thione–thiol rearrangement to afford the corresponding dithiol ester (IIc). However, the rearrangement could not be observed in solvents having low ionizing power, *e.g.*, benzene.

Correlation to E_T Values To examine the general features of the correlation between the reaction rates and empirical parameters of solvent polarity, the logarithms of the rate constants were plotted against the E_T values of Reichardt,[5] based on the transition energy for the longest-wavelength solvatochromic absorption band of pyridinium *N*-phenoxide betaine dye (Fig. 1). As shown in Fig. 1, a plot of log *k* *vs.* E_T values in all solvents used exhibits some scattering of points. Plots of log *k* *vs.* E_T values for aprotic and protic solvent systems show nearly linear relationships with slopes $a=0.143$ and 0.0792, respectively. In the protic solvents, the rate constant for 80% aqueous EtOH deviates from the expected value.

Correlation to *Y* Value A plot of log *k* *vs.* Grunwald–Winstein *Y* values shows an excellent linear relationship for alcohols (*Y* value for 80% aqueous EtOH = 0.0) with slope $m=0.310$ (correlation coefficient, $r=0.999$, see Fig. 2), suggesting that the rate of reaction depends moderately on the ionizing power of the solvent as compared with the case of *O*-allyl *S*-methyl xanthate (Id) ($m=0.141$).[1a] It is of interest to note that a [3,3]-sigmatropic rearrangement of this type is affected by introduction of a γ-substituent into the allylic moiety. The *m* value for the solvolysis of Ib in aqueous EtOH is 0.316 ($r=0.993$) (Fig. 3 and Table IV),

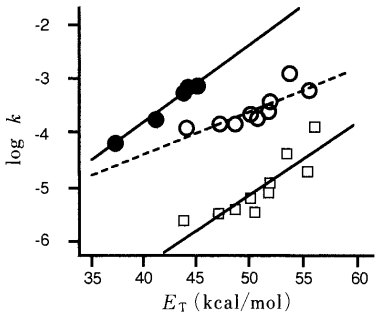

Fig. 1. Plots of log *k* *vs.* E_T Values for the Solvolysis of Ib, c
●, Ib aprotic; ○, Ib protic; □, Ic protic.

TABLE III. First-Order Rate Constants for Solvolyses of Ib, c in Alcohols at 60 °C

Solvent	$k\times10^5$ (s^{-1})		*Y* value
	Ib	Ic	
80% EtOH	132.0	4.52	0.000
MeOH	64.2	1.98	−1.090
AcOH	42.8	1.01	−1.639
EtOH	29.8	0.792	−2.033
tert-BuOH	13.2	0.225	−3.260

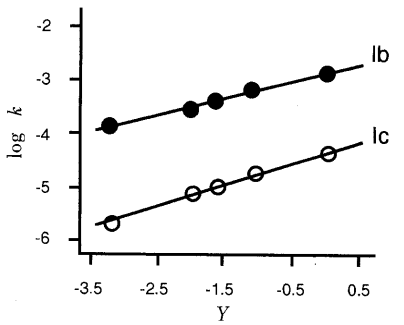

Fig. 2. Plots of log *k* *vs.* *Y* Values for the Solvolysis of Ib, c in Alcohols
1b, slope = 0.310; 1c, slope = 0.402.

TABLE IV. First-Order Rate Constants for Solvolyses of Ib in Aqueous EtOH at 60 °C

Aqueous EtOH (v/v%)	$k\times10^5$ (s^{-1})	*Y* value
100	29.8	−2.033
90	61.9	−0.747
80	132	0.000
70	213	0.595
60	265	1.124

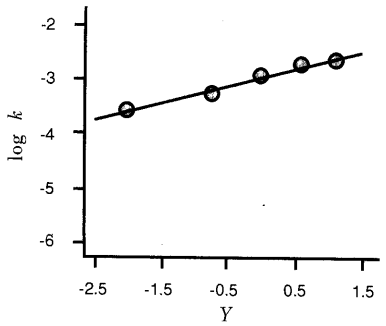

Fig. 3. Plots of log *k* *vs.* *Y* Values for the Solvolysis of Ib in EtOH–H_2O Solvents
Slope = 0.316.

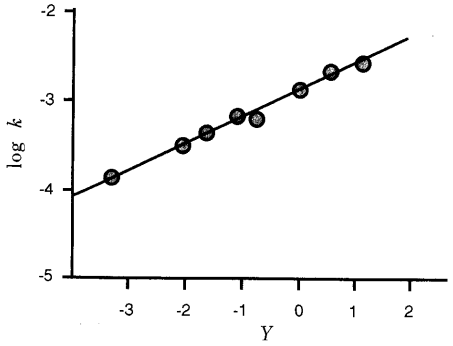

Fig. 4. Plots of log *k* *vs.* *Y* Values for the Solvolysis of Ib in Protic Solvents
Slope = 0.303.

consistent with that for alcoholic solvent ($m=0.310$). The m value for all the protic solvents tested (alcohols and aqueous EtOH) is 0.303 ($r=0.996$) (see Fig. 4).

Correlation to *Y* Value of Binary Mixtures of Phenol with Benzene Next, we studied the correlations between the rate constants and Y values for phenol–benzene solvents (Fig. 5).

In phenol–benzene solvents, linear correlations were observed. The m value for the solvent system is calculated to be 0.583 ($r=0.996$), larger than the value for protic solvents ($m=0.303$), indicating that the phenolysis reaction proceeds through a more ionic intermediate than that for protic solvents.

Solvolysis of *O*-(2-Methylthioethyl) *S*-Methyl Xanthate (Ic) Solvolyses of Ic in various solvents were studied in the same way as mentioned above. The reaction rates in various solvent studied were smaller than those for Ib. The plot of log k *vs.* E_T values showed a scattered pattern (Fig. 1). In contrast, a linear relationship with the Y values was observed ($m=0.402$, $r=0.997$) (Fig. 2).

Structure of the Transition State for the Rearrangement of Allylic Xanthate To understand the solvent effect on the rate for allylic xanthates, we performed modified intermediate neglect of differential overlap (MINDO/3)[6] calculations on the rearrangement reaction. To reduce computation time, the simplest compound, *i.e.*, *O*-allyl *S*-methyl xanthate (Id), was chosen as a model compound.

The molecular geometry of Id was determined by combining the known geometries for *O*-ethyl *S*-carboxyethyl xanthate[7] plus the allyl moiety followed by variation of all the interatomic distances plus bond and dihedral angles, until the heat of formation of the system was minimized. The minimum energy structure (A) is shown in Fig. 6.[8]

Likewise, the minimum energy geometry for the [3,3]-sigmatropic rearrangement product, *i.e.*, *S*-allyl *S*-methyl

TABLE V. First-Order Rate Constants for Solvolyses of Ib, c in Phenol–Benzene at 60 °C

PhOH (w/v%)	$k\times10^5$ (s^{-1})		Y value
	Ib	Ic	
90	556	29.9	1.427
70	307	17.5	1.101
50	166	9.96	0.425
40	—	5.81	—
30	56.9	3.42	−0.192
20	30.4	1.46	−0.711

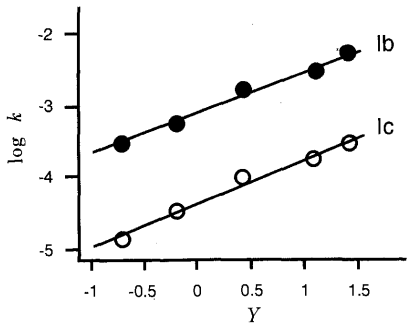

Fig. 5. Plots of log k *vs.* Y Values for the Phenolysis of Ib, c in Phenol–Benzene Solvents

Ib, slope = 0.583; Ic, slope = 0.597.

TABLE VI. Heats of Formation and Dipole Moment Calculated by MINDO/3 for the [3,3]-Sigmatropic Rearrangement of *O*-Allyl *S*-Methyl Xanthate (Id) to *S*-Allyl *S*-Methyl Dithiocarbonate (IId) *via* Concerted Six-Membered Transition State

Distance for >C=S···CH$_2$=C (Å)	ΔH_f (kcal/mol)	Rel. ΔH_f (kcal/mol)	μ_p (debye)
5.790[a]	−47.17	0.0	7.20
5.0	−47.06	+0.11	7.19
4.0	−46.53	+0.64	6.82
3.1	−44.18	+2.09	6.31
2.5	−40.88	+6.29	5.78
2.0	−38.67	+8.50	4.43
1.8	−31.88	+15.29	3.46
1.78	−30.67	+16.50	3.56
1.77	−56.87	−9.70	2.32
1.75	−55.83	−8.66	2.31
1.779[b]	−59.91	−12.74	2.14

a) All parameters were optimized on a conformation in which the methyl group of MeS- is *anti* to the oxygen atom of >C=S. Using this structure as a starting geometry, all parameters except >C=S···CH$_2$=C distance were optimized from 5.0 Å to 1.75 Å. *b*) All parameters were optimized on a conformation in which the methyl group of MeS- is *syn* to the oxygen atom of >C=O.

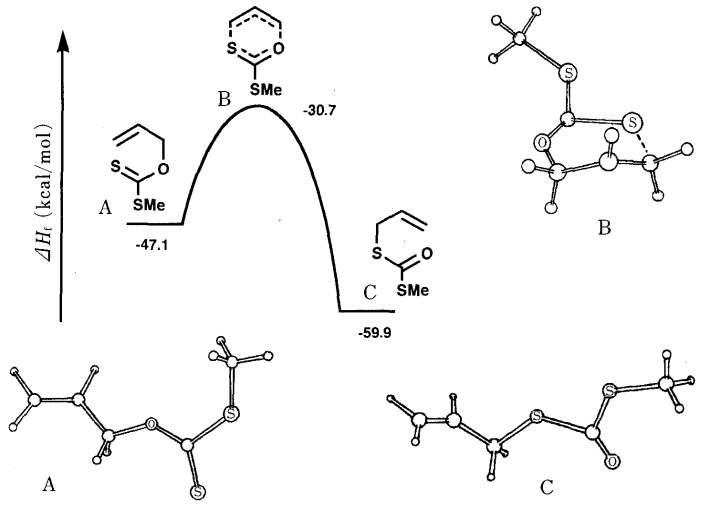

Fig. 6. MINDO/3 Heats of Formation and Optimized Structures of Id, IId and the Transition State for [3,3]-Sigmatropic Rearrangement of Id

dithiocarbonate (IId), was determined. The calculated geometry[9] (C) is shown in Fig. 6.

The relative energies for the related compounds obtained from the MINDO/3 calculations appear in Table VI. Inspection of these values that *S*-allyl *S*-methyl dithiocarbonate (IId) is *ca.* 12 kcal/mol more stable than *O*-allyl *S*-methyl xanthate (Id), suggesting that the thione-to-thiol isomerization is exothermic.[10]

To obtain further information about the nature of the transition state, cyclic transition states were calculated along the reaction coordinate, taking the length of the forming $\geq C=S\cdots CH_2=$ bond as the reaction coordinate. The heat of formation for each structure is summarized in Table VI. As can be seen in Table VI, the optimized structure in which the thione sulfur atom was forced to be located 2.0 Å apart from the γ carbon is *ca.* 8.5 kcal/mol less stable than free *O*-allyl *S*-methyl xanthate (Id). As the $\geq C=S\cdots CH_2=$ distance is decreased, the heat of formation gradually increased and reached a maximum value ($\Delta H_f = -30.7$ kcal/mol) at *ca.* 1.78 Å (see B in Fig. 6). When the $\geq C=S\cdots CH_2=$ distance is 1.77 Å, the transition structure suddenly relaxed and transformed into *S*-allyl *S*-methyl dithiocarbonate (IId). Concomitantly, reorganizations of π- and σ-electrons take place, accompanied with changes of bond distances and angles, resulting in electron delocalization all over the reaction system.

The optimized highest-energy structure along this pathway has a quasi-chair conformation. The structure shows enhanced double bond character at the S=C–O– and =CH–CH_2 bonds and has a heat of formation equal to −30.7 kcal/mol, which is *ca.* 16.5 kcal/mol less stable than the starting material, *O*-allyl *S*-methyl xanthate (Id).

Discussion

In the phenolysis reaction of Ib, the formation of *S*-cinnamyl *S*-methyl dithiocarbonate (IIb′) was observed besides *S*-(1-phenylallyl) *S*-methyl dithiocarbonate (IIb). The magnitude of the *m* value for phenol–benzene solution is considerably larger than the values observed in typical S_N2 reactions.[11] These results provide evidence for the formation of an intimate ion pair or an ion-pair intermediate, which collapses to products before the proper structural orientation for [3,3]-sigmatropic rearrangement is attained.

In the previous paper,[1b] we reported that the catalytic activity of phenols in phenolysis of homoallylic xanthates is probably a consequence of the formation of a complex of the type RO(RS)C=S···H-OAr between the catalyst and substrate (see Chart 3). The mechanism for solvolysis of Ib in protic solvents is very similar to that proposed for phenol-catalyzed thione–thiol rearrangement of homoallylic xanthates.

This assumption is supported by the difference in the activation parameters between protic and aprotic solvents. The activation energies of Ib and Ic in ethanol are 1—3 kcal/mol higher than those in dimethyl formamide (DMF). This may be due to additional desolvation energy in going from the ground state to the transition state. In the rearrangements of Ib and Ic in phenols, the activation entropies are highly negative in comparison with those for EtOH. The low entropy of activation may be due to a highly ordered transition state in which the motion of a phenol molecule might be frozen out. The rate constants in *o*-chlorophenol are smaller than those in *p*-chlorophenol. The rate retardation may be attributed to steric interference and intramolecular hydrogen bonding with the *o*-chloro group.[1b]

According to Swain, the nucleophilic substitution reaction might be pictured as resulting from the combination of "pushing" and "pulling" actions.[12] The "pull" may be exerted by solvent and the "push" is exerted by the nucleophile. The resulting carbonium ion may be stabilized by solvation with solvent molecules. Swain's relationship is $\log k/k_0 = n \times S_n + e \times S_e$ where n is a nucleophilicity parameter associated with a nucleophilic reagent, e is an electrophilicity parameter associated with an electrophilic reagent, S_n is the sensitivity of the reaction under consideration to nucleophilic push, and S_e is the sensitivity of this reaction to electrophilic pull. For a group of substitution reactions that are essentially insensitive to nucleophilic push, the Swain equation may, in principle, be simplified to $\log k/k_0 = e \times S_e$, which is identical to the Grunwald–Winstein equation, $\log k/k_0 = Y \times m$.

While a plot of log k *vs.* Y values shows a linear

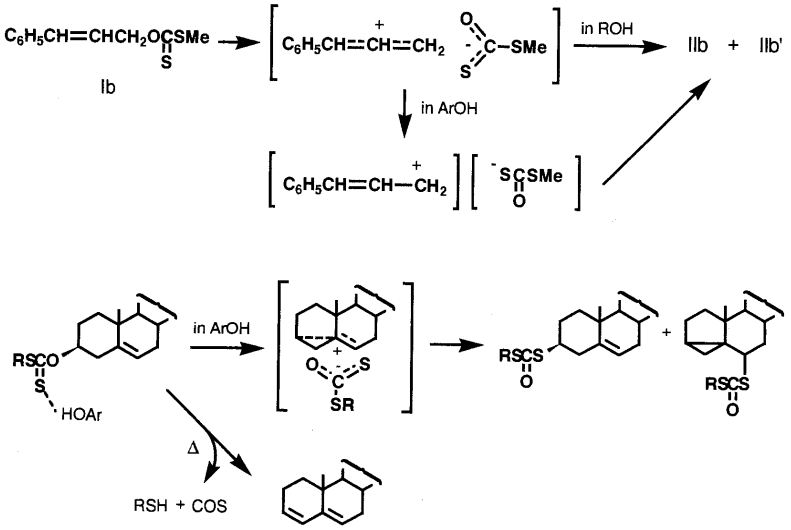

Chart 3

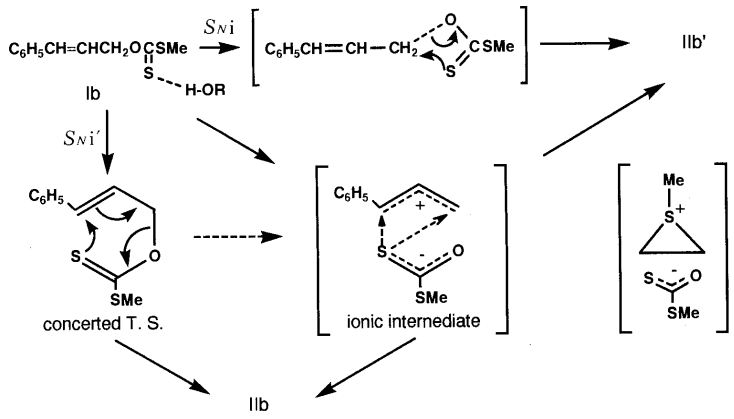

Chart 4

relationship, a plot of log k *vs.* E_T values exhibits some scattering (Fig. 1). In our solvolysis, xanthates mainly act as hydrogen-bond acceptors for protic solvents in a similar manner to *tert*-BuCl, used for evaluation of Y values. As stated above, E_T values are calculated from the results of spectroscopy, and pyridinium *N*-phenoxide betaine dye used for the determination of E_T values exhibits a large permanent dipole moment and has a large π-electron system in addition to being a hydrogen-bond acceptor. In particular, the large dipole moment of the betaine dye reflects the registration of dipole-dipole and dipole-induced dipole interactions between solute and solvent. These considerations may explain why the plot of log k *vs.* E_T values exhibits considerable scattering.

In the dissociation process, the dithiocarbonate moiety, besides being an effective leaving group by hydrogen bonding with protic solvents, acts as a very strong nucleophile by changing the anionic part from $^-O(C=S)SMe$ to $^-S(C=O)SMe$. Consequently, thione–thiol rearrangement of allylic xanthates is considered to be independent of the degree of the nucleophilic push, showing a linear relationship toward Y values.

The mechanism of [3,3]-sigmatropy could involve either a one-stage, concerted process, or ionization to a rigidly oriented intimate ion pair followed by internal return of the sulfur atom of the dithiocarbonate anion (^-SCOSR) to give the rearranged product. For a decision between these alternatives, the response of the rearrangement reaction to changes in solvent composition provides valuable information. The rates of *O*-allyl *S*-methyl dithiocarbonate (Id)[3] are insensitive to the ionizing power of solvents as compared with *O*-(2-methylthioethyl) *S*-methyl xanthate (Ic), which undergoes thione–thiol rearrangement *via* a solvent-separated ion-pair or a free carbonium intermediate [k(80% aqueous EtOH)/k (*tert*-BuOH) = 20, m = 0.402]. In the case of Id, m = 0.141; a threefold increase in rate was observed for the rearrangement in going from *tert*-BuOH to 80% aqueous EtOH [k (80% aqueous EtOH)/k (*tert*-BuOH) = 3.0]. On the other hand, the rearrangement of *O*-cinnamyl *S*-methyl xanthate (Ib) was moderately accelerated by increased polarity of the solvent, m = 0.310; the reaction is about ten times faster in 80% aqueous EtOH than *tert*-BuOH [k (80% aqueous EtOH)/k (*tert*-BuOH) = 10], which indicates a mechanism with more ionic character than that of Id. The solvent effect of phenols is noteworthy. The rearrangement is more than a thousand times faster in phenolic solvent, a highly polar solvent, than in *n*-hexane, which shifts the mechanism of the rearrangement toward an ionic process.

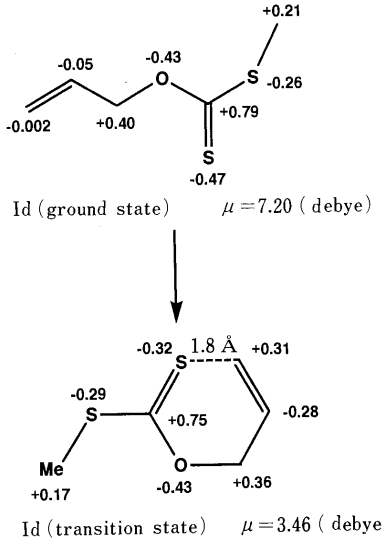

Fig. 7. Change of Net Charges and Dipole Moment in Id Calculated by MINDO/3

These facts indicate that the transition state of allylic xanthate rearrangement has an inherently polarizable structure and may be affected by substituents attached to the allyl moiety and by solvent polarity.

The net charges calculated by MINDO/3 along the reaction coordinate (Table VI) indicate that the electrons participating in the [3,3]-sigmatropic rearrangement delocalize gradually with decreasing $>C=S\cdots CH_2=$ distance, during which the dipole moment changes from 7.20 debye (>5 Å) to 3.46 debye (1.8 Å, cyclic transition state). This indicates that an early stage of the [3,3]-sigmatropic rearrangement may be affected by solvation of the reaction medium used (Table VI and Fig. 7).

In strongly ionizing solvents such as phenols, which have strong hydrogen-bonding ability to the anionic center, the degree of electron delocalization might be affected both in the ground state and in the transition state, causing alteration of the mechanism from nonionic to ionic. The MINDO/3 calculation on phenylallyl cation indicates that the magnitudes of the LUMO (lowest unoccupied molecular orbital) coefficient and net charge of the γ-position of the phenylallyl cation ($[Ph\text{-}C\gamma\ H{=}{=}C\beta\ H{=}{=}C\alpha\ H_2]^+$) are larger

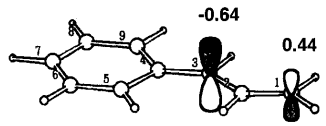

LUMO coefficients

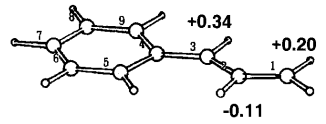

net charges

Fig. 8. The LUMO Coefficients and Net Charges of Cinnamyl Cation Calculated by MINDO/3

than those of the α-position, suggesting that nucleophilic attack at the γ-position predominates over that at the α-position, which is consistent with the product ratio observed in the phenolysis reaction (Fig. 8). It is reasonable to expect that a thermodynamically stable localized ion ($PhCH=CHCH_2^+$)[13] would not intervene in the reaction and the cyclic transition state may ionize to a loosely oriented intimate ion pair (see Chart 4) followed by internal return of the anion (^-SCOSMe) to give the thione–thiol rearranged products.

In summary, the concerted rearrangement of *O*-cinnamyl *S*-alkyl xanthate in aprotic solvents and the ionic rearrangement in phenolic solvents are considered to be the extremes in a continuous spectrum of mechanisms, and the transition state may have considerable polar character.

The rate constants obtained may be useful as a new scale of solvent ionizing power for solvent-sensitive chemical reactions, in particular as a measure of the hydrogen-bonding capacity of solvents with a sulfur atom.

Experimental

^{1}H-NMR spectra were taken with Hitachi R-600 and JEOL GX-400 spectrometers for *ca.* 10% (w/v) solution, with tetramethylsilane (TMS) as an internal standard; chemical shifts are expressed in δ values. Infrared (IR) spectra were recorded on a Hitachi 270-30 infrared spectrophotometer equipped with a grating. Ultraviolet (UV) spectra were recorded on a Hitachi 150-20 spectrophotometer.

Molecular orbital calculations were performed on a Facom M-360 computer in the Computer Center of Kumamoto University. Molecular modeling and least-squares calculations were performed on a Fujitsu FM-16β or FMR-60 personal computer.

Preparation of *O*,*S*-Dialkyl Xanthates (Ia—c) *O*-Cinnamyl[3] (Ib) and *O*-(2-methylthioethyl)[4] (Ic) *S*-methyl xanthates were prepared according to the reported methods.

Compound Ic was purified by column chromatography on silica gel and obtained as an oil (yield 95%). IR (liquid film) cm^{-1}: 1218, 1070 (–O(C=S)SMe). ^{1}H-NMR (in $CDCl_3$): 2.20 (3H, s, SMe), 2.59 (3H, s, –O(C=S)SMe), 2.89 (2H, d, $-SCH_2-$), 4.79 (2H, d, $-OCH_2-$).

Solvolysis of *O*-Cinnamyl *S*-Methyl Xanthate (Ib) in Aqueous EtOH A solution of Ib in aqueous EtOH was heated at 60 °C on a water bath until the completion of the reaction had been confirmed by UV spectrophotometry. The product was extracted with $CHCl_3$. The solvent was evaporated off to leave IIb and IIb′ as a colorless oil.

The solvolysis of Ib in 80% EtOH gave a mixture of IIb (89.7%) and IIb′ (10.3%). The structures of IIb and IIb′ were determined by analysis of the 400 MHz ^{1}H-NMR spectrum. IIb: IR (liquid film) cm^{-1}: 1644, 872 (–S(C=O)S–), 926, 980 (–CH=CH_2). ^{1}H-NMR (in $CDCl_3$): 2.41 (3H, s, SMe), 5.22 (1H, d, =CH_2), 5.27 (1H, d, =CH_2), 5.42 (1H, 2, >CHS–), 6.09 (1H, ddd, –CH=). IIb′: IR (liquid film) cm^{-1}: 1644, 872 (–S(C=O)S–), 968 (–CH=CH–): ^{1}H-NMR (in $CDCl_3$): 2.44 (3H, s, SMe), 3.83 (2H, d, $-CH_2S-$), 6.19 (1H, td, =CH–C–S–), 6.58 (1H, d, PhCH=).

The solvolysis of Ib in 100% EtOH gave a mixture of IIb (96%) and IIb′ (4%).

Phenolysis of Ib in Phenol–Benzene Solution A solution of Ib (200 mg, 0.89 mmol) in phenol (21.3 mmol) was heated at 60 °C for 0.5 h. The product was purified by chromatography on silica gel and obtained as a colorless oil (yield 190 mg, 95%). The ^{1}H-NMR spectrum showed the ratio of IIb: IIb′ to be 64.2: 35.8.

Kinetics The reaction rates were followed at a given temperature by measuring the decrease of the thiocarbonyl absorption at *ca.* 350 nm (14.3—27.7 mmol/l), using a ground-glass-stoppered 10 × 10 mm Pyrex cell, which was thermostated with flowing water at constant temperature. The absorption data were collected automatically. The first-order rate constants were calculated from a plot of ln $(A_t - A_\infty)$ *vs.* time by a least-squares method, where A_t is the absorbance at time t and A_∞ is the absorbance after about 10 half-lives. All spectra were calculated by means of a nonweighted least-squares program written in F-BASIC86 V3.1.

Acknowledgment The authors wish to express their thanks to the members of the Analytical Department of our University, for measurement of NMR spectra. They are also grateful to Mr. H. Nakatomi, President of Hisamitsu Pharmaceutical Co. Inc., for financial support.

References and Notes

1) *a*) K. Harano, H. Kiyonaga and T. Hisano, *Chem. Pharm. Bull.*, **35**, 1388 (1987); *b*) K. Harano, K. Miyoshi and T. Hisano, *Chem. Pharm. Bull.*, **33**, 1861 (1985).
2) *a*) E. Grunwald and S. Winstein, *J. Am. Chem. Soc.*, **70**, 846 (1948); *b*) A. H. Fainberg and S. Winstein, *ibid.*, **78**, 2770 (1956).
3) K. Harano and T. Taguchi, *Chem. Pharm. Bull.*, **23**, 467 (1975).
4) T. Taguchi, Y. Kawazoe, K. Yoshihira, H. Kanayama, T. Tabata, M. Mori and K. Harano, *Tetrahedron Lett.*, **1965**, 2717.
5) *a*) C. Reichardt, *Angew. Chem.*, **77**, 30 (1965); *b*) *Idem*, *Pure Appl. Chem.*, **54**, 1867 (1982).
6) M. J. S. Dewar and J. J. Stewart, "Quantum Chemistry Program Exchange (QCPE), Program No. 464," Indiana University, 1984.
7) *a*) B. Dahlen, *Acta Chem. Scand., Ser. A*, **31**, 407 (1977); *b*) J. Abrahamsson and R. Pearson, *Acta Crystallogr., Sect. B*, **32**, 2745 (1976); *c*) N. J. Brondmo, S. Esperas and S. Husebye, *Acta Chem. Scand., Ser. A*, **29**, 93 (1975).
8) *a*) It is worth noting that the C=S bond length (1.597Å) is shorter than that of 1.6260 Å in X-ray structures of *O*-ethyl *S*-carboxyethyl[7a] and *S*-(11-carboxyundecyl)[7b] xanthates and longer than that found in sulfur di(methylxanthate)[7c] derived from X-ray crystallographic investigation (1.5709 Å).
The conformations of the allyl and methyl groups of the most stable structure are interesting. The two groups lie within the plane of the –O–(C=S)–S– group with *syn* dispositions with regard to the C=S bond (W-shaped conformation). This structural feature has been observed in crystal structures of *O*-ethyl *S*-carboxyethyl xanthate[7a] and *O*-ethyl *S*-(11-carboxyundecyl) xanthate.[7b]
9) The C=O distance of 1.177 Å is shorter than the C=O distance of 1.215 Å in acetone: M. J. S. Dewar, D. H. Lo and C. A. Ramsden, *J. Am. Chem. Soc.*, **97**, 1311 (1975).
10) It was reported that the summation of the bond energies shows thione-to-thiol rearrangement to be an exothermic reaction to the extent of about 20—24 kcal/mol: C. H. DePuy and R. W. King, *Chem. Rev.*, **60**, 431 (1960); F. N. Jones, *J. Org. Chem.*, **33**, 4290 (1968).
11) R. H. DeWolfe and W. G. Young, "The Chemistry of Alkenes," ed. by S. Patai, John Wiley and Sons, Ltd., London, 1974, Chapter 10.
12) C. G. Swain, *J. Am. Chem. Soc.*, **70**, 1119 (1948).
13) P. B. D. de la Mare, "Molecular Rearrangements: Rearrangements in the Chemistry of Allylic Compounds," Part 1, ed. by P. de Mayo, John Wiley and Sons, Inc., New York, 1963, Chapter 2.

New Toxic Metabolites from a Mushroom, *Hebeloma vinosophyllum*. III.[1a] Isolation and Structures of Three New Glycosides, Hebevinosides XII, XIII and XIV, and Productivity of the Hebevinosides at Three Growth Stages of the Mushroom

Haruhiro FUJIMOTO,* Kaijiro MAEDA and Mikio YAMAZAKI

Faculty of Pharmaceutical Sciences, Chiba University, 1–33, Yayoi-cho, Chiba 260, Japan. *Received January 30, 1991*

Three new triterpene glycosides, hebevinosides XII, XIII and XIV, were isolated besides five already known neurotoxic hebevinosides from acetone extract of the mycelium with primordia of a poisonous mushroom, *Hebeloma vinosophyllum*, and their structures were deduced to be 3β,7β,16β-trihydroxycucurbita-5,24-diene-3-*O*-β-D-xylopyranoside-16-*O*-(4-*O*-acetyl)-β-D-glucopyranoside, 3β,7β,16β-trihydroxycucurbita-5, 24-diene-3-*O*-(3,4-di-*O*-acetyl)-β-D-xylopyranoside-16-*O*-(4,6-di-*O*-acetyl)-β-D-glucopyranoside and 3β,7β,16β-trihydroxycucurbita-5,24-diene-3-*O*-(3,4-di-*O*-acetyl)-β-D-xylopyranoside-16-*O*-(6-*O*-acetyl)-β-D-glucopyranoside, respectively.

Productivity of the eight hebevinosides was studied at three growth stages of the organism; mycelium (stage I), mycelium with primordia (stage II) and mycelium with fruit-bodies (stage III). The ratio of production of total hebevinosides at stages I : II : III was approximately 6 : 4 : 25. Production of hebevinosides VII, XIV, XIII, VIII and XII having the acetyl groups at *O*-4 in the glucosyl and/or *O*-3 in the xylosyl moieties, which are comparatively labile, decreased, and that of hebevinosides III and II having the acetyl groups at *O*-6 in the glucosyl and/or *O*-4 in the xylosyl moieties, which are relatively stable, increased in the time course from stage I to stage III. On the other hand, production of hebevinoside VI having no acetyl group was independent of the growth stages. Production of ergostane-type sterols seemed to be activated for the first time at stage III in the organism.

Keywords Basidiomycetes; *Hebeloma vinosophyllum*; neurotoxin; mushroom toxin; hebevinoside; triterpene glycoside; cucurbitane; productivity; growth stage

Recently we isolated eleven new neurotoxic glycosides named hebevinosides I (**1**), II (**2**), III (**3**), IV (**4**), V (**5**), VI (**6**), VII (**7**), VIII (**8**), IX (**9**), X (**10**) and XI (**11**) from a poisonous mushroom, *Hebeloma* (*H.*) *vinosophyllum*,[1] and proved that **2**, **3**, **6**, **7**, **8** and **9**, whose common aglycone is 3β,7β,16β-trihydroxycucurbita-5,24-diene (hydroxyhebevinogenin), are genuine metabolites and the others, whose common aglycone is 3β,16β-dihydroxy-7β-methoxycucurbita-5,24-diene (methoxyhebevinogenin), are artifacts formed from the genuine metabolites during extraction of the mushroom with aqueous methanol.[1a] All of these hebevinosides were isolated from the cultivated mycelium with fruit-bodies. Among six genuine hebevinosides, diglycosidic **2**, **3**, **6**, **7** and **8** were major components and monoglycosidic **9** was minor in the glycoside fraction.[1]

When fresh filamentous hyphae of *H. vinosophyllum* are inoculated on potato dextrose agar (PDA) medium,[2] the hyphae grow first into a mycelium (growth stage I), then into a mycelium with primordia (growth stage II), and further into a mycelium with fruit-bodies (growth stage III). These three growth stages of the organism are distinguishable morphologically. The mycelium is a mass of white filamentous hyphae, the primordium is a pale pink cylindrical projection 2—3 mm across and 5—15 mm high, and the fruit-body is composed of a brown cap 10—40 mm across, many gills having a lot of wine-colored spores and a pale pink stem 20—100 mm high (see Fig. 1). We intended to study whether or not productivity of hebevinosides is related to the growth stages. For this purpose, *H. vinosophyllum* was cultivated in the dark, because any change on cultivation becomes synchronous in the dark, though the growth time from hyphae to mycelium with fruit-bodies on cultivation in the dark is about 1.6 times longer than that in the light. Three new triterpene glycosides

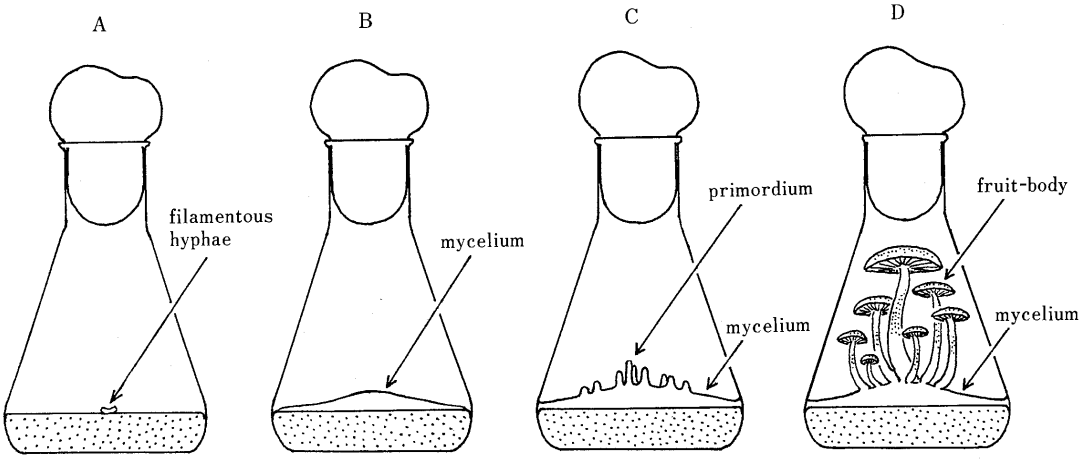

Fig. 1. Three Growth Stages of *H. vinosophyllum* in the Dark

A, inoculation of filamentous hyphae; B, growth stage I (mycelium); C, growth stage II (mycelium with primordia); D, growth stage III (mycelium with fruit-bodies).

named hebevinosides XII (**12**), XIII (**13**) and XIV (**14**) have been isolated in this experiment, besides the five known diglycosidic hebevinosides, from the organism at growth stages I and II.

Isolation of Three New Hebevinosides After drying, *H. vinosophyllum* cultivated in the dark for 12 (stage I), 28 (stage II) or 73 d (stage III) was extracted with acetone. Each acetone extract was then divided into *n*-hexane-soluble (HS) and -insoluble (HI) fractions. Each HI fraction was separated repeatedly by high-performance liquid chromatography (HPLC) using reversed-phase octadecylsilica gel (ODS) columns. On the chromatography, the HI fraction at growth stage II afforded **6**, **3**, **12**, **7**, **2**, **8**, **14** and **13** (yield (%) from the dried organism: 0.061, 0.097, 0.022, 0.092, 0.092, 0.026, 0.067 and 0.036, respectively). Among these eight hebevinosides, **12**, **13** and **14** were unknown, and were named hebevinosides XII, XIII and XIV, respectively.

The ^{1}H-nuclear magnetic resonance (^{1}H-NMR) spectrum of **12** showed that **12** has an acetyl group (δ 2.06 (3H, s, $-COCH_3$)). On acetylation, **12** afforded a heptaacetate which was identical with the heptaacetate of **3** (**15**).[1b] The ^{13}C-nuclear magnetic resonance (^{13}C-NMR) spectrum of **12** was compared with that of **6**, which is identical with the deacetyl derivative of **3** (hydroxyhebevinogenin (**16**)-3-*O*-β-D-xylopyranoside-16-*O*-β-D-glucopyranoside).[1a] All signals in the ^{13}C-NMR spectrum of **12** were quite similar to those of **6** except that the signals of an acetyl group are observed and the signals of C-3, -4 and -5 in the glucosyl moiety are shifted to δ 75.9 (−2.7), 73.1 (+1.0) and 75.9 (−2.2) (see Table I). By considering the acetylation shift rule,[3] it was suggested that the acetyl group in **12**, which is a monoacetyl derivative of **6**, should be present at *O*-4 in the glucosyl moiety. This expectation was also supported by the fact that the signal of H-4 in the glucosyl moiety is seen at δ 5.65 in the ^{1}H-NMR spectrum of **12** (see Experimental). Thus, the structure of **12** was deduced to be **16**-3-*O*-β-D-xylopyranoside-16-*O*-(4-*O*-acetyl)-β-D-glucopyranoside, as shown in Chart 1.

The ^{1}H-NMR spectrum of **13** showed that **13** has four acetyl groups (δ 2.02, 2.08, 2.11 and 2.12 (each 3H, s, $-COCH_3$)). On acetylation, **13** afforded a tetraacetate, which was identical with **15**.[1b] All signals in the ^{13}C-NMR spectrum of **13** were quite similar to those of **6**[1a] except that the signals of four acetyl groups are observed and the signals of C-2, -3, -4 and -5 in the xylosyl moiety are shifted to δ 72.1 (−2.9), 75.4 (−3.1), 70.6 (−0.5) and 62.8 (−4.3) and the signals of C-3, -4, -5 and -6 in the glucosyl moiety are also shifted to δ 75.4 (−3.2), 72.4 (+0.3), 72.4 (−5.7) and 63.5 (+0.3), respectively (see Table I). By considering the additivity rule of acylation shift parameters,[4] it was suggested that the four acetyl groups in **13**, which is a tetraacetyl derivative of **6**, should be present at *O*-3 and -4 in the xylosyl and at *O*-4 and -6 in the glucosyl moieties. This expectation was also supported by the fact that the signals of the glucosyl moiety in the ^{13}C-NMR spectrum of **13** are quite similar to those of **7**, which has the two acetyl groups at *O*-4 and -6 in the glucosyl moiety[1a] (see Table I), and was further supported by the fact that the signals of H-3 and -4 in the xylosyl moiety are present at δ 5.08 and 5.00 and those of H-4, -6a and -6b in the glucosyl moiety at δ 4.90, 4.08 and 4.22, respectively, in the ^{1}H-NMR spectrum of **13** (see Experimental). Thus, the structure of **13** was deduced to be **16**-3-*O*-(3,4-di-*O*-acetyl)-β-D-xylopyranoside-16-*O*-(4,6-di-*O*-acetyl)-β-D-glucopyranoside, as shown in Chart 1.

The ^{1}H-NMR spectrum of **14** showed that **14** has three acetyl groups (δ 2.03, 2.09 and 2.13 (each 3H, s, $-COCH_3$)). On acetylation, **14** afforded a pentaacetate, which was identical with **15**.[1b] All signals in the ^{13}C-NMR spectrum of **14** were quite similar to those of **6** except that the signals of three acetyl groups are observed and the signals of C-2, -3, -4 and -5 in the xylosyl moiety are shifted to δ 72.2 (−2.8), 75.5 (−3.0), 70.6 (−0.5) and 62.7 (−4.4) and the signals of C-5 and -6 in the glucosyl moiety are also shifted to δ 75.5 (−2.6) and 64.7 (+1.5), respectively (see Table I). Based on both the additivity rule of acylation shift

Table I. ^{13}C-NMR Data for Hebevinosides III (**3**), VI (**6**), VII (**7**), XII (**12**), XIII (**13**) and XIV (**14**), δ (ppm) from TMS in C_5D_5N

Position	**3**[1b]	**6**[1a]	**7**[1a]	**12**	**13**	**14**
3	87.4	87.4	87.4	87.5	87.6	87.5
5	146.3	146.2	146.4	146.2	146.1	146.1
6	122.4	122.6	122.5	122.6	122.7	122.7
7	67.5	67.3	67.4	67.3	67.4	67.5
16	82.2	81.9	82.5	82.1	82.5	82.2
24	126.8	126.8	126.9	126.9	126.9	126.8
25	129.9	130.0	130.1	130.0	130.0	130.0
Xylose-1	107.7	107.6	107.6	107.7	106.9	106.8
Xylose-2	75.1	75.0	75.1	75.0	72.1	72.2
Xylose-3	78.4	78.5	78.5	78.5	75.4	75.5
Xylose-4	71.1	71.1	71.1	71.1	70.6	70.6
Xylose-5	66.8	67.1	67.1	67.1	62.8	62.7
Glucose-1	106.6	106.6	106.5	106.5	106.5	106.5
Glucose-2	75.0	75.7	75.6[a]	75.8[b]	75.6	74.9
Glucose-3	78.6	78.6	75.5[a]	75.9[b]	75.4	78.3
Glucose-4	71.9	72.1	72.4	73.1	72.4	71.8
Glucose-5	75.6	78.1	72.4	75.9[b]	72.4	75.5
Glucose-6	64.8	63.2	63.6	62.5	63.5	64.7
$COCH_3$	20.8		20.8	21.1	20.6	20.6
			20.9		20.8	20.8
					20.9	20.9
					20.9	
$COCH_3$	170.8		170.5	170.6	170.2	170.2
			170.7		170.4	170.4
					170.4	170.8
					170.6	

a, *b*) Assignments may be interchanged.

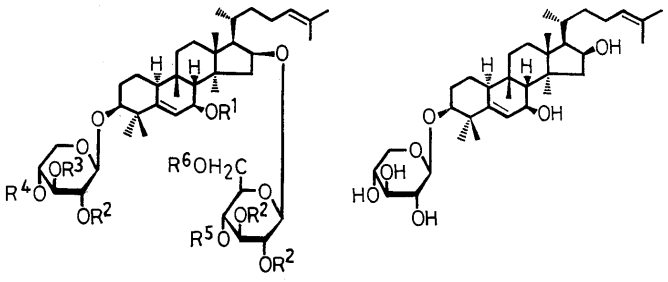

2: $R^1=R^2=R^3=R^5=H$, $R^4=R^6=COCH_3$
3: $R^1=R^2=R^3=R^4=R^5=H$, $R^6=COCH_3$
6: $R^1=R^2=R^3=R^4=R^5=R^6=H$
7: $R^1=R^2=R^3=R^4=H$, $R^5=R^6=COCH_3$
8: $R^1=R^2=R^3=H$, $R^4=R^5=R^6=COCH_3$
12: $R^1=R^2=R^3=R^4=R^6=H$, $R^5=COCH_3$
13: $R^1=R^2=H$, $R^3=R^4=R^5=R^6=COCH_3$
14: $R^1=R^2=R^5=H$, $R^3=R^4=R^6=COCH_3$
15: $R^1=R^2=R^3=R^4=R^5=R^6=COCH_3$

9

Chart 1

parameters[4] and the acetylation shift tule,[3] it was suggested that the three acetyl groups in **14**, which is a triacetyl derivative of **6**, should be present at *O*-3 and -4 in the xylosyl and at *O*-6 in the glucosyl moieties. This expectation was also supported by the fact that the signals of the xylosyl and the glucosyl moieties in the ^{13}C-NMR spectrum of **14** are quite similar to those of the xylosyl moiety of **13** and the glucosyl moiety of **3**, which has an acetyl group at *O*-6 in the glucosyl moiety[1b] (see Table I), and was further supported by the fact that the signals of H-3 and -4 in the xylosyl moiety are present at δ 5.09 and 4.89 and those of H-6a and -6b in the glucosyl moiety at δ 4.03 and 4.16, respectively, in the ^{1}H-NMR spectrum of **14** (see Experimental). Accordingly, the structure of **14** was deduced to be **16**-3-*O*-(3,4-di-*O*-acetyl)-β-D-xylopyranoside-16-*O*-(6-*O*-acetyl)-β-D-glucopyranoside, as shown in Chart 1.

Productivity of the Hebevinosides at Three Growth Stages On HPLC separation using reversed-phase ODS columns, the HI fraction from growth stage I afforded **6**, **3**, **12**, **7**, **2**, **8**, **14** and **13** (yields (%) from the dried organism: 0.079, 0.035, 0.011. 0.269, 0.014, 0.046, 0.211 and 0.073, respectively). On the other hand, the HI fraction from growth stage III afforded **6**, **3**, **7**, **2**, **8** and **14** (yields (%) from the dried organism: 0.391, 0.982, 0.370, 1.110, 0.072 and 0.149, respectively), but afforded none of **12** and **13**. The yields of total hebevinosides from the dried organism at growth stages I, II and III were 0.738, 0.493 and 3.074%, respectively (approximate production ratio of total hebevinosides at stage I : II : III = 6 : 4 : 25). These data indicated that the production of **7**, **14**, **13**, **8** and **12** decreases and that of **3** and **2** increases in the time course from growth stage I to stage III, but **6** is produced constantly throughout the three stages. It is well known that the migration of acyl groups from *O*-4 to -6 and from *O*-3 to -6, or reversible migration of an acyl group between *O*-2 and -3, occurs easily in β-D-glucopyranoside on acid- or base-catalyzed or thermal conditions.[5] Under such conditions, an acyl group migrates easily from *O*-4 to -6 and migrates reversibly between *O*-2 and -3 when the glucoside takes the $^4C_1$ (D) conformation and an acyl group migrates easily from *O*-3 to -6 when the glucoside takes the $^1C_4$ (D) conformation.[5] These considerations suggest that acyl groups at *O*-2, -3 and -4 are more labile than that at *O*-6 in β-D-glucopyranoside. Meanwhile, the stereostructure of the pyranose-ring part in β-D-xylopyranoside seems to be similar to that of the corresponding part in β-D-glucopyranoside. The occurrence of reversible migration of an acyl group between *O*-2 and -3 in the $^4C_1$(D) conformation is therefore considered likely in β-D-xylopyranoside (D-xylose lacks C-6). Consequently, it is considered that acyl groups at *O*-2 and -3 may be more labile than that at *O*-4 in β-D-xylopyranoside. It has been observed that the production of **7**, **14**, **13**, **8** and **12** decreases, whereas that of **3** and **2** increases in passing from growth stage I to III. The former hebevinosides have acetyl groups at *O*-4 in the glucosyl and/or *O*-3 in the xylosyl moieties, which are comparatively labile. On the other hand, the latter hebevinosides have the acetyl groups at *O*-6 in the glucosyl and/or *O*-4 in the xylosyl moieties, which are relatively stable. The productivity of **6** having no acetyl group is independent of the growth stages.

Isolation of Ergostane-Type Sterols from the HS Fraction at Growth Stage III On inspection by HPLC using a silica gel column and gas-liquid chromatography (GLC), the presence of three metabolites was clearly observed in the HS fraction from stage III but not in those from stages I and II. One of these metabolites was proved to be ergosterol, and the other two were obtained as a mixture on HPLC. After acetylation, this mixture afforded two peaks (ratio, 1 : 1) on GLC. Comparison of the ^{13}C-NMR data of the two metabolites with those of known sterols[6] suggested that they are ergosta-7,22-dien-3β-ol and ergost-7-en-3β-ol. Ergosterol was previously isolated from mycelia with fruit-bodies of the organism.[7] Ergosta-7,22-dien-3β-ol and ergost-7-en-3β-ol are the common components in the fugal kingdom.[8] It is well known that ergostane-type sterols are biosynthesized from squalene-2,3-epoxide *via* a lanostane-type precursor in fungi.[9] Biosynthesis of ergostane-type sterols seems to be activated for the first time at stage III in *H. vinosophyllum*.

Experimental

The optical rotations were measured with a JASCO DIP-140 digital polarimeter. The ultraviolet (UV) spectra were recorded with a Hitachi U-3400 recording spectrometer, the infrared (IR) spectra with a Hitachi EPI-G3 grating infrared spectrometer, and the ^{1}H-NMR and ^{13}C-NMR spectra with a JEOL JNM GX-270 or a JEOL FX-270 FT-NMR spectrometer at 270 and 67.8 MHz, respectively. Chemical shifts are expressed in δ (ppm) values from tetramethylsilane (TMS) as an internal standard. The thin layer chromatograhy (TLC) analyses were carried out with silica gel plates (Merck Kieselgel 60G), the HPLC separations with columns of ODS (Senshu 5301-S, 20 i.d. × 300 mm and 4251-S, 10 i.d. × 250 mm) and silica gel (Senshu 5251-N, 20 i.d. × 250 mm) on an HPLC system (Senshu Flow System 3100, Senshu Pressure Control 3110 and Erma RI-Detector ERC-7521 or -7522), and the GLC analyses with a column of Silicon OV-I Chromosorb W AW DMCS (80—100 mesh, 3 i.d. × 2000 mm; column temperature, 245 °C; carrier gas, N_2 42 ml/min) on a Shimadzu GC-5A gas chromatograph equipped with an FID-detector. *H. vinosophyllum* was cultivated on PDA medium[2] at 25 °C in a dark room for 12 d to get mycelia, for 28 d to get mycelia with primordia and for 73 d to get mycelia with fruit-bodies.

Isolation of Hebevinosides II (2), III (3), VI (6), VII (7), VIII (8), XII (12), XIII (13) and XIV (14) Dried mycelia with primordia (73.40 g) at growth stage II were cut into fine pieces and shaken in acetone (1.0 l) at room temperature for 12 h four times to afford an acetone extract (6.70 g). The acetone extract was divided with *n*-hexane (0.5 l) into HS fraction (yield after evaporation of the solvent: 1.710 g) and HI fraction (4.990 g). The HI fraction was chromatographed on an ODS column (Senshu 5301-S) in the HPLC system with 20% aqueous acetone (flow rate: 4.0 ml/min) and an ODS column (Senshu 4251-S) in the HPLC system with 25% aqueous CH_3CN (flow rate: 2.0 ml/min) successively, to afford **6** (44.8 mg), **3** (71.2 mg), **12** (16.1 mg), **7** (67.5 mg), **2** (67.5 mg), **8** (19.1 mg), **14** (49.2 mg) and **13** (26.4 mg).

Dried mycelia (8.95 g) at growth stage I were cut into fine pieces and shaken in acetone (350 ml) at room temperature for 12 h four times to afford an acetone extract (0.38 g), which was divided with *n*-hexane (350 ml) into HS fraction (yield after evaporation of the solvent: 0.181 g) and HI fraction (0.199 g). The HI fraction was chromatographed in a similar way to that described for chromatography of the HI fraction from mycelia with primordia to afford **6** (7.1 mg), **3** (3.1 mg), **12** (1.0 mg), **7** (24.1 mg), **2** (1.3 mg), **8** (4.1 mg), **14** (18.9 mg) and **13** (6.5 mg).

Dried mycelia with fruit-bodies (4.30 g) at growth stage III were cut into fine pieces and shaken in acetone (150 ml) at room temperature for 12 h four times to afford an acetone extract (0.30 g), which was divided with *n*-hexane (150 mg) into HS fraction (yield after evaporation of the solvent: 0.045 g) and HI fraction (0.255 g). The HI fraction was chromatogaphed in a similar way to that described for chromatography of the HI fraction from mycelia with primordia to afford **6** (16.8 mg), **3** (42.2 mg), **7** (15.9 mg), **2** (47.7 mg), **8** (3.1 mg) and **14** (6.4 mg).

Hebevinoside XII (**12**): Amorphous solid. $[\alpha]_D^{22}$ +60° (c=0.36, pyridine). UV in CH_3CN: end absorption. IR ν_{max}^{KBr} cm^{-1}: 3400, 1730, 1640, 1075, 1035. ^{1}H-NMR (C_5D_5N) δ: 0.78, 1.11, 1.20, 1.38, 1.67 (each 3H, s), 1.05 (3H, d, J=6.4 Hz, H_3-21), 1.73, 1.77 (each 3H, s, H_3-26, -27), 2.06 (3H, s, Ac), 4.36 (1H, d, J=4.9 Hz, H-7), 4.75 (1H, d, J=7.6 Hz, H-glc.

1), 4.84 (1H, d, J=7.6 Hz, H-xyl. 1), 5.56 (1H, t, J=7.7 Hz, H-24), 5.65 (1H, t, J=9.6 Hz, H-glc. 4), 6.04 (1H, d, J=4.9 Hz, H-6). Compound **12** (3.0 mg) was acetylated with Ac_2O (0.1 ml) in pyridine (0.2 ml) at 25 °C overnight to afford a heptaacetate (3.0 mg, amorphous solid), which was identical with the heptaacetate of **3** (**15**)[1b] in terms of ^{1}H-NMR spectra ($CDCl_3$) and TLC behavior (solvent: $CHCl_3$–MeOH (50 : 1, v/v)).

Hebevinoside XIII (**13**): Amorphous solid. $[\alpha]_D^{21}$ +35° (c=0.42, $CHCl_3$). UV in CH_3CN: end absorption. IR_{max}^{KBr} cm^{-1}: 3430, 1750, 1645, 1070, 1040. ^{1}H-NMR ($CDCl_3$) δ: 0.66, 1.00, 1.05, 1.08, 1.21 (each 3H, s), 0.95 (3H, d, J=6.6 Hz, H_3-21), 1.61, 1.68 (each 3H, s, H_3-26, -27), 2.02, 2.08 2.11, 2.12 (each 3H, s, Ac), 3.31 (1H, dd, J_1=11.6, J_2=8.7 Hz, H-xyl. 5a), 3.64 (1H, m, H-glc. 5), 3.67 (1H, t-like, H-glc. 3), 4.06 (1H, d, J=5.2 Hz, H-7), 4.08 (1H, dd, J_1=11.8, J_2=5.0 Hz, H-glc. 6a), 4.22 (1H, dd, H-glc. 6b), 4.45 (1H, d, J=7.6 Hz, H-glc. 1), 4.51 (1H, d, J=6.7 Hz, H-xyl. 1), 4.90 (1H, t, J=7.8 Hz, H-glc. 4), 5.00 (1H, br t, J=8.7 Hz, H-xyl. 4), 5.08 (1H, t, J=9.3 Hz, H-xyl. 3), 5.13 (1H, t, J=8.5 Hz, H-24), 5.61 (1H, d, J=5.2 Hz, H-6). Compound **13** (3.1 mg) was acetylated with Ac_2O (0.1 ml) in pyridine (0.2 ml) at 25 °C overnight to afford a tetraacetate (3.1 mg, amorphous solid), which was identical with the heptaacetate of **3** (**15**)[1b] in terms of ^{1}H-NMR spectra ($CDCl_3$) and TLC behavior (solvent: $CHCl_3$–MeOH (50 : 1, v/v)).

Hebevinoside XIV (**14**): Amorphous solid. $[\alpha]_D^{24}$ +15° (c=0.40, $CHCl_3$). UV in CH_3CN: end absorption. IR_{max}^{KBr} cm^{-1}: 3450, 1740, 1635, 1065, 1030. ^{1}H-NMR ($CDCl_3$) δ: 0.66, 1.00, 1.04, 1.07, 1.21 (each 3H, s), 0.94 (3H, d, J=6.4 Hz, H_3-21), 1.61, 1.68 (each 3H, s, H_3-26, -27), 2.03, 2.09, 2.13 (each 3H, s, Ac), 3.31 (1H, dd, J_1=12.2, J_2=9.0 Hz, H-xyl. 5a), 3.52 (1H, m, H-glc. 5), 3.94 (1H, d, J=4.8 Hz, H-7), 4.03 (1H, dd, J_1=11.6, J_2=5.2 Hz, H-glc. 6a), 4.16 (1H, dd, H-glc. 6b), 4.18 (1H, d, J=7.6 Hz, H-glc. 1), 4.35 (1H, d, J=7.3 Hz, H-xyl. 1), 4.89 (1H, dt, J_1=J_2=9.0, J_3=5.2 Hz, H-xyl. 4), 5.09 (1H, t, J=9.0 Hz, H-xyl. 3), 5.13 (1H, t, J=7.3 Hz, H-24), 5.71 (1H, d, J=4.8 Hz, H-6). Compound **14** (3.5 mg) was acetylated with Ac_2O (0.1 ml) in pyridine (0.2 ml) at 25 °C overnight to afford a pentaacetate (3.2 mg, amorphous solid), which was identical with the heptaacetate of **3** (**15**)[1b] in terms of ^{1}H-NMR spectra ($CDCl_3$) and TLC behavior (solvent: $CHCl_3$–MeOH (50 : 1, v/v)).

Isolation of Ergosterol and Other Ergostane-Type Sterols from the HS Fraction at Growth Stage III Comparison of the HS fraction at growth stage III with the corresponding fractions at growth stages I and II by HPLC (column: silica gel (Senshu 5251-N); solvent: $CHCl_3$–acetone (20 : 1, v/v); flow rate: 4.0 ml/min) indicated that the HS fraction at stage III affords two peaks which are not afforded by the HS fractions at stages I and II. Under the HPLC conditions used, the retention times (t_R) of the two peaks were 21.1 and 22.5 min, respectively. The HS fraction at growth stage III (45 mg) was chromatographed under these HPLC conditions to afford one fraction whose t_R is 21.1 min (8.7 mg, colorless amorphous solid), and another fraction whose t_R is 22.5 min (2.8 mg, colorless amorphous solid).

The fraction whose t_R is 21.1 min afforded after crystallization from ether, colorless needles, mp 170—172 °C. This product was identical with authentic ergosterol in terms of mixed melting point, ^{1}H- and ^{13}C-NMR spectra ($CDCl_3$), and TLC behavior (solvent: *n*-hexane–AcOEt (3 : 1, v/v)).

The fraction whose t_R is 22.5 min was supposed to be a mixture of ergosta-7,22-dien-3β-ol (component A) and ergost-7-en-3β-ol (component B) from the following ^{13}C- and ^{1}H-NMR data.

^{13}C-NMR ($CDCl_3$): Component A δ: 12.1 (q, C-18), 13.0 (q, C-19), 17.6 (q, C-28), 19.6 (q, C-26), 19.9 (q, C-27), 21.1 (q, C-21), 21.5 (t, C-11), 22.9 (t, C-15), 28.1 (t, C-16), 29.6 (t, C-6), 31.5 (t, C-2), 33.1 (d, C-25), 34.2 (s, C-10), 37.1 (t, C-1), 38.0 (t, C-4), 39.4 (t, C-12), 40.2 (d, C-5), 40.4 (d, C-20), 42.8 (d, C-24), 43.3 (s, C-13), 49.4 (d, C-9), 55.0 (d, C-14), 56.0 (d, C-17), 71.0 (d, C-3), 117.4 (d, C-7), 131.9 (d, C-23), 135.6 (d, C-22), 139.6 (s, C-8).

Component B δ: 11.8 (q, C-18), 13.0 (q, C-19), 15.4 (q, C-28), 17.6 (q, C-27), 19.0 (q, C-21), 20.5 (q, C-26), 21.5 (t, C-11), 22.9 (t, C-15), 27.9 (t, C-16), 29.6 (t, C-6), 29.6 (t, C-23), 30.7 (t, C-2), 31.5 (d, C-25), 33.6 (t, C-22), 34.2 (s, C-10), 36.6 (d, C-20), 37.1 (t, C-1), 38.0 (t, C-4), 39.0 (d, C-24), 39.5 (t, C-12), 40.2 (d, C-5), 43.3 (s, C-13), 49.4 (d, C-9), 55.1 (d, C-14), 56.0 (d, C-17), 71.0 (d, C-3), 117.4 (d, C-7), 139.6 (s, C-8).

^{1}H-NMR ($CDCl_3$): Component A δ: 0.54, 0.80 (each 3H, s, H_3-18, -19), 0.78 (3H, d, J=6.7 Hz), 0.82 (3H, d, J=6.7 Hz), 0.91 (3H, d, J=7.0 Hz), 1.02 (3H, d, J=6.7 Hz), 3.60 (1H, m, H-3), 5.18 (3H, m, H-7, -22, -23). Component B δ: 0.53, 0.80 (each 3H, s, H_3-18, -19), 0.78 (3H, d, J=5.2 Hz), 0.83 (3H, d, J=5.5 Hz), 0.86 (3H, d, J=5.5 Hz), 0.92 (3H, d, J=6.1 Hz), 3.60 (1H, m, H-3), 5.18 (1H, m, H-7).

The fraction whose t_R is 22.5 min (1.0 mg) was acetylated with Ac_2O (0.05 ml) in pyridine (0.1 ml) at 25 °C overnight to afford a mixture of two acetylated derivatives (1.0 mg), which gave two peaks with t_R values of 8.2 and 9.4 min (intergral ratio, 1 : 1) on GLC.

Acknowledgement We are grateful to Dr. N. Sagara, Kyoto University, and Dr. A. Suzuki, Chiba University, for their kind gift of the strain of *H. vinosophyllum*. We thank Mrs. H. Seki and Miss R. Hara, Chiba University, for their measurements of NMR spectra.

References

1) *a*) Part II: H. Fujimoto, H. Hagiwara, K. Suzuki and M. Yamazaki, *Chem. Pharm. Bull.*, **35**, 2254 (1987); *b*) H. Fujimoto, K. Suzuki, H. Hagiwara and M. Yamazaki, *ibid.*, **34**, 88 (1986).
2) S. Udagawa, K. Tubaki, Y. Horie, K. Miura, K. Minoura, M. Yamazaki, T. Yokoyama and S. Watanabe, "Kinruizukan II," Kodansha, Tokyo, 1978, pp. 1276—1286.
3) H. Ishii, S. Seo, K. Tori, T. Tozyo and Y. Yoshimura, *Tetrahedron Lett.*, **1977**, 1227; K. Tori, *Kagaku No Ryoiki Zokan*, **125**, 221 (1980).
4) K. Yoshimoto, Y. Itatani and Y. Tsuda, *Chem. Pharm. Bull.*, **28**, 2065 (1980).
5) K. Yoshimoto and Y. Tsuda, *Chem. Pharm. Bull.*, **31**, 4324 (1983).
6) J. W. Blunt and J. B. Stothers, *Org. Magne. Reson.*, **9**, 439 (1977).
7) H. Fujimoto, M. Yamazaki and A. Suzuki, *Trans. Mycol. Soc. Jpn.*, **23**, 405 (1982).
8) W. B. Turner, "Fungal Metabolites," Academic Press Inc., London, 1971, pp. 214—279; W. B. Turner and D. C. Aldridge, "Fungal Metabolites II," Academic Press Inc., London, 1983, pp. 225—366.
9) M. Ishimoto, S. Minakami, S. Mizushima, T. Oshima and H. Wada, "Metabolic Maps 1971," Kyoritsu Publishing Co., Ltd., Tokyo, 1971, pp. 19—22.

Studies on Cardiac Ingredients of Plants. VII[1]: Chemical Transformation of Proscillaridin by Means of the Diels–Alder Reaction and Biological Activities of Its Derivatives

Nobutoshi MURAKAMI,[a] Takahiro TANASE,[a] Shin-ichi NAGAI,[a] Yuichi SATO,[a] Taisei UEDA,[a] Jinsaku SAKAKIBARA,*[,a] Hiroaki ANDO,[b] Yoshihiro HOTTA,[b] and Kazumi TAKEYA[b]

Faculty of Pharmaceutical Sciences, Nagoya City University,[a] Tanabe-dori, Mizuho-ku, Nagoya 467, Japan and Department of Pharmacology, Aichi Medical University,[b] Nagakute, Aichi 480–11, Japan. *Received February 4, 1991*

The Diels–Alder reactions of a cardiac glycoside, proscillaridin (1), with some dienophiles were investigated. The reaction of 1 with alkenes such as methyl vinyl ketone and methyl acrylate afforded 3-oxo-2-oxabicyclo[2.2.2]oct-7-enes (2—5) and *para*-substituted benzene derivatives (6 and 7), while 1 reacted with alkynes (3-butyn-2-one, methyl propiolate) to yield *para*- or *meta*-substituted benzene derivatives (6—9). The biological activities of the resulting derivatives were evaluated by the use of isolated guinea-pig papillary muscle preparations and Na^+,K^+-adenosine triphosphatase (ATPase) preparation from dog kidney. Among the proscillaridin derivatives, compounds 4 and 7 moderately inhibited Na^+,K^+-ATPase activity. Furthermore, the concentration range of 7 over which its positive inotropic effect on guinea-pig papillary muscle preparations, increased from 5% to 95% of maximum was broader than that of 1, *i.e.*, concentration dependency was maintained over a greater range of concentration.

Keywords proscillaridin; cardiac glycoside; chemical transformaion; Diels–Alder reaction; guinea-pig papillary muscle; Na^+,K^+-ATPase; positive inotropic effect

The cardiac glycoside, proscillaridin (**1**) has been widely used in the treatment of congestive heart failure.[3] However, this drug develops its positive inotropic effect (PIE) over a very narrow concentration range and sometimes causes arrhythmia.[4] The narrow therapeutic range of this drug makes it desirable to develop improved proscillaridin analogues with a lower risk of toxicity. We have recently reported extensive chemical modifications of **1** and have found that C_{22}–C_{23} hydrogenated proscillaridin, 3β-[(6-deoxy-α-L-mannopyranosyl)oxy]-14β-hydroxybufa-4,20-dienolide has a greatly expanded concentration range of PIE development on guinea-pig papillary muscle preparation and shows a reduced occurrence of arrhythmia.[5] As part of our continuing program aimed at the development of therapeutically advantageous drugs with a high margin of safety, we modified the δ-lactone group of **1** mainly by means of the Diels–Alder reactions with alkenes and alkynes. In this paper, we describe the preparation, the structure determination and the biological evaluation of the Diels–Alder cycloadducts.

Chemistry In a previous paper, we reported that the pyridinone molecule derived from the α-pyrone of **1** underwent the Diels–Alder reaction with dimethyl acetylenedicarboxylate to give the 1,4-cycloadduct in moderate yield.[2] Thus, we initiated the Diels–Alder reaction of **1** with several dienophiles such as methyl vinyl ketone, methyl acrylate, 3-butyn-2-one, and methyl propiolate as shown in Chart 1.

Compound **1** was allowed to react with methyl vinyl ketone in boiling dioxane for 10 h to give a product showing a single spot on thin-layer chromatography (TLC). The proton nuclear magnetic resonance (^{1}H-NMR) spectrum, however, revealed that the product is a mixture of two compounds, which were easily separable by high-performance liquid chromatography (HPLC) using an ODS column without endcapping of residual silanol groups to furnish **2** (54%) and **3** (38%). The infrared (IR) spectrum of **2** (a crystalline powder, mp 155—156 °C, $C_{34}H_{48}O_9$) showed lactone and ketone carbonyl absorptions at 1740 and 1720 cm^{-1}. The ^{1}H-NMR spectrum exhibited signals due to the C-8 olefinic proton at δ 5.99 (1H, dd, J=1.8, 6.3 Hz), the C-4 bridgehead proton at δ 3.76 (1H, dd, J=2.5, 6.3 Hz), the C-5 methine proton at δ3.02 (1H, ddd, J=2.5, 3.8, 9.8 Hz) and the C-1 bridgehead proton at δ 5.38 (1H, br s). The stereochemistry at C-1 and C-4 of **2** was established by circular dichroism (CD) spectroscopy, which showed a positive Cotton effect at 232 nm ($[\theta]$ +1.2 × 10^4). Based on the octant rule, we concluded that compound **2** possesses the 1*R*,4*R*-configuration as illustrated in Fig. 1-i. The configuration at C-5 was then deduced as follows. The signal of an *exo* proton of the 3-oxo-2-oxabicyclo[2.2.2]oct-7-ene ring system is known to be observed at lower field than that of an *endo*-proton in the ^{1}H-NMR spectrum,[6] because of shielding by the double bond between

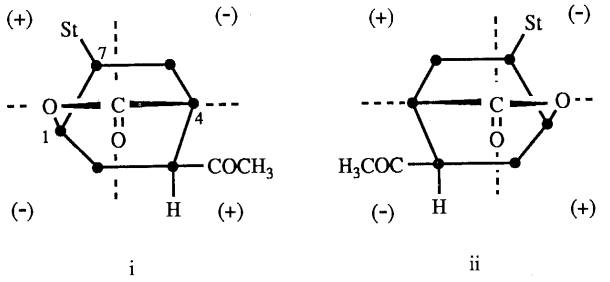

Fig. 1. Perspective Representation of 3-Oxo-2-oxabicyclo[2.2.2]oct-7-ene Derivatives (**2** and **3**)

St: steroid nucleus.

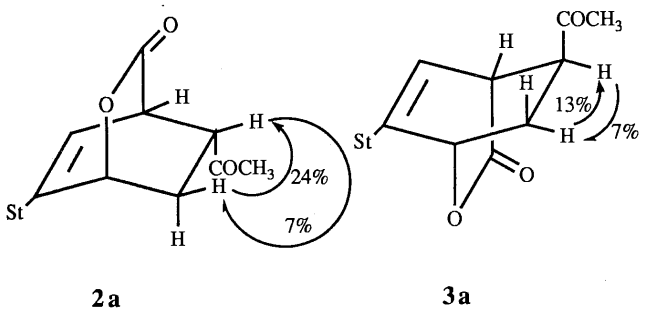

Fig. 2. NOE Data for **2a** and **3a**

C-7 and C-8. Therefore, the signal observed at 2.30 ppm (1H, ddd, $J=3.7$, 9.8, 13.5 Hz) in the ^{1}H-NMR spectrum of **2** was assigned to *exo* 6-H and the signal at 2.23 ppm (1H, dd, $J=3.8$, 13.5 Hz) was assigned to *endo* 6-H. From the coupling constants between the C-5 and C-6 protons, the stereochemistry of the C-5 acetyl group was determined to be *endo*. The assigned configuration is consistent with Alder's rule. The stereochemical assignment was further corroborated by difference nuclear Overhauser effect (NOE) studies of the tri-*O*-acetate of **2** (**2a**); irradiation of *exo* 6-H led to 24% enhancement of the proton resonance at *exo* 5-H, while irradiation at *exo* 5-H resulted in 7% enhancement of *exo* 6-H (Fig. 2). From the observed NOEs, the chemical structure of **2** was confirmed to be (1*R*,4*R*,5*R*)-5-acetyl-7-[3β-[(6-deoxy-α-L-mannopyranosyl)oxy]-14β-hydroxyandrost-4-en-17β-yl]-3-oxo-2-oxabicyclo[2.2.2]oct-7-ene. In contrast, the minor isomeric product (**3**) showed a negative Cotton effect in the CD spectrum, (Fig. 1-ii). In addition, NOE enhancements between *exo* 6-H (δ 2.33, 1H, ddd, $J=3.2$, 9.4, 13.9 Hz) and *exo* 5-H (δ 3.02, 1H, ddd, $J=2.1$, 4.0, 9.4 Hz) were observed in the ^{1}H-NMR spectrum of the tri-*O*-acetate of **3** (**3a**). Consequently, the structure of **3** was determined to be (1*S*,4*S*,5*S*)-5-acetyl-7-[3β-[(6-deoxy-α-L-mannopyranosyl)oxy]-14β-hydroxyandrost-4-en-17β-yl]-3-oxo-2-oxabicyclo[2.2.2]oct-7-ene.

Similarly, the Diels–Alder reaction of **1** with methyl acrylate gave a mixture of 3-oxo-2-oxabicyclo[2.2.2]oct-7-ene derivatives, which were separated by HPLC to give **4** (43%) and **5** (32%). The spectral features of **4** and **5** were very similar to those of **2** and **3** except for those due to the carbomethoxy moiety. The CD spectra of **4** and **5** showed a positive Cotton effect at 228 nm ([θ] 2.3×10^4) and a negative Cotton effect at 221 mn ([θ] -1.4×10^4), respectively. Accordingly, the structures of **4** and **5** were established to be methyl (1*R*,4*R*,5*R*)-7-[3β-[(6-deoxy-α-L-mannopyranosyl)oxy]-14β-hydroxyandrost-4-en-17β-yl]-3-oxo-2-oxabicyclo[2.2.2]oct-7-ene-5-carboxylate and methyl (1*S*,4*S*,5*S*)-7-[3β-[(6-deoxy-α-L-mannopyranosyl)oxy]-14β-hydroxyandrost-en-17β-yl]-3-oxo-2-oxabicyclo[2.2.2]-oct-7-ene-5-carboxylate.

We then conducted the same Diels–Alder reactions at elevated temperature. When compound **1** and methyl vinyl ketone were heated at 150 °C in a sealed tube, compound **6** was obtained as a sole product in 68% yield. The IR spectrum of **6** (a crystalline powder, mp 143—145 °C, $C_{33}H_{46}O_7$) exhibited an absorption band ascribable to an α,β-unsaturated carbonyl group at 1670 cm^{-1}, and the ^{1}H-NMR spectrum showed A_2B_2 type proton signals at 7.41 (2H, d, $J=8.4$ Hz) and 7.91 ppm (2H, d, $J=8.4$ Hz). Based on the above spectral data, compound **6** was confirmed to be 4-[3β-[(6-deoxy-α-L-mannopyranosyl)-oxy]-14β-hydroxyandrost-4-en-17β-yl]phenylethanone, which is obviously formed from the 1,4-cycloadducts (**2** and **3**) by elimination of carbon dioxide *via* a cycloreversion reaction followed by aromatization.[7] In a similar manner, the reaction of **1** with methyl acrylate gave compound **7** in 78% yield. The structure of **7** was established to be methyl 4-[3β-[(6-deoxy-α-L-mannopyranosyl)oxy]-14β-hydroxyandrost-4-en-17β-yl]benzoate by analysis of the spectral data described in Experimental.

On the other hand, the Diels–Alder reactions of **1** with some alkynes such as 3-butyn-2-one[8] and methyl propiolate were expected to afford the isomeric benzenes possessing the substituents at the *meta* and *para* positions. Thus, we undertook the reaction of **1** with 3-butyn-2-one to obtain a mixture of two regioisomers, which were readily separated by HPLC to yield **6** and 3-[3β-[(6-deoxy-α-L-mannopyranosyl)oxy]-14β-hydroxyandrost-4-en-17β-yl]phenylethanone (**8**) in 52% and 43% yields, respectively, as shown in Chart 1. In the ^{1}H-NMR spectrum of **8**, the characteristic signals due to *meta*-substituted benzene [δ 7.35 (1H, dd, $J=7.7$, 7.7 Hz), 7.62 (1H, d, $J=7.7$ Hz), 7.75 (1H, d, $J=7.7$ Hz), 7.93 (1H,s)] were observed. These data were consistent with the assigned structure **8**. The reaction of **1** with methyl propiolate also provided **7** and methyl 4-[3β-[(6-deoxy-α-L-mannopyranosyl)oxy]-14β-hydroxyandrost-

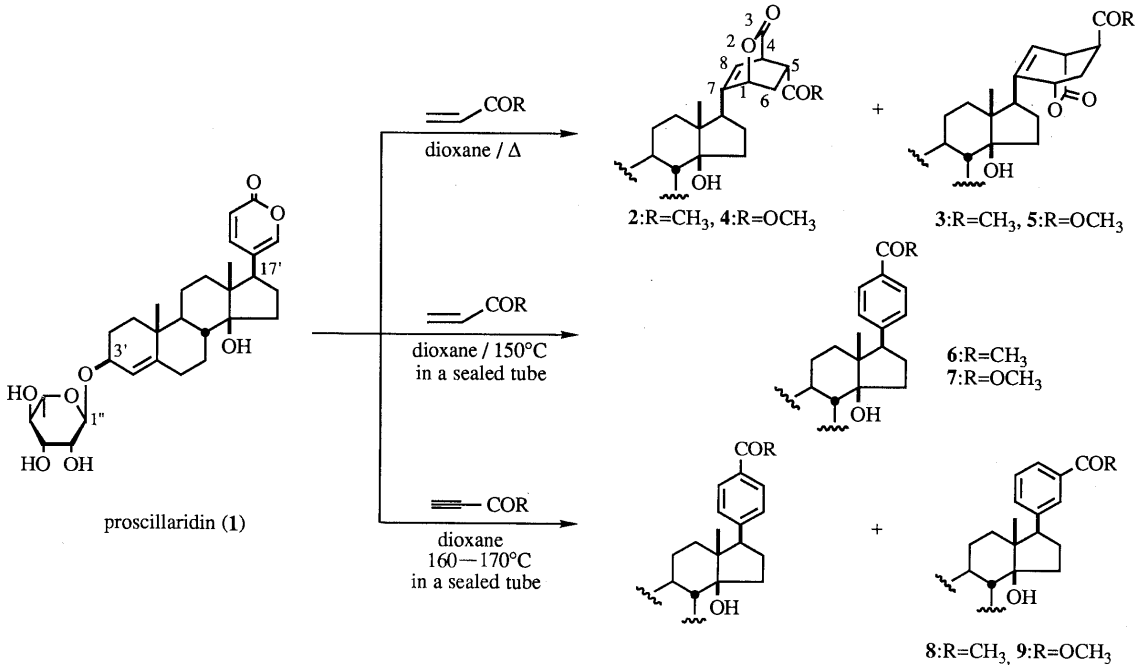

Chart 1

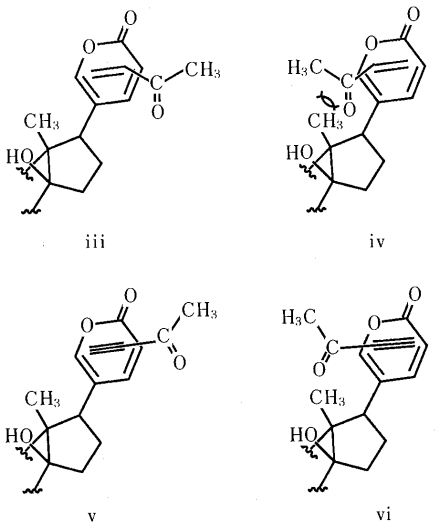

Fig. 3. Possible Transition State in the Diels–Alder Reaction of **1**

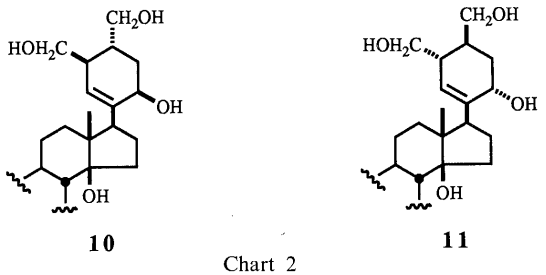

Chart 2

4-en-17β-yl]benzoate (**9**) in 36% and 50% yields. The structures of **7** and **9** were confirmed by the spectral data (see Experimental).

The orientation in the Diels–Alder reactions of **1** with the alkenes is considered to be determined by the steric interaction between the 13′-methyl group and the carbonyl residue in the alkene (Fig. 3). Namely, the cycloaddition may proceed through the transition state (iii) to give the 3-oxo-2-oxabicyclo[2.2.2]oct-7-enes (**2**—**5**) exclusively. In contrast, such selectivity never occurred in the reaction of **1** with the alkynes, since the interactions between the 13′-methyl group and the dienophiles seemed to be negligible (Fig. 3, transition states v and vi).

We finally treated compounds **4** and **5** with lithium aluminum hydride at room temperature. The reductive cleavage of the lactone ring was accomplished within 5 min to give the corresponding alcohols, (1*R*,4*S*,5*S*)-2-[3β-[(6-deoxy-α-L-mannopyranosyl)oxy]-14β-hydroxyandrost-4-en-17β-yl]]-4,5-dihydroxymethyl-2-cyclohexen-1-ol (**10**) and (1*S*,4*R*,5*R*)-2-[3β-[(6-deoxy-α-L-mannopyranosyl)-oxy]-14β-hydroxyandrost-4-en-17β-yl]-4,5-dihydroxy-methyl-2-cyclohexen-1-ol (**11**) quantitatively. The ^{1}H-NMR spectrum of **10** showed one olefinic proton signal (δ 6.04, 1H, d, J=1.8 Hz) and the oxymethine proton signal (δ 5.53, 1H, br s) as well as the signals due to the steroidal and the sugar moieties, while the IR spectrum indicated the absence of a carbonyl group. The spectral data of **11** were almost the same as those of **10**. Based on these data, the structures of **10** and **11** were proved to be as depicted in Chart 2.

Biological Results and Discussion

The biological activities (pIC_{50} and pD_2 values) of proscillaridin derivatives (**2**—**11**) were examined by means of measurements of the enzyme activity of an Na^+,K^+-adenosinetriphosphatase (ATPase) preparation from dog kidney[9] and of PIE in isolated guinea-pig papillary muscle. The results are summarized in Table I.

Table I. Biological Activities of Proscillaridin Derivatives

Compound	pIC_{50}[a]	pD_2[b]
1	7.44±0.02	7.41±0.14
2	5.42±0.03	—
3	5.43±0.08	—
4	<5.0	—
5	<5.0	—
6	6.79±0.01	6.27±0.04
7	6.38±0.10	5.92±0.04
8	6.07±0.02	—
9	5.95±0.09	—
10	<5.0	—
11	<5.0	—

a) pIC_{50} is the concentration of the test compounds required for 50% of the maximum inhibition of Na^+, K^+-ATPase from dog kidney (means±S.E.). *b*) pD_2 is the concentration of the test compounds required for 50% of the maximum PIE in guinea-pig papillary muscles (means±S.E.).

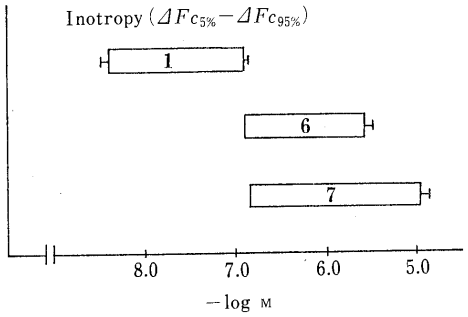

Fig. 4. Concentration-Dependent Range of **1**, **6**, and **7**

The concentration dependency was determined by measuring the range from **5** to 95% of full development of PIE.

Although the biological activities (pIC_{50}) of **2**—**11** were less potent than those of the parent compound (**1**), compounds **6** and **7** bearing a benzene ring at the C-17 position showed moderately potent enzyme-inhibitory activity compared with the other derivatives. Moreover, it is noticeable that the pIC_{50} values of *para*-substituted benzene derivatives (**6** and **7**) were greater than those of *meta*-substituted analogues (**8** and **9**). Compounds **6** and **7** also showed appreciable pD_2 values, and in particular the development of PIE by compound **7** occurred over a rather wider concentration range as compared with **1** (Fig. 4). These biological results suggest that there may be some correlation between the position of the carbonyl oxygen on the C-17 benzene ring and biological activity.

In summary, the δ-lactone of proscillaridin (**1**) was readily transformed to 3-oxo-2-oxabicyclo[2.2.2]oct-7-ene (**2**—**5**) and isomeric benzenes (**6**—**9**) in sufficient yields without prior protection of all the hydroxyl groups in the sugar moiety. Thus, the present modification procedures may be applicable to other cardiac glycosides containing on α-pyrone moiety in the molecule. Additional studies on the correlation between the biological activity and the chemical structure of substituents at C-17 are in progress.

Experimental

All melting points were determined on a Yanagimoto micro melting

point apparatus and are uncorrected. The ultraviolet (UV) spectra were recorded with a Shimadzu UV-2100 spectrometer, the IR spectra with a JASCO IRA-2 spectrometer, and the CD spectra with a JASCO J-600 spectrometer. The ^{1}H-NMR spectra were measured with JEOL JNM-FX-100 and JEOL GSX-400 spectrometers using tetramethylsilane as an internal standard. The following abbreviations are used; s, singlet; d, doublet; t, triplet; q, quartet; m, multiplet. Optical rotations were measured on a JASCO DIP-4 digital polarimeter. HPLC was performed using a JASCO 880-PU pump, and a Shodex RI, SE-11 differential refractometer. Medium pressure chromatography (MPLC) was performed on a C.I.G. column system (Kusano Scientific Co., Ltd., Tokyo; pump KPW-20, UV detector KU-331) with a prepacked column, 20 mm i.d. × 100 mm (octadecyl silica, 20 μm). TLC was carried out on Merck precoated Kieselgel 60F_{254} silanized plates, and spots were detected by illumination with an ultraviolet lamp, or 5% vanillin–70% $HClO_4$, 1% $Ce(SO_4)_2$–10% H_2SO_4 followed by heating. Column chromatography was performed on Silica gel BW-200 or BW-300 (Fuji Davison Chemicals Co., Ltd.).

Reaction of 1 with Methyl Vinyl Ketone A solution of **1** (200 mg, 0.38 mmol) and methyl vinyl ketone (1.6 ml) in dry dioxane (6.4 ml) was heated under reflux for 10 h. The solvent was removed, and the residue was chromatographed on silica gel with $CHCl_3$–$CHCl_3$: MeOH = 8 : 1 to give a mixture of **2** and **3** (213 mg). The mixture was separated by HPLC (Develosil ODS A-5, MeOH : H_2O = 65 : 35, 2.0 ml/min) to yield **2** (123 mg, 54%) and **3** (87 mg, 38%). **2**: a crystalline powder. mp 155—156 °C (MeOH–isopropyl ether). $[\alpha]_D^{26}$ −40.1° (c = 0.5, MeOH). CD (c = 0.02, MeOH) $[\theta]^{25}$ (nm): + 1.2 × 10^4 (232) (positive maximum). IR (KBr) cm^{-1}: 3440 (OH), 1740 (C=O), 1720 ($COCH_3$). ^{1}H-NMR ($CDCl_3$, 400 MHz) δ: 0.80 (3H, s, 13′-CH_3), 1.04 (3H, s, 10′-CH_3), 1.30 (3H, d, J = 6.0 Hz, 5″-CH_3), 2.18 (3H, s, $COCH_3$), 2.23 (1H, dd, J = 3.8, 13.5 Hz, *endo* 6-H), 2.30 (1H, ddd, J = 3.7, 9.8, 13.5 Hz, *exo* 6-H), 3.02 (1H, ddd, J = 2.5, 3.8, 9.8 Hz, 5-H), 3.45 (1H, dd, J = 9.4, 9.4 Hz, 4″-H), 3.76 (1H, dd, J = 2.5, 6.3 Hz, 4-H), 3.75—3.80 (2H, m, 3″-H, 5″-H), 3.92 (1H, br s, 2″-H), 4.12 (1H, dd, J = 7.5, 8.1 Hz, 3′-H), 4.96 (1H, s, 1″-H), 5.31 (1H, s, 4′-H), 5.38 (1H, br s, 1-H), 5.99 (1H, dd, J = 1.8, 6.3 Hz, 8-H). *Anal.* Calcd for $C_{34}H_{48}O_9 \cdot 1/2\,H_2O$: C, 67.00; H, 8.05. Found: C, 66.86; H, 8.03. **3**: a crystalline powder. mp 174—176 °C (MeOH–isopropyl ether). $[\alpha]_D^{26}$ −43.5° (c = 0.5, MeOH). CD (c = 0.02, MeOH). $[\theta]^{25}$ (nm): −7.0 × 10^3 (222) (negative maximum). IR (KBr) cm^{-1}: 3450 (OH), 1740 (C=O), 1710 ($COCH_3$). ^{1}H-NMR ($CDCl_3$, 400 MHz) δ: 0.79 (3H, s, 13′-CH_3), 1.03 (3H, s, 10′-CH_3), 1.30 (3H, d, J = 6.0 Hz, 5″-CH_3), 1.97 (1H, dd, J = 4.0, 13.9 Hz, *endo* 6-H), 2.18 (3H, s, $COCH_3$), 2.33 (1H, ddd, J = 3.2, 9.4, 13.9 Hz, *exo* 6-H), 3.02 (1H, ddd, J = 2.1, 4.0, 9.4 Hz, 5-H), 3.45 (1H, dd, J = 9.4, 9.4 Hz, 4″-H), 3.74 (1H, dd, J = 2.1, 6.2 Hz, 4-H), 3.72—3.80 (2H, m, 3″-H, 5″-H), 3.92 (1H, br s, 2″-H), 4.12 (1H, dd, J = 7.5, 9.3 Hz), 3′-H), 4.95 (1H, s, 1″-H), 5.31 (1H, s, 4-H), 5.38 (1H, dd, J = 2.1, 3.2 Hz, 1-H), 5.88 (1H, dd, J = 2.2, 6.2 Hz, 8-H). *Anal.* Calcd for $C_{34}H_{48}O_9 \cdot 1/2\,H_2O$: C, 67.00; H, 8.05. Found: C, 66.86; H, 8.03.

Acetylation of 2 and 3 Ac_2O (0.5 ml) was added dropwise to an ice-cooled solution of **2** (10 ml, 0.017 mmol) in pyridine (1.0 ml). The mixture was allowed to stand at room temperature for 10 h, then poured into ice-water and extracted with EtOAc. The EtOAc extract was successively washed with 5% HCl, saturated aqueous $NaHCO_3$, and saturated aqueous NaCl, then dried over $MgSO_4$. Removal of the solvent from the EtOAc extract under reduced pressure gave a product which was purified by column chromatography (SiO_2) to furnish **2a** (12 mg, quant.). Acetylation of **3** (10 mg) in the same manner afforded the corresponding acetate (**3a**, 12 mg, quant.). **2a**: a crystalline powder. mp 129—131 °C (EtOH). $[\alpha]_D^{25}$ −38.6° (c = 0.6, $CHCl_3$). IR (KBr) cm^{-1}: 3500 (OH), 1750 (C=O). ^{1}H-NMR ($CDCl_3$, 400 Hz) δ: 0.79 (3H, s, 13′-CH_3), 1.04 (3H, s, 10′-CH_3), 1.20 (3H, d, J = 6.3 Hz, 5″-CH_3), 1.98, 2.04, 2.15, 2.18 (3H each, all s, OAc), 2.23 (1H, dd, J = 4.2, 13.3 Hz, *endo* 6-H), 2.30 (1H, ddd, J = 3.7, 9.6, 13.3 Hz, *exo* 6-H), 3.02 (1H, ddd, J = 2.6, 4.2, 9.6 Hz, 5-H), 3.76 (1H, dd, J = 2.6, 6.2 Hz, 4-H), 3.97 (1H, dq, J = 6.3, 9.9 Hz, 5″-H), 4.11 (1H, m, 3′-H), 4.89 (1H, d, J = 1.6 Hz, 1″-H), 5.05 (1H, dd, J = 9.9, 9.9 Hz, 4″-H), 5.21 (1H, dd, J = 1.6, 3.4 Hz, 2″-H), 5.31 (1H, s, 4′-H), 5.32 (1H, dd, J = 3.4, 9.9 Hz, 3″-H), 5.38 (1H, d-like, 1-H), 5.99 (1H, dd, J = 1.9, 6.2 Hz, 8-H). *Anal.* Calcd for $C_{40}H_{54}O_{12}$: C, 66.17; H, 7.50. Found: C, 65.92; H, 7.61. **3a**: a crystalline powder. mp 115—117 °C (EtOH). $[\alpha]_D^{26}$ −41.6° (c = 0.7, $CHCl_3$). IR (KBr) cm^{-1}: 3440 (OH), 1755 (C=O). ^{1}H-NMR ($CDCl_3$, 400 MHz) δ: 0.79 (3H, s, 13′-CH_3), 1.04 (3H, s, 10′-CH_3), 1.20 (3H, d, J = 6.3 Hz, 5″-CH_3), 1.96 (1H, dd, J = 4.2, 13.7 Hz, *endo* 6-H), 1.98, 2.04, 2.15, 2.18 (3H each, all s, OAc), 2.33 (1H, ddd, J = 4.1, 9.7, 13.7 Hz, *exo* 6-H), 3.02 (1H, ddd, J = 4.2, 6.0, 9.7 Hz, 5-H), 3.73 (1H, dd, J = 2.4, 6.0 Hz, 4-H), 3.97 (1H, dq, J = 6.3, 9.9 Hz, 5″-H), 4.10 (1H, m, 3′-H), 4.89 (1H, d, J = 1.6 Hz, 1″-H), 5.05 (1H, dd, J = 9.9, 9.9 Hz, 4″-H), 5.20 (1H, dd, J = 1.6, 3.5 Hz, 2″-H), 5.30 (1H, s, 4′-H), 5.32 (1H, dd, J = 3.5, 9.9 Hz, 3″-H), 5.83 (1H, d-like, 1-H), 5.87 (1H, dd, J = 2.0, 6.0 Hz, 8-H). *Anal.* Calcd for $C_{40}H_{54}O_{10}$: C, 66.17; H, 7.50. Found: C, 66.24; H, 7.40.

Reaction of 1 with Methyl Acrylate A solution of **1** (200 mg, 0.38 mmol) and methyl acrylate (2.0 ml) in dry xylene (3.0 ml)–dioxane (3.0 ml) was heated under reflux for 24 h. The solvent was removed, and the residue was chromatographed on silica gel using $CHCl_3$–$CHCl_3$: MeOH = 7 : 1 as an eluent to give a mixture of **4** and **5** (190 mg). The mixture was separated by HPLC (Develosil ODS A-5, MeOH : H_2O = 70 : 30, 3.0 ml/min) to yield **4** (100 mg, 43%) and **5** (75 mg, 32%). **4**: a crystalline powder. mp 153—154 °C (MeOH–isopropyl ether). $[\alpha]_D^{26}$ −30.1° (c = 0.6, MeOH). CD (c = 0.01, MeOH) $[\theta]^{25}$ (nm): + 2.3 × 10^4 (228) (positive maximum). IR (KBr) cm^{-1}: 3440 (OH), 1735 (C=O). ^{1}H-NMR ($CDCl_3$, 400 MHz) δ: 0.79 (3H, s, 13′-CH_3), 1.04 (3H, s, 10′-CH_3), 1.30 (3H, d, J = 6.2 Hz, 5″-CH_3), 2.26 (1H, dd, J = 3.3, 13.5 Hz, *endo* 6-H), 2.40 (1H, ddd, J = 3.4, 9.9, 13.5 Hz, *exo* 6-H), 3.02 (1H, ddd, J = 2.7, 3.3, 9.9 Hz, 5-H), 3.45 (1H, dd, J = 9.2, 9.2 Hz, 4″-H), 3.68 (3H, s, CO_2Me), 3.79 (1H, dd, J = 2.7, 6.1 Hz, 4-H), 3.73—3.81 (2H, m, 3″-H, 5″-H), 3.92 (1H, d, J = 1.8 Hz, 2″-H), 4.12 (1H, dd, J = 6.8, 8.2 Hz, 3′-H), 4.95 (1H, s, 1″-H), 5.31 (1H, s, 4′-H), 5.38 (1H, br s, 1-H), 6.04 (1H, dd, J = 2.0, 6.1 Hz, 8-H). *Anal.* Calcd for $C_{34}H_{48}O_{10} \cdot 1/2\,H_2O$: C, 65.28; H, 7.84. Found: C, 64.98; H, 7.54. **5**: a crystalline powder. mp 175—176 °C (MeOH–isopropyl ether). $[\alpha]_D^{26}$ −43.8° (c = 0.5, MeOH). CD (c = 0.02, MeOH) $[\theta]^{25}$ (nm): −1.4 × 10^4 (221) (negative maximum). IR (KBr) cm^{-1}: 3440 (OH), 1735 (C=O). ^{1}H-NMR ($CDCl_3$, 400 MHz) δ: 0.79 (3H, s, 13′-CH_3), 1.04 (3H, s, 10′-CH_3), 1.30 (3H, d, J = 6.4 Hz, 5″-CH_3), 1.98 (1H, dd, J = 3.3, 13.4 Hz, *endo* 6-H), 2.43 (1H, ddd, J = 3.3, 9.6, 13.4 Hz, *exo* 6-H), 3.01 (1H, ddd, J = 2.6, 3.3, 9.6 Hz, 5-H), 3.45 (1H, dd, J = 9.4, 9.4 Hz, 4″-H), 3.78 (1H, dd, J = 2.6, 6.1 Hz, 4-H), 3.75—3.80 (2H, m, 3″-H, 5″-H), 3.92 (1H, br s, 2″-H), 4.12 (1H, dd, J = 7.5, 7.9 Hz, 3′-H), 4.95 (1H, br s, 1″-H), 5.31 (1H, s, 4′-H), 5.82 (1H, br s, 1-H), 5.93 (1H, dd, J = 2.0, 6.1 Hz, 8-H). *Anal.* Calcd for $C_{34}H_{48}O_{10} \cdot 1/2\,H_2O$: C, 65.28; H, 7.84. Found: C, 65.53; H, 8.00.

4-[3β-[(6-Deoxy-α-L-mannopyranosyl)oxy-14β-hydroxyandrost-4-en-17β-yl]phenylethanone (6) A solution of **1** (100 mg, 0.19 mmol) and methyl vinyl ketone (0.8 ml) in dioxane (3.2 ml) was heated at 150 °C for 4 h in a sealed tube. The solvent was removed, and the residue was chromatographed on silica gel with $CHCl_3$–$CHCl_3$: MeOH (10 : 1) to give a crude product, which was purified by MPLC (MeOH : H_2O = 70 : 30, 5.0 ml/min) to yield **6** (71 mg, 68%). **6**: a crystalline powder. mp 143—145 °C (MeOH–isopropyl ether). $[\alpha]_D^{26}$ −49.6° (c = 0.5, MeOH). IR (KBr) cm^{-1}: 3440 (OH), 1670 (C=O). UV (λ_{max}, MeOH) nm (ε): 259.9 (1.4 × 10^4). ^{1}H-NMR ($CDCl_3$, 400 MHz) δ: 0.56 (3H, s, 13′-CH_3), 1.03 (3H, s, 10′-CH_3), 1.30 (3H, d, J = 6.2 Hz, 5″-CH_3), 2.58 (3H, s, $COCH_3$), 2.92 (1H, dd, J = 7.1, 9.3 Hz, 17′-H), 3.46 (1H, dd, J = 9.4, 9.4 Hz, 4″-H), 3.75—3.79 (2H, m, 3″-H, 5″-H), 3.93 (1H, s, 2″-H), 4.12 (1H, dd, J = 7.5, 7.9 Hz, 3′-H), 4.96 (1H, s, 1″-H), 5.32 (1H, s, 4′-H), 7.41 (2H, d, J = 8.4 Hz, 3-H, 5-H), 7.91 (2H, d, J = 8.4 Hz, 2-H, 6-H). *Anal.* Calcd for $C_{33}H_{46}O_7 \cdot 1/2\,H_2O$: C, 69.21; H, 8.44. Found: C, 69.11; H, 8.23.

Methyl 4-[3β-(6-Deoxy-α-L-mannopyranosyl)oxy-14β-hydroxyandrost-4-en-17β-yl]benzoate (7) A solution of **1** (100 mg, 0.19 mmol) and methyl acrylate (1.0 ml) was heated at 150 °C for 9.5 h in a sealed tube. The solvent was removed, and the resulting residue was chromatographed on silica gel using $CHCl_3$–$CHCl_3$: MeOH = 7 : 1 as an eluent to give a crude product, which was purified by HPLC (Develosil ODS A-5, MeOH : H_2O = 65 : 35, 3.0 ml/min) to yield **7** (84 mg) in 78% yield. **7**: a crystalline powder. mp 128—130 °C (MeOH–isopropyl ether). $[\alpha]_D^{26}$ −44.8 °C (c = 0.6, MeOH). IR (KBr) cm^{-1}: 3450 (OH), 1720 (C=O). UV (λ_{max}, MeOH) nm (ε): 246.0 (2.0 × 10^4). ^{1}H-NMR ($CDCl_3$, 400 MHz) δ: 0.56 (3H, s, 13′-CH_3), 1.03 (3H, s, 10′-CH_3), 1.30 (3H, d, J = 6.2 Hz, 5″-CH_3), 2.92 (1H, dd, J = 8.0, 8.0 Hz, 17′-H), 3.46 (1H, dd, J = 9.4, 9.4 Hz, 4″-H), 3.75—3.79 (2H, m, 3″-H, 5″-H), 3.89 (3H, s, CO_2Me), 3.93 (1H, s, 2″-H), 4.12 (1H, dd, J = 7.5, 7.9 Hz, 3′-H), 4.96 (1H, s, 1″-H), 5.32 (1H, s, 4′-H), 7.41 (2H, d, J = 8.4 Hz, 3-H, 5-H), 7.91 (2H, d, J = 8.4 Hz, 2-H, 6-H). *Anal.* Calcd for $C_{33}H_{46}O_8 \cdot 1/2\,H_2O$: C, 68.37; H, 8.17. Found: C, 68.25; H, 8.31.

Reaction of 1 with 3-Butyn-2-one A solution of **1** (200 mg, 0.38 mmol) and 3-butyn-2-one (0.4 ml) in dry dioxane (4.0 ml) was heated at 170 °C for 15 h in a sealed tube. The reaction mixture was concentrated under reduced pressure, then the residue was chromatographed on silica gel with $CHCl_3$: MeOH = 9 : 1 to give a mixture of **6** and **8**. The mixture was separated by HPLC (Develosil ODS-5, MeOH : H_2O = 80 : 20, 2.0 ml/min) to yield **6** (110 mg, 52%) and **8** (91 mg, 43%). **8**: a crystalline powder. mp 135—137 °C (MeOH–isopropyl ether). $[\alpha]_D^{26}$ −51.9° (c = 0.7, MeOH).

IR (KBr) cm^{-1}: 3430 (OH), 1670 (C=O). UV (λ_{max}, MeOH) nm (ε): 250.2 (9.3×10^3). ^{1}H-NMR ($CDCl_3$, 400 MHz) δ: 0.57 (3H, s, 13′-CH_3), 1.04 (3H, s, 10′-CH_3), 1.31 (3H, d, J=6.2 Hz, 5″-CH_3), 2.59 (3H, s, $COCH_3$), 2.94 (1H, dd, J=7.0, 9.2 Hz, 17′-H), 3.45 (1H, dd, J=9.3, 9.3 Hz, 4″-H), 3.75—3.81 (2H, m, 3″-H, 5″-H), 3.94 (1H, s, 2″-H), 4.14 (1H, dd, J=7.5, 8.1 Hz, 3″-H), 4.97 (1H, d, J=1.3 Hz, 1″-H), 5.32 (1H, s, 4′-H), 7.35 (1H, dd, J=7.7, 7.7 Hz, 5-H), 7.62 (1H, d, J=7.7 Hz, 4-H), 7.75 (1H, d, J=7.7 Hz, 6-H), 7.93 (1H, s, 2-H). *Anal.* Calcd for $C_{33}H_{46}O_7 \cdot H_2O$: C, 69.21; H, 8.44. Found: C, 69.51; H, 8.44.

Reaction of 1 with Methyl Propiolate A solution of **1** (500 mg, 0.94 mmol) and methyl propiolate (1.0 ml) in dry dioxane (10.0 ml) was heated at 160 °C for 44 h in a sealed tube. The reaction mixture was concentrated under reduced pressure, then the residue was chromatographed on silica gel with $CHCl_3$: MeOH = 9 : 1 to give a mixture of **7** and **9** (490 mg). The mixture was separated by HPLC (Develosil ODS A-5, MeOH : H_2O = 80 : 20, 3.5 ml/min) to yield **7** (197 mg, 36%) and **9** (272 mg, 50%). **9**: a crystalline powder. mp 144—145 °C (MeOH–isopropyl ether). $[\alpha]_D^{26}$ −51.7° (c=0.7, MeOH). IR (KBr) cm^{-1}: 3440 (OH), 1720 (C=O). UV (λ_{max}, MeOH) nm (ε): 236.0 (8.4×10^3), ^{1}H-NMR ($CDCl_3$, 400 MHz) δ: 0.56 (3H, s, 13′-CH_3), 1.03 (3H, s, 10′-CH_3), 1.31 (3H, d, J=6.3 Hz, 5″-CH_3), 2.92 (1H, dd, J=7.1, 9.3 Hz, 17′-H), 3.47 (1H, dd, J=9.6, 9.6 Hz, 4″-H), 3.76—3.80 (2H, m, 3′-H, 5′-H), 3.90 (3H, s, CO_2Me), 3.94 (1H, s, 2″-H), 4.14 (1H, dd, J=7.3, 8.3 Hz, 3′-H), 4.96 (1H, s, 1″-H), 5.32 (1H, s, 4′-H), 7.32 (1H, dd, J=7.8, 7.8 Hz, 5-H), 7.60 (1H, d, J=7.8 Hz, 4-H), 7.83 (1H, d, J=7.8 Hz, 6-H), 7.98 (1H, s, 2-H). *Anal.* Calcd for $C_{33}H_{46}O_8 \cdot 1/2\,H_2O$: C, 68.37; H, 8.17. Found: C, 68.37; H, 8.50.

$LiAlH_4$ Reduction of 4 $LiAlH_4$ (36 mg, 0.95 mmol) was added portionwise to a solution of **4** (50 mg, 0.073 mmol) in dry THF (10 ml) and the resulting mixture was stirred at room temperature for 10 min under N_2. The reaction mixture was treated with H_2O-saturated ether, H_2O, and 5% aqueous NaOH. The precipitate was removed by filtration, and removal of the solvent from the filtrate gave a product, which was purified by column chromatography (SiO_2, 5 g, $CHCl_3$: MeOH : H_2O = 7 : 3 : 1, lower phase) to furnish **10** (48 mg, quant.). **10**: a crystalline powder. mp 265—267 °C (MeOH–isopropyl ether). $[\alpha]_D^{26}$ −43.3° (c=0.4, MeOH). IR (KBr) cm^{-1}: 3420 (OH). ^{1}H-NMR (pyridine-d_5, 400 MHz) δ: 0.95 (3H, s, 13′-CH_3), 1.23 (3H, s, 10′-CH_3), 1.70 (3H, d, J=5.9 Hz, 5″-CH_3), 3.96—4.10 (4H, m, −$CH_2OH \times 2$), 4.13 (1H, dd, J=5.0, 10.1 Hz, 1-H), 4.30—4.38 (2H, m, 4″-H, 5″-H), 4.42 (1H, dd, J=7.5, 7.9 Hz, 3′-H), 4.54 (1H, dd, J=1.3, 8.6 Hz, 3″-H), 4.58 (1H, br s, 2″-H), 5.53 (1H, s, 1″-H), 5.57 (1H, s, 4′-H), 6.04 (1H, d, J=1.8 Hz, 3-H). *Anal.* Calcd for $C_{33}H_{52}O_9 \cdot H_2O$: C, 64.89; H, 8.93. Found: C, 64.95; H, 9.00.

$LiAlH_4$ Reduction of 5 $LiAlH_4$ (36 mg, 0.95 mmol) was added portionwise to a solution of **5** (50 mg, 0.073 mmol) in dry THF (10 ml) and the resulting mixture was stirred at room temperature for 10 min under N_2. Work-up of the reaction mixture as described above gave a product, which was purified by column chromatography (SiO_2, $CHCl_3$: MeOH : H_2O = 7 : 3 : 1, lower phase) to furnish **11** (48 mg, quant.). **11**: a crystalline powder. mp 266—267 °C. $[\alpha]_D^{24}$ −44.4° (c=0.7, MeOH). IR (KBr) cm^{-1}: 3430 (OH). ^{1}H-NMR (pyridine-d_5, 400 MHz) δ: 0.94 (3H, s, 13′-CH_3), 1.28 (3H, s, 10′-CH_3), 1.71 (3H, d, J=5.7 Hz, 5″-CH_3), 3.96—4.04 (2H, m, 1H in $CH_2OH \times 2$), 4.08 (1H, dd, J=5.6, 10.3 Hz, 1H, in CH_2OH), 4.16 (1H, dd, J=6.0, 10.3 Hz, 1H in CH_2OH), 4.30—4.39 (2H, m, 4″-H, 5″-H), 4.42 (1H, dd, J=7.7, 9.3 Hz, 3′-H), 4.54 (1H, dd, J=1.8, 8.6 Hz, 3″-H), 4.59 (1H, d, J=1.8 Hz, 2″-H), 5.52 (1H, s, 1″-H), 5.57 (1H, s, 4′-H), 6.17 (1H, s, 3-H). *Anal.* Calcd for $C_{33}H_{52}O_9 \cdot H_2O$: C, 64.89; H, 8.93. Found: C, 64.95; H, 9.23.

Acknowledgements The authors thank Misses T. Naito and S. Kato of this Faculty for elemental analyses and NMR measurements. This work was supported in by a Grant-in-Aid for Scientific Research from the Ministry of Education, Science, and Culture of Japan.

References and Notes

1) PartVI: N. Murakami, T. Tanase, S. Nagai, T. Ueda, and J. Sakakibara, *Chem. Pharm. Bull.*, **39**, 1330 (1991).
2) J. Mori, S. Nagai, J. Sakakibara, K. Takeya, and Y. Hotta, *Chem. Pharm. Bull.*, **36**, 48 (1988).
3) H. G. Kurbjuweit, *Arzneim. -Forsch.*, **14**, 716 (1964).
4) A. Schwartz, G. E. Lindenmayer, and J. C. Allen, *Pharmacol. Rev.*, **27**, 3 (1975).
5) J. Sakakibara, J. Mori, S. Nagai, Y. Hotta, and K. Takeya, *Nippon Yakurigaku Zasshi*, **90**, 115 (1987).
6) *a*) H. Behringer and P. Heckmaier, *Chem. Ber.*, **102**, 2835 (1969); *b*) T. Shimo, K. Somekawa, M. Sato, and S. Kumamoto, *Nippon Kagaku Kaishi*, **12**, 1927 (1984); *c*) E. Pufaff and H. Plieniger, *Chem. Ber.*,**115**, 1967 (1982); *d*) G. H. Posner, A. Haces, W. Harrison, and C. M. Kinter, *J. Org. Chem.*, **52**, 4836 (1987).
7) The 1,4-cycloadducts (**2** and **3**) were heated at 150 °C in a sealed tube to provide the aromatized compound (**6**) in 90% yield.
8) E. Reinmann and R. Reitz, *Justus Liebigs Ann. Chem.*, **1976**, 610.
9) W. Schorner, C. von Livery, R. Kramer, and W. Seubert, *Eur. J. Biochem.*, **1**, 334 (1967).

Studies on Reaction Conditions and New Entry to Chiral Ligands in the Chiral Lithium Amide-Mediated Enantioselective Aldol Reaction[1)]

Akira ANDO, Toshiaki TATEMATSU, and Takayuki SHIOIRI*

Faculty of Pharmaceutical Sciences, Nagoya City University, Tanabe-dori, Mizuho-ku, Nagoya 467, Japan. *Received February 12, 1991*

Reaction conditions for the enantioselective aldol reaction of 2,2-dimethyl-3-pentanone (3) and benzaldehyde using the chiral lithium amide 1b as a chiral auxiliary were thoroughly investigated. All three procedures, that is, (1) the combined use of lithium diisopropylamide and the chiral lithium amide 1b, (2) the use of an excess of the chiral lithium amide 1b, and (3) the regeneration of the chiral lithium amide 1b, afforded the aldol 4 in about 90% yield and 70% enantiomeric excess (ee). Investigation of the effects of solvent by utilizing 1-naphthaldehyde revealed that in tetrahydrofuran, (*S*,*S*)-aldol 5 of 77% ee was obtained as the major product, while in ether (*R*,*R*)-5 became the major isomer (38% ee). Furthermore, addition of hexamethylphosphoric triamide caused a dramatic change of stereoselectivity, and (*S*,*S*)-5 of 70% ee was obtained in ether with 20 eq of hexamethylphosphoric triamide. The aldol 4 of 74% ee was obtained when the new chiral lithium amide 6b was used.

Keywords enantioselective aldol reaction; lithium enolate; lithium diisopropylamide; chiral lithium amide; chiral auxiliary; solvent effect; hexamethylphosphoric triamide

The aldol reaction is one of the most representative carbon–carbon bond-forming reactions and many researches have been concerned with the stereoselectivity of this reaction.[2)] We have already reported[3)] the enantioselective aldol reactions of ketone lithium enolates and aldehydes utilizing chiral lithium amides as chiral auxiliaries, covering the substituent effects of chiral lithium amides and the generality of this reaction. It was shown that the chiral lithium amides **1b** and **2b**, derived from (*S*)-2-isopropylamino-1-methoxy-3-methylbutane (**1a**) and (*R*)-2-isopropylamino-1-methoxy-2-phenylethane (**2a**), respectively, are very effective chiral auxiliaries. In the presence of these ligands, the reaction of the enolate of 2,2-dimethyl-3-pentanone (**3**) and benzaldehyde or 1-naphthaldehyde proceeded in good chemical yield (84—93%) and good enantioselectivity (68—77%) to give the aldol **4** or **5**, respectively (Chart 1).[4)] With reference to the stereoselectivity of this reaction, we have thoroughly investigated the reaction conditions and have further become interested in using this reaction as a new entry to chiral ligands which possess two chiral centers. In this report, we would like to present the results of these investigations.

In our previous studies,[3a)] it was clarified that the reaction of a lithium enolate and an aldehyde in the presence of a chiral lithium amide is very important to obtain an aldol in good enantiomeric excess (ee), since the chiral lithium amide is a more effective chiral ligand than the chiral amine itself. We have therefore used the combination of lithium diisopropylamide (LDA) and a chiral lithium amide expecting that LDA would act as a strong base while the chiral lithium amide acts as a chiral auxiliary. We were able to obtain the aldol **4** in 93% chemical yield and 68% ee when the ketone **3** was treated with 1.2 eq of LDA and an equimolar amount of the chiral lithium amide **1b** at −10 °C for 30 min and then the enolate was allowed to react with benzaldehyde at −70 °C for 5 min. However, under these conditions, it seems possible that diisopropylamine, which is formed when the ketone **3** is converted to its enolate, might affect the reaction pathway to change the stereoselectivity. Furthermore, the above conditions, involving the reaction of the enolate in the presence of the chiral lithium amide, could also be produced in the following ways: (1) when the ketone is lithiated with excess chiral lithium amide and (2) when the chiral amine which results when the chiral lithium amide acts as strong base to form the ketone lithium enolate is reconverted to the lithium amide by adding *n*-butyllithium.[5)] So we first examined these points. The results are summarized in Table I. When the ketone **3** was lithiated with 2.4 eq of the chiral lithium amide **1b** at −10 °C for 30 min and then allowed to react with benzaldehyde, the *erythro* aldol **4**[6)] was obtained in 84% yield and 70% ee. Neither lowering of the lithiation temperature to −70 °C nor the use of 5.0 eq of the chiral lithium amide **1b** raised the stereoselectivity of the reaction. On the other hand, almost the same chemical yield (90%) and enantiomeric excess (67% ee) were also realized when 1.2 eq of the chiral lithium amide was employed if 1.0 eq of *n*-butyllithium was added after the lithiation of the ketone **3** with **1b** was completed.

Thus all three procedures, that is, (1) the combination of LDA and the chiral lithium amide **1b**, (2) the use of excess chiral lithium amide **1b** and (3) the regeneration of the chiral lithium amide **1b** after the lithiation of the ketone **3**, afforded the aldol **4** in about 90% yield and 70% ee. These results suggest that the same complex is formed from the enolate and the chiral lithium amide regardless of the formation method. In other words, the chiral amine **1a** or

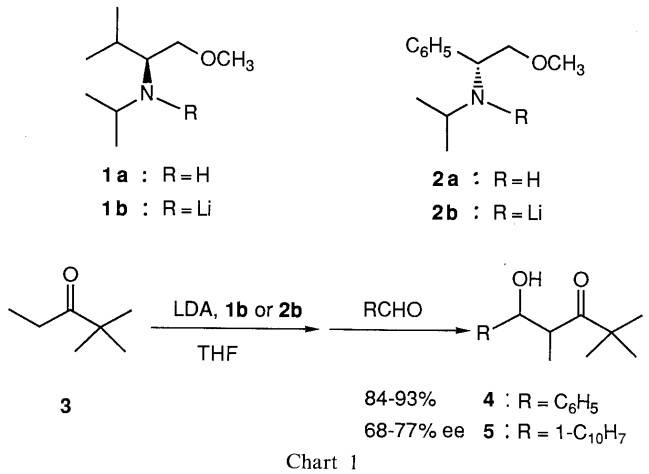

Chart 1

TABLE I. Aldol Reaction of 2,2-Dimethyl-3-pentanone (**3**) with Benzaldehyde in the Presence of the Chiral Lithium Amide **1b**

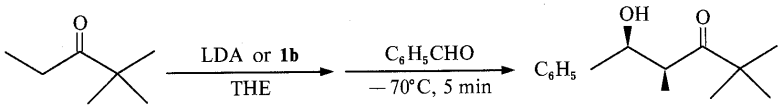

3 **4**

Run	**1a** (eq)	$((CH_3)_2CH)_2NH$ (eq)	n-C_4H_9Li (eq)	Lithiation conditions Temp (°C)	Time (min)	Isolated yield of **4** (%)[a]	% ee (config.)[b]
1	2.4		2.4	−10	30	84	70 (*S*, *S*)
2	2.4		2.4	−70	300	68	69 (*S*, *S*)
3	5.0		5.0	−10	30	59	60 (*S*, *S*)
4	1.2		1.2+1.0[c]	−10	30	90	67 (*S*, *S*)
5	1.2	1.2	2.4	−10	30	93	68 (*S*, *S*)
6	1.2	1.2	2.4	−70	30	88	33 (*S*, *S*)
7	1.2	1.2	2.4	−70	180	79	48 (*S*, *S*)

a) Only the *erythro* isomer was obtained. *b*) Determined by HPLC analysis using a chiral stationary phase column. *c*) This amount of *n*-butyllithium was added after the lithiation of the ketone **3** was completed.

TABLE II. Effects of Solvent and Additive

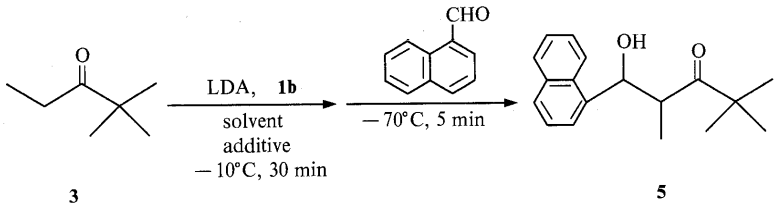

3 **5**

Run	Solvent	Additive[a] (eq)	Isolated yield of **5** (%)	Ratio[b] *Erythro* : *Threo*	% ee of *erythro* isomer	(config.)[b]	% ee of *threo* isomer	(config.)[b]
1	THF		85	97 : 3	77	(*S*, *S*)	21	(*R*, *S*)
2	Ether		76	92 : 8	38	(*R*, *R*)	36	(*R*, *S*)
3	Toluene		58	58 : 42	11	(*R*, *R*)	6	(*S*, *R*)
4	DME[c]		92	85 : 15	24	(*R*, *R*)	59	(*R*, *S*)
5	THF	TMEDA (1.2)	94	97 : 3	78	(*S*, *S*)	28	(*R*, *S*)
6	THF	TMEDA (20.0)	87	95 : 5	75	(*S*, *S*)	18	(*S*, *R*)
7	Ether	TMEDA (1.2)	89	92 : 8	35	(*R*, *R*)	32	(*R*, *S*)
8	Ether	TMEDA (20.0)	71	91 : 9	20	(*R*, *R*)	2	(*R*, *S*)
9	THF	HMPA (1.2)	86	94 : 6	68	(*S*, *S*)	14	(*S*, *R*)
10	Ether	HMPA (1.2)	82	95 : 5	58	(*S*, *S*)	2	(*R*, *S*)
11	Ether	HMPA (20.0)	72	98 : 2	70	(*S*, *S*)	14	(*S*, *R*)

a) TMEDA: *N*,*N*,*N*′,*N*′-tetramethylethylenediamine. HMPA: hexamethylphosphoric triamide. *b*) Determined by HPLC analysis. *c*) 1,2-Dimethoxyethane.

diisopropylamine would not participate in the chiral recognition of this reaction.[7] On the other hand, it has already been revealed[3a] that when the ketone was lithiated by utilizing 1.2 eq of LDA and 1.2 eq of the chiral lithium amide **1b** at −70 °C for 30 min, the enantiomeric excess of the aldol **4** fell to 33%. This temperature effect can be explained by considering the participation of diisopropylamine. When LDA deprotonates the ketone **3** to form the enolate, this enolate would form a complex with diisopropylamine and the conversion of this enolate–diisopropylamine complex to the enolate–chiral lithium amide complex would be slow at −70 °C. In fact, when the ketone **3** was treated with LDA and the chiral lithium amide **1b** at −70 °C for 3 h, the enantiomeric excess of the aldol **4** rose to 48%. From the above investigations, we concluded that the most effective reaction conditions are as follows: the ketone is lithiated by using the combination of LDA and the chiral lithium amide at −10 °C for 30 min, then allowed to react with aldehyde at −70 °C for 5 min. We used these reaction conditions for further studies.

Since tetrahydrofuran (THF) is the most widely used solvent in the reaction of lithium enolates and we had used this solvent for previous studies, we next examined the effects of solvent and then additive using the reaction of the ketone **3** and 1-naphthaldehyde in the presence of the chiral lithium amide **1b**. The results are summarized in Table II. As previously reported,[3b] when this reaction was performed in THF the aldol **5** was obtained in 85% yield with good diastereoselectivity[6] (*erythro* : *threo* = 97 : 3). The enantiomeric excess of the *erythro* isomer was 77% and the absolute configuration of the major enantiomer was (*S*,*S*).[8] On the other hand, when diethyl ether was used as the solvent, the diastereoselectivity was still high (*erythro* : *threo* = 92 : 8). Interestingly, however, the absolute configurations of the major enantiomer were reversed and (*R*,*R*)-**5** of 38% ee was obtained. Both diastereo- and enantioselectivities decreased in toluene or 1,2-dimethoxyethane.

We next studied the effects of additives in THF or

ether. The addition of *N*,*N*,*N*′,*N*′-tetramethylethylenediamine (TMEDA) had little effect on the stereoselectivity in both solvents. However, when hexamethylphosphoric triamide (HMPA) was added, the stereoselectivity changed dramatically. In THF, the addition of 1.2 eq of HMPA lowered the enantiomeric excess of the aldol **5** to 68%. In contrast, when the reaction was performed in ether with 1.2 eq of HMPA, reversal of the enantioselectivity was again observed and (*S*,*S*)-**5** of 58% ee was obtained as the major isomer. Furthermore, the increase of the amount of HMPA caused an increase of the enantiomeric excess and finally 70% ee was achieved when 20 eq of HMPA was added.

From the above results, it is clear that the enolate derived from the ketone **3** reacts with the aldehyde at opposite faces depending on the reaction conditions. In THF or ether–HMPA, the enolate mainly attacks from the *re*-face to afford the (*S*,*S*)-aldol while in ether it attacks from the *si*-face to afford the (*R*,*R*)-aldol. These facts indicate that the structure of the major complex which is formed from the enolate and the chiral lithium amide in THF or ether–HMPA is different from that formed in ether. Although the precise structure of the complex is still unknown,[7] it seems reasonable that the structure of the chiral lithium amide, especially its conformation,[9] plays an important role in the stereoselectivity. According to this assumption, we have prepared many chiral amines which have various substituents on chiral carbon, nitrogen and the chelating group and have investigated the effects of these substituents.[3] However, we have not yet examined chiral amines possessing two chiral centers in the molecule. So we were next interested in the effects of a newly introduced chiral center.

Since the chiral lithium amide **2b** having the phenyl group on the chiral carbon has turned out to be a very effective chiral ligand,[3] we decided to introduce another phenyl group into this molecule. Thus, we designed new chiral amines **6**—**8** and prepared them by the method shown in Chart 2. At first we tried to convert (1*S*,2*R*)-2-amino-1,2-diphenylethanol (**9**)[10] to its N-isopropyl-O-methyl derivative **6a** according to the method developed earlier.[3b] Although the reductive isopropylation using sodium cyanoborohydride and acetone proceeded smoothly, the yield of O-methylation utilizing sodium or potassium hydride and methyl iodide[11] was unsatisfactorily low because of the concomitant formation of N-methyl and N,O-dimethyl derivatives. The use of silver oxide–methyl

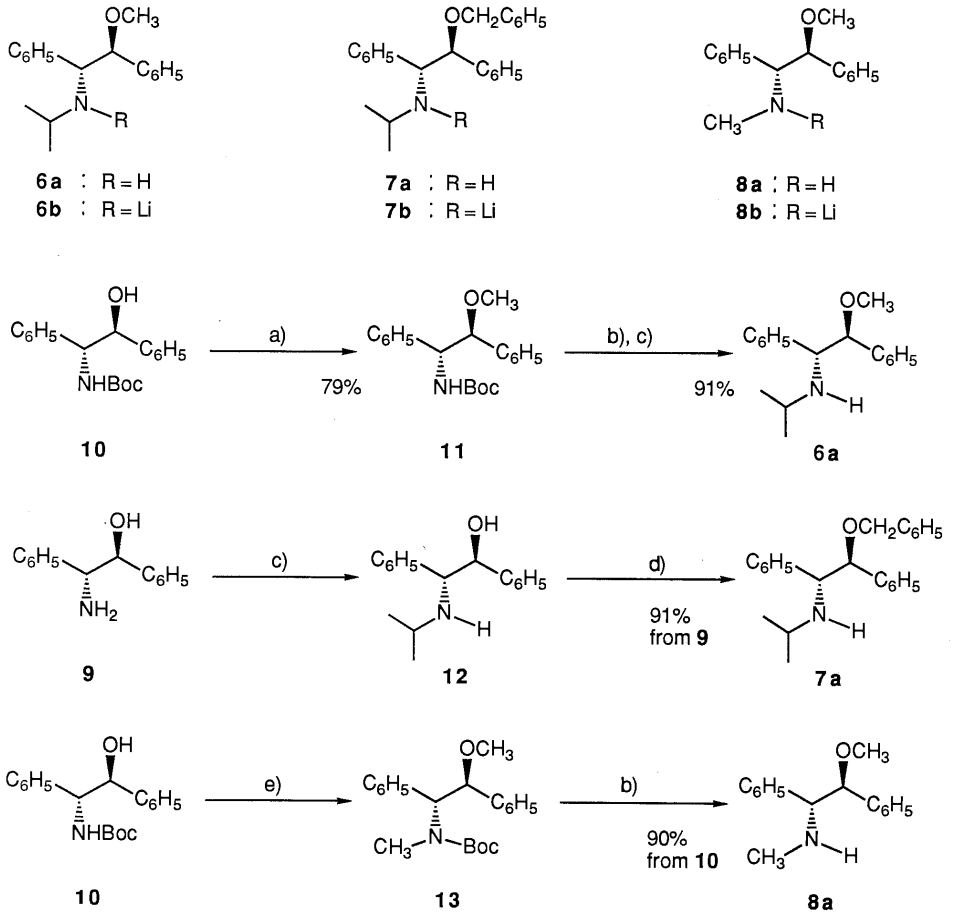

reagents a) NaH(1.1eq), CH_3I(10eq), THF b) CF_3CO_2H, CH_2Cl_2
c) CH_3COCH_3, $NaBH_3CN$, CH_3CO_2H, CH_3OH
d) KH, $C_6H_5CH_2Br$, THF e) NaH(10eq), CH_3I(20eq), THF

Chart 2

TABLE III. Aldol Reaction of 2,2-Dimethyl-3-pentanone (**3**) and Benzaldehyde in the Presence of Various Chiral Lithium Amides

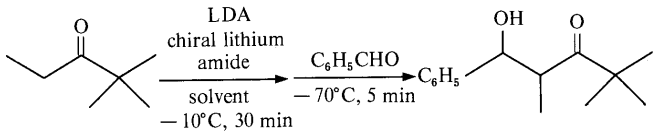

3 **4**

Run	Chiral lithium amide	Solvent	Isolated yield of **4** (%)[a]	% ee	(config.)[b]
1	**6b**	THF	87	74	(*R*, *R*)
2	**6b**	Ether	70	17	(*R*, *R*)
3	*ent*-**6b**	THF	88	62	(*S*, *S*)
4	**7b**	THF	79	58	(*R*, *R*)
5	*ent*-**7b**	THF	73	59	(*S*, *S*)
6	*ent*-**7b**	Ether	74	8	(*S*, *S*)
7	**8b**	THF	78	21	(*R*, *R*)
8	*ent*-**8b**	THF	66	20	(*S*, *S*)
9	*ent*-**8b**	Ether	65	5	(*S*, *S*)

a) Only the *erythro* isomer was obtained. *b*) Determined by HPLC analysis using a chiral stationary phase column.

iodide also proved to be unsuccessful. However, when the N-protected compound **10** was treated with sodium hydride and excess methyl iodide, the O-methylated derivative **11** was obtained in 79% yield. Acid hydrolysis of the *tert*-butoxycarbonyl group followed by reductive alkylation gave the desired chiral amino ether **6a** in good yield. In contrast to O-methylation, O-benzylation of the N-isopropyl derivative **12** using potassium hydride and benzyl bromide afforded the O-benzyl derivative **7a** selectively in excellent yield. We further prepared the N,O-dimethyl derivative **8a** by treatment of the N-protected compound **10** with a large excess of sodium hydride-methyl iodide followed by acid hydrolysis. The enantiomers of **6**—**8** (*ent*-**6**—*ent*-**8**) were also prepared by the same methods from (1*R*,2*S*)-2-amino-1,2-diphenylethanol (*ent*-**9**).[10]

Utilizing these chiral amino ethers, we investigated the aldol reaction of the ketone **3** and benzaldehyde. The results are summarized in Table III. When the chiral lithium amides **6b**—**8b** were used in THF, (*R*,*R*)-**4**[8] was obtained as the major isomer and as a matter of course, when *ent*-**6b**—*ent*-**8b** were used (*S*, *S*)-**4**[8] was predominant. Among them, the N-isopropyl-O-methyl derivative **6b** showed the highest enantioselectivity and 74% ee was realized. The N-isopropyl-O-benzyl derivatives **7b** and *ent*-**7b** gave the aldol **4** of about 60% ee, while the N,O-dimethyl derivatives **8b** and *ent*-**8b** showed poor selectivity. We also performed this reaction in ether in the presence of **6b**—**8b**. In contrast to the chiral lithium amide **1b**, the solvent effects were not so dramatic; we merely obtained the aldol **4** in low enantiomeric excess. Probably, these chiral lithium amides are too sterically bulky to form a complex of similar structure to that formed by the amide **1b** and the enolate of the ketone **3** in ether.

Thus we thoroughly investigated the reaction conditions of the aldol reaction using chiral lithium amide as the chiral auxiliary. We concluded that the combined use of LDA and the chiral lithium amide at −10 °C to form the enolate–chiral lithium amide complex is the condition of choice. Furthermore, we found that both the solvent (THF or ether) and the additive (HMPA) have a large influence on the stereoselectivity. We also examined new chiral ligands possessing two chiral centers in a molecule. Although the effects of the newly introduced chiral center are not as great as we had expected, we believe that further modification of the chiral lithium amide may provide more effective auxiliaries.

Experimental

Melting and boiling points are uncorrected. Infrared (IR) spectra were measured with a JASCO IRA-2 spectrometer using nujol mulls or potassium bromide disks or as films. Proton nuclear magnetic resonance (^{1}H-NMR) spectra were recorded on a JEOL PMX-60, FX-100, EX-270 or GSX-400 spectrometer with tetramethylsilane as an internal standard in deuteriochloroform. Optical rotations were measured with a JASCO DIP-140 automatic polarimeter. High-performance liquid chromatography (HPLC) was carried out with an Erma Optical Works ERC-8710 high-performance liquid chromatograph using a Bakerbond TM (DNBPG) chiral column (RP-7103-0) (i.d. 4.6 × 250 mm, purchased from J. T. Baker Chemical Co.) as described earlier.[3b] Ether was distilled from lithium aluminum hydride and THF was distilled from benzophenone ketyl. Silica gel (BW-820 MH or BW-200, purchased from Fuji-Davison) was used for column chromatography. All reactions involving organometallic reagents were conducted under an argon atmosphere.

General Procedure for the Enantioselective Aldol Reaction First TMEDA or HMPA (if necessary) and then *n*-butyllithium (1.6 M in *n*-hexane, 1.5 ml, 2.4 mmol) were added to a solution of diisopropylamine (121 mg, 1.2 mmol) and the chiral amino ether (1.2 mmol) in a solvent (8 ml) at −10 °C. After 30 min, the ketone **3** (114 mg, 1.0 mmol) in the same solvent (2 ml) was added over 5 min. The mixture was stirred at −10 °C for 30 min then cooled to −70 °C, and benzaldehyde or 1-naphthaldehyde (1.1 mmol) was added in one portion. After 5 min, saturated aqueous ammonium chloride (2 ml) was added and the mixture was warmed to room temperature. Water (20 ml) was added, and the mixture was extracted with ether. The organic layer was washed with 10% aqueous citric acid, water, and saturated aqueous sodium chloride and dried over sodium sulfate. After concentration *in vacuo*, the residue was purified by chromatography on silica gel using *n*-hexane–ethyl acetate (15 : 1, for **4**) or *n*-hexane–ether (15 : 1, for **5**) as an eluent. The enantiomeric excess of each aldol was determined by HPLC according to the method previously reported.[3b] The results are summarized in Tables II and III.

(1*S*,2*R*)-2-*tert*-Butoxycarbonylamino-1-methoxy-1,2-diphenylethane (11) Di-*tert*-butyl dicarbonate (5.98 g, 27.4 mmol) in dioxane (15 ml) was added to a solution of (1*S*,2*R*)-2-amino-1,2-diphenylethanol (**9**)[10] (5.28 g, 25 mmol) in dioxane (35 ml), and the mixture was stirred at room temperature for 4.5 h. After addition of water, the mixture was extracted with ethyl acetate. The organic layer was washed with saturated aqueous sodium chloride and dried over sodium sulfate. Removal of the solvent gave almost pure **10** (7.47 g, 96%), which was used for the next step without further purification. The *N*-protected alcohol **10** (313 mg, 1.0 mmol) and methyl iodide (0.62 ml, 10 mmol) were added to a suspension of sodium hydride (60% oil suspension, 42 mg, 1.1 mmol) in THF (10 ml), and the mixture was stirred at room temperature for 4 h. Water was added to the mixture, and the whole was extracted with ethyl acetate. The extracts were washed with saturated aqueous sodium chloride, dried over sodium sulfate, and concentrated *in vacuo*. The residue was purified by column chromatography on silica gel (*n*-hexane : ethyl acetate = 5 : 1 as an eluent) to give **11** (258 mg, 79%) as a colorless solid, mp 165.5—167 °C (ethyl acetate). $[\alpha]_D^{23}$ +104.9° (*c* = 1, $CHCl_3$). IR ν_{max}^{KBr} cm^{-1}: 3380, 1685, 1510, 1170, 1110, 695. ^{1}H-NMR δ ppm: 1.40 (9H, s), 3.29 (3H, s), 4.56 (1H, s), 4.84 (1H, br s), 5.49 (1H, br s), 6.9—7.0 (4H, s), 7.1—7.3 (6H, s). *Anal.* Calcd for $C_{20}H_{25}NO_3$: C, 73.37; H, 7.70; N, 4.28. Found: C, 73.25; H, 7.66; N, 4.02.

(1*R*,2*S*)-2-*tert*-Butoxycarbonylamino-1-methoxy-1,2-diphenylethane (*ent*-11) This compound was prepared from (1*R*,2*S*)-2-amino-1,2-diphenylethanol (*ent*-**9**)[10] by the same procedure as described above. A colorless solid, mp 171.5 °C (benzene). $[\alpha]_D^{28}$ −97.7° (*c* = 1, $CHCl_3$). The IR and ^{1}H-NMR spectra of this material were in agreement with those of the (1*S*,2*R*)-isomer **11**.

(1*S*,2*R*)-2-Isopropylamino-1-methoxy-1,2-diphenylethane (6a) Trifluoroacetic acid (2.5 ml) was added to a solution of the *tert*-butylurethane **11** (360 mg, 1.1 mmol) in dichloromethane (9 ml). The mixture was stirred at room temperature for 1.5 h and concentrated *in vacuo*. Benzene was added

to the residue and evaporated *in vacuo*. Water was then added to the residue and the solution was made basic with 10% aqueous sodium hydroxide. The solution was salted out with sodium chloride and extracted with ethyl acetate, and the organic layer was dried over sodium sulfate. Removal of the solvent gave the primary amine which was used for the next step without further purification. Sodium cyanoborohydride (117 mg, 1.9 mmol) and acetone (0.45 ml, 6.1 mmol) were added to a solution of the primary amine in methanol (13 ml), and the pH of the solution was adjusted to *ca.* 4 by adding acetic acid. The mixture was stirred for 3.5 h. Aqueous potassium carbonate (10%) was added to the mixture in an ice-bath, and the solution was extracted with ethyl acetate. The extracts were washed with saturated aqueous sodium chloride, and dried over sodium sulfate. Concentration *in vacuo* provided the residue, which was purified by column chromatography on silica gel (*n*-hexane : ethyl acetate = 7 : 1—4 : 1 as an eluent) to give **6a** (270 mg, 91%) as a colorless oil, bp 140 °C (0.3 mmHg) (Kugelrohr). $[\alpha]_D^{20}$ +103.2° (c = 1, CH_3OH). IR ν_{max}^{film} cm^{-1}: 3300, 2950, 1450, 1105, 760, 700. ^{1}H-NMR δ ppm: 0.89 (3H, d, J = 6.2 Hz), 0.96 (3H, d, J = 6.2 Hz), 1.9 (1H, br s), 2.52 (1H, sept, J = 6.2 Hz), 3.18 (3H, s), 3.90 (1H, d, J = 5.1 Hz), 4.43 (1H, d, J = 4.9 Hz), 7.0—7.1 (2H, m), 7.1—7.2 (2H, m), 7.2—7.6 (6H, m). *Anal.* Calcd for $C_{18}H_{23}NO$: C, 80.26; H, 8.61; N, 5.20. Found: C, 80.41; H, 8.77; N, 5.17.

(1*R*,2*S*)-2-Isopropylamino-1-methoxy-1,2-diphenylethane (*ent*-6a) This compound was prepared from the enantiomer of **11** (*ent*-**11**) by the same procedure as described above. A colorless oil, bp 145 °C (0.4 mmHg) (Kugelrohr). $[\alpha]_D^{23}$ −99.3° (c = 1.4, CH_3OH). The IR and ^{1}H-NMR spectra of this material were in agreement with those of the (1*S*,2*R*)-isomer **6a**.

(1*S*,2*R*)-1-Benzyloxy-2-isopropylamino-1,2-diphenylethane (7a) (1*S*,2*R*)-2-Amino-1,2-diphenylethanol (**9**)[10] was N-isopropylated by the same procedure as used for the preparation of **6a** to give **12**. The crude *N*-isopropyl derivative **12** was used in the the next step without further purification. The amino alcohol **12** (79 mg, 0.3 mmol) was added to a suspension of potassium hydride (35% oil suspension, 181 mg, 1.6 mmol) in THF (1.5 ml) and the mixture was stirred for 30 min at room temperature. Benzyl bromide (0.18 ml, 1.5 mmol) was added and the mixture was stirred for another 30 min. Water was added, and the solution was extracted with ether. The organic layer was washed with saturated aqueous sodium chloride, and dried over sodium salfate. The solvent was evaporated off *in vacuo*, and the residue was purified by chromatography on slica gel (*n*-hexane : ethyl acetate = 6 : 1 as an eluent). The desired amino ether **7a** was obtained (97 mg, 91%) as a colorless oil, bp 165 °C (0.2 mmHg) (Kugelrohr). $[\alpha]_D^{24}$ +43.8° (c = 0.6, CH_3OH). IR ν_{max}^{KBr} cm^{-1}: 3320, 2970, 1450, 1105, 1075, 760, 700. ^{1}H-NMR δ ppm: 0.85 (3H, d, J = 6.2 Hz), 0.91 (3H, d, J = 6.3 Hz), 1.62 (1H, s), 2.50 (1H, sept, J = 6.3 Hz), 3.94 (1H, d, J = 6.0 Hz), 4.19 (1H, d, J = 11.8 Hz), 4.41 (1H, d, J = 11.9 Hz), 4.57 (1H, d, J = 5.9 Hz), 7.0—7.3 (15 H, m). *Anal.* Calcd for $C_{24}H_{27}NO$: C, 83.44; H, 7.88; N, 4.05. Found: C, 83.60; H, 7.82; N, 3.67.

(1*R*,2*S*)-1-Benzyloxy-2-isopropylamino-1,2-diphenylethane (*ent*-7a) This compound was prepared from (1*R*,2*S*)-2-amino-1,2-diphenylethanol (*ent*-**9**)[10] by the same procedure as described above. A colorless oil, bp 175°C (0.4 mmHg) (Kugelrohr). $[\alpha]_D^{23}$ −43.7° (c = 1.1, CH_3OH). The IR and ^{1}H-NMR spectra of this material were in agreement with those of the (1*S*,2*R*)-isomer **7a**.

(1*S*,2*R*)-1-Methoxy-2-methylamino-1,2-diphenylethane (8a) The *tert*-butylurethane **10** (626 mg, 2.0 mmol) and methyl iodide (2.5 ml, 40 mmol) were added to a suspension of sodium hydride (60% oil suspension, 800 mg, 20 mmol) in THF (20 ml), and the mixture was stirred at room temperature for 2 h. The work-up procedure was the same as that for the preparation of **6a**. The crude N,O-dimethyl derivative **13** was used for the next step without further purification. Trifluoroacetic acid (1.5 ml) was added to a solution of **13** in dichloromethane (15 ml), and the solution was stirred at room temperature for 2 h. After concentration *in vacuo*, benzene was added to the residue and the mixture was again concentrated *in vacuo*. Saturated aqueous sodium bicarbonate was added to the residue and the mixture was extracted with ethyl acetate. The extracts were washed with saturated aqueous sodium chloride and dried over sodium sulfate. The solvent was removed and the residue was purified by chromatography on silica gel (chloroform: methanol = 20 : 1 as an eluent) to give the *N*,*O*-dimethyl amino ether **8a** (432 mg, 90%) as a colorless solid, mp 133—134 °C (benzene). $[\alpha]_D^{24}$ +39.6° (c = 1, $CHCl_3$). IR ν_{max}^{KBr} cm^{-1}: 3330, 2900, 1450, 1100, 760, 700. ^{1}H-NMR δ ppm: 2.40 (3H, s), 3.28 (3H, s), 3.4—4.4 (1H, br s), 3.94 (1H, d, J = 4.0 Hz), 4.83 (1H, d, J = 4.0 Hz), 6.9—7.3 (10H, m). *Anal.* Calcd for $C_{16}H_{19}NO$: C, 79.63; H, 7.94; N, 5.80. Found: C, 79.82; H, 8.07; N, 5.50.

(1*R*,2*S*)-1-Methoxy-2-methylamino-1,2-diphenylethane (*ent*-8a) This compound was prepared from the enantiomer of **10** (*ent*-**10**) by the same procedure as described above. A colorless solid, mp 129 °C (*n*-hexane). $[\alpha]_D^{23}$ −38.2° (c = 1, $CHCl_3$). The IR and ^{1}H-NMR spectra of this material were in agreement with those of the (1*S*,2*R*)-isomer **8a**.

Acknowledgement We thank Miss Y. Hiraga for her helpful experimental assistance. This work was financially supported in part by a grant (to A. A.) from the Japan Science Society.

References and Notes

1) New Methods and Reagents in Organic Synthesis 89.
2) C. H. Heathcock, "*Asymmetric Synthesis*," Vol. 3, Part B, ed. by. J. D. Morrison, Academic Press, New York, 1984, p. 111 and references cited therein.
3) *a*) A. Ando and T. Shioiri, *J. Chem. Soc., Chem. Commun.*, **1987**, 1620; *b*) *Idem*, *Tetrahedron*, **45**, 4969 (1989).
4) For the aldol reaction of the ketone lithium enolates and aldehydes, see: C. H. Heathcock, C. T. Buse, W. A. Kleschick, M. C. Pirrung, J. E. Sohn, and J. Lampe, *J. Org. Chem.*, **45**, 1066 (1980).
5) M. Muraoka, H. Kawasaki, and K. Koga, *Tetrahedron Lett.*, **29**, 337 (1988).
6) The *erythro* configurations of the aldols were assigned from the ^{1}H-NMR coupling constants. See: C. H. Heathcock, M. C. Pirrung, and J. E. Lampe, *J. Org. Chem.*, **44**, 4294 (1979).
7) D. Seebach, *Angew. Chem. Int. Ed. Engl.*, **27**, 1624 (1988) and references cited therein.
8) Determination of the absolute configurations of the aldols, see ref. 3*b*.
9) R. Shirai, M. Tanaka, and K. Koga, *J. Am. Chem. Soc.*, **108**, 543 (1986).
10) Both enantiomers of 2-amino-1,2-diphenylethanol are commercially available from Aldrich Chemical Company.
11) A. I. Meyers, G. S. Poindexter, and Z. Brich, *J. Org. Chem.*, **43**, 892 (1978).

Selective Monoalkylation of Acyclic Diols by Means of Dibutyltin Oxide and Fluoride Salts[1,2]

Nobuo NAGASHIMA and Masaji OHNO*,[3]

Faculty of Pharmaceutical Sciences, University of Tokyo, 7-3-1, Hongo, Bunkyo-ku, Tokyo 113, Japan. *Received February 12, 1991*

Fluoride anion was found to promote monoalkylation reaction of diols by the stannylene acetal method, and selective monoalkylation of various acyclic diols was accomplished in good yields under mild conditions by employing this new method. Functional groups such as carboxylic acid ester, carboxamide, carbamate, nitrile, alkyl chloride, and ether were not affected under the reaction conditions.

Keywords monoalkylation; stannylene acetal; cesium fluoride; 1,2-diol; 1,3-diol

It is highly desirable to develop an efficient method for selective protection of symmetric and unsymmetric diols, because the monoprotected diols are often useful as synthetic intermediates of bifuntional compounds in organic synthesis. Therefore, various methods have been developed[4] especially for selective protection of unsymmetric diols, though the monoprotection of symmetric diols[5] still remains to be explored. In general, the use of one stoichiometric equivalent of a protecting reagent to a diol results in a statistical mixture of diprotected, monoprotected, and unprotected products. To overcome this difficulty, a large excess of diol is commonly used.[6] However, the method cannot be applied in the case of diols obtained by multi-step synthesis. Therefore, monoprotection[7] of diols with 1 eq amount of protective groups is indeed required. From this point of view, monoprotection of diols through reductive opening of alkylidene acetals[8] or stannylene acetals[9] has been developed successfully, and the latter was found to be particularly efficient for various monofunctionalizations of diols.[10] However, monoalkylation of diols by the stannylene acetal method requires rather strong reaction conditions (*i.e.*, elevated temperature and prolonged reaction time [9,11]) even with the assistance of a stannophilic catalyst, such as a tetraalkylammonium halide.[12] If this reaction could be carried out under milder conditions, its synthetic utility would be considerably increased. In a previous communication,[1] we reported an efficient method for the monoalkylation of dimethyl L-tartrate by use of dibutyltin oxide and cesium fluoride under mild reaction conditions. In this paper, we wish to report the details of the methodology with examples of selective benzylation of unsymmetric diols.

Results and Discussion

Monoalkylation of Dialkyl Tartrates We first used dialkyl tartrates as substrates for monoalkylation, because dialkyl tartrates have been widely used as chiral synthons for the synthesis of various biologically active compounds or enantiomerically pure compounds[13] and also because only a few reports about the monoalkylation of dialkyl tartrates are available.[14] We first examined monobenzylation of dimethyl L-tartrate using the method developed by Moffatt

TABLE I. Monoalkylation of Dialkyl Tartrates

Entry	Tartrate	R'X (eq)	Fluoride salt (eq)	Solvent	Temperature	Time	Product	Yield[a] (%)
1	**1**	$PhCH_2Br$ (2.04)	No salt	DMF	100 °C	3 h	**4**	41
2	**1**	$PhCH_2Br$ (3.00)	*n*-Bu_4NBr (0.5)	PhMe	100 °C	1 h	**4**	13
3	**1**	$PhCH_2Br$ (2.19)	CsF (1.22)	DMF	rt	2 h	**4**	85
4	**1**	$PhCH_2I$ (1.11)	No salt	DMF	100 °C	2 h	**4**	13
5	**1**	$PhCH_2I$ (2.84)	CsF (1.93)	DMF	rt	1 h	**4**	99
6	**1**	$PhCH_2I$ (1.71)	KF (1.53)	DMF	50 °C→rt	2 h→11.0 h	**4**	55
7	**1**	$PhCH_2I$ (2.11)	*n*-Bu_4NF (1.60)	DMF	rt	24 h	**4**	67
8	**1**	$PhCH_2I$ (2.41)	CsF (2.03)	PhMe[b]	rt	25 h	**4**	48
9	**1**	$PhCH_2I$ (2.33)	CsF (1.70)	PhMe[c]	rt	45 h	**4**	75
10	**1**	$PhCH_2I$ (1.91)	CsF (1.30)	PhMe[d]	rt	45 h	**4**	3.8
11	**1**	$PhCH_2I$ (1.52)	CsF (1.64)	THF	rt	25 h	**4**	69
12	**1**	*p*-$NO_2C_6H_4CH_2I$ (2.00)	CsF (1.29)	DMF	rt	3.5 h	**5**	84
13	**1**	*p*-$NO_2C_6H_4CH_2Br$ (1.50)	CsF (1.90)	DMF	rt	46 h	**5**	93
14	**1**	*p*-$MeOC_6H_4CH_2Cl$ (1.12)[e]	*n*-Bu_4NF (1.00)	THF	rt	72 h	**6**	45
15	**1**	*p*-$MeOC_6H_4CH_2Cl$ (1.44)[e]	KF (1.23)	DMF	rt	14 h	**6**	52
16	**1**	*p*-$MeOC_6H_4CH_2Cl$ (1.54)[f]	KF (1.27)	DMF	rt	72 h	**6**	68
17	**1**	*p*-$MeOC_6H_4CH_2Cl$ (1.35)[f]	CsF (1.19)	DMF	0 °C→rt	20 min→1 h	**6**	67
18	**1**	*p*-$MeOC_6H_4CH_2I$ (2.10)	CsF (2.05)	DMF	0 °C→rt	20 min→20 min	**6**	72
19	**1**	$CH_2=CHCH_2Br$ (1.26)	CsF (1.39)	DMF	rt	20 h	**7**	83
20	**1**	$CH_2=CHCH_2I$ (1.53)	CsF (1.62)	DMF	rt	6 h	**7**	98
21	**2**	MeI (4.29)	CsF (1.26)	DMF	rt	21 h	**8**	72
22	**2**	$PhCH_2I$ (1.55)	CsF (1.37)	DMF	rt	3 h	**9**	92
23	**3**	$PhCH_2I$ (2.22)	KF (2.03)	MeCN	rt	50 h	**9**	90
24	**3**	$PhCH_2I$ (2.13)	CsF (1.52)	DMF	rt	5 h	**10**	94

a) Isolated yields after chromatography on silica gel. *b*) The reaction was carried out in the presence of 10 mol% of dibenzo-24-crown-8. *c*) The reaction was carried out in the presence of 10 mol% of dicyclohexano-18-crown-6. *d*) No crown ether was used. *e*) Tetra-*n*-butylammonium iodide (10 mol% in entry 14 and 1 eq in entry 15) was also used as an additive. *f*) Potassium iodide (1.54 eq in entry 16 and 1.33 eq in entry 17) was also used as an additive. rt = room temperature.

et al.,[9] but the yield of the desired product was only 41% (entry 1 in Table I). The same reaction using benzyl iodide gave a much lower yield (entry 4 in Table I) than in the case of benzyl bromide. The results clearly showed that the procedure cannot be applied to monobenzylation of dimethyl L-tartrate. Furthermore, monobenzylation of dimethyl L-tartrate by David's procedure[12a] also gave a low yield of the monoalkylation product (entry 2 in Table I). Therefore, we attempted to improve Moffatt's procedure by the use of additives. By analogy with the fluorodesilylation process, we first examined the effect of fluoride salts in the monoalkylation reaction of dialkyl tartrates (Eq. 1).

The results are listed in Table I. It is apparent from Table I that fluoride anion promoted the reactions, allowing them to proceed even at room temperature with good to excellent yields of the monoalkylated products (entries 3, 5 to 7 *vs.* entries 1 and 4 in Table I). Among the fluoride salts tested, cesium fluoride showed a most remarkable effect. Thus, monobenzylation of tartrate 1 using benzyl iodide and cesium fluoride in *N*,*N*-dimethylformamide (DMF) took place within 1 h at room temperature and gave a quantitative yield of monobenzylated tartrate, **4** (entry 5 in Table I). Other alkyl groups such as *p*-nitrobenzyl, *p*-methoxybenzyl, allyl, and methyl were also introduced in good to excellent yields (entries 13, 18, 20 and 21 in Table I).

As the reaction solvents, polar aprotic solvents such as DMF, tetrahydrofuran (THF) and acetonitrile were successfully employed (entries 5, 11 and 23 in Table I); DMF usually gave the best results. The reactions in nonpolar solvents such as toluene were also possible with the aid of phase transfer catalysts (entries 8 to 10 in Table I). However, the reactions were slower and the yields of products were not so high.

As for the alkylating reagents, the reactions with alkyl iodides usually gave better yields than those with the corresponding bromides (entries 5 *vs.* 3 and 20 *vs.* 19 in Table I), and in the case of an unstable alkyl iodide (entry 18 in Table I), it can be formed *in situ* from the corresponding chloride and the appropriate iodides (entries 14 to 17 in Table I). When dimethyl L-tartrate was treated with 1 eq of benzyl bromide and 1 eq of cesium fluoride in DMF at room temperature, the reaction gave only a 5% yield of the monobenzylated tartrate, **4** (Eq. 2). Therefore, it is evident that the combined use of stannylene acetal of tartrates and cesium fluoride is essential for the selective preparation of the monoalkylated tartrates.

As an efficient method for monoalkylation of symmetric diols had thus been realized, we next examined regioselectivity in monobenzylation of unsymmetrical diols.

Regioselective Benzylation of Unsymmetrical Diols 1-Phenylethanediol was selected as a simple unsymmetrical diol and subjected to monobenzylation under various conditions (Eq. 3). The results are shown in Table II.

The influence of various factors such as benzyl halides, metal fluorides, solvents and temperatures was investigated.

Table II. Regioselective Benzylation of 1-Phenylethanediol

Entry	X in $PhCH_2X$ (eq)	MF (eq)	Solvent	Temperature (°C)	Time (h)	Yield[a] (%) of **29a** and **29b**	Ratio (**29a**: **29b**)
1	I (1.71)	CsF (1.90)	DMF	0—3	1.5	Quant.	90:10
2	I (2.18)	No salt	DMF	0—3	2	0	—
3	I (1.75)	CsF (1.93)	DMF	20—21	1.5	94	91: 9
4	F (1.70)	CsF (1.90)	DMF	0—3	2	0	—
5	Cl (1.71)	CsF (1.92)	DMF	21—22	24	83	87:13
6	Br (1.72)	CsF (1.94)	DMF	21—22	6	95	90:10
7	I (1.72)	CsF (1.96)	THF	20—22	17	96	90:10
8	I (1.82)	CsF (1.93)	MeCN	21—22	5	96	88:12
9	I (1.74)	CsF (1.90)	Me_2CO	21—22	6	99	85:15
10	I (1.71)	CsF (1.97)	$MeNO_2$	21—22	20	N.D.[b]	—
11	I (1.74)	KF (2.01)	DMF	21—22	45	20	88:12
12	I (1.74)	KF (2.26)	MeCN	21—22	50	40	88:12
13	I (1.79)	KF (2.16)	PhMe[c]	21—22	100	64	88:12
14	I (1.81)	KF (2.09)	PhMe[d]	21—22	100	0.6>	—

a) Isolated yields after chromatography on silica gel. *b*) N.D. means not determined. The yield could not be determined because of the formation of an inseparable unknown product together with the monobenzylated products, **29a** and **29b**. *c*) The reaction was carried out in the presence of 5 mol% of dicyclohexano-18-crown-6. *d*) No crown ether was used.

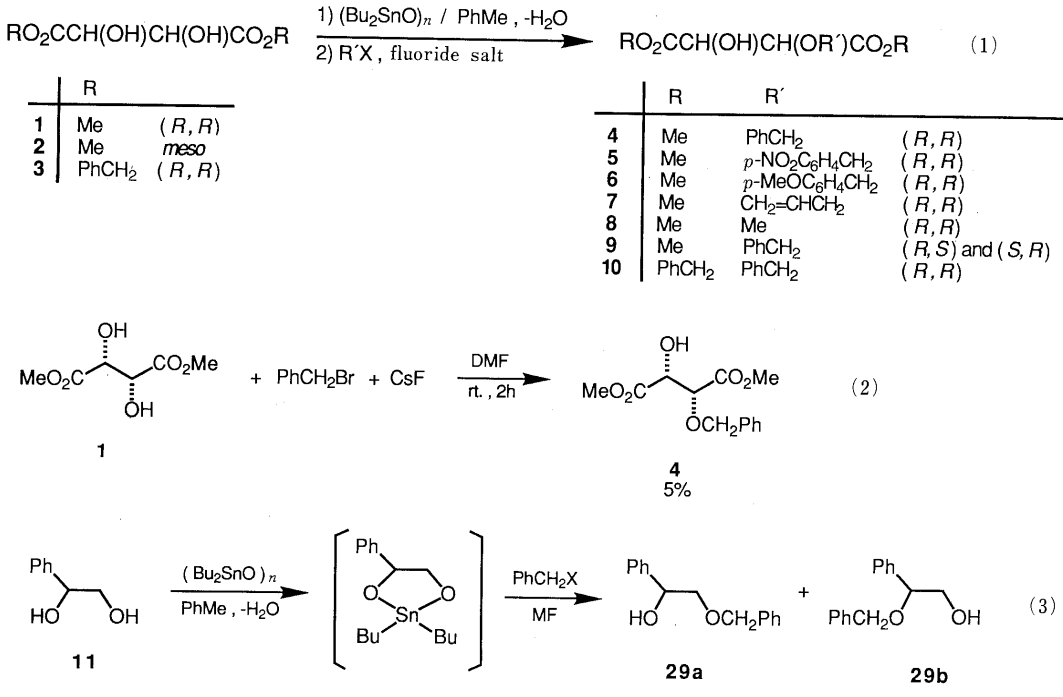

It was shown that the reaction rate increased in the following order (entries 3 to 6 in Table II); benzyl fluoride (no reaction) < benzyl chloride < benzyl bromide < benzyl iodide, while the regioselectivity in the reactions was found to be almost the same. Therefore, among the benzyl halides, benzyl iodide was found to be the best one. Next, the effect of the metal fluorides was investigated. No significant difference in the regioselectivity was observed between cesium fluoride and potassium fluoride, while the reaction rates and yields were markedly reduced in the latter case (entries 3 *vs.* 11; 8 *vs.* 12 in Table II). It is very clear that the reaction requires fluoride salts (entries 2 *vs.* 1 in Table II). Then, the solvent effect on the regioselectivity and the reaction rates was examined. While the reaction rates varied depending upon the solvents used, again no significant solvent effect on the regioselectivity was observed (entries 3, 7 to 9 and 12 to 14 in Table II). Among the solvents used, DMF gave the best result (entry 3 in Table II). No temperature-dependency was observed (entries 1 *vs.* 3 in Table II). Thus, the reaction using benzyl iodide and cesium fluoride in DMF at 0 °C to room temperature was found to proceed most smoothly.

Next, the regioselective benzylation of various acyclic diols (Eqs. 4 and 5) was examined. The results are listed in Tables III and IV. In Table III, the examples of diols containing primary and secondary hydroxyl groups are shown, and the examples of diols containing secondary–secondary or secondary–tertiary hydroxyl groups are shown in Table IV. Some functional groups were introduced into the diols in order to clarify the substituent effects on the regioselection and to examine the compatibility of various functional groups under the reaction conditions. Generally, the monobenzylation reaction of the diols listed in Tables III and IV proceeds in good to excellent yields, although there are some examples of moderate yields (entries 5, 6 and 16 in Table III and entry 5 in Table IV). The reaction of 1,2-diols is faster than that of corresponding 1,3-diols (entries 1 *vs.* 2 and 3 *vs.* 4 in Table III). In addition,

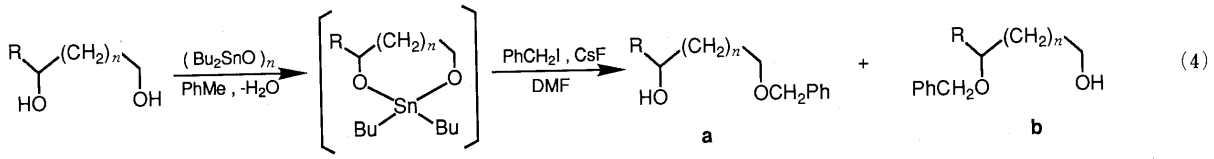

(4)

	R	n
11	Ph	0
12	Ph	1
13	Me	0
14	Me	1
15	$ClCH_2$	0
16	$NCCH_2$	0
17	$MeOCH_2$	0
18	*tert*-$BuOCH_2$	0
19	$PhCH_2OCH_2$	0
20	$PhCOOCH_2$	0
21	$BocNHCH_2$	0
22	$CbzNHCH_2$	0
23	$TsOCH_2$	0
24	CO_2Me	0
25	$CONH_2$	0
26	CONHMe	0
27	$CONMe_2$	0
28	COPh	0

	R	n
29a,b	Ph	0
30a,b	Ph	1
31a,b	Me	0
32a,b	Me	1
33a,b	$ClCH_2$	0
34a,b	$NCCH_2$	0
35a,b	$MeOCH_2$	0
36a,b	*tert*-$BuOCH_2$	0
37a,b	$PhCH_2OCH_2$	0
38a,b	$PhCOOCH_2$	0
39a,b	$BocNHCH_2$	0
40a,b	$CbzNHCH_2$	0
41a,b[a]	$TsOCH_2$	0
42a,b	CO_2Me	0
43a,b	$CONH_2$	0
44a,b	CONHMe	0
45a,b	$CONMe_2$	0
46a,b[a]	COPh	0

a) in the case of the diols **23** and **28**, the expected products were not obtained

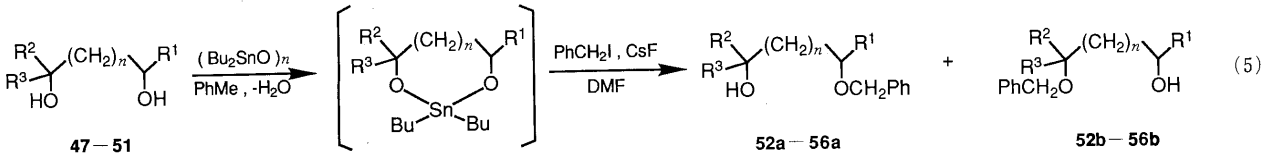

(5)

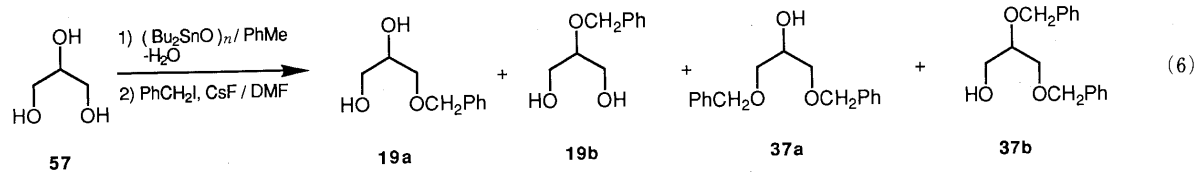

(6)

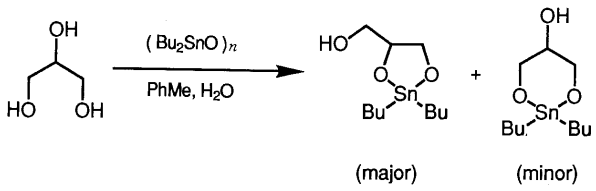

(7)

the reaction can be successfully carried out with diols containing functional groups such as carboxylic acid esters, carboxamides, carbamates, nitriles, alkyl chlorides, and others. However, *O*-tosylate and phenyl ketone groups are not compatible with the reaction conditions (entries 14 and 19 in Table III). For the diols in Table III, selective benzylation occurred at the primary hydroxyl groups[15]

TABLE III. Regioselective Benzylation of Acyclic 1,2- and 1,3-Diols Containing Primary and Secondary Hydroxyl Groups

Entry	Diol	Equiv. of $PhCH_2I$	Equiv. of CsF	Temperature (°C)	Time (h)	Product	Yield[a] (%)	**a**:**b** ratio
1	**11**	1.74	2.01	0—3	1.5	**29a, b**	Quant.	90:10
2	**12**	2.06	2.09	−5—3	21	**30a, b**	80	85:15
3	**13**	1.57	2.07	0—3	24	**31a, b**	Quant.	91: 9
4	**14**	1.65	2.58	0—3	50	**32a, b**	86	97: 3
5	**15**	1.98	1.51	rt	22	**33a, b**	64	81:19
6	**16**	2.10	1.31	rt	24	**34a, b**	51	93: 7
7	**17**	1.66	1.33	rt	44	**35a, b**	77	87:13
8	**18**	1.93	1.72	rt	50	**36a, b**	81	82:18
9	**19a**	2.17	1.91	rt	10	**37a, b**	81	89:11
10	**20**	1.97	1.64	rt	2	**38a, b**	81	87:13[b]
11	**21**	2.00	1.05	rt	120	**39a, b**	71[c]	94: 6
12	**22**	1.85	1.12	rt	140	**40a, b**	74[d]	94: 6
13	**22**	$PhCH_2Br$; 2.00	No salt	100	2	**40a, b**	17	87:13
14	**23**	1.63	1.45	rt	6	[e]	0	—
15	**24**	1.44	1.57	0—3	24	**42a, b**	76	82:18
16	**25**	1.88	1.15	0—3	2	**43a, b**	67[f]	82:18
17	**26**	1.88	1.01	0—3	22	**44a, b**	77[g]	91: 9
18	**27**	1.89	1.11	0—3	20	**45a, b**	98	89:11
19	**28**	1.62	1.21	rt	1	[e]	0	—

a) Isolated yields after chromatography on silica gel. *b*) The ratio was determined after the removal of the benzoyl group. See the experimental section. *c*) *O,O*-Dibenzylated product was also formed in 1.5% yield. *d*) *O,O*-Dibenzylated product was also formed in 3% yield. *e*) The reaction was not clean and no desired product was obtained. *f*) *O,O*-Dibenzylated product was also formed in 17.5% yield. *g*) *O,O*-Dibenzylated product was also formed in 9.7% yield.

TABLE IV. Regioselective Benzylation of Acyclic 1,2- and 1,3-Diols Containing Secondary–Secondary or Secondary–Tertiary Hydroxyl Groups

Entry	Diol	Equiv. of $PhCH_2I$	Equiv. of CsF	Temperature (°C)	Time (h)	Yield[a] (%)	Product ratio
1	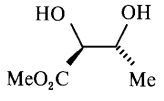 **47**	1.43	1.15	0—3	16	85	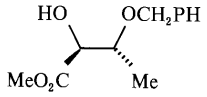 **52a** (65 : 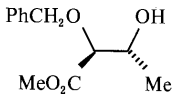 **52b** 35)
2	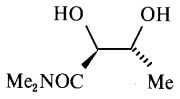 **48**	2.07	1.62	0—3	45	92	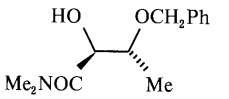 **53a** (81 : 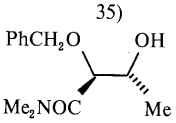 **53b** 19)
3	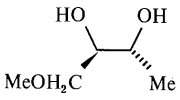 **49**	2.13	1.56	rt	20	76	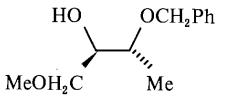 **54a** (50 : 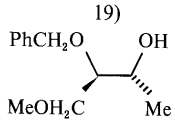 **54b** 50)
4	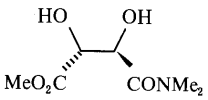 **50**	2.11	1.16	0—3	40	95	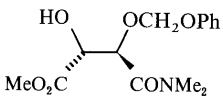 **55a** (75 : 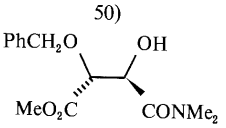 **55b** 25)
5	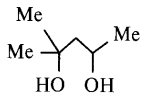 **51**	1.83	1.40	50—53	42	50	Only 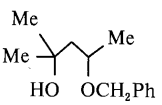 **56a**

a) Isolated yields after chromatography on silica gel.

and the regioselectivity (the ratio of the major isomer to the minor isomer) was in the range of 81:19 to 97:3. Furthermore, the regioselectivity was not necessarily improved when the bulkiness of the substituent R in diols was increased (entries 3 *vs.* 1, 5 to 12 in Table III and entries 4 *vs.* 2 in Table III). This fact seems to show that steric hindrance is not the major factor controlling the regioselectivity in these reactions. It should be emphasized that the present methodology afforded the expected product even in the case of unsuccessful Moffatt's procedure (entries 13 *vs.* 12 in Table III). In some cases (entries 11, 12, 16 and 17 in Table III), dibenzylation of the diols was also observed. This phenomenon was observed only for the diols containing NH groups of carboxamides or carbamates. The NH groups of carboxamides or carbamates form strong hydrogen bonding with fluoride anion.[16] Therefore, activation through the NH group is considered to occur in diols **21**, **22**, **25** and **26**. A similar effect of an OH group was also observed in the benzylation of glycerol (*vide post*). For the diols containing two secondary hydroxyl groups, modest regioselectivity was observed (entries 1, 2 and 4 in Table IV). Thus, preferential benzylation took place at the hydroxyl groups bonding to the carbon atoms which bear more electron-donating substituents (Me *vs.* CO_2Me or $CONMe_2$; $CONMe_2$ *vs.* CO_2Me). The 1,3-glycol **51**, which bears secondary and tertiary hydroxyl groups, was benzylated only at the secondary hydroxyl group (entry 5 in Table IV).

Benzylation of Glycerol Finally, the benzylation reaction of glycerol was examined (Eq. 6). The results are shown in Table V. If the five-membered stannylene acetal of glycerol is formed predominantly over the six-membered one (Eq. 7),[17] the expected benzylation products will be monobenzylated glycerol derivatives, **19a** and **19b**. However, Table V clearly shows that considerable amounts of dibenzylated glycerol derivatives, **37a** and **37b**, are also formed (entries 1 and 2 in Table V). Furthermore, the dibenzylated products, **37a** and **37b**, are also formed even in a reaction using Moffatt's procedure (entry 4 in Table V). These facts imply that the activation of the free OH group toward further benzylation probably occurs through the interactions of the OH group with tin atom and/or fluoride anion (hydrogen bond formation). When more than 2 eq of benzyl iodide and cesium fluoride were used, the reaction gave a good yield (71%) of dibenzylated derivatives, **37a** and **37b**, with the ratio of 9 to 1 (entry 3 in Table V). Thus, a direct and selective dibenzylation for glycerol has been achieved for the first time.

Mechanistic Aspect of the Reaction At present, the precise mechanism of the reaction is not known and mechanistic studies using ^{19}F- and/or ^{119}Sn-NMR remain to be done. However, it seems to be worthwhile to consider the mechanism of the present reaction. It is known that fluoride anion attacks tin atoms of *C*-trialkylstannylated compounds to form carbanion equivalents,[18] and transient formation of pentacoordinated tin complexes[19] is postu-

TABLE V. Benzylation of Glycerol

Entry	Equiv. of $PhCH_2I$	Equiv. of CsF	Temperature (°C)	Time (h)	Yield (%)[a]		Ratio	
					19a, b	**37a, b**	**19a : 58b**	**37a : 37b**
1	1.45	1.90	0—3	24	21	50	86 : 14	81 : 19
2	1.06	1.00	0—3	24	33	24.5	91 : 9	86 : 14
3	2.48	2.12	0—3	41	Trace[b]	71	—	90 : 10
4	$PhCH_2Br$; 2.01	No salt	100	2	27	14	91 : 9	79 : 21

a) Isolated yields after chromatography on silica gel. *b*) Detected on TLC.

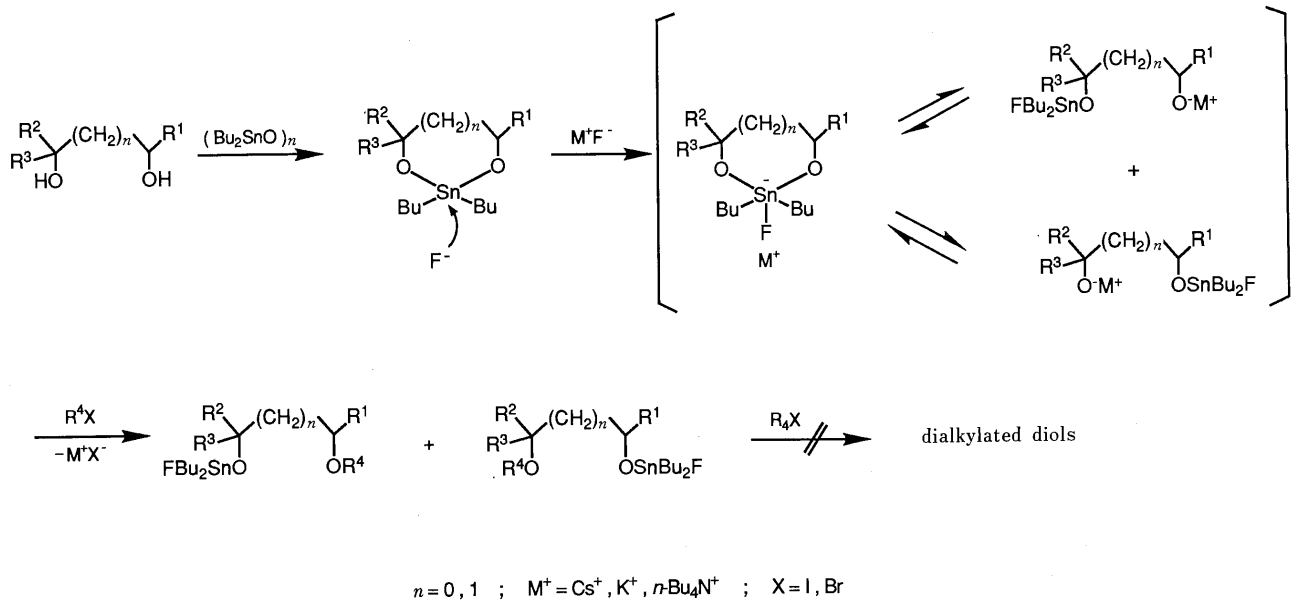

$n = 0, 1$; $M^+ = Cs^+, K^+, n\text{-}Bu_4N^+$; X = I, Br

Chart 1

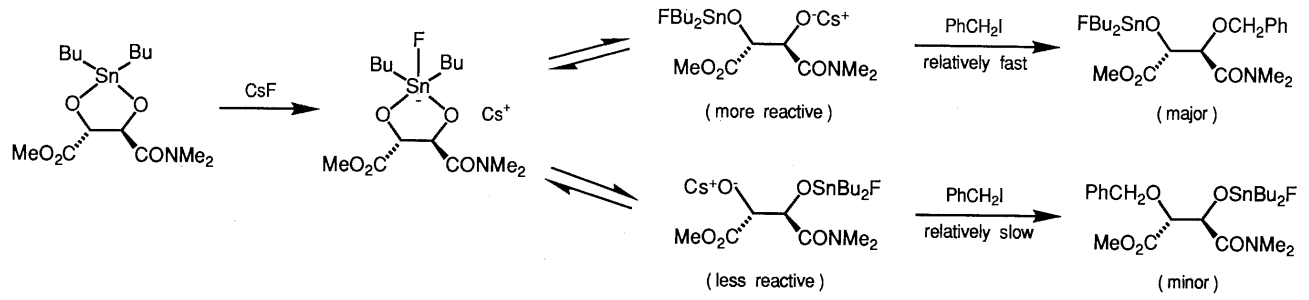

Chart 2

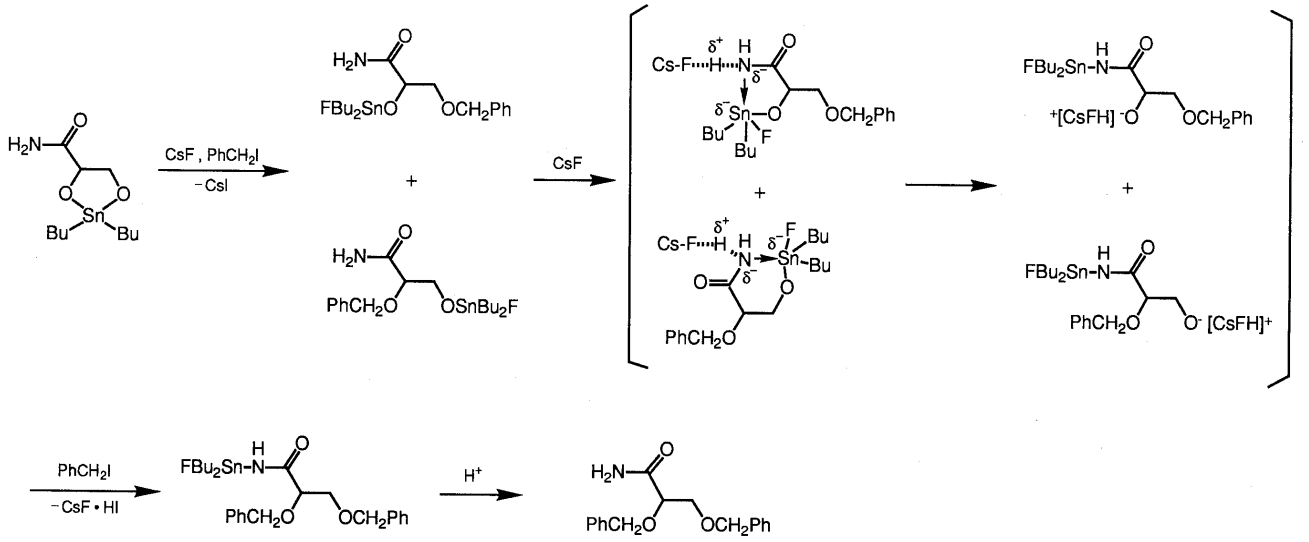

The case of the diol **25** is shown

Chart 3

lated. Recently, Harpp *et al.* reported that fluoride anion attacks tin atoms of organotin sulfides to generate pentacoordinated intermediates.[20] Therefore, it is reasonable to assume that fluoride anion attacks tin atom of the stannylene acetal of a diol to form the pentacoordinated complex, which can reversibly dissociate into a highly reactive alkoxide anion.[21] The resulting alkoxide anion has greater nucleophilicity than the original stannylene acetal and reacts smoothly with alkyl halides to give the monoalkylated derivatives. These monoalkylated derivatives are thought to be inactive to further alkylation under the reaction conditions employed, because dialkylation is not usually observed. The above process is illustrated in Chart 1. On the other hand, the observed regioselectivity can be explained in terms of the reactivity of the alkoxide anions formed. For example, monobenzylation of the diol **50** is thought to proceed through the preferential reaction of the more reactive alkoxide anion with benzyl iodide (Chart 2).

In the case where the diols have NH or OH groups and can form a hydrogen bond with fluoride anion, dibenzylation of the diol occurs (*vide ante*). This phenomenon may be explained as shown in Chart 3. For example, stannylene acetal of the diol **25** is thought to react with cesium fluoride and benzyl iodide to give *O*-fluorostannyl derivatives, whose NH groups may be activated through the hydrogen bonding with cesium fluoride in the reaction mixture. The activated NH groups may interact with Lewis acidic tin atoms to generate reactive anionic oxygen species by the migration of fluorostannyl groups from oxygen to nitrogen. Then the anionic oxygen species may react with benzyl iodide to form the dibenzylated product.

Conclusion

The original Moffatt's procedure for the monoalkylation of diols has been improved by the concomitant use of cesium fluoride. Thus, the alkylation reaction was found to proceed smoothly under very mild reaction conditions and higher yields were obtained. In addition, this new procedure could be successfully applied to the selective alkylation of symmetrical and unsymmetrical diols containing some other functional groups. Therefore, this procedure is expected to be useful synthetically.[21]

Experimental

General Reactions were performed under an inert atmosphere of argon unless otherwise specified, using a standard syringe technique for the transfer of materials. The solvents were generally redistilled before use. Thin-layer chromatography (TLC) was performed on Kieselgel 60 F_{254} precoated plates (0.25 mm), and spots were visualized with molybdophosphoric acid in sulfuric acid. Preparative TLC was accomplished on Kieselgel 60 PF_{254} precoated plates (0.75 mm; 20 × 20 cm^2). Wako-gel C200 and Silicagel BW-200 were used for column chromatography. The melting points were determined on a Yanagimoto micro hot stage melting point apparatus and are uncorrected. The infrared (IR) spectra were recorded with a JASCO A-102 spectrometer. The proton nuclear magnetic resonance (^{1}H-NMR) spectra were measured on a Varian EM390 spectrometer. The chemical shift values (δ) are reported in ppm downfield from

tetramethylsilane as the internal standard. The optical rotations were measured on a JASCO DIP-140 polarimeter. The mass spectra (MS) were recorded with a JEOL JMS-DX 300 apparatus.

Materials Commercially available reagents were used without further purification. Tetrabutylammonium fluoride (*n*-Bu_4NF) was dried according to the reported procedure[23] and was used as a DMF solution (entry 7 in Table I), while commercial *n*-Bu_4NF solution in THF (1 mol·dm^{-3}) was used without drying (entry 14 in Table I). The following compounds were prepared according to the reported methods: dibenzyl (*R,R*)-(+)-tartrate (**3**)[24]; 3,4-dihydroxybutyronitrile (**16**)[25]; 1-*O*-methylglycerol (**17**)[26]; 1-*O*-*tert*-butylglycerol (**18**)[27]; 1-*O*-benzylglycerol (**19a**)[27]; 1-*O*-benzylglycerol (**20**)[27]; 1-*O*-*p*-toluenesulfonylglycerol (**23**)[28]; α,β-dihydroxypropiophenone (**28**)[29] and methyl (2*S*,3*R*)-2,3-dihydroxybutyrate (**47**).[30] 1-Phenyl-1,3-propanediol (**12**) was prepared by the lithium aluminum hydride reduction of ethyl benzoylacetate in THF. 3-((*tert*-Butoxycarbonyl)amino)-1,2-propanediol (**21**) was obtained by the reaction of 3-amino-1,2-propanediol with di-*tert*-butyl pyrocarbonate. 3-((Benzyloxycarbonyl)amino)-1,2-propanediol (**22**) was also prepared from 3-amino-1,2-propanediol and benzyl chloroformate. 2,3-Dihydroxypropionamide (**25**) was synthesized by the aminolysis reaction of methyl glycerate using concentrated ammonia-water in methanol (MeOH). 2,3-Dihydroxy-*N*-methylpropionamide (**26**) and 2,3-dihydroxy-*N,N*-dimethylpropionamide (**27**) were also synthesized in a similar manner, using methyl glycerate and 40% methylamine solution in MeOH or 50% aqueous solution of dimethylamine.

(2*S*,3*R*)-2,3-Dihydroxy-*N,N*-dimethylbutyramide (48) A 50% aqueous solution of dimethylamine (10 ml) was added dropwise to solid potassium hydroxide and the evolved gaseous dimethylamine was collected at −78 °C. To the liquid dimethylamine thus obtained, a solution of ester **47** (206 mg, 1.54 mmol) in dry MeOH (20 ml) was added, and the mixture was stirred at room temperature for 6 d. The solvent was evaporated off and the resulting residue was chromatographed on silica gel (ethyl acetate (EtOAc) : ethanol : water = 7 : 1 : 1) to give 188 mg (83%) of **48** as an oil, $[\alpha]_D^{23}$ +23.6° (*c* = 1.17, MeOH). IR (neat): 3380, 1630 cm^{-1}. NMR (CD_3OD): 1.21 (d, *J* = 6.4 Hz, 3H, $CHC\underline{H}_3$), 2.99 (s, 3H, N-CH_3), 3.14 (s, 3H, N-CH_3), 3.97 (qd, *J* = 6.4, 4.2 Hz, 1H, $C\underline{H}CH_3$), 4.31 (d, *J* = 4.2 Hz, 1H, $C\underline{H}CON(CH_3)_2$), 4.70 (s, 2H, OH × 2). MS *m/z*: 148 ($M^+ + 1$), 103 ($M^+ - 44$ (Me_2N)).

(4*R*,5*R*)-5-Hydroxymethyl-2,2,4-trimethyl-1,3-dioxolane (58) from 47 A mixture of the diol **47** (0.764 g, 5.7 mmol), 2,2-dimethoxypropane (2.5 ml) and *p*-toluenesulfonic acid monohydrate (110 mg, 0.58 mmol) in acetone (25 ml) was stirred at room temperature for 41 h. After the addition of triethylamine (0.5 ml) to the reaction mixture, the acetone and excess 2,2-dimethoxypropane were removed and an aqueous solution of sodium bicarbonate was added to the resulting oily residue. The mixture was extracted three times with methylene chloride and the combined extracts were dried over anhydrous sodium sulfate. Evaporation of the solvent gave 1.15 g of a yellow oil, which was used for the following step without further purification. Lithium aluminum hydride (309 mg, 8.1 mmol) was added in one portion to a solution of this oil (1.15 g) in dry THF (25 ml) under ice-water cooling and the mixture was stirred at room temperature for 61 h. The reaction mixture was cooled to 0 °C, diluted with EtOAc, and quenched by the addition of saturated aqueous sodium bicarbonate. The precipitate formed was filtered through a pad of Celite and washed thoroughly with EtOAc. The filtrate and washings were combined, and concentrated under reduced pressure. The obtained residue was purified by silica gel column chromatography (hexane–EtOAc (20—30%)) to afford 598 mg (72%) of **58** as a colorless oil, $[\alpha]_D^{24}$ −1.37° (*c* = 6.02, $CHCl_3$). IR (neat): 3450, 1380, 1370 cm^{-1}. NMR ($CDCl_3$); 1.31 (d, *J* = 5.8 Hz, 3H, $CHC\underline{H}_3$), 1.42 (s, 3H, C $(CH_3)_2$), 1.43 (s, 3H, $C(CH_3)_2$), 2.83 (br t, *J* = 5.7 Hz, 1H, OH), 3.51—4.17 (m, 4H, $C\underline{H}CH_3$, $C\underline{H}CH_2OH$). MS was measured after *O*-trimethylsilylation. *m/z*: 203 ($M^+ - 15$(Me)), 204 (($M^+ + 1$) −15(Me)), 205 (($M^+ + 2$) −15 (Me)), 145 ($M^+ - 73$ (TMS)).

(2*R*,3*R*)-1-Methoxy-2,3-butanediol (49) A 25% potassium hydride oil dispersion (1 ml, 6.2 mmol) was slowly added to a solution of **58** (552 mg, 3.8 mmol) in dry THF (15 ml) under ice-water cooling. The reaction mixture was stirred at 0 °C for an additional 10 min, and then methyl iodide (1.2 ml, 19.3 mmol) was added. The reaction mixture was stirred at 0 °C for 20 min and then at room temperature for 2.5 h, cooled to 0 °C, and quenched by the addition of water (1.5 ml). Then 6 N hydrochloric acid (3 ml) was added to the resulting mixture, and stirring was continued at room temperature for 17 h. The reaction mixture was neutralized by the addition of solid sodium bicarbonate and then concentrated to give an oil-solid residue. Chloroform ($CHCl_3$) was added to this residue and the resulting insoluble materials were filtered off. The filtrate was concentrated to give an orange oil, which was purified by silica gel column chromatography (hexane: EtOAc = 2 : 1; finally EtOAc) to afford 283 mg (62%) of **49** as a pale yellow oil. $[\alpha]_D^{22}$ +3.83° (*c* = 2.09, $CHCl_3$). IR (neat): 3400 cm^{-1}. NMR ($CDCl_3$): 1.22 (d, *J* = 6.4 Hz, 3H, $CHC\underline{H}_3$), 3.00 (br s, 2H, OH × 2), 3.41 (s, 3H, OCH_3), 3.51 (s, 2H, $C\underline{H}_2OCH_3$), 3.40—3.67 (m, 1H) and 3.67—3.98 (m, 1H) ($CH_3C\underline{H}C\underline{H}CH_2OCH_3$). MS *m/z*: 75 ($M^+ - 45$ ($MeOCH_2$)).

Methyl (2*R*,3*R*)-2,3-Dihydroxy-3-(*N,N*-dimethylcarbamoyl)propionate (50) A mixture of methyl hydrogen (2*R*,3*R*)-2,3-*O*-isopropylidenetartrate[30] (1 g, 4.9 mmol) and dimethylamine (30 ml) in dry MeOH (20 ml) was stirred at room temperature for 9 d. After the evaporation of the solvent and excess dimethylamine, *p*-toluenesulfonic acid monohydrate (1.13 g, 5.96 mmol) and MeOH (50 ml) were added to the oily residue and the mixture was stirred at room temperature for 23 h. The solvent was evaporated off and the resulting residue was dissolved in acetic acid (40 ml) and water (10 ml). This mixture was stirred at 50 °C for 3 h and then the solvent was removed under reduced pressure. The resulting residue was again dissolved in MeOH (50 ml) and the mixture was stirred at room temperature for 21 h. Removal of the solvent gave an oily residue, which was purified twice by silica gel column chromatography (EtOAc then EtOAc : ethanol : water = 7 : 1 : 1) to afford 746 mg (80%) of **50** as a pale yellow oil. This oil solidified upon standing at room temperature, but all attempts to crystallize this solid from various mixed solvents failed. $[\alpha]_D^{21}$ −17.0° (*c* = 1.89, MeOH). IR (KBr): 3425, 1747, 1644 cm^{-1}. NMR (CD_3OD): 3.00 (s, 3H, $N(CH_3)_2$), 3.16 (s, 3H, $N(CH)_3)_2$), 3.81 (s, 3H, CO_2CH_3), 4.44 (d, *J* = 3 Hz, 1H, $C\underline{H}CON(CH_3)_2$), 4.71 (s, 2H, OH × 2), 4.81 (d, *J* = 3 Hz, 1H, $C\underline{H}CO_2CH_3$). MS *m/z*: 192 ($M^+ + 1$), 132 ($M^+ - 59$ (CO_2Me)), 119 ($M^+ - 72$ ($CONMe_2$)).

General Procedure for Monoalkylation of Dialkyl Tartrates An equimolar mixture of dialkyl tartrate (0.5—1 mmol) and dibutyltin oxide (0.5—1 mmol) in toluene (3—5 ml) was heated under reflux for 1—2 h, removing water formed as the azeotropic mixture. The solution was evaporated to complete dryness *in vacuo* to give the stannylene acetal of dialkyl tartrate, which was used for the following step without purification. To the stannylene acetal thus obtained, a fluoride salt (CsF, KF) and an additive (crown ether, *n*-Bu_4NI, KI) were added when they were used; the amounts of these ragents are shown in Table I. The resulting mixture was dried at room temperature *in vacuo* for 1—2 h, and a suitable amount of alkyl halide dissolved in dry solvent (3—5 ml) was added at room temperature or 0 °C. The reaction mixture was stirred vigorously under the conditions given in Table I. When *n*-Bu_4NF was used (entry 7 in Table I), *n*-Bu_4NF in dry DMF and benzyl iodide in dry DMF were successively added to the stannylene acetal at room temperature, and the resulting mixture was stirred under the condition given in Table I. After stirring, the solvent was removed under vacuum and the residue obtained was extracted with ethyl acetate. The organic layer was dried over anhydrous sodium sulfate, concentrated, and purified by silica gel column chromatography using hexane–EtOAc as an eluent. If necessary, further purification by preparative TLC on silica gel was also carried out. The following compounds were obtained in the yields shown in Table I.

Dimethyl (2*R*,3*R*)-2-*O*-Benzyltartrate (4) Colorless needles from ether–hexane, mp 69—70 °C, $[\alpha]_D^{22}$ +87.5° (*c* = 1.17, $CHCl_3$). IR (KBr): 3500, 1730, 748, 705 cm^{-1}. NMR ($CDCl_3$): 3.23 (d, *J* = 9.2 Hz, 1H, OH), 3.69 (s, 3H, CO_2CH_3), 3.85 (s, 3H, CO_2CH_3), 4.35 (d, *J* = 2.4 Hz, 1H, $C\underline{H}OCH_2C_6H_5$), 4.62 (dd, *J* = 9.2, 2.4 Hz, 1H, $C\underline{H}OH$), 4.45 and 4.88 (ABq, *J* = 12.3 Hz, 2H, $C\underline{H}_2C_6H_5$), 7.37 (s, 5H, C_6H_5). *Anal.* Calcd for $C_{13}H_{16}O_6$: C, 58.20; H, 6.01. Found: C, 58.02; H, 5.95.

Dimethyl (2*R*,3*R*)-2-*O*-(*p*-Nitrobenzyl)tartrate (5) Pale yellow prisms from ether–hexane, mp 74.5—75.5 °C, $[\alpha]_D^{24}$ +68.1° (*c* = 1.03, $CHCl_3$). IR (KBr): 3520, 1740, 1605, 1520 cm^{-1}. NMR ($CDCl_3$): 3.29 (br s, 1H, OH), 3.79 (s, 3H, CO_2CH_3), 3.86 (s, 3H, CO_2CH_3), 4.46 (d, *J* = 2.4 Hz, 1H, $C\underline{H}OCH_2C_6H_4NO_2$), 4.70 (d, *J* = 2.4 Hz, 1H, $C\underline{H}OH$), 4.59 and 4.99 (ABq, *J* = 13.2 Hz, 2H, $C\underline{H}_2C_6H_4NO_2$), 7.54 and 8.24 ($A_2B_2q$, *J* = 9 Hz, 4H, C_6H_4). *Anal.* Calcd for $C_{13}H_{15}NO_8$: C, 49.84; H, 4.83; N, 4.47. Found: C, 49.73; H, 4.82; N, 4.55.

Dimethyl (2*R*,3*R*)-2-*O*-(*p*-Methoxybenzyl)tartrate (6) Colorless oil. $[\alpha]_D^{23}$ +84.0° (*c* = 1.72, $CHCl_3$). IR (neat): 3500, 1748, 1612, 1515 cm^{-1}. NMR ($CDCl_3$): 3.12 (d, *J* = 9 Hz, 1H, OH), 3.68 (s, 3H, OCH_3), 3.80 (s, 3H, CO_2CH_3), 3.83 (s, 3H, CO_2CH_3), 4.31 (d, *J* = 2.4 Hz, 1H, $C\underline{H}OCH_2C_6H_4OCH_3$), 4.57 (dd, *J* = 9, 2.4 Hz, 1H, $C\underline{H}OH$), 4.41 and 4.75 (ABq, *J* = 12 Hz, 2H, $C\underline{H}_2C_6H_4OCH_3$), 6.88 and 7.22 ($A_2B_2q$, *J* = 9 Hz, 4H, C_6H_4). MS *m/z*: 298 (M^+).

Dimethyl (2*R*,3*R*)-2-*O*-Allyltartrate (7) Colorless oil. $[\alpha]_D^{22.5}$ +34.1° (*c* = 1.28, $CHCl_3$). IR (neat): 3500, 1748, 1645 cm^{-1}. NMR ($CDCl_3$): 3.29 (d, *J* = 8.6 Hz, 1H, OH), 3.83 (s, 6H, $CO_2CH_3 \times 2$), 3.77—4.10 (m, 1H, $C\underline{H}_2CH=CH_2$), 4.20—4.50 (m, 1H, $C\underline{H}_2CH=CH_2$), 4.35 (d, *J* = 2.4 Hz,

1H, CHOCH$_2$CH=CH$_2$), 4.63 (dd, J=8.6, 2.4 Hz, 1H, CHOH), 5.10—5.40 (m, 2H, CH=CH$_2$), 5.63—6.10 (m, 1H, CH=CH$_2$). MS m/z: 219 (M^++1), 160 (M^+−58 (CH_2=$CHCH_2OH$)).

Dimethyl (2*R*,3*R*)-2-*O*-Methyltartrate (8) Colorless oil. $[\alpha]_D^{21}$ +39.0° (c=1.07, $CHCl_3$). IR (neat): 3500, 1745 cm^{-1}. NMR ($CDCl_3$): 3.33 (d, J=8.7 Hz, 1H, OH), 3.49 (s, 3H, OCH_3), 3.86 (s, 3H, CO_2CH_3), 3.88 (s, 3H, CO_2CH_3), 4.22 (d, J=2.7 Hz, 1H, CHOCH$_3$), 4.63 (dd, J=8.7, 2.7 Hz, 1H, CHOH). MS m/z: 193 (M^++1), 133 (M^+−59 (CO_2Me)).

Dimethyl (2*R*,3*S*) and (2*S*,3*R*)-2-*O*-Benzyltartrate (9) Colorless oil. IR (neat): 3475, 1740, 1603, 1499, 745, 702 cm^{-1}. NMR ($CDCl_3$): 3.37 (d, J=7.2 Hz, 1H, OH), 3.78 (s, 6H, CO_2CH_3 × 2), 4.36 (d, J=3 Hz, 1H, CHOCH$_2$C$_6$H$_5$), 4.63 (dd, J=7.2, 3 Hz, 1H, CHOH), 4.54 and 4.88 (ABq, J=12.2 Hz, 2H, CH$_2$C$_6$H$_5$), 7.40 (s, 5H, C_6H_5). MS m/z: 268 (M^+).

Dibenzyl (2*R*,3*R*)-2-*O*-Benzyltartrate (10) Colorless needles from ether–hexane, mp 57—58 °C, $[\alpha]_D^{23}$ +60.2° (c=1.42, $CHCl_3$), $[\alpha]_D^{20.5}$ +72.6° (c=1.01, EtOAc) (lit.[6c]) mp 50—52 °C, $[\alpha]_D^{20}$ +64.0° (c=1, EtOAc)). IR (KBr): 3520, 1750, 1605, 1499, 738, 730, 700 cm^{-1}. NMR ($CDCl_3$); 3.18 (d, J=9 Hz, 1H, OH), 4.37 (d, J=2.3 Hz, 1H, CHOCH$_2$C$_6$H$_5$), 4.65 (dd, J=9, 2.3 Hz, 1H, CHOH), 4.32 and 4.76 (ABq, J=11.6 Hz, 2H, OCH$_2$C$_6$H$_5$), 5.03 and 5.15 (ABq, J=12 Hz, 2H, $CO_2CH_2C_6H_5$), 5.23 (s, 2H, $CO_2CH_2C_6H_5$), 7.10—7.33 (m, 10H, C_6H_5 × 2), 7.36 (s, 5H, C_6H_5). *Anal.* Calcd for $C_{25}H_{24}O_6$: C, 71.4; H, 5.75. Found: C, 71.17; H, 5.76. This compound was prepared on a 20 mmol scale by the following procedure. A mixture of **3** (6.61 g, 20 mmol) and dibutyltin oxide (5.16 g, 20.7 mmol) in toluene (65 ml) was refluxed for 1 h, while water formed was removed as the azeotropic mixture. After the complete removal of the solvent under vacuum, a white solid was obtained, CsF (assay min. 90%, 5.12 g, 30.4 mmol) was added to this solid and the mixture was dried at room temperature *in vacuo* for 1 h. Benzyl iodide (9.27 g, 42.5 mmol) in dry DMF (65 ml) was added at room temperature and the resulting suspension was vigorously stirred at room temperature for 5 h. The solvent was removed under vacuum and the resulting residue was extracted with ether. The organic layer was dried over anhydrous sodium sulfate, concentrated, and purified by silica gel column chromatography (hexane : EtOAc = 4 : 1) to afford 7.87 g (94%) of **10** as a colorless solid.

Monobenzylation of 1-Phenylethanediol (11). General Procedure A mixture of **11** (91.2 mg, 0.66 mmol) and dibutyltin oxide (164.3 mg, 0.66 mmol) in toluene (3 ml) was refluxed for 1 h, while water formed was removed as the azeotropic mixture. After the complete removal of the solvent under vacuum, a white solid was obtained. To this solid, a suitable amount of fluoride salt was added, and the resulting mixture was further dried at room temperature *in vacuo* for 1—2 h. In the case of entry 13 in Table II, 5 mol% of dicyclohexano-18-crown-6 was also added with the fluoride salt at this stage and the mixture was dried as above. Then, a suitable amount of benzyl halide in dry solvent (3 ml) was added at the temperature shown in Table II and the reaction mixture was stirred vigorously under the conditions given in Table II. After the removal of the solvent under reduced pressure, benzene was added to the residue and the resulting solution was subjected to silica gel column chromatography using hexane–EtOAc as an eluent. The monobenzylated products, **29a** and **29b**, were obtained as a mixture in the yields shown in Table II. The ratios of regioisomers were determined from the peak intensities of benzylic protons of each isomer in the ^{1}H-NMR spectra. The peak corresponding to the benzylic protons of the major isomer **29a** appears at δ 4.57 as a singlet, while that of the minor isomer **29b** appears at δ 4.34 and 4.52 as an ABq signal (J=11.7 Hz).

Mixture of 2-Benzyloxy-1-phenylethanol (29a) and 2-Benzyloxy-2-phenylethanol (29b) IR (neat): 3425, 1604, 1497, 740, 700 cm^{-1}. NMR ($CDCl_3$): 2.94 (br s, 1H, OH), 3.34—3.90 (m, 2H, CHCH$_2$O), 4.34 and 4.52 (ABq, J=11.7 Hz), 4.57 (s) (total 2H, CH$_2$C$_6$H$_5$), 4.51 (dd, J=7.3, 4.8 Hz), 4.87 (dd, J=8.3, 4.2 Hz) (total 1H, C_6H_5CHCH$_2$O), 7.35 (s, 10H, C_6H_5 × 2). MS m/z: 228 (M^+).

General Procedure for Regioselective Benzylation of Unsymmetric Diols An equimolar mixture of a diol (0.5—2.1 mmol) and dibutyltin oxide (0.5—2.1 mmol) in toluene (3—5 ml) was refluxed for 1 h, while water formed was removed as the azeotropic mixture. In the case of the diol **15**, the refluxing time was 15 min, while it was 30 min for the diol **20**. After the complete removal of the solvent under vacuum, the stannylene acetal of the diol was obtained as a solid or a syrup. To this stannylene acetal, a suitable amount of cesium fluoride was added, and the resulting mixture was further dried at room temperature *in vacuo* for 1—2 h. Benzyl iodide, in the amount given in Table III or IV, in dry DMF (3—6 ml) was then added at the temperature shown in Table III or IV and the mixture was vigorously stirred at the same temperature for a suitable period of time. The solvent was removed under vacuum, and the residue was extracted with EtOAc. The organic layer was dried over anhydrous sodium sulfate, concentrated, and purified by silica gel column chromatography; elution was carried out with hexane containing increasing amounts of EtOAc and in some cases finally with EtOAc. If necessary, repeated purifications by column chromatography and/or preparative TLC on silica gel were also employed. The products were obtained in the yields shown in Tables III and IV. The ratios of the products were determined from the peak intensities of benzylic protons of each isomer in the ^{1}H-NMR spectra or from the weights of each isomer separated.

3-Benzyloxy-1-phenylpropanol (30a) and 3-Benzyloxy-3-phenylpropanol (30b) These compounds were completely separated and the ratio of **30a** to **30b** was determined from their weights.

30a: IR (neat): 3420, 1603, 1497, 739, 700 cm^{-1}. NMR ($CDCl_3$): 1.88—2.16 (m, 2H, CHCH$_2$CH$_2$O), 3.33 (br s, 1H, OH), 3.45—3.83 (m (t like), 2H, CHCH$_2$CH$_2$O), 4.51 (s, 2H, CH$_2$C$_6$H$_5$), 4.90 (br t, J=6 Hz, 1H, C_6H_5CH–OH), 7.36 (s, 5H, C_6H_5), 7.37 (s, 5H, C_6H_5). MS m/z: 242 (M^+).

30b: IR (neat): 3415, 1602, 1496, 740, 703 cm^{-1}. NMR ($CDCl_3$): 1.64—2.32 (m, 2H, CHCH$_2$CH$_2$O), 2.81 (br s, 1H, OH), 3.51—3.94 (m (t like), 2H, CHCH$_2$CH$_2$O), 4.29 and 4.47 (ABq, J=11.9 Hz, 2H, CH$_2$C$_6$H$_5$), 4.59 (dd, J=8.5, 4.2 Hz, 1H, C_6H_5CHOH), 7.34 (s, 5H, C_6H_5), 7.41 (s, 5H, C_6H_5). MS m/z: 242 (M^+).

Mixture of 1-Benzyloxy-2-propanol (31a) and 2-Benzyloxypropanol (31b) These compounds could not be separated and the ratio of **31a** to **31b** was determined by ^{1}H-NMR. IR (neat): 3425, 1604, 1498, 740, 700 cm^{-1}. NMR ($CDCl_3$): 1.12 (d, J=6.5 Hz), 1.17 (d, J=6.5 Hz) (total 3H, CH_3), 2.69 (br s, 1H, OH), 3.14—3.87 (m), 3.72—4.25 (m) (total 3H, CHCH$_2$), 4.52 and 4.63 (ABq, J=11.7 Hz), 4.55 (s) (total 2H, CH$_2$C$_6$H$_5$), 7.37 (s, 5H, C_6H_5). MS m/z: 166 (M^+).

Mixture of 4-Benzyloxy-2-butanol (32a) and 3-Benzyloxybutanol (32b) These compounds could not be separated and the ratio of **32a** to **32b** was determined by ^{1}H-NMR. IR (neat): 3400, 1602, 1498, 738, 700 cm^{-1}. NMR ($CDCl_3$): 1.19 (d, J=6.4 Hz), 1.25 (d, J=6.2 Hz) (total 3H, CH_3), 1.58—1.89 (m, 2H, CHCH$_2$CH$_2$O), 3.02 (br s, 1H, OH), 3.46—3.86 (m (t like)), 3.55—4.02 (m), 3.83—4.23 (m) (total 3H, CH_3CHCH$_2$CH$_2$O), 4.52 (s), 4.46 and 4.62 (ABq, J=12Hz) (total 2H, CH$_2$C$_6$H$_5$), 7.36 (s, 5H, C_6H_5). MS m/z: 180 (M^+).

1-Benzyloxy-3-chloro-2-propanol (33a) and 2-Benzyloxy-3-chloropropanol (33b) These compounds were completely separated and the ratio of **33a** to **33b** was determined from their weights.

33a: IR (neat): 3410, 1603, 1497, 740, 700 cm^{-1}. NMR ($CDCl_3$): 2.94 (br s, 1H, OH), 3.40—3.77 (m, 4H, CH$_2$CHCH$_2$), 3.83—4.12 (m, 1H, CH$_2$CHCH$_2$), 4.54 (s, 2H, CH$_2$C$_6$H$_5$), 7.35 (s, 5H, C_6H_5). MS m/z: 202 (M^++2), 200 (M^+).

33b: IR (neat): 3400, 1604, 1499, 742, 702 cm^{-1}. NMR ($CDCl_3$): 2.02 (br t, J=5.7 Hz, 1H, OH), 3.43—3.87 (m, 5H, CH$_2$CHCH$_2$), 4.64 and 4.71 (ABq, J=11.7 Hz, 2H, CH$_2$C$_6$H$_5$), 7.40 (s, 5H, C_6H_5). MS m/z: 202 (M^++2), 200 (M^+).

1-Benzyloxy-3-cyano-2-propanol (34a) and 2-Benzyloxy-3-cyano propanol (34b) These compounds were completely separated and the ratio of **34a** to **34b** was determined from their weights.

34a: IR (neat): 3440, 2255, 1604, 1498, 743, 702 cm^{-1}. NMR ($CDCl_3$): 2.52 (d, J=6 Hz, 2H, CH_2CN), 3.35 (br s, 1H, OH), 3.48 (d, J=5.7 Hz, 2H, CH_2O), 3.76—4.19 (m, 1H, CHOH), 4.52 (s, 2H, CH$_2$C$_6$H$_5$), 7.32 (s, 5H, C_6H_5). MS m/z: 191 (M^+).

34b: IR (neat): 3440, 2250, 1498, 740, 699 cm^{-1}. NMR ($CDCl_3$): 2.07 (br s, 1H, OH), 2.63 (d, J=5.7 Hz, 2H, CH_2CN), 3.47—3.93 (m, 3H, CHCH$_2$OH), 4.64 and 4.68 (ABq, J=11.4 Hz, 2H, CH$_2$C$_6$H$_5$), 7.40 (s, 5H, C_6H_5). MS m/z: 191 (M^+).

1-*O*-Benzyl-3-*O*-methylglycerol (35a) and 2-*O*-Benzyl-1-*O*-methylglycerol (35b) These compounds were partially separated by repeated chromatography and the ratio of **35a** to **35b** was determined by ^{1}H-NMR.

35a: IR (neat): 3450, 1605, 1499, 740, 700 cm^{-1}. NMR ($CDCl_3$): 2.79 (d, J=4.4 Hz, 1H, OH), 3.37 (s, 3H, OCH_3), 3.39—3.63 (m, 4H, CH$_2$CHCH$_2$), 3.83—4.18 (m, 1H, CH$_2$CHCH$_2$), 4.56 (s, 2H, CH$_2$C$_6$H$_5$), 7.38 (s, 5H, C_6H_5). MS m/z: 196 (M^+).

35b: IR (neat): 3425, 1604, 1497, 740, 700 cm^{-1}. NMR ($CDCl_3$): 2.32 (br s, 1H, OH); 3.37 (s, 3H, OCH_3), 3.44—3.80 (m, 5H, CH$_2$CHCH$_2$), 4.65 and 4.69 (ABq, J=12 Hz, 2H, CH$_2$C$_6$H$_5$), 7.38 (s, 5H, C_6H_5). MS m/z: 196 (M^+).

1-*O*-Benzyl-3-*O*-*tert*-butylglycerol (36a) and 2-*O*-Benzyl-1-*O*-*tert*-butylglycerol (36b) These compounds were partially separated by repeated chromatography and the ratio of **36a** to **36b** was determined by ^{1}H-NMR.

36a: IR (neat); 3450, 1604, 1498, 1390, 1368, 738, 700 cm^{-1}. NMR ($CDCl_3$): 1.19 (s, 9H, $(CH_3)_3C$), 2.71 (d, 1H, J=4.2 Hz, OH), 3.27—3.70

(m, 4H, $C\underline{H}_2CHCH_2$), 3.75—4.12 (m, 1H, $CH_2C\underline{H}CH_2$), 4.57 (s, 2H, $C\underline{H}_2C_6H_5$), 7.38 (s, 5H, C_6H_5). MS *m/z*: 238 (M^+).

36b: IR (neat): 3430, 1603, 1496, 1389, 1366, 737, 698 cm^{-1}. NMR ($CDCl_3$): 1.20 (s, 9H, $(CH_3)_3C$), 2.59 (br s, 1H, OH), 3.37—3.82 (m, 5H, $C\underline{H}_2C\underline{H}C\underline{H}_2$), 4.65 and 4.68 (ABq, J=12 Hz, 2H, $C\underline{H}_2C_6H_5$), 7.37 (s, 5H, C_6H_5). MS *m/z*: 223 (M^+-15 (Me)), 181 (M^+-57 (*tert*-Bu)), 165 (M^+-73 (*tert*-BuO)), 147 (M^+-91 ($PhCH_2$)).

1,3-Di-*O*-benzylglycerol (37a) and 1,2-Di-*O*-benzylglycerol (37b) These compounds were partially separated by repeated chromatography and the ratio of **37a** to **37b** was determined by ^{1}H-NMR.

37a: IR (neat): 3440, 1604, 1498, 739, 700 cm^{-1}. NMR ($CDCl_3$): 2.78 (br s, 1H, OH), 3.38—3.76 (m (d like), 4H, $C\underline{H}_2CHC\underline{H}_2$), 3.87—4.16 (m, 1H, $CH_2C\underline{H}CH_2$), 4.53 (s, 4H, $C\underline{H}_2C_6H_5\times2$), 7.35 (s, 10H, $C_6H_5\times2$). MS *m/z*: 272 (M^+).

37b: IR (neat): 3440, 1604, 1498, 740, 701 cm^{-1}. NMR ($CDCl_3$): 2.32 (br s, 1H, OH), 3.47—3.89 (m, 5H, $C\underline{H}_2C\underline{H}C\underline{H}_2$), 4.53 (s, 2H, $C\underline{H}_2C_6H_5$), 4.62 and 4.67 (ABq, J=12 Hz, 2H, $C\underline{H}_2C_6H_5$), 7.35 (s, 10H, $C_6H_5\times2$). MS *m/z*: 272 (M^+).

Mixture of 1-*O*-Benzoyl-3-*O*-benzylglycerol (38a) and 1-*O*-Benzoyl-2-*O*-benzylglycerol (38b) These compounds could not be separated and the ratio of **38a** to **38b** was determined by ^{1}H-NMR after the removal of the benzoyl group. NMR ($CDCl_3$): 2.45 (br s), 2.87 (d, J=5.1 Hz) (total 1H, OH), 3.47—4.07 (m), 4.07—4.33 (m), 4.33—4.57 (m) (total 5H, $C\underline{H}_2C\underline{H}C\underline{H}_2$), 4.58 (s), 4.69 and 4.74 (ABq, J=12 Hz) (total 2H, $C\underline{H}_2C_6H_5$), 7.20—7.72 (m, 3H, C_6H_5CO), 7.33 (s, 5H, $C\underline{H}_2C_6H_5$), 7.97—8.20 (m, 2H, C_6H_5CO).

1-Benzyloxy-3-((*tert*-butoxycarbonyl)amino)propan-2-ol (39a) and 2-Benzyloxy-3-((*tert*-butoxycarbonyl)amino)propanol (39b) A mixture of the diol **21** (340 mg, 1.78 mmol) and dibutyltin oxide (443 mg, 1.78 mmol) in toluene (6 ml) was refluxed for 1 h, while water formed was removed as the azeotropic mixture. The solution was evaporated to complete dryness under vacuum and CsF (314 mg, 1.86 mmol) was added to the residue. The mixture was further dried at room temperature *in vacuo* for 1 h and then dry DMF (5 ml) was added. The resulting solution was stirred at room temperature for 3 h, then benzyl iodide (776 mg, 3.56 mmol) in dry DMF (2 ml) was added. The reaction mixture was further stirred at room temperature for 120 h. The solvent was removed under vacuum and the residue was extracted with EtOAc. The organic layer was dried over anhydrous sodium sulfate, concentrated, and purified repeatedly by silica gel column chromatography (hexane– EtOAc) to afford 356 mg (71%) of **39a** and **39b** as an oil. This mixture was subjected to ^{1}H-NMR measurement to determine the ratio of **39a** to **39b**. Partial separation of **39a** and **39b** was accomplished through the above purification.

39a: IR (neat): 3390, 1700, 1392, 1368, 739, 700 cm^{-1}. NMR ($CDCl_3$): 1.44 (s, 9H, $(CH_3)_3C$), 2.95—3.65 (m, 5H, $C\underline{H}_2CHC\underline{H}_2$ and OH), 3.72—4.07 (m, 1H, $CH_2C\underline{H}CH_2$), 4.54 (s, 2H, $C\underline{H}_2C_6H_5$), 5.17 (br t, J=5.7 Hz, 1H, NH), 7.37 (s, 5H, C_6H_5). MS *m/z*: 208 (M^+-73 (*tert*-BuO)), 180 (M^+-101 (*tert*-BuOCO)).

39b: IR (neat): 3370, 1700, 1392, 1368, 739, 700 cm^{-1}. NMR ($CDCl_3$): 1.45 (s, 9H, $(CH_3)_3C$), 3.10 (br s, 1H, OH), 3.22—3.80 (m, 5H, $C\underline{H}_2C\underline{H}C\underline{H}_2$), 4.61 (s, 2H, $C\underline{H}_2C_6H_5$), 4.97 (br s, 1H, NH), 7.40 (s, 5H, C_6H_5). MS *m/z*: 208 (M^+-73 (*tert*-BuO)), 180 (M^+-101 (*tert*-BuOCO)).

1,2-Di(benzyloxy)-3-((*tert*-butoxycarbonyl)amino)propane (9.7 mg, 1.5%) was also isolated. IR (neat): 3430, 3370, 1700, 1392, 1368, 737, 700 cm^{-1}: NMR ($CDCl_3$): 1.44 (s, 9H, $(CH_3)_3C$), 3.19—3.83 (m, 5H, $C\underline{H}_2C\underline{H}C\underline{H}_2$), 4.56 (S, 2H, $C\underline{H}_2C_6H_5$), 4.63 and 4.68 (ABq, J=12 Hz, 2H, $CH_2C_6H_5$), 4.81 (br s, 1H, NH), 7.39 (s, 10H, $C_6H_5\times2$). MS *m/z*: 314 (M^+-57 (*tert*-Bu)), 298 (M^+-73 (*tert*-BuO)), 270 (M^+-101 (*tert*-BuOCO)).

1-Benzyloxy-3-((benzyloxycarbonyl)amino)propan-2-ol (40a) and 2-Benzyloxy-3-((benzyloxycarbonyl)amino)propanol (40b) These compounds were prepared from the diol **22** in 74% yield in a manner similar to that described for the preparation of compounds **39a** and **39b** from the diol **21**; the ratio of **40a** to **40b** was determined by ^{1}H-NMR. Partial separation of **40a** and **40b** was possible by repeated chromatography.

40a: IR (neat): 3400, 1700, 740, 700 cm^{-1}. NMR ($CDCl_3$): 2.98 (d, J=4.2 Hz, 1H, OH), 3.07—3.63 (m, 4H, $C\underline{H}_2CHC\underline{H}_2$), 3.70—4.05 (m, 1H, $CH_2C\underline{H}CH_2$), 4.51 (s, 2H, $C\underline{H}_2C_6H_5$), 5.10 (s, 2H, $C_6H_5C\underline{H}_2OCO$), 5.31 (br s, 1H, NH), 7.35 and 7.37 (S×2, 5H×2, $C_6H_5\times2$). MS *m/z*: 224 (M^+-91 ($PhCH_2$)), 180 (M^+-135 ($PhCH_2OCO$)).

40b: IR (neat): 3420, 3330, 1700, 740, 700 cm^{-1}. NMR ($CDCl_3$): 2.70 (br s, 1H, OH), 3.20—3.80 (m, 5H, $C\underline{H}_2C\underline{H}C\underline{H}_2$), 4.58 (s, 2H, $C\underline{H}_2C_6H_5$), 5.11 (s, 2H, $C_6H_5C\underline{H}_2OCO$), 5.17 (br s, 1H, NH), 7.36 and 7.38 (S×2, 5H×2, $C_6H_5\times2$). MS *m/z*: 224 (M^+-91 ($PhCH_2$)), 180 (M^+-135 ($PhCH_2OCO$)).

1,2-Di(benzyloxy)-3-((benzyloxycarbonyl)amino)propane was also obtained in 3% yield. IR (neat): 3425, 3330, 1712, 737, 700 cm^{-1}. NMR ($CDCl_3$): 3.14—3.86 (m, 5H, $C\underline{H}_2C\underline{H}C\underline{H}_2$), 4.53 (s, 2H, $C\underline{H}_2C_6H_5$), 4.60 and 4.65 (ABq, J=12 Hz, 2H, $C\underline{H}_2C_6H_5$), 5.08 (br s, 1H, NH), 5.11 (s, 2H, $C_6H_5C\underline{H}_2OCO$), 7.37 (s), 7.39 (s) (total 15H, $C_6H_5\times3$). MS *m/z*: 314 (M^+-91 ($PhCH_2$)), 270 (M^+-135 ($PhCH_2OCO$)).

Methyl 2-Hydroxy-3-(benzyloxy)propionate (42a) and Methyl 2-Benzyloxy-3-hydroxypropionate (42b) These compounds were partially separated by repeated chromatography and the ratio of **42a** to **42b** was determined by ^{1}H-NMR.

42a: IR (neat): 3475, 1740, 1604, 1498, 742, 700 cm^{-1}. NMR ($CDCl_3$): 3.32 (d, J=6.9 Hz, 1H, OH), 3.75 (d, J=3.1 Hz, 2H, $CHC\underline{H}_2$), 3.77 (s, 3H, CO_2CH_3), 4.20—4.44 (m, 1H, $C\underline{H}CH_2$), 4.57 (s, 2H, $C\underline{H}_2C_6H_5$), 7.33 (s, 5H, C_6H_5). MS *m/z*: *210* (M^+).

42b: IR (neat): 3450, 1737, 1604, 1498, 743, 701 cm^{-1}. NMR ($CDCl_3$): 2.58 (br s, 1H, OH), 3.77 (s, 3H, CO_2CH_3), 3.85 (m, 2H, $C\underline{H}_2OH$), 4.08 (dd, J=5.6, 3.9 Hz, 1H, $C\underline{H}CH_2$), 4.52 and 4.80 (ABq, J=11.5 Hz, 2H, $C\underline{H}_2C_6H_5$), 7.39 (s, 5H, C_6H_5). MS *m/z*: 210 (M^+).

2-Hydroxy-3-(benzyloxy)propionamide (43a) and 2-Benzyloxy-3-hydroxypropionamide (43b) These compounds were partially separated by repeated chromatography and the ratio of **43a** to **43b** was determined by ^{1}H-NMR.

43a: Colorless leaflets from hexant–ether–EtOAc. mp 98—98.5 °C. IR (KBr): 3450, 3330, 3200, 1650, 748, 700 cm^{-1}. NMR (CD_3OD): 3.56—3.86 (m, 2H, $CHC\underline{H}_2$), 4.25 (dd, J=5.1, 4.0 Hz, 1H, $C\underline{H}CH_2$), 4.57 (s, 2H, $C\underline{H}_2C_6H_5$), 4.76 (s, 3H, OH and $CONH_2$), 7.38 (s, 5H, C_6H_5). *Anal.* Calcd for $C_{10}H_{13}NO_3$: C, 61.52; H, 6.71; N, 7.18. Found: C, 61.48; H, 6.72; N, 6.99.

43b: Colorless needles from hexane–ether–EtOAc, mp 112.5—113.5 °C. IR (KBr): 3370, 3220, 1658, 740, 700 cm^{-1}. NMR (CD_3OD): 3.52—4.02 (m, 3H, $C\underline{H}C\underline{H}_2$), 4.67 (s, 2H, $C\underline{H}_2C_6H_5$), 4.77 (s, 3H, OH and $CONH_2$), 7.41 (s, 5H, C_6H_5). *Anal.* Calcd for $C_{10}H_{13}O_3N$: C, 61.52; H, 6.71; N, 7.18. Found: C, 61.22; H, 6.58; N, 6.88.

2,3-Di(benzyloxy)propionamide was also formed in 17.5% yield in this reaction. Colorless needles from hexane–ether, mp 74.5—76 °C. IR (KBr): 3377, 3200, 1657, 1498, 742, 700 cm^{-1}. NMR ($CDCl_3$): 3.64—3.99 (m, 2H, $CHC\underline{H}_2$), 4.08 (dd, J=5.0, 3.1 Hz, 1H, $C\underline{H}CH_2$), 4.57 (s, 2H, $C\underline{H}_2C_6H_5$), 4.67 (s, 2H, $C\underline{H}_2C_6H_5$), 6.56 (br s, 1H, $CONH_2$), 6.76 (br s, 1H, $CONH_2$), 7.36 (s, 5H, C_6H_5), 7.38 (s, 5H, C_6H_5). *Anal.* Calcd for $C_{17}H_{19}NO_3$: C, 71.56; H, 6.71; N, 4.91. Found: C, 71.30; H, 6.72; N, 5.16.

***N*-Methyl-2-hydroxy-3-(benzyloxy)propionamide (44a) and *N*-Methyl-2-benzyloxy-3-hydroxypropionamide (44b)** These compounds were completely separated and the ratio of **44a** to **44b** was determined from their weights.

44a: IR (neat): 3350, 1650, 1498, 741, 701 cm^{-1}. NMR ($CDCl_3$): 2.79 and 2.85 (S×2, 3H, $CONHC\underline{H}_3$), 3.46—3.90 (m, 3H, $C\underline{H}_2OCH_2C_6H_5$ and OH), 4.10—4.36 (m, 1H, $C\underline{H}CONHCH_3$), 4.56 (s, 2H, $C\underline{H}_2C_6H_5$), 6.83 (br s, 1H, $CON\underline{H}CH_3$), 7.38 (s, 5H, C_6H_5). MS *m/z*: 210 (M^++1), 179 (M^+-30(MeNH)), 118 (M^+-91 ($PhCH_2$)).

44b: IR (neat); 3360, 1650, 1498, 738, 700 cm^{-1}. NMR ($CDCl_3$): 2.79 and 2.85 (S×2, 3H, $CONHC\underline{H}_3$), 2.92 (br s, 1H, OH), 3.70—4.08 (m, 3H, $C\underline{H}CH_2$), 4.64 and 4.66 (ABq, J=11.7 Hz, 2H, $C\underline{H}_2C_6H_5$), 6.78 (br s, 1H, $CON\underline{H}CH_3$), 7.39 (s, 5H, C_6H_5). MS *m/z*: 210 (M^++1), 179 (M^+-30 (MeNH)).

N-Methyl-2,3-di(benzyloxy)propionamide was also formed in 9.7% yield in this reaction. IR (neat): 3425, 3330, 1660, 1498, 734, 698 cm^{-1}. NMR ($CDCl_3$): 2.79 and 2.85 (S×2, 3H, $CONHC\underline{H}_3$), 3.62—4.0 (m, 2H, $CHC\underline{H}_2$), 4.10 (dd, J=4.8, 2.7 Hz, 1H, $C\underline{H}CH_2$), 4.56 (s, 2H, $CH_2C_6H_5$), 4.63 and 4.69 (ABq, J=11.7 Hz, 2H, $C\underline{H}_2C_6H_5$), 6.77 (br s, 1H, $CON\underline{H}CH_3$), 7.35 (s, 5H, C_6H_5); 7.38 (s, 5H, C_6H_5). MS *m/z*: 300 (M^++1), 208 (M^+-91 ($PhCH_2$)), 192 (M^+-107 ($PhCH_2O$)).

***N,N*-Dimethyl-2-hydroxy-3-(benzyloxy)propionamide (45a) and *N,N*-Dimethyl-2-benzyloxy-3-hydroxypropionamide (45b)** These compounds were completely separated and the ratio of **45a** to **45b** was determined from their weights.

45a: IR (neat): 3400, 1638, 1498, 740, 700 cm^{-1}: MMR ($CDCl_3$): 2.96 (s, 3H, $N(CH_3)_2$), 3.01 (s, 3H, $N(CH_3)_2$), 3.62 (d, J=5.1 Hz, 2H, $CHC\underline{H}_2$), 3.77 (br s, 1H, OH), 4.58 (s, 2H, $C\underline{H}_2C_6H_5$), 4.63 (br t, J=5.1 Hz, 1H, $C\underline{H}OH$), 7.38 (s, 5H, C_6H_5). MS *m/z*: 223 (M^+).

45b: IR (neat): 3400, 1637, 1500, 739, 702 cm^{-1}. NMR ($CDCl_3$): 2.79 (br s, 1H, OH), 2.97 (s, 3H, $N(CH_3)_2$), 3.02 (s, 3H, $N(CH_3)_2$), 3.91 (d, J=5.1 Hz, 2H, $CHC\underline{H}_2$), 4.35 (t, J=5.1 Hz, 1H, $C\underline{H}CH_2$), 4.57 and 4.63 (ABq, J=11.7 Hz, 2H, $C\underline{H}_2C_6H_5$), 7.39 (s, 5H, C_6H_5). MS *m/z*: 224 (M^++1), 151 (M^+-72 ($CONMe_2$)), 132 (M^+-91 ($PhCH_2$)).

Methyl (2*S*,3*R*)-2-Hydroxy-3-(benzyloxy)butyrate (52a) and Methyl

(2*S*,3*R*)-2-Benzyloxy-3-hydroxybutyrate (52b) These compounds were completely separated and the ratio of **52a** to **52b** was determined from their weights.

52a: $[\alpha]_D^{23}$ −27.2° (c=1.59, $CHCl_3$). IR (neat): 3475, 1740, 1604, 1498, 739, 699 cm^{-1}. NMR ($CDCl_3$): 1.30 (d, J=6.4 Hz, 3H, $CHCH_3$), 3.18 (d, J=7.8 Hz, 1H, OH), 3.69 (s, 3H, CO_2CH_3), 3.90 (qd, J=6.4, 2.5 Hz, 1H, $CHCH_3$), 4.06 (dd, J=7.8, 2.5 Hz, 1H, $CHCO_2CH_3$), 4.40 and 4.57 (ABq, J=11.7 Hz, 2H, $CH_2C_6H_5$), 7.31 (s, 5H, C_6H_5). MS m/z: 224 (M^+).

52b: $[\alpha]_D^{23}$ −89.6° (c=1.57, $CHCl_3$). IR (neat) 3475, 1740, 1604, 1499, 748, 702 cm^{-1}. NMR ($CDCl_3$): 1.21 (d, J=6.3 Hz, 3H, $CHCH_3$), 2.52 (d, J=4.8 Hz, 1H, OH), 3.76 (s, 3H, CO_2CH_3), 3.81 (d, J=4.8 Hz, 1H, $CHCO_2CH_3$), 3.89—4.22 (m, 1H, $CHCH_3$), 4.43 and 4.74 (ABq, J=11.4 Hz, 2H, $CH_2C_6H_5$), 7.37 (s, 5H, C_6H_5). MS m/z: 165 (M^+ −59 (CO_2Me)), 91 ($PhCH_2$).

(2*S*,3*R*)-*N*,*N*-Dimethyl-2-hydroxy-3-(benzyloxy)butyramide (53a) and (2*S*,3*R*)-*N*,*N*-Dimethyl-2-benzyloxy-3-hydroxybutyramide (53b) These compounds were completely separated and the ratio of **53a** to **53b** was determined from their weights.

53a: $[\alpha]_D^{23}$ +7.68° (c=2.87, $CHCl_3$). IR (neat): 3425, 1635, 740, 700 cm^{-1}. NMR ($CDCl_3$): 1.22 (d, J=6.3 Hz, 3H, $CHCH_3$), 2.89 (s, 3H, $N(CH_3)_2$), 2.97 (s, 3H, $N(CH_3)_2$), 3.76 (qd, J=6.3, 3.6 Hz, 1H, $CHCH_3$), 3.89 (d, J=7.3 Hz, 1H, OH), 4.42 (dd, J=7.3, 3.6 Hz, 1H, $CHCON(CH_3)_2$), 4.49 and 4.62 (ABq, J=12.3 Hz, 2H, $CH_2C_6H_5$), 7.35 (s, 5H, C_6H_5). MS m/z: 238 (M^++1), 193 (M^+−44 (NMe_2)), 146 (M^+−91 ($PhCH_2$)).

53b: $[\alpha]_D^{23}$ −57.3° (c=1.00, $CHCl_3$). IR (neat): 3410, 1632, 738, 700 cm^{-1}. NMR ($CDCl_3$): 1.21 (d, J=6.2 Hz, 3H, $CHCH_3$), 2.96 (s, 3H, $N(CH_3)_2$), 3.02 (s, 3H, $N(CH_3)_2$), 3.28 (br s, 1H, OH), 3.81—4.24 (m, 1H, $CHCH_3$), 4.09 (d, J=2.6 Hz, 1H, $CHCON(CH_3)_2$), 4.48 and 4.70 (ABq, J=11.7 Hz, 2H, $CH_2C_6H_5$), 7.37 (s, 5H, C_6H_5). MS m/z: 193 (M^+−44 (NMe_2)), 146 (M^+−91 ($PhCH_2$)).

Mixture of (2*R*,3*R*)-1-Methoxy-3-(benzyloxy)butan-2-ol (54a) and (2*R*,3*R*)-1-Methoxy-2-(benzyloxy)butan-3-ol (54b) These compounds could not be separated and the ratio of **54a** to **54b** was determined by ^{1}H-NMR.

This mixture showed the optical rotation; $[\alpha]_D^{22}$ −39.0° (c=5.53, $CHCl_3$). IR (neat): 3440, 1604, 1498; 740, 700 cm^{-1}. NMR ($CDCl_3$): 1.18 (d, J=6.4 Hz) and 1.21 (d, J=6.2 Hz) (total 3H, $CHCH_3$), 2.70 (d, J=5.2 Hz) and 2.82 (d, J=4.2 Hz) (total 1H, OH), 3.36 (s, 3H, OCH_3), 3.36—4.09 (m, 4H, $CH_3CHCHCH_2OCH_3$), 4.49 and 4.63 (ABq, J=11.4 Hz), 4.59 and 4.76 (ABq, J=11.7 Hz) (total 2H, $CH_2C_6H_5$), 7.37 (s) and 7.38 (s) (total 5H, C_6H_5). MS m/z: 210 (M^+).

Methyl (2*R*,3*R*)-2-Hydroxy-3-(*N*,*N*-dimethylcarbamoyl)-3-(benzyloxy)-propionate (55a) and Methyl (2*R*,3*R*)-2-Benzyloxy-3-(*N*,*N*-dimethylcarbamoyl)-3-hydroxypropionate (55b) These compounds were completely separated and the ratio of **55a** to **55b** was determined from their weights.

55a: Pale yellow prisms from hexane–ether–EtOAc. mp 63.5—64.5 °C, $[\alpha]_D^{23}$ +103.7° (c=1.02, $CHCl_3$). IR (KBr): 3410, 1750, 1643, 1500, 750, 703 cm^{-1}. NMR ($CDCl_3$): 2.68 (s, 3H, N $(CH_3)_2$) and 2.93 (s, 3H, $N(CH_3)_2$), 3.86 (s, 3H, CO_2CH_3), 4.14 (d, J=2.7 Hz, 1H, $CHCON(CH_3)_2$), 4.17 (d, J=8.1 Hz, 1H, OH), 4.77 (dd, J=8.1 Hz, 2.7 Hz, 1H, $CHCO_2CH_3$), 4.43 and 4.87 (ABq, J=12.8 Hz, 2H, $CH_2C_6H_5$), 7.37 (s, 5H, C_6H_5). *Anal.* Calcd for $C_{14}H_{19}NO_5$: C, 59.77; H, 6.81; N, 4.98. Found: C, 59.84; H, 6.82; N, 4.88.

55b: $[\alpha]_D^{24}$ +36.6° (c=1.64, $CHCl_3$). IR (neat): 3370, 1744, 1640, 1500, 750, 703 cm.$^{-1}$ NMR ($CDCl_3$): 3.01 (s, 3H, $N(CH_3)_2$) and 3.10 (s, 3H, $N(CH_3)_2$), 3.76 (br s, 1H, OH), 3.73 (s, 3H, CO_2CH_3), 4.55 (d, J=3 Hz, 1H, $CHCON(CH_3)_2$), 4.60 (d, J=3 Hz, 1H, $CHCO_2CH_3$), 4.43 and 4.74 (ABq, J=12 Hz, 2H, $CH_2C_6H_5$), 7.36 (s, 5H, C_6H_5). MS m/z: 282 (M^++1), 222 (M^+−59 (CO_2Me)), 190 (M^+−91 ($PhCH_2$)), 91 ($PhCH_2$), 72 ($CONMe_2$).

2-Methyl-4-(benzyloxy)pentan-2-ol (56a) A mixture of the diol 51 (146 mg, 1.23 mmol) and dibutyltin oxide (307 mg, 1.23 mmol) in toluene (4 ml) was refluxed for 2 h, while water formed was removed as the azeotropic mixture. The solution was evaporated to complete dryness under vacuum and CsF (assay min. 90%, 290 mg, 1.72 mmol) was added to the residue. The mixture was further dried at room temperature *in vacuo* for 1 h and then dry DMF (2 ml) was added. The resulting solution was stirred at 50 to 53 °C for 1 h, then benzyl iodide (490 mg, 2.25 mmol) in dry DMF (4 ml) was added. The reaction mixture was further stirred at the same temperature for 42 h. The solvent was removed under vacuum and the residue was extracted with EtOAc. The organic layer was dried over anhydrous sodium sulfate, concentrated, and purified by silica gel column chromatography (hexane–EtOAc) to give an oil. This oil was further purified by preparative TLC on silica gel (benzene: EtOAc=2:1) to afford 128 mg (50%) of **56a** as a colorless oil. IR (neat): 3475, 1602, 1500, 740, 700 cm^{-1}. NMR ($CDCl_3$): 1.21 (s, 6H, $CH_3\times2$), 1.24 (d, J=7.2 Hz, 3H, $CHCH_3$), 1.37—2.03 (m, 2H, CH_2CHCH_3), 3.77—4.17 (m, 1H, CH_2CHCH_3), 3.98 (s, 1H, OH), 4.42 and 4.64 (ABq, J=11.4 Hz, 2H, $CH_2C_6H_5$), 7.37 (s, 5H, C_6H_5). MS m/z: 208 (M^+).

General Procedure for Benzylation of Glycerol A mixture of glycerol (89 mg, 0.97 mmol) and dibutyltin oxide (241 mg, 0.97 mmol) in toluene (3 ml) was refluxed for 1 h, while water formed was removed as the azeotropic mixture. The solution was evaporated to complete dryness under vacuum and a suitable amount of CsF was added to the resulting white solid. The mixture was further dried at room temperature *in vacuo* for 1 h. Then benzyl iodide, in the amount shown in Table V, in dry DMF (3 ml) was added at 0 °C. The reaction mixture was stirred vigorously at 0 to 3 °C for the period of time shown in Table V. EtOAc was then added to the reaction mixture and the resulting insoluble materials were filtered through a pad of Celite and washed with EtOAc. The filtrate and washings were combined, and concentrated under reduced pressure. The obtained residue was purified by silica gel column chromatography using hexane–EtOAc as an eluent. The monobenzylated products and the dibenzylated products were easily separated, and both of them were isolated as mixtures of regioisomers. The isolated yields are listed in Table V. The ratios of regioisomers were determined from the peak intensities of benzylic protons of each isomer in the ^{1}H-NMR spectra. ^{1}H-NMR data for the mixture are given below.

19a and **19b**: NMR ($CDCl_3$): 3.30—4.03 (m, 7H, CH_2CHCH_2 and OH×2), 4.52 (s) and 4.61 (s) (total 2H, $CH_2C_6H_5$), 7.36 (s, 5H, C_6H_5).

37a and **37b**: NMR ($CDCl_3$): 2.49 (br s) and 2.84 (d, J=3.9 Hz) (total 1H, OH), 3.37—3.79 (m) and 3.84—4.16 (m) (total 5H, CH_2CHCH_2), 4.52 (s), 4.62 and 4.67 (ABq, J=12 Hz) (total 4H, $CH_2C_6H_5\times2$), 7.33 (s, 10H, $C_6H_5\times2$).

References and Notes

1) A part of this work was presented at the 106th Annual Meeting of the Pharmaceutical Society of Japan, Chiba, April 1986, Abstract of Papers, p. 399; and also at the 107th Annual Meeting of the Pharmaceutical Society of Japan, Kyoto, April 1987, Abstract of Papers, p. 234. See also; N. Nagashima and M. Ohno, *Chem. Lett.*, **1987**, 141.
2) An excellent ring closure reaction using stannylene acetal of a diol and CsF was independently reported by Danishefsky *et al.* See; S. Danishefsky and R. Ungate, *J. Am. Chem. Soc.*, **108**, 2486 (1986).
3) Present address: *Eisai Co., Ltd., 1–3, Tokodai 5-chome, Tsukuba-shi, Ibaraki 300–26, Japan.*
4) T. W. Green, "Protective Groups in Organic Synthesis," John Wiley & Sons Inc., New York, 1981, pp. 10—86.
5) For a discussion of this problem, see; C. C. Leznoff, *Acc. Chem. Res.*, **11**, 327 (1978).
6) For example, see; *a*) Y. Ikeda, J. Ukai, N. Ikeda, and H. Yamamoto, *Tetrahedron Lett.*, **25**, 5177 (1984); *b*) B. M. Trost and T. R. Verhoeven, *J. Am. Chem. Soc.*, **102**, 4743 (1980).
7) *a*) P. B. McDougal, J. G. Rico, Young-Im Oh, and B. D. Condon, *J. Org. Chem.*, **51**, 3388 (1986); *b*) A. Gateau-Oleskear, J. Cléphax, and S. D. Géro, *Tetrahedron Lett.*, **27**, 41 (1986); *c*) T. G. Hansson and J. O. Kihlberg, *J. Org. Chem.*, **51**, 4490 (1986); *d*) E. Hungerbühler and D. Seebach, *Helv. Chim. Acta.*, **64**, 687 (1981); *e*) H. Iida, N. Yamazaki and C. Kibayashi, *J. Org. Chem.*, **51**, 1069 (1986); *f*) P. J. Garegg, T. Iversen, and S. Oscarson, *Carbohydr. Res.*, **50**, C12 (1976); *g*) R. D. Walkup and R. T. Cunningham, *Tetrahedron Lett.*, **28**, 4019 (1987).
8) *a*) E. L. Eliel, V. G. Badding, and M. N. Rerick, *J. Am. Chem. Soc.*, **84**, 2371 (1962); *b*) B. E. Leggetter and R. K. Brown, *Can. J. Chem.*, **42**, 990 (1964); *c*) B. Fleming and H. I. Balker, *ibid.*, **52**, 888 (1974); *d*) D. Seeback and E. Hungerbüler, "Modern Synthetic Methods," ed. by R. Scheffold, Salle and Sauerländer, Berlin, 1980, p. 152; *e*) K. Fujita, H. Nakai, S. Kobayashi, K. Inoue, S. Nojima, and M. Ohno, *Tetrahedron Lett.*, **24**, 3507 (1982); *f*) S. Takano, A. Kurotaki, Y. Sekiguchi, S. Satoh, M. Hirama, and K. Ogasawara, *Synthesis*, **1986**, 811; *g*) T. Wakamiya, K. Yamanoi, K. Kanou, and T. Shiba, *Tetrahedron Lett.*, **28**, 5887 (1987); *h*) P. J. Garegg, *Pure Appl. Chem.*, **56**, 845 (1984); *i*) R. Johansson and B. Samuelsson, *J. Chem. Soc., Chem. Commun.*, **1984**, 201; *j*) H. Kotsuki, Y. Ushio, N. Yoshimura, and M. Ochi, *J. Org. Chem.*, **52**, 2594 (1987).
9) For a review, see; S. David and S. Hanessian, *Tetrahedron*, **41**, 643 (1985) and references cited therein. See, particularly; D. Wagner, J. P. H. Verheyden, and J. G. Moffatt, *J. Org. Chem.*, **39**, 24 (1974).
10) *a*) For monoacylation, see: A. Shanzer, *Tetrahedron Lett.*, **21**, 221

(1980); Y. Tsuda, Md. E. Haque, and K. Yoshimoto, *Chem. Pharm. Bull.*, **31**, 1612 (1983); *b*) For monotosylation, see: J. Thiem and Hans-Peter Wessel, *Tetrahedron Lett.*, **21**, 3571 (1980); M. Muraoka, *Chem. Pharm. Bull.*, **29**, 3449 (1981); *c*) For monoacetalization, see: M. A. Nashed, M. S. Chowdhary, and L. Anderson, *Carbohydr. Res.*, **102**, 99 (1982); *d*) For monosilylation, see: A. Ricci, S. Roelens, and A. Vannucchi, *J. Chem. Soc., Chem. Commun.*, **1985**, 1457; U. Berlage, J. Schmidt, U. Peters, and P. Welzel, *Tetrahedron Lett.*, **28**, 3091 (1987); *e*) For monoalkylation, see: C. Augé, S. David, and A. Veyrières, *J. Chem. Soc., Chem. Commun.*, **1976**, 375; M. A. Nashed and L. Anderson, *Carbohydr. Res.*, **56**, 419 (1977); H. Takaku, K. Kamaike, and H. Tsuchiya, *J. Org. Chem.*, **49**, 51 (1984).

11) M. A. Nashed and L. Anderson, *Tetrahedron Lett.*, **1976**, 3503.

12) *a*) S. David, A. Thieffry, and A. Veyrières, *J. Chem. Soc., Perkin Trans., 1*, **1981**, 1796; *b*) J. Alais, A. Maranduba, and A. Veyrières, *Tetrahedron Lett.*, **24**, 2383 (1983).

13) See ref. 8*d*, p. 91 and references cited therein.

14) During the course of our study, two reports on the monoalkylation of dialkyl tartrates were published. See refs. 7*b* and 7*c*.

15) For other examples of selective alkylation of unsymmetric diols, see: *a*) T. Ogawa and T. Horisaki, *Carbohydr. Res.*, **123**, Cl (1983); *b*) O. Sakanaka, T. Ohmori, S. Kozaki, and T. Suami, *Bull. Chem. Soc. Jpn.*, **59**, 3523 (1986); *c*) *Idem*, *ibid.*, **60**, 1057 (1987); *d*) S. Kozaki, O. Sakanaka, T. Yasuda, T. Shimizu, S. Ogawa, and T. Suami, *J. Org. Chem.*, **53**, 281 (1988); *e*) See also ref. 7*g*.

16) *a*) J. Emsley, D. J. Jones, J. M. Miller, R. E. Overill, and R. A. Waddilove, *J. Am. Chem. Soc.*, **103**, 24 (1981); *b*) J. H. Clark and J. M. Miller, *J. Chem. Soc., Perkin Trans., 1*, **1977**, 2063.

17) T. Mukaiyama, Y. Tanabe, and M. Shimizu, *Chem. Lett.*, **1984**, 401.

18) *a*) N. H. Andersen, D. A. McCrae, D. B. Grotjahn, S. Y. Gabhe, L. J. Theodore, R.M. Ippolito, and T. K. Sarkar, *Tetrahedron*, **37**, 4069 (1981); *b*) M. Gielen and R. Fosty, *J. Chem. Res. (s)*, **1977**, 214; *c*) A. Degl'Innocenti, S. Pike, and D. R. M. Walton, *J. Chem. Soc., Chem. Commun.*, **1980**, 1201; *d*) B. A. Pearlman, S. R. Putt, and J. A. Fleming, *J. Org. Chem.*, **50**, 3622 (1985).

19) A formation of pentacoordinate tin complex has also been postulated for trialkyltin alkoxide. See: J. Alais and A. Veyrières, *J. Chem. Soc., Perkin Trans., 1*, **1981**, 377.

20) M. Gingras, T. H. Chan, and D. N. Harpp, *J. Org. Chem.*, **55**, 2078 (1990).

21) Danishefsky makes a similar assumption in ref. 2.

22) For synthetic applications of our procedure, see; *a*) H. Niwa *et al.*, 30th Symposium on the Chemistry of Natural Products, 1988, Abstract, 418; *b*) K.-L. Yu and B. Fraser-Reid, *Tetrahedron Lett.*, **29**, 979 (1988); *c*) Y.-C. Liu and C.-S. Chen, *ibid.*, **30**, 1617 (1989); *d*) C. J. J. Elie, C. E. Dreef, R. Verduyn, G. A. Van Der Marel, and J. H. Van Boom, *Tetrahedron*, **45**, 3477 (1989); *e*) C. Murakata and T. Ogawa, *Tetrahedron Lett.*, **31**, 2439 (1990); *f*) T. Sato, T. Tada, J. Otera, and H. Nozaki, *ibid.*, **30**, 1665 (1989); *g*) T. Sato, J. Otera, and H. Nozaki, *ibid.*, **30**, 2959 (1989).

23) E. J. Corey and A. Venkateswarlu, *J. Am. Chem. Soc.*, **94**, 6190 (1972).

24) H. L. Smith, E. S. Brown, J. D. Smith, and J. Andrako, *J. Pharm. Sci.*, **54**, 1269 (1965).

25) M. E. Jung and T. J. Shaw, *J. Am. Chem. Soc.*, **102**, 6304 (1980).

26) H. Hibbert and N. M. Carter, *J. Am. Chem. Soc.*, **50**, 3120 (1928).

27) J. P. Amma and J. K. Stille, *J. Org. Chem.*, **47**, 468 (1982).

28) J. J. Baldwin, A. W. Raab, K. Mensler, B. H. Arison, and D. E. McClure, *J. Org. Chem.*, **43**, 4876 (1978).

29) M. Cahnmann, *Bull. Soc. Chim. Fr.* **4**, 226 (1937).

30) C. Fuganti, P. Grasselli, and G. Pedrocchi-Fantoni, *Tetrahedron Lett.*, **22**, 4017 (1981).

31) Ref. 8*d*, p. 151.

Lithium Aluminum Hydride Reduction of Glycopyranoside-Monosulfonates: Formation of Branched Furanosides[1)]

Yoshisuke TSUDA,* Makoto NISHIMURA,[2)] and Yoko ITO

Faculty of Pharmaceutical Sciences, Kanazawa University, 13-1 Takara-machi, Kanazawa 920, Japan. *Received February 14, 1991*

Lithium aluminum hydride reduction of glycopyranoside-monotosylates caused three reactions: (1) stereospecific 1,2-shift, producing branched furanosides (path A), (2) reductive O–S bond cleavage, producing the original glycosides (path B), and (3) reductive removal of the tosyloxy group, producing deoxyglycosides (path C). The path A reaction was particularly evident for the monotosylates at 2-*O*, 3-*O*, and 4-*O*: for example, methyl 2-*O*-tosyl-α-D-xylopyranoside gave methyl 2-deoxy-2-*C*-(hydroxymethyl)-α-D-erythrofuranoside in 60% yield. This reaction opens a new and efficient route to branched glycofuranosides of natural and unnatural type. Stereo–electronic requirements of this reaction in relation to the balance of the other two reactions are discussed.

Keywords lithium aluminum hydride; glycopyranoside-monotosylate; branched furanoside; stereospecific 1,2-shift; metalate complex; deoxyglycoside; O–S bond cleavage; reductive detosyloxylation; intramolecular hydride transfer

It is well known that glycoside-tosylates, when treated with bases, give epoxides or products derived therefrom; other products, such as those of skeletal rearrangement, have rarely been observed. In 1985, Bear *et al.*[3)] reported that monotosylates of 6-deoxyhexopyranosides, when treated with lithium triethylborohydride (LTBH), produced branched pentofuranosides in appreciable yields (40—60 %). Binkley[4)] also observed similar rearrangement of a 2,3-ditosylate by LTBH, though in low yield (8%). However, application of this interesting reaction has been limited, because regioselective synthesis of glycoside-monotosylates has required multiple steps.

Various glycopyranoside-monotosylates are now readily available through regioselective monotosylation of unprotected or partially protected glycopyranosides by the dibutyltin oxide method.[5)] By the use of substrates thus obtained, we found, independently of the previous authors, that treatment of glycopyranoside-monotosylates with an excess of lithium aluminum hydride (LAH) under reflux resulted in one or more of the following three reactions: (1) stereospecific 1,2-shift, producing branched glycofuranosides (path A), (2) reductive O–S bond cleavage, producing the original glycosides (path B), and (3) reductive removal of the tosyloxy group, producing deoxyglycosides (path C). The path A reaction was particularly evident for 2-*O*-, 3-*O*-, and 4-*O*-tosylates. Here, we present the results in detail.

Results and Discussion

LAH Reduction of Glycopyranoside-Monotosylates Reduction of methyl 6-*O*-tosyl-α- and β-D-glucopyranoside, **6** and **10**, with LAH gave the 6-deoxy derivatives, **23** and **24**, in 70—75% yield, respectively: path C is the major reaction path of the primary *O*-tosylates.[6)]

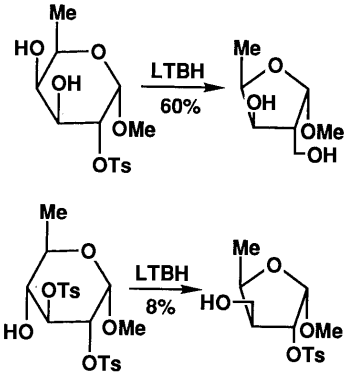

Chart 1. Reported Rearrangement of Glycopyranoside-Tosylates

Methyl α-D-glucopyranoside (Me α-D-Glc)[7)] 2-*O*-tosylate **2** afforded two products, **32** (33%) and Me α-D-Glc **1** (41%), which are path A and path B products, respectively. The oily product **32** showed a peak at *m/z* 147 ($M^+ - OMe$) in the mass spectrum (MS) and formed a crystalline tribenzoate **32b** (**b** indicates perbenzoate, hereafter), mp 118—120 °C. From the formula, $C_{28}H_{26}O_8$, of the tribenzoate, the formula of **32** was determined as $C_7H_{14}O_5$. The furanoside structure was suggested by the ^{13}C-nuclear magnetic resonance (^{13}C-NMR) spectra of **32** and the triacetate **32a** (**a** indicates peracetate, hereafter), which showed the presence of two primary and one secondary hydroxyls, one –CHO–, and one –CH–, besides an anomeric carbon and a methoxyl in **32**. From these data we concluded that it is the product formed from **2** by a stereospecific 1,2-shift of C-4 to C-2 with concomitant reduction of the resulting aldehyde group.

The 2,6-di-*O*-tosylate **7** also gave the rearranged product **33** with concomitant reductive removal of the 6-tosyloxy group, but in low yield (16%). Compound **33** was identical, in terms of the ^{13}C-NMR spectrum, with the product obtained from methyl 6-deoxy-6-iodo-2-*O*-tosyl-α-D-glucopyranoside by Bear *et al.*[3)]

Me α-D-Xyl 2-*O*-tosylate **12**, on similar reduction, gave only the rearranged product **34** (path A) in 62% yield. Me β-L-Ara 2-*O*-tosylate **18** gave three products: **35** (path A, 8%), **17** (path B, 48%), and **26** (path C, 17%). In all of those cases, the rearrangement occurred in only one direction (C-4 to C-2) of the two possible directions: ring-O to C-2 and C-4 to C-2.

The 4-*O*-tosylates also gave stereospecific 1,2-shift products: again the rearrangement occurred in only one direction (C-2 to C-4). Thus Me α- and β-D-Xyl 4-*O*-

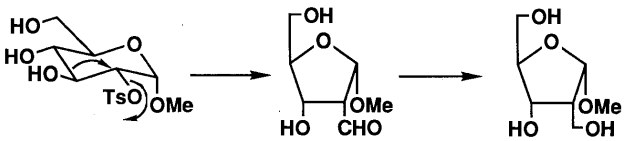

Chart 2. Path A Reaction

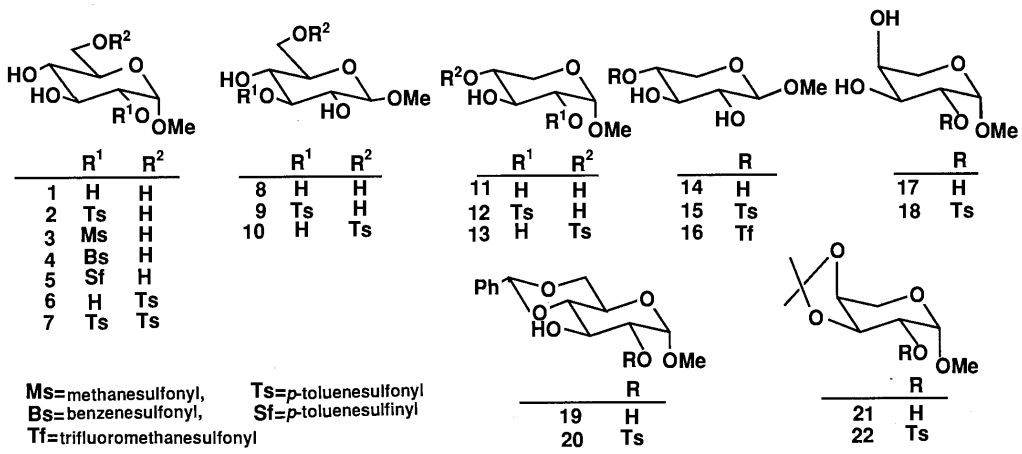

Chart 3. Glycopyranoside Derivatives Used in This Work

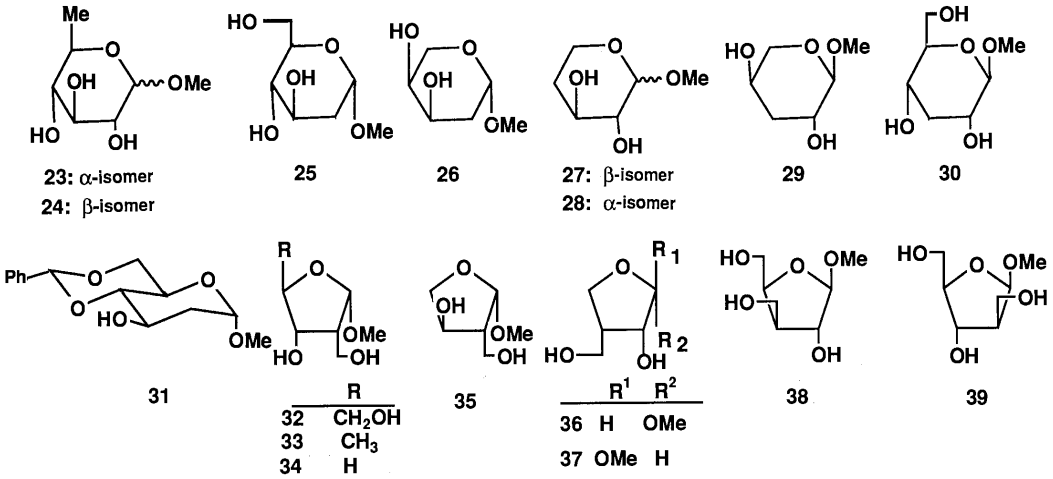

Chart 4. Deoxyglycosides and Rearranged Glycosides

TABLE I. Reaction of Pyranoside-Monotosylates with Lithium Aluminum Hydride

Position of Ts group	Substrate	Rearranging carbon	Product (yield %) Path A	Path B	Path C
2-*O*	Me α-D-Glc	C4	**32** (38)	**1** (41)	**25** (trace)
	Me α-D-Xyl		**34** (62)	—	—
	Me β-L-Ara		**35** (8)	**17** (48)	**26** (17)
4-*O*	Me α-D-Xyl	C2	**36** (44)	**11** (15)	**27** (25)
	Me β-D-Xyl		**37** (17)	**14** (25)	**28** (41)
3-*O*	Me β-D-Glc	C5, C1	**38** (14), **39** (3)	**8** (trace)	**30** (41)

tosylates, **13** and **15**, gave single 1,2-shift producs **36** and **37** in yields of 44% and 17%, respectively, together with variable amounts of the path B and path C producs.

The 3-*O*-tosylate **9** also gave the 1,2-shift product, but rearrangement occurred in two directions (C-1 to C-3 and C-5 to C-3), thus giving two rearrangement products, **38** and **39**, together with the path B and path C products.

The structures of all the products were elucidated, after conversion to the corresponding benzoates, by examination of the ^{1}H-, ^{13}C-NMR, and H–H and C–H correlation spectroscopy (COSY) spectra. The results are summarized in Table I, and the ^{13}C-NMR data of the rearranged and deoxygenated products in Tables II and III.

Table I clearly indicates that the rearranging group is the carbon functionality only; the ring-oxygen does not participate in this rearrangement. Further, when the number of oxygen substituents on the rearranging carbon increased, its rearranging ability decreased.

Mechanistic Study on the Rearrangement (Path A Reaction) It is evident that the above 1,2-shift proceeds through the *C1* conformation with the tosyloxy group in equatorial orientation, or otherwise the reaction would proceed toward epoxide formation. The following mechanistic questions arise: (1) what leaving groups are effective for the rearrangement? (2) what reagents cause the rearrangement?, and (3) what is the factor fixing the conformation in *C1*?

Table IV-1 indicated that when the electronegativity of the leaving group was increased the yield of rearranged product increased, as expected: the *O*-benzenesulfonyl group was more effective than the *O*-*p*-toluenesulfonyl group, and the *O*-methanesulfonyl group was ineffective. The sulfinyloxy group was completely ineffective; the product from **5** was the path B product only. The results prove that the rearrangement does not proceed through initial reduction of the sulfonyl group to a sulfinyl group, and a sufficient electronegativity of the leaving group is necessary for the rearrangement.

The *O*-triflate group was also effective, as expected, if we

TABLE II. ^{13}C-NMR Data for Branched Furanosides (in Chloroform-*d*)

Compd.	**32a**[a]	**32b**	**32c**	**33a**[a]	**34b**	**35b**	**36b**	**37b**	**38b**	**39b**
C-1	106.1	104.8	104.7	105.6 (105.4)[b]	104.1	104.0	101.7	107.3	107.8	104.4
C-2	51.7	46.5	55.3	50.7 (48.2)	46.4	49.2	73.5	77.1	78.7	49.1
C-3	72.8	74.1	72.8	76.9 (77.2)	72.4	77.0	37.3	39.8	45.5	76.9
C-4	88.9	82.3	82.3	82.8 (83.1)	73.3	71.1	68.2	69.3	80.6	81.7
C-5	63.3	64.6	63.9	19.8 (19.4)	—	—	—	—	64.3	65.9
CH_2OR	57.3	59.5	58.8	57.3 (58.1)	59.6	62.2	63.9	61.6	61.6	62.3
OMe	54.7	55.4	55.3	54.6 (54.9)	55.2	55.0	55.3	54.7	55.4	55.2

a) Data in pyridine-d_5. *b*) Reported data (ref. 3) in chloroform-*d*.

TABLE III. ^{13}C-NMR Data for Deoxyglycosides (in Chloroform-*d*)

Compd.	**23a**[a]	**24a**[a]	**26b**	**27b**	**28b**	**29b**	**30b**
C-1	105.1	101.0	98.1	98.1	101.7	97.8	102.8
C-2	75.2	73.6	31.4	72.8	71.5	65.6	68.9
C-3	77.9	74.7	66.7	68.7	70.8	29.9	32.2
C-4	72.2	77.0	68.6	31.2	29.7	69.7	67.1
C-5	76.6	68.2	61.0	57.3	59.8	61.4	74.9
C-6	18.5	18.4	—	—	—	—	63.8
OMe	56.5	54.9	55.2	55.3	56.4	55.3	56.7

a) In pyridine-d_5 (ref. 6).

TABLE IV-1. LAH Reduction of Me α-D-Glc 2-*O*-Sulfonates and Sulfinate

Compd.	Leaving group	Product (%) A (**32**)	B (**1**)	C (**25**)
3	OMs	—	79	Trace
2	OTs	33	41	—
4	OBs	39	22	—
5	OSf	—	78	—

TABLE IV-2. Hydride Reduction of Me β-D-Xyl 4-*O*-Sulfonates

Compd.	Leaving group	Reagent	Product (%) A (**37**)	B (**14**)	C (**28**)	**29**
15	OTs	LAH	17	25	41	—
15	OTs	LBAH	—	—	—	53
16	OTf	LAH	11	10	1	11

TABLE IV-3. Hydride Reduction of Me α-D-Xyl 2-*O*-Tosylate

Compd.	Reagent	Product (%) A (**34**)	B (**11**)
12	LAH	62	—
12	LBAH	54	—
12	LBH	37	5

disregard the instability of the *O*-Tf group: it increased the ratio of the rearranged product (Table IV-2). However, in the reduction of the *O*-triflate **16**, a new product **29** (see also below) was produced in addition to the expected three products.

Tsuchihashi *et al.*[8] reported a similar stereospecific 1,2-shift of 1,2-glycol monomesylate with organoaluminum reagents (Chart 5). In their mechanism, the aluminum reagent chelates to both the sulfonyl and the neighboring hydroxyl group to assist the rearrangement. However, their

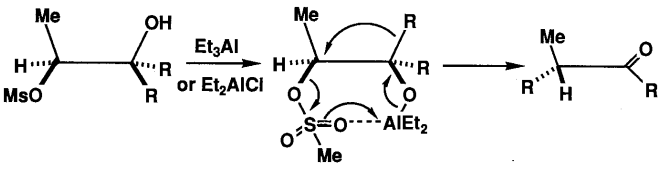

Chart 5. Stereospecific 1,2-Shift of Glycol-Mesylates Reported by Tsuchihashi *et al.*

reagent [$AlEt_3$, diisobutylaluminum hydride (DIBAL), $AlEt_2Cl$, or $AlEt_2Cl$–DIBAL] did not give any rearrangement product for glycoside-monotosylates (**2**, **12**, **13**, and **15**). Neither AlH_3 nor lithium tri-*tert*-butoxyaluminum hydride was effective.

Instead, we observed that metalate complexes such as LAH or lithium *n*-butyl-diisobutylaluminum hydride (LBAH)[9] were effective for rearrangement of glycoside-monotosylates. LTBH reported by previous workers[3,4] is also an ate complex. Reaction of **12** with LBAH gave the path A product **34** in 54% yield. However, in the reduction of **15** with LBAH, the 3-deoxy derivative **29** was the sole product (53%). Apparently this is formed through the epoxide **44**. The difference of the products may be due to the basicity of the reagent. Lithium borohydride (LBH) also gave the rearranged product (**34** from **12**), but it was less effective than LAH in terms of both yield (37%) and reaction time. Sodium borohydride in ethanol was appreciably basic and caused only the epoxide formation, thus giving methyl α-D-3-*O*-ethyl-altropyranoside **41** exclusively from Me α-D-Glc 2-*O*-tosylate **2**. The structure of **41** was confirmed by an alternative synthesis (see Experimental).

4,6-*O*-Benzylidene derivatives are fixed in *C1* conformation. The reaction of **20** with LAH was therefore examined. However, it gave only the path B and path C products, **19** and **31**, no rearrangement product being produced, probably due to the disfavored transition state, as suggested by Bear *et al.*[3]: a highly strained system comprising a six-membered acetal ring *trans*-fused to a five-membered furanose ring. From the isopropylidene derivative **22**, the transition state of rearrangement is, if the reaction occurs, a *cis*-fused five-five membered ring system which would not have such an unfavorable strain. However, LAH reduction of **22** gave the path B product only, again no rearrangement being observed. The result, when compared to the reduction of **18**, implies that the presence of an equatorial hydroxyl group neighboring the (equatorial) tosyloxy group is necessary for the rearrangement.

Therefore, we consider, tentatively, that ate complexes operate to fix the conformation, where lithium cation chelates between the *O*-sulfonyl group and the metal of the

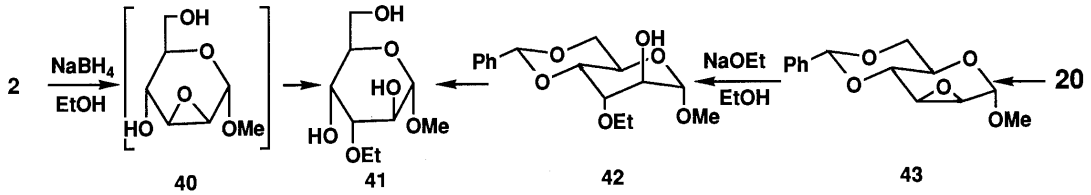

Chart 6. Epoxide Formation by Sodium Borohydride in Ethanol

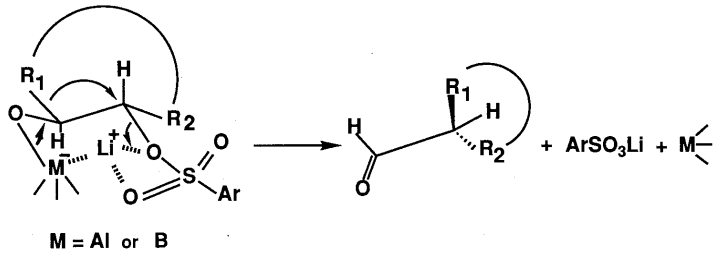

Chart 7. Proposed Mechanism of Stereospecific 1,2-Shift of Glycoside-Sulfonates with Metalate Complexes

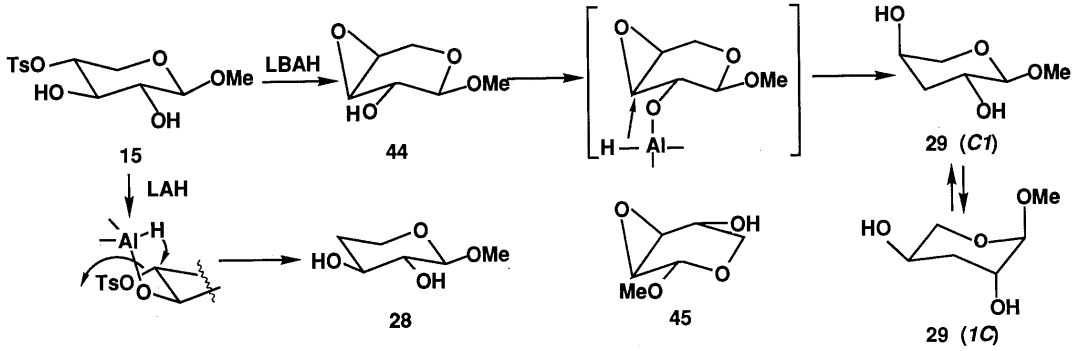

Chart 8. Rearrangement in Deoxygenation

metalated neighboring (equatorial) hydroxyl group as shown in Chart 7. The anionic metal (Al or B) linked to oxygen assists the rearrangement in this mechanism.[10]

On the Formation of Deoxyglycosides (Path C Reaction) Secondary tosyloxy groups on a cyclohexane ring are usually difficult to remove by LAH reduction. The same can be said for primary *O*-tosyl groups neighboring a quaternary carbon. This is due to the steric hindrance for back side attack of a hydride anion. The usual products in such cases are those of O–S bond cleavage (path B reaction).[11] Thus, although the yields are variable depending on the substrates, the formation of path C products by LAH reduction of glycopyranoside-monotosylates needs to be reasonably explained.

The 3-deoxy derivative **29** formed from **15** with LBAH or from **16** with LAH must be produced through the epoxide **44**, since the configuration of 4-OH was inverted. This was proved by independent LAH reduction of the 3,4-anhydro derivative **44** to **29**. The 4-deoxy derivative **28** was not produced in the reduction of **44**, which therefore must be formed directly from **15** (or **16**). The dibenzoate **29b** was suggested to be of *1C* conformation, since the coupling constant between H-1 and H-2 was 2.5 Hz. Formation of a single product **29** in the reduction of **44** can be explained by an intramolecular hydride transfer as shown in Chart 8.

The other deoxyglycosides (*e.g.* **28**) should also be the products of an intramolecular hydride transfer from the intermediary –O–Al–H to the carbon geminal to the tosyloxy group. Such a neighboring group participation has been shown in the reductive detosyloxylation of triterpenoid tosylates with LAH.[11] In support of this consideration, the isopropylidene derivative **22**, which lacks hydroxyl group, gave no deoxy product, while the hydroxy derivative **18** gave the deoxy product **26** in 17% yield, probably through the intermediate **46**.

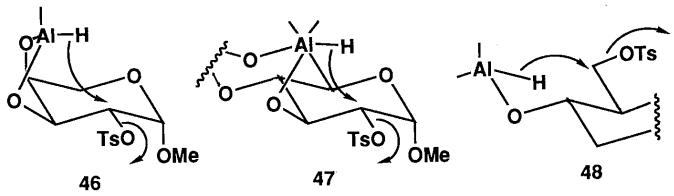

Chart 9. Intramolecular Hydride Transfer

The difference between the reductions of **2** and the corresponding 4,6-*O*-benzylidene derivative **20** is also remarkable: the former gave no path C product, while the latter gave the deoxy product **31** in 15% yield. The reduction of **20** could proceed through the intermediate **47**, while the complex formed from **2** and LAH would have the structure unfavorable for intramolecular hydride transfer. Even in the reductive removal of the primary 6-OTs group, the reaction probably proceeds through an intramolecular hydride transfer, as in **48**.

The above consideration, however, does not necessarily rule out the direct intermolecular *SN2* displacement of the

OTs group by a hydride. Reaction of Me α-D-Xyl 2,3,4-tri-*O*-mesylate with sodium azide gives Me 4-azido-4-deoxy-β-L-Ara 2,3-di-*O*-mesylate[12] indicating that an *SN*2 substitution is possible at C-4. The formation of the 4-deoxy derivative **27** or **28** from **13** or **15** may, at least partially, be the result of direct displacement.

Conclusion

Of the three reactions that occurred in LAH reduction of glycopyranoside-monotosylates, stereospecific 1,2-shift (path A) is the most common, and is always observed except for 6-*O*-tosylates. The reaction is supposed to proceed through the cyclic intermediate shown in Chart 7, where the hydroxyl group neighboring the tosyloxy group is metalated by an ate complex and the lithium cation chelates to both the metal anion and the *O*-sulfonate group, thus assisting the rearrangement. Therefore, the substituent on the carbon bearing that hydroxy group shifts toward the *O*-sulfonate group, so that sufficient electronegativity is necessary to induce rearrangement. The resulting aldehyde is concomitantly reduced by excess reagent to give a branched furanoside. This reaction will be particularly useful for the preparation of branched glycofuranosides of unnatural type.

Of the other paths, O–S bond cleavage producing the original glycosides (path B) is common for a hindered OTs group, and the deoxyglycosides sometimes observed in variable yield (path C) may be the products of intramolecular hydride transfer.

Experimental

General Unless otherwise stated, the following procedures were adopted. Melting points were determined on a Yanaco micro hot stage melting point apparatus and are uncorrected. Infrared (IR) spectra were taken in $CHCl_3$ solutions on a Jasco IR-G spectrometer, and the data are given in cm^{-1}. NMR spectra were taken with a JEOL FX-100 (100 MHz for ^1H and 25 MHz for ^{13}C) or a GX-400 (400 Mz for ^1H and 100 MHz for ^{13}C) spectrometer in chloroform-*d* solution with tetramethylsilane as an internal standard, and the chemical shifts are given in δ values. For benzoates, the data of aromatic protons and carbons are omitted. MS and high resolution MS (HRMS) were taken with a Hitachi M-80 spectrometer and major peaks are indicated in *m/z* (%). Column chromatography was performed on Fuji-Devison silica gel BW-820 MH. Recycling preparative high performance liquid chromatography (HPLC) of the benzoates was performed on a LC-908 analyzer (Nihon Bunseki Kogyo) with a JAIGEL-H column (2 cm i.d. × 60 cm) using $CHCl_3$ as a mobile phase. Peaks were detected by ultraviolet (UV) measurement (254 nm). For thin layer chromatography (TLC), Macherey-Nagel precoated plates $SILG_{254}$ were used and spots were monitored by UV measurement (254 nm), then developed by spraying 10% H_2SO_4 and heating the plates at 100 °C until coloration took place. Gas chromatographic (GC) analyses were carried out with a Shimadzu GC4CM-PF gas chromatograph with a flame ionization detector (FID) using a column (1 m × 2.6 mm i.d.) packed with 1.5% OV-1 on a Shimalite W (80—100 mesh) and N_2 (50—80 ml/min) as a carrier gas. Identities were confirmed by mixed melting point determination (for crystalline compounds) and also by comparisons of TLC behavior, GC of trimethylsilyl derivatives or benzoates, and ^1H-NMR and IR spectra.

LAH Reduction of Glycoside-Sulfonates (General Procedure) The starting sugar sulfonate and LAH in dry tetrahydrofuran (THF, refluxed over Na and benzophenone and freshly distilled) were refluxed with magnetic stirring under an Ar atmosphere with periodic monitoring of the progress of the reaction by TLC. Amounts of materials and reaction times are given for each individual experiment. For processing, the mixture was cooled and excess reagent was decomposed by dropwise addition of aqueous saturated Na_2SO_4 solution, then the whole was filtered. The residue was decomposed with dilute HCl, then neutralized with $NaHCO_3$, concentrated to dryness, and extracted exhaustively with hot EtOH. If the extract contained a large amount of inorganic salts, it was evaporated and again extracted with dry EtOH. The combined filtrate and the extracts were concentrated to give the crude reaction product, which was separated by chromatography or benzoylated with benzoyl chloride in pyridine overnight at room temperature, then the benzoylated product was separated by chromatography.

Reduction of Me α-D-Glc 2-*O*-Sulfonates (1) The reaction was performed with the tosylate **2** (0.5 g) and LAH (291 mg, 5 mol eq) in THF (40 ml) for 21 h. The crude product was chromatographed to give **2** (49 mg, 10%) from the AcOEt eluate, **32** (91 mg, 33%) from the AcOEt–EtOH (9 : 1) eluate, and **1** (114 mg, 41%) from the AcOEt–EtOH (5 : 1) eluate.

Methyl 2-Deoxy-2-*C*-(hydroxymethyl)-α-D-*ribo*-pentofuranoside **32**: Colorless syrup. ^1H-NMR (pyridine-d_5): 5.27 (1H, d, J=4.8 Hz, H-1), 4.78 (1H, dd, J=7.2, 2.0 Hz, H-3), 4.58 (1H, td, J=4.8, 2.0 Hz, H-4), 4.35, 4.42 (each 1H, d, J=5.0 Hz, CH_2O), 3.97 (2H, d, J=4.8 Hz, H-5), 3.36 (3H, s, OMe), 2.69—2.96 (1H, m, H-2). MS: 147 (M^+−OMe, 21), 87 (100). The tribenzoate **32b** was obtained as colorless needles from hexane, mp 118—120 °C. IR: 1715. ^1H-NMR: 5.66 (1H, dd, J=7, 3 Hz, H-3), 5.24 (1H, d, J=4.9 Hz, H-1), 4.75—4.58 (4H, m, H-5 and CH_2O), 4.53 (1H, br dd, J=4.5, 3 Hz, 3Hz, H-4), 3.47 (3H, s, OMe), 3.09—2.82 (1H, m, H-2). *Anal.* Calcd for $C_{28}H_{26}O_8$: C, 68.56; H, 5.34. Found: C, 68.83; H, 5.36. The triacetate **32a** was obtained as a colorless syrup. ^1H-NMR: 5.16 (1H, dd, J=9.2, 2.4 Hz, H-3), 5.03 (1H, d, J=4.8 Hz, H-1), 3.38 (3H, s, OMe), 2.40—2.68 (1H, m, H-2), 2.08 (6H), 2.04 (3H) (each s, OAc).

(2) The reaction of the mesylate **3** (171 mg) with LAH (130 mg, 5 mol eq) in THF (30 ml) for 16 h gave Me α-D-Glc **1** (97 mg, 79%). A trace of the 2-deoxy derivative **25** was detected on TLC, but could not be isolated.

(3) The reaction of the benzenesulfonate **4** (0.5 g) with LAH (455 mg, 8 mol eq) in THF (40 ml) for 13 h gave, after benzoylation, the furanoside **32b** (163 mg, 39%) and Me α-D-Glc tetrabenzoate **1b** (200 mg, 22%).

(4) The reaction of the *p*-toluenesulfinate **5** (30 mg) with LAH (17 mg, 5 mol eq) in THF (10 ml) for 3 h gave, after benzoylation, Me α-D-Glc tetrabenzoate **1b** (43 mg, 78%). Compound **32** was not detected on TLC.

Reduction of Me α-D-Glc 2,6-Di-*O*-tosylate 7 The reaction was performed with **7** (1.3 g) and LAH (563 mg, 5 mol eq) in THF (50 ml) for 14 h. Chromatography of the crude product gave **33** (73 mg, 16%) from the $CHCl_3$–EtOH (9 : 1) eluate. Acetylation of the $CHCl_3$–EtOH (3 : 1) eluate and purification of the product by chromatography gave Me 6-deoxy-α-D-Glc triacetate **23a** (122 mg, 14%).

Methyl 2,5-Dideoxy-2-*C*-(hydroxymethyl)-α-D-*ribo*-pentofuranoside **33**: Colorless syrup (lit. syrup).[3] ^1H-NMR: 5.18 (1H, d, J=4.8 Hz, H-1), 3.33 (3H, s, OMe), 2.56—2.82 (1H, m, H-2), 1.26 (3H, d, J=5.6 Hz, Me).

Methyl 6-Deoxy-α-D-glucopyranoside Tri-*O*-acetate **23a**: Colorless needles from hexane, mp 59—61 °C. ^1H-NMR: 3.40 (3H, s, OMe), 2.00, 2.04, 2.08 (each 3H, s, Ac), 1.20 (3H, d, J=6.4 Hz, Me). This was identical with the compound obtained on acetylation of **23**.[6]

Reduction of Me α-D-Xyl 2-*O*-Tosylate 12 The reaction was performed with **12** (250 mg) and LAH (225 mg, 7.5 mol eq) in THF (20 ml) for 9 h. The crude product was benzoylated and chromatographed to give methyl 2-deoxy-2-*C*-(hydroxymethyl)-α-D-erythrofuranoside di-*O*-benzoate **34b** (170 mg, 62%) as a colorless syrup. IR: 1714. ^1H-NMR: 5.66 (1H, ddd, J=8.2, 5.8, 2.6, Hz, H-3), 5.14 (1H, d, J=4.9 Hz, H-1), 4.70 (1H, dd, J=11.0, 7.0 Hz), 4.62 (1H, dd, J=11.0, 7.9 Hz) (CH_2O), 4.41 (1H, dd, J=10.6, 2.6 Hz), 4.03 (1H, dd, J=10.6, 5.8 Hz) (H-4), 3.64 (3H, s, OMe), 2.85—2.75 (1H, m, H-2). MS: 356 (M^+, 0.2), 325 (M^+−OMe, 2), 105 (100). HRMS: Calcd for $C_{20}H_{20}O_6$ (M^+): 356.1258; $C_{19}H_{17}O_5$ (M^+−OMe): 325.1074. Found: 356.1258; 325.1074.

Reduction of Me β-L-Ara 2-*O*-Tosylate 18 The reaction was performed with **18** (500 mg) and LAH (305 mg, 5.0 mol eq) in THF (45 ml) for 31 h. The crude product was benzoylated and the product was chromatographed to give a mixture of **35b** (44 mg, 8%), **17b** (361 mg, 48%), and **26b** (94 mg, 17%), which were separated by recycling preparative HPLC.

Methyl 2-Deoxy-3,4-di-*O*-benzoyl-β-L-*erythro*-pentopyranoside **26b**: Colorless syrup. IR: 1718. ^1H-NMR: 5.65 (1H, ddd, J=12.8, 4.7, 3.4 Hz, H-3), 5.53 (1H, br s, H-1), 4.97 (1H, br dd, J=3.4, 2.0 Hz, H-4), 4.10 (1H, dd, J=12.8, 1.2 Hz, H-5eq), 3.95 (1H, dd, J=12.8, 3.1 Hz, H-5ax), 3.34 (3H, s, OMe), 2.38 (1H, dt, J=12.2, 3.4 Hz, H-2ax), 2.14 (1H, ddd, J=12.2, 4.7, 2.0 Hz, H-2eq). MS: 356 (M^+, 0.4), 325 (M^+−OMe, 3), 105 (100). HRMS: Calcd for $C_{20}H_{20}O_6$ (M^+): 356.1258; $C_{19}H_{17}O_5$: 325.1074. Found: 356.1229; 325.1091.

Methyl 2-Deoxy-2-*C*-(hydroxymethyl)-β-L-threofuranoside Di-*O*-benzoate **35b**: Colorless syrup. IR: 1715. ^1H-NMR: 5.51 (1H, td, J=6.6, 3.4 Hz, H-3), 5.14 (1H, d, J=4.9 Hz, H-1), 4.64 (1H, dd, J=11.4, 7.0 Hz), 4.51 (1H, dd, J=11.4, 7.9 Hz) (CH_2O), 4.41 (1H, dd, J=10.4, 6.6 Hz), 3.93

(1H, dd, J=10.4, 3.4 Hz) (H-4), 3.38 (3H, s, OMe), 3.02—2.96 (1H, m, H-2). MS: 356 (M^+, 0.2), 325 (M^+−OMe, 2), 105 (100). HRMS: Calcd for $C_{20}H_{20}O_6$ (M^+): 356.1258; $C_{19}H_{17}O_5$ (M^+−OMe): 325.1074. Found: 356.1074. Found: 356.1237; 325.1102.

Reduction of Me α-D-Xyl 4-*O*-Tosylate 13 The reaction was performed with **13** (250 m) and LAH (212 mg, 7 mol eq) in THF (30 ml) for 9 h. The crude product was benzoylated and product was chromatographed to give a mixture of **36b** (110 mg, 44%), **27b** (70 mg, 25%), and **11b** (52 mg, 15%) from the $CHCl_3$–AcOEt (19 : 1) eluate. The products were separated by recycling preparative HPLC.

Methyl 3-Deoxy-3-*C*-(hydroxymethyl)-α-D-erythrofuranoside Di-*O*-benzoate **36b:** Colorless needles from benzene–hexane, mp 82.5—84 °C. IR (KBr): 1710. ^{1}H-NMR: 5.34 (1H, dd, J=9.2, 4.3 Hz, H-2), 5.21 (1H, d, J=4.3 Hz, H-1), 4.74 (1H, dd, J=11.0, 6.4 Hz), 4.53 (1H, dd, J=11.0, 8.5 Hz) (CH_2O), 4.22 (1H, dd, J=9.2, 7.9 Hz), 4.00 (1H, dd, J=9.2, 6.1 Hz) (H-4), 3.39 (3H, s, OMe), 3.13—3.00 (1H, m, H-3). MS: 325 (M^+−OMe, 7), 105 (100). *Anal.* Calcd for $C_{20}H_{20}O_6$: C, 67.41; H, 5.66. Found: C, 67.39; H, 5.68.

Methyl 4-Deoxy-β-L-*threo*-pentopyranoside Di-*O*-benzoate **27b**: Colorless prisms from benzene–hexane, mp 106—107 °C. IR (KBr): 1720. ^{1}H-NMR: 5.62 (1H, td, J=10.1, 5.3 Hz, H-3), 5.19 (1H, dd, J=10.1, 3.7 Hz, H-2), 5.02 (1H, d, J=3.7 Hz, H-1), 3.88 (1H, dt, J=12.1, 2.4 Hz), 3.67 (1H, ddd, J=12.1, 5.3, 1.2 Hz) (H-5), 3.35 (3H, s, OMe), 2.27—2.23 (1H, m), 1.91 (1H, dq, J=12.8, 5.3 Hz) (H-4). MS: 357 (M^++1, 0.2), 325 (M^+−OMe, 2), 105 (100). *Anal.* Calcd for $C_{20}H_{20}O_6$: C, 67.41; H, 5.66. Found: C, 67.14; H, 5.28.

Reduction of Me α-D-Xyl 4-*O*-Sulfonates (1) The reaction was performed with the tosylate **15** (0.5 g) and LAH (300 mg, 5 mol eq) in THF (50 ml) for 8 h. The crude product was benzoylated and chromatographed. The $CHCl_3$ eluate was separated by recycling preparative HPLC to give **37b** (96 mg, 17%), the 4-deoxy derivative **28b** (228 mg, 41%), and Me α-D-Xyl tri-*O*-benzoate **14b** (188 mg, 25%).

Methyl 3-Deoxy-3-*C*-(hydroxymethyl)-α-D-erythrofuranoside Di-*O*-benzoate **37b**: Colorless needles from benzene–hexane, mp 84—85 °C. IR (KBr): 1716. ^{1}H-NMR: 5.50 (1H, br d, J=5.2 Hz, H-2), 5.04 (1H, br s, H-1), 4.60—4.43 (2H, m, CH_2O), 4.29, 4.02 (each 1H, br t, J=9—8.2 Hz, H-4), 3.41 (3H, s, OMe), 3.60—3.15 (1H, m, H-3). MS: 356 (M^+, 0.1), 325 (M^+−OMe, 9), 105 (100). *Anal.* Calcd for $C_{20}H_{20}O_6$: C, 67.41; H, 5.66. Found: C, 67.31; H, 5.62.

Methyl 4-Deoxy-α-L-*threo*-pentopyranoside Di-*O*-benzoate **28b**: Colorless syrup. IR ($CHCl_3$): 1720. ^{1}H-NMR: 5.35—5.27 (2H, m, H-2,3), 4.55 (1H, d, J=5.8 Hz, H-1), 4.13 (1H, dt, J=12.4, 4.3 Hz), 3.64 (2H, ddd, J=12.4, 9.6, 2.8 Hz) (H-5), 3.50 (3H, s, OMe), 2.36—2.30, 1.98—1.89 (each 1H, m, H-4). MS: 325 (M^+−OMe, 0.7), 105 (100). HRMS: Calcd for $C_{19}H_{17}O_5$ (M^+−OMe): 325.1083. Found: 325.1073.

(2) The reaction was performed with the triflate **16** (166 mg) and LAH (110 mg, 5 mol eq) in THF (25 ml) for 11 h. The crude product was benzoylated and chromatographed. Separation of the $CHCl_3$–AcOEt (19 : 1) eluate by recycling preparative HPLC gave **37b** (22 mg, 11%), the 3-deoxy derivative **29b** (22 mg, 11%), the 4-deoxy derivative **28b** (2 mg, 1%), and **14b** (26 mg, 10%). The ratio of the products was determined by GC: relative retention times: **37b**, 1.00; **28b**, 0.82; **29b**, 1.15.

Methyl 3-Deoxy-α-L-*threo*-pentopyranoside Di-*O*-benzoate **29b**: Colorless syrup. IR: 1715. ^{1}H-NMR: 5.53—5.38 (1H, m, H-4), 5.27—5.25 (1H, m, H-2), 4.69 (1H, d, J=2.5 Hz, H-1), 3.94 (1H, dd, J=10.7, 4.9 Hz, H-5 eq), 3.84 (1H, dd, J=10.7, 9.7 Hz, H-5ax), 3.48 (3H, s, OMe), 2.35—2.32 (2H, m, H-3). MS: 325 (M^+−OMe, 2), 105 (100). HRMS: Calcd for $C_{19}H_{18}O_5$ (M^+−OMe): 325.1091. Found: 325.1083.

Reduction of Me β-D-Glc 3-*O*-Tosylate 9 The reaction was performed with **9** (400 mg) and LAH (306 mg, 5 mol eq) in THF (40 ml) for 6 h. The crude product was benzoylated and separated by recycling preparative HPLC to give the 3-deoxy derivative **30b** (229 mg, 41%), Me β-D-Glc tetra-*O*-benzoate **8b** (2 mg, 0.3%), and a mixture of the rearranged products, **38b** and **39b** (93 mg, 17%).

Methyl 3-Deoxy-β-D-*ribo*-hexopyranoside Tri-*O*-benzoate **30b**: Colorless needles from benzene–hexane, mp 117—120 °C. IR (KBr): 1713. ^{1}H-NMR: 5.29 (1H, dt, J=9.8, 5.1 Hz, H-4), 5.15 (1H, ddd, J=10.0, 7.0, 5.1 Hz, H-2), 5.13 (1H, d, J=7.0 Hz, H-1), 4.67 (1H, dd, J=11.6, 3.7 Hz), 4.49 (1H, dd, J=11.6, 5.1 Hz) (H-6), 4.16 (1H, ddd, J=8.9, 5.1, 3.7 Hz, H-5), 3.55 (3H, s, OMe), 2.84 (1H, dt, J=10.0, 5.1 Hz, H-3 eq), 2.01 (1H, td, J=12.8, 10.0 Hz, H-3ax). MS: 489 (M^+−1, 0.05), 459 (M^+−OMe, 0.8), 105 (100). *Anal.* Calcd for $C_{28}H_{26}O_8$: C, 68.56; H, 5.34. Found: C, 68.60; H, 5.32.

Methyl 3-Deoxy-3-*C*-(hydroxymethyl)-β-D-*xylo*-pentofuranoside Tri-*O*-benzoate **38b** and Methyl 2-Deoxy-2-*C*-(hydroxymethyl)-β-D-*arabino*-pentofuranoside Tri-*O*-benzoate **39b**: Although the products were not separated, examination of H–H and C–H COSY spectra allowed the following signal assignments for ^{1}H-NMR. The product ratio (14 : 3) was determined from the peak intensities. **38b**: 5.53 (1H, d, J=2.1 Hz, H-2), 5.13 (1H, s, H-1),4.89 (1H, dt, J=7.0, 5.2 Hz, H-4), 4.73, 4.67 (each 1H, m, CH_2O), 4.57 (2H, m, H-5), 3.43 (3H, s, OMe), 3.08 (1H, m, H-3). **39b**: 5.73 (1H, dd, J=8.7, 5.3 Hz, H-3), 5.16 (1H, d, J=4.9 Hz, H-1), 4.75—4.68 (4H, m, H-5 and CH_2O), 4.58—4.48 (1H, m, H-4), 3.37 (3H, s, OMe), 3.20—3.10 (1H, m, H-2). For ^{13}C-NMR data, see Table II.

Reduction of Methyl 4,6-*O*-Benzylidene-α-D-Glc 2-*O*-Tosylate 20 The reaction was performed with **20** (200 mg) and LAH (57 mg, 3 mol eq) in THF (20 ml) for 10 h. The crude product was chromatographed to give the 2-deoxy derivative **31** (19 mg, 15%) and **19** (44 mg, 69%).

Methyl 4,6-*O*-Benzylidene-2-deoxy-α-D-*arabino*-hexopyranoside **31**: Colorless needles from ether–hexane, mp 136—138 °C. ^{1}H-NMR: 7.6—7.2 (5H, m, ArH), 5.55 (1H, s, $ArCHO_2$), 4.78 (1H, br d, J=4.0 Hz, H-1), 3.33 (3H, s, OMe), 1.61—2.32 (2H, m, H-2). Deprotection of this with 30% AcOH (60 °C, 15 min) followed by acetylation gave methyl 2-deoxy-α-D-*arabino*-hexopyranoside tri-*O*-acetate **25a**, which was identical with an authentic sample.[6]

Reduction of Methyl 3,4-*O*-Isopropylidene-β-L-Ara 2-*O*-Tosylate 22 The reaction was performed with **22** (300 mg) and LAH (96 mg, 3 mol eq) in THF (20 ml) for 31 h. Chromatography of the crude product gave **21** (102 mg, 60%) and the starting material **22** (47 mg, 17%).

LBAH Reduction of Me α-D-Xyl 2-*O*-Tosylate 12 LBAH was prepared by mixing DIBAL (25% in hexane, 1.4 ml, 5.2 mol eq) and *n*-BuLi (1.3 M in hexane, 1.7 ml, 4.9 mol eq) in dry THF (15 ml) at 0 °C and stirring for 30 min. The mixture was cooled to −78 °C and stirred with **12** (150 mg) for 2 h, then refluxed for 3 h. After decomposition of the reagent with ice, the mixture was stirred with AcOEt and filtered. The residue was decomposed with dilute HCl, neutralized with $NaHCO_3$, concentrated to dryness, and extracted with EtOH as described in the reduction with LAH. The combined filtrate and extracts were concentrated and the residue was benzoylated. The product obtained on usual work-up was purified by preparative TLC to yield the di-*O*-benzoate **34b** (91 mg, 54%).

LBAH Reduction of Me β-D-Xyl 4-*O*-Tosylate 15 A mixture of **15** (300 mg) and LBAH (prepared from 2.7 ml of DIBAL and 3.4 ml of *n*-BuLi) in THF (20 ml) was stirred at 0 °C for 30 min, refluxed for 10 h, and worked up as above. The crude product was benzoylated and the product was purified by recycling preparative HPLC to yield the 3-deoxy derivative **29b** (175 mg, 53%).

Methyl 3,4-Anhydro-α-L-arabinopyranoside 44 Me β-D-Xyl 4-*O*-tosylate **15** (711 mg) in 27% aqueous NaOH (7 ml) and EtOH (7 ml) was stirred overnight at room temperature. The mixture was neutralized with dilute HCl and conentrated. Chromatography of the residue gave **44** (76 mg, 22%), Me 2,3-anhydro-α-L-lyxopyranoside **45** (54 mg, 16%), and a mixture of **44** and **45** (114 mg).

44: Colorless prisms from benzene–hexane, mp 64—68 °C. ^{1}H-NMR: 4.24, 3.93, (each 1H, d, J=13.4 Hz, H-5), 4.03 (1H, d, J=6.4 Hz, H-1), 3.70 (1H, dd, J=6.4, 3.7 Hz, changed into d of J=6.4 Hz, H-2), 3.48 (3H, s, OMe), 3.24, 3.17 (each 1H, d, J=3.7 Hz, H-3, 4). ^{13}C-NMR: 103.7 (C-1), 66.8 (C-2), 62.8 (C-5), 56.5 (OMe), 53.8, 49.7 (C-3, 4), HRMS: Calcd for $C_6H_{10}O_4$ (M^+): 146.0578. Found: 146.0566.

45: Colorless needles from $CHCl_3$–hexane, mp 97—102 °C. ^{1}H-NMR: 4.77 (1H, s, H-1), 3.99 (1H, br t, J=5—7 Hz, H-4), 3.63 (1H, dd, J=11.6, 4.9 Hz), 3.50 (1H, dd, J=11.6, 7.0 Hz) (H-5), 3.49 (3H, s, OMe), 3.30, 3.14 (each 1H, d, J=3.8 Hz, H-2, 3). ^{13}C-NMR: 96.5 (C-1), 62.6 (C-4), 60.9 (C-5), 56.1 (OMe), 53.9, 51.1 (C-2, 3). HRMS: Calcd for $C_6H_{10}O_4$ (M^+): 146.0578. Found: 146.0571.

LAH Reduction of 44 Compound **44** (10 mg) and LAH (6 mg) in THF (3 ml) were stirred for 2 h at room temperature and worked up as usual. The crude product was benzoylated and purified by chromatography to give Me 3-deoxy-α-L-*threo*-pentopyranoside di-*O*-benzoate **29b** (18 mg, 74%). The 4-deoxy derivative was not detected on TLC.

LBH Reduction of Me α-D-Xyl 2-*O*-Tosylate 12 Compound **12** (230 mg) and LBH (79 mg, 5 mol eq) in THF (30 ml) were heated under reflux for 40 h, and worked up as described in the reduction with LAH. Chromatography of the crude product gave unchanged **12** (72 mg, 31%) from the AcOEt eluate. The $CHCl_3$–MeOH (2 : 1) eluate was benzoylated and the product was purified by chromatography and recycling preparative HPLC to give **34b** (96 mg, 37%) and **11b** (17 mg, 5%).

Reaction of Me α-D-Glc 2-*O*-Tosylate 2 with $NaBH_4$ Compound **2** (200 mg) and $NaBH_4$ (289 mg, 13 mol eq) in EtOH (10 ml) were refluxed for 3.5 h. The mixture was made slightly acidic dilute HCl, neutralized with $NaHCO_3$, and concentrated to dryness. The residue was extracted

several times with hot EtOH. The combined extracts were concentrated and the residue was purified by chromatography to give Me 3-*O*-ethyl-α-D-altropyranoside **41** (97 mg, 72%) as a colorless syrup. ^{1}H-NMR: 5.05 (1H, d, J=2.4 Hz, H-1), 3.84, 3.67 (each 1H, dq, J=9.5, 7.2 Hz, $OC\underline{H}_2CH_3$), 3.42 (3H, s, OMe), 1.16 (3H, t, J=7.2 Hz, $OCH_2C\underline{H}_3$). This was identical with the compound obtained below.

Methyl 3-*O*-Ethyl-α-D-altropyranoside 41 Me 4,6-*O*-benzylidene-α-D-Glc 2-*O*-tosylate **20** (400 mg) was heated with 6% NaOEt–EtOH (20 ml) for 15 min to give Me 2,3-anhydro-4,6-*O*-benzylidene-α-D-Man **43** (242 mg, 95%) as colorless needles, mp 149.5—150.5 °C (lit. 147 °C).[13]

Compound **43** (114 mg) in 6% NaOEt–EtOH (5 ml) was heated under reflux for 19 h. Chromatography of the product gave Me 3-*O*-ethyl-4,6-*O*-benzylidene-α-D-Alt **42** (86 mg, 64%, syrup) and Me 4,6-*O*-benzylidene-α-D-Glc **19** (18 mg, 15%). **42**: ^{1}H-NMR: 5.77 (1H, s, $PhCHO_2$), 5.02 (1H, s, H-1), 3.35 (3H, s, OMe), 1.14 (3H, t, J=6.8 Hz, $OCH_2C\underline{H}_3$).

Compound **42** (25 mg) in 50% AcOH was heated at 100 °C for 1 h. Evaporation of the solvent *in vacuo* and chromatography of the residue gave **41** (15 mg, 82%), which was identical with the compound obtained above.

Acknowledgement A part of this work was financially supported by a Grant-in-Aid for Scientific Research from the Ministry of Education, Science and Culture of Japan.

References and Notes

1) Utilization of Sugars in Organic Synthesis. XXIII. Part XXII: Y. Tsuda, Y. Okuno, M. Iwaki, and K. Kanemitsu, *Chem. Pharm. Bull.*, **37**, 2673 (1989).
2) Present address: *Fuji Chemical Industry Ltd., 530 Chōkeiji, Takaoka-shi, Toyama 933, Japan.*
3) H. H. Bear, D. J. Astles, H. C. Chin, and L. Siemsen, *Canad. J. Chem.*, **63**, 432 (1985).
4) R. W. Binkley, *J. Org. Chem.*, **50**, 5646 (1985).
5) Our results on regioselective tosylation of carbohydrates in relation to acylation will be reported separately [*c.f.*, Y. Ysuda, M. E. Haque, and K. Yoshimoto, *Chem. Pharm. Bull.*, **31**, 1612 (1983)].
6) M. E. Haque, T. Kikuchi, K. Kanemitsu, and Y. Tsuda, *Chem. Pharm. Bull.*, **35**, 1016 (1987).
7) Abbreviations: Me = methyl, Alt = altropyranoside, Ara = arabinopyanoside, Glc = glucopyranoside, Man = mannopyranoside, Xyl = xylopyranoside.
8) *a*) G. Tsuchihashi, K. Tomooka, and K. Suzuki, *Tetrahedron Lett.*, **25**, 4253 (1984); *b*) K. Suzuki, K. Tomooka, M. Shimazaki, and G. Tsuchihashi, *ibid.*, **26**, 4781 (1985).
9) S. Kim and K. H. Ahn, *J. Org. Chem.*, **49**, 1717 (1984).
10) Tsuchiya *et al.* [T. Tsuchiya, F. Nakamura, and S. Umezawa, *Tetrahedron Lett.*, **30**, 2805 (1979)] reported a similar ring contraction of methyl 6-tosylamido-6-deoxy-α-D-glucopyranoside 2-*O*-triflate to methyl 5-animo-2,5-di-deoxy-2-*C*-(hydroxy-methyl)-α-D-*ribo*-pentofuranoside (45% yield) on reaction with sodium and liquid ammonia and proposed a radical mechanism (cleavage of the 3–4 bond and recombination of C-2 to C-4). However, we argue that the mechanism must be a stereospecific 1,2-shift with concomitant reduction, otherwise the product would be a mixture of stereoisomers. Reduction of Me α-D-Glc 2-*O*-tosylate **2** with Na-liquid NH_3 only removed the tosyl group, producing Me α-D-Glc **1** quantitatively.
11) Y. Tsuda, K. Isobe, T. Sano, and A. Morimoto, *Chem. Pharm. Bull.*, **23**, 98 (1975).
12) A. J. Dick and J. K. N. Jones, *Canad. J. Chem.*, **46**, 425 (1968).
13) N. K. Richtmyer, "Methods in Carbohydrate Chemistry," Vol. I, ed. by R. L. Whistler and M. L. Wolfrom, Academic Press, New York, 1962, p.107.

Research for New Antichagasic Drugs

Brenda MESTER,[a] Rosa M. CLARAMUNT*,[b] José ELGUERO,[c] Juan ATIENZA,[d] Alicia GOMEZ BARRIO[d] and Jose Antonio ESCARIO[d]

Química Farmaceútica, Facultad de Química, Universidad de la República,[a] Montevideo, Uruguay, Dpto. Química Orgánica, Facultad de Ciencias,[b] Uned, 28040-Madrid, Spain, Instituto de Química Médica,[e] Csic, 28006-Madrid, Spain and Dpto. de Parasitología, Facultad de Farmacia, Universidad Complutense,[d] 28040-Madrid, Spain. *Received January 7, 1991*

A series of ten 1-[(5-nitrothenylidene)amino]azoles has been synthesized by the reaction of 5-nitrothiophene-2-carbaldehyde with 1-aminopyrazole, 1-aminoimidazole, 1- and 4- amino-1,2,4-triazoles, 1-aminoindole, 1- and 2-aminoindazoles, 1-aminobenzimidazole and 1- and 2-aminobenzotriazoles. Physical data, spectroscopic characteristics and biological properties of all the derivatives have been examined. The antiprotozoal activity has been tested against *Trypanosoma cruzi*, comparative to Nifurtimox (Lampit).

Keywords 1-[(5-nitrothenylidene)amino]azole; synthesis; ^{1}H-NMR; ^{13}C-NMR; antitrypanosomal activity

Nifurtimox or tetrahydro-3-methyl-4[(5-nitrofurfuryl-idene)]-2*H*-thiazine-1,1-dioxide (nfx) is one of the most effective drugs used in the treatment of Chagas' disease (American trypanosomiasis). However its use is limited due to its mutagenicity, side effects and non curative action in certain cases. Besides, none of the few compounds which have reached the stage of clinical trial in Chagas' disease are considered to be safe, effective, convenient and inexpensive chemotherapeutic agents for extensive use in man, not even to prevent transmission during blood transfusion.[1)]

In these circumstances, the development of new compound alternatives to the currently used nfx is a research area of great interest due to the economic, social and political impact that the control of trypanosomiasis would have.

Chemistry Recently, we have synthesized and examined the antitrypanosomal activity of new derivatives structurally related to nfx **1**, where the thiazine 1,1-dioxide ring of this latter drug was replaced by a *N*-heterocyclic residue. The compounds in which the heterocyclic counterparts were 1,2,4-triazol-4-yl and pyridin-1-yl groups clearly showed superior *in vitro* activity against *T. cruzi*.[2)]

The present work was undertaken in order to examine in a further step what would be the effect on the biological activity when the furan ring of series **2** was replaced by a thiophene.

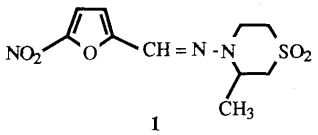

1

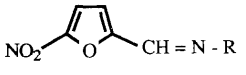

2

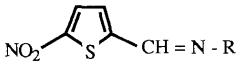

3

a : pyrazol-1-yl
b : imidazol-1-yl
c : 1, 2, 4-triazol-4-yl
d : 1, 2, 4-triazol-1-yl
e : indol-1-yl
f : indazol-1-yl
g : indazol-2-yl
h : benzimidazol-1-yl
i : benzotriazol-1-yl
j : benzotriazol-2-yl

Chart 1

According to the results shown in Table I, the title compounds **3** (**a** to **j**) were obtained from the *N*-aminoderivatives **4** by reaction with 5-nitrothiophene-2-carbaldehyde **5** in boiling toluene with catalytic amounts of *p*-toluene sulfonic acid, the yields ranging from 63 to 98%.

1-Aminopyrazole **4a**,[3)] 1-aminoimidazole **4b**,[4)] 1-amino-1,2,4-triazole **4d**,[5)] 1-aminoindole **4e**,[6)] 1-amino- **4f** and 2-aminoindazoles **4g**,[7)] 1-aminobenzimidazole **4h**,[5)] 1-amino- **4i** and 2-aminobenzotriazoles **4j**,[8)] were prepared according to the literature from the corresponding azoles with hydroxylamine-*O*-sulfonic acid. 5-Nitrothiophene-2-carbaldehyde **5** was synthesized by nitration of thiophene-2-carbaldehyde with fuming nitric acid and anhydrous acetic

TABLE I. Yields, Melting Points and Microanalytical Data

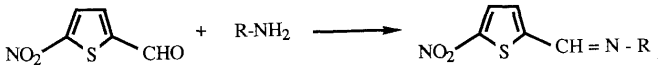

5 **4** **3**

Compd.	Yield (%)	mp (°C) (Solvent)	Formula (Mol. weight)	Calcd (Found) C	H	N
3a	87	172—174 (Acetone–water)	$C_8H_6N_4O_2S$ (222.2)	43.23 (43.28	2.72 2.94	25.22 24.96)
3b	80	149—150 (Chloroform–ethanol)	$C_8H_6N_4O_2S$ (222.2)	43.23 (43.41	2.72 2.65	25.22 25.54)
3c	98	204—206 (Toluene)	$C_7H_5N_5O_2S$ (223.2)	37.66 (37.54	2.26 2.04	31.38 31.62)
3d	85	210 (dec.) (Chloroform)	$C_7H_5N_5O_2S$ (223.2)	37.66 (37.84	2.26 2.85	31.38 31.10)
3e	90	191—193 (Ethyl acetate–hexane)	$C_{13}H_9N_3O_2S$ (271.3)	57.55 (57.64	3.34 3.37	15.49 15.67)
3f	63	251—252 (Chloroform)	$C_{12}H_8N_4O_2S$ (272.3)	52.93 (52.72	2.96 2.90	20.58 20.77)
3g	83	226—228 (Chloroform)	$C_{12}H_8N_4O_2S$ (272.3)	52.93 (53.01	2.96 3.05	20.58 20.35)
3h	81	225—227 (Ethanol–water)	$C_{12}H_8N_4O_2S$ (272.3)	52.93 (53.20	2.96 3.12	20.58 20.39)
3i	85	242—243 (Toluene)	$C_{11}H_7N_5O_2S$ (273.3)	48.34 (48.19	2.58 2.71	25.63 25.65)
3j	85	262—265 (Ethanol)	$C_{11}H_7N_5O_2S$ (273.3)	48.34 (48.53	2.58 2.46	25.63 25.52)

TABLE II. ^{1}H-NMR Data[a,b] (Chemical Shifts, δ, ppm Relative to Internal TMS) in Hexadeuteriodimethylsulphoxide

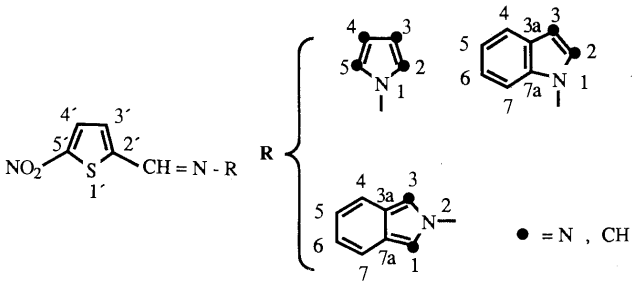

Compound	–CH=N–	H3′	H4′	H2	H3	H4	H5	H6	Hz
3a	9.38 (s)	7.80 (dd)	8.18 (d)	—	7.72 (dd)	6.53 (dd)	8.10 (dd)		
3b	9.18 (s)	7.63 (d)	8.18 (d)	8.17 (s)	—	7.93 (s)	7.12 (s)		
3c	9.30 (s)	7.70 (d)	8.17 (d)	—	9.11 (s)	—	9.11 (s)		
3d	9.40 (s)	7.87 (d)	8.15 (d)	—	8.18 (s)	—	8.90 (s)		
3e	9.08 (s)	7.52 (d)	8.14 (d)	8.16 (d)	6.82 (d)	7.60 (dd)	7.17 (m)	7.30 (m)	7.70 (dd)
3f	9.33 (s)	7.75 (d)	8.13 (d)	—	8.36 (d)	7.85 (dd)	7.31 (ddd)	7.58 (ddd)	7.81 (dd)
3g	9.78 (s)	7.94 (d)	8.20 (d)	—	8.67 (d)	7.75 (dd)	7.12 (ddd)	7.38 (ddd)	7.63 (dd)
3h	9.41 (s)	7.70 (d)	8.17 (d)	8.89 (s)	—	7.73 (dd)	7.33 (ddd)	7.41 (ddd)	7.83 (dd)
3i	9.86 (s)	7.96 (d)	8.23 (d)	—	—	8.15 (dd)	7.54 (ddd)	7.72 (ddd)	7.95 (dd)
3j	9.91 (s)	8.04 (d)	8.20 (d)	—	—	7.96 (m)	7.54 (m)	7.54 (m)	7.96 (m)

a) Apparent multiplicity is given in the table: s, singlet; d, doublet; m, multiplet. *b*) δ values for 5-nitrothiophene-2-carbaldehyde are: CHO, 10.20 (s); H3′, 8.20 (d); H4′, 8.80 (d).

TABLE III. ^{13}C-NMR Data[a] (Chemical Shifts, δ, in ppm Relative to Internal TMS) in Hexadeuteriodimethylsulphoxide

Compound	C2′	C3′	H4′	H5′	–CH=	C2	C3	C4	C5	C6	C7	C3a	C7a
3a	143.9	132.7	130.4	152.2	143.5	—	139.1	107.6	130.0	—			
3b	143.8	132.1	130.3	152.2	146.5	136.5	—	129.1	112.8	—			
3c	142.4	133.3	130.2	153.0	151.3	—	139.1	—	139.1	—			
3d	142.1	133.2	129.5	152.8	147.1	—	149.8	—	142.6	—			
3e	146.4	129.5	130.6	150.8	139.0	119.1	105.9	121.1	121.7	123.7	110.3	126.8	135.7
3f	144.8	130.6	129.9	151.2	139.2	—	134.8	122.6	121.3	128.2	109.7	123.4	137.4
3g	142.9	134.3	130.3	152.8	148.3	—	123.9	121.2	122.4	128.2	117.0	121.4	146.2
3h	144.4	131.6	130.3	152.0	145.6	137.7	—	120.1	123.3	124.2	110.9	141.7	131.4
3i	142.8	133.5	129.9	153.0	146.8	—	—	119.6	125.2	129.2	110.2	144.6	130.0
3j	141.4	135.5	129.9	154.1	152.5	—	—	118.0	128.2	128.2	118.0	142.9	142.9

See Table II for structural formula numbering. *a*) δ values for 5-nitrothiophene-2-carbaldehyde are: C2′, 146.6; C3′, 135.6; C4, 130.0; C5′, 156.0; CHO, 185.8.

anhydride.[9]

Structures of compounds **3a**—**j** were confirmed by proton and carbon-13 nuclear magnetic resonance (^{1}H- and ^{3}C-NMR) spectroscopy (Tables II and III). Assignments of all the signals to the different protons and carbon atoms were achieved on the basis of previous data existing in the literature[2,10] and two dimensional NMR (2D-NMR) techniques [highest occupied molecular orbital (HOMO) (^{1}H–^{1}H) and heteronuclear (^{1}H–^{13}C) correlated experiments][11] for **3e**, **3f**, **3g**, and **3h**. A detailed analysis of the molecular structures of **1**, **2a** and **3a**, in solution by ^{1}H- and ^{13}C-NMR, and in solid state by X-ray crystallography, has been recently published by us.[12]

Chemical shift and coupling constant values (H3′/H4′ 4.0; C3′/H3 177.0; C3′/H4′ 2.5; C4′/H4′ 179.5; C4′/H3′ 4.3 Hz) for the thiophene counterpart were in accordance with the literature data.[13]

The main features observed in the NMR spectra of the azole groups in derivatives **3** are similar to the ones encountered for the furan analogues **2**.[2,10a] Attention must be paid to the fact that an error slipped by in reference 10*a* concerning C3 of the furan ring and C2 of the indole group in 1-[(5-nitrofurfurylidene)amino]indole. ^{13}C-NMR data were reversed, C3 appearing at 114.8 ppm, with *J* values of 184.1 and 7.6 Hz.

Biological Results To determine the activity of compounds (**3a**—**j**) against the Y strain[14] of *Trypanosoma* (*S.*) *cruzi*, three types of tests were carried out: i) *In vitro* tests, directed to determine the trypanocidal activity on *T. cruzi* cultures.[15] ii) *In vivo* tests, to know the possible chemotherapic action of the new synthesis compounds.[16] iii) Mixed tests, based on the previous study of the compounds activity on infected stored blood and posterior inoculation of this blood to recipient animals.[17]

Nifurtimox was used as the reference drug in all of the experiments.

In vitro activity was assayed on epimastigote culture during their exponential growth in liver infusion tryptose (LIT) medium supplemented with 10% fetal calf serum (FCS) (Chart 2). NUNCLON plaques were filled with 2.5 ml/well of an initial culture. Three wells were used for every dose assayed. Compounds were dissolved in phosphate-buffered saline (PBS) containing 0.2% dimethylsulfoxide (DMSO). At this concentration no adverse

effects attributable to the DMSO were noted.

After 6 d of incubation at 28°C, doubled counts with Neubauer chambers were made. The percentage of growth inhibition was calculated as follows:

$$\% \text{ growth inhibition} = \left(1 - \frac{\text{growth of experimental culture}}{\text{growth of control culture}}\right) \times 100$$

In vivo activity was determined (Chart 3) by treatment of infected mice and subsequent determination of parasitaemia and mortality rates in animals. NMRI mice were infected by intraperitoneally (i.p.) injection with 100000 trypanosomes (tryp) obtained from donor animals. Compounds were dissolved in PBS containing 16% ethyleneglycol and administered at 50 mg/kg body weight/d during 3 to 7 postinfection days by i.p. injection.

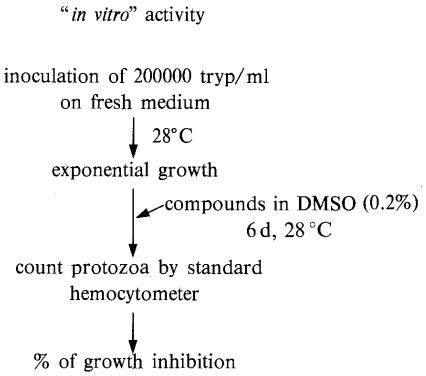

Chart 2

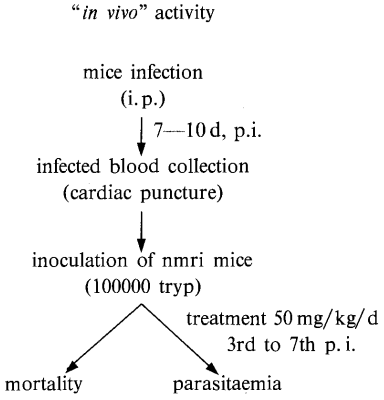

Chart 3

Chemoprophylactic activity of the compounds was studied using infected blood obtained from donor mice and stored in the same conditions as in blood banks (Chart 4). Compounds were dissolved as above and were added at 1 mg/ml to tubes containing infected blood with 250000 trypomastigotes/ml. Tubes were incubated at 4 °C on a shaker placed into a dark room. After incubation times, groups of mice were inoculated (i.p. injection) with 0.5 ml of the stored blood. Parasitaemia and mortality rates were followed in the animals.

As shown in Fig. 1 for *in vitro* activity a complete growth inhibition was obtained at 10 μg/ml with nfx, and compounds named **3b**, **3c** and **3e**. At this concentration level, **3d** and **3h** derivatives were able to only partially inhibit the growth.

In vivo treatment with the reference drug nfx produced a delay in the parasitaemia and reduced the parasitaemia levels. Survival of these animals with nfx (Table IV) was higher than the one obtained in animals treated with the new compounds. All of the new compounds **3** assayed showed parasitaemia curves similar to the control ones.

The treatment of infected stored blood with products named **3c**, **3i** and nfx delayed the beginning of parasitaemia in recipient animals. However, none of the compounds produced a significative reduction in the parasitaemia peaks and only some of them (Table V) prolonged the

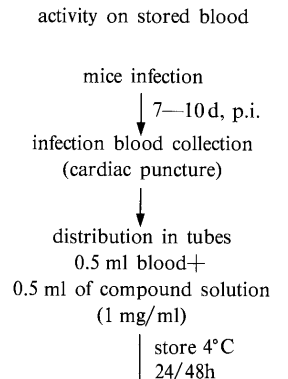

Chart 4

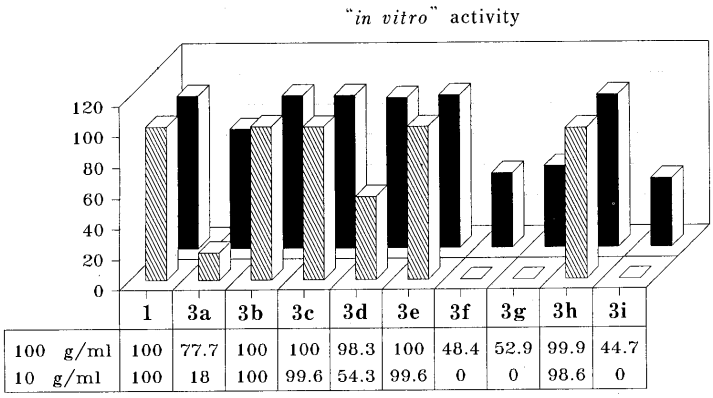

	1	3a	3b	3c	3d	3e	3f	3g	3h	3i
100 g/ml	100	77.7	100	100	98.3	100	48.4	52.9	99.9	44.7
10 g/ml	100	18	100	99.6	54.3	99.6	0	0	98.6	0

Fig. 1. % Growth Inhibition
▨, 10 g/ml; ■, 100 g/ml.

TABLE IV. *In Vivo* Tests. Survival Index (Day 30 Postinfection)

Compound	Survival index[a]
3b	0
3c	0.6
3d	1
3e	0.2
3f	0.8
3g	0.2
3h	1
3i	0.6
1 (nfx)	1.2

a) Survival of treated animals/survival of control animals.

TABLE V. Experiments on Stored Blood. Survival Index (Day 30 Postinfection)

Compound	Survival index[a]
3a	1
3b	1.5
3c	3
3d	1
3e	1.5
3f	2
3g	2.5
3h	1
3i	0.8
1 (nfx)	1.2

a) Survival of animals inoculated with treated blood/survival of animals inoculated with untreated blood.

survival of the animals.

Conclusion

From our results we can conclude that in the *in vitro* tests all the 1-[(5-nitrothenylidene)amino]azoles **3** show trypanocidal activity similar to Nifurtimox, the less active ones being indazole and benzotriazole derivatives. However the *in vivo* assays indicate that they were not able to completely erradicate the infection in treated mice. Furthermore, they did not present good chemoprophylactic activity as neither nfx **1** nor the new compounds **3** could completely kill the surviving trypanosomes in stored blood.

Experimental

Chemistry Melting points were determined on a capillary Büchi 512 apparatus and are uncorrected. The NMR spectra were taken with a Bruker AC 200, working at 200.13 MHz for ^1H and 50.32 MHz for ^{13}C. ^1H and ^{13}C chemical shifts (δ) are given from internal tetramethylsilane with an accuracy of ± 0.01 and ± 0.1 ppm, respectively. Coupling constants (J) were measured with digital resolutions of 0.2 and 0.6 Hz. The 2D-experiments were run according to the following data acquisition parameters: (i) for the 2D (^1H–^1H) COSY, F1 domain (SI1: 1K; SW1; 853 Hz) F2 domain (SI2; 2K; SW2; 1706 Hz), D1 : 1s RD: Os; PW : Os; NS (number of transients per FID): 16; DS (number of preparatory dummy transients per FID): 2. (ii) for the 2D (^1H–^{13}C) COSY, F1 domain (SI1; 256W; SW1 : 822 Hz), F2 domain (SI2 : 2K; SW2 : 10000 Hz), D1 : 1s, RD : 0s; NS : 160; DS : 0. All the 2D experiments were processed with a sine bell window.[11] Analyses were carried out using in-house facilities. Chromatographic purifications were performed through columns at normal pressure using silica gel Merck 60 (70—230 mesh). Thiophene-2-carbaldehyde, azoles, hydroxylamine-*O*-sulfonic acid and 4-amino-1,2,4-triazole were purchased from Aldrich.

Condensation of *N*-Aminoazoles (4) with 5-Nitrothiophene-2-carbaldehyde (5) Equimolar amounts (0.005 mol) of the *N*-amino compounds **4** and **5** in 40—50 ml of toluene were heated under reflux with *p*-toluene sulfonic acid. After 5—10 h the solvent was evaporated off and the crude products were purified by crystallization in derivatives **3a**, **3c**, **3i** and **3j** (Table I). In the other imino compounds, purification was achieved by column chromatography with the appropriate eluent: **3b** (chloroform–ethanol, 9 : 1), **3d** (chloroform), **3e** (ethyl acetate–hexane, 1 : 3), **3f** (chloroform), **3g** (chloroform), and **3h** (chloroform–ethanol, 95 : 5).

References

1) *a*) J. J. Marr and R. Docampo, *Rev. Infect. Dis.*, **8**, 884 (1986); *b*) G. B. Henderson and A. H. Fairlamb, *Parasitology Today*, **3**, 312 (1987); *c*) P. S. Doyle and E. C. Weinbach, *Exp. Parasitol*, **68**, 320 (1989); *d*) A. M. Celentano and S. M. González Cappa, *Medicina* (Buenos Aires), **48**, 265 (1988).
2) B. Mester, J. Elguero, R. M. Claramunt, S. Castanys, M. L. Mascaró, A. Osuna, M. J. Vilaplana and P. Molina, *Arch. Pharm.* (Weinheim), **320**, 115 (1987).
3) H. Neuhoeffer, M. Clausen, H. D. Vofter, H. Ohl, C. Kruger and K. Angermund, *Justus Liebigs Ann. Chem.*, **1985**, 1732.
4) M. C. Foces-Foces, F. H. Cano, R. M. Claramunt, D. Sanz, J. Catalán, F. Fabero, A. Fruchier and J. Elguero, *J. Chem. Soc., Perkin Trans. 2*, **1990**, 237.
5) J. Mendoza, M. L. Castellanos, J. P. Fayet, M. C. Vertut and J. Elguero, *J. Chem. Res. (M)*, **1980**, 514.
6) M. Somei and M. Natsume, *Tetrahedron Lett.*, **5**, 461 (1974).
7) B. M. Adgar, S. Bradbury, M. Keating, C. W. Rees and R. C. Storr, *J. Chem. Soc., Perkin Trans. 1*, **1975**, 31.
8) C. D. Campbell and C. W. Rees, *J. Chem. Soc. (C)*, **1969**, 742.
9) P. Fournari and J. P. Chane, *Bull. Soc. Chim. Fr.*, **1963**, 479.
10) *a*) B. Mester, R. M. Claramunt and J. Elguero, *Magn. Reson. Chem.*, **25**, 260 (1987); *b*) M. Begtrup, J. Elguero, R. Faure, P. Camps, C. Estopá, D. Ilavsky, A. Fruchier, C. Marzin and J. de Mendoza, *ibid.*, **26**, 134 (1988).
11) W. R. Croasmun and R. M. K. Carlson (eds.), "Two-Dimensional NMR Spectroscopy," VCH Publishers, Inc., New York, 1987.
12) M. C. Foces-Foces, F. H. Cano, R. M. Claramunt, A. Fruchier and J. Elguero, *Bull. Soc. Chim. Belg.*, **97**, 1055 (1988).
13) A. R. Katritzky and C. W. Rees, (eds.), "Comprehensive Heterocyclic Chemistry," Vol. 4, Pergamon Press, New York, 1984.
14) H. P. Silva and V. Nussensweig, *Golha Clin. Biol.*, **20**, 191 (1953).
15) M. Wittner, L. Squilante, J. P. Nadler and H. B. Tanowitz, *Exp. Parasitol*, **53**, 255 (1982).
16) J. A. Escario, A. Gómez Barrio, J. Atienza, M. C. De Diego and F. M. Belda Neto, *Mem. Inst. Oswaldo Cruz, Suppl.*, **82**, 174 (1987).
17) J. Atienza, F. M. Belda Neto, J. A. Escario, A. Gómez Barrio, M. C. Averndaño, M. C. De Diego and A. R. Martínez Fernández, Proceeding of the 3rd International Congress on Pharmaceutical Sciences, Barcelona, 1987, p. 455.

Synthesis and Biological Activities of Analogs of a Lipid A Biosynthetic Precursor: 1-*O*-Phosphonooxyethyl-4′-*O*-phosphono-disaccharides with (*R*)-3-Hydroxytetradecanoyl or Tetradecanoyl Groups at Positions 2, 3, 2′ and 3′

Tsuneo KUSAMA,*[,a] Tsunehiko SOGA,[a] Yoshiyuki ONO,[a] Eiji KUMAZAWA,[a] Emiko SHIOYA,[a] Yasuaki OSADA,[a] Shoichi KUSUMOTO[b] and Tetsuo SHIBA[c]

Research Institute, Daiichi Pharmaceutical Co., Ltd.,[a] 16–13, Kitakasai 1-chome, Edogawa-ku, Tokyo 134, Japan, Department of Chemistry, Faculty of Science, Osaka University,[b] 1–1, Machikaneyama-cho, Toyonaka, Osaka 560, Japan, and Peptide Institute, Protein Research Foundation,[c] 1–2, Ina 4-chome, Minoh-shi, Osaka 562, Japan. *Received January 17, 1991*

Two novel analogs of a biosynthetic precursor of lipid A (2) were synthesized. The one analog (3) has acyl groups identical to those of 2, and the other (4) has tetradecanoyl groups in place of the (*R*)-3-hydroxytetradecanoyl groups of 2. Both 3 and 4 possess an α-glycosidically-bound phosphonooxyethyl group in place of the α-glycosyl phosphate group of 2.

Compounds 3 and 4 exhibited definite antitumor activity against Meth A fibrosarcoma and low toxicity in rabbits, as the original compound 2 does. The replacement of the hydroxytetradecanoyl groups with tetradecanoyl groups barely affected the antitumor activity, but slightly enhanced the toxicity in rabbits.

Keywords lipid A analog; phosphate group; phosphonooxyethyl group; antitumor activity; toxicity; Meth A fibrosarcoma; tetradecanoic acid; (*R*)-3-hydroxytetradecanoic acid

Lipid A, which is the lipophilic component of bacterial lipopolysaccharide (LPS), is now known to be responsible for the various biological activities of LPS, both beneficial and toxic. Shiba and his colleagues deduced the complete chemical structure for *Escherichia coli* (*E. coli*) lipid A (**1**)[1] and unequivocally confirmed it by total synthesis.[2] They also synthesized a biosynthetic precursor (**2**)[3] which is characterized by the presence of four fatty acyl groups each with a free hydroxyl, in contrast to lipid A (**1**), which contains only two corresponding groups at positions 2 and 3 and two acyloxyacyl groups at positions 2′ and 3′ of the 1,4′-bisphosphorylated disaccharide backbone.

Biological study with pure synthetic compounds clearly demonstrated that precursor **2** is less endotoxic than the complete lipid A (**1**). Compound **2**, in spite of its low toxicity, exhibits a definite ability to induce activity of interferon-α, β and tumor necrosis activity in adequately primed mice, though in each case the potency is slightly weaker than **1**.[4] This finding suggested that compound **2**, possessing no 3-acyloxyacyl group, could serve as a "key compound" which may lead to the development of new compounds with low toxicity but which retain the beneficial bioactivities.

On the other hand, we recently reported that, with respect to antitumor activity, the 1-*O*-phosphono group of lipid A is not essential, but replaceable by other acidic groups such as a phosphonooxyethyl group.[5] 1-α-*O*-Phosphonooxyethyl derivatives could be more readily synthesized than the corresponding α-phosphate because of the chemical stability of the former. However, the phosphonooxyethyl derivatives of **1** were unfortunately toxic, though they showed high antitumor activity comparable to that of **1**. Therefore, it seemed interesting to test the α-phosphonooxyethyl derivatives which have all four linear fatty acyl groups without the branched 3-acyloxyacyl moieties on the disaccharide backbone.

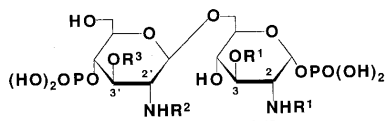

1 : $R^1 = CH_3(CH_2)_{10}CH(OCO(CH_2)_{10}CH_3)CH_2CO$
$R^2 = CH_3(CH_2)_{10}CH(OCO(CH_2)_{12}CH_3)CH_2CO$
$R^3 = CH_3(CH_2)_{10}CH(OH)CH_2CO$

2 : $R^1 = R^2 = R^3 = CH_3(CH_2)_{10}CH(OH)CH_2CO$

Fig. 1

In this paper we describe the synthesis as well as the toxic and antitumor activity of two analogs of **2** having either four 3-hydroxytetradecanoyl (**3**) or four tetradecanoyl groups (**4**), respectively, at positions 2, 3, 2′ and 3′ on the β(1→6)glucosamine disaccharide with 1-α-*O*-phosphonooxyethyl and 4′-*O*-phosphono groups.

Chemistry The basic strategy for the synthesis of **3** and **4** was similar to that employed in our previous synthesis of the 1-*O*-phosphonooxyethylated derivatives of lipid A.[5] In this strategy, glycosyl bromides, as an important key intermediate for the formation of disaccharides, were prepared by treatment of the corresponding glycosyl acetate with HBr–AcOH. The glycosyl bromide required for the synthesis of compound **3** contains a 3-hydroxytetradecanoyl group. By protection of this hydroxyacyl function with an acid-stable 2,2,2-trichloroethoxycarbonyl (Troc) group, the bromide was successfully obtained and used in the following glycosidation reaction. In an earlier work, where the benzyl group was employed for the protection of the hydroxyacyl function, the corresponding bromide was prepared using a Vilsmeier reagent.[6] This latter method was so moisture sensitive that the result was sometimes not satisfactory. The hydroxytetradecanoyl functions bound to the reducing glucosamine were protected with a benzyl group as in the previous works.[2,5]

The protected fatty acid **8** with a Troc group was prepared from (*R*)-3-hydroxytetradecanoic acid (**5**), as shown in Chart 1. Reaction of (*R*)-3-hydroxytetradecanoic acid (**5**) with benzyl bromide in the presence of triethylamine (Et_3N) gave the benzyl ester **6**. Treatment of **6** with Troc–Cl in pyridine afforded a 3-*O*-Troc derivative **7**,

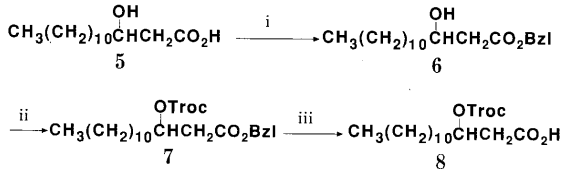

Bzl : $C_6H_5CH_2$ Troc : CCl_3CH_2OCO

i) BzlBr/Et_3N ii) Troc-Cl, Py iii) H_2, Pd/C

Chart 1

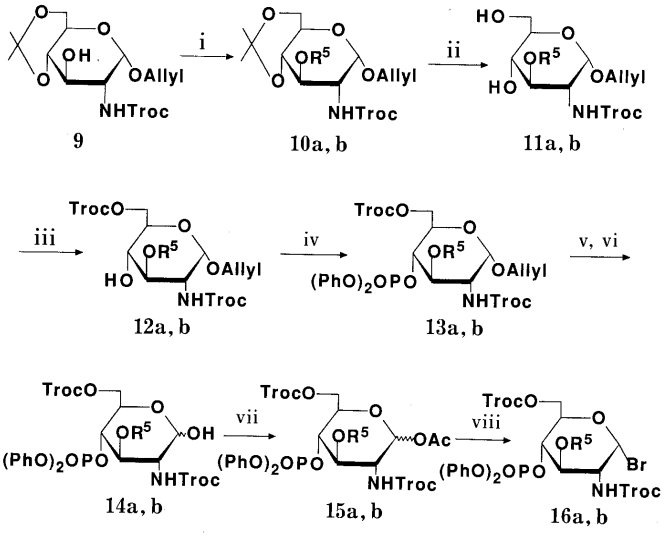

Troc : CCl_3CH_2OCO Allyl : $CH_2=CHCH_2$

a : R^5=(*R*)-3-(2, 2, 2-trichloroethoxycarbonyloxy) tetradecanoyl

b : R^5=tetradecanoyl

i) R^5OH, DMAP, DCC ii) 90% AcOH iii) Troc-Cl, Py iv) $(PhO)_2POCl$, DMAP v) (COD) Ir $[PCH_3(C_6H_5)_2]_2^+PF_6^-$ vi) I_2-H_2O vii) Ac_2O, Py viii) HBr/AcOH

Chart 2

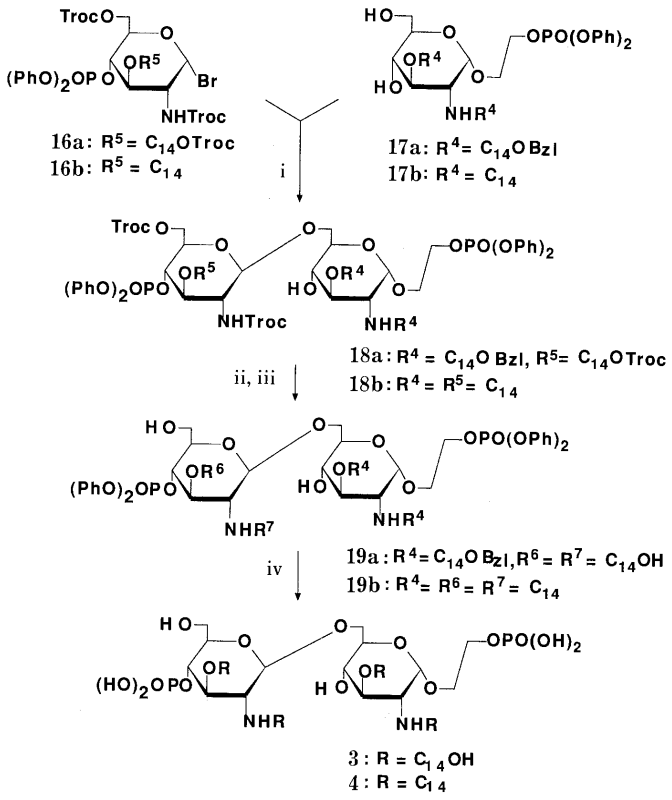

Troc : CCl_3CH_2OCO

C_{14}OTroc : (*R*)-3-(2, 2, 2-trichloroethoxycarbonyloxy)tetradecanoyl

C_{14}OBzl : (*R*)-3-benzyloxytetradecanoyl

C_{14}OH : (*R*)-3-hydroxytetradecanoyl

C_{14} : tetradecanoyl

i) $Hg(CN)_2$ ii) Zn/AcOH iii) C_{14}OH-OBt or C_{14}-OBt iv) H_2

Chart 3

which was subjected to hydrogenolysis over palladium carbon in tetrahydrofuran (THF) to give the desired (*R*)-3-trichloroethoxycarbonyloxytetradecanoic acid (**8**). The optical purity of **8** was confirmed in the following manner. Treatment of **8** with *S*-(−)-1-phenylethylamine in the presence of dicyclohexylcarbodiimide (DCC) gave a single spot (*Rf*, 0.35) on thin layer chromatography (TLC) (benzene–EtOAc, 10 : 1), whereas, treatment of **8** with (±)-1-phenylethylamine under the same reaction conditions gave a mixture of two diastereomers (*Rf*, 0.35 and 0.39). The *Rf* value of 0.39 should correspond to (*R*)-fatty acid-(*R*)-(+)-1-phenylethylamide, which is an enantiomer of (*S*)-fatty acid-(*S*)-(−)-1-phenylethylamide, a possible contamination in the former product. Therefore, a racemization of the (*R*)-fatty acid **8** obtained above can be detected within the sensitivity of TLC.

The glycosyl donors **16a** and **16b** were synthesized from **9** by the method of Imoto *et al.*[2] as shown in Chart 2.

After 3-*O*-acylation of **9** with (*R*)-3-trichloroethoxycarbonyloxytetradecanoic acid (**8**) or tetradecanoic acid by the 1-hydroxybenzotriazole (HOBt) active ester method, removal of the isopropylidene group gave **11a** and **11b**. Selective *O*-trichloroethoxycarbonylation at the 6-position followed by phosphorylation with diphenyl phosphorochloridate and dimethylaminopyridine (DMAP) at position 4 gave **13a** and **13b**. The allyl group in **13a** and **13b** was cleaved off with an iridium complex, followed by reaction with iodine–H_2O. After acetylation of the C-1 hydroxyl group with acetic anhydride, the resulting glycosyl acetates **15a** and **15b** were brominated with 25% HBr–AcOH.

Coupling reactions of bromides **16a** and **16b** with acceptors **17a** and **17b**, respectively, were carried out in the presence of mercuric cyanide to give the corresponding disaccharides **18a** and **18b**, as shown in Chart 3. Cleavage of two Troc groups of **18a** and **18b** was effected with zinc dust in AcOH. The resultant free amino group was acylated with an active ester of (*R*)-3-hydroxy fatty acid without a protecting group or tetradecanoic acid, respectively, to give the fully acylated compounds **19a** and **19b**. Compound **19a** was hydrogenolyzed, first over a palladium catalyst to remove benzyl protection and then over a platinum catalyst to cleave phenyl protection, to give the title compound **3**. Compound **19b** was hydrogenolyzed in the presence of platinum dioxide to give compound **4**.

Antitumor Activity Antitumor activity of the synthetic compounds was tested in BLAB/c mice as described earlier.[5] A group of 8 mice were inoculated intradermally with Meth A syngenic fibrosarcoma cells (2×10^5). The Et_3N salt of each compound was dissolved in a 5% aqueous glucose solution containing 0.1% Et_3N. The resulting solution was then administered to the mice at doses of 100 μg/mouse through the vein on the 7th, 12th and 17th days after implantation. The percentage antitumor effect on

the growth of Meth A was determined on the 21st day by dividing the average tumor weight of the tested group by the average tumor weight of the control group and multiplying the quotient by 100. Table I shows the results.

Toxicity The Et_3N salt of each compound was dissolved in 5% glucose containing 0.1% Et_3N to prepare a 100 μg/ml solution. The solution was administered to 3 NZW rabbits per group at a dose of 50 μg/kg-body weight (b.w.) through the ear vein for 3 consecutive days. Toxicity was evaluated by the number of dead test animals 24 h after the final administration. For comparison, synthetic *E. coli*-type lipid A (**1**) was administered at a level of 5 μg/kg-b.w. The results obtained are shown in Table II.

Discussion

Compounds **3** and **4** with the 1-α-phosphonooxyethyl group in place of a phosphono group exhibited definite high antitumor activity. The activities of these compounds were comparable to the activity of the corresponding original precursor type lipid A (**2**), but slightly less than that of synthetic *E. coli*-type lipid A (**1**). Compound **4**, with four tetradecanoyl groups, showed slightly higher activity than compound **3** with four (*R*)-3-hydroxytetradecanoyl groups.

Concerning toxicity in rabbits, compounds **3** and **4** were weakly toxic as was precursor-type lipid A (**2**), no rabbit being dead with a 50 μg/kg dose. Particularly, it has to be emphasized that compound **3** exhibited no detectable toxicity with that dose in spite of its significant antitumor activity. In the case of *E. coli*-type lipid A (**1**), all four rabbits died with only a single administration of a 5 μg/kg dose within 24 h, manifesting symptoms of endotoxin shock.

In view of the biological activities of compound **3** possessing the same acyl groups as that of compound **2**, the substitution of a glycosidic phosphate group with α-phosphonooxyethyl group appeared likely to yield slightly higher antitumor activity, but similar or slightly less toxicity than that of the original precursor compound **2**. On the other hand, the presence or absence of a hydroxyl group of hydroxytetradecanoic acid residue on the disaccharide back bone (**3** or **4**) exhibits little effect on the antitumor activity, although it influenced the toxicity in rabbits slightly more than the antitumor activity. It is possible that the influence on activity was caused by the capacity for hydrogen bond formation and enlargement of polarity, both by the hydroxyl in the fatty acid residue. In accordance with a previous work,[7] these results indicate that the toxicity of lipid A analogs in rabbits is affected by a slight variation of the component fatty acyl groups. In conclusion, the present study demonstrated that synthesis of lipid A analogs which contain four linear fatty acyl residues on the disaccharide back bone and have a polar moiety such as an α-*O*-phosphonooxyethyl group at the glycosidic position in place of the phosphate can be expected to give promising results in the search for low-toxicity compounds retaining significant antitumor activity.

TABLE I. Antitumor Activity of Lipid A, Its Precursor and Their Analogs Against Meth A Fibrosarcoma[a]

Compound number	Dose (μg/mouse)	T/C (%)[b]	Cured mice[c]/ treated mice
3	100 × 3	32[d]	1/8
4	100 × 3	24[d]	3/8
1	100 × 3	10[e]	1/8
Control		100	0/8
2	100 × 3	41[e]	0/8
1	100 × 3	18[e]	1/8
Control		100	0/8

a) Antitumor tests were conducted twice using compound **1** as a positive control. *b*) (Mean tumor weight in tested group/that in control group) × 100. Results given are at 21 d after tumor inoculation. *c*) Number of tumor-free mice/number of mice tested. *d*) $p<0.01$, *e*) $p<0.001$ *vs.* control (Student's *t*-test).

Experimental

All melting points are uncorrected. Proton nuclear magnetic resonance (^{1}H-NMR) spectra were measured on a Varian XL-200 spectrometer (200 MHz) in chloroform-*d* solutions unless otherwise noted. Tetramethylsilane (TMS) was used as the internal standard. Optical rotations were measured with a Horiba SEDA 200 polarimeter at 25 °C. Mass spectra (MS) were obtained on a JMS-HX 110 or JMX-300 instrument. Precoated Silica gel 150A PLK5F plates (1.0 mm thickness; Whatman) were used for preparative TLC. Organic solutions were dried over sodium sulfate.

Benzyl (*R*)-3-Hydroxytetradecanoate (6) Benzyl bromide (4.20 g, 24.5 mmol) and Et_3N (3.44 ml, 24.5 mmol) were added to a suspension of

TABLE II. Toxicity of Precursor Lipid A Analogs in Rabbits

Observations	Compound				
	3 (Dose 50	**4** 50	**1** 1	5	**2** 50 μg/kg)
Mortality[a]	0/3	0/3	0/5	4/4	0/4
Clinical signs[b]	NO	PT, AD, LY, HE	AD, HE	AD, HE, LY	NO
Decrease in body weight (g)[c]	NO	300—400	0—180	NE	0—160
Decrease in platelets (%)[d]	NO	52	56	NE	33
Hematological examination[e]	NO	GOT↑, GPT↑, UN↑, CRE↑	GOT↑, GPT↑, UN↑, CRE↑	NE	(NE)
Pathology[a]					
Thrombus	NO	3/3 (3+)	4/5 (2+—3+)	4/4 (+—2+)	NO
Liver change[f]	NO	3/3 (2+—3+)	4/5 (+)	4/4 (+)	NO
Kidney change[g]	NO	NO	4/5 (+—3+)	NO	NO
Heart change[h]	NO	3/3 (+—3+)	4/5 (+—3+)	NO	NO

a) Mortality and pathology: Number of rabbits changed/number of rabbits tested. *b*) PT: ptosis. AD: decrease in locomotor activity. HE: hyperemia of eye. LY: lying on side. *c*) 24 h after final injection. *d*) 24 h after first injection. *e*) GOT: glutamate oxaloacetate transaminase. GPT: glutamate pyruvate transaminase. UN: urea nitrogen. CRE: creatinine. *f*) Liver change: degeneration and necrosis of liver cells. *g*) Kidney change: degeneration and necrosis of uriniferous tubular epithelia. *h*) Heart change: degeneration and necrosis of muscle fiber. NO: no change, NE: not examined for early death, (NE): not examined. +: slight. 2+: moderate. 3+: severe.

(*R*)-3-hydroxytetradecanoic acid (2.00 g, 8.18 mmol) in ethyl acetate (EtOAc) (20 ml). The mixture was stirred for 3 d at room temperature. Any insoluble matter was filtered off and the filtrate was concentrated. The residue was purified by silica gel column chromatography (benzene–EtOAc, 19 : 1) to give an oil. Hexane was added to the oil and the resulting precipitate was collected to give **6** as a white powder (1.68 g, 61%). mp 43—44 °C. $[\alpha]_D$ −13.6° (c=1.3, $CHCl_3$). IR (KBr): 3560, 1715, 1470, 1410 cm^{-1}. ^{1}H-NMR δ: 0.88 (3H, t, J=6 Hz, CH_3), 1.25 (s) and 1.7 (m) (total 20H), 2.50 (2H, m, CH_2CO_2), 4.00 (1H, m, CH–OH), 5.15 (2H, s, $CH_2C_6H_5$), 7.35 (5H, s, arom. H).

(*R*)-3-(2,2,2-Trichloroethoxycarbonyloxy)tetradecanoic Acid (8) A solution of Troc–Cl (1.32 ml, 9.56 mmol) in THF (2 ml) was added to a solution of **6** (1.60 g, 4.78 mmol) in 20 ml of pyridine with ice-cooling. The mixture was stirred for 1 h at room temperature, then methanol (4 ml) was added to the reaction mixture and stirred for 1 h. After evaporation of the solvent, the residue was diluted with benzene. The solution was washed with 1 M HCl and then with saturated aqueous NaCl, and dried. Evaporation of the solvent gave a pale yellow oil of crude **7**. Palladium carbon (5%, 0.2 g) was added to a solution of the above oily substance in THF (30 ml), and the mixture was stirred under a hydrogen atmosphere for 2 h. The catalyst was filtered off and the filtrate was concentrated. The resulting oily substance was purified by silica gel column chromatography (benzene–EtOAc, 9 : 1—1 : 1) to give **8** (1.43 g, 71%) as a pale yellow oil. $[\alpha]_D$ 2.7° (c=1.2, $CHCl_3$). ^{1}H-NMR δ: 0.88 (3H, t, J=6 Hz, CH_3), 1.25 (s) and 1.7 (m) (total 20H), 2.72 (2H, m, CH_2CO_2), 4.80 (2H, s, CH_2CCl_3), 5.18 (1H, m, CHOTroc). MS m/z: 418 (M^+).

Allyl 2-Deoxy-4,6-*O*-isopropylidene-2-(2,2,2-trichloroethoxycarbonylamino)-3-*O*-[(*R*)-3-(2,2,2-trichloroethoxycarbonyloxy)tetradecanoyl]-α-D-glucopyranoside (10a) DMAP (67 mg, 0.55 mmol) and DCC (0.68 g, 3.31 mmol) were added to a solution of **8** (1.27 g, 3.04 mmol) and **9** (1.20 g, 2.76 mmol) in CH_2Cl_2 (20 ml) with ice-cooling, and the mixture was stirred for 1 h at room temperature. The precipitate was filtered off, and the filtrate was concentrated by evaporation. The residue was purified by silica gel column chromatography (benzene–EtOAc, 19 : 1) to give **10a** (1.74 g, 75%) as a colorless oil. $[\alpha]_D$ +31.2° (c=1.1, $CHCl_3$). ^{1}H-NMR δ: 0.88 (3H, t, J=6 Hz, CH_3), 1.26 (18H, s, CH_2), 1.39 and 1.49 (each 3H, s, CCH_3), 1.7 (2H, br, CH_2), 2.59 (1H, dd, J=16, 6 Hz, CH_2CO_2), 2.81 (1H, dd, J=16, 8 Hz, CH_2CO_2), 4.22 (1H, m), 4.76 (2H, s, CH_2CCl_3), 4.73 and 4.93 (each 1H, AB type d, J=12 Hz, CH_2CCl_3), 4.92 (1H, d, J=4 Hz, H-1), 5.9 (1H, m, $\underline{CH}=CH_2$). MS m/z: 833 (M^+).

Allyl 2-Deoxy-4,6-*O*-isopropylidene-3-*O*-tetradecanoyl-2-(2,2,2-trichloroethoxycarbonylamino)-α-D-glucopyranoside (10b) As described for **10a**, compound **9** (15.0 g, 34.5 mmol) was treated with tetradecanoic acid (9.46 g, 41.4 mmol) in the presence of DCC (8.54 g, 41.4 mmol) and DMAP (0.84 g, 6.9 mmol) to give **10b** (19.8 g, 89%) as a colorless oil. $[\alpha]_D$ +46.4° (c=1.2, $CHCl_3$). *Anal.* Calcd for $C_{29}H_{48}Cl_3NO_8$: C, 54.00; H, 7.50; N, 2.17. Found: C, 54.07; H, 7.54; N, 2.21. ^{1}H-NMR δ: 0.87 (3H, t, J=6 Hz, CH_3), 1.26 (18H, s, CH_2), 1.38 and 1.49 (each 3H, s, CCH_3), 1.60 (2H, br, CH_2), 2.30 (2H, m, CH_2CO), 4.72 (2H, s, CH_2CCl_3), 4.92 (1H, d, J=4 Hz, H-1), 5.90 (1H, m, $\underline{CH}=CH_2$). MS m/z: 643 (M^+).

Allyl 2-Deoxy-2-(2,2,2-trichloroethoxycarbonylamino)-3-*O*-[(*R*)-3-(2,2,2-trichloroethoxycarbonyloxy)tetradecanoyl]-α-D-glucopyranoside (11a) A solution of **10a** (1.72 g, 2.06 mmol) in 90% AcOH (40 ml) was heated at 90 °C for 30 min. After evaporation of the solvent, the residue was purified by silica gel column chromatography ($CHCl_3$–MeOH, 19 : 1) to give **11a** as a colorless, viscous oil (1.49 g, 91%). $[\alpha]_D$ +53.4° (c=2.0, $CHCl_3$). ^{1}H-NMR δ: 0.88 (3H, t, J=6 Hz), 1.26 (18H, s, CH_2), 1.70 (2H, br, CH_2), 1.94 (1H, t, J=6 Hz, OH), 2.60 (1H, dd, J=16, 4 Hz, CH_2CO_2), 2.8 (2H, m, CH_2CO_2 and OH), 4.24 (1H, m), 4.70 and 4.80 (each 1H, AB type d, J=12 Hz, CH_2CCl_3), 4.73 and 4.88 (each 1H, AB type d, J=12 Hz, CH_2CCl_3), 4.95 (1H, J=4 Hz, H-1), 5.1—5.4 (5H, m, H-3, CHOTroc, NH and $CH=\underline{CH_2}$), 5.9 (1H, m, $\underline{CH}=CH_2$). MS m/z: 793 (M^+).

Allyl 2-Deoxy-3-*O*-tetradecanoyl-2-(2,2,2-trichloroethoxycarbonylamino)-α-D-glucopyranoside (11b) As described for **11a**, compound **10b** (4.43 g, 6.78 mmol) was treated with 90% AcOH to give **11b** (3.20 g, 77%) as a colorless oil. $[\alpha]_D$ +54.4° (c=1.0, $CHCl_3$). *Anal.* Calcd for $C_{26}H_{44}Cl_3NO_8$: C, 51.62; H, 7.33; N, 2.32. Found: C, 51.87; H, 7.30; N, 2.26. ^{1}H-NMR δ: 0.90 (3H, t, J=6 Hz), 1.26 (18H, s, CH_2), 1.60 (2H, br, CH_2), 2.35 (2H, m, CH_2CO), 4.75 (2H, m, CH_2CCl_3), 4.97 (1H, d, J=4 Hz, H-1), 5.92 (1H, m, $\underline{CH}=CH_2$). MS m/z: 603 (M^+).

Allyl 2-Deoxy-6-*O*-(2,2,2-trichloroethoxycarbonyl)-2-(2,2,2-trichloroethoxycarbonylamino)-3-*O*-[(*R*)-3-(2,2,2-trichloroethoxycarbonyloxy)-tetradecanoyl]-α-D-glucopyranoside (12a) Troc–Cl (0.57 ml, 4.19 mmol) was gradually added to a solution of **11a** (1.44 g, 1.81 mmol) in pyridine (20 ml) with ice cooling. After the mixture was stirred for 6 h at room temperature, the mixture was diluted with EtOAc. The solution was washed with 1 M HCl, then with saturated aqueous NaCl and dried. After evaporation of the solvent, the residue was purified by silica gel column chromatography (benzene–EtOAc, 19 : 1—9 : 1) to give **12a** (1.50 g, 85%) as a pale yellow oil. $[\alpha]_D$ +46.2° (c=1.8, $CHCl_3$). ^{1}H-NMR δ: 0.88 (3H, t, J=6 Hz), 1.28 (18H, s, CH_2), 1.70 (2H, br, CH_2), 2.60 (1H, dd, J=16, 4 Hz, CH_2CO_2), 2.78 (1H, dd, J=16, 8 Hz, CH_2CO_2), 2.86 (1H, m, OH), 4.57 (2H, d, J=4 Hz, H-6), 4.8 (6H, m, $CH_2CCl_3\times3$), 4.96 (1H, d, J=4 Hz, H-1), 5.9 (1H, m, $\underline{CH}=CH_2$). MS m/z: 967 (M^+).

Allyl 2-Deoxy-3-*O*-tetradecanoyl-6-*O*-(2,2,2-trichloroethoxycarbonyl)-2-(2,2,2-trichloroethoxycarbonylamino)-α-D-glucopyranoside (12b) As described for **12a**, compound **11b** (3.20 g, 5.29 mmol) was treated with Troc–Cl (1.20 ml, 8.95 mmol) to give **12b** (3.00 g, 73%) as an oil. $[\alpha]_D$ +45.4° (c=1.1, $CHCl_3$). *Anal.* Calcd for $C_{29}H_{45}Cl_6NO_{10}$: C, 44.63; H, 5.81; N, 1.79. Found: C, 44.76; H, 5.67; N, 1.75. ^{1}H-NMR δ: 0.88 (3H, t, J=6 Hz, CH_3), 1.28 (18H, s, CH_2), 1.60 (2H, br, CH_2), 2.36 (2H, t, J=7 Hz, CH_2CO), 4.58 (2H, d, J=4 Hz, H-6), 4.8 (4H, m, CH_2CCl_3), 4.96 (1H, d, J=4 Hz, H-1), 5.9 (1H, m, $\underline{CH}=CH_2$). MS m/z: 777 (M^+).

Allyl 2-Deoxy-4-*O*-diphenylphosphono-6-*O*-(2,2,2-trichloroethoxycarbonyl)-2-(2,2,2-trichloroethoxycarbonylamino)-3-*O*-[(*R*)-3-(2,2,2-trichloroethoxycarbonyloxy)tetradecanoyl]-α-D-glucopyranoside (13a) Diphenyl phosphorochloridate (0.73 g, 2.75 mmol), DMAP (0.33 g, 2.75 mmol) and pyridine (0.18 ml, 2.25 mmol) were added to a solution of **12a** (1.46 g, 1.50 mmol) in CH_2Cl_2. The mixture was stirred for 22 h at room temperature, then $CHCl_3$ was added to the mixture. The solution was washed successively with 1 M HCl, H_2O, 5% aqueous $NaHCO_3$ and saturated aqueous NaCl, and dried. After evaporation of the solvent, the resultant residue was purified by silica gel column chromatography (benzene–EtOAc, 19 : 1) to give **13a** (1.72 g, 95%) as a colorless oil. $[\alpha]_D$ +36.8° (c=1.4, $CHCl_3$). ^{1}H-NMR δ: 0.88 (3H, t, J=6 Hz), 1.26 (18H, s, CH_2), 1.52 (2H, br, CH_2), 2.55 (2H, m, CH_2CO_2), 4.0—4.3 (4H, m, H-2, H-5, and $O\underline{CH_2}CH=CH_2$), 4.42 (2H, m, H-6), 4.60—4.95 (7H, m, H-4, $CH_2CCl_3\times3$), 5.00 (1H, d, J=4 Hz, H-1), 5.10 (1H, m, CHOTroc), 5.3—5.6 (4H, m, H-3, NH and $CH=\underline{CH_2}$), 5.9 (1H, m, $\underline{CH}=CH_2$), 7.2—7.4 (m). MS m/z: 1199 (M^+).

Allyl 2-Deoxy-4-*O*-diphenylphosphono-3-*O*-tetradecanoyl-6-*O*-(2,2,2-trichloroethoxycarbonyl)-2-(2,2,2-trichloroethoxycarbonylamino)-α-D-glucopyranoside (13b) As described for **13a**, compound **12b** (2.95 g, 3.78 mmol) was reacted with diphenylphosphorochloridate (2.40 g, 11.4 mmol) to give **13b** (3.58 g, 94%) as a colorless oil. $[\alpha]_D$ +42.4° (c=0.2, $CHCl_3$). ^{1}H-NMR δ: 0.88 (3H, t, J=6 Hz), 1.1—1.3 (20H, br, CH_2), 2.14 (2H, m, CH_2CO_2), 4.63—4.86 (4H, m, $CH_2CCl_3\times2$), 4.98 (1H, d, J=4 Hz, H-1), 5.9 (1H, m, $CH=\underline{CH_2}$), 7.14—7.46 (10H, m, arom. H). MS m/z: 1009 (M^+).

2-Deoxy-4-*O*-diphenylphosphono-6-*O*-(2,2,2-trichloroethoxycarbonyl)-2-(2,2,2-trichloroethoxycarbonylamino)-3-*O*-[(*R*)-3-(2,2,2-trichloroethoxycarbonyloxy)tetradecanoyl]-D-glucose (14a) 1,5-Cyclooctadienebis(methyldiphenylphosphine)iridium hexafluorophosphate (20 mg) was added to a solution of **13a** (1.68 g, 1.40 mmol) in THF (20 ml) under nitrogen. The mixture was heated at 50 °C under a nitrogen atmosphere for 2 h after activation of the iridium catalyst with hydrogen for 1 min. After cooling, iodine (0.71 g) and H_2O (2.5 ml) were added to the solution and the mixture was stirred for 20 min at room temperature. The solution was neutralized with 5% aqueous Na_2SO_3 and concentrated by evaporation. The residue was dissolved in $CHCl_3$ and the solution was washed with saturated aqueous NaCl, and dried. After evaporation of the solvent, the residue was purified by silica gel column chromatography (benzene–EtOAc, 9 : 1—4 : 1) to give **14a** (1.13 g, 70%). ^{1}H-NMR δ: 0.88 (3H, t, J=6 Hz), 1.26 (18H, s, CH_2), 1.52 (2H, br, CH_2), 2.56 (2H, m, CH_2CO_2), 3.44 (1H, br, OH), 4.06 (1H, m, H-2 or H-5), 4.4 (3H, m), 4.6—5.0 (7H, m, H-4 and $CH_2CCl_3\times3$), 5.11 (1H, m, CHOTroc), 5.40 (1H, m, H-1), 5.55 (2H, m, H-3 and NH), 7.2—7.4 (10H, m, arom. H). MS m/z: 1159 (M^+).

2-Deoxy-4-*O*-diphenylphosphono-3-*O*-tetradecanoyl-6-*O*-(2,2,2-trichloroethoxycarbonyl)-2-(2,2,2-trichloroethoxycarbonylamino)-D-glucose (14b) As described for **14a**, compound **13b** (2.70 g, 2.98 mmol) was treated with 1,5-cyclooctadienebis(methyldiphenylphosphine)iridium hexafluorophosphate (59 mg) to give **14b** (2.32 g, 89%) as a caramel. *Anal.* Calcd for $C_{38}H_{50}Cl_6NO_{13}P$: C, 46.93; H, 5.18; Cl, 21.87; N, 1.44. Found: C, 47.16; H, 5.18; Cl, 22.00; N, 1.42. $[\alpha]_D$ +26.4° (c=0.3, $CHCl_3$). ^{1}H-NMR δ: 0.88 (3H, t, J=6 Hz, CH_3), 1.1—1.5 (20H, br, CH_2), 2.08—2.30 (2H, m, CH_2CO_2), 4.60—4.90 (4H, m, $CH_2CCl_3\times2$), 7.14—7.46 (10H, m, arom.

H). MS *m/z*: 969 (M^+).

1-*O*-Acetyl-2-deoxy-4-*O*-diphenylphosphono-6-*O*-(2,2,2-trichloroethoxycarbonyl)-2-(2,2,2-trichloroethoxycarbonylamino)-3-*O*-[(*R*)-3-(2,2,2-trichloroethoxycarbonyloxy)tetradecanoyl]-D-glucopyranose (15a) Acetic anhydride (0.39 g, 3.82 mmol) and pyridine (0.30 ml, 3.82 mmol) were added to a solution of **14a** (0.89 g, 0.76 mmol) in CH_2Cl_2. The mixture was stirred for 15 h at room temperature and diluted with $CHCl_3$. The solution was washed with 1 M HCl, 5% aqueous $NaHCO_3$ and saturated aqueous NaCl. The solvent was evaporated *in vacuo* to give **15a** (0.92 g, quant.) as an oil. $[\alpha]_D$ +43.2° (c=1.2, $CHCl_3$). *Anal.* Calcd for $C_{43}H_{53}Cl_9NO_{17}P$: C, 42.83; H, 4.43; N, 1.16. Found: C, 42.66; H, 4.09; N, 1.16. ^{1}H-NMR δ: 0.89 (3H, t, J=6 Hz), 1.2—1.3 (20H, s, CH_2), 1.52 (2H, br, CH_2), 2.22 (3H, s, OAc), 2.56 (2H, m, CH_2CO_2), 4.1—4.3 (2H, m, H-2 and H-5), 4.40 (2H, m, H-6), 4.6—5.0 (7H, m, H-4 and $CH_2CCl_3 \times 3$), 5.12 (1H, m, CHOTroc), 5.32 (1H, d, J=10 Hz, NH), 5.50 (1H, t, J=10 Hz, H-3), 6.32 (1H, d, J=4 Hz, H-1), 7.2—7.4 (10H, m, arom. H). MS *m/z*: 1201 (M^+).

1-*O*-Acetyl-2-deoxy-4-*O*-diphenylphosphono-3-*O*-tetradecanoyl-6-*O*-(2,2,2-trichloroethoxycarbonyl)-2-(2,2,2-trichloroethoxycarbonylamino)-α-D-glucopyranose (15b) In the same manner as described for **15a**, compound **14b** (2.28 g, 3.34 mmol) was reacted with acetic anhydride to give **15b** (2.18 g, 91.6%) as an oil. $[\alpha]_D$ +37.2° (c=0.8, $CHCl_3$). *Anal.* Calcd for $C_{40}H_{52}Cl_6NO_{14}P$: C, 47.36; H, 5.17; N, 1.38. Found: C, 47.78; H, 4.95; N, 1.33. ^{1}H-NMR δ: 0.88 (3H, t, J=6 Hz, CH_3), 1.1—1.5 (20H, br, CH_2), 2.16 (2H, CH_2CO_2), 2.24 (3H, s, OAc), 4.60—5.00 (4H, m, $CH_2CCl_3 \times 2$), 5.50 (1H, t, J=10 Hz, H-3), 6.29 (1H, d, J=4 Hz, H-1), 7.04—7.46 (10H, m, arom. H). MS *m/z*: 1011 (M^+).

2-(Diphenylphosphonooxy)ethyl 3-*O*-[(*R*)-3-Benzyloxytetradecanoyl]-2-[(*R*)-3-benzyloxytetradecanoylamino]-2-deoxy-6-*O*-[2-deoxy-4-*O*-diphenylphosphono-6-*O*-(2,2,2-trichloroethoxycarbonyl)-2-(2,2,2-trichloroethoxycarbonylamino)-3-*O*-[(*R*)-3-(2,2,2-trichloroethoxycarbonyloxy)tetradecanoyl]-β-D-glucopyranosyl]-α-D-glucopyranoside (18a) HBr–AcOH (25%, 6 ml) was added to a solution of **15a** (409 mg, 0.34 mmol) in CH_2Cl_2 (2 ml), and the mixture was stirred for 1.5 h at room temperature. The reaction mixture was diluted with $CHCl_3$ and the solution was washed with a mixture of ice-H_2O, 5% aqueous $NaHCO_3$ and saturated aqueous NaCl, and dried. Evaporation of the solvent gave **16a** as an oil. This oil and **17a** (370 mg, 0.34 mmol) were dissolved in CH_2Cl_2 (5 ml), then $CaSO_4$ (0.5 g) and mercuric cyanide (172 mg, 0.68 mmol) were added to the mixture. After being refluxed for 18 h, the reaction mixture was filtered through Celite 545, and the filtrate was washed with 5% aqueous potassium iodide and saturated aqueous NaCl, and dried. After evaporation of the solvent, the residue was purified by silica gel column chromatography (benzene–EtOAc, 9:1—2:1) to give **18a** (577 mg, 76%) as a pale yellow viscous oil. $[\alpha]_D$ +20.2° (c=0.2, $CHCl_3$). ^{1}H-NMR δ: 0.88 (9H, t, J=7 Hz), 1.26 (54H, s, CH_2), 1.56 (6H, br, CH_2), 2.3—2.7 (6H, m), 5.70 (1H, m, H-3′), 7.2—7.4 (30H, m, arom. H). MS *m/z*: 2228 (M^+).

2-(Diphenylphosphonooxy)ethyl 2-Deoxy-6-*O*-[2-deoxy-4-*O*-diphenylphosphono-3-*O*-tetradecanoyl-6-*O*-(2,2,2-trichloroethoxycarbonyl)-2-(2,2,2-trichloroethoxycarbonylamino)-β-D-glucopyranosyl]-3-*O*-tetradecanoyl-2-tetradecanoylamino-α-D-glucopyranoside (18b) As described for **18a**, compound **16b**, obtained from **15b** (706 mg, 0.70 mmol), was reacted with **17b** (543 mg, 0.62 mmol) to give **18b** (885 mg, 78%) as an oil. $[\alpha]_D$ +15.1° (c=0.8, $CHCl_3$). *Anal.* Calcd for $C_{86}H_{126}Cl_6N_2O_{23}P_2 \cdot H_2O$: C, 55.88; H, 6.98; N, 1.52. Found: C, 55.64; H, 6.84; N, 1.51. ^{1}H-NMR δ: 0.89 (9H, t, J=6 Hz), 1.26 (54H, s, CH_2), 1.6 (6H, br, CH_2), 2.01—2.46 (6H, m, $CH_2CO_2 \times 3$), 4.68 (2H, m, CH_2CCl_3), 4.76 (2H, m, CH_2CCl_3), 5.06 (1H, t, J=10 Hz, H-3), 5.60 (1H, t, J=10 Hz, H-3′), 5.75 (1H, d, NH), 6.24 (1H, d, NH), 7.15—7.52 (20H, m, arom. H). MS *m/z*: 1826 (M^+).

2-(Diphenylphosphonooxy)ethyl 3-*O*-[(*R*)-3-Benzyloxytetradecanoyl]-2-(*R*)-3-benzyloxytetradecanoylamino]-2-deoxy-6-*O*-[2-deoxy-4-*O*-diphenylphosphono-3-*O*-[(*R*)-3-hydroxytetradecanoyl]-2-[(*R*)-3-hydroxytetradecanoylamino]-β-D-glucopyranosyl]-α-D-glucopyranoside (19a) Zinc powder (0.6 g) was added to a solution of **18a** (555 mg, 0.25 mmol) in AcOH (12 ml), and the mixture was vigorously stirred for 2 h at room temperature. The reaction mixture was filtered off and the filtrate was concentrated *in vacuo* to give an oil. After dissolution in $CHCl_3$, the solution was washed with 1 M HCl, H_2O, and 5% aqueous $NaHCO_3$ and dried. Separately, (*R*)-3-hydroxytetradecanoic acid (93 mg, 0.38 mmol) was dissolved in THF (2 ml), then 1-hydroxybenzotriazole (61 mg, 0.4 mmol) and DCC (82 mg, 0.4 mmol) were added to the solution with ice cooling. The mixture was stirred for 3 h at room temperature and the precipitate was filtered off to give an active ester solution. The active ester solution was added to the solution of the oily substance mentioned above in CH_2Cl_2 (5 ml), then *N*-methylmorpholine (44 μl, 0.4 mmol) was added to the mixture with ice cooling, and the final mixture was stirred for 13 h at room temperature. After evaporation of the solvent, the residue was purified by silica gel column chromatography ($CHCl_3$–MeOH, 50:1—20:1) to give **19a** (312 mg, 65%) as a colorless oil. $[\alpha]_D$ +6.3° (c=0.7, $CHCl_3$). ^{1}H-NMR δ: 0.90 (12H, t, J=7 Hz), 1.26 (72H, s, CH_2), 1.56 (8H, br, CH_2), 1.9—2.7 (8H, m), 4.7 (2H, m, H-1 and H-4′), 4.84 (1H, d, J=8 Hz, H-1′), 5.16 (1H, m, H-3), 5.59 (1H, m, H-3′), 7.2—7.4 (30H, m, arom. H). MS *m/z*: 1932 (M^+).

2-(Diphenylphosphonooxy)ethyl 2-Deoxy-6-*O*-(2-deoxy-4-*O*-diphenylphosphono-3-*O*-tetradecanoyl-2-tetradecanoylamino-β-D-glucopyranosyl)-3-*O*-tetradecanoyl-2-tetradecanoylamino-α-D-glucopyranoside (19b) As described for **19a**, compound **18b** (402 mg, 0.22 mmol) was treated with Zn dust, and the resulting oil was condensed with the HOBt active ester of tetradecanoic acid (75 mg, 0.33 mmol) to give **19b** (308 mg, 83%) as a white powder. mp 47.0—50.0 °C. *Anal.* Calcd for $C_{94}H_{150}N_2O_{20}P_2 \cdot H_2O$: C, 66.09; H, 8.97; N, 1.64. Found: C, 66.30; H, 8.82; N, 1.69. $[\alpha]_D$ +5.9° (c=0.7, $CHCl_3$). ^{1}H-NMR δ: 0.88 (12H, t, J=6 Hz, $CH_3 \times 4$), 1.26 (72H, s, CH_2), 1.5 (8H, br, CH_2), 1.96—2.46 (8H, m, CH_2CO_2), 4.64—4.94 (3H, H-4′, H-1 and H-1′), 5.10 (1H, t, J=10 Hz, H-3), 5.50 (1H, t, J=10 Hz, H-3′), 5.90 (1H, d, NH), 6.29 (1H, d, NH), 7.10—7.50 (20H, m, arom. H). IR (KBr): 3440, 2930, 1745, 1670, 1630, 1495, 1290, 1195 cm^{-1}. MS *m/z*: 1688 (M^+).

2-Phosphonooxyethyl 2-Deoxy-6-*O*-[2-deoxy-3-*O*-[(*R*)-3-hydroxytetradecanoyl]-2-[(*R*)-3-hydroxytetradecanoylamino]-4-*O*-phosphono-β-D-glucopyranosyl]-3-*O*-[(*R*)-3-*O*-hydroxytetradecanoyl]-2-[(*R*)-3-hydroxytetradecanoylamino]-α-D-glucopyranoside (3) Palladium–carbon (5%, 0.3 g) was added to a solution of **19a** (294 mg, 0.15 mmol) in AcOH (10 ml), and the mixture stirred under a hydrogen atmosphere for 7 h. The catalyst was filtered off and the filtrate was concentrated under reduced pressure, then the resulting oil was dissolved in THF (20 ml). Next, platinum dioxide (180 mg) was added to the solution and the mixture was stirred under a hydrogen atmosphere for 1.5 h. After filtration of the catalyst, the filtrate was concentrated, and the resulting residue was purified by preparative TLC ($CHCl_3$–MeOH–H_2O, 6:4:0.7). The extracted solution with $CHCl_3$–MeOH–H_2O–Et_3N (6:4:1:0.02) was concentrated by evaporation. After dissolution in $CHCl_3$–MeOH–H_2O (6:4:1), the solution was desalted with Dowex 50 (H^+). A part of the desalted solution was concentrated and freeze-dried from a dioxane suspension to give **3** as a white powder. mp 155—158 °C (dec). $[\alpha]_D$ −1.8° (c=0.5, $CHCl_3$–MeOH, 3:1). IR (KBr): 3440, 1740, 1660 cm^{-1}. ^{1}H-NMR ($CDCl_3$–CD_3OD, 3:1) δ: 0.90 (12H, t, J=6 Hz, CH_3), 1.28 (72H, br, CH_2), 1.48 (8H, br, CH_2), 2.3—2.5 (8H, m), 5.2 (2H, m).

The remaining desalted solution was neutralized with MeOH containing 1% Et_3N under ice-cooling to about pH 8. After evaporation of the solvent, the residue was dissolved in 0.1% Et_3N. The solution was lyophilized to give 76 mg of Et_3N salt as a white powder.

2-Phosphonooxyethyl 2-Deoxy-6-*O*-(2-deoxy-4-*O*-phosphono-3-*O*-tetradecanoyl-2-tetradecanoylamino-β-D-glucopyranosyl)-3-*O*-tetradecanoyl-2-tetradecanoylamino-α-D-glucopyranoside (4) In similar manner to that described for **3**, compound **19b** (215 mg, 0.13 mmol) was hydrogenolyzed in the presence of platinum dioxide (210 mg), and the resulting powder was purified by preparative TLC ($CHCl_3$–MeOH–H_2O, 6:4:0.8), and desalted and freezed-dried from a dioxan suspension to give **4** (80 mg, 45%) as a white powder. mp 153.5—155.0 °C (dec). $[\alpha]_D$ +13.3° (c=0.6, $CHCl_3$–MeOH, 9:1). IR (KBr): 3445, 2930, 1740, 1660, 1560 cm^{-1}. ^{1}H-NMR ($CDCl_3$–CD_3OD, 3:1) δ: 0.90 (12H, CH_3), 1.28 (72H, br, CH_2), 1.60 (8H, br, CH_2), 2.10—2.26 (4H, m, CH_2CO_2), 2.26—2.46 (4H, m, CH_2CO_2).

Et_3N salt was prepared in a manner similar to that described for **3**.

References

1) M. Imoto, S. Kusumoto, T. Shiba, H. Naoki, T. Iwashita, E. Th. Rietschel, H. W. Wollenweber, C. Galanos and O. Luderiz, *Tetrahedron Lett.*, **24**, 4017 (1983); M. Imoto, S. Kusumoto, T. Shiba, E. Th. Rietschel, C. Galanos and O. Luderiz, *ibid.*, **26**, 907 (1985).
2) M. Imoto, H. Yoshimura, S. Kusumoto and T. Shiba, *Proc. Jpn. Acad., Ser. B*, **60**, 285 (1984); M. Imoto, H. Yoshimura, N. Sakaguchi, S. Kusumoto and T. Shiba, *Tetrahedron Lett.*, **26**, 1545 (1985); M. Imoto, H. Yoshimura, T. Shimamoto, N. Sakaguchi, S. Kusumoto and T. Shiba, *Bull. Chem. Soc. Jpn.*, **60**, 2205 (1987).
3) M. Imoto, H. Yoshimura, M. Yamamoto, T. Shimamoto, S. Kusumoto and T. Shiba, *Bull. Chem. Soc. Jpn.*, **60**, 2197 (1987); *idem*, *Tetrahedron Lett.*, **25**, 2267 (1984).
4) C. Galanos, V. Lehmann, O. Luderitz, E. Th. Rietschel, O. Westphal, H. Brade, L. Brade, M. A. Freudenberg, T. Hansen-Hagge, T.

Luderitz, G. Mckenzie, U. Schade, W. Strittmatter, K. Tanamoto, U. Zahringer, M. Imoto, H. Yoshimura, M. Yamamoto, T. Shimamoto, S. Kusumoto and T. Shiba, *Eur. J. Biochem.*, **140**, 221 (1984); S. Kotani, H. Takada, M. Tsujimoto, T. Ogawa, K. Harada, T. Shiba, S. Kusumoto, M. Imoto, H. Yoshimura, M. Yamamoto and T. Shimamoto, *Infect. Immun.*, **45**, 293 (1984); H. Takada, S. Kotani, M. Tsujimoto, T. Ogawa, I. Takahashi, K. Harada, C. Katsukawa, S. Tanaka, T. Shiba, S. Kusumoto, M. Imoto, H. Yoshimura, M. Yamamoto and T. Shimamoto, *ibid.*, **48**, 219 (1985); S. Kanegasaki, Y. Kojima, M. Matsuura, J. Y. Homma, A. Yamamoto, Y. Kumazawa, K. Tanamoto, T. Yasuda, T. Tsumita, M. Imoto, H. Yoshimura, M. Yamamoto, T. Shimamoto, S. Kusumoto and T. Shiba, *Eur. J. Biochem.*, **143**, 237 (1984).

5) T. Kusama, T. Soga, E. Shioya, H. Nakayama, Y. Osada, Y. Ono, S. Kusumoto and T. Shiba, *Chem. Pharm. Bull.*, **38**, 3366 (1990).
6) M. Imoto, N. Kusunose, S. Kusumoto and T. Shiba, *Tetrahedron Lett.*, **29**, 2227 (1988).
7) S. Kusumoto, N. Kusunose, M. Imoto, T. Shimamoto, T. Kamikawa, H. Takada, S. Kotani, E. Th. Rietschel and T. Shiba, *Pure Appl. Chem.*, **61**, 461 (1989).

Chem. Pharm. Bull. **39**(8) 2000—2004 (1991) Vol. 39, No. 8

Synthesis and Pharmacological Activity of Sulfate Conjugates at 6-Position of *N*-Substituted Normorphine Derivatives

Takaaki HIRANO, Kazuta OGURI* and Hidetoshi YOSHIMURA

Faculty of Pharmaceutical Sciences, Kyushu University 62, 3–1–1 Maidashi, Higashi-ku, Fukuoka 812, Japan. *Received February 4, 1991*

Three pairs of *N*-substituted normorphine derivatives and the sulfate conjugates at the 6-position were tested for the analgesic and antagonistic activities and the development of physical dependence in mice. The compounds examined were nalorphine, nalorphine-6-sulfate (N-6-S), *N*-cyclopropylmethylnormorphine (CPN), *N*-cyclopropylmethylnormorphine-6-sulfate (C-6-S), *N*-dimethylallylnormorphine (DMN) and *N*-dimethylallylnormorphine-6-sulfate (D-6-S). The latter two pairs were newly synthesized. The analgesic activity of C-6-S and D-6-S was equipotent to that of CPN and DMN by the acetic acid writhing test on the s.c. injection, and the activity of N-6-S was about 2 times more potent than that of nalorphine. The antagonistic activity of N-6-S, C-6-S and D-6-S to morphine analgesia was higher than that of the parent compounds by the tail pinch test on i.c.v. injection. A withdrawal sign was seen in mice treated chronically with CPN, C-6-S and N-6-S by challenge with naloxone, whereas the mice treated with DMN, D-6-S and nalorphine showed no such sign. The effect of sulfation at the 6-position on the development of physical dependence was not well associated with the effect on agonistic and antagonistic activities.

Keywords opioid; *N*-cyclopropylmethylnormorphine; *N*-dimethylallylnormorphine; nalorphine; sulfate conjugate; analgesic activity; antagonistic activity; physical dependence

Previous works from our laboratory have shown that glucuronidation and sulfation of morphine at the 6-position enhance the analgesic activity.[1,2] Morphine-6-glucuronide is receiving considerable attention because of a higher level of this active metabolite than morphine in the blood of cancer patients with chronic dosings of morphine,[3,4] and the potential importance of glucuronide in morphine analgesia was appreciated.[5–7] The strong activity of morphine-6-glucuronide was unequivocally proved to be induced by the glucuronide itself.[8] A mixed agonist–antagonist, nalorphine was also modified in the same way and examined for its effect on agonistic and antagonistic activities and on the development of physical dependence.[9] The antagonistic activity of nalorphine to morphine analgesia was enhanced by glucuronidation and sulfation at the 6-position. These 6-conjugates of nalorphine were found to have potent dependence liability while the liability is low in nalorphine. Knoll *et al.* have reported the pharmacological profile following chemical modification at the 6-position of opiate analgesics with an azido group.[10–12] 6-Azidomorphine and 14-hydroxy-6-azidomorphine were shown to induce more potent analgesia than hydromorphone and oxymorphone, respectively. These derivatives were, further, reported to have a low dependence liability.

The experiments reported here were designed to examine the effects of 6-sulfation of *N*-substituted normorphine derivatives on the agonistic and antagonistic activities, and also on the development of physical dependence in mice. Compounds newly synthesized and tested for pharmacological activities were *N*-cyclopropylmethylnormorphine (CPN, **1**), its 6-sulfate (C-6-S, **3**), *N*-dimethylallylnormorphine (DMN, **2**) and its 6-sulfate (D-6-S, **4**), which are shown in Chart 1.

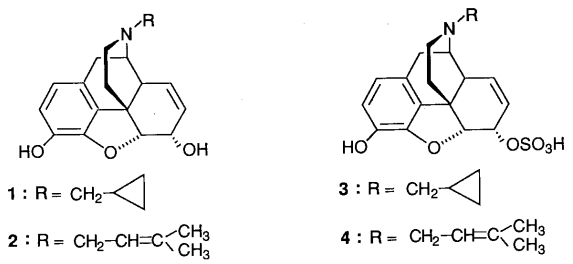

Chart 1

Chemistry Synthetic routes are shown in Chart 2. CPN (**1**) was prepared from normorphine (**5**) according to the method described by Gates and Monzka.[13] The starting material, normorphine (**5**), was synthesized from morphine in three steps according to the method reported by Rapoport.[14] DMN (**2**) was prepared from **5** according to the method described by Iijima *et al.*[15] **5** was alkylated with dimethylallyl bromide, and the resultant product (**2**) was purified by silica gel chromatography. C-6-S (**3**) and D-6-S (**4**) were synthesized following the method for morphine and nalorphine sulfates previously reported.[2,9] The intermediates **7** and **8** were used without further purification. Table I shows synthetic yields and melting points of the *N*-substituted normorphine derivatives newly synthesized in this paper.

Pharmacological Results The analgesic activity of *N*-substituted normorphine derivatives injected i.c. was assessed by the acetic acid writhing test in mice (Table II). The analgesic activity of nalorphine-6-sulfate (N-6-S) was about 2 times that of nalorphine as reported previously.[9] C-6-S and D-6-S, however, showed comparable analgesic activity to that of CPN and DMN, respectively. These compounds, except morphine, showed no analgesic activity when assessed by the tail pinch test in mice even at a high dose of 20 μmol/kg s.c. (data not shown).

The antagonistic activity of *N*-substituted normorphine derivatives and pentazocine to morphine analgesia was assessed by the tail pinch test in mice. All compounds, CPN, C-6-S, DMN, D-6-S, nalorphine, N-6-S, and pentazocine antagonized to the analgesic effect of morphine co-administered i.c.v. at a dose of 8 nmol/body (Table III). The sulfates, C-6-S, D-6-S and N-6-S showed more potent antagonistic activity than the parent compounds.

The effect on the development of physical dependence by 6-sulfation of *N*-substituted normorphine derivatives was examined in mice by 14 times s.c. administrations of the

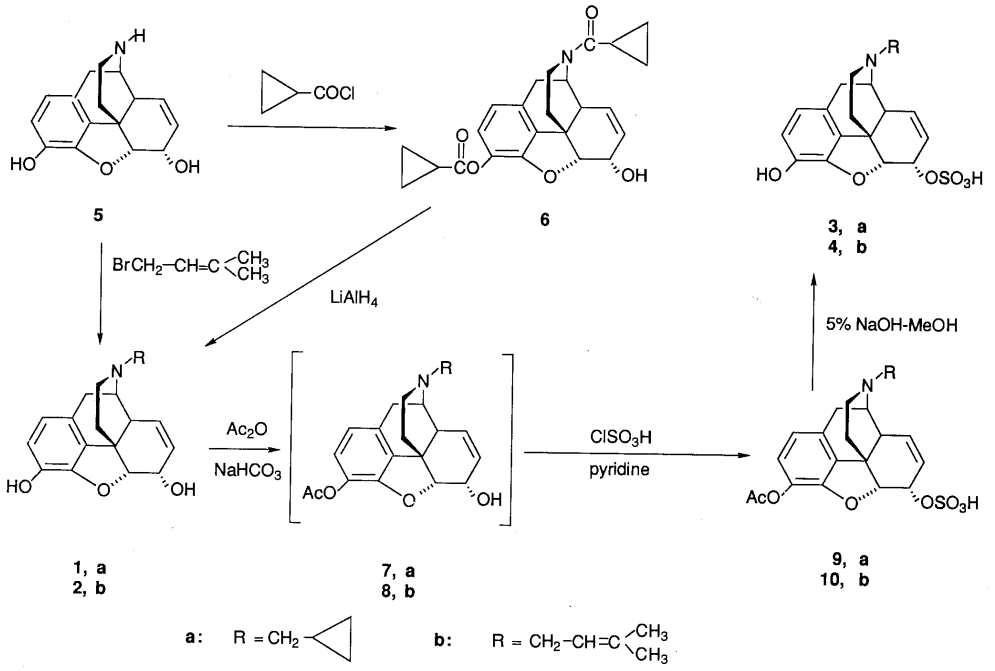

Chart 2

TABLE I. *N*-Substituted Normorphine Derivatives: Synthetic Yield and Melting Points

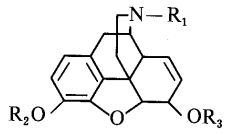

No.	R_1	R_2	R_3	Salt	Yield	mp (°C)	Recryst. solvent	Formula
1	Cyclopropylmethyl	H	H		74	189—191	MeOH	$C_{20}H_{23}NO_3 \cdot \frac{1}{2}CH_3OH \cdot \frac{1}{2}H_2O$
2	Dimethylallyl	H	H		49	97—99	Benzene	$C_{21}H_{25}NO_3 \cdot C_6H_6$
3	Cyclopropylmethyl	H	SO_3H		55	280—285[b]	MeOH	$C_{20}H_{23}NO_6S \cdot 1\frac{1}{2}H_2O$
4	Dimethylallyl	H	SO_3H		70	290—295[b]	MeOH	$C_{21}H_{25}NO_6S \cdot \frac{1}{2}H_2O$
5	H	H	H		63[a]	250—258[b]	MeOH	$C_{16}H_{17}NO_3 \cdot 1\frac{1}{2}H_2O$
6	Cyclopropylcarbonyl	Cyclopropylcarbonyl	H		100	176—178	AcOEt	$C_{24}H_{25}NO_5$
7	Cyclopropylmethyl	$COCH_3$	H		100	Oil		
8	Dimethylallyl	$COCH_3$	H		100	Oil		
9	Cyclopropylmethyl	$COCH_3$	SO_3H		70	245—247[b]	H_2O	$C_{22}H_{25}NO_7S \cdot 2\frac{1}{2}H_2O$
10	Dimethylallyl	$COCH_3$	SO_3H		70	248—250[b]	H_2O	$C_{23}H_{27}NO_7S \cdot H_2O$
11	Cyclopropylmethyl	H	H	HCl	100	191—193	Et_2O	$C_{20}H_{23}NO_3 \cdot \frac{1}{2}H_2O \cdot HCl$
12	Dimethylallyl	H	H	HCl	100	181—183	Et_2O	$C_{21}H_{25}NO_3 \cdot H_2O \cdot HCl$

a) Compound **5** was synthesized from morphine in about a 63% yield *via* three step reactions according to the method described in the literature.[4] *b*) Decomposition.

drugs at 9 a.m., 3 p.m. and 9 p.m. At 4 h after the last injection, the mice were challenged by a s.c. injection of nalorphine HCl at a dose of 10 mg/kg and physical dependence was assessed by using a jumping response as a criterion of precipitated withdrawal. Frequent jumping behavior was seen in mice treated chronically with CPN, C-6-S, N-6-S, morphine and morphine-6-sulfate (M-6-S), while, no such sign was observed by chronic treatment with DMN, D-6-S, nalorphine and pentazocine (Table IV). The development of physical dependence was, thus, strikingly enhanced by the sulfation of nalorphine and morphine at the 6-position, but, the dependence liability was not changed in pairs of *N*-cyclopropylmethyl and *N*-dimethylallyl derivatives by the modification. Tremors and diarrhea were also seen as the precipitated withdrawal signs in mice treated chronically with norphine, M-6-S and N-6-S.

Discussion

The present studies intended to examine the effect of modification on the pharmacological activity of *N*-allyl, *N*-cyclopropylmethyl and *N*-dimethylallyl derivatives of normorphine by sulfation at the 6-position. Newly synthesized C-6-S and D-6-S retained equipotent analgesic activity with that of the parent compounds, when assessed by the acetic acid writhing test with s.c. injection. The analgesic activity of N-6-S reported previously[9] was reconfirmed to be twice as potent as that of nalorphine also in the present study. On the other hand, the antagonistic activity of C-6-S and D-6-S to morphine analgesia was more potent than that of CPN and DMN, respectively. The sulfation appears to be more effective on the antagonistic effect than on the agonistic effect. The effect on the development of physical dependence by the modification

Table II. Analgesic Activity of Normorphine Derivatives Assessed by Acetic Acid Writhing Test in Mice

Drugs[a]	ED_{50}[b]	μmol/kg	Relative potency[c]
CPN	0.122	(0.097—0.151)	3.78
C-6-S	0.182	(0.137—0.242)	2.53
DMN	7.48	(5.10—11.9)	0.062
D-6-S	9.88	(6.98—14.0)	0.047
Nalorphine	1.43	(1.13—1.75)	0.322
N-6-S	0.716	(0.639—0.794)	0.644
Morphine	0.461	(0.384—0.547)	1.00

a) Drugs were injected subcutaneously. *b*) Values in parentheses represent 95% confidence limits. *c*) Values represent relative potency to that of morphine on the basis of ED_{50}.

Table III. Antagonistic Effect of Normorphine Derivatives and Pentazocine on Analgesic Activity of Morphine in Mice

Drugs	Dose nmol/body	Number of animals	Analgesia[a] (%)
Morphine	—	25	78.0
Morphine & CPN	0.1	10	30.0
	0.2	10	15.0
Morphine & C-6-S	0.01	10	30.0
	0.025	10	15.0
	0.05	10	5.0
	0.1	10	0
Morphine & DMN	25.0	20	55.0
	50.0	10	50.0
	100.0	10	40.0
Morphine & D-6-S	5.0	10	40.0
	10.0	10	30.0
	20.0	10	15.0
Morphine & nalorphine	0.8	10	35.0
Morphine & N-6-S	0.1	10	35.0
	0.2	10	20.0
Morphine & pentazocine	32.0	10	40.0

Morphine HCl (8 nmol/body) and antagonists were injected intracerebrally simultaneously. Analgesia was assessed 20 min after the injection by Haffner's tail pinch test. An ambiguous response to the test was counted as 0.5. *a*) Values represent % of mice which responded positively to the analgesic test.

Table IV. Naloxone-Precipitated Jumping in Mice after Chronic Administration of Normorphine Derivatives and Pentazocine

Drugs	Dose μmol/kg	Jumped mice/ total number	% of jumping response
CPN	100	4/15	26.7[a]
C-6-S	100	5/15	33.3[a,c]
DMN	200	0/15	0
D-6-S	200	0/7	0
Nalorphine	200	0/15	0
N-6-S	100	12/15	80.0[a,b]
Morphine	100	4/15	28.6[a]
	200	7/15	46.7[a]
M-6-S	10	9/13	69.2[a,d]
	50	12/13	92.3[a,e]
Pentazocine	200	0/14	0
Saline	—	0/42	0

Drugs were injected s.c. 14 times at 9 a.m., 3 p.m. and 9 p.m. of every day. Doses were raised gradually (1st and 2nd, 1/8; 3rd and 4th, 1/4; 5th and 6th, 1/2; 7th and 8th, 3/4; 9th to the last, the doses shown in this table). Naloxone HCl was challenged at a dose of 10 mg/kg 4 h after the last injection of test drugs, and a jumping response was observed for 15 min. In the drugs of low dependence liability, the doses were raised up to 200 μmol/kg. *a*) Significantly different from saline group, $p<0.01$ [χ^2-test]. *b*) Significantly different from nalorphine group, $p<0.01$ [χ^2-test]. *c*) Not significantly different from CPN group, $p>0.05$ [χ^2-test]. *d*) Significantly different from morphine group (100 μmol/kg), $p<0.05$ [χ^2-test]. *e*) Significantly different from morphine group (200 μmol/kg), $p<0.01$ [χ^2-test].

was not significant to *N*-cyclopropylmethyl and *N*-dimethylallyl derivatives in contrast to the striking effect on *N*-allyl and *N*-methyl derivatives.

The results obtained here extended previous findings on the pharmacological activity of morphine and nalorphine by the modification at the 6-position.[2,9] We first found very potent analgesic activity of morphine-6-glucuronide in mice.[1] Recently, the activity of this morphine metabolite was recognized to be 90- and 650-times as potent as that of morphine in mice when injected i.c.v. and intrathecally, respectively.[16] The sulfation of morphine at the same position also raised the analgesic activity above morphine similarly.[2] Further glucuronate and sulfate conjugates of nalorphine at the 6-position showed more potent antagonistic activity to morphine analgesia.[9] These findings seemed to suggest that the glucuronidation and sulfation of morphine and related compounds at the 6-position raise either agonistic or antagonistic activity directed to the opioid receptors.

In the present study, the analgesic activity of the sulfates of *N*-cyclopropylmethyl and *N*-dimethylallyl derivatives was equipotent to that of the parent compounds by the s.c. route of administration. This also agreed with the previous finding that nalorphine-6-conjugates slightly raised the analgesic effect of nalorphine.[9] This result means that the sulfated antagonists do not lose, but do not raise significantly the analgesic effect when injected s.c.

There was inconsistency in the effect of sulfation on the development of physical dependence. Remarkable withdrawal signs were reconfirmed in mice treated chronically with N-6-S by challenge with naloxone, while no such signs were observed in the case of nalorphine.[9] This effect of nalorphine-6-sulfate made a striking contrast to the indistinguishable activity of CPN and C-6-S, and of DMN and D-6-S. DMN is a weak analgesic and this may be the reason that D-6-S did not produce addiction, the dependence liability of a strong agonist CPN by sulfation was also not changed. Although the reason for this inconsistency has not yet been resolved, it seems to be due to the different affinity and selectivity of the above compounds to the opioid receptors. Gilbert and Martin have indicated that nalorphine is an antagonist at the μ-receptor and a partial agonist at the κ-receptor.[17] They also suggested that each of the κ-receptor-directed mixed agonist–antagonists had a different affinity and selectivity to the κ-receptor, and that cyclazocine possessing a cyclopropylmethyl group like CPN was a strong agonist to the κ-receptor. Therefore, the different effect of the 6-conjugates on the development of physical dependence seems to be induced by the altered interactions with the multiple opioid receptors.[18]

Experimental

1) Chemistry Melting points were determined on a Yanagimoto melting point microscope and were uncorrected. Infrared (IR) spectra were obtained on a JEOL DS-701G spectrometer. Proton nuclear magnetic resonance (^{1}H-NMR) spectra were determined with a JEOL DS-100 spectrometer. Chemical shifts are expressed in ppm (δ) relative to tetramethylsilane as an internal standard and $CDCl_3$ or dimethyl sulfoxide-d_6 (DMSO-d_6) was used as a solvent. Mass spectra (MS) were obtained on a JEOL D-300 spectrometer.

Reaction progress and purity of products were determined by analytical thin layer chromatography (TLC) using precoated plates (either Merck silica gel G or Wako B-5FM, 20 × 5 cm or 20 × 20 cm). Spots were visualized

with a ultraviolet (UV) 254 nm light or iodine vapor. Silica gel type 60 (Merck, 70—230 mesh) and Silicic AR CC-7 (Mallinckrodt) were used for column chromatography. Elemental analyses were performed at the Analytical Section, Kyushu University. Organic extracts were dried over anhydrous Na_2SO_4.

Normorphine (5) Compound **5** was synthesized from morphine according to the method described in the literature[14] in about a 63% yield *via* diacetylmorphine (92% yield) and *N*-cyanodiacetylnormorphine (80% yield) as a light brown powder. UV λ_{max}^{EtOH} nm (log ε): 282 (3.25). MS *m/z*: 271 (M^+). *Anal.* Calcd for $C_{16}H_{17}NO_3 \cdot 1\ 1/2\ H_2O$: C, 64.40; H, 6.76; N, 4.69. Found: C, 64.45; H, 6.66; N, 4.68.

3-*O*,*N*-Dicyclopropylcarbonylnormorphine (6) A solution of cyclopropylcarbonyl chloride (3.74 g, 35.8 mmol) in $CHCl_3$ (11 ml) was added dropwise to a stirring mixture of **5** (2.15 g, 7.2 mmol), triethylamine (6.5 ml), and $CHCl_3$ (43 ml) during a period of 5 min. The mixture was refluxed for 8 h. After being cooled, the mixture was washed twice with 60 ml of 3.6% HCl, and then washed twice with 60 ml of 5% Na_2CO_3. The $CHCl_3$ layer was dried and concentrated *in vacuo*. The oily residue was crystallized from ethyl acetate to give **6** (almost a quantitative yield) as colorless needles. IR ν_{max}^{KBr} cm^{-1}: 1741 (C=O); 1631 (C=O). UV λ_{max}^{EtOH} nm (log ε): 287 (3.17). ^{1}H-NMR ($CDCl_3$) δ: 4.12—4.32 (1H, m, C_6-H), 4.93 (1H, d, J=7 Hz, C_5-H), 5.20—5.40 (1H, m, C_8-H), 5.68—5.96 (1H, m, C_7-H), 6.70 (2H, dd, J=8 Hz, C_1-H, C_2-H). MS *m/z*: 407 (M^+). *Anal.* Calcd for $C_{24}H_{25}NO_5$: C, 70.74; H, 6.18; N, 3.44. Found: C, 70.45; H, 6.16; N, 3.38.

***N*-Cyclopropylmethylnormorphine (1)** To a stirred solution of **6** (2.84 g, 7.0 mmol) in tetrahyrofuran (THF) (70 ml) was added dropwise a suspension of lithium aluminum hydride (1.26 g, 33.2 mmol) in THF (10 ml) at room temperature during a period of 5 min. The resulting mixture was stirred at room temperature for an additional 23 h. The remaining lithium aluminum hydride was allowed to decompose by the cautious addition of ethyl acetate (4 ml) and H_2O (6 ml). After standing, the upper layer was removed, and the lower layer was extracted three times with 75 ml of ethyl acetate. The combined extract was dried and concentrated *in vacuo*. The residue was recrystallized from MeOH to give **1** (1.84 g, 74% yield) as light brown crystals. UV λ_{max}^{EtOH} nm (log ε): 287 (3.19). ^{1}H-NMR ($CDCl_3$) δ: 0—1.10 (5H, m, cyclopropane-H), 2.49 (2H, d, J=6 Hz, *N*-C<u>H</u>$_2$-cyclopropyl), 3.45 (1.5H, s, C<u>H</u>$_3$OH), 4.07—4.27 (1H, d, C_6-H), 4.83 (1H, d, J=6 Hz, C_5-H), 5.12—5.36 (1H, m, C_8-H), 5.53—5.76 (1H, m, C_7-H), 6.53 (2H, dd, C_1-H, C_2-H). MS *m/z*: 325 (M^+). *Anal.* Calcd for $C_{20}H_{23}NO_3 \cdot 1/2H_2O \cdot 1/2CH_3OH$: C, 70.36; H, 7.34; N, 3.34. Found: C, 70.48; H, 7.64; N, 3.79.

***N*-Dimethylallylnormorphine (2)** Dimethylallyl bromide (0.82 g, mmol) was added slowly to a stirred mixture of **5** (1.58 g, 5.3 mmol) and K_2CO_3 (2.5 g, 18.1 mmol) in dimethylformamide (DMF) (25 ml). The resulting mixture was heated at 90—95 °C for 3 h under N_2. After being cooled, the reaction mixture was diluted with H_2O (100 ml), saturated with NaCl, and extracted with three 30 ml parts of $CHCl_3$. The combined extracts were washed with a saturated NaCl solution (100 ml), dried, and concentrated *in vacuo*. The brown oily residue was chromatographed on silica gel ($CHCl_3$ and 2% MeOH/$CHCl_3$) to give **2** (1.50 g, 83% yield) as an oil. It was crystallized from benzene to give **2** (1.06 g, 49% yield) as light brown crystals. UV λ_{max}^{EtOH} nm (log ε): 286.5 (3.16). ^{1}H-NMR ($CDCl_3$) δ: 1.68 and 1.72 (3H×2, s, *gem* CH_3), 3.14 (2H, d, *N*-C<u>H</u>$_2$-CH=), 4.05—4.25 (1H, m, C_6-H), 4.82 (1H, d, C_5-H), 5.12—5.40 (1H×2, m, –CH_2–C<u>H</u>=C and C_8-H), 5.50—5.74 (1H, m, C_7-H), 6.53 (2H, dd, C_1-H), C_2-H), 7.34 (6H, s, benzene-H). *Anal.* Calcd for $C_{21}H_{25}NO_3 \cdot C_6H_6$: C, 77.67; H, 7.48; N, 3.35. Found: C, 77.56; H, 7.53; N, 3.28. MS *m/z*: 339 (M^+).

***N*-Cyclopropylmethylnormorphine·HCl (11)** HCl gas was bubbled into a solution of **1** (436 mg, 1.2 mmol) in dry ether (30 ml). The resulting precipitate was collected by filtration, washed with dry ether, and dried *in vacuo* to give **11** (almost quantitative yield) as colorless crystals. UV λ_{max}^{EtOH} nm (log ε): 285 (3.14). *Anal.* Calcd for $C_{20}H_{23}NO_3 \cdot 1/2H_2O \cdot HCl$: C, 64.77; H, 6.79; N, 3.78. Found: C, 65.13; H, 7.17; N, 3.52.

***N*-Dimethylallylnormorphine·HCl (12)** This compound was prepared from **2** in an almost quantitative yield in the same manner as compound **11**. UV λ_{max}^{EtOH} nm (log ε): 285 (3.16). *Anal.* Calcd for $C_{21}H_{25}NO_3 \cdot H_2O \cdot HCl$: C, 64.03; H, 7.16; N, 3.56. Found; C, 64.02; H, 7.25; N, 3.35.

3-*O*-Acetyl-*N*-cyclopropylmethylnormorphine (7) Acetic anhydride (2.7 ml) was added dropwise to a stirring suspension of **1** (501.9 mg, 1.4 mmol) and $NaHCO_3$ (5 g, 59.5 mmol) in H_2O (100 ml) during a period of 10 min. The resulting mixture was stirred at room temperature for 30 min. The reaction mixture was then extracted three times with 100 ml of $CHCl_3$. The combined extracts were washed with H_2O (200 ml), dried and concentrated *in vacuo* to give **7** (an almost quantitative yield) as an oily product. The product showed a spot (*Rf* 4.8) by silica gel TLC with a solvent system of $CHCl_3$ and MeOH (9 : 1) and detection with potassium platinum iodide reagent. Compound **7** was used without further purification.

3-*O*-Acetyl-*N*-dimethylallylnormorphine (8) This compound was prepared from **2** in an almost quantitative yield in the same manner as compound **7**. The product gave a spot (*Rf* 4.5) by silica gel TLC with a solvent system of $CHCl_3$ and MeOH (9 : 1) and detection with potassium platinum iodide reagent.

3-*O*-Acetyl-*N*-cyclopropylmethylnormorphine-6-*O*-sulfate (9) A mixture of dry pyridine (1.2 ml) and chlorosulfonic acid (0.2 ml) was heated at 60 °C for 10 min. To this, a solution of **7** (593.4 mg, 1.6 mmol) in dry pyridine (0.4 ml) was added and heated at 70 °C for 10 min. To jelly clump separated as a lower layer was added 5 ml of H_2O. After standing for a while, the solution was concentrated *in vacuo* to remove pyridine. H_2O (5 ml) was added to the oily residue, and the resultant precipitate was collected by filtration, recrystallized from H_2O to give **9** (504.7 mg, 70%) as colorless crystals. IR ν_{max}^{KBr} cm^{-1}: 1019 (SO_2), 1240 (SO_2), 1750 (C=O), 2720 (NH)$^+$. UV λ_{max}^{EtOH} nm (log ε): 285 (3.18). *Anal.* Calcd for $C_{22}H_{25}NO_7S \cdot 2\ 1/2H_2O$: C, 53.65; H, 6.14; N, 2.83. Found: C, 53.49; H, 5.99; N, 2.98.

3-*O*-Acetyl-*N*-dimethylallylnormorphine-6-*O*-sulfate (10) This compound was prepared from **8** in a 70% yield in the same manner as compound **9**. IR ν_{max}^{KBr} cm^{-1}: 1022 (SO_2), 1250 (SO_2), 1756 (C=O), 2755 (NH)$^+$. UV λ_{max}^{EtOH} nm (log ε): 281.5 (3.30). *Anal.* Calcd for $C_{23}H_{28}NO_7S \cdot H_2O$: C, 57.61; H, 6.10; N, 2.92. Found: C, 57.38; H, 6.12; N, 3.09.

***N*-Cyclopropylmethylnormorphine-6-*O*-sulfate (3)** A solution of **9** (491.5 mg, 1.0 mmol) in 5% NaOH–MeOH (25 ml) was stirred at room temperature for 1 h. After being adjusted to pH 6.5 with 10% acetic acid, the reaction mixture was concentrated *in vacuo*. The oily residue was crystallized from MeOH to give **3** (223.5 mg, 55%) as colorless crystals. IR ν_{max}^{KBr} cm^{-1}: 1017 (SO_2), 1260 (SO_2), 2720 (NH)$^+$. UV λ_{max}^{EtOH} nm (log ε): 282 (3.31). *Anal.* Calcd for $C_{20}H_{23}NO_6S \cdot 1\ 1/2H_2O$: C, 57.68; H, 6.29; N, 3.36. Found: C, 57.35; H, 5.93; N, 3.34.

***N*-Dimethylallylnormorphine-6-*O*-sulfate (4)** This compound was prepared from **10** in a 70% yield in the same manner as compound **3**. IR ν_{max}^{KBr} cm^{-1}: 1018 (SO_2), 1249 (SO_2), 2760 (NH^+). UV λ_{max}^{EtOH} nm (log ε): 285.5 (3.18). *Anal.* Calcd for $C_{21}H_{25}NO_6S \cdot 1/2H_2O$: C, 58.86; H, 6.12; N, 3.27. Found: C, 59.26; H, 6.15; N, 3.12.

2) Pharmacology Materials Male mice (ddN strain) weighing 15—20 g were used for pharmacological experiments. Nalorphine hydrochloride was supplied from the Ministry of Health and Welfare of Japan. Morphine hydrochloride was purchased from Takeda Chemical Ind., Ltd. (Osaka). Pentazocine and naloxone hydrochloride were kindly given by Sankyo Co., Ltd. (Tokyo). M-6-S and N-6-S were synthesized according to the method reported previously.[2,9] CPN and DMN were used as HCl salt (**11** and **12**), respectively.

Analgesic Activity Analgesic activity was assessed by the acetic acid writhing method developed by Koster *et al.*[19] Writhings were counted for 10 min from 10 min after an i.p. injection of 0.6% acetic acid physiological saline solution. Drugs were dissolved in the saline and injected s.c. 30 min before the injection of acetic acid at a volume of 0.1 ml/10 g body weight. The time to estimate the analgesia was decided following the maximum effect of morphine HCl and morphine-6-glucuronide at about 45 min after the injection s.c.[1]

Antagonistic Activity Antagonistic activity to morphine analgesia was assessed by the tail-pinch method in mice.[20] Drugs were dissolved in physiological saline and injected i.c.v. concomitantly with 8 nmol morphine HCl at a volume of 20 μl/body. Time for determination of the activity was set at 20 min after the injection from the result of a preliminary study for the time point of the most reproducible and potent effect of morphine and test drugs.

Development of Physical Dependence Dependence was induced in 7—42 mice by giving drugs or saline s.c. 14 times totally at 9 a.m., 3 p.m. and 9 p.m. everyday. Dosage was increased gradually (1st-2nd, 1/8; 3th—4th, 1/4; 5th—6th, 1/2; 7th—8th, 3/4; 9th—14th, the same dose of the last injection). The mice were challenged with 10 mg/kg s.c. injection of naloxone HCl 4 h after the last injection. The jumping response and other withdrawal signs (tremor, diarrhea) were observed for 15 min after the injection of naloxone following the method of Way *et al.*[21]

Acknowledgements This work was supported in part by a Grant-in-Aid for scientific research from the Ministry of Education, Science and Culture of Japan, which is gratefully acknowledged.

References

1) K. Shimomura, O. Kamata, S. Ueki, S. Îda, K. Oguri, H. Yoshimura and H. Tsukamoto, *Tohoku J. Exp. Med.*, **105**, 45 (1971).
2) M. Mori, K. Oguri, H. Yoshimura, K. Shimomura, O. Kamata and S. Ueki, *Life Sci.*, **11** (Part 1), 525 (1972).
3) J.-O. Svensson, A. Rane, J. Säwe and F. Sjöqvist, *J. Chromatogr.*, **230**, 427 (1982).
4) J. Säwe, J. -O. Svensson and A. Rane, *Br. J. Clin. Pharmacol.*, **16**, 85 (1983).
5) S. P. Joel, R. J. Osborne, N. S. Nixon and M. L. Slevin, *Lancet*, i, 1099 (1985).
6) C. W. Hand, W. P. Blunnie, L. P. Claffey, A. J. McShane, H. J. McQuay and R. A. Moore, *Lancet*, ii, 1207 (1987).
7) R. J. Osborne, S. P. Joel, D. Trex and M. Slevin, *Lancet*, i, 828 (1988).
8) H. Yoshimura, S. Îda, K. Oguri and H. Tsukamoto, *Biochem. Pharmacol.*, **22**, 1423 (1973).
9) K. Oguri, I. Yamada-Mori, J. Shigezane, T. Hirano and H. Yoshimura, *Eur. J. Pharmacol.*, **102**, 229 (1984).
10) J. Knoll, S. Fürst and K. Keleman, *J. Pharm. Pharmacol.*, **25**, 929 (1973).
11) J. Knoll, *J. Neuropharmacol.*, **14**, 921 (1975).
12) J. Knoll, S. Fürst and S. Makleit, *Arch. Int. Pharmacodyn.*, **228**, 268 (1977).
13) M. Gates and T. A. Monzka, *J. Med. Chem.*, **7**, 127 (1964).
14) H. Rapoport and M. Look, U. S. Patent 2890221 (1959) [*Chem. Abstr.*, **54**, 6125 (1960)].
15) I. Iijima, J. Minamikawa, A. E. Jacobson, A. Brossi and C. Rice, *J. Med. Chem.*, **21**, 399 (1978).
16) D. Paul, Standifer, K. M. C. E. Inturrisi and G. W. Pasternak, *J. Pharmacol. Exp. Ther.*, **251**, 477 (1989).
17) P. E. Gilbert and W. R. Martin, *Drug Alcohol Depend.*, **1**, 373 (1976).
18) K. Oguri, I. Yamada-Mori, J. Shigezane, T. Hirano and H. Yoshimura, *Life Sci.*, **41**, 1457 (1987).
19) R. Koster, M. Anderson and E. I. Debear, *Fed. Proc.*, **18**, 412 (1983).
20) F. Haffner, *Deu. Med. Wochenshr.*, **55**, 731 (1927).
21) E. L. Way, H. H. Loh and F. Shen, *J. Pharmacol. Exp. Ther.*, **167**, 1 (1969).

Chem. Pharm. Bull. **39**(8) 2005—2008 (1991)

Structure–Activity Relationships of Alpha-Human Atrial Natriuretic Peptide (α-hANP) Analogs: Role of Charged Groups in α-hANP[1)]

Yoshiharu MINAMITAKE, Yasuo KITAJIMA,* Mayumi FURUYA, Maki YOSHIDA, and Shoji TANAKA

Suntory Institute for Biomedical Research, Shimamoto-cho, Mishima-gun, Osaka 618, Japan. *Received February 7, 1991*

To determine whether the addition of a methylene unit in the side chain of the Asp or Arg residue in α-human atrial natriuretic peptide (α-hANP) influences its biological activity, analogs of α-hANP, [Glu^{13}]-α-hANP (7—28) (1), [Aad^{13}]-α-hANP (7—28) (2), and [Har^{n}]-α-hANP(7—28) (where *n* is any possible combination of 11, 14 and 27) (3—9), where the original Asp or Arg residue was replaced by a homo-amino acid, were synthesized by the solid-phase synthesis method. All the analogs were evaluated for their receptor binding, cyclic guanosine monophosphate (cGMP) accumulation activity in rat vascular smooth muscle cells (VSMC), and for vasorelaxant activity employing rat aorta. 1 and 2 were 0.9 and 0.03 times as potent as α-hANP (7—28), respectively, in binding. Har-containing analogs (3—9) were as potent as α-hANP (7—28) in binding. Among the Har-containing analogs, [Har^{11,14}]-α-hANP (7—28) (6) and [Har^{11,27}]-α-hANP (7—28) (7) were remarkably vasorelaxant active, being 4.2 and 5.3 times potent than α-hANP (7—28), respectively, in spite of relatively lower cGMP accumulation activity in the case of 7. The roles of the chargeable amino acid residues in biological activity are discussed.

Keywords α-human atrial natriuretic peptide analog; solid phase peptide synthesis; biological activity; receptor binding; cyclic GMP; vasorelaxation; vascular smooth muscle cell (VSMC)

Alpha-human atrial natriuretic peptide (α-hANP) is a 28-amino acid peptide exhibiting a variety of biological functions including natriuresis/diuresis, vasorelaxation, hypotension and inhibition of aldosterone secretion (Fig. 1).[2,3)] It has been suggested that cyclic guanosine monophosphate (cGMP) mediates the effect of α-hANP through a guanylate cyclase coupled receptor. Three major natriuretic peptide receptor (NP-R) subtypes, designated NP-R_A, -R_B and -R_C, have recently been identified and cloned. The NP-R_A and -R_B (*Mr* 120—140 kilodaltons (kDa)) are guanylate cyclase coupled receptors (B-receptor).[4,5)] On the other hand, the NP-R_C (*Mr* 60—70 kDa) is a guanylate cyclase uncoupled receptor (C-receptor), and may function in the clearance or storage of atrial natriuretic peptide (ANP).[6,7)] However, details of the molecular mechanism of signal transduction of α-hANP is still unclear.

Extensive structure activity studies concerning the α-hANP molecule have revealed the minimum requirements for the expression of full biological activity: 1) the cyclic form is esential for full vasorelaxant activity,[8,9)] 2) α-hANP (7—28) is the minimal peptide which possesses activity equal to α-hANP in all assay systems,[10)] 3) the amino acid residues Phe^{8}, Met^{12}, Asp^{13} and Arg^{27} play important roles in the expression of activity.[11)] Especially, the role of the Asp^{13} residue was demonstrated by Chino's study, where the [D-Asp^{13}]-α-hANP (7—28) analog was inactive in the vasorelaxant assay.[12)] In addition, the importance of the Arg^{27} side chain was confirmed by D-Ala substitution or the deletion of this residue, which resulted in inactive analogs.[11,13)]

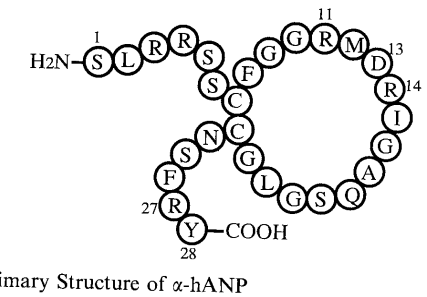

Fig. 1. Primary Structure of α-hANP

Intramolecular disulfide bridge is formed between two cysteine residues.

We were further interested in clarfying the role of chargeable amino acid residues, namely Asp^{13} and Arg^{11,14,27}, by introducing a delicate modification. Previously, we have reported the properties of α-hANP analogs, where the hydrophobic amino acid residues (Phe^{8}, Met^{12}) were replaced by homo-amino acids.[14)] In the course of the evaluation of the activity profile of these analogs we found that these hydrophobic residues are responsible for recognition of the ANP molecule to the B-receptor. In addition, the affinity for the B-receptor was greatly influenced by the side chain length (deletion or addition of a methylene unit) of these hydrophobic residues. We have extended this approach to Asp^{13} and several Arg^{11,14,27} residues, recognized as being critical for vasorelaxation. We prepared [Glu^{13}]-α-hANP (7—28) (**1**), [Aad^{13}]-α-hANP (7—28) (**2**) and 7 analogs of [Har^{n}]-α-ANP (7—28) (where *n* is any possible combination of 11, 14 and 27) (**3**—**9**) to determine whether the addition of a methylene unit in the original Asp or Arg side chain influences biological activity. Alpha-hANP (7—28) was chosen as a parent compound, because of its similar pharmacological profile to α-hANP. In this paper we describe the synthesis of the above analogs and their biological activity.

Results and Discussion

All the peptides were synthesized without difficulty *via* coupling reactions. After HF cleavage, dihydropeptides were subjected to cyclization using $K_3Fe(CN)_6$ with the aid of 8 M urea to minimize the scrambling reaction of disulfide bonds. The desired peptides were purified by carboxymethyl ion-exchange chromatography and by reverse-phase chromatography to homogeneity. Table I shows the physicochemical properties of the analogs synthesized in this study. Purity of all the analogs was more than 97% as judged by analytical HPLC, and the structures were characterized by amino acid analysis and FAB-MS.

The receptor binding potency of the analogs is shown in

TABLE I. Physical Constants of α-hANP (7—28) Analogs

Compd. No.		$[\alpha]_D^{30}/(^\circ)$ $c=0.3$, 1% AcOH	Rf^1	Rf^2	$[M+H]^+$ Found[a]
1	[Glu^{13}]-α-hANP (7—28)	−38.0	0.38	0.56	2406.7
2	[Aad^{13}]-α-hANP (7—28)	−37.7	0.38	0.56	2420.7
3	[Har^{11}]-α-hANP (7—28)	−37.3	0.40	0.52	2407.3
4	[Har^{14}]-α-hANP (7—28)	−38.8	0.40	0.53	2407.2
5	[Har^{27}]-α-hANP (7—28)	−40.0	0.41	0.53	2407.0
6	[Har^{11,14}]-α-hANP (7—28)	−36.7	0.40	0.53	2421.1
7	[Har^{11,27}]-α-hANP (7—28)	−39.2	0.40	0.53	2421.3
8	[Har^{14,27}]-α-hANP (7—28)	−38.1	0.40	0.54	2421.3
9	[Har^{11,14,27}]-α-hANP (7—28)	−45.8	0.42	0.56	2435.1

a) Actual values were in good agreement with calculated values. Satisfactory results were obtained in amino acid composition analysis of the analogs (data not shown).

TABLE II. Biological Activities of α-hANP (7—28) Analogs

Compd. No.	Binding potency		cGMP accumulation activity		Vasorelaxant activity	
	IC_{50} (nM)[a]	R.P.	EC_{50} (nM)[a]	R.P.	EC_{50} (nM)[b]	R.P.
α-hANP (7—28)	1.5	1	160	1	13.8±0.44	1
1	1.6	0.9	800	0.2	183±46	0.06
2	50	0.03	>1000	<0.16	277±35	0.04
3	1.0	1.5	>1000	<0.16	15.5±2.4	0.9
4	2.3	0.7	>1000	<0.16	6.2±1.4	2.2
5	1.6	0.9	630	0.3	6.8±2.8	2.0
6	1.5	1.0	261	0.6	3.3±0.7	4.2
7	1.7	0.9	459	0.3	2.6±0.1	5.3
8	1.7	0.9	401	0.4	5.5±1.3	2.5
9	3.5	0.4	>1000	<0.16	37.2±4.6	0.4

a) Values are means of two separate experiments. *b*) Values are means±S.E. of four separate experiments. R.P.; relative potency.

Table II. Regarding the Asp homolog series, analog **1**, which has one more methylene unit, was 0.9 times as potent as α-hANP (7—28) in binding, whereas **2** (with two more methylene units) showed very weak binding potency (relative potency=0.03). These results indicate that the length of the methylene chain in the Asp residue is a critical factor for binding. The major population (more than 90%) of receptor in this VSMC in the C-receptor.[15] Therefore, apparent receptor binding activity of the analogs in VSMC seems to be attributed mainly to the affinity of the ligand to the C-receptor. Results of the binding assay suggest that **1** (with an additional methylene unit) still has binding affinity to the C-receptor, whereas **2** (with two additional methylene units) does not have affinity to the C-receptor. It should be noted that the ligand recognition of the C-receptor is not as stringent as that of the B-receptor.[16] However, it is interesting that the introduction of only two additional methylene units in the Asp residue resulted in the non-binding analog **2**. Thus, the length of the methylene chain of the Asp residue in the α-hANP molecule is important for the recognition of ANP receptors. On the other hand, analogs containing Har residues **3** through **9** showed almost equal binding potency to that of α-hANP (7—28), indicating that the introduction of Har residues did not strongly affect the binding potency of these analogs.

We then compared cGMP accumulation activity of the analogs (Table II). This activity is assumed to be correlated with affinity of the ligand to the B-receptor. Regarding the Asp homolog series, **1** and **2** were inactive in this cGMP accumulation assay. Among the Har-containing analogs, **3**, **4**, and **9** were relatively weak in the cGMP accumulation assay; **6** was most potent.

Vasorelaxant activities of the analogs were evaluated employing norepinephrine contracted rat aorta (Table II). **1** and **2** were inactive in this assay, consistent with the results of the cGMP accumulation assay. In the group of Har-containing analogs, **6** and **7** were remarkably active in the vasorelaxation assay, despite relatively weak cGMP accumulation activity in the case of **7**. Although the tri-Har-containing analog **9** displayed considerably low vasorelaxant activity, there is a tendency for di-Har-containing analogs (**6**, **7**) to be stronger than mono-Har-containing analogs (**3**—**5**). From the CPK model building study, we speculate that Arg^{11,14,27} may participate in ionic stabilization with the two carboxyl groups of Asp^{13}, C-terminal Tyr^{28} and/or receptor protein on the reverse side of the hydrophobic cluster (formed by the side chains of Phe^8, Met^{12}, Ile^{15} and Leu^{21}).[17] We propose that the introduction of two Har residues into the ANP molecule (analogs **6**, **7**) enhanced vasorelaxant activity by strongly stabilizing possible ionic interactions. However, the three Har residues contained in **9** might actually destabilize the proposed ionic interactions, resulting in weak vasorelaxant activity. We also speculate that these ionic interactions might be destabilized in analogs **1** and **2**.

The results of cGMP accumulation and vasorelaxant activity of the analogs should be carefully discussed due to the complexity of a receptor system.[4-7] In our study, **7** was remarkably potent in the vasorelaxation assay in spite of relatively weak cGMP accumulation activity. A lack of correlation between these two activities was observed in several previous reports,[11,18,19] showing the difficulty of correlating cGMP elevation in cultured cells with vasorelaxation in the intact aortic tissue. We have previously reported that C-type natriuretic peptide (CNP) more potently elevates a cGMP level in VSMC than α-hANP.[20] However, in the assay of aortic tissues, the vasorelaxant activity of CNP was 1/16 that of α-hANP. For this reason we speculated that natriuretic peptide receptors in the VSMC might be different from those in intact aortic smooth muscle.[20] In fact, the existence of two kinds of B-receptor subtypes (NP-R_A and -R_B) has been reported. Although the relationships between the ligands and the receptors are still unclear, we consider that analogs **6** and **7** might have a high affinity to a subtype (which is responsible for vasorelaxation) of B-receptors in aortic tissue; thereby, **6** and **7** showed strong vasorelaxant activity.

In conclusion, we have found that in VSMC the binding potency of analogs **1** and **2** decreased depending upon the length of the methylene units in the Asp side chain, showing the crucial role of the Asp residue. Analog **7** exhibited enhanced vasorelaxant activity in spite of its relatively low cGMP accumulation activity. A lack of correlation between cGMP accumulation and vasorelaxant activity was observed. Further investigations are in progress to define the proposed charge-network which would stabilize the α-hANP molecule intramolecularly and/or intermolecularly with the receptor protein. Also, we further intend to clarify the mechanism of ANP action by using the guanylate cyclase coupled receptor which is specifically expressed in mammalian cells.

Experimental

General Specific optical rotations were measured with a Jasco DIP-360 polarimeter using half dm microcells. *Rf* values on TLC of silica gel (Merck 5714) were determined in the following solvent systems: Rf^1, *n*-BuOH : AcOH : Py : H_2O = 4 : 1 : 1 : 2; Rf^2, *n*-BuOH : AcOH : Py : H_2O = 30 : 6 : 20 : 24. Analytical HPLC was performed on a Shimadzu LC-6A system by using an ODS column (YMC A-302, 4.6 × 150 mm). Amino acid analysis was performed on a Hitachi 835 analyzer after aminopeptidase M digestion, or 24 h of hydrolysis in 6 M HCl containing 0.1% phenol in an evacuated and sealed ampule. The FAB mass spectra were taken on a JEOL mass spectrometer Model JMS-HX100 equipped with FAB ion source. The high-resolution FAB mass spectra were obtained with a JEOL JMS-HX110 spectrometer. Chemicals for peptide synthesis were obtained from Applied Biosystems. The nonnative amino acids (Aad and Har) were obtained from Aldrich and Sigma, and converted to Boc–Aad(OBzl)–OH·DCHA and Z(OMe)–Har(Tos)–OH·CHA by conventional methods. These protected-amino acid DCHA or CHA salts were converted to base-free forms, then used for the coupling reactions.

Boc–Aad(OBzl)–OH·DCHA This compound was prepared according to the modified method of Ratcliffe *et al.*[21]; mp 123—124 °C, $[\alpha]_D^{30}$ +9.0° (c = 1.3, MeOH), Rf^1 0.77, Rf^2 0.77. *Anal.* Calcd for $C_{30}H_{48}N_2O_6 \cdot 1/5 \cdot H_2O$: C, 67.19; H, 9.10; N, 5.22. Found: C, 67.08; H, 8.91; N, 5.24.

Z(OMe)–Har–OH To a solution of HCl·H–Har–OH (20.0 g, 89.0 mmol) and Et_3N (24.9 ml, 178 mmol) in H_2O (220 ml) was added *S*-*p*-methoxybenzyloxycarbonyl-4,6-dimethyl-2-mercaptopyrimidine (32.5 g, 106.8 mmol) in CH_3CN (200 ml). The reaction mixture was stirred at room temperature for 24 h, concentrated to a smaller volume (250 ml) by evaporation and washed with AcOEt (3 × 500 ml). The aqueous layer was saturated with NaCl and its pH was adjusted to 10 with 20% NH_4OH. The resulting residual oil was extracted into *n*-BuOH (500 ml). The solution was concentrated and the residue was triturated with MeOH–AcOEt to give an amorphous solid; yield 26.5 g (84.5%), $[\alpha]_D^{30}$ +6.2° (c = 1.1, MeOH), Rf^1 0.55, Rf^2 0.56. High-resolution FAB-MS for $C_{16}H_{24}N_4O_5$ ($[M+H]^+$): Calcd m/z: 353.1827. Found: 353.1836. This compound was used for the next reaction without further purification.

Z(OMe)–Har(Tos)–OH·CHA Z(OMe)–Har–OH (25.5 g, 72.4 mmol) was dissolved in a mixture of 100 ml of 4 M NaOH and 400 ml of acetone, cooled to 0 °C, and stirred vigorously. *para*-Toluenesulfonyl chloride (41.4 g, 217.2 mmol) dissolved in acetone (200 ml) was added dropwise to the above solution under stirring at 0 °C. The reaction mixture was stirred at 0 °C for 1 h and at room temperature for 3 h. After acetone was removed by evaporation, the resulting aqueous solution was washed with AcOEt (3 × 2 l). The aqueous layer then was cooled to 0 °C, and acidified to pH 3 with 5 M HCl. The resulting oil was extracted into AcOEt (1 l), and evaporated to dryness, leaving an oily product. This crude product was dissolved in $CHCl_3$, and the solution was put on a column of silica gel (Merck Kieselgel 60H) (8 cm × 20 cm), eluted with $CHCl_3$ (2 l), $CHCl_3$–MeOH–AcOH (95 : 5 : 3, v/v/v) (500 ml) and $CHCl_3$–MeOH–AcOH (85 : 15 : 5, v/v/v) (2 l). The pure fractions were pooled and concentrated, washed with H_2O, dried over Na_2SO_4, and concentrated. To the concentrated solution, cyclohexylamine (2.80 ml, 24.5 mmol) was added under cooling with ice-H_2O, triturated with *n*-hexane to give an amorphous solid; yield 13.5 g (31%), $[\alpha]_D^{30}$ +5.9° (c = 1.3, MeOH), Rf^1 0.72, Rf^2 0.74. High-resolution FAB-MS for $C_{23}H_{30}N_4O_7S$ ($[M+H]^+$): Calcd m/z: 507.1915. Found: 507.1913.

Peptide Synthesis All the analogs were synthesized on an Applied Biosystems Peptide Synthesizer, Model 430A, employing Boc chemistry. Starting from 0.5 mmol Boc–Tyr(BrZ)–O–CH_2–Pam resin, Boc-amino acids were successively coupled by DCC–HOBt in NMP. Cleavage from the resin and deprotection was achieved by treating the peptide-resin with HF (8.5 ml per gram of peptide-bound resin) in the presence of *p*-cresol (1.5 ml) at −2 °C for 60 min. The following oxidative cyclization of the crude dihydropeptide was carried out using potassium ferricyanide (1.4 eq) in an 8 M urea solution at pH 7.4. After removal of ferri- and ferrocyanide anions, the peptide was purified to homogeneity (more than 97% pure) by carboxymethyl ion-exchange HPLC (2 cm × 15 cm) followed by reverse-phase HPLC (2 cm × 25 cm). The net content of each peptide for evaluation of biological activity was determined by amino acid analysis after 6 M HCl hydrolysis.

Biological Assays All the analogs were studied according to a competitive receptor binding assay, the accumulation activity of cGMP using VSMC, and a vasorelaxation assay using rat aorta as reported previously.[19] The assay procedures are described briefly below.

Receptor Binding VSMC were derived from explants of rat aorta and were cultured in 24-well plates. VSMC were incubated with 5×10^{-10} M [^{125}I]-α-hANP with various doses of the analog for 45 min at 25 °C. The bound [^{125}I]-α-hANP to VSMC was solubilized with 0.5 N NaOH and the radioactivity was counted by γ-spectrophotometer. Non-specific binding was routinely less than 10% of the total binding. IC_{50} values of the analogs were obtained after creating displacement curves.

cGMP Determination VSMC were cultured in 24-well multiplates as described above and the confluent cells were incubated with the analogs in the presence of 0.5 mM 1-methyl-3-isobutylxanthine for 15 min at 37 °C. The incubation was terminated by aspiration of the assay medium and the addition of 6% perchloric acid. The cells were disrupted by sonication, and cellular cGMP was measured using a cGMP radioimmunoassay kit (Yamasa Shoyu). Activity curves were generated for the EC_{50} calculation.

Vasorelaxant Activity Aortic strips were prepared from the thoracic aorta of male Sprague-Dawley rats. The aortic strip was contracted with 2×10^{-7} M norepinephrine and the vasorelaxant activity of various doses of analog were determined. Maximum relaxation was obtained by the addition of 5×10^{-7} M papaverine. Dose–response curves were obtained for the determination of EC_{50} values.

Acknowledgements We are grateful to Professor Y. Shimonishi and Dr. T. Takao, Institute for Protein Research of Osaka University, for the measurement of FAB-MS. H. Naoki and T. Fujita, Suntory Institute for Bioorganic Research, are gratefully acknowledged for the measurement of high-resolution FAB-MS. We also thank Dr. Y. Shimohigashi, Kyushu University, for helpful comments, and Dr. P. T. M. Kenny, Suntory Institute for Bioorganic Research, for reading the manuscript.

References and Notes

1) The amino acids used in this study are of an L-configuration. Abbreviations used are according to IUPAC-IUB. Commissions, *Eur. J. Biochem.*, **138**, 9 (1984). Other abbreviations: *Mr*, relative molecular mass; DCC, dicyclohexylcarbodiimide; HOBt, 1-hydroxybenzotriazole; NMP, *N*-methylpyrrolidone; FAB-MS, fast atom bombardment mass spectrometry; HPLC, high-performance liquid chromatography; TLC, thin layer chromatography; Aad, 2-aminoadipic acid; Har, homoarginine, Boc, *tert*-buthoxycarbonyl; Z(OMe), *p*-methoxybenzyloxycarbonyl; Tos, tosyl; BrZ, 2-bromobenzyloxycarbonyl; CHA, cyclohexylamine; DCHA, dicyclohexylamine.
2) K. Kangawa and H. Matsuo, *Biochem. Biophys. Res. Commun.*, **118**, 131 (1984).
3) D. B. Northridge and J. McMurray, "Atrial Natriuretic Factor," ed. by A. D. Struthers, Blackwell Scientific Publications, Oxford, London, 1990, pp. 57—87.
4) M. Chinkers, D. L. Garbers, M.-S. Chang, D. G. Lowe, H. Chin, D. V. Goeddel, and S. Schulz, *Nature* (London), **338**, 78 (1989).
5) M.-S. Chang, D. G. Lowe, M. Lewis, R. Hellmiss, E. Chen, and D. V. Goeddel, *Nature* (London) **341**, 68 (1989).
6) T. Maack, M. Suzuki, F. A. Alemedia, D. Nussenzveig, R. M. Scarborough, G. A. McEnroe, and J. A. Lewicki, *Science*, **238**, 675 (1987).
7) F. Fuller, J. G. Porter, A. E. Arfsten, J. Miller, J. W. Schilling, R. M. Scarborough, J. A. Lewicki, and D. B. Schenk, *J. Biol. Chem.*, **263**, 9395 (1988).
8) Y. Hirata, M. Tomita, S. Takada, and H. Yoshimi, *Biochem. Biophys. Res. Commun.*, **128**, 538 (1985).
9) Y. Kitajima, Y. Minamitake, M. Furuya, M. Takehisa, T. Katayama, and S. Tanaka, *Biochem. Biophys. Res. Commun.*, **164**, 1295 (1989).
10) T. X. Watanabe, Y. Noda, N. Chino, Y. Nishiuchi, T. Kimura, S. Sakakibara, and M. Imai, *Eur. J. Pharmacol.*, **147**, 49 (1988).
11) R. F. Nutt and D. F. Veber, *Endocrinology and Metabolism Clinics of North America*, **16**, 19 (1987).
12) N. Chino, Y. Nishiuchi, Y. Noda, T. X. Watanabe, T. Kimura, and S. Sakakibara, "Peptides: Structure and Function, Proceedings of the 9th American Peptid Symposium," ed. by C. M. Deber, V. J. Hruby, and K. D. Kopple, Pierce Chemical Co., Rockford, Illinois, 1986, pp. 945—948.
13) Y. Hayashi, F. Iwasa, M. Furuya, Y. Kanai, Y. Minamitake, I. Kubota, N. Ohnuma, K. Kanagawa, and H. Matsuo, "Peptide Chemistry 1985," ed. by Y. Kiso, Protein. Res. Foundation, Osaka, 1986, pp. 27—32.
14) Y. Minamitake, Y. Kitajima, M. Furuya, M. Yoshida, and S. Tanaka, *Biochem. Biophys. Res. Commun.*, **172**, 971 (1990).
15) G. M. Olins, D. R. Patton, P. R. Bovy, and P. P. Mehta, *J. Biol. Chem.*, **263**, 10989 (1988).

16) P. R. Bovy, J. M. O'Neal, G. M. Olins, and D. R. Patton, *J. Med. Chem.*, **32**, 869 (1989).
17) T. M. Williams, R. F. Nutt, S. F. Brady, T. A. Lyle, T. M. Ciccarone, C. D. Colton, W. J. Palaveda, G. M. Smith, D. F. Veber, and R. J. Winquist, "Peptides: Chemistry, Structure and Biology, Proceedings of the 11th American Peptide Symposium," ed. by J. E. River and G. R. Marshall, ESCOM Sci. Pub., B. Leiden, Netherlands, 1990, pp. 258—259.
18) G. P. Budzik, S. L. Firestone, E. N. Bush, P. J. Connolly, T. W. Rockway, V. K. Sarin, and W. H. Holleman, *Biochem. Biophys. Res. Commun.*, **144**, 422 (1987).
19) Y. Minamitake, M. Furuya, Y. Kitajima, M. Takehisa, and S. Tanaka, *Chem. Pharm. Bull.*, **38**, 1920 (1990).
20) M. Furuya, M. Takehisa, Y. Minamitake, Y. Kitajima, Y. Hayashi, N. Ohnuma, T. Ishihara, N. Minamino, K. Kanagawa, and H. Matsuo, *Biochem. Biophys. Res. Commun.*, **170**, 201 (1990).
21) R. W. Ratcliffe and B. G. Christensen, *Tetrahedron Lett.*, 2907 (1972).

Studies on Antiatherosclerotic Agents.[1] Synthesis and Inhibitory Activities on Platelet Aggregation of 4-Aryl Derivatives of 7-Ethoxycarbonyl-6,8-dimethyl-1(2*H*)-phthalazinone

Yukuo EGUCHI,* Yuko SATO, Satomi SEKIZAKI, and Masayuki ISHIKAWA

Institute for Medical and Dental Engineering, Tokyo Medical and Dental University, 2–3–10, Surugadai, Kanda, Chiyoda-ku, Tokyo 101, Japan.
Received February 21, 1991

4-Aryl derivatives of 7-ethoxycarbonyl-6,8-dimethyl-1(2*H*)-phthalazinone and related derivatives were newly synthesized in order to test for their inhibitory activities on platelet aggregation. 4-(2-Anisyl) compound and the corresponding 1-chloro derivative demonstrated significant activity.

Keywords synthesis; arylcadmium reagent; coupling reaction; 4-(2-anisyl)-7-ethoxycarbonyl-6,8-dimethyl-1(2*H*)-phthalazinone; inhibitory effect; platelet aggregation

In the course of studies on the search for antiatherosclerotic agents, we have found that 7-ethoxycarbonyl-6,8-dimethyl-4-hydroxymethyl-1(2*H*)-phthalazinone[1b] (I) showed potent inhibitory activity on platelet aggregation and cyclic-adenosine monophosphate (AMP) phosphodiesterase. In subsequent studies, compound I was examined for its bioavailability in animals as a potential agent. The examination revealed rapid metabolism of the 4-hydroxymethyl group to the 4-carboxylic acid, which was devoid of the biological activity. It was considered difficult to maintain the activity as an effective plasma level in animals due to low solubility of compound I in water and lipid. Compound I was therefore modified[1a,d,2] in part or the 4-hydroxymethyl group was replaced with other alkyl moieties[1a,b] to improve bioavailability without loss of the activity. Some of the other compounds exhibited fairly potent inhibitory activity on platelet aggregation, however they did not show good balance as a potential agent.

According to the literature, the phthalazines with substituents on their α (1 and/or 4) position such as azelastine[3] with a benzyl, carbazeran[4] with a cyclic amino, and MY-5445[5] with a phenyl, and also aromatic amino moieties have been reported to possess anti-allergic, phosphodiesterase inhibitory, and anti-platelet aggregatory effects, respectively. Considering the structure–activity requirements of the phthalazines, the activities might be primarily attributable to the ring system, but the substituents are also considered to have a role in providing adequate bioavailability.

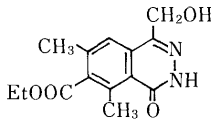

I

Fig. 1

Based on the structure–activity requirements of the phthalazines, compound I was subjected to construction of an aryl moiety in place of the 4-hydroxymethyl group, and a series of derivatives was synthesized.

This paper deals with the synthesis and inhibitory activities on platelet aggregation of 4-aryl derivatives of 7-ethoxycarbonyl-6,8-dimethyl-1(2*H*)-phthalazinone and the related α substituted phthalazines.

Chemistry The synthesis of 4-aryl compounds (**3a—k**) and the analogous 4-(2-thienyl) compound (**4**) were attainable as outlined in Chart 1 by the reactions of 4-ethoxycarbonyl-3,5-dimethylphthalic anhydride (**1**)[1b] with the corresponding arylcadmium reagents to afford the aroyl benzoic acid intermediates (**2**), which, in turn, were condensed by treatment with hydrazine hydrate in ethanol (EtOH). Since the reactions were accompanied by an amount of 1,1-diarylphthalides (**2′**), which arose from subsidiary reaction between the initially formed intermediate **2** and cadmium reagents, column chromatographical purification of the compounds was necessary, and the yields were rather low: 23—60%. Compounds **3k**, **3i**, and **3e** were further modified as shown in Chart 2; oxidation of 4-(2-thioanisyl) compound **3k** using an equimolar amount of *m*-chloroperbenzoic acid (*m*-CPBA) afforded 4-(2-methylsulfinylphenyl) derivative (**3l**) in 75% yield,

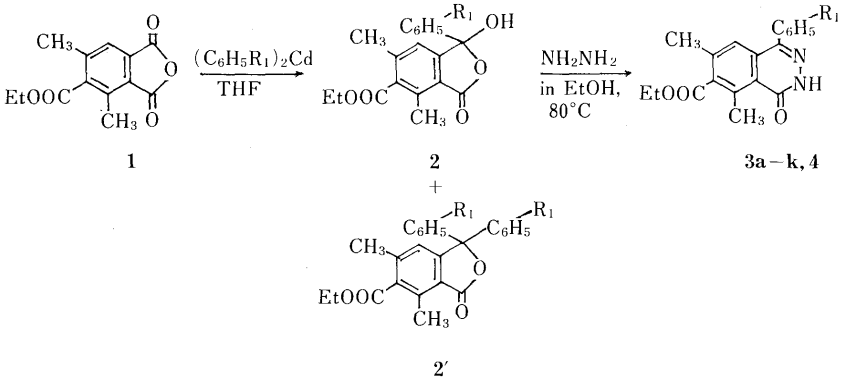

	R_1	yield (%)
3a	H	37
3b	*o*-Me	60
3c	*m*-Me	25
3d	*p*-Me	23
3e	*o*-OMe	51
3f	*p*-OMe	38
3g	*o*-Cl	43
3h	*p*-Cl	38
3i	*o*-OCH_2Ph	24
3j	*p*-OCH_2Ph	32
3k	*o*-SMe	36
4	$C_6H_5R_1$ = 	49

Chart 1

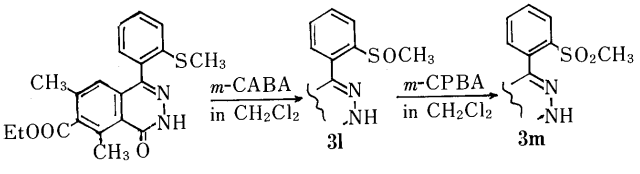

3k 3l 3m

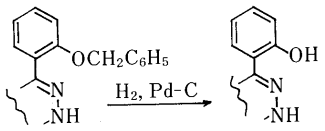

3i 3n

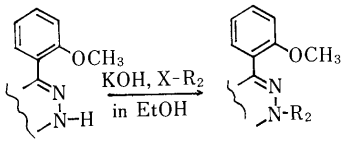

3e 3o, p

	R_2	yield (%)
3o	Me	62
3p	$(CH_2)_2N(Me)_2$	40

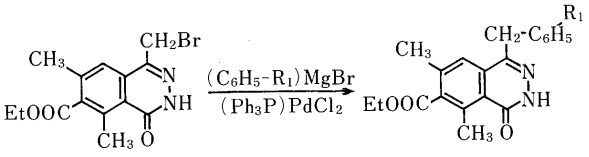

5 6a, b

	R_1	yield (%)
6a	H	72
6b	*o*-OMe	58

Chart 2

while the treatment of an excess *m*-CPBA gave 4-(2-methylsulfonylphenyl) derivative (**3m**) in good yield. Catalytic debenzylation of **3i** over palladium on carbon (Pd–C) under atmospheric pressure led smoothly to the corresponding 4-(2-hydroxyphenyl) derivative (**3n**). Meanwhile, compound **3e** was reacted with methyl iodide and dimethylaminoethyl chloride in 5% potassium hydroxide (KOH) in EtOH, and the N^2-alkylated derivatives (**3o, p**) were obtained in 62 and 40% yields, respectively.

Additionally, the other 4-benzyl analogues (**6a, b**) were prepared by coupling reactions of a related 4-bromomethyl compound (**5**)[1b] with aryl magnesium reagents catalyzed by bis(triphenylphosphine)palladium(II) chloride in the described manner.[6,7]

Conversion of the phthalazinone to phthalazine was readily accomplished by heating **3e** with $POCl_3$ for half an hour to afford an α chlorinated derivative (**7a**) in 80% yield. The resulting compound **7a** was transformed into the requisite α substituted phthalazines by the following procedures (a—d): (a) The chlorine atom of **7a** was substituted with methoxy and ethylthio moieties by the conventional synthetic procedure[8] to afford **7b** and **7c**, respectively. (b) Several amino derivatives (**7d—j**) were derivatized from **7a** by treatment of the corresponding amines without solvents, with moderate yields. Since dimethylamino and *o*-chloroanilino derivatives (**7d, h**) were obtained as an oil, they led to oxalate and HCl salt, respectively. (c) Dechlorination of **7a** by hydrogen in the presence of Pd–C afforded a naked phthalazine (**7k**). The compound was converted into HCl salt with high solubility in water. (d) Phenylacetylenic moiety was also introduced

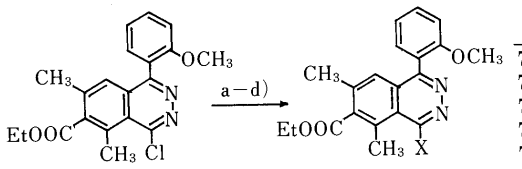

7a 7b—m

	method	agent	temp. (°C)	time (h)	X	yield (%)
7b	a	NaOEt	60	0.5	OEt	68
7c	a	NaSEt	80	0.5	SEt	63
7d	b	40%-dimethylamine	r.t.	12	$N(Me)_2 \cdot C_2O_4H_2$	76
7e	b	piperidine	80	3	N⟨⟩	58
7f	b	*N*-benzylpiperazine	100	2	N⟨⟩NCH2Ph	63
7g	b	*m*-chloroaniline	80	3	NHC_6H_4 (*m*-Cl)	65
7h	b	*o*-chloroaniline	80	3	NHC_6H_4 (*o*-Cl)·HCl	71
7i	b	*p*-methoxybenzylamine	80	3	$NHCH_2C_6H_4$ (*p*-OMe)	77
7j	b	benzylamine	90	2	$NHCH_2Ph$	81
7k	c	H_2, Pd-C	r.t.	8	H·HCl	44
7l	d	PhC≡CH, $(Ph_3P)PdCl_2$	90	4	C≡CPh	51
7m	d	H_2, Pd-C	r.t.	6	CH_2CH_2Ph	88

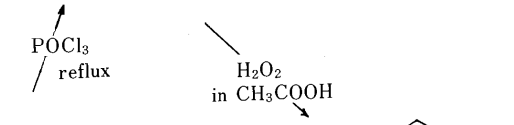

3e 8

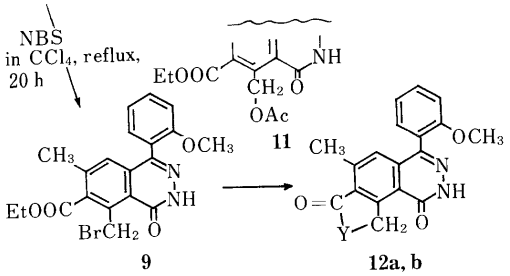

9 11 12a, b

	Y	yield (%)
12a	O	82
12b	NH	84

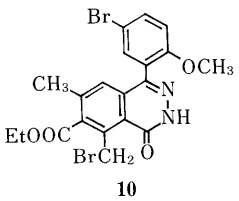

10

Chart 3

to afford **7l** by the manner described[9] using phenylacetylene with a catalyst of palladium complex. This **7l** was then reduced in hydrogen over Pd–C, affording an α phenethyl derivative (**7m**) in good yield.

Since compound **7a** was considerably susceptible to hydrolysis to regenerate **3e** under conditions of even a weak hydrolytic medium, such as hot EtOH–water, it was possible that if **7a** were N^2-oxidized, it would not undergo hydrolytic change to generate **3e**. Compound **7a** was then subjected to *N*-oxidation reaction by means of hydrogen peroxide in glacial acetic acid; fortunately, an oxygen atom was directed to the N^2 position near the chlorine atom of **7a**, despite there being a result obtained[10] that an oxygen atom was introduced to the N^3 position, when *N*-oxidation reaction was carried out on related 1-chloro-4-methylphthalazine under a similar reaction condition. Location of the oxygen atom introduced was confirmed by the fact that compound **8** remained intact with prolonged heating in 5% KOH–EtOH. Presumably, an electronic repulsion of the 4-(2-anisyl) moiety near the N^3 atom resulted in a settlement of the oxygen atom on the N^2 position in the *N*-oxidation reaction.

When **3e** was reacted with *N*-bromosuccinimide in CCl_4, the 8-methyl hydrogen of **3e** was selectively brominated to give **9** with a minor quantity of dibrominated compound (**10**). The structure of **9** was determined by comparison of proton nuclear magnetic resonance (^{1}H-NMR) spectra of **3e** and **9**. 6-Methyl protons of **3e** appeared at 2.32 ppm, while the 8-methyl protons at 2.94 ppm. The latter signals demonstrated a lower value under influence of both carbonyls on adjacent sides of the 8-methyl protons. On the other hand, methyl signals of **9** exhibited at 2.37 ppm. The value approximates the 2.32 ppm observed in 6-methyl protons of **3e**. Compound **10** was consistent with an analysis[11] of spectra taken by high frequency ^{1}H-NMR spectroscopy. Checking on the signals appearing at 6.93 ppm in a doublet pattern with a coupling constant of 8.8 Hz suggests the existence of a methoxy group as well as a proton at the *ortho* position; the signals thus correspond to H_3 of the 4-(2-anisyl) moiety. Signals appearing at 7.61 ppm in a doublet-doublet with 8.8 and 2.5 Hz correspond to H_4 of the moiety due to a downfield shift by bromine effect with couplings between the *ortho* H_3 and the *meta* H_6. The 6-proton designated at 7.43 ppm was in a doublet pattern with 2.5 Hz.

Finally, compound **9** was converted to an acetoxy derivative (**11**) by reaction with acetic acid which, in turn, was reacted with 5% KOH in EtOH to provide the lactone derivative (**12a**). When **9** was reacted with ammonia in EtOH, the lactam derivative (**12b**) was obtained in good yield.

Results and Discussion

Compounds listed in Tables I and II were tested for their inhibitory activities on platelet aggregation induced by both arachidonic acid (AA, 100 μM) and adenosine diphosphate (ADP, 30 μM). The optical density method of Born[12] was used to assess the ability of test compounds. The inhibitory activities were expressed by the term IC_{50} as the concentration that inhibited the induced aggregation by 50%. The data obtained at several concentrations were presented as means of three runs.

Table I. Biological Activities of Compounds

Compd.	Inhibition of AA and ADP-induced platelet aggregation (IC_{50}, μM)	
	AA (100 μM)	ADP (30 μM)
3a	3—7	100
3b	20	100
3c	100	100
3d	50—70	100
3e	1—3	100
3f	50—70	100
3g	5—10	100
3h	30—50	100
3i	100	100
3j	100	100
3k	20	60
3l	50—70	100
3m	50—70	100
3n	20	100
3o	5—7	60
3p	100	60
4	30—50	100
6a	100	40
6b	70	40

Table II. Biological Activities of Compounds

Compd.	Inhibition of AA and ADP-induced platelet aggregation (IC_{50}, μM)	
	AA (100 μM)	ADP (30 μM)
7a	1—2	100
7b	50—100	60
7c	100	100
7d	30—50	60
7e	50—70	100
7f	70	100
7g	100	100
7h	100	100
7i	70	100
7j	70	60
7k	3—7	60
7l	100	100
7m	100	100
8	20—50	100
12a	100	100
12b	100	100

In a preliminary test, the reference phthalazinone I marked the IC_{50} 1—5 μM on AA, and 10—20 μM on ADP, respectively.

As can be seen, the results showed no effective compounds marked on ADP, except 4-benzyl compounds **6a**, **b** which exhibited activity to some extent. On the contrary, some compounds demonstrated considerable inhibitory activity on AA when compared to the referenced phthalazinone I. Among them, the 4-phenyl **3a**, *o*-anisyl **3e**, *o*-chlorophenyl **3g**, N^2-methylated *o*-anisyl compounds **3o** in Table I, an α chloro **7a** and its dechlorinated compound **7k** in Table II showed fairly potent activity, and *o*-anisyl and its α chlorinated compounds **3e**, **7a** demonstrated particularly significant activities. The potencies of the activities on AA of both compounds were comparable to the referenced phthalazinone I.

From the results of this test, the structure–activity relation of **3e** and **7a**, together with the tested compounds may be explained as follows.

TABLE III. Data for Compounds **3a**—**p**, **4**, and **6a**, **b**

Compd.	mp (°C) (Solvent)[a]	Formula	Analysis (%) Calcd (Found) C	H	N	UV (EtOH, nm)	^{1}H-NMR ($CDCl_3$, J=Hz)
3a	207—209 (EtOH)	$C_{19}H_{18}N_2O_3$	70.79 (70.72	5.63 5.65	8.69 8.72)	277, 293, 322	1.43 (3H, t, 7), 2.38 (3H, s), 2.96 (3H, s), 4.48 (2H, q, 7), 7.36 (1H, s), 7.51 (5H, s), 10.37 (1H, s)
3b	223—224 (EtOH)	$C_{20}H_{20}N_2O_3$	71.41 (71.31	5.99 6.00	8.33 8.46)	219, 298, 311, 324	1.42 (3H, t, 7), 2.14 (3H, s), 2.31 (3H, s), 2.95 (3H, s), 4.42 (2H, q, 7), 6.93 (1H, s), 7.34 (4H, s), 10.79 (1H, s)
3c	175—176 (EtOH)	$C_{20}H_{20}N_2O_3$	71.41 (71.41	5.99 6.04	8.33 8.38)	215, 225, 300, 312, 325	1.42 (3H, t, 7), 2.37 (3H, s), 2.45 (3H, s), 2.95 (3H, s), 4.46 (2H, q, 7), 7.34 (5H, s), 10.44 (1H, s)
3d	205—207 (EtOH)	$C_{20}H_{20}N_2O_3$	71.41 (71.37	5.99 6.05	8.33 8.40)	227, 301, 311, 325	1.42 (3H, t, 7), 2.36 (3H, s), 2.46 (3H, s), 2.95 (3H, s), 4.48 (2H, q, 7), 7.37 (5H, s), 10.43 (1H, s)
3e	185—187 (EtOAc–ether)	$C_{20}H_{20}N_2O_4$	68.17 (68.20	5.72 5.68	7.95 7.89)	217, 282, 295, 310, 321	1.41 (3H, t, 7), 2.32 (3H, s), 2.94 (3H, s), 3.72 (3H, s), 4.45 (2H, q, 7), 6.96—7.50 (5H, m), 10.46 (1H, s)
3f	210—211 (MeOH)	$C_{20}H_{20}N_2O_4$	68.17 (68.15	5.72 5.75	7.95 8.00)	229, 262, 303, 310	1.42 (3H, t, 7), 2.37 (3H, s), 2.95 (3H, s), 3.89 (3H, s), 4.46 (2H, q, 7), 7.22 (4H, d, d, 9, 4), 7.38 (1H, s), 10.66 (1H, s)
3g	224—225 (EtOH)	$C_{19}H_{17}ClN_2O_3$	63.90 (63.85	4.96 5.03	7.84 7.90)	227, 260, 297, 310, 323	1.41 (3H, t, 7), 2.34 (3H, s), 2.95 (3H, s), 4.48 (2H, q, 7), 6.92 (1H, s), 7.45 (4H, m), 10.62 (1H, s)
3h	245—247 (MeOH)	$C_{19}H_{17}ClN_2O_3$	63.90 (63.86	4.96 4.99	7.84 7.88)	265, 296, 320	1.42 (3H, t, 7), 2.35 (3H, s), 2.95 (3H, s), 4.50 (2H, q, 7), 6.95 (1H, s), 7.43 (4H, d, d, 9, 4), 10.46 (1H, s)
3i	186—188 (EtOH)	$C_{26}H_{24}N_2O_4$	72.88 (72.85	5.65 5.70	6.54 6.60)	218, 282, 296, 320	1.42 (3H, t, 7), 2.31 (3H, s), 2.95 (3H, s), 4.48 (2H, q, 7), 5.05 (2H, s), 7.19 (10H, m), 10.54 (1H, s)
3j	245—247 (MeOH)	$C_{26}H_{24}N_2O_4$	72.88 (73.00	5.65 5.70	6.54 6.59)	209, 227, 303	1.42 (3H, t, 7), 2.38 (3H, s), 2.95 (3H, s), 4.48 (2H, q, 7), 5.16 (2H, s), 7.00—7.50 (10H, m), 10.19 (1H, s)
3k	182—184 (EtOAc–ether)	$C_{20}H_{20}N_2O_3S$	65.21 (65.19	5.47 5.51	7.61 7.64)	219, 296	1.41 (3H, t, 7), 2.32 (3H, s), 2.38 (3H, s), 2.95 (3H, s), 4.46 (2H, q, 7), 6.92 (1H, s), 7.42 (4H, m), 10.77 (1H, s)
3l	210—212 (MeOH–ether)	$C_{20}H_{20}N_2O_4S$	62.49 (62.65	5.24 5.30	7.29 7.30)	202, 221, 300	1.41 (3H, t, 7), 2.32 (3H, s), 2.79 (3H, s), 2.92 (3H, s), 4.48 (2H, q, 7), 7.03 (1H, s), 7.26—8.40 (4H, m), 11.01 (1H, s)
3m	252—254 (MeOH)	$C_{20}H_{20}N_2O_5S$	59.99 (59.92	5.04 5.08	7.00 7.05)	219, 297	1.40 (3H, t, 7), 2.30 (3H, s), 2.91 (3H, s), 3.19 (3H, s), 4.45 (2H, q, 7), 6.80 (1H, s), 7.27—8.36 (4H, m), 11.01 (1H, s).
3n[b]	222—223 (EtOAc)	$C_{19}H_{18}N_2O_4$	67.44 (67.54	5.36 5.32	8.28 8.30)	217, 236, 284, 295, 310, 321	1.41 (3H, t, 7), 2.32 (3H, s), 2.89 (3H, s), 4.41 (2H, q, 7), 6.90—7.50 (5H, m), 9.12 (1H, OH), 12.07 (1H, s)
3o	113—115 (Ether–*n*-hexane)	$C_{21}H_{22}N_2O_4$	68.83 (68.87	6.05 6.07	7.65 7.69)	219, 235, 283, 301, 312, 325	1.40 (3H, t, 7), 2.30 (3H, s), 2.93 (3H, s), 3.72 (3H, s), 3.83 (3H, s), 4.45 (2H, q, 7), 6.80—7.65 (5H, m)
3p	106—108 (Ether)	$C_{24}H_{29}N_3O_4$	68.06 (68.13	6.90 6.94	9.92 9.98)	219, 302	1.41 (3H, t, 7), 2.33 (9H, s), 2.79 (2H, m), 2.93 (3H, s), 3.73 (3H, s), 4.25 (2H, m), 4.47 (2H, q, 7), 6.92—7.55 (5H, m)
4	186—188 (EtOAc)	$C_{17}H_{16}N_2O_3S$	62.19 (62.16	4.91 4.89	8.53 8.60)	213, 231, 263, 312	1.43 (3H, t, 7), 2.43 (3H, s), 2.95 (3H, s), 4.49 (2H, q, 7), 7.32 (3H, m), 7.76 (1H, s), 10.85 (1H, s)
6a	140—141 (EtOAc)	$C_{20}H_{20}N_2O_3$	71.41 (71.37	5.99 6.13	8.33 8.23)	216, 260, 296, 309, 321	1.40 (3H, t, 7), 2.36 (3H, s), 2.89 (3H, s), 4.22 (2H, s), 4.42 (2H, q, 7), 7.26 (5H, s), 7.41 (1H, s), 10.35 (1H, s)
6b	166—168 (EtOAc–ether)	$C_{21}H_{22}N_2O_4$	68.83 (68.85	6.05 6.02	7.65 7.70)	217, 260, 282, 296, 311, 323	1.40 (3H, t, 7), 2.37 (3H, s), 2.89 (3H, s), 3.92 (3H, s), 4.20 (2H, s), 4.45 (2H, q, 7), 6.80—7.20 (4H, m), 7.54 (1H, s), 10.10 (1H, s)

a) Recrystallization solvent. *b*) NMR spectra were taken in $CDCl_3$+DMSO-d_6.

In comparing the 4-tolyl compounds **3b**, **c**, **d**, the activities decreased in *ortho*-, *para*-, and *meta*-order. This tendency was also observed in the anisyl **3e**, **f**, chlorophenyl **3g**, **h**, and benzyloxyphenyl **3i**, **j** compounds. With regard to the *ortho*-substituents on the 4-aryl moieties, the unsubstituted and methoxy moieties seemed to be effective. Replacing the methoxy oxygen with sulfur decreased the activity. The aryl moiety had to be connected directly to the phthalazinone for the activity in this test.

In the derivatives of **3e** in Table II, the potencies of the activities were generally decreased only when the α carbonyl moiety was substituted for the other moieties. However, it was clear that the chlorine moiety **7a** significantly enhanced the activity of **3e**. Meanwhile, hydrolytic change of the chlorine moiety from **7a** to **3e** was definitely observed in a diluted hydrolytic media. The N^2-oxide **8** gained considerable durability from the change, but the activity was greatly decreased. Compound **7a** thus appeared to act as a precursor for **3e**.

The modified compound **3e**, and both **12a** and **12b** lost their activity. It was found that the 7-ethyl ester might have a role[1b] in the platelet aggregation inhibitory activity.

As described, although compounds **3e**, **7a** did not show the activity on ADP, these compounds were selected as candidates for further pharmacological evaluations from this experiment. Concerning the solubility in lipid, both compounds increased their ability in organic solvents. The 4-(*o*-anisyl) moiety might provide an adequate bioavailability, and hopefully protect from the rapid metabolic degradation which was seen in the referenced phthalazinone I.

Experimental

All melting points were determined in a capillary tube and are uncorrected. Mass spectra (MS) were recorded by a Hitachi RMU-7L spectrometer, ultraviolet (UV) spectra with a Hitachi model 323 and U-3200 spectrometers, infrared (IR) spectra were determined with a Hitachi model 285 spectrometer, and ^{1}H-NMR spectra with a JEOL JUM-C-60 HL machine. ^{1}H-NMR spectra of compound **10** were taken by a JEOL JNM-FX 270 spectrometer. Merck Silica gel 60 was used for column chromatography.

TABLE IV. Data for Compounds **7a—m**, **8**, and **12a, b**

Compd.	mp (°C) (Solvent)[a]	Formula	Analysis (%) Calcd (Found) C	H	N	^{1}H-NMR ($CDCl_3$, J=Hz)
7a	125—126 (Ether)	$C_{20}H_{19}ClN_2O_3$	64.70 (64.81)	5.12 5.11	7.54 7.61)	1.43 (3H, t, 7), 2.38 (3H, s), 2.94 (3H, s), 3.69 (3H, s), 4.51 (2H, q, 7), 6.90—7.70 (4H, m), 7.10 (1H, s)
7b	113—115 (Ether)	$C_{22}H_{24}N_2O_4$	69.45 (69.41)	6.36 6.41	7.36 7.39)	1.42 (3H, t, 7), 1.54 (3H, t, 7), 2.36 (3H, s), 2.85 (3H, s), 3.69 (3H, s), 4.46 (2H, q, 7), 4.73 (2H, q, 7), 6.95—7.50 (5H, m)
7c	119—121 (Ether)	$C_{22}H_{24}N_2O_3S$	66.65 (66.62)	6.10 6.13	7.07 7.12)	1.39 (3H, t, 7), 1.48 (3H, t, 7), 2.34 (3H, s), 2.69 (3H, s), 3.44 (2H, q, 7), 3.69 (3H, s), 4.41 (2H, q, 7), 6.92—7.65 (5H, m)
7d	170—172 (Acetone–ether)	$C_{24}H_{27}N_3O_7$	61.40 (61.31	5.80 5.90	8.95 9.05)	1.44 (3H, t, 7), 2.42 (3H, s), 2.80 (3H, s), 3.18 (6H, s), 3.75 (3H, s), 4.49 (2H, q, 7), 6.90—7.71 (5H, m), 13.32 (2H, s, $(COO\underline{H})_2$)
7e	140—142 (Ether)	$C_{25}H_{29}N_3O_3$	71.57 (71.47	6.97 7.01	10.02 10.13)	1.42 (3H, t, 7), 1.77 (6H, br), 2.35 (3H, s), 2.94 (3H, s), 3.03 (2H, br), 3.56 (2H, br), 3.69 (3H, s), 4.47 (2H, q, 7), 6.94—7.52 (5H, m)
7f	196—198 (MeOH)	$C_{31}H_{34}N_4O_3$	72.91 (72.87	6.71 6.73	10.97 11.04)	1.41 (3H, t, 7), 2.36 (3H, s), 2.92 (3H, s), 2.50—3.10 (4H, m), 3.51 (4H, br), 3.60 (2H, s), 3.69 (3H, s), 4.46 (2H, q, 7), 6.90—7.55 (10H, m)
7g	151—153 (Ether)	$C_{26}H_{24}ClN_3O_3$	67.60 (67.58	5.41 5.43	9.10 9.20)	1.41 (3H, t, 7), 2.29 (3H, s), 2.91 (3H, s), 3.73 (3H, s), 4.46 (2H, q, 7), 6.75—7.50 (9H, m), 8.88 (1H, s)
7h	117—120 (Ether)	$C_{26}H_{25}Cl_2N_3O_3$	52.20 (52.17	5.22 5.27	8.43 8.72)	1.43 (3H, t, 7), 2.46 (3H, s), 2.95 (3H, s), 3.76 (3H, s), 4.49 (2H, q, 7), 7.00—8.20 (9H, m)
7i	120—121 (Ether)	$C_{28}H_{29}N_3O_4$	71.32 (71.31	6.20 6.25	8.91 8.94)	1.39 (3H, t, 7), 2.32 (3H, s), 2.77 (3H, s), 3.69 (3H, s), 3.82 (3H, s), 4.41 (2H, q, 7), 4.12 (2H, d, 4), 5.38 (1H, br), 6.80—7.48 (8H, m)
7j	136—138 (Benzene–ether)	$C_{27}H_{27}N_3O_3$	73.45 (73.50	6.16 6.20	9.52 9.60)	1.39 (3H, t, 7), 2.33 (3H, s), 2.79 (3H, s), 3.69 (3H, s), 4.42 (2H, q, 7), 4.90 (2H, d, 5), 5.50 (1H, br), 7.00—7.65 (5H, m), 7.35 (5H, m)
7k	110—112 (Ether)	$C_{20}H_{20}N_2O_3$	71.41 (71.39	5.99 5.90	8.33 8.29)	1.44 (3H, t, 7), 2.42 (3H, s), 2.76 (3H, s), 3.69 (3H, s), 4.50 (2H, q, 7), 7.00—7.65 (5H, m), 9.72 (1H, s)
7l	185—187 (EtOAc–ether)	$C_{28}H_{24}N_2O_3$	77.04 (77.01	5.54 5.60	6.42 6.49)	1.43 (3H, t, 7), 2.40 (3H, s), 3.19 (3H, s), 3.69 (3H, s), 4.49 (2H, q, 7), 7.00—7.75 (10H, m)
7m	123—125 (EtOAc)	$C_{28}H_{28}N_2O_3$	76.34 (76.31	6.41 6.43	6.36 6.38)	1.43 (3H, t, 7), 2.38 (3H, s), 2.87 (3H, s), 3.45 (2H, m), 3.69 (3H, s), 3.78 (2H, m), 4.45 (2H, q, 7), 7.70—8.59 (10H, m)
8	217—219 (MeOH)	$C_{20}H_{19}ClN_2O_4$	62.03 (62.21	4.91 5.07	7.23 7.31)	1.41 (3H, t, 7), 2.34 (3H, s), 2.93 (3H, s), 3.71 (3H, s), 4.44 (2H, q, 7), 6.88—7.55 (5H, m)
12a[b]	300 (MeOH)	$C_{18}H_{14}N_2O_4$	67.07 (67.06	4.38 4.40	8.69 8.70)	2.70 (3H, s), 3.76 (3H, s), 5.79 (2H, s), 7.31 (5H, m), 13.08 (1H, s)
12b[b]	285—287 (MeOH)	$C_{18}H_{15}N_3O_3$	67.28 (67.28	4.71 4.73	13.08 13.13)	2.67 (3H, s), 3.71 (3H, s), 4.79 (2H, s), 7.28 (5H, m), 8.79 (1H, s), 12.86 (1H, s)

a) Recrystallization solvent. *b*) NMR spectra were taken in DMSO-d_6.

Preparation of 3a—k, and 4. 4-(2-Anisyl)-7-ethoxycarbonyl-6,8-dimethyl-1(2*H*)-phthalazinone (3e) To the Grignard reagent [prepared from *o*-bromoanisole (9.35 g, 0.05 mol), Mg turning (1.94 g, 0.08 mol)] in anhydrous ether (120 ml) was added portionwise anhydrous $CdCl_2$ (9.2 g, 0.05 mol). The mixture was stirred for 30 min at room temperature, then was added dropwise a solution of **1** (8.68 g, 0.035 mol) in tetrahydrofuran (THF) (50 ml). The mixture was heated to reflux for 1 h. The reaction mixture was decomposed by addition of 5% H_2SO_4. The organic layer (A) was extracted with 10% K_2CO_3. The alkaline extract was acidified with 1 N HCl, and it was re-extracted with EtOAc. Working-up afforded an oil, which was dissolved in EtOH (100 ml) and treated with hydrazine hydrate (4 ml). The new mixture was heated to 80 °C for 2 h. Evaporation of the solvent and purification of the residue by column chromatography with benzene–EtOAc (100:3) afforded 6.8 g (51%) of **3e**, melted at 185—187 °C (EtOAc–ether). *Anal.* Calcd for $C_{20}H_{20}N_2O_4$: C, 68.17; H, 5.72; N, 7.95. Found: 68.20; H, 5.68; N, 7.89. MS *m/z*: 352 (M^+), 323 (M^+-Et), 321 (M^+-OMe), 307 (M^+-OEt), 293. UV λ_{max}^{EtOH} nm: 217, 282, 295, 310, 321. ^{1}H-NMR ($CDCl_3$) δ: 1.41 (3H, t, J=7 Hz), 2.32 (3H, s), 2.94 (3H, s), 3.72 (3H, s), 4.45 (2H, q, J=7 Hz), 6.96—7.50 (5H, m), 10.46 (1H, s).

The organic mother layer (A) was purified by column chromatography with benzene to afford 2.1 g (13.4%) of 1,1-(2-anisyl)-5-ethoxycarbonyl-4,6-dimethylphthalide, melted at 147—149 °C (MeOH). *Anal.* Calcd for $C_{27}H_{26}O_6$: C, 72.63; H, 5.87. Found: C, 72.59; H, 5.88. MS *m/z*: 446 (M^+), 401 (M^+-OEt), 387, 371. ^{1}H-NMR ($CDCl_3$) δ: 1.40 (3H, t, J=7 Hz), 2.38 (3H, s), 2.68 (3H, s), 3.50 (6H, s), 4.42 (2H, q, J=7 Hz), 6.60—7.41 (9H, m).

7-Ethoxycarbonyl-6,8-dimethyl-4-(2-methylsulfinylphenyl)-1(2*H*)-phthalazinone (31) A mixture of **3k** (368 mg, 1 mmol) and *m*-CPBA (173 mg, 1 mmol) in CH_2Cl_2 (20 ml) was placed for 5 h with external water cooling. The mixture was washed with 10% K_2CO_3 and water. Evaporation of the solvent and recrystallization of the residue from MeOH–ether afforded 290 mg (75.5%) of **3k**, melted at 210—212 °C. *Anal.* Calcd for $C_{20}H_{20}N_2O_4S$: C, 62.49; H, 5.24; N, 7.29. Found: C, 62.65; H, 5.30; N, 7.30. MS *m/z*: 384 (M^+), 369 (M^+-Me), 355 (M^+-Et), 339 (M^+-OEt). UV λ_{max}^{EtOH} nm: 202, 221, 300. ^{1}H-NMR ($CDCl_3$) δ: 1.41 (3H, t, J=7 Hz), 2.32 (2H, s), 2.79 (3H, s), 2.92 (3H, s), 4.48 (2H, q, J=7 Hz), 7.03 (1H, s), 7.26—8.40 (4H, m), 11.01 (1H, s).

Compound **3m** was prepared from **3k** in a similar manner using 3 times the amount of *m*-CPBA in a molar ratio.

7-Ethoxycarbonyl-4-(2-hydroxyphenyl)-6,8-dimethyl-1(2*H*)-phthalazinone (3n) Compound **3i** (350 mg) in EtOH (50 ml) was shaken in H_2 in the presence of 5% Pd–C (20 mg) under atmospheric pressure for 2 h. The catalyst was filtered off and the filtrate was evaporated to afford 250 mg (90.5%) of **3n**. mp 222—223 °C (EtOAc). *Anal.* Calcd for $C_{19}H_{18}N_2O_4$: C, 67.44; H, 5.36; N, 8.28. Found: C, 67.54; H, 5.32; N, 8.30. MS *m/z*: 338 (M^+), 323, 309 (M^+-Et), 293 (M^+-OEt). UV λ_{max}^{EtOH} nm: 217, 236, 284, 295, 310, 321. ^{1}H-NMR ($CDCl_3$ + DMSO-d_6) δ: 1.41 (3H, t, J=7 Hz), 2.32 (3H, s), 2.89 (3H, s), 4.41 (2H, q, J=7 Hz), 6.90—7.50 (5H, m), 9.12 (1H, OH), 12.07 (1H, s).

Preparation of 3o, p. 4-(2-Anisyl)-7-ethoxycarbonyl-2-(2-dimethylamino)ethyl-6,8-dimethyl-1(2*H*)-phthalazinone (3p) A mixture of **3e** (250 mg, 0.7 mmol) and dimethylaminoethylchloride (100 mg, 0.9 mmol) in MeOH (10 ml) containing 5% NaOH (2 ml) was stirred at room temperature for 2 d. The mixture was concentrated and extracted with EtOAc. Purification by chromatography with chloroform–MeOH (50:1) afforded 120 mg (40%) of **3p**. mp 106—108 °C (ether). *Anal.* Calcd for $C_{24}H_{29}N_3O_4$: C, 68.06; H, 6.90; N, 9.92. Found: C, 68.13; H, 6.94; N, 9.90. UV λ_{max}^{EtOH} nm: 219, 302. ^{1}H-NMR ($CDCl_3$) δ: 1.41 (3H, t, J=7 Hz), 2.33 (9H, s), 2.79 (2H, m), 2.93 (3H, s), 3.73 (3H, s), 4.25 (2H, m), 4.47 (2H, q, J=7 Hz), 6.92—7.55 (5H, m).

Preparation of 6a, b. 4-(2-Anisyl)methyl-7-ethoxycarbonyl-6,8-dimethyl-1(2*H*)-phthalazinone (6b) To the Grignard reagent [prepared from *o*-bromoanisole (9.35 g, 0.05 mol), Mg turning (1.94 g, 0.08 mol)] in an-

hydrous THF (120 ml) was added **5** (4.0 g, 0.01 mol), and then bis-(triphenylphosphine)palladium(II) chloride (50 mg, 0.07 mmol). The reaction mixture was stirred at room temperature for 20 h and was decomposed by addition of 5% H_2SO_4. The organic layer was separated and washed with water, then evaporated to afford crude oil. The oil was purified by column chromatography with benzene–EtOAc (10 : 1) to afford 2.5 g (58%) of **6b**, melted at 166—168 °C (EtOAc–ether). *Anal.* Calcd for $C_{21}H_{22}N_2O_4$: C, 68.83; H, 6.05; N, 7.65. Found: C, 68.85; H, 6.02; N, 7.70. MS *m/z*: 366, 335, 321, 307. UV λ_{max}^{EtOH} nm: 217, 260, 282, 296, 311, 323. ^{1}H-NMR ($CDCl_3$) δ: 1.40 (3H, t, J=7 Hz), 2.37 (3H, s), 2.89 (3H, s), 3.92 (3H, s), 4.20 (2H, s), 4.45 (2H, q, J=7 Hz), 6.80—7.20 (4H, m), 7.54 (1H, s), 10.10 (1H, s).

4-(2-Anisyl)-1-chloro-7-ethoxycarbonyl-6,8-dimethylphthalazine (7a) A mixture of **3e** (3.0 g, 0.08 mol) and $POCl_3$ (10 ml) was refluxed for 30 min. Excess $POCl_3$ was concentrated under reduced pressure. The mixture was poured into ice-water with vigorous stirring. The aqueous mixture was neutralized with 5% K_2CO_3, then extracted with chloroform. The extract was washed with water and evaporated to afford crude **7a**. Recrystallization from ether gave 2.7 g (85.7%) of pale yellow crystals. mp 125—126 °C (ether). *Anal.* Calcd for $C_{20}H_{19}ClN_2O_3$:C, 64.70; H, 5.12; N, 7.54. Found: C, 64.81; H, 5.11; N, 7.61. MS *m/z*: 370 (M^+), 341 (M^+-Et), 335 (M^+-Cl), 325 (M^+-OEt). UV ν_{max}^{EtOH} nm: 235, 280, 292, 320. ^{1}H-NMR ($CDCl_3$) δ: 1.43 (3H, t, J=7 Hz), 2.38 (3H, s), 2.94 (3H, s), 3.69 (3H, s), 4.51 (2H, q, J=7 Hz), 6.90—7.70 (4H, m), 7,10 (1H, s).

Compounds **7b—j** were prepared from **7a** by the conventional synthetic procedure.[6]

1-(2-Anisyl)-6-ethoxycarbonyl-5,7-dimethylphthalazine (7k) A suspension of **7a** (500 mg, 1.3 mmol) in EtOH (30 ml) containing a few drops of concd. NH_4OH was shaken in H_2 over 5% Pd–C (70 mg) under atmospheric pressure. Completion of the reaction took about 8 h at room temperature. Purification by column chromatography with chloroform–MeOH (50 : 1) afforded 200 mg (44%) of **7k**. mp 110—112 °C (ether). *Anal.* Calcd for $C_{20}H_{20}N_2O_3$: C, 71.41; H, 5.99; N, 8.33. Found: C, 71.39; H, 5.90; N, 8.29. MS *m/z*: 336, 335, 319, 308, 307, 291. UV λ_{max}^{EtOH} nm: 232, 282. ^{1}H-NMR ($CDCl_3$) δ: 1.44 (3H, t, J=7 Hz), 2.42 (3H, s), 2.76 (3H, s), 3.69 (3H, s), 4.50 (2H, q, J=7 Hz), 7.00—7.65 (5H, m), 9.72 (1H, s). Oxalate: mp 172—173 °C (acetone–ether), HCl salt: mp 206—207 °C (acetone).

4-(2-Anisyl)-1-chloro-7-ethoxycarbonyl-6,8-dimethylphthalazine N^2-Oxide (8) A mixture of **7a** (185 mg, 0.5 mmol) in acetic acid (5 ml) containing 30% H_2O_2 (0.5 ml) was heated at 80 °C for 2 h. The mixture was concentrated to a volume of 2 ml and was left at room temperature. Precipitated crystals were filtered. Recrystallization from acetone–ether afforded 105 mg (54.4%) of **8**. mp 218—219 °C. *Anal.* Calcd for $C_{20}H_{19}ClN_2O_4$: C, 62.03; H, 4.91; N, 7.23. Found: C, 62.21; H, 5.07; N, 7.31. MS *m/z*: 386 (M^+), 357 (M^+-Et), 341 (M^+-OEt), 200. UV λ_{max}^{EtOH} nm: 221, 260, 294, 310, 323. ^{1}H-NMR ($CDCl_3$) δ: 1.41 (3H, t, J=7 Hz), 2.34 (3H, s), 2.93 (3H, s), 3.71 (3H, s), 4.44 (2H, q, J=7 Hz), 6.88—7.55 (5H, m).

Test on 8 for Hydrolytic Reaction A mixture of **8** (100 mg) in MeOH (10 ml) containing 5% NaOH (1 ml) was heated at reflux for 5 h. Working-up gave crystals melted at 217—219 °C. Spectral data of this compound were identical with those of **8** in all respects.

1-(2-Anisyl)-6-ethoxycarbonyl-5,7-dimethyl-4-(2-phenylethynyl)-phthalazine (71) A mixture of **7a** (370 mg, 1 mmol), phenylacetylene (150 mg, 1.5 mmol), bis(triphenylphosphine)palladium(II) chloride (16 mg, 0.02 mmol), CuI (8 mg), and triethylamine (3 ml) in benzene (10 ml) was heated at reflux for 4 h. The mixture was applied to column chromatography with benzene–EtOAc (10 : 1) to afford 223 mg (51%) of **71** melted at 185—187 °C (EtOAc–ether). *Anal.* Calcd for $C_{28}H_{24}N_2O_3$: C, 77.04; H, 5.54; N, 6.42. Found: C, 77.01; H, 5.60; N, 6.49. MS *m/z*: 436, 421, 407, 391. UV λ_{max}^{EtOH} nm: 242, 333. ^{1}H-NMR ($CDCl_3$) δ: 1.43 (3H, t, J=7 Hz), 2.40 (3H, s), 3.19 (3H, s), 3.69 (3H, s), 4.49 (2H, q, J=7 Hz), 7.00—7.75 (10H, m).

Compound **7m** was obtained from **71** by hydrogenolysis in H_2 in the presence of 5% Pd–C.

4-(2-Anisyl)-8-bromomethyl-7-ethoxycarbonyl-6-methyl-1(2*H*)-phthalazinone (9) A suspension of **3e** (2.0 g, 5.6 mmol), *N*-bromosuccinimide (NBS) (1.2 g, 6.7 mmol), and benzoylperoxide (0.05 g) in CCl_4 (100 ml) was heated to reflux for 20 h. The reaction mixture was diluted with chloroform (20 ml) and filtered. The filtrate was washed with water and dried over anhyd. Na_2SO_4, then evaporated. The residue was purified by column chromatography with benzene–EtOAc (10 : 1). The later fractions afforded 900 mg (38%) of **9**, which did not melt at 280 °C (EtOAc). *Anal.* Calcd for $C_{20}H_{19}BrN_2O_4$: C, 55.68; H, 4.64; N, 6.49. Found: C, 55.65; H, 4.65; N, 6.56. MS *m/z*: 432 (M+2), 430 (M^+), 385 (M^+-OEt), 350 (M^+-HBr), 321 (M^+-Et, HBr). IR ν_{max}^{KBr} cm^{-1}: 3400, 1710, 1660, 1600. ^{1}H-NMR ($CDCl_3$) δ: 1.48 (3H, t, J=7 Hz), 2.37 (3H, s), 3.75 (3H, s), 4.60 (2H, q, J=7 Hz), 5.51 (2H, m), 7.28 (5H, m), 10.38 (1H, br). The early fractions afforded 8-bromomethyl-7-ethoxycarbonyl-6-methyl-4-(2-methoxy-5-bromophenyl)-1(2*H*)-phthalazinone (**10**) in 260 mg (9.2%) yield. mp 300 °C (acetone). *Anal.* Calcd for $C_{20}H_{18}Br_2N_2O_4$: C, 47.05; H, 3.72; N, 5.49. Found: C, 47.10; H, 3.75; N, 5.60. MS *m/z*: 512, 510, 508, 463. ^{1}H-NMR (270 MHz in $CDCl_3$) δ: 1.47 (3H, t, J=7.4 Hz), 2.38 (3H, s), 3.72 (3H, s), 4.54 (2H, q, J=7.4 Hz), 5.48 (2H, q, J=9.4 Hz), 6.93 (1H, d, J=8.8 Hz), 7.09 (1H, s), 7.43 (1H, d, J=2.5 Hz), 7.61 (1H, dd, J=8.8, 2.5 Hz), 10.23 (1H, s).

8-Acetoxymethyl-4-(2-anisyl)-7-ethoxycarbonyl-6-methyl-1(2*H*)-phthalazinone (11) A mixture of **9** (400 mg) in acetic acid (20 ml) containing triethylamine (2 ml) was heated at 100 °C for 30 min. The mixture was diluted with water and extracted with EtOAc. The extract was evaporated to afford a crude product. It was recrystallized from acetone. Yield: 200 mg (53%), mp 210—212 °C. *Anal.* Calcd for $C_{22}H_{22}N_2O_6$: C, 64.38: H, 5.40; N, 6.83. Found. C, 64.41; H, 5.36; N, 6.91. MS *m/z*: 410 (M^+), 367 (M^+-Ac), 350 (M^+-OAc), 337 (M^+-CH_2OAc). ^{1}H-NMR ($CDCl_3$) δ: 1.40 (3H, t, J=7 Hz), 2.07 (3H, s), 2.38 (3H, s), 3.73 (3H, s), 4.38 (2H, q, J=7 Hz), 5.97 (2H, s), 7.17 (5H, m), 10.53 (1H, br).

Preparation of 12a A mixture of **11** (200 mg) in EtOH (10 ml) containing 5% KOH (1 ml) was heated at 60 °C for 2 h. The solvent was removed and the residue was extracted with EtOAc. The extract was purified by column chromatography with chloroform–EtOAc (20 : 1) to afford 130 mg of **12a**, which did not melt at 290 °C. *Anal.* Calcd for $C_{18}H_{14}N_2O_4$: C, 67.07; H, 4.38; N, 8.69. Found: C, 67.06; H, 4.40; N, 8.70. MS *m/z*: 322, 294. IR ν_{max}^{KBr} cm^{-1}: 3300, 1730, 1670, 1600. ^{1}H-NMR (DMSO-d_6) δ: 2.70 (3H, s), 3.76 (3H, s), 5.79 (2H, s), 7.31 (5H, m), 13.08 (1H, s).

Preparation of 12b A mixture of **9** (200 mg) in ammonia saturated EtOH (10 ml) was heated at 60 °C for 2 h. The solvent was evaporated and the residue was purified by column chromatography with chloroform–EtOAc (5 : 1) to afford 105 mg of **12b**, which melted at 285—287 °C (MeOH). *Anal.* Calcd for $C_{18}H_{15}N_3O_3$: C, 67.28; H, 4.71; N, 13.08. Found: C, 67.2; H, 4.73; N, 13.13. MS *m/z*: 321, 250. IR ν_{max}^{KBr} cm^{-1}: 3400, 3300, 1690, 1660, 1590. ^{1}H-NMR (DMSO-d_6) δ: 2.67 (3H, s), 3.71 (3H, s), 4.79 (2H, s), 7.28 (5H, m), 8.79 (1H, s), 12.86 (1H, s).

Preparation of Rabbit Platelet-Rich Plasma (PRP) Blood was collected from a catheter inserted into the carotid artery of ethyl ether anesthesized rabbits. The blood was citrated with 3.8% aqueous sodium citrate solution (1 ml of citrate/9 ml of blood) and separated from the red blood cells by centrifugation for 15 min at 150 g at room temperature. The supernatant thus obtained was used as PRP.

Platelet Aggregation Test The optical density method of Born[12] was used to assess the ability of test compounds to inhibit platelet aggregation induced by ADP and AA. A silicone treated cuvette containing 0.435 ml of the PRP sample was placed in an aggregometer (Sienco, DP-247E) set at 37 °C and 1200 rpm, and a solution of the test compound in 2.5 μl of DMSO was added. After preincubation for 3 min, 20 μl of an aqueous solution of ADP (30 μM) or 10 μM of an aqueous solution of AA (100 μM) was added to induce platelet aggregation. Inhibition of platelet aggregation by a test compound was calculated by dividing the maximum deflection in the optical density curve by that observed with the control (2.5 μl of DMSO alone).

References

1) *a*) Y. Eguchi, F. Sasaki, Y. Takashima, M. Nakajima, and M. Ishikawa, *Chem. Pharm. Bull.*, **39**, 795 (1991); *b*) M. Ishikawa, Y. Eguchi, and A. Sugimoto, *ibid.*, **28**, 2770 (1980); *c*) S. Kaneko, Y. Eguchi, Y. Takashima, M. Nakajima, and M. Ishikawa, *Ketsueki To Myakkan*, **12**, 433 (1981); *d*) Y. Eguchi, and M. Ishikawa, *Chem. Pharm. Bull.*, **39**, 1846 (1991); *e*) Y. Eguchi, F. Sasaki, A. Sugimoto, H. Ebisawa, and M. Ishikawa, *ibid.*, **39**, 1753 (1991).

2) S. Ito, Y. Komoda, S. Sekizaki, H. Azuma, and M. Ishikawa, *Chem. Pharm. Bull.*, **36**, 2669 (1988).

3) K. Tasaka and M. Akagi, *Arzneim.-Forsch.*, **29**, 488 (1979).

4) C. R. Taylor, J. R. C. Baird, K. J. Blackburn, D. Cambridge, J. W. Constantine, M. S. Ghaly, M. L. Hayden, H. M. McIlhenny, P. F. Moore, A. Y. Olukotun, L. G. Pullman, D. S. Salsburg, C. A. P. D. Saxton, and S. Shevde, *Am. Hert J.*, **102**, 515 (1981).

5) M. Hagiwara, T. Endo, T. Kanayama, and H. Hidaka, *J. Pharm. Exp. Ther.*, **228**, 467 (1984).

6) F. A. Vingiello, S-G. Quo, and J. Sheridan, *J. Org. Chem.*, **26**, 3202 (1961).

7) T. Hayashi, M. Konishi, and M. Kumada, *Tetrahedron Lett.*, **21**,

1871 (1979).
8) E. Ochiai, "Aromatic Amine Oxides," ed. by Elsevier Publishing Company, 1967, pp. 382—395.
9) T. Sakamoto, M. Shiraiwa, Y. Kondo, and H. Yamanaka, *Synthesis*, **1983**, 312.
10) Y. Eguchi, A. Sugimoto, S. Ito, M. Nakajima, S. Kaneko, and M. Ishikawa, *Reports Inst. Med. Dent. Eng.*, **18**, 17 (1984).
11) L. M. Jackman and S. Sternhell, "Nuclear Magnetic Resonance Spectroscopy in Organic Chemistry," ed. by Pergamon Press, 1972, pp. 201—214.
12) G. V. R. Born, *Nature* (London), **194**, 927 (1962).

Structure–Activity Relationships of Rat Neuromedin U for Smooth Muscle Contraction

Naoki SAKURA,* Satoru OHTA, Yoshiki UCHIDA, Katsuro KUROSAWA, Keiko OKIMURA and Tadashi HASHIMOTO

Faculty of Pharmaceutical Sciences, Hokuriku University, Kanagawa-machi, Kanazawa 920–11, Japan. *Received February 27, 1991*

Rat neuromedin U (r-NMU) and its fragment peptide amides were synthesized by solid-phase methodology. Using a chicken crop smooth muscle contraction assay, the potency of r-NMU and its fragments relative to porcine neuromedin U-8 (p-NMU-8) was r-NMU: 10.25±2.88, r-NMU (6—23): 8.01±1.04, r-NMU (10—23): 2.76±0.46, r-NMU (13—23): 2.81±0.52, and r-NMU (16—23): 0.88±0.19, respectively. Two heptapeptides, r-NMU (17—23) and r-NMU (16—22), had a relative potency of 0.61 and 0.03 respectively, and elicited maximal contraction at a dose of 10 μM to a similar degree to p-NMU-8. The other shorter C-terminal fragments did not elicit the maximal contraction or any activity. In a rat uterus contraction assay, r-NMU (13—23), but not r-NMU (16—23), at a dose of 4 nM retained as high a stimulatory activity as r-NMU itself. r-NMU (17—22) was the smallest peptide fragment to elicit the maximal sustained contraction at 10 μM. These results indicate that the amino acid sequence Phe–Leu–Phe–Arg–Pro–Arg, corresponding to positions 17 to 22 of r-NMU, may be essential for contractile activity. N-terminal peptide segments Tyr–Gln–Gly–Pro corresponding to positions 6 to 9, and Ser–Gly–Gly corresponding to positions 13 to 15, appear to be of special importance for potent activity.

Keywords neuromedin U; rat; structure–activity relationship; smooth muscle contraction; chicken crop; rat uterus

Introduction

Neuromedin U (NMU) is a newly discovered neuropeptide originally isolated from porcine spinal cord in two molecular forms: a pentacosapeptide amide neuromedin U-25 (p-NMU-25) and an octapeptide amide (p-NMU-8).[1] Rat neuromedin U (r-NMU) was subsequently isolated from rat small intestine and sequenced as a tricosapeptide amide.[2,3] NMU has a potent stimulatory effect on the isolated rat uterus and increases blood pressure in the rat.[1,3] It also affects splanchnic blood flow[4] and ion transport in the porcine jejunum.[5] It regulates gut motility in the turtle[6] and has a direct contractile effect on the isolated human ileum and urinary bladder.[7] The C-terminal heptapeptide amide of r-NMU is identical to that of p-NMU-8 and p-NMU-25. The remainder of r-NMU has limited sequence homology with p-NMU-25. The dibasic sequence, which is the postulated cleavage site of the p-NMU-25 molecule located at the positions preceding the p-NMU-8 sequence, is not present in the corresponding position in r-NMU. The rat uterus stimulatory activity of r-NMU is higher than p-NMU-25, which in turn is three times more potent than p-NMU-8. Thus it has been suggested that the C-terminal regions of NMUs are essential for their biological activity and the N-terminal may also play an important role.[1,3] We have already reported the structure–activity relationships of p-NMU-8 and the development of an antagonist against p-NMU-8,[8] employing an isolated chicken crop preparation as the bioassay system. This paper describes the structure–activity relationships of r-NMU in relation to its peptide chain length.

Synthesis r-NMU-related peptide amides (Fig. 1) were synthesized by solid-phase techniques conducted on benzhydrylamine resin employing N^{α}-Boc protected amino acids. Each crude peptide obtained after HF treatment was revealed as a main peak on analytical reverse phase high performance liquid chromatography (RP-HPLC). The peptides were highly purified simply by semi-preparative RP-HPLC with 0.1% trifluoroacetic acid (TFA)–acetonitrile in an isocratic system, followed by gel filtration. The isolated yield of r-NMU was 8.1%, and most of the other shorter fragments were attainable in higher yields. Homogeneity of the product was ascertained by analytical

	1	6	10	13	16	17	18	19	20	21	22	23
r-NMU	H-Tyr-Lys-Val-Asn-	Glu-Tyr-	Gln-Gly-	Pro-Val-Ala-Pro-	Ser-	Gly-	Gly-	Phe-	Phe-	Leu-	Phe-	Arg-Pro-Arg-Asn-NH_2
r-NMU (6—23)		H-Tyr-	Gln-Gly-	Pro-Val-Ala-Pro-	Ser-	Gly-	Gly-	Phe-	Phe-	Leu-	Phe-	Arg-Pro-Arg-Asn-NH_2
r-NMU (10—23)			H-Val-	Ala-Pro-	Ser-	Gly-	Gly-	Phe-	Phe-	Leu-	Phe-	Arg-Pro-Arg-Asn-NH_2
r-NMU (13—23)				H-Ser-	Gly-	Gly-	Phe-	Phe-	Leu-	Phe-	Arg-	Pro-Arg-Asn-NH_2
r-NMU (16—23)					H-Phe-	Phe-	Leu-	Phe-	Arg-	Pro-	Arg-	Asn-NH_2
r-NMU (17—23)					H-	Phe-	Leu-	Phe-	Arg-	Pro-	Arg-	Asn-NH_2
r-NMU (18—23)						H-	Leu-	Phe-	Arg-	Pro-	Arg-	Asn-NH_2
r-NMU (19—23)							H-	Phe-	Arg-	Pro-	Arg-	Asn-NH_2
r-NMU (16—22)					H-Phe-	Phe-	Leu-	Phe-	Arg-	Pro-	Arg-NH_2	
r-NMU (16—21)					H-Phe-	Phe-	Leu-	Phe-	Arg-	Pro-NH_2		
r-NMU (17—22)					H-	Phe-	Leu-	Phe-	Arg-	Pro-	Arg-NH_2	
r-NMU (18—22)						H-	Leu-	Phe-	Arg-	Pro-	Arg-NH_2	
r-NMU (17—21)					H-	Phe-	Leu-	Phe-	Arg-	Pro-NH_2		
p-NMU-8					H-Tyr-	Phe-	Leu-	Phe-	Arg-	Pro-	Arg-	Asn-NH_2

Fig. 1. Synthetic Peptides Related to Rat Neuromedin U (r-NMU)

TABLE I. Amino Acid Analysis of Synthetic r-NMU-Related Peptides

Peptide	Asp	Ser	Glu	Pro	Gly	Ala	Val	Leu	Tyr	Phe	Lys	Arg	NH_3	Recovery (%)
r-NMU	2.03 (2)	0.96 (1)	2.14 (2)	2.88 (3)	3.02 (3)	1.02 (1)	1.96 (2)	1.03 (1)	1.98 (2)	3.01 (3)	0.97 (1)	2.00 (2)	4.77 (4)	83.4
r-NMU (6—23)	1.00 (1)	0.96 (1)	1.04 (1)	2.86 (3)	3.03 (3)	1.03 (1)	1.03 (1)	1.04 (1)	0.99 (1)	2.99 (3)	—	2.02 (2)	3.85 (3)	86.7
r-NMU (10—23)	1.04 (1)	0.98 (1)	—	1.95 (2)	2.03 (2)	1.02 (1)	0.95 (1)	1.02 (1)	—	2.99 (3)	—	2.03 (2)	2.66 (2)	78.8
r-NMU (13—23)	1.07 (1)	0.98 (1)	—	0.97 (1)	2.01 (2)	—	—	1.02 (1)	—	2.95 (3)	—	2.00 (2)	3.03 (2)	79.9
r-NMU (16—23)	1.01 (1)	—	—	1.05 (1)	—	—	—	0.99 (1)	—	2.87 (3)	—	2.07 (2)	2.15 (2)	84.6
r-NMU (17—23)	1.02 (1)	—	—	0.91 (1)	—	—	—	1.03 (1)	—	2.04 (2)	—	1.99 (2)	2.30 (2)	75.2
r-NMU (18—23)	1.05 (1)	—	—	0.93 (1)	—	—	—	1.03 (1)	—	1.03 (1)	—	1.96 (2)	2.21 (2)	76.4
r-NMU (19—23)	1.06 (1)	—	—	0.94 (1)	—	—	—	—	—	0.95 (1)	—	1.92 (2)	2.14 (2)	81.5
r-NMU (16—22)	—	—	—	0.99 (1)	—	—	—	1.05 (1)	—	2.92 (3)	—	2.04 (2)	1.24 (1)	69.8
r-NMU (16—21)	—	—	—	0.93 (1)	—	—	—	1.05 (1)	—	3.02 (3)	—	1.00 (1)	1.30 (1)	76.1
r-NMU (17—22)	—	—	—	1.01 (1)	—	—	—	0.96 (1)	—	1.99 (2)	—	2.05 (2)	1.12 (1)	73.1
r-NMU (18—22)	—	—	—	0.94 (1)	—	—	—	0.93 (1)	—	0.94 (1)	—	2.05 (2)	1.15 (1)	64.2
r-NMU (17—21)	—	—	—	0.98 (1)	—	—	—	1.03 (1)	—	2.00 (2)	—	1.00 (1)	1.08 (1)	64.2
p-NMU-8	1.01 (1)	—	—	0.97 (1)	—	—	—	1.00 (1)	0.98 (1)	1.97 (2)	—	2.33 (2)	1.73 (2)	82.0

Hydrolysis: at 130 °C for 3.0 h by vapor of 6 N hydrochloric acid containing phenol (3%). Numbers in parentheses are theoretical values.

TABLE II. Characteristics of Synthetic r-NMU-Related Peptides

Peptide	Yield[a] (%)	$[\alpha]_D^{23}$ ($c=0.5$) (2 M AcOH)	HPLC[b] t_R (min)	HP-TLC[c] Rf^1	HP-TLC[c] Rf^2
r-NMU	8.1	−80.1	31.65	0.35	0.39
r-NMU (6—23)	29.7	−75.7	31.42	0.39	0.41
r-NMU (10—23)	8.6	−72.6	30.47	0.39	0.42
r-NMU (13—23)	14.2	−41.7	28.42	0.40	0.43
r-NMU (16—23)	13.6	−40.3	27.00	0.45	0.45
r-NMU (17—23)	32.5	−44.4	19.13	0.39	0.43
r-NMU (18—23)	30.1	−33.2	10.65	0.31	0.19
r-NMU (19—23)	11.5	−43.8	4.13	0.26	0.10
r-NMU (16—22)	11.5	−33.1	27.10	0.49	0.46
r-NMU (16—21)	25.8	−30.4	30.50	0.58	0.52
r-NMU (17—22)	44.4	−39.3	18.96	0.46	0.44
r-NMU (18—22)	32.5	−23.2	11.39	0.41	0.40
r-NMU (17—21)	15.0	−38.5	23.62	0.56	0.48
p-NMU-8	23.4	−36.4	24.30	0.45	0.44

a) Based on the C-terminal amino acid incorporated on BHA resin. *b*) Column; Nova-pak C_{18} (3.9 × 150 mm), elution; linear gradient (30 min) from 3.5 to 31.5% MeCN in 20 mM phosphate buffer (pH 3.0), flow rate; 1 ml/min; detection; 210 mm. *c*) Rf^1, *n*-BuOH–pyridine–AcOH–H_2O (30:20:6:24), Rf^2, *n*-BuOH–AcOEt–AcOH–H_2O (1:1:1:1).

TABLE III. Contractile Activity of Rat Neuromedin U (r-NMU) and Its Fragments on Isolated Chicken Crop

Peptide	pD_2	α	*RA*	*n*
p-NMU-8	7.23±0.14	1.00	1.00	10
r-NMU	8.08±0.08	0.92±0.06	10.25±2.88	10
r-NMU (6—23)	8.05±0.06	0.93±0.04	8.01±1.04	7
r-NMU (10—23)	7.80±0.14	1.01±0.04	2.76±0.46	9
r-NMU (13—23)	7.63±0.14	0.91±0.03	2.81±0.52	9
r-NMU (16—23)	6.87±0.19	1.11±0.03	0.88±0.19	9
r-NMU (17—23)	6.57±0.05	1.05±0.03	0.61±0.04	7
r-NMU (18—23)	5.57±0.03	0.52±0.12	0.05±0.01	6
r-NMU (19—23)	NA	0.27±0.05	NA	7
r-NMU (16—22)	5.62±0.03	0.90±0.04	0.03±0.007	8
r-NMU (16—21)	NA	NA	NA	6
r-NMU (17—22)	NA	0.28±0.02	NA	6
r-NMU (18—22)	NA	NA	NA	6
r-NMU (17—21)	NA	NA	NA	6

Isolated chicken crop was suspended in an organ bath at 28 °C containing Tyrode's solution under 0.5 g tension. Peptide dissolved in saline was added cumulatively to obtain a dose–response curve, from which the pharmacological parameters were calculated; α: intrinsic activity taking p-NMU-8 as 1.00, *RA*: relative affinity to p-NMU-8. NA: not assessed. *n*: number of experiments.

RP-HPLC with a phosphate buffer–acetonitrile system and high performance thin layer chromatography (HP-TLC) with two solvent systems. Amino acid analysis of the acid hydrolysates reconfirmed the purity (Table I). Characteristics of the synthetic peptides are shown in Table II. The stability of r-NMU and p-NMU-8 in solution was examined by HPLC. Quantitative recovery of both peptides from saline at a concentration of 0.1 mM was proven after storage at 4 °C or 27 °C for 7 d without any significant changes in their chromatograms. The results suggested that NMU-related peptide solutions in saline (0.1 mM) are available for the bioassay for at least a week after storage at 4 °C.

Smooth Muscle Contraction Activity Synthetic peptides were tested on isolated chicken crop and rat uterus smooth muscle preparations for contractile activity. The activity of p-NMU-8 was taken as a reference. In the chicken crop assay, the dose–response curves were obtained by cumulative administration of peptides. In order to estimate the activity of each peptide, the pharmacological parameters of pD_2, α (intrinsic activity) and *RA* (relative affinity to p-NMU-8) were used. r-NMU, r-NMU (6—23), r-NMU (10—23) and r-NMU (13—23) exerted dose–dependent contractions with a similar pattern to p-NMU-8. Their dose–response curves shifted slightly to the left compared to p-NMU-8, the threshold doses were 1 to 3 nM, and the maximal responses, represented by α values, were almost the same as that of p-NMU-8. On the other hand, the dose–response curves of r-NMU (16—23), r-NMU (17—23) and r-NMU (16—22) shifted slightly to the right compared to p-NMU-8. The other shorter C-terminal fragments did not produce responses of the same degree as p-NMU-8, even at high concentrations (10 μM). The pharmacological parameters of each peptide obtained from the dose–response curve are given in Table III.

In the rat uterus assay, the single dose–response pattern for each peptide was examined at a concentration of 4 nM, 1 μM and/or 10 μM. The traces of the representative response patterns of the peptide fragments are illustrated in Fig. 2.

Results and Discussion

In the chicken crop contraction assay, r-NMU exhibited

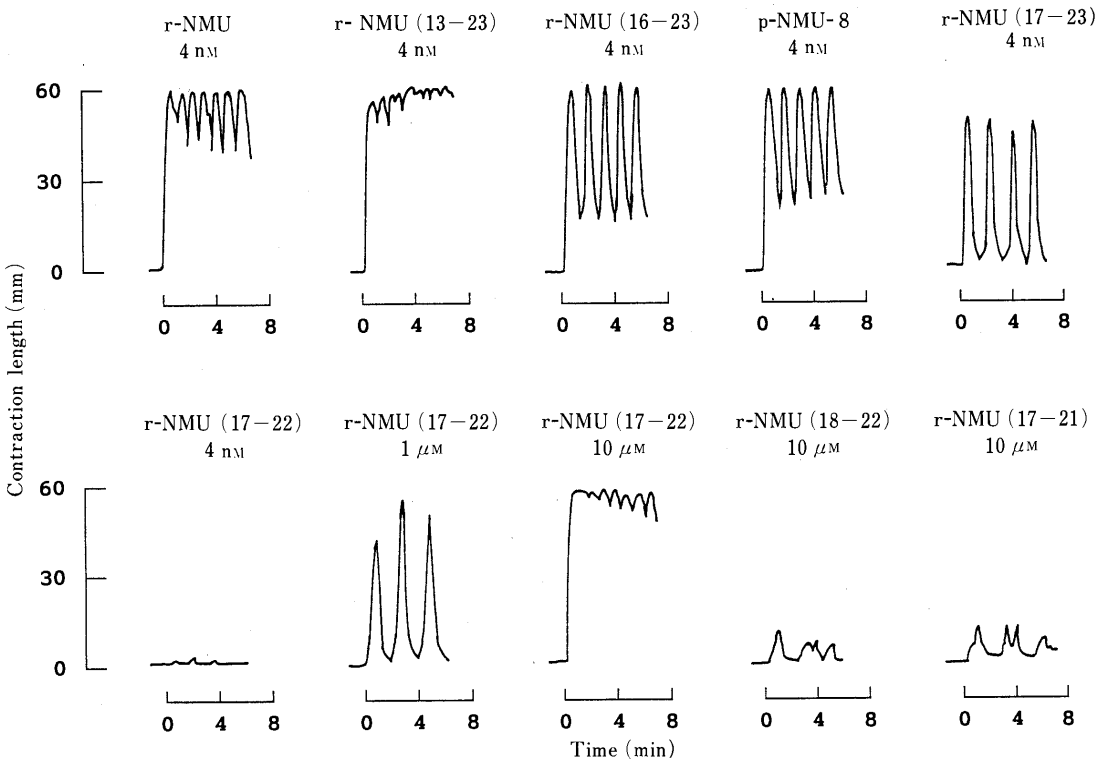

Fig. 2. Typical Traces of Contractile Responses of Isolated Rat Uteri Induced by Rat Neuromedin U (r-NMU)-Related Peptides

potent activity. The pD_2 of r-NMU was significantly higher than that of p-NMU-8, and the relative potency, represented by *RA* values, was 10-fold higher. Elimination of the N-terminal peptide fragments decreased the activity step by step. The removal of the N-terminal 9 amino acid residues reduced the activity [*RA* value of r-NMU (10—23), 2.76] more significantly than removal of the N-terminal 5 residues [*RA* value of r-NMU (6—23), 8.01]. However, the C-terminal undecapeptide amide, r-NMU (13—23), still retained high activity with a pD_2 value of 7.63; the maximal contractile response in terms of the α value was 0.91, and the relative potency in terms of the *RA* value was 2.81.

r-NMU (16—23) had slightly less activity than p-NMU-8. The structural differences between the two octapeptide amides lie in the N-terminal Phe and Tyr, suggesting that the hydroxy group of Tyr is preferable for affinity to NMU receptor(s) in the chicken crop.

These results clearly show that the elongation of peptide chain length from the C-terminal octapeptide amide of r-NMU to the undecapeptide amide brings about three times more potent contractile activity. A significant increase of the activity is also shown when the peptide chain is elongated from the C-terminal tetradecapeptide amide of r-NMU to the octadecapeptide amide. Thus, a special contribution of the N-terminal peptide segments of r-NMU (6—23) and r-NMU (13—23) is suggested to enhance the activity.

Further deletion of an N-terminal amino acid from r-NMU (16—23) gave the C-terminal heptapeptide amide r-NMU (17—23), which retained the activity with a relative potency of 0.61. Another heptapeptide amide, r-NMU (16—22), without the C-terminal Asn residue, showed weak activity with a relative potency of 0.03. Both heptapeptides, which are the N- or C-terminal deletion analogs of p-NMU-8, still elicited maximal contractions as shown by α values of 1.05 and 0.90 at a high concentration of 10 μM. The results suggest that the common sequence Phe–Leu–Phe–Arg–Pro–Arg, overlapping the above two heptapeptide amides, is an essential part of the r-NMU molecule for contractile activity on the chicken crop smooth muscle preparation. The importance of the sequence was supported by the weak but significant activity of the hexapeptide amide, r-NMU (17—22), with an α value of 0.28.

In the rat uterus stimulation assay, synthetic peptide amides were tested as a single dose. At a dose of 4 nM, which is a ten-fold higher concentration than the threshold dose of p-NMU-8 or r-NMU previously reported,[1,3] r-NMU, r-NMU (6—23), r-NMU (10—23) and r-NMU (13—23) caused sustained tetanic contractions with similar patterns to each other. The representative traces of r-NMU and r-NMU (13—23) are shown in Fig. 2. It is interesting that all peptides containing the C-terminal undecapeptide amide had potent activity on rat uterus smooth muscle. On the other hand, r-NMU (16—23) at a dose of 4 nM gave rise to rhythmic contractions. The lower potency of this octapeptide amide compared with the above fragments is comparable to that of p-NMU-8. A heptapeptide amide, r-NMU (17—23) reduced the activity, and a hexapeptide amide, r-NMU (17—22), produced almost no activity at a dose of 4 nM. However, this hexapeptide definitely elicited rhythmic contractions at a concentration of 1 μM, and a sustained tetanic contraction at 10 μM. Further shortening of the peptide chain resulted in almost complete loss of activity, as shown in Fig. 2 for two pentapeptides, r-NMU (18—22) and r-NMU (17—21).

The present study on structure–activity relationships of r-NMU indicates that the amino acid sequence of Phe–Leu–Phe–Arg–Pro–Arg corresponding to positions 17—22 of the

r-NMU molecule appears to be essential for the smooth muscle contractile activity in both isolated chicken crop and rat uterus preparations. This peptide segment is common to mammalian NMUs so far elucidated from rat, porcine, guinea pig[9] and dog.[10] Heptapeptide chain length including this portion was necessary for full intrinsic activity on chicken crop smooth muscle. The results are consistent with the previous study on the contractile activities of p-NMU-8 analogs in isolated chicken crop preparations, suggesting that the active site of p-NMU-8 may exist between positions 2 and 8,[8] since the C-terminal heptapeptide amides of p-NMU-8 and r-NMU share the same structure. Furthermore, the present results reveal that the C-terminal Arg–Asn portion of r-NMU and p-NMU-8 makes relatively higher contributions to the activity than the N-terminal Tyr^1–Phe^2 portion of p-NMU-8, or the Phe^{16}–Phe^{17} of r-NMU. For more potent activity, elongation of the peptide chain from the C-terminal octapeptide amide of r-NMU towards the N-terminal is required. The peptide segment Ser–Gly–Gly at positions 13 to 15, as well as Tyr–Gln–Gly–Pro at positions 6 to 9, may be of special importance in the N-terminal 15 amino acid sequence, which may serve to maintain a favorable molecular form for interaction with NMU receptor(s).

Experimental

All reagents and solvents for peptide synthesis were obtained from Watanabe Chem. Ind. Ltd. or Wako Pure Chem. Ind. Ltd., Japan, unless otherwise mentioned, and were used without further purification. Evaporation of solvents was carried out *in vacuo* below 40 °C in a rotary evaporator.

Peptide Synthesis Peptides were synthesized by a solid-phase method[11] with N^{α}-Boc amino protection on benzhydrylamine (BHA) resin employing a model 990C peptide synthesizer (Beckman Instruments Ltd., U.S.A.) Anchoring of the first amino acid was achieved through dicyclohexylcarbodiimide (DCC) coupling in the presence of 1-hydroxybenzotriazole (HOBt) of 0.4 mmol eq of N^{α}-Boc–amino acid (Peptide Institute Inc., Japan) with 1 g eq of BHA resin (1% DVB polymer, available amine of the resin: 0.66 mmol/g; Peptide Institute Inc., Japan), followed by acetylation with acetic anhydride (2 mmol eq)–pyridine (1 mmol eq) in *N,N'*-dimethylformamide (DMF)–dichloromethane (DCM) (1 : 1). Deprotection of the N^{α}-Boc group was accomplished with 33% TFA in DCM for 30 min. N^{α}-Boc–amino acids (2.5 eq) were coupled for 1—2 h *via* DCC (2.5 eq) for the first coupling, or DCC (2.5 eq)–HOBt (2.5 eq) for further repeated coupling in DCM and/or DMF. Every introduction reaction of an amino acid was repeated until the resin became negative to the Kaiser test,[12] then the acetylation procedure with acetic anhydride–pyridine described above was performed. N^{α}-Boc–Asn and N^{α}-Boc–Gln were coupled in the presence of a 2-fold excess of HOBt. Side-chain protection of N^{α}-Boc–amino acids was as follows: Arg(Tos), Ser(Bzl), Tyr(Cl_2-Bzl), Glu(OBzl) and Lys(ClZ). After assembling the respective amino acids, the protected peptide-resin was washed with 33% TFA/DCM and ethanol and dried. Final deprotection and cleavage from the resin was achieved in liquid HF in the presence of 10% anisole at 0 °C for 45 min. HF was removed *in vacuo* with ice-cooling. The residue was washed with ethyl acetate–ether (1 : 1) and non-peptide materials were removed by filtration. The crude peptides were extracted with 12% acetic acid (AcOH) and the extracts were then lyophilized.

Peptide Purification Crude peptides were purified by semi-preparative RP-HPLC. The apparatus consisted of a model 590 pump, a model U6K injector (Waters, U.S.A.), an S310 model II ultraviolet (UV) detector (Soma, Japan) and a model 561-3003 recorder (Hitachi, Japan) connected to a column of μ-Bondasphere C_{18} (19 × 150 mm) (Waters) or YMC-pack D-ODS-5-A (20 × 250 mm) (YMC Co., Japan). The lyophilized crude peptides (2—8 mg) dissolved in aqueous AcOH were loaded onto the column, and eluted with an acetonitrile (MeCN)–0.1% TFA solvent system in an isocratic manner at a flow rate of 8 ml/min. Concentration of MeCN in the solvent system for each peptide was specified to keep the retention time of the main peak between 30—60 min. The UV absorption of the eluate was monitored at 210 nm. Fractions containing the purified peptide were pooled, MeCN was removed under reduced pressure, and the residual solution was lyophilized. The peptide was finally gel-filtered on a Sephadex G-25 superfine column (1.5 × 58 cm) using 12% AcOH as an eluent, and the desired fractions were lyophilized. The final yields of the peptides based on the C-terminal amino acid on the resin are shown in Table I.

Peptide Characterization Analytical RP-HPLC was performed on an HPLC system comprising two model 510 pumps, a model U6K injector, a model 680 gradient controller, a model 730 data module (Waters) and a model UV-8011 UV detector (Tosoh Co., Japan). HPLC analysis of synthetic peptides was carried out using a Nova pak C_{18} column (3.9 × 150 mm) (Waters) with a linear gradient elution of 3.5—31.5% MeCN over a period of 30 min in 20 mM sodium phosphate buffer (pH 3.0) (flow rate, 1 ml/min; UV detection, 210 nm).

For stability test of the NMU-related peptides, r-NMU and p-NMU-8 were dissolved in saline, both at a concentration of 0.1 mM, and three aliquots of each peptide solution were kept at −40, 4, and 27 °C for 7 d. The peptide solutions were then analyzed by HPLC on a YMC-pack ODS-AM column (4.6 × 150 mm) with elution using a gradient of 4—40% MeCN in 0.1% TFA over a period of 30 min at the flow rate of 1 ml/min. No peaks other than those of p-NMU-8 and r-NMU (retention time, 24.8 min for p-NMU-8 and 27.9 min for r-NMU) were detectable at 210 nm in the HPLC chromatograms of three aliquots stored at different temperatures, respectively. The peak areas of p-NMU-8, or r-NMU, from three aliquots after storage, were almost the same respectively (differences within ±6%) supporting high stability of the NMUs in saline.

Acid hydrolysis of the peptides was carried out with 6 N HCl vapor; peptide powder (30—200 μg) was taken in a test tube (6 × 50 mm) and placed in a 40-ml vial, at the bottom of which 6 N HCl containing 3% phenol (0.5 ml) was added. The vial was evacuated under cooling and then closed with a Teflon valve stopper and kept in an aluminum block heater at 130 °C for 3 h. Amino acid analysis of the acid hydrolysate was performed on a Beckman model 7300 amino acid analyzer system. The results are shown in Table I.

Optical rotations of peptides were measured with a DIP-370 digital polarimeter (Nippon Bunko Co., Ltd., Japan) employing a 3 × 50 mm cell. Peptides were dissolved in 12% AcOH at a concentration of 0.50%, *i.e.* 4—5 mg peptide in 0.8—1.0 ml, uncorrected for counterions toward the amino and guanidino groups of the peptides or water. Values shown in Table I were obtained by calculation from the means of 5 successive 20-s integrations.

The *Rf* values in HP-TLC, performed on precoated silica gel (Kieselgel 60; Merck), refer to the following solvent systems: Rf^1, *n*-BuOH–pyridine–AcOH–H_2O (30 : 20 : 6 : 24) and Rf^2, *n*-BuOH–AcOEt–AcOH–H_2O (1 : 1 : 1 : 1).

Isolated Smooth Muscle Contraction Assay A chicken (age: 8—12 d) was sacrificed after fasting for 12 h and the crop was removed rapidly and then cut vertically (about 2 × 20 mm). The tissue was mounted longitudinally at a resting tension of 0.5 g in an organ bath (10 ml) containing Tyrode's solution of the following composition (mM): NaCl 137, KCl 2.7, $CaCl_2$ 1.8, $MgCl_2$ 1.1, NaH_2PO_4 0.4, $NaHCO_3$ 12, glucose 5.6. This was kept at 28 °C and bubbled with a mixture of 95% O_2 and 5% CO_2. The tissue preparation was equilibrated for 60 min, challenged twice with carbachol (1 μM) and once with p-NMU-8, and then re-equilibrated for 40—50 min prior to estimation of the contractile activity of each peptide in comparison with that of p-NMU-8. Peptides were added cumulatively and the contractile responses of the tissue preparation were recorded using a model TD-111T isotonic transducer (Nihon Khoden, Japan) on a model 561-3003 recorder (Hitachi). The pharmacological parameters pD_2, α [an intrinsic activity; maximum contractions induced by each peptide (10 μM)/maximum contraction induced by p-NMU-8 (10 μM)] and *RA* (relative affinity; EC_{50} of p-NMU-8/EC_{50} of each peptide) were calculated from the dose–response curves, which were obtained from six to ten experiments using different tissue preparations (Table II).

Female rats (weighing 250—300 g) were killed by a blow on the head and bleeding from the neck, and their uteri were removed rapidly. Isolated segments of uterine horns (about 15 mm long) were suspended in an organ bath at 28 °C containing oxygenated Tyrode's solution and equilibrated for 1 h and challenged twice with saturated KCl solution (0.1 ml). After re-equilibration for 30 min, the contractile activity of a single dose (4 nM, 1 μM and/or 10 μM) of peptide was tested with interval rest periods of 30—90 min, during which the solution in the organ bath was changed every 15—20 min. Three to four tests were performed on the same isolated uterus preparation. The contractile activity of each peptide was examined on four to five different uterus preparations, and the trace of a representative response pattern is shown in Fig. 2.

References

1) N. Minamino, K. Kangawa and H. Matsuo, *Biochem. Biophys. Res. Commun.*, **130**, 1078 (1985).
2) J. M. Conlon, J. Domin, L. Thim, V. DiMarzo, H. R. Morris and S. R. Bloom, *J. Neurochem.*, **51**, 988 (1988).
3) N. Minamino, K. Kangawa, M. Honzawa and H. Matsuo, *Biochem. Biophys. Res. Commun.*, **156**, 355 (1988).
4) S. Sumi, K. Inoue, M. Kogire, R. Doi, K. Takaori, T. Suzuki, H. Yajima and T. Tobe, *Life Sci.*, **41**, 1585 (1987).
5) D. R. Brown and F. L. Quito, *Eur. J. Pharmacol.*, **155**, 159 (1988).
6) C. S. Bockman, P. W. Abel, J. W. Hicks and J. M. Conlon, *Eur. J. Pharmacol.*, **171**, 255 (1989).
7) C. A. Maggi, R. Patacchini, S. Guiliani, D. Turini, G. Barbanti, P. Rovero and A. Meli, *Br. J. Pharmacol.*, **99**, 186 (1990).
8) *a*) T. Hashimoto, H. Masui, N. Sakura, K. Okimura and Y. Uchida, "Peptides, Chemistry, Structure and Biology," ed. by J. E. Rivier and G. R. Marshall, ESCOM Science Publishers, Leiden, 1990, p. 116; *b*) Y. Uchida, K. Okimura, H. Masui, N. Sakura and T. Hashimoto, "Peptide Chemistry 1989," ed. by N. Yanaihara, Protein Research Foundation, Osaka, 1990, p. 181; *c*) T. Hashimoto, H. Masui, Y. Uchida, N. Sakura and K. Okimura, *Chem. Pharm. Bull.*, **39**, 2319 (1991).
9) R. Murphy, C. A. Turmer, J. B. Furness, L. Parker and A. Giraud, *Peptides*, **11**, 613 (1990).
10) F. O'Harte, C. S. Bockman, P. W. Abel and J. M. Conlon, *Peptides*, **12**, 11 (1991).
11) J. Stewart and J. Young, "Solid Phase Peptide Synthesis," Pierce Chem. Co., Rockford, 1984.
12) E. Kaiser, R. L. Colescott, C. S. Bossinger and P. I. Cook, *Anal. Biochem.*, **34**, 595 (1970).

Chem. Pharm. Bull. **39**(8) 2021—2023 (1991)

New Quassinoids from *Picrasma javanica*. Structures of Javanicins U, V, W, X and Y

Kazuo KOIKE, Kiyoshi ISHII, Katsuyoshi MITSUNAGA and Taichi OHMOTO*

School of Pharmaceutical Sciences, Toho University, 2–2–1 Miyama, Funabashi, Chiba 274, Japan. *Received December 21, 1990*

Five new quassinoids, javanicins U, V, W, X and Y were isolated from *Picrasma javanica* (Simaroubaceae) collected in Indonesia. Their structures were determined by spectroscopic evidence.

Keywords *Picrasma javanica*; Simaroubaceae; javanicin U; javanicin V; javanicin W; javanicin X; javanicin Y; picrasane; des-4-methylpicrasane; quassinoid

Picrasma javanica BL. (Simaroubaceae) is used as a traditional antimalarial medicine in Indonesia. In previous phytochemical studies of the plant,[1] we isolated a new type of quassinoid, des-4-methylpicrasane, which has bitter qualities. Further investigation of the bitter fractions of MeOH extract of the same plant had led to the isolation of five new quassinoids. We report herein the isolation and structural elucidation of these five new javanicins U (**1**), V (**2**), W (**3**), X (**4**) and Y (**5**).

Results and Discussion

Javanicin U (**1**), $C_{23}H_{32}O_8$, was obtained as colorless prisms, mp 257—259 °C. The infrared (IR) and ultraviolet (UV) spectra of **1** indicated the presence of hydroxyl (ν_{max} 3450 cm^{-1}), δ-lactone (ν_{max} 1750 cm^{-1}) and α,β-unsaturated ketone (ν_{max} 1680 and 1645 cm^{-1} and λ_{max} 272 nm) groups. The proton (^{1}H)- and carbon-13 (^{13}C)-nuclear magnetic resonance (NMR) spectral data of **1** were very similar to those of nigakilactone F (**6**),[2] except that the methoxyl group in **6** was replaced by an acetoxyl group in **1**. Comparing the ^{1}H-NMR chemical shifts of **1** with those of **6** revealed a clear downfield shift for H-12 ($\Delta\delta = 1.68$ ppm), which suggested that the acetoxyl group was located at C-12. Furthermore, in a nuclear Overhauser effect (NOE) experiment, irradiation of methoxyl protons at δ 3.49 induced 15% NOE enhancement in H-3, suggesting the location of the methoxyl and the acetoxyl groups to be C-2 and C-12, respectively.

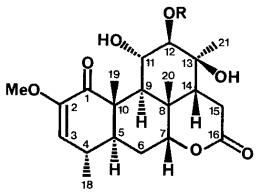

1 : R=Ac
6 : R=Me

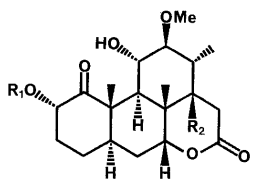

2 : R_1=R_2=H
2a : R_1=Ac, R_2=H
3 : R_1=H, R_2=OH

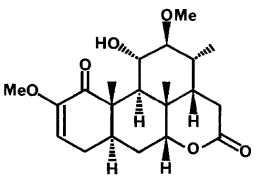

7

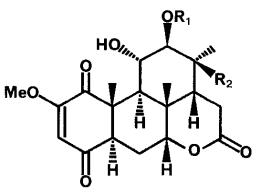

4 : R_1=Me, R_2=H
5 : R_1=H, R_2=OH

Chart 1

Javanicin V (**2**), $C_{20}H_{30}O_6$, was obtained as colorless prisms, mp 107—108 °C. The IR spectrum of **2** indicated the presence of hydroxyl (ν_{max} 3480 cm^{-1}) and δ-lactone (ν_{max} 1730 cm^{-1}) groups. The ^{1}H- and ^{13}C-NMR spectra of **2** were similar to those of javanicin A (**7**),[3] however, **2** has no olefinic signals at C-2 and C-3. Another difference between **2** and **7** was the lack of one methoxyl group in **2**. The ^{1}H–^{1}H COSY suggested the presence of isolated structure unit, ■–C(2)H–C(3)H_2–C(4)H_2–C(5)H–C(6)H_2–C(7)H–■ in the structure of **2**. These data indicated that α,β-unsaturated ketone group in **7** was replaced by the 2,3-saturated ketone group in **2**, and one of the methoxyl groups in **7** was replaced by a hydroxyl group in **2**. In the ^{1}H-NMR spectrum of the acetyl derivative **2a**, the signal of H-2 at δ 5.86 gave a clear downfield shift ($\Delta\delta = 0.81$ ppm), when compared with the corresponding signal in **2**. This ^{1}H signal of **2** observed 10% NOE enhancement when Me-10 was irradiated. These data indicated that the hydroxyl group in **2** is located at C-2 with an α-orientation.

Javanicin W (**3**), $C_{20}H_{30}O_7$, was obtained as colorless needles, mp 169—171 °C. The IR spectrum of **3** indicated the presence of hydroxyl (ν_{max} 3470 cm^{-1}) and carbonyl (ν_{max} 1710 (br) cm^{-1}) groups. The ^{1}H- and ^{13}C-NMR spectral data of javanicin W (**3**) and javanicin V (**2**) were closely related. From the molecular weight, **3** contains 16 more mass units than **2**, and the presence of an extra hydroxyl group was suggested for **3**. The downfield shift of the lactone terminus proton (H-7) at δ 4.79 relative to **2** (H-7, δ 4.10) revealed the extra hydroxyl group was located at C-14 with β-orientation[4] in **3**. This was confirmed by the signals of H-15 appearing at δ 3.04 and 3.32 as a doublet of geminal coupling (each, J = 19 Hz). The downfield shifts (β-effect) were observed for the C-8 ($\Delta\delta = 7.32$ ppm), C-13 ($\Delta\delta = 8.23$ ppm) and C-15 ($\Delta\delta = 10.69$ ppm) resonances and the upfield shift (γ-effect) was demonstrated by the C-7 ($\Delta\delta = 2.74$ ppm) resonance in **3**, when compared with the corresponding signals in **2**, which also suggested that the extra hydroxyl group is attached at C-14.

Javanicin X (**4**), $C_{21}H_{28}O_7$, was obtained as colorless prisms, mp 138—140 °C. The IR and UV spectra of **4** indicated the presence of hydroxyl (ν_{max} 3450 cm^{-1}), α,β-unsaturated ketone (ν_{max} 1650 and 1608 cm^{-1} and λ_{max} 258 nm) and carbonyl (ν_{max} 1710 (br) cm^{-1}) groups. The presence of these carbonyl carbons was indicated by the ^{13}C signals at δ 169.67, 193.94 and 199.94. The ^{1}H- and ^{13}C-NMR spectra of javanicin X (**4**) showed close correspondence with those of javanicin A (**7**).[3] The ^{1}H–^{1}H COSY suggested the presence of two isolated structure units, ■–C(5)H–C(6)H_2–C(7)H–■ and ■–C(9)H–C(11)H–C(12)H–C(13)H–C(21)H_3–C(14)H–C(15)H_2–■ in the

TABLE I. ^{1}H-NMR Spectral Data for Compounds **1**—**7**

Proton	**1**[a]	**6**[a]	**2**[b]	**3**[b]	**7**[b]	**4**[b]	**5**[b]
H-2			5.05 dd (11, 8)	5.12 dd (10, 8)			
H-3	5.61 d (2)	5.58 d (2)	1.49 m 2.45 m	1.54 m 2.49 m	5.49 dd (6, 2)	6.03 s	6.03 s
H-4	2.51 m	2.50 m	1.20 m 1.74 m	1.25 m 1.78 m	1.86 ddd (18,6,4) 2.16 ddd (18,11,2)		
H-5	1.61 ddd (12,9,4)	1.59 ddd (12,9,4)	1.95 ddd (13,3,3)	1.99 ddd (13,3,3)	2.28 m	2.58 dd (6, 2)	2.60 dd (6, 2)
H-6	1.82 ddd (15,4,3) 2.02 m	1.80 ddd (14,4,3) 1.99 ddd (14,12,2)	1.60 ddd (13,3,3) 1.86 ddd (13,13,2)	1.71 ddd (14,3,3) 1.89 ddd (14,13,2)	1.55 ddd (14,3,3) 1.96 ddd (14,11,3)	2.22 ddd (15,7,3) 3.22 m	2.36 ddd (15,7,3) 3.24 m
H-7	4.23 dd (3, 2)	4.17 dd (3, 2)	4.10 dd (3, 2)	4.79 dd (3, 2)	4.10 t (3)	4.23 t (3)	4.29 t (3)
H-9	2.11 d (10)	2.06 d (10)	2.87 d (11)	2.99 d (12)	2.43 d (11)	3.08 d (11)	3.26 d (11)
H-11	3.87 q (10)	3.82 q (10)	3.97 dd (12, 11)	4.14 ddd (12,11,9)	3.96 ddd (11,9,8)	4.00 m	4.38 m
H-12	4.83 d (10)	3.15 d (10)	3.17 dd (12, 9)	3.19 dd (11, 9)	3.08 dd (10, 8)	3.22 m	4.00 d (8)
H-13			2.08 m	2.30 m	2.08 m	2.02 m	
H-14	1.98 dd (12, 8)	1.99 dd (12, 8)	1.65 m		1.66 ddd (12,8,5)	1.67 m	2.21 dd (12, 7)
H-15	2.39 dd (19, 12) 2.56 dd (19, 8)	2.45 dd (19, 12) 2.53 dd (19, 8)	2.65 dd (19, 8) 2.74 dd (19, 12)	3.04 d (19) 3.32 d (19)	2.67 dd (20, 12) 2.76 dd (20, 8)	2.62 dd (19, 7) 2.91 dd (19, 12)	2.78 dd (19, 7) 2.99 dd (19, 12)
Me-4	1.07 d (7)	1.06 d (7)					
Me-8	1.41 s	1.37 s	1.08 s	1.29 s	1.07 s	1.10 s	1.67 s
Me-10	1.36 s	1.35 s	1.38 s	1.48 s	1.35 s	1.50 s	1.64 s
Me-13	1.00 s	1.11 s	0.97 d (7)	1.30 d (7)	0.99 d (8)	0.95 d (7)	1.45 s
OMe-2	3.49 s	3.50 s			3.45 s	3.43 s	3.46 s
OMe-12		3.56 s	3.65 s	3.71 s	3.71 s	3.66 s	
OAc-12	2.07 s						
11-OH	3.44 d (10)	3.48 d (10)		4.49 br d (9)	4.60 d (9)		

Coupling constants (J in Hz) are given in parentheses. *a*) In DMSO-d_6. *b*) In C_5D_5N.

TABLE II. ^{13}C-NMR Spectral Data for Compounds **1**—**7**

Carbon	**1**[a]	**6**[a]	**2**[b]	**3**[b]	**7**[b]	**4**[b]	**5**[b]
C-1	204.42	204.44	218.67	218.55	204.75	199.94	201.19
C-2	147.34	147.45	71.43	71.41	149.72	166.24	166.63
C-3	118.70	118.37	25.66	25.73	112.47	108.68	108.55
C-4	31.15	31.03	42.87	40.76	28.08	193.94	194.17
C-5	43.38	43.37	39.13	38.94	36.72	51.32	51.48
C-6	24.49	24.77[c]	29.69	29.53	29.61	24.91	25.24[e]
C-7	80.52	80.56	82.68	79.94	82.42	82.54	82.35
C-8	35.98	35.68	35.69	43.01[d]	37.96	35.44	36.57
C-9	38.02	37.63	37.44	36.97	37.96	41.84	42.55
C-10	47.27	47.16	51.05	51.26	48.16	49.36	49.68
C-11	67.50	70.11	73.62	73.43	74.05	71.41	69.60
C-12	79.22	87.96	88.32	89.26	88.78	88.17	78.33
C-13	73.94	74.83	34.90	43.13[d]	34.95	34.02	75.28
C-14	48.98	48.27	45.52	74.62	44.85	46.30	50.75
C-15	29.67	29.39	28.53	39.22	28.64	27.95	30.34
C-16	169.46	169.49	170.11	170.21	169.99	169.67	169.95
C-18	19.06	18.88					
C-19	12.16	11.90	12.54	11.15	11.27	16.61	16.76
C-20	24.49	24.44[c]	21.88	15.21	21.38	22.34	25.91[e]
C-21	22.71	22.48	14.76	12.78	14.68	14.83	24.70[e]
OMe-2	54.81	54.71			55.08	56.16	56.14
OMe-12		61.35	60.91	60.85	61.28	61.15	
OCOMe-12	20.74						
OCOMe-12	170.38						

a) In DMSO-d_6. *b*) In C_5D_5N. *c*—*e*) Values may be interchanged.

structure of **4**. The difference between **4** and **7** suggested that methylene proton signals in **7** were replaced by a ketone group in **4** at C-4. Therefore, the A-ring of **4** has a conjugated 1,4-diketone moiety (two carbonyl carbons; ^{13}C, δ 199.94 and 193.94). The downfield shifts were observed for the H-3 ($\Delta\delta = 0.54$ ppm), H-5 ($\Delta\delta = 0.30$ ppm) and H-6 ($\Delta\delta = 0.67$ and 1.26 ppm) in **4**, compared with the corresponding signals in **7**. These downfield shifts are influenced by the ketone group at C-4.

Javanicin Y (**5**), $C_{20}N_{26}O_8$, was obtained as colorless needles mp 155—157 °C. The IR and UV spectra of **5** indicated the presence of hydroxyl (ν_{max} 3450 cm^{-1}), α,β-unsaturated ketone (ν_{max} 1650 and 1605 cm^{-1} and λ_{max} 252 nm) and carbonyl (ν_{max} 1710 (br) cm^{-1}) groups. The presence of these carbonyl carbons was indicated by the ^{13}C signals at δ 169.95, 194.17 and 201.19. The ^{1}H- and ^{13}C-NMR spectra of **5** were very similar to those of **4**, apart from the absence in **5** of the signals for methoxyl and H-13 protons. Instead of secondary methyl protons at C-13 in **4**, compound **5** exhibited the signal for tertiary methyl protons. The chemical shift of Me-13 in **5** was also shifted downfield by about 0.5 ppm. Therefore, the methine carbon at C-13 in **4** had to be changed to a quarternary carbon bearing a hydroxyl group in **5**. These results agreed with the ^{13}C-NMR data which showed the signals at δ 34.02 (C-13) and 14.83 (Me-13) in the spectrum of **4** being replaced by signals at δ 75.28 (C-13) and 24.70 (Me-13) in **5**. The position of a methoxyl group in **5** was determined by an NOE experiment. Irradiation of the methoxyl protons at δ 3.46 induced 33% NOE enhancement in H-3, suggesting that the location of the methoxyl group was at C-2.

The relative stereochemistry of five new javanicins U (**1**), V (**2**), W (**3**), X (**4**) and Y (**5**) was determined by NOE measurements (see Experimental section) and comparison of coupling constants. From these observations, all the angular chiral centers (C-5, C-7, C-8, C-9, C-10 and C-14) and other chiral centers (C-2, C-4 and C-13) were compatible with the usual picrasane skeleton,[5] and H-2 (**2** and **3**), H-11 and H-12 were deduced to be β-, β- and α- axials, respectively. On the basis of the above results, the structures of javanicins U, V, W, X and Y were determined to be **1**, **2**, **3**, **4** and **5**, respectively.

Experimental

All melting points were determined on a Yanagimoto micromelting point apparatus and are uncorrected. The UV and IR spectra were recorded on Hitachi 340 and Hitachi 260-30 spectrophotometers, respectively. The ^{1}H-NMR and ^{13}C-NMR spectra were recorded with a JEOL JNM GX-400 (^{1}H, 400 MHz; ^{13}C, 100 MHz) spectrometer. Chemical shifts are given on the δ-scale (with ppm downfield from tetramethylsilane as internal standard) and coupling constants (J) in hertz (Hz). Electron-impact mass spectrometry (EIMS) and high-resolution MS (HRMS) were run on JEOL JMS D-300 and JEOL JMS DX-303 mass spectrometers, respectively. Optical rotations were determined on a JASCO DIP-4 digital polarimeter. Column chromatography was carried out on silica gel (BW-820MH, Fuji Davison) and Diaion HP-20 (Mitsubishi Kasei). Low-pressure liquid chromatography (LC) and high performance LC (HPLC) were carried out on silica gel (CQ-3, 24 i.d. × 360 mm, Fuji Gel, detector: 254 nm) and silica gel (Senshu Pak SSC-Silica 3251-N, 8 i.d. × 250 mm, detector: 254 nm), respectively.

Isolation of Javanicins U (1), V (2) and W (3) The dried stems (3.7 kg) of *Picrasma javanica* collected in Indonesia, in July, 1986, were extracted with MeOH (49 l). The extract was evaporated to dryness and residue, to which an equal volume of water was added. The aqueous solution was

extracted with $CHCl_3$ (12 l) and then *n*-BuOH (3.6 l). The $CHCl_3$ soluble fraction (73 g) was repeatedly subjected to column chromatography on silica gel. Elution was performed with 1, 5, 10, 25, 50% MeOH in $CHCl_3$ and MeOH. The 10% MeOH in $CHCl_3$ fraction was subjected to preparative low-pressure LC (silica gel) and HPLC (silica gel) with the solvent system, CH_2Cl_2–MeOH (20 : 1), to afford javanicins U (**1**, 29 mg), V (**2**, 28 mg) and W (**3**, 10 mg).

Isolation of Javanicins X (4) and Y (5) Dried bark (1.8 kg) of the same plant was extracted with MeOH (16 l). The extract was concentrated under reduced pressure to give a residue (263 g), to which an equal volume of water was added. The aqueous solution was extracted with $CHCl_3$ (4 l) and then *n*-BuOH (4 l). The *n*-BuOH-soluble fraction (38 g) was applied to a column of Diaion HP-20. Elution with MeOH gave some fractions, which were chromatographed on silica gel columns. Elution was performed with 1, 5, 10, 25, and 50% MeOH in $CHCl_3$ and MeOH. The 10% MeOH in $CHCl_3$ fraction was subjected to preparative low-pressure LC (silica gel) and HPLC (silica gel) with the solvent system, CH_2Cl_2–MeOH (20 : 1), to afford javanicins X (**4**, 9 mg) and Y (**5**, 8 mg).

Javanicin U (1) Colorless prisms (MeOH), mp 257—259 °C, $[\alpha]_D^{24}$ +46.2° (*c*=0.8, C_5H_5N). UV λ_{max}^{MeOH} nm (log ε): 272 (3.51). IR ν_{max}^{KBr} cm^{-1}: 3450, 1750, 1710, 1680, 1645, 1610, 1460, 1375, 1270, 1235, 1145, 1110, 1050, 1035. ^{1}H-NMR and ^{13}C-NMR data are given in Tables I and II, respectively. MS *m/z*: 436 (M^+, 6%), 418 (68), 376 (75), 361 (100), 343 (27), 315 (48), 299 (17), 262 (19), 165 (22). HRMS *m/z*: 436.2084 $[M]^+$ (Calcd for $C_{23}H_{32}O_8$: 436.2088). NOE difference spectra: irradiated proton→observed proton (enhancement NOE %), δ 3.87→δ 1.41 (Me-8, 10) and 1.36 (Me-10, 10); δ 4.23→δ 1.41 (Me-8, 6), 1.36 (Me-10, 5), 1.98 (H-14, 13) and 2.39 (H-15β, 7); δ 1.00→δ 4.83 (H-12, 9) and 2.56 (H-15α, 17).

Javanicin V (2) Colorless prisms (MeOH), mp 107—108 °C, $[\alpha]_D^{23}$ +16.3° (*c*=0.9, MeOH). IR ν_{max}^{KBr} cm^{-1}: 3480, 1730, 1465, 1450, 1390, 1260, 1230, 1145, 1115, 1090, 1045. ^{1}H-NMR and ^{13}C-NMR data are given in Tables I and II, respectively. MS *m/z*: 366 (M^+, 31%), 348 (24), 320 (89), 288 (39), 276 (44), 261 (37), 245 (37), 229 (47), 143 (91), 98 (100). HRMS *m/z*: 366.2032 $[M]^+$ (Calcd for $C_{20}H_{30}O_6$: 366.2034). NOE difference spectra: irradiated proton→observed proton (enhancement NOE %), δ 1.22→δ 4.14 (H-7, 9), 3.73 (H-11, 11), 1.76 (H-14, 6) and 1.40 (Me-10, 10); δ 1.40→δ 4.73 (H-2, 10) and 3.73 (H-11, 7); δ 1.04→δ 2.90 (H-12, 4).

Acetylation of Javanicin V (2) Javanicin V (**2**, 15 mg) was acetylated with acetic anhydride (1 ml) and pyridine (1 ml) at room temperature for 6 h. After MeOH (20 ml) was added, evaporation of the reaction mixture gave a residue (17 mg) which was purified by low-pressure LC (silica gel) to give a pure monoacetyljavanicin V (**2a**, 15 mg). **2a**: mp 89—91 °C, $[\alpha]_D^{20}$ −29.7° (*c*=1.5, $CHCl_3$). IR ν_{max}^{KBr} cm^{-1}: 3490, 2930, 1730, 1250, 1115. MS *m/z*: 408 (M^+, 19%), 390 (12), 342 (45), 310 (35), 270 (23), 43 (100). ^{1}H-NMR (400 MHz, C_5D_5N) δ: 5.86 (1H, dd, *J*=12, 7 Hz, H-2), 4.11 (1H, br t, *J*=2 Hz, H-7), 3.96 (1H, dd, *J*=12, 10 Hz, H-11), 3.65 (3H, s, OMe-12), 3.15 (1H, dd, *J*=10, 9 Hz, H-12), 2.78 (1H, dd, *J*=19, 9 Hz, H-15), 2.70 (1H, d, *J*=12 Hz, H-9), 2.64 (1H, dd, *J*=19, 7 Hz, H-15), 2.01 (3H, s, OAc-2), 1.46 (3H, s, Me-10), 1.06 (3H, s, Me-8), 0.96 (3H, d, *J*=7 Hz, Me-13).

Javanicin W (3) Colorless needles (MeOH), mp 169—171 °C, $[\alpha]_D^{23}$ +31.0° (*c*=1.0, MeOH). IR ν_{max}^{KBr} cm^{-1}: 3540, 3470, 3320, 1710 (br), 1633, 1388, 1375, 1270, 1250, 1115, 1080, 1037. ^{1}H-NMR and ^{13}C-NMR are given in Tables I and II, respectively. MS *m/z*: 382 (M^+, 2%), 364 (82), 346 (10), 332 (30), 277 (100), 220 (17). HRMS *m/z*: 364.1889 $[M-H_2O]^+$ (Calcd for $C_{20}H_{28}O_6$: 364.1878). NOE difference spectra: irradiated proton→observed proton (enhancement NOE %), δ 1.29→δ 1.48 (Me-10, 13), 4.79 (H-7, 21), 4.14 (H-11, 14); δ 1.48→δ 5.12 (H-2, 14), 4.14 (H-11, 8), 1.29 (Me-8, 9); δ 1.30→δ 3.19 (H-12, 4), 4.49 (OH-11, 8).

Javanicin X (4) Colorless prisms (MeOH), mp 138—140 °C, $[\alpha]_D^{23}$ +39.8° (*c*=1.1, MeOH). UV λ_{max}^{MeOH} nm (log ε): 258 (3.61). IR ν_{max}^{KBr} cm^{-1}: 3450, 1710 (br), 1650, 1608, 1450, 1370, 1250, 1220, 1105, 1050. ^{1}H-NMR and ^{13}C-NMR are given in Tables I and II, respectively. MS *m/z*: 392 (M^+, 19%), 374 (31), 359 (15), 315 (13), 299 (15), 232 (26), 217 (21), 167 (37), 143 (55), 98 (100). HRMS *m/z* 392.1824 $[M]^+$ (Calcd for $C_{21}H_{28}O_7$: 392.1827). NOE difference spectra: irradiated proton→observed proton (enhancement %), δ 1.10→δ 4.23 (H-7, 9), 4.00 (H-11, 6), 2.02 (H-13, 9), 1.67 (H-14, 7) and 1.50 (Me-10, 9); δ 0.95→δ 3.22 (H-12, 4) and 2.91 (H-15α, 5).

Javanicin Y (5) Colorless needles (MeOH), mp. 155—157 °C, $[\alpha]_D^{18}$ +25.8° (*c*=0.8, MeOH). UV λ_{max}^{MeOH} nm (log ε): 252 (3.61). IR ν_{max}^{KBr} cm^{-1}: 3450, 2920, 1710 (br), 1650, 1605, 1460, 1250, 1220, 1195, 1070, 1035. ^{1}H-NMR and ^{13}C-NMR data are given in Tables I and II, respectively. MS *m/z*: 376 ($[M-H_2O]^+$, 17%), 361 (22), 343 (9), 315 (18), 291 (20), 271 (20), 167 (44), 43 (100). HRMS *m/z*: 395.1731 $[M+H]^+$ (Calcd for $C_{20}H_{27}O_8$: 395.1698). NOE difference spectra: irradiated proton→observed proton (enhancement NOE %), δ 4.29→δ 1.67 (Me-8, 5), 2.99 (H-15β, 3); δ 4.38→δ 1.67 (Me-8, 3), 1.64 (Me-10, 2); δ 2.21→δ 1.67 (Me-8, 3), δ 1.45→δ 4.00 (H-12, 3), 2.78 (H-15α, 5).

Acknowledgement We are grateful to P. T. Indonesia Eisai Co., Ltd., and Eisai Co., Ltd., for their kind supply of the plant material.

References and Notes

1) K. Koike, K. Ishii, K. Mitsunaga and T. Ohmoto, *J. Nat. Prod.*, "in press" and references cited therein.
2) T. Murae, T. Tsuyuki, T. Ikeda, T. Nishihama, S. Masuda and T. Takahashi, *Tetrahedron*, **27**, 1545 (1971).
3) T. Ohmoto, K. Koike, K. Mitsunaga, H. Fukuda and K. Kagei, *Chem. Pharm. Bull.*, **37**, 2991 (1989).
4) T. Murae, A. Sugie, T. Tsuyuki, S. Masuda and T. Takahashi, *Tetrahedron*, **29**, 1515 (1973); K. Koike, K. Ishii, K. Mitsunaga and T. Ohmoto, *Chem. Pharm. Bull.*, **39**, 939 (1991).
5) J. Polonsky, *Fortschr. Chem. Org. Naturst.*, **30**, 101 (1973); *idem*, *ibid.*, **43**, 221 (1986).

Isolation and Characterization of Phenolic Compounds from Magnoliae Cortex Produced in China

Shoji YAHARA,*[,a] Takashi NISHIYORI,[b] Akihide KOHDA,[b] Toshihiro NOHARA[a] and Itsuo NISHIOKA[c]

Faculty of Pharmaceutical Sciences, Kumamoto University,[a] Oe-honmachi 5–1, Kumamoto 862, Japan, Gifu Pharmaceutical University,[b] Gifu 502, Japan and Faculty of Pharmaceutical Sciences, Kyushu University 62,[c] Maidashi, Higashi-ku, Fukuoka 812, Japan. *Received December 25, 1990*

A chemical examination of Magnoliae Cortex produced in China (*Magnolia officinalis* REHD. *et* WILS., Magnoliaceae) has led to the isolation of eighteen new lignans and related compounds [four monoterpenyl-lignans: piperitylmagnolol (3), dipiperitylmagnolol (4), piperitylhonokiol (5) and bornylmagnolol (6); seven lignans: magnaldehydes B(8), C(9), magnolignans A(10), B(11), C(12), D(13) and E(14); three norlignans: magnatriol B(16), magnaldehydes D(17) and E(18); and four dilignans: magnolignans F(19), G(20), H(21) and I(22)], together with randainal (7), randaiol (15), sinapic aldehyde, syringaresinol, syringaresinol 4′-*O*-β-D-glucopyranoside and 6′-*O*-methylhonokiol. Their structures were determined by the chemical and spectral methods.

Keywords *Magnolia officinalis*; Magnoliaceae; lignan; piperitylmagnolol; piperitylhonokiol; bornylmagnolol; magnatriol; magnaldehyde; magnolignan; randainal

Magnoliae Cortex, the bark of *Magnolia officinalis* REHD. *et* WILS. (Magnoliaceae) is a Chinese crude drug used as a repression drug for turgescence of the thoreco-abdominal region, and a stomachic.[1)] With regard to the ingredients of the magnoliae species, lignans such as magnolol (**1**)[2)] and honokiol (**2**),[3)] and alkaloids[4)] are known, however, the minor constituents of this crude drug have not yet been surveyed. We have now obtained eighteen new lignans and related compounds together with **1**, **2**, randainal (**7**),[5)] randaiol (**15**),[5)] 1-(4-hydroxy-3-methoxyphenyl)-2-[4-(ω-hydroxypropyl)-2-methoxyphenoxy]propane-1,3-diol (**23**),[6)] sinapic aldehyde (**24**), syringaresinol (**25**), syringaresinol 4′-*O*-β-D-glucopyranoside (**26**), 6′-*O*-methylhonokiol (**27**).[7)] This paper deals with the structural characterization of the new compounds of monoterpenyl-lignans: piperitylmagnolol (**3**), dipiperitylmagnolol (**4**), piperitylhonokiol (**5**) and bornylmagnolol (**6**); lignans: magnaldehydes B(**8**) and C(**9**), magnolignans A(**10**), B(**11**), C(**12**), D(**13**) and E(**14**); norlignans: magnatriol B(**16**), magnaldehyde D(**17**) and E(**18**); and dilignans: magnolignans F(**19**), G(**20**), H(**21**) and I(**22**).

Monoterpenyl-Lignans Piperitylmagnolol (**3**), colorless viscous oil, $[\alpha]_D$ −146.0° ($CHCl_3$), showed the ultraviolet (UV) absorption [λ_{max}^{MeOH} (ε): 290 nm (8500)] and circular dichroism (CD) spectrum [$\theta]_{max}^{MeOH}$ (nm): $+7.22\times10^3$ (254), $+2.50\times10^3$ (292). It has a molecular formula $C_{28}H_{34}O_2$ (*m/z* 402.257), which is based on its electron impact mass spectrum (EI-MS) and nuclear magnetic resonance (NMR) spectra. It afforded a dimethyl ether (**3a**) on methylation. In the ^{1}H-NMR spectrum of **3**, signals at δ 0.80, 0.88 (each 3H, d, $J=6$ Hz), and 1.70 (3H, br s) were assignable to the methyl groups, and signals at δ 3.30 (4H, d, $J=6$ Hz), 5.00 (2H, br d, $J=11$ Hz), 5.02 (2H, br d, $J=18$ Hz) and 5.75—6.20 (2H, m) were similar to those of the allyl group in magnolol and five aromatic protons at δ 6.79 (m) were observed. The ^{13}C-NMR spectrum (Table I) of **3** revealed the presence of twelve aromatic carbons at δ 116.4 (d), 125.0×2 (s), 129.0×2 (d), 129.8 (d), 131.1 (d), 132.0×2 (s), 132.4 (s), 148.9 (s) and 150.8 (s) and two allyl group carbons at δ 39.3×2 (t), 115.3×2 (t) and 137.3×2 (d). Moreover, the remaining ten carbon signals indicated the occurrence of three methyl groups at δ 16.8, 21.6 and 23.5, a trisubstituted olefinic carbon at δ 124.3 (d) and 136.8 (s), three methine carbons at δ 27.0, 41.0 and 44.8, and two methylene carbons at δ 21.6 and 30.1. From the above evidence, **3** was assumed to be a monoterpenyl magnolol derivative. The monoterpenyl residue consisting of $C_{10}H_{17}$ was suggested by the ^{1}H-NMR spectrum to contain two methyl groups at δ 0.80 and 0.88, a trisubstituted olefinic proton at δ 5.40 (1H, br s), a methine proton at δ 3.60 (1H, m) coupled with the olefinic proton and a methyl group at δ 1.70 attached to a double bond. These signals were almost the same as those of a menthane-type monoterpene. Comparison of the ^{13}C-NMR spectra of the substituent in **3** with those of menthane, menthol, limonene and *p*-menth-1-ene (piperityl) moiety of linderatin[8)] revealed that the chemical shifts of the carbon atoms were similar to those of the *p*-menth-1-ene moiety of linderatin. Oxidation of the tetrahydrogenated compound (**3b**), obtained by the mild hydrogenation over Pd–C of **3**, with *m*-chloroperbenzoic acid, yielded a product (**3c**) (Chart 2), whose ^{1}H-NMR spectrum showed an epoxy methine proton signal at δ 4.27 (1H, d, $J=6$ Hz) and a benzylic methine proton signal at δ 3.02 (1H, dd, $J=6$, 11 Hz) coupled with the epoxy methine proton and C-4″ (δ 1.10, 1H, m) methine proton, suggesting the occurrence of a partial structure of *p*-menth-1″-ene-3″,4″-*trans* system (piperityl) for the substituent in **3**, and this result furthermore indicated that the magnolol moiety in **3** was linked at the C-3 carbon atom of the piperityl structure. As regards the bonding location into the magnolol side, the signal of one magnolol unit was shifted by +15.5 ppm at C-5 in the ^{13}C-NMR spectrum. Therefore, the structure of **3** was deduced to be 3″, 4″-*trans*-piperityl-(3″→5)-magnolol. In order to establish this structure involving the configurations at C-3″ and C-4″ on the piperityl moiety in **3**, dimethyltetrahydrate (**3d**), obtained by the methylation and hydrogenation of **3**, was treated with SeO_2 to give an oxidative product (**3e**). Next, **3e** was subjected to reduction with $NaBH_4$ to afford two C-6″-hydroxyl products **3f** and **3g** (Chart 2). Both compounds **3f** and **3g** showed a peak at *m/z* 450 due to M^+ in the EI-MS. Respective signals at δ 4.35 (1H, dd, $J=11$, 4 Hz) and 4.04 (1H, br t, $J=4$ Hz) in the ^{1}H-NMR spectra of **3f** and **3g** could be assigned to H-6″. Consequently, **3f** and **3g** could be represented as 6″-equatorial and 6″-axial hydroxyl products, respectively. The configuration at C-6″ of the two epimeric products were determined by the modified Horeau's method[9)] to be *S* for **3f** (6″-equatorial

hydroxyl) and *R* for **3g** (6″-axial hydroxyl). Consequently, the configuration on C-3″ and C-4″ of the piperityl moiety in **3** could be represented as 3 (*S*), 4 (*S*). The structure of **3** was concluded to be as shown in the formula.

Dipiperitylmagnolol (**4**), a white powder, $[\alpha]_D$ −140.0° ($CHCl_3$) showed a maximum absorption band at 290 nm ($\varepsilon = 10200$) in the UV spectrum. The EI-MS of **4** presented a molecular ion peak at *m/z* 538.373, indicating the molecular formula to be $C_{38}H_{50}O_2$. In the ^{1}H-NMR spectrum, the characteristic signals were due to the piperityl groups and substituted magnolol moiety. These spectral data indicated that **4** was a magnolol substituted symmetrically by the two piperityl groups. The ^{13}C-NMR (Table I) signals also indicated the presence of the piperityl moieties and the magnolol moiety di-substituted at C-5 and C-5′ in a symmetrical structure, showing down-field shifts at C-5 and C-5′ carbons (+15.8 ppm) by comparing with those of magnolol. Compound **4** was therefore considered to be dipiperityl-(3″→5 and 3‴→5′)-magnolol. The configurations at C-3″, C-3‴, C-4″ and C-4‴ in **4** were established as *S*, *S*, *S* and *S*, respectively, by reason of a comparative study of the Cotton curves in the CD spectra of **3** and **4** [255 nm (+1.04 × 10^4) and 294 nm (+4.96 × 10^3)]. Therefore, the structure of **4** could be represented as shown in the formula.

Piperitylhonokiol (**5**) was obtained as a colorless viscous oil, $[\alpha]_D$ −97.0° ($CHCl_3$), $C_{28}H_{34}O_2$, showed a maximum absorption at 290 nm in the UV spectrum. In the EI-MS, the same molecular ion peak at *m/z* 402 as that of **3** was obtained, thus **5** was estimated to be an isomer of **3**. The ^{13}C-NMR spectrum (Table I) of **5** exhibited piperityl moiety and honokiol moiety signals, in which the C-5 or C-5′ signal

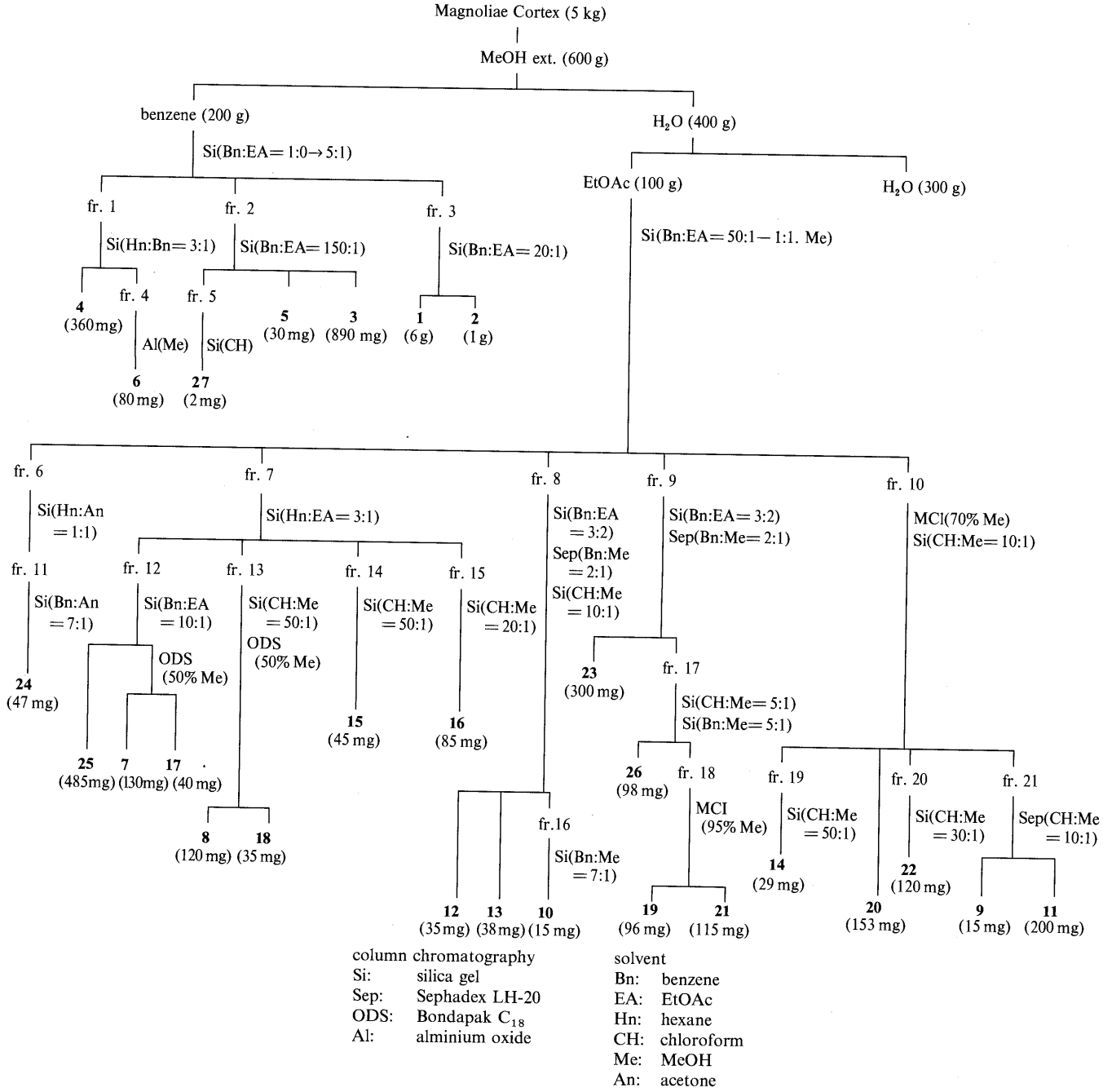

Chart 1. Extraction and Separation of Magnoliae Cortex

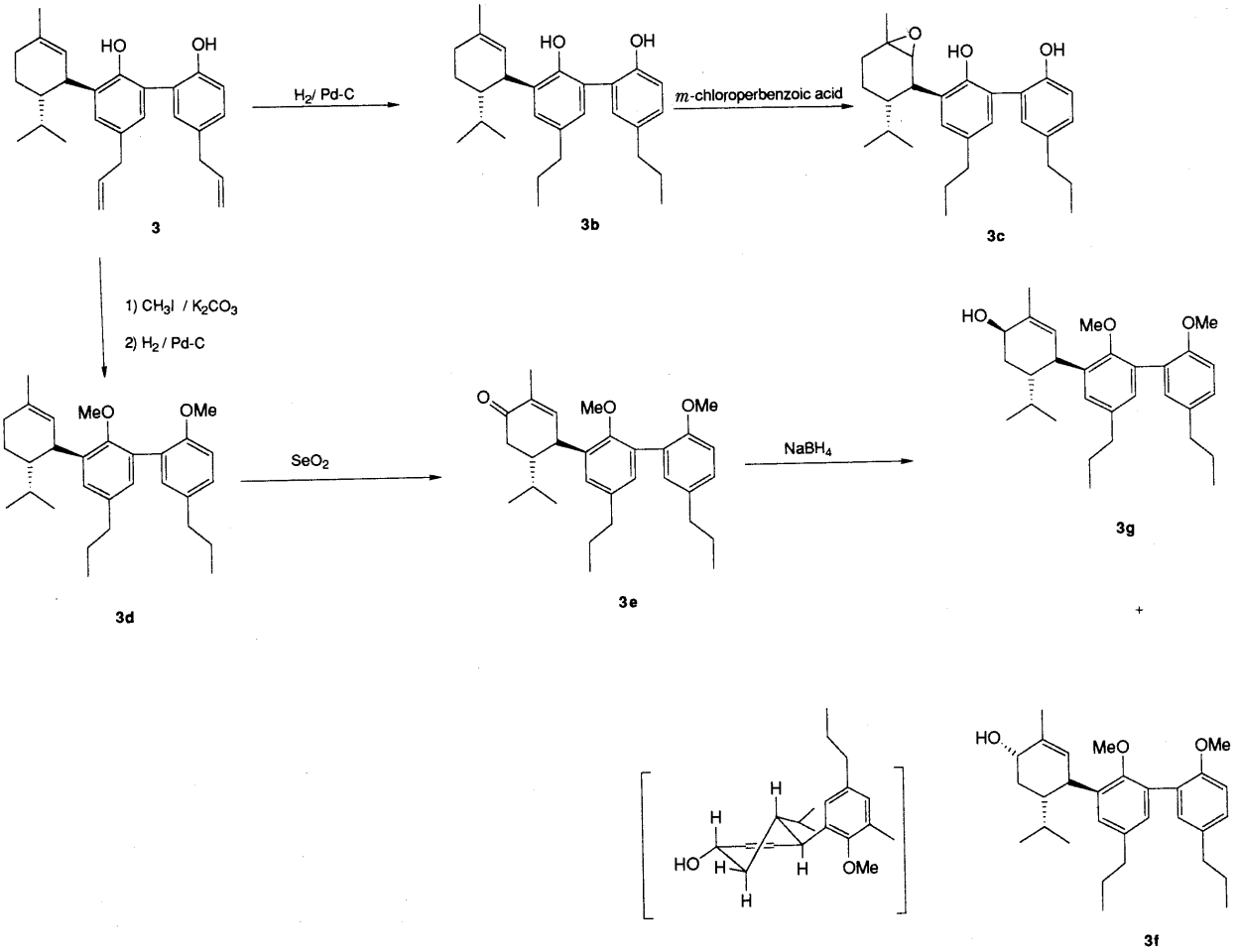

Chart 2

known compounds

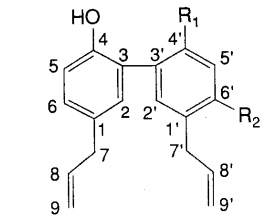

magnolol (1) : R_1= OH, R_2= H
honokiol (2) : R_1= H, R_2= OH

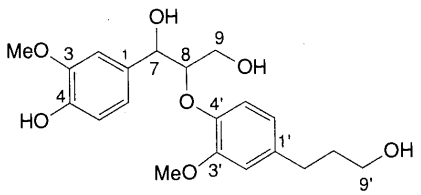

23

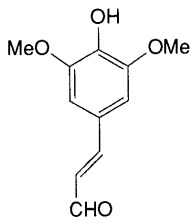

sinapic aldehyde (24)

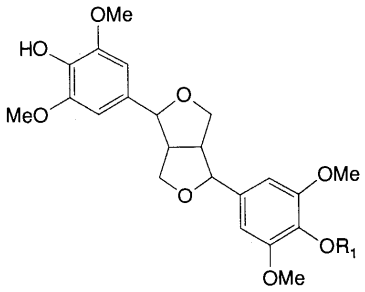

syringaresinol (25) : R_1= H
syringaresinol 4'-*O*-glucopyranoside (26) : R_1= glc

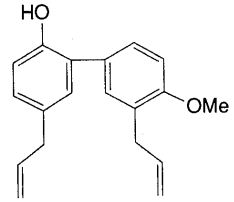

6'-*O*-methylhonokiol (27)

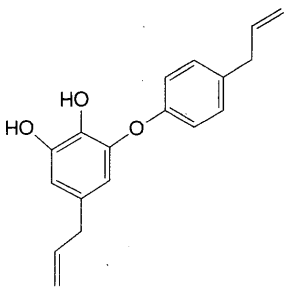

obovatol (29)

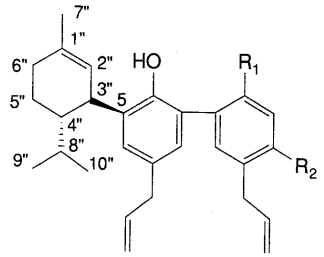

piperitylmagnolol (3) : R_1= OH, R_2= H
piperitylhonokiol (5) : R_1= H, R_2= OH

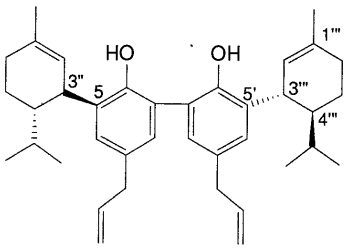

dipiperitylmagnolol (4)

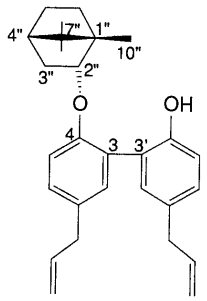

bornylmagnolol (6)

TABLE I. ^{13}C-NMR Data for **1**, **2**, **3**, **4**, **5**, **6** and Borneol ($CDCl_3$)

	1	2	3	4	5	6	Borneol
C-1	132.9	132.1	132.0[a]	132.0	131.2	133.4	
C-2	131.2	130.7	129.0[b]	129.9	131.4	132.3[a]	
C-3	124.7	126.4	125.0	125.4	125.7	128.0	
C-4	150.8	150.1	148.9	149.5	149.3	153.3	
C-5	116.5	115.3	132.0	132.2	131.0	117.2	
C-6	129.3	130.0	129.0[b]	129.2	129.4	129.1[b]	
C-7	39.5	39.2	39.3	39.5	39.5	39.4	
C-8	137.2	137.4	137.3	137.5	138.0	137.9[c]	
C-9	115.2	115.4	115.3	115.4	115.3	115.7[d]	
C-1′	132.9	127.7	132.4[a]	132.0	128.2	131.9	
C-2′	131.2	128.0	131.1	129.9	128.2	131.0[a]	
C-3′	124.7	129.3	125.0	125.4	130.7	126.6	
C-4′	150.8	128.4	150.8	149.5	128.9	152.0	
C-5′	116.5	116.0	116.4	132.2	116.0	114.7	
C-6′	129.3	153.2	129.8[b]	129.2	153.5	128.9[b]	
C-7′	39.5	34.6	39.3	39.5	35.2	39.4	
C-8′	137.2	135.8	137.3	137.5	136.3	137.4[c]	
C-9′	115.2	116.2	115.3	115.4	116.7	115.3[d]	
C-1″			136.8	136.5	137.0	49.5	49.4
C-2″			124.3	124.8	124.7	87.0	76.9
C-3″			44.8	44.9	44.4	36.7	38.7
C-4″			41.0	40.7	41.4	44.9	45.1
C-5″			21.6	21.6	21.6	26.7	26.0
C-6″			30.1	30.1	30.2	27.8	28.3
C-7″			23.5	23.6	23.5	47.7	47.9
C-8″			27.0	27.6	27.5	19.3	20.2
C-9″			16.8	17.0	16.7	18.9	18.7
C-10″			21.6	21.6	21.6	13.6	13.3
C-1‴				136.5			
C-2‴				124.8			
C-3‴				44.9			
C-4‴				40.7			
C-5‴				21.6			
C-6‴				30.1			
C-7‴				23.6			
C-8‴				27.6			
C-9‴				17.0			
C-10‴				21.6			

a—d) Assignments are interchangeable in each column.

was shifted to δ 131.0, thus **5** was presumed to be bonding through the C-3″ of the piperityl moiety and C-5 or C-5′ of the honokiol moiety. The proton selective decoupling ^{13}C-NMR spectrum of **5** showed a long-range coupling between the H-3″ proton signal at δ 3.50 and the C-4 carbon signal at δ 149.3, thus **5** was concluded to be linked through C-3″ and C-5. The CD spectrum of **5** showed positive Cotton curves at 248 and 293 nm suggesting configurations at C-3″ and C-4″ to be *S* and *S*, respectively. Therefore, the structure of **5** could be represented as shown in the formula.

Bornylmagnolol (**6**), a colorless viscous oil, $[\alpha]_D$ −7.6° ($CHCl_3$) has a molecular formula, $C_{28}H_{34}O_2$ (*m/z* 402.254) based on its EI-MS, and afforded a monoacetate (*m/z* 444 in EI-MS) on acetylation. The ^{1}H-NMR spectrum of **6** showed three singlets of methyl groups at δ 0.80, 0.83 and 0.87, a signal at δ 4.38 (1H, dd, J=9, 3 Hz) for an axial hydrogen geminal to the ether linkage (this signal showed non-shift on acetylation), two allyl groups signals at δ 3.36 (4H, br d, J=7 Hz), 4.90—5.20 (4H, m) and 5.75—6.23 (2H, m), a hydroxy proton signal at δ 6.28 and six aromatic proton signals at δ 6.79—7.23, which suggested **6** to be a monoterpenyl-magnolol. The ^{13}C-NMR (Table I) signals also indicated the presence of a magnolol moiety and a monoterpenyl moiety, the latter of which consisted of three methyl groups (δ 13.6, 18.9 and 19.3), an oxygenated methine (δ 87.0), three methylenes (δ 26.7, 27.8 and 36.7), a methine (δ 44.9) and two quaternary carbons (δ 47.7 and 49.5). These signals were almost the same as those of borneol except for the C-2 carbon signal, which was shifted down-field by +10.1 ppm. From the above evidence, the chemical structure of **6** was estimated to involve an ether linkage through C-4-OH in magnolol and C-2 in borneol. As regards the configuration of the bornyl moiety, the optical rotation ($[M]_D$ −30.6°) of **6** was compared with that of (−)-borneol methyl ether ($[M]_D$ −82.5°), thus suggesting **6** should be (−)-bornyl group. Consequently, the structure of **6** could be represented as shown in the formula.

Lignans Randainal (**7**) was obtained as pale yellow needles, mp 135—138 °C, showed a molecular ion peak at *m/z* 280 in the EI-MS. The infrared (IR) spectrum showed the presence of a hydroxyl group (3550 cm^{-1}), α,β-unsaturated carbonyl group (1675 and 1625 cm^{-1}) and aromatic group (1605 cm^{-1}). The compound **7** was identified as randainal isolated previously from *Sassafras randaiense*.[5]

Magnaldehyde B(**8**), pale yellow needles, mp 155—158 °C, $C_{18}H_{16}O_3$, showed absorption bands due to a hydroxyl (3550 cm^{-1}), an α,β-unsaturated carbonyl (1675 and 1625 cm^{-1}) and aromatic groups (1605 cm^{-1}) in the IR spectrum. In the EI-MS, the same molecular ion peak at *m/z* 280 as that of **7** was obtained, thus **8** was estimated to be an isomer of **7**. The ^{1}H-NMR spectrum of **8** exhibited two ABX type aromatic signals [δ 6.92, 7.03 (each 1H, d, J=8 Hz, H-5, 5′), 7.33, 7.51 (each 1H, dd, J=8, 2 Hz, H-6, 4′) and 7.37, 7.60 (each 1H, d, J=2 Hz, H-2, 2′)], an allyl

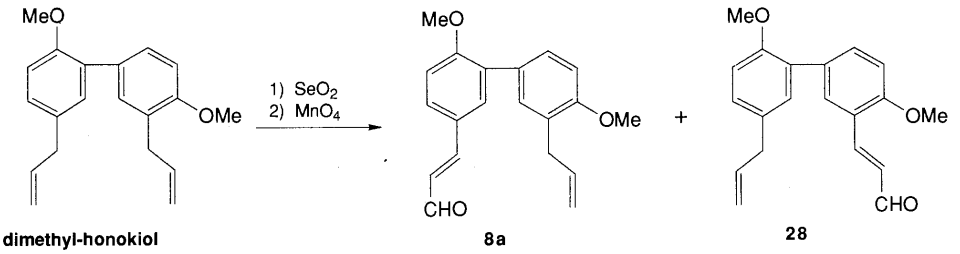

dimethyl-honokiol — **8a** — **28**

Chart 3

TABLE II. ^{13}C-NMR Data for **7**, **8**, **9**, **10**, **11**, **12**, **13** and **14** (in Acetone-d_6)

	7	8	9	10	11	12	13	14
C-1	127.7	126.8	127.0[a]	131.9[a]	132.6[a]	130.8[a]	130.9[a]	131.7[a]
C-2	133.6	131.6	130.1[b]	132.4	128.1	131.9[b]	130.3[b]	128.7[b]
C-3	127.0	126.8	128.0[a]	131.0[a]	126.7[b]	128.8	129.0[a]	129.6[c]
C-4	158.1	158.2	158.5	153.0	153.0[c]	153.0	154.8[c]	153.1
C-5	117.7	117.7	117.8	117.2[b]	117.1[d]	115.3[c]	115.4[d]	116.8
C-6	132.2	132.3	133.2[c]	133.3	132.5	131.6[b]	131.7[b]	131.7[d]
C-7	154.8	155.0	155.0	40.0	77.2	39.7	85.1	39.8
C-8	126.3	126.2	126.5	74.1	74.5	74.0	76.7	139.1
C-9	195.2	195.1	195.3	66.5	63.9	66.1	63.5	115.4
C-1′	132.2	129.6[a]	131.2	133.2[a]	135.2[a]	126.5	126.8	132.3[a]
C-2′	130.1	128.9	130.8[b]	130.5	130.9	128.8	129.0[b]	127.4[b]
C-3′	125.5	130.1[a]	125.4[a]	131.9[a]	127.2[b]	130.9[a]	130.8[a]	129.0[c]
C-4′	152.9	129.5	153.2	153.0	154.0[c]	129.3[b]	127.8[b]	131.2[d]
C-5′	116.9	115.4	115.8	117.4[b]	117.4[d]	116.5[c]	116.8[d]	110.1
C-6′	129.8	155.0	133.8[c]	129.8	129.6	154.5	154.6[c]	161.7
C-7′	39.7	34.9	39.5	40.0	40.0	34.9	35.0	92.0
C-8′	138.7	137.9	73.9	139.1	139.1	138.0	138.1	73.8
C-9′	115.6	115.5	66.0	115.5	115.5	115.3	115.5	62.7
OMe							56.7	

a—*d*) Assignments are interchangeable in each column.

group and an α,β-unsaturated aldehyde group signal [δ 6.75 (1H, dd, $J=16$, 8 Hz, H-8), 7.60 (1H, d, $J=16$ Hz) and 9.62 (1H, d, $J=8$ Hz, H-9)], thus suggesting that **8** was an isomer (honokiol type) of **7**. The ^{13}C-NMR spectrum of **8** exhibited a benzylic methylene signal (δ 34.9) and a terminal vinyl carbon signal (δ 115.5 and 137.9), which were similar with the allyl group signals in the *ortho*-allyl-phenol type, thus suggesting that **8** might be the 9-aldehyde type of honokiol. Treatment of honokiol dimethyl ether with SeO_2 and then with MnO_2 resulted in the formation of two oxidative products (**8a** and **28**) (Chart 3). The physical constants of **8a** agreed well with those of dimethylmagnaldehyde B prepared by methylation. Compound **28** was estimated as the 9′-aldehyde type of honokiol, an isomer of **8a**, by the nuclear Overhauser effect (NOE) experiment. All physical data of **8** were identical with those of the synthetic product.[10] Consequently, the structure of **8** could be represented as shown in the formula.

Magnaldehyde C(**9**), a pale yellow powder, $[\alpha]_D$ −15.5° (MeOH), IR ν_{max}^{KBr} 1655 cm^{-1} (α,β-unsaturated carbonyl), has a molecular ion peak at m/z 314 in the field desorption (FD)-MS. The ^{1}H-NMR spectrum of **9** exhibited signals due to a benzylic methylene [δ 2.65 (1H, dd, $J=14$, 8 Hz) and 2.84 (1H, dd, $J=14$, 5 Hz)], which coupled with an oxygenated methine proton [δ 3.80 (m)], two oxygenated methylene protons [δ 3.56 (m)], an α,β-unsaturated aldehyde group [δ 6.66 (1H, dd, $J=16$, 8 Hz), 7.70 (1H, d, $J=16$ Hz) and 9.62 (1H, d, $J=8$ Hz)] and six aromatic protons [δ 6.97—7.62 (m)]. The ^{13}C-NMR spectrum (Table II) of **9**, indicated distinctions in the two signals at C-8′ and C-9′ in the propyl moiety in comparison with those of **7**.

lignans

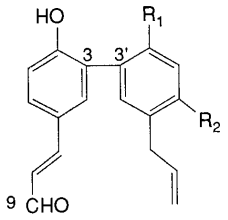

randainal (7) : R_1= OH, R_2= H
magnaldehyde B (8) : R_1= H, R_2= OH

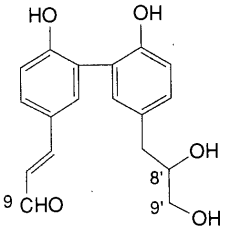

magnaldehyde C (9)

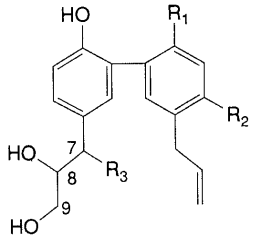

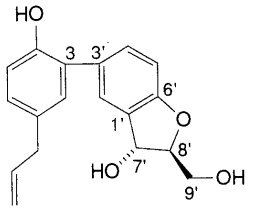

magnolignan A (10) : R_1= OH, R_2=R_3= H
magnolignan B (11) : R_1=R_3= OH, R_2= H
magnolignan C (12) : R_1=R_3= H, R_2= OH
magnolignan D (13) : R_1= H, R_2= OH, R_3= OMe

magnolignan E (14)

norlignans

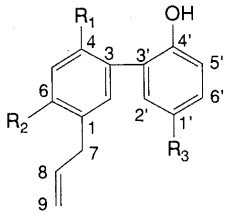

randaiol (15) : R_1=R_3= OH, R_2= H
magnatriol B (16) : R_1= H, R_2=R_3= OH
magnaldehyde D (17) : R_1= OH, R_2= H, R_3= CHO
magnaldehyde E (18) : R_1= H, R_2= OH, R_3= CHO

The above evidence suggested that the structure of **9** corresponds to that of **7** possessing two hydroxy groups at C-8′ and C-9′. The structure of **9** was thus concluded to be as shown in the formula.

Magnolignan A(**10**), a white powder, $[\alpha]_D$ −0.8° (MeOH) showed a molecular ion peak at m/z 300.134, along with m/z 239 ($M^+ - C_2H_5O_2$), indicating a molecular formula to be $C_{18}H_{20}O_4$ in the EI-MS, and was transformed into a tetraacetate on acetylation. The ^{1}H-NMR spectrum of **10** exhibited a benzylic methylene signal [δ 2.64 (1H, dd, $J=14$, 7 Hz) and 2.80 (1H, dd, $J=14$, 5 Hz)], one oxygenated methine and one oxygenated methylene signal [δ 3.82 (1H, m) and 3.50 (2H, m)], an allyl group signal and six aromatic

proton signals. The above evidence suggested that the structure of **10** was 8,9-dihydroxydihydro-magnolol. The ^{13}C-NMR spectrum (Table II) of **10**, when compared with those of **1** and **9**, indicated that the signals in **10** were nearly the same as those in the *para*-8,9-dihydroxypropyl-phenol moiety of **9** and as those in the *para*-allyl-phenol moiety of magnolol. The structure of **10** was then concluded to be as shown in the formula.

Magnolignan B(**11**), a white powder, $[\alpha]_D$ +0.3° (MeOH), showed a molecular ion peak at *m/z* 316 in the FD-MS, suggesting the one additional oxygen atom on **10**. The ^{1}H-NMR spectrum of **11** displayed an allyl group signal, two ABX-type aromatic proton signals [δ 6.90, 6.92 (each 1H, d, J=8 Hz), 7.07, 7.25 (each 1H, dd, J=8, 2 Hz), 7.11, 7.31 (each 1H, d, J=2 Hz)], a benzylic methine proton signal adjacent to the oxygen [δ 4.65 (d, J=6 Hz, H-7)] and one oxygenated methine and one oxygenated methylene signal [δ 3.70 (1H, m) and 3.52 (2H, m), respectively], suggesting that **11** had a hydroxyl group at C-7 in **10**. This inferential structure was supported with the ^{13}C-NMR data as listed in Table II. Therefore, the structure of **11** could be represented as shown in the formula.

Magnolignan C(**12**), a white powder, $[\alpha]_D$ −6.8° (MeOH), afforded a molecular ion peak at *m/z* 300.138 along with *m/z* 239 ($M^+ - C_2H_5O_2$) in the EI-MS, indicating the molecular formula to be $C_{18}H_{20}O_4$, and was transformed into a tetraacetate (**12a**) on acetylation. The ^{1}H-NMR spectrum of **12** exhibited the presence of an allyl group, a benzylic methylene group [δ 2.65 (1H, dd, J=12, 8 Hz), 2.79 (1H, dd, J=12, 6 Hz), H_2-7], one oxygenated methine and one oxygenated methylene group [δ 3.82 (1H, m) and 3.50 (2H, m)] and six aromatic proton signals. From the spectral data analogous to those of **10**, **12** was estimated to be a honokiol type isomer of **10**. The ^{13}C-NMR spectrum (Table II) of **12**, compared with those of **2** and **9**, the location of the hydroxyl groups were revealed to be at C-8 and C-9 positions in the honokiol skeleton. The structure of **12** could be represented as shown in the formula.

Magnolignan D(**13**), a white powder, $[\alpha]_D$ +3.0° (MeOH), exhibited a molecular ion peak at *m/z* 330.150, providing a molecular formula of $C_{19}H_{22}O_5$, besides strong peaks at *m/z* 300, 269 (base peak, $M^+ - C_2H_4O_2$) and 239 (*m/z* 269 − CH_2O) in the EI-MS. Its ^{1}H-NMR spectrum showed the signals of four protons consisting of an oxygenated benzyl methine signal [δ 4.17 (1H, d, J=7 Hz, H-7)] and one oxygenated methylene and one oxygenated methine signal [δ 3.66 (2H, m) and 4.00 (1H, m)]. Besides the above signals, an aliphatic methoxyl signal (δ 3.21), an allyl group signal and two ABX type aromatic signals [δ 6.89, 6.96 (each 1H, d, J=8 Hz), 7.12, 7.50 (each 1H, dd, J=8, 2 Hz) and 7.42, 7.56 (each 1H, d, J=2 Hz)] were observed. This signal pattern was similar to that of one side in **11**, except for the methoxyl signal. The ^{13}C-NMR spectrum, compared with that of **12**, indicated shifts of +45.4, +2.7 and −2.6 ppm in the *para*-propylphenol type C-7, C-8 and C-9, respectively, supporting that the structure of **13** could be 7-methoxylated **12**. Therefore, the structure of **13** was concluded to be as shown in the formula.

Magnolignan E(**14**), a white powder, $[\alpha]_D$ −2.0° (MeOH), showed a molecular ion peak at *m/z* 298 together with fragment peaks at *m/z* 280 ($M^+ - H_2O$) and 250 (*m/z* 280 − CH_2OH) in the FD-MS. The ^{1}H-NMR spectrum of **14** showed signals ascribable to two mutually coupled methines bearing oxygen [δ 4.53 (dd, J=10, 6 Hz) and 5.28 (m, after D_2O exchange J=4 Hz)], an oxygenated methylene proton [δ 3.75 (2H, d, J=6 Hz)], an allyl group and six aromatic proton signals. On methylation, **14** afforded a monomethyl ether (**14a**) [^{1}H-NMR: δ 3.78 (3H, s)]. On acetylation, **14** yielded a triacetate (**14b**) [EI-MS *m/z*: 424 (M^+)]. The location of the acetyl groups in **14b** was determined by comparing the ^{1}H-NMR spectra with those of **14a**. Signals due to the benzylic methine and terminal methylene appeared at δ 6.11 (1H, d, J=4 Hz, H-7′), and at 4.28 (1H, dd, J=6, 12 Hz, H-9′) and 4.42 (1H, dd, J=5, 12 Hz, H-9′) showing acetylation shifts. Taking the chemical shift of the H-8′ signal into account, the C-7′ and C-8′ position were concluded to be on the dihydrobenzofuran ring, compared with those of **2** and **13**. The ^{13}C-NMR spectrum of **14** exhibited to oxygenated methine carbons (δ 73.8 and 92.0) and one oxygenated methylene carbon (δ 62.7). Moreover, the ^{13}C-NMR spectrum of **14**, compared with that of **2**, indicated shifts of +8.5 and −5.9 ppm at C-6′ and C-5′, respectively, also supporting the above deduced structure. The relative stereochemistry of the two substituents on the dihydrobenzofuran ring was concluded to be *trans*, based on the fact that irradiation of the hydroxymethyl H_2-9′ signal (δ 3.75) caused the enhancement of the benzylic H-7′ signal (δ 5.28) in the NOE experiment of **14**. Therefore, the structure of **14** could be represented as shown in the formula.

Norlignans Randaiol (**15**) showed a molecular peak at *m/z* 242 in the EI-MS. The ^{1}H-NMR spectrum of **15** revealed the presence of an allyl group and two ABX type aromatic protons [δ 6.75, 7.05 (each 1H, dd, J=9, 2 Hz), 6.84, 6.94 (each 1H, d, J=9 Hz) and 6.79, 7.11 (each 1H, d, J=2 Hz)]. The compound **15** was identified as randaiol isolated previously from *Sassafras randaiense*.[5]

Magnatriol B(**16**), pale yellow needles, mp 99—100 °C, showed an absorption maximum at 306 nm (ε=5100) in the UV spectrum. In the EI-MS, the same molecular ion peak at *m/z* 242 ($C_{15}H_{14}O_3$) as that of **15** was obtained, thus **16** was estimated to be an isomer of **15**. The ^{1}H-NMR spectrum of **16** showed signals ascribable to an allyl group and two

Table III. ^{13}C-NMR Data for **15**, **16**, **17** and **18** (in Acetone-d_6)

	15	16	17	18
C-1	132.6	126.7	132.5	130.0
C-2	132.2	128.8	131.1[a]	128.9
C-3	127.2[a]	129.9[a]	125.3	129.3
C-4	152.7[b]	131.5	153.4	130.6
C-5	116.2[c]	115.4[b]	117.1[b]	115.5
C-6	129.7	154.6	130.1	155.1
C-7	39.8	34.6	39.9	34.8
C-8	138.8	137.9	139.0	137.8
C-9	115.7	115.4	115.6	115.5
C-1′	151.6[b]	151.2	130.7	130.5
C-2′	118.2[c]	117.5[c]	134.9	133.2
C-3′	127.9[a]	130.9[a]	127.8	127.0
C-4′	147.3	147.6	160.9	160.5
C-5′	117.4[c]	117.4[c]	117.8[b]	117.2
C-6′	118.1[c]	115.0[b]	132.5[a]	131.6
C-7′			191.2	191.3

a—*c*) Assignments are interchangeable in each column.

ABX type aromatic signals. The ^{13}C-NMR spectrum (Table III) of **16**, when compared with that of **15**, indicated shifts of +24.9, −4.9 and −21.2 ppm at C-6, C-7 and C-4, respectively, and other signals were almost the same pattern. On methylation of **16** it afforded a trimethyl ether, which was then hydrogenated to yield a dihydrotrimethyl ether (**16a**) [EI-MS *m/z*: 286 (M^+)]. In the NOE experiments of **16a**, irradiation on the benzylic methylene (H_2-7) signal at δ 2.76 caused enhancement of the H-2 [δ 7.53 (J=3 Hz)], on the other hand, irradiation on the center of the two methoxyl signals (δ 3.36 and 3.37) caused enhancements of the H_2-7 (δ 2.76), H-5 [δ 6.64 (d, J=9 Hz)] and H-5′ [δ 6.66 (d, J=9 Hz)], and irradiation on the methoxyl signal (δ 3.42) caused enhancements of the H-2′ [δ 7.15 (d, J=3 Hz)] and H-6′ [δ 6.80 (dd, J=9, 3 Hz)]. On the basis of these NOE, the structure of **16** was concluded to be as shown in the formula.

Magnaldehyde D(**17**), pale yellow needles, mp 140—143 °C, showed a molecular ion peak at *m/z* 254.093, indicating the molecular formula to be $C_{16}H_{14}O_3$ in the EI-MS. The ^{1}H-NMR spectrum of **17** revealed the presence of an aldehyde proton signal [δ 9.89 (s)], six aromatic proton signals and an allyl group. The above evidence suggested that the structure of **17** was presumed to be allyl-formyl-dihydroxy-biphenyl. In the ^{13}C-NMR spectrum (Table III), signals due to one allyl group [δ 39.9 (t), 115.6 (t) and 139.0 (d)] of the *ortho*-hydroxy-allyl-phenol type, the twelve aromatic signals and an aldehyde signal [δ 191.2 (d)] were observed. These signals were similar to those of **7**, except for the olefinic carbons at C-7 and C-8 in **7**. Therefore, the structure of **17** was concluded to be as shown in the formula.

Magnaldehyde E(**18**), pale yellow needles, mp 160—162 °C, showed a molecular ion peak at *m/z* 254 in the EI-MS, whose molecular weight was the same as that of **17**, thus **18** was estimated to be an isomer of **17**. To decide the location of hydroxyl, aldehyde and allyl groups on the biphenyl, a comparative investigation of the ^{13}C-NMR spectra (Table III) of **8** and **18** had almost the same chemical shifts, except for the olefinic carbons at C-7 and C-8 in **8**. Therefore, the structure of **18** was concluded to be as shown in the formula.

Dilignans Magnolignan F(**19**) showed a molecular ion peak at *m/z* 564 together with fragment ions at *m/z* 546, 282 and 266 in the FD-MS. In the ^{1}H-NMR spectrum, the signals due to three allyl groups, a benzylic methine [δ 4.64 (d, J=5 Hz)] and twelve aromatic protons were observed, which suggested **19** to be a dimeric lignan. The ^{13}C-NMR spectrum of **19** showed signals due to thirty-six carbons, including three signals [δ 70.2 (t), 74.1 (d) and 74.9 (d)] assignable to C-9″, C-8″ and C-7″, whose signal patterns were similar to those of 7,8,9-trihydroxypropyl moiety in **11**, signals of the magnolol type three allyl group and four oxygenated aromatic carbons. On methylation, **19** afforded a trimethyl ether (**19a**) [^{1}H-NMR: δ 3.68, 3.69, 3.73 (each 3H, s)]. Subsequent acetylation of **19a** yielded a diacetate (**19b**). The ^{1}H-NMR spectrum of **19b** exhibited mutually coupled two methine protons [δ 5.30 (m) and 5.82 (d, J=8 Hz)] connecting to the acetoxyl groups (δ 1.92 and 1.99). Hydrogenation of **19a** over Pd–C afforded a hexahydrogenated derivative (**19c**) [EI-MS *m/z*: 612 (M^+)]. From the above evidence, **19** was assumed to be a dilignan compound possessing an ether bonding between **1** and **11**. To determine the location of the ether bond, oxidation of **19c** with sodium metaperiodate was undertaken to yield two products (**19d** and **19e**) (Chart 4). The product **19d** showed a molecular ion at *m/z* 284 in the EI-MS. The ^{1}H-NMR spectrum of **19d** exhibited signals due to an aldehyde proton [δ 9.91 (s)], two methoxy groups (δ 3.75 and 3.87), a propyl group and two ABX type aromatic protons. The product **19d** was found to be identical with the dimethyldihydrogenated compound of **17**. Another

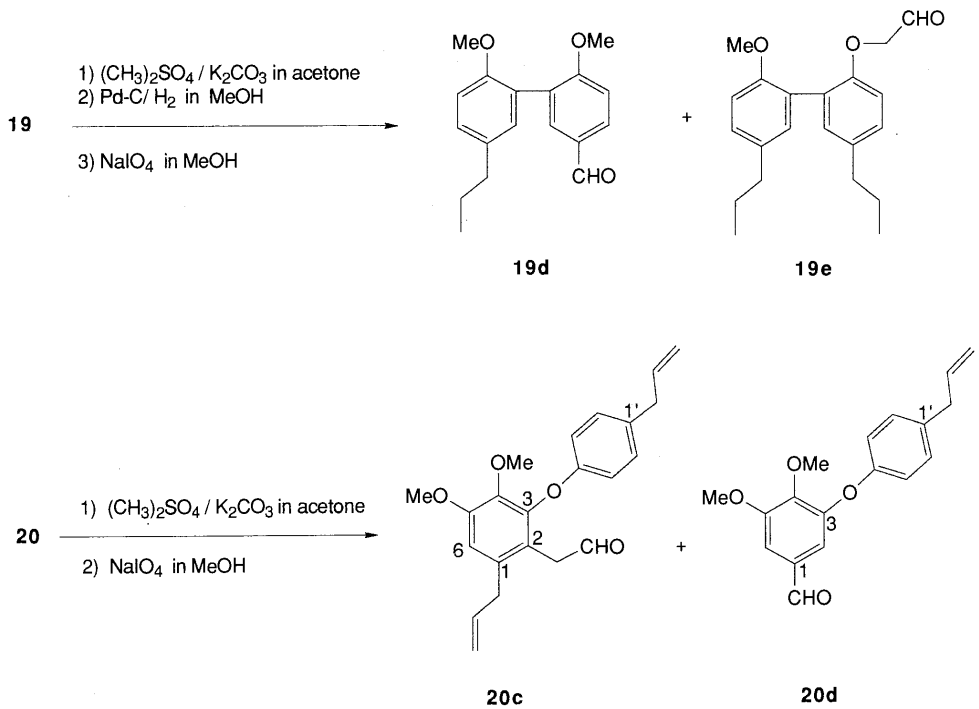

19d **19e**

20c **20d**

Chart 4

dilignans

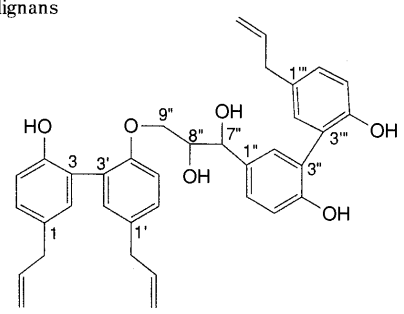

magnolignan F (19)

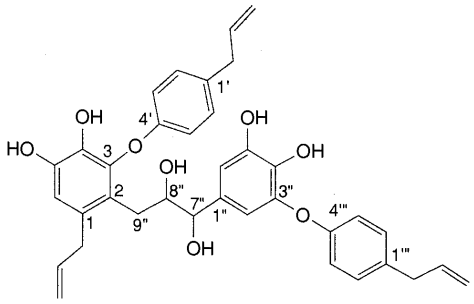

magnolignan G (20)

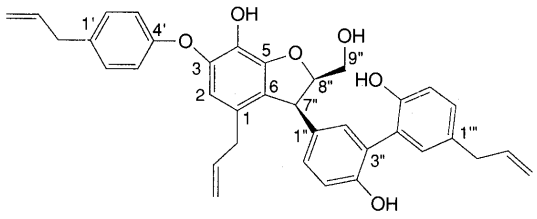

magnolignan H (21)

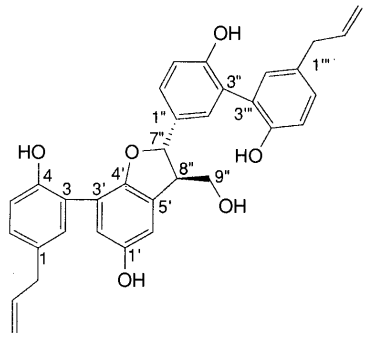

magnolignan I (22)

TABLE IV. ^{13}C-NMR Data for **19**, **20**, **21**, **22** (in Acetone-d_6) and Obovatol (**29** in $CDCl_3$)

	19	29	20	21	22
C-1	132.3[a]	132.5	131.1	126.7[a]	131.8[a]
C-2	129.3[b]	111.3	123.1	114.7	127.1[b]
C-3	127.1[c]	144.7	141.7[a]	144.6	125.3[c]
C-4	153.0[d]	135.1	134.1[b]	134.3[b]	152.6[d]
C-5	117.0[e]	143.8	144.9[a]	149.1	117.1[e]
C-6	132.5	110.9	114.3	127.9[a]	131.5[f]
C-7	39.3	39.6[a]	39.6	36.7	39.7
C-8	138.8[f]	137.4[b]	138.5[c]	137.1	138.7
C-9	115.5[g]	115.8[c]	115.2[d]	115.7	115.6
C-1′	133.2[a]	133.0	133.7	132.4	150.3[d]
C-2′	129.3[b]	129.8	129.7[e]	130.1[c]	116.6[e]
C-3′	126.8	117.9	115.2[f]	117.2	129.5[c]
C-4′	155.0	155.0	156.6[g]	152.8[e]	154.3[d]
C-5′	112.8	117.9	117.2[f]	117.2	121.2
C-6′	132.5	129.8	129.7[e]	130.1[c]	112.0
C-7′	39.3	39.4[a]	39.6	39.7	
C-8′	139.0[f]	137.2[b]	138.5[c]	138.6	
C-9′	115.5[g]	115.7[c]	115.5[d]	115.7	
C-1″	129.5		133.2	126.7[a]	132.4[a]
C-2″	127.9		110.5[h]	129.5[c]	127.1
C-3″	128.8		143.6[a]	127.5[a]	127.1[c]
C-4″	154.1[d]		137.1[b]	153.6[d]	153.0[d]
C-5″	117.4[e]		146.9[a]	117.2	117.2[e]
C-6″	130.8		111.6[h]	129.5[c]	129.8
C-7″	74.9[h]		76.8[i]	48.9	87.5
C-8″	74.1[h]		77.7[i]	89.0	54.5
C-9″	70.2		37.3	63.2	64.2
C-1‴	134.7[a]		133.7	134.3[b]	134.6[a]
C-2‴	129.5[b]		130.0[e]	132.6	129.5[b]
C-3‴	127.5[c]		117.2[f]	130.9	126.6[c]
C-4‴	153.5[d]		157.0[g]	157.6[d]	151.9[d]
C-5‴	117.6[e]		117.2[f]	117.2	117.5[e]
C-6‴	132.5		130.0[e]	132.3	132.2[f]
C-7‴	39.3		39.6	39.7	39.7
C-8‴	139.0[f]		138.7[c]	138.6	138.7
C-9‴	115.7[g]		115.7[d]	115.7	115.6

a—*i*) Assignments are interchangeable in each column.

product (**19e**) showed a molecular ion at *m/z* 326 in the EI-MS. The ^{1}H-NMR spectrum of **19e** exhibited mutually coupled aldehyde and oxygenated methylene signals [δ 9.69 (1H, d, J=1.5 Hz) and 4.45 (2H, d, J=1.5 Hz)], a methoxy signal (δ 3.73), two propyl and six aromatic proton signals. The above evidence suggested that the structure of **19e** was represented as shown in the formula. The structure of **19** was thus estimated to involve the ether bonding through C-9 in **11** and C-4-OH in **1**, and concluded to be as shown in the formula.

Magnolignan G(**20**) showed a molecular peak at *m/z* 596 in the FD-MS. In the ^{1}H-NMR spectrum, the signal due to a benzylic methylene [δ 2.43 (2H, d, J=6 Hz)], a benzylic methine having oxygen [δ 4.22 (d, J=6 Hz)] whose signals were coupled with the oxygenated methine proton [δ 3.77 (1H, m)], three allyl groups and eleven aromatic proton signals were observed, which suggested **20** to be a dimeric lignan. The ^{13}C-NMR spectrum of **20** showed the following signals: thirty-six carbon signals including two signals at δ 76.8 (d) and 77.7 (d) assignable to C-7″ and C-8″ on the propyl moiety, a benzylic methylene signal (δ 37.3), three allyl group signals of the magnolol-type, two *para*-substituted phenoxyl carbons, 1-substituted-3,4,5-trioxybenzene-type carbons and 1,2-di-substituted-3,4,5-trioxybenzene-type carbons. From the above evidence, **20** was assumed to be a dilignan of an obovatol (**29**)[11] and obovatol 7,8-dihydroxy derivative. As regards the bonding location, the signal of an obovatol unit in **20** was shifted by +11.8 ppm at C-2 or C-6, and another unit possessed the C-9″ methylene carbon (δ 37.3), thus indicating that the molecule has a bonding between C-2 (or C-6) and a terminal C-9″ of the propyl unit. On methylation, **20** afforded a tetramethyl ether (**20a**) [^{1}H-NMR: δ 3.53, 3.65, 3.79 and 3.81 (each 3H, s)]. On acetylation, **20** afforded a hexaacetate (**20b**), which showed signals of two aliphatic acetoxyl groups (δ 1.81 and 1.83) and four aromatic acetoxyl groups (δ 2.00,

2.18, 2.21 and 2.28) in the ^{1}H-NMR spectrum. These chemical data were coincident with the above evidence. To determine the bonding location, oxidation of **20a** with sodium metaperiodate was carried out to yield two products (**20c** and **20d**) (Chart 4), **20c** or which showed a molecular ion at *m/z* 352 in the EI-MS. The signal assignable to the ethanal group connected to the benzene ring appeared at δ 3.50 (2H, d, $J=2$ Hz) and 9.46 (1H, t, $J=2$ Hz), in the ^{1}H-NMR spectrum of **20c**. Furthermore, two methoxyl signals (δ 3.62 and 3.81), two allyl groups, two AB type aromatic signals [δ 6.67, 6.98 (each 2H, d, $J=9$ Hz)] and a singlet aromatic signal (δ 6.62) appeared. In the NOE experiment of **20c**, irradiation of the methoxyl signal (δ 3.81) caused the enhancement at the aromatic signal [δ 6.62 (s), H-6] and the methoxyl signal (δ 3.62, C-4-OMe). The structure of **20c** was represented as 3-*O*-(*para*-allyl-phenyl)-1-allyl-2-ethanal-4,5-dimethoxy-3-oxybenze ether. Another product (**20d**) showed a molecular ion at *m/z* 298 in EI-MS. The ^{1}H-NMR spectrum of **20d** exhibited signals due to an aldehyde group [δ 9.77 (s)], two AB and an AX type aromatic signals [δ 6.91, 7.15 (each 2H, d, $J=9$ Hz) and 7.07, 7.24 (each 1H, d, $J=2$ Hz)], an allyl group and two methoxyl groups [δ 3.96 (6H, s)]. In the NOE experiment of **20d**, irradiation on the methoxyl signal (δ 3.96) caused the enhancement at the aromatic H-6 (δ 7.24). Consequently, **20d** was concluded to be 3-*O*-(*para*-allyl-phenyl)-1-formyl-4,5-dimethoxy-3-oxybenzene ether. The above evidence suggested that the bonding location of **20** was through the C-2 of obovatol (**29**) and the C-9 in a 7,8-dihydroxypropyl derivative of obovatol. Therefore, the structure of **20** was concluded to be as shown in the formula.

Magnolignan H(**21**) showed a quasi-molecular ion peak $[M+H]^+$ at *m/z* 563 in the FD-MS, which suggested **21** to be a dilignan. The ^{1}H-NMR spectrum of **21** exhibited signals ascribable to the allyl groups, and eleven aromatic signals including a singlet signal at δ 6.36. Moreover, it showed the following signals: an oxygenated methylene signal [δ 3.51 (d, $J=6$ Hz)], an oxygenated methine [δ 4.78 (m)] and a down-field shifted benzylic methine proton [δ 4.68 (d, $J=9$ Hz)], which could be assigned to H_2-9″, H-8″ and H-7″, respectively, in the dihydrobenzofuran moiety, on the basis of spin-decoupling experiments. The ^{13}C-NMR spectrum (Table IV) disclosed the presence of thirty-six carbon signals including an oxygeneted methylene group [δ 63.2 (t)] and two methine groups [δ 48.9 (d), 89.0 (d)], suggesting the presence of a dihydrobenzofuran ring. Furthermore, it showed the following signals: two allyl group signals of the *para*-allyl-phenol type, an upper-field shifted benzylic methylene (C-7) in one allyl group, twelve aromatic carbons of the mono-substituted obovatol type and twelve aromatic carbons of the magnolol type. Methylation of **21** yielded a trimethyl ether (**21a**). Hydrogenation of **21a** provided a hexahydroganate (**21b**) and subsequent acetylation of **21a** yielded a monoacetate (**21c**). From this evidence, **21** could contain a benzofuran, a primary alcohol, three allyl and three aromatic hydroxyl groups. In the NOE experiments of **21b**, irradiation of a signal at δ 2.16 (2H, m, H_2-7) resulted in the observation of NOE at the signal of H-2 [δ 6.33 (s)] and irradiation of the methoxyl signals at δ 3.67, 3.72 and 3.88 resulted in the enhancement of signals around at δ 6.80—7.12, respectively. From these facts, **21** was assumed to be a dilignan constituted of obovatol (**29**) and magnolignan A (**10**). Careful examination of the ^{1}H-NMR spectrum of **21**, showed that the up-field shift of the H_2-7 signal (δ 2.97) in 3,4,5-trihydroxy-phenyl-allyl moiety could be reasonably explained when the aromatic ring in the other lignan moiety and the H_2-7 are located on the same side, thus indicating that the molecule has a bond between C-6 in obovatol and C-7″ on the dihydroxy-propyl moiety in **10**, and the dihydrobenzofuran ring could be formed around C-6→C-7″→C-8″-O→C-5 positions. The relative stereochemistry of the two substituents on the dihydrobenzofuran ring was concluded to be *cis*, based on the fact that irradiation of the benzylic H-7″ signal (δ 4.58) caused the enhancement of the oxygenated methine H-8″ (δ 5.02) in the NOE experiment in **21b**. Consequently, the structure of **21** was concluded to be as shown in the formula.

Magnolignan I(**22**) exhibited a molecular ion peak at *m/z* 522 in the FD-MS. The ^{1}H-NMR spectrum showed three ABX type aromatic signals [δ 6.86, 6.93, 7.00 (each 1H, d, $J=8.1$ Hz), 7.01, 7.05, 7.33 (each 1H, dd, $J=8.1$, 2.2 Hz), 7.10, 7.19, 7.37 (each 1H, d, $J=2.2$ Hz)], an AX type aromatic signal [δ 6.78, 6.83 (each 1H, d, $J=2.2$ Hz)] shifted toward up-field, and two allyl group signals. Moreover, it showed the following signals: two methine signals [δ 5.63 (1H, d, $J=6.2$ Hz), 3.60 (1H, m)] and a hydroxymethyl signal [δ 3.89 (2H, m)], which could be assigned to H-7″, H-8″ and H_2-9″, respectively, in the dihydrobenzofuran moiety, on the basis of spin-decoupling experiments. The ^{13}C-NMR spectrum of **22** revealed the presence two allyl groups of the magnolol type and four aromatic rings. The carbon signals at δ 54.5 (d), 64.2 (t), 87.5 (d), 112.0 (d), 116.6 (d), 121.2 (s), 129.5 (s), 150.3 (s) and 154.3 (s) were assigned to the moiety of the dihydrobenzofuran ring. That is, their signals disclosed a partial structure, 5-hydroxy-3-hydroxymethyl-2,7-diphenyl-dihydrobenzofuran for **22** by comparing the ^{13}C- and ^{1}H-NMR spectra with those of **15**, leptolepisol C[12] and lappaol A.[13] On methylation under the same condition as for **20**, **22** yielded a tetramethyl ether (**22a**) [^{1}H-NMR δ 3.64, 3.68, 3.73, 3.77 (each 3H, s)]. Hydrogenation of **22a** yielded a tetrahydrogenated derivative (**22b**) and subsequent acetylation of **22b** yielded a monoacetate (**22c**). The ^{1}H-NMR spectrum of **22c** afforded an acetyl methyl signal (δ 2.04), two propyl group signals, two methine of the 3-hydroxymethyl-dihydrobenzofuran type signals [δ 3.79 (1H, m) and 5.43 (1H, d, $J=6.6$ Hz)] and one methylene signal [δ 4.31 (1H, dd, $J=11.0$, 7.7 Hz) and 4.46 (1H, dd, $J=11.0$, 5.8 Hz)] and an AX type and three ABX type aromatic signals. These chemical and spectral data suggested that **22** possessed a bond between C-5′ in **15** and C-8 on the propyl moiety in the 9-hydroxy derivative of magnolol, and the dihydrofuran ring was formed around the C-4′-O→C-7″→C-8″→C-5′ position. The relative stereochemistry of the two substituents on the dihydrobenzofuran ring was concluded to be *trans*, based on the fact that irradiation on the oxygenated benzylic H-7″ signal (δ 5.43) caused the enhancement of the hydroxymethyl signal (H_2-9″, δ 4.31 and 4.46) in the NOE experiment of **22c**. Consequently, the structure of **22** was concluded to be as shown in the formula.

Compounds **3**, **4**, **5** and **6** are unique in respect to having the structures linked by the two parts of monoterpene and neolignan, and are the first reported monoterpenoid-

neolignan. These monomeric and dimeric lignans occur rarely in nature.

Experimental

Melting points were determined with a Yanagimoto micromelting apparatus and are uncorrected. The optical rotation were measured with a JASCO DIP-4 digital polarimeter. The IR and UV spectra were obtained with JASCO IR-G and Hitachi UV-340 spectrometers, respectively. The EI- and FD-MS were measured with a JEOL DX-300 and DX-303. The ^{1}H- and ^{13}C-NMR spectra were recorded with JEOL PS-100 (100 MHz for ^{1}H-NMR), FX-100 (100 MHz for ^{1}H-NMR and 25 MHz for ^{13}C-NMR) and GX-400 (400 MHz for ^{1}H-NMR) spectrometers, chemical shifts are given on a δ (ppm) scale with tetramethylsilane as an internal standard. Column chromatography was carried-out with MCI-gel CHP 20P (75—150 μ, Mitsubishi Chemical Industries, Ltd.), Kieselgel 60 (70—230 mesh, Merck), Bondapak C_{18} (Waters) and Sephadex LH-20 (25—100 μ, Pharmacia Fine Chemicals). TLC was performed on precoated Kieselgel 60 F_{254} plates (0.2 mm, Merck) using benzene–EtOAc (40 : 1) as the developing solvent for the compounds **1**—**6** and benzene–MeOH (5 : 1) as the solvent for the compounds **7**—**22**, and detection was achieved by spraying 10% H_2SO_4 reagent followed by heating, or by irradiating with a UV-lamp (254 nm). Purity was checked by highe performance liquid chromatography (HPLC) (Toso HPLC 803D, UV-8 model II system (280 nm); column, Toso TSK-80TM (ODS, 4.6 mm × 150 mm); solvent, 50—90% MeOH.

Isolation Commercial Magnoliae Cortex (*Magnolia officinalis* REHD *et* WILS.) produced in China (5 kg) was extracted at room temperature with MeOH and its extract was evaporated under reduced pressure to afford a residue (600 g). The MeOH extract was partitioned between H_2O and benzene, and the aqueous layer was extracted with EtOAc (100 g). The benzene extract (200 g) was chromatographed over silica gel (1 kg) using benzene–EtOAc as the solvent to give frs. 1—3, which were further separated by means of various chromatographies on silica gel and alumina afforded compounds **1** (6 g), **2** (1 g), **3** (890 mg), **4** (360 mg), **5** (30 mg), **6** (80 mg) and **27** (2 mg). The EtOAc extract (100 g) was chromatographed over silica gel (500 g) using benzene–EtOAc and MeOH as the solvent to give frs. 1—5. These frs. were subjected to column chromatographies on silica gel, Bondapak C_{18} and Sephadex LH-20 furnished compounds **7** (130 mg), **8** (120 mg), **9** (15 mg), **10** (15 mg), **11** (200 mg), **12** (35 mg), **13** (38 mg), **14** (29 mg), **15** (45 mg), **16** (85 mg), **17** (40 mg), **18** (35 mg), **19** (96 mg), **20** (153 mg), **21** (115 mg), **22** (120 mg), **23** (300 mg), **24** (47 mg), **25** (485 mg) and **26** (98 mg) (Chart 1).

Magnolol (1) ^{1}H-NMR ($CDCl_3$) δ: 3.35 (4H, br d, J=7 Hz, H_2-7, H_2-7′), 5.01 (2H, br d, J=11 Hz, H-9, H-9′), 5.06 (2H, br d, J=18 Hz, H-9, H-9′), 5.94 (2H, ddt, J=18, 11, 7 Hz, H-8, H-8′), 6.81 (2H, d, J=8 Hz), 7.02 (2H, dd, J=8, 2 Hz), 7.07 (2H, d, J=2 Hz).

Honokiol (2) ^{1}H-NMR ($CDCl_3$) δ: 3.27, 3.36 (each 2H, br d, J=7 Hz, H_2-7, H_2-7′), 5.05 (4H; m, H_2-9, H_2-9′), 5.93 (2H, m, H-8, H-8′), 6.74, 6.91 (each 1H, d, J=8 Hz), 6.97, 7.15 (each 1H, dd, J=8, 2 Hz), 7.00, 7.17 (each 1H, d, J=2 Hz).

1-(4-Hydroxy-3-methoxyphenyl)-2-[4-(ω-hydroxypropyl-2-methoxy)-phenoxy]-propane-1,3-diol (23)[6] **(7,8-*threo* and *erythro* Mixture)** EI-MS m/z: 378 (M^+). UV λ_{max}^{MeOH} nm (ε): 281 (12000). ^{1}H-NMR (acetone-d_6) δ: 1.62—1.97 (2H, m, H-8′), 2.50—3.90 (4H, m, H_2-9, H_2-9′), 3.80 (6H, s, OMe), 4.17—4.40 (1H, m, H-8), 7.91 (1/2H, d, J=4 Hz, H-7), 4.92 (1/2H, d, J=7 Hz, H-7), 6.60—7.15 (6H, m, Ar-H). ^{13}C-NMR (acetone-d_6) δ: 32.1 (C-8′), 35.0 (C-7′), 56.2, 55.5 (OMe × 2), 61.9 (61.1, 61.3) (C-9, C-9′), 73.2 (73.1) (C-8), 85.6 (86.4) (C-7), 111.5 (C-2′), 113.6 (113.4) (C-2), 115.2 (C-5), 118.3 (117.9) (C-5′), 120.3 (C-6), 121.4 (C-6′), 133.8 (133.6) (C-1), 137.2 (C-1′), 146.4 (C-3, C-4), 184.0 (C-3′), 150.9 (150.7) (C-4′).

Sinapic Aldehyde (24) ^{1}H-NMR ($CDCl_3$) δ: 3.90 (6H, s), 6.60 (1H, dd, J=8, 16 Hz), 6.80 (2H, s), 7.37 (1H, d, J=16 Hz), 9.62 (1H, d, J=8 Hz).

Syringaresinol (25) Colorless needles, mp 174—177 °C (benzene–acetone). $[\alpha]_D^{20}$ 0 (c=2.40, $CHCl_3$). ^{1}H-NMR ($CDCl_3$) δ: 3.11 (2H, m, H-1, H-5), 3.86 (12H, s), 3.94 (2H, dd, J=9, 4 Hz, H-4, H-8), 4.30 (2H, dd, J=8, 9 Hz, H-4, H-8), 4.76 (2H, d, J=5 Hz, H-2, H-6), 5.83 (2H, s, OH), 6.59 (4H, s, Ar-H).

Syringaresinol 4′-*O*-β-D-Glucopyranoside (26) Colorless needles, mp 192—194 °C ($CHCl_3$). $[\alpha]_D^{19}$ −19.3° (c=1.10, MeOH). FD-MS m/z: 580 (M^+). ^{13}C-NMR (DMSO-d_6) δ: 53.6, 85.1, 71.2, 53.6, 85.4, 71.2 (C-2—8), 131.5, 103.5, 147.8, 134.5, 147.8, 103.9 (C-1′—6′), 137.4, 103.5, 152.5, 133.5, 152.5, 103.9 (C-1″—6″), 102.7, 73.9, 76.1, 69.6, 76.9, 60.7 (glc C-1—6).

6′-*O*-Methylhonokiol (27) ^{1}H-NMR ($CDCl_3$) δ: 3.35, 3.43 (each 2H, br d, J=7 Hz, H_2-7, H_2-7′), 3.88 (3H, s, OMe), 5.00—5.19 (5H, m, H_2-9, H_2-9′, OH), 5.78—6.22 (2H, m, H-8, H-8′), 6.86—7.34 (6H, m, Ar-H).

Piperitylmagnolol (3) Colorless viscous oil, $[\alpha]_D^{26}$ −146.0° (c=1.18, $CHCl_3$). UV λ_{max}^{MeOH} nm (ε): 290 (8500). CD (c=1.77 × 10^{-3}, MeOH) [θ] (nm): +7.22 × 10^3 (254), +2.25 × 10^3 (292). EI-MS m/z: 402.257 (M^+, $C_{28}H_{34}O_2$, requires 402.255). ^{1}H-NMR ($CDCl_3$) δ: 0.80, 0.88 (each 3H, d, J=6 Hz, H_3-9″, 10″), 1.70 (3H, br s, H_3-7″), 1.20—1.80 (4H, m, H-4″, H-8″, H_2-5″), 2.06 (2H, m, H_2-6″), 3.30 (4H, d, J=6 Hz, H_2-7, H_2-7′), 3.60 (1H, m, H-3″), 5.00 (2H, br d, J=11 Hz, H-9, H-9′), 5.02 (2H, br d, J=18 Hz, H-9, H-9′), 5.40 (1H, br s, H-2″), 6.75—6.20 (2H, m, H-8, H-8′), 6.30 (2H, br s, OH), 6.79 (5H, m, H-2, H-2′, H-5′, H-6, H-6′). ^{13}C-NMR: Table I.

Methylation of 3 A mixture of **3** (200 mg), dimethyl sulfate (3 ml) and anhydrous potassium carbonate (5 g) in dry acetone (50 ml) was refluxed for 2 h with stirring. After removal of inorganic salts by filtration, the filtrate was concentrated to a syrup, which was subjected to silica gel chromatography with benzene to afford **3a** (210 mg) as a colorless viscous oil, EI-MS m/z: 430.285 (M^+, $C_{30}H_{38}O_2$, requires 430.287). ^{1}H-NMR ($CDCl_3$) δ: 0.82, 0.90 (each 3H, d, J=6 Hz, H_3-9″, H_3-10″), 1.71 (3H, br s, H_3-7″), 1.40—1.80 (4H, m, H_2-5″, H-4″, H-8″), 2.07 (2H, m, H_2-6″), 3.35 (4H, d, J=6 Hz, H_2-7, H_2-7′), 3.77 (1H, m, H-3″), 3.73 (3H, s, C-4-OMe), 3.81 (3H, s, C-4′-OMe), 5.02 (2H, br d, J=11 Hz, H-9, H-9′), 5.06 (2H, br d, J=18 Hz, H-9, H-9′), 5.48 (1H, br d, J=7 Hz, H-2″), 5.77—6.20 (2H, m, H-8, H-8′), 6.83—7.722 (5H, m, Ar-H).

Partial Hydrogenation of 3 **3** (100 mg) was hydrogenated over 10% Pd–C (25 mg) in MeOH (20 ml) under a hydrogen atmosphere for 1 h. After removal of the catalyst by filtration, the filtrate was evaporated under reduced pressure to give a residue. The residue was purified by silica gel chromatography with benzene to give **3b** (90 mg) as a colorless viscous oil, EI-MS m/z: 406 (M^+). ^{1}H-NMR ($CDCl_3$) δ: 0.80—1.01 (12H, m, H_3-9, H_3-9′, H_3-9″, H_3-10″), 1.40—1.85 (8H, m, H-4″, H-8″, H_2-5″, H_2-8, H_2-8′, H_2-6″), 1.77 (3H, br s, H_3-7″), 2.57 (4H, br t, J=6 Hz, H_2-7, H_2-7′), 3.52 (1H, m, H-3″), 5.49 (1H, br s, H-2″), 6.00 (2H, br s, OH), 6.85—7.15 (5H, m, Ar-H).

Oxydation of 3b with *m*-Chloroperbenzoic Acid A solution of **3b** (90 mg) and *m*-chloroperbenzoic acid (100 mg) in dry $CHCl_3$ was stirred overnight at room temperature. The reaction mixture was evaporated under reduced pressure to give a residue. The residue was purified by silica gel chromatography with benzene–EtOAc (200 : 7) to give **3c** (33 mg), as a white powder, $[\alpha]_D^{20}$ −1.0° (c=3.30, $CHCl_3$). ^{1}H-NMR ($CDCl_3$) δ: 0.80—1.02 (12H, m, H_3-9, H_3-9′, H_3-9″, H_3-10″), 1.43 (3H, s, H_3-7″), 1.40—2.10 (10H, m, H-4″, H-8″, H_2-5″, H_2-6″, H_2-8, H_2-8′), 2.59, 2.61 (each 2H, t, J=6 Hz, H_2-7, H_2-7′), 3.02 (1H, dd, J=6, 11 Hz, H-3″), 4.27 (1H, d, J=6 Hz, H-2″), 6.90—7.20 (5H, m, Ar-H), 7.02 (2H, br s, OH).

Partial Hydrogenation of 3a **3a** (550 mg) was hydrogenated in the same way as **3** to yield **3d** (374 mg) as a colorless viscous oil, EI-MS m/z: 434 (M^+). ^{1}H-NMR ($CDCl_3$) δ: 0.80—1.01 (12H, m, H_3-9, H_3-9′, H_3-9″, H_3-10″), 1.71 (3H, br s, H_3-7″), 1.40—1.80 (8H, m, H-4″, H-8″, H_2-5″, H_2-8, H_2-8′), 2.03 (2H, m, H_2-6″), 2.58 (4H, br t, J=6 Hz, H_2-7, H_2-7′), 3.45 (3H, s, C-4-OMe), 3.77 (3H, s, C-4′-OMe), 3.82 (1H, m, H-3″), 5.35 (1H, br s, H-2″), 6.82—7.20 (5H, m, Ar-H).

Oxidation of 3d with Selenium Dioxide A mixture of **3d** (100 mg) and selenium dioxide (200 mg) in dioxane (10 ml) was heated at 80 °C for 5 h with stirring. The reaction mixture was filtered after cooling, diluted with water, and extracted with $CHCl_3$. The $CHCl_3$ extract was evaporated under reduced pressure to give a residue, which was purified by silica gel chromatography using hexane–EtOAc (10 : 1) to afford **3e** (25 mg) as a white powder, $[\alpha]_D^{27}$ −109.5° (c=1.49, $CHCl_3$). EI-MS m/z: 448.298 (M^+, $C_{30}H_{40}O_3$, requires 448.297). ^{1}H-NMR ($CDCl_3$) δ: 0.83—1.01 (12H, m, H_3-9, H_3-9′, H_3-9″, H_3-10″), 1.83 (3H, br s, H_3-7″), 1.50—1.80 (6H, m, H_2-8, H_2-8′, H-4″, H-8″), 2.20—2.50 (2H, m, H_2-5″), 2.57, 2.59 (each 2H, t, J=6 Hz, H_2-7, H_2-7′), 3.30, 3.77 (each 3H, s, OMe), 4.05 (1H, m, H-3″), 6.61 (1H, br s, H-2″), 6.85—7.20 (5H, m, Ar-H).

$NaBH_4$ Reduction of 3e **3e** (20 mg) was reduced with $NaBH_4$ (50 mg) in MeOH (10 ml) at room temperature for 5 h. The reaction mixture (20 mg) was purified by silica gel chromatography using benzene–EtOAc (30 : 1) to give two products, **3f** (15 mg) and **3g** (1 mg). **3f**: A white powder. $[\alpha]_D^{27}$ −118.8° (c=1.12, $CHCl_3$). EI-MS m/z: 450.313 (M^+, $C_{30}H_{42}O_3$, requires 450.313). ^{1}H-NMR ($CDCl_3$) δ: 0.81—1.01 (12H, m, H_3-9, H_3-9′, H_3-9″, H_3-10″), 1.43—1.80 (7H, m, H-4″, H-5″, H-8″, H_2-8, H_2-8′), 1.82 (3H, br s, H_3-7″), 2.16 (1H, m, H-5″), 2.56, 2.58 (each 2H, t, J=6 Hz, H_2-7, H_2-7′), 3.28, 3.75 (each 3H, s, OMe), 3.55 (1H, m, H-3″), 4.35 [1H, dd, J=11, 4 Hz, H-6″ (axial)], 5.38 (1H, br s, H-2″), 6.83—7.17 (5H, m, Ar-H). **3g**: A white powder. EI-MS m/z: 450 (M^+). ^{1}H-NMR ($CDCl_3$) δ: 0.80—1.01 (12H, m, H_3-9, H_3-9′, H_3-9″, H_3-10″), 1.40—1.80 (7H, m, H-4″, H-5″, H-8″, H_2-8, H_2-8′), 1.80 (3H, br s, H_3-7″), 2.10 (1H, m, H-5″), 2.56, 2.58 (each 2H, t, J=6 Hz, H_2-7, H_2-7′), 3.27, 3.75 (each 3H, s, OMe), 3.78

(1H, m, H-3″), 4.04 [1H, br t, J=4 Hz, H-6″ (equatorial)], 5.48 (1H, br s, H-2″), 6.80—7.20 (5H, m, Ar-H).

Determination of the Configuration (By Modified Horeau's Method) at C-6″ of 3f and 3g **3f** (5 mg) and **3g** (1 mg) in pyridine (10 μl) were each treated with (±)-α-phenylbutylic anhydride (6 μl) and kept in a sealed tube at 40 °C for 2 h. Then, (+)-(*R*)-α-phenylethylamine (6 μl) was added. After 30 min, the mixture was diluted with dry ethyl acetate (100 μl) and a sample was analyzed by gas chromatography (GLC) at 215 °C on a 2 mm × 2 m column packed with 2% OV-17 (N_2 1 kg/cm^2). The relative proportion of the amides of (−)-*R*- and (+)-*S*-phenylbutylic acid was indicated by the peak height. The peak retention indices % were: **3f**, 55 : 45 (6″*S*); **3g**, 51 : 49 (6″*R*).

Dipiperitylmagnolol (4) A white powder. $[\alpha]_D^{21}$ −140.0° (c=0.31, $CHCl_3$). EI-MS m/z: 538.373 (M^+, $C_{38}H_{50}O_2$, requires 538.380), UV λ_{max}^{MeOH} nm (ε): 290 (10200). CD ($c=2.41\times10^{-3}$, MeOH) [θ] (nm): $+1.04\times10^4$ (255), $+4.96\times10^3$ (294). ^{1}H-NMR ($CDCl_3$) δ: 0.83, 0.90 (each 6H, d, J=6 Hz, H_3-9″, H_3-9‴, H_3-10″, H_3-10‴), 1.72 (6H, br s, H_3-7″, H_3-7‴), 1.20—1.90 (8H, m, H-4″, H-4‴, H-8″, H-8‴, H_2-5″, H_2-5‴), 2.05 (4H, m, H_2-6″, H_2-6‴), 3.32 (1H, br d, J=7 Hz, H_2-7, H_2-7′), 3.65 (2H, m, H-3″, H-3‴), 5.02 (2H, br d, J=11 Hz, H-9, H-9′), 5.06 (2H, br d, J=18 Hz, H-9, H-9′), 5.40 (2H, br s, H-2″, H-2‴), 5.99 (2H, ddt, J=18, 11, 7 Hz, H-8, H-8′), 5.93 (2H, s, OH), 6.93 (4H, m, Ar-H). ^{13}C-NMR (Table I).

Methylation of 4 **4** (50 mg) was methylated in the same way as **3** to give a dimethyl ether (50 mg) as a white powder. ^{1}H-NMR ($CDCl_3$) δ: 0.81, 0.85 (each 6H, d, J=6 Hz, H_3-9″, H_3-9‴, H_3-10″, H_3-10‴), 1.40—1.85 (8H, m), 1.71 (6H, br s, H_3-7″, H_3-7‴), 2.05 (4H, m, H_2-6″, H_2-6‴), 3.32 (6H, s, OMe), 3.36 (4H, br d, J=7 Hz, H_2-7, H_2-7′), 3.74 (2H, m, H-3″, H-3‴), 5.01 (2H, br d, J=11 Hz, H-9, H-9′), 5.04 (2H, br d, J=18 Hz, H-9, H-9′), 5.24 (2H, br s, H-2″, H-2‴), 5.98 (2H, ddt, J=18, 11, 7 Hz, H-8, H-8′), 6.95 (4H, m, Ar-H).

Piperitylhonokiol (5) Colorless viscous oil. $[\alpha]_D^{24}$ −97.0° (c=0.69, $CHCl_3$). EI-MS m/z: 402.250 (M^+, $C_{28}H_{34}O_2$, requires 402.255). UV λ_{max}^{MeOH} nm (ε): 290 (7800). CD ($c=1.74\times10^{-3}$, MeOH) [θ] (nm): $+4.59\times10^3$ (248), $+2.30\times10^3$ (293). ^{1}H-NMR ($CDCl_3$) δ: 0.83, 0.89 (each 3H, d, J=6 Hz, H_3-9″, H_3-10″), 1.72 (3H, br s, H_3-7″), 1.30—1.90 (4H, m, H-4″, H-8″, H_2-5″), 2.05 (2H, m, H_2-6″), 3.30, 3.42 (each 2H, d, J=7 Hz, H_2-7, H_2-7′), 3.50 (1H, m, H-3″), 4.92—5.30 (4H, m, H_2-9, H_2-9′), 5.12, 5.51 (each 1H, s, OH), 5.41 (1H, br s, H-2″), 5.78—6.25 (2H, m, H-8, H-8′), 6.80—6.93 (3H, m, Ar-H), 7.22 (2H, br s, Ar-H). ^{13}C-NMR (Table I).

Acetylation of 5 A mixture of **5** (7 mg), acetic anhydride (0.5 ml) and pyridine (0.5 ml) was kept standing overnight at room temperature and evaporated under reduced pressure to give a residue, which was subjected to silica gel chromatography with benzene–EtOAc (20 : 1) to afford an acetate (**5a**, 7 mg) as a white powder. ^{1}H-NMR ($CDCl_3$) δ: 0.78, 0.86 (each 3H, d, J=6 Hz, H_3-9″, H_3-10″), 1.40—1.75 (4H, m, H-4″, H-8″, H_2-5″), 1.69 (3H, br s, H_3-7″), 2.02 (2H, m, H_2-6″), 1.98, 2.31 (each 3H, s, Ac), 3.28, 3.37 (each 2H, br d, J=7 Hz, H_2-7, H_2-7′), 3.35 (1H, m, H-3″), 4.95—5.20 (2H, m, H-8, H-8′), 5.20 (1H, br s, H-2″), 5.70—6.20 (2H, m, H-8, H-8′), 7.03 (3H, m, Ar-H), 7.24 (2H, m, Ar-H).

Bornylmagnolol (6) Colorless viscous oil. $[\alpha]_D^{26}$ −7.6° (c=1.67, $CHCl_3$). EI-MS m/z: 402.254 (M^+, $C_{28}H_{34}O_2$, requires: 402.255), 266, 137. UV λ_{max}^{MeOH} nm (ε): 290 (8000). ^{1}H-NMR ($CDCl_3$) δ: 0.80, 0.83, 0.87 (each 3H, s, H_3-8″, H_3-9″, H_3-10″), 0.70—2.45 (7H, m, H_2-3″, H_2-5″, H_2-6″, H-4″), 3.36 (4H, br d, J=7 Hz, H_2-7, H_2-7′), 4.38 (1H, dd, J=9, 3 Hz, H-2″), 4.90—5.20 (4H, m, H_2-9, H_2-9′), 5.75—6.23 (2H, m, H-8, H-8′), 6.28 (1H, br s, OH), 6.79—7.23 (6H, m, Ar-H). ^{13}C-NMR (Table I).

Acetylation of 6 **6** (10 mg) was acetylated in the same way as **5** to yield a monoacetate (10 mg) as a white powder. EI-MS m/z: 444.266 (M^+, $C_{30}H_{36}O_3$, requires: 444.266), 308, 266, 137. ^{1}H-NMR (CCl_4) δ: 0.73, 0.82, 0.87 (each 3H, s, H_3-8″, H_3-9″, H_3-10″), 0.70—2.35 (7H, m, H_2-3″, H-4″, H_2-5″, H_2-6″), 1.89 (3H, s, Ac), 3.25, 3.36 (each 2H, br d, J=7 Hz, H_2-7, H_2-7′), 4.18 (1H, dd, J=3, 9 Hz, H-2″), 4.85—5.15 (2H, m, H_2-9, H_2-9′), 5.70—6.17 (2H, m, H-8, H-8′), 6.62 (1H, d, J=8 Hz, H-5), 6.90—7.11 (5H, m, Ar-H).

Randainal (7)[5] Pale yellow needles, mp 135—138 °C ($CHCl_3$). UV λ_{max}^{MeOH} nm (ε): 330 (28000), 373 (26000). EI-MS m/z: 280.110 (M^+, $C_{18}H_{16}O_3$, requires: 280.109). IR $\nu_{max}^{CHCl_3}$ (cm^{-1}): 3550 (OH), 1675, 1625 (α,β-unsaturated aldehyde), 1605 (aromatic ring). ^{1}H-NMR (acetone-d_6) δ: 3.35 (2H, d, J=7 Hz, H_2-7′), 4.60 (2H, br, OH), 5.02 (1H, br d, J=10 Hz, H-9′), 5.06 (1H, br d, J=18 Hz, H-9′), 5.98 (1H, ddt, J=18, 10, 7 Hz, H-8′). 6.65 (1H, dd, J=16, 8 Hz, H-8), 6.92—7.13 (4H, m, Ar-H), 7.58 (1H, d, J=8 Hz, Ar-H), 7.60 (1H, d, J=2 Hz, Ar-H), 7.62 (1H, d, J=16 Hz, H-7), 9.61 (1H, d, J=8 Hz, H-9). ^{13}C-NMR (Table II).

Magnaldehyde B (8) Pale yellow needles, mp 155—158 °C ($CHCl_3$). UV λ_{max}^{MeOH} nm (ε): 284 (40000), 324 (33000). EI-MS m/z: 280.109 (M^+, $C_{18}H_{16}O_3$, requires: 280.109), IR $\lambda_{max}^{CHCl_3}$ (cm^{-1}): 3550 (OH), 1675, 1625 (α,β-unsaturated aldehyde), 1605 (aromatic ring). ^{1}H-NMR (acetone-d_6) δ: 3.44 (2H, d, J=7 Hz, H_2-7′), 3.46 (2H, br s, OH), 5.00 (1H, br d, J=11 Hz, H-9′), 5.11 (1H, br d, J=18 Hz, H-9′), 6.07 (1H, ddt, J=18, 11, 7 Hz, H-8′), 6.75 (1H, dd, J=16, 8 Hz, H-8), 6.92, 7.03 (each 1H, d, J=8 Hz, H-5, H-5′), 7.33, 7.51 (each 1H, dd, J=8, 2 Hz, H-6, H-4′), 7.37, 7.60 (each 1H, d, J=2 Hz, H-2, H-2′), 7.60 (1H, d, J=16 Hz, H-7), 9.62 (1H, d, J=8 Hz, H-9). ^{13}C-NMR (Table II).

Methylation of 8 **8** (12 mg) was methylated in the same way as **3** to yield a dimethyl ether (**8a**) (5 mg) as a pale yellow powder. ^{1}H-NMR ($CDCl_3$) δ: 3.42 (2H, d, J=7 Hz, H_2-7′), 3.87, 3.88 (each 3H, s, OMe), 5.65 (1H, br d, J=11 Hz, H-9′), 5.08 (1H, br d, J=18 Hz, H-9′), 6.04 (1H, ddt, J=18, 11, 7 Hz, H-8′), 6.64 (1H, dd, J=16, 8 Hz, H-8), 7.45 (1H, d, J=16 Hz, H-7), 6.87—7.50 (6H, m, Ar-H), 9.67 (1H, d, J=8 Hz, H-9).

Oxidation of Honokiol Dimethyl Ether A mixture of honokiol dimethyl ether (200 mg) and selenium dioxide (110 mg) in dioxane (5 ml) was heated at 90 °C for 1.5 h. It was filtered after cooling, diluted with water, and extracted with $CHCl_3$. The $CHCl_3$ extract was washed with 10% aqueous sodium bicarbonate, then with water and dried over anhydrous sodium sulfate. The organic solvent was evaporated under reduced pressure to give a residue. Next, an active manganese dioxide (50 mg) was added to a solution of the residue (35 mg) in $CHCl_3$ (10 ml) and the mixture was stirred at room temperature overnight. After removal of the inorganic by filtration, the filtrate was concentrated to a syrup, which was subjected to silica gel chromatography with hexane–EtOAc (10 : 1) to afford two products [**8a** (4 mg) and **28** (3 mg)]. **28**: Pale yellow powder. ^{1}H-NMR ($CDCl_3$) δ: 3.37 (2H, d, J=7 Hz, H_2-7), 3.80, 3.94 (each 3H, s, OMe), 5.06 (1H, br d, J=11 Hz, H-9), 5.13 (1H, br d, J=18 Hz, H-9), 6.18 (1H, ddt, J=18, 11, 7 Hz, H-8), 6.81 (1H, dd, J=8, 16 Hz, H-8′), 6.95—7.80 (6H, m, Ar-H), 7.89 (1H, d, J=16 Hz, H-7′), 9.70 (1H, d, J=8 Hz, H-9′).

Magnaldehyde C(9) A pale yellow powder. $[\alpha]_D^{29}$ −15.5° (c=1.50, MeOH). FD-MS m/z: 314 (M^+), 337 $[M+Na]^+$. IR $\lambda_{max}^{CHCl_3}$ (cm^{-1}): 3500 (OH), 1655, 1622 (α,β-unsaturated aldehyde), 1600 (aromatic ring). ^{1}H-NMR (acetone-d_6) δ: 2.65 (1H, dd, J=14, 8 Hz, H-7′), 2.84 (1H, dd, J=14, 5 Hz, H-7′), 3.56 (2H, m, H-9′), 3.80 (1H, m, H-8′), 6.66 (1H, dd, J=16, 8 Hz, H-8), 6.97—7.20 (4H, m, Ar-H), 7.62 (2H, m, Ar-H), 7.70 (1H, d, J=16 Hz, H-7), 9.62 (1H, d, J=8 Hz, H-9). ^{13}C-NMR (Table II).

Magnolignan A(10) A white powder. $[\alpha]_D^{17}$ −0.8° (c=1.50, MeOH). EI-MS m/z: 300.134 (M^+, $C_{18}H_{20}O_4$, requires: 300.136), 282 (M^+-H_2O), 269 (M^+-CH_2OH), 239 ($M^+-C_2H_5O_2$). UV λ_{max}^{MeOH} nm (ε): 256 (18000), 293 (18600). ^{1}H-NMR (acetone-d_6) δ: 2.64 (1H, dd, J=14, 7 Hz, H-7), 2.80 (1H, dd, J=14, 5 Hz, H-7), 3.35 (2H, br d, J=7 Hz, H_2-7′), 3.50 (2H, m, H-9), 3.82 (1H, m, H-8), 5.01 (1H, br d, J=11 Hz, H-9′), 5.06 (1H, br d, J=18 Hz, H-9′), 6.00 (1H, ddt, J=18, 11, 7 Hz, H-8′), 6.80—7.35 (6H, m, Ar-H). ^{13}C-NMR (Table II).

Acethylation of 10 **10** (5 mg) was acetylated in the same way as **5** to yield a tetraacetate (4 mg) as a white powder. ^{1}H-NMR ($CDCl_3$) δ: 2.03, 2.04, 2.07, 2.08 (each 3H, s, Ac), 2.93 (2H, d, J=7 Hz, H_2-7), 3.41 (2H, br d, J=7 Hz, H_2-7′), 3.98 (1H, dd, J=12, 6 Hz, H-9), 4.36 (1H, dd, J=12, 4 Hz, H-9), 5.10 (2H, m, H_2-9′), 5.25 (1H, m, H-8), 5.80—6.20 (1H, m, H-8′), 7.13 (6H, m, Ar-H).

Magnolignan B(11) A white powder. $[\alpha]_D^{28}$ +0.3° (c=2.50, MeOH). FD-MS m/z: 316 (M^+), 254. ^{1}H-NMR (acetone-d_6) δ: 3.35 (2H, br d, J=6 Hz, H_2-7′), 3.52 (2H, m, H_2-9), 3.70 (1H, m, H-8), 4.65 (1H, d, J=6 Hz, H-7), 5.01 (1H, br d, J=11 Hz, H-9′), 5.06 (1H, br d, J=18 Hz, H-9′), 5.99 (1H, ddt, J=18, 11, 6 Hz, H-8′), 6.90, 6.92 (each 1H, d, J=8 Hz), 7.07, 7.56 (each 1H, dd, J=8, 2 Hz), 7.11, 7.31 (each 1H, d, J=2 Hz). ^{13}C-NMR (Table II).

Magnolignan C(12) A white powder. $[\alpha]_D^{22}$ −6.8° (c=0.91, MeOH), EI-MS m/z: 300.138 (M^+, $C_{18}H_{20}O_4$, requires: 300.136). UV λ_{max}^{MeOH} nm (ε): 259 (19400), 293 (17800). ^{1}H-NMR (acetone-d_6) δ: 2.65 (1H, dd, J=12, 8 Hz, H-7), 2.79 (1H, dd, J=12, 6 Hz, H-7), 3.40 (2H, br d, J=6 Hz, H_2-7), 3.50 (2H, m, H_2-9), 3.82 (1H, m, H-8), 4.93 (1H, br d, J=11 Hz, H-9′), 5.08 (1H, br d, J=18 Hz, H-9′), 6.02 (1H, ddt, J=18, 11, 6 Hz, H-8), 6.80—7.37 (6H, m, Ar-H). ^{13}C-NMR (Table II).

Acetylation of 12 **12** (20 mg) was acetylated in the same way as **5** to afford a tetraacetate (19 mg) as a white powder, $[\alpha]_D^{19}$ +2.9° (c=1.88, $CHCl_3$). ^{1}H-NMR ($CDCl_3$) δ: 2.02, 2.04, 2.05, 2.32 (each 3H, s, Ac), 2.94 (2H, d, J=7 Hz, H_2-7), 3.33 (2H, br d, J=6 Hz, H_2-7′), 4.03 (1H, dd, J=12, 6 Hz, H-9), 4.26 (1H, dd, J=12, 4 Hz, H-9), 5.05 (1H, br d, J=11 Hz, H-9′), 5.06 (1H, br d, J=18 Hz, H-9′), 5.23 (1H, m, H-8), 5.91 (1H, ddt, J=18, 11, 6 Hz, H-8′), 6.97—7.30 (6H, m, Ar-H). ^{13}C-NMR ($CDCl_3$) δ: 131.2, 129.3, 134.1, 146.6, 122.4, 131.2, 36.5, 71.9, 64.1 (C-1—9), 127.9, 134.5, 135.2, 130.8, 123.0, 148.5, 34.7, 135.7, 116.4 (C-1′—9′), 20.8 × 2, 20.9 × 2, 169.4 × 2, 170.2, 170.6 ($COCH_3$).

Magnolignan D(13) A white powder. $[\alpha]_D^{17}$ +3.0° (c=0.88, MeOH). EI-MS m/z: 330.150 (M^+, $C_{19}H_{22}O_5$, requires: 330.147), 300, 269 $[M-C_2H_4O_2]^+$, 239 $[269-CH_2O]^+$. UV λ_{max}^{MeOH} nm (ε): 259 (14500), 293 (11500). ^{1}H-NMR (acetone-d_6) δ: 3.21 (3H, s, OMe), 3.42 (2H, br d. J=7 Hz, H_2-7'), 3.66 (2H, m, H_2-9), 4.00 (1H, m, H-8), 4.17 (1H, d, J=7 Hz, H-7), 4.94 (1H, br d, J=11 Hz, H-9'), 5.11 (1H, br d, J=18 Hz, H-9'), 6.05 (1H, ddt, J=18, 11, 7 Hz, H-8'), 6.89, 6.96 (each 1H, d, J=8 Hz, H-5, H-5'), 7.12, 7.50 (each 1H, dd, J=8, 2 Hz, H-6, H-4'), 7.42, 7.56 (each 1H, d, J=2 Hz, H-2, H-2').

Acetylation of 13 **13** (10 mg) was acetylated in the same way as **5** to afford a tetraacetate (10 mg) as a white powder, $[\alpha]_D^{17}$ −0.3° (c=1.25, $CHCl_3$). ^{1}H-NMR ($CDCl_3$) δ: 2.03×2, 2.10, 2.33 (each s, $COCH_3$), 3.29 (3H, s, OMe), 3.35 (2H, br d, J=7 Hz, H_2-7'), 3.92 (1H, dd, J=12, 7 Hz, H-9), 4.33 (1H, dd, J=12, 4 Hz, H-9), 4.59 (1H, d, J=6 Hz, H-7), 5.08 (2H, m, H_2-9'), 5.26 (1H, ddd, J=7, 6, 4 Hz, H-8), 5.75—6.20 (1H, m, H-8'), 7.02—7.36 (6H, m, Ar-H).

Methylation of 13 **13** (6 mg) was methylated in the same way as **3** to afford a dimethyl ether (3 mg) as a white powder, $[\alpha]_D^{20}$ −2.0° (c=0.20, $CHCl_3$). ^{1}H-NMR ($CDCl_3$) δ: 3.26, 3.81, 3.87 (each 3H, s, OMe), 3.42 (2H, br d, J=7 Hz, H_2-7'), 3.53 (1H, dd, J=12, 6 Hz, H-9), 3.62 (1H, dd, J=12, 4 Hz, H-9), 4.10 (1H, d, J=8 Hz, H-7), 4.29 (1H, ddd, J=8, 6, 4 Hz, H-8), 5.05 (1H, br d, J=11 Hz, H-9'), 5.08 (1H, br d, J=18 Hz, H-9'), 6.00 (1H, ddt, J=18, 11, 7 Hz, H-8'), 6.89, 6.92 (each 1H, d, J=8 Hz), 7.20, 7.35 (each 1H, dd, J=8, 2 Hz), 7.25, 7.32 (each 1H, d, J=2 Hz).

Magnolignan E(14) A white powder, $[\alpha]_D^{29}$ −2.0° (c=2.06, MeOH). FD-MS m/z: 298 (M^+), 280, 250. ^{1}H-NMR (acetone-d_6) δ: 3.32 (2H, br d, J=6 Hz, H_2-7), 3.75 (2H, d, J=6 Hz, H_2-9'), 4.53 (1H, dd, J=10, 6 Hz, H-8'), 5.03 (1H, br d, J=11 Hz, H-9), 5.05 (1H, br d, J=18 Hz, H-9), 5.28 (1H, br s, H-7', after D_2O exchange J=4 Hz), 5.98 (1H, ddt, J=18, 11, 6 Hz, H-8), 6.77 (1H, d, J=8 Hz, H-5'), 6.94 (1H, d, J=8 Hz, H-5), 6.96 (1H, dd, J=8, 2 Hz, H-6), 7.42 (1H, dd, J=8, 2 Hz, H-4'), 7.08 (1H, d, J=2 Hz, H-2), 7.56 (1H, d, J=2 Hz, H-2'). NOEs: δ 3.75 (irr)→5.28 (5% NOE); 5.28 (irr)→3.75 (5% NOE), 7.56 (4% NOE).

Methylation of 14 **14** (10 mg) was methylated in the same way as **3** to afford a dimethyl ether (**14a**) (5 mg) as a white powder. ^{1}H-NMR ($CDCl_3$) δ: 3.34 (2H, m, H_2-7), 3.78 (3H, s, OMe), 3.60—3.98 (2H, m, H_2-9'), 4.78 (1H, m, H-8'), 5.05 (1H, br d, J=11 Hz, H-9), 5.08 (1H, br d, J=18 Hz, H-9), 5.13 (1H, d, J=6 Hz, H-7'), 5.79—6.12 (1H, m, H-8), 6.83—7.60 (6H, m, Ar-H).

Acetylation of 14 **14** (7 mg) was acetylated in the same way as **5** to afford a triacetate (**14b**) (7 mg) as a white powder. EI-MS m/z: 424 (M^+). ^{1}H-NMR ($CDCl_3$) δ: 2.05 (3H, s, Ac), 2.11 (6H, s, Ac×2), 3.41 (2H, m, H_2-7), 4.28 (1H, dd, J=12, 6 Hz, H-9'), 4.42 (1H, dd, J=12, 5 Hz, H-9'), 4.85 (1H, m, H-8'), 5.08 (1H, br d, J=10 Hz, H-9), 5.10 (1H, br d, J=18 Hz, H-9), 5.82 (1H, m, H-8), 6.11 (1H, d, J=4 Hz, H-7'), 6.86—7.40 (6H, m, Ar-H).

Randaial[5] **(15)** A pale yellow powder. EI-MS m/z: 242.094 (M^+, $C_{15}H_{14}O_3$, requires: 242.094). UV λ_{max}^{MeOH} nm (ε): 298 (5700). ^{1}H-NMR (acetone-d_6) δ: 3.35 (2H, br d, J=7 Hz, H_2-7), 5.01 (1H, br d, J=11 Hz, H-9), 5.06 (1H, br d, J=18 Hz, H-9), 5.99 (1H, ddt, J=18, 11, 7 Hz, H-8), 6.75, 7.05 (each 1H, dd, J=9, 2 Hz, H-6, H-6'), 6.84, 6.94 (each 1H, d, J=9 Hz, H-5, H-5'), 6.79, 7.11 (each 1H, d, J=2 Hz, H-2, H-2'). ^{13}C-NMR (Table III).

Methylation and Hydrogenation of 15 **15** (30 mg) was methylated in the same way as **3** to afford a trimethyl ether (30 mg) as a pale yellow powder. ^{1}H-NMR ($CDCl_3$) δ: 3.40 (2H, br d, J=7 Hz, H_2-7), 3.70, 3.71, 3.88 (each 3H, s, OMe), 5.02 (1H, br d, J=11 Hz, H-9), 5.06 (1H, br d, J=18 Hz, H-9), 6.00 (1H, ddt, J=18, 11, 7 Hz, H-8), 6.65—7.30 (6H, m, Ar-H). The trimethyl ether (30 mg) was hydrogenated over 10% Pd–C (30 mg) in MeOH (20 ml) under a hydrogen atmosphere for 3 h. After removal of the catalyst by filtration, the filtrate was evaporated under reduced pressure. The residue was purified by chromatography over silica gel with benzene–hexane (1 : 1) to give a dihydrotrimethyl ether (**15a**) (33 mg) as a pale yellow powder. EI-MS m/z: 286 (M^+). ^{1}H-NMR ($CDCl_3$) δ: 0.88 (3H, t, J=8 Hz, H_3-9), 1.50 (2H, m, H_2-8), 2.48 (2H, br t, J=7 Hz, H_2-7), 3.34, 3.35, 3.37 (each 3H, s, OMe), 6.66 (1H, d, J=9 Hz, H-5'), 6.68 (1H, d, J=8 Hz, H-5), 6.83 (1H, dd, J=9, 3 Hz, H-6'), 7.00 (1H, dd, J=8, 2 Hz, H-6), 7.05 (1H, d, J=3 Hz, H-2'), 7.19 (1H, d, J=2 Hz, H-2). NOEs: δ 2.48 (irr)→7.00 (11% NOE), 7.19 (21% NOE); δ 3.34, 3.35, 3.37 (center irr)→6.66 (12% NOE), 6.68 (12% NOE), 6.83 (11% NOE), 7.03 (11% NOE).

Magnatriol B(16) Pale yellow needles, mp 99—100 °C ($CHCl_3$–benzene). EI-MS m/z: 242.094 (M^+, $C_{15}H_{14}O_3$, requires: 242.094). UV λ_{max}^{MeOH} nm (ε): 306 (5100). ^{1}H-NMR (acetone-d_6) δ: 3.40 (2H, br d, J=7 Hz, H_2-7), 5.01 (1H, br d, J=11 Hz, H-9), 5.06 (1H, br d, J=18 Hz, H-9), 6.06 (1H, ddt, J=18, 11, 7 Hz, H-8), 6.65 (1H, dd, J=8, 2 Hz, H-6'), 6.80 (1H, d, J=2 Hz, H-2'), 6.84 (1H, d, J=8 Hz, H-5), 6.96 (1H, d, J=8 Hz, H-5'), 7.28 (1H, dd, J=8, 2 Hz, H-4), 7.33 (1H, d, J=2 Hz, H-2). ^{13}C-NMR (Table III).

Methylation and Hydrogenation of 16 **16** (30 mg) was methylated in the same way as **3** to afford a trimethyl ether (25 mg) as a pale yellow powder. ^{1}H-NMR ($CDCl_3$) δ: 3.41 (2H, br d, J=7 Hz, H_2-7), 3.67, 3.72, 3.79 (each 3H, s, OMe), 5.02 (1H, br d, J=11 Hz, H-9), 5.07 (1H, br d, J=18 Hz, H-9), 6.02 (1H, ddt, J=18, 11, 7 Hz, H-8), 6.67—7.42 (6H, m, Ar-H). The trimethyl ether (25 mg) was hydrogenated in the same way as **15** to give a dihydrotrimethyl ether (**16a**) (25 mg) as a pale yellow powder. EI-MS m/z: 286 [M^+]. ^{1}H-NMR ($CDCl_3$) δ: 0.96 (3H, t, J=7 Hz, H_3-9), 1.61 (2H, m, H_2-8), 2.76 (2H, t, J=7 Hz, H_2-7), 3.36, 3.37, 3.42 (each 3H, s, OMe), 6.64 (1H, d, J=9 Hz, H-5), 6.66 (1H, d, J=9 Hz, H-5'), 6.80 (1H, dd, J=9, 3 Hz, H-6'), 7.15 (1H, d, J=3 Hz, H-2'), 7.51 (1H, dd, J=9, 3 Hz, H-4), 7.53 (1H, d, J=3 Hz, H-2). NOEs: δ 2.76 (irr)→δ 7.53 (20% NOE); δ 3.56, 3.57 (center irr)→δ 2.76 (2% NOE), 6.64 (13% NOE), 6.66 (13% NOE); δ 3.42 (irr)→δ 6.80 (23% NOE), 7.15 (21% NOE).

Magnaldehyde D(17) Pale yellow needles, mp 140—143 °C ($CHCl_3$–benzene). EI-MS m/z: 254.093 (M^+, $C_{16}H_{14}O_3$, requires: 254.094). ^{1}H-NMR (acetone-d_6) δ: 3.38 (2H, br d, J=7 Hz, H_2-7), 5.02 (1H, br d, J=11 Hz, H-9), 5.08 (1H, br d, J=18 Hz, H-9), 6.02 (1H, ddt, J=18, 11, 7 Hz, H-8), 7.00—7.21 (4H, m, Ar-H), 7.77 (1H, dd, J=9, 2 Hz), 7.83 (1H, d, J=2 Hz), 9.89 (1H, s, H-7'). ^{13}C-NMR (Table III).

Magnaldehyde E(18) Pale yellow needles, mp 160—162 °C ($CHCl_3$–benzene). EI-MS m/z: 254.094 (M^+, $C_{16}H_{14}O_3$, requires: 254.094). ^{1}H-NMR (acetone-d_6) δ: 3.46 (2H, br d, J=7 Hz, H_2-7), 5.01 (1H, br d, J=11 Hz, H-9), 5.07 (1H, br d, J=18 Hz, H-9), 6.00 (1H, ddt, J=18, 11, 7 Hz, H-8), 6.92, 7.13 (each 1H, d, J=9 Hz, H-5, H-5'), 7.40, 7.72 (each 1H, dd, J=9, 2 Hz, H-4, H-6'), 7.40, 7.80 (each 1H, d, J=2 Hz, H-2, H-2'), 9.86 (1H, s, H-7'). ^{13}C-NMR (Table III).

Magnolignan F(19) A pale brown powder. $[\alpha]_D^{28}$ −1.5° (c=1.04, MeOH). FD-MS m/z: 564 (M^+), 546, 282, 273, 266, 182. ^{1}H-NMR (acetone-d_6) δ: 3.20—3.40 (6H, m, H_2-7, H_2-7', H_2-7''), 3.80—4.20 (3H, m, H-8'', H_2-9''), 4.64 (1H, d, J=5 Hz, H-7''), 4.85—5.20 (6H, m, H_2-9, H_2-9', H_2-9'''), 5.70—6.20 (3H, m, H-8, H-8', H-8'''), 6.80—7.25 (12H, m, Ar-H). ^{13}C-NMR (Table IV).

Methylation of 19 **19** (20 mg) was methylated in the same way as **3** to afford a trimethyl ether (**19a**, 14 mg) as a pale brown powder. $[\alpha]_D^{20}$ +0.8° (c=1.47, $CHCl_3$). ^{1}H-NMR ($CDCl_3$) δ: 3.35 (6H, br d, J=7 Hz, H_2-7, H_2-7', H_2-7'''), 3.68, 3.69, 3.73 (each 3H, s, OMe), 3.90 (3H, m, H-8'', H_2-9''), 4.50 (1H, m, H-7''), 4.85—5.16 (6H, m, H_2-9, H_2-9', H_2-9'''), 5.77—6.18 (3H, m, H-8, H-8', H-8'''), 6.60—7.28 (12H, m, Ar-H).

Acetylation of 19a **19a** (2 mg) was acetylated in the same way as **5** to yield a diacetyl-trimethyl ether (**19b**, 2 mg) as a white powder. ^{1}H-NMR ($CDCl_3$) δ: 1.92, 1.99 (each 3H, s, $COCH_3$), 3.30 (6H, m, H_2-7, H_2-7', H_2-7'''), 3.64, 3.72, 3.76 (each 3H, s, OMe), 3.62 (1H, dd, J=11, 4 Hz, H-9''), 4.04 (1H, dd, J=11, 3 Hz, H-9''), 4.85—5.15 (6H, m, H_2-9, H_2-9', H_2-9'''), 5.30 (1H, m, H-8''), 5.82 (1H, d, J=8 Hz, H-7''), 5.78—6.18 (3H, m, H-8, H-8', H-8'''), 6.60—7.15 (12H, m, Ar-H).

Hydrogenation of 19a **19a** (11 mg) was hydrogenated in the same way as **15** to give a hexahydroganate (**19c**, 11 mg) as a white powder. EI-MS m/z: 612 (M^+). ^{1}H-NMR ($CDCl_3$) δ: 0.95 (9H, m, H_3-9, H_3-9', H_3-9'''), 1.60 (6H, m, H_2-8, H_2-8', H_2-8'''), 2.55 (6H, m, H_2-7, H_2-7', H_2-7'''), 3.62, 3.71, 3.76 (each 3H, s, OMe), 3.65 (1H, dd, J=10, 4 Hz, H-9''), 4.02 (2H, m, H-8'', H-9''), 4.60 (1H, d, J=8 Hz, H-7''), 6.63—7.15 (12H, m, Ar-H).

Periodate Oxidation of 19c A mixture of **19c** (11 mg) and sodium metaperiodate (3 mg) in MeOH (5 ml) was stirred at room temperature for 3 h. The reaction mixture was concentrated to a syrup, which was subjected to silica gel chromatography with hexane–EtOAc (20 : 1) furnished two products [**19d** (1.5 mg) and **19e** (1.8 mg)]. **19d**: EI-MS m/z: 284 (M^+). ^{1}H-NMR ($CDCl_3$) δ: 0.95 (3H, t, J=7 Hz, H_3-9), 1.60 (2H, m, H_2-8), 2.57 (2H, t, J=7 Hz, H_2-7), 3.75, 3.87 (each 3H, s, OMe), 6.89, 7.06 (each 1H, d, J=8 Hz, H-5, H-5'), 7.04, 7.78 (each 1H, d, J=2 Hz, H-2, H-2'), 7.17, 7.87 (each 1H, dd, J=8, 2 Hz, H-6, H-6'), 9.91 (1H, s, CHO). **19e**: EI-MS m/z: 326 (M^+). ^{1}H-NMR ($CDCl_3$) δ: 0.95 (6H, t, J=7 Hz, H_3-9, H_3-9'), 1.61 (4H, m, H_2-8, H_2-8'), 2.44 (4H, m, H_2-7, H_2-7'), 3.73 (3H, s, OMe), 4.45 (2H, d, J=1.5 Hz, O–$\underline{CH_2}$–CHO), 6.72—7.18 (6H, m, Ar-H), 9.69 (1H, d, J=1.5 Hz, O–CH_2–$\underline{CHO}$).

Magnolignan G(20) A pale brown powder. $[\alpha]_D^{29}$ +0.1° (c=1.25, MeOH). FD-MS m/z: 596 (M^+), 578, 446, 298, 289. ^{1}H-NMR (acetone-d_6 + D_2O) δ: 2.43 (2H, d, J=6 Hz, H_2-9''), 3.30 (6H, m, H_2-7, H_2-7', H_2-7'''), 3.77 (1H, m, H-8''), 4.22 (1H, d, J=6 Hz, H-7''), 4.80—5.15 (6H, m, H_2-9, H_2-9', H_2-9'''), 5.68—6.15 (3H, m, H-8, H-8', H-8'''), 6.38 (1H, d, J=2 Hz, H-2''), 6.51—7.08 (10H, m, Ar-H). ^{13}C-NMR (Table IV).

Methylation of 20 **20** (40 mg) was methylated in the same way as **3** to yield a tetramethyl ether (**20a**, 15 mg) as a pale brown powder. $[\alpha]_D^{20}$ +0.8° (c=1.50, $CHCl_3$). ^{1}H-NMR (acetone-d_6) δ: 2.59 (2H, d, J=6 Hz, H_2-9″), 3.30 (6H, m, H_2-7, H_2-7′, H_2-7‴), 3.53, 3.65, 3.79, 3.81 (each 3H, s, OMe), 3.80 (1H, m, H-8″), 4.35 (1H, m, H-7″), 5.02 (6H, m, H_2-9, H_2-9′, H_2-9‴), 5.96 (3H, m, H-8, H-8′, H-8‴), 6.55—7.17 (11H, m, Ar-H).

Acetylation of 20 **20** (17 mg) was acetylated in the same way as **5** to yield a hexaacetate (**20b**, 15 mg) as a white powder. $[\alpha]_D^{25}$ +0.7° (c=1.50, $CHCl_3$). ^{1}H-NMR ($CDCl_3$) δ: 1.81, 1.83, 2.00, 2.18, 2.21, 2.28 (each 3H, s, Ac), 2.76 (2H, d, J=7 Hz, H_2-9″), 3.32 (6H, m, H_2-7, H_2-7′, H_2-7‴), 5.05 (6H, m, H_2-9, H_2-9′, H_2-9‴), 5.34 (1H, td, J=7, 6 Hz, H-8″), 5.65 (1H, d, J=6 Hz, H-7″), 5.88 (3H, m, H-8, H-8′, H-8‴), 6.63—7.17 (11H, m, Ar-H).

Hydrogenation of 20b **20b** (3 mg) was hydrogenated in the same way as **15** to give a hexahydro-hexaacetate (2 mg) as a white powder. ^{1}H-NMR ($CDCl_3$) δ: 0.93 (9H, m, H_3-9, H_3-9′, H_3-9‴), 1.59 (6H, m, H_2-8, H_2-8′, H_2-8‴), 1.79, 1.82, 1.99, 2.17, 2.20, 2.27 (each 3H, s, Ac), 2.53 (6H, m, H_2-7, H_2-7′, H_2-7‴), 2.73 (2H, d, J=7 Hz, H_2-9″), 5.32 (1H, td, J=7, 6 Hz, H-8″), 5.66 (1H, d, J=6 Hz, H-7″), 6.58—7.16 (11H, m, Ar-H).

Periodate Oxidation of 20a A mixture of **20a** (15 mg) and sodium metaperiodate (5 mg) in MeOH (5 ml) was stirred at room temperature for 3 h. The reaction mixture was concentrated to a syrup, which was subjected to silica gel chromatography with hexane–EtOAc (20 : 1) to afford two products [**20c** (3.5 mg) and **20d** (2.8 mg)]. **20c**: EI-MS m/z: 352 (M^+). ^{1}H-NMR ($CDCl_3$) δ: 3.23 (4H, br d, J=6 Hz, H_2-7, H_2-7′), 3.50 (2H, d, J=2 Hz, $\underline{CH_2}$–CHO), 3.62 (3H, s, C-4-OMe), 3.81 (3H, s, C-5-OMe), 5.00 (4H, m, H_2-9, H_2-9′), 5.67—6.06 (2H, m, H-8, H-8′), 6.62 (1H, s, H-6), 6.67 (2H, d, J=9 Hz, H-3′, H-5′), 6.98 (2H, d, J=9 Hz, H-2′, H-6′), 9.46 (1H, d, J=2 Hz, CH_2–$\underline{CHO}$). NOEs: δ 3.81 (irr)→6.62 (28% NOE) and 3.62 (10% NOE), 3.62→3.81 (10% NOE), 3.50→3.23 (9% NOE). **20d**: EI-MS m/z: 298 (M^+). ^{1}H-NMR ($CDCl_3$) δ: 3.37 (2H, br d, J=6 Hz, H_2-7′), 3.96 (6H, s, C-4-OMe, C-5-OMe), 5.05 (1H, br d, J=11 Hz, H-9′), 5.06 (1H, br d, J=17 Hz, H-9′), 5.97 (1H, ddt, J=17, 11, 6 Hz, H-8′), 6.91 (2H, d, J=9 Hz, H-3′, 5′), 7.07 (1H, d, J=2 Hz, H-2), 7.15 (2H, d, J=9 Hz, H-2′, H-6′), 7.24 (1H, d, J=2 Hz, H-6), 9.77 (1H, s, C-1-CHO). NOE: δ 3.96 (irr)→7.24 (18% NOE).

Magnolignan H(21) A pale brown powder, $[\alpha]_D^{28}$ +2.0° (c=2.65, MeOH). FD-MS m/z: 563 $[M+H]^+$, 544, 531, 337, 239. ^{1}H-NMR (acetone-d_6) δ: 2.97 (2H, br d, J=6 Hz, H_2-7), 3.31 (4H, br d, J=6 Hz, H_2-7′, H_2-7‴), 3.51 (2H, d, J=6 Hz, H_2-9″), 4.68 (1H, d, J=9 Hz, H-7″), 4.78 (1H, m, H-8″), 4.75—5.16 (6H, m, H_2-9, H_2-9′, H_2-9‴), 5.46—6.17 (3H, m, H-8, H-8′, H-8‴), 6.36 (1H, s, H-2), 6.80—7.14 (10H, m, Ar-H). ^{13}C-NMR (Table IV).

Methylation of 21 **21** (50 mg) was methylated in the same way as **3** to yield a trimethyl ether (**21a**, 40 mg) as a pale yellow powder. $[\alpha]_D^{28}$ +0.4° (c=4.00, MeOH). ^{1}H-NMR ($CDCl_3$) δ: 2.93 (2H, br d, J=7 Hz, H_2-7), 3.35 (4H, br d, J=7 Hz, H_2-7′, H_2-7‴), 3.58 (2H, m, H_2-9″), 3.67, 3.71, 3.87 (each 3H, s, OMe), 4.59 (1H, d, J=9 Hz, H-7″), 4.78—5.20 (7H, m, H-8″, H_2-9, H_2-9′, H_2-9‴), 5.60 (1H, ddt, J=17, 11, 7 Hz, H-8), 5.75—6.20 (2H, m, H-8′, H-8‴), 6.35 (1H, s, H-2), 6.84—7.19 (10H, m, Ar-H).

Hydrogenation of 21a **21a** (20 mg) was hydrogenated in the same way as **15** to give a hexahydrogenate (**21b**, 18 mg) as a white powder. EI-MS m/z: 610 (M^+). ^{1}H-NMR ($CDCl_3$) δ: 0.71, 0.92, 0.94 (each 3H, t, J=7 Hz, H_3-9, H_3-9′, H_3-9‴), 1.27 (1H, m, H_2-8), 1.62 (4H, m, H-8′, H-8‴), 2.16 (2H, m, H_2-7), 2.55 (4H, br t, J=8 Hz, H_2-7′, H_2-7‴), 3.50 (1H, dd, J=12, 6 Hz, H-9″), 3.69 (1H, dd, J=12, 8 Hz, H-9″), 3.67, 3.73, 3.88 (each 3H, s, OMe), 4.58 (1H, d, J=9 Hz, H-7″), 5.02 (1H, ddd, J=9, 8, 6 Hz, H-8″), 6.33 (1H, s, H-2), 6.80—7.12 (10H, m, Ar-H). NOEs: δ 2.16 (irr)→6.33 (20% NOE), 3.50 (irr)→5.02 (8% NOE), 3.67 (irr)→6.80—7.12 (8% NOE); δ 3.73 (irr)→6.80—7.12 (8% NOE), 3.88 (irr)→6.80—7.12 (3% NOE); δ 4.58 (irr)→5.02 (12% NOE); δ 5.02 (irr)→4.58 (10% NOE).

Acetylation of 21a **21a** (5 mg) was acetylated in the same way as **5** to yield a tetraacetyltrimethyl ether (**21c**, 5 mg) as a white powder. ^{1}H-NMR ($CDCl_3$) δ: 2.03 (3H, s, Ac), 2.93 (2H, br d, J=7 Hz, H_2-7), 3.35 (4H, br d, J=7 Hz, H_2-7′, H_2-7‴), 3.67, 3.75, 3.90 (each 3H, s, OMe), 4.02 (1H, dd, J=12, 8 Hz, H-9″), 4.13 (1H, dd, J=12, 4 Hz, H-9″), 4.58 (1H, d, J=9 Hz, H-7″), 4.76—5.15 (7H, m, H-8″, H_2-9, H_2-9′, H_2-9‴), 5.61 (1H, ddt, J=18, 11, 7 Hz, H-8), 5.77—6.17 (2H, m, H-8′, H-8‴), 6.35 (1H, s, H-2), 6.85—7.18 (m, 10H, Ar-H).

Magnolignan I(22) A pale brown powder, $[\alpha]_D^{28}$ +2.1° (c=0.97, MeOH), FD-MS m/z: 522 (M^+). ^{1}H-NMR (acetone-d_6, 400 MHz) δ: 3.32 (4H, m, H_2-7, H_2-7‴), 3.60 (1H, m, H-8″), 3.89 (2H, m, H_2-9″), 5.01 (4H, m, H_2-9, H_2-9‴), 5.63 (1H, d, J=6.2 Hz, H-7″), 5.95 (2H, m, H-8, H-8‴), 6.78, 6.83 (each 1H, d, J=2.2 Hz, H-2′, H-6′), 6.86, 6.93, 7.00 (each 1H, d, J=8.1 Hz, H-5, H-5″, H-5‴), 7.01, 7.05, 7.33 (each 1H, dd, J=8.1, 2.2 Hz, H-6, H-6″, H-6‴), 7.10, 7.19, 7.37 (each 1H, d, J=2.2 Hz, H-2, H-2″, H-2‴). ^{13}C-NMR (Table IV).

Methylation of 22 **22** (30 mg) was methylated in the same way as **3** to yield a tetramethyl ether (**22a**, 19 mg) as a white powder. ^{1}H-NMR ($CDCl_3$) δ: 3.33 (4H, br d, J=6 Hz, H_2-7, H_2-7‴), 3.64, 3.68, 3.73, 3.77 (each 3H, s, OMe), 3.60 (1H, m, H-8″), 3.86 (2H, m, H_2-9″), 5.04 (4H, m, H_2-9, H_2-9‴), 5.51 (1H, d, J=7 Hz, H-7″), 5.73—6.17 (2H, m, H-8, H-8‴), 6.77—7.21 (11H, m, Ar-H).

Hydrogenation of 22a **22a** (12 mg) was hydrogenated in the same way as **15** to give a tetrahydrogenate (**22b**, 12 mg) as a white powder. EI-MS m/z: 582 (M^+), 564, 552. $[\alpha]_D^{30}$ +1.7° (c=1.18, $CHCl_3$). ^{1}H-NMR ($CDCl_3$) δ: 0.91, 0.92 (each 3H, t, J=7 Hz, H_3-9, H_3-9‴), 1.65 (4H, m, H_2-8, H_2-8‴), 2.53 (4H, t, J=7 Hz, H_2-7, H_2-7‴), 3.63, 3.68, 3.43, 3.77 (each 3H, s, OMe), 3.60 (1H, m, H-8″), 3.91 (2H, m, H_2-9″), 5.52 (1H, d, J=7 Hz, H-7″), 6.58—7.20 (11H, m, Ar-H).

Acetylation of 22b **22b** (12 mg) was acetylated in the same way as **5** to yield a monoacetate (**22c**, 13 mg) as a white powder. ^{1}H-NMR ($CDCl_3$, 400 MHz) δ: 0.92, 0.94 (each 3H, t, J=7.3 Hz, H_3-9, H_3-9‴), 1.61 (4H, m, H_2-8, H_2-8‴), 2.04 (3H, s, Ac), 2.52 (4H, m, H_2-7, H_2-7‴), 3.65, 3.70, 3.76, 3.78 (each 3H, s, OMe), 3.79 (1H, m, H-8″), 4.31 (1H, dd, J=11.0, 7.7 Hz, H-9″), 4.46 (1H, dd, J=11.0, 5.8 Hz, H-9″), 5.43 (1H, d, J=6.6 Hz, H-7″), 6.77 (1H, d, J=2.3 Hz, H-6′), 6.81 (1H, d, J=2.3 Hz, H-2′), 6.84, 6.86 (each 1H, d, J=8.4 Hz, H-5, H-5‴), 6.92 (1H, d, J=8.4 Hz, H-5″), 7.01, 7.17 (each 1H, d, J=2.2 Hz, H-2, H-2‴), 7.26 (1H, d, J=2.2 Hz, H-2″), 7.09, 7.10 (each 1H, dd, J=8.4, 2.2 Hz, H-6, H-6‴), 7.35 (1H, dd, J=8.4, 2.2 Hz, H-6″). NOEs: δ 4.31 (irr)→3.79 (22% NOE), 5.43 (22% NOE), 6.77 (3% NOE); δ 4.46 (irr)→3.79 (16% NOE), 5.43 (5% NOE); δ 5.43 (irr)→4.31 (9% NOE), 4.46 (4% NOE), 7.26 (12% NOE), 7.35 (10% NOE).

References and Notes

1) Jiangsu New Medical College (ed.), "Chinese Drug Dictionary," Shanghai Science and Technology Publishing Co., Shanghai, 1977, pp. 1628—1630.
2) Y. Sugii, *Yakugaku Zasshi*, **50**, 183 (1930).
3) M. Fujita, H. Itokawa and Y. Sashida, *Chem. Pharm. Bull.*, **20**, 212 (1972).
4) K. Ito and S. Asahi, *Yakugaku Zasshi*, **94**, 729 (1974).
5) F. C. Chen, J. S. Lee and Y. M. Lin, *Phytochemistry*, **22**, 616 (1983).
6) K. Miki and T. Sasaya, *Mokuzai Gakkaishi*, **25**, 361 (1979).
7) F. S. El-Feraly and W. S. Li, *Lloydia*, **41**, 442 (1978).
8) K. Ichino, H. Tanaka and K. Ito, *Tetrahedron*, **44**, 3251 (1988).
9) C. J. Brooks and J. D. Gilbert, *J. Chem. Soc., Chem. Commun.*, **1973**, 194.
10) T. Takeya, T. Okubo and S. Tobinaga, *Chem. Pharm. Bull.*, **35**, 1755 (1987).
11) K. Ito, T. Iida, K. Ichino, M. Tsunezuka, M. Hattori and T. Namba, *Chem. Pharm. Bull.*, **30**, 3347 (1982).
12) K. Miki, T. Takehara, T. Sasaya and A. Sakakibara, *Phytochemistry*, **19**, 449 (1980).
13) A. Ichihara, Y. Numata, S. Kanai and S. Sakamura, *Agric. Biol. Chem.*, **41**, 1813 (1977); S. Yamanouchi, M. Takido, U. Sankawa and S. Shibata, *Yakugaku Zasshi*, **96**, 1942 (1976); A. Ichihara, K. Oda, Y. Numata and S. Sakamura, *Tetrahedron Lett.*, **1976**, 3961.

Studies on the Constituents of *Solidago virga-aurea* L. I. Structural Elucidation of Saponins in the Herb

Yoshinori INOSE, Toshio MIYASE* and Akira UENO

School of Pharmaceutical Sciences, University of Shizuoka, 395, Yada, Shizuoka 422, Japan. *Received January 7, 1991*

Nine new oleanane-type saponins, solidagosaponins I—IX (1—9), were isolated from *Solidago virga-aurea* L. (Compositae). Interestingly, these saponins, except 9, have a sugar chain at the 16 position of the aglycone. Moreover, four of them contain a β-hydroxy butyrate group at a portion of the sugar chain. The structures of these compounds were established on the basis of spectroscopic and chemical evidence.

Keywords *Solidago virga-aurea*; Compositae; β-hydroxy butyrate; polygalacic acid; oleanane-type saponin; solidagosaponin

Solidago virga-aurea L. is widely distributed in Eurasia. In China the decoction of this whole plant has been used as an expectorant, an anti-inflammatory agent for bronchitis and an anti-bacterial agent.[1)]

In connection with a study on the terpenic glycosides of some plants in Compositae, we have also studied *Solidago virga-aurea* L. Several other groups have already investigated this plant and reported the presence of virgaureaside A,[2)] leiocarposide[3)] and solidagolactone[4)] *etc.* Especially, Hiller *et al.*[5)] reported some saponins whose aglycone was polygalacic acid; they named them virgaureasaponin. During the course of further investigation, we obtained nine new oleanane-type triterpene saponins, designated as solidagosaponins I—IX (**1**—**9**). This paper deals with the isolation and structure elucidation of these saponins.

The water extract of the whole plants was passed through a Diaion HP-20 column, and the absorbed materials were eluted with 50% methanol and 100% methanol, successively. The 100% methanol eluate was chromatographed on silica gel and an ODS column, followed by repeated

TABLE I. ^{13}C-NMR Spectral Data of Aglycone and Ester Moieties in C_5D_5N

Carbon No.	**1b**	**1c**	**1**	**2**	**3**	**4**	**5**	**6**	**7**	**8**	**9**
Aglycone moiety											
1	44.9	44.9	44.7	44.8	44.8	44.9	44.8	44.8	44.7	44.8	44.2
2	71.5	71.7	71.6	71.6	71.6	71.6	71.6	71.4	71.4	71.5	70.6
3	73.0	73.0	73.0	73.4	73.4	73.4	73.1	73.2	73.0	73.2	83.1
4	42.4	42.5	42.4	42.4	42.4	42.4	42.4	42.3	42.3	42.4	42.8
5	48.3	48.1	48.3	48.4	48.3	48.3	48.3	48.3	48.3	48.3	48.0
6	18.3	18.3	18.2	18.3	18.2	18.3	18.3	18.3	18.2	18.3	18.1
7	33.2	33.0	33.0	33.1	33.1	33.1	33.0	33.1	33.0	33.1	33.3
8	40.0	39.9	39.9	39.9	40.0	40.0	40.1	40.1	40.0	40.0	40.1
9	47.6	47.6	47.6	47.7	47.5	47.6	47.6	47.6	47.5	47.6	47.7
10	37.3	37.2	37.2	37.3	37.2	37.3	37.2	37.3	37.2	37.3	37.1
11	24.0	24.0	23.9	24.0	24.1	24.1	24.0	24.0	24.0	24.0	24.1
12	122.9	122.7	122.2	122.2	122.7	122.7	122.8	122.7	122.7	122.7	122.6
13	144.5	144.3	145.1	145.5	144.3	144.5	144.3	144.6	144.4	144.7	145.2
14	42.1	41.7	41.4	41.4	41.4	41.4	41.5	41.4	41.4	41.4	42.3
15	35.9	30.0	29.6	29.9	29.6	29.8	29.6	29.9	29.6	29.8	36.2
16	74.3	78.9	77.8	78.2	77.1	77.5	77.5	77.6	77.2	77.6	74.7
17	49.0	48.6	48.4	48.4	49.1	49.0	48.9	48.7	48.9	48.8	48.9
18	41.3	41.2	41.2	41.1	41.3	41.2	41.0	40.8	40.9	40.8	41.5
19	47.0	46.2	45.3	45.3	45.0	44.9	45.2	45.2	45.3	45.2	47.3
20	30.9	30.7	31.0	31.0	30.8	30.8	30.9	30.8	30.9	30.9	31.0
21	35.9	36.0	36.5	36.5	36.2	36.1	36.3	36.2	36.4	36.3	36.3
22	32.5	32.1	32.4	32.6	32.1	32.2	31.8	32.0	31.9	32.1	32.8
23	67.6	67.8	68.0	68.2	68.1	68.1	68.0	68.0	67.8	68.0	65.6
24	14.6	14.6	14.5	14.6	14.6	14.6	14.6	14.5	14.5	14.5	15.0
25	17.4	17.3	17.2	17.3	17.3	17.3	17.3	17.3	17.3	17.3	17.3
26	17.4	17.3	17.4	17.5	17.8	17.8	17.6	17.6	17.5	17.6	17.6
27	27.2	27.4	27.0	27.0	26.9	26.9	27.0	27.0	26.9	27.0	27.3
28	177.9	177.3	179.6	179.8	175.4	175.5	175.9	176.0	175.9	175.9	180.0
29	33.2	33.2	33.4	33.3	33.2	33.1	33.2	33.1	33.3	33.2	33.3
30	24.6	24.7	25.1	25.1	24.7	24.7	25.0	24.9	25.0	24.9	24.8
OMe	51.8	51.9									
Ester moiety											
1				172.3		172.2		172.3		172.3	
2				45.3		45.3		45.1		45.1	
3				64.5		64.5		64.4		64.4	
4				24.2		24.3		24.1		24.2	

Recorded on JEOL GSX-270 (67.80 MHz).

semi-preparative high performance liquid chromatography (HPLC) on a reversed phase column (ODS, PhA). We identified all nine saponins.

Solidagosaponin I (**1**) revealed the $[M+Na]^+$ ion peak at m/z 821 and the $[M+H]^+$ ion peak at m/z 799 in the fast atom bombardment mass spectrum (FAB-MS) and elemental analysis data were consistent with $C_{41}H_{66}O_{15}\cdot 2H_2O$. The ^{1}H-nuclear magnetic resonance (^{1}H-NMR) spectrum showed six singlet methyl signals (δ 1.03, 1.14, 1.14, 1.33, 1.55 and 1.77), an olefinic proton signal ([δ 5.57 (t-like)] and two anomeric proton signals [δ 4.95 (d, $J=8$ Hz) and 5.28 (d, $J=8$ Hz)]. The ^{13}C-nuclear magnetic reasonance (^{13}C-NMR) spectrum showed two anomeric carbon signals (δ 98.5 and 106.3), trisubstituted olefinic carbon signals (δ 122.2 and 145.1) and a signal of carboxylic acid (δ 179.6). Mild methanolysis of **1a**, obtained by methylation of **1** with diazomethane, yielded sapogenin methyl ester (**1b**) and prosapogenin methyl ester (**1c**). The ^{1}H-NMR spectrum of **1b** exhibited signals due to three oxygenated methine protons [δ 4.28 (d, $J=4$ Hz), 4.55 (dd, $J=3$, 4 Hz) and 5.03 (br s)], a hydroxymethyl proton [δ 3.72 (d, $J=11$ Hz) and 4.17 (d, $J=11$ Hz)], six singlet methyl signals and an olefinic proton signal. This data suggested that the sapogenin is a polygalacic acid.[6,7] Comparing ^{1}H- and ^{13}C-NMR data with those of the reference, we concluded **1b** to be methyl polygalacate. In the ^{13}C-NMR of **1c**, signals due to a sugar moiety were observed at δ 101.3 (anomeric carbon), 75.6, 79.4, 72.3, 78.2 and 63.2, indicating the presence of a β-glucopyranosyl unit. Furthermore, when signals due to the sapogenin moiety of **1c** were compared with those of **1b**, glycosylation shifts[8] were observed at C-15 (-5.9 ppm) and C-16 ($+4.6$ ppm). So the linkage site of the glycoside moiety was determined to be C-16 in the

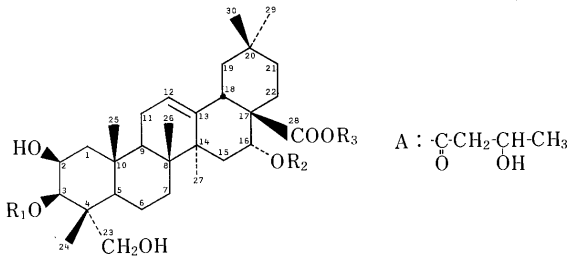

	R_1	R_2	R_3
1:	–H	–glc(2→1)ara	–H
1a:	–H	–glc(2→1)ara	–Me
1c:	–H	–glc	–Me
1b:	–H	–H	–Me
2:	–H	–glc(2→1)ara(4→1)A	–H
3:	–H	–glc(2→1)ara	–rham
4:	–H	–glc(2→1)ara(4→1)A	–rham
5:	–H	–glc(2→1)ara	–xyl
6:	–H	–glc(2→1)ara(4→1)A	–xyl
7:	–H	–glc(2→1)ara	–ara
8:	–H	–glc(2→1)ara(4→1)A	–ara
9:	–glc(4→1)glc	–H	–H

Chart 1

TABLE II. ^{13}C-NMR Spectral Data of Sugar Moieties in C_5D_5N

Carbon No.	1c	1	2	3	4	5	6	7	8	9
Sugar moiety										
C-16										
Glc-1	101.3	98.5	98.8	98.4	98.7	98.4	98.5	98.4	98.6	
Glc-2	75.6	82.9	80.4	83.0	80.5	83.0	80.3	82.7	80.4	
Glc-3	79.4	79.3	79.6	79.4	79.6	79.4	79.4	79.1	79.4	
Glc-4	72.3	71.9	72.3	71.8	72.2	71.7	71.9	71.6	72.0	
Glc-5	78.2	78.2	78.2	78.3	78.3	78.2	78.0	78.1	78.1	
Glc-6	63.2	62.9	63.0	62.9	63.0	62.8	62.7	62.8	62.8	
Ara-1		106.3	105.3	106.5	105.4	106.4	105.1	106.2	105.1	
Ara-2		73.5	73.1	73.6	73.1	73.6	73.2	73.3	73.1	
Ara-3		74.8	72.7	74.9	72.6	74.9	72.5	74.6	72.5	
Ara-4		69.6	72.7	69.6	72.6	69.6	72.7	69.4	72.7	
Ara-5		67.5	64.2	67.6	64.3	67.5	64.1	67.4	64.1	
C-28				Rham	Rham	Xyl	Xyl	Ara	Ara	
-1				95.3	95.3	96.4	96.4	95.5	95.5	
-2				72.6	72.6	73.5	73.2	71.1	71.1	
-3				72.8	72.9	77.3	77.3	72.9	73.0	
-4				73.1	73.4	70.6	70.4	66.8	66.8	
-5				71.5	71.5	67.3	67.2	64.6	64.7	
-6				18.8	18.8					
C-3										
Glc-1 (inner)										105.4
Glc-2										75.0
Glc-3										76.8
Glc-4										81.0
Glc-5										76.4
Glc-6										62.1
Glc-1 (terminal)										104.9
Glc-2										74.7
Glc-3										78.2
Glc-4										71.5
Glc-5										78.4
Glc-6										62.4

Recorded on JEOL GSX-270 (67.80 MHz).

sapogenin. On the other hand, acid hydrolysis of **1** with 5% H_2SO_4 afforded glucose and arabinose in a ratio of 1 : 1. The assignment of a glycoside moiety in **1** was achieved by analysis of a detailed proton decoupling experiment and C–H COSY spectrum. For the purpose of investigating the binding site of two sugars, we obtained a nuclear Overhauser effect (NOE) difference spectra by irradiation at the frequencies of two anomeric protons. When the signal at δ 4.95, due to the H-1 of glucose, was irradiated, NOE was observed at the signal of H-16. Irradiation at frequency δ 5.28, due to the H-1 of arabinose, yielded NOE at the signal of the H-2 of glucose. Based upon the above evidence, the structure of solidagosaponin I was elucidated to be **1**.

Solidagosaponin II (**2**) revealed a $[M+Na]^+$ ion peak at *m/z* 907 and the $[M+H]^+$ ion peak at *m/z* 885. This means that its molecular weight was 884. Its analysis data was consistent with $C_{47}H_{72}O_{17}\cdot 2H_2O$. The ^{1}H- and ^{13}C-NMR spectra of **2** were similar to those of **1**, except for the presence of an ester moiety. The ^{1}H-NMR data due to the ester moiety was observed at δ 1.48 (3H, d, $J=6$ Hz), 4.64 (1H, m), 2.76 (1H, dd, $J=15$, 5 Hz) and 2.88 (1H, dd, $J=15$, 8 Hz). Judging from these and the ^{13}C-NMR data (Table I), we assumed that the ester moiety was β-hydroxy butyrate. The ^{1}H-NMR spectrum of an authentic β-hydroxy butyric acid showed signals at δ 1.39 (3H, d, $J=6$ Hz), 4.55 (1H, m), 2.68 (1H, dd, $J=15$, 5.5 Hz) and 2.79 (1H, dd, $J=15$, 7.5 Hz). This data supported our assumption. The location of β-hydroxy butyrate was determined to be at C-4 of the arabinose moiety by ^{13}C-NMR analysis; because of acylation,[8] the C-4 signal of the arabinose moiety shifted down-field by 3.1 ppm compared with that of **1**, while the neighboring C-3 and C-5 signals were shifted up-field by 2.1 and 3.3 ppm, respectively. Therefore, the structure of solidagosaponin II was elucidated to be **2**.

Solidagosaponins III (**3**), V (**5**) and VII (**7**), on acid hydrolysis, gave rhamnose, xylose and arabinose, respectively, together with common monosaccharides (glucose and arabinose). According to the ^{1}H- and ^{13}C-NMR spectra of **3**, **5** and **7**, these three saponins were found to contain the same partial structure as **1** and to have one more sugar than **1**. The above evidence indicated that **3**, **5** and **7** consisted of **1** plus rhamnose, **1** plus xylose and **1** plus arabinose, respectively. Three reasons confirmed that the binding site of each sugar was at the C-28 of the aglycone. First, anomeric proton signals [**3**: δ 6.76 (br s), **5**: 6.24 (d, $J=7$ Hz) and **7**: 6.40 (d, $J=3.5$ Hz)] shifted relatively down-field. Second, anomeric carbon signals [**3**: δ 95.3, **5**: 96.4 and **7**: 95.5] appeared at a higher field than usual. Third, carbon signals due to the C-28 of sapogenin [**3**:δ 175.5, **5**: 175.9 and **7**: 175.9] were displaced up-field, compared with the C-28 signal of **1** (δ 179.6). These three shifts were characteristic of ester-type-glycoside linkage. Thus, the structures of solidagosaponins III, V and VII were determined to be **3**, **5** and **7**, respectively.

Solidagosaponins IV (**4**), VI (**6**) and VIII (**8**), on acid hydrolysis, afforded the same monosaccharides as **3**, **5** and **7**, respectively (**4**: Glc, Ara, Ram, **6**: Glc, Ara, Xyl and **8**: Glc, 2 × Ara). The ^{1}H- and ^{13}C-NMR spectra of **4**, **6** and **8** remarkably resembled those of **3**, **5** and **7**, respectively, except for the existence of an ester moiety. The ^{1}H- and ^{13}C-NMR data due to the ester moiety of **4**, **6** and **8** were similar to those of **2**. Moreover, acylation shifts were observed at C-4 of each arabinose attaching to C-2 of the respective glucoses. This data suggested that **4**, **6** and **8** had β-hydroxy butyrate which linked to the C-4 of the arabinose moiety as **2** did. Therefore, the structure of solidagosaponins IV, VI and VIII were characterized as **4**, **6** and **8**, respectively.

Solidagosaponin IX (**9**) yielded only glucose as a sugar moiety on acid hydrolysis. The ^{13}C-NMR spectrum of **9** showed two anomeric carbon signals at δ 105.4 and 104.9. Namely, **9** had two glucose units. All of the alycone carbon signals of **9** were almost superimposable on those of **1b**, which meant that **9** had the same aglycone as **1**—**8**. In order to determine the sugar sequence and the position of the sugar linkage, a differentiating NOE spectral experiment was employed. When the signals at δ 5.09 and 5.16 (two anomeric protons of each glucose) were irradiated, NOEs were observed at signals due to the H-3 of the aglycone and the H-4 of glucose, respectively. This experiment made it clear that the glucose (1 → 4) glucose unit attached to the C-3 of polygalacic acid. Thus, the structure of solidagosaponin IX was elucidated to be **9**.

The anomeric configurations of arabinose which belongs to the C-16 sugar chain, glucose and xylose in these saponins, were determined to be α, β and β, respectively, from the *J* values of its anomeric proton signals.

As far as we know, solidagosaponins I—VIII (**1**—**8**) represent the first examples of saponins whose sugar chain attached to C-16 of the aglycone. Moreover, solidagosaponins II, IV, VI and VIII (**2**, **4**, **6** and **8**, respectively) are original saponins possessing β-hydroxy butyrate.

Experimental

General Procedures ^{1}H- and ^{13}C-NMR spectra were obtained with a JOEL GSX-270 and GSX-500 FT NMR, and chemical shifts were given in ppm with tetramethylsilane as an internal standard. FAB-MS was recorded on a JOEL JMS-SX102 mass spectrometer. Optical rotations were measured with a JASCO DIP-360 Digital Polarimeter. Gas chromatography (GC) was run on a HITACHI G-3000 Gas Chromatograph. Semi-preparative HPLC was carried out on a column of YMC ODS-7 (20 mm × 25 cm) and Develosil PhA-7 (Phenyl Alkyl) (20 mm × 25 cm).

Extraction and Isolation *Solidago virga-aurea* L. was collected in Shizuoka, Japan in October, 1989. The fresh whole plants (*ca.* 17 kg) were extracted twice with hot water. The extract was passed through a Diaion HP-20 column. After the content of the column was washed with water, the absorbed materials were eluted with 50% methanol and 100% methanol successively. The 100% methanol eluate (113 g) was rechromatographed on silica gel with $CHCl_3$–MeOH–AcOEt–H_2O (35 : 25 : 35 : 15) to give three fractions, frs. 1—3. Fraction 2 (53 g) was subjected to rechromatography on silica gel with $CHCl_3$–MeOH–AcOEt–H_2O (40 : 20 : 37 : 3) to afford 17 fractions, frs. A—Q. Fraction G (780 mg) was chromatographed on an ODS packed column with 20, 22.5, 25, 27.5 and 30% CH_3CN to give 22 fractions, frs. 1′—22′. Compound **9** was obtained from fr. 17′ by semi-preparative HPLC [ODS-7, 55% MeOH]. Fraction H (3.5 g) was chromatographed on a Silica gel (Fuji Gel, 2061) column with $CHCl_3$–MeOH–AcOEt–H_2O (40 : 20 : 37 : 3) to give six fractions, frs. a—f. Chromatography of fr. c (800 mg) on a medium pressure ODS packed column with 60% MeOH and semi-preparative HPLC [ODS-7, 27.5% CH_3CN] afforded **1** (287 mg) and **2** (185 mg). Repeated chromatography of fr. e (1.749 g) on ODS-7 and PhA column yielded **3** (51 mg), **4** (51 mg), **5** (17 mg), **6** (13 mg), **7** (11 mg) and **8** (15 mg).

Solidagosaponin I (**1**): Amorphous powder, $[\alpha]_D^{18}$ +6.9° ($c=0.97$, MeOH). *Anal.* Calcd for $C_{41}H_{66}O_{15}\cdot 2H_2O$: C, 58.99; H, 8.44. Found: C, 58.73; H, 8.26. FAB-MS *m/z*: 821 $(M+Na)^+$, 799 $(M+H)^+$. ^{1}H- and ^{13}C-NMR: Tables I—IV.

Solidagosaponin II (**2**): Amorphous powder, $[\alpha]_D^{18}$ +24.3° ($c=1.51$, MeOH). *Anal.* Calcd for $C_{45}H_{72}O_{17}\cdot 2H_2O$: C, 58.68; H, 8.32. Found: C, 58.86; H, 8.05. FAB-MS *m/z*: 907 $(M+Na)^+$, 885 $(M+H)^+$. ^{1}H- and ^{13}C-NMR: Tables I—IV.

TABLE III. ^{1}H-NMR Spectral Data of Aglycone and Ester Moieties in C_5D_5N

Proton No.	1c	1	2	3	4
Aglycone moiety					
2	4.55 (1H, dd, J=4, 3 Hz)	4.48 (1H, dd, J=4, 3 Hz)	4.52 (1H, dd, J=4, 3 Hz)	4.50 (1H, dd, J=4, 3 Hz)	4.53 (1H, dd, J=4, 3 Hz)
3	4.28 (1H, d, J=4 Hz)	4.18 (1H, d, J=3.5 Hz)	4.22 (1H, d, J=3.5 Hz)	4.23 (1H, d, J=3.5 Hz)	4.25 (1H, d, J=3 Hz)
12	5.53 (1H, t-like)	5.57 (1H, t-like)	5.62 (1H, t-like)	5.60 (1H, t-like)	5.62 (1H, t-like)
16	5.15 (1H, br s)	5.39 (1H, br s)	5.36 (1H, br s)	5.31 (1H, br s)	5.23 (1H, br s)
18	3.36 (1H, dd, J=14, 4 Hz)	3.53 (1H, dd, J=14, 4 Hz)	3.58 (1H, dd, J=14, 4 Hz)	3.42 (1H, dd, J=14, 4 Hz)	3.43 (1H, dd, J=14, 4 Hz)
19	2.65 (1H, t, J=14 Hz)	2.89 (1H, t, J=14 Hz)	2.92 (1H, t, J=13.5 Hz)	2.86 (1H, t, J=14 Hz)	2.85 (1H, t, J=14 Hz)
23	3.76 (1H, d, J=11 Hz)	3.68 (1H, d, J=11 Hz)	3.70 (1H, d, J=11 Hz)	3.71 (1H, d, J=10 Hz)	3.72 (1H, d, J=10 Hz)
23	4.19 (1H, d, J=11 Hz)	4.11 (1H, d, J=11 Hz)	4.15 (1H, d, J=11 Hz)	4.15 (1H, d, J=10 Hz)	4.17 (1H, d, J=10 Hz)
24	1.40 (3H, s)	1.33 (3H, s)	1.36 (3H, s)	1.37 (3H, s)	1.39 (3H, s)
25	1.66 (3H, s)	1.55 (3H, s)	1.60 (3H, s)	1.64 (3H, s)	1.67 (3H, s)
26	0.94 (3H, s)	1.03 (3H, s)	1.06 (3H, s)	1.00 (3H, s)	1.06 (3H, s)
27	1.82 (3H, s)	1.77 (3H, s)	1.77 (3H, s)	1.74 (3H, s)	1.74 (3H, s)
29	0.74 (3H, s)	1.14 (3H, s)	1.10 (3H, s)	1.03 (3H, s)	1.09 (3H, s)
30	1.02 (3H, s)	1.14 (3H, s)	1.14 (3H, s)	1.10 (3H, s)	1.00 (3H, s)
OMe	3.66 (3H, s)				
Ester moiety					
2			2.76 (1H, dd, J=15, 5 Hz)		2.70 (1H, dd, J=15, 5.5 Hz)
2			2.88 (1H, dd, J=15, 8 Hz)		2.82 (1H, dd, J=15, 8 Hz)
3			4.64 (1H, m)		4.62 (1H, m)
4			1.48 (3H, d, J=6 Hz)		1.46 (3H, d, J=6 Hz)

Recorded on JEOL GSX-500 (500 MHz). *a*) Obscured by other signals; therefore, couplings could not be accurately determined.

TABLE IV. ^{1}H-NMR Spectral Data of Sugar Moieties in C_5D_5N

Proton No.	1c	1	2	3	4
Sugar moiety					
C-16					
Glc-1	4.94 (1H, d, J=8 Hz)	4.95 (1H, d, J=8 Hz)	4.91 (1H, d, J=8 Hz)	4.91 (1H, d, J=8 Hz)	4.85 (1H, d, J=8 Hz)
Glc-2	4.04 (1H, t, J=8.5 Hz)	4.17 (1H, t, J=9 Hz)	4.29 (1H, t, J=8.5 Hz)	4.16 (1H, t, J=8 Hz)	4.23 (1H, t, J=8 Hz)
Glc-3	4.31 (1H, t, J=8.5 Hz)	4.40 (1H, t, J=9 Hz)	4.42 (1H, t, J=9 Hz)	4.36 (1H, t, J=9 Hz)	4.37 (1H, t, J=9 Hz)
Glc-4	4.29 (1H, t, J=9 Hz)	4.17 (1H, t, J=9 Hz)	4.16 (1H, t, J=10 Hz)	4.18 (1H, t, J=9 Hz)	4.16 (1H, t, J=9 Hz)
Glc-5	4.02 (1H, m)	3.96 (1H, m)	3.96 (1H, m)	3.87 (1H, m)	3.86 (1H, m)
Glc-6	4.40 (1H, dd, J=11, 5 Hz)	4.32 (1H, dd, J=12, 5.5 Hz)	4.33 (1H, dd, J=12.5, 3.5 Hz)	4.33 (1H, dd, J=12, 5.5 Hz)	4.38[a]
Glc-6	4.59 (1H, dd, J=11, 2 Hz)	4.54 (1H, dd, J=12, 2 Hz)	4.57 (1H, dd, J=12.5, 2 Hz)	4.58 (1H, dd, J=12, 3 Hz)	4.57[a]
Ara-1		5.28 (1H, d, J=8 Hz)	5.49 (1H, d, J=8 Hz)	5.26 (1H, d, J=8 Hz)	5.55 (1H, d, J=8 Hz)
Ara-2		4.45 (1H, t, J=8 Hz)	4.34 (1H, t, J=8.5 Hz)	4.46 (1H, t, J=8 Hz)	4.32 (1H, t, J=8 Hz)
Ara-3		4.11 (1H, dd, J=9, 3.5 Hz)	4.20 (1H, dd, J=9, 3.5 Hz)	4.11 (1H, dd, J=9.5, 3.5 Hz)	4.19 (1H, dd, J=9, 3.5 Hz)
Ara-4		4.22 (1H, br s)	5.48 (1H, br s)	4.20 (1H, br s)	5.50 (1H, br d, J=2 Hz)
Ara-5		3.65 (1H, d, J=12 Hz)	3.62 (1H, d, J=13 Hz)	3.65 (1H, d, J=12 Hz)	3.62 (1H, d, J=13 Hz)
Ara-5		4.24 (1H, br d, J=12 Hz)	4.27 (1H, br d, J=12 Hz)	4.23 (1H, br d, J=12 Hz)	4.22 (1H, br d, J=13 Hz)
C-28				Rham	Rham
-1				6.76 (1H, br s)	6.77 (1H, br s)
-2				4.56[a]	4.56[a]
-3				4.57[a]	4.57[a]
-4				4.36 (1H, t, J=9 Hz)	4.36 (1H, t, J=9 Hz)
-5				4.43 (1H, m)	4.43 (1H, m)
-5					
-6				1.71 (3H, d, J=6 Hz)	1.72 (3H, d, J=6 Hz)
C-3 (inner)					
Glc-1					
Glc-2					
Glc-3					
Glc-4					
Glc-5					
Glc-6					
Glc-6 (terminal)					
Glc-1					
Glc-2					
Glc-3					
Glc-4					
Glc-5					
Glc-6					
Glc-6					

Recorded on JEOL GSX-500 (500 MHz). *a*) Obscured by other signals; therefore, couplings could not be accurately determined.

Proton No.	5	6	7	8	9
Aglycone moiety					
2	4.49[a]	4.51[a]	4.50[a]	4.50[a]	4.74 (1H, dd, J=4, 3 Hz)
3	4.24[a]	4.20 (1H, d, J=3 Hz)	4.22 (1H, d, J=3.5 Hz)	4.19 (1H, d, J=3.5 Hz)	4.27 (1H, d, J=3 Hz)
12	5.60 (1H, t-like)	5.62 (1H, t-like)	5.59 (1H, t-like)	5.61 (1H, t-like)	5.65 (1H, t-like)
16	5.46 (1H, br s)	5.40 (1H, br s)	5.48 (1H, br s)	5.39 (1H, br s)	5.22 (1H, br s)
18	3.54 (1H, dd, J=14, 4 Hz)	3.56 (1H, dd, J=14.5, 4 Hz)	3.56 (1H, dd, J=13.5, 4 Hz)	3.55 (1H, dd, J=14, 4 Hz)	3.61 (1H, dd, J=14, 3 Hz)
19	2.89 (1H, t, J=14 Hz)	2.90 (1H, t, J=14 Hz)	2.90 (1H, t, J=13.5 Hz)	2.87 (1H, t, J=14 Hz)	2.80 (1H, t, J=14 Hz)
23	3.71 (1H, d, J=10 Hz)	3.70 (1H, d, J=10 Hz)	3.70 (1H, d, J=10 Hz)	3.68 (1H, d, J=11 Hz)	3.66 (1H, d, J=10 Hz)
23	4.15 (1H, d, J=10 Hz)	4.16 (1H, d, J=10 Hz)	4.20[a]	4.11 (1H, d, J=11 Hz)	4.32 (1H, d, J=10 Hz)
24	1.36 (3H, s)	1.38 (3H, s)	1.37 (3H, s)	1.36 (3H, s)	1.33 (3H, s)
25	1.61 (3H, s)	1.64 (3H, s)	1.61 (3H, s)	1.61 (3H, s)	1.58 (3H, s)
26	1.15 (3H, s)	1.17 (3H, s)	1.09 (3H, s)	1.09 (3H, s)	1.11 (3H, s)
27	1.77 (3H, s)	1.76 (3H, s)	1.77 (3H, s)	1.75 (3H, s)	1.81 (3H, s)
29	1.12 (3H, s)	1.08 (3H, s)	1.13 (3H, s)	1.07 (3H, s)	1.04 (3H, s)
30	1.09 (3H, s)	1.07 (3H, s)	1.12 (3H, s)	1.11 (3H, s)	1.17 (3H, s)
OMe					
Ester moiety					
2		2.72 (1H, dd, J=14.5, 5 Hz)		2.72 (1H, dd, J=15, 5.5 Hz)	
2		2.82 (1H, dd, J=14.5, 8 Hz)		2.84 (1H, dd, J=15, 8 Hz)	
3		4.62 (1H, m)		4.60 (1H, m)	
4		1.46 (3H, d, J=6 Hz)		1.46 (3H, d, J=6 Hz)	

Proton No.	5	6	7	8	9
Sugar moiety					
C-16					
Glc-1	4.90 (1H, d, J=8 Hz)	4.83 (1H, d, J=8 Hz)	4.92 (1H,d, J=8 Hz)	4.84 (1H, d, J=8 Hz)	
Glc-2	4.20[a]	4.23 (1H, t, J=8.5 Hz)	4.19 (1H, t, J=8 Hz)	4.21 (1H, t, J=8 Hz)	
Glc-3	4.36 (1H, t, J=9 Hz)	4.34 (1H, t, J=9 Hz)	4.35 (1H, t, J=9 Hz)	4.34 (1H, t, J=9 Hz)	
Glc-4	4.18[a]	4.17[a]	4.16 (1H, t, J=9 Hz)	4.10 (1H, t, J=9 Hz)	
Glc-5	3.81 (1H, m)	3.80 (1H, m)	3.81 (1H, m)	3.81 (1H, m)	
Glc-6	4.29 (1H, dd, J=12, 5.5 Hz)	4.15[a]	4.25 (1H, dd, J=12.5, 3 Hz)	4.24[a]	
Glc-6	4.48[a]	4.49[a]	4.50[a]	4.46[a]	
Ara-1	5.29 (1H, d, J=7 Hz)	5.47 (1H, d, J=8 Hz)	5.28 (1H, d, J=7 Hz)	5.41 (1H, d, J=7.5 Hz)	
Ara-2	4.47 (1H, d, J=7.5 Hz)	4.30 (1H, t, J=8 Hz)	4.47 (1H, dd, J=9, 7 Hz)	4.30 (1H, dd, J=9, 8 Hz)	
Ara-3	4.11 (1H, dd, J=9.5, 3.5 Hz)	4.19[a]	4.12 (1H, dd, J=9.5, 3 Hz)	4.18 (1H, dd, J=9, 3.5 Hz)	
Ara-4	4.20[a]	5.48 (1H, br s)	4.20[a]	5.47 (1H, br s)	
Ara-5	3.66 (1H, d, J=12 Hz)	3.61 (1H, d, J=12.5 Hz)	3.67 (1H, d, J=12 Hz)	3.61 (1H, d, J=13 Hz)	
Ara-5	4.25 (1H, dd, J=12, 2 Hz)	4.24[a]	4.25 (1H, br d, J=12 Hz)	4.23[a]	
C-28	Xyl	Xyl	Ara	Ara	
-1	6.24 (1H, d, J=7 Hz)	6.24 (1H, d, J=6.5 Hz)	6.40 (1H, d, J=3.5 Hz)	6.36 (1H, d, J=4 Hz)	
-2	4.20[a]	4.18[a]	4.52 (1H, t, J=3.5 Hz)	4.55 (1H, t, J=4.5 Hz)	
-3	4.20[a]	4.20[a]	4.49[a]	4.47[a]	
-4	4.18[a]	4.17[a]	4.58[a]	4.55 (1H, br s)	
-5	3.82 (1H, dd, J=12, 9 Hz)	3.82 (1H, dd, J=12, 8.5 Hz)	3.96 (1H, dd, J=11, 3 Hz)	3.94 (1H, dd, J=12, 3 Hz)	
-5	4.39 (1H, dd, J=12, 5 Hz)	4.39 (1H, dd, J=12, 5 Hz)	4.42[a]	4.51 (1H,d, J=12 Hz)	
-6					
C-3					
(inner)					
Glc-1					5.09 (1H, d, J=8 Hz)
Glc-2					3.99 (1H, t, J=8.5 Hz)
Glc-3					4.18 (1H, t, J=9 Hz)
Glc-4					4.29 (1H, t, J=9 Hz)
Glc-5					3.85 (1H, m)
Glc-6					4.37 (1H, dd, J=12, 2 Hz)
Glc-6					4.49 (1H, br d, J=12 Hz)
(terminal)					
Glc-1					5.16 (1H, d, J=8 Hz)
Glc-2					4.06 (1H, t, J=8.5 Hz)
Glc-3					4.18 (1H, t, J=9 Hz)
Glc-4					4.16[a]
Glc-5					3.97[a]
Glc-6					4.27[a]
Glc-6					4.49 (1H, br d, J=12 Hz)

Solidagosaponin III (**3**): Amorphous powder, $[\alpha]_D^{18}$ −9.2° (c=0.85, MeOH). *Anal.* Calcd for $C_{47}H_{76}O_{19}\cdot 9/2H_2O$: C, 55.01; H, 8.35. Found: C, 55.14; H, 8.08. FAB-MS m/z: 967 $(M+Na)^+$. ^{1}H- and ^{13}C-NMR: Tables I—IV.

Solidagosaponin IV (**4**): Amorphous powder, $[\alpha]_D^{18}$ +18.3° (c=0.51, MeOH). *Anal.* Calcd for $C_{51}H_{82}O_{21}\cdot 5H_2O$: C, 54.63; H, 8.27. Found: C, 54.89; H, 8.12. FAB-MS m/z: 1054 $(M+Na)^+$. ^{1}H- and ^{13}C-NMR: Tables I—IV.

Solidagosaponin V (**5**): Amorphous powder, $[\alpha]_D^{18}$ −8.6° (c=0.76, MeOH). *Anal.* Calcd for $C_{46}H_{74}O_{19}\cdot 7/2H_2O$: C, 55.58; H, 8.21. Found: C, 55.43; H, 8.08. FAB-MS m/z: 953 $(M+Na)^+$, 931 $(M+H)^+$. ^{1}H- and ^{13}C-NMR: Tables I—IV.

Solidagosaponin VI (**6**): Amorphous powder, $[\alpha]_D^{18}$ +6.1° (c=0.99, MeOH). *Anal.* Calcd for $C_{50}H_{80}O_{21}\cdot 2H_2O$: C, 57.0; H, 8.04. Found: C, 57.16; H, 8.03. FAB-MS m/z: 1039 $(M+Na)^+$, 1017 $(M+H)^+$. ^{1}H- and ^{13}C-NMR: Tables I—IV.

Solidagosaponin VII (**7**): Amorphous powder, $[\alpha]_D^{18}$ −2.0° (c=0.93, MeOH). *Anal.* Calcd for $C_{46}H_{74}O_{19}\cdot 4H_2O$: C, 55.08; H, 8.24. Found: C, 55.31; H, 8.12. FAB-MS m/z: 953 $(M+Na)^+$, 931 $(M+H)^+$. ^{1}H- and ^{13}C-NMR: Tables I—IV.

Solidagosaponin VIII (**8**): Amorphous powder, $[\alpha]_D^{18}$ +9.1° (c=1.35, MeOH). *Anal.* Calcd for $C_{50}H_{80}O_{21}\cdot 2H_2O$: C, 57.02; H, 8.04. Found: C, 57.23; H, 7.82. FAB-MS m/z: 1039 $(M+Na)^+$, 1017 $(M+H)^+$. ^{1}H- and ^{13}C-NMR: Tables I—IV.

Solidagosaponin IX (**9**): Amorphous powder, $[\alpha]_D^{18}$ +8.8° (c=1.01, MeOH). *Anal.* Calcd for $C_{42}H_{68}O_{16}\cdot 3H_2O$: C, 57.13; H, 8.45. Found: C, 57.15; H, 8.34. FAB-MS m/z: 851 $(M+Na)^+$, 829 $(M+H)^+$. ^{1}H- and ^{13}C-NMR: Tables I—IV.

Acid Hydrolysis of 1—9 Compound **1** (*ca.* 0.2 mg) was heated at 100 °C with 3 drops of 5% H_2SO_4 and 3 drops of dioxane for 1 h. The reaction mixture was diluted with H_2O and passed through an Amberlite IR-45 column. The eluate was concentrated to give a residue, which was reduced with $NaBH_4$ (*ca.* 1 mg) in water (0.2 ml) for 1 h at room temperature and passed through an Amberlite IR-120 column. The eluate was concentrated to dryness under reduced pressure and then the reaction mixture was heated at 100 °C with acetic anhydride (2 drops) and pyridine (2 drops) for 1 h. The acetylated mixture was subjected to GC, which revealed two peaks for the derivatives of arabinose and glucose (1 : 1, respectively). Acid hydrolysis of **2**—**8** and **9** was performed by the same method used for **1**, and the sugar components of each saponin were confirmed by the same method employed for **1**. GC conditions: column, Supelco SP-2380 capillary column (0.25 mm × 30 m); column temperature, 250 °C; carrier gas, N_2; t_R, glucitol acetate, 11.8 min; arabinitol acetate, 6.5 min; rhamnitol acetate, 5.0 min; xylitol acetate, 7.3 min.

Methylation and Mild Methanolysis of 1 Compound **1** (14 mg) was dissolved in MeOH (1 ml) and treated with CH_2N_2–ether (5 ml) at room temperature for 1 h. The reaction mixture was concentrated to give **1a**. Compound **1a** (14 mg) was refluxed with AcCl–MeOH (1 : 10) (5 ml) for 7 h and the reagents were evaporated to afford a residue, which was subjected to HPLC [ODS-7: 50% CH_3CN] to give **1b** (2.6 mg) and **1c** (1 mg). **1b**: amorphous powder, $[\alpha]_D^{18}$ +42.3° (c=0.26, MeOH). ^{1}H-NMR (C_5D_5N): 0.99 (3H, s, H_3-26), 1.00 (3H, s, H_3-30), 1.10 (3H, s, H_3-29), 1.40 (3H, s, H_3-24), 1.68 (3H, s, H_3-25), 1.76 (3H, s, H_3-27), 2.76 (1H, t, J=14 Hz, H-19), 3.41 (1H, dd, J=14, 4 Hz, H-18), 3.70 (3H, s, OMe), 3.72 (1H, d, J=11 Hz, H-23), 4.17 (1H, d, J=11 Hz, H-23), 4.28 (1H, d, J=4 Hz, H-3), 4.55 (1H, dd, J=4, 3 Hz, H-2), 5.03 (1H, br s, H-16), 5.58 (1H, t-like, H-12). ^{13}C-NMR: Table I. **1c**: amorphous powder, $[\alpha]_D^{18}$ 0° (c=0.10, MeOH). FAB-MS m/z: 703 $(M+Na)^+$. ^{1}H- and ^{13}C-NMR: Tables I—IV.

Acknowledgment We are grateful to the staff of the Central Analytical Laboratory of this university for elemental analysis and measurement of MS.

References

1) H. Mitsuhashi (ed.), "Illustrated Medical Plants of the World in Colour," 1st, Hokuryukan, Tokyo, 1988, p. 575.
2) K. Hiller, G. Dube and D. Zeigan, *Pharmazie*, **40**, 795 (1985).
3) K. Hiller and G. Fotsh, *Pharmazie*, **41**, 415 (1986).
4) A. Goswami, R. N. Barua, R. P. Sharma, J. N. Baruah, P. Kulanthaivel and W. Herz, *Phytochemistry*, **23**, 837 (1984).
5) K. Hiller, G. Bader and H. R. Schulten, *Pharmazie*, **42**, 541 (1987).
6) Y. Asada, T. Ueoka and T. Furuya, *Chem. Pharm. Bull.*, **37**, 2139 (1989).
7) H. Ishii, K. Tori, T. Tozyo and Y. Yoshimura, *J. Chem. Soc., Perkin Trans. 1*, **1981**, 1928.
8) O. Tanaka, *Yakugaku Zasshi*, **105**, 323 (1985).

Chem. Pharm. Bull. **39**(8) 2043—2045 (1991)

Transfructosylation of Rebaudioside A (a Sweet Glycoside of *Stevia* Leaves) with *Microbacterium* β-Fructofuranosidase

Hiroshi ISHIKAWA,[a] Sumio KITAHATA,*[,b] Kazuhiro OHTANI[c] and Osamu TANAKA[c]

Hokkaido Sugar Co., Ltd.,[a] 2–1 Jinbocho, Kanda, Chiyoda-ku, Tokyo 101, Japan, Osaka Municipal Technical Research Institute,[b] 1–6–50 Morinomiya, Jyoto-ku, Osaka 536, Japan and Institute of Pharmaceutical Sciences, Hiroshima University School of Medicine,[c] Kasumi, Minami-ku, Hiroshima 734, Japan. *Received February 8, 1991*

It was found that a β-fructofuranosidase produced by *Microbacterium* sp. H-1 has potent trans-β-fructofuranosylation activity from sucrose (donor). By means of this enzyme system, rebaudioside A (RA), the second major sweet steviol glycoside of the leaves of *Stevia rebaudiana*, was subjected to transfructosylation, affording a mono-β-fructofuranosylated product (RA-F) in a high yield. The structure of RA-F was elucidated as β-D-fructofuranosyl-(2→6)-β-D-glucopyranosyl ester of steviol-13-*O*-[β-D-glucopyranosyl-(1→2)]-[β-D-glucopyranosyl-(1→3)]-β-D-glucopyranoside. Some improvement in the quality of sweetness was observed for RA-F.

Keywords rebaudioside A; *Stevia rebaudiana*; sweet natural glycoside; trans-β-fructofuranosylation; β-fructofuranosidase; *Microbacterium* sp. H-1; β-fructofuranosyl-rebaudioside A; steviol glycoside

Introduction

Stevioside (S),[1] the major sweet steviol glycoside from the leaves of *Stevia rebaudiana* BERTONI (Compositae) is commercially used as a low calorie sweetener in Japan. Several related sweet steviol glycosides called rebaudiosides-A (RA),[2] -C[3] (=dulcoside B[4]), -D, and -E[5] and dulcoside A[4] were also isolated from the leaves of this plant. Of these, RA which is the second most plentiful sweet glycoside of the leaves, has greater sweetness than S, and is now commercially utilized as a good sweetener in Japan.

To further improve the sweetness, enzymic glycosylation of S and its congeners has been extensively studied by our group. It has been reported that the 1,4-α-transglucosylation of S with soluble starch and cyclomaltodextrin glucanotransferase (CGTase) resulted in improvement of the taste[6] and a mixture of the glucosylated products (so-called glucosylstevioside) is now commercially used as a better sweetener than S. In this enzymic reaction, 1,4-α-glucosylation occurs to both the 13-*O*-β-sophorosyl and 19-*O*-β-glucosyl moieties of S, affording a complex mixture. We recently succeeded in the separation of all of the mono-, di- and tri-glucosylated products from this complex mixture and evaluated the sweetness of each product.[7] Rubusoside (desglucostevioside, RU),[8] the major sweet component from leaves of *Rubus suavissimus* S. LEE (Rosaceae) growing in Southern China, was also subjected to transglucosylation by the CGTase system, and separation and sweetness evaluation of the mono-, di-,[9] tri- and tetra-[10] glucosylated products were achieved. Based on these results, the structure–sweetness relationship of these steviol glycosides was investigated, disclosing that the glucosylation of the 13-*O*-glycosyl chain led to increased sweetness. It has been reported that a galactosyl group is not an efficient acceptor for the 1,4-α-transglucosylation by CGTase.[11] Selective elongation of the 13-*O*-glycosyl moiety of S or RU for production of the superior sweeteners was established by means of the chemical[12] or enzymic[10,13] protection of 19-*O*-glycosyl moiety with a β-galactosyl group against CGTase glucosylation.

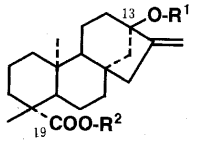

	R^1	R^2
S	-β-D-Glc^{2}—β-D-Glc	-β-D-Glc
RA	-β-D-Glc^{2}(β-D-Glc, ^{3}β-D-Glc)	-β-D-Glc
RA-F	-β-D-Glc^{2}(β-D-Glc, ^{3}β-D-Glc)	-β-D-Glc^{6}^{2}β-D-Fru
RU	-β-D-Glc	-β-D-Glu
S-F	-β-D-Glc^{2}—β-D-Glc	-β-D-Glc^{6}^{2}β-D-Fru
R-B	-β-D-Glc^{2}(β-D-Glc, ^{3}β-D-Glc)	-H

Chart 1

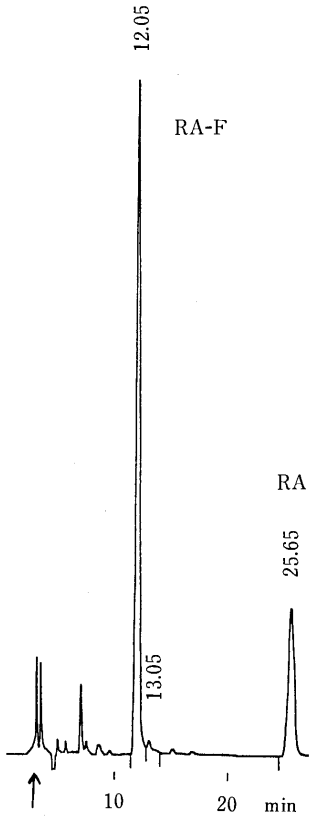

Fig. 1. High Performance Liquid Chromatogram of Trans-β-fructofuranosylation Products [on ODS-Column with CH_3CN–H_2O (31 : 69)]

TABLE I. Influence of Concentration of RA and Reaction Time on Yield of RA-F

Conc. of RA (M)	Yield (%) of RA-F			
	Reaction time (h)			
	0.5	1.0	3.0	21.0
0.025	79	82	81	50
0.05	55	67	75	60
0.1	45	58	54	36
0.5	11	16	19	19

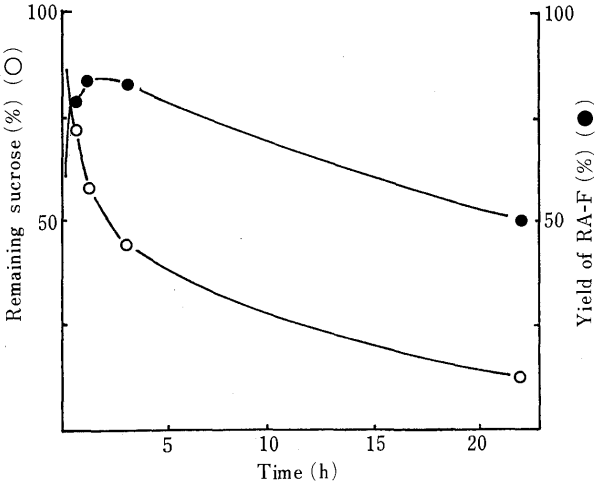

Fig. 2. Time Course of Trans-β-fructosylation (0.025 M RA)

Very recently, it was found that treatment of S or RU with sucrose and β-fructofuranosidase from *Arthrobacter* sp. K-1 afforded the corresponding product by β- fructofuranosylation at 6-hydroxyl group of the 19-*O*-β-glucosyl moiety in high yield.[14] It was also revealed that, by this fructosylation, the character of taste of both S and RU was greatly improved in every respect. Especially, the fructosylated stevioside (S-F) was proved to be more delicious than RA, being almost equivalent to aspartame, a flavorful synthetic dipeptide-sweetener. As a continuation of the studies on enzymic glycosylation of steviol glycosides, the present paper reports the enzymic fructosylation of RA.

Results and Discussion

It was found that β-fructofuranosidase (FFase) produced by a bacterium isolated from soil exhibited potent trans-β-fructofuranosylation activity from sucrose (donor); this is described more fully in Experimental. A solution of RA, sucrose and the FFase in phosphate buffer (pH 6.5) was incubated at 40 °C for 2 h. The products were chromatographed on a Diaion HP-20 column with water and then methanol. The methanolic eluate was subjected to high performance liquid chromatography (HPLC) on a reverse phase (ODS) column to give a fructosylated product (RA-F).

Compound RA-F, $C_{44}H_{70}O_{23}$ (from elemental analysis and fast atom bombardment mass spectrum (FAB-MS)), afforded fructose and glucose on acid hydrolysis. Comparison of the ^{13}C-nuclear magnetic resonance (^{13}C-NMR) spectrum of RA-F with that of RA indicated that one β-fructofuranoside unit was introduced to RA. Alkaline saponification of the esteric glycosyl linkage at 19-carboxyl group of RA-F gave rebaudioside B (RB)[2] which had already been obtained from RA by alkaline saponification. This indicated that the fructosylation occurred not at the 13-*O*-glycosyl moiety but at the 19-*O*-glucosyl moiety. Methylation analysis of RA-F demonstrated the presence of 6-linked glucopyranosyl and 2,3-linked glucopyranosyl units together with terminal fructofuranosyl and glucopyranosyl units, proving that the fructosylation occurred at 6-hydroxyl group of the 19-*O*-glucosyl moiety. It follows that RA-F can be formulated as illustrated in Chart 1.

The yield of transglycosylation with glycosidases essentially depends upon the concentrations of acceptor, donor and enzyme as well as the reaction time. By means of HPLC analysis (Fig. 1), the influence of the reaction time and the concentration of the acceptor (RA) on the yield of RA-F was investigated. As summarized in Table I and Fig. 2, RA-F was more efficiently produced at relatively lower concentration of RA and the yield was decreased with increased RA concentration. It was also found that the maximum yield was obtained at the early stage of the reaction and prolonged reaction resulted in lowered yield of RA-F owing to enzymic hydrolysis of the fructosyl linkage of RA-F. The maximum yield, 82%, was obtained by the reaction at a concentration of 0.025 M RA for 1 h. The yield of RA-F at the concentration of 0.5 M RA for 21 h was only 19%.

The intensity and quality of sweetness of RA-F were compared with those of RA and a commercial glucosyl-stevioside (*vide supra*) as summarized in Table II (see Experimental). In this fructosylation, some decrease of bitterness and an increase in tastiness over RA were observed, although the aftertaste of RA-F was somewhat stronger than RA. The intensity of sweetness of RA-F was found to be similar to that of RA. As mentioned, remarkable improvement in the quality of sweetness was observed for S-F, which is thus promising as a good commercial sweetener. The present results are significant for the industrial scale production of S-F from crude S which contains some RA.

Experimental

Materials and Method Rebaudioside A (RA) was purchased from Morita Kagaku Kogyo Co., Ltd., Osaka. NMR and FAB-MS spectra were recorded with a JEOL JNM GX-400 spectrometer and with a JEOL JMS SX-102 spectrometer, respectively.

Preparation of Crude FFase A bacterium, strain H-1, which was one of those isolated from soil as a fructose-transferring enzyme producer, was used in the present study. This bacterium is classified as a member of the genus *Microbacterium* by the National Collection of Industrial and Marine Bacteria, Ltd. in Scotland and tentatively called *Microbacterium* sp. H-1 by the present authors. The bacterium was cultivated in a 500 ml shaking flask containing the following medium at 28 °C for 48 h on a reciprocal shaker (110 rpm): 1% sucrose, 0.3% $NaNO_3$, 0.1% KH_2PO_4, 0.05% $MgSO_4 \cdot 7H_2O$, 0.02% $MnCl_2$ and 0.05% yeast extract (pH 7.0). The supernatant obtained by centrifuging the culture broth was salted out with 60% $(NH_4)_2SO_4$. After standing overnight at 10°C, the resulting precipitate was collected by centrifugation and dissolved in 20 mM phosphate buffer (pH 7.0), and then the solution was dialyzed against the same buffer overnight. The non-dialyzed solution was used as FFase solution.

Assay of FFase Activity A mixture of 5% sucrose solution in 50 mM phosphate buffer (pH 6.5, 200 μl) and the enzyme solution (50 μl) was incubated at 40 °C for 10 min. The released glucose was measured by an F-kit reagent (Boehringer Manheim GMBH Biochemica). One unit of FFase activity was defined as the amount of enzyme releasing 1 μmol of

glucose per minute under this condition.

Chromatography Conditions of thin layer chromatography (TLC): on Kiesel gel 60 plate (Merck Co., Ltd.); solvent system, $CHCl_3$–MeOH–H_2O (10:5:1 or 6:4:1); detection, spraying methanolic H_2SO_4 followed by heating at 110 °C. HPLC conditions for analysis of glycosides: on a column of TSK gel ODS-120T (4.6 mm i.d. × 250 mm, Tosoh Co. Ltd.); detection, ultraviolet (UV) 213 nm; mobile phase, CH_3CN–H_2O (25—30: 75—70); flow rate, 0.5 ml/min (see Fig. 1). HPLC condition for analysis of saccharides: on a column of Shimpack CLC-NH_2 (4.6 mm i.d. × 250 mm, Shimadzu Co., Ltd.); detection, refraction index; mobile phase, CH_3CN–H_2O (75:25); flow rate 0.8 ml/min.

Isolation and Properties of RA-F A solution of RA (0.05 M), sucrose (2.0 M), FFase (50 units) in 50 mM phosphate buffer (pH 6.5, final volume 31 ml) was incubated at 40 °C. The reaction process was followed by HPLC analysis of aliquots of the mixture. After 2 h, the mixture was heated at 100 °C for 15 min and chromatographed on Diaion HP-20 with H_2O and then MeOH. The MeOH eluate was separated by HPLC on TSKgel ODS 120T (21.5 mm i.d. × 30 cm) with 32% CH_3CN (flow rate: 6 ml/min) to give RA-F (800 mg) together with recovered RA.

RA-F: a white powder, $[\alpha]_D^{21}$ +68.5° (c=0.97, MeOH). Anomeric carbon signals in C_5D_5N: 13-*O*-glycosyl moiety δ: 97.9 (13-*O*-Glc), 104.5, 104.6; 19-*O*-glycosyl moiety δ: 95.8 (β-Glc), 105.7 (β-Frc). Negative FAB-MS: 1127. $[M-H]^-$. *Anal.* Calcd. for $C_{50}H_{80}O_{28}\cdot H_2O$: C, 52.35; H, 7.20. Found: C, 52.30; H, 7.09. A solution of RA-F in 8% aqueous KOH was heated at 80 °C for 1 h. The reaction mixture was acidified with 2 N HCl and extracted with 1-BuOH (saturated with H_2O). The BuOH layer was washed with H_2O and concentrated to dryness, affording RB which was identified by comparison of TLC and the ^{13}C-NMR spectrum with those of an authentic sample. Methylation analysis of RA-F was conducted by the procedure reported previously.[14]

Effect of Acceptor Concentration and Reaction Time on Formation of RA-F A solution of the FFase (0.6 units) and 2.0 M sucrose in 50 mM phosphate buffer (pH 6.5, 400 μl) was incubated in the presence of various concentrations of RA at 40 °C. After 0.5, 1.0, 3.0 and 21 h, the amounts of RA-F in the reaction mixture were determined by HPLC. The results are summarized in Table I and Fig. 2.

Sensory Evaluation Sweetness of RA-F was evaluated and compared with RA and commercial glucosyl-stevioside (*vide supra*) by human sensory panels. All samples were dissolved in water to make appropriate concentrations which corresponded to 3—5% (w/v) sucrose solutions in intensity of sweetness, and standard sucrose solutions were prepared at graduated concentrations from 3 to 6% (w/v) with intervals of 0.5%. The panelists were asked to taste a sucrose solution and estimate its total taste intensity relative to that of the sample solutions. Panelists tested each sample several times. The relative sweetness to sucrose was calculated according to the following formula.

$$\frac{\sum A/B}{\text{number of tests} \times \text{number of panelists}}$$

A, concentration (w/v, %) of sucrose solution with the same intensity of sweetness as the sample solution; B, concentration (w/v, %) of the sample solution.

The qualities of taste, aftertaste, bitterness and deliciousness were evaluated for each sample solution at a concentration corresponding to 5% (w/v) sucrose solution in intensity of sweetness and were calculated according to the following formula.

$$\frac{\sum T}{\text{number of tests} \times \text{number of panelists}}$$

T, evaluation point of each sample; 5, much better; 4, somewhat better; 3, better; 2, slightly better; 1, no good.

TABLE II. Sensory Evaluation

Compd.	Bitterness	Aftertaste	Deliciousness	Sweetness[a]
RA	4.0	4.0	2.0	198
RA-F	4.3	3.7	2.1	200
Glucosyl-stevioside[b]	3.8	3.6	1.6	53

a) Relative sweetness to sucrose. *b*) Commercial sample.

Acknowledgements We are grateful to Professor K. Yamasaki, Hiroshima University for his encouragement.

References and Notes

1) E. Mosettig, U. Beglinger, F. Dolder, H. Lichiti, P. Quitt and J. A. Waters, *J. Am. Chem. Soc.*, **85**, 2305 (1963) and references cited therein.
2) H. Kohda, R. Kasai, K. Yamasaki and O. Tanaka, *Phytochemistry*, **15**, 981 (1976).
3) I. Sakamoto, K. Yamasaki and O. Tanaka, *Chem. Pharm. Bull.*, **25**, 844 (1977).
4) M. Kobayashi, S. Horikawa, I. Degrandi, J. Ueno and H. Mitsuhashi, *Phytochemistry*, **15**, 1405 (1977).
5) I. Sakamoto, K. Yamasaki and O. Tanaka, *Chem. Pharm. Bull.*, **25**, 3437 (1977).
6) R. Kasai, N. Kaneda, O. Tanaka, K. Yamasaki, I. Sakamoto, K. Morimoto, S. Okada, S. Kitahata and H. Furukawa, *Nippon Kagakukaishi*, **1981**, 726.
7) Y. Fukunaga, T. Miyata, N. Nakayasu, K. Mizutani and O. Tanaka, *Agric. Biol. Chem.*, **53**, 1603 (1989).
8) T. Tanaka, H. Kohda, O. Tanaka, F. H. Chen, W. H. Chou and J. L. Leu, *Agric. Biol. Chem.*, **45**, 2165 (1981). In this paper, we tentatively called this sweet plant *Rubus chingii* HU. However, further botanical and chemotaxonomical investigation led to its designation as a new species, *R. suavissimus* S. LEE (S. K. Lee, *Guihaia* (China), **1**, 17 (1981).
9) M. Muchsin, K. Mizutani, R. Kasai, O. Tanaka, S. Kitahata, S. Okada, S. Ogawa, F. Murakami and F. H. Chen, *Agric. Biol. Chem.*, **48**, 2483 (1984).
10) K. Ohtani, Y. Aikawa, H. Ishikawa, R. Kasai, S. Kitahata, K. Mizutani, S. Doi, M. Nakamura and O. Tanaka, *Agric. Biol. Chem.*, **55**, 449 (1991).
11) S. Kitahata, S. Okada and T. Fukui, *Agric. Biol. Chem.*, **42**, 2369 (1978).
12) K. Mizutani, T. Miyata, R. Kasai, O. Tanaka, S. Ogawa and S. Doi, *Agric. Biol. Chem.*, **53**, 395 (1989).
13) S. Kitahata, H. Ishikawa, T. Miyata and O. Tanaka, *Agric. Biol. Chem.*, **53**, 2923 (1989).
14) H. Ishikawa, S. Kitahata, K. Ohtani, C. Ikuhara and O. Tanaka, *Agric. Biol. Chem.*, **54**, 3137 (1990).

Chem. Pharm. Bull. **39**(8) 2046—2048 (1991) Vol. 39, No. 8

Evaluation of Angelicae Radix (Touki) by the Inhibitory Effect on Platelet Aggregation[1)]

Mineo SHIMIZU,* Takayasu MATSUZAWA, Syoichi SUZUKI, Masao YOSHIZAKI and Naokata MORITA

Faculty of Pharmaceutical Sciences, Toyama Medical and Pharmaceutical University, 2630 Sugitani, Toyama 930-01, Japan. *Received February 15, 1991*

Quality evaluation of Angelicae Radix (Touki) was discussed referring to its inhibitory effect on platelet aggregation. No better correlation was observed in quality determined morphologically from the above-ground part of Touki and that determined by anti-platelet aggregation (APA) effects. Phthalides and adenosine, known to be the major components of Touki, were found not sufficient to evaluate the Touki quality as regards APA. Other APA active components have been studied and it was concluded that the APA effect of Touki results from the combined action of plural components. The importance of determining quality based on the action of total extract to meet the purpose for which the substance is to be used was suggested.

Keywords Angelicae Radix; *Angelica acutiloba*; evaluation; anti-platelet aggregation; morphological variety; habitat; phthalide; adenosine

Angelicae Radix (Touki) is one of the crude drugs applied most frequently in Sino–Japanese therapy. The commercial preparation is from the dried root of the Angelicae plant which differs by habitat and species: *Angelica acutiloba* KITAGAWA (Obuka Touki) and *A. acutiloba* var. *sugiyamae* HIKINO (Hokkai Touki) in Japan, and *A. sinensis* (OLIV.) DIELS (Kara Touki) in China. The result of any evaluation depends mainly on the habitat or external appearance as judged by experts, who require severe cultivation conditions. Especially, self-pollination is not adapted for the propagation of Angelicae plants, which have highly genetic inhomogeneity, and it is thus very difficult to supply the market with Angelicae Radix of a uniform and stable quality. It is fundamentally desirable to evaluate the crude drugs from their clinical aspects, although to date yield of the major component or total volume of the extracts have been the factors primarily used. Quantitative analyses of the dried material extract and several specific constituents, such as phthalides, nicotinic acid, Vitamine B_{12}, niacin, biotin, choline *etc.*, have been reported,[2-7)] but no evaluative study of the real therapeutic purpose has been reported. Among the various beneficial effects of Angelicae Radix, its use as a homeostatic remedy for women's disorders has empirically been known.[8)] From the view point of this clinical effect, we report here an evaluation of the anti-platelet aggregation (APA) effect with certain varieties of Angelicae Radix; this is considered to be one of the important factors in improvement of the 'Oketsu' syndrome, which is regarded as a kind of peripheral circulatory disorder and clinically recognized as blood stagnation.

Experimental

The following instruments were used: gas chromatography (GC), Shimadzu GC-9A; high performance liquid chromatography (HPLC), Shimadzu LC-6A; Platelet aggregation tester-counter: TOA Medical Electron Co., Ltd., PL-100, Aggregometer: NKK Hematracer I, Niko Bio-Science Inc., Tokyo.

Plant Material *Angelica acutiloba* KITAGAWA cultivated in Sibukawa, Fujimi-mura and Azumagun-Rokugomura, Gunma Prefecture (Japan) were offered by Mr. T. Hashimoto. A commercial product was purchased from Tochimoto Tenkaido Co., Ltd., Osaka, and morphologically different varieties cultivated in the same place were obtained from Toyama Medicinal Plant Instructive Center and the herbal garden of this university. *A. acutiloba* var. *sugiyamae* HIKINO cultivated in Nayoro, Hokkaido, was offered by Mr. Y. Hatakeyama. All materials except the commercial one were used after treatment with hot water (60 °C, 30 min) (so-called yu-doshi).

Sample Preparation for Analysis and Bioassay 1 g of the ground plant material was extracted with 5 ml of 80% MeOH (40—50 °C, 1 h × 2). The combined extract was concentrated *in vacuo*, and dried for use as the sample for the experiment.

Platelet Aggregation Measurement Platelets were obtained as platelet-rich plasma (PRP), which was prepared by centrifugation of fresh human (male) blood (1100 × *g* for 10 min) with a 1/10 volume of 3.8% sodium citrate aq. Platelet density was adjusted to 3.0×10^5 per μl with platelet-poor plasma (PPP), which was obtained by centrifugation of the same blood at 3000 × *g* for 10 min. 200 μl of PRP was incubated with 25 μl of the test solution (80% MeOH extract was dissolved in distilled water or 2% dimethylsulfoxide (DMSO) solution and diluted to 1.0% with saline) at 37° C for 4 min, then 25 μl of collagen (collagen reagent "HORM," Hormon Chemie Co., Ltd., Munich, Germany) was added to the reaction mixture as aggregating agent. It was confirmed that 2% DMSO in saline had no effect on platelet aggregation so this was used as the control. The aggregation profile was recorded in terms of the change of PRP light transmittance with constant stirring (5—7 min). Inhibition (percent) was calculated by the following equation.

$$\text{inhibition (\%)} = (1 - \text{sample value/control value}) \times 100$$

Quantitative Analysis of Ligustilide and Butylidenephthalide 80% MeOH extract prepared from 0.5 g of the ground material was extracted with 5 ml of $CHCl_3$ containing 50 μg/ml of naphthol as an internal standard (room temp., 30 min) and the upper layer after centrifugation (3000 × *g*, 10 min) was determined by GC. GC conditions-column: silicon OV-17 on Chromosorb W (AW-DMCS) (3 × 200 mm), column temperature: 200 °C, detector: FID, injector temperature: 250 °C, carrier gas: N_2 (30 ml/min), internal standard: α-naphthol.

Quantitative Analysis of Adenosine 0.5 g of the ground material was extracted with 5 ml of distilled water with continuous stirring (room temp., 40 min). 2 ml of MeOH containing 1.3 mg/ml of *p*-toluene sulfonic acid was added to 2 ml of the extracted solution as an internal standard and after centrifugation the supernatant was analyzed by HPLC. HPLC conditions-column: YMC A-303 (s-5 120A ODS) 4.6 × 250 mm, column temperature: 30 °C, detector: UV 254 nm, eluent: 5% CH_3CN/0.05 N phosphate buffer (pH 4.5), flow rate: 0.7 ml/min.

Results

Comparison of APA by Habitats Whether a wild or cultured material, the quality of a crude drug differs by habitat in many cases; on Touki cultured in various districts, a study was therefore made of the difference in APA effect. In this study Obuka Touki was employed, and all materials were treated with hot water to assure uniformly prepared samples. Meanwhile, in consideration of individual differences, samples were prepared using 3 to 5 stocks each from a respective habitat. Results indicated that even with the same species APA greatly differs by habitat (Table I).

TABLE I. Inhibitory Effect of Angelicae Radix (Obuka Touki) Cultivated in Different Districts on Collagen[a]-Induced Platelet Aggregation

Material[b]	Yield of ext. (%)	Inhibition activity (%)		
		2×10^{-3}	1×10^{-3}	5×10^{-4} (g/ml)[c]
1	36.4	86	75	31
2	33.1	38	13	—
3	39.2	63	25	—
4	29.9	79	48	15
5	35.5	88	86	70

a) At 1.0 μg/ml (final concentration). *b*) Material 1: commercial product (Tochimoto Tenkaido Co., Osaka), 2: Sibukawa, Gumma, 3: Fujimi-mura, Gumma, 4: Azuma-gun, Gumma, 5: Herbal Garden, Toyama Medical and Pharmaceutical University. *c*) Extract was dissolved in H_2O or 2% DMSO solution.

TABLE II. Inhibitory Effects of Morphologically Different Groups of Obuka Touki (I—III) and Hokkai Touki on Collagen[a]-Induced Platelet Aggregation

Group	Sampling No.	Yield of ext. (%)	Inhibition activity (%)	
			1×10^{-3}	5×10^{-4} (g/ml)[b]
I	-1	36.8	35	—
	-2	33.6	35	—
	-3	43.5	31	—
	-4	34.2	28	—
	-5	39.4	32	—
II	-1	37.2	66	39
	-2	31.2	90	46
	-3	35.0	72	42
III	-1	44.5	46	—
	-2	39.1	32	—
	-3	39.8	48	26
Hokkai	-1	34.8	17	—
	-2	36.1	10	—
	-3	35.3	25	—
	-4	33.6	22	—

a) At 1.0 μg/ml (final concentration). *b*) Extract was dissolved in H_2O or 2% DMSO solution. Aspirin IC_{50}: 3.8×10^{-5} g/ml.

Relationship between Appearance and APA Even with the same species grown in the same district, the form differed largely, therefore, the morphological factor is one of the important aims for evaluation of the quality. Obuka Touki grown in the same location (Toyama Medicinal Plant Instructive Center) were divided morphologically into the following 3 groups to study their correlation with APA effects. Group I: Typical Obuka Touki showing glossy dark green leaves with many lobations, purplish stems and veins on the back of leaves. Group II: A slightly different morphologically from group I, showing very light purple stem color, with leaf veins being lighter green and not as glossy. Group III: Showing almost no characteristics of groups I and II: glossless leaves, shallow lobations, and strongly greenish as a whole. As shown in Table II, no correlation was observed in qualities determined morphologically from the above-ground part of Touki and those determined by their APA effects. In other words, group I, noted as good quality, did not show the APA effect as strongly as did group II, being rather uncharacteristic Obuka Touki. The same comparison was made using Hokkai Touki obtained from Nayoro, Hokkaido. Although yield of the extract was found to be nearly the same as that of Obuka Touki, the APA effect was markedly lower

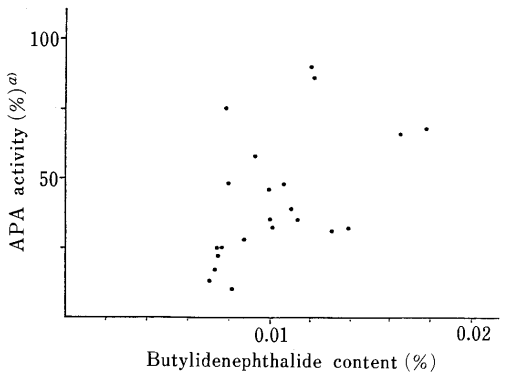

Fig. 1. Relationship between Butylidenephthalide Content and APA Activity in Total Extract of *Angelica acutiloba* ($n=22$)

a) At 10^{-3} g/ml of extract.

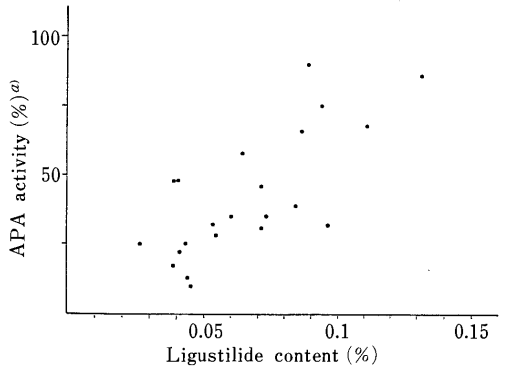

Fig. 2. Relationship between Ligustilide Content and APA Activity in Total Extract of *Angelica acutiloba* ($n=22$)

a) At 10^{-3} g/ml of extract.

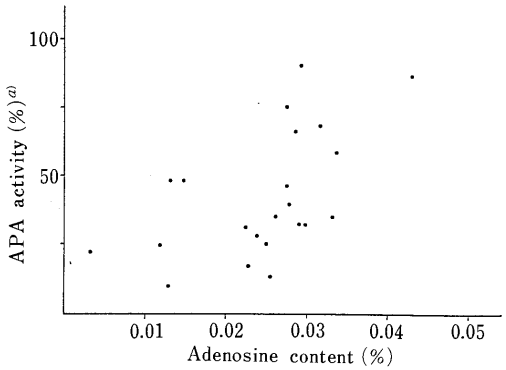

Fig. 3. Relationship between Adenosine Content and APA Activity in Total Extract of *Angelica acutiloba* ($n=22$)

a) At 10^{-3} g/ml of extract.

(Table II).

Relationship between APA and Ingredients The APA effect of Touki has been reported in the past,[9,10] but only adenosine[10] in the water soluble fraction is known as an active material. Thus, for the purpose of clarifying the components that support the APA effect of total extracts other than adenosine, ligustilide and butylidenephthalide, considered to be the major components of Touki, were first studied for their content in extracts and APA effect in each sample. Next, to determine whether or not adenosine can be a guide for quality evaluation of Touki, adenosine content in each sample and its correlation with the APA

effect were examined in the same manner. No clear correlation was noted between butylidenephthalide content in any extract and the APA effect (correlation coefficient: 0.5) (Fig. 1). On the other hand, a certain correlation was noted between ligustilide content and the APA effect (correlation coefficient: 0.7) (Fig. 2). Touki, which contains much phthalide, was not however always strong in the APA effect, making it rather difficult to evaluate the quality with this component. No better correlation was noted between adenosine, which itself shows a strong APA effect, content and APA (correlation coefficient: 0.5): thus it is not sufficient to evaluate the quality of Touki with adenosine only, because a sample containing about 0.03% of adenosine indicated a larger fluctuation in APA effect (Fig. 3).

Discussion

Within the same species of Touki, the APA effect has been suggested to be quite different by habitat. Conventional morphological evaluation as to the quality of Touki by its appearance is not always the same as that of the APA effect shown by Touki extract, and the samples assumed to be of better quality (group I in Table II) showed lower APA effect. Further, studies on ligustilide, butylidenephthalide, and adenosine isolated as active material in APA, which are considered to be used as indices for quality evaluation, as to their contents related to their APA effects, revealed no superior correlation that enables to obtain knowledge of endorsing the APA effect of Touki. APA active components other than adenosine have been studied, and the results will be reported in detail elsewhere, but it is concluded that the APA effect of Touki results from the combined action of plural components. That is, when the qualitly of Touki is evaluated in view of APA, estimation is very difficult if based solely on the content of a specific component. The quality of a crude drug is conventionally evaluated by certain of its specific components; however, the result of this study indicated the importance of making this determination based on the action of total extracts combined to assure that the purpose of use is met. Also important is that the efficacy of a natural drug, which is often not scientifically explainable, be more seriously studied.

Acknowledgements The authors are deeply grateful to Mr. T. Hashimoto and the Toyama Medicinal Plant Instructive Center for supplies of *Angelica acutiloba* KITAGAWA (Obuka Touki), and to Mr. Y. Hatakeyama for the supply of *A. acutiloba* var. *sugiyamae* HIKINO (Hokkai Touki). Further, they express their sincere appreciation to Dr. K. Toriizuka of this University for his generous guidance in measurement of platelet aggregation, and to Profs. M. Tabata and H. Fukui, Faculty of Pharmaceutical Sciences, Kyoto University for valuable advice.

References

1) A part of this work was presented at the 110th Annual Meeting of the Pharmaceutical Society of Japan, Sapporo, August 1990.
2) S. Tanaka, T. Hoshino, Y. Ikeshiro, M. Tabata and M. Konoshima, *Yakugaku Zasshi*, **97**, 14 (1977).
3) S. Takahashi, H. Hikino and Y. Sasaki, *Yakugaku Zasshi*, **78**, 1156 (1958).
4) H. Hikino, Y. Hikino, O. Tamura and S. Takahashi, *Syoyakugaku Zasshi*, **16**, 12 (1962).
5) T. Watanabe and M. Goto, *Yakugaku Zasshi*, **73**, 841 (1953).
6) T. Yamagishi, H. Kaneshima, Y. Kinoshita and M. Mori, *Hokkaido Institute of Public Health Report*, **24**, 47 (1974).
7) M. Goto, *Yakugaku Zasshi*, **75**, 1180 (1955).
8) K. Terasawa, A. Imadaya, H. Tosa, T. Mitsuma, K. Toriizuka, K. Takeda, M. Mikage, M. Hattori and T. Namba, *Fitoterapia*, LVI, 201 (1985).
9) Z.-Z. Yin, *Yao Hsueh Hsueh Pao*, **6**, 321 (1980).
10) K. Toriizuka, P. Nishiyama, I. Adachi, N. Kawashiri, M. Ueno, K. Terasawa and I. Horikoshi, *Chem. Pharm. Bull.*, **34**, 5011 (1986).

Isolation of 10-*O*-Acyl Iridoid Glucosides from a Philippine Medicinal Plant, *Oldenlandia corymbosa* L. (Rubiaceae)

Hideaki OTSUKA,*[,a] Kayoko YOSHIMURA,[a] Kazuo YAMASAKI,[a] and Magdalena C. CANTORIA[b]

Institute of Pharmaceutical Sciences, Hiroshima University School of Medicine,[a] 1-2-3 Kasumi, Minami-ku, Hiroshima 734, Japan, Faculty of Pharmaceutical Sciences, University of the Philippines at Manila,[b] Padre Fauna St., Ermita, Manila, Philippines. *Received February 18, 1991*

From the aerial parts of *Oldenlandia corymbosa*, nine iridoid glucoside derivatives were isolated. On spectroscopic investigation, five known compounds were identified, that is, deacetyl asperuloside, asperuloside, asperulosidic acid, deacetyl asperulosidic acid and scandoside methyl ester. The structures of four new compounds were determined to be acylated derivatives of the known compounds, that is, 10-*O*-benzoyl deacetyl asperulosidic acid methyl ester, and 10-*O*-benzoyl, 10-*O*-*p*-hydroxybenzoyl, and 10-*O*-*p*-*trans*, *cis*-coumaroyl scandoside methyl esters.

Keywords *Oldenlandia corymbosa*; *Hedyotis corymbosa*; Rubiaceae; iridoid; asperuloside; scandoside methyl ester; 10-*O*-benzoyl deacetyl asperulosidic acid methyl ester; 10-*O*-acyl scandoside methyl ester

The constituents of *Hedyotis corymbosa* LAM. (syn. *Oldenlandia corymbosa* L., 水線草, Rubiaceae), which was imported from China, have been investigated by Takagi *et al.*, and the isolation of six iridoid glucosides was reported.[1] The same group isolated some 6-*O*-acyl scandoside methyl esters from a related plant, *Hedyotis diffusa* WILLD. (白花蛇舌草) which was also imported from China through a Hong Kong market.[2] These two plants are now used in Chinese medicine as anti-tumor drugs. During further studies on Philippine medicinal plants,[3,4] we investigated the constituents of *O. corymbosa* harvested in the Philippines. The whole plant, as a decoction, is used as a febrifuge and a stomachic, and the juice is applied for the burning sensation in the palms of the hands and soles of the feet caused by fever.[5] Of the nine iridoid glucosides isolated, four are new compounds. In this paper, determination of the structure of these compounds is described.

Results and Discussion

The aerial part of *O. corymbosa* was extracted with MeOH. The MeOH extract was separated by means of a combination of highly porous synthetic resin, Diaion HP-20, silica gel column chromatography, droplet counter-current chromatography (DCCC) and preparative high performance liquid chromatography (HPLC). The isolation and purification procedures are described in detail in the Experimental section.

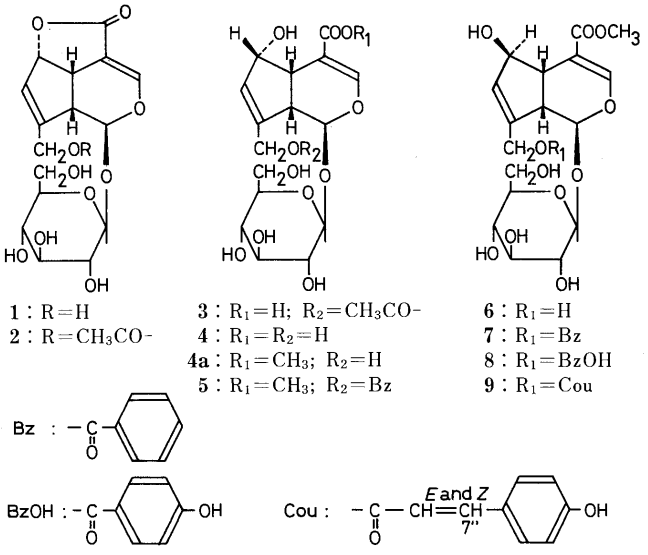

From the spectroscopic data, compounds **1**, **2** and **3** were identified as deacetyl asperuloside, asperuloside and asperulosidic acid, respectively. Compound **4** was characterized as its methyl ester (**4a**).[6] Since the structure of **4a** was determined to be deacetyl asperulosidic acid methyl ester, the parent compound is the free acid of **4a**, namely, deacetyl asperulosidic acid.

Compound **5** was obtained as an amorphous powder, whose elemental composition was determined to be $C_{24}H_{28}O_{12}$ by high resolution (HR)-fast atom bombardment-mass spectrometry (FAB-MS), a cluster ion peak being observed at m/z 531.1494 $[M+Na]^+$ on the addition of NaI. Its ultraviolet (UV) spectrum showed maximum absorption at 231 nm for an aromatic ring, conjugated with a ketone function, and its infrared (IR) spectrum showed the presence of a conjugated ester (1710 and 1635 cm^{-1}). Its ^{13}C-nuclear magnetic resonance (carbon-13 NMR)

TABLE I. ^{13}C-NMR Data for Compounds **4a**—**9** (CD_3OD, 100 MHz)

Carbon number	**4a**	**5**	**6**	**7**	**8**	**9** *trans*	**9** *cis*
1	101.6	101.4	98.7	98.5	98.5	98.52	98.58
3	155.4	155.4	153.9	154.0	154.0	153.99	153.99
4	108.3	108.2	110.9	110.7	110.7	110.65	110.65
5	42.7	42.5	45.8	45.6	45.6	45.63	45.70
6	75.4	75.4	82.5	82.3	82.5	82.34	82.34
7	129.9	132.0	130.4	132.9	132.6	132.59	132.80
8	151.5	146.0	147.5	142.1	142.4	142.30	142.08
9	45.9	46.5	47.3	47.8	47.8	47.64	47.58
10	61.7	64.3	61.1	63.7	63.7	63.00	63.00
11	169.5	170.3	170.3	170.3	170.3	170.29	170.29
-COOMe	51.9	52.1	52.1	52.1	52.1	52.14	52.14
1′	100.5	100.8	100.5	100.6	100.6	100.53	100.53
2′	75.0	75.0	74.9	74.8	74.8	74.80	74.80
3′	78.5	78.6	78.4	78.5	78.5	78.45	78.47
4′	71.6	71.6	71.6	71.5	71.5	71.48	71.54
5′	77.8	77.9	78.0	78.0	78.0	77.95	77.95
6′	62.8	63.0	62.9	62.8	62.8	62.82	62.82
1″		131.3		131.3	122.0	127.13	127.61
2″, 6″		130.7		130.7	133.0	131.32	133.75
3″, 5″		129.7		129.7	116.3	116.89	115.96
4″		134.4		134.5	163.8	161.43	161.18
7″		167.7		167.7	167.8	147.10	145.71
8″						116.22	114.80
9″						168.85	167.86

TABLE II. ^{1}H-NMR Data for Compounds **4a**—**9** (CD_3OD, 400 MHz)

Proton(s) at	**4a**	**5**	**6**	**7**	**8**	**9** *trans*	**9** *cis*
1	5.055 (d, 8)	5.122 (d, 9)	5.190 (d, 7)	5.268 (d, 7)	5.257 (d, 7)	5.216 (d, 7)	5.179 (d, 7)
3	7.651 (d, 2)	7.669 (d, 2)	7.507 (d, 1)	7.537 (d, 2)	7.533 (d, 2)	7.532 (d, 2)	7.520 (d, 1)
5	3.018 (ddd, 2/6/8)	3.086 (dd, 2/8)	2.993 (ddd, 1/5/8)	3.056 (ddd, 1/5/8)	3.047 (ddd, 2/5/8)	*ca.* 3.02 (m)	
6	4.794 (m)	*a)*	4.544 (dt, 2/5)	4.539 (td, 2/5)	4.581 (td, 2/5)	*ca.* 4.58 (m)	
7	6.019 (d, 2)	6.113 (d, 2)	5.081 (t, 2)	5.925 (d, 2)	5.891 (d, 2)	5.867 (d, 2)	5.801 (d, 2)
9	2.565 (dd, 7/8)	2.724 (br t, 8)	3.030 (br t, 7)	3.149 (br t, 7)	3.129 (br t, 8)	3.091 (br t, 7)	
10a	4.207 (br d, 15)	5.023 (br d, 15)	4.181 (br d, 15)	5.011 (br d, 15)	4.938 (br d, 15)	*b)*	
10b	4.453 (dd, 2/15)	5.224 (br d, 15)	4.336 (br d, 15)	5.114 (br d, 15)	5.071 (br d, 15)	4.978 (br d, 15)	
–COOMe	3.741 (s)	3.745 (s)	3.751 (s)	3.757 (s)	3.754 (s)	3.754 (s)	3.750 (s)
1′	4.716 (d, 8)	4.749 (d, 8)	4.667 (d, 8)	4.699 (d, 8)	4.694 (d, 8)	4.697 (d, 8)	4.690 (d, 8)
2′	3.239 (dd, 8/9)	3.277 (dd, 8/9)	3.205 (dd, 8/9)	3.237 (dd, 8/9)	3.234 (dd, 8/9)	3.240 (dd, 8/9)	
3′	*a)*	*a)*	*a)*	*a)*	*a)*	*a)*	
4′	3.389 (t, 9)	3.392 (t, 9)	*a)*	3.370 (t, 9)	*a)*	*ca.* 3.36	
5′	*a)*	*a)*	*a)*	*a)*	*a)*	*a)*	
6′a	3.617 (dd, 6/12)	3.630 (dd, 6/12)	3.633 (dd, 6/12)	3.637 (dd, 6/12)	3.639 (dd, 7/12)	*ca.* 3.64	
6′b	3.847 (dd, 2/12)	3.861 (dd, 2/12)	3.863 (dd, 2/12)	3.849 (dd, 2/12)	3.852 (dd, 2/12)	3.869 (br d, 12)	
2″, 6″		8.067 (dd, 1/8)		8.067 (dd, 1/8)	7.919 (d, 9)	7.476 (d, 9)	7.636 (d, 9)
3″, 5″		7.495 (t, 8)		7.496 (t, 8)	6.840 (d, 9)	6.810 (d, 9)	6.757 (d, 9)
4″		7.621 (tt, 1/8)		7.622 (tt, 1/8)			
7″						7.663 (d, 16)	6.902 (d, 13)
8″						6.378 (d, 16)	5.829 (d, 13)

The letters and figures in parentheses are multiplicities and coupling constants in Hz. *a)* Signals overlapped by the envelope of the solvent signal. *b)* Signal merged with the water signal.

spectrum closely resembled that of **4a**, except for the presence of additional four sp^2 signals, two of which were of double strength and a carboxyl carbon signal. Thus, compound **5** was expected to be an acylated derivative of **4a** (Tables I and II). The acyl portion was actually composed of six aromatic signals and a carboxyl carbon signal, which is in accordance with those for benzoic acid.[7] Five aromatic proton signals, observed in the proton nuclear magnetic resonance (^{1}H-NMR) spectrum, were coupled in the system, which also reflected that the acyl portion is benzoic acid. On acetylation of **5** in Ac_2O and pyridine, pentaacetate was obtained, the ^{1}H-NMR spectrum of which showed the presence of five alcoholic acetyl groups. The position of esterification was determined to be the 10-hydroxyl group of aglucone, since, when the ^{13}C-NMR spectra of compounds **4a** and **5** were compared, the C-10 signal of **4a** was found to be significantly shifted downfield, by +2.6 ppm, on acylation, the β-position (C-8) shifted upfield by −5.5 ppm, and the γ-position (C-7) downfield by +2.1 ppm (Table I).[8] This was also supported by the results of ^{1}H-NMR spectroscopy, *i.e.*, the two protons on C-10 were shifted downfield, by about 0.8 ppm on acylation (Table II). Therefore, the structure of compound **5** was concluded to be 10-*O*-benzoyl-deacetyl asperulosidic acid methyl ester.

Compound **6** was obtained as an amorphous powder and determined to be scandoside methyl ester from the spectroscopic data.[1]

Compound **7** was obtained as an amorphous powder. On HR-FAB-MS, its molecular composition was determined to be $C_{24}H_{28}O_{12}$. On comparison of the spectroscopic data for compounds **6** and **7**, compound **7** was expected to be an acylated derivative of **6**, as in the case for compounds **4a** and **5**. The acyl portion was also determined to be benzoic acid and from substitution shift trends, induced by acylation, the esterified position was concluded to be the C-10 hydroxyl group of aglucone. Thus, the structure of compound **7** was consequently determined to be 10-*O*-benzoyl scandoside methyl ester.

Compound **8**, $C_{24}H_{28}O_{13}$, was also obtained as an amorphous powder. The molecular composition determined by HR-FAB-MS indicated that this compound has one more oxygen atom than compound **7**. The chemical shifts in ^{1}H- and ^{13}C-NMR spectra were essentially the same as those in the case of compound **6**, except for in the acyl portion (Tables I and II). Of four aromatic carbon signals, two were of double strength, which indicated that the acyl portion included a *para*-substituted benzene system (δ 116.3 and 133.0); one of the substituents was assumed to be a hydroxyl group, taking into account that the ^{13}C-NMR signal appeared at δ 163.8 ppm. The observation of two aromatic proton signals coupled in an AA'BB' system [δ 6.840 (d, J=9 Hz) and 7.919 (d, J=9 Hz)] confirmed that the structure of the acyl moiety was *p*-hydroxybenzoic acid.[9] The position of esterification was also determined to be the C-10 hydroxyl group from the acylation induced shift trend, which was similar to previous cases. On acetylation with a mixture of Ac_2O and pyridine, hexaacetate was obtained. The ^{1}H-NMR spectrum indicated that there were five acetyl groups attached to alcoholic groups and one to a phenolic hydroxyl group. Therefore, compound **8** was determined to be 10-*O*-*p*-hydroxybenzoyl scandoside methyl ester.

Compound **9** was obtained as an inseparable amorphous mixture; however, it showed a single spot on thin layer chromatogram ($CHCl_3$: MeOH : H_2O = 15 : 6 : 1 and EtOAc : EtOH : H_2O = 8 : 2 : 1) and one peak by HPLC. Its molecular composition was determined to be $C_{26}H_{30}O_{13}$ by HR-FAB-MS. The ^{1}H- and ^{13}C-NMR spectra indicated that compound **9** was also an acylated derivative of scandoside methyl ester. However, these NMR spectra showed some complexity. The ^{13}C-NMR signals for

aglucone and glucose moieties unexceptionally appeared with smaller satellite peaks. In the ^{1}H-NMR spectrum, two sets of doublets at δ 6.378 (d, J=16 Hz) and 7.663 (d, J=16 Hz), and δ 5.829 (d, J=13 Hz) and 6.902 (d, J=13 Hz) indicated the existence of *trans* and *cis* double bonds, respectively. Aromatic proton signals were observed as doublets at δ 6.810 (d, J=9 Hz), and 7.476 (d, J=9 Hz), were accompanied by smaller similar signals at δ 6.757 (d, J=9 Hz) and 7.636 (d, J=9 Hz), which are assumed to be due to a *cis* isomer. This data implied the acyl portion is a *para*-substituted cinnamic acid, and the ^{13}C-NMR data reported for the *trans* and *cis-p*-coumaric acids showed good agreement with those for the acyl moiety.[10] The *trans* and *cis* ratio was calculated to be approximately 70:30 from the proton signal integrals. The position of acylation was determined to be at the C-10 hydroxyl group, as in the cases of the compounds previously discussed, since between compounds **6** and **9**, similar acylation-induced shift trends were observed at the C-10, C-8 and C-7 positions. Thus, the structure of **9** was concluded to be 10-*O*-*p*-coumaroyl scandoside methyl ester.

Experimental

Each melting point was determined with a Yanagimoto micro melting point apparatus and is uncorrected. ^{1}H- and ^{13}C-NMR spectra were recorded on a JEOL GX-400 spectrometer at 400 MHz and 100 MHz, respectively, and chemical shifts are given in ppm, with tetramethylsilane as an internal standard. Dioxane (δ_C=67.4 ppm) and HDO (δ_H=4.70 ppm) were used as internal standards for ^{13}C- and ^{1}H-NMR in D_2O, respectively. IR and UV spectra were obtained with Shimadzu IR-408 and UV-200S spectrophotometers, respectively. Optical rotations were measured with a Union Giken PM-101 automatic digital polarimeter. Mass spectra were recorded on a JEOL SX-102 mass spectrometer under the following conditions: electron impact (EI)-MS, 70 eV; FAB-MS, glycerol as a matrix for non-acetates, and *m*-nitrobenzyl alcohol for acetates. DCCC separation was carried out by an ascending method with $CHCl_3$–MeOH–H_2O–*n*-PrOH (9:12:8:2) as a solvent system and with 500 columns (2 mm × 40 cm). Four gram fractions were obtained and numbered according their elution with the mobile phase.

Isolation Procedure The plant material (460 g) was extracted with *n*-hexane three times under reflux to give 7.0 g of a hexane extract. The residue was extracted four times with MeOH for 3 h under reflux. The MeOH extract (42 g) was dissolved in 95% aq. MeOH and then extracted with *n*-hexane. The MeOH layer was concentrated to dryness to give 40 g of a brown mass. This was separated by a highly porous synthetic resin, Diaion HP-20, with the solvent system of 20%, 40%, 60% (a, b) and 80% (a, b, c) MeOH in water, and then with MeOH.

The 20% MeOH fraction (1.48 g) was again subjected to Diaion HP-20 column chromatography with a 5% stepwise increase in the MeOH content from 100% H_2O, which gave 711 mg of a compound **4**-rich fraction in the 5% MeOH eluate. After checking by ^{1}H-NMR that the compounds in this fraction did not have any methoxyl groups, the MeOH solution of the fraction (364 mg) was treated with ethereal diazomethane and then purified by DCCC (frs. 33—42) to give 169 mg of compound **4a**. An aliquot (317 mg) of the 40% MeOH fraction (645 mg) was subjected to DCCC to give 115 mg of compound **1** (frs. 26—35). Purification of the 60% (a) MeOH eluate (0.69 g) by silica gel column chromatography ($CHCl_3$–MeOH, 9:1) afforded 212 mg of compound **6**. A portion (511 mg) of the b fraction of the 60% MeOH eluate (1.18 g) was first separated by two runs of DCCC to give 140 mg of a compound **2**-rich (frs. 68—88) fraction and 289 mg of a compound **3**-rich (frs. 36—48) fraction. Compound **2** (39 mg) was obtained as colourless needles by recrystallization of the fraction from H_2O. Compound **3** (87 mg) was isolated by silica gel column chromatography ($CHCl_3$–MeOH–H_2O, 30:12:1) from the compound **3**-rich fraction. The b fraction of the 80% MeOH eluate (2.25 g) gave compound **8** (15 mg), after separation by both silica gel column chromatography ($CHCl_3$–MeOH–H_2O, 150:30:1) and preparative HPLC (TSK gel, octadecyl silica (ODS), 50% MeOH). The c fraction (2.27 g) of the 80% MeOH eluate was subjected to silica gel column chromatography. The second fraction (305 mg), eluted with $CHCl_3$–MeOH–H_2O (150:30:1), was further separated by silica gel column chromatography ($CHCl_3$–MeOH, 96:4) and preparative HPLC (TSK gel, ODS, 60% MeOH) to give 24 mg of compound **7**. Compounds **5** and **9** were isolated from the third fraction (441 mg), with elution with $CHCl_3$–MeOH–H_2O (150:30:1). Further column chromatography on silica gel ($CHCl_3$–MeOH, 96:4) of the fraction led to the condensation of compounds **5** and **9** (155 mg). Finally, preparative HPLC with 65% MeOH afforded 40 mg of compound **9** from the slower-eluted portion, and 22 mg of compound **5** was isolated by repeated preparative HPLC of the faster-eluted portion (60% MeOH) with 45% MeOH. Analytical HPLC of **9** was performed on an Inertsil ODS column (6 × 250 mm, 45% aq. MeOH, at 22 °C, 1.5 ml/min; detection: UV at 310 nm). The t_R (min) of compound **9** was 17.3 (a single peak).

Known Compounds Isolated Deacetyl asperuloside (**1**), an amorphous powder. $[\alpha]_D^{22}$ −140.0° (c=0.75, MeOH). FAB-MS m/z: 373 ($[MH]^+$), 395 ($[M+Na]^+$) (+NaI), 411 ($[M+K]^+$)(+KI). ^{13}C-NMR (CD_3OD) δ: 37.5 (d, C-5), 45.0 (d, C-9), 60.1 (t, C-10), 62.8 (t, C-6′), 71.6 (d, C-4′), 74.7 (d, C-2′), 77.9 (d, C-5′), 78.4 (d, C-3′), 86.7 (d, C-6), 93,4 (d, C-1), 99.9 (d, C-1′), 106.5 (s, C-4), 125.8 (d, C-7), 149.8 (s, C-8), 150.3 (d, C-3), 172.9 (s, C-11). The spectroscopic data for the pentaacetate of deacetyl asperuloside were indistinguishable from those for the tetraacetate of asperuloside.

Asperuloside (**2**): Colorless needles (H_2O), mp 124—126 °C, lit.[1] 120—123 °C. $[\alpha]_D^{22}$ −190.0° (c=1.60, MeOH). FAB-MS m/z: 415 ($[MH]^+$), 437 ($[M+Na]^+$) (+NaI), 453 ($[M+K]^+$)(+KI); ^{13}C-NMR (CD_3OD) δ: 20.7 (q, $\underline{C}H_3CO$–), 37.5 (d, C-5), 45.2 (d, C-9), 60.9 (t, C-10), 62.8 (t, C-6′), 71.5 (d, C-4′), 74.6 (d, C-2′), 77.8 (d, C-5′), 78.3 (d, C-3′), 86.3 (d, C-6), 93.3 (d, C-1), 100.0 (d, C-1′), 106.2 (s, C-4), 128.9 (d, C-7), 144.2 (s, C-8), 150.3 (d, C-3), 172.2, 172.5 (both s, C-11 and $CH_3\underline{C}O$–). ^{13}C-NMR (D_2O) δ: 21.0, 36.7, 44.4, 61.6, 62.3, 70.4, 73.4, 76.3, 77.2, 87.1, 93.7, 99.4, 105.5, 128.9, 143.0, 150.7, 174.2, 174.5.[11]

Asperulosidic Acid (**3**): An amorphous powder. $[\alpha]_D^{23}$ +21.7° (c=0.69, MeOH). FAB-MS m/z: 455 ($[M+Na]^+$) (+NaI), 471 ($[M+K]^+$) (+KI). ^{13}C-NMR (CD_3OD) δ: 20.8 (q, $\underline{C}H_3CO$–), 42.6 (d, C-5), 46.3 (d, C-9), 63.0 (t, C-6′), 63.8 (t, C-10), 71.5 (d, C-4′), 74.9 (d, C-2′), 75.4 (d, C-6), 77.8 (d, C-5′), 78.5 (d, C-3′), 100.5 (d, C-1′), 101.2 (d, C-1), 131.9 (d, C-7), 145.9 (s, C-8), 155.0 (d, C-3), 171.2, 172.5 (both s, C-11 and $CH_3\underline{C}O$–).[12] The signal for C-4 at around 110 ppm was missing, maybe due to formation of the carboxylate anion.[13]

Deacetyl Asperulosidic Acid (**4**): Characterized as its methyl ester (deacetyl asperulosidic acid methyl ester) (**4a**). An amorphous powder, $[\alpha]_D^{23}$ +22.6° (c=1.33, MeOH), FAB-MS m/z: 427 ($[M+Na]^+$) (+NaI), 443 ($[M+K]^+$) (+KI). ^{13}C-NMR (CD_3OD): see Table I. ^{1}H-NMR (D_2O) δ: 2.61 (H, br t, J=8.3 Hz, 9-H), 3.08 (H, H, br t, J=6.8 Hz, 5-H), 3.32 (H, dd, J=8.0, 9.2 Hz, 2′-H), 3.55 (H, t, J=9.2 Hz, 3′-H), 3.46 (H, t, J=9.2 Hz, 4′-H), 3.64 (H, dd, J=5.1, 12.1 Hz, 6′-H_a), 3.71 (3H, s), 3.82 (H, dd, J=1.5, 12.1 Hz, 6′-H_b), 4.22 (H, br d, J=15.7 Hz, 10-H_a), 4.40 (H, dd, J=1.3, 15.7 Hz, 10-H_b), 4.79 (H, d, J=8.0 Hz, 1′-H), 4.81 (H, br dd-like, 6-H), 4.93 (H, d, J=9.0 Hz, 1-H), 5.99 (H, d, J=1.8 Hz, 7-H), 7.66 (H, d, J=1.3 Hz, 3-H).[14]

Scandoside Methyl Ester (**6**): An amorphous powder, $[\alpha]_D^{23}$ −34.8° (c=0.69, MeOH). FAB-MS m/z: 427 ($[M+Na]^+$) (+NaI), 443 ($[M+K]^+$) (+KI). ^{13}C-NMR (CD_3OD): see Table I. ^{1}H-NMR (D_2O) δ: 3.03 (H, dd, J=3.4, 7.5 Hz, 5-H), 3.16 (H, br t, J=5.5 Hz, 9-H), 3.25 (H, dd, J=8.3, 9.0 Hz, 2′-H), 3.33 (H, t, J=9.0 Hz, 3′-H), 3.39 (H, ddd, J=1.9, 5.7, 9.0 Hz, 5′-H), 3.44 (H, t, J=9.0, 4′-H), 3.65 (H, dd, J=5.7, 12.3, 6′-H_a), 3.71 (3H, s), 3.82 (H, dd, J=1.9, 12.3 Hz, 6′-H_b), 4.20 (H, br d, J=15.2 Hz, 10-H_a), 4.28 (H, br d, J=15.2 Hz, 10-H_b), 4.57 (H, very br s, 6-H), 4.72 (H, d, J=8.3 Hz, 1′-H), 5.34 (H, d, J=5.1 Hz, 1-H), 5.78 (H, br s, 7-H), 7.45 (H, s, 3-H).[1,15]

10-*O*-Benzoyl Deacetyl Asperulosidic Acid Methyl Ester (5) An amorphous powder, $[\alpha]_D^{22}$ +21.4° (c=1.40, MeOH). IR ν_{max}^{KBr} cm^{-1}: 3420, 2925, 1710, 1635, 1445, 1315, 1275, 1150, 1100, 1075, 1045, 780, 715. UV λ_{max}^{MeOH} nm (log ε): 211 (3.65) inf, 231 (4.21). HR-FAB-MS m/z: 531.1494 ($[M+Na]^+$) (+NaI) ($C_{24}H_{28}O_{12}Na$ requires 531.1478). ^{1}H- and ^{13}C-NMR: see Tables I and II.

10-*O*-Benzoyl Scandoside Methyl Ester (7) An amorphous powder, $[\alpha]_D^{22}$ −22.5° (c=0.71, MeOH). IR ν_{max}^{KBr} cm^{-1}: 3375, 2875, 1705, 1630, 1440, 1380, 1310, 1275, 1155, 1110, 1070, 805, 770, 715. UV λ_{max}^{MeOH} nm (log ε): 213 (3.60) inf, 232 (4.26). HR-FAB-MS m/z: 531.1503 ($[M+Na]^+$) (+NaI) ($C_{24}H_{28}O_{12}Na$ requires 531.1478). ^{1}H- and ^{13}C-NMR: see Tables I and II.

10-*O*-*p*-Hydroxybenzoyl Scandoside Methyl Ester (8) An amorphous powder, $[\alpha]_D^{22}$ −17.0° (c=1.00, MeOH). IR ν_{max}^{KBr} cm^{-1}: 3420, 2955, 1700, 1630, 1605, 1515, 1440, 1385, 1310, 1275, 1165, 1100, 1080, 895, 850, 770.

UV λ_{max}^{MeOH} nm (log ε): 213 (3.94), 251 (4.11). HR-FAB-MS *m/z*: 547.1497 ($[M+Na]^+$) (+NaI) ($C_{24}H_{28}O_{13}Na$ requires 547.1427). ^1H- and ^{13}C-NMR: see Tables I and II.

10-*O*-*p*-*trans*, *cis*-Coumaroyl Scandoside Methyl Ester (9) An amorphous powder, $[\alpha]_D^{22}$ −20.0° (*c*=1.35, MeOH). IR ν_{max}^{KBr} cm^{-1}: 3425, 2920, 1700, 1635, 1605, 1515, 1440, 1385, 1310, 1280, 1170, 1100, 1080, 955, 890, 840, 770. UV λ_{max}^{MeOH} nm (log ε): 215 (4.03), 230 (4.15), 302 (4.10), 313 (4.15). HR-FAB-MS *m/z*: 573.1557 ($[M+Na]^+$) (+NaI) ($C_{26}H_{30}O_{13}Na$ requires 573.1584). ^1H- and ^{13}C-NMR: see Tables I and II.

Acetates of Compounds 5, 7, 8 and 9 Compounds **5**, **7**, **8** and **9** (about 3 mg each) were acetylated with a mixture of Ac_2O (3 drops) and pyridine (3 drops) at 25 °C overnight. Each reaction solution was evaporated to dryness. Compound **5** pentaacetate. FAB-MS *m/z*: 741 ($[M+Na]^+$), 169 (+NaI), 757 ($[M+K]^+$) (+KI). EI-MS *m/z* (rel. int.): 718 ($[M]^+$) (<1), 368 (14), 331 ($[Gluc(Ac)_4]^+$) (87), 169 (100), 133 (50), 109 (44). ^1H-NMR ($CDCl_3$) δ: 1.95, 2.02 (×2), 2.09, 2.03. Compound **7** pentaacetate. FAB-MS *m/z*: 741 ($[M+Na]^+$), 169 (+NaI), 757 ($[M+K]^+$) (+KI). EI-MS *m/z* (rel. int.): 368 (19), 331 ($[Gluc(AC)_4]^+$) (65), 169 (100), 133 (67), 108 (48). ^1H-NMR ($CDCl_3$) δ: 1.95, 2.006, 2.010, 2.02, 2.06. Compound **8** hexaacetate. FAB-MS *m/z*: 799 ($[M+Na]^+$), 172, 169 (+NaI), 815 ($[M+K]^+$) (+KI). EI-MS *m/z* (rel. int.): 538 (4), 331 ($[Gluc(Ac)_4]^+$) (65), 169 (100), 109 (42). ^1H-NMR ($CDCl_3$) δ: 1.94, 2.01, 2.02, 2.03, 2.07, 2.32. Compound **9** hexaacetate. FAB-MS *m/z*: 825 ($[M+Na]^+$) (+NaI), 841 ($[M+K]^+$) (+KI). EI-MS *m/z* (rel. int.): 386 (12), 368 (22), 331 ($[Gluc(Ac)_4]^+$) (59), 169 (100), 157 (48), 133 (39), 109 (52). ^1H-NMR ($CDCl_3$) δ: 1.955 (*E*), 2.006 (*E*+*Z*), 2.027 (*E*+*Z*), 2.059 (*E*), 2.062 (*Z*), 2.068 (*Z*), 2.098 (*E*+*Z*), 2.302 (*Z*), 2.314 (*E*).

Acknowledgment This study was supported by a Research Study Grant under the JSPS International Joint Research Project.

References

1) S. Takagi, M. Yamaki, K. Masuda, Y. Nishihama, and K. Sakina, *Yakugaku Zasshi*, **101**, 657 (1981).
2) Y. Nishihama, K. Masuda, M. Yamaki, S. Takagi, and K. Sakina, *Planta Med.*, **43**, 28 (1981).
3) A. Rimando, S. Inoshiri, H. Otsuka, H. Kohda, K. Yamasaki, W. G. Padolina, L. Torres, E. G. Quintana, and M. C. Cantoria, *Jpn. J. Pharmacog.*, **41**, 242 (1987).
4) H. Otsuka, N. Kubo, K. Yamasaki, and W. G. Padolina, *Phytochemistry*, **28**, 3065 (1989).
5) A. Quisumbing, "Medicinal Plants of the Philippines," Katha Publishing Co., Quezon City, 1978, pp. 920—921.
6) C. A. Boros and F. R. Stermitz, *J. Nat. Prod.*, **53**, 1055 (1990).
7) R. K. Chaudhuri and O. Sticher, *Helv. Chim. Acta*, **63**, 117 (1980).
8) V. M. Chari, M. Jordan, H. Wagner, and P. W. Thies, *Phytochemistry*, **16**, 1110 (1977).
9) S. F. El-Naggar and R. W. Doskotch, *J. Nat. Prod.*, **43**, 524 (1980).
10) J. Garcia and A. J. Chulia, *Planta Med.*, **1986**, 101.
11) F. Bailleul, P. Delaveau, A. Rabaron, M. Plat, and M. Koch, *Phytochemistry*, **16**, 723 (1977).
12) R. K. Chaudhuri, F. U. Afifi-Yazar, O. Sticher, and T. Winkler, *Tetrahedron*, **36**, 2317 (1980).
13) G. König, H. Rimpler, and D. Hunkler, *Phytochemistry*, **26**, 423 (1987).
14) A. Bianco, M. Guiso, C. Iavarone, P. Passacantilli, and C. Trogolo, *Gazz. Chim. Ital.*, **108**, 13 (1978).
15) H. Inouye, Y. Takeda, and H. Nishimura, *Phytochemistry*, **13**, 2219 (1974).

Studies on the Constituents of Palmae Plants. VI.[1a] Steroid Saponins and Flavonoids of Leaves of *Phoenix canariensis* hort. ex CHABAUD, *P. humilis* ROYLE var. *hanceana* BECC., *P. dactylifera* L., and *Licuala spinosa* WURMB.

Akitoshi ASAMI, Yasuaki HIRAI, and Junzo SHOJI*

School of Pharmaceutical Sciences, Showa University, Hatanodai, Shinagawa-ku, Tokyo 142, Japan. *Received February 12, 1991*

Steroid saponins and flavonoids of the leaves of *Phoenix canariensis* hort. ex CHABAUD, *P. humilis* ROYLE var. *hanceana* BECC., *P. dactylifera* L., and *Licuala spinosa* WURMB. have been investigated. Tricin 7-*O*-β-D-glucopyranoside (1), isorhamnetin 3-*O*-β-D-glucopyranoside (2), isoquercitrin (3), isorhamnetin 3-*O*-β-rutinoside (4), rutin (5), and methyl (25*S*)-proto-Pb (6) from *P. canariensis*, 1, 6, glucoluteolin (7), tricin 7-*O*-α-L-rhamnopyranosyl(1→2)-β-D-glucopyranoside (8), and methyl (25*S*)-proto-loureiroside (9) from *P. humilis* var. *hanceana*, 1, 2, 8, methyl proto-prosapogenin A of dioscin (10), methyl proto-reclinatoside (11) and methyl proto-Pb (12) from *P. dactylifera*, and vitexin (13) and methyl (25*S*)-proto-dioscin (14) from *Licuala spinosa* have been isolated and identified.

Keywords *Phoenix canariensis*; *Phoenix humilis* var. *hanceana*; *Phoenix dactylifera*; *Licuala spinosa*; Palmae; steroid saponin; furostanol oligoside; diosgenin; flavone glycoside; flavonol glycoside

A series of chemotaxonomical studies on plants of the Palmae family was undertaken,[1] and the constituents of steroid saponin and flavonoids from Palmae plants, *Phoenix rupicola* T. ANDERSON, *P. loureirii* KUNTH, *P. reclinata* N. J. JACQUIN, and *Arecastrum romanzoffianum* BECCARI reported.[1a] The present paper is mainly concerned with studies on the constituents of *Phoenix canariensis* hort. ex CHABAUD, *P. humilis* ROYLE var. *hanceana* BECC., *P. dactylifera* and *Licuala spinosa* WURMB.

The habitat of *P. canariensis* (Japanese name: kanariiyashi) is the Canary Islands, and the plant is cultivated in warm areas of Japan as a shade tree. The habitat of *P. humilis* var. *hanceana* (Sotetsujuro) is Formosa; that of *P. dactylifera* (Natsumeyashi) is along the bay of Persia and the fruit is used for food. Finally, the habitat of *L. spinosa* (Togegoheiyashi) is Malaya.

The leaves of *Phoenix canariensis*, *P. humilis* var. *hanceana*, and *P. dactylifera* harvested in Hachijo island, off the mainland from Tokyo, in January 1986 and *Licuala spinosa* harvested in Okinawa in January 1987 were individually chopped and extracted with methanol at room temperature. Each methanol extract was treated by the method described in the Experimental section.

Six compounds (**1**—**6**) were separated from the methanol extract of *P. canariensis*. Compounds **1**—**5** were identified as tricin 7-*O*-β-D-glucopyranoside,[2] isorhamnetin 3-*O*-β-D-glucopyranoside,[3] isoquercitrin,[4] isorhamnetin 3-*O*-β-rutinoside[2] and rutin[5] by comparing the thin layer chromatographic (TLC) behavior, and the infrared (IR) and nuclear magnetic resonance (NMR) spectra with those of respective authentic samples.

6 was positive in the Liebermann–Burchard reaction and in the Ehrlich reaction.[6] The IR spectrum of **6** shows a strong absorption band due to hydroxyl groups and the ^{13}C-NMR spectrum of **6** shows five anomeric carbon signals and methoxyl group signal. Accordingly, **6** was suggested to be a furostanol pentaoside. On enzymatic hydrolysis with almond emulsion, **6** afforded D-glucose and a prosapogenin (**6a**). On acidic hydrolysis, **6a** gave the aglycone, D-glucose and L-rhamnose. The absolute configuration of these sugars was determined using the method of Oshima *et al.*[7] On acetylation, the aglycone of **6a** afforded yamogenin acetate and diosgenin acetate. It is well known that the methyl group at C-25 of yamogenin is easily isomerized under an acidic condition to afford diosgenin.[8] Finally, the genuine aglycone was concluded to be yamogenin by examination of IR and ^{13}C-NMR spectra. The ^{13}C-NMR spectrum of **6a** showed four anomeric carbon signals and three methyl signals corresponding to C-6 methyl group of L-rhamnose. By comparison of ^{13}C-NMR spectra, the structure of sugar moiety of **6a** was deduced to be the same as that of Pb, which has been isolated from the Palmae plant.[1] Finally, **6a** was characterized to be the (25*S*)-isomer of Pb and **6** was the (25*S*)-isomer of methyl proto-Pb. Both these compounds are new steroid saponins hitherto isolated from Palmae plants.

Five compounds, **1** and **6**—**9**, were isolated from the methanol extract of *P. humilis* var. *hanceana*. **7** and **8** were deduced to be glucoluteolin[1e] and tricin 7-neohesperidoside[9] by comparing the TLC behavior, and the IR and NMR spectra with those of the respective authentic sample. The latter compound, **8**, is a known compound, but this is the first report of its isolation from the palmae plant.

Compound **9** was positive in the Liebermann–Burchard reaction and in the Ehrlich reaction. Based on the IR and ^{13}C-NMR spectra, **9** was suggested to be a furostanol pentaoside. On enzymatic hydrolysis with almond emulsion, **9** afforded D-glucose and a prosapogenin (**9a**), which was suggested to be (25*S*)-spirostanol tetraglycoside by IR and ^{13}C-NMR spectra. On acidic hydrolysis, **9a** gave L-arabinose, D-glucose, L-rhamnose and an aglycone, which was deduced to be a mixture of yamogenin and diosgenin. The ^{13}C-NMR spectrum of **9a** showed four anomeric carbon signals and one methyl signal corresponding to C-6 methyl group of L-rhamnose. By comparison of ^{13}C-NMR spectra, the structure of sugar moiety of **9a** was deduced to be the same as that of loureiroside which has been isolated from a palmae plant.[1a] Finally, the structures of new steroid saponins **9a** and **9** were established to be (25*S*)-isomer of loureiroside and (25*S*)-isomer of methyl proto-loureiroside, respectively.

Six compounds, **1**, **2**, **8**, **10**, **11** and **12**, were separated from the methanol extract of *P. dactylifera*; **10**, **11** and **12** were identified as methyl proto-prosapogenin A of dio-

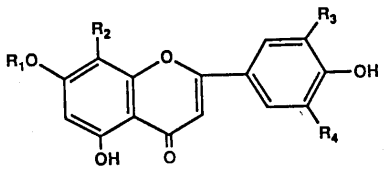

1 : R_1=I, R_2=H, R_3=R_4=OCH_3
7 : R_1=I, R_2=R_4=H, R_3=OH
8 : R_1=IV, R_2=H, R_3=R_4=OCH_3
13 : R_1=R_3=R_4=H, R_2= I

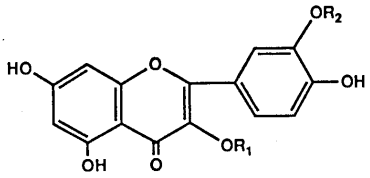

2 : R_1=I, R_2=CH_3
3 : R_1=I, R_2=H
4 : R_1=II, R_2=CH_3
5 : R_1=II, R_2=H

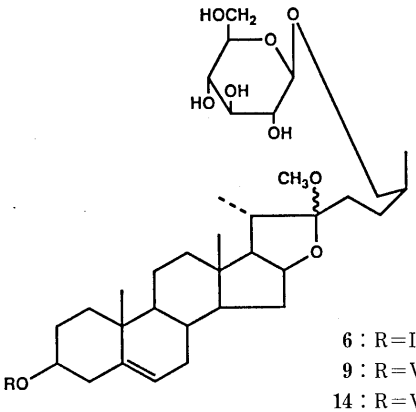

6 : R=III
9 : R=V
14 : R=VII

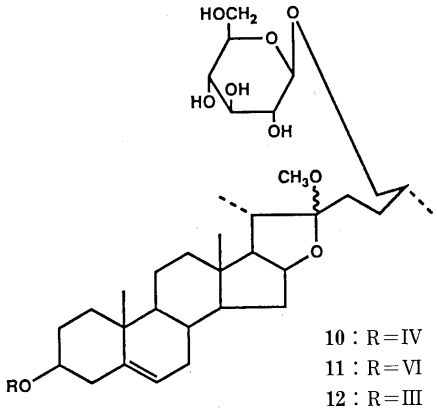

10 : R=IV
11 : R=VI
12 : R=III

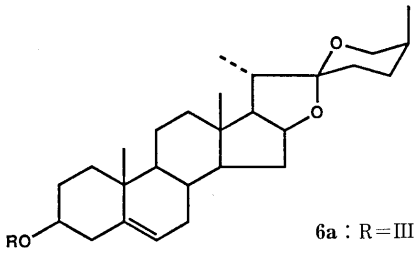

6a : R=III
9a : R=V
14a : R=VII

I :

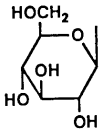

II :

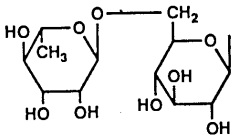

III :

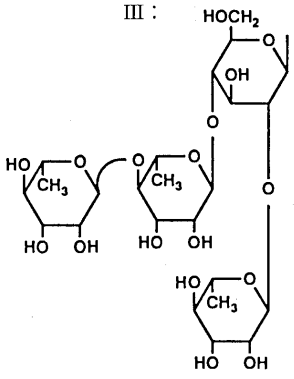

IV :

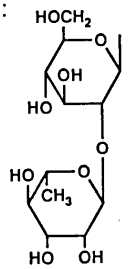

V :

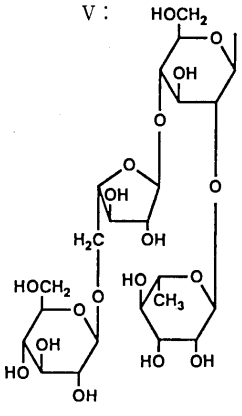

VI :

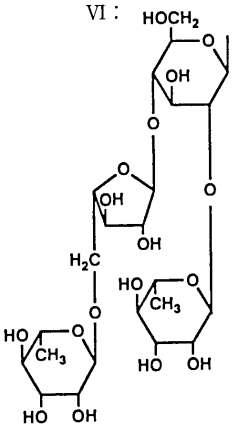

VII :

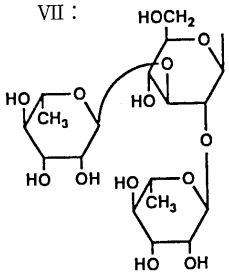

Chart 1

scin,[1d] methyl protoreclinatoside[1a] and methyl proto-Pb,[1e] respectively.

Two compounds, **13** and **14**, were separated from the methanol extract of *Licuala spinosa*, and **13** was identified as vitexin[1d] by direct comparison.

14 was positive in the Liebermann–Burchard reaction and in the Ehrlich reaction. Based on the IR and ^{13}C-NMR spectra, **14** was suggested to be a furostanol tetraoside. On enzymatic hydrolysis with almond emulsin, **14** afforded D-glucose and a prosapogenin (**14a**), which was suggested to be (25*S*)-spirostanol triglycoside by IR and ^{13}C-NMR spectra. On acidic hydrolysis, **14a** gave D-glucose, L-rhamnose and an aglycone, which was suggested to be a mixture of yamogenin and diosgenin. The ^{13}C-NMR spectrum of **14a** showed three anomeric carbon signals and two methyl signals corresponding to C-6 methyl group of L-rhamnose. By comparison of ^{13}C-NMR spectra, the structure of sugar moiety of **13a** was deduced to be the same as that of dioscin, which has been obtained from the Palmae plant, *Trachycarpus fortunei*.[1e] Finally, the structure of **14a** was established to be as the (25*S*)-isomer of dioscin,[10] and that of **14** was the (25*S*)-isomer of methyl proto-dioscin.

We are reporting the isolation of three new steroid saponins, methyl (25*S*)-proto-Pb, methyl (25*S*)-proto-loureiroside and methyl (25*S*)-proto-dioscin, along with three known steroid saponins and eight known flavonoid glycosides. We also described the isolation of tricin 7-neohesperidoside from *P. humilis* var. *hanceana* and *P. dactylifera*. In 1974, Williams and Harborne carried out a chemotaxonomical study on the leaf flavonoids of Saccharum and related genera,[9] and they reported that tricin 7-rutinoside, the isomer of **8**, was found in palms, while 7-neohesperidoside (**8**) was found only in the Saccharinae of the Gramineae. This conclusion is incompatible with our present study and our investigation on the Palmae plants will be continued.

Experimental

All melting points were determined on a Yanaco micro-melting point apparatus (hot-stage type) and are uncorrected. The optical rotations were measured with a JASCO DIP-140 polarimeter at room temperature. The IR spectra were recorded with a JASCO IR-810 and the NMR spectra were recorded with a JEOL GX-400 spectrometer (400 MHz for ^{1}H-NMR and 100 MHz for ^{13}C-NMR). Chemical shifts are given on a δ (ppm) scale with tetramethylsilane (TMS) as an internal standard. Gas-liquid chromatography (GLC) was run on a Shimadzu GC-6A unit equipped with a flame ionization detector. Experimental conditions for sugars: (a) column, 5% SE-52 on Chromosorb W 3 mm × 2 m; column temp., 180 °C; injection temp., 200 °C; carrier gas N_2, 1.2 kg/cm^2; samples, trimethylsilyl (TMS) ether. (b) column, 5% SE-52 on Chromosorb W 3 mm × 2 m; column temp., 170 °C; injection temp., 180 °C; carrier gas N_2, 1.1 kg/cm^2; samples, TMS ether. TLC was performed on precoated Kieselgel 60 F_{254} plates (Merck) using the following solvents: solvent 1 (solvent for the identification of glycosides); $CHCl_3$–MeOH–H_2O (7:3:0.4, v/v), solvent 2; CH_2Cl_2–acetone (99:1, v/v). Detection was made by spraying 10% H_2SO_4 followed by heating.

Extraction and Isolation of the Compounds from the Leaves Fresh leaves of *P. canariensis* hort. ex CHABAUD (5.66 kg), *P. dactylifera* L. (3.74 kg) and *P. humilis* ROYLE var. *hanceana* BECC. (2.4 kg) harvested in Hachijo island, in Tokyo, in January 1986 and dried leaves of *Licuala spinosa* WURMB. (2.40 kg) harvested in Okinawa in January 1987 were respectively chopped and extracted with MeOH at room temperature. a) *P. canariensis*: The MeOH extract was evaporated to dryness *in vacuo*. The residue (294.36 g) was suspended in water (800 ml) and partitioned with ether (200 ml × 5). The ether layer was concentrated *in vacuo* to afford the ether extract (12.38 g), and the aqueous layer was partitioned with BuOH saturated with water (200 ml × 5). The BuOH-soluble layer was concentrated under reduced pressure to afford the BuOH extract (25.49 g) and the aqueous layer was concentrated *in vacuo* to give the water extract (224.86 g). The BuOH extract was subjected to column chromatography on Sephadex LH-20 with MeOH to afford four fractions, fr. I (0.18 g), fr. II (2.56 g), fr. III (19.20 g), and fr. IV (0.99 g). Fraction II was subjected to column chromatography on silica gel with $CHCl_3$–MeOH–H_2O (7:3:0.4, v/v) followed with $CHCl_3$–MeOH–H_2O (75:25:3, v/v) to yield **6** (0.11 g). Fraction III was rechromatographed on Sephadex LH-20 with MeOH to fractionate into three fractions (fr. I′ (7.78 g), fr. 2′ (8.92 g), fr. 3′ (0.23 g)). Fraction 2′ was subjected to column chromatography on Avicel with $CHCl_3$–MeOH–H_2O (7:3:1, v/v, lower phase) to afford five fractions (fr. A′ (2.29 g), fr. B′ (1.94 g), fr. C′ (1.79 g), fr. D′ (0.66 g), fr. E′ (1.91 g)). Fraction B′ was crystallized from MeOH to afford **1** (0.16 g), and the filtrate was subjected to column chromatography on octadecyl silica (ODS) with 60% MeOH to afford **2** (0.68 g). Fraction C′ was chromatographed on Avicel with $CHCl_3$–MeOH–H_2O (75:25:10, v/v, lower phase) followed by ODS with 60% MeOH to afford **3** (0.54 g) and **4** (0.20 g). Fraction D′ was chromatographed on Avicel with $CHCl_3$–MeOH–H_2O (75:25:10, v/v, lower phase) to afford **5** (0.28 g).

b) *P. humilis* var. *hanceana*: The MeOH extract (426.81 g) was treated by the same method to afford the ether extract (9.80 g), the BuOH extract (68.05 g) and the water extract (147.95 g). The BuOH extract was subjected to column chromatography on Sephadex LH-20 with MeOH to give four fractions, fr. I (0.15 g), fr. II (7.19 g), fr. III (42.82 g) and fr. IV (14.64 g). Fraction II was subjected to column chromatography on silica gel with $CHCl_3$–MeOH–H_2O (a: 13:7:1, v/v; b: 7:3:0.4, v/v; c: 13:7:1, v/v) to afford **6** (0.14 g) and **9** (0.95 g). Fraction III was subjected column chromatography on Sephadex LH-20 (MeOH) followed by Avicel ($CHCl_3$–MeOH–H_2O = 7:3:1, v/v, lower phase) to give **1** (0.10 g), **7** (0.25 g) and **8** (0.30 g).

c) *P. dactylifera*: The MeOH extract (156.27 g) was treated in the same way as described in a), and afforded the ether extract (6.57 g), the BuOH extract (11.55 g) and the water extract (137.87 g). The BuOH extract was subjected to column chromatography on Sephadex LH-20 with MeOH to give four fractions, fr. I (0.03 g), fr. II (5.34 g), fr. III (6.04 g) and fr. IV (0.61 g). Fraction II was subjected to column chromatography on silica gel with $CHCl_3$–MeOH–H_2O (a: 13:7:1, v/v; b: 75:25:3, v/v; c: 7:3:0.4, v/v) to afford **10** (0.04 g), **11** (0.95 g) and **6** (0.41 g). Fraction III was subjected to column chromatography on Sephadex LH-20 (MeOH), Avicel ($CHCl_3$–MeOH–H_2O = 7:3:1, v/v, lower phase) and ODS (60% MeOH) to give **1** (0.01 g), **2** (0.02 g) and **8** (0.03 g).

d) *Licuala spinosa*: The MeOH extract (401.33 g) was treated in the same way as described in a), and afforded the ether extract (84.49 g), the BuOH extract (46.57 g) and the water extract (215.90 g). The BuOH extract was subjected to column chromatography on Sephadex LH-20 with MeOH to afford five fractions, fr. I (0.25 g), fr. II (11.17 g), fr. III (19.79 g), fr. IV (4.66 g) and fr. V (6.09 g). Fraction II was subjected to column chromatography on silica gel with $CHCl_3$–MeOH–H_2O (a: 7:3:0.4, v/v; b: 75:25:3, v/v; c: 8:2:0.2, v/v) to afford **14** (0.26 g). Fraction IV was subjected to column chromatography on Avicel with $CHCl_3$–MeOH–H_2O = 7:3:1, v/v, lower phase) to afford **13** (0.11 g).

Properties of 1—14 **1**: Yellow needles from MeOH, mp 228—231 °C (dec.), $[\alpha]_D$ −50.7° (c=0.34, pyridine). **2**: Yellow prisms from MeOH, mp 161—163 °C (dec.), $[\alpha]_D$ −10.6° (c=0.39, MeOH). **3**: Yellow needles from aqueous MeOH, mp 181—183 °C (dec.), $[\alpha]_D$ −9.0° (c=0.34, MeOH). **4**: A pale yellow powder from MeOH–AcOEt, (mp 178—180 °C (dec.)), $[\alpha]_D$ −12.4° (c=0.37, MeOH). **5**: Pale yellow needles from H_2O, mp 183—185 °C (dec.), $[\alpha]_D$ +3.8° (c=0.45, EtOH). **7**: Pale yellow needles from aqueous MeOH, mp 239—242 °C (dec.), $[\alpha]_D$ −46.9° (c=0.37, MeOH). **8**: Pale yellow needles from aqueous MeOH, mp 179—181 °C (dec.), $[\alpha]_D$ −84.8° (c=0.34, MeOH). IR ν_{max}^{KBr} cm^{-1}: 3520—3300, 1660, 1620. UV λ_{max}^{MeOH} nm (log ε): 250 (4.21), 271 (4.18), 349 (4.31). $\lambda_{max}^{MeOH+AlCl_3}$ nm: 276, 300, 394. $\lambda_{max}^{MeOH+CH_3COONa}$ nm: 250, 271, 349. *Anal.* Calcd for $C_{29}H_{34}O_{16}\cdot 3/2H_2O$: C, 52.33; H, 5.60. Found: C, 52.08; H, 5.28. The properties of tricin 7-*O*-neohesperidoside were not reported in detail in the literature.[9] **13**: Yellow needles from MeOH, mp 255—258 °C (dec.) $[\alpha]_D$ −84.8° (c=0.34, MeOH). **6**: A white powder from MeOH–AcOEt, (mp 177—179 °C (dec.)), $[\alpha]_D$ −87.2° (c=0.35, pyridine). IR ν_{max}^{KBr} cm^{-1}: 3500—3300 (OH). ^{13}C-NMR (in C_5D_5N at 50 °C) δ: aglycone; 38.1 (C_1), 30.7 (C_2), 78.6 (C_3), 39.5 (C_4), 141.0 (C_5), 121.8 (C_6), 32.9 (C_7), 32.3 (C_8), 50.9 (C_9), 37.7 (C_{10}), 21.7 (C_{11}), 40.3 (C_{12}), 41.0 (C_{13}), 57.1 (C_{14}), 32.8 (C_{15}), 81.7 (C_{16}), 63.4 (C_{17}), 16.7 (C_{18}), 20.0 (C_{19}), 41.3 (C_{20}), 18.1 (C_{21}), 112.9 (C_{22}), 35.0 (C_{23}), 32.7 (C_{24}), 31.5 (C_{25}), 64.6 (C_{26}), 16.8 (C_{27}), 47.8 (OCH_3). Sugar moiety; glucose (→^{3}aglycone) 100.6 (C_1), 80.6 (C_2), 78.4

(C_3), 77.2 (C_4), 78.9 (C_5), 61.9 (C_6); rhamnose ($\rightarrow^2$glucose) 102.2 (C_1), 72.7 (C_2), 73.1 (C_3), 74.5 (C_4), 69.8 (C_5), 19.3 (C_6); rhamnose ($\rightarrow^4$glucose) 103.2 (C_1), 73.1 (C_2), 70.6 (C_3), 78.0 (C_4), 68.8 (C_5), 19.1 (C_6); rhamnose ($\rightarrow^4$rhamnose) 102.5 (C_1), 72.9 (C_2), 73.0 (C_3), 74.3 (C_4), 73.4 (C_5), 18.9 (C_6); glucose ($\rightarrow^{26}$aglycone) 105.1 (C_1), 75.5 (C_2), 78.9 (C_3), 72.3 (C_4), 78.6 (C_5), 64.6 (C_6). *Anal.* Calcd for $C_{58}H_{96}O_{26}\cdot 2H_2O$: C, 55.93; H, 0.89. Found: C, 55.69; H, 7.68. **9**: A white powder from MeOH–AcOEt, (mp 185—187 °C (dec.)), $[\alpha]_D$ −78.3° ($c=0.37$, pyridine). IR ν_{max}^{KBr} cm^{-1}: 3500—3300 (OH). ^{13}C-NMR (in C_5D_5N at 50 °C) δ: Each signal of the aglycone moiety of **9** was analogous to that of **6**. Sugar moiety; glucose ($\rightarrow^3$aglycone) 100.5 (C_1), 78.9 (C_2), 78.1 (C_3), 76.9 (C_4), 78.5 (C_5), 62.0 (C_6); rhamnose ($\rightarrow^2$glucose) 102.2 (C_1), 73.1 (C_2), 72.6 (C_3), 74.5 (C_4), 69.8 (C_5), 19.1 (C_6); arabinose ($\rightarrow^4$glucose) 109.9 (C_1), 83.4 (C_2), 78.6 (C_3), 84.6 (C_4), 70.6 (C_5); glucose ($\rightarrow^4$arabinose) 105.4 (C_1), 75.3 (C_2), 78.3 (C_3), 72.1 (C_4), 77.9 (C_5), 63.4 (C_6); glucose ($\rightarrow^{26}$aglycone) 105.1 (C_1), 75.5 (C_2), 78.9 (C_3), 72.3 (C_4), 78.6 (C_5), 64.6 (C_6). *Anal.* Calcd for $C_{57}H_{94}O_{27}\cdot H_2O$; C, 55.69; H, 7.87. Found: C, 55.45; H, 7.89. **10**: A white powder from MeOH–AcOEt, (mp 173—177 °C (dec.)), $[\alpha]_D$ −87.6° ($c=0.53$, pyridine). **11**: A white powder from MeOH–AcOEt, (mp 150—152 °C (dec.)), $[\alpha]_D$ −86.7° ($c=0.43$, pyridine). **12**: A white powder from MeOH–AcOEt, (mp 176—179 °C (dec.)), $[\alpha]_D$ −83.1° ($c=0.43$, pyridine). **14**: A white powder from MeOH–AcOEt, (mp 166—168 °C (dec.)), $[\alpha]_D$ −73.0° ($c=0.69$, pyridine). IR ν_{max}^{KBr} cm^{-1}: 3500—3300 (OH). ^{13}C-NMR (in C_5D_5N at 50 °C) δ: Each signal of the aglycone moiety of **9** was analogous to that of **6**. Sugar moiety; glucose ($\rightarrow^3$aglycone) 100.6 (C_1), 79.7 (C_2), 78.2 (C_3), 77.1 (C_4), 78.3 (C_5), 62.0 (C_6); rhamnose ($\rightarrow^2$glucose) 102.1 (C_1), 72.7 (C_2), 73.1 (C_3), 74.5 (C_4), 69.7 (C_5), 19.1 (C_6); rhamnose ($\rightarrow^4$glucose) 103.3 (C_1), 73.2 (C_2), 70.6 (C_3), 78.0 (C_4), 68.8 (C_5), 19.1 (C_6); glucose ($\rightarrow^{26}$aglycone) 105.2 (C_1), 75.3 (C_2), 78.9 (C_3), 72.3 (C_4), 78.7 (C_5), 64.6 (C_6). *Anal.* Calcd for $C_{52}H_{86}O_{22}\cdot 3/2H_2O$: C, 57.28; H, 8.23. Found: C, 57.13; H, 7.82.

Enzymatic Hydrolysis of 6, 9 and 14 Each aqueous solution (30 ml) of **6** (50 mg), **9** (50 mg) and **14** (100 mg) was incubated with almond emulsin (50 mg) at 37 °C for 12 h. The precipitate was collected by filtration and dried. Crude hydrolysates of **6** and **9** were purified on silica gel column chromatography with $CHCl_3$–MeOH–H_2O (75:25:3 v/v) to afford **6a** (28 mg) and **9a** (12 mg), while that of **14** was subjected to silica gel column chromatography with $CHCl_3$–MeOH–H_2O (8:2:0.2 v/v) to afford **14a** (43 mg). **6a**: Colorless needles from aqueous MeOH, mp 243—245 °C (dec.), $[\alpha]_D$ −115.2° ($c=0.42$, pyridine). IR ν_{max}^{KBr} cm^{-1}: 3580—3300 (OH), 988, 920, 900, 842 (intensity 920 > 900, (25*S*)-spiroketal). ^{13}C-NMR (in C_5D_5N at 50 °C) δ: aglycone; 38.1 (C_1), 30.7 (C_2), 78.6 (C_3), 39.6 (C_4), 141.0 (C_5), 121.8 (C_6), 32.9 (C_7), 32.3 (C_8), 50.9 (C_9), 37.7 (C_{10}), 21.8 (C_{11}), 40.5 (C_{12}), 41.0 (C_{13}), 57.2 (C_{14}), 32.8 (C_{15}), 81.5 (C_{16}), 63.3 (C_{17}), 16.9 (C_{18}), 20.0 (C_{19}), 43.0 (C_{20}), 15.4 (C_{21}), 109.9 (C_{22}), 28.1 (C_{23}), 27.1 (C_{24}), 26.8 (C_{25}), 65.5 (C_{26}), 16.9 (C_{27}). Each signal of the sugar moiety attached to C_3 hydroxyl group of the aglycone was analogous to that of **6**. *Anal.* Calcd for $C_{51}H_{82}O_{20}\cdot 3/2H_2O$: C, 58.77; H, 8.22. Found: C, 58.80; H, 8.27. **9a**: Colorless needles from aqueous MeOH, mp 237—239 °C (dec.), $[\alpha]_D$ −85.7° ($c=0.19$, pyridine). IR ν_{max}^{KBr} cm^{-1}: 3500—3300 (OH), 970, 922, 900, 856 (intensity 922 > 900, (25*S*)-spiroketal). ^{13}C-NMR (in C_5D_5N at 50 °C) δ: Each signal of the aglycone moiety of **9a** was analogous to that of **6a**, and each signal of the sugar moiety attached to C_3 hydroxyl group of the aglycone was analogous to that of **9**. *Anal.* Calcd for $C_{50}H_{80}O_{21}\cdot 3H_2O$: C, 56.06; H, 8.09. Found: C, 56.29; H, 7.81. **14a**: Colorless needles from aqueous MeOH, mp 278—282 °C (dec.), $[\alpha]_D$ −111.0° ($c=0.33$, pyridine). IR ν_{max}^{KBr} cm^{-1}: 3500—3310 (OH), 990, 920, 898, 840 (intensity 920 > 900, (25*S*)-spiroketal). ^{13}C-NMR (in C_5D_5N at 50 °C) δ: Each signal of the aglycone moiety of **14a** was analogous to that of **6a**, and each signal of the sugar moiety attached to C_3 hydroxyl group of the aglycone was analogous to that of **14**. *Anal.* Calcd for $C_{45}H_{72}O_{16}\cdot 3/2H_2O$: C, 60.32; H, 8.44. Found: C, 60.14; H, 8.24.

Each filtrate was evaporated to dryness *in vacuo* and the residue was examined by GLC (condition a). GLC t_R (min) 7.5, 11.3 (TMS-glucose).

Acidic Hydrolysis of 6a, 9a and 14a **6a** (10 mg), **9a** (8 mg) and **14a** (10 mg) were separately heated with 2 N HCl–50% dioxane (0.2 ml/mg prosapogenin) for 3 h in a boiling water bath. Each reaction mixture was cooled and neutralized with $NaHCO_3$. The mixture was then diluted with water (1 ml/mg prosapogenin) and extracted with $CHCl_3$. The $CHCl_3$ extract was evaporated to dryness *in vacuo* and the residue was acetylated in the usual way. Each acetate was compared by TLC with solvent 2. The aqueous layer was evaporated to dryness *in vacuo* and the residue was examined by GLC. **6a** and **14a**: Aglycone; TLC *Rf* 0.73 (diosgenin acetate), 0.70 (yamogenin acetate). Sugars: GLC (condition a) t_R (min) 2.4, 3.2 (TMS-rhamnose), 7.5, 11.3 (TMS-glucose). **9a**: Aglycone; TLC *Rf* 0.73 (diosgenin acetate), 0.70 (yamogenin acetate). Sugars: GLC (condition b) t_R (min) 3.2, 3.7, 4.1 (TMS-arabinose), 3.3, 4.4 (TMS-rhamnose), 11.0, 17.1 (TMS-glucose).

Acidic Hydrolysis of 8 **8** (10 mg) was heated in a water bath with 10% H_2SO_4 (10 ml) for 2 h. The reaction mixture was cooled and the precipitate was collected by filtration to afford an aglycone (**8a**; 4 mg) as pale yellow needles from MeOH, mp 264—267 °C (dec.). The aqueous layer was evaporated to dryness *in vacuo* and the residue was examined by GLC. GLC (condition a) t_R (min) 2.4, 3.2 (TMS-rhamnose), 7.5, 11.3 (TMS-glucose).

Determination of Absolute Configurations of Sugars by HPLC Each solution of **6a**, **8**, **9a** and **14a** (1 mg) in 2 N HCl–50% dioxane (2 ml) was heated in a sealed tube for 3 h at 100 °C. The reaction mixture was diluted with water and evaporated to remove dioxane. The solution was neutralized with Amberlite IRA-93ZU (OH^- form) and passed through a SEP-PAK C_{18} cartridge to give a sugar fraction. Each component sugar in the solution was reduced to 1-(*N*-acetyl-L-α-methylbenzylamino)-1-deoxyalditol acetate using the method of Asada *et al.*[11] and analyzed by HPLC. Condition: column, supermicro bead Silica gel B-5, 5 μm (10 × 250 mm); solvent, hexane–EtOH (9:1); flow rate, 4 ml/min; detection, ultraviolet (UV) (230 nm). t_R (min) **6a**, **8** and **14a**: L-rhamnose 22.8, D-glucose 37.7. **9a**: L-arabinose 33.0, L-rhamnose 22.8, D-glucose 37.7.

Enzymatic Hydrolysis of 8 **8** (5 mg) was dissolved in McIlvaine buffer (pH 4) and incubated with hesperidinase (1 mg) at 37 °C for 0.5 h to afford **1** (2 mg), which was identified by direct comparison.

Acknowledgment The authors are grateful to Mr. K. Okuyama, Hachijo-cho, Tokyo, Mr. M. Ohbayashi, director of the Southeast Botanical Garden, Okinawa, and Mr. S. Isoda of the Medicinal Plant Garden of Showa University for providing the plant materials. Thanks are also due to the staff of the Analytical Laboratory of this school for elemental analysis, IR and NMR spectral measurements.

References

1) *a*) K. Idaka, Y. Hirai and J. Shoji, *Chem. Pharm. Bull.*, **39**, 1455 (1991); *b*) *Idem*, *ibid.*, **36**, 1783 (1988); *c*) Y. Hirai, S. Sanada, Y. Ida and J. Shoji, *ibid.*, **34**, 82 (1986); *d*) *Idem*, *ibid.*, **32**, 4003 (1984); *e*) *Idem*, *ibid.*, **32**, 295 (1984).
2) S. Kuwazuka and Y. Oshima, *Nippon Nogeikagaku Kaishi*, **38**, 351 (1964).
3) L. Hörhammer, H. Wagner, H. G. Arndt and H. Kraemer, *Chem. Ber.*, **99**, 1384 (1966).
4) C. D. Douglass, W. L. Howard and S. H. Wender, *J. Am. Chem. Soc.*, **1949**, 2658.
5) Ibarahim El-Sayed El-Kholy and Mohammed Abdel Monem Shaban, *J. Chem. Soc.* (*C*), **1966**, 1140.
6) S. Kiyosawa, M. Hutoh, T. Komori, T. Nohara, I. Hosokawa and T. Kawasaki, *Chem. Pharm. Bull.*, **16**, 1162 (1968).
7) R. Oshima, Y. Yamauchi and J. Kumanotani, *Carbohydr. Res.*, **107**, 169 (1982).
8) R. E. Marker, R. B. Wagner, P. R. Ulshafer, E. L. Wittbecker, D. P. J. Goldsmith and C. H. Ruof, *J. Am. Chem. Soc.*, **69**, 2167 (1947).
9) C. A. Williams and J. B. Harborne, *Phytochemistry*, **13**, 1141 (1974).
10) K. Miyahara, K. Kudo and T. Kawasaki, *Chem. Pharm. Bull.*, **31**, 348 (1983).
11) Y. Asada, M. Ikeno, T. Ueoka and T. Furuya, *Chem. Pharm. Bull.*, **37**, 2747 (1989).

Thermospray Liquid Chromatographic/Mass Spectrometric Analysis of Iridoid Glycosides from *Gardenia jasminoides*

Junko IIDA,*[,a] Masami ONO,[b] Kenichiro INOUE[b] and Tetsuro FUJITA[b]

Analytical Applications Department, Shimadzu Corporation,[a] Nishinokyo-kuwabara-cho, Nakagyo-ku, Kyoto 604, Japan and Faculty of Pharmaceutical Sciences, Kyoto University,[b] Sakyo-ku, Kyoto 606, Japan. *Received January 10, 1991*

Thermospray liquid chromatography/mass spectrometry (TSP LC/MS) was applied to the determination of iridoid glycosides. Monosaccharide glycosides exhibited dependence, in terms of sensitivity and mass spectra, on the ion source block temperature. Disaccharide glycosides exhibited dependence in sensitivity and peak shape on the block temperature. The resulting mass spectra gave qualitative information concerning both the aglycon and sugar moieties as well as molecular weights. A methanol extract from the fruit of *Gardenia jasminoides* was analyzed for iridoid glycosides which were identified by mass spectra and mass chromatograms.

Keywords thermospray; LC/MS; iridoid glycoside; *Gardenia jasminoides*; monosaccharide glycoside; disaccharide glycoside; aglycon moiety; sugar moiety

Introduction

There are many kinds of glycosides which are very important as drugs or natural products. Because glycosides are highly polar and thermally labile, mass spectrometric analyses of these substances have been mainly performed with soft ionization techniques such as fast atom bombardment (FAB),[1-6] field desorption (FD)[2,7] and laser desorption (LD).[8,9] Although each method has its merits, these techniques require isolation and purification of object compounds prior to measurement. This isolation and purification is inconvenient and time-consuming, especially when the object compounds are minor components and/or thermally labile.

From this point of view, liquid chromatography/mass spectrometry (LC/MS) which includes a soft ionization process, is thought to be useful in the determination of polar and thermally labile substances. If LC/MS can be made to give adequate structural information for aglycon and sugar moieties as well as molecular weights of glycosides, it would be the appropriate technique for the identification of these substances. Analytical attempts using a moving belt LC/MS system[10] and a frit FAB LC/MS system[11] have been reported. In those reports, samples used were mixtures of two or three glycosides, but there have been no reports concerning the application of LC/MS to analysis of crude extracts from plants. We investigated iridoid glycosides in the fruit of *Gardenia jasminoides* using thermospray (TSP) LC/MS. Iridoid glycosides are contained in many kinds of crude drug plants[12-13] and these plants have been widely used as antipyretics, anti-inflammatories, laxatives and so on. The fruit of *G. jasminoides* holds an important position in Chinese medicines used as anti-inflammatories and tranquilizers,[14] and some part of its efficacy is due to the iridoid glycosides it contains.[15] To date, ten kinds of iridoid glycosides, which are shown in Fig. 1 (**2**—**11**), have been isolated from this plant.[16-22] We now report the results of the experiments using standard samples of the ten iridoids and extracts from the fruit of *G. jasminoides* to evaluate TSP LC/MS for the determination of glycosides in crude drugs.

Experimental

Preparation of the Extract and Standard Iridoids The fruit of *G. jasminoides* (1 kg) was extracted three times with MeOH (totally 6 l) and

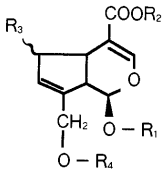

1 : $R_1 = R_3 = R_4 = H$, $R_2 = CH_3$; genipin (M.W. 226)
2 : $R_1 = \beta$-D-Glc, $R_2 = CH_3$, $R_3 = R_4 = H$; geniposide (M.W. 388)
3 : $R_1 = \beta$-D-Glc (6, 1 β) Glc (= gentiobiose), $R_2 = CH_3$, $R_3 = R_4 = H$; genipin gentiobioside (M.W. 550)
4 : $R_1 = \beta$-D-Glc, $R_2 = R_3 = R_4 = H$; geniposidic acid (M.W. 374)
5 : $R_1 = \beta$-D-Glc, $R_2 = R_4 = H$, $R_3 = \alpha$-OH ; deacetylaspelurosidic acid (M.W. 390)
6 : $R_1 = \beta$-D-Glc, $R_2 = CH_3$, $R_3 = \alpha$-OH, $R_4 = H$; methyl deacetylaspelurosidate (M.W. 404)
7 : $R_1 = \beta$-D-Glc, $R_2 = CH_3$, $R_3 = \beta$-OH, $R_4 = H$; scandoside methyl ester (M.W. 404)
8 : $R_1 = \beta$-D-Glc, $R_2 = CH_3$, $R_3 = H$, $R_4 = Ac$; acetylgenipioside (M.W. 430)

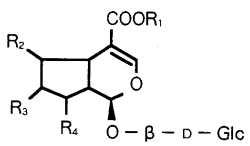

9 : $R_1 = CH_3$, $R_2 = H$, $R_3 = \beta$-OH, $R_4 = CH_2$; gardoside (M.W. 388)
10: $R_1 = H$, $R_2 = \beta$-OH, $R_3 = H$, $R_4 = \alpha$-CH_3, β-OH ; shanziside (M.W. 390)

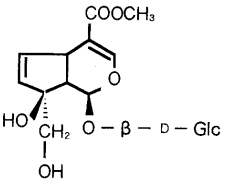

11 gardenoside (M.W. 404)

Fig. 1. Structural Formula of the Iridoids in *Gardenia jasminoides*

the combined extracts were concentrated to 4 l. Insoluble compounds were removed by filtration (0.45 μm mesh). Ten μl of the filtrate was injected onto the LC column.

The standard iridoids (**1**—**11**) which were used for the investigation of chromatographic and mass spectrometric conditions were isolated and purified according to the previously reported methods.[20]

Chemicals and Reagents Ammonium acetate (special grade) was purchased from Wako Pure Chemical Industries, Ltd. Pure water from a Toraypure still (Toray Co., Ltd.) was used in the mobile phase. All other chemicals and reagents used were reagent or chromatographic grade.

LC/MS The standard mixture of iridoid glycoside and the extract were resolved on Shim-pack CLC-ODS (M) (5 μm, 4.6 i.d. × 150 mm) (Shimadzu Co.) at 50 °C with 0.1 M ammonium acetate and acetonitrile (93 : 7, v/v). The mobile phase was degassed prior to use and was delivered at 1.0 ml/min with a Shimadzu LC-6A. Samples were injected with a Model 7125 injector (Rheodyne, U.S.A.). The eluent was introduced into a Shimadzu LCMS-QP1000, which is a quadrupole mass spectrometer equipped with a Vestec TSP interface. Vaporization and ionization were achieved by heating the capillary vaporizer. The ionization mode used was filament off mode. It has been said that a fairly large fraction of low-molecular-weight compounds can be analyzed by setting the vaporizer control temperature about 2—5 °C below the take off point[23] (the temperature at which complete vaporization occurs). The observed take off point was 135—137 °C with the mobile phase and flow rate used, consequently the vaporizer control temperature was maintained at 130—135 °C. The mass range was m/z 120—900.

Results and Discussion

The ionization efficiencies and mass spectra of some compounds have been found to depend upon the ion source block temperature.[24] Thus, the effect of variation in source block temperature on ionization efficiencies and mass spectra were investigated for iridoid glycoside standards. Total ion current (TIC) and characteristic ion intensities as a function of ion source block temperature were monitored. As examples, results for compounds **2** (geniposide) and **3** (genipin gentiobioside) are given. First, mass spectra of compounds **2** and **3** were measured with a block temperature of 300 °C for the purpose of determining their characteristic ions. Figure 2 illustrates the mass spectra of 2.5 μg of **2** and 5 μg of **3**. In Fig. 2a, the ions observed at m/z 209, 227 and 244 correspond to $[\text{aglycon}-17]^+$, $[\text{aglycon}+\text{H}]^+$ and $[\text{aglycon}+\text{NH}_4]^+$, respectively. The ion appearing at m/z 406 is attributed to $[\text{M}+\text{NH}_4]^+$. Ions at m/z 198 ($[\text{glucose}+\text{NH}_4]^+$) and m/z 180 are ascribed to the sugar moiety. In Fig. 2b, the base peak observed at m/z 209 is considered to be $[\text{aglycon}-17]^+$, with the intense ions appearing at m/z 227, 551 and 568 corresponding to $[\text{aglycon}+\text{H}]^+$, $[\text{M}+\text{H}]^+$ and $[\text{M}+\text{NH}_4]^+$, respectively. The ions at m/z 406, 389 and 371 are attributed to $[\text{M}-\text{C}_6\text{H}_{10}\text{O}_5+\text{NH}_4]^+$, $[\text{M}-\text{C}_6\text{H}_{10}\text{O}_5+\text{H}]^+$ and $[\text{M}-\text{C}_6\text{H}_{10}\text{O}_5+\text{H}-\text{H}_2\text{O}]^+$, respectively. The ion at m/z 342 is derived from the sugar moiety ($[\text{gentiobiose}+\text{NH}_4-\text{H}_2\text{O}]^+$). These characteristic ions were used to examine the dependence of mass spectra of **2** and **3** upon ion source temperature. Figure 3 shows the change in TIC and characteristic ion intensities as a function of the ion source block temperature. In Fig. 3a (compound **2**), it is observed that TIC and the intensity of m/z 406 ($[\text{M}+\text{NH}_4]^+$) are maximized at 220 and 210 °C, respectively. Below 240 °C, the base peak is m/z 406 and above this temperature it changes to m/z 209 ($[\text{aglycon}-17]^+$). The changes in TIC and mass spectra with respect to ion source block temperature are similar to

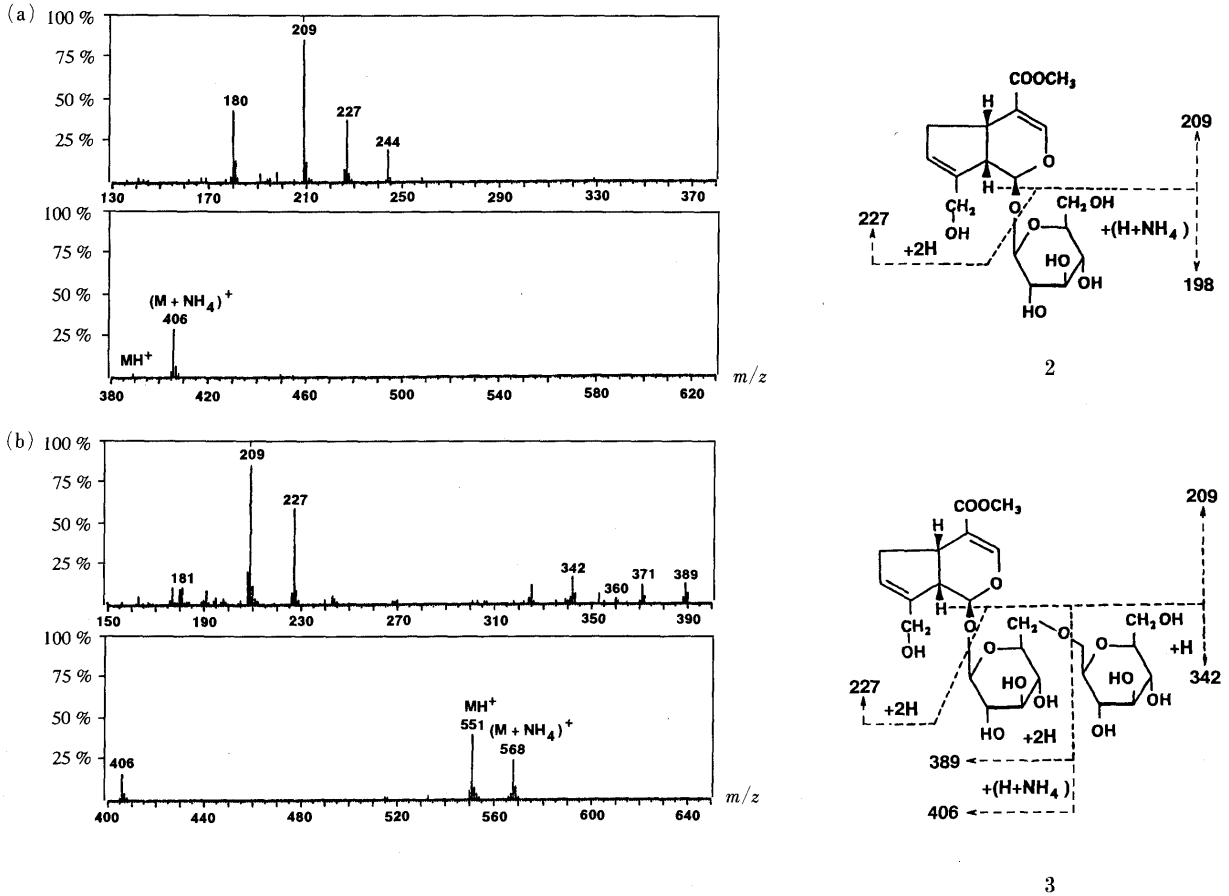

Fig. 2. Mass Spectra of (a) Compound **2** (Geniposide) and (b) Compound **3** (Genipin Gentiobioside) (at Ion Source Block Temperature 300 °C)

the phenomena observed in chemical ionization (CI).[25,26] On the other hand, the maximum of TIC of **3** is at about 300 °C, as shown in Fig. 3b. Although **3** is more thermally labile than **2**, the former requires higher temperatures for ionization. This is in contrast to the results with CI.[25,26] In addition, the chromatographic peak of **3** is affected drastically by the temperature. The peak shape of **3** is much better when the ion source temperature is above 270 °C, and the chromatographic peak height at 300 °C is ten times greater than at 240 °C, because of the improved in peak shape. These facts suggest that the ionization of **3** is affected not only by the gas phase ion-molecular reaction (*i.e.*, CI) but also by other factors. It has been reported that the gas phase ion-molecular reaction is the main ionization mechanism of TSP and that ionization in the liquid phase may contribute to TSP ionization.[23,27] Although it is controversial whether the mechanism in the liquid phase is ion vaporization[23] or ionization by desolvation,[28] it has been accepted that some part of TSP ionization occurs by the electric field on the surface of the fine droplets which are produced by heating of vaporizer and ion source. The strength of the electric field required might be different depending on the polarity or volatility of compound, and highly polar and/or highly non-volatile compounds are believed to require stronger fields. The strength of the electric field on the surface of the fine droplets increases as their diameters decrease, which would result from increasing ion source block temperature. The fact that the ionization of **3** needs a higher ion source block temperature than that of **2** indicates that for the former, the contribution of ionization in the liquid phase is greater than that for the latter, and that in order to promote ionization in the liquid phase, a stronger electric field might be necessary. Since both compounds have the same aglycon, *i.e.*, genipin (**1**), the difference in behavior with changing ion source block temperature must be related to the difference in the sugar moieties. As for other iridoid glycosides in *G. jasminoides* which are linked with a glucose, their total ion intensities are maximized around 220 °C and the base peak ions change in a manner similar to compound **2**. We tested the response of other kinds of glycosides containing disaccharides (ex. saikosaponin a, rutin *etc.*). They provided results similar to those for **3**, suggesting that the sugar moieties contribute more to this temperature dependence than the aglycon moieties.[29]

Figure 4 shows the TIC of the standard mixture of the iridoid glycosides, **1**, **2**, **5**, **7** and **11**. The good response confirms the applicability of the mobile phase to mixtures including iridoid glycosides. The mass spectra of peaks 1—5 in Fig. 4 are shown in Fig. 5, and reveal $[M+NH_4]^+$ as the quasimolecular ions with fragment ions indicating aglycon moieties and sugar moieties. Table I shows relative intensities of diagnostic ions, which give structural information, of iridoid glycosides and iridoid in Fig. 5 and compound **3** in Fig. 2. As can be seen from this table, compounds **5**, **11** and **7** which have two hydroxy groups in their aglycon moieties give $[M+NH_4]^+$ as quasimolecular ions and intense $[M+NH_4-H_2O]^+$. They give $[A+NH_4]^+$ and $[A+NH_4-H_2O]^+$ as the ions ascribed to their aglycon moieties. On the other hand, compounds **2** and **3** give $[M+NH_4]^+$ and $[M+H]^+$ as quasimolecular ions and $[A+H]^+$ as well as $[A+NH_4]^+$ as the fragment ions derived from the aglycon moieties. The aglycon moiety of these compounds is genipin (**1**) which has a hydroxy group. All glycosides shown in Table I give [glucose+NH_4]$^+$ and [glucose+NH_4-H_2O]$^+$ as the fragment ions derived from sugar moieties. In the spectrum of compound **3**, [gentiobiose+NH_4]$^+$ (*m/z* 360) and [gentiobiose+NH_4-H_2O]$^+$ (*m/z* 342) are observed. Using these ions,

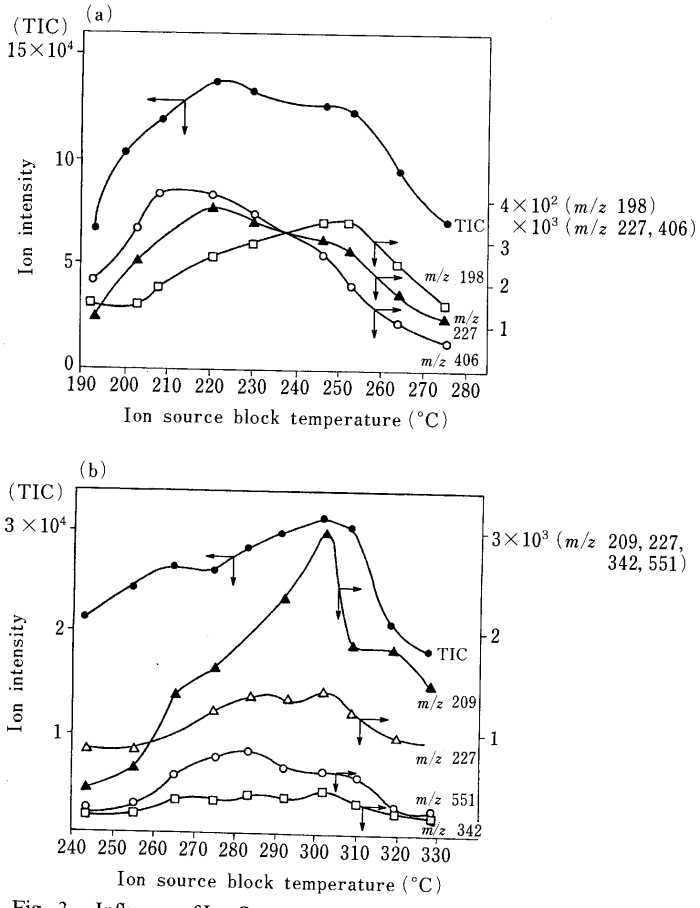

Fig. 3. Influence of Ion Source Block Temperature on Intensities of Total Ion Current and Characteristic Ions of (a) Compound **2** and (b) Compound **3**

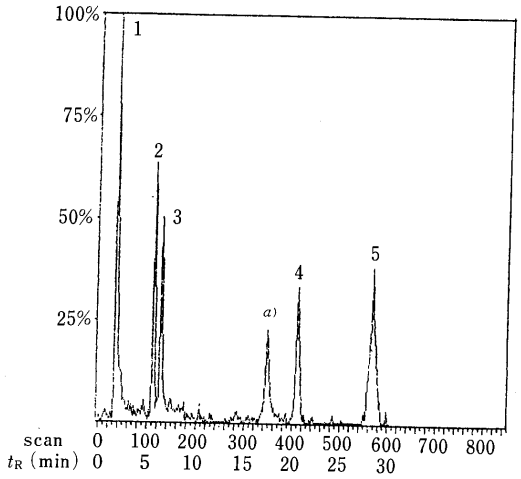

Fig. 4. Total Ion Current of a Mixture of Five Standard Iridoids (at Ion Source Block Temperature 220°C)

Peak 1: compound**5**, peak 2: compound **11**, peak 3: compound **7**, peak 4: compound **2**, peak 5: compound **1**. (Peak *a*) is a decomposition product of scandside methyl ester. It may be produced during storage because iridoide glycosides are unstable.)

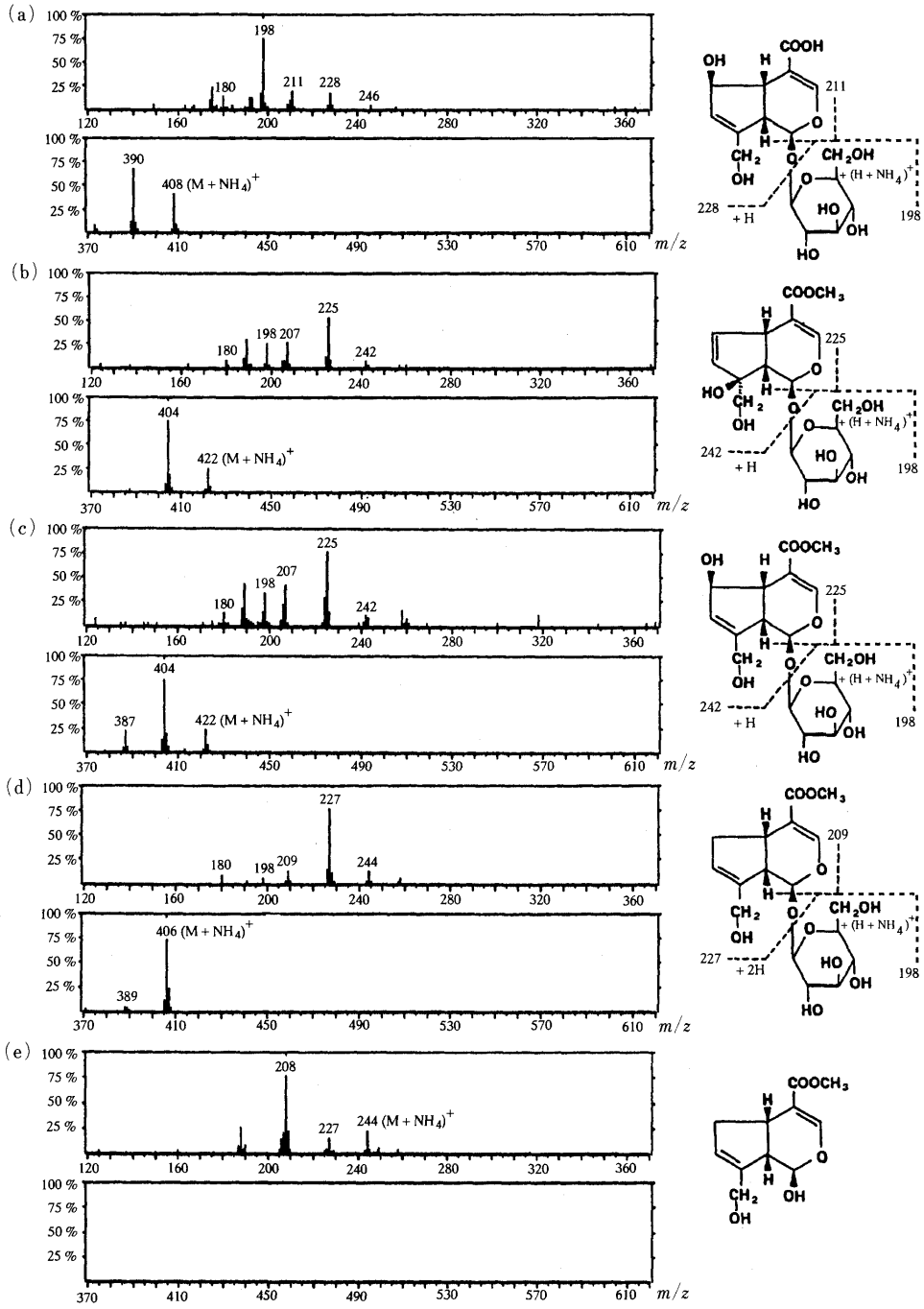

Fig. 5. Mass Spectra of Peaks 1—5 (a—e) of Fig. 4

(a) peak 1; (b) peak 2; (c) peak 3; (d) peak 4; (e) peak 5.

TABLE I. Relative Intensities (%) of Characteristic Ions of Iridoid Glycosides and Iridoid Observed in Fig. 5a—e (Peaks 1—5)[a] and Fig. 2b[b]

Compound	Characteristic ions[c]										
	$[M+NH_4]^+$	$[M+H]^+$	$[M+NH_4-H_2O]^+$	$[A+NH_4]^+$	$[A+H]^+$	$[A+NH_4-H_2O]^+$	$[A-OH]^+$	$[A-OH-H_2O]^+$	$[A-OH-2H_2O]^+$	$[Glc+NH_4]^+$	$[Glc+NH_4-H_2O]^+$
5 (Peak 1)	43	—	68	5	—	19	21	14	24	100	15
11 (Peak 2)	26	—	100	4	—	9	54	28	30	27	9
7 (Peak 3)	24	—	100	8	—	13	78	44	45	35	16
2 (Peak 4)	100	5	—	19	81	—	15	4	—	8	11
1 (Peak 5)[e]	25	17									
3[d]	24	40	—	4	60	—	100	10	—	2	10

a) Ion source block temperature: 220 °C. *b*) Ion source block temperature: 300 °C. *c*) A, aglycon; Glc, glucose. *d*) The base peak (relative intensity: 100%) is *m/z* 208 which is assumed to be $[M+NH_4-2H_2O]^+$. *e*) Other characteristic ions observed in Fig. 2b and their relative intensities (%) are: *m/z* 406: $[M+NH_4-C_6H_{10}O_5]^+$ (16%), *m/z* 389: $[M+H-C_6H_{10}O_5]^+$ (13%), *m/z*: 360 [gentiobiose + NH_4]$^+$ (4%), *m/z* 342: [gentiobiose + NH_4-H_2O]$^+$ (18%).

each iridoid glycoside can be clearly identified. In compound **1**, $[M+H]^+$ and $[M+NH_4]^+$ appear as quasi-molecular ions and an ion eighteen mass unit lower than molecular ion as the base peak. Comparing the mass spectra of **2** obtained with ion source block temperatures at 220 and 300 °C (Fig. 5d with Fig. 2a), respectively, the intensities of the fragment ions ascribed to the aglycon moiety and sugar moiety at 300 °C are greater than those at 220 °C. Although the sensitivity to monosaccharide glycosides is maximized at about 220 °C, the ion source block temperature for the analysis of the extract from the fruit of *G. jasminoides* was fixed at 300 °C, based on the amount of structural information of these glycosides obtainable at this temperature and the increased ionization efficiency of **3**.

At this point, in order to confirm that mass chromatograms produced by characteristic ions could be effective in detecting and identifying iridoid glycosides, an extract from *G. jasminoides* was analyzed. The TIC of the extract is shown in Fig. 6. The compounds of peaks 1—6 were identified by mass spectra, mass chromatograms and retention times. The sample amount for this injection was equivalent to 2.5 mg of the fruit. As an example, the mass spectra of the gardenoside standard (**11**) and that of the corresponding peak 2 in the extract are exhibited in Fig. 7a and b, respectively. The spectra compare well and the latter is not interfered with by co-eluting compounds. Figure 8 shows three peaks, 2, 3 and 4, on the mass chromatograms produced by *m/z* 422 and 404. These ions correspond to $[M+NH_4]^+$ and $[M+NH_4-H_2O]^+$ of both **11** (gardenoside; peak 2) and **7** (scandoside methyl ester; peak 4), which have the same molecular weight. However, only two peaks, 2 and 4, appear on the TIC. Considering the retention time of peak 3 and mass spectrum constructed from the mass chromatogram peak, peak 3 was identified as **6** (methyl deacetylaspelurosidate). It was confirmed by checking mass spectra and mass chromatograms that peaks other than peaks 1—6 were not iridoids.

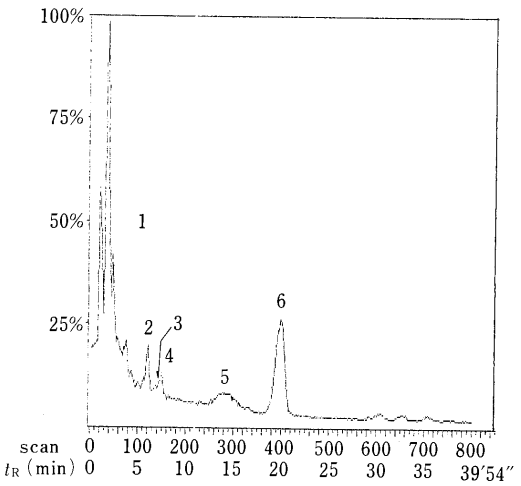

Fig. 6. Total Ion Current of the Extract from the Fruit of *Gardenia jasminoides*

Peak 1: compound **5**, peak 2: compound **11**, peak 3: compound **6**, peak 4: compound **7**, peak 5: compound **3**, peak 6: compound **2**.

Conclusion

The results indicate that TSP LC/MS can be successfully applied to the identification of iridoid glycosides in methanolic extracts from plants. The TSP LC/MS gives qualitative information concerning aglycon and sugar

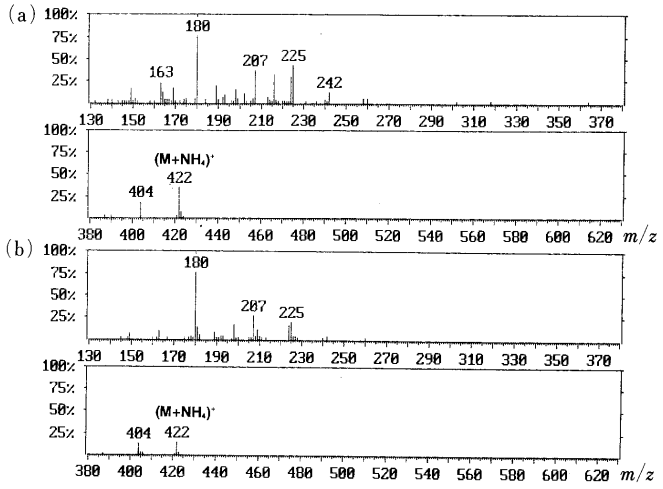

Fig. 7. Mass Spectra of Compound **11**

(a) standard and (b) peak 2 shown in Fig. 6.

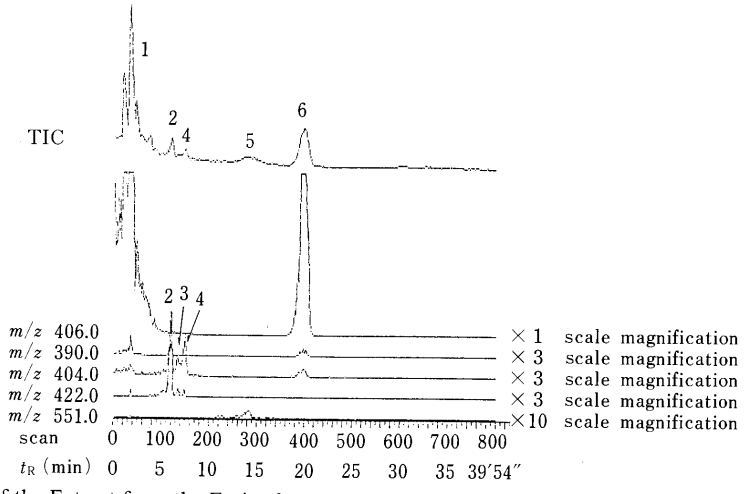

Fig. 8. Mass Chromatograms of the Extract from the Fruit of *Gardenia jasminoides*

m/z 406: $[M+NH_4]^+$ of compound **2**, *m/z* 390: $[M+NH_4-18]^+$ of compound **5**, *m/z* 404: $[M+NH_4-18]^+$ of compounds **6**, **7** and **11**, *m/z* 422: $[M+NH_4]^+$ of compounds **6**, **7** and **11**, *m/z* 551: $[MH]^+$ of compound **3**.

moieties as well as molecular weights. TSP LC/MS allows rapid and reliable identification with a minute amount of material, not only by using mass spectra but also by considering retention time. Furthermore, the detection of minor components can be made by mass chromatograms. The ratio of components contained in a crude drug varies with the producing area and harvest time. It is also known that there are differences in the quantities of glycosides between natural and cultivated products, such as tissue culture. Methods to detect the efficacious components and to evaluate the quality of crude drugs are required as biotechnological cultivation comes to be extensively used for their production. The results of this investigation indicate that TSP LC/MS is appropriate for this purpose.

References

1) D. Fraisse, J. C. Tabet, M. Becci and J. Raynaud, *Biomed. Environ. Mass Spectrom.*, **13**, 1 (1986).
2) R. Isobe, T. Komori, F. Abe and T. Yamauchi, *Biomed. Environ. Mass Spectrom.*, **13**, 585 (1986).
3) Y. Chen, N. Chen, H. Li, F. Zhao and N. Chen, *Biomed. Environ. Mass Spectrom.*, **14**, 9 (1987).
4) M. Stobiecki, W. Olechnowicz-stepien, H. Rzadkowska-bodalska, W. Cisowski and E. Bunda, *Biomed. Environ. Mass Spectrom.*, **15**, 589 (1988).
5) A. Sakushima, S. Nishibe, T. Takeda and Y. Ogihara, *Shitsuryo Bunseki*, **36**, 71 (1988).
6) R. Higuchi, Y. Tokimitsu and T. Komori, *Phytochemistry*, **27**, 1165 (1988).
7) F. Asai, M. Mizuno, M. Iinuma, T. Takeda, C. Phengklai, A. Inada and T. Nakanishi, *Shoyakugaku Zasshi*, **41**, 349 (1987).
8) M. L. Coates and C. L. Wilkins, *Biomed. Environ. Mass Spectrom.*, **13**, 199 (1986).
9) R. E. Shomo, A. Chandrasekaran, A. G. Marshall, R. H. Renning and L. W. Robertson, *Biomed. Environ. Mass Spectrom.*, **15**, 295 (1988).
10) D. E. Games, M. A. McDowall, K. Levsen, K. H. Schafer, P. Dobberstein and J. L. Gower, *Biomed. Environ. Mass Spectrom.*, **11**, 87 (1984).
11) M. Hattori, Y. Kawata, N. Kaniuchi, K. Matuura and T. Namba, *Shoyakugaku Zasshi*, **43**, 228 (1988).
12) H. Limpler, *J. Med. Plant Res.*, **33**, 313 (1978).
13) L. J. El-Naggar and J. L. Bael, *J. Nat. Prod.*, **43**, 649 (1980).
14) T. Kariyone, "Syoyakugaku," Hirokawa Syoten, Tokyo, 1973, p. 245.
15) K. Yamauchi, N. Fujimoto, S. Kuwano, H. Inoue and K. Inoue, *Planta Medica*, **30**, 39 (1976).
16) H. Inoue, S. Saito, H. Taguchi and T. Endo, *Tetrahedron Lett.*, **1969**, 2347.
17) H. Inoue, S. Saito and T. Shingu, *Tetrahedron Lett.*, **1970**, 3581.
18) T. Endo and H. Taguchi, *Chem. Pharm. Bull.*, **18**, 1066 (1970).
19) T. Endo and H. Taguchi, *Chem. Pharm. Bull.*, **21**, 2684 (1973).
20) H. Inoue, Y. Takeda, S. Saito, H. Nishimura and R. Sakurai, *Yakugaku Zasshi*, **94**, 577 (1974).
21) H. Inoue, Y. Takeda and H. Nishimura, *Phytochemistry*, **13**, 2219 (1974).
22) Y. Takeda, H. Nishimura, O. Kadota and H. Inoue, *Chem. Pharm. Bull.*, **24**, 2644 (1976).
23) D. A. Garteiz and M. L. Vestal, *LC Mag.*, **3**, 334 (1985); A. L. Yergey, C. G. Edmonds, I. A. S. Lewis and M. L. Vestal, "Liquid Chromatography/Mass Spectrometry," Plenum Press, New York, 1990, Chapter IV.
24) P. Arpino, *Mass Spectrom. Rev.*, **9**, 631 (1990).
25) F. H. Field, *J. Am. Chem. Soc.*, **91**, 2827 6334 (1969).
26) H. Miyazaki, Y. Hashimoto, M. Iwanaga and T. Kubodera, *J. Chromatogr.*, **99**, 575 (1974).
27) A. J. Alexander and P. Kebarle, *Anal., Chem.*, **58**, 471 (1986).
28) G. Schmelzeisen-Redeker, L. Bütfering and F. W. Röllgen, *Int. J. Mass Spectrom. Ion Proc.*, **90**, 139 (1989).
29) In preparation.

Action of Phosphatidylinostiol-Specific Phospholipase C from *Bacillus thuringiensis* is Significantly Influenced by Coexisting Lipids in Substrate-Detergent Micelles

Takashi KUME,*[,1] Ryo TAGUCHI and Hiroh IKEZAWA

Faculty of Pharmaceutical Sciences, Nagoya City University, 3-1 Tanabe-dori, Mizuho-ku, Nagoya, Aichi 467, Japan. *Received December 25, 1990*

The effects of phosphatidylcholine (PC), phosphatidylethanolamine (PE), sphingomyelin (SM), and cholesterol on the activity of phosphatidylinositol-specific phospholipase C (PI-PLC) from *Bacillus thuringiensis* were studied in detail in phosphatidylinositol (PI)/detergent mixed micelles. By addition of PC, the enzymatic hydrolysis of PI was significantly stimulated in PI/Triton X-100 as well as PI/sodium deoxycholate (SDC) mixed micelles. SM stimulated enzyme activity toward PI/Triton X-100 micelles at a lower molar ratio of SM to PI, but was rather inhibitory at a ratio higher than 2.0. The enzyme activity became significantly lower with an increase of PE or cholesterol in PI/Triton X-100 micelles. Actually, both PE and cholesterol were intensively inhibitory when added at a higher molar ratio to PI in Triton X-100-containing micelles. In the system of PI/SDC mixed micelles, not only PC but also SM, PE and cholesterol enhanced the enzymatic hydrolysis of PI. The difference between PI/Triton X-100 and PI/SDC micelles regarding the effects of these lipids on PI-PLC action, must be dependent on the physical state of micelles formed by these detergents and lipids.

Keywords phosphatidylinositol; PI/detergent micelle; phosphatidylinositol-specific phospholipase C; *Bacillus thuringiensis*

Phosphatidylinositol (PI)-specific phospholipase C (EC 3.1.4.10, PI-PLC), which catalyzes the hydrolysis of PI to yield diacylglycerol and *myo*-inositol 1,2-cyclic phosphate, is known to be produced by several gram-positive bacteria such as *Staphylococcus aureus*,[2] *Clostridium novyi*,[3] *Bacillus cereus*[4,5] and *Bacillus thuringiensis*.[6,7] These bacterial PI-PLCs are now being used in order to investigate glycosylphosphatidylinositol (GPI)-anchored antigens and enzymes, since most of these membranous proteins have been shown to be solubilized by the action of PI-PLCs.[5,8,9] Especially, PI-PLC from *B. thuringiensis* has now become widely used in studies on GPI-anchored proteins. Recently, complementary deoxyribonucleic acid (cDNA) cloning of this enzyme disclosed its amino acid sequence.[10,11] However, the mechanism of action of this enzyme was not sufficiently clarified.

PI exists as one of the minor components in the biomembranes, where the PI content is only 5—10% of the total phospholipids. Therefore, the action of PI-PLC on membranous PI must be significantly interfered with by other lipid constituents in these membranes. In the present study, as one model for membrane circumstances surrounding PI, we examined the influence of other phospholipids and cholesterol on the action of PI-PLC from *B. thuringiensis* toward PI-detergent micelles.

Materials and Methods

Materials PI was purified from an autolysate of baker's yeast by batch operation with diethylaminoethyl (DEAE)-cellulose or silicic acid column chromatography.[12,13] Phosphatidylcholine (PC) and phosphatidylethanolamine (PE) were prepared from egg yolk, and sphingomyelin (SM) from bovine brain by silicic acid column chromatography.[13] According to the method described in the previous report,[7] PI-PLC was purified from the culture broth of *B. thuringiensis* IAM 12077 in a homogeneous state, as indicated by polyacrylamide gel electrophoresis. All other chemicals used were of analytical reagent grade unless otherwise stated.

Enzyme Assay The activity of PI-PLC was determined by the method reported previously.[6]

Action of PI-PLC on Mixed Micelles Containing PI, Other Lipids and Detergents Reaction mixtures containing 10 munits of PI-PLC, 0.02% bovine serum albumin and PI/one of other lipids (PC, PE, SM and cholesterol)/Triton X-100 or sodium deoxycholate (SDC) mixed micelles in 40 mM borate-NaOH, pH 7.5, were incubated at 37°C for 10 min. The reaction was terminated by the addition of chloroform-methanol-HCl (66:33:1), and the mixtures were centrifuged at $3000 \times g$ for 5 min. Then, aliquots of the upper layer were withdrawn from the mixtures and subjected to phosphate analysis according to the method of Eibl and Lands,[14] after oxidation of the organic phosphate by the method of Fiske and Subbarow.[15]

Results

When PI in the mixed micelles containing detergents such as Triton X-100 and SDC was hydrolyzed by PI-PLC, there were optimal molar ratios of the detergents to PI; that of Triton X-100 was 0.8 and that of SDC, 1.93.[6] Thus, in the present experiments, the molar ratio of Triton X-100 or SDC to total lipids was kept at 0.8 or 1.93, respectively, according to the above results.

Influence of Other Phospholipids and Cholesterol on PI-PLC Action toward PI/Triton X-100 Mixed Micelles At first, the action of PI-PLC toward PI/Triton X-100

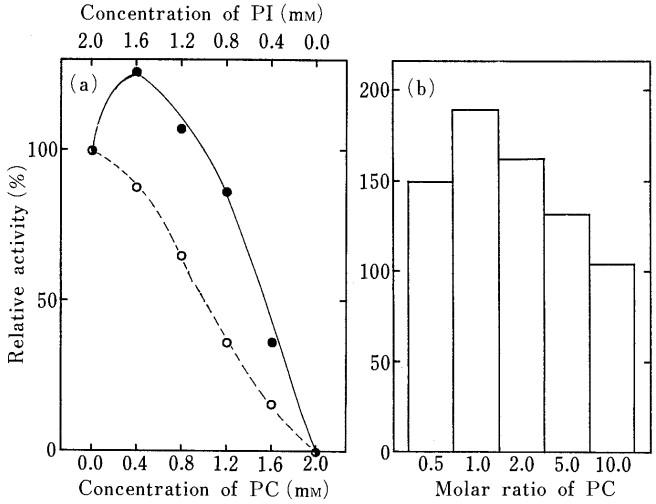

Fig. 1. Effect of PC Addition on PI-PLC Activity toward PI/Triton X-100 Mixed Micelles

The molar ratio of total lipids to Triton X-100 was kept at 0.8. (a) The molar ratio of PI to PC was varied, keeping the total lipid concentration at 2 mM. ○, PI/detergent; ●, PC/PI/detergent. The enzyme activity toward PI/Triton X-100 at 2 mM PI was considered the control (100%). (b) At 1 mM PI in mixed micelles, only the concentration of PC was varied from 0.5—10 mM. The value in the absence of PC was considered 100%.

mixed micelles was studied in binary mixtures with varying molar ratios of PC *versus* PI at 2 mM total phospholipids. As shown in Fig. 1a, the enzymatic hydrolysis of PI was significantly enhanced by the addition of PC, compared with the hydrolysis in the control runs at each concentration of PI without PC. Secondly, when the concentration of PI was fixed at 1 mM, the hydrolysis of PI was also enhanced by the addition of 0.5—10 mM PC (Fig. 1b). Especially, the enhancing effect reached a maximum at 1 mM PC; *i.e.* the enzymatic hydrolysis of PI nearly doubled in the presence of equimolar PC.

Similarly, SM was added to PI/Triton X-100 mixed micelles, and the enzymatic activity was also estimated in binary mixtures with varying molar ratios of SM *versus* PI at 2 mM total phospholipids. As shown in Fig. 2a, the hydrolysis of PI seemed to be slightly stimulated in the presence of SM at not more than 1.2 mM (the molar ratio SM/PI = 1.5). When the concentration of PI was fixed at 1 mM, however, the stimulating effect of SM on the enzyme activity proved to be limited only at a low molar ratio of SM *versus* PI (Fig. 2b). Actually, the enzymatic hydrolysis of PI decreased against the increase in molar ratio. At ratios higher than 2.0, the activity of PI–PLC was significantly inhibited by coexisting SM.

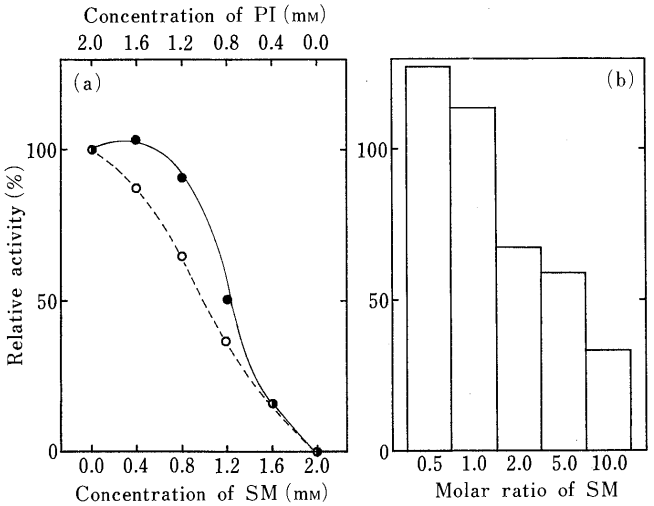

Fig. 2. Effect of SM Addition on PI–PLC Activity toward PI/Triton X-100 Mixed Micelles

The condition of SM addition was the same as that of PC addition, shown in Fig. 1. (a) The molar ratio of PI to SM was varied, keeping the total lipid concentration at 2 mM. ○, PI/detergent; ●, SM/PI/detergent. The enzyme activity toward PI/Triton X-100 at 2 mM PI was considered the control (100%). (b) At 1 mM PI in mixed micelles, only the concentration of SM was varied from 0.5—10 mM. The value in the absence of SM was considered 100%.

At 2 mM total phospholipids, addition of PE with varying molar ratios to PI seemed to have no effect on the enzyme activity toward PI/Triton X-100 mixed micelles, although the activity was significantly inhibited in the presence of 1.6 mM PE with 0.4 mM PI (Fig. 3a). Under a PI concentration fixed at 1 mM, the enzymatic hydrolysis of PI decreased against an increase in the molar ratio of PE to PI (Fig. 3b), as observed in the case of SM addition to PI/Triton X-100 micelles (Fig. 2b). Especially, the hydrolysis of PI was reduced to a level not more than 1/5 that of the control, at the molar ratio of more than 5.0.

As shown in Figs. 4a and 4b, the effect of cholesterol addition was similar to that of PE addition, although inhibition by cholesterol became much greater at the molar ratio of cholesterol *versus* PI above 2.0 (Fig. 4b). Especially, the enzymatic hydrolysis of PI was almost completely inhibited by 10 molar-excess cholesterol.

Influence of Other Phospholipids and Cholesterol on PI–PLC Action toward PI/SDC Mixed Micelles In contrast with PI/Triton X-100 mixed micelles, all the lipid additives tested stimulated the enzymatic hydrolysis of PI in PI/SDC mixed micelles. When PC was added to PI/SDC micelles with a varying molar ratio of PC *versus* PI at 2 mM total phospholipids, the activation profile obtained (Fig. 5a) was almost the same as that obtained in PI/Triton X-100 micelles (Fig. 1a). When the concentration of PI was fixed at 1 mM, however, the stimulating effect of PC on PI–PLC activity toward PI/SDC micelles (Fig. 5b) was much greater

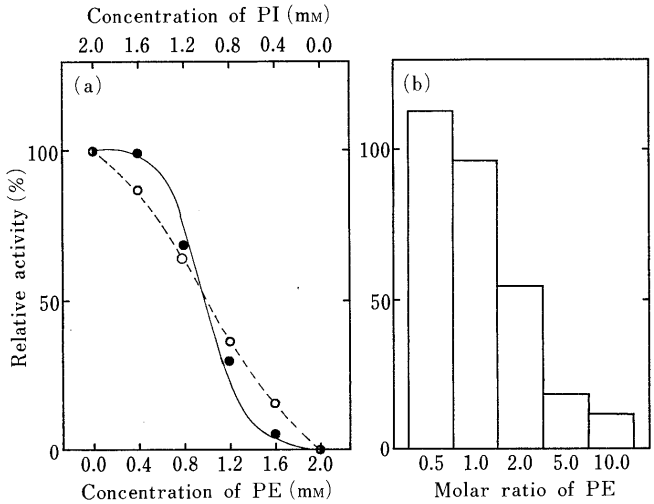

Fig. 3. Effect of PE Addition on PI–PLC Activity toward PI/Triton X-100 Mixed Micelles

The condition of PE addition was the same as that of PC addition, shown in Fig. 1. (a) The molar ratio of PI to PE was varied, keeping the total lipid concentration at 2 mM. ○, PI/detergent; ●, PE/PI/detergent. The enzyme activity toward PI/Triton X-100 at 2 mM PI was considered the control (100%). (b) At 1 mM PI in mixed micelles, only the concentration of PE was varied from 0.5—10 mM. The value in the absence of PE was considered 100%.

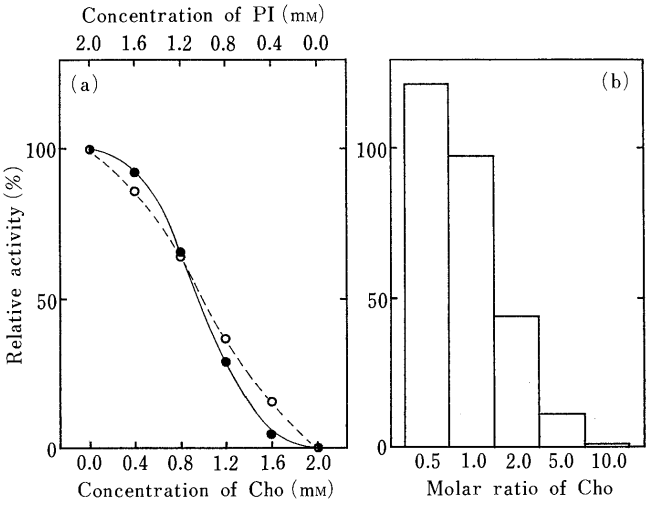

Fig. 4. Effect of Cholesterol Addition on PI–PLC Activity toward PI/Triton X-100 Mixed Micelles

The condition of cholesterol (Cho) addition was the same as that of PC addition, shown in Fig. 1. (a) The molar ratio of PI to cholesterol was varied, keeping the total lipid concentration at 2 mM. ○, PI/detergent; ●, cholesterol/PI/detergent. The enzyme activity toward PI/Triton X-100 at 2 mM PI was considered the control (100%). (b) At 1 mM PI in mixed micelles, only the concentration of cholesterol was varied from 0.5—10 mM. The value in the absence of cholesterol was considered 100%.

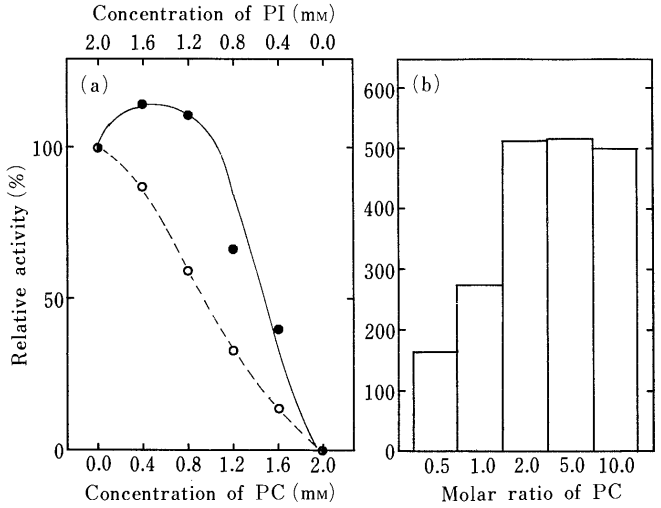

Fig. 5. Effect of PC Addition on PI–PLC Activity toward PI/SDC Mixed Micelles

The molar ratio of total lipids to SDC was kept at 1.93. The graphic illustrations in (a) and (b) were the same as in Fig. 1, except that SDC was used as the detergent instead of Triton X-100.

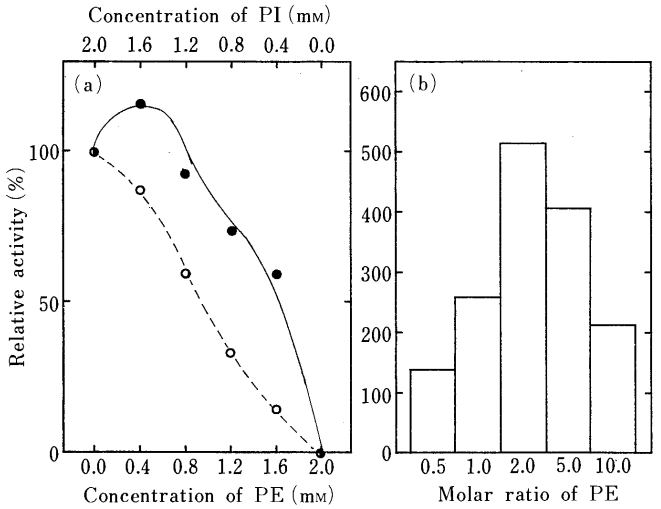

Fig. 7. Effect of PE Addition on PI–PLC Activity toward PI/SDC Mixed Micelles

The condition of PE addition was the same as that of PC addition, shown in Fig. 5. The graphic illustration in (a) and (b) were the same as in Fig. 3, except that SDC was used as the detergent instead of Triton X-100

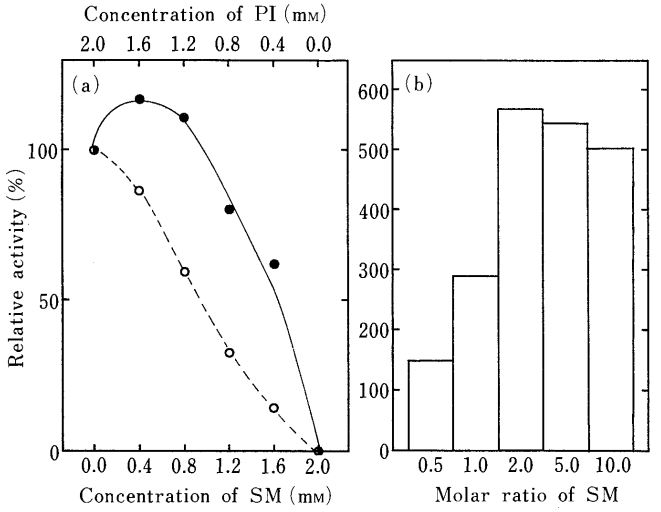

Fig. 6. Effect of SM Addition on PI–PLC Activity toward PI/SDC Mixed Micelles

The condition of SM addition was the same as that of PC addition, shown in Fig. 5. The graphic illustrations in (a) and (b) were the same as in Fig. 2, except that SDC was used as the detergent instead of Triton X-100.

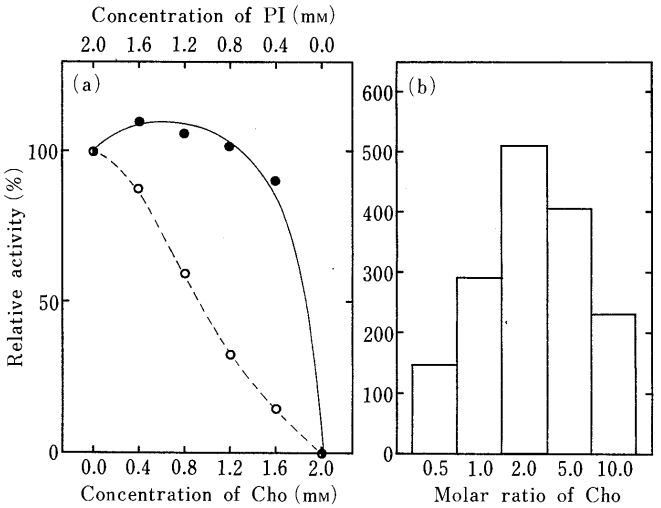

Fig. 8. Effect of Cholesterol Addition on PI–PLC Activity toward PI/SDC Mixed Micelles

The condition of cholesterol addition was the same as that of PC addition, shown in Fig. 5. The graphic illustrations in (a) and (b) were the same as in Fig. 4, except that SDC was used as the detergent instead of Triton X-100.

than that toward PI/Triton X-100 micelles (Fig. 1b). Especially, when the molar ratio of PC *versus* PI was greater than 2.0, the enzymatic hydrolysis of PI became five times as great as that of the control in the absence of PC.

By the addition of SM to PI/SDC mixed micelles, activation profiles (Fig. 6) similar to those by PC addition (Fig. 5) were obtained, contrary to the results of adding SM to PI/Triton X-100 micelles (Fig. 2). Figure 6a shows that PI–PLC activity was stimulated at any molar ratio of SM *versus* PI at 2 mM total phospholipids. When the PI concentration was fixed at 1 mM, the enzymatic hydrolysis of PI was maximally enhanced when the molar ratio of added SM *versus* PI was 2.0, reaching 5.7-fold the enzymatic hydrolysis in the absence of SM (Fig. 6b), while the addition of SM to PI/Triton X-100 micelles at the same molar ratio resulted in significant inhibition of enzyme activity (Fig. 2b).

The effects of PE and cholesterol on the enzymatic hydrolysis of PI in SDC-containing micelles were also different from those in Triton X-100-containing micelles. As shown in Figs. 7 and 8, the activity of PI–PLC was extensively stimulated by the addition of PE or cholesterol to PI/SDC mixed micelles, while enzyme activity toward PI/Triton X-100 micelles was significantly inhibited in the presence of PE or cholesterol at a molar ratio not less than 2.0 (Figs. 3b and 4b). Especially, when the concentration of PI was fixed at 1 mM, both PE and cholesterol exhibited the maximal activation of PI–PLC in PI/SDC micelles at the molar ratio of each (lipid *versus* PI) of 2.0 (Figs. 7b and 8b).

Discussion

In previous studies,[6,7] we found PI–PLC from *B. thuringiensis*, isolated it from the culture broth in a

homogeneous state, and reported its enzymatic properties. The enzyme shows weak activity toward the sonicated suspension of pure PI. However, when substrate micelles are formed by sonication in the presence of Triton X-100 or SDC, the enzyme activity toward PI is markedly increased, reaching a 5-fold or 8-fold level at maximum activation, respectively.[6] Thus, in the present study we examined the effects of membranous lipid components on the action of PI–PLC toward PI/Triton X-100 and PI/SDC mixed micelles, since PI is a minor component in several biomembranes and PI–PLC activity must be greatly influenced by the physical state of the substrate PI, which is surrounded by various membrane lipids.

Therefore, this may be the first study on the modulation of PI–PLC activity toward PI by lipid circumstances, although similar studies were carried out by Dennis and his colleagues on the action of *Naja naja* phospholipase A_2 toward phosphoglycerides.[16]

Triton X-100, a neutral detergent, has long, hydrophilic chains extending from the surface of the micelles into an aqueous medium, and it becomes an activator of PI–PLC, though it is slightly weaker than SDC. When lipids were added at low molar ratio to PI, the enzymatic breakdown of PI in Triton X-100-containing micelles was enhanced, probably due to a dilution effect in which each of the added lipids diluted the hydrophobic moiety of PI as a substitute, expanding the substrate area in the mixed micelles. By this effect, PI–PLC must become more accessible to micellar PI. The differences in the molecules of individual lipids, however, were reflected in the PI–PLC activity toward PI/Triton X-100 micelles at a high molar ratio of each lipid to PI. For instance, the activation of PI–PLC in the presence of PC is not explicable only by the dilution effect, but also by the charges of substrate micelles and enzyme molecule. Since PC is cylindrical in its molecular form,[17] it seems to be without significant effect on the form of PI/Triton X-100 micelles. Both PI and PI–PLC (pI 4.9) have a negative net charge in the reaction medium at pH 7.5, and might repulse each other in the interface of micelles. Since the molecule of PC is nearly neutral, the addition of PC might result in a dispersion of the negatively charged area on the micellar surface of PI/Triton X-100, leading to an increase in the accessibility of PI–PLC to PI.

With regard to molecular properties, SM shares similar characteristics with PC; both PC and SM have cylindrical forms[17] with a choline residue in each polar head. At a high molar ratio of SM to PI, however, SM was rather inhibitory for PI–PLC activity toward PI/Triton X-100 micelles, in contrast with PC. Sphingosine base, existing in the molecule of SM, might be responsible for this difference, since sphingosine has an amide bond and a hydroxyl group located at neighboring C atoms in its framework. These two groups must interact inter- and intramolecularly with each other at a high concentration of SM, inhibiting PI–PLC activity toward PI/Triton X-100 mixed micelles.

PE, one of the neutral phosphoglycerides, has a cone-shaped molecule,[17] in contrast to Triton X-100, which is known to form spherical of oblate-ellipsoid micelles.[18] Thus, the interface of PI/Triton X-100 micelles might be significantly perturbed at a high molar ratio of PE to PI. Probably, such perturbation led to the inhibition of enzyme activity toward micellar PI.

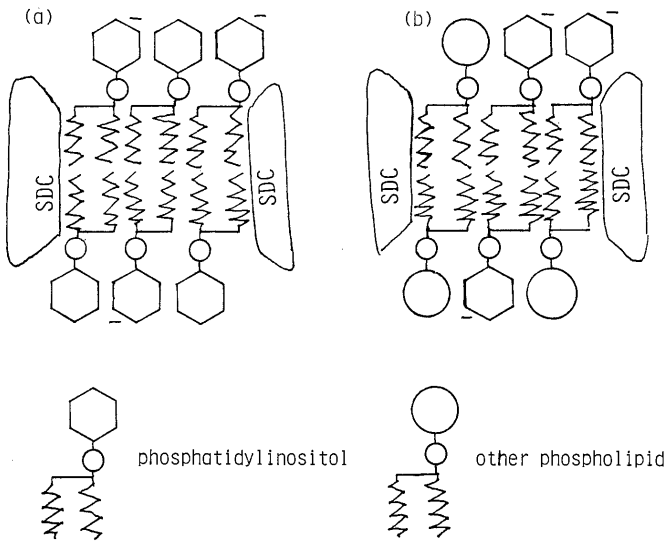

Fig. 9. The Models of PI/SDC (a) and PI/Other Phospholipid/SDC (b) Mixed Micelles

The effect of cholesterol on PI–PLC activity toward PI/Triton X-100 micelles was apparently similar to that of PE. Cholesterol has been shown to reduce the fluidity of the phospholipid bilayer containing unsaturated fatty acids.[19] Also, the presence of cholesterol at a high molar ratio to PI might cause reduction in the fluidity of PI/Triton X-100 mixed micelles, resulting in inhibition of PI–PLC activity. In contrast with PI/Triton X-100 micelles, all the lipids added were stimulative for PI–PLC activity toward PI/SDC mixed micelles. SDC is an amphiphile, which might form the bilayer of mixed micelles with phospholipids by environing diacylglycerol or ceramide moiety of these lipids with its hydrophobic area. Furthermore, SDC-containing micelle usually tend to form a small disk, which might be insignificantly affected by the molecular forms of the individual lipids added. Thus, even at high molar ratio of each lipid to PI, dilution of the hydrophobic moiety of PI with phospholipids or cholesterol seems to favor PI–PLC activity toward PI/SDC mixed micelles due to the dilution effect. In addition, the molecules of SDC and PI contain anionic groups in their hydrophilic regions, a carboxyl group in SDC, and a primary phosphate in PI. Therefore, the dispersion of an anionic charge must also be related to the enhancement of PI–PLC activity toward PI/SDC mixed micelles, as shown in Fig. 9. The interface of PI/SDC mixed micelles (Fig. 9a) must be covered with a negative charge at neutral pH, since the components contain anionic groups. As mentioned above, both PI–PLC and PI have a negative net charge in the reaction medium at pH 7.5, where electrostatic repulsion might be expected between them. However, the activity of PI–PLC is activated by SDC and not affected by cetyltrimethylammonium bromide, a cationic detergent.[6] Therefore, the molecule of PI–PLC might contain a partially cationic region which is involved in the catalytic process. When a neutral lipid such as PC, SM or PE is added to PI/SDC micelles (Fig. 9b), dispersion of a negative charge must take place in the interface of the micelles, rendering the catalytic site of PI–PLC more accessible to PI and resulting in the enhancement of PI hydrolysis.

In the outer leaflet of plasma membrane, PI is diluted

mainly with choline-containing phospholipids such as PC and SM, which usually exhibit a stimulative effect on PI–PLC activity. Therefore, solubilization of PI-anchored proteins by PI–PLC must proceed effectively, in that the PI-moiety in these proteins is sufficiently exposed to the attack of the enzyme under these circumstances.

From the present study, it is concluded that the action of PI–PLC toward micellar PI is significantly influenced in the presence of other membranous lipids. The effect of these lipids on PI–PLC activity toward liposomal PI has been also studied in our laboratory and will be reported elsewhere.

Acknowledgment This study was supported in part by a Grant-in-Aid for Scientific Research from the Ministry of Education, Science and Culture of Japan.

References and Notes

1) Present adress: *Central Research Laboratory, Ishihara Sangyo Kaisha, Ltd., 2–3–1 Nishi-shibukawa, Kusatsu, Shiga 525, Japan.*
2) H. M. Doery, B. J. Magnusson, J. Gulasekharam and J. E. Pearson, *J. Gen. Microbiol.*, **40**, 283 (1965).
3) R. Taguchi and H. Ikezawa, *Arch. Biochem. Biophys.*, **186**, 196 (1978).
4) M. W. Slein and G. F. Logan, Jr., *J. Bacteriol.*, **90**, 69 (1965).
5) H. Ikezawa, M. Yamanegi, R. Taguchi, T. Miyashita and T. Ohyabu, *Biochim. Biophys. Acta*, **450**, 154 (1976).
6) R. Taguchi, Y. Asahi and H. Ikezawa, *Biochim. Biophys. Acta*, **619**, 48 (1980).
7) H. Ikezawa, T. Nakabayashi, K. Suzuki, M. Nakajima, T. Taguchi and R. Taguchi, *J. Biochem.* (Tokyo), **93**, 1717 (1983).
8) M. G. Low, *Biochem. J.*, **244**, 1 (1987).
9) H. Ikezawa, *J. Toxicol. Toxin Rev.*, **5**, 1 (1986).
10) D. J. Henner, M. Yang, E. Chen, R. Hellmiss, H. Rodriguez and M. G. Low, *Nucleic Acids Res.*, **16**, 10383 (1988).
11) M. Lechner, T. Kupke, S. Stefanovic and F. Götz, *Molec. Microbiol.*, **3**, 621 (1989).
12) W. E. Trevelyan, *J. Lipid Res.*, **7**, 445 (1966).
13) S. Spanner, "Form and Function of Phospholipids," ed. by G. B. Ansell, J. N. Hawthorne and R. M. C. Dawson, Elsevier, Amsterdam, 1973, pp. 43—65.
14) H. Eibl and W. E. M. Lands, *Anal. Biochem.*, **30**, 51 (1969).
15) H. Fiske and Y. Subbarow, *J. Biol. Chem.*, **66**, 375 (1925).
16) E. A. Dennis, P. L. Darke, R. A. Deems, C. R. Kensil and A. Plückthun, *Molec. Cell. Biochem.*, **36**, 37 (1981).
17) P. R. Cullis and B. de Kruijff, *Biochim. Biophys. Acta*, **559**, 399 (1979).
18) A. Helenius and K. Simmons, *Biochim. Biophys. Acta*, **415**, 29 (1975).
19) A. Seelig and J. Seelig, *Biochemistry*, **13**, 4839 (1984).

Reticuloendothelial System-Potentiating and Alkaline Phosphatase-Inducing Activities of Plantago-Mucilage A, the Main Mucilage from the Seed of *Plantago asiatica*, and Its Five Modification Products

Masashi TOMODA,* Katsutoshi TAKADA, Noriko SHIMIZU, Ryōko GONDA and Naoko ŌHARA

Kyoritsu College of Pharmacy, Shibakōen, Minato-ku, Tokyo 105, Japan. *Received January 21, 1991*

Five kinds of chemically modified products were prepared from Plantago-mucilage A, the representative mucous polysaccharide isolated from the seed of *Plantago asiatica* L., and their reticuloendothelial system-potentiating and alkaline phosphatase-inducing activities have been investigated. Both activities were markedly enhanced when the mucilage was de-*O*-acetylated. The products obtained by periodate oxidation, controlled Smith degradation, and partial acid hydrolysis under the two conditions were not effective. Structural features of the partial hydrolyzates were elucidated, and it was shown that these products lost all *O*-acetyl groups, all xylose branches and many hexuronosyl arabinose side chains.

Keywords Plantago-mucilage A; *Plantago asiatica*; seed; polysaccharide; chemical modification; immunological activity; reticuloendothelial system; alkaline phosphatase; deacetylation effect

Plantago-mucilage A is a representative mucous polysaccharide obtained from the seed of *Plantago asiatica* L.[1] The seed of this plant is a well-known crude drug used as an antiphlogistic, a diuretic, an antidiarrheic and cough medicine. Structural studies[1,2] on Plantago-mucilage A were performed by controlled Smith degradation and methylation analysis, and the results indicated that the mucilage possesses a backbone chain composed of β-1,4-linked D-xylopyranose residues having three kinds of branches composed of a β-D-xylopyranose, α-D-glucopyranosyluronic acid-(1→3)-α-L-arabinofuranose and α-D-galactopyranosyluronic acid-(1→3)-α-L-arabinofuranose at position 3. Thus the all D-xylose residues in the backbone carry side chains, and the ratio of these three types of branches is 15:10:2. In addition, the mucilage contains 4.8% *O*-acetyl groups, and these groups were located at position 2 of a part of L-arabinofuranosyl and D-xylopyranosyl residues. The results of structural studies showed that the molar ratios of D-xylopyranose and 2-*O*-acetyl-D-xylopyranose are approximately 3:2 in the terminal units and approximately 8:1 in the intermediate units, and that the molar ratio of L-arabinose and 2-*O*-acetyl-L-arabinose is approximately 3:1.[2]

Recently, Tomoda *et al.* reported on the anti-complementary activity[3] and the hypoglycemic activity[4] of Plantago-mucilage A and its modified products. Because of the importance of macrophages and lymphocytes for the body's defense system against microbial infections and tumors, the present paper describes two immunological activities of this mucous polysaccharide and the five products obtained by chemical modification of it on both reticuloendothelial system (RES)-potentiating and alkaline phosphatase-inducing activities. The modification products were examined for the purpose of studies on the relationship between structures and biological activities.

Materials and Methods

Isolation of Polysaccharide This was performed as described in a previous report.[1]

Deacetylation The mucilage (50 mg) was dissolved in water (5 ml), then 0.02 N sodium hydroxide (5 ml) was mixed. After standing at room temperature for 10 min, the solution was neutralized with 1 M acetic acid. The resulting mixture was applied to a column (5 × 82 cm) of Sephadex G-25, and the column was eluted with water. Fractions of 20 ml were collected and analyzed by the phenol–sulfuric acid method.[5] The eluates obtained from tubes 32 to 44 were combined, concentrated and lyophilized. Yield, 42 mg. The disappearance of a signal at δ 2.16 ppm, corresponding to acetyl groups was confirmed by proton nuclear magnetic resonance (^{1}H-NMR) spectrum. The ^{1}H-NMR spectrum was recorded on a JEOL JNM-GX 270 FT NMR spectrometer in heavy water containing sodium 2,2-dimethyl-2-silapentane-5-sulfonate as an internal standard at 70 °C.

Periodate Oxidation The deacetylated product (200 mg) was oxidized with 0.05 M sodium metaperiodate (100 ml) at 4 °C in the dark. The periodate consumption was measured by a spectrophotometric method.[6] Oxidation was completed after 7 d. The reaction mixture was successively treated with ethylene glycol (1 ml) at 4 °C for 1 h and sodium borohydride (1 g) at 4 °C for 16 h, then adjusted to pH 5.0 by the addition of acetic acid. The solution was concentrated and applied to a column (5 × 85 cm) of Sephadex G-25. The column was eluted with water, and fractions of 20 ml were collected. The eluates obtained from tubes 33 to 41 were combined, concentrated and lyophilized. Yield, 147 mg.

Controlled Smith Degradation The product (200 mg) obtained by periodate oxidation was dissolved in 0.5 N sulfuric acid (10 ml). After standing at room temperature for 16 h, the solution was neutralized with barium carbonate. The filtrate was concentrated and passed through a column (0.7 × 4 cm) of Dowex 50W-X8 (H^+). The eluate with water was concentrated and dialyzed against water, then the non-dialyzable fraction was applied to a column (5 × 80 cm) of Sephadex G-25. The column was eluted with water, and fractions of 20 ml were collected. The eluates obtained from tubes 33 to 44 were combined, concentrated and lyophilized. Yield, 80 mg.

Partial Acid Hydrolysis The mucilage (300 mg) was dissolved in 0.1 M trifluoroacetic acid (45 ml) and heated under reflux at 60 °C for 1 h. After removal of acid by evaporation, the residue was dissolved in water and applied to a column (5 × 85 cm) of Sephadex G-25. The column was eluted with water, and fractions of 20 ml were collected. The eluates obtained from tubes 33 to 37 were combined, concentrated and lyophilized. Yield, 161 mg. On the other hand, the partial hydrolysis was carried out at 80 °C for 1 h under conditions similar to those described above. In this case, the yield was 157 mg from 300 mg of the mucilage.

Determination of Component Sugars Neutral sugars were analyzed by gas chromatography (GC) after conversion of the hydrolyzate into alditol acetates as described in a previous report.[7] Hexuronic acid was determined by the *m*-hydroxybiphenyl method.[8]

Determination of Molecular Mass The sample (3 mg) was dissolved in 0.1 M Tris–HCl buffer (pH 7.0) and applied to a column (2.6 × 87 cm) of Toyopearl HW 65F, pre-equilibrated and developed with the same buffer. Fractions of 5 ml were collected and analyzed by the phenol–sulfuric acid method. Standard pullulans (Shōwa Denkō Co.) having known molecular masses were run on the column to obtain a calibration curve.

Reduction of Carboxyl Groups This was performed with 1-cyclohexyl-3-(2-morpholinoethyl)carbodiimide metho-*p*-toluenesulfonate and sodium borohydride as described in a previous report.[9]

Methylation Analysis Methylation was performed with powdered sodium hydroxide and methyl iodide in dimethyl sulfoxide as described in a previous report.[10] This product was hydrolyzed with dilute sulfuric acid in acetic acid, then reduced and acetylated as described in a previous report.[11] The partially methylated alditol acetates obtained were analyzed

TABLE I. Relative Retention Times on GC and Main Fragments in MS of Partially Methylated Alditol Acetates

	Relative retention time[a)]	Main fragments (*m/z*)
1,4-Ac_2-2,3,5-Me_3-L-arabinitol	0.69	43, 45, 71, 87, 101, 117, 129, 161
1,3,4-Ac_3-2,5-Me_2-L-arabinitol	1.04	43, 87, 113, 117, 233
1,4,5-Ac_3-2,3-Me_2-D-xylitol	1.21	43, 87, 101, 117, 129, 189
1,3,4,5-Ac_4-2-Me-D-xylitol	1.54	43, 117, 261
1,5-Ac_2-2,3,4,6-Me_4-D-glucitol	1.00	43, 45, 71, 87, 101, 117, 129, 145, 161, 205
1,5-Ac_2-2,3,4,6-Me_4-D-galactitol	1.09	43, 45, 71, 87, 101, 117, 129, 145, 161, 205

a) Relative to 1,5-di-*O*-acetyl-2,3,4,6-tetra-*O*-methyl-D-glucitol. Abbreviations: Ac=acetyl; Me=methyl (*e.g.*, 1,4-Ac_2-2,3,5-Me_3-=1,4-di-*O*-acetyl-2,3,5-tri-*O*-methyl-).

by gas chromatography-mass spectrometry (GC-MS) using a fused silica capillary column (0.32 mm i.d. × 30 m) of SP-2330 (Supelco Co.) with a programmed temperature increase of 4 °C per min from 160 to 220 °C at a helium flow of 1 ml per min. GC-MS was performed with a JEOL JMS-GX mass spectrometer. The relative retention times of the products with respect to 1,5-di-*O*-acetyl-2,3,4,6-tetra-*O*-methyl-D-glucitol in GC and the main fragments in MS are listed in Table I.

Phagocytic Activity This was measured as described in a previous report.[7)] The sample and a positive control, zymosan (Tokyo Kasei Co.), were each dissolved and suspended in physiological saline and dosed i.p. (50 and 20 mg/kg body weight) once a day. The phagocytic index, K, was calculated by means of the following equation:

$$K=(\ln OD_1-\ln OD_2)/(t_1-t_2)$$

where OD_1 and OD_2 are the optical densities at times t_1 and t_2, respectively. Results were expressed as the arithmetic mean ± S.D. of five male mice (ICR-SPF). The comparison of results was performed by means of Student's t-test.

Alkaline Phosphatase Assay ICR-SPF male mice were killed by cervical dislocation and the cell suspension from the spleen was prepared by teasing the organ in ice cold RPMI-1640 medium (Nissui Seiyaku Co.) supplemented with 5 mM HEPES (Sigma Co.), 100 U/ml penicillin and 100 μg/ml streptomycin (Meiji Seika Co.). After centrifugation (1200 rpm for 5 min at 4 °C), the packed cells were treated with ACK buffer (8.29 g ammonium chloride, 1 g potassium bicarbonate and 37.2 mg disodium ethylenediaminetetraacetate in 1 l, pH 7.2) to lyse red cells. The treated cells were washed with fresh medium three times, resuspended with the above medium containing 10% FCS (Flow Lab.) and viability was assessed by the trypan blue dye exclusion test. The cell suspension was adjusted to 5×10^6 viable cells per ml. Each test sample solution (100 μl) was placed in a flat bottomed 96-well tissue culture plate and 100 μl of the cell suspension prepared above were added to each well. The cell cultures were incubated at 37 °C for 48 h in a humidified atmosphere of 5% CO_2. Each of the resultant cell suspensions (150 μl) was placed in an appropriate test tube. To these tubes, 600 μl of 10% diethanolamine–HCl buffer (pH 9.8) containing 0.1% *p*-nitrophenylphosphate was added. The reaction mixture was incubated at 37 °C for 1 h and was terminated by the addition of 600 μl of 0.25 N sodium hydroxide. The absorbance at 405 nm was measured and the results were expressed as the arithmetic mean ± S.D. of triplicate cultures.

Results

The deacetylated product (DAP) of Plantago-mucilage A was obtained by treatment with alkali under a very mild condition. DAP was subjected to periodate oxidation followed by reduction. The product (POP) was treated with dilute sulfuric acid at room temperature overnight, then the controlled Smith degradation product (SDP) was isolated. As reported previously,[2)] DAP had the same composition and almost the same molecular mass as Plantago-mucilage A. Both POP and SDP were composed of D-xylose and L-arabinose in a molar ratio of 9:4,[2)] and their molecular masses were 15.4×10^4 and 11.1×10^4, respectively.

TABLE II. Methylation Analysis of HP60, HP80 and Their Carboxyl-Reduced Derivatives

Methylated sugars (as alditol acetates)	Molar ratios from HP60		Molar ratios from HP80	
	Original	Carboxyl-reduced	Original	Carboxyl-reduced
2,3,5-Me_3-L-arabinose	1	2	1	1
2,5-Me_2-L-arabinose	6	12	15	14
2,3-Me_2-D-xylose	18	36	60	60
2-Me-D-xylose	7	14	15	15
2,3,4,6-Me_4-D-glucose	—	11	—	13
2,3,4,6-Me_4-D-galactose	—	1	—	1

In addition, the mucilage was partially hydrolyzed under the two conditions with dilute trifluoroacetic acid at 60°C or 80°C for 1 h. Both the products (HP60 and HP80) gave a single peak on gel chromatography, respectively. Gel chromatography gave values of 8.6×10^4 and 2.26×10^4 for the molecular masses of HP60 and HP80, respectively. Quantitative analyses of component sugars showed that HP60 was composed of D-xylose, L-arabinose, D-glucuronic acid and D-galacturonic acid in the molar ratio of 52:14:11:1, and that HP80 was composed of the same components as HP60 in the molar ratio of 80:15:13:1. ^{1}H-NMR spectra showed no acetyl signals in HP60 and HP80.

The carboxyl groups of hexuronic acid residues in both HP60 and HP80 were reduced to give the corresponding neutral sugar residues.[12)] The ratio of two hexuronic acids was confirmed by analysis of the carboxyl-reduced derivatives. Both the original products (HP60 and HP80) and their carboxyl-reduced derivatives were methylated with solid sodium hydroxide and methyl iodide in dimethyl sulfoxide.[13)] The methylated products were hydrolyzed, then converted into the partially methylated alditol acetates. Hexuronic acid methyl ethers from the original samples were removed from the hydrolyzates by treatment with an anion-exchange resin. Analysis by GC-MS[14)] gave the results shown in Tables II and III.

The structural feature of Plantago-mucilage A[2)] and the results of methylation analysis described above indicated that HP60 and HP80 contain the units shown in Chart 1, respectively.

The effects of Plantago-mucilage A and five kinds of chemical modification products, DAP, POP, SDP, HP60 and HP80, on the RES were demonstrated by a modification[7)] of the *in vivo* carbon clearance test[15)] using zymosan as a positive control. As shown in Fig. 1, the phagocytic index was significantly increased, suggesting the activation of RES by i.p. injection of Plantago-mucilage A. The activity was markedly enhanced when the mucilage was deacetylated. HP60 showed weak activity, but the other three products, POP, SDP and HP80, had no effect.

The alkaline phosphatase activity of murine spleen cell was induced by stimulating directly with B cell mitogen or indirectly *via* lymphokines with T cell mitogen.[16)] So the measurements of alkaline phosphatase with Plantago-

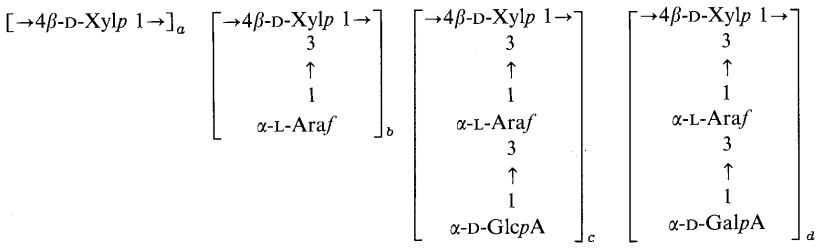

Chart 1. Component Units in the Structures of HP60 and HP80

HP60, $a:b:c:d=38:2:11:1$.
HP80, $a:b:c:d=65:1:13:1$.
Abbreviations: Xyl*p*, xylopyranose; Ara*f*, arabinofuranose; Glc*p*A, glucopyranosyluronic acid; Gal*p*A, galactopyranosyluronic acid.

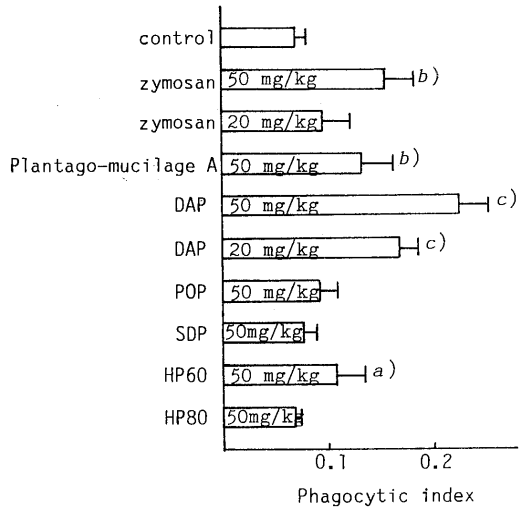

Fig. 1. Effects of Plantago-Mucilage A and Its Chemical Modification Products on Phagocytosis

Significantly different from the control, *a*) $p<0.05$, *b*) $p<0.01$, *c*) $p<0.001$.

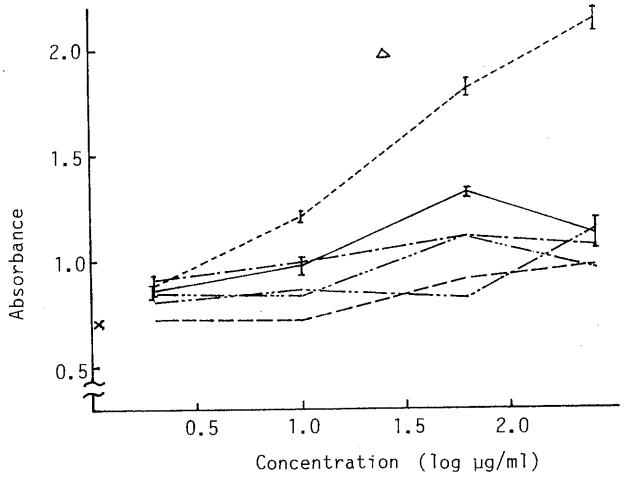

Fig. 2. Mitogenic Activity of Plantago-Mucilage A and Its Chemical Modification Products Assessed by Alkaline Phosphatase Activity

Plantago-mucilage A, ——; DAP, ------; POP, — —; SDP, — · —; HP60, — · · —; HP80, — — — —. Control, ×; positive control, lipopolysaccharide from *E. coli* serotype 0111 (Sigma Co.), △.

mucilage A and its five products were performed by the *in vitro* murine spleen cell assay.[16] As shown in Fig. 2, Plantago-mucilage A was not so effective. However, when the cells were stimulated with DAP, the alkaline phosphatase activity was induced in a dose dependent manner. The other four modification products, POP, SDP, HP60 and HP80, on the contrary, showed no effect.

Discussion

We have already investigated the structure-complement activation relationship of Plantago-mucilage A.[3] Plantago-mucilage A showed considerable anti-complementary activity. Its activity was in almost the same level as that of a positive control, AR-arabinogalactan, from the root of *Angelica acutiloba*.[17] POP gave an effect similar to the original mucilage, and the activity of HP80 was slightly enhanced on this assay. Structural features of this partial hydrolyzate were not clear at that time. The anti-complementary activity was markedly enhanced when the mucilage was deacetylated. It was concluded that the *O*-acetyl groups in Plantago-mucilage A prevent the activation of the complement *via* the classical pathway.[3]

Four years previous, Plantago-mucilage A and DAP were tested for hypoglycemic activity on administration to normal mice.[4] The deacetylation product of the mucilage showed a pronounced elevation in the activity. Thus, DAP belongs to the substances having the highest levels of activity by these two assays.

We have already found the RES activities of two polysaccharides obtained from the root and rhizome of *Saposhnikovia divaricata*,[7,18] three polysaccharides from the seed of *Malva verticillata*,[10,19,20] a polysaccharide from the bark of *Cinnamomum cassia*,[21] three polysaccharides from the rhizome of *Curcuma longa*,[22-24] three polysaccharides from the root of *Glycyrrhiza uralensis*[25,26] and two polysaccharides from the bark of *Eucommia ulmoides*.[27,28] Saposhnikovan A,[7] MVS-IIIA,[19] -IVA[20] and -VI,[10] ukonans A[23] and B,[22] and glycyrrhizan UA[25] possess acidic arabino-3,6-galactan structure as their major parts. Ukonan C[24] and glycyrrhizan UC[26] belong to arabino-3,6-galactoglucan. Saposhnikovan C,[18] glycyrrhizan UB,[25] and eucommans A[27] and B[28] are essentially rhamnogalacturonans having various arabinogalactan type side chains. Cinnaman AX[21] is not arabinogalactan but arabinoxylan having a β-1,4-linked D-xylose backbone mostly bearing L-arabinosyl side chains at position 3.

Plantago-mucilage A is a partially acetylated acidic arabinoxylan having a similar backbone to that of cinnaman AX, but its side chains are composed of terminal D-xylose and D-glucurono- or D-galacturono-L-arabinose. This substance also showed significant RES activity, although its value of the phagocytic index was lower than those of the other active polysaccharides described above. However, the RES activity was greatly increased by deacetylation of this mucous polysaccharide. A similar effect of deacetylation

was observed on the alkaline phosphatase inducing activity.

Deacetylation of Plantago-mucilage A does not cause any reduction of molecular weight of polysaccharide itself.[3] Of course DAP has the same sugar composition as that of the original mucilage. So it is conceivable that the deacetylation effect on these biological activities may be attributed to steric factors. The difference in RES activity between HP60 and HP80 indicated that both the degree of branching and molecular mass seem to be the other factors in the immunological activity.

Acknowledgements We wish to thank Prof. T. Yadomae, Tokyo College of Pharmacy, for his advice on the alkaline phosphatase assay. This work was supported in part by The Science Research Promotion Fund of the Japan Private School Promotion Foundation.

References

1) M. Tomoda, M. Yokoi and K. Ishikawa, *Chem. Pharm. Bull.*, **29**, 2877 (1981).
2) M. Tomoda, N. Shimizu, K. Shimada, R. Gonda and H. Sakabe, *Chem. Pharm. Bull.*, **32**, 2182 (1984).
3) H. Yamada, T. Nagai, J.-C. Cyong, Y. Otsuka, M. Tomoda, N. Shimizu and R. Gonda, *Carbohydr. Res.*, **156**, 137 (1986).
4) M. Tomoda, N. Shimizu, Y. Oshima, M. Takahashi, M. Murakami and H. Hikino, *Planta Medica*, **53**, 8 (1987).
5) M. Dubois, K. A. Gilles, J. K. Hamilton, P. A. Rebers and F. Smith, *Anal. Chem.*, **28**, 350 (1956).
6) G. O. Aspinall and R. J. Ferrier, *Chem. Ind.* (London), **1957**, 1216.
7) N. Shimizu, M. Tomoda, R. Gonda, M. Kanari, N. Takanashi and N. Takahashi, *Chem. Pharm. Bull.*, **37**, 1329 (1989).
8) N. Blumenkrantz and G. Asboe-Hansen, *Anal. Biochem.*, **54**, 484 (1973).
9) M. Tomoda and M. Ichikawa, *Chem. Pharm. Bull.*, **35**, 2360 (1987).
10) R. Gonda, M. Tomoda, M. Kanari, N. Shimizu and H. Yamada, *Chem. Pharm. Bull.*, **38**, 2771 (1990).
11) M. Tomoda, K. Shimada, Y. Saito and M. Sugi, *Chem. Pharm. Bull.*, **28**, 2933 (1980).
12) R. L. Taylor and H. E. Conrad, *Biochemistry*, **11**, 1383 (1972).
13) I. Ciucanu and F. Kerek, *Carbohydr. Res.*, **131**, 209 (1984).
14) H. Björndall, B. Lindberg and S. Svensson, *Carbohydr. Res.*, **5**, 433 (1967).
15) G. Biozzi, B. Benacerraf and B. N. Halpern, *Br. J. Exp. Pathol.*, **34**, 441 (1953).
16) N. Ohno, Y. Arai, I. Suzuki and T. Yadomae, *J. Pharmacobio-Dyn.*, **9**, 593 (1986).
17) H. Yamada, H. Kiyohara, J.-C. Cyong, Y. Kojima, Y. Kumazawa and Y. Otsuka, *Planta Medica*, **50**, 163 (1984).
18) N. Shimizu, M. Tomoda, R. Gonda, M. Kanari, Aki. Kubota and Ake. Kubota, *Chem. Pharm. Bull.*, **37**, 3054 (1989).
19) M. Tomoda, M. Kanari, R. Gonda and N. Shimizu, *Phytochemistry*, **28**, 2609 (1989).
20) R. Gonda, M. Tomoda, N. Shimizu and M. Kanari, *Planta Medica*, **56**, 73 (1990).
21) M. Kanari, M. Tomoda, R. Gonda, N. Shimizu, M. Kimura, M. Kawaguchi and C. Kawabe, *Chem. Pharm. Bull.*, **37**, 3191 (1989).
22) R. Gonda, M. Tomoda, N. Shimizu and M. Kanari, *Chem. Pharm. Bull.*, **38**, 482 (1990).
23) M. Tomoda, R. Gonda, N. Shimizu, M. Kanari and M. Kimura, *Phytochemistry*, **29**, 1083 (1990).
24) R. Gonda and M. Tomoda, *Chem. Pharm. Bull.*, **39**, 441 (1991).
25) M. Tomoda, N. Shimizu, M. Kanari, R. Gonda, S. Arai and Y. Okuda, *Chem. Pharm. Bull.*, **38**, 1667 (1990).
26) N. Shimizu, M. Tomoda, M. Kanari, R. Gonda, A. Satoh and N. Satoh, *Chem. Pharm. Bull.*, **38**, 3069 (1990).
27) R. Gonda, M. Tomoda, N. Shimizu and M. Kanari, *Chem. Pharm. Bull.*, **38**, 1966 (1990).
28) M. Tomoda, R. Gonda, N. Shimizu and M. Kanari, *Phytochemistry*, **29**, 3091 (1990).

Effects of Metal Elements on β-Hexosaminidase Release from Rat Basophilic Leukemia Cells (RBL-2H3)

Yukio TANAKA,* Yutaka TAKAGAKI and Takahiro NISHIMUNE

Osaka Prefectural Institute of Public Health, 3–69, Nakamichi 1-chome, Higashinari-ku, Osaka 537, Japan. *Received January 28, 1991*

Immediate allergy is caused by a chemical mediator released from basophile and mast cells *via* cell degranulation due to reaction between an immunoglobulin E (IgE) antibody, bound with the IgE receptor on the cell membrane, and an antigen. The present authors have established a new method for assaying the enzyme activity of β-hexosaminidase as an index of chemical mediator release. Using cultured cells instead of conventional methods based on histamine release from mast cells, the present method permits highly accurate mass screening since it uses a well-established cell line of rat basophilic leukemia cells (RBL-2H3). The effects of metal elements on immediate allergic reaction were evaluated using a newly developed assay system.

A total of 38 metal elements were investigated for effects on immediate allergic reactions *in vitro*. These elements were classified by five types on the basis of action on β-hexosanimidase release: 1) those which showed very strong inhibitory action, such as $ZnCl_2$ and $ZrCl_4$, 2) those which showed relatively strong inhibitory action, such as $CdCl_2$ and $CuCl_2$, 3) those which showed relatively weak inhibitory action, such as $CoCl_2$ and $Pb(NO_3)_2$, 4) those which showed neither inhibitory nor promoting action, such as $MnCl_2$ and $SrCl_2$, and 5) $AgNO_3$, which alone showed promoting action.

Keywords immediate allergy; immunoglobulin E; rat basophilic leukemia cell (2H3); chemical mediator; β-hexosaminidase release; metal element

Immediate allergy occurs due to an antigen–antibody reaction involving the immunoglobulin E (IgE) antibody,[1] and includes food allergy, urticaria, pollinosis, bronchial asthma and atopic dermatitis. These diseases have been increasing steadily with changes in lifestyle. Although the definite causes remain unknown, a number of factors are considered as involved, including environmental changes, dietary life changes, aggravated atmospheric pollution, somatic constitution and increased mental stress. Among the factors involved, metal elements were selected and examined using an assay system incorporating cultured cells.

In general, *in vitro* experiments on immediate allergic reactions have often been conducted by the method in which mast cells isolated and purified from the rat peritoneal cavity are stimulated with an antigen or a degranulation inducer, followed by determination of histamine release from the mast cells.[2,3] However, this method is faulty in that, since the mast cells are collected from rats, high purity cells are difficult to obtain, thus preventing accurate mass screening. The present authors developed a method of determining the enzyme activity of β-hexosaminidase,[4,5] as an index of chemical mediator release, in which cultured rat basophilic leukemia cells (RBL-2H3)[6] of a well-established cell line are stimulated with a complex of avidin and biotinylated mouse anti-dinitrophenyl IgE antibody (monoclonal antibody derived from hydridoma cells[7]).

The reported effects of metal elements on immediate allergic reactions *in vitro* include inhibition of rat mast cell degranulation by zinc and manganese,[8] inhibition of human basophilic histamine release by zinc,[9,10] and inhibition of RBL-2H3 cells histamine release by lanthanum and zinc,[11,12] but there are no reports dealing with a variety of metal elements. This paper presents the results of a study of the effects of 38 metal elements on immediate allergic reactions, determined using a newly developed assay method.

Materials and Methods

Cultured Cells Rat basophilic lekemia cells (RBL-2H3)[6] were cultured, at 37 °C in an atmosphere containing 5% CO_2, in a medium prepared by supplementing RPM1-1640 medium (Sigma Chemical Co.) with 3% fetal calf serum (HyClone Laboratories Inc.) and 0.2% bovine serum albumin (fraction V, Seikagaku Kogyo Co.). The resulting suspended cells were used for the experiment.

Biotinylation of Mouse Anti-DNP IgE Antibody Reaction was carried out between 4.0 mg of mouse anti-DNP IgE antibody,[7] isolated and purified from hybridoma cells, and 4.7 mg of a 6-fold molar concentration of NHS-LC-biotin (Pierce Chemical Co.) in a solution of 0.1 M sodium hydrogen carbonate at room temperature for 1 h. The resulting reaction product was filtered through a cellulose acetate filter (0.45 μm) and applied to a fast protein liquid chromatography (FPLC, Pharmacia Co.) to collect biotinylated IgE alone. The chromatography was conducted using a series of two columns of Superose 12 HR 10/30 (Pharmacia Co.). Phosphate buffered saline solution (PBS, pH 7.4) was used as the eluent; the resulting eluate was collected with a cutoff value of 5%.

Stimulated Degranulation of RBL-2H3 Cells The cells were stimulated with the complex of avidin (Sigma Chemical Co.) and biotinylated mouse anti-DNP IgE antibody prepared as above.

Subject Metal Elements and Reagents Salts of the subject metal elements were each dissolved in ultra-pure water to a concentration of 100 mM. The resulting solution was appropriately diluted before use. The metals were selected in the form of a hydrochloride, nitrate or sulfate compound, insofar as possible. The releasing medium used was a solution containing 117 mM NaCl, 5.4 mM KCl, 2.0 mM $CaCl_2$, 0.8 mM $MgSO_4$, 5.6 mM D-glucose, 25 mM *N*-(2-hydroxyethyl)piperazine-*N'*-2-ethanesulfonic acid (HEPES, Sigma Chemical Co.) and 1 mg/ml bovine serum albumin (globulin-free, Sigma Chemical Co.) adjusted at a pH of 7.70. The substrate used to determine β-hexosaminidase activity was a solution of 5.0 mM *p*-nitrophenyl-2-acetamide-2-deoxy-β-D-glucopyranoside (Nakalai Tesque Co.) in 0.05 M citrate buffer, pH 4.5. The stop solution was 0.2 M glycine buffer (pH 10.7). All other reagents used in the experiment were chemicals of Wako Pure Chemical Industries.

Determination Procedure RBL-2H3 cells were seeded onto a 48-well microplate (Costar Co.) at 5×10^5 cells/well and incubated in a CO_2 incubator for 24 h. The medium was removed by aspiration and the monolayer cultures were washed twice with 500 μl of the releasing medium warmed at 37 °C. To the microplate was added 250 μl/well of a reaction mixture (prepared by adding biotinylated mouse anti-DNP IgE antibody and avidin, and 10 μl of a metal element solution, to the releasing medium and diluting the mixture to a total quantity of 1 ml), prepared separately and warmed at 37 °C, followed by incubation at 37 °C for 1 h. Then 100 μl of the extracellular fluid was taken, and the residue was removed by aspiration. Next, 250 μl/well of 0.2% Triton X-100 was added. Ten min later, 100 μl of the lysed cell solution (intracellular fluid) was taken. The collected extracellular and intracellular fluids were assayed for the enzyme activity of β-hexosaminidase,[4,5] as the index of chemical mediator. Namely, 400 μl of a solution of *p*-nitrophenyl-2-acetamide-2-deoxy-β-D-

glucopyranoside (as substrate) was added, followed by incubation at 37 °C for 30 min. After the addition of 1 ml of the stop solution, the resulting *p*-nitrophenol was measured at an OD of 405 nm, and the net percent release of β-hexosaminidase was calculated using the following equation:

$$\text{net \% release} = (A - C)/[(A + B) - C] \times 100$$

where *A*: amount of β-hexosaminidase in the extracellular fluid, *B*: amount of β-hexosaminidase in the intracellular fluid, *C*: amount of β-hexosaminidase in the extracellular fluid from control cells.

The cell viability was determined by the trypan blue staining method.

Results

Optimum Composition and Optimum Dose of Stimulator The optimum mixing ratio of biotinylated IgE and avidin for the stimulation was determined by varying the composition of the biotinylated IgE–avidin complex used as the stimulator (Fig. 1).

The avidin content was varied from 0 to 10 μg/ml while the biotinylated IgE content was kept constant at 3.0 μg/ml.

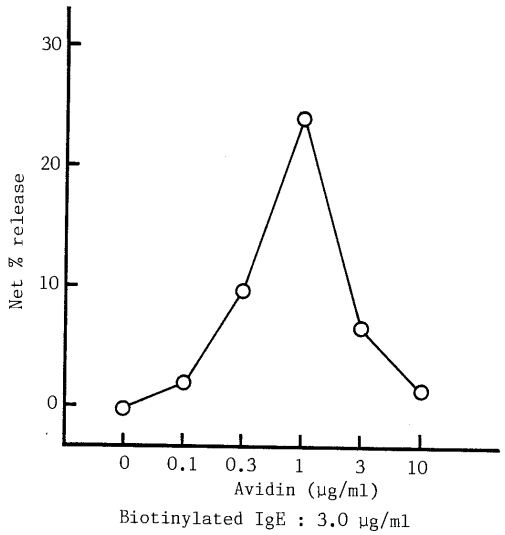

Fig. 1. Effect of Ratio in Biotinylated IgE and Avidin on β-Hexosaminidase Release

The cells were stimulated with the stimulator alone, which was prepared by adding biotinylated IgE and avidin to the releasing medium and diluting the mixture to a total quantity of 1 ml. Each plotting point was obtained in triplicate.

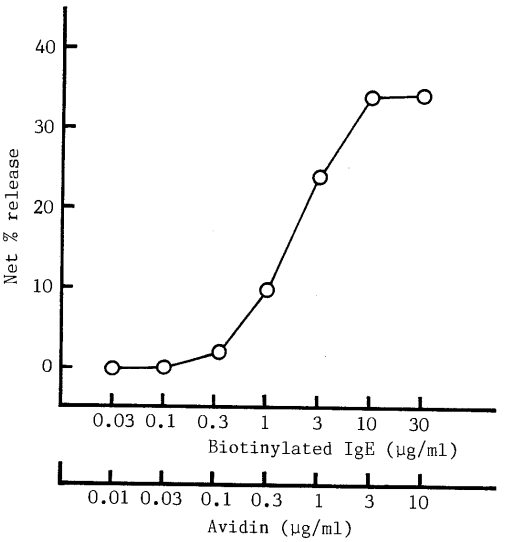

Fig. 2. Dose Response Curve of Biotinylated IgE–Avidin Complex

For details see Fig. 1.

Maximum β-hexosaminidase release was obtained when the avidin content was 1 μg/ml. Thus, it was found that the maximum is reached at a molar ratio of about 1 to 1, since the molecular weight of biotinylated IgE is about 200000 and that of avidin is about 68000.

Next, the amount of the complex was serially varied with a molar ratio of about 1 of biotinylated IgE to 1 of avidin, and the dose response curve was drawn (Fig. 2).

The release amount increased as the amount of the complex increased, and reached a plateau when the amount of biotinylated IgE exceeded 10 μg/ml. On the basis of this finding, a complex composition of 3 μg/ml biotinylated IgE and 1 μg/ml avidin was selected for the cell stimulation, permitting the observation of the release inhibition or promotion.

Effect of Metal Elements on β-Hexosaminidase Release from RBL-2H3 Cells A total of 38 metal elements were investigated as to effects on β-hexosaminidase release from RBL-2H3 cells *in vitro* by the group, according to the periodic table of the elements.

Elements in Groups Ia and IIa: The dose response curves of an alkali metal element in group Ia and alkaline earth metal elements in group IIa are given in Fig. 3. Note that Fig. 3 through 9 below give the dose response curves drawn from the relative % release obtained after the stimulation with different concentrations of each metal element, expressed in percent ratio to the net % release obtained when the cells were stimulated with the stimulator alone (prepared by adding 3 μg of biotinylated IgE and 1 μg of avidin to the releasing medium and diluting the mixture to a total quantity of 1 ml). Each plotting point was obtained in triplicate.

Alkali metals were investigated as LiCl, RbCl and CsCl.

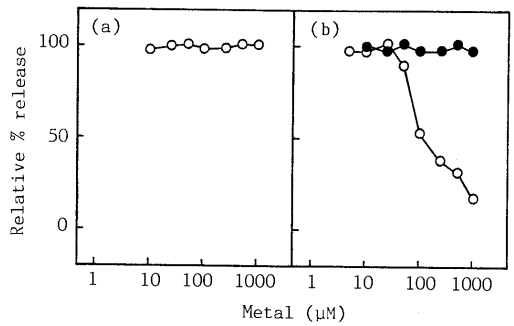

Fig. 3. Dose Response Curves of Groups Ia and IIa Elements

(a) shows an alkali metal element in group Ia. ○, LiCl. (b) shows alkaline earth metal elements in group IIa. ○, $BeSO_4$; ●, $SrCl_2$.

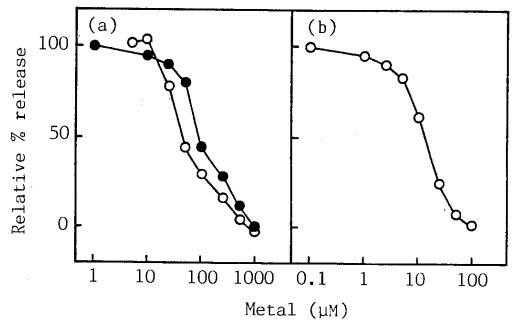

Fig. 4. Dose Response Curves of Groups IIIa and IVa Elements

(a) shows rare earth elements in group IIIa. ○, $Er(NO_3)_3$; ●, $LaCl_3$. (b) shows a titanium series element in group IVa. ○, $ZrCl_4$.

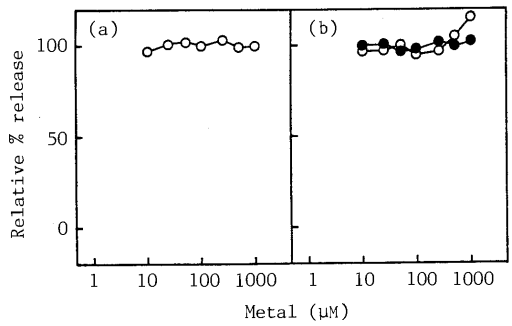

Fig. 5. Dose Response Curves of Groups Va and VIa Elements

(a) shows a vanadium series element in group Va. ○, $NaVO_3$. (b) shows chromium series elements in group VIa. ○, $CrCl_3$; ●, K_2CrO_4.

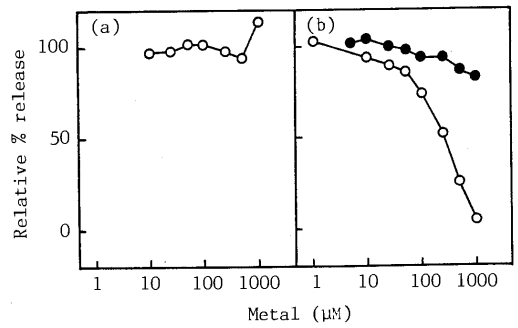

Fig. 6. Dose Response Curves of Groups VIIa and VIII Elements

(a) shows a manganese series element in group VIIa. ○, $MnCl_2$. (b) shows iron/platinum series elements in group VIII. ○, $CoCl_2$; ●, $FeSO_4$.

None of the three metals had the effect (RbCl and CsCl did not show the data). Alkaline earth metals were investigated as $BeSO_4$, $SrCl_2$ and $BaCl_2$. $BeSO_4$ showed inhibitory action on β-hexosaminidase release, while neither $SrCl_2$ nor $BaCl_2$ (data not shown) had the effect.

Elements in Groups IIIa and IVa: The dose response curves of rare earth elements in group IIIa and a titanium series element in group IVa are given in Fig. 4.

Rare earth elements were investigated as $LaCl_3$, $CeCl_3$, $NdCl_3$, $SmCl_3$, $GdCl_3$, $Dy(NO_3)_3$, $HoCl_3$ and $Er(NO_3)_3$, all of which belong to the lanthanide series. All eight of these inhibited the release ($CeCl_3$, $NdCl_3$, $SmCl_3$, $GdCl_3$, $Dy(NO_3)_3$ and $HoCl_3$ did not show the data). In the titanium series, $ZrCl_4$ alone was investigated, and was found to be much more inhibitory of the release than the above-mentioned rare earth elements.

Elements in Groups Va and VIa: The dose response curves of a vanadium series element in group Va and chromium series elements in group VIa are give in Fig. 5.

$NaVO_3$ in the vanadium series showed no action. The chromium series metals examined were $CrCl_3$, K_2CrO_4 and Na_2MoO_4. All three of these metal elements showed almost no effect (Na_2MoO_4 did not show the data); there was no difference between the valencies, *i.e.*, between trivalent and hexavalent chromium species. Trivalent chromium showed slight release-promoting action at 1000 μM.

Elements in Groups VIIa and VIII: The dose response curves of a manganese series element in group VIIa and iron/platinum series elements in group VIII are given in Fig. 6.

$MnCl_2$ in the manganese series had almost no effect, though it showed slight release-promoting action at 1000 μM.

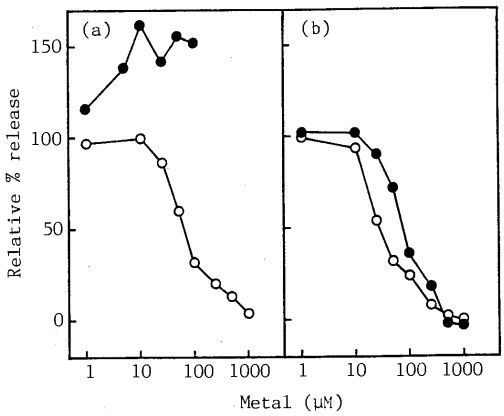

Fig. 7. Dose Response Curves of Groups Ib and IIb Elements

(a) shows copper series elements in group Ib. ○, $CuCl_2$; ●, $AgNO_3$. (b) shows zinc series elements in group IIb. ○, $ZnCl_2$; ●, $CdCl_2$.

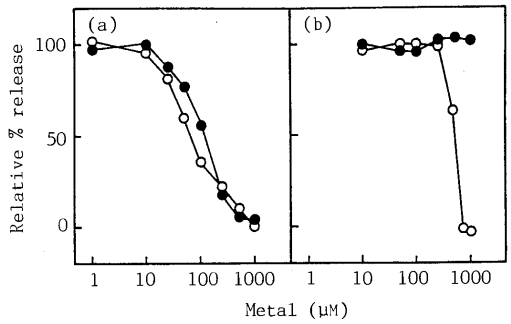

Fig. 8. Dose Response Curves of Groups IIIb and IVb Elements

(a) shows aluminium series elements in group IIIb. ○, $Al(NO_3)_3$; ●, Tl_2SO_4. (b) shows carbon series elements in group IVb. ○, $Pb(NO_3)_2$; ●, GeO_2.

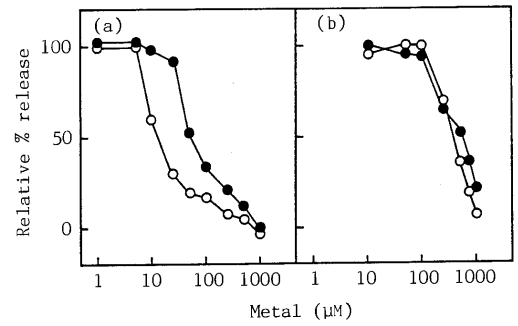

Fig. 9. Dose Response Curves of Groups Vb and VIb Elements

(a) shows a nitrogen series element in group Vb. ○, As_2O_3; ●, As_2O_5. (b) shows an oxygen series element in group VIb. ○, Na_2SeO_3; ●, Na_2SeO_4.

Iron/platinum series elements were investigated as $FeSO_4$, $CoCl_2$, $NiCl_2$ and H_2PtCl_6. $CoCl_2$ and $NiCl_2$ (data not shown) showed inhibitory action on the release, while $FeSO_4$ and H_2PtCl_6 (data not shown) showed almost no effect.

Elements in Groups Ib and IIb: The dose response curves of copper series elements in group Ib and zinc series elements in group IIb are given in Fig. 7.

Copper series elements were investigated as $HAuCl_4$, $AgNO_3$ and $CuCl_2$. $CuCl_2$ showed inhibitory action on the release, while $AgNO_3$ showed promoting action. $HAuCl_4$ showed no action (data not shown). In the zinc series, both $ZnCl_2$ and $CdCl_2$ showed inhibitory action on the release, with stronger inhibition obtained with $ZnCl_2$. $HgCl_2$ completely inhibited β-hexosaminidase activity itself at a

TABLE I. Median Inhibitory Concentration (IC_{50}) of Metal Elements on β-Hexosaminidase Release

Metal	IC_{50} (μM)	Metal	IC_{50} (μM)
$ZrCl_4$	15	$LaCl_3$	100
As_2O_3	15	$NiCl_2$	100
$ZnCl_2$	25	Tl_2SO_4	100
As_2O_5	50	$SmCl_3$	110
$Er(NO_3)_3$	50	$CoCl_2$	250
$Al(NO_3)_3$	75	$Dy(NO_3)_3$	250
$CdCl_2$	75	$GdCl_3$	250
$CeCl_3$	75	$NdCl_3$	250
$CuCl_2$	75	Na_2SeO_3	400
$HoCl_3$	75	Na_2SeO_4	500
$BeSO_4$	100	$Pb(NO_3)_2$	500

IC_{50} values represented the final concentration in the reaction mixture, respectively.

TABLE II. pH in Reaction Mixture and Viability of RBL-2H3 Cells

Metal	pH	Viability (%)	Metal	pH	Viability (%)
$AgNO_3$	7.58	97	$HgCl_2$	7.50	98
$Al(NO_3)_3$	7.49	>99	$HoCl_3$	7.59	>99
As_2O_3	7.70	>99	$LaCl_3$	7.53	>99
As_2O_5	7.52	>99	$NdCl_3$	7.51	>99
$BeSO_4$	7.63	>99	$NiCl_2$	7.52	>99
$CdCl_2$	7.55	>99	$Pb(NO_3)_2$	7.56	99
$CeCl_3$	7.58	99	Na_2SeO_3	7.52	>99
$CoCl_2$	7.59	>99	Na_2SeO_4	7.59	>99
$CuCl_2$	7.60	99	$SmCl_3$	7.54	>99
$Dy(NO_3)_3$	7.51	>99	Tl_2SO_4	7.40	>99
$Er(NO_3)_3$	7.48	>99	$ZnCl_2$	7.55	>99
$GdCl_3$	7.56	>99	$ZrCl_4$	7.58	>99

The metal concentration was 1 mM (final concentration), respectively. The viability of the control cells was 99% or above.

concentration exceeding 50 μM (data not shown).

Elements in Group IIIb and IVb: The dose response curves of aluminium series elements in group IIIb and carbon series elements in group IVb are given in Fig. 8.

In the aluminium series, $Al(NO_3)_3$ and Tl_2SO_4 showed almost equal inhibitory action on the release. In the carbon series, GeO_2 showed no action, and $Pb(NO_3)_2$ began to show remarkable release-inhibitory action when its concentration exceeded 500 μM.

Elements in Groups Vb and VIb: The dose response curves of a nitrogen series element in group Vb and an oxygen series element in group VIb are given in Fig. 9.

In the nitrogen series, trivalent and pentavalent arsenic were investigated. The former was found to be more inhibitory than the latter. In the oxygen series, tetravalent and hexavalent selenium were investigated. They showed almost equal inhibitory action on the release, involving no difference between the valencies.

Median Inhibitory Concentration of Metal Element on β-Hexosaminidase Release For each of the metal elements found to be inhibitory of β-hexosaminidase release, the median inhibitory concentration (IC_{50}) in the reaction mixture was determined. The results are given in Table I.

$ZrCl_4$, As_2O_3 and $ZnCl_2$ were in the group of the strongest inhibitory action, having a IC_{50} of 15 to 25 μM. The second ranking group comprised As_2O_5 through $SmCl_2$, with a IC_{50} of 50 to 110 μM. The group comprising $CoCl_2$ through $Pb(NO_3)_2$ showed weak inhibitory action,

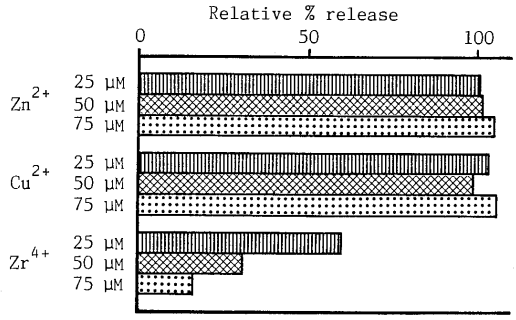

Fig. 10. Effect of Pre-culture in Metal Elements on β-Hexosaminidase Release

The stimulator consisted of biotinylated IgE (3 μg/ml) and avidin (1 μg/ml). The results were obtained in triplicate.

with a IC_{50} of 250 to 500 μM. Chlorine ions, nitrate ions and sulfate ions proved to have no effect, as evidenced with $BaCl_2$, $Mn(NO_3)_2$ and Li_2SO_4.

Reaction Mixture pH and RBL-2H3 Cells Viability With respect to the metal elements found to be inhibitory or promotive of β-hexosaminidase release, the pH at a metal concentration of 1 mM in the reaction mixture and RBL-2H3 cells viability after 1 h incubation at 37 °C in the presence of the reaction mixture were determined (Table II).

The reaction mixture pH which was physiologically favorable for the cells was between 7.40 and 7.70. As for the cell viability, slightly lower values of 97 to 99% were obtained with $AgNO_3$, $CeCl_2$, $CuCl_2$, $HgCl_2$ and $Pb(NO_3)_2$, but there were no changes in the viability from the control cells in the other metals.

Effects of Pre-culture on β-Hexosaminidase Release The pre-culture was conducted in a medium containing 25, 50 or 75 μM $ZnCl_2$, $CuCl_2$ or $ZrCl_4$. 24 h later, the cells were stimulated with the stimulator and the effects of the pre-culture on β-hexosaminidase release were investigated (Fig. 10).

Neither $ZnCl_2$ nor $CuCl_2$ inhibited the release at any concentration in the pre-culture. On the other hand, $ZrCl_4$ showed marked release-inhibitory action in proportion to an increase in the concentration; the relative % release below 20% was obtained in the pre-culture at 75 μM.

Discussion

The present study reviewed three methods of stimulating RBL-2H3 cells to cause their degranulation. In the first method, which offers the best approximation of an actual immediate allergic reaction, DNP_{30}·BSA was used as an antigen to crosslink IgE molecules after sensitizing RBL-2H3 cells with an IgE antibody. In the second method, an anti-IgE receptor antibody was prepared and bound directly to an IgE receptor to cause the receptor aggregation. In the third method, a complex of biotinylated IgE antibody and avidin was used as the stimulator to cause the IgE molecule crosslinking. Although all these methods caused degranulation, the third was adopted for the present study. Histamine is often measured as an index of chemical mediator release, but in the present study, β-hexosaminidase was used as the index, and its enzyme activity was determined, since good correlation exists between the amounts of histamine and β-hexosaminidase released from human and rat mast cells.[4,5] In addition, metal elements

proved to have no inhibitory action for β-hexosaminidase activity itself (excepting for $HgCl_2$), as evidenced that RBL-2H3 cells were degranulated with the stimulator alone, then the extracellular fluid was added to a metal element solution of 1 mM, followed by determination for the enzyme activity.

Among the reports dealing with the effects of metal elements on immediate allergic reactions is one stating that zinc (Zn^{2+}) and manganese (Mn^{2+}) inhibited the degranulation of thrombin-induced mouse mast cells while copper (Cu^{2+}) did not.[8] Concerning the inhibitory action mechanism of Zn^{2+} and Mn^{2+}, suggestions have been made as to the possibilities of inhibition by proteolysis of a mast cell surface protein, interference with intracellular microtubule assembly associated with mast cell degranulation, or by blockage of the calcium channels of stimulated cells. It is also reported that zinc, at physiologic concentrations (10^{-5} or 10^{-6} M), inhibited *in vitro* histamine release from human basophils,[9,10] of which inhibition is estimated as occurring due to the microtubule system, directly or *via* its interaction with calcium. Beaven *et al.*[11,12] made an intensive investigation, using RBL-2H3 cells, to clarify the mechanism of the calcium signal and correlation with histamine release. They stated that lanthanum (La^{3+}) causes a rapid and reversible block of the calcium signal and histamine release, Mn^{2+} does not inhibit histamine release, and Zn^{2+} is the only agent that uncouples the calcium signal from subsequent histamine release. In a study on correlation with histamine release and breakdown of phosphatidylinositol (PI), which coincided with the generation of the calcium signal, Zn^{2+}, Co^{2+} and La^{3+} selectively blocked histamine release without affecting PI breakdown, while Sr^{2+}, Mn^{2+} and Li^{+} did not affect the release of histamine.

In the present study, $LaCl_3$ (Fig. 4a), $CoCl_2$ (Fig. 6b) and $ZnCl_2$ (Fig. 7b) showed inhibitory action on β-hexosaminidase release, while LiCl (Fig. 3a) and $SrCl_2$ (Fig. 3b) did not show such action, results in good agreement with previous reports. As for $MnCl_2$ (Fig. 6a) and $CuCl_2$ (Fig. 7a), the former showed no inhibitory action, while the latter showed inhibitory action; this finding is the reverse of the report of Baranes *et al.*[8] This discrepancy is attributable to differences in the cell type and cell stimulation method used.

As for rare earth elements, seven lanthanoid series elements, namely $CeCl_3$, $NdCl_3$, $SmCl_3$, $GdCl_3$, $Dy(NO_3)_3$, $HoCl_3$ and $Er(NO_3)_3$ (Fig. 4a), as well as $LaCl_3$ (Fig. 4a), were examined. All eight showed release-inhibitory action, relatively uniform in an ion radius at about 1.0 to 1.3 Å because of lanthanide contraction, blocked the calcium signal in the same mode of inhibition as with $LaCl_3$, showing inhibitory action on β-hexosaminidase release.

It should be noted that of the metal elements found to be release-inhibitory action (Table I), $ZrCl_4$ and As_2O_3 showed very strong inhibitory action. Concerning the relationship between the valency and the release-inhibitory action of the metals, trivalent arsenic was found to be more than 3 times stronger than pentavalent arsenic, as assessed by IC_{50} value, while there was almost no difference among the valencies in the case of selenium, as shown in Fig. 9. Even when RBL-2H3 cells were treated with these metal elements which showed release-inhibitory action, the cell viability remained almost unchanged from that of the control cells (Table II), which finding ensures that this release-inhibitory action was not caused by the cell death. The lowest viability, 97% obtained with $AgNO_3$, was given in Table II; it is speculated that the cell damage triggered the release-promoting action (Fig. 7a). In addition, from the results of an experiment on the effects of the pre-culture on β-hexosaminidase release, illustrated in Fig. 10, it is considered that the release inhibition occurs to reversible blocking of Ca^{2+} incorporation in the case of $ZnCl_2$ and $CuCl_2$, or to irreversible blocking of Ca^{2+} incorporation, or of the intracellular activation path, as in the case of $ZrCl_4$.

Of the metal elements investigated in the present study, zinc and copper are quite interesting as β-hexosaminidase release inhibitors, from the viewpoint of suppression of immediate allergic reactions *in vivo*. It is noteworthy that $ZnCl_2$ has a IC_{50} of 25 μM (corresponding to 1.6 ppm as Zn), which is in the physiological range. With respect to the nutritive requirements of zinc, Japan has no specifications, while the United States government specifies a recommended nutritional requirement value at 15 mg/d for males and females aged 11 or above.[13] The average zinc ingestion by adult females in Osaka prefecture is reported as about 7.5 mg/d,[14,15] which is a value significantly lower than the US recommendation mentioned above. In conclusion, it is desirable that a sufficient ingestion of trace metal elements such as zinc and copper be recommended to establish good dietary status for the prevention of immediate allergic diseases.

References

1) K. Ishizaka, T. Ishizaka and M. M. Hornbrook, *J. Immunol.*, **97**, 75 (1966).
2) K. Nakagomi, M. Yamamoto, H. Tanaka, N. Tomizuka, T. Masui and H. Nakazawa, *Agric. Biol. Chem.*, **51**, 1723 (1987).
3) Y. Maeda, M. Yamamoto, T. Masui, K. Sugiyama, M. Yokota, K. Nakagomi, H. Tanaka, I. Takahashi and T. Kobayashi, *J. Food Hyg. Soc. Jpn.*, **30**, 295 (1989).
4) L. B. Schwartz, K. F. Austen and S. I. Wasserman, *J. Immunol.*, **123**, 1445 (1979).
5) L. B. Schwartz, R. A. Lewis, D. Seldin and K. F. Austen, *J. Immunol.*, **126**, 1290 (1981).
6) E. L. Barsumian, C. Isersky, M. G. Petrino and R. P. Siraganian, *Eur. J. Immunol.*, **11**, 317 (1981).
7) F.-T. Liu, J. W. Bohn, E. L. Ferry, H. Yamamoto, C. A. Molinaro, L. A. Sherman, N. R. Klinman and D. H. Katz, *J. Immunol.*, **124**, 2728 (1980).
8) D. Baranes, F.-T. Liu, G. Marx, M. Shalit and E. Razin, *Immunol. Lett.*, **12**, 95 (1986).
9) G. Marone, S. R. Findlay and L. M. Lichtenstein, *J. Pharmacol. Exp. Ther.*, **217**, 292 (1981).
10) G. Marone, M. Columbo, A. Paulis, R. Giugliano and M. Condorelli, *Agents Actions*, **18**, 103 (1986).
11) M. A. Beaven, J. Rogers, J. P. Moore, T. R. Hesketh, G. A. Smith and J. C. Metcalfe, *J. Biol. Chem.*, **259**, 7129 (1984).
12) M. A. Beaven, J. P. Moore, G. A. Smith, T. R. Hesketh and J. C. Metcalfe, *J. Biol. Chem.*, **259**, 7137 (1984).
13) The Welfare Ministry of Japan (ed.), "Nutritive Requirements in Japanese," 4th ed., Dai-ichi Shuppan, Inc., Tokyo, 1989, p. 188.
14) K. Ikebe, Y. Tanaka and R. Tanaka, *J. Food Hyg. Soc. Jpn.*, **29**, 52 (1988).
15) K. Ikebe, Y. Tanaka, T. Nishimune and R. Tanaka, *J. Food Hyg. Soc. Jpn.*, **29**, 440 (1988).

Mode of Complement Activation by Acidic Heteroglycans from the Leaves of *Artemisia princeps* PAMP

Haruki YAMADA,* Takayuki NAGAI, Jong-Chol CYONG, and Yasuo OTSUKA

Oriental Medicine Research Center of the Kitasato Institute, 5-9-1, Shirokane, Minato-ku, Tokyo 108, Japan. *Received January 31, 1991*

The mode of action of the anti-complementary acidic heteroglycans, AAF-IIb-2 and IIb-3 which consisted of rhamnogalacturonan core and arabinogalactan moieties, purified from the leaves of *Artemisia princeps* PAMP (Japanese name = Gaiyo) were investigated. The anti-complementary activities of AAF-IIb-2 and IIb-3 were reduced partially in the absence of Ca^{2+} ions. A marked consumption of C4 was observed to have occurred when serum was incubated with both polysaccharides in the presence of Ca^{2+} ions. AAF-IIb-2 showed more potent C4 consumption than IIb-3. After the incubation of the serum with AAF-IIb-2 in the absence of Ca^{2+} ions, a cleavage of C3 in the serum was detected by immunoelectrophoresis. AAF-IIb-2 showed more significant consumption of the complement than IIb-3 when rabbit erythrocytes were used in the assay system in the absence of Ca^{2+} ions. These results indicate that AAF-IIb-2 activates the complement *via* both the alternative and classical pathways, whereas IIb-3 mainly activates the complement *via* the classical pathway. The absorption of serum with Protein A-Sepharose results in a decrease of the activity of AAF-IIb-2 and IIb-3. However, the decrease of the activity was restored by the replacement of the immunoglobulin G (IgG) fraction after its recovery from the Protein A-Sepharose. These results suggest that IgG dependent mechanisms are both involved in the anti-complementary activity of AAF-IIb-2 and IIb-3.

Keywords *Artemisia princeps*; anti-complementary activity; polysaccharide; action mode; immunoglobulin G

The complement system plays an important role in host defence, inflammation or allergic reactions, and activation occurs *via* both the classical and alternative pathways. The classical pathway is activated by an immune complex containing immunoglobulin M (IgM) and IgG antibodies, the acute phase protein such as C-reactive protein, and ribonucleic acid (RNA) tumor viruses. The alternative pathway is directly activated by polysaccharides, certain immunoglobulins, viruses, fungi, bacteria, certain animal cells and parasites. Some anti-complementary polysaccharides, for example, lipopolysaccharide (LPS),[1] β-(1→3)glucan,[2] 6-branched β-(1→3)glucan[2] and inulin,[3] have already been isolated from bacteria, fungi and plants. Potent anti-complementary activity has also been observed in the extracts of some Chinese herbs.[4] One of these, the extract of the leaves of *Artemisia princeps* PAMP also contained potent anti-complementary activity.[5] Artemisiae Argyi Folium, the leaves of *A. princeps* PAMP (Japanese name = Gaiyo) is a well known crude drug clinically used in the treatment of colic pain, vomiting and diarrhea, and irregular bleeding from the uterus. In previous papers, we have reported the purification and structural characterization of the anti-complementary acidic polysaccharides, AAF-IIb-2 and IIb-3, from the leaves of *A. princeps* PAMP.[5,6] AAF-IIb-2 and IIb-3 are suggested to be structurally related acidic heteroglycans which contained rhamnogalacturonan and arabinogalactan moieties in different proportions.[6]

The present paper describes the mode of action of these anti-complementary polysaccharides.

Materials and Methods

Purification of Anti-complementary Polysaccharides, AAF-IIb-2 and IIb-3, from *A. princeps* PAMP AAF-IIb-2 and IIb-3 were purified from the leaves of *A. princeps* PAMP as reported previously.[5] The crude polysaccharide was prepared by hot-water extraction and dialysis, and was purified by ion exchange chromatography on diethylaminoethyl (DEAE)-Sepharose, affinity chromatography on *Ricinus communis*-agglutinin conjugated Sepharose and gel filtrations on Sephadex G-100 and Sepharose CL-4B.

Anti-complementary Activity The anti-complementary activity was measured as described previously.[7] Gelatin–veronal-buffered saline (pH 7.4) containing 500 μM Mg^{2+} and 150 μM Ca^{2+} (GVB^{++}) was prepared as previously described, and normal human serum (NHS) was obtained from a healthy adult. Various dilutions of AAF-IIb-2 or IIb-3 in water (50 μl) were incubated with 50 μl of NHS and 50 μl of GVB^{++}. The mixtures were incubated at 37 °C for 30 min and the residual total hemolytic complement (TCH_{50}) was determined by a method using IgM-hemolysin-sensitized sheep erythrocytes (EA) at 1×10^8 cells/ml. NHS was incubated with water and GVB^{++} to provide a control. The anti-complementary activity of the polysaccharide was expressed as the percentage inhibition of the TCH_{50} of the control.

Determination of the Complement Hemolysis through the Alternative Complement Pathway (ACH_{50}) ACH_{50} was determined[8] in 10 mM EGTA (ethyleneglycol-bis(β-aminoethylether)*N*,*N*,*N*′,*N*′-tetraacetic acid) containing 2 mM $MgCl_2$ in GVB^{--} (Mg^{2+}–EGTA–GVB^{--}). A sample of AAF-IIb-2 or IIb-3 was incubated with Mg^{2+}–EGTA–GVB^{--} and NHS at 37 °C for 30 min, and the residual complement of the mixtures was measured by the hemolysis of rabbit erythrocytes (5×10^7 cells/ml) incubated with Mg^{2+}–EGTA–GVB^{--}.

Crossed Immunoelectrophoresis NHS was incubated with a half volume of the solution of the anti-complementary polysaccharide with Mg^{2+}–EGTA–GVB^{--} for 30 min at 37 °C. The serum was then subjected to crossed immunoelectrophoresis to locate the C3 cleavage products.[9] Shortly after the first run (barbital buffer pH 8.6, ionic strength 0.025, with 1% of agarose), the second run was carried out on a gel plate (2.0 mm layer) containing 3% of a rabbit anti-human C3 serum at a potential gradient of 0.8 mA/cm for 15 h. After the electrophoresis, the plate was fixed and stained with Ponceau 3R.

Determination of C4 Titration of C4 was performed[10] using intermediate cells $EAC1^{gp}$ for C4. $EAC1^{gp}$ cells were prepared from EA (1×10^9 cells/ml) incubated with C1 solution (1×10^{12} SFU/ml) in the ratio of 28 : 1 at 4 °C for 1 h.

Analytical Procedures The total carbohydrate content was determined by the phenol–sulfuric acid method,[11] using glucose as the respective standard. Protein was assayed by measuring the absorption at 280 nm.

Affinity Absorption of NHS NHS (2 ml) was applied to an asialofetuin-Sepharose 4B column (1.26 × 2.0 cm) and washed with veronal-buffered saline (pH 7.3) containing 500 μM Mg^{2+} and 150 μM Ca^{2+} (VBS^{++}) at 4 °C. The asialofetuin-unbound fraction was used for the measurement of anti-complementary activity. NHS (2 ml) was also applied to a Protein A-Sepharose CL-4B column (1.26 × 1.7 cm) and washed with VBS^{++} at 4 °C. The Protein A-unbound fraction was used for the measurement of anti-complementary activity. IgG was eluted from the Protein A-Sepharose column with 0.05 M sodium citrate (pH 4.5), and dialyzed against VBS^{++}. The TCH_{50} values of both asialofetuin-Sepharose-passed serum and Protein A-Sepharose-passed serum were the same as that of Sepharose passed serum.

Immunoadsorption of Protein A-Unbound Fraction The wells of 96-well polystylene plate (Sumitomo Bakelite Co., Ltd.) were coated with 100 μl of $F(ab')_2$ fragment of rabbit anti-human IgG (0.7 mg/ml as antibody

protein) in 0.01 M sodium bicarbonate (pH 9.6) containing 0.02% NaN_3 by incubation at 4 °C for 4 h. The wells washed three times with 0.01 M phosphate-buffered saline, pH 7.2 (PBS^-). Then the Protein A-unabsorbed fraction was added to the wells, and the filled plate was incubated at 0 °C for 24 h. The resulting IgG-depleted solution was used for the measurement of anti-complementary activity.

Materials Protein A-Sepharose CL-4B, CNBr-activated Sepharose 4B, and Sepharose 4B and CL-4B were obtained from Pharmacia-LKB Biotechnology, and Bio-Gel P-2 (200—400 mesh) from Bio-Rad. $F(ab')_2$ fragment of rabbit anti-human IgG was purchased from Cappel Lab. Inc. (U.S.A.). Fetuin was purchased from Sigma. Asialofetuin was prepared by mild acid hydrolysis (80 °C, 1 h) and dialysis.[12] Asialofetuin-Sepharose 4B was prepared by the coupling of asialofetuin and CNBr-Sepharose 4B.[13] An anti-complementary polysaccharide, LR-polysaccharide IIa as a positive control, was purified from the root of *Lithospermum euchromum* ROYLE.[14]

Results

Mode of Action of Anti-complementary Polysaccharides, AAF-IIb-2 and IIb-3 AAF-IIb-2 and IIb-3 were shown to have potent dose-dependent anti-complementary activity, and AAF-IIb-2 was more active than IIb-3 (Fig. 1). However, the anti-complementary activities of these polysaccharides were less in the absence of Ca^{2+} ions with surplus Mg^{2+} ions (Fig. 1). When NHS was incubated with AAF-IIb-2 or IIb-3 in GVB^{++} at 30 °C for 30 min and the residual activity of C4 estimated by hemolytic assay, AAF-IIb-2 was shown to decrease the C4 content of NHS drastically (Fig. 2). About 100% of the hemolytic titer of C4 was consumed by the use of 100 μg/ml of AAF-IIb-2, and this result was similar to the consumption by LR-polysaccharide IIa, an anti-complementary polysaccharide from *L. euchromum* ROYLE. AAF-IIb-3 also decreased the C4 content of NHS significantly: when NHS incubated with 100 μg/ml of AAF-IIb-3 was used for C4 titration, *ca.* 50% of the hemolytic titer of C4 was consumed. These results show that these polysaccharides can activate the complement *via* the classical pathway, and AAF-IIb-2 was shown to be twice as active as IIb-3. When these polysaccharides were incubated with NHS in Mg^{2+}–EGTA–GVB^{--} at 37 °C for 30 min and the residual complement titer was determined by hemolytic assay using rabbit erythrocytes (ACH_{50}), AAF-IIb-2 and IIb-3 also showed anti-complementary activity on ACH_{50} (ACP activity) (Fig. 3). AAF-IIb-2 was more active than IIb-3.

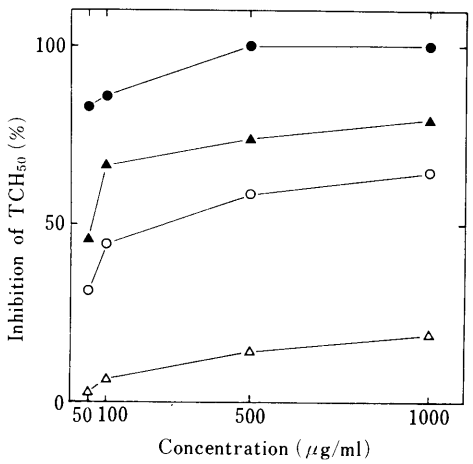

Fig. 1. Change of TCH_{50} by Incubation with AAF-IIb-2 or AAF-IIb-3 in the Presence or Absence of Ca^{2+} Ions

AAF-IIb-2 in GVB^{++} (●), AAF-IIb-2 in Mg^{2+}–EGTA–GVB^{--} (○), AAF-IIb-3 in GVB^{++} (▲), AAF-IIb-3 in Mg^{2+}–EGTA–GVB^{--} (△).

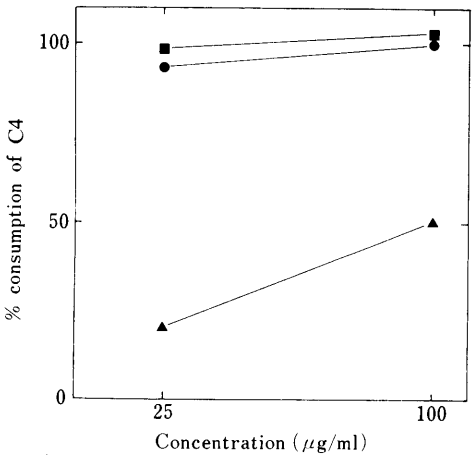

Fig. 2. Consumption of C4 by AAF-IIb-2 or AAF-IIb-3 Treatment

AAF-IIb-2 (●), AAF-IIb-3 (▲), LR-polysaccharide IIa (■).

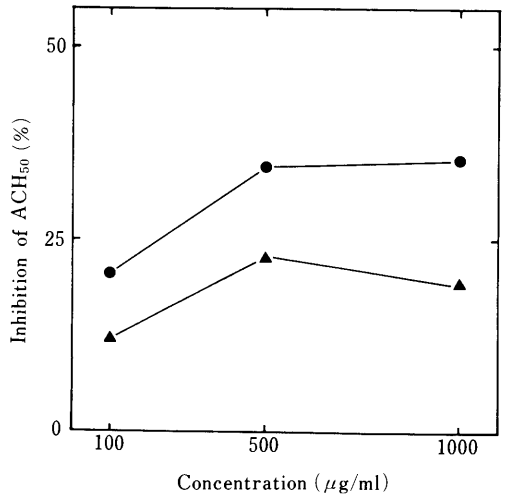

Fig. 3. ACP Activity of AAF-IIb-2 or AAF-IIb-3

AAF-IIb-2 (○), AAF-IIb-3 (▲).

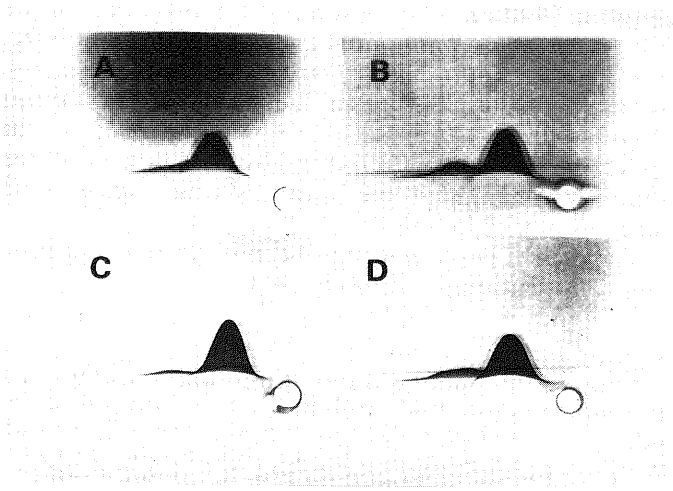

Fig. 4. C3 Activation by AAF-IIb-2 or AAF-IIb-3 Treatment

NHS was incubated with a half volume of (A) PBS^-, or 1 mg/ml of (B) AAF-IIb-2, (C) AAF-IIb-3 and (D) LR-polysaccharide IIa solution with Mg^{2+}–EGTA–GVB^{--} at 37 °C for 30 min. The sera were then subjected to crossed immunoelectrophoresis to locate C3 cleavage products. The anode is to the left.

Therefore, crossed immunoelectrophoresis was carried out after the incubation of NHS with these polysaccharides in Mg^{2+}–EGTA–GVB^{--} to determined whether C3 activation had occurred (Fig. 4). A cleavage of the C3 precipitin line was observed in the serum treated with AAF-IIb-2, but AAF-IIb-3 could not cleave C3 significantly. These results indicate that AAF-IIb-2 also activate the complement *via* the alternative pathway.

Effects of Serum Factors on the Anti-complementary Activity of AAF-IIb-2 and IIb-3 To know how these polysaccharides activate the complement, we examined the effects of serum factors on the anti-complementary activity. AAF-IIb-2 and IIb-3 contained galactose as a predominant component sugar.[5] Therefore, we first examined the possibility as to whether some galactose specific lectin-like molecule in the serum is involved in the activity. After serum was passed through an asialofetuin-Sepharose 4B column at 4 °C, an unabsorbed fraction was used for the measurement of the anti-complementary activity of AAF-IIb-2 and IIb-3. However, the activity of the use of this fraction did not change in comparison with that by the use of Sepharose 4B column-passed serum as a control (data not shown). Asialofetuin is possessing Gal-β-(1→4)-GlcNAc as the non-reducing terminal structure of *N*-linked sugar chains and Gal-β-(1→3)-GalNAc as *O*-linked sugar chain. Therefore, this result denied the possibility of the involvement of galactose binding protein in serum having specificity for these galactosyl structures to the appearance of anti-complementary activity by AAF-IIb-2 and IIb-3. Next, serum was passed through a Protein A-Sepharose CL-4B column at 4 °C, and an unabsorbed fraction was used for the measurement of the anti-complementary activity of AAF-IIb-2 and IIb-3. As shown in Figs. 5a and b, both AAF-IIb-2 and IIb-3 decreased their anti-complementary activity dramatically by the use of this serum, comparing with the use of Sepharose CL-4B column-passed serum. When Protein A-Sepharose-absorbed fraction was added to the Protein A-Sepharose-passed serum again and the resulting serum was used for measurement of anti-complementary activity, the activity was recovered to a similar level with the activity by the use of NHS (Fig. 5c). These results suggested that IgG molecules are involved in the appearance of the activity by the polysaccharides. When these polysaccharides were measured for anti-complementary activity by the use of Protein A-Sepharose-passed serum, the remaining significant activity was still observed. Therefore, to know whether this remaining activity was caused by the IgG molecule unabsorbed to the Protein A-Sepharose, this Protein A-Sepharose-passed serum was absorbed with anti-human IgG antibody. However, no more reduction of the activity was observed (Fig. 5d). When Protein A-Sepharose-passed serum was used for measurement of consumption of C4 by AAF-IIb-2 and IIb-3, the consumption of C4 by both polysaccharides was decreased partially comparing with the use of Sepharose passed serum (data not shown).

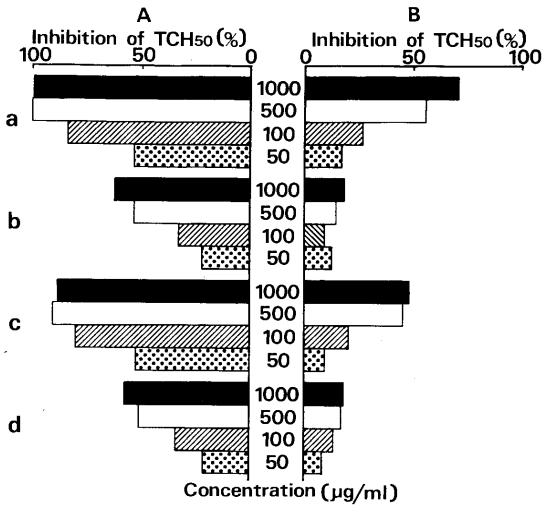

Fig. 5. Effects of Protein A-Sepharose and Anti-IgG Treatments of the Serum on Anti-complementary Activity of AAF-IIb-2 (A) or AAF-IIb-3 (B)

Sepharose-passed serum (a), Protein A-Sepharose-passed serum (b), Protein A-Sepharose-passed serum plus Protein A-Sepharose-absorbed fraction (c) or anti-IgG-treated Protein A-Sepharose-passed serum (d) was incubated with an equal volume of indicated concentration of AAF-IIb-2 or AAF-IIb-3 solution with GVB^{++} at 37 °C for 30 min. The sera were then subjected to total hemolytic complement (TCH_{50}) assay.

Discussion

We have purified two kinds of anti-complementary acidic polysaccharides, AAF-IIb-2 and IIb-3, from the leaves of *A. princeps* PAMP.[5] AAF-IIb-2 and IIb-3 were composed of rhamnose, xylose, arabinose, galactose, glucose, galacturonic acid and glucuronic acid in the molar ratios of 7.6:7.6:13.0:10.9:3.0:51.2:6.7 and 3.9:2.6:24.7:19.7:2.6:15.0:31.5, respectively.[6] AAF-IIb-3 has a main chain consisting of (1→4)-linked galacturonic acid and (1→2)-linked rhamnopyranosyl residues which is mostly substituted with arabino-3,6-galactan and arabino-4-galactan at position 4 of rhamnosyl residues.[6] Most of the arabinosyl residues of arabino-3,6-galactan in AAF-IIb-3 exist in α-L-furanosyl form and are mostly attached to position 3 of (1→6)-linked galactosyl residues as in the non-reducing terminals and highly branched side chains.[6] The basic structure of AAF-IIb-3 is similar to that of IIb-2, but AAF-IIb-3 has a higher arabinogalactan content than IIb-2.[5,6] AAF-IIb-3 activated the complement mainly *via* the classical pathway. The mode of action of AAF-IIb-3 was similar to that of another anti-complementary polysaccharide, AR-arabinogalactan (AG) IIb-1, which was isolated from the root of *Angelica acutiloba* KITAGAWA.[15] The structure of AAF-IIb-3 was also similar to that of AGIIb-1. AGIIb-1 is a complex arabinogalactan consisting of four carbohydrate units; one neutral and two acidic arabinogalactans and one neutral arabinan, which are linked to each other by acid labile linkage.[15b,c] The acidic arabinogalactan units in AGIIb-1 consist of a rhamnogalacturonan core possessing at least three kinds of arabinogalactan side chains.[15b,c] When the neutral arabino-3,6-galactan unit in AGIIb-1 was digested with exo-α-arabinofuranosidase, the activity was markedly enhanced through the alternative pathway.[15d] These results suggest that the arabinofuranosyl side-chains of AAF-IIb-3 might inhibit the expression of activity through the alternative pathway. AAF-IIb-2 showed more potent activation of the complement *via* both the classical and alternative pathways than IIb-3. The mode of action of AAF-IIb-2 was similar to that of LR-polysaccharide IIa (acidic heteroglycan) from the root of *L. euchromum* ROYLE,[14] Plantago-mucilage A (partially *O*-acetylated

glucuronoarabinofuranoxylan) from the seed of *Plantago asiatica*,[16b,17] and AR-2IId (pectin) from the root of *A. acutiloba* KITAGAWA.[18] AR-2IId contained polygalacturonan regions and "ramified" regions consisting of rhamnogalacturonan cores with β-(1→6)-linked galactooligosaccharides and a trace of arabino-3,6-galactan moiety.[18] AAF-IIb-2 also has a low arabino-3,6-galactan,[6] and it may be related to the mode of action of AAF-IIb-2. But further studies of the structure and the anti-complementary activity are required to clarify the more detailed correlation of structure and mode of activity.

It is known that lipid A,[19] RNA virus,[20] heparin–protamine complex[21] and C-reactive protein–C-polysaccharide complex[22] bind to C1q directly, and enhance the activation of the C1 molecule by antibody independent mechanism. Ihara *et al.*[23] find complement activating antimicrobial protein (camp) in several animal sera. Camp has a specific affinity to the carbohydrate moieties of LPS in the presence of Ca^{2+} and Mg^{2+} ions.[23,24] Camp activates the complement *via* the classical pathway,[25] and is a different molecule from several classes of IgG molecule.[26] Therefore, we examined whether a lectin-like molecule or IgG is involved in the anti-complementary activity by AAF-IIb-2 and IIb-3, but an asialofetuin-Sepharose-passed fraction did not reduce the activity. When Protein A-Sepharose-passed serum was used for the measurement of the anti-complementary activity by AAF-IIb-2 and IIb-3, the activity was much reduced, and recovered by the addition of the absorbed fraction into the IgG-depleted serum. These results indicate that the IgG molecule or some natural antibody is involved in the appearance of the anti-complementary activity of AAF-IIb-2 and IIb-3. It is known that sera of various animals contain "natural" antibodies to carbohydrate components such as blood type antibody.[27] Sela *et al.*[28] find that normal sera from various animals contained anti-carbohydrate IgG antibodies which are purified by fetuin-Sepharose. Because asialofetuin-Sepharose treatment of NHS did not diminish the activity by AAF-IIb-2 and IIb-3, we do not know if the IgG molecule in our experiment is related to this anti-carbohydrate antibody. Schenkein and Ruddy[29] also reported that naturally occurring IgG antibody to zymosan contributes to the function of the alternative pathway by enhancing the rate of deposition of C3 from the fluid phase to the zymosan surface and thus increasing the rate of formation of the alternative pathway C3 convertase. Recently, Galili *et al.*[30] reported that all humans (except for immunosuppressed patients) are producing a large amount of anti-galactosyl IgG as a natural antibody in their sera, and bacteria within normal intestinal flora may provide constant antigenic stimulation for the synthesis of this antibody. Pectic arabinogalactans and pectins are characteristically associated with the cell wall of both higher and lower plants, and several of these polysaccharides have been isolated from many kinds of plants, such as corn,[31] soybean,[32] jujube,[33] cabbage[34] and rice.[35] Therefore, when humans take vegetables and/or fruits as foods, it is possible to synthesize the anti-polysaccharide antibodies. But, we do not know yet whether anti-galactosyl natural antibody in human serum recognizes these plant polysaccharides or another anti-plant polysaccharide antibody is present in the serum.

AAF-IIb-2 and IIb-3 still showed anti-complementary activity even when Protein A-unabsorbed serum was used. This observation suggests that both polysaccharides activate the complement by IgG dependent and independent mechanisms. The present results also showed that these polysaccharides activated the complement through the classical pathway by an IgG dependent mechanism, but we do not know the involvement of this mechanism to the activation of the alternative pathway. Further studies on this subject are now in progress.

Acknowledgment A part of this work was supported by Tsumura & Co. Ltd., Tokyo, Japan.

References

1) H. Gewurz, H. S. Shin and S. E. Mergenhagen, *J. Exp. Med.*, **128**, 1049 (1968); R. L. Marcus, H. S. Shin and M. M. Mayer, *Proc. Natl. Acad. Sci. U.S.A.*, **68**, 1351 (1971); L. Pillemer, M. D. Schoenberg, L. Blum and L. Wurz, *Science*, **122**, 545 (1955).
2) T. Okuda, Y. Yoshioka, T. Ikekawa, G. Chihara and K. Nishioka, *Nature New Biol.*, **238**, 59 (1972); J. Hamuro, U. Hadding and D. Bitter-Suermann, *Immunology*, **34**, 695 (1978).
3) O. Götze and H. J. Müler-Eberhard, *J. Exp. Med.*, **134**, 90s (1971).
4) M. Shindoh, J.-C. Cyong, H. Yamada, H. Kiyohara and Y. Otsuka, *Proc. Symp. Wakan-yaku*, **16**, 76 (1983).
5) H. Yamada, K. Ohtani, H. Kiyohara, J.-C. Cyong, Y. Otsuka, Y. Ueno and S. Ōmura, *Planta Med.*, **1985**, 121 (1985).
6) H. Yamada, Y. Otsuka and S. Ōmura, *Planta Med.*, **1986**, 311 (1986); H. Yamada, H. Kiyohara and Y. Otsuka, *Carbohydr. Res.*, **170**, 181 (1987).
7) *a*) H. Yamada, H. Kiyohara, J.-C. Cyong, Y. Kojima, Y. Kumazawa and Y. Otsuka, *Planta Med.*, **50**, 163 (1984); *b*) H. Yamada, H. Kiyohara, J.-C. Cyong and Y. Otsuka, *Mol. Immunol.*, **22**, 295 (1985).
8) T. A. E. Platts-Mills and K. Ishizaka, *J. Immunol.*, **113**, 348 (1974).
9) J.-C. Cyong, S. S. Witkin, B. Rieger, E. Barbarese, R. A. Good and N. K. Day, *J. Exp. Med.*, **155**, 587 (1982).
10) M. E. Wilson and D. C. Morrison, *Eur. J. Biochem.*, **128**, 137 (1982).
11) M. Dubois, K. A. Gilles, J. K. Hamilton, P. A. Rebers and F. Smith, *Anal. Chem.*, **28**, 350 (1956).
12) R. G. Spiro and V. D. Bhoyroo, *J. Biol. Chem.*, **249**, 5704 (1974).
13) P. Cuatrecasas, *J. Biol. Chem.*, **245**, 3059 (1970).
14) H. Yamada, J.-C. Cyong and Y. Otsuka, *Int. J. Immunopharmacol.*, **8**, 71 (1986).
15) *a*) H. Yamada, H. Kiyohara, J.-C. Cyong and Y. Otsuka, *Carbohydr. Res.*, **159**, 275 (1987); *b*) H. Kiyohara, H. Yamada and Y. Otsuka, *ibid.*, **167**, 221 (1987); *c*) H. Kiyohara and H. Yamada, *ibid.*, **193**, 173 (1989); *d*) H. Kiyohara, J.-C. Cyong and H. Yamada, *ibid.*, **193**, 193 (1989).
16) *a*) M. Tomoda, M. Takahashi and S. Nakatsuka, *Chem. Pharm. Bull.*, **21**, 707 (1973); *b*) H. Yamada, T. Nagai, J.-C. Cyong, Y. Otsuka, M. Tomoda, N. Shimizu and K. Shimada, *Carbohydr. Res.*, **144**, 101 (1985).
17) M. Tomoda, M. Yokoi and K. Ishikawa, *Chem. Pharm. Bull.*, **29**, 2877 (1981); M. Tomoda, N. Shimizu, K. Shimada, R. Gonda and H. Sakabe, *ibid.*, **32**, 2182 (1984).
18) H. Kiyohara, J.-C. Cyong and H. Yamada, *Carbohydr. Res.*, **182**, 259 (1988); *idem*, *ibid.*, **193**, 201 (1989).
19) N. R. Cooper and D. C. Morison, *J. Immunol.*, **120**, 1862 (1978).
20) N. R. Cooper, F. C. Jensen, R. M. Welsh Jr. and M. B. A. Oldstone, *J. Exp. Med.*, **144**, 970 (1976).
21) A. B. Fiedel, R. Rent, R. Myhrman and H. Gewurz, *Immunology*, **30**, 161 (1976).
22) M. H. Kaplan and J. E. Volanakis, *J. Immunol.*, **112**, 2135 (1974).
23) I. Ihara, Y. Harada, S. Ihara and M. Kawakami, *J. Immunol.*, **128**, 1256 (1982).
24) M. Kawakami, I. Ihara, S. Ihara, A. Suzuki and K. Fukui, *J. Immunol.*, **132**, 2578 (1984).
25) I. Ihara and M. Kawakami, *Microbiol. Immunol.*, **25**, 751 (1981).
26) M. Kawakami, I. Ihara, A. Suzuki and Y. Harada, *J. Immunol.*, **129**, 2198 (1982).
27) A.-M. Staub and P. Grabar, *Ann. Inst. Pasteur*, **69**, 368 (1943); J. L.

Turk, *Br. J. Exp. Pathol.*, **40**, 97 (1959).
28) B.-A. Sela, J. L. Wang and G. M. Edelman, *Proc. Natl. Acad. Sci. U.S.A.*, **72**, 1127 (1975).
29) H. A. Schenkein and S. Ruddy, *J. Immunol.*, **126**, 7 (1981); *idem*, *ibid.*, **126**, 11 (1981).
30) U. Galili, R. E. Mandrell, R. M. Hamadeh, S. B. Shohet and J. M. Griffiss, *Infect. Immun.*, **56**, 1730 (1988).
31) Y. Kato and D. J. Neins, *Plant Physiol.*, **74**, 562 (1984).
32) G. O. Aspinall, K. Hunt and I. M. Morrison, *J. Chem. Soc., C*, 1080 (1967).
33) N. Shimizu and M. Tomoda, *Chem. Pharm. Bull.*, **31**, 499 (1983).
34) B. H. J. Stevens and R. R. Selvendran, *Phytochemistry*, **23**, 107 (1984).
35) N. Shibuya and R. Nakane, *Phytochemistry*, **23**, 1425 (1984).

Characterization of a Polysaccharide Having Activity on the Reticuloendothelial System from the Stolon of *Glycyrrhiza glabra* var. *glandulifera*

Noriko SHIMIZU, Masashi TOMODA,* Makiko SATOH, Ryōko GONDA and Naoko ŌHARA

Kyoritsu College of Pharmacy, Shibakōen, Minato-ku, Tokyo 105, Japan. *Received February 5, 1991*

An acidic polysaccharide, named glycyrrhizan GA, was isolated from the stolon of *Glycyrrhiza glabra* L. var. *glandulifera* REG.*et* HERD. It produced a single band on electrophoresis and a single peak on gel chromatography, and its molecular mass was estimated to be 85000. Glycyrrhizan GA is composed of L-arabinose: D-galactose: L-rhamnose: D-galacturonic acid: D-glucuronic acid in the molar ratio of 22:10:1:2:1, in addition to small amounts of *O*-acetyl groups. Part of the hexuronic acid residues exist as methyl esters. Methylation analysis, carbon-13 nuclear magnetic resonance and periodate oxidation studies indicated that its structural features include mainly α-arabino-β-3,6-galactan type structural units. Glycyrrhizan GA showed remarkable reticuloendothelial system-potentiating activity in a carbon clearance test.

Keywords *Glycyrrhiza glabra* var. *glandulifera*; stolon; licorice; glycyrrhizan GA; polysaccharide; acidic arabinogalactan; immunological activity; reticuloendothelial system; structural features

In previous papers,[1,2] the isolation and structural features of two acidic polysaccharides, called glycyrrhizans UA and UB, and a neutral polysaccharide, called glycyrrhizan UC, from the root of *Glycyrrhiza uralensis* FISCHER were reported. These substances showed significant immunological activity on the reticuloendothelial system (RES). The root of this plant is a representative Chinese licorice, and in addition, *Glycyrrhiza glabra* L. var. *glandulifera* REG. *et* HERD. is one of the other material plants of Chinese licorice in the Japanese market. We now report the isolation of a novel acidic polysaccharide from the stolon of the latter plant, and present its structural features and RES activity.

Materials and Methods

Isolation of Polysaccharide The material was imported from China. The sliced stolons (2 kg) were extracted with hot water (20 l) under stirring for 30 min in a boiling water bath. After suction filtration, the filtrate was poured into two volumes of ethanol. After centrifugation and treatment with 70% ethanol, the precipitate was heated with water (7 l) by stirring for 30 min in a boiling water bath. After centrifugation, the supernatant was added to 1/9 volumes of 0.1% sodium sulfate; 5% cetyltrimethylammonium bromide (CTAB, 1.1 l) was then added to the solution. The supernatant obtained was poured into two volumes of ethanol. The precipitate was dissolved in water, then dialyzed, centrifuged, concentrated and lyophilized. The yield of this fraction (CTAB-Sup) was 1.56 g. The resulting precipitate by treatment with CTAB was dissolved in 0.1 M sodium chloride (1.4 l). After centrifugation, the supernatant was poured into two volumes of ethanol. The resulting precipitate was dissolved in water, then dialyzed, centrifuged, concentrated and lyophilized. The yield of this fraction (CTAB-Ppt) was 1.67 g.

Fraction CTAB-Sup (300 mg) was dissolved in water and applied to a column (5 × 82 cm) of Sephacryl S-300. The column was equilibrated and eluted with 0.1 M Tris–HCl buffer (pH 7.0), and fractions of 20 ml were collected and analyzed by the phenol–sulfuric acid method.[3] Fraction 1 was obtained from tubes 27 to 33, fr. 2 from tubes 34 to 45, and fr. 3 from tubes 46 to 61. Fraction 2 was dialyzed and rechromatographed using the same column of Sephacryl S-300. After dialysis and gel chromatography using a column (5 × 82 cm) of Sephadex G-25 with water, fr. A was obtained; the yield was 60 mg.

Fraction A (140 mg) was dissolved in a 1/15 M phosphate buffer (pH 7.0) containing 0.15 M NaCl, 1 mM $MgCl_2$ and 1 mM $CaCl_2$, and applied to a column (1.5 × 39 cm) of Con A-Sepharose (Pharmacia Co.). The column was equilibrated and eluted with the same buffer at 4 °C, and fractions of 10 ml were collected. The eluates obtained from tubes 6 to 9 were combined, dialyzed and then concentrated. The solution from 280 mg of fr. A was applied to a column (5 × 83 cm) of Sephadex G-25. The column was eluted with water and fractions of 20 ml were collected. The eluates obtained from tubes 30 to 34 were combined, concentrated and lyophilized. Glycyrrhizan GA was obtained as a white powder. Qualitative nitrogen analysis and thin-layer chromatography (TLC) of the hydrolyzate showed that it contains no nitrogen component. Yield, 140 mg.

Polyacrylamide Gel Electrophoresis (PAGE) This was carried out in an apparatus with gel tubes (4 × 140 mm each) and a 5 mM Tris–glycine buffer (pH 8.3) at 5 mA/tube for 40 min. Gels were stained by the periodate-Schiff (PAS) procedure. Glycyrrhizan GA gave a distinct band at a distance of 74 mm from the origin.

Gel Chromatography The sample (3 mg) was dissolved in a 0.1 M Tris–HCl buffer (pH 7.0) and applied to a column (2.6 × 95 cm) of Sephacryl S-300HR, pre-equilibrated and developed with the same buffer. Fractions of 5 ml were collected and analyzed by the phenol–sulfuric acid method. Standard pullulans (Shōwa Denkō Co.) having known molecular masses were run on the column to obtain a calibration curve.

Qualitative Analysis of Component Sugars Hydrolysis and cellulose TLC of component sugars were performed as described in a previous report.[4] The configurations of component neutral sugars and neutral derivatives from hexuronic acids were identified by gas chromatography (GC) of trimethylsilylated α-methylbenzylaminoalditol derivatives.[5] GC was carried out on a Shimadzu GC-14A gas chromatograph equipped with a hydrogen flame ionization detector.

Determination of Components Neutral sugars were analyzed by GC after conversion of the hydrolyzate into alditol acetates as described in a previous report.[6] Hexuronic acid was determined by the *m*-hydroxybiphenyl method.[7] For the determination of the ratio of galacturonic acid and glucuronic acid, the sample (6 mg) was hydrolyzed with 2 N sulfuric acid at 100 °C for 6 h, then neutralized with barium carbonate. The filtrate was passed through a column (0.5 × 1 cm) of Dowex 50WX8 (H^+), and the eluate with water was concentrated and applied to a column (0.7 × 4 cm) of DEAE-Sephadex A-25 (formate form). The column was eluted successively with water and 0.3 M formic acid (30 ml each). The eluate with formic acid was evaporated for removal of the acid, then the residue was dissolved in water and reduced with sodium borohydride (5 mg) at room temperature for 2 h. After neutralization with Dowex 50WX8 (H^+), boric acid was removed by the repeated addition and evaporation of methanol. The residue was dissolved in methanol (1 ml), and dry Dowex 50WX8 (H^+) (10 mg) was added to the solution. The mixture was heated at 67 °C for 23 h in a sealed tube, followed by filtration, washing with methanol and evaporation. The residue was dissolved in water (1 ml) and reduced with sodium borohydride (10 mg) at room temperature for 18 h. The resulting alditols were acetylated and analyzed by GC as described above.

Determination of *O*-Acetyl Groups The sample was hydrolyzed with 0.2 N hydrochloric acid and analyzed by GC using propionic acid as an internal standard as described previously.[8]

Determination of *O*-Methyl Groups in Methyl Esters This was performed by GC after saponification using ethanol as an internal standard as described previously.[9]

Nuclear Magnetic Resonance (NMR) NMR spectrum was recorded on a JEOL JNM-GX 270 FT NMR spectrometer in heavy water containing sodium 2,2-dimethyl-2-silapentane-5-sulfonate as an internal standard at 30 °C.

Reduction of Carboxyl Groups This was carried out with 1-cyclohexyl-3-(2-morpholinoethyl)carbodiimide metho-*p*-toluenesulfonate and sodium borohydride as described in a previous report.[10] The reduction was repeated four times under the same conditions. Yield was 23 mg from 33 mg of glycyrrhizan GA.

Methylation Analysis Methylation was performed with powdered sodium hydroxide and methyl iodide in dimethyl sulfoxide as described in a previous report.[11] The yields were 4 mg from 6 mg of glycyrrhizan GA and 4.5 mg from 5.3 mg of the carboxyl-reduced product. The products were hydrolyzed with dilute sulfuric acid in acetic acid, then reduced and acetylated as described in a previous report.[12] The partially methylated alditol acetates obtained were analyzed by gas chromatography-mass spectrometry (GC-MS) using a fused silica capillary column (0.32 mm i.d. × 30 m) of SP-2330 (Supelco Co.) with a programmed temperature increase of 4 °C per min from 160 to 220 °C at a helium flow of 1 ml per min. GC-MS was performed with a JEOL JMS-GX303 mass spectrometer. The relative retention times of the products with respect to 1,5-di-*O*-acetyl-2,3,4,6-tetra-*O*-methyl-D-glucitol in GC and the main fragments in MS are listed in Table I.

Periodate Oxidation Periodate oxidation followed reduction with sodium borohydride was performed as described in a previous report.[1] Oxidation was completed after 3 d. Yield of the product was 4 mg from 5.5 mg of glycyrrhizan GA. Determination of the surviving component sugars was carried out as described above.

Phagocytic Activity This was measured as described in a previous report.[6] The samples and a positive control, zymosan (Tokyo Kasei Co.), were each dissolved and suspended physiological saline and dosed i.p. (20 mg/kg body weight) once a day. The phagocytic index, K, was calculated by means of the following equation:

$$K=(\ln OD_1-\ln OD_2)/(t_2-t_1)$$

where OD_1 and OD_2 are the optical densities at times t_1 and t_2, respectively. Results were expressed as the arithmetic mean ± S.D. of five male mice (ICR-SPF). The comparison of results was performed using the Student's t-test.

Results

The crude polysaccharide fraction was isolated from the stolon of *G. glabra* var. *glandulifera* by hot water extraction followed by precipitation with ethanol. The precipitate was again extracted with hot water, then treatd with CTAB in the presence of small amounts of sodium sulfate. The supernatant obtained was poured into ethanol, then the precipitate was purified by gel chromatography with Sephacryl S-300 twice. The main fraction (fr. A) obtained was subjected to affinity chromatography on Con A-Sepharose. A pure polysaccharide designated as glycyrrhizan GA was obtained from the passed-through fraction with a phosphate buffer, followed by dialysis and gel chromatography with Sephadex G-25. The isolation method of the polysaccharide is summarized in Fig. 1.

Glycyrrhizan GA gave a single band on PAGE, and gave a single peak on gel chromatography. It had $[\alpha]_D^{23}$ −67.6° (H_2O, $c=0.1$). Gel chromatography gave a value of 8.5×10^4 for the molecular mass.

The effects of glycyrrhizan GA, fr. A and fr. CTAB-Ppt on the RES were demonstrated by a modification[6] of the *in vivo* carbon clearance test[13] using zymosan as a positive control. As shown in Fig. 2, the phagocytic index was

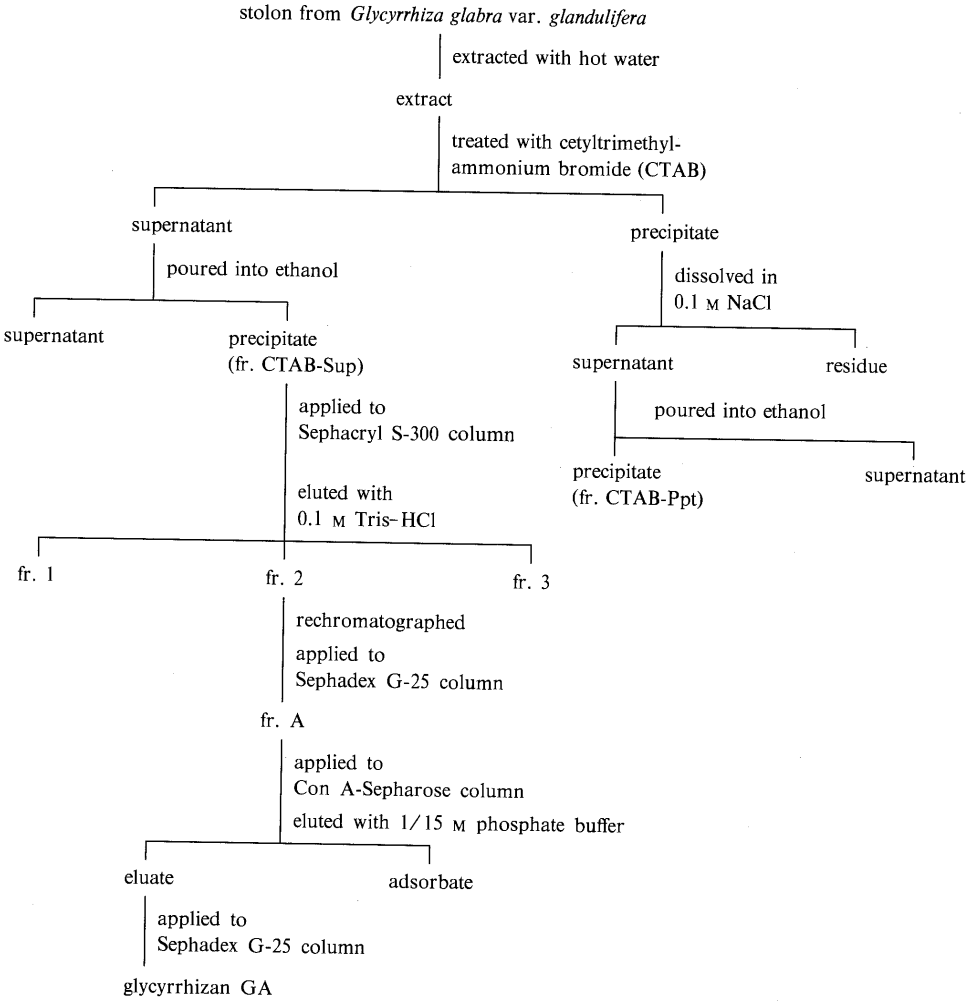

Fig. 1. Isolation of Glycyrrhizan GA

TABLE I. Relative Retention Times on GC and Main Fragments in MS of Partially Methylated Alditol Acetates

	Relative retention time[a]	Main fragments (*m/z*)
1,4-Ac_2-2,3,5-Me_3-L-arabinitol	0.69	43, 45, 71, 87, 101, 117, 129, 161
1,3,4-Ac_3-2,5-Me_2-L-arabinitol	1.05	43, 87, 113, 117, 233
1,4,5-Ac_3-2,3-Me_2-L-arabinitol	1.14	43, 87, 101, 117, 129, 189
1,2,4,5-Ac_4-3-Me-L-arabinitol	1.51	43, 87, 129, 189
1,2,5-Ac_3-3,4-Me_2-L-rhamnitol	0.96	43, 89, 129, 131, 189
1,2,4,5-Ac_4-3-Me-L-rhamnitol	1.30	43, 87, 101, 129, 143, 189, 203
1,5-Ac_2-2,3,4,6-Me_4-D-glucitol	1.00	43, 45, 71, 87, 101, 117, 129, 145, 161, 205
1,5-Ac_2-2,3,4,6-Me_4-D-galactitol	1.10	43, 45, 71, 87, 101, 117, 129, 145, 161, 205
1,3,5-Ac_3-2,4,6-Me_3-D-galactitol	1.38	43, 45, 87, 101, 117, 129, 161
1,4,5-Ac_3-2,3,6-Me_3-D-galactitol	1.46	43, 45, 87, 99, 101, 113, 117, 233
1,5,6-Ac_3-2,3,4-Me_3-D-galactitol	1.62	43, 87, 99, 101, 117, 129, 161, 189
1,3,5,6-Ac_4-2,4-Me_2-D-galactitol	2.02	43, 87, 117, 129, 189

a) Relative to 1,5-di-*O*-acetyl-2,3,4,6-tetra-*O*-methyl-D-glucitol. Abbreviations: Ac=acetyl; Me=methyl (*e.g.*, 1,4-Ac_2-2,3,5-Me_3-=1,4-di-*O*-acetyl-2,3,5-tri-*O*-methyl-).

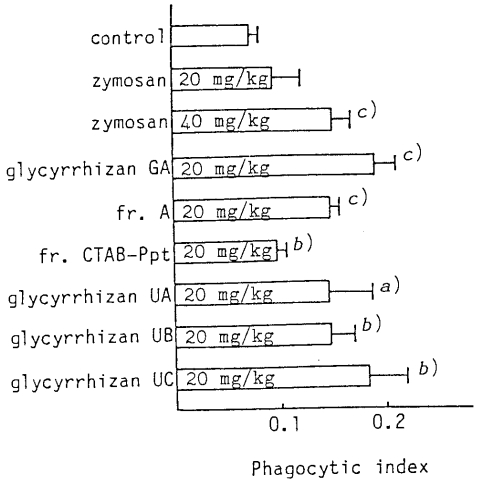

Fig. 2. Effects of Glycyrrhizans GA, UA, UB and UC, Fr. A, and Fr. CTAB-Ppt on Carbon Clearance Index in ICR Mice

Significantly different from the control, *a*) $p<0.05$, *b*) $p<0.01$, *c*) $p<0.001$.

significantly increased, suggesting the activation of RES by i.p. injection of glycyrrhizan GA. Its value was notably higher than that of fr. A, but by contrast, the activity of fr. CTAB-Ppt was very low.

Glycyrrhizan GA is composed of L-arabinose, D-galactose, L-rhamnose, D-galacturonic acid and D-glucuronic acid. Quantitative analysis showed that it contained 54.6% arabinose, 30.2% galactose, 2.8% rhamnose, 6.8% galacturonic acid and 3.4% glucuronic acid. The molar ratio of these components was 22: 10: 1: 2: 1.

The carbon-13 NMR (^{13}C-NMR) spectrum of glycyrrhizan GA showed signals at δ 21.75 and 178.26 ppm, suggesting the presence of an *O*-acetyl group. In addition, the ^{13}C-NMR spectrum showed a signal at δ 57.04 ppm, suggesting the presence of *O*-methyl groups as carboxylic

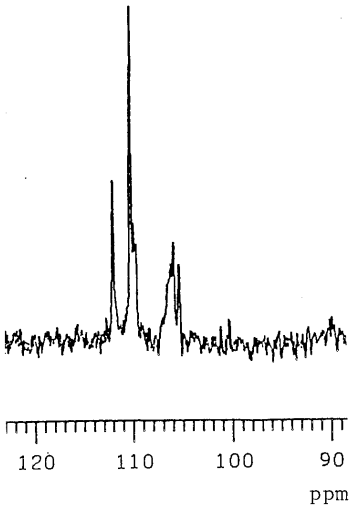

Fig. 3. ^{13}C-NMR Spectrum of Glycyrrhizan GA in Its Anomeric Region

TABLE II. Methylation Analysis of Glycyrrhizan GA and Its Carboxyl-Reduced Derivative

Methylated sugars (as alditol acetates)	Molar ratio	
	Original	Carboxyl-reduced
2,3,5-Me_3-L-arabinose	13	13
2,5-Me_2-L-arabinose	4	4
2,3-Me_2-L-arabinose	22	22
3-Me-L-arabinose	5	5
3,4-Me_2-L-rhamnose	1	1
3-Me-L-rhamnose	1	1
2,3,4,6-Me_4-D-glucose	—	2
2,3,4,6-Me_4-D-galactose	1	1
2,4,6-Me_3-D-galactose	6	6
2,3,6-Me_3-D-galactose	—	4
2,3,4-Me_3-D-galactose	3	3
2,4-Me_2-D-galactose	10	10

acid methyl esters. The presence of these groups was confirmed by GC of the hydrolyzate, and the contents of acetyl and methoxyl groups were 2.0% and 0.18%, respectively. Thus about 10% of the hexuronic acid residues in the polysaccharide exist as methyl esters.

In addition, the ^{13}C-NMR spcetrum showed six signals due to anomeric carbons at δ 100.26, 101.21, 105.31, 105.87, 110.16 and 111.94 ppm (Fig. 3). The first and the second were assigned to the anomeric carbons of α-D-galactopyranosyluronic acid and α-L-rhamnopyranose, respectively.[14] The signals at δ 105.31 and 105.87 ppm were assigned to the anomeric carbons of β-D-glucopyranosyluronic acid and β-D-galactopyranose, respectively.[14,15] The signals at δ 110.16 and 111.94 ppm were assigned to the anomeric carbons of α-L-arabinofuranose.[16]

The carboxyl groups of hexuronic acid residues in the polysaccharide were reduced to give corresponding neutral sugar residues.[17] Both the original polysaccharide and the carboxyl-reduced derivative were methylated with solid sodium hydroxide and methyl iodide in dimethyl sulfoxide.[18] The methylated products were hydrolyzed, then converted into partially methylated alditol acetates. The hexuronic acid methyl ethers were removed from the hydrolysis products of the methylated native sample by

(thirteen)[a] α-L-Araf 1→
(four)[a] →3 α-L-Araf 1→
(twenty-two)[a] →5 α-L-Araf 1→
(five)[a] →5 α-L-Araf 1→
2
↑
(one)[a] →2 α-L-Rhap 1→
↓
4
(one)[a] →2 α-L-Rhap 1→

(one)[a] β-D-Galp 1→
(six)[a] →3 β-D-Galp 1→
(three)[a] →6 β-D-Galp 1→
↓
6
(ten)[a] →3 β-D-Galp 1→
(four)[a] →4 α-D-GalpA 1→
(two)[a] β-D-GlcpA 1→

Chart 1. Component Sugar Residues in the Minimal Unit in the Structure of Glycyrrhizan GA

a) Number of residues. Araf, arabinofuranose; Rhap, rhamnopyranose; Galp, galactopyranose; GalpA, galactopyranosyluronic acid; GlcpA, glucopyranosyluronic acid.

treatment with anion-exchange resin. Analysis by GC-MS[19] gave the results shown in Table II. The results indicate that D-galacturonic acid and D-glucuronic acid residues in the native polysaccharide produced 2,3,6-tri-*O*-methyl D-galactose and 2,3,4,6-tetra-*O*-methyl D-glucose in the methylation products obtained from the carboxyl-reduced derivative, respectively.

The polysaccharide was subjected to periodate oxidation followed by reduction with sodium borohydride. The periodate oxidation-reduction product contained 11.8% arabinose, 23.9% galactose and 1.5% rhamnose. Neither galacturonic acid nor glucuronic acid was found in the product. Thus, these results were consistent with those of methylation analysis.

The accumulated evidence described above indicates that the minimal unit of glycyrrhizan GA is composed of twelve kinds of component sugar units, as shown in Chart 1.

Discussion

We have reported the RES activities of glycyrrhizans UA, UB and UC,[1,2] the three polysaccharides obtained from the root of *G. uralensis*. The main part of glycyrrhizan UA is occupied by arabino-3,6-galactan type structures. In contrast to glycyrrhizan UA, the major structural units of glycyrrhizan UB are composed of rhamnogalacturonan residues. Glycyrrhizan UC possesses many β-3,6-branched D-galactose units, terminal and α-1,5-linked L-arabinose residues in analogy with glycyrrhizan UA. However, this substance is a unique neutral polysaccharide, rich in β-1,4-linked and 4,6-branched D-galactose units, and terminal, α-1,3- and 1,4-linked and 4,6-branched D-glucose residues. Evidently, glycyrrhizan GA belongs to an α-1,5-linked L-arabino-β-3,6-branched D-galactan type polysaccharide group. About three quarters of the component units in this substance are occupied by the components of arabino-3,6-galactan elements. Glycyrrhizan GA showed the highest RES activity of the four active polysaccharides obtained from Chinese licorices.

Further, we have already reported the RES activities and structural features of two polysaccharides from the root and rhizome of *Saposhnikovia divaricata*,[6,20] three polysaccharides from the seed of *Malva verticillata*,[11,21,22] a polysaccharide from the bark of *Cinnamomum cassia*,[23] three polysaccharides from the rhizome of *Curcuma longa*[24-26] and two polysaccharides from the bark of *Eucommia ulmoides*.[27,28] Most of these RES-activating polysaccharides obtained by us possess α-1,5-linked L-arabino-β-3,6-branched D-galactan moieties as their major parts. Saposhnikovan A,[6] MVS-IIIA,[21] -IVA[22] and -VI,[11] ukonans A[24] and B[25] are examples of this type. Both glycyrrhizan UC[2] and ukonan C[26] belong to arabino-3,6-galacto-glucan.

Other reported examples of RES-activating polysaccharides having α-L-arabino-β-3,6-branched D-galactan type structures as the major parts include sanchinan-A from the root of *Panax notoginseng*,[29] polysaccharide F from *Echinacea purpurea* cell culture,[30] and PS-I, -II and -III from the flower of *Calendula officinalis*.[31]

The presence of α-2,5-branched L-arabinose and terminal β-D-glucuronic acid residues in glycyrrhizan GA is characteristic. 2,5-Branched arabinose units have already been found in both MVS-VI and ukonan C; however, glycyrrhizan GA is the first example having terminal glucuronic acid units in addition to the usual rhamnogalacturonan residues among the known RES-activating acidic polysaccharides.

Acknowledgements We wish to thank Dr. M. Okada, Tsumura Laboratory, for the identification of the material. This work was supported in part by The Science Research Promotion Fund of the Japan Private School Promotion Foundation.

References

1) M. Tomoda, N. Shimizu, M. Kanari, R. Gonda, S. Arai and Y. Okuda, *Chem. Pharm. Bull.*, **38**, 1667 (1990).
2) N. Shimizu, M. Tomoda, M. Kanari, R. Gonda, A. Satoh and N. Satoh, *Chem. Pharm. Bull.*, **38**, 3069 (1990).
3) M. Dubois, K. A. Gilles, J. K. Hamilton, P. A. Rebers and F. Smith, *Anal. Chem.*, **28**, 350 (1956).
4) M. Tomoda, S. Kaneko, M. Ebashi and T. Nagakura, *Chem. Pharm. Bull.*, **25**, 1357 (1977).
5) R. Oshima, J. Kumanotani and C. Watanabe, *J. Chromatogr.*, **259**, 159 (1983).
6) N. Shimizu, M. Tomoda, R. Gonda, M. Kanari, N. Takanashi and N. Takahashi, *Chem. Pharm. Bull.*, **37**, 1329 (1989).
7) N. Blumenkrantz and G. Asboe-Hansen, *Anal. Biochem.*, **54**, 484 (1973).
8) M. Tomoda, N. Shimizu, K. Shimada and M. Suga, *Chem. Pharm. Bull.*, **33**, 16 (1985).
9) M. Tomoda, M. Ichikawa and N. Shimizu, *Chem. Pharm. Bull.*, **34**, 4992 (1986).
10) M. Tomoda and M. Ichikawa, *Chem. Pharm. Bull.*, **35**, 2360 (1987).
11) R. Gonda, M. Tomoda, M. Kanari, N. Shimizu and H. Yamada, *Chem. Pharm. Bull.*, **38**, 2771 (1990).
12) M. Tomoda, K. Shimada, Y. Saito and M. Sugi, *Chem. Pharm. Bull.*, **28**, 2933 (1980).
13) G. Biozzi, B. Benacerraf and B. N. Halpern, *Br. J. Pathol.*, **34**, 441 (1953).
14) N. Shimizu and M. Tomoda, *Chem. Pharm. Bull.*, **33**, 5539 (1985).
15) K. Bock, C. Pedersen and H. Pedersen, "Advances in Carbohydrate Chemistry and Biochemistry," Vol. 42, ed. by R. S. Tipson and D. Horton, Academic Press Inc., Orland, 1984, pp. 193—214.
16) J. -P. Joseleau, G. Chambat, M. Vignon and F. Barnoud, *Carbohydr. Res.*, **58**, 165 (1977).
17) R. L. Taylor and H. E. Conrad, *Biochemistry*, **11**, 1383 (1972).
18) I. Ciucanu and F. Kerek, *Carbohydr. Res.*, **131**, 209 (1984).
19) H. Björndall, B. Lindberg and S. Svensson, *Carbohydr. Res.*, **5**, 433 (1967).
20) N. Shimizu, M. Tomoda, R. Gonda, M. Kanari, Aki. Kubota and Ake. Kubata, *Chem. Pharm. Bull.*, **37**, 3054 (1989).
21) M. Tomoda, M. Kanari, R. Gonda and N. Shimizu, *Phytochemistry*, **28**, 2609 (1989).
22) R. Gonda, M. Tomoda, N. Shimizu and M. Kanari, *Planta Medica*, **56**, 73 (1990).
23) M. Kanari, M. Tomoda, R. Gonda, N. Shimizu, M. Kimura, M. Kawaguchi and C. Kawabe, *Chem. Pharm. Bull.*, **37**, 3191 (1989).
24) M. Tomoda, R. Gonda, N. Shimizu, M. Kanari and M. Kimura,

Phytochemistry, **29**, 1083 (1990).
25) R. Gonda, M. Tomoda, N. Shimizu and M. Kanari, *Chem. Pharm. Bull.*, **38**, 482 (1990).
26) R. Gonda and M. Tomoda, *Chem. Pharm. Bull.*, **39**, 441 (1991).
27) R. Gonda, M. Tomoda, N. Shimizu and M. Kanari, *Chem. Pharm. Bull.*, **38**, 1966 (1990).
28) M. Tomoda, R. Gonda, N. Shimizu and M. Kanari, *Phytochemistry*, **29**, 3091 (1990).
29) K. Ohtani, K. Mizutani, S. Hatono, R. Kasai, R. Sumino, T. Shiota, M. Ushijima, J. Zhou, T. Fuwa and O. Tanaka, *Planta Medica*, **53**, 166 (1987).
30) H. Wagner, H. Stupper, W. Schäfer and M. Zenk, *Phytochemistry*, **27**, 119 (1988).
31) J. Varljen, A. Lipták and H. Wagner, *Phytochemistry*, **28**, 2379 (1989).

Glassy State of Pharmaceuticals. V.[1] Relaxation during Cooling and Heating of Glass by Differential Scanning Calorimetry[2]

Eihei FUKUOKA,* Midori MAKITA and Yasuo NAKAMURA

School of Pharmaceutical Sciences, Toho University, 2–2–1 Miyama, Funabashi, Chiba 274, Japan. *Received November 15, 1990*

Glassy pharmaceuticals were prepared by cooling the melts and their state was confirmed by measuring the glass transition temperature (T_g) and the anomalous endothermic peak (heat capacity maximum) in the differential scanning calorimetry (DSC) curves. Glass formation was newly discovered for 24 pharmaceuticals including acetaminophen, chloramphenicol, flufenamic acid and proxyphylline. The value of the ratio of T_g and melting temperature (T_m) of these pharmaceuticals lay between 0.69 and 0.85. The rate and quantity of relaxation of glass was determined by the area under the anomalous endothermic peak of the DSC curves of glasses prepared at various cooling rates, that of glassy griseofulvin was found to have the largest among the pharmaceuticals examined. The apparent activation energy of glass transition of chenodeoxycholic acid, griseofulvin and tolnaftate prepared at the cooling rate of −1.25 K/min was calculated to be 273.6, 270.3 and 127.6 kJ/mol, respectively. The influence of heating rate on T_g and the area under the anomalous endothermic peak of the DSC curve of glassy aspirin both immediately and after standing for 60 min at 232 K following preparation of the glass was examined. Both factors decreased as heating rate decreased. The apparent activation energy of glass transition of both samples of aspirin was calculated to be 105.6 kJ/mol.

Keywords glassy state; pharmaceutical; glass transition temperature; apparent activation energy; relaxation process; differential scanning calorimetry; X-ray analysis

In previous papers,[1,3] the existence of the glassy state of indomethacin was confirmed by detection of a jump of heat capacity and the anomalous endothermic peak in differential scanning calorimetry (DSC) curves. The thermal properties, the relaxation process, the rate of dissolution and the rate of crystallization of glassy pharmaceuticals were investigated. Their mechanical properties were also studied by TMA (thermomechanical analysis). For indomethacin it was reported that the bioavailability of glass was better than that of crystal.[3]

In the present paper, 24 glassy pharmaceuticals were newly prepared by cooling the melts and the glassy state was confirmed by detection of a jump of heat capacity and the anomalous endothermic peak in the DSC curves. The relationship between the glass transition temperature (T_g) and melting temperature (T_m) was investigated. It was found earlier[3] that relaxation of glassy indomethacin occurred during cooling, heating and isothermal aging below T_g. Here the influence of cooling and heating rates on relaxation of some glassy pharmaceuticals was investigated and the apparent activation energy of glass transition was calculated.

Experimental

Materials Materials used were all of reagent grade.

Preparation of Glass The glass was prepared in the same way as reported previously.[3]

Thermal Analysis A Perkin Elmer DSC-2 differential scanning calorimeter equipped with an Intracooler I system was used. Measurement conditions were the same as those reported,[3] as was determination of the area under the anomalous endothermic peak.

Thin-Layer Chromatography (TLC) The chemical stability of pharmaceuticals during treatment of the sample was checked using TLC. Measurement conditions of TLC were the same as reported earlier[1] and spots were detected under ultraviolet light.

Results and Discussion

1) Glass Transition Temperature of Glassy Pharmaceuticals Table I shows the T_g, T_m and the T_g/T_m values of the pharmaceuticals newly found. The T_g values of glassy dibucaine and mephenesin were the lowest among these pharmaceuticals, while glassy brucine, griseofulvin and 4 cholic acid had relatively high T_g values. No decomposition during treatment of the sample was observed by TLC.

2) Relationship between T_g and T_m It is known that T_g/T_m is, as a rough rule, about 0.5 for many symmetrical polymers such as polyethylene and 0.7 for many asymmetrical polymers such as polyisoprene.[4] It was reported[1] that the T_g/T_m values of glassy pharmaceuticals lay between 0.59 and 0.84 and were slightly larger than those of polymers. As shown in Table I, the T_g/T_m values of glassy pharmaceuticals lay between 0.69 and 0.85. Figure 1 shows the relationship between T_g and T_m of glassy pharmaceuticals containing the samples previously reported.[1] Pharmaceuticals newly found to form glass are

TABLE I. Pharmaceuticals Newly Found to Form Glass

Pharmaceutical	T_g (K)	T_m (K)	T_g/T_m
Dibucaine	246	336	0.73
Mephenesin	247	340	0.73
Ethacrynic acid	282	398	0.71
Tolbutamide	284	403	0.70
Tolnaftate	287	384	0.75
Flufenamic acid	290	406	0.71
Proxyphylline	295	403	0.73
Eserine	297	378	0.79
Nialamide	297	427	0.70
Chlorotrianisene	298	393	0.76
Acetaminophen	302	441	0.69
Chloramphenicol	306	414	0.74
Estradiol-17β-cypionate	309	425	0.73
Dyphylline	315	438	0.72
Norethynodrel	324	453	0.72
Spironolactone	331	478	0.69
Chlormadinone acetate	334	483	0.69
β-Estradiol-3-benzoate	336	472	0.71
Brucine	365	451	0.81
Griseofulvin	370	497	0.74
Chenodeoxycholic acid	371	436	0.85
Deoxycholic acid	377	447	0.84
Ursodeoxycholic acid	378	477	0.79
Cholic acid	393	473	0.83

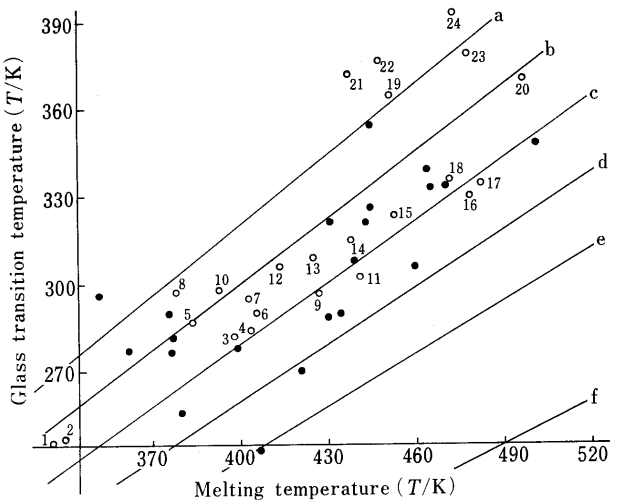

Fig. 1. Relationship between T_g and T_m of Various Pharmaceuticals

The oblique lines originate from the absolute zero point and the slopes give T_g/T_m. The pharmaceuticals newly found to form glass are expressed as open circles and those previously reported to form glass as closed circles. a, 0.80; b, 0.75; c, 0.70; d, 0.65; e, 0.60; f, 0.50. 1, dibucaine; 2, mephenesin; 3, ethacrynic acid; 4, tolbutamide 5, tolnaftate; 6, flufenamic acid; 7, proxyphylline; 8, eserine; 9, nialamide; 10, chlorotrianisene; 11, acetaminophen; 12, chloramphenicol; 13, estradiol-17β-cypionate; 14, dyphylline; 15, norethynodrel; 16, spironolactone; 17, chlormadinone acetate; 18, β-estradiol-3-benzoate; 19, brucine; 20, griseofulvin; 21, chenodeoxycholic acid; 22, deoxycholic acid; 23, ursodeoxycholic acid; 24, cholic acid.

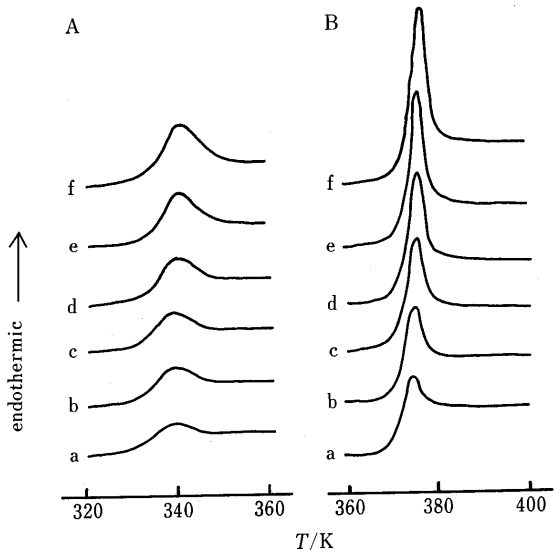

Fig. 2. DSC Curves at Heating Rate of 40 K/min of Glassy Spironolactone and Griseofulvin Prepared at Various Cooling Rates

A, spironolactone; B, griseofulvin. Cooling rate in preparation: a, quenching; b, −10; c, −5; d, −2.5; e, −1.25; f, −0.62 K/min.

expressed as open circles and those previously reported to form glass as closed circles. The oblique lines originate from the absolute zero point and the slopes of the lines give the T_g/T_m. The T_g/T_m values of almost all pharmaceuticals were distributed in the range of 0.65 to 0.80, those of chenodeoxycholic acid, deoxycholic acid and cholic acid having steroid structure were the largest among the samples examined.

3) Relaxation of Glass during Preparation at Various Cooling Rates It has been recognized that T_g of the glass formed increased and the anomalous endothermic peak became larger with decrease in the cooling rate of the melt.[3] Also, for isothermal aging of glassy indomethacin below T_g

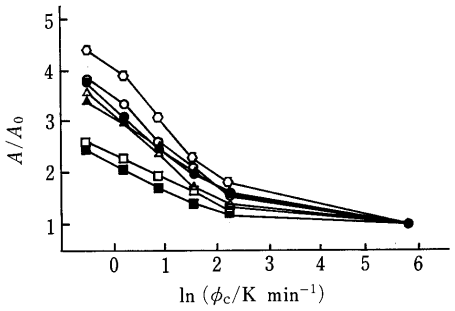

Fig. 3. Effect of Cooling Rate on the Area under the Anomalous Endothermic Peak

ϕ_c, cooling rate. ○, griseofulvin; ○, proxyphylline; ●, chloramphenicol; △, spironolactone; ▲, brucine; □, acetaminophen; ■, nialamide.

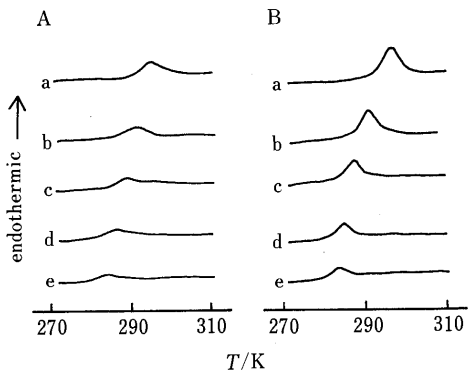

Fig. 4. Influence of Heating Rate on the DSC Curves of Glassy Tolnaftate Prepared at Two Different Cooling Rates

A, quenching; B, cooling rate of −1.25 K/min. Heating rate; a, 40; b, 20; c, 10; d, 5; e, 2.5 K/min.

the presence of an optimum temperature at which the area under the anomalous endothermic peak and T_g was maximum was recognized and could be explained by the relaxation theory.[5]

Thus, relaxation of the glass during preparation at various cooling rates was studied for 7 pharmaceuticals remaining stable at room temperature. The Intracooler I was used to cool the sample to 232 K. The melt was cooled to a specified temperature below T_g at various cooling rates, then heated to above T_g. Measurements were made at a heating rate of 40 K/min.

Figure 2 shows the DSC curves of glassy spironolactone and griseofulvin prepared at various cooling rates.

The T_g of glassy spironolactone varied from 331 K in the case of quenching to 333.5 K in the case of a cooling rate of −0.62 K/min.

The T_g of glassy griseofulvin varied from 370 to 373.6 K under these conditions. Thus, T_g increased and the area under the anomalous endothermic peak became larger with decrease in the cooling rate of the melts. Glassy spironolactone showed a broad anomalous endothermic peak, while glassy griseofulvin showed a sharp anomalous endothermic peak. The area under the anomalous endothermic peak of the DSC curve of glass prepared at each cooling rate and quenching are denoted by A and A_0, respectively. Then, to examine the rate and quantity of relaxation during cooling, A/A_0 was plotted against the logarithm of cooling rate. The results are shown in Fig. 3.

The samples were grouped into three classes by the rate

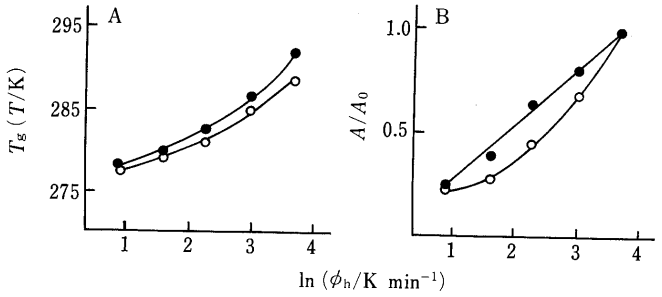

Fig. 5. Influence of Heating Rate on T_g and the Area under the Anomalous Endothermic Peak of Glassy Tolnaftate Prepared at Two Different Cooling Rates

A, T_g; B, A/A_0; ϕ_h, heating rate; ○, quenching; ●, cooling rate of −1.25 K/min.

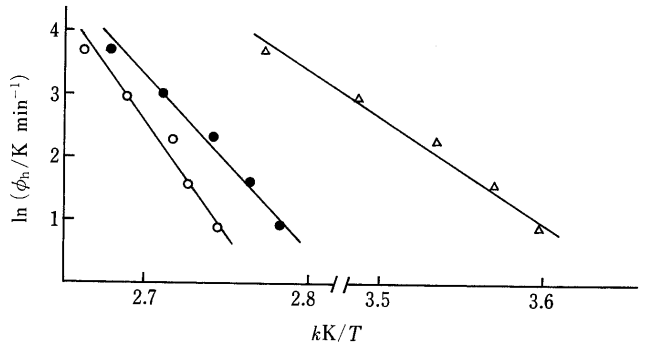

Fig. 6. Plots of ln ϕ_h *vs.* $1/T_g$ of Glassy Chenodeoxycholic Acid, Griseofulvin and Tolnaftate Prepared at the Cooling Rate of −1.25 K/min

ϕ_h, heating rate; ○, chenodeoxycholic acid; ●, griseofulvin; △, tolnaftate.

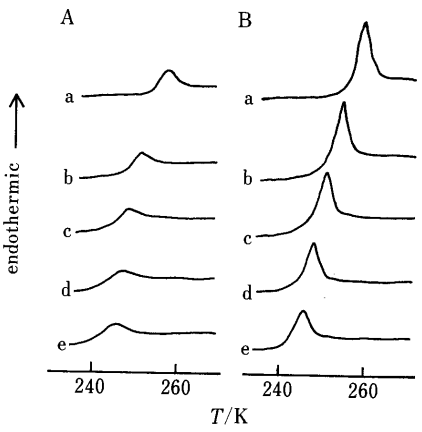

Fig. 7. Influence of Heating Rate of Glassy Aspirin Both Immediately and after Standing for 60 min at 232 K after Preparation of the Glass

A, 0 min; B, 60 min. Heating rate: a, 40; b, 20; c, 10; d, 5; e, 2.5 K/min.

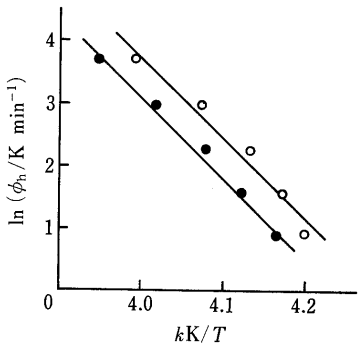

Fig. 8. Plots of ln ϕ_h *vs.* $1/T_g$ of Glassay Aspirin

○, 0 min; ●, 60 min; ϕ_h, heating rate.

and quantity of relaxation. Griseofulvin showed the most remarkable change in both factors, while acetaminophen and nialamide showed the smallest change. The effects of cooling rate during glass preparation on the anomalous endothermic peak of the glass formed varied with the samples. This indicates that a relaxation takes place during cooling in all 7 pharmaceuticals.

4) Influence of Heating Rate on Glass Transition The influence of heating rate of the glass on T_g was examined for three pharmaceutical samples: chenodeoxycholic acid had the largest T_g/T_m value of 0.85; griseofulvin had the highest T_m value of 497 K and with T_g nearly equal to that of chenodeoxycholic acid; and tolnaftate having comparatively low T_g value was examined as a sample with T_g/T_m nearly equal to that of griseofulvin. The influnce of heating rate of glassy tolnaftate prepared at two different cooling rates of −1.25 K/min and quenching on T_g and the area under the anomalous endothermic peak was examined. Measurements were made at heating rates ranging from 2.5 to 40 K/min.

Figure 4 shows the DSC curves of glassy tolnaftate prepared at a cooling rate of −1.25 K/min and quenching, respectively. The glass showed different DSC curves due to the structural relaxation during heating at different rates. The T_g decreased and the area under the anomalous endothermic peak became smaller with the decrease in the heating rate.

Figure 5 shows the influence of heating rate on T_g and the area under the anomalous endothermic peak of glassy tolnaftate prepared at two different cooling rates.

The area under the anomalous endothermic peak of the DSC curve of glass obtained at each heating rate and at the rate of 40 K/min are denoted by A and A_0, respectively. A/A_0 was plotted against the logarithm of the rate. The T_g and A/A_0 of both samples decreased as the heating rate decreased. Earlier studies on the effect of heating rate on T_g[3] revealed that T_g increased as the heating rate increased. From a logarithmic plot of the heating rate *vs.* $1/T_g$, the apparent activation energy of glass transition was calculated according to an equation derived by Barton.[6] Then, to compare two glassy pharmaceuticals with glassy tolnaftate, the influence of heating rate of glass prepared at the cooling rate of −1.25 K/min on T_g was examined.

A linear relationship was observed when the logarithm of the heating rate was plotted against $1/T_g$ (Fig. 6). The apparent activation energy of glass transition of chenodeoxycholic acid, griseofulvin and tolnaftate was calculated to be 273.6, 270.3 and 127.6 kJ/mol, respectively.

5) Influence of Isothermal Aging below T_g of Aspirin Aspirin exists as supercooled liquid at room temperature,[1] and was used as sample with low T_g of 243 K in examining the influence of isothermal aging below T_g on glass transition. After the melt was rapidly cooled to 232 K below T_g, the sample was kept at 232 K for 0 min or 60 min, then reheated to above T_g at various rates. Measurements were made at rates ranging from 2.5 to 40 K/min.

Figure 7 shows the influence of heating rate of glassy aspirin both immediately and after standing for 60 min at 232 K following preparation of the glass. The glass showed different DSC curves due to the structural relaxation during

continuous heating at different rates.

The T_g decreased and the area under the anomalous endothermic peak became smaller with decrease in the heating rate. Influence of heating rate on T_g was examined (Fig. 8).

A linear relationship was observed when the logarithm of the heating rate was plotted against $1/T_g$. The apparent activation energy of glass transition of both samples of aspirin was calculated as 105.6 kJ/mol.

Aspirin had the lowest T_g and T_g/T_m and the smallest apparent activation energy of glass transition, in contrast with chenodeoxycholic acid which had high T_g, the highest T_g/T_m and the largest apparent activation energy of glass transition examined in the present study.

References and Notes

1) Part III: E. Fukuoka, M. Makita and S. Yamamura, *Chem. Pharm. Bull.*, **37**, 1047 (1989); Part IV: E. Fukuoka, M. Makita and Y. Nakamura, *ibid.*, **37**, 2782 (1989).
2) This work was presented at the 101st (Kumamoto, April 1981) and 104th (Sendai, March 1984) Annual Meeting of the Pharmaceutical Society of Japan.
3) E. Fukuoka, M. Makita and S. Yamamura, *Chem. Pharm. Bull.*, **34**, 4314 (1986); *idem*, *ibid.*, **35**, 2943 (1987).
4) R. G. Beaman, *J. Polym. Sci.*, **9**, 470 (1952); R. F. Boyer, *J. Appl. Phys.*, **25**, 825 (1954); C. A. Angell, J. M. Sare and E. J. Sare, *J. Phys. Chem.*, **82**, 2622 (1978); K. Kisbore and G. Prasad, *Colloid Polym. Sci.*, **258**, 125 (1980); P. D. Gujrati and M. Goldstein, *J. Phys. Chem.*, **84**, 859 (1980).
5) B. Wunderlich and D. M. Bodily, *J. Polym. Sci., Part C*, **6**, 137 (1964); N. Hirai and H. Eyring, *J. Appl. Phys.*, **29**, 810 (1958); T. Yoshimoto and A. Miyagi, *Kogyo Kagaku Zasshi*, **69**, 1771 (1966); T. Hatakeyama and H. Kanetsuna, *J. Polym. Sci., Part A-2*, **11**, 815 (1973).
6) J. M. Barton, *Polymer*, **10**, 151 (1969).

Chem. Pharm. Bull. **39**(8) 2091—2095 (1991)

Drug Release from Spray-Dried and Spray-Embedded Microparticles of Diltiazem Hydrochloride

Flavio FORNI, Gilberto COPPI, Maria Angela VANDELLI, and Riccardo CAMERONI*

Department of Pharmaceutical Sciences, University of Modena, Via G. Campi 183, 41100 Modena, Italy. *Received November 26, 1990*

Spray-dried and spray-embedded ethylcellulose microparticles were prepared using a spray-drying technique. The structure of the microparticles (microcapsules or microspheres) changed according to whether the drug (diltiazem hydrochloride) was dispersed or dissolved in the ethylcellulose solution to be spray-dried. The drug release rate from the microparticles was not affected by the physical state of the drug (amorphous or crystalline state), but by the microparticle structure.

Keywords diltiazem hydrochloride; ethylcellulose; microparticles; spray-dried microparticles; microcapsules; spray-embedded microparticles; microspheres; drug physical state; drug release

For a long time the spray-drying technique has been applied in the pharmaceutical field to obtain powders for direct compression,[1] to prepare granulates,[2] agglomerates,[3,4] and microparticles.[5]

The microparticle structure changes according to whether the drug is dispersed or dissolved in the polymer solution to be spray-dried.[5] When the spray-drying procedure is applied to dispersions of drug crystals in polymer solutions, the microparticles are set up by one or more drug crystals surrounded by a polymeric coating. The microparticles therefore have a microcapsule structure.

The spray-drying procedure applied to solutions of drug and polymer can be better defined as a spray-embedding technique.[6] In this case the microparticles are formed by a polymeric matrix where the drug is dispersed. The microparticles can therefore be defined as being microspheres.

In the microspheres the drug can be dispersed either as extremely fine particles or even in a molecular state. The last condition involves a decrease in the degree of drug crystallinity.

Obviously, the presence of the drug in the amorphous state and in the conditions of molecular dispersion increases the drug dissolution rate. However, the effect of these parameters on the release process is a less known factor.

This work aims to evaluate the physical state of diltiazem hydrochloride according to whether the spray-drying technique was applied to solutions of ethylcellulose in which the drug was dispersed or dissolved. Since the polymorphic form affected the drug release process from matrices,[7] the role of the drug's physical state on the release process was evaluated with reference to the reservoir- (microcapsule) or matrix-type (microsphere) structure of the microparticles.

Experimental

Materials Diltiazem hydrochloride (JP XI) was obtained from Profarmaco (Milan, Italy). The drug density ($1.27 \pm 0.03\ g\,cm^{-3}$) was the average of the values obtained using a Beckmann 930 air comparison pycnometer (Fullerton, CA, U.S.A.) on the original drug crystals and a WDF United Engineers & Constructors torsion balance (Markus Hook, PA, U.S.A.) on needle-like crystals (about 2.0×0.1 mm) recrystallized from H_2O–HCl (90:10, v/v). Ethylcellulose (EC) [Ethocel 100 PG (Dow Corning, Midland, MI, U.S.A.); viscosity of the 5% (w/w) solution at 25 °C in toluene–ethanol (80:20, w/w) was 90—110 cP; ethoxy content 48.0—49.6; density $1.11\ g\,cm^{-3}$ [8]] was used as received from the manufacturer. All the solvents were of analytical grade (Carlo Erba, Milan, Italy).

Preparation of the Spray-Dried Drug Crystals The spray-dried drug crystals were prepared using a Buechi 190 mini spray-dryer (Flawil, Switzerland). Diltiazem hydrochloride crystals weighing 1 g were dispersed in 100 ml of benzene or dissolved in 100 ml of methanol. The experimental parameters of the process were set as follows: inlet temperature: 130 °C (benzenic dispersions), 100 °C (methanolic solutions); outlet temperature: 95—98 °C (benzenic dispersions), 65—70 °C (methanolic solutions); aspirator setting: 5; pump setting: $10\ ml\,min^{-1}$; spray-flow: $500\ Nlh^{-1}$. A 0.5 mm nozzle was used throughout the experiments.

Preparation of the Spray-Dried and Spray-Embedded Microparticles Diltiazem hydrochloride (1 g) was dispersed in 100 ml of a benzenic solution of EC (spray-dried microparticles: microcapsules) or dissolved in 100 ml of a methanolic solution of EC (spray-embedded microparticles: microspheres). The microparticles were prepared using 1:1, 1:2.5, 1:5 (microcapsules) and 1:1, 1:1.75, 1:2, 1:2.5 and 1:5 (microspheres) drug/EC ratios. All the preparations were spray-dried with a Buechi 190 mini spray-dryer to prepare microparticles characterized by the theoretical drug/EC ratios of the EC solutions where the drug was dispersed or dissolved. The experimental parameters of the process of the microcapsule and microsphere preparation were set as described above for the preparation of the spray-dried drug crystals from the benzenic dispersions and methanolic solutions, respectively.

Drug Content The amount of diltiazem hydrochloride both in the microcapsules and microspheres was determined: (a) microanalytically on the basis of the percentage of nitrogen and sulfur using a Carlo Erba 1102 elemental analyzer (Milan, Italy) and according to the method proposed by White,[9] respectively; (b) according to Merkle and Speiser.[10] The results obtained with the two methods differed for a maximum of ±7%.

Wall Thickness of the Microcapsules The wall thickness of the microcapsules was calculated according to Si-Nang *et al.*[11]

Morphological Analysis The morphology of drug crystals and microparticles was determined by observation on Philips 500 scanning electron microscopy (Eindhoven, The Netherlands). The particle size and circularity parameter[12] were evaluated using a TESAK FAS image analysis apparatus (Sesto Fiorentino, Italy) to enable the following of a computerized procedure on scanning electron microscopy (SEM) micrographs showing at least 100 crystals or microparticles. The circularity parameter (C)[12] had been suggested for use in shape description and defined as the ratio between the measured perimeter and the perimeter of circle of equal area.

Differential Scanning Calorimetry (DSC) The DSC curves were recorded on a Perkin-Elmer DSC-4 differential scanning calorimeter equipped with a computerized data station (Norwalk, CT, U.S.A.). Indium (99.99%, Perkin-Elmer) (mp 156.60; ΔH $28.45\ J\,g^{-1}$) was used to check the instrument. All the samples (3—4 mg) were heated in crimped aluminium pans (Perkin-Elmer) at the scanning rate of $10\ °C\,min^{-1}$ using dry nitrogen flow ($30\ ml\,min^{-1}$).

X-Ray Diffractometry The X-ray diffraction patterns were recorded using a PW 1050 powder diffractometer (Philips). Experimental settings: Ni filtered Cu radiation ($\lambda = 1.5418$ Å); tube settings 40 kV, 20 mA; angular speed 1° (2θ) per minute; 1-0.1-1 slits.

Drug Dissolution and Drug Release from Microparticles The drug dissolution and the drug release from microparticles were carried out using a Dissotest CE-1 column-type apparatus[13] (Sotax, Basel, Switzerland) in 250 ml deionized water at a flow rate of $25\ ml\,min^{-1}$. All experiments were carried out under perfect sink conditions at a temperature of 37 ± 0.2 °C using either 5 mg of original drug crystals or microparticle samples equivalent to 5 mg of drug. Drug content in the solution was determined spectrophotometrically with a 550 Perkin-Elmer UV-Vis spectrophotometer at fixed time intervals and a wavelength of 237 nm.

Results and Discussion

Spray-Dried Drug Crystals As pointed out by the SEM microphotographs, the spray-dried crystals obtained from benzenic dispersions of diltiazem hydrochloride (Fig. 1A) showed rounder corner-edges than those of the original drug crystals (Fig. 1B). The rounder corner-edges are the consequence of the passage through the pump and the nozzle during the spray-drying procedure. The value of the particle size and circularity parameter were similar (Table I). On the contrary, the spray-dried crystals obtained from methanolic solutions (Fig. 1C) showed a lower particular size than that of the original drug crystals (Table I).

The spray-drying technique applied to the drug solution could modify the original polymorphic phase of the drug or decrease the drug crystallinity.[14] However, both the DSC curves (Fig. 2) and the X-ray diffraction patterns (Fig. 3) of the spray-dried drug crystals obtained from methanolic solutions showed no phase changes or drug crystallinity decrease in comparison with the original drug crystals. Obviously, also the spray-dried drug crystals obtained from benzenic dispersions showed no phase changes.

Spray-Dried Microparticles The spray-drying procedure allowed the preparation of microparticles of shrivelled aspect regardless of whether diltiazem hydrochloride crystals were dispersed or dissolved in the EC solutions (Fig. 4). The shrivelled aspect is due to the EC coating. In confirmation of our hypothesis, the spray-drying procedure of a methanolic solution of EC produced shrivelled EC microparticles. The reasons for the shrivelled aspect have been previously discussed by other authors.[3]

The drug content of the microparticles and the wall thickness of the microcapsules are reported in Table II.

When the microcapsules were prepared in the 1 : 1 drug/EC ratio using the spray-drying method, some crystals were not completely coated. Only little agglomerates of EC were pointed out on the surface of the biggest uncoated crystals (Fig. 5). On the contrary, the microcapsules

TABLE I. Values of the Particle Size (μm) and Circularity Parameter (C) of Diltiazem Hydrochloride Crystals, Microcapsules and Microspheres Prepared Using Different Drug/EC Ratios

	Diameter (μm)	$C^{a)}$
Original drug crystals	7.1 (5.1)	0.72 (0.08)
Spray-dried drug crystals:		
a) from benzenic dispersion	6.5 (4.6)	0.86 (0.07)
b) from methanolic solution	1.7 (0.8)	0.73 (0.08)
Microcapsules		
1 : 1	7.5 (3.5)	0.77 (0.07)
1 : 2.5	8.7 (3.4)	0.77 (0.06)
1 : 5	10.6 (4.6)	0.78 (0.06)
Microspheres		
1 : 1	3.2 (1.4)	0.65 (0.10)
1 : 1.75	5.9 (2.7)	0.75 (0.08)
1 : 2	7.1 (3.8)	0.79 (0.06)
1 : 2.5	8.8 (3.6)	0.68 (0.09)
1 : 5	9.4 (5.6)	0.78 (0.06)

Standard Deviation in Parentheses.
a) C = (measured perimeter)/(perimeter of circle of equal area).

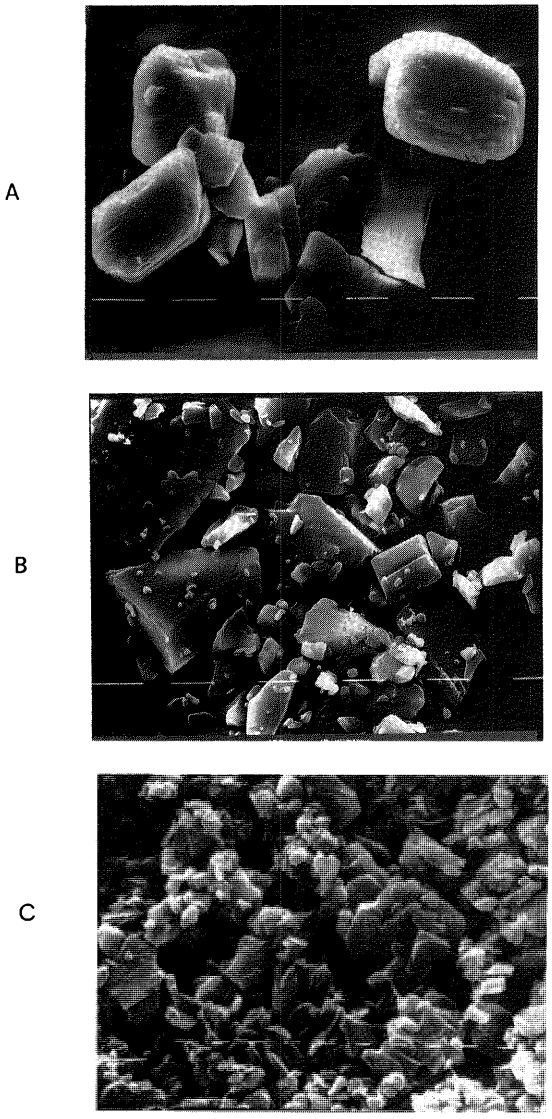

Fig. 1. Scanning Electron Micrographs of Diltiazem Hydrochloride Crystals

A) Drug crystals spray-dried from benzenic dispersion (scale bar: 10 μm); B) original drug crystals (scale bar: 10 μm); C) drug crystals spray-dried from methanolic solution (scale bar: 1 μm).

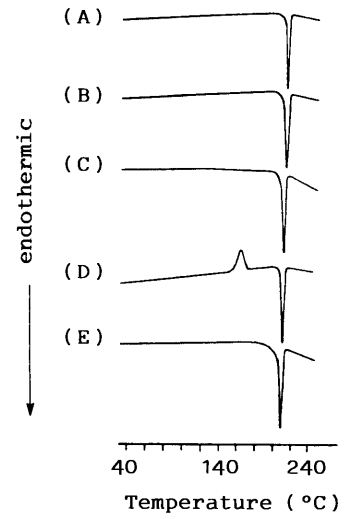

Fig. 2. DSC Thermograms of Diltiazem Hydrochloride Crystals and Microparticles

A) Original drug crystals; B) drug crystals spray-dried both from benzenic dispersion and ethanolic solution; C) microcapsules; D) microspheres; E) microspheres after heating at 170 °C.

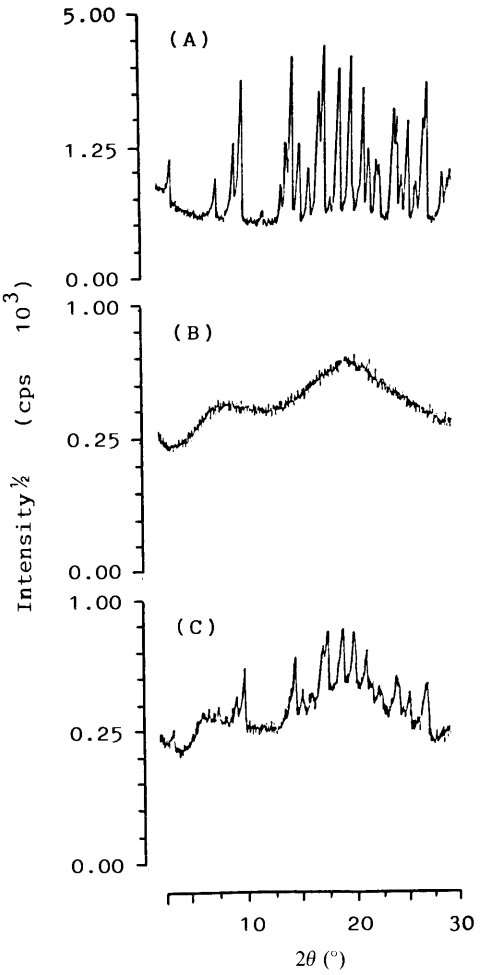

Fig. 3. X-Ray Diffraction Patterns of Diltiazem Hydrochloride Crystals and Microparticles

A) Original drug crystals and microcapsules; B) microspheres; C) microspheres after heating at 170 °C.

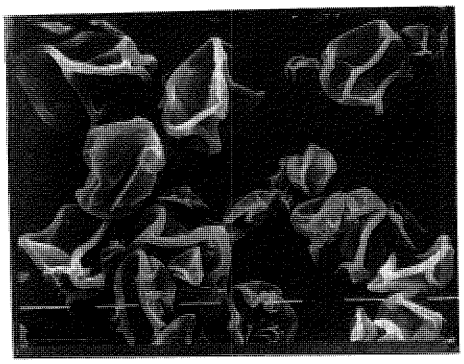

Fig. 4. Scanning Electron Micrograph of Diltiazem Hydrochloride Microparticles (scale bar: 10 μm)

prepared using lower drug/EC ratios (1 : 2.5 and 1 : 5) were completely coated. As the spray-dried drug crystals and the microcapsules are very similar in size and shape (Table I), it is reasonable to hypothize a microcapsule structure where each crystal is surrounded by an EC coating. Therefore, the microcapsules can be defined as being of the "film-type."[15]

As far as the microspheres are concerned, the X-ray diffractometry (Fig. 3) showed the amorphous state of the drug dispersed in the EC matrix.

TABLE II. Parameters of Microcapsules and Microspheres Prepared Using Different Drug/EC Ratios

Drug/EC ratio	Microcapsules		Microspheres
	Drug content (%)	Wall thickness (μm)	Drug content (%)
1 : 1	45.0 (2.0)	0.73 (0.34)	46.6 (2.7)
1 : 1.75	—	—	33.1 (3.1)
1 : 2	—	—	32.4 (0.9)
1 : 2.5	22.2 (0.9)	1.16 (0.45)	27.7 (1.3)
1 : 5	12.5 (1.1)	1.57 (0.66)	16.1 (2.2)

Standard Deviation in Parentheses.

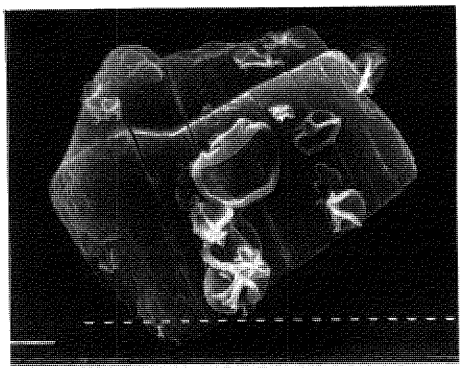

Fig. 5. Scanning Electron Micrograph of an Uncoated Crystal in the Microcapsules Prepared at 1 : 1 Drug/EC Ratio (scale bar: 1 μm).

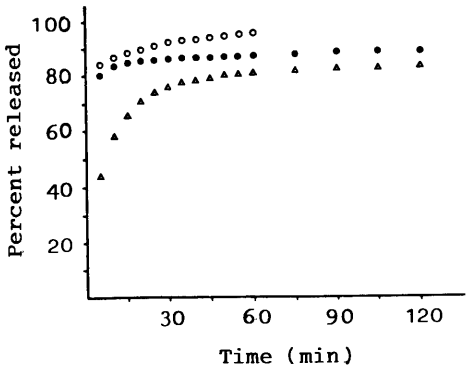

Fig. 6. Percentage Release of Diltiazem Hydrochloride from Microcapsules

Drug/EC ratio: (○) 1 : 1; (●) 1 : 2.5; (△) 1 : 5.

In all the microsphere formulations, the DSC curves showed a broad exothermic peak (150—170 °C) (Fig. 2) owing to the crystallization process of the amorphous drug. As the scanning procedure went on, the endothermic peak due to the melting of the crystallized diltiazem hydrochloride (210—211 °C) appeared. After having heated the microspheres at 170 °C, the exothermic peak did not appear and the X-ray diffraction patterns showed an increase of the drug crystallinity in confirmation of the crystallization process by the thermal energy.

Obviously, both the differential scanning calorimetry and the X-ray diffractometry showed no crystallinity changes of the drug crystals being the microcapsule cores.

Drug release profiles in the dissolution medium (deionized water) from microparticles are depicted in Figs. 6 and

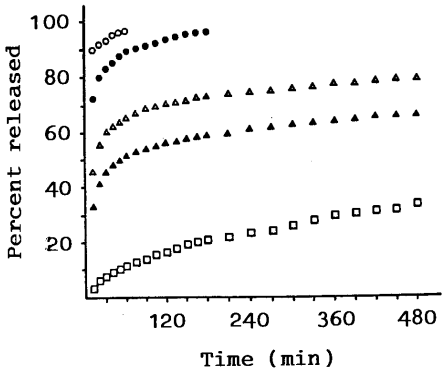

Fig. 7. Percentage Release of Diltiazem Hydrochloride from Microspheres

Drug/EC ratio: (○) 1:1; (●) 1:1.75; (△) 1:2; (▲) 1:2.5; (□) 1:5.

TABLE III. Parameters of the Drug Release Process from Microcapsules and Microspheres Prepared Using Different Drug/EC Ratios Calculated According to the Weibull Function

Drug/EC ratio	Microcapsules		Microspheres	
	T_d[a] (h)	b[b]	T_d[a] (h)	b[b]
1:1	c)	c)	c)	c)
1:1.75	—	—	0.1 (0.01)	0.32 (0.02)
1:2	—	—	1.0 (0.1)	0.38 (0.05)
1:2.5	c)	c)	5.0 (1.2)	0.23 (0.01)
1:5	0.29 (0.1)	0.42 (0.04)	37.1 (4.4)	0.60 (0.01)

95% Confidence Limits in Parentheses.
a) T_d is the dissolution time, *i.e.* the time interval necessary to dissolve 63.2% of the drug. *b*) b is the shape parameter characterizing the release curve. *c*) Not calculated owing to the too fast drug release rate ($T_d < 0.01$ h).

7. The drug release rate from the microparticles decreased with decreasing the drug/EC ratio as shown by the T_d (dissolution time) values[16] (Table III). The drug/EC ratio being equal, the release rate of diltiazem hydrochloride from the microcapsules was faster than that from the microspheres as demonstrated by the T_d values (Table III). The faster drug release rate from the microcapsules is due to the lack of a continuous coating for the 1:1 microcapsules and probably to the thin wall for those having lower drug/EC ratios (Table II). Only the 1:5 microcapsules showed a remarkable decrease of the drug release rate. The lower release rate of the drug from the microspheres can be justified as follows. Although dispersed in the amorphous state, the drug in the microspheres could be surrounded by a non-porous structure (as the SEM microphotographs showed) hampering the drug release. The shape parameter "b" is always less than unity, indicating a steeper initial slope for the plot of the release process (Table III).

As the drug dissolution rate is much higher than the drug release rate from the microparticles, it is reasonable to hypothize a key role of either the diffusion-type or solvent penetration processes.

A useful tool to clarify the release mechanism could be the following power law expression[17]

$$M_t/M_\infty = kt^n \quad (1)$$

where M_t/M_∞ is the drug fraction released at the time "t", and "k" and "n" are the constant and the kinetic exponent of release, respectively. The value of the kinetic exponent "n" defines the mechanism of the drug release process. This equation was applied to the release from matrices of several geometries (slabs, spheres, discs) and recently was proposed to confirm the diffusion-type mechanism of drug release from microcapsules.[18] It should be noted that the "n" value indicating the release mechanism is dependent from the geometry of the system.[19]

TABLE IV. Values of Kinetics Exponent of Drug Release (n) for Microparticles Prepared Using Different Drug/EC Ratios According to Eq. 1 ($M_t/M_\infty = kt^n$)

Drug/EC ratio	Microcapsules	Microspheres
	n	n
1:1	a)	a)
1:1.75	—	0.40 (0.08)
1:2	—	0.37 (0.06)
1:2.5	a)	0.34 (0.06)
1:5	0.39 (0.05)	0.55 (0.01)

95% Confidence Limits in Parentheses.
a) Not calculated owing to the too fast drug release rate.

As far as the diltiazem hydrochloride release from microparticles (spherical systems) is concerned, the values of the kinetic exponent suggested a release process where a diffusion-type mechanism predominates (Table IV).

Conclusion

Diltiazem hydrochloride in the microspheres is dispersed in an amorphous state in an EC matrix, whereas a drug crystal is surrounded by a thin membrane in the microcapsules. As the drug release rate in the amorphous state from the microspheres is lower than that of the crystalline drug from the microcapsules, it is reasonable to suppose that the release process was not affected by the drug dissolution process. Therefore, the drug release from the microparticles was not affected by the physical state of the drug (amorphous or crystalline state), but by the microparticle structure.

Acknowledgement This work was supported by a grant from the Ministero dell' Università e della Ricerca Scientifica e Tecnologica, Rome, Italy. The authors are grateful to Profarmaco S.p.A. for their gift of diltiazem hydrochloride.

References

1) W. C. Gunsel and L. Lachman, *J. Pharm. Sci.*, **52**, 178 (1963).
2) S. S. Kornblum, *J. Pharm. Sci.*, **58**, 125 (1969).
3) Y. Kawashima, K. Matsuda, and H. Takenaka, *J. Pharm. Pharmacol.*, **24**, 505 (1972).
4) Y. Kawashima and H. Takenaka, *J. Pharm. Sci.*, **63**, 1546 (1974).
5) C. Voellmy, P. Speiser, and M. Soliva, *J. Pharm. Sci.*, **66**, 631 (1977).
6) H. Takeuchi, T. Handa, and Y. Kawashima, *Chem. Pharm. Bull.*, **35**, 3800 (1987).
7) M. T. Bernabei, G. Gamberini, V. Ferioli, and R. Cameroni, *Boll. Chim. Farm.*, **122**, 20 (1983).
8) M. Samejima, G. Hirata, and Y. Koida, *Chem. Pharm. Bull.*, **30**, 2894 (1982).
9) D. C. White, *Mikrochim. Acta*, **1962**, 807.
10) H. P. Merkle and P. Speiser, *J. Pharm. Sci.*, **62**, 1444 (1973).
11) L. Si-Nang, P. F. Carlier, P. Delort, J. Gazzola, and D. Lafont, *J. Pharm. Sci.*, **62**, 452 (1973).
12) B. H. Kaye, "Particle Characterization in Technology," Vol. 1, ed. by J. K. Beddow, CRC Press, Boca Raton, 1986, pp. 81—100.

13) F. Langenbucher, *J. Pharm. Sci.*, **58**, 1265 (1969).
14) O. I. Corrigan, K. Sabra, and E. M. Holohan, *Drug Dev. Ind. Pharm.*, **9**, 1 (1983).
15) S. Benita and M. Donbrow, *Int. J. Pharm.*, **12**, 251 (1982).
16) F. Langenbucher, *J. Pharm. Pharmacol.*, **24**, 979 (1972).
17) R. W. Korsmeyer, R. Gurny, E. Doelker, P. Buri, and N. A. Peppas, *Int. J. Pharm.*, **15**, 25 (1983).
18) F. Forni, G. Coppi, M. A. Vandelli, and M. T. Bernabei, *Int. J. Pharm.*, **60**, 83 (1990).
19) P. L. Ritger and N. A. Peppas, *J. Controlled Release*, **5**, 23 (1987).

Evaluation of New Pasty-Type Implantable Devices Consisting of Poly(ε-caprolactone/δ-valerolactone) and Estracyt or Estramustine

Kazumichi IMASAKA,*[,a] Masaru YOSHIDA,[b] Hironobu FUKUZAKI,[b] Masaharu ASANO,[b] Minoru KUMAKURA,[b] Tohru MASHIMO,[c] Hidetoshi YAMANAKA,[c] and Tsuneji NAGAI[a]

Department of Pharmaceutics, Hoshi University,[a] Ebara-2-4-41, Shinagawa-ku, Tokyo 142, Japan, Department of Development, Takasaki Radiation Chemistry Research Establishment, Japan Atomic Energy Research Institute,[b] Watanuki-machi 1233, Takasaki, Gunma 370-12, Japan and Department of Urology, School of Medicine, Gunma University,[c] Maebashi, Gunma 371, Japan. *Received January 17, 1991*

Biodegradable pasty-type copolyesters with a relatively low molecular weight of 4500 were synthesized by direct copolycondensation of ε-caprolactone (CL) and δ-valerolactone (VL) in the absence of catalysts to evaluate *in vivo* capabilities of the polymer for implantable controlled release devices in drug delivery systems. The devices in cylindrical shape were prepared by the melt-pressing technique using pasty-type copoly(CL/VL) with 53 mol% CL unit, in which Estracyt and estramustine were used as a water soluble and insoluble drug, respectively. The degradation and drug release *in vivo* of the devices were examined by subcutaneous implantation in the backs of male rats. The degradation of the device was remarkably accelerated by the presence of hydrophilic Estracyt, and was slightly suppressed by hydrohobic estramustine. The estramustine release profile roughly corresponded to the polymer degradation one. It was found that the degradation of the polymer in the device was affected by hydrophilicity of the drug. A reasonable release of estramustine from the device was kept for a period of more than 20 weeks. Furthermore, the release of the drugs *in vivo* was able to lead to an atrophy of accessory sex organs such as ventral prostates (VP) and right-side seminal vesicle (SV), resulting in pharmacological influence.

Keywords implant; biodegradable polymer; pasty-polymer; lactone polymer; controled release drug; prostate cancer; estramustine; Estracyt

Introduction

The incorporation of anticancer drugs in biodegradable polymers has been considered to be a useful method for obtaining implantable controlled release drugs and for maintaining the drug release.[1-5]

In previous papers,[6,7] the synthesis methods of low molecular weight polymers have been investigated by direct copolycondensation of lactones such as ε-caprolactone (CL) and δ-valerolactone (VL) without catalysts applied as high safty biodegradable polymers for implantable controlled release drug devices. Such low molecular weight polymers without impurities were convenient for the preparation of implantable controlled release drug devices in cylindrical shape using the melt pressing technique. Furthermore, we have investigated *in vivo* capabilities such as biodegradability and drug release in the devices by implantation into the backs of male rats. The degradation was greatly affected by the polymer composition of CL and VL, and the biodegradation and controlled drug release for long periods of time were observed on the *in vivo* studies of the devices prepared by copoly(CL/VL) in a polymer composition of 92 mol% CL unit. A controlled release of estramustine from the waxy devices was kept throughout an experimental period of 20 weeks. In this case the release pattern of the drug was parallel to the degradation pattern of the polymer.

In this paper, we report on *in vivo* degradation properties and drug release phenomena in the implantable devices consisting of pasty-type copoly(CL/VL) with 53 mol% CL unit obtained by the melt-pressing technique,[8-11] in which Estracyt (estradiol 3-bis(2-chloroethyl)carbamate-17β-phosphate) and estramustine (estradiol 3-bis(2-chloroethyl)carbamate are used as a model compound of water-soluble and water-insoluble drugs. Pharmacological influences of the devices with Estracyt and estramustine were evaluated by *in vivo* test on the sex organs of rat.

Experimental

Materials CL and VL were purchased from Tokyo Kasei Kogyo Co., Ltd. Estracyt and estramustine (A/B Leo, Helsingborg, Sweden) having an excellent palliative effect on advanced prostatic cancer, were used as chemotherapeutic agents and their structural formulas are shown in Fig. 1. All other chemicals were of special grades.

Synthesis The pasty-type low molecular weight polymer was synthesized by direct copolycondensation of 0.25 mol CL and 0.25 ml VL without catalysts at 200 °C by bubbling nitrogen gas through the monomer solution.

Analysis of Polymer Melting point (T_m) was measured with a Perkin Elmer differential scanning calorimeter (DSC), model DSC-7. Polymer composition was determined by proton nuclear magnetic resonance (^{1}H-NMR) spectroscopy using a Jeol GSX-270 spectrometer, and number-average molecular weight ($\bar{M}_n$) and weight-average molecular weight ($\bar{M}_w$) and polydispersity ($\bar{M}_w/\bar{M}_n$) were measured with Waters ALC-244 gel permeation chromatography (GPC).

Preparation of Devices The small cylindrical devices (3 mm diameter, 130 mm length) containing Estracyt or estramustine were prepared by the melt pressing technique as follows; a mixture of 80 mg polymer and 20 mg powdered drug was first melted at about 30 °C to obtain a homogeneous mixture, then allowed to cool to 0 °C, and crushed. The crushed mixture was charged into a Teflon® tube of 3 mm inner diameter. The piston rods were inserted from both sides of the tube under a pressure of 100 kg/cm^2

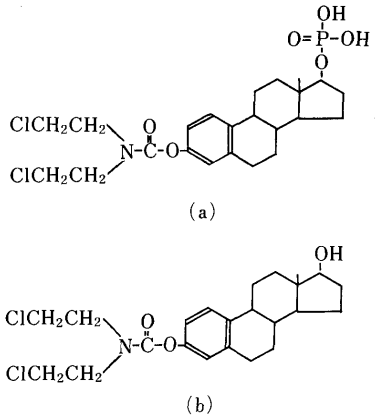

Fig. 1. Structural Formula of Estracyt (a), Estramustine (b)

at 30 °C to mold the mixture, obtaining pasty-type cylinders of the mixture charged into the tube. After preparation, the devices were immediately stored at 5 °C. The device without 100 mg of the drug was prepared by the same method.

***In Vivo* Polymer Degradation** The site of surgical insertion of the device *in vivo* experiments is shown in Fig. 2. The degree of *in vivo* degradation in the device with or without drugs was evaluated by measuring the weight loss of the device. The devices were implanted subcutaneously in the backs of male adult Wistar strain rats weighing 350—400 g (1 (with drugs) or 3 (without drugs) devices per rat, 3 rats per group). At certain time intervals, the devices were taken out from sacrificed rats, pooled after being freed of surrounding connective tissue, lyophilized, and weighed to estimate the degree of *in vivo* degradation (%) from the equation $[100(D_0-D)/D_0]$, where D_0 is the weight of the device before degradation and D is the weight of the device after treatment for the desired period of time.

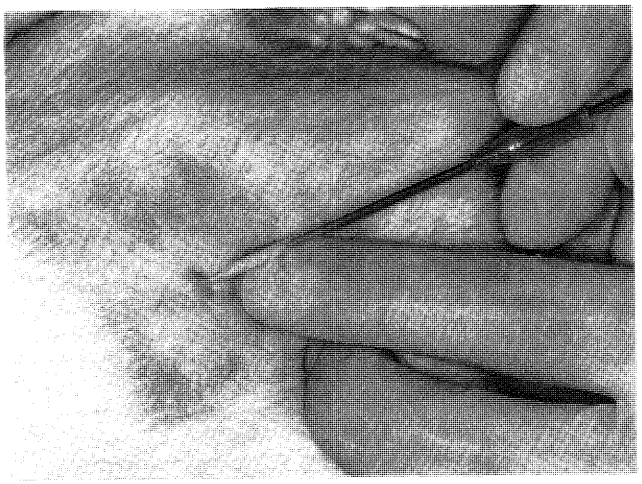

Fig. 2. Surgical Insertion Site of the Device

***In Vivo* Drug Release** The cumulative amount of Estracyt or estramustine released *in vivo* from the device was estimated from the amount of drug remaining in the device which was taken from sacrificed rats at appropriate time intervals. The drug remaining in the device was extracted with ethanol and, after centrifugation, its concentration in the supernatant solution was assayed at 269 nm with a Hitachi U-3210 spectrophotometer.

Pharmacological Influence The pharmacological influences of Estracyt or estramustine in the devices were estimated in male rats by measuring the change in weight of sex organs such as ventral prostates (VP) and right-side seminal vesicle (SV). For this purpose, each drug-containing device (one device per rat, 5 rats per group) was administered subcutaneously in the backs of male adult Wistar strain rats weighing 350—400 g. At the required time intervals, the rats were sacrificed. Each organ was freed from surrounding connective tissue, then pooled, and weighed. The organ weight is expressed in mg per 100 g of body weight at the sacrifice.

Results

Changes in Shape of Devices The change in shape of the devices implanted subcutaneously into the rats is shown in Fig. 3. Figure 3a shows the state of the device before implantation. The shape of the device was markedly changed by implantation, and it gradually degradaded from the surface of the device and disappeared. The degree of *in vivo* degradation in the device was found to be approximately 26% at 3 weeks, 42% at 7 weeks and 75% at 20 weeks.

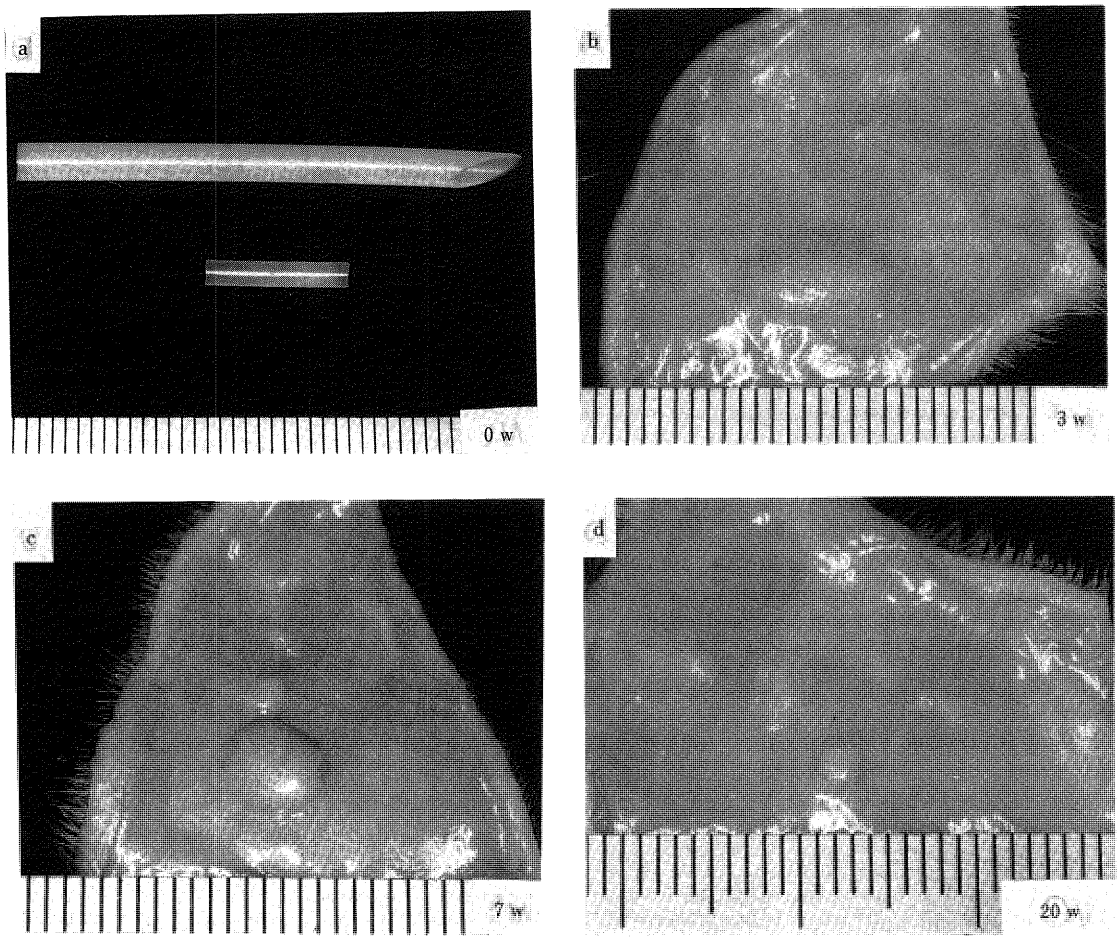

Fig. 3. Change of the Device Shape Throughout Implantation Time

a, before implantation; b, 3 weeks implantation; c, 7 weeks implantation; d, 20 weeks implantation.

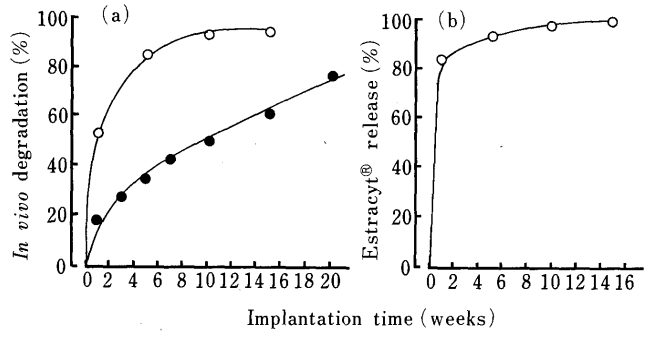

Fig. 4a. *In Vivo* Degradation Curves in the Devices with and without Estracyt

○—○, with Estracyt, ●—●; without Estracyt.

Fig. 4b. *In Vivo* Drug Release Curves in the Device with Estracyt

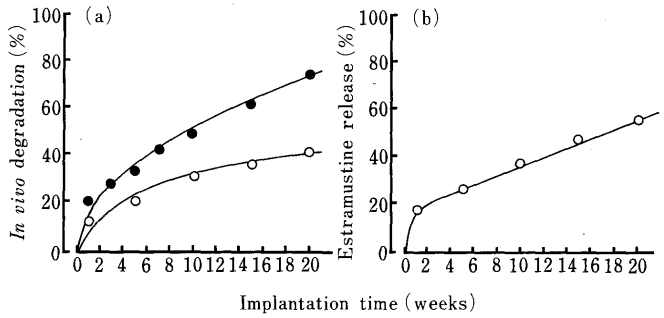

Fig. 5a. *In Vivo* Degradation Curves in the Devices with and without Estramustine

○—○, with estramustine; ●—●, without estramustine.

Fig. 5b. *In Vivo* Drug Release Curves in the Device with Estramustine

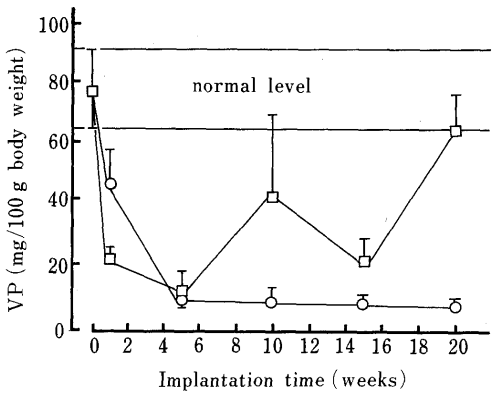

Fig. 6. Changes of VP Weight in Rats Implanted with the Devices Containing (□) Estracyt, (○) Estramustine

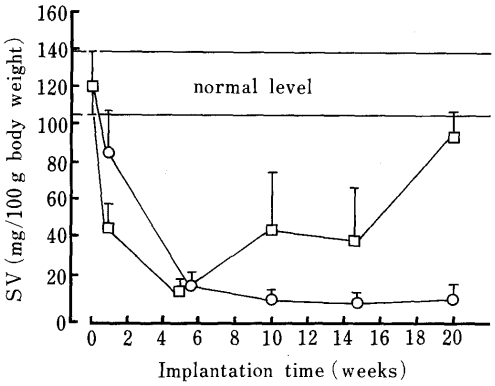

Fig. 7. Changes of SV Weight in Rats Implanted with the Devices Containing (□) Estracyt, (○) Estramustine

Estracyt Release and Degradation in Devices Estracyt release and degradation curve in the devices with and without Estracyt are shown in Fig. 4 as a function of implantation time. In the degradation curve, the degradation yield in the devices with the drug was higher than that in the devices without the drug. The *in vivo* degradation curves in the devices with and without drugs showed a parabola type, in which the degrees of the degradation at the 5th week were about 85% and 35%, respectively. The time required for 80% release was within 1 week due to burst phenomena, and the remaining drug was released over 15 weeks.

Estramustine Release and Degradation in Devices Estramustine release and degradation curve in the devices with and without estramustine are shown in Fig. 5 as a function of implantation time. In the degradation curve, the degradation yield in the device with the drug was lower than that in the devices without the drug. The release curve in the device with estramustine was roughly similar to the degradation curve. The time required for 55% release was about 20 weeks.

Pharmacological Influences The pharmacological influences of the devices were estimated by measuring the change in weight of the organs such as VP and SV in the rat. The results in SV and VP are shown in Figs. 6 and 7 as a function of implantation time. When the device without the drug was implanted in the rats, the weights of VP and SV in the rat were 63—90 and 105—140 mg/100 g body weight, respectively. The weight of the organs decreased, reached about 10—20 mg/100 g body weight at the initial implantation stage, and after that these values were kept until the 15—20th week, though the values in the case of Estracyt were scattered. Although the initial burst release occured in the case of Estracyt as seen in Fig. 4a, the death of the rat due to drug toxicity was not observed. Duration periods in the devices Estracyt and estramustine were about 15 and above 20 weeks, respectively. These results indicated that the drugs were effectively released from the devices to atrophy the organs for long periods of time.

Discussion

In this study, after the implantation, the shape of the device was gradually changed from cylinder to sphere by an increase of the implantation time depending on the body temperature of the rat as shown in Fig. 3. The shape of the spherical device changed at the initial implantation stage, however, was kept without dispersion or special deformation for long periods of time. The change in the shape of the device at the initial stage was not observed when the waxy polymer was used for the device.[7] It was found that the feature of the shape of the device implanted in the rat was markedly affected by morphology relating to the glass temperature (T_g) and T_m of the polymer.

In general, the rate of drug release in controlled release drugs using high molecular weight biodegradable polymer depends on the diffusion rate of the drug, in which the polymer is gradually degradaded after release of the drug.[12-14] In the degradation and drug release studies using the device with and without Estracyt, the degradation yield in the devices with the drug was higher than that in

the devices without the drug at the initial implantation time as seen in Fig. 4a. This high degradation yield was similar to the high release yield in the devices at the initial implantation time. Most of the Estracyt contained in the devices was released at the initial implantation time (0—2 weeks) as seen in Fig. 4b. Thus, it was found that the degradation of the devices was accelerated by the mixing of the water soluble drug (Estracyt).

On the other hand, the degradation yield in the devices with estramustine was lower than that in the devices without estramustine and the profiles of the estramustine release curve resembled that of the degradation curve of the device with estramustine, indicating that the degradation of the device was suppressed by the mixing of the water-insoluble drug (estramustine). From these results, it was found that the degradation of the devices was affected by the hydrophilicity of the drug. In the present preparation method, the drug was mixed with the polymer taking a molecular dispersion state, in which the chemical bonds between the polymer and the drug were not formed. Accordingly, the drugs are physically dispersed in the polymer without interacting with each other. It is, therefore, proposed that the degree of the degradation of the polymer is intimately dependent on the mixture ratio of the drug in the devices.

The water-soluble drugs dispersed in a micro-particle state in the polymer could play the role of a driving force for the increase of polymer degradation accompanying an increase of polymer swelling because the drugs are first dissolved to release them from the polymer forming a porous structure (capillary tube structure) with a large surface area.[15,16] The formation of a capillary tube structure in the pasty-type polymer due to drug release seems to be favorable compared with that in a hard polymer such as a waxy polymer. On the other hand, the water-insoluble drugs were not able to form a porous structure in the polymer because the drugs are not easily dissolved. The affinity of the polymer matrix to water in the rat-body accompanying a swelling should be decreased owing to such a reason, so that the degradation of the polymer may be suppressed. But, this supression appeared to be effective for the control of drug release for long periods of time from the aspect of pharmacological influence.

In pharmacological study using both the devices with Estracyt or estramustine, the atrophy of SV and VP was maintained for adequate times. The atrophy of the sex organs in the devices with Estracyt was recovered at the 20th week and that in the devices with estramustine was maintained for more than 20 weeks as can be seen in Figs. 4 and 5. The effective maintenance of the atrophy in these sex organs should be based on reasonable drug release from the devices. The *in vivo* data here demonstrated that the biodegradable pasty-type polymer was very useful as a matrix of implantable controlled release drugs in drug delivery systems.

References

1) S. Yolles, T. D. Leate, and F. J. Meyer, *J. Pharm. Sci.*, **64**, 115 (1975).
2) B. Hecquet, F. Chabot, J. C. D. Gonzalez, C. Fournier, S. Hilali, L. Cambier, G. Depadt, and M. Vert, *Aaticancer Res.*, **6**, 1251 (1986).
3) T. Iwa, M. Hirano, R. Yamashita, and M. Sakatoku, *Igaku No Ayumi*, **128**, 655 (1984).
4) I. Kawaguchi, M. Nakano, K. Juni, S. Inoue, and Y. Yoshida, *Chem. Pharm. Bull.*, **31**, 4157 (1983).
5) Y. Machida, T. Nagai, M. Abe, and T. Sannan, *Drug Design and Del.*, **1**, 119 (1986).
6) K. Imasaka, T. Nagai, M. Yoshida, H. Fukuzaki, M. Asano, and M. Kumakura, *Eur. Polym. J.*, **26**, 831 (1990).
7) K. Imasaka, M. Yoshida, H. Fukuzaki, M. Asano and M. Kumakura, T. Mashimo, H. Yamanaka, and T. Nagai, *Int. J. Pharm.*, **68**, 87 (1991).
8) H. Fukuzaki, M. Yoshida, M. Asano, M. Kumakura, T. Mashimo, H. Yuasa, K. Imai, H. Yamanaka, U. Kawaharada, and K. Suzuki, *J. Contr. Rel.*, **10**, 293 (1989).
9) M. Asano, H. Fukuzaki, M. Yoshida, M. Kumakura, T. Mashimo, H. Yuasa, K. Imai, and H. Yamanaka, *Biomaterials*, **10**, 569 (1989).
10) M. Asano, H. Fukuzaki, M. Yoshida, M. Kumakura, T. Mashimo, H. Yuasa, K. Imai, and H. Yamanaka, *Drug Design and Del.*, **5**, 301 (1990).
11) H. Fukuzaki, M. Yoshida, M. Asano, M. Kumakura, K. Imasaka, T. Nagai, T. Mashimo, H. Yuasa, K. Imai, and H. Yamanaka, *Eur. Polym. J.*, **26**, 1273 (1990).
12) A. Kishida, S. Yoshioka, Y. Takeda, and M. Uchiyama, *Chem. Pharm. Bull.*, **37**, 1954 (1989).
13) Y. Cha and C. G. Pitt, *J. Contr. Rel.*, **7**, 69 (1988).
14) V. V. Ranade, *J. Clin. Pharmacol.*, **30**, 871 (1990).
15) K. Imasaka, H. Ueda, T. Azuma, T. Kawaguchi, and T. Nagai, *Drug Design and Del.*, **4**, 273 (1989).
16) K. Imasaka, H. Ueda, T. Azuma, and T. Nagai, *Drug Design and Del.*, **5**, 159 (1989).

Relationship between the Biological Potency of Polychlorinated Dibenzo-*p*-dioxins and Their Electronic States

Shigeki KOBAYASHI,*[,a] Akio SAITO,[a] Yoko ISHII,[a] Akira TANAKA,[b] and Seisho TOBINAGA*[,a]

Showa College of Pharmaceutical Sciences,[a] Machida, Tokyo 194, Japan and National Institute of Hygienic Sciences,[b] 1–18–1, Setagaya-ku, Tokyo 158, Japan. *Received February 8, 1991*

The molecular orbital (MO) method, as one approach explaining the structure–activity of polychlorinated dibenzo-*p*-dioxins (PCDDs), was used to understand the relationship between the biological activities and electronic state or highest occupied molecular orbital (homo) phase symmetry of PCDDs. The structure–activity relationship of PCDDs could be explained by the difference between the homo and lowest unoccupied molecular orbital (lumo) energy levels ($\Delta\varepsilon$: difference of ε_{homo} and ε_{lumo}) which indicates orbital mixing with other molecules. The magnitude of biological activity was consistent with the following order: 2,3,7,8-tetraCDD > 1,2,3,7,8-pentaCDD > 1,2,3,7,8,9-hexaCDD > 2,3,7-triCDD > 2,8-diCDD, with the order of decreasing $\Delta\varepsilon$ by Hückel MO calculation. Our method can also estimate a magnitude of biological activity for PCDDs. The structure requirement for high toxicity suggested that the electronic states of PCDDs showed a small value difference ($\Delta\varepsilon$) and S_1S_2 phase symmetry on the homo for PCDDs. These results indicate that the electron states of PCDDs, which are based on the binding interaction of PCDDs to a cytosolic Ah receptor, play an important role in the appearance of their activity.

Keywords polychlorinated dibenzo-*p*-dioxin; molecular orbital calculation; electronic state; orbital symmetry; toxicity; biological activity; structure–activity relationship

Polychlorinated dibenzo-*p*-dioxins (PCCDs) are three-ring hetero aromatic compounds and nearly planar molecules,[1] as shown in Chart 1. A number of recent investigations have reported the toxicities and structure–activity relationships in various PCDDs.[2–5] These compounds have striking biological properties, such as specific binding activity to affinity sites (Ah receptor)[4,6] in hepatic cytosol of C57BL/6J mice,[7] and potent inducement of enzymes, namely, aryl hydrocarbons hydroxylase (AHH)[7–10] and δ-aminolevulinic acid (δ-ALA) synthetase.[8] The specific structural properties for these compounds have been studied regarding their biological mechanisms of toxicity and the relation between the PCDDs' structure–enzyme induction and structure–toxicity relationships.[4,5,9,11] In these relationships, the differences in physiological activities of PCDDs are strongly dependent on the substitution pattern in the PCDD molecule. For example, 2,3,7,8-tetraCDD of PCDDs shows the highest biological activity, but the reason why the number and substituted position of the chlorine atom in the dibenzo-*p*-dioxin (DD) molecule influenced the toxicity and biological activities of the compound is not clear at present. Poland *et al.* concluded that: (i) three positions of C-2, -3, -7, and -8 on the PCDD skeleton must contain halogen substituents, (ii) at least one hydrogen atom must be on the PCDD nucleus, and (iii) biological activity by the halogen substituent effects decreases in the following order, *i.e.*, Br > Cl > F.[10]

Several approaches have been carried out to understand the structure–activity relationship involved in these xenobiotics. Among those, it was described that the quantum structure–activity relationship (QSAR) method, which presented the structural relationship for the biological potency of PCDDs, indicates that a receptor protein (ex. Ah receptor) binds with the PCDDs at a common binding site on the receptor, and introduces the essential highly hydrophobic interaction of PCDDs with a binding site.[5,9] Therefore, it is considered that the Ah receptor-ligand interaction is dependent on substituent lipophilicity.

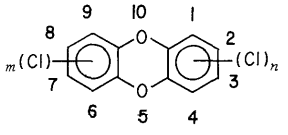

Chart 1. Structure of PCDDs

We suggest that the magnitude of biological potency or toxicity for PCDD congeners may be proportional to the intensity for stabilization energy forming the interaction between PCDD congeners and Ah receptor protein. The difference in energies ($\varepsilon_{homo} - \varepsilon_{lumo} = \Delta\varepsilon$) of a number of PCDD congeners has been determined by the Hückel molecular orbital (MO) method, and these $\Delta\varepsilon$ were compared with the biological activities of PCDDs. As a result, it was found that the magnitude of $\Delta\varepsilon$ has relevance to the structure–activity relationship for PCDDs. Naturally, the interaction of PCDD congeners with an Ah receptor is a molecular recognition process in which it seemed that the above process would be under the control of hydrophobic action, electrostatic potential, and spatial conformation. The PCDDs' orbital energy brings out the participation of the structure–activity relationship for the bioactivity of PCDDs.

The orbital phase symmetry of homo for PCDDs is different from the position of substituent chlorine on the DD skeleton. This homo phase analysis can predict the potency of biological activity and toxicity for PCDDs, and it is possible to use this homo phase analysis for the prediction of biological potency for PCDDs.

Theoretical Methods

MO calculations are performed using a simple Hückel approximation (HMO) using the semiempirical parameters shown in Table I.[12] Alfa and β are coulomb and resonance integrals, respectively, and the following indices were calculated for the PCDD system: the MO energies of the ε_{homo} (the highest occupied molecular orbital energy), ε_{lumo} (the lowest unoccupied molecular orbital energy), the

difference ($\Delta\varepsilon$) of ε_{homo} and ε_{lumo}. The results obtained are shown in Table II.

McKinney *et al.* have reported an Ah receptor stacking interaction model, showing polarization through π-complexation, and a nonstacking lateral chlorine polarization interaction model.[13] The mechanism of stabilization, except for the delocalization interaction, was explained by the polarization interaction,[14] dispersion interaction,[13,15] electrostatic interaction,[16] charge transfer interaction,[17] hydrophobic interaction,[5] and so on.

The PCDDs' orbital energy gap, $\Delta\varepsilon$, implies the magnitude of stabilization energy by polarization interaction by means of a perturbation theory,[14] and a small $\varepsilon_{homo}-\varepsilon_{lumo}$ gap indicates high reactivity.

TABLE I. Empirical Parameters Used in the Simple Hückel MO Calculations

Bond	No. of electron	Coulomb integral (a_X)	Resonance integral (b)
C–C	1	$a_C=0.0$	$b=1.0$
C–O	2	$a_O=2.0$	$b=0.6$
		$a_C=0.2$	
C–Cl	2	$a_{Cl}=1.8$	$b=0.8$
		$a_C=0.18$	

a) Coulomb integral of the substituent X: $\alpha_X=\alpha+a_X\beta$. *b*) Coulomb integral of the carbon atom adjacent to X:$\alpha_{adj}=\alpha+a_C\beta$. *c*) Resonance integral of the carbon atom and X: $\beta_{C-X}=b\beta$.

Results and Discussion

The structure–enzyme activity relationship of PCDDs for AHH induction ability, in the chick embryo liver, is similar to the induction of δ-ALA synthetase.[7-10] From these structure–enzyme activity relationships, it is recognized that 2,3,7,8-tetraCDD is the most potent inducer of AHH and δ-ALA synthetase because the abilities become lower in the order of 1,2,3,4,7,8-hexaCDD > 1,2,3,4,7-pentaCDD > 2,3,7-triCDD. Although several approaches have been carried out to examine the structure–activity relationships for these PCDDs, it is concluded that the lipophilicity or distortion polarizability[18] of PCDDs plays an essential role in ligand–receptor protein complex formation.

On one hand, we used MO property to determine the relation between the chlorine substituent effects of PCDDs and their biological activity ability. Our calculated Hückel MO energies and $\Delta\varepsilon$ for PCDDs are presented in Table II.

TABLE II. Calculated Hückel MO Energies of Various PCDDs

Chlorine position	MO energy			Chlorine position	MO energy		
	ε_{homo} (β)	ε_{lumo} (β)	$\Delta\varepsilon$ (β)		ε_{homo} (β)	ε_{lumo} (β)	$\Delta\varepsilon$ (β)
2,3,7,8-	0.64647	−0.92017	1.5666	1,3,6,8-	0.70466	−0.90777	1.6124
1,2,3,7,8-	0.64644	−0.92025	1.5667	1,3,7,9-	0.68856	−0.90739	1.5960
1,2,3,7,8,9-	0.64641	−0.92033	1.5667	1,3,7,8-	0.66771	−0.91356	1.5813
1,2,3,6,7,8-	0.64642	−0.92035	1.5668	2,3,7-	0.67191	−0.91355	1.5855
1,2,3,4,7,8-	0.64644	−0.92038	1.5668	2,8-	0.70943	−0.90738	1.6168
1,2,3,4,6,7,8-	0.64641	−0.92047	1.5669	2,7-	0.71429	−0.90776	1.6221
1,2,4,7,8-	0.65782	−0.91388	1.5717	Non	0.78782	−0.89553	1.6834

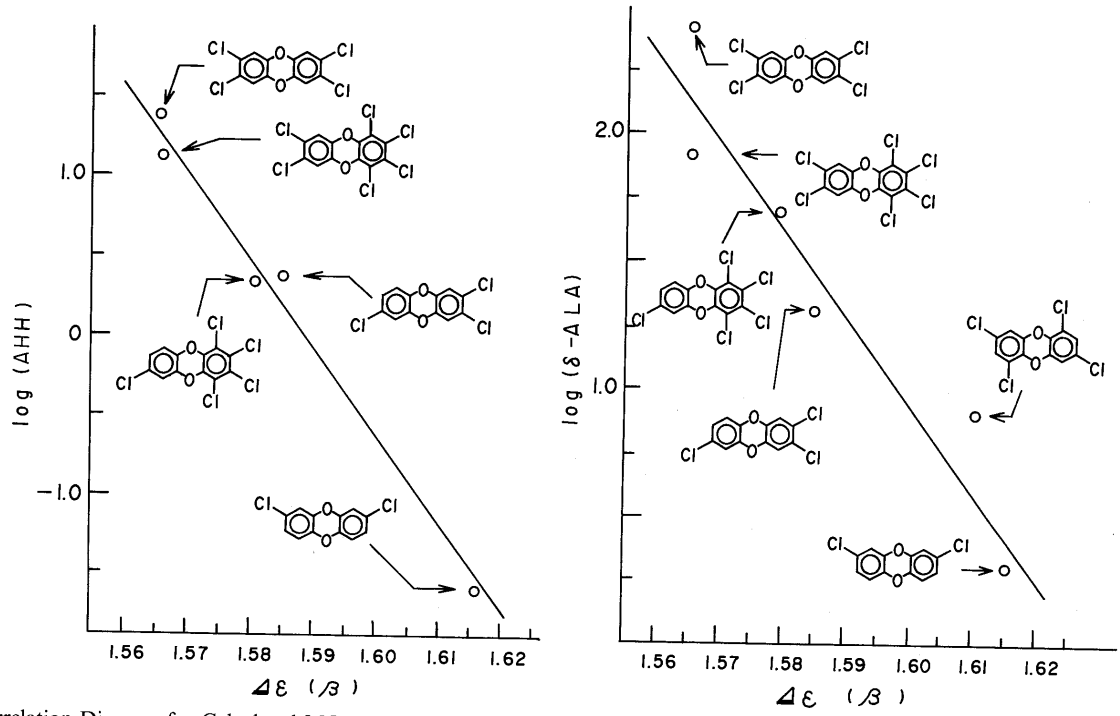

Fig. 1. Correlation Diagram for Calculated MO Energy Levels, $\Delta\varepsilon$, of Aryl Hydrocarbon Hydroxylase Activity in the Chick Embryo Liver (Left) and δ-ALA Synthetase Activity in the Chick Embryo (Right)

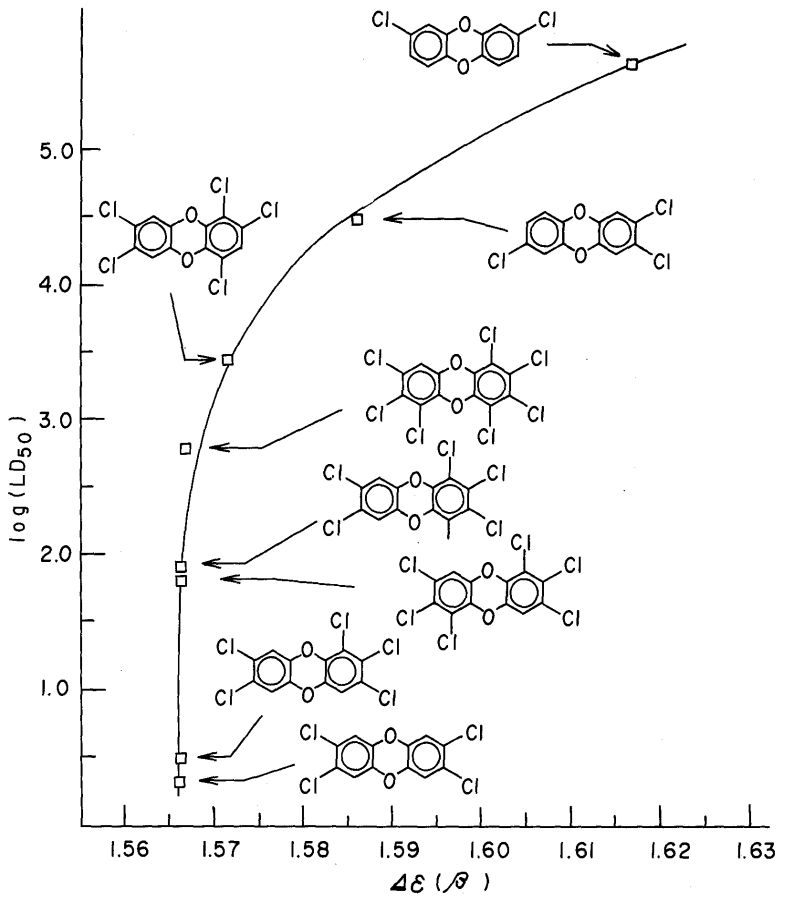

Fig. 2. Plot of Calculated MO Energy Levels, $\Delta\varepsilon$, for PCDDs and Acute Oral log(LD_{50}) (μg/kg Body Weight) in Guinea Pig

The enzyme induction ability for PCDDs was practically proportional to the calculated values $\Delta\varepsilon$ for PCDDs, that is, a plot of $\Delta\varepsilon$ *vs.* $\log_{10}$(AHH) and $\log_{10}$(δ-ALA) of AHH and δ-ALA synthetase induction ability assayed by Poland *et al.*[7,8,10,19] gave a linear equation, as in Fig. 1.

This calculated $\Delta\varepsilon$ can predict the influence of the chlorine substitution pattern on a DD skeleton, and this index indicates the relation between PCDD structure and AHH or δ-ALA synthetase induction ability. The enzyme induction ability of PCDDs increased with decreasing the values of calculated $\Delta\varepsilon$ for PCDDs. PCDDs having a chlorine atom at least at the C-2, -3, -7, and -8 positions have a lower $\Delta\varepsilon$ compared to PCDDs without chlorine at these positons. However, the magnitude of $\Delta\varepsilon$ values is not related to the number of chlorine atoms on the DD skeleton. The order of enzyme induction potencies for PCDDs is in proportion to assay order for cytosolic receptor binding affinity.[8,9] In these results, the magnitude of Ah receptor binding affinity may in fact be supported by quantum chemical expressions for the interaction between Ah receptor and PCDDs.

The major toxicities of PCDD isomers cause a decrease in bodyweight, acnegenic, teratogenic, edema, liver disorder, and immunosuppressive *etc.*[4] 2,3,7,8-TetraCDD isomer is the most toxic compound, and the LD_{50} or $LD_{50\text{-}30}$ values of PCDDs have been reported regarding acute toxicities in guinea pigs or mice.[2,3] An interesting feature in these toxicities depends on the position or number of the chlorine atom on the DD skeleton as well as the structure–enzyme induction abilities of PCDDs. This finding seems to relate the toxicities of various PCDDs to their structures. Plots of the estimated log(LD_{50}) or log($LD_{50\text{-}30}$) values *vs.* $\Delta\varepsilon$ obtained by MO calculations for PCDDs are given in Figs. 2, 3, and 4. In these results, (a) a low $\Delta\varepsilon$ suggests highly potent toxicity, and a high $\Delta\varepsilon$ points to a weakly potent toxic property; (b) the structure–activity relationship can be recognized the relation between the log(LD_{50}) or log($LD_{50\text{-}30}$) values and the calculated $\Delta\varepsilon$ values; (c) the structure–activity relationship for PCDDs is dependent on the structure of PCDDs, but has no relation to animal species.

TABLE III. Point Groups and homo Phase Symmetry for Various PCDDs

Chlorine position	Point group	Irreducible representation	Homo phase
2,3,7,8-	D_{2h}	$4a_u+5b_{1u}+5b_{2g}+4b_{3g}$	S_1S_2
1,2,3,7,8-	C_s	19a	S_1S_2
1,2,3,7,8,9-	C_{2v}	$9a_2+11b_1$	S_1S_2
1,2,3,6,7,8-	C_{2h}	$10a_u+10b_g$	S_1S_2
1,2,3,4,7,8-	C_s	20a	S_1S_2
1,2,3,4,6,7,8-	C_s	21a	S_1A_2
1,2,4,7,8-	C_s	19a	A_1A_2
2,3,7-	C_s	17a	A_1A_2
2,7-	C_{2h}	$8a_u+8b_g$	A_1A_2
2,8-	C_{2v}	$7a_2+9b_1$	S_1A_2
1,3,6,8-	C_{2h}	$9a_u+9b_g$	A_1A_2

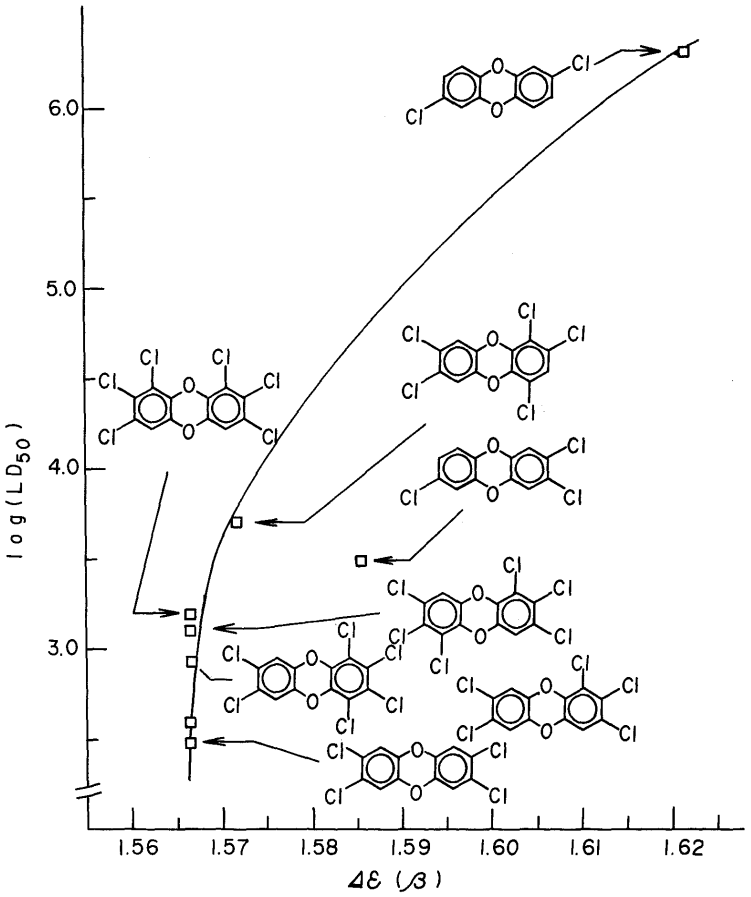

Fig. 3. Plot of Calculated MO Energy Levels, $\Delta\varepsilon$, for PCDDs and Acute Oral log(LD_{50}) (μg/kg Body Weight) in Mouse

TABLE IV. homo Phase Symmetry and Acute Toxicity (LD_{50} and LD_{50-30}) of PCDDs

Chlorine position	Acute toxicity (LD_{50})[a]		Acute toxicity (LD_{50-30})[b]		homo phase
	Guinea pig (μg/kg)	Mouse (μg/kg)	Guinea pig (μmol/kg)	Mice (μmol/kg)	
2,7-	—	2000000	—	—	A_1A_2
2,8-	300000	—	>1180	—	S_1A_2
2,3,7-	30000	3000	120.41	10	A_1A_2
2,3,7,8-	2	280	0.006	0.88	S_1S_2
1,2,3,7,8-	3	340	0.009	0.94	S_1S_2
1,2,4,7,8-	1100	5000	3.15	14	A_1A_2
1,2,3,4,7,8-	73	825	0.185	2.11	S_1S_2
1,2,3,6,7,8-	70—100	1250	0.178—0.255	3.19	S_1S_2
1,2,3,7,8,9-	60—100	1440	0.153—0.255	3.67	S_1S_2
1,2,3,4,6,7,8-	600	—	>1.400	—	S_1A_2
1,3,6,8-	—	—	—	—	A_1A_2
1,3,7,9-	—	—	—	—	S_1A_2

a) Taken from ref. 3. *b*) Taken from ref. 2.

Further, we studied the relation between the potency of toxicity and homo-phase symmetry for PCDDs. The irreducible representation (τ) of 2,3,7,8-tetraCDD, which belongs to a D_{2h} point group, is $4a_u+5b_{1u}+5b_{2g}+4b_{3g}$. Moreover, two reflection planes of plane $1(\sigma_{xz})$ and plane $2(\sigma_{yz})$ exist on the DD ring, including the rotation axis (Table III). As shown in Fig. 5, the hatched and unhatched areas symbolize the positive and negative regions of the atomic orbitals in the homo energy level of PCDDs, respectively. The authors examined the homo-phase symmetry concerning the reflction plane, except for the phase of a chlorine atom on the DD skeleton, such as plane 1 and plane 2 for PCDDs. The same sign of π atomic orbital ϕ_r at the r number of the atom means symmetry (S) for plane 1 and plane 2, whereas the opposite sign indicates the assymmetry (A) for the plane. According to the methods described above, it is found that 2,3,7,8-tetraCDD has S_1S_2 symmetry, while 2,3,7-triCDD has A_1A_2 symmetry for the DD skeleton.

In connection with acute toxicities and the symmetry of homo phase, high toxicity requires S_1S_2 symmetry for PCDDs. On the other hand, low toxic PCDDs have S_1A_2

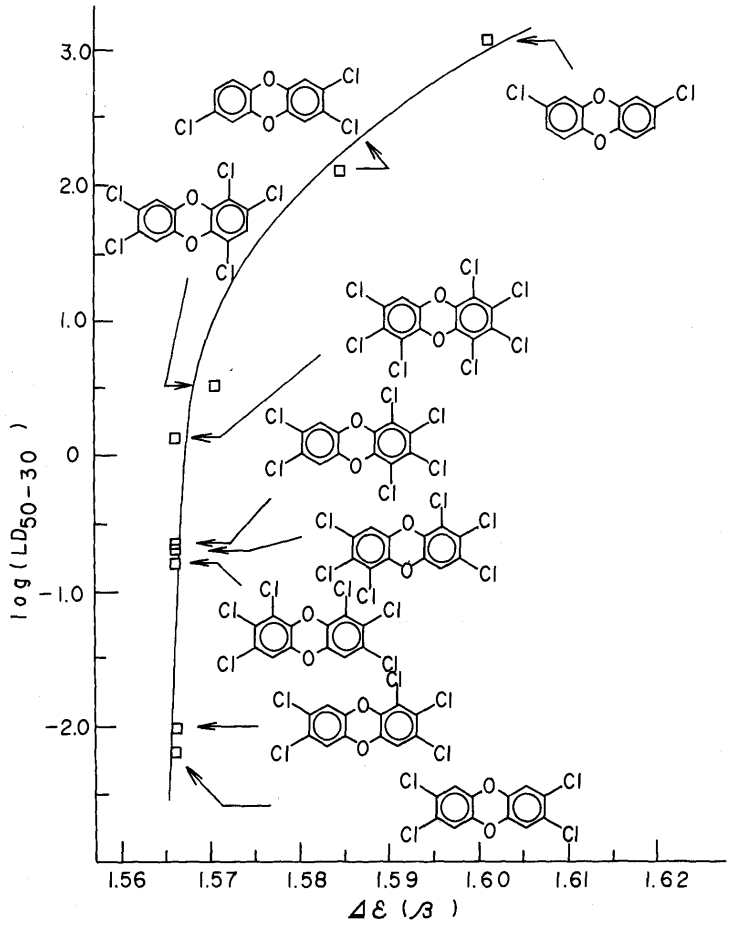

Fig. 4. Plot of Calculated MO Energy Levels, $\Delta\varepsilon$, for PCDDs and Acute Oral $\log(LD_{50-30})$ (μmol/kg Body Weight) in Guinea Pig

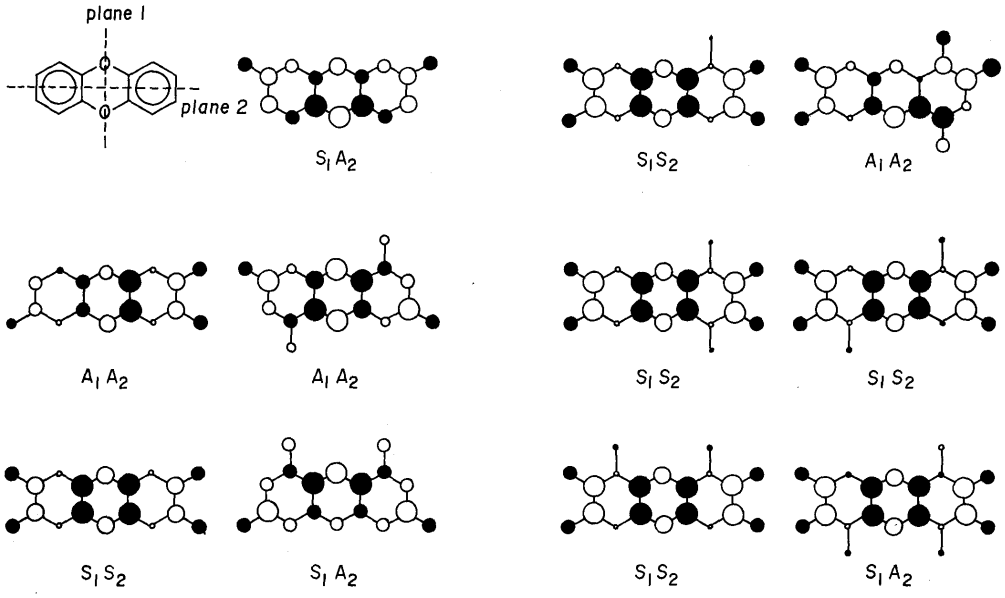

Fig. 5. homo (Highest Occupied Molecule Orbital) Phase Representations of Several PCDDs
S = symmetry, A = assymmetry.

(or A_1A_2 *etc.*) symmetry in the homo phase. The $\Delta\varepsilon$ values of 1,2,3,4,7,8-hexaCDD and 1,2,3,4,6,7,8-heptaCDD, for example, do not show a large difference, but the former has S_1S_2 symmetry and the latter S_1A_2 symmetry; hence it is predicted that 1,2,3,4,7,8-hexaCDD with S_1S_2 symmetry has high toxic potency. The toxicity of 1,3,6,8-tetraCDD or 1,3,7,9-tetraCDD, having the same number of chlorine in comparison with 2,3,7,8-tetraCDD, is low because the

homo phase and $\Delta\varepsilon$ for these compounds have A_1A_2 symmetry and are small, respectively (Table IV).

Thus, the homo phase analysis for PCDDs is a useful method when we surmise the induction ability of AHH and δ-ALA synthetase and the toxicity of PCDDs. The potency of biological activity, *e.g.* $LD_{50\text{-}30}$ and ability of AHH or δ-ALA synthetase induction of PCDDs, is in the following order: 2,3,7,8-tetraCDD > 1,2,3,7,8-pentaCDD > 1,2,3,4,7,8-hexaCDD > 1,2,3,6,7,8-hexa-CDD > 1,2,3,7,8,9-hexaCDD > 1,2,3,4,6,7,8-heptaCDD > 1,2,4,7,8-pentaCDD > 1,2,3,4,7-pentaCDD > 2,3,7-triCDD ≫ 2,8-di CDD. It was found that this order was consistent with that of the magnitude of MO calculated $\Delta\varepsilon$ of PCDDs; therefore, toxic potency can be predicted by the MO calculated $\Delta\varepsilon$ values or orbital symmetry using the homo phase analysis of these PCDDs.

It is reported that there is a linear correlation between cytosolic receptor (*e.g.* Ah receptor) binding affinity and AHH induction ability.[5,9] These findings indicate that $\Delta\varepsilon$ may show the relationship between PCDDs and Ah receptor binding affinity, since $\Delta\varepsilon$ for PCDD congeners is related to the potency of AHH induction. We have concluded that the magnitude of these $\Delta\varepsilon$ values has a relation to the binding affinity with an Ah receptor in hepatic cytosol. The interaction between Ah receptor protein and PCDDs does not involve the formation of any covalent bonds.

Delta ε values for PCDDs indicate the magnitude of complex formation with the binding site of Ah receptors such as aromatic amino acid residues.[20] Hence, it is concluded that lower $\Delta\varepsilon$ values define the ability of highly potent toxicity and the enzyme induction, *e.g.* AHH and δ-ALA synthetase, toward a series of PCDD congeners. This paper showed that the structure–activity relationship for PCDDs can be explained by means of the $\Delta\varepsilon$ and homo phase symmetry. These results suggest one possbility that the structure–activity relationship for PCDDs may be connected with MO energy and the MO phase.

References and Notes

1) *a*) M. Senma, Z. Taira, T. Taga, and K. Osaki, *Cryst. Struct. Commun.*, **2**, 311 (1973); *b*) G. Distefano, V. Galasso, K. J. Irgolic, and G. C. Pappalardo, *J. Chem. Soc., Perkin Trans. 2*, **1983**, 1109.
2) E. E. McConnell, J. A. Moore, J. K. Haseman, and M. W. Harris, *Toxicol. Appl. Pharmacol.*, **44**, 335 (1978).
3) K. Payne, "Chemistry and Toxicology of Polychlorodibenzo-*p*-dioxins. In: Study on State of Art of Dioxin From Combustion Sources (MT-3)," Arthur D. Little Inc., 1981.
4) A. Poland and J. C. Kuntson, *Ann. Rev. Pharmacol. Toxicol.*, **22**, 517 (1982).
5) S. H. Safe, *Ann. Rev. Pharmacol. Toxicol.*, **26**, 371 (1986).
6) *a*) K. D. Courtney, *Bull. Environ. Contam. Toxicol.*, **16**, 674 (1976); *b*) N. J. Bunce, J. P. Landers, and S. H. Safe, *Arch. Biochem. Biophys.*, **267**, 384 (1988).
7) A. Poland, E. Glover, and A. S. Kende, *J. Biol. Chem.*, **251**, 4936 (1976).
8) A. Poland and E. Glover, *Mol. Pharmacol.*, **9**, 736 (1973).
9) G. Mason, K. Farrell, B. Keys, J. Diskoraska-Plisczynska, L. Safe, and S. Safe, *Toxicology*, **41**, 21 (1986).
10) A. S. Kende, J. J. Wade, D. Ridge, and A. Poland, *J. Org. Chem.*, **39**, 931 (1974).
11) A. Poland, J. Knutson, and E. Glover, *Clin. Physiol. Biochem.*, **3**, 147 (1985).
12) C. Chin and P. Song, "Reactivity Indices for Biomolecules," Texas Tech Press, Lubbock, Texas, 1981, p. 175.
13) J. D. McKinney, K. Chae, E. E. McConnell, and L. S. Birnbaum, *Environ. Health Perspectives*, **60**, 57 (1985).
14) *a*) K. Fukui and H. Fujimoto, *Bull. Chem. Soc. Jpn.*, **41**, 1989 (1968); H. Fujimoto and S. Inagaki, *J. Am. Chem. Soc.*, **99**, 7424 (1977).
15) S. Bandiera, S. Safe, and A. B. Okey, *Chem. Biol. Instract.*, **39**, 259 (1982).
16) J. S. Murray, B. A. Zilles, K. Jayasuriya, and P. Politzer, *J. Am. Chem. Soc.*, **108**, 915 (1986).
17) *a*) G. Miller, S. Sontum, and D. G. Crosby, *Bull. Environ. Contam. Toxicol.*, **18**, 611 (1977); *b*) B. V. Cheney and T. Tolly, *Int. J. Quantum Chem.*, **16**, 87 (1979); *c*) W. Veerkamp, P. Serne, and O. Hutzinger, *J. Chem. Soc., Perkin Trans. 2*, **1983**, 353.
18) P. W. Albro and J. D. Mckinney, *Chem. Biol. Interactions*, **34**, 373 (1981).
19) The order of difference ($\Delta\varepsilon$) of ε_{homo} and ε_{lumo} for PCDDs is also proportional to the effects of structures on the *in vivo* toxic effect of PCDDs. See ref. 9, p. 26.
20) In this model, it was found that the quantity of charge transfer on the molecular complex between PCDDs and aromatic amino acids, such as phenylalanine, tyrosine, and tryptophane, increased with an increase in the toxicity of PCDDs.

Chem. Pharm. Bull. **39**(8) 2106—2114 (1991) Vol. 39, No. 8

A Novel Oxidative Intramolecular [4+2]Cycloaddition of Silylene-Protected Dihydroxystyrene Derivatives Leading to *peri*-Hydroxy Polycyclic Aromatic Compounds: A Synthesis of the ABCD Ring System of Fredericamycin A

Yasuyuki KITA,* Ryuichi OKUNAKA, Takao HONDA, Maiko KONDO, Osamu TAMURA, and Yasumitsu TAMURA

Faculty of Pharmaceutical Sciences, Osaka University, 1–6 Yamada-oka, Suita, Osaka 565, Japan. *Received March 13, 1991*

Heating of the silylene protected dihydroxystyrene generated from the *o*-hydroxyacetophenone (3a) at 130—150 °C for 15—48 h in a sealed tube gave intramolecular [4+2]cycloaddition products (5 and 6). The addition of chloranil to the reaction mixture brought about an oxidative intramolecular [4+2]cycloaddition to give the linearly condensed *peri*-hydroxy aromatic compound (7a) in excellent yield. The generality of this cycloaddition and application to a short and efficient synthesis of the ABCD ring system of fredericamycin A are described.

Keywords intramolecular [4+2]cycloaddition; *peri*-hydroxy polycyclic aromatic compound; oxdative cycloaddition; silylene derivative; fredericamycin A

Development of an efficient synthesis of naturally occurring *peri*-hydroxy aromatic compounds,[1] such as anthracyclines,[2] nogalamycin,[3] olivomycin,[4] bostrycin,[5] granaticin,[6] fredericamycin A,[7] and other antitumor polycyclic antibiotics, has been the subject of intensive study. The regioselective ring annulation is the critical step in the synthesis of these compounds. Among many approaches to them,[1] an intramolecular [4+2]cycloaddition reaction of alkoxystyrene derivatives having a suitable dienophile in the side chain, was expected to be a useful and straightforward method. The trials, however, were unsuccessful. One reason for this failure was the elimination of the alkoxy (or hydroxy) group from the cyclized product under the thermal conditions, leading to stable aromatization products.[8] Several years ago, we found a novel oxidative cycloaddition reaction of silylene-protected dihydroxystyrene derivatives with dienophiles, which gave the *peri*-hydroxy polycyclic aromatic compounds without loss of the α-hydroxyl group (Chart 1).[9] This approach should provide a short and efficient synthetic method for *peri*-hydroxy polycyclic compounds if the cycloaddition reaction can be extended to the intramolecular system. The conditions, however, were not suitable and gave a miserable yield of the intramolecular cycloaddition products. In connection with that work, we have recently communicated an efficient oxidative intramolecular [4+2]cycloaddition of *o*-hydroxyphenyl ketone having a suitable dienophile in the side chain leading to the *peri*-hydroxy aromatic compound in extremely high yield.[10] We now give a full account of this work and additional studies on the intramolecular [4+2]cycloaddition of other *o*-hydroxyphenyl ketones leading to the ABCD ring system of fredericamycin A.

Synthesis of 2,3-Dihydro-1*H*-benz[*f*]isoindol-1-ones (7a—c) and 2,3-Dihydro-1*H*-benz[*f*]indene Derivatives (21a, b and 22) The starting *o*-hydroxyphenyl ketones (**3a—c**) were prepared from *o*-hydroxyacetophenone in 4 steps. Hydroxymethylation of the acetyl group of *o*-hydroxyacetophenone with formaldehyde vapor under basic condition followed by dehydration with concentrated H_2SO_4 in benzene gave the known vinyl ketone (**1**).[11] Michael addition of aniline to **1** gave the terminal amino compound (**2**), which was condensed with α,β-unsaturated carboxylic acids by using a dehydrating agent, dicyclohexylcarbodiimide (DCC) or (trimethylsilyl)ethoxyacetylene,[12] to give the amides (**3a—c**) in considerable yields (Chart 2).

Initially, the dimethylsilylene derivative (**4a**) isolated by the reaction of **3a** with dichlorodimethylsilane (Me_2SiCl_2)/triethylamine (Et_3N) was heated under the same conditions as in the case of the intermolecular cycloaddition to give the cycloaddition products, **5** and **6**, in 15% and 11% yields, respectively. The yield of the products was dramatically improved when the reaction was performed without isolation of **4a** to give a 92% combined yield of **5** and **6** in a 35 : 57 ratio. Variation of the substituents on the silicon atom among dimethyl, diethyl, and diphenyl groups resulted in a slight increase in the ratio of **5** *vs.* **6** from 35 : 57 to 48 : 52. Although the yield of cycloadducts (**5** and **6**) was improved, the desired fully aromatized *peri*-hydroxy adduct (**7a**) could not be obtained at all.[13] After many unsuccessful trials,[14–16] an excellent result was obtained by addition of chloranil (0.136 mmol) in the reaction of **3a** (0.054 mmol), dichlorosilane (0.108 mmol), and Et_3N (0.217 mmol), which produced **7a** selectively in high yield (97%) (Chart 3).

Other *o*-hydroxyphenyl ketones (**3b, c**) gave the corresponding *peri*-hydroxy polycyclic compounds (**7b, c**) in excellent yeilds (Table I). It should be noted that the initially formed moisture-sensitive *Z*-olefin intermediates (**4**)[17] could be regenerated under the reaction conditions and underwent intramolecular Diels–Alder reaction to give the adducts, which were readily oxidized with chloranil to the stable *peri*-hydroxy polycyclic aromatic compounds (**7a—c**) irreversibly in high yields.

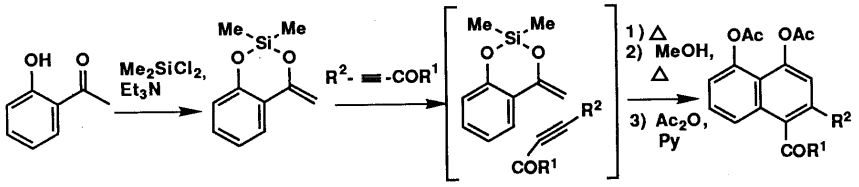

Chart 1

Next, we examined the generality of the cycloaddition in other *o*-hydroxyphenyl ketone systems. The starting *o*-hydroxyphenyl ketones (**16a—c** and **17**) were prepared from *o*-anisaldehyde (**8a**) or 2,5-dimethoxybenzaldehyde (**8b**) in several steps through intermediates (**12a—c** and **13a, b**) as outlined in Chart 4. The iodide (**10**) was prepared from γ-butyrolactone *via* the intermediates **18**, **19**, and **20** in 4 steps. Details of the preparation of **16a—c** and **17** are given in the experimental section.

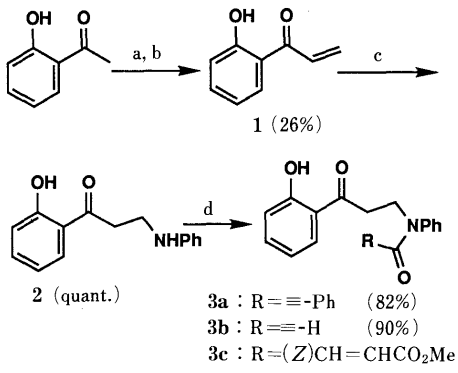

reagents : (a) LDA, $(HCHO)_n$, THF; (b) conc. H_2SO_4, C_6H_6; (c) aniline, EtOH; (d) α,β-unsaturated carboxylic acid (RCO_2H), CH_2Cl_2/DCC or TMS-≡-OEt, HgO

Chart 2

Thermal treatment of the dimethylsilylene derivatives of dihydroxystyrene derivatives (**16a—c** and **17**) as in the case of the synthesis of **7a—c** from **3a—c** gave the corresponding *peri*-hydroxy compounds (**21a, b**, **22**) in fair yields (Table II). The terminal silyl groups [trimethylsilyl (TMS) and *tert*-butyldimethylsilyl (TBDMS)] were eliminated under the reaction conditions and the bulky TBDMS group merely decreased the yield (entry 2). Even though the electron-withdrawing carbonyl function of the dienophile part was present on the opposite side of the acetylene bond, cyclization occurred smoothly (entry 4).

Application for Synthesis of the ABCD Ring System of Fredericamycin A (23) Fredericamycin A (**23**), isolated from *Streptomyces griseus*,[7] exhibits a potent *in vitro* cytotoxic activity[18] and has a unique structure involving a single chiral center at the spiro junction of the CD ring system. Although extensive efforts to achieve a total synthesis of **23**,[19] including one completed total synthesis of racemic **23**,[20] have been made, there is no report on

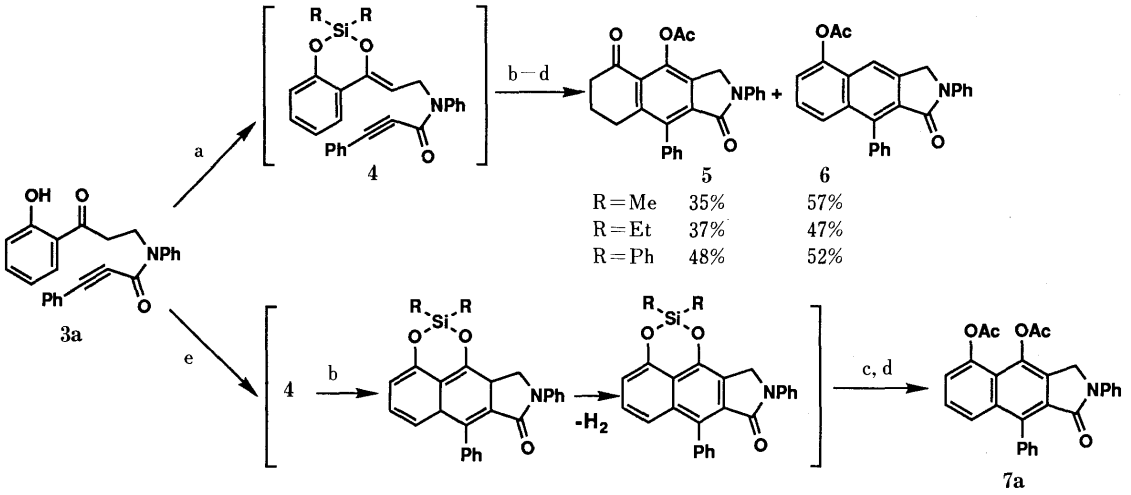

reagents : (a) R_2SiCl_2, Et_3N, C_6H_6; (b) heat in a sealed tube; (c) MeOH, reflux; (d) Ac_2O, pyridine; (e) R_2SiCl_2, Et_3N, chloranil, C_6H_6

Chart 3

TABLE I. Oxidative Intramolecular [4+2]Cycloaddition of **3a—c**

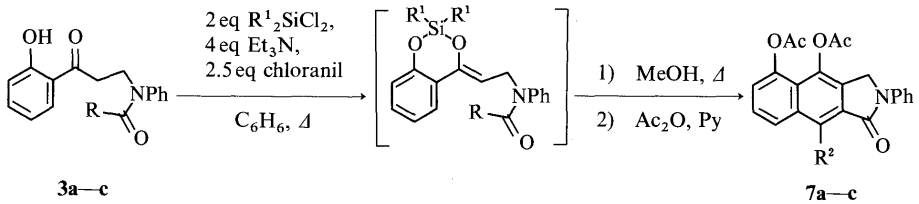

3a—c **7a—c**

Entry	R	R^1	Reaction time (h)		R^2	Product Yields (%)
1	—≡—Ph	Me	48	**7a**	Ph	97
2	—≡—Ph	Ph	48	**7a**	Ph	92
3	—≡—H	Me	7	**7b**	H	84
4	—≡—H	Ph	48	**7b**	H	75
5	(Z) -CH=$CHCO_2Me$	Me	18	**7c**	CO_2Me	64
6	(Z) -CH=$CHCO_2Me$	Ph	48	**7c**	CO_2Me	65

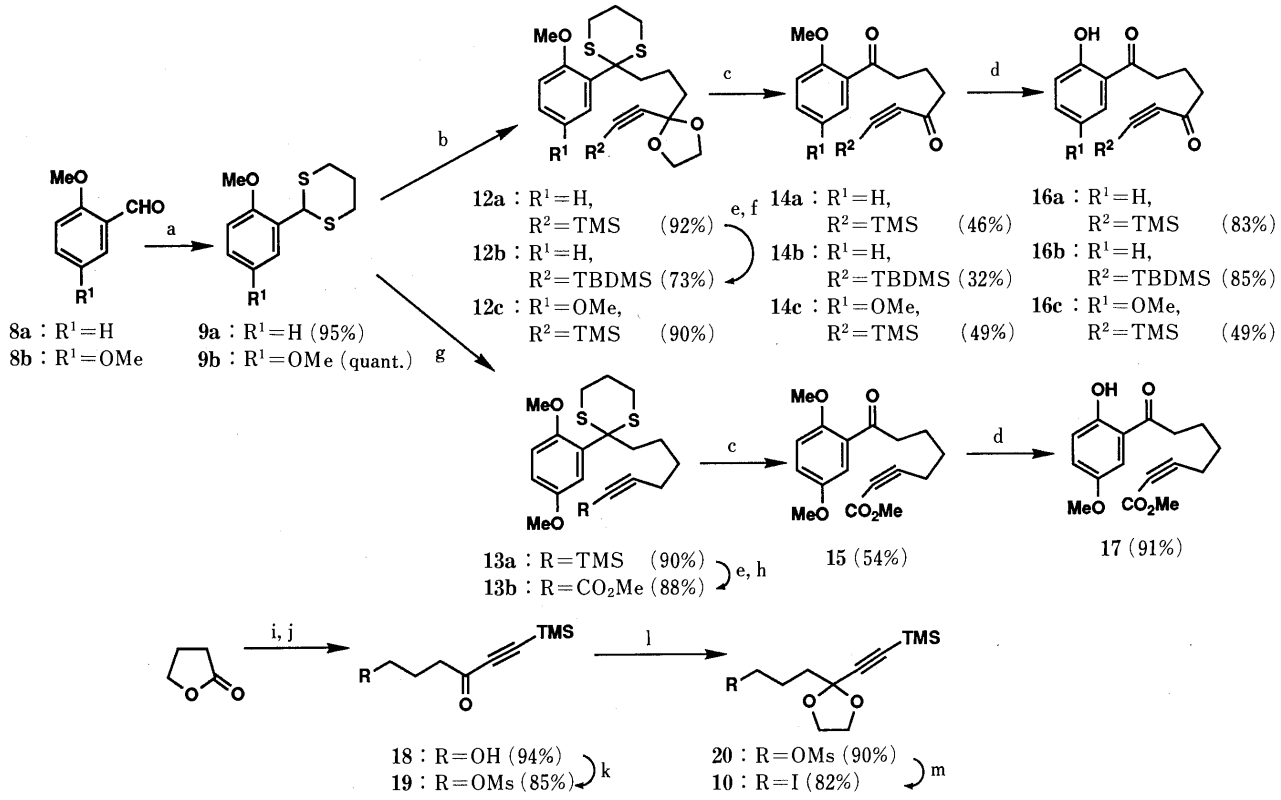

reagents : (a) propanedithiol, BF_3 Et_2O, CH_2Cl_2; (b) LDA, **10**, THF; (c) PIDA, *p*-TsOH, MeOH; (d) $AlCl_3$, CH_2Cl_2; (e) TBAF, THF; (f) *n*-BuLi, TBDMSCl, THF; (g) LDA, 6-iodo-1-(trimethylsilyl)-1-hexyne (**11**), THF; (h) *n*-BuLi, $ClCO_2Me$, THF; (i) TMS-≡-Li, THF; (j) AcOH, CH_2Cl_2; (k) MsCl, pyridine, CH_2Cl_2; (l) $(CH_2OH)_2$, *p*-TsOH, C_6H_6; (m) NaI, acetone

Chart 4

TABLE II. Oxidative Intramolecular [4+2]Cycloaddition of **16a—c** and **17**

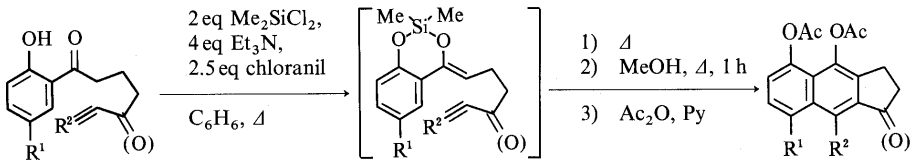

Entry	Starting compound	Reaction time (h)	Product	Yield (%)
1	**16a**: R^2=TMS	15	**21a**	66
2	**16b**: R^2=TBDMS	48		22
3	**16c**	15	**21b**	61
4	**17**	22	**22**	62

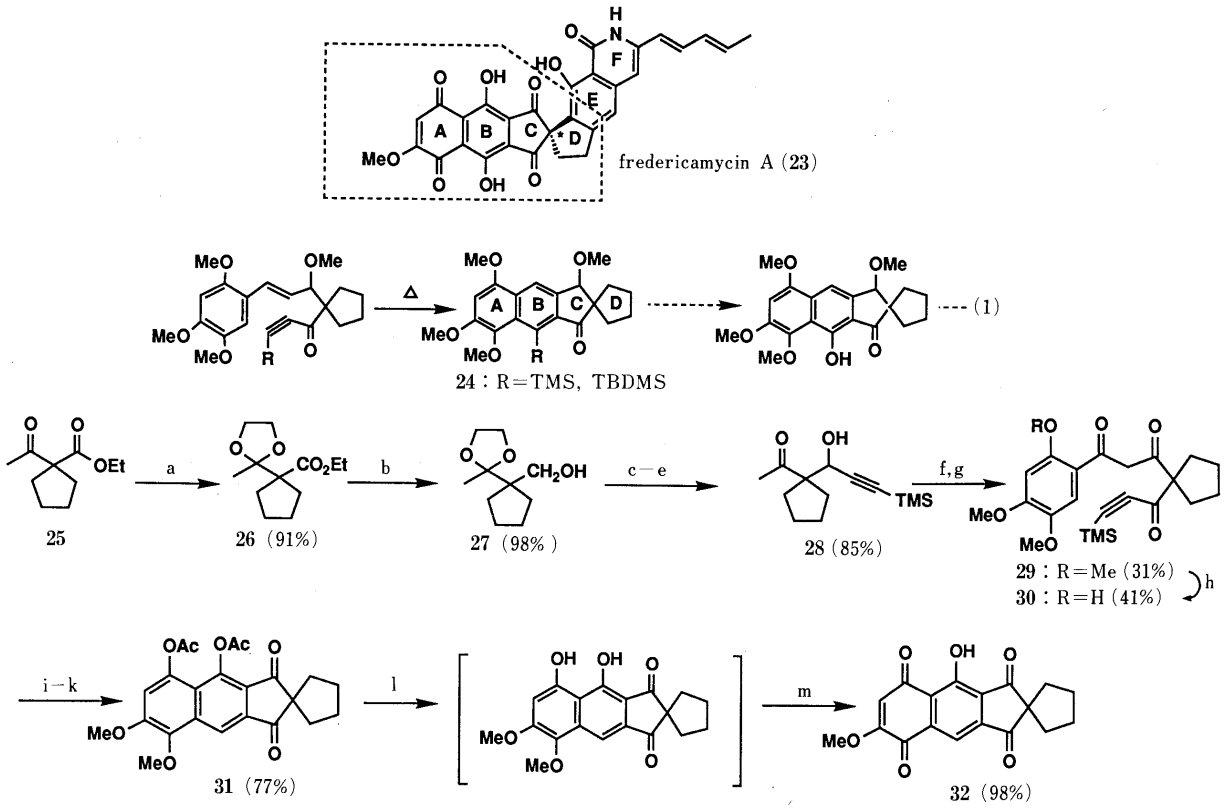

reagents : (a) $(CH_2OH)_2$, *p*-TsOH, C_6H_6; (b) $LiAlH_4$, Et_2O; (c) $(COCl)_2$, DMSO, Et_3N, CH_2Cl_2; (d) TMS-≡-Li, THF; (e) *p*-TsOH, acetone; (f) 2 eq LDA, HMPA, 2,4,5-trimethoxybenzoyl chloride, THF; (g) DMSO, DCC, pyridinium trifluoroacetate, C_6H_6; (h) 4 eq $AlCl_3$, CH_2Cl_2; (i) Me_2SiCl_2, Et_3N, chloranil, C_6H_6, heat in a sealed tube; (j) MeOH, reflux; (k) Ac_2O, pyridine; (l) 80% aqueous CF_3CO_2H; (m) PIFA, 33% aqueous CH_3CN

Chart 5

the synthesis of optically active **23**. Very recently, Toyota and Terashima reported an elegant synthesis of 2,2-tetramethylene-benz[*f*]indanes (**24**) by an intramolecular Diels–Alder reaction of dienynes as exemplified in Eq. 1.[21] It is expected to be a useful method for the synthesis of optically active **23**, because it has potential for construction of the asymmetric spiro junction of the CD ring system. The conversion of the silyl group on the B-ring of **24** thus obtained into an OH group was, unfortunately, quite difficult and failed in our hands. Therefore, we examined the synthesis of the ABCD ring system of **23** using the present oxidative intramolecular [4+2]cycloaddition reaction of silylene-protected dihydroxystyrene derivatives.

The requisite *o*-hydroxyphenyl ketone (**30**) was prepared from the known β-ketoester (**25**)[22] in 8 steps. Acetalization of **25** followed by reduction of the acetal (**26**) gave the alcohol (**27**) in 89% yield. Oxidation of **27** followed by treatment with lithium trimethylsilylacetylide gave the ethynyl alcohol, which was deprotected to give the β-ketoalcohol (**28**) in 85% overall yield from **27**. The dianion of **28** was aroylated with 2,4,5-trimethoxybenzoyl chloride to give the β-diketoalcohol, which was oxidized to give the triketone (**29**) in 31% overall yield from **28**. Selective demethylation of **29** with aluminum trichloride ($AlCl_3$) at room temperature gave the requisite *o*-hydroxyphenyl ketone (**30**) in 41% yield. Thermal treatment of **30** under the conditions described above caused oxidative intramolecular cycloaddition to give the desired *peri*-hydroxy aromatic compound, which was acetylated to give the acetate (**31**) in 77% overall yield from **30**. Deacetylation of **31** followed by oxidation with phenyliodosyl bis(trifluoroacetate)[PIFA, $PhI(OCOCF_3)_2$][23] gave the quinone (**32**), which is a key partial structure of **23** (Chart 5).

Application of this methodology to a total synthesis of optically active fredericamycin A is under investigation.

Experimental

All boiling and melting points are uncorrected. Infrared (IR) absorption spectra were recorded on a JASCO HPIR-102 spectrophotometer, ^{1}H-nuclear magnetic resonance (^{1}H-NMR) spectra were determined on a Hitachi R-22 (90 MHz) or JEOL JNM-GX500 (500 MHz) spectrometer with tetramethylsilane as an internal standard. Mass spectra (MS) were obtained by the electron impact (EI) method on an ESCO EMD-05A (for EI-MS) or a JEOL JMS-D300 (for EI- and exact MS) mass spectrometer. E. Merck silica gel 60 (70—230 mesh ASTM) for column chromatography and E. Merck precoated thin layer chromatography (TLC) plates, Silica gel F_{254} for preparative TLC (prep. TLC) were used. Organic layers were dried with anhydrous $MgSO_4$. Tetrahydrofuran (THF) was distilled from the sodium benzophenone dianion under nitrogen.

2-Hydroxyphenyl Vinyl Ketone (1) *o*-Hydroxyacetophenone (7.23 ml, 60.0 mmol) was added dropwise at −78 °C under nitrogen to an anhydrous THF solution of lithium diisopropylamide (LDA), prepared from *n*-BuLi (1.6 N in hexane, 89.0 ml, 144 mmol), diisopropylamine (20.1 ml, 144 mmol) and anhydrous THF (100 ml), and the mixture was stirred for 1 h under the same conditions. Then HCHO vapor obtained by heating paraformaldehyde (7.00 g) at 180 °C was introduced into the reaction vassel with vigorous stirring under nitrogen at 0 °C. The reaction mixture was poured into saturated aqueous NH_4Cl, and acidified (pH=3) with concentrated HCl. After extraction with Et_2O and AcOEt, the organic layer was washed with saturated aqueous $NaHCO_3$ and brine successively, dried, and then evaporated under reduced pressure. Purification of the residue by column chromatography on silica gel (benzene : AcOEt=

5:1—1:1, and Et_2O) followed by recrystallization from hexane–CH_2Cl_2 gave 3.50 g (35%) of pure 2'-hydroxyethyl 2-hydroxyphenyl ketone.

Concentrated H_2SO_4 (50.0 mg) was added to a benzene solution (21 ml) of 2'-hydroxyethyl 2-hydroxyphenyl ketone (1.00 g, 6.02 mmol). The reaction mixture was refluxed for 80 min with a Dean–Stark apparatus. The resultant mixture was poured into saturated aqueous $NaHCO_3$, and extracted with ether. The organic layer was washed with brine, dried, and concentrated under reduced pressure. The residue was purified by column chromatography on silica gel (benzene) to give 670 mg (75%) of pure **1** as a yellow oil: bp 65—67 °C (1.2—1.3 mmHg) (lit.[11] bp 67—68 °C (1—2 mmHg)). IR ($CHCl_3$) ν: 3040, 1640, 1620 cm^{-1}. ^{1}H-NMR ($CDCl_3$) δ: 5.92 (dd, 1H, J=10, 2 Hz, vinyl-H), 6.51 (dd, 1H, J=16, 2 Hz, vinyl-H), 6.77—7.59 (m, 4H, vinyl-H and ArH×3), 7.78 (dd, 1H, J=8, 2 Hz, 3-H), 12.50 (s, 1H, OH).

3-Anilino-1-(2-hydroxyphenyl)-1-propanone (2) An EtOH (160 ml) solution of **1** (1.99 g, 13.4 mmol) was added dropwise over 30 min to an EtOH (100 ml) solution of aniline (1.25 g, 13.4 mmol) at room temperature. The solvent was removed by evaporation under reduced pressure to give a crude solid. Recrystallization from hexane–AcOEt gave 3.40 g (quant.) of pure **2** as colorless crystals: mp 65—67 °C. IR ($CHCl_3$) ν: 3010, 1640, 1600 cm^{-1}. ^{1}H-NMR ($CDCl_3$) δ: 3.23 (t, 2H, J=6 Hz, $COCH_2$), 3.58 (t, 2H, J=6 Hz, NCH_2), 6.51—7.71 (m, 10H, ArH×9 and NH), 12.26 (s, 1H, OH). MS m/z: 241 (M^+). *Anal.* Calcd for $C_{15}H_{15}NO_2$: C, 74.67; H, 6.27; N, 5.80. Found: C, 74.59; H, 6.19; N, 5.78.

***N*-[3-(2-Hydroxyphenyl)-3-oxo-propyl]-*N*-phenyl-phenylpropiolamide (3a)** DCC (206 mg, 1.00 mmol) was added to a CH_2Cl_2 (2 ml) solution of **2** (241 mg, 1.00 mmol) and phenylpropiolic acid (146 mg, 1.00 mmol) at room temperature. The reaction mixture was stirred under the same conditions for 25 h. After filtration to remove the precipitate, the filtrate was evaporated under reduced pressure to give a crude residue. The residue was purified by column chromatography on silica gel (hexane: AcOEt=5:1) to give 302 mg (82%) of pure **3a** as colorless crystals: mp 111—112 °C (hexane–CH_2Cl_2). IR ($CHCl_3$) ν: 3000, 2210, 1640, 1630, 1595 cm^{-1}. ^{1}H-NMR ($CDCl_3$) δ: 3.40 (t, 2H, J=8 Hz, $COCH_2$), 4.24 (t, 2H, J=8 Hz, NCH_2), 6.71—7.82 (m, 14H, ArH×14), 12.02 (s, 1H, OH). MS m/z: 369 (M^+). *Anal.* Calcd for $C_{24}H_{19}NO_3$: C, 78.03; H, 5.18; N, 3.79. Found: C, 78.19; H, 4.94; N, 3.80.

***N*-[3-(2-Hydroxyphenyl)-3-oxo-propyl]-*N*-phenyl-Propiolamide (3b)** This was prepared from **2** (241 mg, 1.00 mmol) and propiolic acid (75.0 μl, 1.20 mmol) by the same procedure as described for the preparation of **3a**. Purification by column chromatography on silica gel (hexane: AcOEt=2:1) gave pure **3b** (262 mg, 90%) as colorless crystals: mp 134—135 °C (hexane–CH_2Cl_2). IR ($CHCl_3$) ν: 3300, 3010, 2100, 1640, 1595 cm^{-1}. ^{1}H-NMR ($CDCl_3$) δ: 2.80 (s, 1H, C≡CH), 3.36 (t, 2H, J=8 Hz, $COCH_2$), 4.20 (t, 2H, J=8 Hz, NCH_2), 6.76—7.78 (m, 9H, ArH×9), 12.04 (s, 1H, OH). MS m/z: 293 (M^+). *Anal.* Calcd for $C_{18}H_{15}NO_3$: C, 73.71; H, 5.15; N, 4.78. Found: C, 73.47; H, 5.02; N. 4.69.

***N*-[3-(2-Hydroxyphenyl)-3-oxo-propyl]maleinanilic Acid, Methyl Ester (3c)** A CH_2Cl_2 (0.3 ml) solution of maleic acid monomethyl ester (49.0 mg, 0.373 mmol) was added dropwise to a mixture of (trimethylsilyl)ethoxyacetylene (90.0 μl, 0.525 mmol), a catalytic amount of HgO (0.24 mg, 1.1 μmol) and dry CH_2Cl_2 (1.2 ml), and the mixture was stirred at room temperature for 1 h. Then a CH_2Cl_2 solution of **2** (75.0 mg, 0.311 mmol) was added dropwise and the whole was stirred at room temperature for 6 h. After addition of (trimethylsilyl)ethoxyacetylene (90.0 μl, 0.525 mmol) and maleic acid monomethyl ester (49.0 mg, 0.373 mmol), the reaction mixture was stirred at room temperature for 15 h. Removal of the solvent under reduced pressure gave the crude product. Purification by column chromatography on silica gel (hexane: AcOEt=3:1) gave pure **3c** (63.2 mg, 58%) as colorless crystals: mp 105—107 °C (hexane–CH_2Cl_2). IR ($CHCl_3$) ν: 1725, 1640, 1600 cm^{-1}. ^{1}H-NMR ($CDCl_3$) δ: 3.42 (t, 2H, J=8 Hz, $COCH_2$), 3.73 (s, 3H, OCH_3), 4.18 (t, 2H, J=8 Hz, NCH_2), 5.73 (d, 1H, J=12 Hz, vinyl-H), 6.22 (d, 1H, J=12 Hz, vinyl-H), 6.72—7.89 (m, 9H, ArH×9). 12.09 (s, 1H, OH). MS m/z: 353 (M^+). *Anal.* Calcd for $C_{20}H_{19}NO_5$: C, 67.98; H, 5.42; N, 3.96. Found: C, 67.86; H, 5.25, N, 3.87.

General Procedure for Intramolecular [4+2]Cycloaddition Reaction of Silylene-Protected Dihydroxystyrene Derivatives Obtained from *o*-Hydroxyphenylketones (3a—c, 16a—c, 17, and 30) Method A: A mixture of *o*-hydroxyphenyl ketone (0.100 mmol), Me_2SiCl_2 (0.200 mmol), Et_3N (0.400 mmol) in benzene (10 ml) was refluxed under nitrogen for 6 h and then stirred at room temperature for 12 h. The reaction mixture was diluted with dry benzene. The precipitate was filtered off, and the filtrate was concentrated under reduced pressure. The residue was diluted with dry benzene and heated in a sealed tube at 130—150 °C for 48 h. The reaction mixture was evaporated under reduced pressure, then diluted with MeOH and refluxed for 1 h. After concentration, the crude desilylated product was acetylated by a usual method with acetic anhydride in pyridine to give the acetate, which was purified by preparative TLC to give the pure acetylated cycloadducts.

Method B: A mixture of *o*-hydroxyphenyl ketone (0.100 mmol), dichlorodialkylsilane (0.200 mmol), Et_3N (0.400 mmol) and benzene (10 ml) was heated in a sealed tube at 130—150 °C for 48 h. The reaction mixture was worked up as described under method A to give the acetylated cycloadducts.

Method C: A suspension of *o*-hydroxyphenyl ketone (0.100 mmol), dichlorodialkylsilane (0.200 mmol), Et_3N (0.400 mmol), chloranil (0.250 mmol) and benzene (10 ml) was heated in a sealed tube at 130—150 °C for 15—48 h. The reaction mixture was worked up as described under method A to give the acetylated cycloadducts.

4-Acetoxy-2,9-diphenyl-2,3,5,6,7,8-hexahydro-1*H*-benz[*f*]isoindole-1,5-dione (5) and 5-Acetoxy-2,9-diphenyl-2,3-dihydro-1*H*-benz[*f*]isoindol-1-one (6) These were prepared from **3a** by method A or B. Purification by preparative TLC gave pure **5** and **6**. **5**: pale yellow crystals; mp 227—229 °C (hexane–CH_2Cl_2). IR ($CHCl_3$) ν: 1770, 1705, 1690 cm^{-1}. ^{1}H-NMR ($CDCl_3$) δ: 1.97—2.07 (m, 2H, 7-CH_2), 2.49 (s, 3H, $COCH_3$), 2.66 (t, 2H, J=7 Hz, 6-CH_2), 2.73 (t, 2H, J=7 Hz, 8-CH_2), 4.78 (s, 2H, 3-CH_2), 7.08—7.79 (m, 10H, ArH×10). MS m/z: 411 (M^+). *Anal.* Calcd for $C_{26}H_{21}NO_4$: C, 75.90; H, 5.14; N, 3.40. Found: C, 75.66; H, 5.02; N, 3.29. **6**: colorless crystals; mp 235—238 °C (hexane–CH_2Cl_2). IR ($CHCl_3$) ν: 1760, 1695 cm^{-1}. ^{1}H-NMR ($CDCl_3$) δ: 2.54 (s, 3H, $COCH_3$), 5.03 (s, 2H, 3-CH_2), 7.15 (t, 1H, J=8.0 Hz, ArH), 7.33—7.48 (m, 6H, ArH×6), 7.49—7.58 (m, 3H, ArH×3), 7.66 (d, 1H, J=8.5 Hz, ArH), 7.86 (dd, 2H, J=8.0, 1.0 Hz, ArH×2), 8.02 (s, 1H, 4-CH). MS m/z: 393 (M^+). *Anal.* Calcd for $C_{26}H_{19}NO_3$: C, 79.37; H, 4.87; N, 3.56. Found: C, 79.28; H, 4.69; N, 3.58.

4,5-Diacetoxy-2,9-diphenyl-2,3-dihydro-1*H*-benz[*f*]isoindol-1-one (7a) This was prepared from **3a** (20.0 mg, 54.2 μmol) by method C. Purification by preparative TLC gave pure **7a** (23.6 mg, 97%) as colorless crystals: mp 280—285 °C (dec.) (hexane–CH_2Cl_2). IR ($CHCl_3$) ν: 1775, 1765, 1700 cm^{-1}. ^{1}H-NMR ($CDCl_3$) δ: 2.47 (s, 3H, $COCH_3$), 2.53 (s, 3H, $COCH_3$), 4.83 (s, 2H, 3-CH_2), 7.15 (t, 1H, J=7.3 Hz, ArH), 7.26 (dd, 1H, J=7.0, 1.2 Hz, ArH), 7.34—7.46 (m, 6H, ArH×6), 7.51—7.57 (m, 4H, ArH×4), 7.71 (dd, 1H, J=8.5, 1.2 Hz, ArH), 7.79 (br d, 1H, J=8.0 Hz, 8-CH). MS m/z: 451 (M^+). *Anal.* Calcd for $C_{28}H_{21}NO_5$: C, 74.49; H, 4.69; N, 3.10. Found: C, 74.28; H, 4.49; N, 3.06.

4,5-Diacetoxy-2-phenyl-2,3-dihydro-1*H*-benz[*f*]isoindol-1-one (7b) This was prepared from **3b** (40.0 mg, 0.136 mmol) by method C. Purification by preparative TLC gave pure **7b** (43.0 mg, 84%) as colorless crystals: mp 241—243 °C (hexane–CH_2Cl_2). IR ($CHCl_3$) ν: 1775, 1700 cm^{-1}. ^{1}H-NMR ($CDCl_3$) δ: 2.44 (s, 3H, $COCH_3$), 2.49 (s, 3H, $COCH_3$), 4.84 (s, 2H, 3-CH_2), 7.22 (tt, 1H, J=7.3, 1.2 Hz, 4'-CH), 7.27 (dd, 1H, J=8.5, 1.2 Hz, 6-CH), 7.45 (td, 2H, J=7.3, 1.2 Hz, 3' and 5'-CH), 7.56 (t, 1H, J=8.5 Hz, 7-CH), 7.86 (dd, 2H, J=7.3, 1.2 Hz, 2' and 6'-CH), 7.98 (dd, 1H, J=8.5, 1.2 Hz, 8-CH), 8.41 (s, 1H, 9-CH). MS m/z: 375 (M^+). *Anal.* Calcd for $C_{22}H_{17}NO_5$: C, 70.39; H, 4.56; N, 3.73. Found: C, 70.58; H, 4.58; N, 3.81.

4,5-Diacetoxy-9-methoxycarbonyl-2-phenyl-2,3-dihydro-1*H*-benz[*f*]-isoindol-1-one (7c) This was prepared from **3c** (20.0 mg, 56.7 μmol) by method C. Purification by preparative TLC gave pure **7c** (16.0 mg, 65%) as colorless crystals: mp 230—232 °C (hexane–CH_2Cl_2). IR ($CHCl_3$) ν: 1770, 1740, 1710 cm^{-1}. ^{1}H-NMR ($CDCl_3$) δ: 2.44 (s, 3H, $COCH_3$), 2.49 (s, 3H, $COCH_3$), 4.15 (s, 3H, OCH_3), 4.84 (s, 2H, 3-CH_2), 7.22 (tt, 1H, J=7.3, 1.2 Hz, 4'-CH), 7.31 (dd, 1H, J=8.5, 1.2 Hz, 6-CH), 7.43 (td, 2H, J=7.3, 1.2 Hz, 3' and 5'-CH), 7.62 (t, 1H, J=8.5 Hz, 7-CH), 7.82 (dd, 1H, J=7.3, 1.2 Hz, 2' and 6'-CH), 7.91 (dd, 1H, J=8.5, 1.2 Hz, 8-CH). MS m/z: 433 (M^+). *Anal.* Calcd for $C_{24}H_{19}NO_7$: C, 66.50; H, 4.41; N, 3.23. Found: C, 66.63; H, 4.36; N, 3.50.

6-Hydroxy-3-oxo-1-trimethylsilyl-1-hexyne (18) A solution of *n*-BuLi (1.6 N in hexane, 6.30 ml, 10.2 mmol) was added dropwise to an anhydrous THF (7 ml) solution of trimethylsilylacetylene (1.44 ml, 10.2 mmol) at −40 °C under nitrogen. The mixture was stirred under the same conditions for 30 min, then added dropwise to an anhydrous THF (13 ml) solution of γ-butyrolactone (0.854 ml, 11.2 mmol) at −40 °C under nitrogen. The reaction mixture was stirred under the same conditions for 1 h and kept at −40 °C. The mixture was introduced into a CH_2Cl_2 (200 ml) solution of acetic acid (0.600 ml, 10.5 mmol) at room temperature, and the whole was washed with brine. The aqueous layer was extracted with CH_2Cl_2, and the combined organic layer was dried, and concentrated under reduced pressure. Purification of the residue by column chromatography on silica

gel (hexane : AcOEt = 2 : 1) gave **18** (1.69 g, 94%) as a colorless oil: bp 145—165 °C (0.11 mmHg) (dec.). IR ($CHCl_3$) *v*: 2960, 2150, 1670 cm^{-1}. ^{1}H-NMR ($CDCl_3$) δ: 0.24 (s, 9H, $Si(CH_3)_3$), 1.91 (quint, 2H, J = 6 Hz, CH_2), 2.69 (t, 2H, J = 6 Hz, $COCH_2$), 3.67 (t, 2H, J = 6 Hz, OCH_2). MS *m/z*: 184 (M^+). *Anal.* Calcd for $C_9H_{16}O_2Si$: C, 58.65; H, 8.75. Found: C, 58.91; H, 8.85.

4-Oxo-6-trimethylsilyl-5-hexynyl Methanesulfonate (19) A mixture of **18** (1.46 g, 7.90 mmol), pyridine (0.960 ml, 11.9 mmol), methanesulfonyl chloride (0.735 ml, 9.50 mmol), and CH_2Cl_2 (80 ml) was stirred at room temperature for 14 h. Further methanesulfonyl chloride (0.37 ml, 4.8 μmol) and pyridine (0.48 ml, 5.9 μmol) were added to the mixture, and the whole was stirred at room temperature for 22 h. Then MeOH (1 ml) was added, and the mixture was washed with brine. The aqueous layer was extracted with CH_2Cl_2, and the combined organic layer was dried, and evaporated under reduced pressure. Purification of the residure by column chromatography on silica gel (hexane : AcOEt = 2 : 1) gave **19** (1.76 g, 85%) as a colorless oil: bp 106 °C (0.19 mmHg) (dec.). IR ($CHCl_3$) *v*: 2150, 1675, 1360, 1175 cm^{-1}. ^{1}H-NMR ($CDCl_3$) δ: 0.24 (s, 9H, $Si(CH_3)_3$), 2.11 (quint, 2H, J = 6 Hz, CH_2), 2.77 (t, 2H, J = 6 Hz, $COCH_2$), 3.02 (s, 3H, SO_2CH_3), 4.28 (t, 2H, J = 6 Hz, OCH_2). Exact MS Calcd for $C_9H_{15}O_4SSi$ ($M^+ - CH_3$): 247.0458. Found: 247.0438, and Calcd for $C_9H_{15}O_2Si$ ($M^+ - SO_2CH_3$): 183.0838. Found: 183.0818.

4,4-Ethylenedioxy-6-trimethylsilyl-5-hexynyl Methanesulfonate (20) A benzene (30 ml) solution of **19** (500 mg, 1.91 mmol), ethylene glycol (1.06 ml, 19.1 mmol), and a catalytic amount of *p*-TsOH (150 mg, 0.871 mmol) was refluxed for 3 h under azeotropic conditions. The resulting mixture was diluted with AcOEt, washed with saturated aqueous $NaHCO_3$, dried, and concentrated under reduced pressure. Purification by column chromatography on silica gel (hexane : AcOEt = 2 : 1) gave **20** (525 mg, 90%) as a colorless oil: bp 105—115 °C (0.25 mmHg) (dec.). IR ($CHCl_3$) *v*: 2970, 1355, 1170 cm^{-1}. ^{1}H-NMR ($CDCl_3$) δ: 0.18 (s, 9H, $Si(CH_3)_3$), 1.96—2.11 (m, 4H, $CH_2 \times 2$), 3.00 (s, 3H, SO_2CH_3), 3.91—4.16 (m, 4H, OCH_2CH_2O), 4.20—4.38 (m, 2H, OCH_2). Exact MS Calcd for $C_{12}H_{22}O_5SSi$ (M^+): 306.0956. Found: 306.0931.

3,3-Ethylenedioxy-6-iodo-1-trimethylsilyl-1-hexyne (10) A Mixture of **20** (1.19 g, 3.89 mmol), sodium iodide (1.46 g, 9.72 mmol), and acetone (30 ml) was stirred at room temperature for 4 d. The reaction mixture was diluted with CH_2Cl_2, then washed with aqueous $Na_2S_2O_3$, and brine successively. The organic layer was dried an evaporated under reduced pressure. Purification of the residure by column chromatography on silica gel (hexane : AcOEt = 10 : 1) gave **10** (1.13 g, 82%) as a colorless oil: bp 95—105 °C (0.26 mmHg). IR ($CHCl_3$) *v*: 2970, 2910, 845 cm^{-1}. ^{1}H-NMR ($CDCl_3$) δ: 0.16 (s, 9H, $Si(CH_3)_3$), 1.94—2.10 (m, 4H, $CH_2 \times 2$), 3.25 (t, 2H, J = 7 Hz, ICH_2), 3.92—4.07 (m, 4H, OCH_2CH_2O). Exact MS Calcd for $C_{11}H_{19}O_2SiI$ (M^+): 338.0199. Found: 338.0204.

2-(2-Methoxyphenyl)-1,3-dithiane (9a) $BF_3 \cdot Et_2O$ (2.44 ml, 20.0 mmol) was added dropwise to a dry CH_2Cl_2 (20 ml) solution of *o*-anisaldehyde (**8a**, 2.41 ml, 20.0 mmol) and propanedithiol (2.00 ml, 19.9 mmol) at 0 °C under nitrogen. The reaction mixture was stirred at room temperature for 20 h, and then poured into aqueous KOH. The organic layer was separated, and the aqueous layer was extracted with CH_2Cl_2. The combined organic layer was washed with brine, dried, and evaporated under reduced pressure. Purification of the residure by column chromatography on silica gel (benzene) gave **9a** (4.28 g, 95%) as colorless crystals: mp 127—128.5 °C (benzene). IR ($CHCl_3$) *v*: 2910, 2840, 1590, 1490, 1250 cm^{-1}. ^{1}H-NMR ($CDCl_3$) δ: 1.79—2.26 (m, 2H, CH_2), 2.71—3.26 (m, 4H, $SCH_2 \times 2$), 3.83 (s, 3H, OCH_3), 5.65 (s, 1H, SCH), 6.75—7.59 (m, 4H, ArH × 4). MS *m/z*: 226 (M^+). *Anal.* Calcd for $C_{11}H_{14}OS_2$: C, 58.37; H, 6.23; S, 28.33. Found: C, 58.39; H, 6.30; S, 28.33.

3,3-Ethylenedioxy-7-(2-methoxyphenyl)-7,7-propylenedithio-1-trimethylsilyl-1-heptyne (12a) *n*-BuLi (1.6 N in hexane, 0.150 ml, 0.243 mmol) was added dropwise to an anhydrous THF (1 ml) solution of **9a** (50.0 mg, 0.221 mmol) at −78 °C under nitrogen, and the mixture was stirred under the same conditions for 30 min. An anhydrous THF (2 ml) solution of **10** (75.0 mg, 0.221 mmol) was added dropwise to the anion solution at the same temperature. The reaction mixture was stirred at −78 °C for 1 h, and then allowed to warm to room temperature for 1 h. Aqueous NH_4Cl was added to the solution, and the organic layer was separated. The aqueous layer was extracted with CH_2Cl_2. The combined organic layer was washed with brine, dried, and concentrated under reduced pressure. Purification of the residue by column chromatography on silica gel (hexane : AcOEt = 5 : 1) gave pure **12a** (93.7 mg, 97%) as a colorless oil: IR ($CHCl_3$) *v*: 2960, 2900, 2840, 1595 cm^{-1}. ^{1}H-NMR ($CDCl_3$) δ: 0.11 (s, 9H, $Si(CH_3)_3$), 1.39−1.41 (m, 2H, CH_2), 1.76—1.80 (m, 2H, CH_2), 1.95—1.97 (m, 2H, CH_2), 2.50—2.53 (m, 2H, SCH_2CH_2), 2.77—2.79 (m, 4H, $SCH_2 \times 2$), 3.85 (s, 3H, OCH_3), 3.87—4.01 (m, 4H, $OCH_2 \times 2$), 6.90—6.95 (m, 2H, ArH × 2), 7.23—7.24 (m, 1H, ArH), 7.87 (dd, 1H, J = 7.3, 1.2 Hz, ArH). Exact MS Calcd for $C_{22}H_{32}O_3S_2Si$ (M^+): 436.1559. Found: 436.1541.

1,5-Dioxo-1-(2-methoxyphenyl)-7-trimethylsilyl-6-heptyne (14a) Phenyliodosyl diacetate [PIDA, $PhI(OCOCH_3)_2$] (1.12 g, 3.47 mmol) was added to a MeOH (10 ml) solution of **12a** (1.01 g, 2.32 mmol), and the mixture was stirred at room temperature for 15 min, then the reaction was quenched with saturated aqueous $NaHCO_3$, and the whole was extracted with CH_2Cl_2. The extract was dried, and concentrated under reduced pressure. A catalytic amount of *p*-TsOH was added to an acetone (10 ml) solution of the residue, and the solution was stirred for 10 min at room temperature. The reaction was quenched with saturated aqueous NH_4Cl, and the mixture was extracted with CH_2Cl_2. The combined organic layer was washed with brine, dried, and evaporated under reduced pressure. The residue was purified by column chromatography on silica gel (hexane : AcOEt = 5 : 1) to give **14a** (320 mg, 46%) as a colorless oil: IR ($CHCl_3$) *v*: 3000, 2960, 2145, 1670, 1595 cm^{-1}. ^{1}H-NMR ($CDCl_3$) δ: 0.23 (s, 9H, $Si(CH_3)_3$), 2.05 (quint, 2H, J = 7.3 Hz, CH_2), 2.67 (t, 2H, J = 7.3 Hz, $COCH_2$), 3.03 (t, 2H, J = 7.1 Hz, $COCH_2$), 3.90 (s, 3H, OCH_3), 6.95 (d, 1H, J = 7.9 Hz, ArH), 7.00 (t, 1H, J = 7.9 Hz, ArH), 7.45 (td, 1H, J = 7.9, 1.8 Hz, ArH), 7.68 (dd, 1H, J = 7.9, 1.8 Hz, ArH). Exact MS Calcd for $C_{17}H_{22}O_3Si$ (M^+): 302.1336. Found: 302.1336.

1,5-Dioxo-1-(2-hydroxyphenyl)-7-trimethylsilyl-6-heptyne (16a) Powdered anhydrous $AlCl_3$ (155 mg, 1.16 mmol) was added to a dry CH_2Cl_2 (10 ml) solution of **14a** (87.8 mg, 0.291 mmol). The mixture was stirred at room temperature for 90 min. The reaction was quenched with aqueous $(CO_2H)_2$, and the whole was extracted with $CHCl_3$. The combined organic layer was washed with brine, dried, and concentrated under reduced pressure. Purification of the residue by preparative TLC (hexane : AcOEt = 5 : 1) gave **16a** (69.8 mg, 83%) as a pale yellow oil. IR ($CHCl_3$) *v*: 2960, 2150, 1670, 1635, 1610 cm^{-1}. ^{1}H-NMR ($CDCl_3$) δ: 0.24 (s, 9H, $Si(CH_3)_3$), 2.11 (quint, 2H, J = 7.3 Hz, CH_2), 2.73 (t, 2H, J = 7.3 Hz, $COCH_2$), 3.06 (t, 2H, J = 7.3 Hz, $COCH_2$), 6.90 (t, 1H, J = 8.0 Hz, ArH), 6.98 (d, 1H, J = 8.0 Hz, ArH), 7.47 (td, 1H, J = 8.0, 1.2 Hz, ArH), 7.75 (dd, 1H, J = 8.0, 1.2 Hz, ArH), 12.25 (s, 1H, OH). Exact MS Calcd for $C_{16}H_{20}O_3Si$ (M^+): 288.1181. Found: 288.1181.

1-*tert*-Butyldimethylsilyl-3,3-ethylenedioxy-7-(2-methoxyphenyl)-7,7-propylenedithio-1-heptyne (12b) A mixture of **12a** (707 mg, 1.62 mmol) and tetrabutylammonium fluoride (1 M in anhydrous THF, 4.86 ml, 4.86 mmol) was stirred at room temperature overnight. The mixture was diluted with CH_2Cl_2, washed with H_2O and brine, dried, and evaporated under reduced pressure. Purification of the residue by column chromatography on silica gel (hexane : AcOEt = 2 : 1) gave 3,3-ethylenedioxy-7-(2-methoxyphenyl)-7,7-propylenedithio-1-heptyne (500 mg, 85%). *n*-BuLi (1.6 N in hexane, 0.613 ml, 0.992 mmol) was added dropwise to an anhydrous THF (3 ml) solution of the desilylated compound (300 mg, 0.827 mmol) at −78 °C under nitrogen, and the mixture was stirred under the same conditions for 1 h. A THF (3 ml) solution of *tert*-butyldimethylchlorosilane (249 mg, 1.65 mmol) was added to the anion solution at −78 °C. The mixture was stirred under the same condition for 30 min, and then allowed to warm to room temperature for 3 h. The reaction was quenched with saturated aqueous NH_4Cl, and the mixture was extracted with CH_2Cl_2. The combined organic layer was washed with brine, dried, and concentrated under reduced pressure. Purification of the residue by column chromatography on silica gel (hexane : AcOEt = 10 : 1) gave **12b** (343 mg, 86%) as a colorless oil: IR ($CHCl_3$) *v*: 2960, 2860, 1590 cm^{-1}. ^{1}H-NMR ($CDCl_3$) δ: 0.05 (s, 6H, $Si(CH_3)_2$), 0.88 (s, 9H, $SiC(CH_3)_3$), 1.39—1.44 (m, 2H, CH_2), 1.77—1.80 (m, 2H, CH_2), 1.94—1.96 (m, 2H, CH_2), 2.50—2.53 (m, 2H, SCH_2CH_2), 2.76—2.79 (m, 4H, $SCH_2 \times 2$), 3.84 (s, 3H, OCH_3), 3.88—4.01 (m, 4H, $OCH_2 \times 2$), 6.91 (d, 1H, J = 8.0 Hz, ArH), 6.93 (t, 1H, J = 8.0 Hz, ArH), 7.24 (td, 1H, J = 8.0, 1.2 Hz, ArH), 7.86 (dd, 1H, J = 8.0, 1.2 Hz, ArH). Exact MS Calcd for $C_{25}H_{38}O_3S_2Si$ (M^+): 478.2031. Found: 478.2036.

7-*tert*-Butyldimethylsilyl-1,5-dioxo-1-(2-methoxyphenyl)-6-heptyne (14b) This was prepared from **12b** by the same procedure as described for the synthesis of **14a**. The reaction of **12b** (295 mg, 0.617 mmol) and PIDA (298 mg, 0.926 mmol) gave **14b** (68.3 mg, 32%) as a pale yellow oil: IR ($CHCl_3$) *v*: 2930, 2850, 2145, 1665, 1595 cm^{-1}. ^{1}H-NMR ($CDCl_3$) δ: 0.17 (s, 6H, $Si(CH_3)_2$), 0.96 (s, 9H, $SiC(CH_3)_3$), 2.06 (quint, 2H, J = 7.3 Hz, CH_2), 2.67 (t, 2H, J = 7.3 Hz, $COCH_2$), 3.03 (t, 2H, J = 7.3 Hz, $COCH_2$), 3.89 (s, 3H, OCH_3), 6.95 (d, 1H, J = 8.0 Hz, ArH), 6.99 (t, 1H, J = 8.0 Hz, ArH), 7.45 (td, 1H, J = 8.0, 1.8 Hz, ArH), 7.68 (dd, 1H, J = 8.0, 1.8 Hz, ArH). Exact MS Calcd for $C_{20}H_{28}O_3Si$ (M^+): 344.1805. Found: 344.1787.

7-*tert*-Butyldimethylsilyl-1,5-dioxo-1-(2-hydroxyphenyl)-6-heptyne (16b)

Reaction of **14b** (56.8 mg, 0.165 mmol) with anhydrous $AlCl_3$ (88.0 mg, 0.660 mmol) by the same procedure as described for the synthesis of **16a** gave **16b**. Purification by column chromatography on silica gel (hexane : AcOEt = 8 : 1) gave pure **16b** (46.2 mg, 85%) as a pale yellow oil: IR ($CHCl_3$) ν: 2950, 2930, 2850, 2150, 1670, 1640, 1610 cm^{-1}. ^{1}H-NMR ($CDCl_3$) δ: 0.18 (s, 6H, $Si(CH_3)_2$), 0.96 (s, 9H, $SiC(CH_3)_3$), 2.11 (quint, 2H, J=7.3 Hz, CH_2), 2.73 (t, 2H, J=7.3 Hz, $COCH_2$), 3.07 (t, 2H, J=7.3 Hz, $COCH_2$), 6.89 (td, 1H, J=8.5, 1.2 Hz, ArH), 6.99 (dd, 1H, J=8.5, 1.2 Hz, ArH), 7.47 (td, 1H, J=8.5, 1.2 Hz, ArH), 7.76 (dd, 1H, J=8.5, 1.2 Hz, ArH), 12.25 (s, 1H, OH). Exact MS Calcd for $C_{19}H_{26}O_3Si$ (M^+): 330.1649. Found: 330.1643.

2-(2,5-Dimethoxyphenyl)-1,3-dithiane (9b) This was prepared from 2,5-dimethoxybenzaldehyde (**8b**) by the same procedure as described for the synthesis of **9a**. Reaction of **8b** (0.913 g, 5.50 mmol) and propanedithiol (0.500 ml, 4.98 mmol) with $BF_3 \cdot Et_2O$ (0.46 ml, 5 mmol) gave **9b** (1.45 g, quant.) as colorless crystals: mp 126—129 °C (hexane–AcOEt). IR ($CHCl_3$) ν: 3010, 2950, 2910, 2850, 1500 cm^{-1}. ^{1}H-NMR ($CDCl_3$) δ: 1.84—2.37 (m, 2H, CH_2), 2.77—3.33 (m, 4H, $SCH_2 \times 2$), 3.79 (s, 3H, OCH_3), 3.84 (s, 3H, OCH_3), 5.66 (s, 1H, SCH), 6.76—7.25 (m, 3H, ArH × 3). MS m/z: 256 (M^+). *Anal.* Calcd for $C_{12}H_{16}O_2S_2$: C, 56.22; H, 6.29; S, 25.01. Found: C, 55.92; H, 6.32; S, 25.15.

7-(2,5-Dimethoxyphenyl)-3,3-ethylenedioxy-7,7-propylenedithio-1-trimethylsilyl-1-heptyne (12c) Reaction of **9b** (250 mg, 0.977 mmol) and **10** (330 mg, 0.977 mmol) by the same procedure as described for the synthesis of **12a** gave **12c**. Purification by column chromatography on silica gel (hexane : AcOEt = 10 : 1) gave pure **12c** (412 mg, 90%) as a colorless oil: IR ($CHCl_3$) ν: 2970, 2910, 2840, 1610, 1580 cm^{-1}. ^{1}H-NMR ($CDCl_3$) δ: 0.10 (s, 9H, $Si(CH_3)_3$), 1.29—2.89 (m, 12H, $CH_2 \times 3$ and $CH_2 \times 3$). 3.82 (s, 3H, OCH_3), 3.84 (s, 3H, OCH_3), 3.81—4.13 (m, 4H, OCH_2CH_2O), 6.68—6.93 (m, 2H, 3′ and 4′-CH), 7.53 (d, 1H, J=2 Hz, 6′-CH). Exact MS Calcd for $C_{23}H_{34}O_4S_2Si$ (M^+): 466.1665. Found: 466.1660.

1-(2,5-Dimethoxyphenyl)-1,5-dioxo-7-trimethylsilyl-6-heptyne (14c) Reaction of **12c** (2.20 g, 4.72 mmol) with PIDA (2.28 g, 7.09 mmol) by the same procedure as described for the synthesis of **14a** gave **14c**. Purification by column chromatography on silica gel (hexane : AcOEt = 5 : 1) gave pure **14c** (862 mg, 49%) as a colorless oil: IR ($CHCl_3$) ν: 3010, 2970, 2840, 2160, 1670 cm^{-1}. ^{1}H-NMR ($CDCl_3$) δ: 0.16 (s, 9H, $Si(CH_3)_3$), 1.98 (quint, 2H, J=7.1 Hz, CH_2), 2.61 (t, 2H, J=7.1 Hz, $COCH_2$), 2.97 (t, 2H, J=7.1 Hz, $COCH_2$), 3.72 (s, 3H, OCH_3), 3.79 (s, 3H, OCH_3), 6.76—7.19 (m, 3H, ArH × 3). Exact MS Calcd for $C_{18}H_{24}O_4Si$ (M^+): 332.1444. Found: 332.1445.

1,5-Dioxo-1-(2-hydroxy-5-methoxyphenyl)-7-trimethylsilyl-6-heptyne (16c) Reaction of **14c** (140 mg, 0.422 mmol) and anhydrous $AlCl_3$ (224 mg, 1.68 mmol), by the same proceudre as described for the synthesis of **16a**, gave **16c**. Purification by column chromatography on silica gel (hexane : AcOEt = 5 : 1) gave pure **16c** (66.0 mg, 49%) as pale yellow crystals: mp 50.5—52 °C (hexane–CH_2Cl_2). IR ($CHCl_3$) ν: 2960, 2150, 1670, 1645 cm^{-1}. ^{1}H-NMR ($CDCl_3$) δ: 0.25 (s, 9H, $Si(CH_3)_3$), 2.09 (quint, 2H, J=7.0 Hz, CH_2), 2.74 (t, 2H, J=7.0 Hz, $COCH_2$), 3.03 (t, 2H, J=7.0 Hz, $COCH_2$), 3.81 (s, 3H, OCH_3), 6.86—7.26 (m, 3H, ArH × 3), 11.90 (s, 1H, OH). Exact MS Calcd for $C_{17}H_{22}O_4Si$ (M^+): 318.1285. Found: 318.1268.

2-(2,5-Dimethoxyphenyl)-2-(6-trimethylsilyl-5-hexynyl)-1,3-dithiane (13a) This was prepared from **9b** (2.00 g, 7.81 mmol) and 6-iodo-1-trimethylsilyl-1-hexyne[24] (**11**, 2.54 g, 8.59 mmol) by the same procedure as described for the synthesis of **12a**. Purification by column chromatography on silica gel (hexane : AcOEt = 10 : 1) gave pure **13a** (2.87 g, 90%) as a pale yellow oil: IR ($CHCl_3$) ν: 3000, 2950, 2900, 2820, 2160 cm^{-1}. ^{1}H-NMR ($CDCl_3$) δ: 0.08 (s, 9H, $Si(CH_3)_3$), 1.19—2.83 (m, 14H, $CH_2 \times 3$ and $CH_2 \times 4$), 3.78 (s, 6H, $OCH_3 \times 2$), 6.72—7.45 (m, 3H, ArH × 3). Exact MS Calcd for $C_{21}H_{32}O_2S_2Si$ (M^+): 408.1613. Found: 408.1613.

Methyl 8-(2,5-Dimethoxyphenyl)-8,8-propylenedithio-2-octynoate (13b) A mixture of **13a** (1.18 g, 2.89 mmol) and tetrabutylammonium fluoride (1 M in anhydrous THF, 14.5 ml, 14.5 mmol) was stirred at room temperature for 3 d. The mixture was diluted with CH_2Cl_2, washed with H_2O and brine, dried, and evaporated under reduced pressure. Purification of the residue by column chromatography on silica gel (AcOEt) gave 2-(2,5-dimethoxyphenyl)-2-(5-hexynyl)-1,3-dithiane (950 mg, 98%) as a colorless oil. IR ($CHCl_3$) ν: 3310, 3000, 2950, 2830, 2120 cm^{-1}. ^{1}H-NMR ($CDCl_3$) δ: 1.73—2.84 (m, 15H, $CH_2 \times 3$, $CH_2 \times 4$, and C≡CH), 3.79 (s, 6H, $OCH_3 \times 2$), 6.76—7.51 (m, 3H, ArH × 3). MS m/z: 336 (M^+). *Anal.* Calcd for $C_{18}H_{24}O_2S_2$: C, 64.25; H, 7.19; S, 19.05. Found: C, 64.10; H, 7.35; S, 18.89. *n*-BuLi (1.6 N in hexane, 1.90 ml, 2.46 mmol) was added dropwise to a THF (10 ml) solution of 2-(2,5-dimethoxyphenyl)-2-(5-hexynyl)-1,3-dithiane (750 mg, 2.23 mmol) at −78 °C under nitrogen, and the mixture was stirred under the same conditions for 30 min. Methyl chloroformate (0.517 ml, 6.70 mmol) was added to the anion solution at −78 °C. The mixture was stirred under the same conditions for 10 min, and then allowed to warm to room temperature for 20 min. The reaction mixture was quenched with saturated aqueous NH_4Cl and the mixture was extracted with CH_2Cl_2. The combined organic layer was washed with brine, dried, and concentrated under reduced pressure. Purification by column chromatography on silica gel (hexane : AcOEt = 10 : 1) gave **13b** (790 mg, 90%) as a colorless oil. IR ($CHCl_3$) ν: 3000, 2950, 2830, 2230, 1710 cm^{-1}. ^{1}H-NMR ($CDCl_3$) δ: 1.79—2.83 (m, 14H, $CH_2 \times 3$ and $CH_2 \times 4$), 3.70 (s, 3H, OCH_3), 3.88 (s, 6H, $OCH_3 \times 2$), 6.74—7.45 (m, 3H, ArH × 3). MS m/z: 394 (M^+). *Anal.* Calcd for $C_{20}H_{26}O_4S_2$: C, 60.89; H, 6.64; S, 16.25. Found: C, 60.74; H, 6.71; S, 16.04.

Methyl 8-(2,5-Dimethoxyphenyl)-8-oxo-2-octynoate (15) This was prepared from **13b** (20.0 mg, 50.8 μmol) by the same procedure as described for the synthesis of **14a**. Purification of the residue by column chromatography on silica gel (hexane : AcOEt = 4 : 1) gave **15** (8.40 mg, 54%) as colorless crystals: mp 62—62.5 °C (hexane–CH_2Cl_2). IR ($CHCl_3$) ν: 3010, 2960, 2840, 2240, 1710, 1670 cm^{-1}. ^{1}H-NMR ($CDCl_3$) δ: 1.62—1.85 (m, 4H, $CH_2 \times 2$), 2.36 (t, 2H, J=7 Hz, C≡CCH_2), 2.98 (t, 2H, J=7 Hz, $COCH_2$), 3.73 (s, 3H, OCH_3), 3.78 (s, 3H, OCH_3), 3.86 (s, 3H, OCH_3), 6.81—7.25 (m, 3H, ArH × 3). MS m/z: 304 (M^+). *Anal.* Calcd for $C_{17}H_{20}O_5$: C, 67.09; H, 6.62. Found: C, 66.95; H, 6.63.

Methyl 8-(2-Hydroxy-5-methoxyphenyl)-8-oxo-2-octynoate (17) This was prepared from **15** (235 mg, 0.774 mmol) by the same procedure as described for the synthesis of **16a**. Purification of the residue by preparative TLC (hexane : AcOEt = 10 : 1) gave **17** (203 mg, 91%) as pale yellow crystals: mp 47.5—48 °C (hexane). IR ($CHCl_3$) ν: 3020, 2960, 2240, 1705, 1645, 1620 cm^{-1}. ^{1}H-NMR ($CDCl_3$) δ: 1.70 (quint, 2H, J=7.3 Hz, CH_2), 1.89 (quint, 2H, J=7.3 Hz, CH_2), 2.42 (t, 2H, J=7.3 Hz, C≡CCH_2), 3.02 (t, 2H, J=7.3 Hz, $COCH_2$), 3.75 (s, 3H, OCH_3), 3.81 (s, 3H, OCH_3), 6.93 (d, 1H, J=9 Hz, 3-CH), 7.11 (dd, 1H, J=9, 3 Hz, 4-CH), 7.18 (d, 1H, J=3 Hz, 6-CH), 11.9 (s, 1H, OH). MS m/z: 290 (M^+). *Anal.* Calcd for $C_{16}H_{18}O_5$: C, 66.20; H, 6.25. Found: C, 66.21; H, 6.29.

4,5-Diacetoxy-2,3-dihydro-1*H*-benz[*f*]indene-1-one (21a) This was prepared from **16a** (26.2 mg, 91.0 μmol) by method C. Purification by preparative TLC (hexane : AcOEt = 1 : 1) gave **21a** (17.9 mg, 66%) as colorless crystals: mp 177.5—179.5 °C (hexane–benzene). IR ($CHCl_3$) ν: 3020, 1760, 1715 cm^{-1}. ^{1}H-NMR ($CDCl_3$) δ: 2.43 (s, 3H, $COCH_3$), 2.46 (s, 3H, $COCH_3$), 2.79 (t, 2H, J=6.4 Hz, 2-CH_2 or 3-CH_2), 3.11 (t, 2H, J=6.4 Hz, 2-CH_2 or 3-CH_2), 7.25—7.28 (m, 1H, 6-CH or 8-CH), 7.51 (t, 1H, J=8.5 Hz, 7-CH), 7.95 (d, 1H, J=8.5 Hz, 6-CH or 8-CH), 8.27 (s, 1H, 9-CH). Exact MS Calcd for $C_{17}H_{14}O_5$ (M^+): 298.0842. Found: 298.0844.

4,5-Diacetoxy-7-methoxy-2,3-dihydro-1*H*-benz[*f*]indene-1-one (21b) This was prepared from **16c** (20.3 mg, 63.0 μmol) by method C. Purification by preparative TLC (hexane : AcOEt = 1 : 1) gave **21b** (12.8 mg, 61%) as colorless crystals: mp 158—160.5 °C (hexane–CH_2Cl_2). IR ($CHCl_3$) ν: 3030, 1770, 1760, 1715 cm^{-1}. ^{1}H-NMR ($CDCl_3$) δ: 2.40 (s, 3H, $COCH_3$), 2.45 (s, 3H, $COCH_3$), 2.78 (t, 2H, J=6.8 Hz, 2-CH_2 or 3-CH_2), 3.09 (t, 2H, J=6.8 Hz, 2-CH_2 or 3-CH_2), 4.01 (s, 3H, OCH_3), 6.78 (d, 1H, J=8.5 Hz, 6-CH or 7-CH), 7.15 (d, 1H, J=8.5 Hz, 6-CH or 7-CH), 8.75 (s, 1H, 9-CH). Exact MS Calcd for $C_{18}H_{16}O_6$ (M^+): 328.0944. Found: 328.0929.

8,9-Diacetoxy-5-methoxy-4-methoxycarbonyl-2,3-dihydro-1*H*-benz[*f*]-indene (22) This was prepared from **17** (25.4 mg, 87.6 μmol) by method C. Purification by preparative TLC (hexane : AcOEt = 3 : 1) gave **22** (20.2 mg, 62%) as colorless crystals: mp 167—169 °C (hexane–benzene). IR ($CHCl_3$) ν: 3010, 2840, 1775, 1765, 1730 cm^{-1}. ^{1}H-NMR ($CDCl_3$) δ: 2.14 (quint, 2H, J=7.3 Hz, 2-CH_2), 2.36 (s, 3H, $COCH_3$), 2.37 (s, 3H, $COCH_3$), 2.88 (t, 2H, J=7.3 Hz, 1-CH_2 or 3-CH_2), 2.99—3.08 (m, 2H, 1-CH_2 or 3-CH_2), 3.92 (s, 3H, OCH_3), 3.94 (s, 3H, OCH_3), 6.78 (d, 1H, J=8.2 Hz, 6-CH or 7-CH), 6.99 (d, 1H, J=8.2 Hz, 6-CH or 7-CH). Exact MS Calcd for $C_{20}H_{20}O_7$ (M^+): 372.1209. Found: 372.1215.

Ethyl 1-Acetylcyclopentane-1-carboxylate (25) A mixture of ethyl acetoacetate (21.3 g, 0.164 mol), 1,4-dibromobutane (29.5 g, 0.137 mol), K_2CO_3 (113 g, 0.819 mol), and acetone (530 ml) was stirred at room temperature for 24 h. After removal of the solvent, the reaction mixture was diluted with AcOEt, washed with H_2O, dried, and concentrated under reduced pressure. The residue was purified by distillation under reduced pressure to give **25** (9.25 g, 37%) as a colorless oil: bp 116—120 °C (30 mmHg) (lit.[22] 120—128 °C (30 mmHg)). IR ($CHCl_3$) ν: 2970, 1710 cm^{-1}. ^{1}H-NMR ($CDCl_3$) δ: 1.26 (t, 3H, J=7 Hz, CH_2CH_3), 1.53—1.76 (m, 4H, $CH_2 \times 2$), 1.99—2.22 (m, 4H, $CH_2 \times 2$), 2.13 (s, 3H, $COCH_3$), 4.20 (q, 2H, J=7 Hz, CH_2CH_3).

Ethyl 1-(1,1-Ethylenedioxyethyl)cyclopentane-1-carboxylate (26) Compound **25** (6.20 g, 33.7 mmol) was reacted with ethylene glycol (18.8 ml, 0.337 mol) under the same conditions as described for the synthesis of **20** to give **26** (7.00 g, 91%) as a colorless oil: bp 101 °C (0.31 mmHg). IR ($CHCl_3$) *v*: 3000, 2970, 2890, 1710 cm^{-1}. ^{1}H-NMR ($CDCl_3$) δ: 1.24 (t, 3H, J=7 Hz, $CH_2\underline{CH_3}$), 1.33 (s, 3H, CH_3), 1.45—2.29 (m, 8H, $CH_2 \times 4$), 3.94 (s, 4H, $OCH_2 \times 2$), 4.15 (q, 2H, J=7 Hz, $\underline{CH_2}CH_3$). MS *m/z*: 213 ($M^+ - CH_3$). *Anal.* Calcd for $C_{12}H_{20}O_4$: C, 63.14; H, 8.83. Found: C, 62.95; H, 9.03.

3,3-Ethylenedioxy-2,2-tetramethylene-1-butanol (27) An ether (1 ml) solution of **26** (38.6 mg, 0.169 mmol) was added dropwise to a suspension of $LiAlH_4$ (14.1 mg, 0.372 mmol) in ether (2 ml) at 0 °C, and the mixture was stirred for 15 min at the same temperature. The reaction was quenched with 5% HCl at 0 °C and the mixture was washed with H_2O. The aqueous layer was extracted with ether. The combined organic layer was washed with brine, dried, and concentrated under reduced pressure. Purification of the residue by column chromatography on silica gel (hexane : AcOEt = 3 : 1) gave **27** (31.0 mg, 98%) as a colorless oil: bp 95 °C (0.25 mmHg). IR ($CHCl_3$) *v*: 3530, 2975, 2890 cm^{-1}. ^{1}H-NMR ($CDCl_3$) δ: 1.31 (s, 3H, CH_3), 1.44—2.04 (m, 8H, $CH_2 \times 4$), 2.87—3.11 (br s, 1H, OH), 3.49 (s, 2H, OCH_2), 3.98 (s, 4H, $OCH_2 \times 2$). MS *m/z*: 171 ($M^+ - CH_3$). *Anal.* Calcd for $C_{10}H_{18}O_3$: C, 64.49; H, 9.74. Found: C, 64.28; H, 9.93.

4-Hydroxy-3,3-tetramethylene-6-trimethylsilyl-5-hexyn-2-one (28) A dry CH_2Cl_2 (10 ml) solution of **27** (2.96 g, 15.9 mmol) was added dropwise to a mixture of $(COCl)_2$ (5.56 ml, 63.7 mmol), dimethyl sulfoxide (DMSO) (6.77 ml, 95.4 mmol), and dry CH_2Cl_2 (150 ml) at −78 °C, and the mixture was stirred at the same temperature for 30 min. Then Et_3N (15.5 ml, 0.111 mol) was added at −78 °C and the whole was stirred for 15 min. The reaction was quenched with H_2O, and the mixture was extracted with $CHCl_3$. The extract was washed with 3% HCl, saturated aqueous $NaHCO_3$, and brine, dried, and concentrated under reduced pressure to give the aldehyde (3.34 g). A THF (50 ml) solution of lithium trimethylsilylacetylide, which was prepared from trimethylsilyl acetylene (5.13 ml, 36.3 mmol) and *n*-BuLi (1.6 N in hexane, 22.4 ml, 36.3 mmol) was added dropwise to a THF (50 ml) solution of the above aldehyde at −45 °C and the mixture was stirred at the same temperature for 20 min and at room temperature for 20 min. The reaction was quenched with saturated aqueous NH_4Cl, and the mixture was extracted with CH_2Cl_2. The organic layer was washed with brine, dried, and concentrated under reduced pressure. A mixture of the residue, *p*-TsOH (200 mg, 1.16 mmol), and acetone (60 ml) was stirred at room temperature for 17 h. The reaction was quenched with saturated aqueous NH_4Cl, and the mixure was extracted with CH_2Cl_2. The extract was washed with brine, dried, and concentrated under reduced pressure. Purification of the residue by column chromatography on silica gel (hexane : AcOEt = 4 : 1) gave **28** (3.21 g, 85% from **27**) as colorless crystals. mp 49—50 °C (hexane). IR ($CHCl_3$) *v*: 2960, 2175, 1685 cm^{-1}. ^{1}H-NMR ($CDCl_3$) δ: 0.15 (s, 9H, $Si(CH_3)_3$), 1.56—2.11 (m, 8H, $CH_2 \times 4$), 2.21 (s, 3H, $COCH_3$), 3.03 (d, 1H, J=7 Hz, OH), 4.54 (d, 1H, J=7 Hz, OCH). MS *m/z*: 238 (M^+). *Anal.* Calcd for $C_{13}H_{22}O_2Si$: C, 65.50; H, 9.30. Found: C, 65.44; H, 9.46.

4,4-Tetramethylene-1-(2,4,5-trimethoxyphenyl)-7-trimethylsilyl-6-heptyn-1,3,5-trione (29) A solution of **28** (1.01 g, 4.24 mmol) in anhydrous THF (8 ml) and hexamethylphosphoric triamide (HMPA, 1.61 ml, 9.24 mmol) were added dropwise at −78 °C to a solution of LDA in anhydrous THF (9 ml), obtained from dry diisopropylamine (1.29 ml, 9.24 mmol) and *n*-BuLi (1.6 N in hexane, 5.72 ml, 9.24 mmol). The mixture was stirred at the same temperature for 45 min. Then a solution of 2,4,5-trimethoxybenzoyl chloride (1.16 g, 5.04 mmol) in anhydrous THF (16 ml) was added dropwise at −78 °C and the whole was stirred at the same temperature for 35 min and at room temperature for 35 min. The reaction was quenched with saturated aqueous NH_4Cl, and the mixture was extracted with CH_2Cl_2. The organic layer was washed with brine, dried, and concentrated under reduced pressure to give a mixture of the *C*-acylated and the *O*-acylated products. A mixture of the crude acylated product (398 mg), DMSO (0.261 ml, 3.68 mmol), DCC (380 mg, 1.84 mmol), pyridinium trifluoroacetate (88.8 mg, 0.460 mmol), and dry benzene (7 ml) was stirred at room temperature for 5 h. The reaction was quenched with water, and the mixture was extracted with ether. The extract was washed with saturated aqueous $NaHCO_3$ and brine, dried, and concentrated under reduced pressure. Purification of the residue by column chromatography on silica gel (hexane : AcOEt = 2 : 1) gave **29** (227 mg, 31% from **28**) as yellow crystals: mp 93—95 °C (hexane–CH_2Cl_2). IR ($CHCl_3$) *v*: 2970, 2150, 1665, 1605, 1570 cm^{-1}. ^{1}H-NMR ($CDCl_3$) δ: 0.19 (s, 9H, $Si(CH_3)_3$), 1.64—1.71 (m, 4H, $CH_2 \times 2$), 2.18—2.22 (m, 2H, CH_2), 2.33—2.38 (m, 2H, CH_2), 3.888 (s, 3H, OCH_3), 3.893 (s, 3H, OCH_3), 3.95 (s, 3H, OCH_3), 6.50 (s, 1H, vinyl-H), 6.58 (s, 1H, ArH), 7.50 (s, 1H, ArH). MS *m/z*: 430 (M^+). *Anal.* Calcd for $C_{23}H_{30}O_6Si$: C, 64.16; H, 7.02. Found: C, 64.14; H, 7.06.

4,4-Tetramethylene-1-(4,5-dimethoxy-2-hydroxyphenyl)-7-trimethylsilyl-6-heptyn-1,3,5-trione (30) This was prepared from **29** (48.3 mg, 0.112 mmol) by the same procedure as described for the synthesis of **16a**. Purification by preparative TLC (hexane : AcOEt = 2 : 1) gave **30** (19.1 mg, 41%) as a yellow oil. IR ($CHCl_3$) *v*: 2950, 2150, 1660, 1610 cm^{-1}. ^{1}H-NMR (C_6D_6) δ: 0.03 (s, 2/3 × 9H, $Si(CH_3)_3 \times 2/3$), 0.05 (s, 1/3 × 9H, $Si(CH_3)_3 \times 1/3$), 2.08—2.57 (m, 8H, $CH_2 \times 4$), 3.13 (s, 3H, OCH_3), 3.36 (s, 2/3 × 3H, $OCH_3 \times 2/3$), 3.59 (s, 1/3 × 3H, $OCH_3 \times 1/3$), 3.84 (s, 1/3 × 2H, $COCH_2CO \times 1/3$), 6.24 (s, 2/3 × 1H, vinyl-H × 2/3), 6.32 (s, 1/3 × 1H, ArH × 1/3), 6.37 (s, 2/3 × 1H, ArH × 2/3), 6.99 (s, 2/3 × 1H, ArH × 2/3), 7.09 (s, 1/3 × 1H, ArH × 1/3), 12.6 (s, 2/3 × 1H, OH × 2/3), 13.1 (s, 1/3 × 1H, OH × 1/3). Exact MS Calcd for $C_{22}H_{28}O_6Si$ (M^+): 416.1652. Found: 416.1652.

4,5-Diacetoxy-7,8-dimethoxy-2,2-tetramethylene-benz[*f*]indane-1,3-dione (31) This was prepared from **30** (19.1 mg, 45.9 μmol) by method C. Purification by preparative TLC (hexane : AcOEt = 2 : 1) gave **31** (15.1 mg, 77%) as pale yellow crystals: mp 144—146 °C (hexane–CH_2Cl_2). IR ($CHCl_3$) *v*: 3020, 2980, 1770, 1735, 1710 cm^{-1}. ^{1}H-NMR ($CDCl_3$) δ: 1.96—1.97 (m, 8H, $CH_2 \times 4$), 2.44 (s, 3H, $COCH_3$), 2.54 (s, 3H, $COCH_3$), 4.02 (s, 3H, OCH_3), 4.03 (s, 3H, OCH_3), 7.15 (s, 1H, ArH), 8.68 (s, 1H, ArH). MS *m/z*: 426 (M^+). *Anal.* Calcd for $C_{23}H_{22}O_8$: C, 64.78; H, 5.20. Found: C, 64.77; H, 5.05.

4-Hydroxy-7-methoxy-2,2-tetramethylene-benz[*f*]indane-1,3,5,8-tetrone (32) A mixture of **31** (24.6 mg, 57.7 μmol) and 80% aqueous trifluoroacetic acid (10 ml) was refluxed for 3 h. The reaction mixture was concentrated under reduced pressure. The residue was dissolved in 33% aqueous CH_3CN. To this solution, phenyliodosyl bistrifluoroacetate (PIFA) (245 mg, 0.570 mmol) was added at room temperature and the mixture was stirred at the same temperature overnight, then concentrated under reduced pressure. Purification by preparative TLC (CH_2Cl_2 : MeOH = 30 : 1) gave **32** (18.4 mg, 98%) as pale yellow crystals: mp 220—230 °C (dec.) (hexane–CH_2Cl_2). IR ($CHCl_3$) *v*: 2940, 1710, 1690, 1630, 1605 cm^{-1}. ^{1}H-NMR ($CDCl_3$) δ: 1.97 (m, 8H, $CH_2 \times 4$), 3.99 (s, 3H, OCH_3), 6.25 (s, 1H, vinyl-H), 8.17 (s, 1H, ArH), 13.28 (s, 1H, OH). Exact MS Calcd for $C_{18}H_{14}O_6$ (M^+): 326.0791. Found: 326.0801.

References and Notes

1) *a*) R. H. Thompson, "Naturally Occuring Quinones," Academic Press, New York, 1971; *b*) S. Neidle, "Topics in Antibiotic Chemistry," ed. by P. G. Sammes, Halstead Press, New York, 1978; Vol. 2, p. 242; *c*) T. Oki and T. Takeuchi, *Yuki Gousei Kagaku Kyokaishi*, **40**, 2 (1982).

2) For reviews on synthetic studies, see: *a*) S. Terashima, *Yuki Gousei Kagaku Kyokaishi*, **40**, 20 (1982); *b*) Tetrahedron Symposia-in-Print Number 17, T. R. Kelly (ed.), *Tetrahedron*, **40**, 4537 (1984); *c*) M. J. Broadhurst, C. H. Hassall, and G. Thomas, *J. Chem. Ind.* (London), **1985**, 106; *d*) K. Krohn, *Angew. Chem., Int. Ed. Engl.*, **25**, 790 (1986); *e*) Y. Tamura and Y. Kita, *Yuki Gosei Kagaku Kyokaishi*, **46**, 205 (1988); *f*) K. Krohn, "Progress in the Chemistry of Organic Natural Products," W. Herz, H. Griselbach, G. W. Kirby, and Ch. Tamm (eds.), Springer-Verlag, New York, 1989, p. 37; *g*) K. Krohn and V. S. Ekkundi, "Studies in Natural Product Chemistry," Vol. 4, ed. by Atta-ur-Rahman, Elsevier, Amsterdam, 1989, p. 317.

3) *a*) M. A. Bates and P. G. Sammes, *J. Chem. Soc., Chem. Commun.*, **1983**, 896; *b*) F. M. Hauser and T. C. Adams Jr., *J. Org. Chem.*, **49**, 2296 (1984); *c*) P. DeShong and J. M. Leginus, *Tetrahedron Lett.*, **25**, 5355 (1984); *d*) R. P. Joyce, M. Parvez, and S. M. Weinreb. *ibid.*, **27**, 4885 (1986); *e*) K. Krohn and H.-J. Kohle, *Liebig Ann.* Chem., **1987**, 1037; *f*) M. Kawasaki, F. Matsuda, and S. Terashima, *Tetrahedron*, **44**, 5695, 5713, 5727 (1988); *g*) R. Kind, K. Hutter, A. Zeeck, K. S-Base, and E. Ergert, *J. Antibiot.*, **42**, 7 (1989).

4) *a*) J. H. Dodd, R. S. Garigipati, and S. M. Weinreb, *J. Org. Chem.*, **47**, 4045 (1982); *b*) R. W. Franck, V. Bhat, and C. S. Subramaniam, *J. Am. Chem. Soc.*, **108**, 2455 (1986); *c*) W. R. Roush, M. R. Michaelides, D. F. Tai, B. M. Lesur, W. K. M. Chong, and D. J. Harris, *ibid.*, **111**, 2984 (1989).

5) *a*) K. Krohn, K. Tolkiehn, V. Lehne, H. W. Schmalle, H.-F. Grutzmacher, *Liebig Ann. Chem.*, **1985**, 1311; *b*) T. R. Kelly and J. K. Saha, *J. Org. Chem.*, **50**, 3679 (1985); *c*) T. R. Kelly, A. Whiting, and N. S. Chandrakumar, *J. Am. Chem. Soc.*, **108**, 3510 (1986); *d*) B. Beagley, D. S. Larsen, R. G. Pritchard, and R. J. Stoodley, *J. Chem.*

Soc., Chem. Commun., **1989**, 17.
6) K. Nomura, K. Okazaki, K. Hori, and E. Yoshii, *J. Am. Chem. Soc.*, **109**, 3402 (1987).
7) *a*) R. C. Dandey, M. W. Toussaint, R. M. Stroshane, C. C. Kalita, A. A. Aszalos, A. L. Garretson, T. T. Wei, K. M. Byrne, R. F. Geoghegan Jr., and R. J. White, *J. Antibiot.*, **34**, 1389 (1981); *b*) R. Misra, R. C. Pandey, J. V. Silverton, *J. Am. Chem. Soc.*, **104**, 4478 (1982).
8) W. B. Manning and D. J. Wilbur, *J. Org. Chem.*, **45**, 733 (1980).
9) Y. Kita, H. Yasuda, O. Tamura, and Y. Tamura, *Tetrahedron Lett.*, **25**, 1813 (1984).
10) Y. Kita, R. Okunaka, T. Honda, M. Shindo, and O. Tamura, *Tetrahedron Lett.*, **30**, 3995 (1989).
11) A. I. Turbina, V. G. Sinyavskii, and M. Ya. Romankevich, *Ukr. Khim. Zh.* (*Russ. Ed.*), **31**, 85 (1965) [*Chem. Abstr.*, **62**, 14555*f* (1965)].
12) Y. Kita, S. Akai, N. Ajimura, M. Yoshigi, T. Tsugoshi, H. Yasuda, and Y. Tamura, *J. Org. Chem.*, **51**, 4150 (1986).
13) Efforts to obtain **7a** from **5** under dehydrogenation conditions failed.
14) Heating of the boronate or stannylene derivative, obtained by the reaction of **3a** with $PhB(OH)_2$ in benzene[15] or $(n\text{-}Bu)_2SnO$ in benzene,[16] caused intramolecular cycloaddition and subsequent oxidative deprotection gave **7a**, but the yield never exceeded 44%.
15) *a*) M. J. Broadhurst, C. H. Hassall, and G. J. Thomas, *J. Chem. Soc., Perkin Trans. 1*, **1982**, 2239; *b*) Y. Tamura, S. Akai, H. Kishimoto, M. Sasho, M. Kirihara, and Y. Kita, *Chem. Pharm. Bull.*, **36**, 3897 (1988).
16) *a*) W. J. Considine, *J. Organometallic Chem.*, **5**, 263 (1966); *b*) J. C. Pommier and M. Pereyre, *Adv. Chem. Ser.*, **157**, 82 (1976); *c*) S. David and A. Thieffry, *J. Chem. Soc., Perkin Trans. 1*, **1979**, 1568.
17) Spectrospecific generation of the *Z*-olefin was ascertained in the reaction of *o*-hydroxypropiophenone with Me_2SiCl_2/Et_3N.
18) *a*) D. J. W.-Pickle, K. M. Byrne, R. C. Pandey, and R. J. White, *J. Antibiot.*, **34**, 1402 (1981); *b*) D. D. von Hoff, J. C. Cooper, E. Bradley, J. Sandbach, J. Jones, and R. Makuch, *Am. J. Med.*, **70**, 1027 (1981); *c*) K. M. Byrne, B. D. Hilton, R. J. White, R. Misra, and R. C. Pandey, *Biochemistry*, **24**, 478 (1985).
19) *a*) A. V. R. Rao, D. R. Reddy, and V. H. Deshpande, *J. Chem. Soc., Chem. Commun.*, **1984**, 1119; *b*) K. A. Parker, K. A. Koziski, and G. Breault, *Tetrahedron Lett.*, **26**, 2181 (1985); *c*) A. S. Kende, F. H. Ebetino, and T. Ohta, *ibid.*, **26**, 3063 (1985); *d*) D. L. Boger and I. C. Jacobson, *J. Org. Chem.*, **55**, 1919 (1990).
20) T. R. Kelly, N. Ohashi, R. J. Armstrong-Chong, S. H. Bell, *J. Am. Chem. Soc.*, **108**, 7100 (1986).
21) M. Toyota and S. Terashima, *Tetrahedron Lett.*, **30**, 829 (1989).
22) L. J. Goldworthy, *J. Chem. Soc.*, **1934**, 377.
23) *a*) Y. Tamura, T. Yakura, J. Haruta, and Y. Kita, *J. Org. Chem.*, **52**, 3927 (1987); *b*) Y. Tamura, T. Yakura, H. Tohma, K. Kikuchi, and Y. Kita, *Synthesis*, **1989**, 126.
24) Y. Kita, R. Okunaka, T. Honda, M. Shindo, M. Taniguchi, M. Kondo, and M. Sasho, *J. Org. Chem.*, **56**, 119 (1991).

Binding Characteristics of DOPA (3,4-Dihydroxyphenylalanine) and Its Metabolites to Bovine Serum Albumin as Measured by Ultrafiltration Technique

Nobuo OKABE,* Yukiko SAGIMORI and Misa HOKAZE

Faculty of Pharmaceutical Sciences, Kinki University, Kowakae 3-4-1, Osaka 577, Japan. *Received March 11, 1991*

The interaction between 3,4-dihydroxyphenylalanine (DOPA), dopamine, 3-methoxytyramine and homovanillic acid and bovine serum albumin (BSA) was investigated by the ultrafiltration technique. The apparent binding constants were determined assuming the equivalence and independence of the binding sites on the BSA molecule. The binding constants were in the range of log $K = 2.85$ to 3.77 with 1 to 2 binding sites. The affinity of ligands to BSA strengthened with progression of the metabolism in the order of DOPA < dopamine < 3-methoxytyramine < homovanillic acid.

Keywords DOPA metabolite; dopamine; 3-methoxytyramine; homovanillic acid; bovine serum albumin; binding constant; ultrafiltration; serum albumin binding

Introduction

Many studies have revealed that the plasma levels of catecholamines and their metabolites are related to many neuropathic diseases.[1-4] Therefore, it is important to clarify the binding characteristics of catecholamines and/or their metabolites to serum albumin, which is well known to bind many drugs and hormones.[5] To date, however, very few investigations have been reported on the interaction between catecholamines and/or their metabolites and serum albumin. This paper describes studies made on this interaction using the ultrafiltration technique,[6,7] and presents some fundamental information concerning the binding characteristics of 3,4-dihydroxyphenylalanine (DOPA), dopamine, 3-methoxytyramine and homovanillic acid to bovine serum albumin (BSA).

Materials and Methods

BSA (lot. No. 86) was obtained from Seikagaku Kogyo Co., Ltd., Tokyo. L-DOPA (lot. No. MOA 9542), dopamine (lot. No. KPG 7332), 3-methoxytyramine (lot. No. 89F-3680), homovanillic acid (lot. No. SAN 0962) and other reagents of the highest quality were from Wako Pure Chemical Ind., Ltd., Osaka. The ultrafiltration device, Ultrafree C3 (Catalogue No. UFC3LGCOO) was obtained from Nihon Millipore Ltd., Tokyo. The binding reaction was performed as follows: 500 μl of the reaction mixture in 0.1 M sdoium phosphate buffer, pH 5.6, 0.3 mM ethylenediaminetetraacetic acid (EDTA) containing BSA (10^{-4} M) and appropriate concentrations of ligands (0.5—2.5 $\times 10^{-4}$ M) were shaken for 1 h at room temperature (25 $\pm$ 1 °C) in the dark. Then, 400 μl of the sample was ultrafiltrated using a Taitec micro clever CR-12 ultrafiltration device (Taiyo Kogyo Ltd., Tokyo) at 2000 $\times g$ (6000 rpm) for 5 min at room temperature. DOPA and its metabolites have similar fluorescence characteristics at around 310—320 nm (excitation wavelength: 280 nm). The concentrations of free ligands could therefore be determined fluorometrically using a Hitachi 850 spectrofluorometer from the calibration curves of the known concentrations. Protein leakage through the membrane and adsorption of the ligands to the ultrafiltration device were also determined and corrected. The concentration of BSA was determined spectrophotometrically using $E^{1\%}_{1cm} = 6.54$ at 280 nm and the molecular weight of 66300.[8,9] The binding constants and the number of binding sites were determined by the double-reciprocal method described by Hughes and Klotz[10] using the following expression:

$$\frac{1}{r} = \frac{1}{nK}\left(\frac{1}{C}\right) + \frac{1}{n}$$

where r is the number of moles of ligands bound per mole of BSA, n is the number of binding sites, K is the binding constant and c is the concentration of free ligands. The solvent and the sample solutions were degassed carefully under vacuum before preparing the reaction mixtures.

Results and Discussion

DOPA and dopamine are oxidized and easily discolored, especially in an alkaline solution. This discoloration could be prevented for a few hours by lowering pH and degassing the sample. Because of this, however, it is difficult to determine the binding parameters by a general equilibrium dialysis method which usually requires a long period of over 15 h for equilibrium. In this study, therefore, we used the ultrafiltration technique which has the advantage that it takes only 0.5—2 h for equilibrium.[6,7] The binding reaction was performed under somewhat acidic conditions at pH 5.6, because BSA is stable between pH 5—7.[5] Figure 1 shows the typical double-reciprocal plot of the binding data of dopamine to BSA and DOPA, 3-methoxy tyramine and homovanillic acid showed similar results (data are not shown here). The binding parameters determined from the double-reciprocal plots are summarized in Table I. The binding constants for all ligands are in the range of

TABLE I. Parameters of Binding of DOPA and Its Metabolites to BSA at pH 5.6 at 25 °C

	Binding constant K (S.D.) $\times 10^{-3}$ (M^{-1})	Number of binding sites n (S.D.)
DOPA	0.70 (0.08)	1.97 (0.36)
Dopamine	2.95 (0.25)	0.83 (0.22)
3-Methoxytyramine	4.33 (0.26)	0.89 (0.18)
Homovanillic acid	5.92 (0.72)	0.88 (0.17)

Standard deviations (S.D.) were obtained from seven measurements.

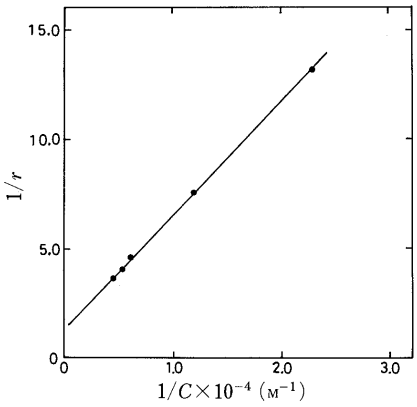

Fig. 1. Double-Reciprocal Plot of Dopamine Binding to BSA

BSA concentration was 10^{-4} M and dopamine concentrations were in the range of 0.5—2.5 $\times 10^{-4}$ M. The fluorescence was measured at 315 nm (excitation: 280 nm). Temperature was 25 $\pm$ 1 °C. The results were calculated as described in the text.

log $K=2.85$ to 3.77. These values seems to be somewhat lower than the values for binding of many organic anions to BSA with the range of log $K=4$ to 6, although metal ions such as calcium or zinc ions bind in a similar range with log $K=3$.[5] The affinity of DOPA (log $K=2.85$) is the weakest and that of homovanillic acid (log $K=3.77$) is strongest. The small number of 1 to 2 binding sites indicates the specific binding. It is to be noted that the affinity is strengthened with the progress of metabolism in the order of DOPA < dopamine < 3-methoxytyramine < homovanillic acid. This may indicate some physiological impact on the circulation of these metabolites in the serum. By comparing the substituent groups on the phenyl ring, it is clear that both the methoxy and carboxyl groups have an important role in the affinity of these metabolites to BSA. Nozaki *et al.*[11] reported that the association of an anionic surfactant on a serum albumin molecule would be more favourable than a cationic one, because the positively charged arginyl and lysyl side chains project more from the surface than the negatively charged glutamyl and aspartyl side chains. This explanation might be applicable to the results of this study, that homovanillic acid with a carboxyl group could bind more favourably on the negatively charged BSA molecule at pH 5.6 (pI = 4.8[5]) than other DOPA metabolites with an amino group. The arginyl and/or lysyl side chains might be located in the vicinity of the binding site of homovanillic acid.

References

1) K. H. DeTruck and W. H. Vogel, *Pharmac. Biochem. Behav.*, **13**, 129 (1980).
2) D. S. Goldstein, *Acta Physiol. Scand.*, **527**, 39 (1984).
3) T. Hata, E. Itoh, Y. Kamanaka, K. Kawabata and S. Honda, *J. Auton. Pharmacol.*, **11**, 15 (1991).
4) T. Ishimitsu and S. Hirose, *Chem. Pharm. Bull.*, **29**, 3403 (1981).
5) T. Peters, Jr., *Adv. Protein Chem.*, **37**, 161 (1985).
6) T. Oshima, I. Johno and S. Kitazawa, *Therapeutic Drug Monitoring*, **10**, 310 (1988).
7) R. Matsushita, Y. Deguchi, K. Yokogawa, E. Nakashima and F. Ichimura, *Yakugaku*, **49**, 221 (1989).
8) W. H. Pealman and I. F. F. Fong, *J. Biol. Chem.*, **247**, 8078 (1972).
9) R. G. Reed, F. W. Putnum and T. Peters, Jr., *Biochem. J.*, **191**, 867 (1980).
10) T. R. Hughes and I. M. Klotz, *Methods Biochem. Anal.*, **3**, 265 (1956).
11) Y. Nozaki, J. A. Reynolds and C. Tanford, *J. Biol. Chem.*, **249**, 2252 (1974).

Revised Structure of *N*-Oxidation Products of 4,5,6-Triaryltriazines: 1,2,3-Triazine 2-Oxides

Akio OHSAWA,* Takashi ITOH, Kentaro YAMAGUCHI, and Chikako KAWABATA

School of Pharmaceutical Sciences, Showa University, 1–5–8 Hatanodai, Shinagawa-ku, Tokyo 142, Japan. *Received January 21, 1991*

The *N*-oxidation products of 4,5,6-triaryl-1,2,3-triazines were decided to be the 2-oxides on the basis of spectral data and X-ray crystallography; the structures are different from those reported previously.

Keywords 1,2,3-triazine; oxidation; triaryl-1,2,3-triazine; triaryl-1,2,3-triazine *N*-oxide; *m*-chloroperbenzoic acid; peracetic acid; X-ray crystallography

In the field of heteroaromatic chemistry, there is considerable interest in the selectivity on *N*-oxidation of polyazaheteroaromatic compounds,[1] and several studies have appeared on the position of *N*-oxidation of 1,2,3-triazines **2**.[2-5] However, there have been conflicting results. The present authors have reported[2] that some phenyl-substituted triazines (**1a** and **1b**) underwent the oxidation with *m*-chloroperbenzoic acid (*m*CPBA) at N-2 exclusively, whereas there are reviews[4] and articles[5] in which predominant formation of the 1-oxides **3** upon oxidation of 4,5,6-triaryl-1,2,3-triazines with peracetic acid (PAA) is claimed. These reports prompted us to re-investigate the structure of 1,2,3-triazine *N*-oxide, and whether or not changes in the oxidation conditions would alter the reaction sites.

As model reactions, we employed the oxidation of 4,5,6-triphenyl-1,2,3-triazine **1b** with PAA and of 4,5,6-tris(*p*-tolyl)-1,2,3-triazine **1c** with *m*CPBA and PAA, and the structure of a major product (the sole *N*-oxide) from

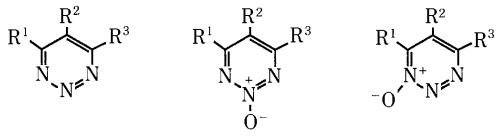

1 2 3

a : $R^1=R^3=Ph$, $R^2=H$
b : $R^1=R^2=R^3=Ph$
c : $R^1=R^2=R^3=p$-MeC_6H_4
d : $R^1=R^3=Ph$, $R^2=p$-MeC_6H_4
e : $R^1=R^2=Ph$, $R^3=p$-MeC_6H_4

Chart 1

1c was definitively determined by X-ray crystallography.

First, **1b** was oxidized with PAA according to Neunhoeffer's method (with 40% AcOOH–AcOH/$CHCl_3$, under reflux for 4 h).[5] The major product (77% from consumed **1b**) of the reaction was identical with the one that had been obtained as the major product of the reaction of **1b** with *m*CPBA, and whose structure had been determined as the 2-oxide **2b**.[2] Other compounds isolated were the starting material **1b** and 3,4,5-triphenylisoxazole (**4**, trace), and the 1-oxide was not found despite careful examination of the reaction mixture.

Secondly, the oxidation of **1c** with *m*CPBA in methylene chloride at room temperature gave a single product (95%). The proton and carbon-13 nuclear magnetic resonance (^{1}H- and ^{13}C-NMR) spectra revealed a highly symmetrical character, indicating it to be the 2-oxide **2c**. An X-ray crystallographic analysis was carried out to elucidate the structure unequivocally, and the result are shown in Fig. 1 and Table I.

The oxidation of **1c** with PAA under Neunhoeffer's

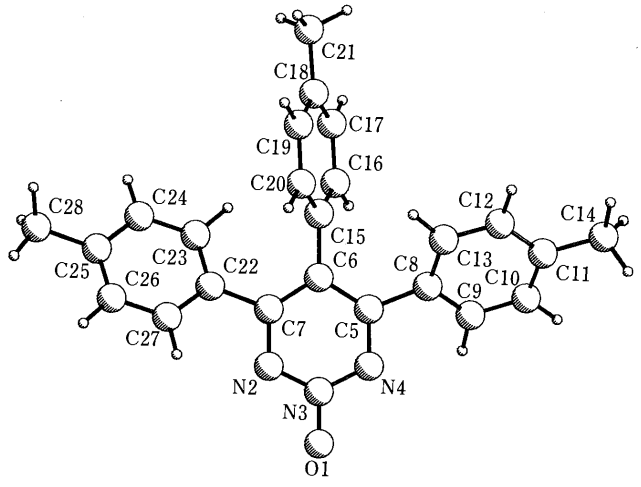

Fig. 1. Structure of 4,5,6-Tris(*p*-tolyl)-1,2,3-triazine *N*-Oxide (**2c**)

TABLE I. Fractional Atomic Coordinates and Isotropic Thermal Parameters of **2c**

	x	*y*	*z*	B_{eq} [a]
O(1)	0.0951 (0)	0.1084 (0)	0.7742 (0)	5.97 (10)
N(2)	0.2536 (5)	0.3151 (5)	0.9957 (8)	4.16 (9)
N(3)	0.2309 (4)	0.2077 (4)	0.8305 (8)	4.01 (9)
N(4)	0.3406 (5)	0.1968 (5)	0.7204 (8)	3.89 (9)
C(5)	0.4870 (5)	0.3041 (5)	0.7797 (8)	3.51 (10)
C(6)	0.5258 (5)	0.4232 (5)	0.9510 (8)	3.47 (10)
C(7)	0.4014 (5)	0.4226 (5)	1.0557 (8)	3.82 (11)
C(8)	0.5972 (5)	0.2766 (5)	0.6443 (8)	3.75 (10)
C(9)	0.5380 (5)	0.2070 (5)	0.4150 (9)	3.90 (11)
C(10)	0.6325 (6)	0.1687 (5)	0.2895 (9)	4.51 (12)
C(11)	0.7872 (6)	0.1936 (6)	0.3846 (9)	5.00 (13)
C(12)	0.8459 (6)	0.2646 (6)	0.6139 (10)	5.35 (14)
C(13)	0.7543 (5)	0.3055 (6)	0.7418 (9)	4.51 (12)
C(14)	0.8863 (8)	0.1446 (9)	0.2530 (12)	7.49 (22)
C(15)	0.6873 (5)	0.5430 (5)	1.0122 (8)	3.66 (10)
C(16)	0.7431 (5)	0.6406 (5)	0.8594 (9)	4.15 (11)
C(17)	0.8895 (5)	0.7579 (5)	0.9226 (9)	4.53 (12)
C(18)	0.9858 (5)	0.7785 (5)	1.1371 (9)	4.44 (12)
C(19)	0.9299 (6)	0.6787 (5)	1.2880 (9)	4.52 (12)
C(20)	0.7836 (6)	0.5627 (5)	1.2276 (9)	4.27 (11)
C(21)	1.1423 (6)	0.0060 (7)	1.2079 (11)	5.84 (16)
C(22)	0.4097 (5)	0.5358 (5)	1.2418 (9)	4.23 (12)
C(23)	0.5056 (7)	0.6830 (5)	1.2540 (10)	5.31 (15)
C(24)	0.5041 (8)	0.7848 (6)	1.4256 (10)	6.03 (16)
C(25)	0.4054 (7)	0.7438 (6)	1.5832 (10)	6.17 (17)
C(26)	0.3125 (7)	0.5977 (7)	1.5727 (10)	6.09 (16)
C(27)	0.3134 (6)	0.4949 (6)	1.4053 (10)	4.98 (13)
C(28)	0.4044 (13)	0.8574 (9)	1.7634 (12)	9.29 (32)

a) $B_{eq}=(1/3)\Sigma_i\Sigma_j B_{ij}a_i^*a_j^*\mathbf{a}_i\mathbf{a}_j$.

TABLE II. *N*-Oxidation of Aryl-1,2,3-triazines **1**

Triazine (**1**)	Reagent	Product(s)	Yield (%)	Recovery of **1** (%)	By-product
1a	*m*CPBA[a]	**2a**	81	Trace	—
1b	*m*CPBA[a]	**2b**	53 (72)[b]	26	—
1b	PAA[c]	**2b**	54[d] (77)[b]	30	Isoxazole (**4**) (Trace)[e]
1c	*m*CPBA	**2c**	95	Trace	—
1c	PAA[c]	**2c**	51[f]	Trace	mp 208 °C (16%)[g]
1c	PAA[h]	**2c**	55 (74)[b]	25	mp 208 °C (Trace)[g]
1d+**e**[i]	*m*CPBA	**2d**+**2e**	90	Trace	—
1d+**e**[i]	PAA[c]	**2d**+**2e**	34 (50)[h]	22	mp 209 °C (5%)[j]

a) See ref.[2]. *b*) Percent from consumed **1**. *c*) At 80 °C (bath temp.). *d*) Neunhoeffer *et al.* reported a yield of 65% for **3b**[5]; yield 35% by reaction with H_2O_2–AcOH, reflux.[2] *e*) Yield 4% by reaction with H_2O_2–AcOH, reflux.[2] *f*) Ref. 5 reports a yield of 70% for **3c**. *g*) See note.[6] *h*) At 65 °C (bath temp.). *i*) See note.[7] *j*) See note.[10]

conditions gave **2c** as a major product (51%), accompanied with a minor product(s) described in the experimental section.[6] Thorough inspection of the reaction mixture proved that the corresponding 1-oxide (**3c**) was not formed. The oxidation of **1c** under milder condition (heated at 65 °C) afforded a 74% yield (base on the consumed **1c**) of **2c**.

Finally, the oxidation of a mixture[7] of 4,6-diphenyl-5-tolyl **2d** and 4,5-diphenyl-6-tolyltriazines **2e** with *m*CPBA and with PAA also gave their 2-oxides (mixture) as major products (see Experimental and Notes). The data are summarized in Table II. In conclusion, we have proved that *N*-oxidation of the triaryltriazines gives exclusively the corresponding 2-oxides, irrespective of the reaction conditions.[8]

Experimental

All melting points were taken on a Yanaco micro melting point apparatus and are uncorrected. The mass spectra (MS) were measured with a JEOL JMS-D300 instrument. The NMR spectra were taken on a JEOL GX400 spectrometer using tetramethylsilane as an internal standard.

Oxidation of 1b with *m*CPBA The procedure and results are described in our previous paper,[2] yield of **2b** 53%, recovery of **1b** 26%, and no by-products were detected.

Oxidation of 1b with PAA A 1 ml aliquot of 90% H_2O_2 was added to 5 ml of Ac_2O under cooling on an ice bath, and the mixture was allowed to stand at room temperature for 24 h (aging), then used as the reagent; the calculated content of PAA is *ca.* 42%. PAA solution (PAA, 200 mg, *ca.* 1.11 mmol) was added to a solution of **1b** (100 mg, 0.32 mmol) in $CHCl_3$ (10 ml), and the mixture was refluxed for 4 h at 80 °C. The CH_2Cl_2 (90 ml) was added, and the solution was washed with 10% aqueous $KHCO_3$, dried over $MgSO_4$, and evaporated. Thin layer chromatography (TLC, Merck Aluminiumoxid 5713/Et_2O–hexane–trace acetone) of the reaction mixture showed two major (**1b** and **2b**) and one minor (**4**)[2] spots. Recrystallization of the mixture gave 22 mg of prisms (**2b**). The residual solvent was evaporated off and the residue was subjected to preparative TLC (Merck Aluminiumoxid 5726/Et_2O–hexane–trace acetone) to give a trace of **4**,[9] 30 mg (30%) of **1b**, and an additional 35 mg of **2b** (total 54%).[5] No other products were obtained.

Oxidation of 1c with *m*CPBA A solution of **1c** (110 mg, 0.31 mmol) and *m*CPBA (100 mg, 0.58 mmol) in CH_2Cl_2 (25 ml) was allowed to stand at room temperature for 24 h. The reaction mixture was washed with aqueous $KHCO_3$, dried over $MgSO_4$, and evaporated. TLC of the residue showed only two spots. The residue (130 mg) was recrystallized from MeOH–Et_2O–hexane to give 85 mg of colorless thick needles (**2c**). The mother liquor was evaporated and the residue, which contained *m*-chlorobenzoic acid, was submitted to alumina column chromatography (Et_2O–hexane–trace acetone) to give a trace of **1c** and additional **2c** (25 mg). The total yield of **2c** was 95%. No other products were detected. **2c**: mp 219 °C (ref.[5] gives mp 223 °C for **3c**). *Anal.* Calcd for $C_{24}H_{21}N_3O$: C, 78.45; H, 5.76; N, 11.44. Found: C, 78.21; H, 5.67; N, 11.38. IR (KBr): 1600 (strong), 1523, 1431 (strongest), 1345, 1275, 1170, 1018, 815, 780, 733 cm^{-1}. MS (MS, EI/70 eV); *m/z*: 367 (40%, M^+), 337 (20%, M^+-NO), 309 (13%, M^+-N_3O), 220 (35%, Tol_2C_2N), 206 (100%, Tol_2C_2), 205 (28%), 202 (9%), 191 (22%), 189 (20%), 119 (7%), 117 (8%), 103 (25%). (Ref.[5]) gives values for **3c**, 367 (6%), 206 (100%), 205, 202, 191, 189, 119, 117). ^{1}H-NMR ($CDCl_3$) δ: 2.32 (9H, s), 6.84 (2H, d, J=8 Hz), 7.02 (2H, d, J=8 Hz), 7.05 (4H, d, J=8 Hz), 7.21 (4H, d, J=8 Hz). ^{13}C-NMR ($CDCl_3$) δ: 21.19, 21.25, 119.81, 128.76, 129.47, 129.66, 129.76, 130.26, 130.40, 138.32, 140.59, 166.21.

Oxidation of 1c with PAA under Reflux A mixture of **1c** (160 mg, 0.456 mmol), PAA solution (260 mg, *ca.* 1.44 mmol), and $CHCl_3$ (10 ml) was refluxed for 4 h at 80 °C. The reaction mixture was treated as described for **1b**. The residue showed one major (**2c**) and one minor TLC spots. Repeated cautious separation by preparative TLC (Et_2O–hexane–trace acetone) gave 85 mg (51%) of **2c**, a minor product (30 mg, 16%, mp 208 °C, colorless prisms from MeOH–Et_2O–hexane), and a trace of **1c**. Spectral data of the minor product excluded the structure of **3c**[6]: ^{1}H-NMR; three methyl signals, two benzylic signals at δ 4.54 and 4.55, intensity ratio *ca.* 8:5 together with rather complex signals in the aromatic region: The ^{13}C-NMR spectrum showed five signals in the aliphatic region and twenty signals in the aromatic region, some signals appearing as shoulders. MS *m/z*: 403 (35%, exact mass; 403.129. This value is consistent with $C_{24}H_{20}N_3{}^{37}ClO$=403.127), 401 (100%, exact mass; 401.130. This value is consistent with $C_{24}H_{20}N_3{}^{35}ClO$=401.130, M^+), 373 (22%, M^++2−NO), 371 (65%, M^+-NO), 366 (18%, M^+-Cl), 256 (22%, $C_{16}H_{13}N^{37}Cl$), 254 (66%, $C_{16}H_{13}N^{35}Cl$), 242 (20%, $C_{16}H_{13}{}^{37}Cl$), 240 (60%, $C_{16}H_{13}{}^{35}Cl$), 220 (60%, Tol_2C_2N), 219 (22%), 206 (78%), 195 (95%), 103 (54%): The IR spectrum was analogous to that of **2c**.

Oxidation of 1c with PAA at 65 °C A mixture of **1c**, PAA, and $CHCl_3$ was heated at 65 °C for 4 h. Then the reaction mixture was washed with $KHCO_3$, dried over $MgSO_4$, and evaporated. The residue was chromatographed on alumina to give **1c**, **2c**, and a trace amount of by-product.

Oxidation of 1d+1e with *m*CPBA A mixture of **1d** and **1e**[7] (260 mg, 0.80 mmol) in CH_2Cl_2, was treated with 280 mg (1.6 mmol) of *m*CPBA, and the solution was allowed to stand at room temperature for 24 h. Then the reaction mixture was treated as mentioned above. The residue showed two spots on TLC, one of which was due to *m*-chlorobenzoic acid. The residue was recrystallized from $CHCl_3$–CH_3OH(trace)–hexane to give 155 mg of colorless needles. The mother liquor, which contained mainly *m*-chlorobenzoic acid, was evaporated and the residue was subjected to alumina preparative TLC to give a trace amount of starting material and an additional 90 mg of the same product (the total yield 90% (145 mg); mp 196—210 °C (br); ref. 5 gives mp 198 °C for **3d**). The constitution of the product was suggested to be a mixture of the *N*-oxides **2d** and **2e** from the data shown below. *Anal.* Calcd for $C_{22}H_{17}N_3O$: C, 77.85; H, 5.05; N, 12.38. Found: C, 78.15; H, 5.28; N, 12.11. MS *m/z*: 339 (78%, M^+), 309 (20%, M^+-NO), 281 (5%, M^+-N_3O), 206 (30%, $Tol(Ph)C_2N$), 192 (100%, $Tol(Ph)C_2$), 191, 189, 178 (22%, Ph_2C_2. This peak suggests the presence of two phenyl groups on adjacent carbons). Reference 5 reports a similar *m/z* for **3d**. ^{1}H-NMR ($CDCl_3$) δ: 2.31 (3H, br s), 6.72—7.43 (10H, m). The ^{13}C-NMR spectrum showed two signals due to the C-5 in triazine rings at δ 119.2 and 120.1. These data are inconsistent with the structure of **3d** in the literature.[5]

Oxidation of 1d+1e with PAA A mixture of **1d**+**1e**[7] (260 mg, 0.80 mmol), PAA solution (650 mg, *ca.* 3.60 mmol), and $CHCl_3$ (10 ml) was refluxed at 80 °C for 4 h, and treated as described before. The residue thus obtained consisted of the starting material, major products (**2d**+**2e**), and a minor product, as detected by TLC. The residue was chromatographed on alumina, and overlapping fractions were submitted repeatedly to preparative TLC to give the starting material (58 mg), a major product (colorless needles, 107 mg), and a by-product (mp 190—209 °C (br)). The major product was identical with that from the *m*CPBA oxidation. The minor one showed spectral data which were inconsistent with the structure **3d**, and contained a chlorine atom.[10]

Structural Analysis of 2c by X-Ray Crystallography The observed cell parameters for **2c** (0.30×0.20×0.50 mm, from MeOH–Et_2O–hexane) were as follows: M.W. 367.45 ($C_{24}H_{21}N_3O$), space group $P\bar{1}$ (monoclinic), Z=1, a=9.333(1), b=10.073(1), c=5.903(1) Å, α=94.23(1), β=98.62(1), γ=113.01(1)°, V=116.9(2) Å^3, D_C=1.222 g cm^{-3}. Data were collected on a Rigaku AFC-5 diffractometer using graphite monochromated Cu$K\alpha_1$ radiation by the θ–2θ scan method. The scan speed was 16° min^{-1}. The data were corrected for Lorentz and polarization factors, but no absorption correction was applied. A total of 1697 reflections were measured within the 2θ angle of 120°. The crystal structure was determined by the direct method and refined by the full-matrix least-squares method. The final R value was 0.042 for 1459 reflections above $3\sigma(F)$ including anisotropic thermal factors for nonhydrogen atoms and isotropic ones for hydrogen

atoms. The final atomic coordinates are listed in Table I.

References and Notes

1) A. R. Katritzky and J. M. Lagowski, "Chemistry of the Heterocyclic *N*-Oxides," Academic Press, London, 1971, p. 70, and references cited therein.
2) A. Ohsawa, H. Arai, H. Ohnishi, T. Kaihoh, K. Yamaguchi, H. Igeta, and Y. Iitaka, *Chem. Pharm. Bull.*, **34**, 109 (1986).
3) *a*) R. J. Kobylecki and A. Mckillop: 1,2,3-Triazines," Advances in Heterocyclic Chemistry," Vol. 19, ed. by A. R. Katritzky and A. J. Boulton, Academic Press, London, 1971, p. 241, and references cited therein; *b*) A. J. Boulton, M. Kiss, and J. D. K. Saka, *J. Chem. Soc., Perkin Trans. 1*, **1988**, 1509.
4) H. Neunhoeffer: Chemistry of 1,2,3-Triazine," The Chemistry of Heterocyclic Compounds," ed. by A. Weissberger and E. C. Taylor, Wiley, New York, 1978, p. 6, and references cited therein.
5) H. Neunhoeffer, M. Clausen, H.-D. Vötter, H. Ohl, C. Krüger, and K. Angermund, *Justus Liebigs Ann. Chem.*, **1985**, 1732.
6) This product is assumed to be mixed crystals of 4-(*p*-chloromethylphenyl)-5,6-bis(*p*-tolyl)-1,2,3-triazine 2-oxide and 5-(*p*-chloromethylphenyl)-4,6-bis(*p*-tolyl)-1,2,3-triazine 2-oxide, although the formation mechanism is unclear (they were probably derived from **2c** *via* radical abstraction of a chlorine atom from the solvent molecule). TLC of the compound(s) using alumina or silica gel showed one clear spot with all solvents examined, and the separation was unsuccessful.
7) The report by Neunhoeffer *et al.*[11] claimed that the reaction of 1,2-diphenyl-3-(*p*-tolyl)cyclopropenyl salt with sodium azide (a modification of the method of Chandross *et al.*, *Tetrahedron Lett.*, **1960**, 19) gave 4,6-diphenyl-5-(*p*-tolyl)-1,2,3-triazine (**1d**) predominantly (isomer 0—15%) because of the electron-donating effect of the methyl group. However, we obtained different results: the procedure according to Neunhoeffer *et al.* afforded a major product in 24% yield, whose melting point was 218 °C (lit. 222 °C as **1d**). Its ^{13}C-NMR spectrum showed signals at δ 21.25 and 21.28 due to methyl groups. The ^{1}H-NMR spectrum showed methyl signals at δ 2.34 and 2.36 (shoulder), and they were split into two signals at δ 2.48 and 2.60 in the ratio of *ca.* 63 : 37 upon addition of Eu(FOD)$_3$, which also suggested the presence of two kinds of methyl groups. The MS showed intense peaks at *m/z* 178 (30%, Ph_2C_2) and 192 (100%, Tol(Ph)C_2). The former fragment implied the presence of two phenyl groups on adjacent carbons. Thus the product is thought to be a mixture of **1d** and its isomer, 4,5-diphenyl-6-(*p*-tolyl)-1,2,3-triazine **1e**. All attempts to separate them were unsuccessful.
8) We think that the misassignment in the previous report[4,5] is due to misreading of the mass fragmentation and the lack of high resolution NMR spectra.
9) Compound **4** was obtained in 4% yield on oxidation with H_2O_2–AcOH under reflux.
10) This compound is probably a mixture of 5-(*p*-chloromethylphenyl)-4,6-diphenyl-1,2,3-triazine 2-oxide and 4-(*p*-chloromethylphenyl)-5,6-diphenyl-1,2,3-triazine 2-oxide. The MS showed peaks at *m/z* 375 (33%, $C_{22}H_{16}N_3{}^{37}ClO$) and 373 (100%, $C_{22}H_{16}N_3{}^{35}ClO$). The ^{1}H-NMR spectrum showed two chloromethyl signals at δ 4.52 and 4.53.
11) H. Neunhoeffer, H-D. Vötter, and H. Ohl, *Chem. Ber.*, **103**, 3695 (1972).

Hydride Reduction of Erythrinan-7,8-diones and 7-*O*-Methanesulfonyl-8-oxo-erythrinans[1)]

Yoshisuke TSUDA,*[,a] Yuki SAKAI,[a] Katsuko AKIYAMA,[a] and Kimiaki ISOBE[b]

Faculty of Pharmaceutical Sciences, Kanazawa University,[a] 13–1 Takara-machi, Kanazawa 920, Japan and Showa College of Pharmaceutical Sciences,[b] 3–3165 Higashi-tamagawagakuen, Machida-shi, Tokyo 194, Japan. *Received January 28, 1991*

The stereochemistry of hydride reduction of erythrinan-7,8-diones was markedly affected by the bulkiness of the reagent and the polarity of the solvent: sodium borohydride in ethanol–tetrahydrofuran gave the 7β-hydroxy isomers and tetrabutylammonium borohydride in methanol gave the 7α-hydroxy isomers, stereoselectively. This can be explained in terms of fluctuation of the balance between product development control and approach control. The structures of the products were established by chemical and spectroscopic means. Their *O*-mesylates were hydrolyzed under basic conditions with epimerization to give a mixture of alcohols with a preference for the 7β-hydroxy derivatives. A similar epimerization of the mesyloxy group was also observed in lithium aluminum hydride reduction.

Keywords erythrinan-7,8-dione; hydride reduction; sodium borohydride; solvent effect; stereochemistry; epimerization; 7-*O*-methanesulfonyl-8-oxoerythrinan; lithium aluminum hydride

Erythrinan-7,8-diones **1** exist mainly in a diosphenol form (B) rather than a 7-oxo form (A), as evidenced from infrared (IR) and ultraviolet (UV) spectra, from the color reaction to ferric chloride solution, and from their solubility in alkaline solutions. Previously Mondon *et al.*[2)] reported that the reduction of **1a** with sodium borohydride in ethanol yielded the 6βH-7αOH isomer **2a** as a single product. On reinvestigation of their reduction, however, we observed that the product was a mixture of two stereoisomeric alcohols, **2a** and **3a**, and that the ratio of these isomers was largely dependent on the polarity of the solvents. This paper deals with this finding in detail.

Results and Discussion

The results of hydride reductions of **1a** and other erythrinan-7,8-dione (**1b—d**) with various hydride reagents in various solvents are summarized in Table I. Contrary to the previous report,[2)] $NaBH_4$ in EtOH usually produced the 6βH-7βOH isomers **3** preferentially. These two products, **2** and **3**, are characterized by the coupling constants between 6-H and 7-H, which are 7 Hz in **2** and 10 Hz in **3**.

The stereochemistries of the products were conclusively proved for **2a** and **3a** as follows. (1) The derived *O*-mesylate **4** from **2a** gave the olefin **6** on heating with 1,8-diazabicyclo[5.4.0]undec-7-ene (DBU), while the *O*-mesylate **5** from **3a** was recovered unchanged after a similar treatment, indicating that 6-H and 7-OH in **2** were *trans* and those in **3** were *cis*. (2) Treatment of **4** and **5** with 10% KOH–MeOH produced a mixture of the same compounds, the alcohols **2a** and **3a** and the olefin **6**, respectively. These facts indicate that, though the reaction was accompanied with an epimerization of the C-7 substituent (see also below), **2a** and **3a** are different only in the configuration of the 7-OH group and have the same configuration at the ring juncture (C-6). The ratio of **2a**/**3a** is 1/2.2 from **4**, and 1/9 from **5**, with **3a** always being predominant, suggesting that **3a** is thermodynamically more stable than **2a**. (3) The two mesylates, **4** and **5**, gave the olefin **6** on heating with LiCl in dimethylformamide (DMF). In this reaction, **4** afforded the chloro compound **7** as a by-product, which was reduced to the oxo-erythrinan **8** with Zn/AcOH. This compound **8** was also formed on hydrogenation of **6** and was reduced, with lithium aluminum hydride (LAH), to the *cis*-erythrinan **9**,[3)] thus confirming the relative stereochemistry of C-5 and C-6.

Tetra-*n*-butylammonium borohydride (BBH) also reduced **1**, though the ratio of **2**/**3** was the reverse of that in the case of $NaBH_4$ reduction (for **1c**). Lithium borohydride gave a similar stereochemical result to that with $NaBH_4$.

TABLE I. Hydride Reduction of Erythrinan-7,8-diones

Run	Compd.	Reagent[a)]	Solvent	Conditions	Products (2:3)[b)]	Total yield (%)
1	**1a**	$NaBH_4$	EtOH	0 °C 1.5 h	1:1	96
2	**1a**	$NaBH_4$	MeOH	r.t. 2 h	1.6:1	93
3	**1b**	$NaBH_4$	EtOH–THF	0 °C 2 h	1:2	95
4	**1c**	$NaBH_4$	EtOH–THF	0 °C 1.5 h	1:1.7	96
5	**1c**	$NaBH_4$	MeOH	0 °C 1 h	2:1	100
6	**1c**	$NaBH_4$	PrOH	0 °C 2 h	1:1.3	99
7	**1c**	$NaBH_4$	H_2O–NaOH	0 °C	Unchanged	
8	**1c**	Bu_4NBH_4	MeOH	r.t. 2 h	2.9:1	81
9	**1c**	Bu_4NBH_4	THF	r.t. 0.3 h	1.8:1	100
10	**1c**	$LiBH_4$	THF	r.t. 10 h	1:1.3	92
11	**1d**	$NaBH_4$	EtOH	0 °C 2 h	1:2.5	56[c)]

a) The amount of reagent used was 0.3—0.5 mol eq. *b*) The yields and the ratio were determined after isolation of the products by PTLC. *c*) Considerable amounts of the starting material **1d** were recovered. r.t. = room temperature.

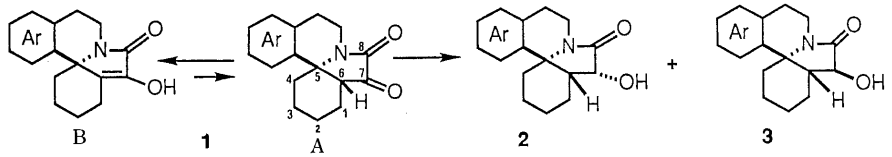

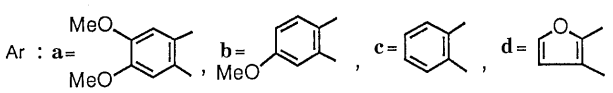

Chart 1

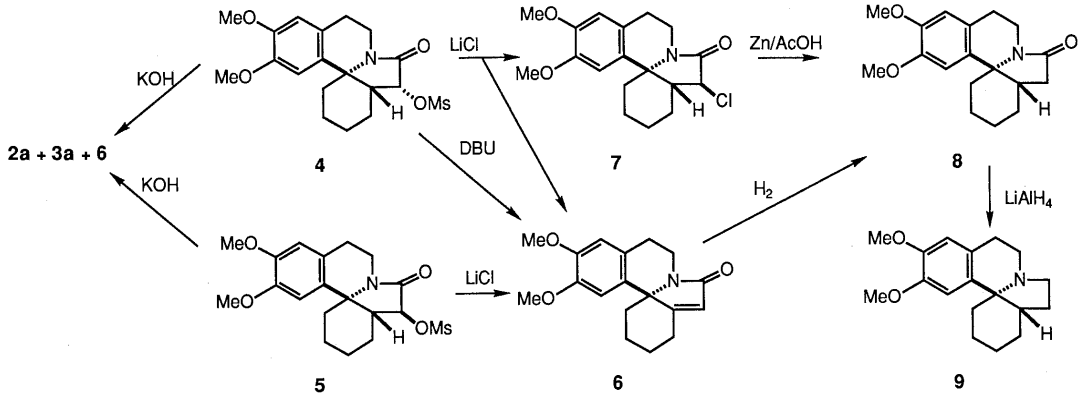

Chart 2

Sodium bis(2-methoxyethoxy)aluminum hydride, diisobutyl aluminum hydride, lithium tri-*sec*-butyl borohydride, and lithium aluminum tri-*tert*-butoxide did not reduce **1c**, the starting material being recovered. When these reagents were added, **1c** rapidly moved to the starting point on thin layer chromatography (TLC), indicating the enolate formation. The same phenomenon was observed in the reduction with $NaBH_4$ in aqueous NaOH solution, again the starting material being recovered. These results indicate that hydride reduction of erythrinan-7,8-diones proceeds through 1,2-addition to the 7-oxo form (A), and not through 1,4-addition to the diosphenol form (B).

A remarkable solvent effect was observed on the stereochemical result of this reduction. In the reduction of **1c** with $NaBH_4$, MeOH was the best solvent to produce the 6βH-7αOH isomer **2c**, the proportion of which decreased on decrease of the solvent polarity, with increase of the proportion of **3c**. A bulkier reagent such as BBH produced **2c** more preferentially when the same solvent was used. Thus, either **2** or **3** can be prepared stereoselectively by employing an appropriate combination of the reagent and solvent: BBH in MeOH gives the 6βH-7αOH isomers **2** and $NaBH_4$ in EtOH–tetrahydrofuran (THF) gives the 6βH-7βOH isomers **3** preferentially.

The above changes in stereochemistry depending on the reagent and solvent used can be explained in terms of a balance between approach control and product development control.[4] We argue that the transition state of this reduction is originally product-like, thus giving the thermodynamically more stable product **3** preferentially. A bulkier reagent increases the ratio of steric approach controlled product **2**. Increase of the solvent polarity may accelerate the reaction; this effect also increases the ratio of the early transition state product **2** in MeOH rather than in EtOH–THF or *n*-propanol. In agreement with this argument, reduction of **10** with $NaBH_4$ in EtOH–THF gave **11** and **12** in a ratio of 1 : 2 and that with BBH in MeOH gave the same products but in a reversed ratio (2 : 1).

LAH reduction of the *O*-mesylates, **4** and **5**, gave a mixture of **13** and **14** from either compound, suggesting that a partial epimerization of the *O*-mesyl group had taken place. Since the erythrinan **9** was not found as a product and **2a** or **3a** was reduced with LAH to a single amine, **13** or **14**, the epimerization should have occurred for the *O*-mesylates **4** and **5**. As indicated above, alkaline hydrolysis of the *O*-mesylates, **4** and **5**, was always accompanied with an epimerization of the substituent, with preferred formation of the thermodynamically more stable 7β-isomer. Hydrolysis of the 6β-ethoxycarbonyl-7β-*O*-mesyl derivative **15** with 10% KOH gave the product of original configuration, the 7β-hydroxy isomer **16**, as a sole product (the tertiary carbethoxy group was unaffected), suggesting that *SN*2 substitution is an insignificant path in the alkaline treatment of 7-*O*-mesyl-8-oxo-erythrinan derivatives and that the OMs group was epimerized prior to O–S bond cleavage.[5]

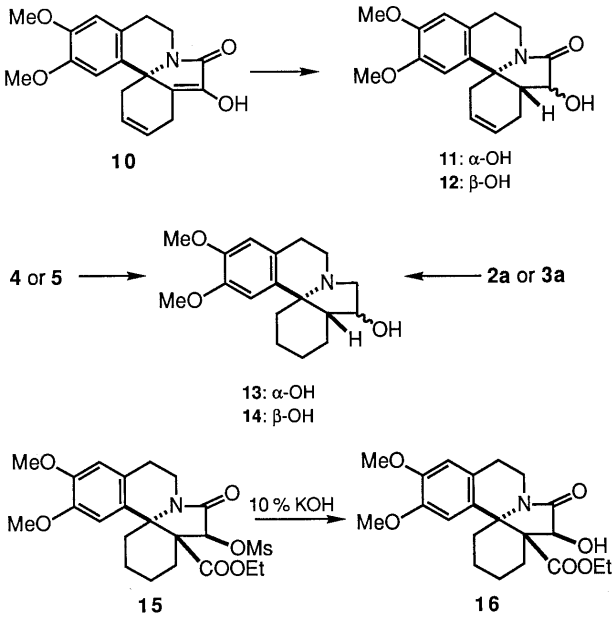

Chart 3

Experimental

General See Experimental in ref. 1.

Hydride Reduction of Erythrinan-7,8-diones 1 Compounds **1a**—**d**[6] (each 0.1 g) were reduced under the conditions shown in Table I, and the products were analyzed after isolation by preparative TLC (PTLC).

The 7α-Hydroxy Isomer **2a**: Colorless needles from benzene, mp 103—131 °C, which on drying at 80 °C over P_2O_5 *in vacuo* showed mp 163 °C. IR: 3200, 1670. ^{1}H-NMR: 6.68, 6.45 (each 1H, s, ArH), 4.04 (1H, d, J=7 Hz, CHOH), 3.84, 3.78 (each 3H, s, OMe), 7.26 (3H, s, 1/2C_6H_6). *Anal.* Calcd for $C_{18}H_{23}NO_4 \cdot 1/2C_6H_6$: C, 70.79; H, 7.30; N, 3.93. Found: C, 70.35; H, 7.27; N, 3.76. This was identical with Mondon's 6βH-7αOH isomer (mp 163 °C),[2] and gave the *O*-mesylate **4** on usual mesylation (MsCl–pyridine), as colorless prisms from MeOH, mp 171.5—172.5 °C. IR: 1718, 1705. ^{1}H-NMR; 6.85, 6.49 (each, 1H, s, ArH), 4.91 (1H, d, J=7 Hz, CHOMs), 3.84, 3.80 (each 3H, s, OMe), 3.21 (3H, s, Ms). *Anal.* Calcd for $C_{19}H_{25}NO_6S$: C, 57.72; H, 6.33; N, 3.54. Found: C, 57.64; H, 6.55; N, 3.45.

The 7β-Hydroxy Isomer **3a**: Colorless prisms from benzene, mp 185—186 °C. IR: 3250, 1670. ^{1}H-NMR: 6.92, 6.56 (1H, s, ArH), 4.35 (1H, d, J=10 Hz, CHOH), 3.83 (6H, s, OMe×2), 7.26 (3H, s, 1/2C_6H_6). *Anal.* Calcd for $C_{18}H_{23}NO_4 \cdot 1/2C_6H_6$: C, 70.79; N, 3.93. Found: C, 70.26; H, 7.33; N, 4.05. This was identical with Mondon's minor product (mp 177 °C) obtained by hydrogenation of **1a** over platinum.[2] This compound gave the *O*-mesylate **5** as colorless prisms from MeOH, mp 180—181 °C. IR: 1702. ^{1}H-NMR: 6.86, 6.57 (each 1H, s, ArH), 5.21 (1H, d, J=10 Hz, CHOMs), 3.83 (6H, s, OMe×2), 3.21 (3H, s, OMs). *Anal.* Calcd for $C_{19}H_{25}NO_6S$: C, 57.72; H, 6.33; N, 3.54. Found: C, 57.51; H, 6.42; N, 3.56.

The 7α-Hydroxy Isomer **2b**: Colorless prisms from AcOEt, mp 172—174 °C. IR; 3320, 1655. ^{1}H-NMR: 6.6—7.3 (3H, m, ArH), 4.07 (1H, d, J=7 Hz, CHOH), 3.76 (3H, s, OMe). *Anal.* Calcd for $C_{17}H_{21}NO_3$: C, 71.05; H, 7.37; N, 4.87. Found: C, 71.06; H, 7.42; N, 4.87.

The 7β-Hydroxy Isomer **3b**: Colorless prisms from AcOEt, mp 168—170 °C. IR: 3280, 1685—1660. ^{1}H-NMR: 6.6—7.3 (3H, m, ArH), 4.38 (1H, d, J=10 Hz, CHOH), 3.89 (3H, s, OMe). *Anal.* Calcd for $C_{17}H_{21}NO_3$: C, 71.05; H, 7.37; N, 4.87. Found: C, 70.64: H, 7.46; N, 4.62.

The 7α-Hydroxy Isomer **2c**: Colorless prisms from AcOEt, mp 169—170 °C. IR: 3250, 1660. ^{1}H-NMR: 7.0—7.3 (4H, m, ArH), 4.75 (1H, d, J=7 Hz, CHOH). *Anal.* Calcd for $C_{16}H_{19}NO_2$: C, 74.68; H, 7.44; N, 5.44. Found: C, 74.75; H, 7.68; N, 5.51.

The 7β-Hydroxy Isomer **3c**: Colorless prisms from AcOEt, mp 207—208 °C. IR: 3160, 1680—1660. ^{1}H-NMR: 7.0—7.5 (4H, m, ArH), 4.42 (1H, d, J=10 Hz, CHOH). *Anal.* Calcd for $C_{16}H_{19}NO_2$: C, 74.68; H, 7.44; N, 5.44. Found: C, 74.68; H, 7.52; N, 5.54.

The 7α-Hydroxy Isomer **2d**: Colorless prisms from ether, mp 207—208°C. IR (Nujol): 3250, 1665. ^{1}H-NMR: 7.27, 6.38 (each 1H, d, J=2 Hz, furan), 4.22 (1H, d, J=7 Hz, CHOH). HRMS m/z: (M^+): Calcd for $C_{14}H_{17}NO_3$: 247.1207. Found: 247.1211.

The 7α-Hydroxy Isomer **2d**: Colorless prisms from ether, mp 207—208 °C. IR (Nujol): 3250, 1665. ^{1}H-NMR: 7.27, 6.38 (each 1H, d, J=2 Hz, furan), 4.22 (1H, d, J=7 Hz, CHOH). HRMS m/z: (M^+): Calcd for $C_{14}H_{17}NO_3$: 247.1207. Found: 247.1211.

The 7β-Hydroxy Isomer **3d**: Colorless prisms from ether, mp 160—163 °C. IR (Nujol): 3270, 1680. ^{1}H-NMR: 7.29, 6.46 (each 1H, d, J=2 Hz, furan), 4.42 (1H, d, J=12 Hz, CHOH). HRMS m/z: (M^+): Calcd for $C_{14}H_{17}NO_3$: 247.1207. Found: 247.1220.

Reaction of the *O*-Mesylates with DBU (1) The 7α-*O*-mesylate **4** (51 mg) and DBU (1 g) in benzene (10 ml) were heated under reflux for 4.5 h. The cooled mixture was diluted with benzene and washed with 1 N HCl. Concentration of the benzene layer gave the olefin **6** (47 mg, 100%) as a gum. IR: 1650. ^{1}H-NMR: 7.00, 6.64 (each 1H, s, ArH), 5.82 (1H, s, =CH), 3.83, 3.81 (each 3H, s, OMe). HRMS m/z: (M^+): Calcd for $C_{18}H_{21}NO_3$: 299.1520. Found: 299.1532.

(2) The 7β-*O*-mesylate **5** (47 mg) was treated with DBU and worked up as described above. The starting material **5** (47 mg) was recovered unchanged.

Reaction of the *O*-Mesylates with LiCl (1) The 7α-*O*-mesylate **4** (40 mg) and LiCl (160 mg) in DMF (7 ml) were heated at 145 °C for 3 h. After evaporation of DMF under reduced pressure, water was added and the mixture was extracted with $CHCl_3$ to give a 5:2 mixture of the olefin **6** and the chloro derivative **7** (32 mg), which were separated by chromatography. **7**: Colorless gum. IR ($CHCl_3$): 1650. ^{1}H-NMR: 6.92, 6.60 (each 1H, s, ArH), 4.36 (1H, d, J=10 Hz, CHCl), 3.83, 3.81 (each 3H, s, OMe). HRMS m/z: (M^+): Calcd for $C_{18}H_{22}NO_3{}^{35}Cl$: 335.1287. Found: 335.1269.

(2) Treatment of the 7β-*O*-mesylate **5** (29 mg) with LiCl as described above gave the olefin **6** quantitatively.

Reaction of the *O*-Mesylates with 10% KOH–MeOH (1) The 7α-*O*-mesylate **4** (110 mg) in 10% KOH–MeOH (10 ml) was heated under reflux for 1.5 h. After addition of water, the mixture was extracted with $CHCl_3$. Purification of the product by PTLC (solvent: CH_2Cl_2: AcOEt=2:1) gave **2a** (12 mg, 14%), **3a** (26 mg, 29%), and **6** (44 mg, 53%).

(2) The 7β-*O*-mesylate **5** (50 mg) was treated and worked up as above to give **2a** (2.3 mg, 6%), **3a** (23 mg, 57%), and **6** (12 mg, 32%).

Conversion of the Chloro Derivative 7 to the *cis*-Erythrinan 9 Zn powder (1.5 g) was added in portions to a stirred, refluxing solution of **7** (220 mg) in AcOH (15 ml) and the mixture was refluxed for 4 h. After cooling, the mixture was filtered, and the filtrate was diluted with water and extracted with $CHCl_3$. Purification of the product by PTLC gave the starting material **7** (100 mg) and the oxoerythrinan **8** (30 mg, 17%). IR($CHCl_3$): 1685. ^{1}H-NMR: 6.85, 6.57 (each 1H, s, ArH), 3.87, 3.82 (each 3H, s, OMe). The same compound was obtained (74% yield) on hydrogenation of the olefin **6** over PtO_2 in AcOH.

The oxoerythrinan **8** (80 mg) was reduced with LAH (70 mg) in THF (10 ml) under reflux for 2.5 h. After decomposition of the reagent with water, the mixture was filtered and the filtrate was concentrated to give an amine (38 mg, 50%) as an oil. ^{1}H-NMR: 6.70, 6.50 (each 1H, s, ArH), 3.87, 3.84 (each 3H, s, OMe). The IR and ^{1}H-NMR spectra of this compound were identical with those reported for 15,16-dimethoxy-*cis*-erythrinan **9**.[3] The picrate: yellow prisms from EtOH, mp 186—190 °C (lit. 183 °C).[3] *Anal.* Calcd for $C_{18}H_{25}NO_2 \cdot C_6H_3N_3O_7$: C, 55.81; H, 5.46; N, 10.85. Found: C, 55.75; H, 5.32; N, 10.82.

Hydride Reduction of 15,16-Dimethoxy-7,8-dioxo-Δ^2-erythrinan 10 (1) A mixture of 10 (98 mg) and $NaBH_4$ (10 mg) in THF–EtOH (1:1, 10 ml) was stirred at 0 °C for 1 h. The product showed a single spot on TLC, but gave the following ^{1}H-NMR spectrum, indicating that it is a 1:2 mixture of **11** and **12**. ArH: δ 6.77 (1/3H, s), 6.67 (2/3H, s) 6.51 (1H, s).

(2) Compound **10** (580 mg) was reduced with BBH (1 g) in MeOH (100 ml) for 1 h at room temperature to give a 2:1 mixture (500 mg) of **11** and **12**. Fractional crystallizations of this mixture from MeOH gave **11** as colorless prisms, mp 185—187 °C (lit. 175 °C).[2b] The acetate: colorless prisms from AcOEt, mp 187—189 °C (lit. 183—184 °C).[2b] IR: 1735, 1690. ^{1}H-NMR: 6.70, 6.53 (each 1H, ArH), 5.6—6.2 (2H, m, CH=CH), 5.42 (1H, d, J=6.5 Hz, CHOAc), 3.82, 3.78 (each 3H, s, OMe), 2.09 (3H, s, Ac).

Hydrogenation of 11 and 12 The above mixture of **11** and **12** (1:2.5, 40 mg) in EtOH (10 ml) was hydrogenated over PtO_2 (5 mg) for 2 h to give **2a** and **3a** (1:2.5, 38 mg), which were separated by PTLC and identified.

7α-Hydroxy-15,16-dimethoxyerythrinan 13 The 7α-hydroxy isomer **2a** (50 mg) and LAH (50 mg) in THF (5 ml) were heated under reflux for 4 h. The cooled mixture was decomposed with aqueous saturated Na_2SO_4 solution and filtered. The residue was washed several times with hot CH_2Cl_2. Concentration of the combined filtrate and washings left an oil, which was dissolved in 1 N HCl and washed with ether. Basification of the acidic layer with K_2CO_3 and extraction with $CHCl_3$ gave, on concentration of the extract, an oil which was purified by chromatography (solvent: $CHCl_3$: diethylamine=10:1) to give the amine **13** (36 mg, 71%) as an oil. ^{1}H-NMR; 6.51, 6.37 (each 1H, s, ArH), 3.82 (6H, s, OMe×2). The picrate: yellow prisms from EtOH, mp 209—210 °C. *Anal.* Calcd for $C_{18}H_{24}NO_3 \cdot C_6H_3N_3O_7$: C, 54.23; H, 5.08; N, 10.55. Found: C, 53.90; H, 5.46; N, 10.51.

7β-Hydroxy-15,16-dimethoxyerythrinan 14 The 7β-hydroxy isomer **3a** (50 mg) was reduced and worked up as above to give the amine **14** (22 mg, 46%). ^{1}H-NMR: 6.63, 6.46 (each 1H, s, ArH), 3.81 (6H, s, OMe×2). The picrate: yellow prisms from MeOH, mp 169—172 °C. *Anal.* Calcd for $C_{18}H_{24}NO_3 \cdot C_6H_3N_3O_7$: C, 54.23; H, 5.08; N, 10.55. Found: C, 53.97; H, 5.31; N, 10.66.

LAH Reduction of the *O*-Mesylates (1) The 7α-*O*-mesylate **4** (0.1 g) was reduced with LAH (50 mg) and worked up as described above. Purification of the basic product by PTLC gave **13** (68 mg, 85%) and **14** (8 mg, 10%).

(2) The 7β-*O*-mesylate **5** (0.1 g) was reduced with LAH (55 mg) and worked up as above to give **13** (21 mg, 26%) and **14** (59 mg, 74%).

LAH Reduction of the 7,8-Dioxoerythrinan 1a Compound **1a** (0.1 g) was reduced with LAH (0.1 g) and worked up as described above to give **13** (30 mg, 32%) and **14** (27 mg, 28%).

6β-Ethoxycarbonyl-7β-methanesulfonyloxy-15,16-dimethoxy-8-oxoerythrinan 15 This compound was prepared by usual methanesulfonylation of **16**.[6] Colorless needles from MeOH, mp 195—197 °C. IR (KBr): 1720, 1705. ^{1}H-NMR: 6.77, 6.52 (each 1H, s, ArH), 5.46 (1H, s, CHOMs), 3.81 (6H, s, OMe×2), 3.32 (3H, s, Ms), 0.82 (3H, t, J=7 Hz, $COOCH_2\underline{CH}_3$). *Anal.* Calcd for $C_{22}H_{29}NO_8S$: C, 56.52; H, 6.25; N, 3.00. Found: C, 56.57; H, 6.01; N, 2.89.

Alkaline Hydrolysis of 15 The *O*-mesylate **15** (120 mg) in 10% KOH–MeOH (10 ml) was heated under reflux for 2 h. Dilution with water and extraction with $CHCl_3$ of the mixture gave the original compound **16** (100 mg).

References and Notes

1) Synthesis of *Erythrina* and Related Alkaloids. XXVI. Part XXV: Y. Tsuda, Y. Sakai, T. Sano, and J. Toda, *Chem. Pharm. Bull.*, **39**, 1402 (1991).
2) *a*) A. Mondon, *Justus Liebigs Ann. Chem.*, **628**, 123 (1959); *b*) A. Mondon, K. F. Hansen, K. Boehme, H. P. Faro, H. J. Nestler, H. G. Vilhuber, and K. Böttcher, *Chem. Ber.*, **103**, 615 (1970).
3) *a*) A. Mondon, *Chem. Ber.*, **92**, 1461 (1959); *b*) A. Mondon and K. F. Hansen, *Tetrahedron Lett.*, **14**, 5 (1960); *c*) A. Mondon and P. R.

Seidel, *Chem. Ber.*, **104**, 2937 (1971).
4) We use here the terms approach control and product development control following the definition by Wigfield and Phelps [D. C. Wigfield and D. J. Phelps, *Cand. J. Chem.*, **50**, 388 (1972)]. They correspond to kinetic control and thermodynamic control, respectively. However, since these reductions of ketones are purely kinetically controlled, the **2**/**3** ratio must depend on, and only on, the relative free energies of the two transition states leading to the two diastereomeric products, so the above terms are more precise.
5) A similar base-catalyzed epimerization of the *O*-mesyl group was suggested in the cyclization reaction of 7α-*O*-mesyl-2,8-dioxoerythrinans to 2,8-dioxo-1,7-cycloerythrinans [Y. Tsuda, Y. Sakai, A. Nakai, T. Ohshima, S. Hosoi, K. Isobe, and T. Sano, *Chem. Pharm. Bull.*, **38**, 2136 (1990)].
6) Y. Tsuda, Y. Sakai, A. Nakai, M. Kaneko, Y. Ishiguro, K. Isobe, J. Taga, and T. Sano, *Chem. Pharm. Bull.*, **38**, 1462 (1990).

Studies on Hindered Phenols and Analogues. V.[1] Synthesis, Identification, and Antidiabetic Activity of the Glucuronide of CS-045

Takao YOSHIOKA,*,[a] Yuichi AIZAWA,[a] Takashi FUJITA,[a] Kan-ichi NAKAMURA,[b] Kunihiro SASAHARA,[c] Harumitsu KUWANO,[b] Takeshi KINOSHITA,[b] and Hiroyoshi HORIKOSHI[d]

Medicinal Chemistry Research Laboratories,[a] Analytical and Metabolic Research Laboratories,[b] Product Development Laboratories,[c] and Biological Research Laboratories,[d] Sankyo Co., Ltd., 2–58 Hiromachi 1-chome, Shinagawa-ku, Tokyo 140, Japan. *Received December 25, 1990*

The glucuronide of a new oral antidiabetic agent, (±)-5-[4-(6-hydroxy-2,5,7,8-tetramethylchroman-2-ylmethoxy)benzyl]thiazolidine-2,4-dione (CS-045) (1), was synthesized to confirm the structure of a metabolite in monkeys (*Macaca fascicularis*) and to examine its antidiabetic activity. The glucuronide also had antidiabetic activity in KK-mice.

Keywords glucuronide; CS-045; antidiabetic activity; hindered phenol; *Macaca fascicularis*; KK-mice

(±)-5-[4-(6-Hydroxy-2,5,7,8-tetramethylchroman-2-ylmethoxy)benzyl]thiazolidine-2,4-dione (**1**, CS-045) is undergoing clinical trial (phase II study)[2] as a new oral antidiabetic agent.[3] This compound **1** is not only effective in insulin resistant diabetic animals such as the KK-mouse, ob/ob mouse, and Zucker fatty rat,[4] but also lowers lipid peroxide (LPO) which is thought to be one of the causes of macro- and microangiopathy.[3]

It has been well known that phenolic compounds can be metabolized to give the corresponding glucuronide as exemplified in Chart 2.[5] The hindered phenolic compound **1** also appeared to be metabolized to the corresponding glucuronide. We actually isolated a metabolite from the bile of a monkey (*Macaca fascicularis*), whose mass spectral data indicated the structure of the glucuronide **2**.[6]

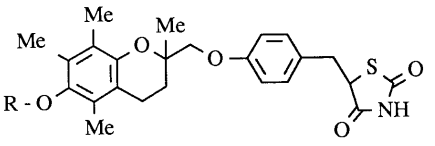

1: R=H CS-045

2: R= 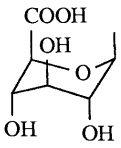

Chart 1

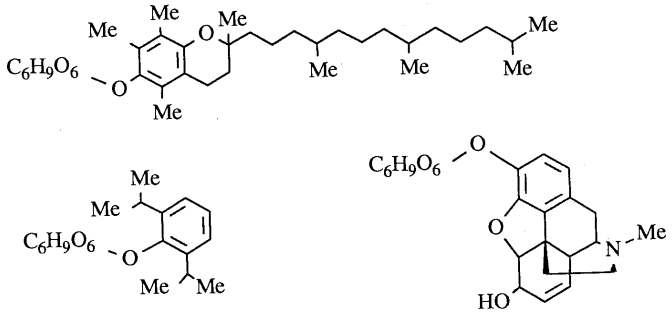

Chart 2. Examples of Phenolic Glucuronides

The presence of the glucuronide **2** might contribute to the long duration of antidiabetic activity based on so-called enterohepatic recirculation accompanying the hydrolysis of glucuronide **2**, giving the parent drug **1** in the intestine.

In this paper, we wish to report the chemical synthesis of the glucuronide **2**, its identification with the monkey metabolite isolated from bile, and the oral antidiabetic activity of **2** together with the synthetic precursor **3** in KK-mice.

Synthesis Compound **2** was synthesized by a method similar to that previously reported.[7] A mixture of compound **1** and freshly prepared methyl 1,2,3,4-tetra-*O*-acetyl-β-D-glucopyranuronate (**4**)[8] in nitrobenzene was heated under reduced pressure in the presence of an acid catalyst to give the corresponding protected glucuronide **3** in a 23% yield. Deprotection of compound **3** by alkaline hydrolysis gave the desired glucuronide **2** in a moderate yield.

Identification The glucuronide isolated from the bile of *M. fascicularis* was identified with the authentic glucuronide **2**, based on fast atom bombardment (FAB) mass spectrum and high performance liquid chromatography (HPLC) analysis. Also, both glucuronides gave compound **1** quantitatively by treatment with β-glucuronidase originated from *Escherichia coli*.

Antidiabetic Activity According to a manner similar to that described in reference 4, the antidiabetic activity was evaluated by the percent decrease of the serum glucose level when the test compounds were administered orally at a

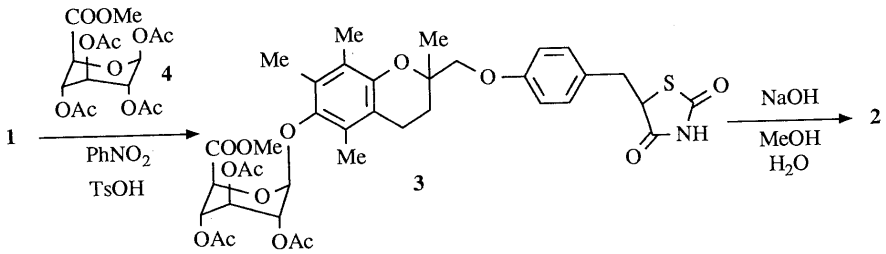

Chart 3

single dose of 50 mg/kg to genetically diabetic male KK-mice under a fed condition, which is a model animal of non-insulin dependent diabetes mellitus (NIDDM). Glucuronides **2** and **3** respectively showed 26 and 29% decreases from the control group, and these values were smaller than compound **1** which had a value of 38.5% ($p<0.05$).

Experimental

FAB mass spectra were recorded on a JEOL JMS-HX100 mass spectrometer with a 3-nitrobenzyl alcohol matrix. Proton-nuclear magnetic resonance (^{1}H-NMR) spectrum was recorded on a 500 MHz JEOL JNM-GX500 FT NMR spectrometer with tetramethylsilane as an internal standard. The abbreviation "nd" indicates that precise identification of the signal was not possible because of overlap by other signals.

Isolation of the Metabolic Glucuronide 2 from the Bile CS-045 (**1**) was administered to a bile duct cannulated monkey (*M. fascicularis*) as an infusion injection from the great saphenous vein at a dose of 5 mg/kg. During 2 h of infusion, bile was collected under anesthesia. Tweny-four ml of bile was applied to the isolation: Each 4-ml portion of bile was charged into a Sep-pak C_{18}^{TM} cartridge (Millipore, U.S.A.). Then the cartridge was washed with 10 ml of water and 2 ml of 5% methanol successively, and the objective fraction was eluted by 4 ml of 25% acetonitrile. The combined fraction was freeze-dried, and the residue was reconstituted with 10 ml of benzene–methanol (3 : 1). The solution was passed through a Sep-pak Florisil™ cartridge to remove polar contaminants. After evaporation of the solvent, the residue was reconstituted with a small amount of acetonitrile and charged into a Sep-pak C_{18} column again, to remove inorganic contaminants from Florisil. After washing with water and 5% methanol in the same manner, glucuronide **2** was eluted by 4 ml of 100% acetonitrile. The eluent was evaporated to dryness. After the residue was dissolved in a small amount of methanol, water was added until the solution became turbid. White powdered glucuronide **2** was collected by filtration after standing overnight in a refrigerator.

Methyl 2,3,4-Tri-*O*-acetyl-1-*O*-[2,[4-(2,4-dioxothiazolidin-5-ylmethyl)-phenoxymethyl]-2,5,7,8-tetramethylchroman-6-yl]-β-D-glucopyranuronate (3) A mixture of 31.0 g of (±)-5-[4-(6-hydroxy-2,5,7,8-tetramethylchroman-2-ylmethoxy)benzyl]thiazolidine-2,4-dione (**1**), 9.8 g of methyl 1,2,3,4-tetra-*O*-acetyl-β-D-glucopyranuronate (**4**), 1.0 g of *p*-toluenesulfonic acid monohydrate, and 87 ml of nitrobenzene was heated at 85 °C for 4 h at 20 mmHg. The reaction mixture was subjected to silica gel column chromatogaphy [eluent; benzene : ethyl acetate = 1 : 0 to 3 : 1], to give 4.6 g (23%) of caramel-like compound **3**. FAB MS *m/z*: 757 ($M^+\cdot$). ^{1}H-NMR ($CDCl_3$) δ: 1.40 (3H, s, 2-Me [chroman]), 1.82—1.96 (1H, m, 3-H [chroman]), 2.0—2.2 (1H, nd, 3-H [chroman]), 2.02 (3H, s, OAc), 2.05 (3H, s, OAc), 2.06 (3H, s, Ar-Me), 2.109 and 2.111 (total 3H, each s, OAc), 2.14 (3H, s, Ar-Me), 2.17 (3H, s, Ar-Me), 3.11 (1H, dd, J=14.3, 9.5 Hz, $C_6H_4C\underline{H}_2$), 3.44 (1H, dd, J=14.3, 4.0 Hz, $C_6H_4C\underline{H}_2$), 3.68 and 3.69 (total 3H, each s, COOMe), 3.85 (1H, d, J=9.8 Hz, 5-CH [sugar]), 3.88, 3.95 (each 1H, each d, J=9.2 Hz, $C\underline{H}_2OC_6H_4$), 4.49 (1H, dd, J=9.5, 4.0 Hz, 5-CH [thiazolidine]), 4.75 (1H, d, J=7.7 Hz, 1-CH [sugar]), 5.24 (1H, dd, J=9.8, 8.8 Hz, 4-CH [sugar]), 5.32 (1H, dd, J=9.6, 8.8 Hz, 3-CH [sugar]), 5.34 (1H, dd, J=9.6, 7.7 Hz, 2-CH [sugar]), 6.87, 7.13 (each 2H, each d, J=8.6 Hz, Ar-H), 7.98 (1H, br s, NH).[9]

1-*O*-[2-[4-(2,4-Dioxothiazolidin-5-ylmethyl)phenoxymethyl]-2,5,7,8-tetramethylchroman-6-yl]-β-D-glucopyranuronic Acid (2) To a solution of 3.9 g of **3** in 150 ml of methanol was added, dropwise, 20.63 g of 2.4% aq. sodium hydroxide solution under ice cooling. After stirring at room temperature for 1 h, dry carbon dioxide gas was bubbled into the reaction mixture. The solvent was removed under reduced pressure, the resulting residue was subjected to silica gel column chromatography [eluent; ethyl acetate : acetic acid = 5 : 1], and the residual substance was dissolved in ethyl acetate. The solution was washed with water and dried over sodium sulfate, and the solvent was removed under reduced pressure, to give 2.4 g of a pale yellow caramel-like substance. The caramel was triturated with water to give a paste, which was freeze-dried to give 1.85 g of compound **2** as a pale yellow powder. The powder was identical with the authentic metabolite from the data on the retention time of HPLC carried out with a reverse-phase column (YMC A-312 (ODS), Yamamura Chemical Laboratories Co., Ltd.) using an acetonitrile–distilled water–phosphoric acid (42 : 58 : 0.05, v/v) mixture. The powder was treated with β-glucuronidase as follows: about 1 mg of the powder was dissolved in 10 ml of a 0.1 M acetate buffer (pH 4) and the solution was treated with 260000 units of β-glucuronidase that originated from *E. coli.* at 37 °C for 2 h to give quantitatively the compound **1**, as detected by HPLC analysis with a reverse-phase column (YMC A-314) using an acetonitrile–distilled water–phosphoric acid (62 : 38 : 0.05, v/v) mixture. Compound **2**: FAB MS *m/z*: 616 $(M-H)^-$, 618 $(M+H)^+$. *Anal.* Calcd for $C_{30}H_{35}NO_{11}S\cdot 1.5H_2O$: C, 55.89; H, 5.94; N, 2.17; S. 4.97. Found: C, 56.02; H, 5.82; N, 2.19; S, 4.73.

References and Notes

1) Part IV: Y. Aizawa, T. Kanai, T. Fujita, H. Horikoshi, and T. Yoshioka, *Heterocycles*, **32**, 285 (1991).
2) Y. Iwamoto and T. Kuzuya, *Sogorinsho*, **39**, 2053 (1990).
3) T. Yoshioka, T. Fujita, T. Kanai, Y. Aizawa, T. Kurumada, K. Hasegawa, and H. Horikoshi, *J. Med. Chem.*, **32**, 421 (1989).
4) T. Fujiwara, S. Yoshioka T. Yoshioka, I. Ushiyama, and H. Horikoshi, *Diabetes*, **37**, 1549 (1988).
5) D. Sklan and S. Donoghue, *J. Nutr.*, **112**, 759 (1982); P. J. Simons, I. D. Cookshott, E. J. Douglas, E. A. Gordon, K. Hopkins, and M. Rowland, *Xenobiotica*, **18**, 429 (1988); E. Del Villar, E. Sanchez, and T. R. Tephly, *Drug Metab. Disposit.*, **2**, 370 (1974); R. T. Williams, "Detoxication Mechanisms," Chapman & Hall Ltd. London, 1959, Chapter 9.
6) H. Iwabuchi and K. Nakamura, *Proc. Jpn. Soc., Med. Mass Spectrom.*, **14**, 111 (1989). Details will be reported elsewhere in the near future.
7) T. Sato, H. Miyataka, Y. Masamoto, T. Asai, K. Hasegawa, and H. Kakegawa, *Jpn. Kokai Tokkyo Koho*, Japan. Patent, 86-30594 (1986) [*Chem. Abstr.*, **104**, 213266*u* (1986)].
8) G. N. Bollenback, J. W. Long, D. G. Benjamin, and J. A. Lindquist, *J. Am. Chem. Soc.*, **77**, 3310 (1955).
9) This compound was found to occur as a diastereomeric mixture in the ratio of approximately 1 : 1.

Studies on Immunostimulating Derivatives: Synthesis of Some Pyrrolo[1,2-*c*]pyrimidines

El Houssain BAHAJI,[a] Pierre TRONCHE,*,[a] Joële COUQUELET,[a] Said HARRAGA,[b] Jacqueline PANOUSE-PERRIN[b] and Catherine RUBAT[a]

Groupe de Recherche en Pharmacochimie, Faculté de Pharmacie,[a] 28, place Dunant, 63001 Clermont-Ferrand Cēdex, France and Laboratoire d'Immunologie et de Microbiologie Pharmaceutique, Faculté de Médecine et de Pharmacie,[b] 4, place Saint-Jacques, 25030 Besancon Cédex, France.
Received December 25, 1990

In a search for potential immunomodulating agents novel pyrrolo[1,2-*c*]pyrimidines were synthesized and their structures elucidated by spectroscopic means. Unfortunately, most of them were cytotoxic and devoid of effects on T lymphocyte lymphoblastic transformation. Furthermore, they were inactive in the locomotor activity test in mice.

Keywords pyrrolo[1,2-*c*]pyrimidine; pyrrolopyrimidine dione; ethoxycarbonyl pyrrolopyrimidine; immunomodulating activity; sedative activity; cytotoxicity

In a previous paper[1] we described the synthesis of thiadiazabicyclic compounds containing a bridgehead nitrogen atom and we reported their immunomodulating activity on human T lymphocytes. These considerations prompted us to extend our investigations to some structurally related pyrrolo[1,2-*c*]pyrimidines.

The accesses to the two series of these compounds **3** and **4** were performed from the same starting material, ethyl pyrrolidinylidene-2 acetate **1** the structure and the reactivity of which have been recently developed.[2,3] Formerly we investigated the reactivity of this compound towards acid chlorides and isocyanates.[4,5] In the two synthetic pathways

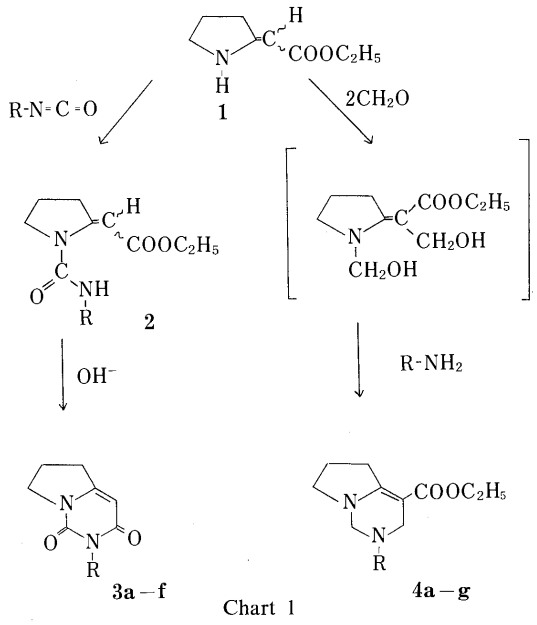

Chart 1

TABLE I. Physical Constants of 2-Substituted 1*H*,5*H*-2,3,6,7-Tetrahydropyrrolo[1,2-*c*]pyrimidine-1,3-diones

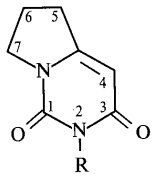

Compd. No.	R	Yield (%)	mp (°C)	Formula (MW)	Calcd (Found) C	H	N
3a	CH_3	90	116	$C_8H_{10}N_2O_2$ (166)	57.83 (57.83	6.02 6.10	16.87 17.00)
3b	*n*-C_4H_9	86	44	$C_{11}H_{16}N_2O_2$ (208)	63.46 (63.71	7.69 7.89	13.46 13.37)
3c	*n*-C_6H_{13}	85	61	$C_{13}H_{20}N_2O_2$ (236)	66.10 (66.13	8.47 8.52	11.86 11.92)
3d		90	135	$C_{13}H_{18}N_2O_2$ (234)	66.67 (66.41	7.69 7.71	11.96 11.78)
3e	CH_2 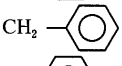	91	89	$C_{14}H_{14}N_2O_2$ (242)	69.42 (69.63	5.78 5.87	11.57 11.45)
3f		74	188	$C_{13}H_{12}N_2O_2$ (228)	68.42 (68.29	5.26 5.15	12.28 12.43)

TABLE II. Spectral Data for 2-Substituted 1*H*,5*H*-2,3,6,7-Tetrahydropyrrolo[1,2-*c*]pyrimidine-1,3-diones

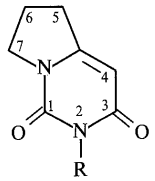

Compd. No.	IR (KBr) cm^{-1} C=O	C=C	^{1}H-NMR (60 MHz, $CDCl_3$) δ ppm 6-CH_2	5-CH_2	7-CH_2	=CH	R
3a	1700, 1670	1640	2.20 (m)	3.05 (t)	4.05 (t)	5.70 (s)	3.3 (s) CH_3
3b	1710, 1680	1630	2.25 (m)	3.05 (t)	4.05 (m)	5.70 (s)	0.90 (m) CH_3, 1.35 (m) $2CH_2$, 4.05 (m) CH_2–N
3c	1710, 1660	1630	2.20 (m)	3.10 (t)	4.05 (m)	5.70 (s)	0.90 (m) CH_3, 1.40 (m) $4CH_2$, 4.05 (m) CH_2–N
3d	1690, 1670	1635	2.20 (m)	3.05 (t)	4.05 (m)	5.65 (s)	1.60 (m) $5CH_2$, 4.05 (m) CH–N
3e	1710, 1650	1630	2.25 (m)	2.95 (t)	3.95 (t)	5.70 (s)	5.00 (s) CH_2–N, 7.30 (m) 5H arom.
3f	1720, 1690	1645	2.20 (m)	3.05 (t)	4.05 (t)	5.70 (s)	7.30 (m) 5H arom.

represented on Chart 1 the starting material **1** was a mixture of the *Z* and *E* isomers which were obtained by the procedure described in a previous paper.[6] Compounds **3a**—**f** were obtained in two steps: reaction of an alkyl or aryl isocyanate with the enaminoester **1** leading mainly to the urea derivatives **2** then cyclisation under alkaline conditions in refluxing ethanol. All structural features of the bicyclic products **3** may be found in the spectroscopic data (Tables I and II).

On the infrared spectrum two intensive carbonyl absorption bands corresponding to the sequence of >N–C(=O)–NH–C(=O)– appear at about 1700 and 1670 cm^{-1}. A third band near 1630 cm^{-1} corresponds to the ethylenic band. On the proton nuclear magnetic resonance spectra (^{1}H-NMR) the following signals were identified: H-6 protons as multiplets near 2.2 ppm, H-5 protons as triplets near 3.0 ppm, H-7 protons as triplets near 4.0 ppm. The H-1 ethylenic proton signal appeared near 5.7 ppm as a singlet (Table II).

Compounds **4a**—**g** were obtained from enaminoester **1** by reaction with formaldehyde and a primary amine. The access to nitrogenic heterocycles through Mannich reaction is reported in the literature and has been the matter of a general review.[7] In the case of enaminoester **1** the use of two formaldehyde molecules leads very likely in a first step to a double hydroxymethylation, one on the nitrogen atom and the other on the carbon atom bearing the ethylenic proton (Chart 1). The mobility of the latter is increased because it belongs to an enamine moiety and it conjugates with an ester carbonyl.[8] The dihydroxymethylated inter-

TABLE III. Physical Constants of 2-Substituted 4-Ethoxycarbonyl-1*H*,5*H*,2,3,6,7-tetrahydropyrrolo[1,2-*c*]pyrimidines

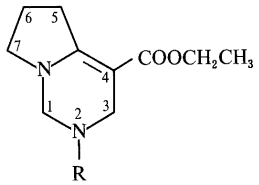

Compd. No.	R	Yield (%)	n_D^{20} mp °C	Formula (MW)	Analysis (%) Calcd (Found) C	H	N	F
4a	$CH(CH_3)_2$	33	Oil, 1.5495 107 (maleate)	$C_{13}H_{22}N_2O_2$ (238)	65.55 (65.65	9.24 9.32	11.76 11.86)	
4b	CH_2–$CH(CH_3)_2$	37	Oil, 1.5563	$C_{14}H_{24}N_2O_2$ (252)	66.67 (66.74	9.52 9.52	11.11 11.21)	
4c	CH_2–C$_6$H$_5$	34	Oil 1.5682 114 (maleate)	$C_{17}H_{22}N_2O_2$ (286)	71.33 (71.43	7.69 7.72	9.79 9.70)	
4d	CH_2–C$_6$H$_4$–F	44	Oil 1.5450 112 (maleate)	$C_{17}H_{21}FN_2O_2$ (304)	67.10 (66.98	6.91 7.04	9.21 9.07	6.25 6.33)
4e	CH_2–C$_6$H$_4$–OCH_3	28	Oil 1.5608	$C_{19}H_{26}N_2O_4$ (346)	65.89 (65.76	7.51 7.60	8.09 8.14)	
4f	CH_2–C$_5$H$_4$N	37	Oil 1.5590	$C_{16}H_{21}N_3O_2$ (287)	66.90 (66.96	7.32 7.32	14.63 14.80)	
4g	H	31	Oil, 1.5375 122 (maleate)	$C_{16}H_{26}N_2O_2$ (278)	69.06 (69.25	9.35 9.50	10.07 9.87)	

MW = molecular weight.

TABLE IV. Spectral Data for 2-Substituted 4-Ethoxycarbonyl-1*H*,5*H*-2,3,6,7-tetrahydropyrrolo[1,2-*c*]pyrimidines

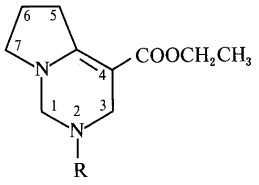

Compd. No.	IR (KBr) cm^{-1} C=O	C=C	^{1}H-NMR (60 MHz, $CDCl_3$) δ ppm 6-CH_2	3-CH_2 5-CH_2	7-CH_2	1-CH_2	$COOCH_2\underline{CH_3}$	$COO\underline{CH_2}CH_3$	R
4a	1670	1600	2.0 (m)	3.3 (m)	3.3 (m)	4.2 (m)	1.25 (m)	4.2 (m)	1.2 (m) $CH(C\underline{H}_3)_2$, 3.3 (m) $C\underline{H}(CH_3)_2$
4b	1680	1600	2.0 (m)	3.2 (m)	3.4 (m)	4.0 (m)	1.25 (m)	4.2 (q)	0.9 (d) $2C\underline{H}_3$, 2.0 (m) $C\underline{H}(CH_3)_2$
4c	1670	1600	2.0 (m)	3.2 (m)	3.7 (m)	4.1 (m)	2.3 (t)	4.1 (m)	3.7 (m) $C\underline{H}_2C_6H_5$, 7.4 (m) arom.
4d	1680	1600	2.0 (m)	3.2 (m)	3.7 (m)	4.2 (m)	1.25 (t)	4.2 (m)	3.7 (m) $C\underline{H}_2C_6H_5$, 7.2 (m) arom.
4e	1680	1600	2.0 (m)	3.2 (m)	3.6 (m)	3.6 (m)	1.25 (t)	4.2 (m)	3.6 (m) $C\underline{H}_2C_6H_4$, 3.9 (s) $2OCH_3$, 7.0 (m) arom.
4f	1670	1600	2.0 (m)	3.2 (m)	3.6 (m)	4.1 (m)	1.3 (t)	4.1 (m)	3.8 (s) $C\underline{H}_2$ pyridine
4g	1680	1600	2.0 (m)	3.1 (m)	3.6 (m)	4.2 (m)	1.25 (t)	4.2 (m)	1.5 (m) $5CH_2$, 4.2 (m) NCH

mediates are not isolated and the azabicyclic compounds **4** are directly obtained (Table III). The crude oily bases are changed into maleic acid salts.

The infrared (IR) spectra of free bases **4** exhibit only one highly intensive carbonyl band near 1670 cm^{-1} assigned to the ester group. The other absorption bands near 1610 cm^{-1} are assigned to the ethylenic group. On the ^{1}H-NMR spectra the signals for the bicyclic ring system and the ethyl ester group are perceived: triplet at 1.2 ppm (3H, CH_3); multiplet centred on 2.0 ppm (2H, H-6); multiplet centred on 2.7 ppm (2H, H-3) and 3.3 ppm (2H, H-5); two singlets at 3.6 and 4.0 ppm (H-7 and H-1); quartet centred on 4.2 ppm (2H, $C\underline{H}_2$–CH_3) (Table IV).

Biological Results and Discussion

Immunomodulating Effect In a first step the study was carried out by determining the effect on the T lymphocyte lymphoblastic transformation induced by phytohemagglutinin (PHA): in a second time the study of rosettes E formation in trypsinated T lymphocytes was carried out on the previously selected compounds. The test was performed on the T lymphocytes of a single person for compounds **3a**—**f**. Noted was a weak activity for **3a** which was not found with the other compounds of the same series. As for compounds of structure **4**, it was observed that **4a** proved itself toxic long before exhibiting a possible immunostimulating effect. The toxicity was confirmed through a microscopic slide examination. Compound **4g** had no effect in the PHA test; as for compound **4c**, it decreased the PHA activity at any concentration of the compound from 1 to 5 μg/ml; it is not toxic at 50 μg/ml towards T lymphocyte.

If comparing these results with those previously observed[1] on thia-7 diaza-1,3 bicyclo[3.3.0]octanes, it may be inferred that unsaturated compounds described here are inactive, or even toxic, in the same experimental testing. However, it must be considered that other structural features are different: lack of an intracyclic sulfur atom in the present case, unlike disposition of carbonyl groups, a six membered ring instead of a five membered in the bicyclic ring system.

Neuromodulating Effect Referring to a possible relationship between central nervous system disorders and immune response[9-11] we performed a tentative evaluation of the ability of these compounds to modify spontaneous locomotor activity in mice. When **3a**—**f** and **4a**—**g** were given intraperitoneally only compound **3a** exhibited a weak and significant neurosedative activity at the dose level of 50 mg/kg and reduced the locomotor activity by 35%; comparatively the observed reducing rate of chlorpromazine was 80% at 2 mg/kg.

The inactive compound **3e** became rapidly so toxic as to kill animals at the level dose of 100 mg/kg. The acute toxicity of compounds **4a**—**e** remained within the range of 800—1200 mg/kg; the locomotor activity was increased but unsignificantly except for compound **4c** for which this activity was raised up 70% at 100 mg/kg. So it seems that the introduction of an unsaturated bond in the azabicyclic ring system is not favourable because it induces cytotoxicity and removes the sedative effects which were observed with the corresponding saturated compounds.[1]

Experimental

Melting points were determined on a Kofler apparatus and are uncorrected. The IR spectra were recorded on a Beckman 4240 spectrophotometer. The ^{1}H-NMR spectra were recorded on a Varian EM 360 A spectrometer. Resonance positions are given on the scale (ppm) relative to internal tetramethylsilane. The NMR signals were designated as follows: s, singlet; d, doublet; t, triplet; m, multiplet. Elementary analysis were performed in the CNRS Analysis Central Service at Vernaison.

When required, the separation of the crude reactional products was performed by chromatography on a silica gel column (70—230 mesh) with a Merck Duramat pump.

2-Substituted 1*H*,5*H*-2,3,6,7-Tetrahydropyrrolo[1,2-*c*]pyrimidine-1,3-diones (3a—f) To a solution of 0.02 mol of carbamoylated derivative **2**[6] in 10 ml of ethanol was added dropwise 10 ml a 10% aqueous sodium hydroxide solution while stirring. The reaction mixture was refluxed for 15 to 20 min. After cooling it was diluted with water, neutralized with hydrochloric acid, then evaporated to dryness. The residue was treated with chloroform. The organic phase was washed with water, separated, and dried on sodium sulfate. After removing the solvent, the residue was chromatographied on a silical gel column, using a mixture of ethyl acetate–hexane (5 : 5) as an eluent.

2-Substituted 4-Ethoxycarbonyl-1*H*,5*H*-2,3,6,7-tetrahydropyrrolo[1,2-*c*]pyrimidines (4a—g) To a solution of 0.023 mol of enaminoester **1** in 20 ml of ethanol was added slowly 5 ml of a solution of 35% aqueous formaldehyde then dropwise 0.025 mol of the appropriate primary amine. The mixture was stirred for 12 h at room temperature. After removing the solvent, the residue was treated with 100 ml of chloroform, the organic phase was washed with distilled water, separated and dried on sodium sulfate. The solvent was concentrated and the remaining solution was chromatographied on a silica gel column using a mixture of ethyl acetate–hexane (7 : 3) as an eluent.

The maleic acid salts were obtained by the dropwise addition of a solution of 0.002 mol of diazabicyclic derivative in 20 ml of anhydrous ether into 20 ml of ethereous solution containing 0.002 mol of maleic acid. The salt precipitated out as a white powder.

Immunomodulating Activity The human mononuclears from peripheral blood taken from healthy donors were separated by a Ficoll gradient and the T cells proliferation in the presence of PHA was investigated by the tritiated thymidine procedure with and without assayed compounds.[12]

It is noteworthy that the right transmembrane mechanism of T lymphocytes activation by mitogenes is just coming to be elucidated.[13]

Sedative Activity This was evaluated by a study of spontaneous motor activity. Groups of ten mice were used. The test was carried out by using the method of Boissier and Simon[14] in photoelectric activity cages (Apelex). Test drugs were administered 30 min before evaluation of spontaneous activity and the number of passages was scored during 10 min. Statistical analysis of the results was performed by using the method of Schwartz.[15] The level of significance was $p < 0.05$ in the Student's t test.

References

1) B. Refouvelet, P. Tronche, J. Couquelet, J. F. Robert, G. Bonnefoy-Claudet and J. Panouse-Perrin, *Eur. J. Med. Chem.*, **22**, 11 (1987).
2) J. P. Celerier, E. Deloisy, F. Lhommet and P. Maitte, *J. Org. Chem.*, **44**, 3089 (1979).
3) P. Brunerie, J. P. Celerier, H. Petit and G. Lhommet, *J. Heterocycl. Chem.*, **23**, 1183 (1986).
4) E. H. Bahaji, B. Refouvelet, J. Couquelet and P. Tronche, *C. R. Acad. Sci., Ser. II*, **303** 455 (1986).
5) E. H. Bahaji, J. Couquelet and P. Tronche, *C. R. Acad. Sci.*, **305**, 441 (1987).
6) E. H. Bahaji, P. Bastide, J. Bastide, C. Rubat and P. Tronche, *Eur. J. Med. Chem.*, **23**, 193 (1988).
7) M.Miocque, *Ann. Pharm. Fr.*, **27**, 381. (1969).
8) J. Mathieu and J. Weill-Raynal, "Introduction of an α Functional Carbon Chain. Formation of C–C Bonds. III," Georg Thieme Publ., Stutgart, 1979, p.238.
9) C. M. Blatteis, *Yale J. Biol. Med.*, **63**, 133 (1990).
10) N. E. Kay, J. E. Morley an J. I. Allen., *Immunology*, **70**, 485 (1990).
11) R. N. Spengler, R. M. Allen, D. G. Remick, R. M. Stricter and S. L. Kunkel, *Immunology*, **145**, 1430 (1990).
12) J. W. Hadden, E. M. Hadden and R. G. Coffey, *Infect. Immun.*, **13**, 382 (1975).
13) J. W. Hadden, *Immunol. Today*, **9**, 235 (1988).
14) J. R. Boissier and P. Simon, *Arch. Int. Pharmacodyn. Ther.*, **158**, 212 (1965).
15) D. Schwartz, "Méthodes Statistiques à l' Usage des Médecins et des Biologistes," ed. Médicales Flammarion, 1984, p. 263.

Cytotoxic Activity of Marine Algae and a Cytotoxic Principle of the Brown Alga *Sargassum tortile*

Atsushi NUMATA,*[,a] Syoichi KANBARA,[a] Chika TAKAHASHI,[a] Ryoko FUJIKI,[a] Michiko YONEDA,[a] Eiichi FUJITA,[a] and Yasunobu NABESHIMA[b]

Osaka University of Pharmaceutical Sciences,[a] 2–10–65 Kawai, Matsubara, Osaka 580, Japan and Osaka Prefectural Fisheries Experimental Station,[b] Misaki-cho, Sennan-gun, Osaka 599–03, Japan. *Received January 7, 1991*

Partition fractions of hexane, CCl_4 and $CHCl_3$ from methanolic extracts of marine algae were each examined for cytotoxic activities against cultured P-388 lymphocytic leukemia cells. Cytotoxic activities were found for partition fractions of 21 species of seaweed. Bioactivity-guided fractionation of the CCl_4 partition fraction from *Sargassum tortile*, exhibiting the most prominent activity, afforded dihydroxysargaquinone (1) and sargatriol (2) previously isolated from this alga. The former was evaluated as a cytotoxic principle, and the latter, showing moderate activity, was suggested to be an artifact derived from 1 during the isolation procedure.

Keywords marine alga; *Sargassum tortile*; cytotoxicity; dihydroxysargaquinone; sargatriol; benzoquinone; chromene

Previously it was reported that water extracts from some seaweeds showed tumor-inhibiting effects against Sarcoma-180 implanted subcutaneously in mice, or against Ehrlich ascites carcinoma in mice, and the tumor-inhibiting principle was a polysaccharide, whose tumor-inhibiting effect was suggested to be mainly host-mediated.[1] We initiated a survey of marine algae for antineoplastic and/or cytotoxic constituents other than polysaccharides. This paper describes the screening results of various seaweeds in the P-388 lymphocytic leukemia test system *in vitro*, in which a cytotoxic principle was found from the brown alga *Sargassum tortile* C. AGARDH (yoremoku in Japanese) (Sargassaceae).

Twenty-four species of fresh seaweed, collected along the coast of Tanabe Bay in Japan in May 1985, were extracted with MeOH, and a solution of each extract in aqueous MeOH was partitioned successively with hexane, CCl_4 and $CHCl_3$. The resulting fractions of each seaweed were tested for their growth-inhibitory activity on P-388 cultured cells. As a result, some partition fractions of 21 species of seaweed were shown to exhibit growth inhibition against P-388 cells, and the most prominent activity was found to be located in the CCl_4 partition fraction of *S. tortile* (Table I). This result led us to investigate the cytotoxic principle of *S. tortile*.

The CCl_4 partition fraction from the MeOH extract of *S. tortile* was purified by bioassay-directed fractionation employing Sephadex LH-20 and silica gel column chromatographies to afford dihydroxysargaquinone (**1**) and sargatriol (**2**), already isolated from this alga (Chart 1).[2] These compounds were identified by comparison of their spectral data with the reported values.[2]

For sargatriol (**2**), Kikuchi *et al.* proposed the C_2-α-methyl structure (**2a**) on the basis of a Cotton effect in the 265—275 nm region of circular dichroism (CD).[2a] The CD data of **2** obtained herein was consistent with the published values.[2a] However, in the carbon-13 nuclear magnetic resonance (^{13}C-NMR) spectrum of **2**, each of C-3, C-10, C-4′ and C-16′ appeared as two signals (*ca.* 1 : 1) as shown in Table II. The proton nuclear magnetic resonance (^{1}H-NMR) spectrum of **2** also exhibited signals due to an epimeric mixture (see Experimental). The same feature was observed in the ^{1}H- and ^{13}C-NMR spectrum of the methyl ether (**3**) derived from **2**. In addition, optical rotation and CD curves were not observed in the aldehyde (**4**) derived by oxidation of **3** with a chromium trioxide–pyridine complex. Furthermore, cyclization of **1** with hot pyridine afforded a chromene derivative identical to **2**. The sum of this evidence shows that sargatriol, obtained herein and previously,[2a] is a mixture of two epimers with respect to C-2. In addition to this evidence, the fact that crude dihydroxysargaquinone (**1**) converted into **2** on standing in a bit of MeOH at room temperature for about one month suggests the possibility that **2** is an artifact of the isolation procedure. The 265 nm CD value of **2**, identical to the published one,[2a] is one-tenth that of general chiral styrenes.[3] This weak Cotton effect is considered to appear as the sum of Cotton effects of two C-2 epimers, in which the signs are opposite and the absolute values are different due to the prenyl side-chain with asymmetric centers.

The absolute configuration of **1** has not yet been established. The above-mentioned transformation of **1** to **2** demonstrates that **1** has an *R* configuration at both

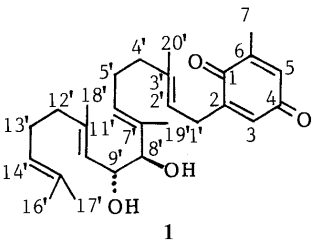

1

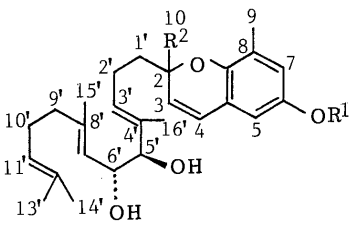

2 : R^1=H, R^2=CH_3 ; C_2 epimeric mixture

2a : R^1=H, R^2=β-CH_3

3 : R^1=R^2=CH_3, C_2 epimeric mixture

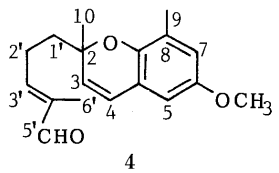

4

Chart 1

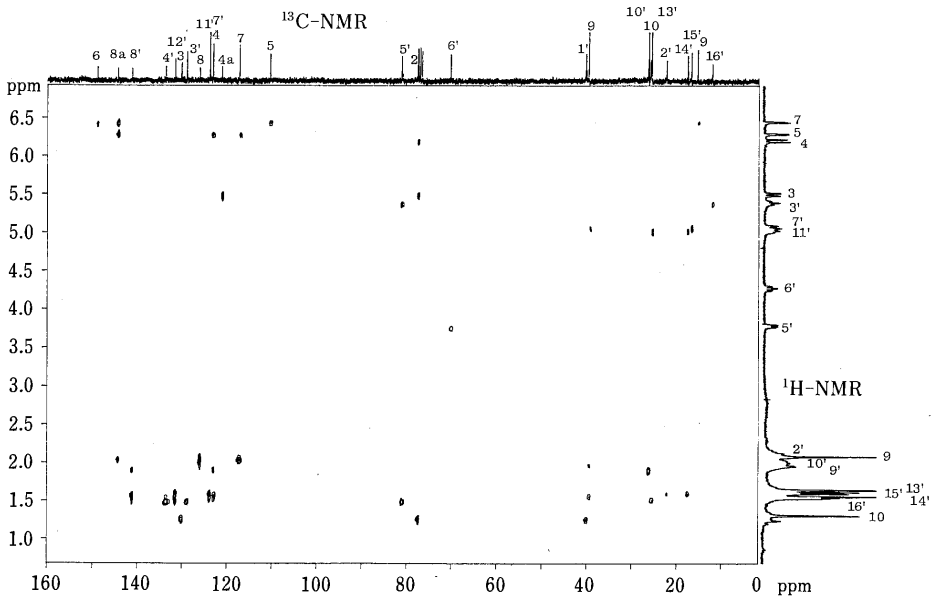

Fig. 1. The XCORFE Spectrum of Sargatriol (**2**)

TABLE I. Cytotoxicity of Partition Fractions of Algal Extracts toward P-388 Cells

Marine algae	ED_{50} (μg/ml)		
	Hexane fr.	CCl_4 fr.	$CHCl_3$ fr.
Brown algae			
Cystophyllum sisymbrioides	22.0	43.5	>100
Hizikia fusiforme	>100	>100	>100
Ecklonia cava	>100	>100	48.2
S. ringgoldianum	>100	>100	26.9
Padina arborescens	>100	>100	48.0
S. tortile	18.0	3.6	7.1
S. thunbergii	>100	13.6	5.6
Eisenia bicyclis	>100	46.5	>100
Dictyopteris prolifera	>100	>100	38.1
Undaria pinnatifira	>100	32.7	36.0
Laminaria japonica	>100	>100	98.8
S. hemiphyllum	>100	56.0	23.3
S. piluliferum	>100	>100	>100
Colpomenia sinuosa	>100	30.6	23.5
Red algae			
Gelidium amansii	>100	18.0	8.2
Scinaia japonica	13.0	>100	30.0
Amphiroa ephedraea	>100	30.5	>100
Schizymenia dubyi	>100	>100	>100
Acrosorium yendoi	25.0	14.0	>100
Chondrus ocellatus	>100	22.3	>100
Carpopeltis flabellata	>100	19.1	15.2
Gracilaria textorii	>100	22.2	32.2
Pterocladia capillacea	>100	>100	16.2
Green algae			
Ulva pertusa	>100	30.6	23.5

Cytotoxicity of etoposide as standard was ED_{50} 0.2 μg/ml.

TABLE II. ^{13}C-NMR Chemical Shifts (δ ppm) of **1**—**4**[a]

Position	**1**	**2**		**3**		**4**
1	187.93					
2	148.65	77.65		77.70		77.67
3	132.24	130.27	130.13	130.30	130.24	129.54
4	188.47	123.11		123.33		123.93
4a		121.17		121.01		120.72
5	133.14	110.49		108.86		109.03
6	146.25	148.97		152.96		153.14
7	15.82	117.30		116.10		116.33
8		126.12		126.14		126.17
8a		144.43		144.85		144.64
9		15.45		15.63		15.66
10		25.79	25.91	25.94	26.01	26.25
1′	27.48	40.24		40.35		39.49
2′	118.36	22.37		22.38		24.14
3′	139.63	129.03		128.75		154.63
4′	39.06	133.72	133.65	133.89	133.96	139.32
5′	25.60	81.15		81.04		195.27
6′	127.94	70.25		70.19		9.10
7′	134.71	123.18		123.33		
8′	80.79	141.32		141.19		
9′	70.11	39.59		39.62		
10′	123.47	26.35		26.39		
11′	141.01	123.86		123.88		
12′	39.71	131.61		131.66		
13′	26.47	25.69		25.69		
14′	123.92	17.68		17.70		
15′	131.65	16.86		16.88		
16′	25.68	12.20	12.00	12.28	12.22	
17′	17.74					
18′	16.89					
19′	12.53					
20′	16.05					
OCH_3				55.66		55.69

a) The data was taken in $CDCl_3$ at 75.4 MHz.

assymmetric centers (C-8′ and C-9′). Assignments of the ^{1}H- and ^{13}C-NMR spectra of **1** and **2** were based on the application of the ^{1}H-homonuclear decoupling technique and ^{1}H–^{13}C heteronuclear shift-correlated (HETCOR) and X-nucleus-proton correlation with fixed evolution time (XCORFE)[4] (Fig. 1) 2D-NMR spectra. Appearance of only one methyl resonance above 20 ppm in the ^{13}C-NMR spectra of **1** and **2** supports the theory that the prenyl side-chain double bonds are all-*E*-oriented.[5]

Compounds **1** and **2** exhibited significant and moderate cytotoxicities (ED_{50} 1.2 and 18.0 μg/ml) against P-388 cultured cells, respectively. However, these compounds did not demonstrate significant activity against the *in vivo* murine P-388 lymphocytic leukemia test system.

Experimental

CD curves were recorded on a JASCO J-500A Spectrometer. Other spectral measurements were carried out with the instruments described in the previous paper.[4]

Extraction and Fractionation of Marine Algae Each fresh alga, collected in May 1985 at the coast of Tanabe Bay, was finely cut and extracted three times with boiling MeOH. The combined extracts were evaporated *in vacuo*. The residue was successively partitioned between MeOH–H_2O (9 : 1) and hexane, MeOH–H_2O (8 : 2) and CCl_4, and MeOH–H_2O (1 : 1) and $CHCl_3$. Removal of the solvents gave hexane, CCl_4, $CHCl_3$ and MeOH–H_2O fractions.

Cytotoxic Activity Evaluation of cytotoxic activity for test material was made according to the procedure previously reported.[4]

Separation of Extract from *S. tortile* A second collection of *S. tortile* (8.8. kg) in Oct. 1985 was extracted with aqueous MeOH, and the resulting extract (586 g) was partitioned according to the procedure described above to afford hexane (58.9 g), CCl_4 (60.8 g), $CHCl_3$ (29.0 g) and MeOH–H_2O (430 g) fractions. The CCl_4 fraction (60 g) was passed through a Sephadex LH-20 column using MeOH–$CHCl_3$ (1 : 1) as the eluent. The cytotoxic activities of the resulting fifth, sixth and seventh fractions were evaluated as ED_{50} 13.7, 3.4 and 18.5 μg/ml, respectively. The sixth fraction (18 g) was repeatedly chromatographed on a silica gel column with a MeOH–$CHCl_3$ gradient as the eluent. Elution with 1% MeOH in $CHCl_3$ and 2% MeOH in $CHCl_3$ gave **1** (500 mg) and **2** (6 g), respectively.

Dihydroxysargaquinone (1) A pale brown oil, $[\alpha]_D^{22}$ +2.1° (c=0.95, $CHCl_3$). High resolution mass spectrum (HR-MS) m/z: 426.2774 (M^+) (Calcd for $C_{27}H_{38}O_4$: 426.2771). ^{1}H-NMR ($CDCl_3$, 300 MHz) δ ppm: 1.59 (6H, s, 17′, 20′-H), 1.61 (3H, s, 19′-H), 1.67 (6H, s, 16′, 18′-H), 2.02 (2H, m, 12′-H), 2.06 (2H, m, 13′-H), 2.07 (3H, d, J=1.1 Hz, 7-H), 2.13 (2H, m, 4′-H), 2.18 (2H, m, 5′-H), 2.43 (1H, s, OH), 3.13 (2H, br d, J=8 Hz, 1′-H), 3.16 (1H, s, OH), 3.85 (1H, d, J=8 Hz, 8′-H), 4.30 (1H, t, J=8 Hz, 9′-H), 5.07 (1H, t, J=7 Hz, 14′-H), 5.14 (1H, d, J=8 Hz, 10′-H), 5.15 (1H, t, J=8 Hz, 2′-H), 5.39 (1H, t, J=6 Hz, 6′-H), 6.49 (1H, dt, J=2.5, 1.6 Hz, 3-H), 6.56 (1H, dq, J=2.5, 1.1 Hz, 5-H). The ultraviolet (UV) and infrared (IR) spectral data of this compound were in accord with the published values.[2b]

Salgatriol (2) A pale brown oil, $[\alpha]_D^{22}$ +15.4° (c=1.0, $CHCl_3$). HR-MS m/z: 426.2772 (M^+) (Calcd for $C_{27}H_{38}O_4$: 426.2771). ^{1}H-NMR ($CDCl_3$) δ ppm: 1.34, 1.35 (3H, each s, 10-H), 1.57, 1.58 (3H, each br s, 16′-H), 1.59 (3H, s, 14′-H), 1.648, 1.653 (3H, each s, 15′-H), 1.67 (3H, s, 13′-H), 1.69 (2H, m, 1′-H), 1.98 (2H, m, 9′-H), 2.03 (2H, m, 10′-H), 2.12 (3H, s, 9-H), 2.15 (2H, m, 2′-H), 2.40 (1H, br s, OH), 3.80, 3.81 (1H, each d, J=8 Hz, 5′-H), 4.29, 4.30 (1H, each dd, J=9, 8 Hz, 6′-H), 4.70 (1H, s, OH), 5.05 (1H, br t, J=6 Hz, 11′-H), 5.11 (1H, br d, J=9 Hz, 7′-H), 5.43 (1H, br t, J=7 Hz, 3′-H), 5.54, 5.55 (1H, each d, J=10 Hz, 3-H), 6.246, 6.251 (1H, each d, J=10 Hz, 4-H), 6.31 (1H, d, J=3.5 Hz, 5-H), 6.47 (1H, d, J=3.5 Hz, 7-H). CD (c=5.54 × 10^{-4} mol/l, MeOH, 20 °C): $\Delta\varepsilon$ (nm): 0 (382), −0.40 (327), −0.19 (290), −0.28 (271), −0.89 (265), −0.70 (247), −2.26 (221), 0 (214). The UV and IR data of this compound were in accord with the published values.[2a]

Sargatriol Methyl Ether (3) Methylation of **2** (91 mg) with diazomethane followed by chromatography on silica gel under elution with 0.5% MeOH in CH_2Cl_2 yielded methyl ether **3** (43 mg) as a pale brown oil, $[\alpha]_D^{26}$ +17.6° (c=0.17, EtOH). HR-MS m/z: 440.2906 (M^+) (Calcd for $C_{28}H_{40}O_4$: 440.2924). ^{1}H-NMR ($CDCl_3$) δ ppm: 1.350, 1.354 (3H, each s, 10-H), 1.57 (3H, br s, 16′-H), 1.58 (3H, s, 14′-H), 1.63, 1.65 (3H, each d, J=1.3 Hz, 15′-H), 1.67 (3H, s, 13′-H), 1.70 (2H, m, 1′-H), 1.98 (2H, m, 9′-H), 2.03 (2H, m, 10′-H), 2.14 (2H, m, 2′-H), 2.15 (3H, s, 9-H), 2.40 (1H, br s, OH), 3.73 (3H, s, OCH_3), 3.79, 3.80 (1H, each d, J=7.6 Hz, 5′-H), 4.27, 4.28 (1H, each dd, J=8.8, 7.6 Hz, 6′-H), 5.05 (1H, br t, J=7 Hz, 11′-H), 5.09 (1H, br d, J=8.8 Hz, 7′-H), 5.42 (1H, br t, J=7 Hz, 3′-H), 5.55, 5.56 (1H, each d, J=10 Hz, 3-H), 6.287, 6.292 (1H, each d, J=10 Hz, 4-H), 6.38 (1H, d, J=3 Hz, 5-H), 6.55 (1H, d, J=3 Hz, 7-H).

Preparation of Aldehyde 4 Oxidation of **3** (40 mg) with a chromium trioxide–pyridine complex in the usual way, followed by chromatography on silica gel under elution with CH_2Cl_2, gave aldehyde **4** (12 mg) as a colorless oil. HR-MS m/z: 286.1568 (M^+) (Calcd for $C_{18}H_{22}O_3$: 286.1568). ^{1}H-NMR ($CDCl_3$) δ ppm: 1.40 (3H, s, 10-H), 1.70 (3H, s, 6′-H), 1.85 (2H, m, 1′-H), 2.16 (3H, s, 9-H), 2.51 (2H, m, 2′-H), 3.74 (3H, s, OCH_3), 5.56 (1H, d, J=9.8 Hz, 3-H), 6.34 (1H, d, J=9.8 Hz, 4-H), 6.40 (1H, d, J=3 Hz, 5-H), 6.51 (1H, br t, J=6.5 Hz, 3′-H), 6.57 (1H, d, J=3 Hz, 7-H), 9.36 (1H, s, 5′-H).

Transformation of 1 to 2 A solution of **1** (15 mg) in pyridine was heated at 50 °C for 48 h and evaporated *in vacuo*. The residue was chromatographed on silica gel and eluted with 5% MeOH in $CHCl_3$ to give **2** (8 mg).

Acknowledgement We are grateful to Drs. O. Shiratori and S. Takase, Research Laboratory, Shionogi & Co., Ltd., for advice on cell culture. Thanks are also due to Drs. S. Tsukagoshi and T. Tashiro, Cancer Chemotherapy Center, Japanese Foundation for Cancer Research, for *in vivo* screening tests, and to Miss M. Danjyo, this university, for MS measurements.

References

1) S. Nakazawa, H. Kuroda, F. Abe, T. Nishino, M. Ohtsuki, and I. Umezaki, *Chemotherapy*, **22**, 1435 (1974); S. Nakazawa, F. Abe, H. Kuroda, K. Kohno, T. Higashi, and I. Umezaki, *ibid.*, **24**, 443 (1976); S. Nakazawa, F. Abe, H. Kuroda, K. Kohno, T. Higashi, and I. Umezaki, *ibid.*, **24**, 448 (1976); M. Fujihara, K. Komiyama, I. Umezawa, and T. Nagumo, *ibid.*, **32**, 1004 (1984); I. Yamamoto, T. Nagumo, K. Yagi, H. Tominaga, and M. Aoki, *Jpn. J. Exp. Med.*, **44**, 543 (1974); I. Yamamoto, T. Nagumo, M. Fujihara, M. Takahashi, Y. Ando, M. Okada, and K. Kawai, *ibid.*, **47**, 133 (1977); M. Fujihara, N. Iizima, I. Yamamoto, and T. Nagumo, *Carbohydr. Res.*, **125**, 97 (1984); H. Ito and M. Sugiura, *Chem. Pharm. Bull.*, **24**, 1114 (1976).
2) *a*) T. Kikuchi, Y. Mori, T. Yokoi, S. Nakazawa, H. Kuroda, Y. Masada, K. Kitamura, and K. Kuriyama, *Chem. Pharm. Bull.*, **31**, 106 (1983); *b*) M. Ishitsuka, T. Kusumi, Y. Nomura, T. Konno, and H. Kakisawa, *Chem. Lett.*, **1979**, 1269.
3) P. Crabbé, *Chem. Ind.*, **1969**, 917.
4) A. Numata, P. Yang, C. Takahashi, R. Fujiki, M. Nabae, and E. Fujita, *Chem. Pharm. Bull.*, **37**, 648 (1989).
5) G. Englert, *Helv. Chim. Acta*, **58**, 2367 (1975).

Presence of Protein Polymorphism in Karasurin, an Abortifacient and Anti-tumor Protein, Identified with Physicochemical Properties

Shunsuke TOYOKAWA,[a] Tadahiro TAKEDA,[a] Yukio KATO,[b] Katsumi WAKABAYASHI[b] and Yukio OGIHARA*,[a]

Faculty of Pharmaceutical Sciences, Nagoya City University,[a] Tanabe-dori, Mizuho-ku, Nagoya 467, Japan and Hormone Assay Center, Institute of Endocrinology, Gunma University,[b] Showa-machi, Maebashi 371, Japan. *Recieved January 28, 1991*

Karasurin is an abortifacient plant protein isolated from fresh root tubers of *Trichosanthes kirilowii* MAXIMOWICZ var. *japonicum* KITAMURA (Cucurbitaceae). This study describes the presence of protein polymorphism in karasurin (karasurin-A and karasurin-B) separated by ion-exchange chromatography. Two components showed no differences in the molecular weight (*ca.* 28000), the amino acid composition, the neutral sugar content and part of the amino acid sequence. A unique difference was observed in their isoelectric points (10.1 for karasurin-A and 10.2 for karasurin-B). However, modifications of glycosylation or phosphorylation were not found. Biological assays for inducing mid-term abortion in pregnant mice and inhibition of the growth of BeWo cells gave no significant differences between them. The presence of protein polymorphism in karasurin, whose biological significance is not yet understood, is a first finding among several abortifacient proteins.

Keywords plant protein; karasurin; *Trichosanthes kirilowii* var. *japonicum*; abortifacient protein; anti-tumor protein; ion-exchange chromatograhy; isoelectric focusing; amino acid sequence

Karasurin, which was isolated from fresh root tubers of *Trichosanthes kirilowii* MAXIMOWICZ var. *japonicum* KITAMURA (Cucurbitaceae), was a highly basic protein with pI 10.1, and showed potent activity in inducing mid-term abortion in pregnant mice.[1] We have previously determined the complete amino acid sequence.[2]

In Cucurbitaceae, many abortifacient proteins are now known and show similar physicochemical properties to karasurin.[1-9] They are present as a single molecular form. It is interesting that this protein family has several biological roles such as anti-tumor, ribosome-inactivation and anti-human immunodeficiency virus (HIV) (the virus causing aquired immune deficiency syndrome (AIDS).[10-14]

We report herein the finding of an electrophoretic variant of karasurin, which was effective in inducing mid-term abortion in mice and showed strong inhibition of the growth of BeWo cells (human choriocarcinoma cell line) *in vitro* for the first time.

Materials and Methods

Purification Karasurin-A whose primary structure[2] was previously determined and karasurin-B (newly found in this study) were isolated from the acetone precipitate obtained from root tubers of *T. kirilowii* MAX. var. *japonicum* KITAM. (collected in the botanical garden of Nagoya City University) as previously described.[1]

Acetone powder (100 mg), fraction P1,[1] was separated by ion-exchange chromatography on Toyopearlpak SP 650S (2.2 × 20 cm: Tosoh) with a linear gradient of 0—0.1 M NaCl in 20 mM potassium phosphate buffer (pH 6.5) at a flow rate of 4 ml/min. The eighth and tenth peaks, karasurin-A and -B, respectively, were collected, dialyzed against distilled water, and lyophilized.

Biological Assays The assay of mid-term abortifacient activity was performed by the administration of karasurin-A or -B intraperitoneally on day 12 post coitum (PC). Mice were autopsied on day 14 PC. The total number of implantation sites in uterine was recorded and their sizes measured. The numbers of live fetuses, dead fetuses whose hearts had stopped pulsating, and resorbing fetuses were recorded.[1]

The assay of the inhibition of cell growth was performed essentially according to the MTT (3-[4,5-dimethylthiazol-2-yl]-2,5-diphenyl-tetrazolium bromide) method[15] using a human choriocarcinoma cell line, BeWo (kindly supplied by Japanese Cancer Research Resources Bank). About 2×10^3 cells in 0.1 ml of culture medium (RPMI 1640 supplemented with 10% fetal calf serum) were inoculated into 96-well culture plates. After 24 h of incubation in a humidified 5% CO_2 atmosphere at 37 °C, karasurin-A or -B in culture medium was added to each well at various concentrations. Cells were incubated for 48 h. The inhibition of cell growth with karasurin-A or -B was assayed by measurement of dehydrogenase activity using MTT (Sigma). After incubation with MTT (50 μg in 10 μl phosphate-buffered saline per well) for 6 h, the resulting products were dissolved by adding 100 μl/well of 10% sodium dodecyl sulfate (SDS) for 24 h at 37 °C. The optical density (OD) measured the difference between 550 and 630 nm using an automatic plate reader (Corona Electric). The results were computed for each well against the incubate without karasurin as a control.

Physicochemical Analyses The molecular weight was determined by SDS-polyacrylamide gel electrophoresis[16] with 15% gel using the molecular weight standards (MW 14400—97400: Bio-Rad).

Deglycosylation was performed for sample (50 μg) with glycopeptidase F (2 munits: Takara) in 0.16 M sodium phosphate buffer, pH 8.6, at 37 °C for 16 h. Dephosphorylation was performed for sample (50 μg) with bacterial alkaline phosphatase (250 units: Bethesda Research Laboratories) in 0.01 M Tris–HCl, pH 8.0, at 37 °C for 30 min. Isoelectric focusing was performed with PhastSystem and PhastGel IEF 3—9 (Pharmacia) using the pI-Marker kit (pI 4.1—10.6: Oriental Yeast).

The neutral sugar content was analyzed by the phenol–sulfuric acid method,[17] with glucose as a standard. The amino acid composition was determined as previously described.[1] The amino acid sequence of the N-terminal region was determined by automated Edman degradation using an Applied Biosystems model 477A automated gas phase sequencer.

Results and Discussion

Separation by ion-exchange chromatography on Toyopearlpak SP 650S (Fig. 1) revealed that karasurin-B was

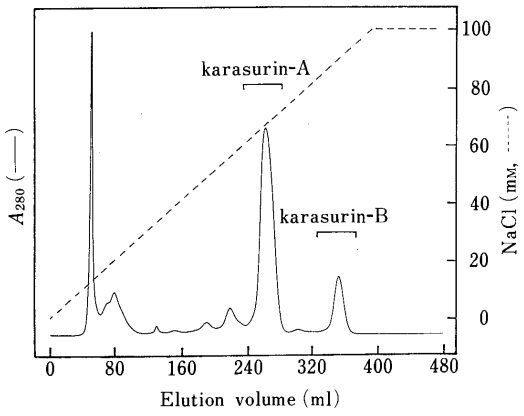

Fig. 1. Ion-Exchange Chromatography on Toyopearlpak SP 650S of Fraction P1

TABLE I. Mid-Term Abortifacient Activities of Karasurin-A and -B

	Dose (mg/kg)	No. of mice	No. of aborted mice[a] per No. of treated mice
Control	0.2 ml saline	5	0/5 (0%)
Karasurin-A	2.5	5	5/5 (100%)
Karasurin-B	2.5	6	6/6 (100%)

a) Mice were considered to be aborted when the dead fetuses were more than 50% of the total number of implantation sites on day 14 PC.

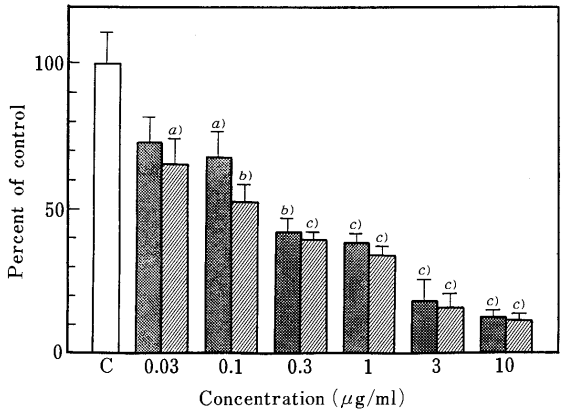

Fig. 2. Effects of Karasurin-A and -B on Growth of BeWo Cells

□, control (C); ▩, karasurin-A; ▨, karasurin-B. Each bar and vertical line represent the mean and S.E. of 6—8 experiments in each experimental group. *a*) $p<0.05$, *b*) $p<0.01$, *c*) $p<0.001$ *vs.* control.

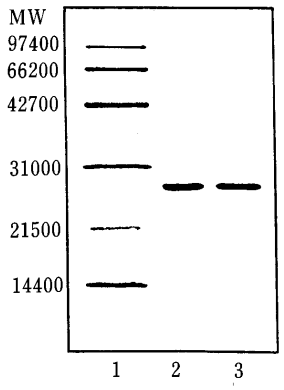

Fig. 3. SDS-Polyacrylamide Gel Electrophoreses of Karasurin-A and -B

Samples were: lane 1, marker proteins (molecular sizes are indicated at the left); lane 2, karasurin-A; lane 3, karasurin-B. The gel was stained with Coomassie brilliant blue R-250.

eluted at the tenth peak, whereas karasurin-A was present at the eighth peak.[1] Karasurin-B was adsorbed on a column more strongly than karasurin-A. Karasurin-A and -B comprised 60% and 10% of the protein loaded, respectively.

The biological activity of *in vivo* mid-term abortifacient activity in mice was assayed for karasurin-A and -B. The results (Table I) show that a single intraperitoneal injection of a dose of 2.5 mg/kg of karasurin-A or -B on day 12 PC induced abortion in all pregnant mice.

The effects of karasurin-A and -B on the growth of BeWo cells are assayed (Fig. 2). Both proteins significantly inhibited the cell growth above 0.1 μg/ml. The biological activities of both proteins were dose dependent and almost the same.

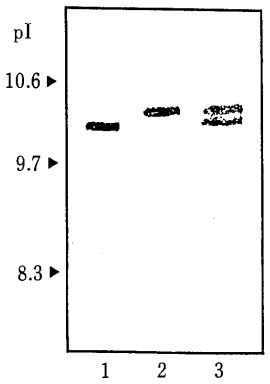

Fig. 4. Isoelectric Focusing Profiles of Karasurin-A and -B

Samples were: lane 1, karasurin-A; lane 2, karasurin-B; lane 3, karasurin-A plus -B. The positions of pI markers are indicated at the left. The gel was stained with PhastGel Blue R.

TABLE II. Amino Acid Compositions (mol%) and Neutral Sugar Contents (mol/mol protein) of Karasurin-A and -B

	Karasurin-A	Karasurin-B
Asn/Asp	11.2	11.1
Thr	6.6	6.6
Ser	8.9	8.8
Gln/Glu	8.5	8.6
Pro	3.2	2.8
Gly	4.7	5.0
Ala	11.1	11.5
Cys	0.0	0.0
Val	6.1	6.1
Met	0.8	1.2
Ile	7.3	7.2
Leu	10.7	10.6
Tyr	5.9	5.8
Phe	3.8	3.8
Lys	4.8	4.8
His	0.3	0.3
Arg	5.7	5.7
Trp	0.4	0.4
Neutral sugar	<0.60	<0.63

TABLE III. The N-Terminal Sequences of Karasurin-A and -B

	1	10	20	30
Karasurin-A	DVSFRLSGA	TSSSYGVFIS	NLRKALPYER	KLYDIPLL
Karasurin-B	DVSFRLSGA	TSSSYGVFIS	NLRKALPYER	KLYDIPLL

SDS–polyacrylamide gel electrophoresis of karasurin-A and -B showed an identical mobility with the molecular weight estimated to be 28000 (Fig. 3).

Since karasurin-B is more basic than karasurin-A on ion-exchange chromatography, non-equilibrium isoelectric focusing was performed by running the proteins from cathode to anode. Karasurin-B gave a single band and was shown to be more basic (pI 10.2) than karasurin-A (pI 10.1) (Fig. 4). To search for a modification of the karasurins, treatment of glycosidase or phosphatase was performed. The isoelectric focusing profiles of karasurin-A and -B did not change (data not shown).

Analyses of the amino acid composition of karasurin-A and -B showed no significant differences between them. The neutral sugar contents of two proteins were less than 0.63 mol/mol protein (Table II).

Table III shows the amino acid sequences of the N-terminal 37 residues of karasurin-A and -B and the sequences were identical.

Karasurin-B, which was newly isolated in this study, was obtained at about one-sixth of karasurin-A.[1] Karasurin-B showed a strong abortion effect in pregnant mice and strong anti-tumor activity in BeWo cells, the same as karasurin-A. Moreover, physicochemical properties in the molecular weight, the neutral sugar content, the amino acid composition and the amino acid sequence of the N-terminal 37 residues showed no differences between karasurin-A and -B. The only difference between them is basicity as found in ion-exchange chromatography and isoelectric focusing. These facts suggested that electrophoretic variants are present in karasurin. However, the isoelectric focusing profiles of glycosidase- or phosphatase- treated karasurin-A and -B indicate the absence of glycosylation or phosphorylation. Furthermore, microheterogeneity of the amino acid sequence of karasurin is not convinced by the partial analyses of the peptides of karasurin-B (unpublished data). An alternative explanation of the polymorphism is a difference in the contents of Asn and Gln/Asp and Glu between Karasurin-A and -B.

Recently, it is becoming known that some abortifacient and anti-tumor proteins, a family of karasurin, obtained from the Cucurbitaceae subspecies have additional biological activities such as ribosome-inactivation[11-13] and anti-HIV.[10] It will be interesting to know how the polymorphic karasurin molecules perform various biological activities in the future.

Acknowledgments The authors are grateful to Dr. K. Sakamoto and Mr. Y. Waki of the Tumura Research Institute for Pharmacology for their valuable suggestions and encouragement.

References

1) S. Toyokawa, T. Takeda and Y. Ogihara, *Chem. Pharm. Bull.*, **39**, 716 (1991).
2) S. Toyokawa, T. Takeda, Y. Kato, K. Wakabayashi and Y. Ogihara, *Chem. Pharm. Bull.*, **39**, 1244 (1991).
3) E. J. Collins, J. D. Robertus, M. LoPresti, K. L. Stone, K. R. Williams, P. Wu, K. Hwang and M. Piatak, *J. Biol. Chem.*, **265**, 8665 (1990).
4) T. P. Chow, R. A. Feldman, M. Lovett and M. Piatak, *J. Biol. Chem.*, **265**, 8670 (1990).
5) H. W. Yeung, T. B. Ng, N. S. Wong and W. W. Li, *Int. J. Peptide Protein Res.*, **30**, 135 (1987).
6) H. W. Yeung and W. W. Li, *Int. J. Peptide Protein Res.*, **29**, 289 (1987).
7) H. W. Yeung, T. B. Ng, W. W. Li and W. K. Cheung, *Planta Medica*, **1987**, 164.
8) Y. Wang, R. Q. Qian, Z. W. Gu, S. W. Jin, L. Q. Zhang, Z. X. Xia, G. Y. Tian and C. Z. Ni, *Pure & Appl. Chem.*, **58**, 789 (1986).
9) H. W. Yeung, W. W. Li, W. Y. Chan, L. K. Law and T. B. Ng, *Int. J. Peptide Protein Res.*, **28**, 518 (1986).
10) M. S. McGrath, K. M. Hwang, S. E. Caldwell, I. Gaston, K.-C. Luk, P. Wu, V. L. Ng, S. Crowe, J. Daniels, J. Marsh, T. Deinhart, P. V. Lekas, J. C. Vennari, H.-W. Yeung and J. D. Lifson, *Proc. Natl. Acad. Sci. U.S.A.*, **86**, 2844 (1989).
11) H. W. Yeung, W. W. Li, Z. Feng, L. Barbieri and F. Stirpe, *Int. J. Peptide Protein Res.*, **31**, 265 (1987).
12) P. Casellas, D. Dussossoy, A. I. Falasca, L. Barbieri, J. C. Guillemot, P. Ferrara, A. Bolognesi, P. Cenini and F. Stirpe, *Eur. J. Biochem.*, **176**, 581 (1988).
13) J. M. Maraganore, M. Joseph and M. C. Bailey, *J. Biol. Chem.*, **262**, 11628 (1987).
14) S. W. Tsao, K. T. Yan and H. W. Yeung, *Toxicon*, **24**, 831 (1986).
15) T. Mosmann, *J. Immunol. Methods*, **65**, 55 (1983).
16) U. K. Laemmli, *Nature* (London), **227**, 680 (1970).
17) J. E. Hodge and B. T. Hofreiter, "Methods in Carbohydrate Chemistry," Vol. 1, ed. by R. L. Whistler and M. L. Wolfrom, Academic Press, 1962, p. 388.

Hematological Studies on Naturally Occurring Substances. VI.[1] Effects of an Animal Crude Drug "Chan Su" (Bufonis Venenum) on Blood Coagulation, Platelet Aggregation, Fibrinolysis System and Cytotoxicity

Jen-Der WANG,[a] Takao NARUI,[a] Satoshi TAKATSUKI,[a] Takao HASHIMOTO,[b] Fumiko KOBAYASHI,[c] Hisao EKIMOTO,[c] Hideo ABUKI,[c] Kunihiro NIIJIMA,[c] and Toru OKUYAMA*,[a]

Department of Pharmacognosy and Phytochemistry,[a] Pharmacology,[b] Meiji College of Pharmacy, Nozawa 1–35–23, Setagaya-ku, Tokyo 154, Japan and Research Laboratories, Nippon Kayaku Co., Ltd.,[c] Shimo 3–31–12, Kita-ku, Tokyo 115, Japan. *Received February 26, 1991*

During the screening test of the animal crude drug "Chan su" (Chinese name, toad-cake), the venom of *Bufo bufo gargorizans* CANTOR (Bufonidae), on blood coagulation, platelet aggregation, fibrinolysis system and cytotoxicity, the ethyl acetate extract showed promotive action on platelet aggregation and remarkable cytotoxic activity on HeLa-S_3 cells. Nine kinds of bufadienolides were isolated from the ethyl acetate extract by bioactivity-guided fractionation and were identified by chemical and spectral analysis.

Keywords hematological study; Chan su; *Bufo bufo gargorizans*; blood coagulation; platelet aggregation; fibrinolysis system; cytotoxicity; HeLa-S_3 cell; bufadienolide; Bufonidae

"Chan su" (Bufonis Venenum) is a dry toad venom collected by squeezing the secretion directly from the parotid gland and sebaceous gland of Chinese toads, either *Bufo bufo gargorizans* CANTOR or *B. melanosticus* SCHNEIDER (Bufonidae). It is used in clinical therapy to stimulate heart contraction, for diuresis, to relieve pain and as an anti-tumor remedy in oriental medicine.[2]

We previously reported the screening test of animal crude drugs on blood coagulation and the fibrinolysis system.[3] To carry out systematic studies on the physiological activities of the animal crude drug Chan su, we extracted and separated the material in the manner shown in Experimental to obtain the corresponding AcOEt-, MeOH- and H_2O extracts, respectively, and investigated the hematological effect and cytotoxicity on HeLa-S_3 cells. The MeOH- (56%) and H_2O extract (88%) showed relatively strong activity on the fibrinolytic system, and the AcOEt- (82%) and H_2O extract (64%) showed promotive action on platelet aggregation (see Fig. 1). As shown in Table I, the AcOEt extract was recognized to have a remarkable cytotoxic effect on HeLa-S_3 cells, and was subsequently submitted to column chromatography on silica gel to provide twelve fractions (fr. 1—12). Fractions 5—8 and 10, exhibiting more potent cytotoxicity against HeLa-S_3 cells, were purified by high performance liquid chromatography (HPLC) on a reversed phase column and recrystallized to obtain 9 kinds of bufadienolides: bufalin (**1**), cinobufagin (**2**), resibufogenin (**3**), gamabufotalin (**4**), hellebrigenin (**5**), telocinobufagin (**6**), desacetylcinobufagin (**7**), bufotalin (**8**) and cinobufotalin (**9**), as shown in Chart 1. Each compound was identified by comparison of mp and $[\alpha]_D$, infrared (IR), fast atom bombardment mass spectra (FAB-MS), electron impact mass spectra (EI-MS), proton and carbon-13 nuclear magnetic resonance (^{1}H- and ^{13}C-NMR) spectral data of authentic samples.[4–8]

Further, all of them were examined for blood coagulation by plasma recalcification time method, platelet aggregation by adenosine diphosphate (ADP)-induced aggregation of

TABLE I. Cytotoxic Activity of Extracts, Fractions and Bufadienolides Obtained from Chan Su on HeLa-S_3 Cells (IC_{50} Value)

Sample name	IC_{50} (μg/ml)	Sample name	IC_{50} (μg/ml)
AcOEt extr.	0.0096	Fr.11	0.0470
MeOH extr.	0.021	Fr.12	0.235
Fr. 1	>1	**1**	0.000615
Fr. 2	>1	**2**	0.0208
Fr. 3	0.412	**3**	0.550
Fr. 4	0.0126	**4**	0.014
Fr. 5	0.00789	**5**	0.014
Fr. 6	0.00240	**6**	0.037
Fr. 7	0.0313	**7**	0.025
Fr. 8	0.0228	**8**	0.020
Fr. 9	0.0450	**9**	0.11
Fr.10	0.00438		

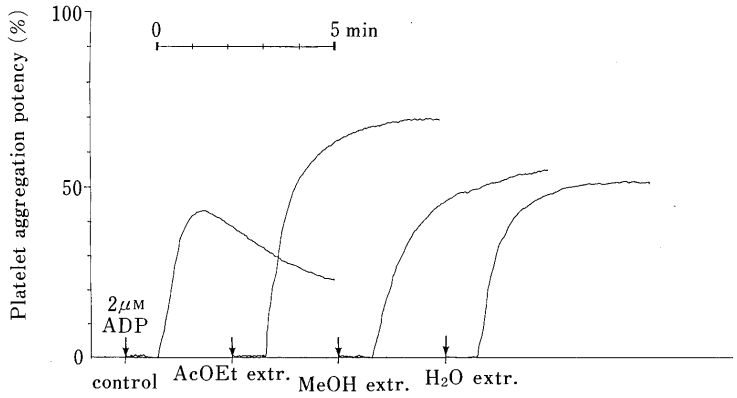

Fig. 1. Effects of Extracts of Chan Su on ADP-Induced Blood Platelet Aggregation (Rabbit)

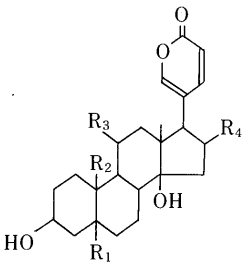

	R_1	R_2	R_3	R_4
1	H	CH_3	H	H
4	H	CH_3	OH	H
5	OH	CHO	H	H
6	OH	CH_3	H	H
8	H	CH_3	H	OAC

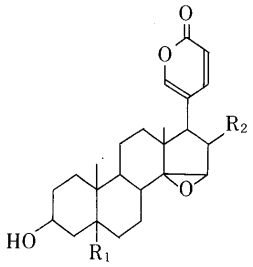

	R_1	R_2
2	H	OAC
3	H	H
7	H	OH
9	OH	OAC

Chart 1. Structures of Bufadienolides Isolated from Chan Su

TABLE II. Effects of Bufadienolides on Blood Coagulation, Platelet Aggregation and Fibrinolysis System

Bufadienolide	Coagulation (%)	Platelet aggregation (%)	Fibrinolysis (%)
1	1	−16	−31
2	−1	32	−29
3	−3	5	−8
4	3	−14	−23
5	−3	19	−22
6	−2	22	2
7	−6	0	−18
8	−10	13	−3
9	−5	14	4

TABLE III. Contents of Adrenaline and Noradrenaline in Chan Su

Sample	Contents of catecholamine (%)	
	Adrenaline	Noradrenaline
Powder of Chan su	2.94	0.13
AcOEt extr.	Trace	Trace
MeOH extr.	1.72	0.06
H_2O extr.	4.37	0.08

rabbit platelet, fibrinolysis system by fibrin plate method (see Table II) and cytotoxicity against HeLa-S_3 cells (see Table I).

It was found that compound **1** showed the most excellent cytotoxic activity, and **4** and **5** also exhibited relatively strong activity. Most compounds, however, had less activity in blood coagulation, platelet aggregation and the fibrinolysis system.

In addition, we determined adrenaline and noradrenaline content in Chan su by a HPLC method owing to the promotive effect of platelet aggregation.[9a,b] The data presented in Table III, in conjunction with Fig. 1, suggest that the promotive effect on platelet aggregation of Chan su is not only due to adrenaline but also to the synergism of interaction in bufadienolides or to other active substance existing in it.

Experimental

Spectroscopy All melting points were taken on a micro hot-stage apparatus and are uncorrected. Optical rotations were measured with a JASCO model DIP-4 automatic polarimeter. IR spectra were recorded by Hitachi model 215, JASCO model IRA-1 and IR-S spectrometers. Mass spectral measurements were run on a JEOL model JMS-DX 302 and a JASCO model ZABHF spectrometer. NMR spectra were recorded with tetramethylsilane (TMS) as an internal standard on a JEOL model FT-NMR GSX-400 and a Varian FT-NMR GEMA-200 spectrometer at 50 and 200 MHz, respectively. HPLC was carried out on a Beckman model 110A pump equipped with a SSC Y-1000 UV detector and a Senshu pak. ODS-3251 column (i.d. 8 × 250 mm).

Materials The crude drug Chan su was imported from the Chinese market by Mikuni Co. (Osaka, Japan). All reagents were of fine grade.

Extraction of Chan Su The materials (315 g) were crushed and pulverized, then successively extracted with AcOEt, MeOH and water (3 l × 3, 2 h per extraction) under reflux. The AcOEt and MeOH solutions were evaporated *in vacuo* to dryness and the water solution was lyophilized to yield AcOEt (A: 6 g), MeOH (M: 82 g) and water (W: 112 g) extract, respectively.

Isolation of Bufadienolides 1—9 The AcOEt extract (6 g) was subjected to column chromatography on silica gel and eluted successively with acetone–chloroform–cyclohexane (3 : 3 : 4) to give 12 fractions (Frs. 1—12). Fractions 5 (0.51 g) and 6 (1.24 g) were separated by HPLC using MeOH–H_2O (7 : 3) as a solvent and were further purified by recrystallization to give compounds **1** (16 mg), **2** (28 mg) and **3** (46 mg). Fractions 10 (0.68 g) and 11 (0.92 g) were separated by HPLC using MeOH–H_2O (2 : 1) as a solvent and were further purified by recrystallization to give compounds **4** (18 mg), **5** (21 mg), **6** (24 mg) and **7** (12 mg). Fractions 7 (0.38 g) and 8 (0.46 g) were separated by HPLC using MeOH–H_2O (2 : 1) as a solvent and were further purified by recrystallization to give compounds **8** (11 mg) and **9** (14 mg).

Compound **1** was recrystallized from acetone–MeOH to give bufalin (**1**) as colorless needles. mp 225—234 °C. $[\alpha]_D^{22.5}$ −8.7° (c=0.32, $CHCl_3$). EI-MS m/z: 386 (M^+). ^{1}H-NMR (in $CDCl_3$, 400 MHz) δ: 0.70 (s), 0.95 (s), 2.46 (dd, J=9.53, 6.76 Hz), 4.14 (br s), 6.26 (d, J=9.84 Hz), 7.23 (d, J=2.29 Hz), 7.84 (dd, J=9.84, 2.29 Hz).

Compound **2** was recrystallized from ether–acetone to give cinobufagin (**2**) as colorless prisms. mp 210—215 °C. $[\alpha[_D^{22.5}$ −3.7° (c=0.26, $CHCl_3$). EI-MS m/z: 442 (M^+). FAB-MS m/z: 443 ($M+H^+$). ^{1}H-NMR (in $CDCl_3$, 200 MHz) δ: 0.82 (s), 0.99 (s), 1.89 (s), 2.80 (d, J=9.33 Hz), 3.66 (d, J=1.32 Hz), 4.16 (br s), 5.46 (dd, J=9.33, 1.32 Hz), 6.22 (d, J=9.24 Hz), 7.17 (br s), 7.93 (d, J=9.24 Hz).

Compound **3** was recrystallized from acetone–H_2O to give resibufogenin (**3**) as colorless amorphous substance. mp 153—156 °C. $[\alpha]_D^{22}$ −7.4° (c=0.92, $CHCl_3$). EI-MS m/z: 384 (M^+), FAB-MS m/z: 385 ($M+H^+$). ^{1}H-NMR (in $CDCl_3$, 200 MHz) δ: 0.78 (s), 0.99 (s), 2.48 (d, J=10.14 Hz), 3.53 (s), 4.14 (br s), 6.25 (dd, J=9.74, 1.06 Hz), 7.25 (dd, J=2.64, 1.06 Hz), 7.80 (dd, J=9.74, 2.64 Hz).

Compound **4** was recrystallized from acetone–MeOH to give gamabufotalin (**4**) as colorless prisms. mp 260—264 °C. $[\alpha]_D^{22}$ 1.5° (c=0.36, MeOH). EI-MS m/z: 402 (M^+). FAB-MS m/z: 403 ($M+H^+$). ^{1}H-NMR (in DMSO-d_6, 200 MHz) δ: 0.61 (s), 0.96 (s), 3.44 (br s), 3.89 (br s), 4.04 (d, J=6.14), 4.14 (s), 4.14 (s), 6.29 (d, J=9.67 Hz), 7.55 (d, J=2.53 Hz), 7.90 (dd, J=9.67, 2.53 Hz).

Compound **5** was recrystallized from acetone to give hellebrigenin (**5**) as colorless plates. mp 154—159/232—236 °C. $[\alpha]_D^{22}$ 21.9° (c=0.42, $CHCl_3$). EI-MS m/z: 416 (M^+). FAB-MS m/z: 417 ($M+H^+$); ^{1}H-NMR (in DMSO-d_6, 200 MHz), δ: 0.55 (s), 2.44 (d, J=8.43 Hz), 4.02 (br s), 4.33 (br s), 5.20 (s), 5.37 (br s), 6.30 (d, J=9.84 Hz), 7.52 (d, J=2.01 Hz), 7.92 (dd, J=9.84, 2.01 Hz), 10.05 (s).

Compound **6** was recrystallized from acetone to give telocinobufagin (**6**) as colorless needles. mp 154—157/204—206 °C. $[\alpha]_D^{22}$ 5.4° (c=0.48, $CHCl_3$). EI-MS m/z: 402 (M^+). FAB-MS m/z: 403 ($M+H^+$). ^{1}H-NMR (in DMSO-d_6, 200 MHz), δ: 0.60 (s), 0.82 (s), 2.45 (d, J=9.44 Hz), 4.01 (br s), 4.18 (s), 4.82 (s), 5.22 (d, J=4.03 Hz), 6.29 (d, J=9.81 Hz), 7.52 (d, J=2.52 Hz), 7.93 (dd, J=9.81, 2.52 Hz).

Compound **7** was recrystallized from acetone–ether to give desacetylcinobufagin (**7**) as colorless particles. mp 180—220 °C. $[\alpha]_D^{22}$ 18.4° (c=0.24, $CHCl_3$). EI-MS m/z: 400 (M^+). FAB-MS m/z: 401 ($M+H^+$). ^{1}H-NMR (in $CDCl_3$, 200 MHz) δ: 0.80 (s), 0.99 (s), 2.61 (d, J=9.23 Hz), 3.58 (d, J=1.19 Hz), 4.15 (br s), 4.75 (dd, J=9.23, 1.19 Hz), 6.22 (d, J=9.79 Hz), 7.24 (dd, J=2.59, 0.96 Hz), 7.99 (dd, J=9.79, 2.59 Hz).

Compound **8** was recrystallized from acetone to give bufotalin (**8**) as colorless prisms. mp 226—229 °C. $[\alpha]_D^{22.5}$ 4.0° (c=0.16, $CHCl_3$). EI-MS m/z: 444 (M^+). FAB-MS m/z: 445 ($M+H^+$). ^{1}H-NMR (in $CDCl_3$, 200 MHz) δ: 0.78 (s), 0.95 (s), 1.87 (s), 2.65 (dd, J=15.49, 8.95 Hz), 2.88 (d, J=8.95 Hz), 4.15 (br s), 5.54 (m), 6.20 (dd, J=9.39, 0.93 Hz).

Compound **9** was recrystallized from acetone–ether to give cinobufotalin

(**9**) as colorless plates. mp 249—255 °C. $[\alpha]_D^{22.5}$ 13.3° ($c=0.28$, $CHCl_3$). EI-MS *m/z*: 458 (M^+). FAB-MS *m/z*: 459 ($M+H^+$). ^{1}H-NMR (in $CDCl_3$, 200 MHz) δ: 0.83 (s), 0.98 (s), 1.90 (s), 2.81 (d, $J=9.43$ Hz), 3.26 (d, $J=1.34$ Hz), 4.21 (br s), 5.45 (dd, $J=9.43$, 1.34 Hz), 6.22 (d, $J=9$, 12 Hz), 7.1 (d, $J=1.10$ Hz), 7.92 (d, $J=9$, 12 Hz).

Blood Coagulation A water soluble test sample (5 mg) was dissolved in 250 μl of saline or a water insoluble sample (5 mg) was dissolved in 250 μl of DMSO. A mixture containing 30 μl of test solution and 150 μl of platelet poor plasma (PPP) obtained from a healthy Japanese white male rabbit in the manner reported previously[3] was incubated for 60 s with stirring, then dropped into 150 μl of 0.025 M $CaCl_2$ solution at 37 °C. Saline or DMSO was used as a control. Coagulation time was evaluated by an automatic recording apparatus (KC-4A, Amelung GmbH, Lemgo) based on the viscosity change of the plasma. Each sample was tested at least 3 times on the plasma of each of 3—5 test animals. The average time was calculated by the following equation: ratio of anti-coagulation (%) = [(coagulation time of each test solution/coagulation time of control) − 1] × 100.

Platelet Aggregation By the same method as the blood coagulation test, fresh blood (9 ml) containing 3.8% sodium citrate (1 ml) was centrifuged at 1000 rpm for 20 min at room temperature to obtain a clear supernatant as platelet-rich plasma (PRP). PPP was prepared by centrifugation of the remaining blood at 3000 rpm for 10 min. A water soluble sample (5 mg) was dissolved in 1 ml of saline, 25 μl of which was added to 175 μl of PRP; a sample (5 mg) of low saline solubility was dissolved in 200 μl of MeOH, 5 μl of which was added to 195 μl of PRP, then dropped into 25 μl 50 mM $CaCl_2$ and incubated at 37 °C for 1 min with stirring. The platelet aggregation was induced in a final concentration of 2 μM ADP and determined by a light transmission method slightly modified from that of Okuyama *et al.*[10a] as reported previously,[10b] using a platelet aggregometer of PAM-8T (Mebanix Corporation). Saline or MeOH was used as a control. As shown in Fig. 1 the ratio of platelet aggregation potency is assigned as 0% PRP transmission and 100% PPP transmission.[11] The activity of anti-platelet aggregation (%) was calculated by the following equation: ratio of anti-platelet aggregation (%) = [(platelet aggregation potency of sample/platelet aggregation potency of control) − 1] × 100.

Fibrinolytic Activity Preparation of the fibrin plate was carried out according to the procedure previously reported.[3] A mixture of 100 μl of each test solution, 30 μl of urokinase solution (600 U/ml) and 10 μl of aliquot was placed in each of the two wells in two plates. The control used phosphate buffer in place of the sample. After incubation at 37 °C for 18 h, the diameters of the sample- and control-lysed area were measured. This procedure was repeated at least 3 times. The value of activity (%) was calculated by the following equation: fibrinolytic activity (%) = [(lysed area of test solution/lysed area of control) − 1] × 100.

Cytotoxic Activity HeLa-S_3 cells were adjusted to the concentration of 7.5×10^3 cells/ml and 0.2 ml of cells suspension were seeded into each well of a 96 well tissue culture plate (Coster). The cells were precultured for 24 h at 37 °C in a 5% CO_2 incubator. Then, 10 μl of various concentrations of samples was put into each well and the plates were incubated for 72 h at 37 °C in a 5% CO_2 incubator. Following incubation, the medium in the well was discarded. The cells were fixed with MeOH for 2 min and then stained for 30 min with a solution of 0.05% methylene blue in 10 mM Tris–HCl buffer (pH 8.5). The plates were washed 3 times with distilled water and left to dry at room temperature. Each well as filled with 200 μl of 3% HCl in order to dissolve the dye on the adherent cells. The optical density of HCl solution was measured on an automatic photometer (Dynatech Laboratories Inc., Tokyo, Japan) at 660 nm. Percents of growth inhibition rates (%) were calculated by the following formula: percent of growth inhibition (%) = [1 − A_{660} (treated cells)/ A_{660} (control cells)] × 100. IC_{50} values were calculated from the growth inhibition curve drawn on a piece of logarithmic-probability graph paper.

Determination of Adrenaline Content Chan su powder and its extracts (50 mg of each) were dissolved in 5 ml of Ringer solution (NaCl 6.0 g, KCl 0.075 g, $CaCl_2$ 0.1 g, $NaHCO_3$ 0.1 g) and were centrifuged at 3000 rpm for 20 min, then filtered to obtain a supernatant as the test solution. The adrenaline content determined by two point calibration method of HPLC (flow rate: 1 ml/min) was carried out on a Capcell pak C-18 column (i.d. 4.6 × 250 mm) (Shiseido) using phosphate buffer solution (pH 3.0) as solvent.

References

1) Part V of this series: J. D. Wang, T. Narui, K. Yoshikawa, S. Arihara and T. Okuyama, *Shoyakugaku Zasshi*, in press.
2) "The Dictionary of Chinese Material Medica," Shogakukan printed, Shanghai Scientific and Technical Publishing Co., 1985, p. 3141.
3) J. D. Wang, T. Narui, H. Kurata, K. Takeuchi, T. Hashimoto and T. Okuyama, *Chem. Pharm. Bull.*, **37**, 2236 (1989).
4) M. Komatsu, Y. Kamano and M. Suzuki, *Jpn. Analyst*, **14**, 1049 (1965).
5) E. Iseeli, M. Kotake, E. K. Weiss and T. Reichstein, *Helv. Chim. Acta*, **48**, 1093 (1965).
6) L. Gsell and Ch. Tamm, *Helv. Chim. Acta*, **52**, 551 (1969).
7) R. Verpoorte, P. Kinh and A. B. Svendsen, *J. Nat. Prod.*, **43**, 347 (1980).
8) P. Brown, Y. Kamano and G. R. Pettit, *Org. Mass Spectrom.*, **6**, 47 (1972).
9) *a*) T. Matsubara, M. Ueno, Y. Yokota, T. Kawasuji and H. Saito, *Pharmacometrics*, **38**, 71 (1989); *b*) *Idem*, *Wakan-Yaku*, **6**, 75 (1989).
10) *a*) T. Okuyama, C. Kawasaki, S. Shibata, M. Hoson, T. Kawada, H. Osada and T. Noguchi, *Planta Medica*, **1986**, 132; *b*) T. Okuyama, J. D. Wang, E. C. Tsu, T. Narui, M. Hoson, T. Kawada and N. Kawate, Abstracts of Papers, 33th Annual Congress of Pharm. Soc. of Kan-Ton Japan, 1989, p. 58.
11) M. Kubo, H. Matsuda, T. Tani and S. Arichi, *Proc. Symp. Wakan-Yaku*, **15**, 36 (1982).

Determination of Sulfur in Pharmaceutical Preparations Using Reversed-Phase High-Performance Liquid Chromatography

Kaori KUROSAKA,* Akira KUCHIKI, and Hiroshi NAKAGAWA

Pharmaceutical Resarch Center, Kanebo Ltd., 1–5–90, Tomobuchi-cho, Miyakojima-ku, Osaka 534, Japan. *Received November 16, 1990*

A reversed-phase high-performance liquid chromatographic method was developed for the determination of sulfur in topical pharmaceutical preparations. The mobile phase consisted of methanol–5% acetic acid water (85 : 15). The analysis was carried out using an octadecyl silica column (5 μm, 4.0 mm i.d. × 125 mm), with spectrophotometrical detection at 254 nm. Pyrene was used as an internal standard. The calibration curve was linear with a correlation coefficient >0.9996 in the range of 1—3 μg sulfur injected. This method is very useful in determination of sulfur in ointments containing other antibacterial or antiinflammatory drugs.

Keywords sulfur; reversed-phase HPLC; pharmaceutical preparation; ultraviolet detection; quantification

Sulfur (S) is frequently prescribed as an antiinflammatory, an antibacterial, or a keratolitic for topical pharmaceutical preparations.

Official assay methods for the determination of S include the gravimetric analysis (JP XI "Sulfur," USP XXI "Sulfur Ointment") and the titration after an oxidative reaction (USP XXI "Precipitated Sulfur," "Resorcinol and Sulfur Lotion"). The former, however, needs a large quantity of sample for accurate quantification, and the latter involves a complicated and dangerous procedure for an oxidative reaction. Some spectroscopic analysis methods for S are reported, such as measuring the ultraviolet (UV) absorption in organic solvent[1] or the visible absorption from thiocyanate ion with Fe^{3+} after the reaction with sodium cyanate.[2] A UV method is not advisable for the analysis of the pharmaceutical preparations, because some excipients might have ultraviolet absorbance. The thiocyanate method seems to have disadvantages in terms of routine analysis since it requires sodium cyanate as a reagent. Some high-performance liquid chromatographic (HPLC) methods have been reported using octadecyl silica[3] or styrene–divinylbenzen co-polymers[4] as a stationary phase. These methods use no internal standard. For use in routine analysis of S in pharmaceutical preparations, another method is needed which have the internal standard for simplicity of procedure.

This study was of an analytical method which uses reversed-phase HPLC. The procedure involves one step of solvent extraction followed by HPLC determination with UV detection.

Experimental

Apparatus The chromatographic system consisted of a Model 510 solvent delivery system, a Model 710 B WISP sampler, a Model 440 UV detector (all from Waters Assoc., Milford, MA., U.S.A.), and a Chromatopac C-R3A integrator (Shimadzu Co., Ltd., Kyoto, Japan). The spectrophotometer was Model UV-260 (Shimadzu Co., Ltd.).

Materials S (JP XI) was obtained from Fuji Kagaku Sangyo Co., Ltd. (Tokyo, Japan), and pyrene (internal standard) was from Tokyo Kasei Co., Ltd. (Tokyo, Japan). Other chemicals were of reagent grade. Pharmaceutical preparations containing S were obtained from commercial sources.

HPLC Conditions The mobile phase was methanol–5% acetic acid water (85 : 15), which had been filtered through a 0.45 μm membrane filter and degassed under vacuum. Pyrene was used as an internal standard. UV absorption was measured at 254 nm. Samples are chromatographed at room temperature on a LiChroCART 125-4, LiChrospher RP-18e (5 μm, 4.0 mm i.d. × 125 mm, E. Merck, Darmstadt, F.R.G.). The flow rate was 1.2 ml/min (1200 psi).

Sample Preparation for HPLC Analysis Fifteen milliliters of water and 15 ml of internal standard solution (150 mg of pyrene in 1 l of methylene chloride) were added to a sample. The tube was vigorously shaken for 10 min, then centrifuged at 3000 rpm for 10 min. A 1 ml aliquot of the organic layer was removed and diluted to 50 ml with methanol–5% acetic acid water (8 : 2). A 50 μl aliquot was injected into the HPLC apparatus.

Analysis of S by UV Measurement Fifteen ml of water and 15 ml of cyclohexane were added to a sample. The tube was vigorously shaken for 10 min and the centrifuged at 3000 rpm for 10 min. A one ml of aliquot of the organic layer was removed and diluted to 50 ml with cyclohexane, and the UV absorbance was measured at 265 nm.

Results and Discussions

Figure 1 shows a chromatogram of the test solution obtained from 1 g of an ointment B (see Table I) undr the conditions described above. No interference peak for S or the internal standard was observed. The retention times were about 12 min for S and 5.5 min for an internal standard.

The calibration curve used for quantification of S exhibited excellent linearity, with a correlation coefficient >0.9996 in the S infection range of 1—3 μg S. The coefficient of variation was 0.67% after 6 injections. Average recoveries from the emulsion ointment base were 101.0 ± 0.60% ($n=3$).

In four ointments S was determined by our HPLC method, and in two ointments by the UV method. S content was 3—4%; 1 g of ointments was used for analysis

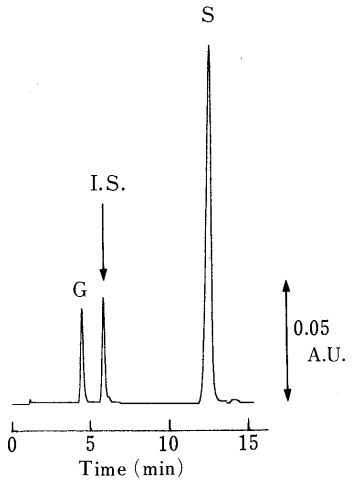

Fig. 1. Chromatogram of Sulfur and Pyrene (Internal Standard) from a Sample of an Ointment Containing 3% of Sulfur and 0.5% of Glycyrrhetinic Acid

S, sulfur; I.S., pyrene (internal standard); G, glycyrrhetinic acid.

TABLE I. Results of Quantitative Analyses of S in Four Ointments on the Market

		Ointments			
		A	B	C	D
HPLC	mean (%)	96.1	101.3	100.3	100.9
	S.D.	2.06	0.306	2.70	2.75
UV	mean (%)	100.1	113.9	—	—
	S.D.	2.16	1.81	—	—

Declaration of ingredients: (A) S 3%, resorcin (R) 2%, bentonite 10%; (B) S 3%, R 2%, glycyrrhetinic acid (GA) 0.5%; (C) S 3%, R 2%, GA 0.3%; (D) S 4%, R 2%, zinc oxide 2%. —, Not determined.

by our HPLC method and 0.5 g by the UV method.

Table I shows the results of S content against the declaration and standard deviations after three analyses, and reveals that our HPLC method is more excellent than the UV method in respect to accuracy and selectivity. Ointment B may contain some excipients with UV absorption, so the result of S content against the declaration was actually more than 100% by the UV method.

In conclusion, the results of this study indicate that our resolution method using reversed phase chromatography is useful for the routine analysis of S.

References

1) T. Ozawa, *Nippon Kagaku Zasshi*, **87**, 578 (1966).
2) J. K. Bartlett and D. A. Skoog, *Anal. Chem.*, **26**, 1008 (1954).
3) K. Wenzel, *Z. Lebensm. Unters. Forsch.*, **170**, 5 (1980); D. R. Lauren and J. H. Watkinson, *J. Chromatogr.*, **348**, 317 (1985); G. Fedeli, D. Moltrasiol, and M. Aeotli, *ibid.*, **447**, 263 (1988).
4) R. M. Cassidy, *J. Chromatogr.*, **117**, 71 (1976).

Studies of Stability Constants of Several Metal Complexes with *N*-(2-Naphthyl)ethylenediamine-*N*,*N*′,*N*′-triacetic Acid

Taketsune MIYAHARA,* Kusuo NARITA and Yoshio TAKINO

School of Pharmaceutical Sciences, University of Shizuoka, 395 Yada, Shizuoka 422, Japan. *Received December 17, 1990*

Stability constants of Cd(II), Cu(II), Hg(II), Pb(II) and Zn(II) chelates with *N*-(2-naphthyl)ethylenediamine-*N*,*N*′,*N*′-triacetic acid (NEDTA) were determined by spectrophotometric and fluorophotometric methods at 25±1 °C. The composition of the NEDTA chelate with each metal ion was 1:1 both by the molar ratio and the continuous variation methods with spectrophotometry. The stability constants (log *K*) determined by the spectrophotometric method were as follows: Cd(II), 9.49; Cu(II), 14.62; Hg(II), 15.08; Pb(II), 11.77; and Zn(II), 11.00. Those by the fluorophotometric method were as follows: Cd(II), 9.67; Cu(II), 14.05; Hg(II), 15.93; Pb(II), 11.32 and Zn(II), 10.99. The conditional stability constants (log *K*′) of these metal–NEDTA chelates at pH 4 were in the range of 6 to 11, which were large values compared to usual metal indicators. NEDTA should be a useful indicator for micro chelatometric titration and applicable to detection of a trace amount of several metal ions.

Keywords *N*-(2-naphthyl)ethylenediamine-*N*,*N*′,*N*′-triacetic acid; metallofluorescent indicator; stability constant; spectrophotometry; fluorophotometry

In order to study titration conditions such as pH and constituents of buffer solution at micro chelatometric titration by fluorophotometric detection, knowledge of the stability constants of metal chelates is necessary. The stability constants of ethylenediamine-*N*,*N*,*N*′,*N*′-tetraacetic acid (EDTA) and indicator chelates are especially important. We previously reported that *N*-(2-naphthyl) ethylenediamine-*N*,*N*′,*N*′-triacetic acid (NEDTA) was synthesized and could be used as a metallofluorescent indicator for several heavy metal ions in the range of pH 4 to 10 because it reacted with various heavy metal ions to quench the fluorescence.[1)]

In this report, to study the titration conditions the stability constants of metal NEDTA chelates for Cd(II), Cu(II), Hg(II), Pb(II) and Zn(II) were determined by spectrophotometric and fluorophotometric methods.

Results and Discussion

In the previous report,[1)] three acid dissociation constants of NEDTA were determined to be 2.2 (pK_{a1}), 3.95 (pK_{a2}) and 9.21 (pK_{a3}). The dissociation constants of two carboxyl protons less than pK_{a1} were ignored in the determination of stability constants because they did not influence the side reaction coefficients by hydrogen ions in the pH range of the titration.

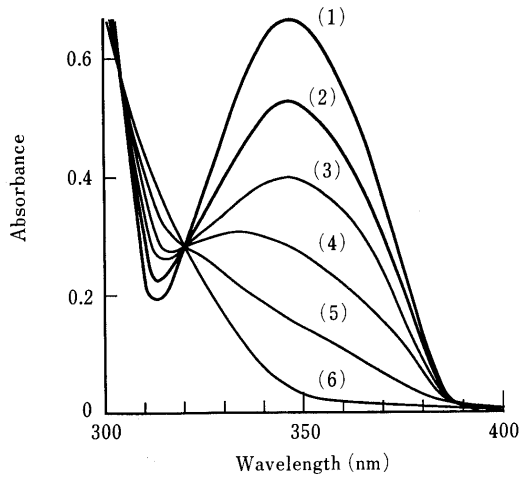

Fig. 1. Absorption Spectra of NEDTA and Its Hg(II) Complexes at pH 5.3

NEDTA concentration was 10^{-5} M. Ratio of [Hg(II)]/[NEDTA]: (1) 0, (2) 0.2, (3) 0.4, (4) 0.6, (5) 0.8, (6) 2.0 in 0.1 M KNO_3.

Absorption spectra of NEDTA at pH 4.6 showed maximum absorption at 347 nm and the absorption decreased by the chelate formation. Absorption spectra of the solutions containing NEDTA and varying concentrations of Hg(II) at pH 5 are shown in Fig. 1.

Since the isosbestic point was observed at 320 nm in Fig. 1, one species of chelate was expected to be formed. By applying the molar ratio and the continuous variation methods, each NEDTA chelate of Cd(II), Cu(II), Hg(II), Pb(II) and Zn(II) was 1:1 complex and no other species were observed.

The stability constants of the NEDTA chelate of Cd(II), Pb(II) and Zn(II) were measured at pH 5.4, 4.2 and 4.6 (347 nm; $\mu=0.1$ with KNO_3), respectively. Since the stability constants of Cu(II) and Hg(II) chelates were larger than other metal chelates, the same method used with other chelates could not measure the concentration of NEDTA dissociated from these chelates. Therefore, by decreasing the conditional stability constants of Cu(II) and Hg(II) chelates in a 5×10^{-3} M solution of iminodiacetic acid (IDA), the stability constant of Cu(II) chelate was measured at pH 5.4 and that of Hg(II) chelate at pH 4.2.

Fluorophotometric measurement was performed to confirm the stability constants by the spectrophotometric method. The addition of equimolar amounts of Cd(II), Pb(II) and Zn(II) ions into 1×10^{-6} M NEDTA solution resulted in about a 50% decrease of fluorescent intensity but those of Cu(II) and Hg(II) ions nearly quenched the fluorescence of NEDTA.

As shown in Fig. 2, the fluorescent intensity of 1×10^{-6} M NEDTA solution decreased in proportion to the amount of Hg(II). In such a manner as the spectrophotometric method, the stability constants of Cu(II) and Hg(II) chelates were measured in 0.001 M solution of nitrilotriacetic acid (NTA).

The stability constants of metallo–NEDTA chelates were obtained by spectrophotometric and fluorophotometric methods and are shown in Table I. The agreement between

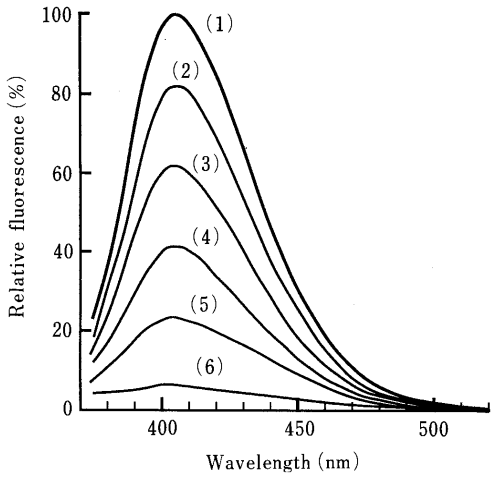

Fig. 2. Fluorescence Spectra of NEDTA and Its Hg(II) Complexes at pH 4.22

NEDTA concentration was 10^{-6} M. Ratio of [Hg(II)]/[NEDTA]: (1) 0, (2) 0.2, (3) 0.4, (4) 0.6, (5) 0.8, (6) 2.0. Excitation wavelength was 365 nm.

TABLE I. Stability Constants of NEDTA Chelates with Some Metal Ions at 25 °C[a)]

Metal ion	Spectrophotometry[b)] log K	Fluorophotometry log K
Cd (II)	9.49 (0.04)	9.67 (0.03)
Cu (II)	14.62 (0.08)[c)]	14.05 (0.11)[d)]
Hg (II)	15.08 (0.02)[c)]	15.93 (0.003)[d)]
Pb (II)	11.77 (0.03)	11.32 (0.06)
Zn (II)	11.00 (0.07)	10.99 (0.07)

a) Values in parentheses are the calculated standard deviations. *b*) $\mu=0.1$ with KNO_3. *c*) Determined in 0.005 M IDA solution. *d*) Determined in 0.001 M NTA solution.

the results of the spectrophotometric and the fluorophotometric methods was given within practical values.

The conditional stability constants of Cu(II) chelate with calcein[2)] and calcein blue[3)] as metallofluorescent indicators at pH 5 were 4.0×10^7 and 6.8×10^7, respectively, and that of Cu(II)–NEDTA chelate was 7.94×10^9, that was about 100 times larger. Similarly, the conditional stability constant of Zn(II) chelate with methylthymol blue (MTB)[4)] as a metallochromic indicator at pH 5 was 4.3×10^4 and that of Zn(II)–NEDTA chelate was 4.71×10^6. From these facts, NEDTA was expected to show a sufficient quenching effect by a diluted metal solution. This should be a useful indicator for micro chelatometric titration and applicable to detection of a trace amount of several metal ions.

Experimental

Equipment Spectrophotometer: A Hitachi spectrophotometer model 124 was used for the measurement of absorption spectra and a Hitachi spectrophotometer model 139 for that of absorbance. Fluorophotometer: A Hitachi fluorophotometer model 204 was used with a Hg-lamp (365 nm) and no correction of fluorospectra was done. The measurements of absorbance and fluorescence were performed at 25±1 °C. pH-meter: A Horiba pH-meter model F-7 was equipped with a combined electrode (Horiba 6028-10T) and hydrogen ion activity $\{H^+\}$ was calculated from $\{H^+\}=\text{antilog}(-\text{pH})$.

Reagents NEDTA: NEDTA synthesized by the method in a previous report[1)] was used (purity of 98.7%). NEDTA solution: About 90 mg of NEDTA were weighed precisely and dissolved in water containing a small amount of $NaHCO_3$ to make 100 ml of solution (2.5×10^{-3} M). It was stored in a cold, dark place and was used after diluting appropriately with water. Metal ion solutions: Cd(II) [$CdSO_4\cdot4H_2O$], Cu(II) [$CuSO_4\cdot5H_2O$], Hg(II) [$Hg(AcO)_2$], Pb(II) [$Pb(NO_3)_2$] and Zn(II) [$ZnSO_4\cdot7H_2O$] of special grade were used to prepare 0.01 M metal ion solutions which were standardized by chelatometric titration.[5)] Each solution was appropriately diluted with water before use. IDA and NTA solution: about 0.33 g of IDA or about 0.48 g of NTA were weighed precisely and dissolved by adding an equivalent of 1 N KOH aqueous solution to accurately make 100 ml with water (2.5×10^{-2} M). Buffer solution: 0.2 M acetic acid/ammonium acetate buffer solution (pH 4.0—5.5), 0.1 M KH_2PO_4/Na_2HPO_4 buffer (pH 5.0—6.0) were used. All other materials used here were special grade reagents.

Stability Constants in a Spectrophotometric Method Solutions containing 0.01 M buffer, 2×10^{-4} M NEDTA, 0.1 M KNO_3, and 1.8×10^{-4} M to 2×10^{-4} M Cd(II) (phosphate buffer, pH 5.4) or Pb(II) (acetate buffer, pH 4.2) or Zn(II) (phosphate buffer, pH 5.0) were prepared to measure the absorbance (As) at 347 nm and the stability constants (K_{MR}) were calculated from Eqs. 1 and 2.

$$As=\varepsilon_{MR}[MR]+\varepsilon_R([R]_0-[MR]) \quad (1)$$

$$K_{MR}=\frac{[MR]\cdot\alpha(H)_R}{([M]_0-[MR])\cdot([R]_0-[MR])} \quad (2)$$

$$\alpha(H)_R=1+\frac{\{H^+\}}{K_{a3}}+\frac{\{H^+\}^2}{K_{a3}\cdot K_{a2}}+\frac{\{H^+\}^3}{K_{a3}\cdot K_{a2}\cdot K_{a1}}$$

Where $[M]_0$ and $[R]_0$ indicate the total concentration of metal ion and NEDTA in each solution, respectively, and ε_R and ε_{MR} indicate the molar absorption coefficient of NEDTA and those of metallo–NEDTA chelates, respectively. $\alpha(H)_R$ is a side reaction coefficient of NEDTA by hydrogen ion. The stability constnat of Pb(II)–NEDTA in acetate buffer was corrected according to the Ringbom method.[6)]

Stability Constants of Cu(II) and Hg(II) Chelates Solutions containing buffer (0.01 M acetate buffer for Hg(II), pH 4.22 or 0.02 M phosphate buffer for Cu(II), pH 5.40), 2×10^{-4} M NEDTA, 5×10^{-3} M IDA, 0.1 M KNO_3 and 1.8×10^{-4} to 2×10^{-4} M Cu(II) ion or Hg(II) ion were prepared to measure the absorbance (As) at 347 nm.

When IDA and metallo–IDA chelates are expected to show no absorbance, the concentration of metallo–NEDTA [MR] is calculated from Eq. 1. In the solution, Eqs 3 to 5 are held, where K_{1MIDA} and K_{2MIDA} are stepwise stability constants of MIDA and $M(IDA)_2$ chelates, $[R]_0$, $[M]_0$ and $[IDA]_0$ are the total concentration of NEDTA, metal ion and IDA, respectively and [IDA], [MIDA] and $[M(IDA)_2]$ are the concentrations of free IDA, MIDA chelate and $M(IDA)_2$ chelate, respectively.

$$[R]_0=[MR]+[R] \quad (3)$$

$$[M]_0=[M]+[MR]+\frac{K_{1MIDA}[M][IDA]}{\alpha(H)_{IDA}}+\frac{K_{1MIDA}\cdot K_{2MIDA}[M][IDA]^2}{(\alpha(H)_{IDA})^2} \quad (4)$$

$$[IDA]_0=[IDA]+\frac{K_{1MIDA}[M][IDA]}{\alpha(H)_{IDA}}+\frac{2\cdot K_{1MIDA}\cdot K_{2MIDA}[M][IDA]^2}{(\alpha(H)_{IDA})^2} \quad (5)$$

$$\alpha(H)_{IDA}=1+\frac{\{H^+\}}{K_{a2}}+\frac{\{H^+\}^2}{K_{a2}\cdot K_{a1}}$$

Where $\alpha(H)_{IDA}$ is a side reaction coefficient by hydrogen ion when acid dissociation constats of IDA are K_{a1} (2.88×10^{-3}) and K_{a2} (7.58×10^{-10}).[7)] The stability constants of metallo–IDA chelates of 3.55×10^{10}, 4.47×10^5, 5.75×10^{11} were used for CuIDA,[7)] $Cu(IDA)_2$[7)] and HgIDA,[8)] respectively. The formation of $Hg(IDA)_2$ chelate is not known and the last terms of Eqs. 4 and 5 were neglected.

Since [M] is obtained from Eqs. 4 and 5, the stability constant (K_{MR}) is given by substituting [M] and [MR] into Eq. 6.

$$K_{MR}=\frac{[MR]\cdot\alpha(H)_R}{[M]\cdot([R]_0-[MR])} \quad (6)$$

Stability Constants in a Fluorophotometric Method Relative fluorescence intensity, F (%), was measured of 1×10^{-6} M NEDTA solution (acetate buffer, 0.08 M, pH 5.0) containing 9×10^{-7} M to 1.05×10^{-6} M Cd(II), Pb(II) and Zn(II) at 365 nm of excitation wavelength and 405 nm

of fluorescence wavelength. The stability constant of metallo–NEDTA chelate (K_{MR}) is obtained from Eq. 7.

$$K_{MR}=\frac{(100-F)\cdot\alpha(H)_R\cdot\alpha(M)_{AcOH}}{[R]_0\cdot F\cdot\left(\frac{[M]_0}{[R]_0}-\frac{100-F}{100}\right)} \quad (7)$$

Where $\alpha(M)_{AcOH}$ indicates a side reaction coefficient of each metal ion with AcOH and $[R]_0$, $[M]_0$ and $\alpha(H)_R$ indicates the same use as in Eq. 2. Each $\alpha(M)_{AcOH}$ was calculated by the Ringbom method.[6]

Stability Constants of Cu(II) and Hg(II) Chelates Relative fluorescence intensity, F (%), was measured of the solution (acetate buffer, 0.08 M, pH 5.0) with 1×10^{-6} M NEDTA and 10^{-3} M NTA containing Cu(II) (2×10^{-5} to 4×10^{-5} M) or Hg(II) (4×10^{-5} to 8×10^{-5} M) at 365 nm of excitation wavelength and 405 nm of fluorescence wavelength. With the relative fluorescence intensity, the stability constant (K_{MR}) is obtained from Eq. 8.

$$K_{MR}=\frac{\alpha(H)_R\cdot K_{MNTA}\cdot[NTA]_0\cdot(100-F)}{\alpha(H)_{NTA}\cdot[R]_0\cdot F\cdot\left(\frac{[M]_0}{[R]_0}-\frac{100-F}{100}\right)} \quad (8)$$

$$\alpha(H)_{NTA}=1+\frac{\{H^+\}}{K_{a3}}+\frac{\{H^+\}^2}{K_{a3}\cdot K_{a2}}+\frac{\{H^+\}^3}{K_{a3}\cdot K_{a2}\cdot K_{a1}}$$

Where K_{MNTA} is the stability constant of metallo–NTA chelate and $\alpha(H)_{NTA}$ is the coefficient of a side reaction produced by hydrogen ion when the acid dissociation constants of NTA are K_{a1} (1.29×10^{-2}), K_{a2} (3.24×10^{-3}), K_{a3} (1.86×10^{-10}).[9] Because [NTA] is greater than $[M]_0$ ($[M]_0\ll[NTA]_0$), [NTA] is approximated by $[NTA]_0$ ($[NTA]\approx[NTA]_0$). Stability constants of metallo–NTA chelates are obtained by those of Cu(II)–NTA[9] and Hg(II)–NTA[10] chelates as 9.12×10^{12} and 3.98×10^{14}, respectively.

References

1) T. Miyahara and Y. Takino, *Chem. Pharm. Bull.*, **37**, 1304 (1989).
2) T. Miyahara, *Bunseki Kagaku*, **26**, 615 (1977).
3) T. Miyahara, *Bunseki Kagaku*, **29**, 11 (1980).
4) T. Yoshino, M. Imada, S. Murakami and M. Kagawa, *Talanta*, **21**, 211 (1974).
5) K. Ueno, "Kireto Tekiteiho (in Japanese)," 12ed., Nankodo, Tokyo, 1975.
6) A. Ringbom, "Complexation in Analytical Chemistry," Interscience Publishers, Inc., New York, 1963, p. 38, 320.
7) S. Chaberek Jr. and A. E. Martell, *J. Am. Chem. Soc.*, **74**, 5052 (1952).
8) N. A. Skorik and V. N. Kumok, *Zh. Obshch. Khim.*, **37**, 1722 (1967).
9) G. Schwarzenbach, G. Anderegg, W. Schneider and H. Senn, *Helv. Chim. Acta*, **38**, 1147 (1955).
10) N. A. Skorik, V. N. Kumok and V. V. Serebrennikov, *Zh. Neorg. Khim.*, **12**, 2711 (1967) [*Chem. Abstr.*, **68**, 53995*p* (1968)].

Separation and Characterization of Three Positional Isomers of Dimaltosyl-cyclomaltoheptaose (Dimaltosyl-β-cyclodextrin)[1)]

Kyoko KOIZUMI,*,[a] Yasuyo OKADA,[a] Emi FUJIMOTO,[a] Yosuke TAKAGI,[b] Hiroshi ISHIGAMI,[b] Kozo HARA,[b] and Hitoshi HASHIMOTO[b]

Faculty of Pharmaceutical Sciences, Mukogawa Women's University,[a] 11–68 Koshien Kyuban-cho, Nishinomiya 663, Japan and Carbohydrate Research Laboratory, Ensuiko Sugar Refining Co., Ltd.,[b] 13–46 Daikoku-cho, Tsurumi-ku, Yokohama 230, Japan. *Received January 21, 1991*

A mixture of maltosylcyclomaltoheptaoses (maltosyl-β-cyclodextrins, G_2-βCDs) was prepared from maltose and β-cyclodextrin (βCD) through the reverse action of *Klebsiella pneumoniae* pullulanase. Three positional isomers of dimaltosyl-βCD in the mixture were separated by high-performance liquid chromatography on a reversed phase column and a graphitized carbon column. Their molecular weights were measured by fast-atom bombardment mass spectrometry, and the structures were established by methylation analysis, hydrolysis with glucoamylase to the known compounds, three positional isomers of diglucosyl-βCD, and ^{13}C-nuclear magnetic resonance spectroscopy.

Keywords maltosyl-β-cyclodextrin; dimaltosyl-β-cyclodextrin; positional isomer; HPLC; reversed phase column; graphitized carbon column; methylation analysis; glucoamylolysis; FAB-MS; ^{13}C-NMR

Maltosylcyclomaltoheptaoses (maltosyl-β-cyclodextrins, G_2-βCDs) have been prepared from maltose and β-cyclodextrin (βCD) by the reverse condensation reaction of debranching enzymes such as pullulanase[2–4)] or isoamylase[4–6)] and have one or more maltosyl branches linked by α-1,6 glucosidic linkage to glucose residues in βCD. Dimaltosyl-βCDs [$(G_2)_2$-βCDs] are expected, having analogue characteristics with diglucosyl-βCDs[7–9)] to have higher solubility both in water and in organic solvents, lower hemolytic activity, and to be safer in other metabolism experiments than parent βCD and even monomaltosyl-βCD [G_2-βCD], and hence are expected to be very useful for the solubilization of water-insoluble or slightly soluble drugs.

We describe here the separation and structural analyses of three positional isomers of $(G_2)_2$-βCD (Chart 1) in a mixture of maltosyl-βCDs which was prepared from maltose and βCD using an enzymatic reaction.

Experimental

Materials βCD (Ensuiko Sugar Refining) and maltose (Sanwa Denpun Kogyo) were commercial products. Pullulanase from *Klebsiella pneumoniae* "Pullulanase Amano 3" (3000 U/ml) and glucoamylase from *Rhizopus niveus* "Gurukuzaimu AF" (6000 U/ml) were both commercial products (Amano Pharmaceutical). One unit of pullulanase activity is defined as the amount of enzyme causing an increase of reduction corresponding to 1 μmol of glucose from pullulan per minute, and one unit of glucoamylase activity is the amount of enzyme that forms 10 mg of glucose from soluble starch in 30 min at 40 °C, pH 4.5. All reagents were of analytical grade. Reagent-grade organic solvents used for chromatography were dried and freshly distilled before use. Water used in solvent preparations was distilled, deionized, an redistilled.

General Methods Optical rotations were measured with a JASCO digital polarimeter, model DIP 360. High-performance liquid chromatography (HPLC) was performed with a JASCO 880-PU pump, a Waters U6K universal injector, and a Showa Denko SE-61 refractive index monitor. The columns used were a YMC-Pack AQ-323 ODS (250 × 10 mm i.d.) and a Hypercarb (100 × 4.6 mm i.d.) (Shandon Scientific). HPLC analyses at constant temperature were conducted using a column oven SSC 3510C (Senshu Scientific Co.). A Shimadzu Chromatopac C-R3A digital integrator was used for integration of peak areas. Fast-atom bombardment-mass spectrometry (FAB-MS) was performed with a JEOL JMS-DX 303 mass spectrometer using xenon atoms having a kinetic energy equivalent to 6 kV at an accelerating voltage of 3 kV. The mass marker was calibrated with perfluoroalkylphosphazine (Ultra Mark), and glycerol was used as the matrix. ^{13}C-Nuclear magnetic resonance (^{13}C-NMR) spectra (125.65 MHz) of 2—3% solutions in D_2O were recorded at ambient temperature with a JEOL GSX-500 spectrometer. Chemical shifts were expressed in ppm downfield from the signal of Me_4Si using 1,4-dioxane (67.40 ppm) as the external standard.

Preparation of a Mixture of Maltosyl-βCDs Maltose (25 g) was dissolved in 5 ml of 25 mM acetate buffer (pH6.0) at 90 °C and βCD (5 g) was added to the solution. After cooling to 55 °C, 0.6 ml of Pullulanase Amano 3 (3000 U/ml) was added, the mixture was incubated for 72 h, and inactivated by heating. Using a C_{18}-bonded silica column (1000 × 26.4 mm i.d., Organo) with water, the remaining maltose in the reaction mixture was removed, and then a mixture of maltosyl-βCDs was eluted from the column with ethanol–water (10 : 90 v/v) at a flow rate of 15 ml/min, concentrated, and lyophilized (4.8 g).

Methylation Analysis Methylation of dimaltosyl-βCDs was performed by the method of Prehm[10)] with 2,6-di-(*tert*-butyl)-pyridine and methyl trifluoromethane-sulfonate in trimethyl phosphate. The products were hydrolyzed, converted to their alditol acetates, and then analyzed with a Hitachi gas chromatograph model 063 fitted with a flame-ionization detector.

Hydrolysis of Dimaltosyl-βCDs with Glucoamylase $(G_2)_2$-βCD sample

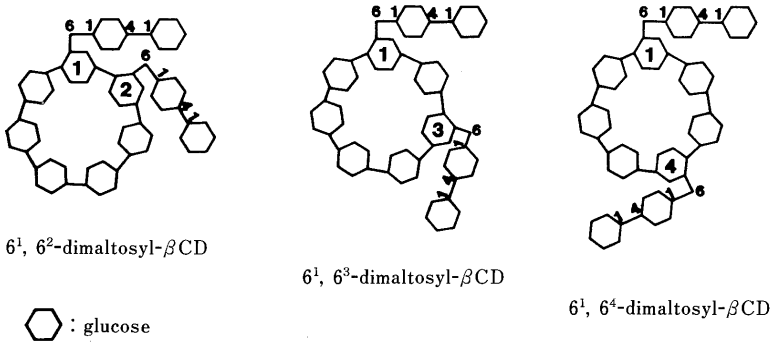

6^1, 6^2-dimaltosyl-βCD

6^1, 6^3-dimaltosyl-βCD

6^1, 6^4-dimaltosyl-βCD

⬡ : glucose

Chart 1

(5 mg) and glucoamylase (37.8 U) were dissolved in 0.5 ml water, and the solution was incubated at 40 °C for 24 h. The reaction mixture was heated at 100 °C for 5 min and then the denatured enzyme was removed by filtration through a 0.2-μm membrane filter. The hydrolyzate, that is, diglucosyl-β CD was characterized by HPLC.

Results and Discussion

Separation Figure 1 shows a chromatogram of a mixture of maltosyl-β CDs prepared from maltose and β CD through the reverse action of *Klebsiella pneumoniae* pullulanase. The components corresponding to peaks 1 and 2 were separated. Although two components should be contained in the peak 1, separation of those was impossible on the reversed column. A new type column packed with graphitized carbon made the separation possible (Fig. 2). The graphitized carbon column, Hypercarb has been demonstrated to have unique ability of resolving isomeric and closely related compounds, and has been used for the analyses of samples such as pharmaceutical products, amino acids, peptides,[11] and phenols.[12] However, it has some disadvantages, *e.g.*, a small loading capacity (less than 1 mg) and a marked tendency of tailing owing to the main mechanism of retention on the column, namely adsorption. Consequently, although this column is very useful for the analysis, it is hardly used for preparative HPLC. In this work isolation of component B corresponding to peak 1B was extremely difficult, though isolation of the first eluting component A was relatively easy. In order to exclude any trace cotamination of A in the fraction of B, many repetitive chromatographic separations of the latter fraction were necessary.

The ratios of G_2- and $(G_2)_2$-βCDs were 7:3, and those of three isomers of $(G_2)_2$-βCD, A, B, and C corresponding to peak 2 in Fig. 1 were 3.4:4.2:1.0, as measured from the chromatograms of Figs. 1 and 2.

Determination of Molecular Weight The molecular weights of A, B, and C confirmed by FAB-MS were all 1782, that is, comprised of 11 glucose units. Moreover, two peaks for fragment ions $[M-G-H]^-$ (m/z 1619) and

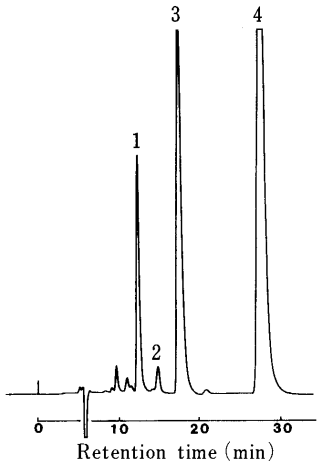

Fig. 1. Chromatogram of a Mixture of Maltosyl-βCDs on ODS Column

1, dimaltosyl-βCDs (A and B); 2, dimaltosyl-βCD (C); 3, monomaltosyl-βCD; 4, βCD. Chromatographic conditions: column, YMC-Pack AQ-323 (250 × 10 mm i.d.); eluent, CH_3OH–H_2O (10:90); flow rate, 2.5 ml/min; temperature, 30 °C.

Fig. 2. Separation of Two Positional isomers of Dimaltosyl-βCD on Graphitized Carbon Column

1A, dimaltosyl-βCD (A); 1B, dimaltosyl-βCD (B). Chromatographic conditions: column, Hypercarb (100 × 4.6 mm i.d.); eluent, CH_3CN–H_2O (16:84); flow rate, 1 ml/min; temperature, 50 °C.

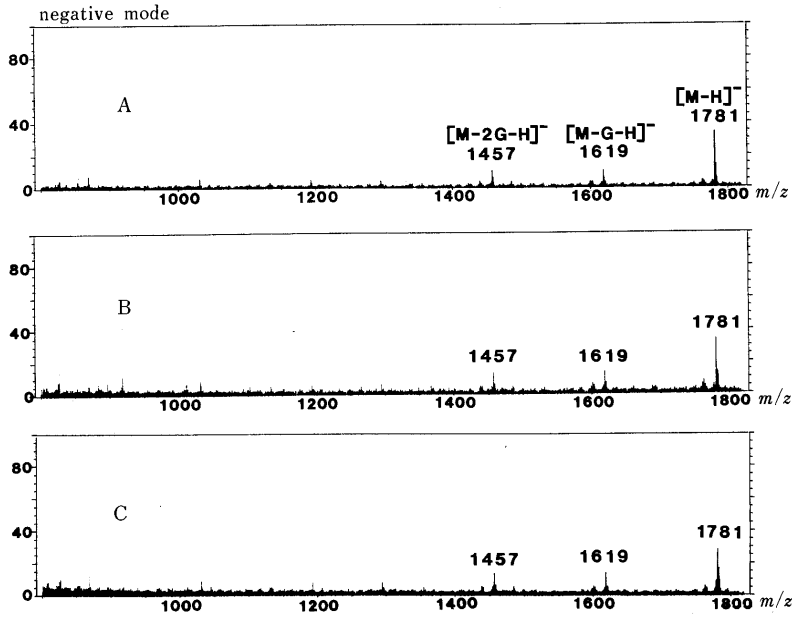

Fig. 3. FAB-MS Spectra of Compounds A, B, and C in Negative Mode

TABLE I. Methylation Analyses of Compounds A, B, and C

Product	t_R (min)	Molar ratio A	B	C
1,5-Di-*O*-acetyl-2,3,4,6-tetra-*O*-methyl-D-glucitol	6.4	2	2	2
1,4,5-Tri-*O*-acetyl-2,3,6-tri-*O*-methyl-D-glucitol	18.0	7	7	7
1,4,5,6-Tetra-*O*-acetyl-2,3-di-*O*-methyl-D-glucitol	38.4	2	2	2

Gas chromatographic conditions: column, 0.3% OV-275—0.4% GEXF-1150 on Shimalite W (AW-DMCS), 80—100 mesh (2 m × 3 mm i.d.); column temperature, 160 °C; carrier gas and flow rate, N_2, 30 ml/min.

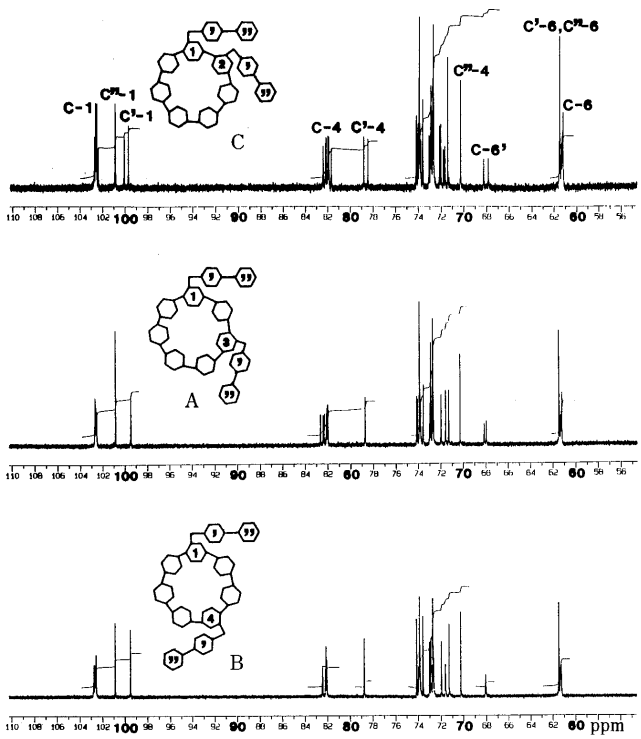

Fig. 4. ^{13}C-NMR Spectra of Compounds A, B and C Measured in D_2O at 125.65 MHz

C: the carbon atom of the ring D-glucose unit. C′ and C″: the carbon atom of the branched unit. C-6′: the carbon atom of the branch point.

$[M-2G-H]^-$ (m/z 1457) were observed in all spectra of A, B, and C (Fig. 3). These fragment ions must be formed through a single cleavage of the side-chain (primary fragments). Thus it was proved that the side-chains of A, B, and C were each two maltosyl residues, and not 6^2-maltosylmaltosyl residues from which two other kinds of primary fragments, $[M-3G-H]^-$ (m/z 1295) and $[M-4G-H]^-$ (m/z 1133) could be generated.[6]

Methylation Analysis The results of methylation analyses of A, B, and C indicated that all of them are 6^1,6^n-di-*O*-maltosyl-βCDs (Table I).

Hydrolysis with Glucoamylase Three isomers of dimaltosyl-βCD (A, B, and C) were hydrolyzed with glucoamylase to corresponding diglucosyl-βCDs whose structures had been established by HPLC analysis of partial hydrolyzates, ^{13}C-NMR spectroscopy, and chemical synthesis.[13] The results show that A, B, and C are 6^1,6^3-, 6^1,6^4-, and 6^1,6^2-di-*O*-maltosyl-βCDs, respectively.

^{13}C-NMR Spectroscopy Figure 4 shows ^{13}C-NMR spectra of dimaltosyl-βCDs (A, B, and C). Assignments of signals in the spectra could be made by analogy with those in the spectra of diglucosyl-βCDs. The assignments of C-6 signals were confirmed by the insensitive nuclei enhanced by polarization transfer (INEPT) method,[14] using $\Delta = 3/4J$. The large downfield shift of two C-6 signals indicates that the side-chain maltose residues are attached to oxygens on these carbon atoms. The ratios in the signal intensities of CD ring C-6 (at δ *ca.* 61.3), side-chain C-6 (at δ *ca.* 61.5, C′- and C″-6) and branch-point C-6 (at δ *ca.* 68.1, C-6′) were 5 : 4 : 2. Those of ring C-4 (at δ 81.7—82.7), side-chain C-4 involved in α(1→4)-linkage (at δ *ca.* 78.8, C′-4) and at nonreducing end (at δ *ca.* 70.3, C″-4) were 7 : 2 : 2, and those of ring C-1 (at δ 102.4—102.7), side-chain C-1 involved in α(1→4)-linkage (at δ *ca.* 100.9, C″-1) and in α(1→6)-linkage (at δ *ca.* 99.5, C′-1) were also 7 : 2 : 2. In the spectrum of C, C-6′, C′-4, and C′-1 signals are each split into two peaks; the C-6′ signal of A is also split and in the expanded spectrum of A, C′-4 and C′-1 signals were each slightly split into two peaks. Those signals of B, except for the very slightly split C-6′ signal were observed as single peaks, respectively, even in the expanded spectrum. These facts indicate the difference of magnitude of interaction between two side-chain maltosyl residues in each molecule of A, B, and C.

Optical Rotation The $[\alpha]_D^{30}$ values in H_2O were +170.0° ($c = 0.3$) for A, +170.0° ($c = 0.3$) for B, and +171.7° ($c = 0.3$) for C.

Acknowledgements We thank Ms. K. Suwa and Ms. S. Horiyama (Mukogawa Women's University) for measurements of the NMR spectra and the FAB-MS spectra.

References and Notes

1) This work was presented at The 9th Cyclodextrin Symposium, Tsukuba, November 1990.
2) S. Kobayashi, K. Nakashima, and M. Arahira, *Carbohydr. Res.*, **192**, 223 (1989).
3) T. Shiraishi, S. Kusano, Y. Tsumuraya, and Y. Sakano, *Agric. Biol. Chem.*, **53**, 2181 (1989).
4) Y. Yoshimura, S. Kitahata, and S. Okada, *Carbohydr. Res.*, **168**, 285 (1987).
5) J. Abe, N. Mizowaki, S. Hizukuri, K. Koizumi, and T. Utamura, *Carbohydr. Res.*, **154**, 81 (1986).
6) J. Abe, S. Hizukuri, K. Koizumi, Y. Kubota, and T. Utamura, *Carbohydr. Res.*, **176**, 87 (1988).
7) K. Koizumi, Y. Okada, Y. Kubota, and T. Utamura, *Chem. Pharm. Bull.*, **35**, 3413 (1987).
8) Y. Okada, Y. Kubota, K. Koizumi, S. Hizukuri, T. Ohfuji, and K. Ogata, *Chem. Pharm. Bull.*, **36**, 2176 (1988).
9) M. Yamamoto, A. Yoshida, F. Hirayama, and K. Uekama, *Int. J. Pharm.*, **49**, 163 (1989).
10) P. Prehm, *Carbohydr. Res.*, **78**, 372 (1980).
11) Application notes, Shandon Scientific Ltd., Chadwick Road, Astmoor, Runcorn, Cheshire WA7 1PR, England.
12) B. J. Bassler and R. A. Hartwick, *J. Chromatogr. Sci.*, **27**, 162 (1989).
13) K. Koizumi, Y. Okada, N. Nakanishi, T. Tanimoto, Y. Takagi, M. Ishikawa, H. Ishigami, K. Hara, and H. Hashinoto, *J. Carbohydr. Chem.*, **10**, in press (1991).
14) G. A. Morris and R. Freeman, *J. Am. Chem. Soc.*, **101**, 760 (1979).

Bimane Fluorogenic Substrates for Microdetermination of Angiotensin Converting Enzyme Level in Serum[1)]

Eisuke SATO,*,[2)] Hiromi HATTORI, Satoko NISHIKAWA, and Yuichi KANAOKA

Faculty of Pharmaceutical Sciences, Hokkaido University, Kita-12, Nishi-6, Kita-ku, Sapporo 060, Japan. *Received January 25, 1991*

The fluorescence of 9,10-dioxa-*syn*-3,4,6,7-tetramethylbimane (bimane) was found to be quenched in the presence of nitrated aromatic amino acid. Bimane peptides containing nitrated amino acid (1a, b) were shown to be useful fluorogenic substrates for the assay of angiotensin I converting enzyme (ACE) from rabbit lung, similar to bimane substrate containing tryptophan (3) previously reported. Among these bimane substrates, substrate 3 was shown to be a potent fluorogenic substrate for microdetermination of the ACE level in human serum.

Keywords bimane; nitrophenylalanine; nitrotryptophan; fluorogenic substrate; angiotensin I converting enzyme; serum

Proteolytic enzymes play a key role not only in the regulation of cellular protein turnover but also in the control of many other physiological functions such as digestion, blood coagulation, inflammation, control of blood pressure and so on. In recent years, the sensitivity of their determination has been increased substantially by the use of fluorogenic substrates with 7-amino-4-methylcoumarin derivatives as fluorophores.[3)] In our search for an improved fluorescent group, we have proposed 9,10-dioxa-*syn*-3,4,6,7-tetramethylbimane (bimane) as a fluorophore for hydrolytic enzyme substrates.[4)] We have recently reported that Bim–SCH_2CO–Phe–Trp–Pro–OH was a fluorogenic substrate which allowed the sensitive determination of angiotensin I converting enzyme (ACE).[4c)]

In this paper, we wish to report a new combination of fluorophore (bimane) and quencher (nitrated aromatic amino acid) for the intramolecularly quenched substrate for the assay of ACE, and also a microdetermination of human serum ACE, which is an exopeptidase and a dipeptidyl-carboxypeptidase that cleaves the C-terminal dipeptide of substrates containing a free carboxyl group and participates in the renin-angiotensin system of blood pressure regulation.

It was found that the fluorescence of bimane can be quenched in the presence of a nitrated aromatic amino acid. To evaluate the influence of a nitrated aromatic amino acid on the fluorescence of bimane, the fluorescence intensity of bimane in the presence and in the absence of a nitrated aromatic amino acid was measured; the intermolecular relative fluorescence intensity of bimane (1.10×10^{-5} M) in the presence (*versus* absence) of large excess 4-nitrophenylalanine (1.00×10^{-1} M) was 0.01. The attempted intermolecular quenched experiment for 6-nitrotryptophan was difficult bacause of significant absorption at the wavelength of excitation for bimane (*ca.* 400 nm). This quenching efficiency of 4-nitrophenylalanine was quantitatively analyzed. Stern–Volmer plots of the quenching of bimane fluorescence with 4-nitrophenylalanine is shown in Fig. 1. From this plot, the Stern–Volmer constant ($k_q\tau$) is determined to be 100 M^{-1} for 4-nitrophenylalanine, which is almost a comparable value with that of tryptophan (115 M^{-1}).[4a)] This observation suggested that quenching by nitrated aromatic amino acids of the bimane fluorescence may be utilized in the design of fluorogenic substrates for ACE.

Bimane substrates (**1a, b**) were synthesized using an active ester method from bimane-thioglycolic acid *N*-hydroxysuccinimide ester and tripeptides. The relative fluorescence intensity (RFI) of substrates **1a** and **1b** are 0.25 and 0.058, respectively, *versus* the fluorescence intensity of Bim–

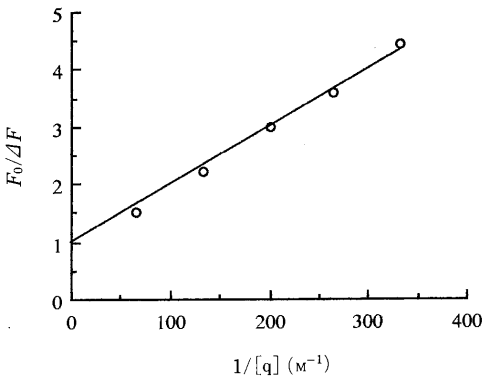

Fig. 1. Stern–Volmer Plots for Quenching of Bimane Fluorescence in the Presence of 4-Nitrophenylalanine

F_0, fluorescence intensity of bimane in the absence of 4-nitrophenylalanine. F, fluorescence intensity of bimane in the presence of 4-nitrophenylalanine. ΔF: $F_0 - F$. [q], concentration of quencher.

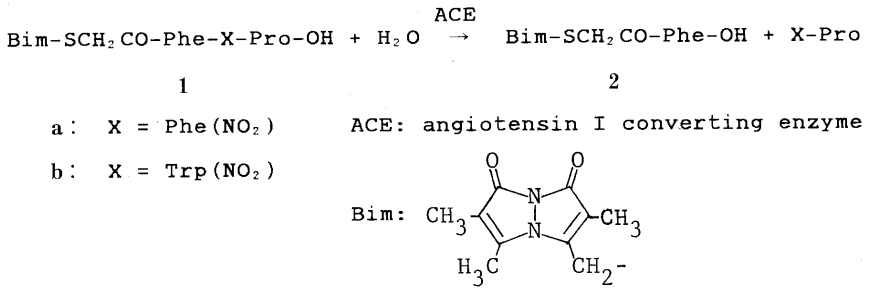

Chart 1

TABLE I. Kinetic Parameters of the Substrates for ACE

Substrate	K_m (M)	k_{cat} (s^{-1})	k_{cat}/K_m ($M^{-1}s^{-1}$)
1a	1.7×10^{-5}	5.1	3.0×10^{5}
1b	1.9×10^{-5}	5.4	2.9×10^{5}
Bim–SCH_2CO–Phe–Trp–Pro–OH (**3**)	2.6×10^{-5}	6.9	2.6×20^{5}
Hip–His–Leu (**4**)	1.1×10^{-3}	11	9.8×10^{3}

Hip–: benzoylglycyl-.

SCH_2CO–Phe–OH (excitation at 401 nm, emission at 481 nm). Although the substrate containing nitrophenylalanine (**1a**) has a higher RFI value than that of the previously reported bimane substrate (**3**) (0.15[4c]), the substrate containing nitrotryptophan (**1b**) has a smaller value than that of **3**, indicating a more intense quenching of nitrotryptophan than of tryptophan on the bimane system.

Kinetic parameters of **1a**, **b** for rabbit lung ACE were obtained by direct continuous spectrofluorometric assay, and the results are listed in Table I. In order to compare the characteristics of substrates containing nitrated aromatic amino acid with those of previously reported fluorogenic substrates (**3** and **4**), the kinetic parameters of **3**, **4** were also measured with the same lot of ACE under the same assay conditions. Both values of K_m and k_{cat} of **1a**, **b** are comparable to those of **3**, so bimane substrates with nitrated aromatic amino acid are also useful for the assay of ACE. Compared with the kinetic parameters of benzoylglycyl-histidyl-leucine (Hip–His–Leu) (**4**),[5] which is the most frequently used substrate for the assay of ACE, K_m values of **1a**, **b** are smaller by about two orders of magnitude compared to those of **4**, though the k_{cat} values of **1a**, **b** are smaller than **4**. So, the values of k_{cat}/K_m of **1a**, **b** are higher than those of **4**. For examination of the linearity of relationship between ACE concentration and fluorescence intensity, substrate **1b** was chosen because of its smaller RFI value compared to **1a**. The rates of hydrolysis for **1b** are proportional to enzyme concentration at least in the range 10^{-12}—10^{-10} M. This is almost the same value as that of the lowest detection limit of ACE with a bimane substrate of **3**.[4c]

As demonstrated above, bimane substrates with nitrated aromatic amino acids (**1a**, **b**) have almost comparable kinetic parameters and sensitivity as the previously reported bimane substrate with tryptophan (**3**). Therefore, substrate **3** and **1b** were used for the assay of ACE activity in human serum. The effect of substrate concentration on reaction velocity for serum ACE is given in Fig. 2. It showed human serum ACE activities with **3** and **1b** as substrate plateaus at a substrate concentration above 1.0×10^{-4} and 4.5×10^{-5} M, respectively. This value of substrate concentration is nearly one range lower in concentration of substrate compared with Hip–His–Leu as a substrate (5×10^{-3} M). The value of units (24) for **3** is almost comparable to the value of units (23) obtained with Hip–His–Leu for the same lot of human serum, though the value of units (12) for **1b** is small.[5] The ACE activities measured with **3** and **1b** are proportional to the serum volume over the range of 2—30 μl for **3** and 2—20 μl for **1b** as shown in Fig. 3, and it increased with time for at least 16 min. Thus, routine assays employ 20 μl serum and a 6 min-incubation.

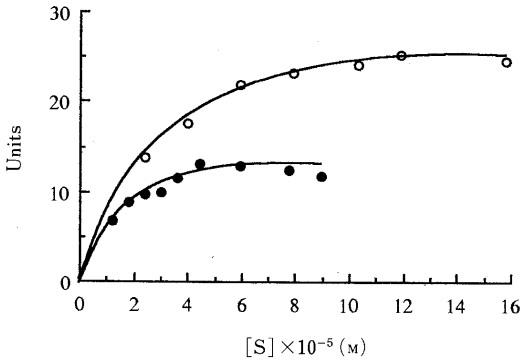

Fig. 2. The Effect of Substrate Concentration on Reaction Velocity

The unit values for Bim–SCH_2CO–Phe–Trp–Pro–OH (**3**) and Bim–SCH_2CO–Phe–Trp(NO_2)–Pro–OH (**1b**) catalyzed by human serum as a function of the concentration of the substrate. ○—○—○, **3**; ●—●—●, **1b**.

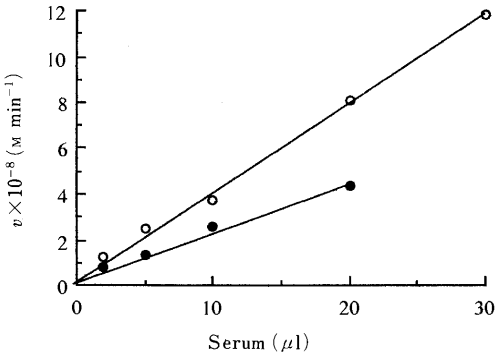

Fig. 3. Linearity with Respect to Serum Concentration of the Velocity

Linearity with respect to serum concentration of the velocity of Bim–SCH_2CO–Phe–OH formation catalyzed by human serum using Bim–SCH_2CO–Phe–Trp–Pro–OH (**3**) and Bim–SCH_2CO–Phe–Trp(NO_2)–Pro–OH (**1b**) as substrate. ○—○—○, **3**; ●—●—●, **1b**.

To make sure that the activities measured with **3** and **1b** are indeed due to ACE activity in the serum, the following experiments were carried out. These bimane substrates have a phenylalanine redsidue, so there is a possibility that they are susceptible to the action of chymotrypsin-like enzymes. However, the hydrolytic activities of serum assayed with **3** and **1b** were not affected by the treatment of human serum with L-1-*p*-tosylamino-2-phenylethyl chloromethyl ketone (TPCK), a selective inhibitor of chymotrypsin. Further, to exclude the participation of any cysteine proteinase activity on the fluorimetric assay, the assay was carried out in the present of *p*-chloromercuribenzoic acid (PCMB), a cysteine proteinase inhibitor. Again, the activities of human serum utilizing **3** and **1b** were not influenced. Therefore, this assay of human serum with bimane substrates **3** and **1b** is free from chymotrypsin-like enzyme activity and cysteine proteinase activity. Although enkephalinase has a similar substrate specificity to ACE, the concentration of chloride ion in buffer discriminates between their activities. Enkephalinase activity is inhibited in the presence of a chloride ion, while ACE activity is activated by it.[6] Therefore, the assay of ACE activity in human serum was carried out in the presence of 300 mM sodium chloride.

Further evidence that assay with bimane substrates of **3** and **1b** monitors specific ACE activity is shown by experiments utilizing captopril, which is a potent and specific inhibitor of ACE.[7] The K_i values for this inhibitor are similar for both substrates employed, with captopril

displaying a K_i of about 1.8 and 1.6 nM by assay with **3** and **1b**, respectively, and they are closely similar to the value of 1.7 nM obtained for ACE utilizing an assay with Hip–His–Leu.[7] Based on these experimental results, it may be concluded that fluorimetric assay in human serum using these bimane substrates selectively evaluates ACE activity in serum.

In summary, it could be illustrated that bimane substrates containing nitrated aromatic amino acid can also be used together with the already reported substrate **3** in continuous fluorimetric assay for ACE, and based on the results of assay for human serum as shown in Figs. 2 and 3, bimane substrate **3** is a potent fluorogenic substrate for the assay of ACE level in human serum. Compared with previously reported fluorescent substrates for the microanalysis of ACE level in human serum, the bimane system has the following advantages. 1) Although Hip–His–Leu is most widely utilized for assay of ACE activity,[8] it is a time-consuming end-point assay. With Hip–His–Leu, hydrolysis of the substrate has been monitored by quantitation of His–Leu liberated by the reaction with *o*-phthalaldehyde. The bimane system can provide a continuous and rapid fluorimetric assay. Recently, it was reported that the values were underestimated in the Hip–His–Leu assay in earlier studies for ACE activity, which depended on the fluorimetric determination of His–Leu. This dipeptide can be rapidly hydrolyzed by membrane dipeptidase.[9] 2) As a continuous fluorescent method, Abz–Gly–Phe(NO_2)–Pro was reported as an intramoleculary quenched fluorogenic substrate for the assay of human serum ACE activity,[10] but the fluorescence intensity of the bimane group is higher than that of the *o*-aminobenzoyl (Abz) group, and the emission wavelength of the bimane system (480 nm) is longer than that of the Abz group (360 nm). These fluorescence characteristics of the bimane system are useful to sensitive assay for serum ACE activity.

In the present work, we extended the usefulness of the bimane system to a fluorogenic substrate for the microdetermination of ACE activity. The proposed method is widely applicable, and further application of these bimane substrates to the clinical field is expected.

Experimental

Melting points were determined on a Yamato MP-21 apparatus and are uncorrected. Infrared (IR) spectra were obtained with a JASCO IRA-1 infrared spectrometer. Ultraviolet (UV) and visible absorption spectra were obtained with a Hitachi 210-10 spectrophotometer. Fluorescence spectra were recorded on a Hitachi 650-10 fluorescence spectrophotometer.

Tripeptides were prepared from *N*-boc-amino acid *N*-hydroxysuccinimide ester and either amino acid or dipeptide by the standard active ester method, followed by deblocking of the protective group with 5 M hydrogen chloride in dioxane. Angiotensin converting enzyme (rabbit lung) was purchased from Sigma Chemical Company. Human serum was obtained from the Hokkaido Red Cross Blood Center.

Synthesis of Substrates (1a, b) **1a**: To a solution of Phe–Phe-(4-NO_2)–Pro·HCl (196 mg, 0.4 mmol) and sodium bicarbonate (101 mg, 1.2 mmol) in water (10 ml), a solution of bimane-thioglycolic acid *N*-hydroxysuccinimide ester (Bim–OSu) (152 mg, 0.4 mmol) in acetonitrile (10 ml) was added. The solution was stirred at room temperature overnight, and concentrated to about 1/2 of the original volume under reduced pressure, diluted with water (50 ml), and then washed with ethyl acetate. The aqueous solution was acidified with concentrated hydrochloric acid and salted out, then extracted with ethyl acetate. The extract was washed with saturated sodium chloride solution, then dried over anhydrous sodium sulfate. **1a** was obtained from methanol–ethyl acetate by condensation as a pale yellow powder of mp 120—139 °C. 192 mg, 67%. IR (Nujol): 1740, 1630, 1520 cm^{-1}. $[\alpha]_D^{25}$ −9.3° (c=0.332, MeOH). *Anal.* Calcd for $C_{35}H_{38}N_6O_9S \cdot CH_3OH$: C, 57.59; H, 5.64; N, 11.19; S, 4.27. Found: C, 57.50; H, 5.52; N, 10.98; S, 4.45.

1b: From Bim–SCH_2CO–OSu (60 mg, 0.16 mmol) and Phe–Trp-(6-NO_2)–Pro (74 mg, 0.15 mmol) with triethylamine (42 μl, 0.3 mmol) using the same procedure as **1a**, **1b** was obtained from methanol–ethyl acetate by condensation as a yellow powder of mp 147—157 °C. 70 mg, 62%. IR (Nujol): 3280, 1735, 1630, 1520 cm^{-1}. $[\alpha]_D^{29}$ −17° (c=0.3165, dimethylformamide (DMF)). *Anal.* Calcd for $C_{37}H_{39}N_7O_9S \cdot 5/3H_2O$: C, 56.41; H, 5.42; N, 12.44; S, 4.07. Found: C, 56.67; H, 5.15; N, 12.17; S, 4.21.

Hydrolyses of 1a, b by Angiotensin I Converting Enzyme a) Kinetic Parameters (K_m, k_{cat}) Measurement: A solution (50 μl) of angiotensin I converting enzyme (from rabbit lung, 3.1 units/mg protein) (2.745×10^{-7} M) was added to the substrate solution (30—100 μl) of **1a** or **1b** (1.46×10^{-3} or 1.68×10^{-3} M, respectively, 25% dimethylsulfoxide) in 50 mM Tris–HCl buffer (pH 8.0) containing 300 mM sodium chloride and 2 ml buffer solution, with additional buffer solution (70—0 μl) to compensate for the substrate solution to the same tatal volume at 37 °C. The increase in emission at 480 nm (appearance of 2) was measured (excitation at 400 nm). Rates of hydrolyses were established from the rates of increase in fluorescence intensity based on the fluorescence intensity of 2. Kinetic parameters for the hydrolyses were obtained from Lineweaver–Burk plots.

b) Linear Relation of the Fluorescence Intensity *vs.* Enzyme Concentration: A solution (5—200 μl) of ACE (6.38×10^{-10} M) was added to the solution of **1b** (20 μl, 1.68×10^{-4} M) in 50 mM Tris–HCl buffer containing 300 mM sodium chloride and the same buffer (2.195—2.000 ml) at 37 °C, and measurement was carried out in the manner described in a).

Assay for Human Serum a) ACE Activity in Human Serum (Fig. 2): Instead of ACE, human serum (20 μl) was used, and the concentrations of the substrate were 2.38×10^{-5}—15.8×10^{-5} M for **3** and 1.19×10^{-5}—8.92×10^{-5} M for **1b**. The unit values were defined as Bim–SCH_2CO–Phe–OH liberated n moles/min/ml serum. Measurement was carried out in the manner described in a) of the hydrolyses of **1a**, **b** by ACE.

b) Linear Relation of the Initial Velocity *vs.* Serum Volume (Fig. 3): Serum (2—30 μl) was added to the solution of 2.0 ml of buffer and 130 μl for **3**, 75 μl for **1b** (1.40×10^{-3} M for **3**, 1.56×10^{-3} M for **1b**: 25% DMSO, finally 1.5% DMSO) of substrate stock solution (final concentration of substrate: 8.44×10^{-5} M for **3**, 5.39×10^{-5} M for **1b**) at 37 °C. Measurement was carried out in the same way described in b) of the hydrolyses of **1a**, **b** by ACE.

Inhibition of ACE Activity by Captopril The K_i values for captopril were measured using **3** and **1b** as substrates in the manner described for the assay for human serum. Final substrate concentrations used were 6.87×10^{-6} and 1.37×10^{-5} M for **3**, 7.01×10^{-6} and 1.40×10^{-5} M for **1b**, and the final captopril concentration was 7.94×10^{-10}—3.97×10^{-9} M for both **3** and **1b**. The human serum amount was 20 μl. The values of K_i were obtained using Dixon plots.

References and Notes

1) Part XX of "Organic Fluorescent Reagents," Part XIX: E. Sato, S. Itoh, and Y. Kanaoka, *J. Pharmacobio-Dyn.*, **14**, 43 (1991).
2) On leave from Nippon Glaxo Ltd., *Yahara, Nerima-ku, Tokyo 177, Japan.*
3) E. Sato, A. Matsuhisa, M. Sakashita, and Y. Kanaoka, *Chem. Pharm. Bull.*, **36**, 3496 (1988) and references cited therein.
4) *a*) E. Sato, M. Sakashita, Y. Kanaoka, and E. M. Kosower, *Bioorg. Chem.*, **16**, 298 (1988); *b*) E. Sato and Y. Kanaoka, *Chem. Pharm. Bull.*, **36**, 4494 (1988); *c*) E. Sato, S. Nishikawa, and Y. Kanaoka, *ibid.*, **37**, 145 (1989); *d*) E. Sato, K. Matsuda, and Y. Kanaoka, *ibid.*, **38**, 2043 (1990); *e*) E. Sato, M. Yoshikawa, and Y. Kanaoka, *ibid.*, **38**, 2287 (1990).
5) J. Friedland and E. Silverstein, *Am. J. Clin. Pathol.*, **66**, 416 (1976).
6) J.-C. Schwartz, B. Malfroy, and S. De La Baume, *Life Sci.*, **29**, 1715 (1981).
7) D. W. Cushman, H. S. Cheung, E. F. Sabo, and M. A. Ondetti, *Biochemistry*, **25**, 5484 (1977).
8) D. W. Cushman and H. S. Cheung, *Biochem. Pharmacol.*, **20**, 1637 (1971).
9) N. M. Hooper, *Biochem. J.*, **270**, 840 (1990).
10) H. M. Neels, S. L. Scharpe, G. A. Fonteyne, A. Yaron, and M. E. van Sande, *Clinica Chemica Acta*, **141**, 281 (1984).

Correlation between Glycated Lipoproteins and Fructosamine Level in Serum

Kunio KOBAYASHI,*[,a] Naomi OGASAHARA,[b] Takafumi SAKOGUCHI,[b] Kaoru TAISHI,[b] Hiroyuki MAKIMURA[b] and Akira MATSUOKA[b]

Biomedical Laboratories, Shionogi & Co., Ltd.,[a] 2–5–1, Mishima, Settsu 566, Japan and Department of Clinical Pathology and Clinical Laboratories, Hyogo College of Medicine,[b] 1–1, Mukogawa-cho, Nishinomiya 663, Japan. *Received January 10, 1991*

The correlation between the level of fructosamine and glycated proteins, including glycated lipoproteins, in serum from diabetic and nondiabetic subjects was studied. Assay of glycated proteins in serum was performed using an agarose gel film electrophoresis with nitroblue tetrazolium coloration. Glycated albumin correlated well with the fructosamine level in the diabetics ($r=0.83$—0.92, $p<0.01$) but showed no correlation with the nondiabetics ($r=0.25$—0.26). Also, a high correlation between the glycated β-lipoprotein and fructosamine levels was observed in diabetic patients with hyperglycemia and in nondiabetic subjects with a high risk of atherogenesis (atherogenic index, low-density lipoprotein-cholesterol/high-density lipoprotein-cholesterol >2.8) ($r=0.51$—0.66, $p<0.01$). Nondiabetics with a high level of β-lipoprotein, which is well known to cause high atherogenesity, showed a high level of glycated β-lipoprotein similar to that in the diabetic groups with hyperglycemia; therefore, the high level of glycated β-lipoprotein seems to be attributable not only to the hyperglycemia-accelerated glycation of β-lipoprotein but also to an increase in the level of β-lipoprotein in serum.

Consequently, the present results show that the fructosamine level in serum reflects not only the glycation of albumin but also that of lipoproteins which are known to increase in diabetes mellitus.

Keywords fructosamine; glycated albumin; glycated lipoprotein; glycation; diabetes mellitus; hyperglycemia; atherogenic index

Fructosamine and glycated hemoglobin are widely accepted as reliable indicators of metabolic control in diabetes mellitus.[1,2] However, in some diseases, such as renal insufficiency with hypoproteinemia, the fructosamine value varies widely without changes in the level of glycated albumin (glc albumin).[3] In addition, not only albumin but also apolipoprotein B in pre β- and β-lipoproteins are nonenzymatically glycated, and in diabetic hyperglycemia, the glycations are accelerated.[4,5] The fructosamine value represents the sum of glycated proteins in serum such as glc albumin and glycated lipoproteins (glc Lps),[4] but it has been considered to reflect the glycation of albumin since glc albumin is a major component of the glycated proteins in serum.[6]

We observed a discrepancy in the correlation between glc albumin and fructosamine levels in serum from diabetic and nondiabetic subjects,[4] suggesting that a different protein from albumin may contribute to changes in the fructosamine value.[7] If the glycation of different proteins from albumin, *e.g.*, lipoproteins, affect the fructosamine value, it may become useful not only as an indicator of glycemic control but also of the extent of glycation of lipoproteins related to the risk of atherogenesis based on the abnormal metabolism of lipoproteins.[8]

In the present study, correlation between the value of fructosamine and other proteins, such as α-, pre β- and β-lipoproteins, in serum were examined using sera from diabetic and nondiabetic populations, and the clinical significance of fructosamine was evaluated.

Materials and Methods

Subjects The nondiabetic groups (I, AI: atherogenic index, low-density lipoprotein-cholesterol/high-density lipoprotein-cholesterol $\leqq 2.8$, $n=31$; II, AI >2.8, $n=31$) consisted of a population (aged 33 to 74 years) certified as being healthy in a group medical examination. The diabetic groups (III, AI $\leqq 2.8$, $n=20$; IV, AI >2.8, $n=63$) consisted of inpatients with or without complications (aged 21 to 76 years) who were undergoing medical treatment at Hyogo College of Medicine Hospital and had been classified as having diabetes mellitus in a glucose tolerance test (75-g glucose load) on the basis of World Health Organization (WHO) criteria.[9] Blood was sampled preprandially without an anticoagulant. After the blood had clotted, the tube was centrifuged at $1400\times g$ for 10 min and the supernatant serum was separated and stored at 4 °C until use.

Fructosamine Assay The fructosamine was essentially assayed by the method of Johnson *et al.* based on the nitroblue tetrazolium (NBT) reducing method.[2] The fructosamine value (mM) was expressed in terms of 1-deoxy-1-morpholino fructose (DMF).

Other Measurements Glc α-Lp, glc pre β-Lp, glc β-Lp, and glc albumin were quantified by the electrophoretic method using agarose gel film.[4] Concentrations of albumin, total protein, β-Lp, total cholesterol and high-density lipoprotein-cholesterol (HDL-cholesterol) were measured with an automated clinical analyzer (JCA RX-30; Japan Electronic Optical Laboratory Ltd., Tokyo, Japan) in our clinical laboratory.

Statistical Analysis The results were recorded with a Lotus 1-2-3 version R2-1J plus (Lotus Development Corp., Cambridge, MA, U.S.A.), which we programmed to perform statistical calculations. Statistical significance was assessed by the Student's *t*-test for paired or unpaired data, as appropriate.

Results and Discussion

Figure 1 illustrates the distribution of fructosamine levels in sera from the nondiabetic (I and II) and diabetic populations (III and IV). All histograms showed typical Gaussian distribution, similar to the profile demonstrated by Lim and Staley.[10] The mean fructosamine levels (mM) in groups III and IV were significantly higher than those in groups I and II. The nondiabetic groups I and II showed a slim bell-type curve with a small standard deviation (S.D.), whereas the diabetic groups III and IV showed a flatter bell-type curve with a large S.D., suggesting the existence of various complicating factors which influence the fructosamine value of diabetic patients.

The levels of AI, fructosamine, glc albumin, glc Lps and other measures of atherogenesis risk in the diabetic and nondiabetic groups are given in Table I. The fructosamine levels in diabetic groups III and IV were about 1.2-fold higher (3.00—3.09 mM) than those in the nondiabetic groups I and II (2.49—2.52 mM). Of the nondiabetic groups, group II showed a 3.5-fold higher level (0.45 mM) of glc pre β-Lp than group I (0.13 mM). The diabetic groups III and IV showed a 3.3—4.2-fold higher level of glc pre β-Lp than

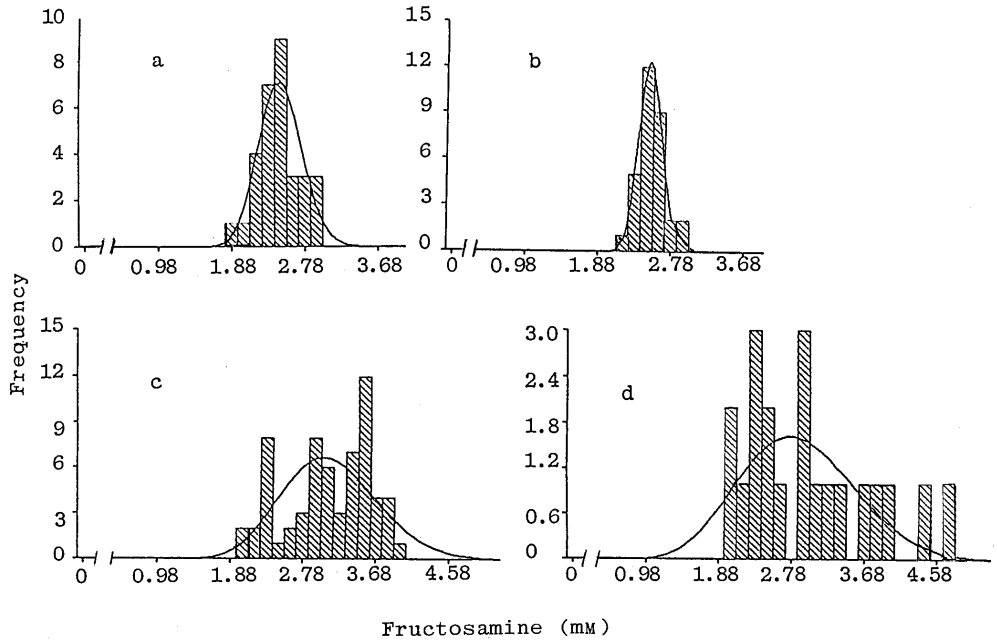

Fig. 1. Frequency Distribution of Fructosamine Levels in Diabetic and Nondiabetic Groups

Mean value of fructosamine (mM, mean±S.D.): a, 2.48±0.27 (I, $n=31$); b, 2.52±0.14 (II, $n=29$); c, 2.82±0.68 (III, $n=18$); d, 3.09±0.59 (IV, $n=61$).

TABLE I. Fructosamine, Glc Lps Levels and Other Measures of Atherosclerosis Risk in Diabetic and Nondiabetic Subjects

Analyte	Found (mean±S.D.)				p (group–group)	
	I ($n=31$)	II ($n=31$)	III ($n=20$)	IV ($n=63$)		
AI	1.95±0.40	3.37±0.47	2.19±0.40	5.00±1.92	<0.001	(I–II), (III–IV)
Fructosamine (mM)	2.49±0.25	2.52±0.17	3.00±0.76	3.09±0.51	<0.001	(II–III); <0.6 (I–II), (III–IV)
Glc α-LP (mM)	0.26±0.09	0.27±0.04	0.37±0.10	0.35±0.09	<0.001	(II–III)
Glc pre β-LP (mM)	0.13±0.08	0.45±0.15	0.54±0.17	0.43±0.16	<0.001	(I–II), (I–IV)
Glc β-LP (mM)	0.39±0.17	0.69±0.19	0.63±0.24	0.82±0.26	<0.001	(I–II), (III–IV)
Glc albumin (mM)	1.65±0.25	1.12±0.22	1.47±0.48	1.45±0.39	<0.001	(I–II, III, IV)
β-LP (g/l)	4.10±0.75	4.63±0.68	3.70±0.75	4.87±1.08	<0.001	(I–II), (III–IV)
Total protein (g/l)	78±7	69±4	67±5	66±5	<0.05	(II–III); <0.005 (II–IV)
Albumin (g/l)	45±4	40±2	38±3	38±3	<0.01	(II–III)

group I. Group IV, which seems to have a highly abnormal metabolism of lipoprotein showed a lower level of glc pre β-Lp than group III, in compensation for the glc β-Lp level. However, we cannot explain this finding in the present study. Group II had 0.69 mM of glc β-Lp, which was 1.8-fold more than that of group I (0.39 mM). Group IV showed the highest level of glc β-Lp (0.82 mM), which was 1.3-fold higher than that of group III (0.63 mM). Groups II and IV, which had high values of AI (II, 3.37; IV, 5.00), showed higher levels of β-Lp (II, 4.63 g/l; IV, 4.87 g/l) than groups I and III (I, 4.10 g/l; III, 3.70 g/l). For group III, the levels of glc β-Lp and β-Lp were 0.63 mM and 3.70 g/l, respectively, suggesting that the glycation of β-Lp was accelerated by diabetic hyperglycemia. The glc β-Lp level was the highest (0.82 mM) in group IV, which showed a high level of β-Lp and hyperglycemia. Although the level of β-Lp in group III was lower than that of group IV, the ratio of glc β-Lp/β-Lp (0.17 mmol/g) of group III was the same as that of group IV. Therefore, this result suggests that the high level of glc β-Lp in group IV is attributable not only to an increase in the level of β-Lp but also to the accelerated glycation of β-Lp in diabetic groups III and IV.

Neither the level of glc albumin nor total albumin paralleled the changes in the fructosamine level in this study. The fructosamine level was around 2.5 mM in the nondiabetic groups I and II, and around 3.0 mM in the diabetic groups III and IV. The levels of total protein and albumin in the diabetic groups were slightly lower (−15%) than those in the nondiabetic groups. Of the nondiabetic groups showing similar fructosamine levels (2.49—2.52 mM), group II, with the high risk of atherogenesis (AI>2.8), showed higher levels of glc pre β-Lp, glc β-Lp and β-Lp than group I, which had a low AI value (AI≦2.8). On the other hand, the level of glc albumin seems to decrease in

TABLE II. Correlation between Glc Lps and Fructosamine

Analyte	Correlation (r)			
	I	II	III	IV
Glc α-LP	0.68[a]	0.27	0.40	0.13
Glc pre β-LP	0.25	0.03	0.80[a]	0.23
Glc β-LP	0.20	0.51[a]	0.63[a]	0.66[a]
Glc albumin	0.25	0.26	0.92[a]	0.83[a]
β-LP	0.12	0.31	0.43[b]	0.46[a]

a) $p<0.01$, *b*) $p<0.05$.

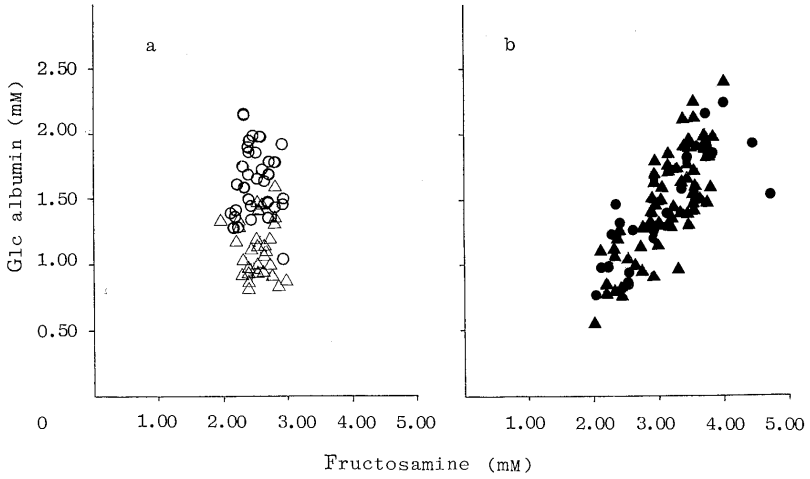

Fig. 2. Correlations between Glc Albumin and Fructosamine Levels in Diabetic and Nondiabetic Subjects

a, nondiabetic groups I (○, $y=4.00x+4.12$, $r=0.25$, $n=31$), II (△, $y=2.86x+0.45$, $r=0.26$, $n=31$); b, diabetic groups III (●, $y=1.72x+0.45$, $r=0.92$, $n=20$), IV (▲, $y=1.59x+0.75$, $r=0.83$, $n=61$).

compensation for the glc Lps levels in group II.

Table II shows the correlations between the fructosamine level and the glc Lps, glc albumin and β-Lp levels in the diabetic and nondiabetic groups. In group I, only the glc α-Lp level correlated with the fructosamine level. Although the level of α-Lp was not measured, the serum from group I probably contained a high level of α-Lp because the AI value was small and the β-Lp level was not particularly low.

Correlations with fructosamine were observed for the four parameters other than glc α-Lp in group III, and glc β-Lp and glc albumin in group IV. Glc albumin and glc β-Lp were also correlated with the fructosamine level only in groups III and IV; therefore, these parameters seem to reflect diabetic hyperglycemia. High correlation between the glc β-Lp and fructosamine levels was also found in group II, suggesting that an increase in the level of glc β-Lp reflects hyperglycemia or a high level of β-Lp in serum.

Figure 2 shows profiles of the correlation between glc albumin and fructosamine levels in the diabetic and nondiabetic populations. There was a significant difference between the correlation with the fructosamine level in the diabetic ($r=0.83$—0.92, $p<0.01$) and nondiabetic subjects ($r=0.25$—0.26).

As shown in Fig. 2, the level of glc albumin of group I was distributed in a slightly higher range (around 1.7 mM) than in group II (around 1.1 mM). In spite of the glc albumin level not having increased in group II, the fructosamine level changed by 2.0 to 3.0 mM. On the other hand, although the range of the glc albumin level was similar to that of the nondiabetics, the fructosamine level increased significantly, up to around 4.0 mM, in the diabetic groups.

In conclusion, the present results suggest that the fructosamine level in serum reflects not only the glycation of proteins, especially albumin, but also that of lipoproteins such as pre β- or β-LPs related to the risk factor of atherogenesis based on abnormal metabolism of lipoproteins.

References

1) M. J. McDonald, R. Shapiro, M. Bleichman, J. Solway and H. F. Bunn, *J. Biol. Chem.*, **253**, 2527 (1978).
2) R. N. Johnson, P. A. Metcalf and J. R. Baker, *Clin. Chim. Acta*, **127**, 87 (1983).
3) R. Wagner, I. Löwenstein, B. Gieshoff, N. Graben, Th. Olbricht, R. Windeck, G. Benker and D. Reinwein, *Dtsch. Med. Wschr.*, **112**, 175 (1987).
4) K. Kobayashi, N. Ogasahara, T. Sakoguchi, M. Kimura, K. Taniuchi and A. Matsuoka, *Clin. Chem.*, **36**, 65 (1990).
5) E. Scleicher, T. Deuffel and O. H. Wieland, *FEBS Lett.*, **129**, 1 (1981).
6) F. Zoppi, A. Mosca, S. Granata and N. Montabetti, *Clin. Chem.*, **33**, 1895 (1987).
7) N. R. Johnson and J. R. Baker, *Clin. Chem.*, **32**, 368 (1986).
8) M. Brownlee, A. Cerami and H. Vlassara, *N. Eng. J. Med.*, **318**, 1315 (1988).
9) WHO Expert Committee on Diabetes Mellitus, Second report, *WHO Tech. Rep. Ser.*, **646**, 1 (1980).
10) Y. S. Lim and M. J. Staley, *Clin. Chem.*, **31**, 731 (1985).

Change of *ras*-Transformed NRK-Cells Back to Normal Morphology by Mycalamides A and B, Antitumor Agents from a Marine Sponge

Hiroshi OGAWARA,*[,a] Kyoichiro HIGASHI,[a] Keijiro UCHINO[b] and Nigel B. PERRY[c]

Department of Biochemistry, Meiji College of Pharmacy,[a] Nozawa-1, Setagaya, Tokyo 154, Japan, Central Laboratory, Nippon Flour Mills Co., Ltd.,[b] Nurumizu-2114, Atsugi, Kanagawa 243, Japan and Department of Chemistry, University of Canterbury,[c] Christchurch, New Zealand.
Received March 7, 1991

Mycalamide A and mycalamide B, isolated as antiviral and antitumor agents from a New Zealand sponge of the genus *Mycale*, converted the morphology of *ras*-transformed NRK-cells to normal morphology at 10 and 1 ng/ml, respectively. The effect on protein synthesis suggests that these agents converted the morphology by preferentially inhibiting the biosynthesis of p21 protein.

Keywords *ras* oncogene; mycalamide; morphological change; antitumor agent; protein synthesis; marine sponge

Oncogenes are the genes which can convert normal cells to transformed or cancer cells. They were originally found in ribonucleic acid (RNA) tumor viruses, but it has recently been revealed that they carry out essential functions in the course of human life even in normal cells.[1] However, once these oncogenes are activated by mutagenesis, such as point mutation and translocation, or rearrangement and amplification of desoxyribonucleic acid (DNA) fragments, they play a critical role in the initiation of carcinogenesis and the proliferation of cancer cells. It is possible, therefore, to overcome human cancer by inhibiting oncogene products or their functions. This proposal is the basis of a new screening method for effective antitumor agents.

In this line of screening, we isolated genistein from fermentation broths of *Pseudomonas* and *Streptomyces* as a specific inhibitor for tyrosine protein kinase, a function of the *src* oncogene family.[2] Genistein inhibited the tyrosine protein kinase activities of the epidermal growth factor (EGF) receptor, $pp60^{src}$ and $pp110^{gag\text{-}fes}$, while it did not inhibit the serine/threonine kinase activities of adenosine 3′,5′-cyclic monophosphate (cAMP)-dependent protein kinase, protein kinase C and phosphorylase kinase and related enzyme activities like 5′-nucleotidase and phosphodiesterase.[3] For this reason, genistein is used widely as a specific inhibitor of tyrosine protein kinase activities in various basic research fields.[4] However, *ras* oncogenes are more interesting because they have been detected in a variety of human cancers at very high frequencies.[5] Thus, we have screened extracts of fermentation broths of some *Streptomyces* species and other bacteria for agents, which can convert the morphology of *ras*-transformed rat NRK cells back to normal. As a result, we found acetoxycycloheximide and cycloheximide to be such agents.[6] Here, we report that mycalamides A and B, antiviral and antitumor agents isolated from marine sponge,[7] also exhibit such activity.

Materials and Methods

Chemicals Dulbecco's modified Eagle medium (DME) and Eagle's minimum essential medium (MEM) which did not contain methionine were purchased from Nissui Pharmaceutical Co., and fetal calf serum came from Filton Pty Ltd., Australia. Anti-RAS monoclonal antibody and p21 protein were purchased from Oncogene Science Inc. [^{35}S]Methionine was obtained from ICN Radiochemicals, U.S.A. Mycalamides A and B were isolated from a New Zealand sponge of the genus *Mycale*. The structures are shown in Fig. 1.

Cells NRK cells and Harvey sarcoma virus-transformed NRK (Hav-NRK) cells were generous gifts from Hiroshi Yoshikura of the University of Tokyo. NRK and Hav-NRK cells were cultured in Dulbecco's modified Eagle medium supplemented with 10% fetal calf serum in a 5% CO_2 and water-saturated incubator. For determination of the activity, the Hav-NRK cells were seeded at 2×10^3 cells in 200 μl in a 96-well plate and were grown overnight at 37 °C. Test samples (usually 10 μl) were added to a well, incubation was continued for 24 and 48 h at 37 °C, and then the cell morphology was observed under an optical microscope.

Inhibition of Protein Synthesis Inhibition of protein synthesis was determined by the method of Kerridge[8] with a slight modification as follows: Hav-NRK cells grown in a 3.5 cm diameter dish were washed with 1 ml of MEM and then suspended in MEM. Ten μl of solution containing mycalamide A or mycalamide B at an appropriate concentration was added and the mixture was incubated for 1 h at 37 °C. Then, 10 μl of [^{35}S]methionine solution (10 μCi/ml) was added and the incubation was continued for 30 more min at 37 °C. After removing the medium and washing with 1 ml each of phosphate-buffered saline twice, 1 ml of 5% trichloroacetic acid was added, and the mixture was kept for 30 min at 0 °C. Radioactivity of the precipitate dissolved in 200 μl of 0.2 N NaOH was determined by a liquid scintillation counter. The percentage inhibition of protein synthesis was calculated on the basis of the number of cells.

The effect of mycalamides A and B on p21 synthesis was assayed as follows: Hav-NRK cells grown in a 6.0 cm diameter dish were washed with 1 ml each of MEM two times and 10 μl of solution containing mycalamide A or mycalamide B and 4 μl of [^{35}S]methionine (30 μCi) were added, then the cells were incubated overnight at 37 °C. After removing the medium and washing with 1 ml each of phosphate-buffered saline four times at 4 °C, 500 μl of PBS-TDS (10 mM Na_2PO_4, 0.155 M NaCl, 1% Triton X-100, 0.5% sodium deoxycholate, 0.1% sodium dodecyl sulfate (SDS), 0.2% sodium azide and 0.004% NaF, pH 7.2) was added and the mixture was incubated for 10 min at 4 °C. The supernatant was collected by centrifugation at $15000 \times g$ for 30 min. p21 protein in the supernatant was analyzed using anti-RAS monoclonal antibody according to the manual of the producer. Electrophoresis was performed by the method of Laemmli.[9]

Results and Discussion

The morphology of the transformed cells (Hav-NRK

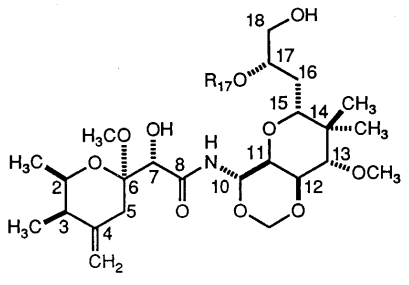

1 : R_{17} = H
2 : R_{17} = CH_3

Fig. 1. Chemical Structures of Mycalamide A (**1**) and Mycalamide B (**2**)

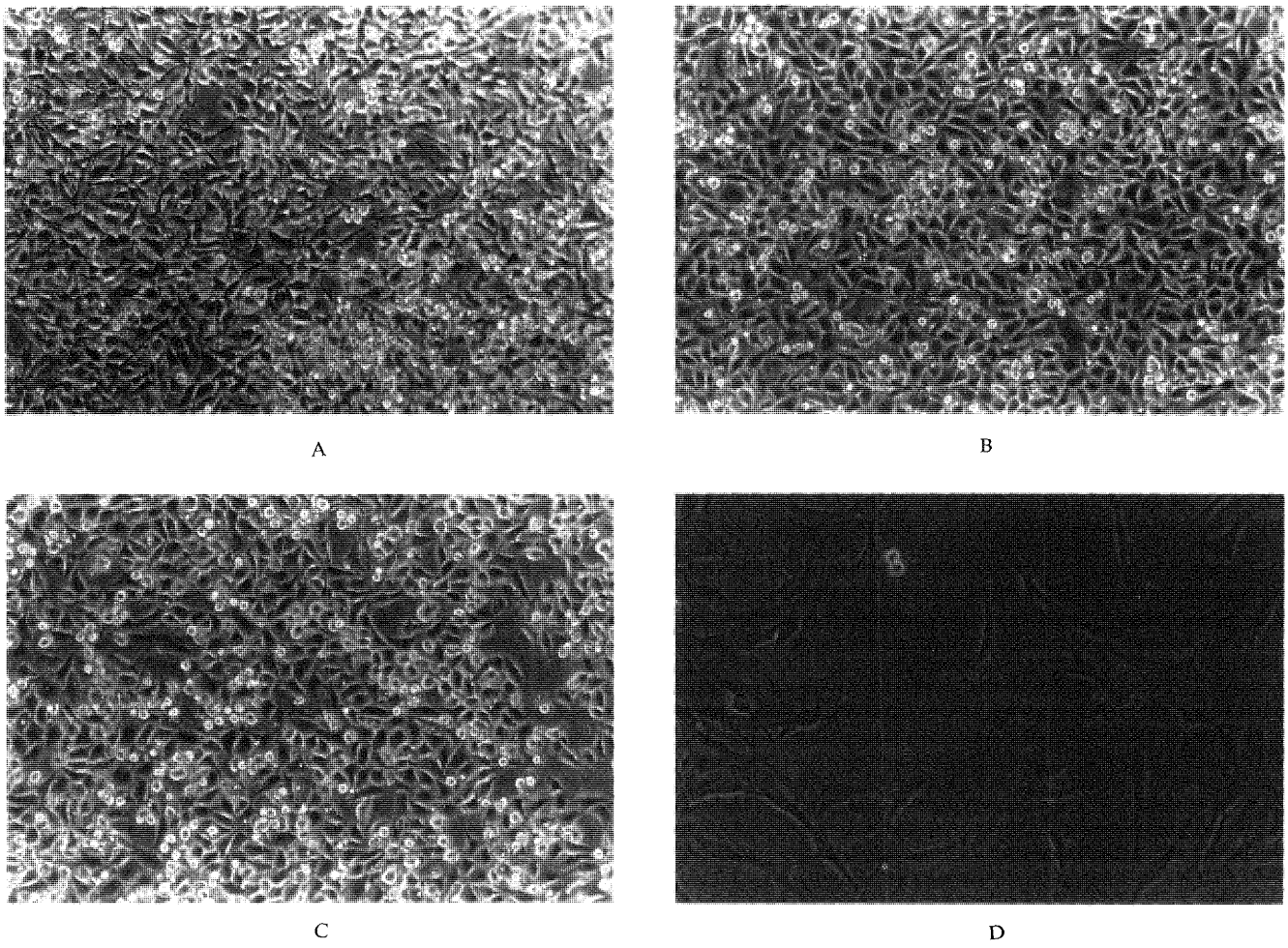

Fig. 2. Microscopic Pictures of Hav-NRK Cells (A), Hav-NRK Cells Treated with 10 ng/ml of Mycalamide A (B), Hav-NRK Cells Treated with 1 ng/ml of Mycalamide B (C), and NRK Cells (D)

cells) characterized by small-sized, densely stuffed and spindle-shaped cells is shown in Fig. 2A. These cells can reach high cell densities. On the other hand, the normal cells are flattened out and sensitive to contact inhibition. When mycalamide A or mycalamide B was added to a Hav-NRK cell culture, the cells changed their morphology from a transformed shape to the normal one. With mycalamide A, the morphological changes were observed at concentrations of 10 ng/ml (20 nM, Fig. 2B) or more, while with mycalamide B the morphology was recovered to normal at a concentration of 1 ng/ml (2 nM, Fig. 2C) or more. When the cells were washed free of these agents and allowed to grow in a fresh medium, the normal morphology was reverted gradually to the transformed one.

Mycalamides A and B are known to be inhibitors of protein synthesis of eukaryotic cells.[10] The inhibition of protein synthesis was therefore determined in Hav-NRK cells. Mycalamide A and mycalamide B inhibited protein synthesis by 50% at concentrations of 6.3 and 1.4 ng/ml, respectively. These results suggest that inhibition of protein synthesis might be related to the recovery of the transformed morphology of Hav-NRK cells to normal morphology. This suggestion is in accord with the results of a comparative study of cytotoxicity, *in vivo* efficacy and the ability to inhibit the protein synthesis of mycalamides A and B,[10] which indicates that the inhibitory activity of protein synthesis is

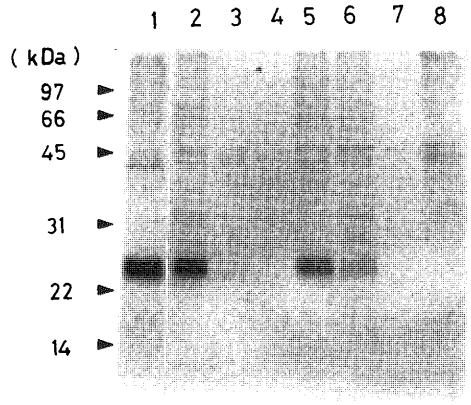

Fig. 3. Analysis of the Proteins Precipitated with Anti-RAS Monoclonal Antibody by SDS-Polyacrylamide Gel Electrophoresis and Autoradiography

1, no inhibitor; 2 to 4, mycalamide A, 3 ng/ml, 10 ng/ml and 30 ng/ml, respectively; 5 to 7, mycalamide B, 0.3 ng/ml, 1 ng/ml and 3 ng/ml, respectively; 8, the precipitate with rat serum.

a determinant of the antitumor action of these marine products. However, antibiotics known to inhibit protein synthesis of eukaryotic organisms such as puromycin and blasticidin S did not change the morphology of Hav-NRK cells at concentrations of 50 μg/ml or less, although puromycin at 50 μg/ml and blasticidin S at 200 μg/ml almost

killed the cells. It is suggested, therefore, that general inhibition of protein synthesis is not directly related to the morphological change. Thus, it was determined whether the biosynthesis of p21 was inhibited preferentially by analyzing the proteins precipitated by anti-RAS monoclonal antibodies using SDS polyacrylamide gel electrophoresis. Under the experimental condition, the biosynthesis of total protein was inhibited by 64 and 33% by 10 ng per ml of mycalamide A and 1 ng per ml of mycalamide B, respectively. Figure 3 revealed that the synthesis of p21 protein was inhibited by mycalamide A and mycalamide B more strongly than were other proteins, and that the biosynthesis of p21 protein was inhibited to 3.6 and 12%, by the same concentrations of mycalamides A and B as above, respectively. These results, very similar to those with acetoxycyclo-heximide and cycloheximide,[6] indicate that mycalamides A and B change the morphology of the transformed cells by preferentially inhibiting the biosynthesis of p21 protein. The detailed mechanism, however, remains to be clarified. Recently, we observed that ergosterol peroxide could weakly convert the morphology of Hav-NRK cells back to normal morphology (unpublished result). This compound is reported to show antitumor activity against L1210[11] and Walker 256 carcinoma cells.[12] It is possible, therefore, to discover an effective antitumor agent against *ras*-related human cancers, when this line of screening is continued on marine as well as bacterial sources.

Acknowledgments We thank H. Yoshikura for the gift of the cell line and J. W. Blunt and M. H. G. Munro for the mycalamides. This work was supported in part by the Grants-in-Aid for Cancer Research from the Ministry of Education, Science and Culture of Japan.

References

1) J. M. Bishop, *Ann. Rev. Biochem.*, **52**, 301 (1983).
2) H. Ogawara, T. Akiyama, J. Ishida, S. Watanabe and K. Suzuki, *J. Antibiot.*, **39**, 606 (1986).
3) T. Akiyama, J. Ishida, S. Nakagawa, H. Ogawara, S. Watanabe, N. Itoh, M. Shibuya and Y. Fukami, *J. Biol. Chem.*, **262**, 5592 (1987).
4) T. Akiyama and H. Ogawara, *Methods Enzymol.*, in press.
5) S. Nishimura and T. Sekiya, *Biochem. J.*, **243**, 313 (1987).
6) H. Ogawara, Y. Hasumi, K. Higashi, Y. Ishii, T. Saito, S. Watanabe, K. Suzuki, N. Kobori, K. Tanaka and T. Akiyama, *J. Antibiot.*, **42**, 1530 (1989).
7) N. B. Perry, J. W. Blunt, M. H. G. Munro and A. M. Thompson, *J. Org. Chem.*, **55**, 223 (1990).
8) D. Kerridge, *J. Gen. Microbiol.*, **19**, 497 (1958).
9) U. K. Laemmli, *Nature* (London), **227**, 680 (1970).
10) N. S. Burres and J. J. Clement, *Cancer Res.*, **49**, 2935 (1989).
11) S. Matsueda and Y. Katsukura, *Chem. Ind.* (London), **1985**, 411.
12) K. Kahlos, L. Kangas and R. Hiltunen, *Planta Medica*, **55**, 389 (1989).

Study of Nasal Enzyme Activity towards Insulin. *In Vitro*

Sveinbjörn GIZURARSON*,[1] and Erik BECHGAARD

Royal Danish School of Pharmacy, Department of Pharmaceutics, Universitetsparken 2, DK-2100 Copenhagen Ø, Denmark and NOVO SYMBION, Drug Delivery Group, Haraldsgade 68[2], DK-2100 Copenhagen Ø, Denmark. *Received November 30, 1990*

The possibility of insulin being enzymatically degraded in contact with the nasal mucosa has been studied *in vitro*. The insulin concentration was followed during 3 h incubation at 37 °C with freshly collected human nasal wash, isolated enzymes from pig and rabbit nasal mucosal tissue, leucine aminopeptidase and microsomal aminopeptidase, respectively. The rate of degradation with human nasal wash was found to be $\leq 0.02\,\mu g/min$, which indicates that less than 0.5% of an intranasally applied insulin dose may be destroyed by local enzymes during the time of absorption. The observed degradation was not found to be limiting for an intranasal application of insulin.

Keywords aminopeptidase; enzyme; insulin; intranasal; mucosa; nasal

Introduction

Among different non-parenteral routes, the intranasal route seems to be the most promising alternative for peptides and proteins.[2] Insulin is an example of a peptide that has been extensively studied in recent years. The bioavailability of insulin is very low, when it is administered intranasally as a simple solution.[3] Many investigations, however, have shown that insulin, in combination with an enhancer system[4] or as a powder dosage form,[5] can be delivered across the nasal mucosa in clinically relevant amounts.

The reason for the observed low bioavailability could be; (1) the high molecular weight[6] of insulin, in aqueous formulations, human insulin exists as dimers and tetramers (molecular weight: about 12 and 24 kilodaltons (kDa)); (2) short contact time in the nasal cavity,[7] the mucociliary clearance mechanism is extremely effective, inhaled particles (or droplets) are removed from the nasal cavity with a clearance half-life of 10—15 min[7] or (3) local enzymatic degradation, the possibility exists that insulin may be degraded locally by peptidases prior to or during absorption.[3,8,9]

Previous investigators have shown that insulin is degraded by enzymes isolated from rat[3] and rabbit[10] nasal mucosal tissue homogenate. The clinical relevance of this observation may have to be studied further, where some enzymes isolated from whole tissue may not be involved, *in vivo*, and the insulin doses studied may be too low.

The objective of this study is to investigate the enzymatic degradation of insulin at higher doses using the described animal tissue enzymes, as well as free enzymes isolated from the nasal cavity from humans after intranasal wash. The intention is to obtain a rough indication of whether enzymatic degradation is clinically important with respect to the low bioavailability of insulin after intranasal application.

Materials and Methods

Materials Zinc-free human insulin powder was obtained as a gift from Novo Nordisk A/S and prepared as a 0.08% w/v solution in 0.1 M Tris-buffer (Tris(hydroxy-methyl)-aminomethane, pH = 7.4).

Leucine aminopeptidase (LAP, EC 3.4.11.1; 200000 mU/mg protein), porcine kidney microsomal aminopeptidase (MAP, EC 3.4.11.2; 28000 mU/mg protein) and L-leucine-4-methoxynaphthylamide were obtained from Sigma Chemicals (Sigma Chemie GmbH, Germany). The enzymes were dissolved by adding 0.04 M Tris-buffer (pH = 7.4), containing 0.008 M manganese sulphate (manganese(II) sulphate monohydrate) to either LAP or MAP to obtain a final concentration of 0.05% w/v.[11] All other chemicals were of reagent grade.

Collection of Pig and Rabbit Mucosal Tissues Mucosal tissues from slain female DLR/Yorkshire bred pig (9 months, 90 kg) were kindly isolated and donated by Novo Nordisk A/S and stored at −70 °C.

Rabbit mucosal tissue was obtained from male New Zealand white rabbits (about 2.3 kg), fasted overnight and killed by an injection of Nembutal. The mucosae was removed by making an incision along the length of the lateral wall on each side of the nasal septum followed by cutting and lifting the nasal bone frontally to expose the nasal cavity fully. Mucosal tissue was then carefully removed from underlying cartilage and bone and stored at −70 °C.

Isolation of Nasal Enzymes The enzymes were isolated from the mucosal tissues as described by Stratford and Lee,[12] but with slight modifications. Immediately before each experiment, about 400 mg of pig or about 100 mg rabbit mucosal tissue were thawed at room temperature for about 10 min and homogenized for 5 min in 1 ml of 0.1 M Tris-buffer at 4 °C using an Ultra-turax (TP 18/10 no: 71713) homogenizer. 3 ml Tris-buffer were added and this mixture was homogenized for a few more minutes using a manual Teflon-glass homogenizer. The homogenates were centrifuged at 7000 rpm ($3840 \times g$) in a Beckman refrigerated centrifuge (model J-21) at 4 °C for 10 min to remove cellular and nuclear debris. The resulting supernatants, were isolated and used directly to study the degradation of human insulin.

Collection of Human Nasal Wash Human nasal wash samples were collected by using a modification of the nasal washing method introduced by Rossen *et al.*[13] While the volunteer was in a Moffats position[14] with the head inclined forward, 2 ml of isotonic sodium chloride solution was instilled into each nasal cavity. After one min, specimens consisting of saline and a variable amount of secretion were collected into small glass vials while the volunteer's head was still inclined forward. The volunteers did not blow their noses during the collection procedure. The specimens obtained were used immediately after sampling.

Design of Degradation Study The enzymatic degradation of insulin was determined by using the optimal conditions for the enzymes. A modified assay method for LAP was used.[11] 500 μl of the above mentioned enzyme preparations were mixed with 1.0 ml of 0.1 M Tris-buffer, at 37 °C. The reaction was initiated by adding 1.0 ml of 800, 80 or 10 μg/ml insulin solutions. The change in the insulin concentration was measured by withdrawal of 25 μl samples, at various time intervals up to 3 h, for direct analysis on high performance liquid chromatography (HPLC).

Analysis of Insulin Insulin was analyzed by an HPLC method modified from the method described by Snel, Damgaard and Mollerup.[15] The Hitachi HPLC-system was from Merck and consisted of a model 655A-11 pump, a model 655A variable wavelength ultraviolet (UV)-detector and a Rheodyne model 7125 injection valve. The column was a 4 × 250 mm LiChrosorb® RP-18, 5 μm, from Merck and the guard column was a 4 × 25 mm Perisorb® RP-8, 30—40 μm, from Merck.

The mobile phase was a mixture of two solutions A and B (4 : 3). Solution A consisted of 0.04 M phosphoric acid, 0.2 M sodium sulphate, 10% acetonitrile and pH at 2.5 with ethanolamine. Solution B was a 50% acetonitrile solution. Detection at 214 nm; flow rate 1 ml/min; column temperature 25 °C and injection volume 20 μl. The retention time (t_R) was about 10 min. Sample concentration was calculated on the basis of peak height × t_R relative to external insulin standard (0.8 mg/ml in 0.1 N hydrochloric acid). The detection limit was found to be about 5 ng injected,

and the reproducibility was about 5%.

Assay of Aminopeptidase Activity Aminopeptidase activity was determined as described by Stratford and Lee,[12] but with slight modifications. 100 μl of a tissue supernatant or nasal wash was preincubated in 2.8 ml 0.04 M Tris-buffer containing 0.008 M manganese sulphate (pH = 7.4) for 15 min in a waterbath at 37 °C. The reaction was initiated by adding to the mixture, 100 μl of 10 mM L-leucine-methoxy-2-naphthylamide. The fluorescence intensity was monitored at an excitation wavelength of 342 nm and an emission wavelength of 426 nm (Hitachi, Fluorescence spectrophotometer F-2000). The initial fluorescence intensity was found to be linear for all samples studied, and was expressed in terms of mIU per mg protein after correcting for chemical hydrolysis.

The protein concentration for tissue supernatant or nasal wash was kindly determined by standard methods at the Department of Clinical Chemistry, Bispebjerg Hospital (Copenhagen, Denmark).

Results

The enzymatic activity in human nasal wash and in isolated enzymes from rabbit and pig nasal tissue homogenate are shown in Table I. The table shows that all preparations contain active enzymes under the experimental conditions, characterized as mU/mg protein.

Table II shows the degradation rate of insulin after incubation with human nasal wash, enzymes isolated from pig and rabbit nasal mucosa and pure enzymes, respectively. The rate of degradation, if any, in human nasal wash, isolated pig and rabbit enzymes, were measured to be ≤ 0.02, 0.09 and 0.03 μg/min, respectively. The table shows that the recovery of insulin, after 3 h incubation at 37 °C, was above 96%, except for enzymes isolated from rabbit nasal mucosa. Experiments performed with rabbit nasal mucosa were carried out using amounts of insulin which are much lower than clinically relevant amounts.

Discussion

This study shows that clinically relevant amounts of insulin, incubated in freshly collected human nasal wash or in isolated enzymes from rabbit and pig nasal mucosa, do not show any pronounced degradation. The incubation of insulin with human nasal wash imitates the exposure of insulin to the enzymes present in the nasal cavity. The incubation with enzymes isolated from animal mucosal tissue also imitates the exposure taking place during the passage of insulin through the membrane into the circulation.[12]

As shown in Table II the rate of degradation (if any) in human nasal wash, was found to be ≤ 0.02 μg/min. This rate is very slow in relation to one clinical intranasal dose of about 2000 μg insulin. Based on the above results, this would indicate that a max. 0.5% of the applied insulin may be destroyed by local enzymes during the time of absorption (about 30 min). Incubation with lower doses of insulin was not of clinical relevance.

Previously, Hirai *et al.*[3] and Hayakawa *et al.*[10] have studied the enzymatic degradation in isolated enzymes from rat and rabbit nasal mucosa, respectively. Hirai *et al.*[3] incubated 1.67 μg insulin with the enzyme preparations finding that 0.025 μg/min was degraded. Hayakawa *et al.*[10] incubated 0.3 and 0.03 μg insulin, and showed that the rates of degradation were 0.00035 and 0.00098 μg/min, respectively. Compared to Table II, the rates of degradation from various preparations were found to be about 0.017 to 0.092 μg/min. Having in mind that one clinically relevant dose is about 2000 μg, these rates may not be able to degrade significant amounts of insulin within the time of absorption.[16]

As seen in Table II, incubation at higher concentrations makes rate determination difficult because the observed degradation of insulin after 3 h is only a few %, which is close to the analytical variation of about 5%. Although not all tissue enzymes may be relevant, the observed low degradation rate for insulin may indicate a low degradation potential. Besides, enzymes may leak out from the cells *in vivo*[12] and some penetration enhancers may promote transcellular absorption of insulin.[17] In order to estimate a significant degradation rate 10 μg/ml insulin was incubated with rabbit tissue enzymes. The total amount of incubated insulin was 10 μg, which is only about 0.5% of a possible clinical intranasal dose of 2000 μg insulin. Only about 0.025 μg/min was degraded. Results obtained with enzymes from rabbit mucosal homogenate were, as mentioned, performed with a very low concentration so as to estimate the rate of degradation more precisely and to compare our observations with previously published results. The experiments showed a linear decrease in the insulin concentration with time, indicating that the degradation of insulin followed zero order kinetics. Furthermore, our results did not differ from those previously published.

Hirai *et al.*[3] reported that the pure enzymes, such as LAP, cleave the B-chain of insulin. No significant degradation of insulin was found together with pure LAP or MAP, when clinically relevant amounts of insulin were used.

In conclusion, only a relatively small degradation of

TABLE I. The Enzymatic Activity towards L-Leucine-4-methoxy-2-naphthylamide and Protein Concentration in Various Preparations

Preparation	Enzymatic activity (mU/mg protein)	Protein concentration (mg/ml)
Human nasal wash	37	0.35
Isolated pig enzymes	25	2.8
Isolated rabbit enzymes	36	1.0
No enzymes	0	0.0

TABLE II. Recovery of Insulin during 3 h Incubation at 37 °C in the Presence of Various Nasal Enzymes

Preparations	Insulin conc. (μg/ml)	Number of experiments	Degradation rate (ng/min)	% recovery	Range
Human nasal wash	32	6	17	96	94— 98
Isolated pig enzymes	320	3	92	98	95—102
Isolated rabbit enzymes	4	4	25	73	67— 81
LAP (EC 3.4.11.1)	320	2	46	99	99— 99
MAP (EC 3.4.11.2)	320	5	46	99	86—107
No enzymes	4	6	6	89	85— 93

intranasally applied insulin was observed in this study. These observations may be studied further *e.g.* in tissue and enzymes isolated from human nasal mucosa and at other insulin concentrations. The apparently low degradation of insulin in combination with the various isolated enzymes indicates that the suggested "enzymatic barrier" to the absorption of insulin *via* the nasal route may not be limiting. It is therefore likely that the low absorption rate in combination with a rapid ciliary clearance of insulin from the nose are responsible for the low bioavailability of nasally applied insulin in simple solutions.[16] Our results seem to correlate with the results observed by Hirai *et al.*[3] and Hayakawa *et al.*,[10] and due to the observed low degradation, even with lyzosomal enzymes, it may be concluded that enzymatic degradation in the nasal cavity is not limiting for the intranasal application of insulin.

Acknowledgements This work was supported by Novo Nordisk A/S, Bagsværd, Denmark. The authors thank Mr. H. M. Højrup, Mrs. T. M. Larsen, Mrs. L. L. Rasmussen, Mr. K. Riis and Mrs. M. Ravn for their skillful technical assistance.

References and Notes

1) Present address: *LYF hf, The Icelandic Drug Delivery Group, Gardaflöt 16–18, IS-210 Gardabær, Iceland.*
2) K. S. E. Su, *Pharm. Int.*, **1986**, 8.
3) S. Hirai, T. Yashiki, and H. Mima, *Int. J. Pharm.*, **9**, 173 (1981).
4) J. P. Longenecker, A. C. Moses, J. S. Flier, R. D. Silver, M. C. Carey, and E. J. Dubovi, *J. Pharm. Sci.*, **76**, 351 (1987).
5) T. Nagai, Y. Nishimoto, N. Nambu, Y. Suzuki, and K. Sekine, *J. Contr. Rel.*, **1**, 15 (1984).
6) C. McMartin, L. E. F. Hutchinson, R. Hyde, and G. E. Peters, *J. Pharm. Sci.*, **76**, 535 (1987).
7) N. Mygind, "Nasal Allergy," ed. by N. Mygind, Blackwell Sci. Publ., New York, 1981, p. 51.
8) X. H. Zhou and A. L. W. Po, *Int. J. Pharm.*, **62**, 259 (1990).
9) A. A. Hussain, K. Iseki, M. Kagoshima, and L. W. Dittert, *J. Pharm. Sci.*, **79**, 947 (1990).
10) E. Hayakawa, A. Yamamoto, Y. Shoji, and V. H. L. Lee, *Life Sci.*, **45**, 167 (1989).
11) E. L. Smith, "Methods in Enzymology," Vol. 2, ed. by S. P. Colowick and N. Q. Kaplan, Academic Press Ltd., London, 1969, pp. 88—93.
12) R. E. Stratford and V. H. L. Lee, *Int. J. Pharm.*, **30**, 73 (1986).
13) R. D. Rossen, W. T. Butler, C. F. Cate, C. F. Szwed, and R. B. Couch, *Proc. Soc. Exp. Biol. Med.*, **119**, 1169 (1965).
14) M. Canciani and G. Mastella, *Acta Pædiatr. Scand.*, **77**, 612 (1988).
15) L. Snel, U. Damgaard, and I. Mollerup, *Chromatographia*, **24**, 329 (1987).
16) S. Gizurarson, S. N. Rasmussen, and F. Larsen, *J. Pharm. Sci.*, **80**, 505 (1991).
17) B. Guldhammer, K. Drejer, A. Engesgaard, P. E. Hansen, R. K. Hjortkjær, N. Mygind, and A. R. Sørensen, *Diab. Res. Clin. Pract.*, Suppl. 1, **5**, S164 (1988).

Improvement of Dissolution and Bioavailability for Mebendazole, an Agent for Human Echinococcosis, by Preparing Solid Dispersion with Polyethylene Glycol

Yukihiro CHIBA, Naonori KOHRI, Ken ISEKI and Katsumi MIYAZAKI*

Department of Pharmacy, Hokkaido University Hospital, School of Medicine, Hokkaido University, Kita-14-jo, Nishi-5-chome, Kita-ku, Sapporo 060, Japan. *Received February 12, 1991*

The solid dispersion of mebendazole was prepared with polyethylene glycol (PEG) to enhance the dissolution rate of mebendazole, an agent for the chemotherapy of human echinococcosis. The dissolution rate of the solid dispersion increased compared with the physical mixture, and also increased with the incorporation of an increasing amount of PEG-6000. An extensive improvement of the dissolution rate was observed when the ratio of the solid dispersion of mebendazole to PEG-6000 was more than 1 : 2. Furthermore, greater bioavailability in rabbits was obtained after oral administration of the solid dispersion compared with the physical mixture.

Keywords echinococcosis; chemotherapy; mebendazole; solid dispersion; solvent method; polyethylene glycol; bioavailability

Introduction

Human echinococcosis is caused by the larval forms of *Echinococcus granulosus* or *E. multilocularis*. It is well known that *E. multilocularis* is an important zoorotic parasite in Japan, especially in eastern Hokkaido.[1] Two hundred and sixty four patients with the disease caused by the larval *E. multilocularis* were found in Hokkaido between 1937 and 1987, and it is indicated that the number of patients will increase.[2] For these patients, surgery has been the only available treatment, but it is often ineffective due to extensive secondary alveolar echinococcosis.[3] Thus, it is proposed that an effective chemotherapy is needed before or after the surgery. For this purpose, benzimidazole derivatives have been used.[3] However, absorption from the gastro-intestinal (GI) tract is very poor, since these drugs are slightly soluble in GI fluid.[4] Therefore, it is necessary to increase the drug's GI absorption and bioavailability for effective medical treatment of hepatic or pulmonary echinococcosis. It is well known that various preparation of the solid dispersion can be used to enhance[5,6] or retard[7,8] the dissolution rate of the drug. Previously we prepared sustained release formulations for nifedipine[9] and ketoprofen[10] by using a solvent method technique for the solid dispersion.

In the present study, we used mebendazole and prepared the solid dispersion of this drug using polyethylene glycol (PEG) to enhance the dissolution rate. Furthermore, we administered this formulation to rabbits, and evaluated the GI absorption.

Experimental

Materials Mebendazole was kindly provided by Janssen Kyowa (Tokyo, Japan, lot No. IF 401). PEG-4000 and PEG-6000 were of JP XI grade. All other reagents were of the highest grade commercially available and used without further purification.

Solubility Studies The solubility of mebendazole in distilled water containing 0 or 0.0011% (w/v) PEG-6000 was determined by adding excess mebendazole to the medium at 37 °C. After equilibrium was reached, the aliquot was filtered immediately by a membrane filter with a pore size of 0.45 μm (Toyo Roshi Co.) and diluted appropriately with the same medium. The samples were analyzed by high performance liquid chromatography (HPLC). Each solubility was determined in triplicate.

Preparaion of Dosage Forms 1) Physical Mixture: Mebendazole and PEG-4000 or 6000 were mixed with a mortar and pestle, and the mixture was passed through a 100-mesh sieve.

2) Solid Dispersions: Solid dispersions of mebendazole with PEG were prepared using a solvent method.[5] The drug and PEG were dissolved in methanol at room temperature, then the solvent was removed *in vacuo* by using a rotary evaporator at 45 °C on a water bath. The residue was dried *in vacuo* at room temperature for 24 h and passed through a 100-mesh sieve.

Dissolution Studies The dissolution of mebendazole was tested in 900 ml of distilled water using the beaker method[11] at an agitation speed of 100 rpm at 37 °C. After the sample, the physical mixture or solid dispersions containing 2 mg of mebendazole, was added to the medium, 4 ml of the test medium was removed at appropriate intervals through a membrane filter (Toyo Roshi Co., pore size 0.45 μm) and immediately replaced with an equal volume of fresh test medium to maintain the original volume.

Plasma Level of Mebendazole in Rabbits Two white male rabbits (2.5—3.5 kg), which had been fasted for 24 h but allowed free access to water, were administered the physical mixture or the solid dispersion at a dose of 20 mg/kg of mebendazole with 20 ml of water. The administration study was performed on a crossover design. About 1.5 ml of blood was drawn from marginal ear veins at 0, 20, 40 min, 1, 2, 3, 4, 6 and 8 h after administration.

Assay Procedure To 0.5 ml of plasma or dissolution test solution in a 15 ml test tube, 3 ml of borate buffer (0.1 M $Na_2B_4O_7$–0.1 M NaOH, pH 10.5) and 4 ml of chloroform was added. The tube was shaken for 10 min, then the tube was centrifuged at $1000 \times g$ for 5 min. After aspiration of the water layer, 2 ml of chloroform was removed to another test tube and the chloroform layer was evaporated to dryness *in vacuo* at 40 °C. The residue in the tube was reconstituted with 100 μl of acetonitrile containing 50 ng of albendazole as an internal standard. Usually, 20—40 μl of the samle solution was injected into the HPLC system.

HPLC Conditions A liquid chromatograph (Hitachi 635A) equipped with a high-pressure sampling valve (Hitachi 638-0801, 1—150 μl) was used. For the stationary phase, a reversed-phase column (Hitachi 3053, 4.6 mm i.d. × 25 cm) was used; the column was warmed at 55 °C using a constant-temperature water bath circulator. The mobile phase consisted of a 0.05 M phosphate buffer (pH 7.0)–acetonitrile (55 : 45). The pH of this mobile phase was adjusted to pH 6.5 with phospholic acid. The flow rate was 0.75 ml/min and the pressure was approximately 60 kg/cm^2. Detection was at 310 nm using a variable wavelength ultraviolet (UV) monitor (Hitachi 638-41) at 0.005 absorbance unit full scale (a.u.f.s.). The retention times for mebendazole and an internal standard were 8.0 and 10.0 min, respectively.

Results and Discussion

Dissolution Studies Figure 1 shows the dissolution profiles of mebendazole from the solid dispersions with PEG-4000 (mebendazole : PEG-4000 = 1 : 5) and with PEG-6000 (mebendazole : PEG-6000 = 1 : 5). The dissolution profile of the physical mixture of mebendazole–PEG-4000 is also shown for comparison. Mebendazole concentrations of two kinds of solid dispersions were significantly higher than that of the mebendazole–PEG-4000 physical mixture, indicating that the dissolution of mebendazole was improved by preparing solid dispersions with PEG.

In the following studies, we used the solid dispersion with PEG-6000, since the dissolution rate of the solid dispersion with PEG-6000 was superior to that of PEG-4000, as shown

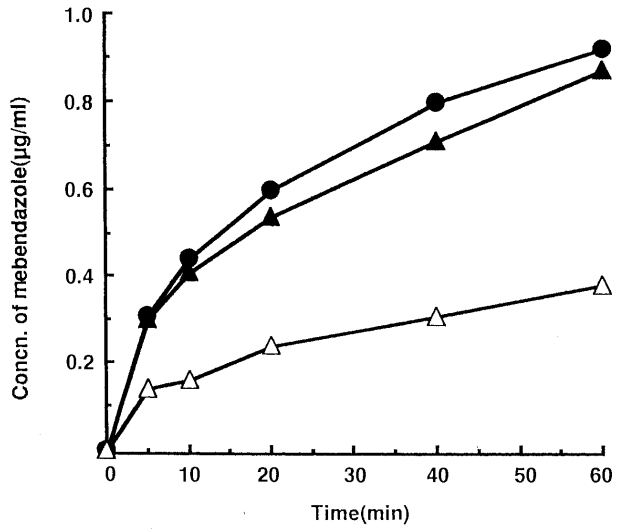

Fig. 1. Dissolution Profiles of Mebendazole

Each point is the mean of two determinations. —●—, mebendazole: PEG-6000 = 1 : 5 solid dispersion; —▲—, mebendazole : PEG-4000 = 1 : 5 solid dispersion; —△—, mebendazole : PEG-4000 = 1 : 5 physical mixture.

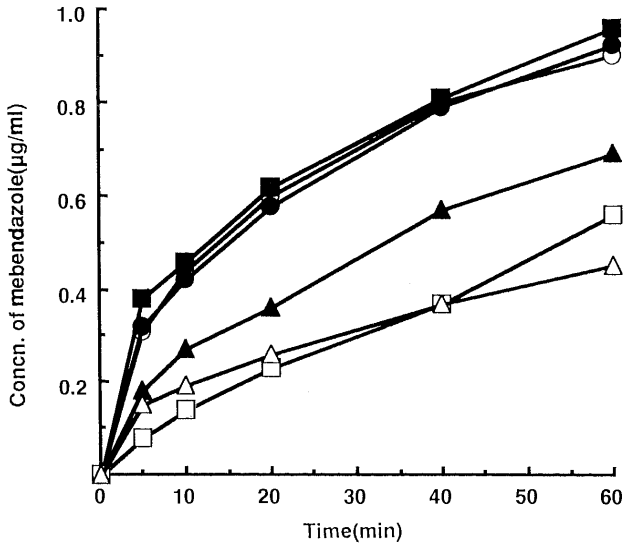

Fig. 2. Dissolution Profiles of Mebendazole from Various Preparations Using PEG-6000

Each point is the mean of two determinations. —○—, 1 : 10 solid dispersion; —●—, 1 : 5 solid dispersion; —■—, 1 : 2 solid dispersion; —▲—, 1 : 1 solid dispersion; —□—, 1 : 0.5 solid dispersion; —△—, 1 : 10 physical mixture.

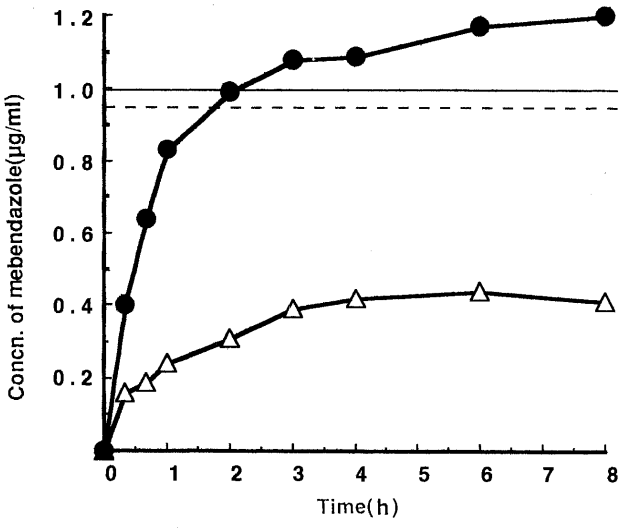

Fig. 3. Dissolution Profiles of Mebendazole

Each point is the mean of two determinations. —●—, 1 : 5 solid dispersion; —△—, 1 : 5 physical mixture; – – –, solubility of mebendazole (distilled water); ——, solubility of mebendazole (distilled water containing 0.0011% PEG-6000).

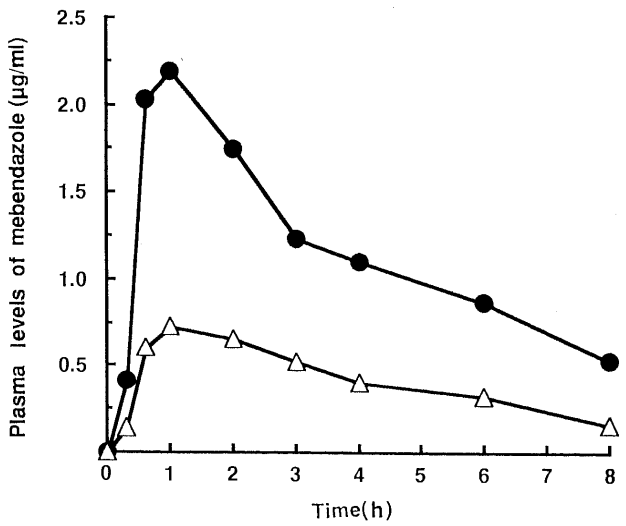

Fig. 4. Mean Plasma Levels of Mebendazole Following Oral Administration at a Dose of 20 mg/kg to Rabbits

—●—, solid dispersion; —△—, physical mixture. Each point is the mean of two determinations.

in Fig. 1. Figure 2 shows dissolution profiles for several solid dispersions of mebendazole containing various amounts of PEG-6000 in the formulations. When the ratio of PEG to drug was greater than one, an enhanced dissolution rate was observed compared with the physical mixture of mebendazole–PEG-6000 (1 : 10). There was no significant difference in the dissolution rate among the solid dispersions which had the following ratios of mebendazole to PEG-6000: 1 : 2, 1 : 5, 1 : 10. Duclos *et al.* reported that the amorphous and crystalline progesterones were found in the solid dispersion with PEG-6000 by differential scanning calorimetry and X-ray diffraction.[12,13] Chiou *et al.* reported the possibility of ultrafine or colloidal dispersions of drugs in the solid dispersion using PEG-6000.[5] Therefore, it is considered that improvement of the dissolution rate of mebendazole might be due to the amorphous phase of mebendazole, the reduction of the drug particle size, or an improvement in wettability, which resulted from the interaction of mebendazole and PEG-6000.

We have also studied the dissolution rate of the solid dispersion of mebendazole–PEG-6000 (1 : 5) and the physical mixture which have the same ratio until 8 h (Fig. 3). Mebendazole was dissolved over its solubility (0.95 μg/ml; distilled water, 0.99 μg/ml; distilled water containing 0.0011% w/v PEG-6000). It was also found that a post-peak decline was observed when the dissolution test was continued to 32 h (data not shown). This was considered a supersaturation phenomenon was caused by the amorphous mebendazole.[14] Thus, we used the solid dispersion of mebendazole with PEG-6000 for the study of GI absorption.

Absorption Studies Figure 4 shows the mean plasma levels of mebendazole following the oral administration of solid dispersion (mebendazole : PEG-6000 = 1 : 5) and phys-

ical mixture (mebendazole : PEG-6000 = 1 : 5) to rabbits. An increased initial dissolution rate of the solid dispersion (Fig. 3) was reflected in the high plasma levels for the solid dispersions. It was found that the C_{max} for the solid dispersion was about 3-fold that of the physical mixture. The area under the plasma concentration–time curves of the solid dispersion and physical mixture up to 8 h were 19.5 and 3.3 ($\mu g \cdot h/ml$), respectively. Conclusively, the larger bioavailability of mebendazole resulted from improvement of the dissolution rate. From the present results, it is assumed that oral administration of the solid dispersion of mebendazole with PEG-6000 is more effective for the chemotherapy of human echinococcosis.

References

1) M. Sakui, M. Ishige, S. Fukumoto, A. Ueda and M. Ohbayashi, *Jpn. J. Parasitol.*, **33**, 291 (1984).
2) M. Kumagai, *Hokkaido J. Public Health*, **2**, 31 (1988).
3) P. M. Schantz, H. V. Bossche and J. Eckert, *Z. Parasitenkunde*, **67**, 5 (1982).
4) G. J. Munst, G. Karlagains and J. Bircher, *Eur. J. Clin. Pharmacol.*, **17**, 375 (1980).
5) W. L. Chiou and S. Riegelman, *J. Pharm. Sci.*, **60**, 1281 (1971).
6) S. Yakou, S. Yamazaki, T. Sonobe, T. Nagai and M. Sugihara, *Chem. Pharm. Bull.*, **34**, 3408 (1986).
7) S. A. El-Fattuh, N. N. Salil and M. El-Assik, *Drug Dev. Ind. Pharm.*, **10**, 649 (1984).
8) M. P. Oth and A. J. Moes, *Int. J. Pharmaceut.*, **55**, 157 (1989).
9) N. Kohri, K. Mori, K. Miyazaki and T. Arita, *J. Pharm. Sci.*, **75**, 57 (1986).
10) N. Kohri, K. Iwasa, J. Kurihara, K. Miyazaki and T. Arita, *Int. J. Pharmaceut.*, **49**, 213 (1989).
11) G. Levy and B. A. Hayes, *New Engl. J. Med.*, **262**, 1053 (1960).
12) J. Grenet and R. Duclos, *J. Therm. Anal.*, **34**, 559 (1988).
13) R. Duclos, J. Grenet, J. M. Saiter, P. Besancon and A. M. Orecchioni, *Drug Dev. Ind. Pharm.*, **16**, 255 (1990).
14) I. Sugimoto, A. Kuchiki, H. Nakagawa, K. Tohgo, S. Kondo, I. Iwane and K. Takahashi, *Drug Dev. Ind. Pharm.*, **6**, 137 (1980).

CONFORMATIONAL ANALYSIS OF [N-DEMETHYL-TYR(OCH3)-3]RA-VII, CONFORMATIONALLY RESTRICTED MODEL APPROACH

Hideji ITOKAWA,* Keiko SAITOU, Hiroshi MORITA and Koichi TAKEYA

Department of Pharmacognosy, Tokyo College of Pharmacy, Horinouchi 1432-1, Hachioji, Tokyo 192-03, Japan

A molecular design was carried out in a way that locked the type II β-turn conformation of RA-VII, which was isolated from *Rubia cordifolia* and *R.akane*, by removing the N-methyl group of the Tyr-3 residue. Conformational analysis of [N-Demethyl-Tyr(OCH3)-3]RA-VII, derived from RA-VII by hepatic microsomal biotransformation, was conducted by 2D-NMR techniques, temperature effect on NH protons, and NOE experiments. It showed a restricted conformational state with a typical type II β-turn structure between Ala-2 and Tyr-3 in solution.

KEYWORDS [N-Demethyl-Tyr(OCH3)-3]RA-VII; RA-VII; RA-V; *Rubia cordifolia*; *Rubia akane*; conformational analysis; type II β-turn

A cyclic hexapeptide, RA-VII isolated from *Rubia cordifolia* and *R. akane* (Rubiaceae) is a potent antitumor agent.[1] Recently, we reported the conformational analysis of the RA series.[2] RA-VII has two conformational states in $CDCl_3$ on the basis of a *cis/trans* isomerism of N-methyl amide bond at residues 2 and 3, and a main conformer with typical type II β-turn structure constructed by Ala-2 and Tyr-3 may play an important role in its antitumor activity.[2]

Specific N-demethylation of Tyr-3 in RA-VII was examined as one of the methods to lock the conformation. The *cis/trans* isomerization of the N-methyl amide bond in cyclic peptides was observed at times.[3] But generally, the amide bond stabilizes in the *trans* form.[4]

On the other hand, an important characteristic of cytochrome P-450 is that it oxidizes a wide variety of xenobiotics in various types of reaction by the reductive activation of molecular oxygen.[5] Certain cytochrome P-450 monooxygenases catalyze the dealkylation of amines.[5] An example is the reaction in which oxygenation of a methyl group bonded to an amino group creates a hydroxymethylamine and an amine adduct of formaldehyde, which decompose to the amine and formaldehyde. These reactions are important in detoxification and secondary metabolism.

In this communication, we describe hepatic microsomal biotransformation from RA-VII (**1**) to [N-Demethyl-Tyr(OCH3)-3]RA-VII (**3**) and the conformational analysis of **3** as a molecular design by conformationally restricted modeling.

RA-VII (**1**) was converted by rat liver microsomes mainly to compounds **2** and **3**,[6] which were purified by HPLC. Compound

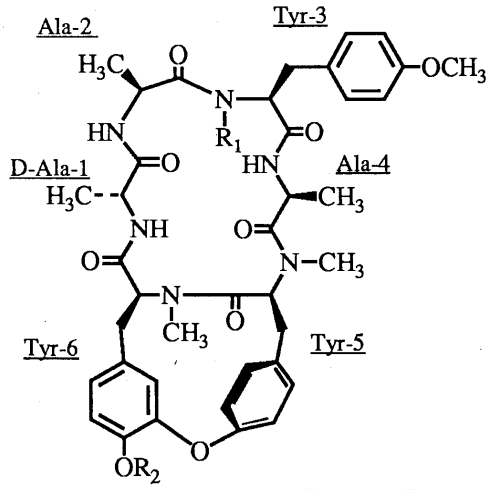

	R_1	R_2
RA-VII (**1**)	Me	Me
RA-V (**2**)	Me	H
[N-Demethyl-Tyr(OCH_3)-3] RA-VII (**3**)	H	Me

Fig. 1. Structures of RA-VII (**1**), V (**2**) and [N-Demethyl-Tyr(OCH_3)-3]RA-VII (**3**)

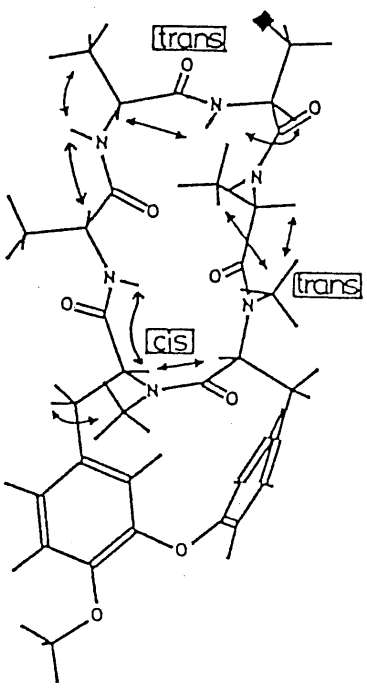

Fig. 2.

The arrows show the negative NOE relationships confirmed by 1D-NOE and NOESYPH experiments in DMSO-d_6 at 303K.

Table I. ^{1}H and ^{13}C-NMR Chemical Shifts of 3 in DMSO-d_6 at 303K (^{1}H: 500MHz, ^{13}C: 125MHz)

Amino acid	Proton	δ (ppm), J (Hz)	Carbon	δ (ppm)
D-Ala-1	Hα	4.28 Jαβ=7.0	Cα	47.09
	Hβ	1.11 JαN=7.8	Cβ	20.51
	HN	7.80	$C_{C=O}$	170.85
Ala-2	Hα	4.24 Jαβ=7.1	Cα	48.56
	Hβ	1.13 JαN=8.5	Cβ	16.65
	HN	8.21	$C_{C=O}$	172.01
Tyr-3	Hα	3.92 Jαβ1=10.4	Cα	54.58
	Hβ1(pro-R)	2.97 Jαβ2=4.0	Cβ	33.72
	Hβ2(pro-S)	3.16 Jβ1β2=13.7	Cγ	130.67
	2Hδ	7.06 Jδε=8.6	Cδ	130.16
	2Hε	6.83 JαN=7.9	Cε	113.41
	HN	8.36	Cζ	157.61
	MeO	3.72	$C_{C=O}$	168.77
			C_O	54.87
Ala-4	Hα	4.61 Jαβ=6.7	Cα	45.50
	Hβ	1.04 JαN=8.0	Cβ	18.49
	HN	6.98	$C_{C=O}$	170.31
Tyr-5	Hα	5.32 Jαβ1=11.4	Cα	53.05
	Hβ1(pro-S)	3.45 Jαβ2=3.3	Cβ	35.72
	Hβ2(pro-R)	2.66 Jβ1β2=11.4	Cγ	135.13
	Hδ1	7.12 Jδ1δ2=2.2	Cδ1	132.73
	Hδ2	7.43 Jδ1ε1=8.5	Cδ2	130.37
	Hε1	6.77 Jδ2ε2=8.4	Cε1	123.78
	Hε2	7.25 Jε1ε2=2.4	Cε2	125.71
	MeN	3.00	Cζ	157.98
			$C_{C=O}$	169.12
			C_N	29.99
Tyr-6	Hα	4.47 Jαβ1=11.9	Cα	56.67
	Hβ1(pro-R)	2.84 Jαβ2=3.5	Cβ	34.83
	HB2(pro-S)	3.13 Jβ1β2=17.6	Cγ	129.53
	Hδ1	6.63 Jδ1δ2=1.7	Cδ1	120.95
	Hδ2	4.50 Jδ1ε1=8.4	Cδ2	114.34
	Hε1	6.88	Cε1	112.60
	MeN	2.51	Cε2	152.28
	MeO	3.83	Cζ	145.79
			$C_{C=O}$	169.83
			C_N	28.97
			C_O	55.73

2 was identical with RA-V, previously isolated from the *Rubia* plant, as shown by direct comparison. Compound 3 with the molecular formula $C_{40}H_{48}O_9N_6$ (756.3561) was obtained as a colorless powder, mp >300°, $[\alpha]_D$ -126.7° (c 0.3, $CHCl_3$-MeOH=1:1).

In the NMR spectra of **3**, suggesting the presence of one stable conformational state in DMSO-d_6, lack of the N-methyl group corresponding to N-methyl-Tyr(OCH_3)-3 was observed. Then, the complete assignments of the ^{1}H and ^{13}C-NMR signals of **3** were made by the combination of the ^{1}H-^{1}H COSY, HMQC and HMBC[7] spectra, as shown in Table I. To confirm the locking of the type II β-turn structure constructed at Ala-2 and Tyr-3, conformational analysis was conducted by NOE experiments (1D-NOE and NOESYPH[8]).

If a type II β-turn occurs, NOE is expected to appear between Ala-2-Hα and Tyr-3-NH, and between Tyr-3-NH and Tyr-3-Hα, whose β-turn is stabilized by a 4-1 hydrogen bond. The signal intensities of the Ala-2-Hα and Tyr-3-Hα decreased when the NH proton of Tyr-3 was saturated. The relationship of NOE enhancements (all negative NOEs) is shown in Fig. 2. The N-methyl amide bond between Tyr-5 and Tyr-6 was shown to be a *cis* bond by the NOE enhancements observed between Tyr-5-Hα and Tyr-6-Hα. Also, the NOE enhancements between the Tyr-5-NCH_3 protons and Ala-4-CH_3/Ala-4-Hα supported to maintain the *trans* in the remaining N-methyl amide bond between Ala-4 and Tyr-5.

The first step in the determination of the secondary structure of peptides in solution by NMR is to distinguish the NH protons exposed to the solvent or shielded from the solvent either sterically or through hydrogen bonding. The most common procedure for that is to determine the temperature effects on the NH protons.[9] The temperature coefficients (dδ/dT) of **3** as

shown in Table II clearly show that Ala-4-NH is involved in a strong intramolecular hydrogen bond and similarly to the active main conformer A of RA-VII.[2] This indicates an antiparallel β-structure stabilized by a 4-1 hydrogen bond.

These NMR examinations show that [N-demethyl-Tyr (OCH_3)-3]RA-VII (**3**) took the typical type II β-turn conformation between Ala-2 and Tyr-3. It is also interesting that the specific N-demethylation of Tyr-3 occurs in the process of metabolism.

Table II. Effect of Temperatures on the NH Chemical Shifts of RA-VII and [N-Demethyl-Tyr(OCH3)-3]RA-VII in DMSO-d_6, $-\Delta\delta/\Delta T$ (10^3 ppm/K)

Compounds	Conformers	D-Ala-1	Ala-2	Tyr-3	Ala-4
RA-VII	A	6.0	4.7	-----	0.0
	B	4.3	4.0	-----	0.0
	C	3.7	4.0	-----	0.7
[N-Demethyl-Tyr (OCH3)-3]RA-VII	A	6.0	4.8	8.3	0.0

A=main conformer, B and C=minor conformers in DMSO-d_6 cited in ref. 2.

Isolation of metabolites *in vivo* , their antitumor activities,[10] and further work to clarify the structure-activity relationship of RAs are in progress.

ACKNOWLEDGEMENT We thank Dr. A. Hiratsuka for useful discussion about hepatic microsomal biotransformation and Mrs. C. Sakuma for NMR measurements.

REFERENCES AND NOTES

1) H.Itokawa, K.Takeya, K.Mihara, N.Mori, T.Hamanaka, T.Sonobe and Y.Iitaka, *Chem.Pharm.Bull.*, **31**, 1424 (1983); H.Itokawa, K.Takeya, N.Mori, T.Hamanaka, T.Sonobe and K.Mihara, *ibid.*, **32**, 284 (1984); H.Itokawa, K.Takeya, N.Mori, T.Sonobe, S.Mihashi and T.Hamanaka, *ibid.*, **34**, 3762 (1986).

2) H.Morita, K.Kondo, Y.Hitotsuyanagi, K.Takeya, H.Itokawa, N.Tomioka, A.Itai and Y.Iitaka, *Tetrahedron*, **47**, 2757(**1991**); H.Itokawa, H.Morita, K.Takeya, N.Tomioka, A.Itai and Y.Iitaka, *ibid.*, in press.

3) D.E.Stewart, A.Sarkar and J.E.Wampler, *J.Mol.Biol.*, **214**, 253 (1990).

4) Recently, a few examples about cyclic cis peptides without N-substituted amides have been reported.; D.F.Mierke, T.Yamazaki, O.E.Said-Nejad, E.R.Felder and M.Goodman, *J.Am.Chem.Soc.*, **111**, 6847 (1989); H.Kessler, U.Anders and M.Schudok, *ibid.*, **112**, 5908 (1990).

5) Some examples of the role of cytochrome P-450 in oxygen activation for drug metabolism; a) J.W.Gorrod, "Biological Oxidation of Nitrogen" Elsevier/North Holland Biomedical Press: New York, (1978); b) R.W.Estabrook and J.Werrigloer, American Chemical Society Symp. Ser., **44**, 1 (1979); c) R.E.White and M.J.Coon, *Annu. Rev. Biochem.*, **49**, 315 (1980); d) J.P.Shea, G.L.Valentine and S.D.Nelson, *Biochem. Biophys. Res. Commun.*, **109**, 231 (1982).

6) RA-VII in 5% DMSO soln. was incubated with rat liver microsomes and cofactor ($MgCl_2$ 8μmol, KCl 33μmol, G-6-P 5μmol, NADPH 4μmol, NADH 4μmol, Na-Phoshate buffer PH 7.4 100μmol) at 37°C for 5h.; B.N.Ames, W.E.Durston, E.Yamasaki and F.D.Lee, *Proc.Nat.Acad.Sci., USA*, **70**, 2281 (1973).

7) A.Bax and M.F.Summers, *J.Am.Chem.Soc.*, **108**, 2094 (1986).

8) G.Bodenhauser, H.Koger, R.R.Ernst, *J.Magn.Res.*, **58**, 370 (1984); NOESYPH experiments were acquired with mixing times of 0.4 and 0.6s.

9) Some examples; a) H.Kessler, *Angew.Chem.*, **94**, 509 (1982); b) A.Ravi, B.V.V.Prasad and P.Balaram, *J.Am.Chem.Soc.*, **105**, 105 (1983); c) M.Iqbal and P.Balaram, *ibid.*, **103**, 5548 (1981); d) K.D.Kopple, M.Ohnishi and A.Go, *ibid.*, **91**, 4264 (1969); e) M.Ohnishi and D.W.Urry, *Biochem. Biophys. Res. Commun.*, **36**, 194 (1969).

10) [N-demethyl-Tyr(OCH_3)-3]RA-VII showed cytotoxic activities against P388 cells; IC_{50} 0.09μg/ml.

(Received May 8, 1991)

DIELS-ALDER REACTION OF 4,6-DIHYDROTHIENO[3,4-c]FURAN-5,5-DIOXIDE WITH QUINONES: STEREOSELECTIVE SYNTHESIS OF QUINONE-ANNELATED 2,3-BIS(METHYLENE)-7-OXABICYCLO[2.2.I]HEPTANES

Takayoshi SUZUKI, Kan KUBOMURA, and Hiroaki TAKAYAMA*
Faculty of Pharmaceutical Sciences, Teikyo University, Sagamiko, Kanagawa 199-01, Japan

4,6-Dihydrothieno[3,4-c]furan-5,5-dioxide (**1**), a novel precursor of a bis-diene, reacts with quinones to afford the normal Diels-Alder adducts, the quinone-annelated 2,3-bis (methlene)-7-oxabicyclo[2.2.1]-heptane derivatives. Promising building blocks(**3b** and **5**) for the synthesis of the antineoplastic antibiotics are prepared by this method.

KEYWORDS 4,6-dihydrothieno[3,4-c]furan-5,5-dioxide; bis-diene precursor; Diels-Alder reaction; tandem cycloaddition; p-bezoquinone; 1,4-naphthoquinone; juglone; quinone-annelated 2,3-bis(methylene)-7-oxabicyclo-[2.2.1] heptane

Furan-annelated 3-sulfolene (**1**) has been used as a masked bis-diene which, depending on the dienophiles and the reaction conditions, could sequentially react with a variety of dienophiles to construct four types of cycloadducts: a monocycloadduct bearing bis-*exo*methylenes (Type A), a tandemadduct (Type B), a monocycloadduct containing a furan ring (Type C), and a monocycloadduct with a 3-sulfolene ring (Type D).[1] Furthermore, even with unfavorable dienophiles such as dimethyl maleate and dimethyl fumarate whose Diels-Alder adducts with furan have not been isolated under thermal conditions, the furansulfolene (**1**) reacted to afford mainly type A and type B adducts.[1]

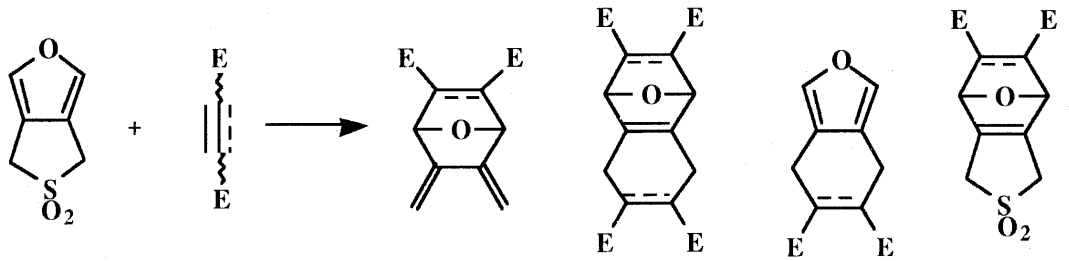

The current interest in brief construction of clinically important polycyclic quinones such as anthracyclinones,[2] pradimicinone A (anti HIV),[3] and their analogues prompted us to examine the reaction of **1** with the quinones whose Diels-Alder adducts with furan have not been isolated before. We reporrt here the successful Diels-Alder reaction of furansulfolene (**1**) with several commercially available quinones, especially with juglone to construct 1,4-epoxy-2,3-bis(methylene)-1,4,4a,9a-tetrahydroanthraquinone system (**3**), and that of dimethyl 5,6-bis(methylene)-7-oxanorbornane-2-*endo*-3-*endo*-dicarboxylate (**4**)[1] (a type A adduct readily available from the reaction of **1** with dimethyl maleate) with juglone to furnish **5**.

The Diels-Alder reaction of **1** with 2 eq mol of p-benzoquinone was achieved at 120°C for 3 h (benzene, sealed tube), affording 6,7-bis(methylene)-5,8-epoxy-4a,5,8,8a-tetrahydro-1,4-naphthoquinone (**2a**) as a single product in 78% yield, and **1** was recovered in 22% yield (Table I, entry 1). Under the same conditions, the reaction of **1** with 2,6-xyloquinone was very sluggish, and heating at 120°C for 12 h resulted in only a 2% yield of **2b** with the recovery of **1** (88%) (entry 2). Next, treatment of **1** with 1,4-naphthoquinone at 150° C for 4 h gave 1,4-epoxy-

2,3-bis(methylene)-1,4,4a,9a-teytrahydro-anthraquinone (**3a**) in 58% yield together with a small amount of a type B adduct (entry 4). In examining of the solvent effect in the cycloaddition of 1 with this dienophile, we found benzene to be the most favorable one (entries 4,5,6,7). Finally, treating 1 with juglone under the same conditions produced the desired product (**3b**) in 60% yield (entry 8). This should permit the ready assemblage of anthracyclinones through the [BCD→ABCD] cycloaddition strategy.[2] The structures of the new compounds thus obtained were confirmed by their ^{1}H- and ^{13}C-NMR spectral data.[4]

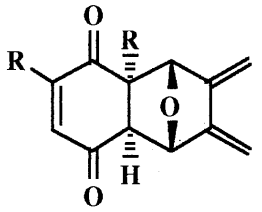

2 a: R= H
b: R= Me

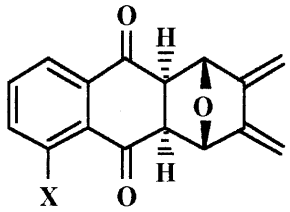

3 a: X= H
b: X= OH

Table I. Reaction of Furansulfolene (1) with Quinones

Entry	Quinone	Solvent	Temp[a] (°C)	Time (h)	Type A (%)[b]	Recovery of 1 (%)[b]
1	p-Benzoquione	Benzene	120	3	2a(*exo* 78)	
2	2,6-Xyloquinone	Benzene	120	12	2b(*exo* 2)	22
3	1,4-Naphthoquinone	Benzene	120	4	3a(*exo* 50)	88
4		Benzene	150	4	3a(*exo* 58)[c]	47
5		Toluene	150	4	3a(*exo* 21)[d] (*endo* 4)	
6		CH_2Cl_2	150	16	3a(*exo* 31)	13
7		$CHCl_3$	150	9	3a(*exo* 24)	2
8	Juglone	Benzene	120	4	3b(*exo* 60)	13

a) In a sealed tube. b) Isolated yield. The reaction conditions were not optimized.
c) A type B adduct was isolated(4% yield). d) A type C adduct was isolated(12% yield).

Isolation of a cycloadduct bearing bismethylene (Type A) in this case is noteworthy because the Diels-Alder adducts of furan and quinones are thermally unstable and either decompose to furan and the dienophiles or are cleaved to Michael-type adducts.[5] In our case, ready desulfonylation of the initially formed furan-adduct (Type D) to the type A adduct should circumvent the unfavorable equilibrium between 1 and the type D adduct. Furthermore, it is significant that the configuration of all of the type A adducts is *exo*, whereas ring annelated furans, for example 5,6-dimethoxy-isobenzofuran, reacted with these quinones to give a mixture of *endo/exo* isomers.[6] This may reflect another important role in the cycloaddition of the furan moiety of 1: the transition state for *endo* addition is unfavorable because of steric repulsion between the sulfonyl group of 1 and the dienophiles. Configuration of all cycloadducts could be readily determined by inspection of their ^{1}H-NMR spectra. Thus the bridgehead protons appeared as singlets in the reasonable region (δ, 5.0 - 6.0), and those of *endo*-isomer appeared as a doublet.[4]

Finally, we examined the reaction of dimethyl 5,6-bis(methylene)-7-oxanorbornane-2-*endo*-3-*endo*-dicarboxylate (4) with juglone. Reaction of the bis-exomethylene (4) with 1.1 eq of juglone in anhyd. CH_2Cl_2

under Argon atmosphere at 80°C for 10 h gave a 58% isolated yield of the tetracyclic quinone (5).[4] This approach to tetracyclic quinones starting from the readily available type A adducts with naphthoquinone may well have fruitful application in constructing the important polycyclic quinones including pentacyclic quinone pradimicin A analogues.

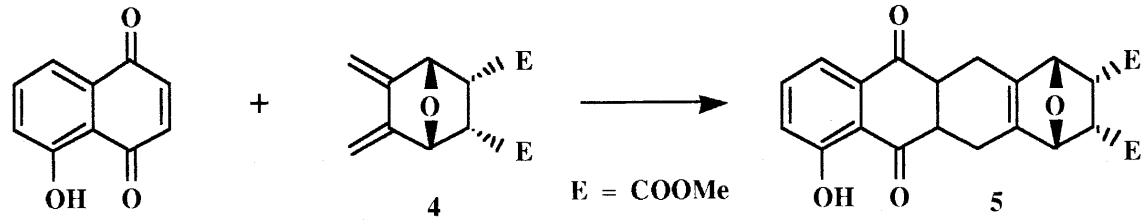

In conclusion, in addition to the role of a precursor of *s-cis*-butadiene, the sulfolene moiety of furansulfolene (1) enhanced the reactivity of the furan ring toward unfavorable dienophiles in Diels-Alder cycloadditions, and thus introduces the use of **1** as a source of important intermediates in the synthesis of natural products.

Further studies along this line are in progress in our laboratory.

REFERENCES AND NOTES

1) T. Suzuki, K. Kubomura, H. Fuchii, and H. Takayama, J. Chem. Soc., Chem. Commun., **1990**,1687 .

2) For recent representative examples: a) S. Terashima, Yuki Gosei Kagaku Kyokai Shi (J. Synth. Org. Chem. Jpn.,**49**, 99 (1991); b) T. Antonsson and P. Vogel, Tetrahedron Lett., **31**, 89 (l990).

3) T. R. Kelly, Q. Li, and V. Bhushan, Tetrahedron Lett., **31**, 161 (1990). For a recent representative example, M. Kakushima, Y. Sawada, M. Nishino, and T. Oki, J. Org. Chem., **54**, 1019 (1989).

4) **2a**: ^{1}H- NMR (90 MHz, $CDCl_3$/TMS) δ: 3.13 (2H, s), 5.15 (2H, s), 5.20(2H, s), 5.35(2H, s), 6.81(2H, s).
2b: δ; 1.24 (3H, s), 2.01(3H, s), 2.66(1H, s), 4.94(1H, s), 4.97(1H, s), 5.14(1H, s), 5.16(1H, s), 5.33(1H, s), 5.51(1H, s), 6.72(1H, s).
3a: δ; 3.33(2H, s), 5.24(2H, s), 5.28(2H, s), 5.34(2H, s), 7.76(2H, d, J=3.4Hz), 8.09(2H, d, J=3.4Hz). ^{13}C-NMR(100 MHz, $CDCl_3$/TMS) δ; 54.46(d), 86.82(d), 103.30(t), 127.20(d), 134.45(d), 145.70(s), 194.66(s).
3b: ^{1}H -NMR δ; 3.30(1H, d, J=1.4Hz), 3.35(1H, d, J=1.4Hz), 5.26(2H, s), 5.27(2H, s), 5.37(, s), 7.27(1H, s), 7.66(2H, m), ^{13}C -NMR δ; 53.96(d), 54.43(d), 87.15(d), 87.20(d), 103.52(t), 118.22(s), 118.78(d), 123.93(d), 35.19(s), 137.50(d), 145.39(s), 145.50(s), 162.18(s), 194.02(s), 201.24(s).
5: ^{1}H -NMR δ; 2.68(2H, m), 3.10(2H, m), 3.53(2H, m), 3.61(3H, s), 3.62(3H, s), 3.65(2H, m, decoupling method showed these protons were coupled with the protons appeared at δ 5.00), 5.00(2H, d, J=4.0Hz), 7.25(1H, m), 7.61(2H, m), ^{13}C- NMR δ; 23.90(t), 25.15(t), 46.33(d), 46.75(d), 47.66(d), 47.82(d), 51.84(q), 81.86(d), 81.90(d), 117.57(s), 117.86(d), 123.66(d), 136.11(s), 136.88(d), 139.87(d), 170.50(s), 170.70(s), 196.82(s), 203.64(s).

5) G. A. Kraus and S. H. Woo, J. Org. Chem., **51**, 114 (1986); J. A. Moore and E. M. Partain III, *ibid*, **48**, 1105, (1983); J. H. Bridson, S. M. Bennett, and G. Butler, J. Chem. Soc., Chem. Commun., **1980**,413 ; T. A. Eggelte, H. D. Koning, and H. O. Huisman, Tetrahedron, **29**, 2491 (1973); C. H. Eugster and A. Hoffmann, Helv. Chim. Acta, **47**, 769 (1964); J. Jolivet, Ann. Chimi., **5**, 1165 (1960).

6) B. A. Keay, D. K. W. Lee, and R. Rodrigo, Tetrahedron Lett., **21**, 3663 (l980).

(Received May 20, 1991)

REGIO- AND STEREOSELECTIVE HYDROXYLATION OF GRINDELIC ACID AND ITS 3α-HYDROXY DERIVATIVE

Sayoko HIRANUMA, Takeshi SHIMIZU* and Hirosuke YOSHIOKA

RIKEN (Institute of Physical and Chemical Research), Wako-shi, Saitama, 351-01, Japan

A hydroxyl group was selectively introduced at the C-17 or C-6 position of grindelic acid (**1a**) and 3α-hydroxygrindelic acid (**1b**) via the 17- or 7β-bromo derivatives (**6a,b** or **9a,b**) given respectively by bromination with Br_2 or NBA. The 7β-hydroxy derivatives (**17a,b**) were obtained via the 8β–methyl-7-one derivatives (**14a,b**) by reduction with $NaBH_4$. The 7α-hydroxy derivatives (**18a,b**) were obtained selectively from the 8,9-en-7-one derivatives (**15a,b**) which contain a cleaved structure at the C-9 position.

KEYWORDS grindelic acid; 3α-hydroxygrindelic acid; bromination; epoxide cleavage; stereoselective reduction; 6-hydroxygrindelic acid; 7-hydroxygrindelic acid; 17-hydroxygrindelic acid

A number of diterpenoids which contain a labdane skelton with hydroxyl group(s) on the decalin ring are biologically active. Examples are 6β- and 18-hydroxygrindelic acids (**3a** and **3b**) as aphid antifeedants,[1] forskolin (**4**) as a cardiac or vasodilator,[2] and salvic acid (**5**) as an antitumor agent.[3] As a part of our consecutive study on designs and syntheses of bioactive diterpenoids from biologically renewable resources, our interest has been focused on the regio- and stereoselective oxygenation of grindelic acid (**1a**) and its 3α-hydroxy derivative (**1b**). The acid (**1a**) occurs abundantly in plants of *Grindelia* species,[4] and **1b** has been produced from **1a** in preparative scale by the microbial transformation developed by Hoffmann.[5] The 3-hydroxyl group of **1b** can be a good candidate for further chemical modification on the A ring.

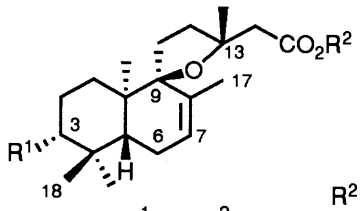

1a R^1= H, R^2= H
1b R^1= OH, R^2= H
2a R^1= H, R^2= Me
2b R^1= OH, R^2= Me

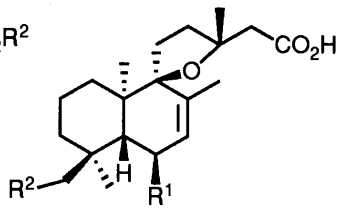

3a R^1= OH, R^2= H
3b R^1= H, R^2= OH

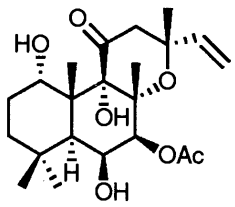

4
forskolin

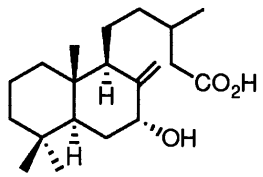

5
salvic acid

Regarding the hydroxylation of **1a** at the C-6 position, Sierra has reported the conversion of **1a** to 6-hydroxygrindelic acids which include **3a** through many steps involving the auto-oxidation of **2a** under intensive UV irradiation.[6] Here we describe the bromination of **2a** and **2b**, which will serve as new pathways leading to the 17-hydroxy derivatives (**8a,b**) and to the 6α-hydroxy derivative (**12b**). We also report a selective method for the synthesis of the 7α- and 7β-hydroxy derivatives via the 7,8β-epoxides (**13a,b**) on the controlled rearrangement

with BF_3•OEt_2 that optionally yielded either the 7-oxo derivatives (**14a,b**) containing a spiro-ether ring or the 8,9-en-7-ones (**15a,b**) with a cleaved sub-structure at C-9.

Treatment of **2a** with bromine under mild conditions (see Chart 1) gave mainly the 17-bromide (**6a**) along with the 7β-bromide (**9a**). **6a** was converted to methyl 17-acetoxygrindelate (**7a**)[7] by treatment with CsOAc in the presence of 18-crown-6 in high yield. Alkaline hydrolysis of **7a** gave 17-hydroxygrindelic acid (**8a**)[8] quantitatively. Methyl 3α-hydroxygrindelate (**2b**) also gave **6b**, **7b** and **8b** in good yields when treated as described for **2a** (see Chart 1).

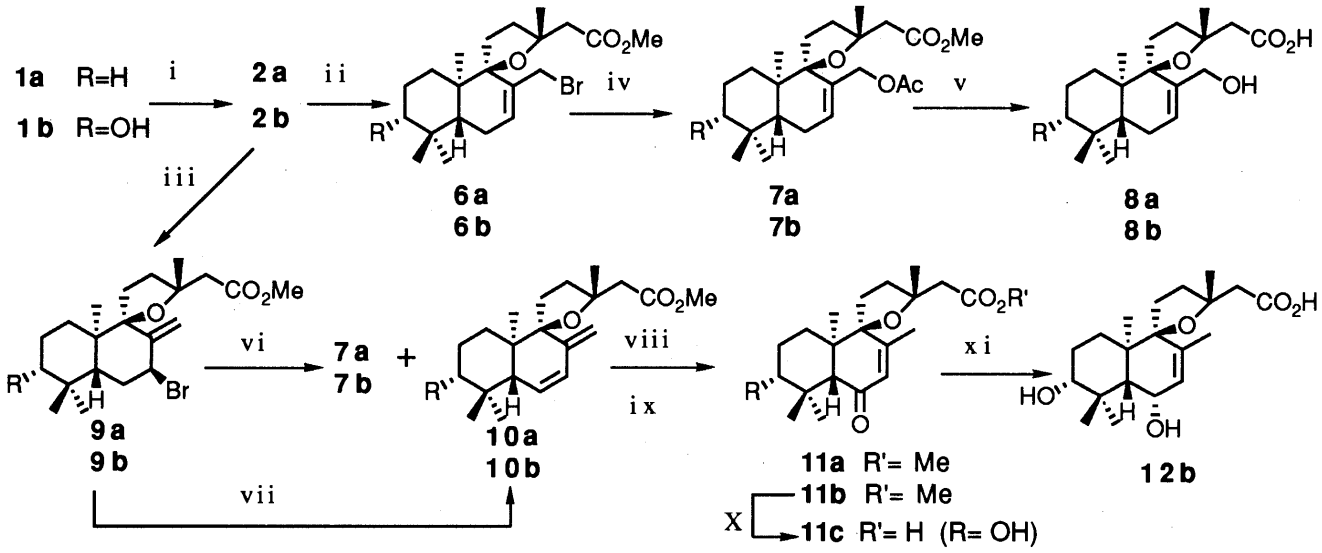

Chart 1 i, CH_2N_2, Et_2O-MeOH (**2a** 90%, **2b** 95%); ii, Br_2, added slowly (2 h), 0°C (**6a** 81% plus **9a** 10%, **6b** 70% plus **9b** 15%); iii, NBA, aq. acetone (5%), r.t., 8 h (**9a** 85%, **9b** 74%); iv, CsOAc (1.1 eq), 18-crown-6, benzene, reflux, 3.5 h (**7a** 93%, **7b** 90%); v, 5% aq. KOH, MeOH, reflux, 8 h (**8a** 93%, **8b** 95%); vi, CsOAc (5 eq), 18-crown-6, benzene, reflux, 8 h (**10a** 14% plus **7a** 73%, **10b** 30% plus **7b** 45%); vii, LiBr, Li_2CO_3, DMF, 80°C, 3 h (**10a** 91%, **10b** 88%); viii, MCPBA (2 eq), 0°C, 3 h; ix, BF_3•OEt_2 (10 eq), benzene, r.t., 10 min, then Al_2O_3 (**11b** 57% from **10b**); x, 5% KOH, MeOH, reflux, 8 h (**11c** 95%); xi, DIBAL, toluene-THF, -78°C to r.t., 3 h (**12b** 70%).

Bromination of **2a** with freshly recrystallized NBA gave the 7β-bromide (**9a**), but treating **9a** with CsOAc/18-crown-6 resulted in the formation of **7a** and the diene (**10a**). Dehydrobromination of **9a** with LiBr and Li_2CO_3 in anhydrous DMF afforded **10a** in high yield. Similarly, **2b** was converted via **9b** to **10b**, which was then led to the 6-enone (**11b**) through epoxidation followed by BF_3•OEt_2 treatment in accordance with Sierra's method.[6] Although reduction of the enone (**11a**) with $Zn(BH_4)_2$ has been known,[6] this proceeded sluggishly with a moderate selectivity to the 6-oxo group in **11b** and affected its ester group in part. **11b** was best converted to the 6α-hydroxy derivative (**12b**) via reduction of the acid (**11c**) with DIBAL.

Oxygenation of **1a** at C-7 was first attempted by Bruun,[8] who treated **1a** with $Na_2Cr_2O_7$ to get **15a** as a result of the concurrent cleavage of the spiro-ether ring at C-9. Later, Sierra obtained the 7β-hydroxy-8,17-ene ester (**16a**) from **1a** through either the auto-oxidation or the epoxidation followed by treatment with $Al(O\textit{i}\text{-}Pr)_3$.[6] We found that the mild BF_3•OEt_2 treatment (see Chart 2) of **13a,b** in benzene afforded the 7-oxo compounds (**14a,b**), in which the spiro-ether ring remained intact while the epoxide ring was rearranged. In contrast, the

BF_3•OEt_2 treatment of **14a,b** in DMSO on heating gave the enone (**15a,b**) in high yield on the concurrent cleavage of the ether bond at C-9. Interestingly, the spiro-ketones (**14a,b**) afforded the 7β-hydroxy derivatives (**17a,b**) when reduced with $NaBH_4$, but the cleaved enones (**15a,b**) selectively gave the 7α–hydroxy derivatives (**18a,b**) .

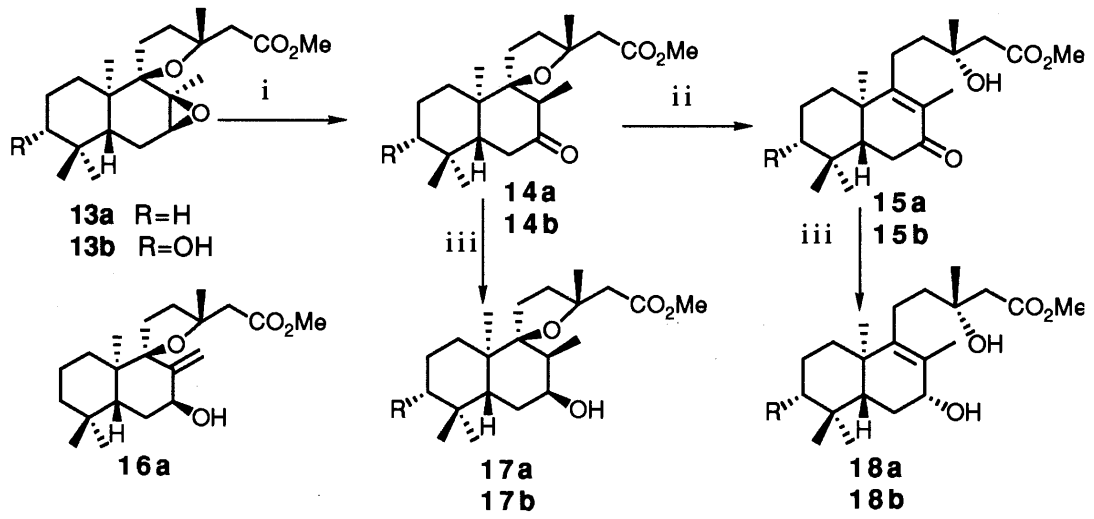

Chart 2 i, BF_3•OEt_2 (10 eq), benzene, r.t., 10 min (**14a** 95%, **14b** 92%); ii, BF_3•OEt_2 (10 eq), DMSO, 80°C, 4.5 h (**15a** 85%, **15b** 90%); iii, $NaBH_4$, EtOH, 0°C to r.t (**17a** 82% **17b**, 93%; **18a** 90%, **18b** 80%).

ACKNOWLEDGEMENTS The authors are thankful to E. I. Du Pont de Nemours & Co. Ltd for financial support, and to Dr. J. J. Hoffmann for supplying grindelic acid and 3α-hydroxygrindelic acid.

REFERENCES AND NOTES

1) A. F. Rose, K. C. Jones, W. F. Haddon and D. L. Dreyer, *Phytochemistry*, **20**, 2249 (1981).
2) S. V. Bhat, B. S. Bajwa, H. Dornauer, N. J. de Souza and H. W. Fehlhaber, *Tetrahedron Lett.*, **1977**, 1669.
3) M. Hoeneisen, P. G. Sammes M. de Silva and W.H. Watson, *Rev. Latinoamer. Quim.*, **10**, 37 (1979).
4) L.Panizzi, L. Mangoni and M. Berlardini, *Tetrahedron Lett.*, **11**, 376 (1961) .
5) J. J. Hoffmann, H. Punnapayak, S. D. Jold, R. B. Bates, and F. A. Camou, *J. Nat. Prod.*, **51**, 125(1988).
6) M. G. Sierra, M. I. Colombo, A. C. Olivieri, M. E. Zudenigo and E. A. Rúveda, *J. Org. Chem.*, **49**, 4984 (1984).
7) F. Bohlmann, M. Ahmed, N. Borthakur, M. Wallmeyer, J. Jakupovic, R. M. King and H. Robinson, *Phytochemistry*, **21**, 167 (1982).
8) T. Bruun, L. M. Jackman and E. Stenhagen, *Acta Chem. Scand.*, **16**, 1675 (1962).

(Received June 5, 1991)

A NEW GENERAL SYNTHETIC ROUTE FOR 1-SUBSTITUTED 4-OXYGENATED β-CARBOLINES[1)]

Hideharu SUZUKI, Yuusaku YOKOYAMA, Chiemi MIYAGI, and Yasuoki MURAKAMI*
School of Pharmaceutical Sciences, Toho University,
2-2-1, Miyama, Funabashi, Chiba 274, Japan

Two naturally occurring 1-substituted 4-methoxy-β-carboline (**1b,c**) were synthesized from ethyl indole-2-carboxylate (**5b**) and its 1-benzyl derivative (**5a**), respectively. The synthesis routes involved elaboration of the ester group of **5a,b**, cyclization of the substituent at the 2-position toward the 3-position of the indole nucleus, and functionalization at the 1-position of the β-carboline nucleus by a modified Reissert reaction. The β-carbolines (**1b,c**) thus prepared should be mother compounds for the synthesis of their congeners.

KEYWORDS indole; β-carboline; cyclization; PPA; Reissert reaction; synthesis

4-Oxygenated β-carboline alkaloids[2)] have become a large family in β-carboline alkaloids recently. Representative examples (**1,2,3,**and **4**) are shown in Fig. 1. Some compounds of them show interesting biological activities,[3,4,5)] but systematic research for biological evaluation has not been done, probably because of their poor isolation yields from natural sources. Thus, we are sure that their syntheses will have some pharmaceutical importance. Two compounds, crenatine[1c,6,7)] (**1a**) and 1-methoxycanthin-6-one[9)] (**3**), were synthesized earlier, but their synthetic routes are not suitable for the general synthesis of their congeners. In this paper we report a new synthesis of 1-functionalized 4-methoxy-β-carbolines (**1b** and **1c**), which are natural products themselves and at the same time mother compounds leading to the general synthesis of their congeners.

Fig. 1

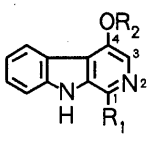

1, 2

	R_1	R_2	
1a	Et	Me	(crenatine)
1b	COMe	Me	
1c	CO_2Me	Me	
1d	$CH=CH_2$	Me	
1e	$CH(OH)CH_2OH$	Me	
2a	CHO	H	
2b	CO_2Me	H	

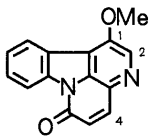

3

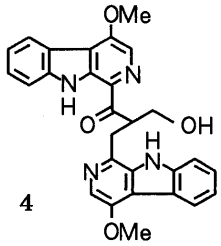

4

Strategy for the synthetic route is based on our route for crenatine,[1c,7)] in which construction of the C-ring consisted of very little cyclization[8)] from the C_2- to C_3-position of the indole nucleus. The synthesis shown in Chart 1 was started with the N-protected ethyl indole-2-carboxylate (**5a**), which was elaborated to the glycine derivative (**7a**) in a good yield. Cyclization of **7a** with PPA occurred naturally at the C_3-position to give the cyclic ketone (**8a**). It is an advantageous feature in the present route

that the cyclization step simultaneously forms the C_4-oxygen functionality of the β-carboline nucleus. A combination of O-methylation and the following dehydrogenation of **8a** to **9a** was conducted by modification of Cook's methods[9]; that is, use of chloranil as a dehydrogenating agent resulted in shortening the reaction time and increasing the yield. C_1-Functionalization of **9a** was achieved by a modified Reissert reaction with diethyl phosphorocyanidate[10] (DEPC) via the N-oxide (**10a**). The modification of the cyano group of **11a** with HCl/MeOH [to methyl ester (**12**)] or with DIBAL [to the aldehyde (**13**)] for converting the nitrile (**11a**) into natural products was unsuccessful, while **11a** was converted to the 1-acetyl compound (**14**) by the reaction with MeLi, followed by treatment with SiO_2. And last, the debenzylation of **14** by our method[11] gave the target compound (**1b**) very smoothly. The synthetic **1b** (mp 211-212.5°C) was identical with the natural one (mp 208°C) in all respects.

To overcome the difficulty that the cyano group of the 9-benzyl compound (**11a**) could not be converted to ester group as mentioned above, debenzylation of **11a** to **11b** was tried. However, no debenzylation occurred. Thus, **11b** was synthesized from ethyl indole-2-carboxylate (**5b**) according to the synthesis of the N-benzyl compound (**11a**). A problem in the NH-series was at the cyclization of the NH-glycine derivative (**7b**). Two cyclization directions were possible[12] for **7b** (1- and 3-positions, giving **8b** and **15**). Fortunately cyclization occurred exclusively at the desired 3-position. Reissert reaction of the N-oxide (**10b**) with DEPC gave the N-phosphorylated 1-cyano compound (**11c**) but not the NH 1-cyano compound (**11b**); that is, N-phosphorylation occurred concurrently with the Reissert reaction. Dephosphorylation was successful with KOH to give **11b** quantitatively. Treatment of both **11b** and **11c** with HCl/MeOH easily gave the 1-ester

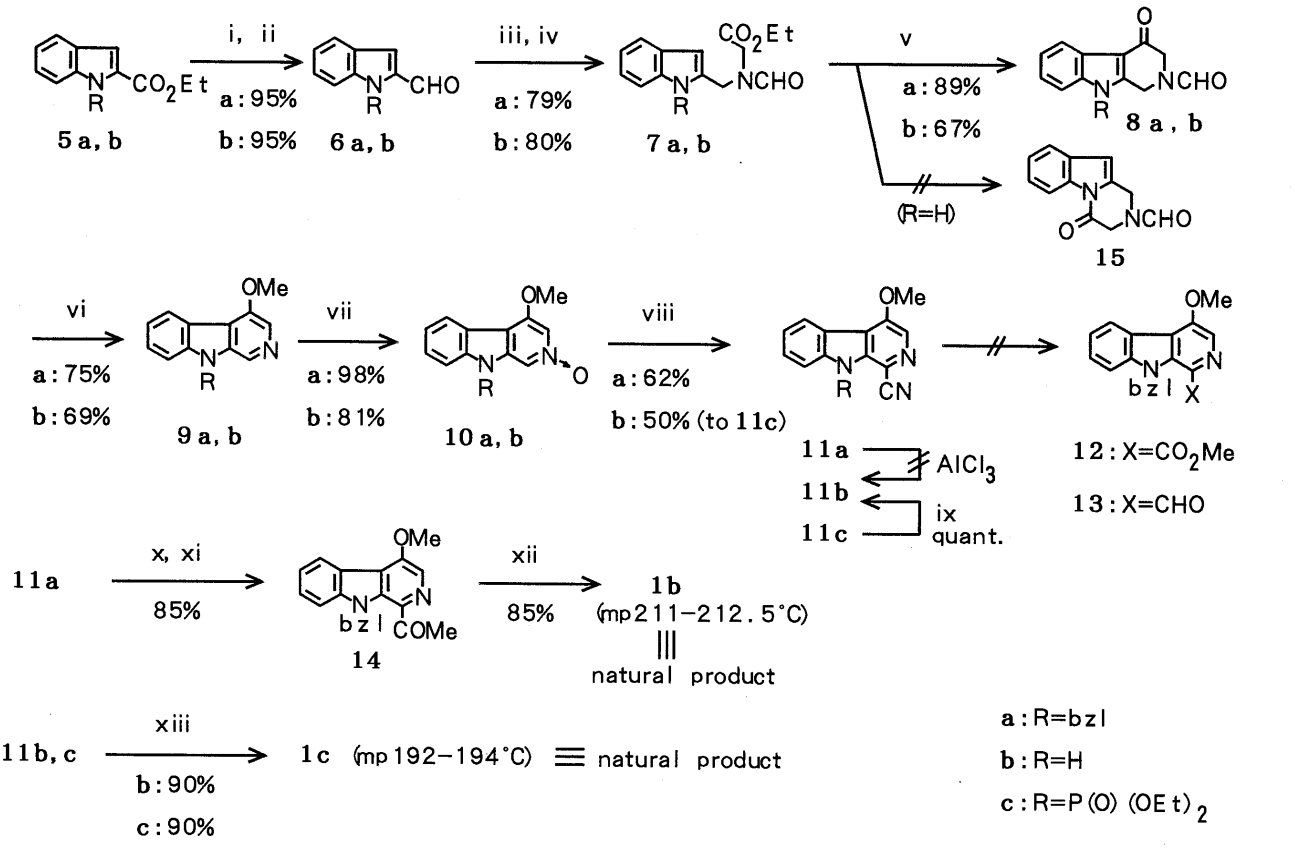

Reagents and conditions : i) $LiAlH_4$ / THF, rt, ii) MnO_2 / CH_2Cl_2, rt, iii) H-Gly-OEt, $NaBH_3CN$ / MeOH, rt, iv) HCO_2Et, rt, v) PPA, 60° C, vi) $(CH_3O)_2C(CH_3)_2$, TsOH, chloranil / benzene, rt, vii) m-CPBA / CH_2Cl_2, rt, viii) DEPC, Et_3N / dioxane, reflux, ix) KOH / CH_3CN-H_2O, rt, x) MeLi / THF -50° C, xi) SiO_2, xii) $AlCl_3$ / benzene, rt, xiii) HCl-MeOH, rt.

Chart 1[13]

(**1c**, mp 192-194°C), which was identical with the natural product (mp 191-192°C).

The synthetic **1b** and **1c** should also serve as starting compounds for the synthesis of their congeners (**1**, **2**, **3**, and **4**). Yields of the benzyl series was superior to those of the NH series in each step. However, debenzylation by $AlCl_3$ in benzene is not necessarily successful for various 1-substituents, while the NH series is feasible for every step. Thus, the two routes are complementary.

REFERENCES AND NOTES

1) This report is part XXX of "Synthetic Studies on Indoles and Related Compounds." a) Part XXIX: T. Watanabe, H. Takahashi, H. Kamakura, S. Sakaguchi, M. Osaki, S. Toyama, Y. Mizuma, I. Ueda, and Y. Murakami, Chem. Pharm. Bull., submitted. b) Part XXVIII: Y. Yokoyama, H. Suzuki, S. Matsumoto, Y. Sunaga, M. Tani, and Y. Murakami, ibid., in press. c) Part XXVII: Y. Murakami, Y. Yokoyama, C. Aoki, H. Suzuki, K. Sakurai, T. Shinohara, C. Miyagi, Y. Kimura, T. Takahashi, T. Watanabe, and T. Ohmoto, ibid., in press.

2) a) T. Ohmoto, R. Tanaka, and T. Nikaido, Chem. Pharm. Bull., **24**, 1532 (1976); b) T. Ohmoto, K. Koike, and Y. Sakamoto, ibid., **29**, 390 (1981); c) T. Ohmoto and K. Koike, ibid., **31**, 3198 (1983); d) T. Ohmoto and K. Koike, ibid., **32**, 170 (1984); e) K. Koike and T. Ohmoto, ibid., **34**, 2090 (1986); f) E. Sánchez and J. Comin, Phytochemistry, **10**, 2155 (1971); g) S. R. Johns, J. A. Lamberton, and A. A. Sioumis, Aust. J. Chem., **23**, 629 (1970); h) B. S. Joshi, V. N. Kamat, and D. H. Gawad, Heterocycles, **7**, 193 (1977); i) E. Varga, K. Szendrei, J. Reisch, and G. Maróti, Planta Medica, **40**, 337 (1980).

3) S. Matsumura, H. Enomoto, Y. Aoyagi, Y. Nomiyama, T. Kono, M. Matsuda, and H. Tanaka, Ger. Offen., 29 41 449, April 17 (1980) [Chem. Abstr. **93**, p114495r (1980)].

4) T. Ohmoto, T. Nikaido, K. Koike, K. Kohda, and U. Sankawa, Chem. Pharm. Bull., **36**, 4588 (1988).

5) a) N. Fukamiya, M. Okano, and T. Aratani, J. Nat. Prod. **49**, 428 (1986); b) L. A. Anderson, A. Harris, and J. D. Phillipson, ibid., **46**, 374 (1983).

6) M. Cain, R. Mantei, and J. M. Cook, J. Org. Chem., **47**, 4933 (1982).

7) Y. Murakami, Y. Yokoyama, C. Aoki, C. Miyagi, T. Watanabe, and T. Ohmoto, Heterocycles, **26**, 875 (1987).

8) Cyclization of C_2-substituent to C_3-position of the indole nucleus to construct the 2,3-fused indole nucleus was only a few examples; a) P. Rosenmund, W. Trommer, D. Dorn-Zachertz, and U. Ewerdwalbesloh, Liebigs Ann. Chem., **1979**, 1643; b) T. Martin and C. J. Moody, J. Chem. Soc., Perkin Trans. 1, **1988**, 235.

9) T. J. Hagen, K. Narayanan, J. Names, and J. M. Cook, J. Org. Chem., **54**, 2170 (1989).

10) S. Harusawa, Y. Hamada, and T. Shioiri, Heterocycles, **15**, 981 (1981).

11) Y. Murakami, T. Watanabe, A. Kobayashi, and Y. Yokoyama, Synthesis, **1984**, 738.

12) There is a report which describes that cyclization of 2-substituted indole occurred both at 1- and 3-positions; J. R. Johnson, A. A. Larsen, A. D. Holley, and K. Gerzon, J. Am. Chem. Soc., **69**, 2364 (1947).

13) All compounds in Chart 1 show satisfactory elemental analyses and spectral data.

(Received June 17, 1991)

PHOTOCHEMISTRY OF 2-(3, 4, 5-TRIMETHOXYPHENYL)-4-(3, 4-METHYLENEDIOXYPHENYL)-4-OXO-2-BUTENONITRILE (β-CYANOCHALCONE): ANOMALOUS DIMERIZATION THROUGH ISOMERIZATION IN THE SOLID STATE[1)]

Hisashi ISHII,*, [a] Eri SAKURADA (nee KAWANABE),[a] Tomoko FURUKAWA,[a] Chiharu KOSEKI,[a] Koreharu OGATA,[b] Nobuyuki KOSEKI,[a] Tsutomu ISHIKAWA,[a] and Takashi HARAYAMA[a]

Faculty of Pharmaceutical Sciences[a] and Chemical Analysis Center,[b] Chiba University, 1-33 Yayoi-cho, Chiba 260, Japan

Exposure of the (*E*)-isomer (**4E**) of 2-(3, 4, 5-trimethoxyphenyl)-4-(3, 4-methylenedioxyphenyl)-4-oxo-2-butenonitrile (β-cyanochalcone) in the solid state to sunlight led to unusual dimerization through isomerization to give an unsymmetrical E-Z dimer (**7**) along with a symmetrical Z-Z dimer (**5**) obtainable from the photoreactive (*Z*)-isomer (**4Z-b**).

KEYWORDS solid state photochemistry; photoisomerization; [2+2] cycloaddition reaction; cyclobutane dimer; X-ray crystallographic analysis; β-cyanochalcone

Solid state photoreactions[2)] of alkenic compounds including chalcone[3)] normally cause dimerizations most of which are strictly controlled by the topochemistry either of the bulk or the defect regions in the crystal to give a single dimer. In the course of synthesis studies on benzo[*c*]phenanthridine alkaloids showing antitumor activity, we occasionally found that the (*E*)-isomer (**4E**) of 2-(3, 4, 5-trimethoxyphenyl)-4-(3, 4-methylenedioxyphenyl)-4-oxo-2-butenonitrile (β-cyanochalcone), prepared for mechanistic consideration on formation of the unsaturated acid (**2**) in alkaline hydrolysis[4)] of the amide (**1**), isomerized in the solid state to yield unexpected dimers (**5** and **7**) when exposed to sunlight. Here we present the anomalous photobehavior of **4E** in addition to the predictable photoreaction of the (*Z*)-isomer (**4Z**).

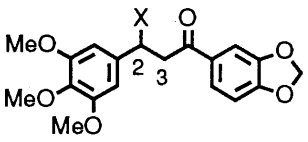

1 : X=$CONH_2$
2 : X=CO_2H, 2,3-dehydro
3 : X=CN

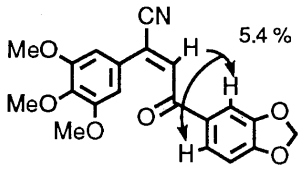

4E

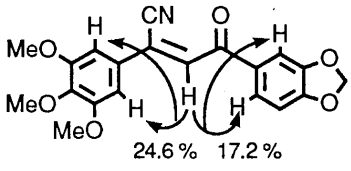

4Z (4Z-a, 4Z-b)

Dehydrogenation of the saturated nitrile[5)] (**3**) with 2, 3-dichloro-5, 6-dicyano-1, 4-benzoquinone (DDQ) in the dark provided the unsaturated nitriles[6)] (**4E** and **4Z**) in 40.2 % and 44.4 % yields, respectively. The stereochemistry of each nitrile was confirmed by difference NOE experiments in their ^{1}H-NMR spectra. In the (*E*)-isomer (**4E**) irradiation of the signal at δ 5.55, due to an olefinic proton, enhanced the integrals of both aromatic protons at ortho positions in the methylenedioxybenzoyl group. But in the (*Z*)-isomer (**4Z**), an additional NOE enhancement appeared between the aromatic protons in the trimethoxyphenyl group and an olefinic proton.

The (*Z*)-isomer (**4Z**) was crystallized into dimorphic forms [**4Z-a**: yellow fine prisms (from benzene-hexane), mp 153-156 °C; **4Z-b**: yellow fine needles (from benzene or ethanol), mp 168-169.5 °C]. Though the crystal (**4Z-a**) with a lower melting point was found to be quite stable to light, the other crystal (**4Z-b**) smoothly underwent solid state photoreaction to yield colorless needles (**5**), mp 169-170 °C[7)], as a single product in 65.0 % yield. Easy thermal regeneration[8)] of **4Z** from **5** suggested that **5** was a symmetrical cyclobutane dimer derived from **4Z**. This was supported by its ^{1}H-NMR spectrum showing only one singlet at δ 4.89 due to a newly born methine proton in place of the disappearance of an olefinic proton. The mirror symmetry structure of **5** was established by X-ray crystallographic analysis[9)] showing that the starting **4Z-b**[11)] crystallizes in the β-modification responsible for topochemical translation to a mirror symmetry dimer such as β-truxinic acid (**6**).[12)]

Exposure of the (*E*)-isomer (**4E**), yellow fine needles, mp 112-114 °C, to sunlight or Daylight lamp®[13)] for 37.5 h afforded two dimers along with the starting **4E** (33.7 %) and the isomerized **4Z** (27.7 %) monomers. One of the dimers yielded in 11.0 % was identified as the same symmetrical dimer (**5**) that was derived from the photoreactive (*Z*)-isomer

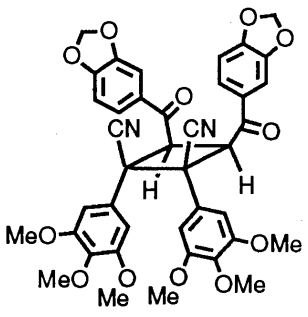

5

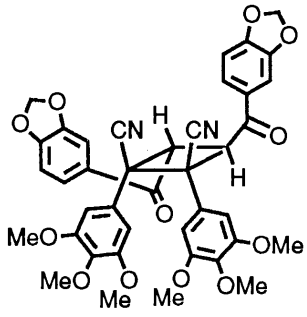

7

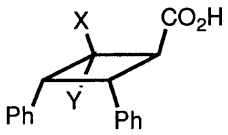

6 : X=CO_2H, Y=H
8 : X=H, Y=CO_2H

(**4Z-b**). The second dimer (**7**) was given as colorless fine needles, mp 117-120°C, in 14.6 % yield. Thermal generation[8] of the isomeric monomers (**4E** and **4Z**) from this dimer (**7**) and isomerization of the symmetrical dimer (**5**) to the alternative dimer (**7**) by silica gel suggested that **7** belonged to an unsymmetrical E-Z dimer with the configuration of *neo*-truxinic acid (**8**).[14] The ^{1}H-NMR spectrum showed coupled 1H doublets (J=10.5 Hz) at δ 5.34 and δ 5.44 attributable to newly born methine protons. NOE enhancements appeared between the methine proton at δ 5.34 and four aromatic protons at ortho positions of two trimethoxyphenyl rings. This allowed us to depict a chiral structure shown as **7** for the second dimer. The correctness of the structure was unambiguously confirmed by X-ray crystallographic analysis.[15] Thus sunlight irradiation to **4E** in the solid state preferentially induced isomerization followed by dimerization, and the formation of the dimers (**5** and **7**) suggested that the starting **4E**[11] also crystallized in β-modification.

Solid state photoisomerization of alkenic compounds is not so common as dimerization. Schmidt and co-workers[16] interpreted the photoreactions of *cis*-cinnamic acids yielding the *trans* isomers and/or dimers as lattice-controlled isomerization which is exerted through a metastable complex formed between the excited molecule and its closest neighbor. Recently an Indian group[17] reinvestigated the solid state cycloaddition reaction of (*E*)-β-nitrostyrene giving an unusual E-Z dimer like **7** and accounted for the dimerization by the disordered crystal structure of the starting nitrostyrene permitting isomerization. Unfortunately precise discussion on the solid state photochemistry[18] of **4E** has failed because of lack of the crystal data of **4E**, but three-dimensional studies of the supposed metastable complex[16] (**9**) using a Dreiding model shows that direct [2+2] cycloaddition from the complex (**9**) would be impossible due to a severe steric repulsion by the *cis* arrangement of all of the trimethoxyphenyl and the methylenedioxybenzoyl substituents in a formed dimer, even if the dimerization is topochemically favored. Thus in our case the steric restriction effect may also trigger generation of possible monomers (**4E**, **4Z-a**, and **4Z-b**) with partial isomerization, the photoreactive (*Z*)-isomer (**4Z-b**) among which could react with either another **4Z-b** or **4E** to produce the [2+2] cycloadducts (**5** and **7**).

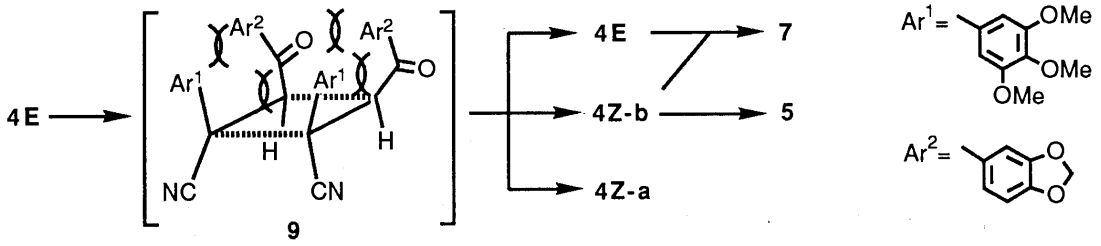

9

As a comparable experiment we examined the photochemistry in solution. Exporsure of each isomer (**4E** and **4Z**) to light in solution led to quantitative isolation of **4E** indicating that photosensitive **4E** in solid state exsisted as a photostable isomer in solution.

For detailed knowledge further examination of the photochemistry of some β-substituted chalcones including the β-cyanochalcone (**4**) is now in progress.

ACKNOWLEDGEMENTS We thank Prof. M. Suzuki and Dr. K.-I. Harada, Meijo University, for the measurement of mass spectrometry and Dr. K. Yamamoto, our universiry, for his assistance in powdered X-ray diffraction measurements.

REFERENCES AND NOTES

1) This paper forms Part 71 of "Studies on the Chemical Constituents of Rutaceous Plants," by H. Ishii. Part 70: H. Ishii, S. Takeda, K. Ogata, M. Hanaoka, and T. Harayama, *Chem. Pharm. Bull.*, accepted.
2) G. M. J. Schmidt, *Pure Appl. Chem.*, **27**, 647(1971); H. Nakanishi and F. Nakanishi, *Yuki Gosei Kagaku Kyokai Shi*, **33**, 661(1975); V. Ramamurthy and K. Venkatesan, *Chem. Rev.*, **87**, 433(1987): M. Hasegawa, *Yuki Gosei Kagaku Kyokai Shi*, **46**, 767(1988).
3) D. Rabinovich and G. M. J. Schmidt, *J. Chem. Soc. (B)*, **1970**, 6; D. Rabinovich, *ibid.*, **1970**, 11.
4) H. Ishii, E. Kawanabe, K.-I. Harada, T. Deushi, E. Ueda, T. Watanabe, Y.-I. Ichikawa, M. Sakamoto, T. Ishida, T. Takahashi, and T. Ishikawa, *Chem. Pharm. Bull.*, **31**, 3039(1983).
5) H. Ishii, T. Ishikawa, T. Deushi, K.-I. Harada, T. Watanabe, E. Ueda, T. Ishida, M. Sakamoto, E. Kawanabe, T. Takahashi, Y.-I. Ichikawa, K. Takizawa, T. Masuda, and I.-S. Chen, *Chem. Pharm. Bull.*, **31**, 3024(1983).
6) All new compounds except **5** described in this paper provided satisfactory analytical and spectroscopic data.
7) TLC of **5** after metling showed only one spot corresponded to the spot of **4Z**. Thus the observed melting point would be attributed to the starting **4Z-b**.
8) Heating a solution of a dimer in ethyl acetate completely gave the corresponding monomer(s).
9) Crystal data for **5**: $C_{40}H_{34}N_2O_{12}$ C_3H_6O, M=792.77, monoclinic, space group $P2_1/n$ with unit cell dimensions a=19.076(7), b=15.176(1), c=13.999(5) Å, β=102.64(4)°, U=3954.73 Å^3, Z=4, and D_C=1.332 g/cm^3. The reflection data were collected on a Rigaku AFC-5 diffractometer for 3°<2θ<120° using Cu$K\alpha$ radiation (λ=1.54178 Å) and the ω<30°<ω-2θ scan method at a 2θ scan speed of 4°/min. The structure was solved by the direct method using the MULTAN (UNICS-III system[10]) program and refined by full-matrix least-squares. The final R value was 0.0606 for 4279 independent reflections [$F_O>3\sigma(F_O)$].
10) T. Sakurai and K. Kobayashi, *Rep. Inst. Phys. Chem. Res.*, **55**, 69(1979).
11) Trials to prepare a single crystal for X-ray analysis have not been successful.
12) M. D. Cohen and G. M. J. Schmidt, *J. Chem. Soc.*, **1964**, 1996; M. D. Cohen, G. M. J. Schmidt, and F. I. Sonntag, *ibid.*, **1964**, 2000; G. M. J. Schmidt, *ibid.*, **1964**, 2014.
13) Toshiba DR-250/T(L) was used.
14) R. Stoemer and E. Laage, *Chem. Ber.*, **54**, 77(1921).
15) Crystal data for **7**: $C_{40}H_{34}N_2O_{12}$ 2(C_3H_6O), M=850.84, triclinic, space group $P\bar{1}$ with unit cell dimensions a=12.155(4), b=16.978(4), c=11.612(9) Å, α=107.95(4)°, β=105.25(4)°, γ=78.77(1)°, U=2182.785 Å^3, Z=2, and D_C=1.118 g/cm^3. The reflection data were collected on a Rigaku AFC-5 diffractometer for 3°<2θ<120° using Cu$K\alpha$ radiation (λ=1.54178 Å) and the ω<30°<ω-2θ scan method at a 2θ scan speed of 4°/min. The structure was solved by the direct method using the MULTAN (UNICS-III system[10]) program and refined by full-matrix least-squares. The final R value was 0.1622 for 3928 independent reflections [$F_O>3\sigma(F_O)$]. The crystal contains acetone with a high thermal factor, especially on the oxygen atom (B=*ca.* 16), as a crystal solvent. This may cause the unsatisfactory refinement.
16) J. Bergman, K. Osaki, G. M. J. Schmidt, and F. I. Sonntag, *J. Chem. Soc.*, **1964**, 2021.
17) G. R. Desiraju and V. R. Pedireddi, *J. Chem. Soc., Chem. Commun.*, **1989**, 1112.
18) Trace of the photoreaction by powdered X-ray diffraction resulted in observation of only peak broadenings.

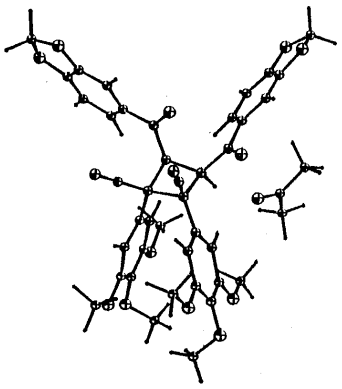

ORTEP drawing of **5**

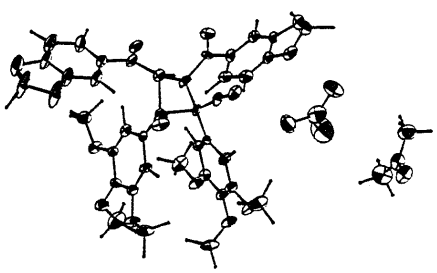

ORTEP drawing of **7**

(Received June 18, 1991)

ORBITAL DISTORTION ARISING FROM REMOTE SUBSTITUENTS NITRATION AND REDUCTION OF SPIRO[CYCLOPENTA-1,9'-FLUORENE]-2-ONES

Tomohiko OHWADA and Koichi SHUDO *

Faculty of Pharmaceutical Sciences, University of Tokyo, 7-3-1 Hongo, Bunkyo-ku, Tokyo 113, Japan

Nitration of spiro[cyclopenta-1, 9'-fluorene]-2-one with acetyl nitrate predominantly gave the 4-nitro derivative. In the reduction of substituted spiro[cyclopenta-1, 9'-fluorene]-2-ones, the anti-alcohols were favored in all cases. Both anomalous distributions of the products can be interpreted in terms of interactions of the π orbitals of the aromatic and the carbonyl moieties. This example of stereoelectronic effects demonstrates intrinsic reciprocal distortion between sterically unbiased π frameworks of the molecule.

KEYWORDS stereoelectronic effect; orbital distortion; reciprocal perturbation; nitration; reduction; fluorene

Stereoelectronic effects take place only when the bonding electrons are properly oriented in space: [1] the reactivity of most types of organic molecules depends upon the three-dimensional array of particular orbitals occupied or unoccupied by electrons. The stereoelectronic effect can emerge evidently as the determinant effect upon the course of attack of a reagent, particularly when the stereogenic center is free from steric bias. Such influence of electronic modifications of the inducing center has been demonstrated in recent studies on methylenecyclohexanes, [2] 5-substituted 2-adamantanones [3] and 2,2-diarylcyclopentanones, [4] in addition to the classic examples of norbornenes. [5] Since stereoelectronic effects stem from orbital interactions between the σ and π frameworks in the molecule, [6] each of the interactive fragments should be subject to *reciprocal* perturbations. In this paper we will describe anomalous distributions of products formed by nitration and by reduction of spiro[cyclopenta-1, 9'-fluorene]-2-one. These reactivities can be interpreted in terms of the interaction between the π-orbitals of the aromatic ring and that of the carbonyl group: the perturbation of the aromatic ring arising from the bisected carbonyl group, and the reciprocal perturbation of the carbonyl group arising from the orthogonal aromatic ring.

Fluorene **1** exhibits more nucleophilicity at C-2 than at C-4, due to increased conjugation of the aromatic rings and steric congestion at C-4. In the nitration of the parent fluorene **1** at -43 °C with acetyl nitrate, the isomer distribution was observed to be 67 % at C-2 and 33 % at C-4. [7] A spiro-substitution, on the other hand, was found to have an

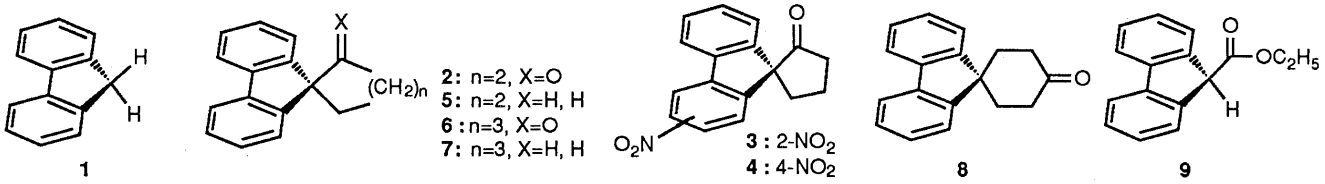

1 **8** **9**

unexpectedly significant effect on the nitration, resulting in a great change of the distribution of products: instead of the 2-nitro derivative (**3**; 11 %), spiro[cyclopenta-1,9'-fluorene]-2-one **2** [8] predominantly gave the 4-nitro derivative (**4**; 77 % yield) with the nitrating reagent at -75 °C (Table I). The bisected carbonyl group of **2** plays the significant role in this divergent nitration: the nitration of spirocyclopenta-1,9'-fluorene **5**, [9] a decarbonylated compound, resulted in

Table I. Distributions of Isomers in Mononitro Derivatives Formed by Nitration in Acetic Anhydride

Substrate	Temp. (°C)	Time (h)	Nitro products (%) 2-Nitro	4-Nitro	4-/2- Ratio
1	-43	6	67	33	0.5 [a]
2	-75	5	11	77	7.0
5	-43	8	81	14	0.2
6	-43	10	26	52 [b]	2.0 [c]
7	-43	7	74	26	0.4
8	-22	5	65	17	0.3
9	-22	3	54	34	0.6

a) At 0 °C the yields of 2-nitro and 4-nitro derivatives are 63 % and 34 %, respectively. The 4-/2-ratio is 0.5. Reference 7a. b) **6** (14 % yield) c) At -22 °C for 6 h, the yields of 2-nitro and 4-nitro derivatives are 41 % and 56 %, respectively. The 4-/2- ratio is 1.4.

the generally expected distribution of nitrated fluorenes. A similar divergence in the distributions of nitrated compounds was also observed in the case of the reactions of the spirofluorenes bearing a six-membered ring, spiro[cyclohexa-1,9'-fluorene]-2-one **6** and spiro[cyclohexa-1,9'-fluorene] **7** [8), 9)] (Table I). Neither the cyclohexane ring nor the cyclopentane ring, in the spiro-geometry, encouraged the nitration at C-4, or rather both enhanced the reactivities at the C-2 position of the fluorene rings. These results also exclude possible steric congestion around the C-2 position owing to the spiro-substitution of the C-9 position. Moreover, the nitration of spiro[cyclohexa-1,9'-fluorene]-4-one **8** [9)] also favored the 2-nitro derivative (65 %) rather than the 4-nitro derivative (17 %), suggesting the requisite proximity for interaction between the carbonyl and the aromatic moieties. Even a carbonyl substituent at the C-9 position of the fluorene, has an indirect effect on the nitration reaction. The nitration of 9-ethoxycarbonylfluorene **9** by acetyl nitrate gave the 2-nitro derivative (54 %), together with the 4-nitro derivative (34 %) (Table I). All the results, therefore, indicate perturbation of the fluorene ring arising from the bisected carbonyl group of **2**.

In the reverse direction, the perturbation on the fluorene ring in the spiro[cyclopenta-1,9'-fluorene]-2-one system should transfer to the carbonyl group. This reciprocal perturbation of the carbonyl group can be demonstrated by the biased reduction of the carbonyl groups of substituted spiro[cyclopenta-1,9'-fluorene]-2-ones (**3**, **4**, **10** and **11**) . [8)] The ketones were reduced to the alcohols (**12** and **13**) by the action of sodium borohydride in methanol at -43 °C.

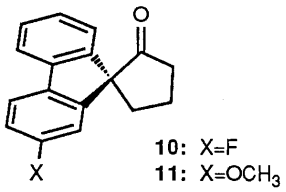

10: X=F
11: X=OCH_3

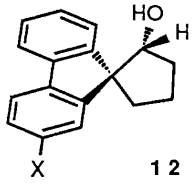

12

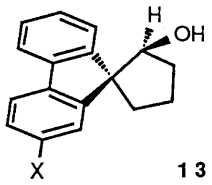

13

Although the yields of the products partially depend on the substituent at C-2 or C-4 of the fluorene ring (Table II), the anti-alcohol **12**, i. e., the syn addition of the reducing reagent with respect to the substituent, is favored in all cases. [10)] A coordinative interaction of the substituent with the reducing agent can be excluded, in view of the great distances between the substituents and the carbonyl group.[11)] Furthermore, the similar behavior of the two isomeric nitro-fluorenes (2-nitro **3** and 4-nitro **4**) also excluded this possibility. The carbonyl group would be perturbed by the asymmetric orbitals of the fluorene ring with respect to reflection in the mirror plane passing through C-9 and the carbonyl group, induced by the sterically unbiased substituent at the C-2 or C-4. [12)]

Table II. Distributions of Isomers in Alcohols Formed by Reduction of Substituted Spiro[cyclopenta-1,9'-fluorene]-2-ones [a)]

Substrate	Substituent (X)	Yield of alcohol	*anti/syn* Ratio
2	H	75 %	50 : 50
3	2-NO_2	81 %	68 : 32
4	4-NO_2	67 %	71 : 29
10	2-F	58 %	72 : 28
11	2-OCH_3	73 %	74 : 26

a) All the reactions were carried out at -43 °C.

In summary, we have described the stereoelectronic effect in spiro[cyclopenta-1,9'-fluorene]-2-one, which probably stems from the interactions between the π frameworks of the carbonyl group and the fluorene ring . These perturbations might be interpreted in terms of the homoconjugative interaction of systems of π orbitals which are separated by insulating atoms, in a similar manner to the spiro conjugation. [13)] Efforts to account for stereoselective transformations in terms of electronic influences arising from orbital interactions are still worthwhile.

REFERENCES AND NOTES

1) P. Deslongchamps, " *Stereoelectronic Effects in Organic Chemistry*" , Pergamon Press Ltd (1983).
2) C. R. Jonson, B. D. Tait and A. S. Cieplak. *J. Am. Chem. Soc.*, ***109***, 5875 (1987) .
3) C. K. Chung, L. T. Tseng, M.-H. Lin, S. Srivastava and W. J. le Noble. *J. Am. Chem. Soc.*, ***108***, 1598 (1986); Chung, W. -S.; Turro, N. J.; Srivastava, S.; Li, H.; le Noble, W. J. *J. Am. Chem. Soc.*, ***110***, 7882 (1988); S. Srivastava and W. J. le Noble. *J. Am. Chem. Soc.*, ***109***, 5874 (1987).
4) R. L. Halterman and M. A. McEvoy. *J. Am. Chem. Soc.*, ***112***, 6690 (1990).
5) a) K. Alder and G. Stein. *Liebigs Ann. Chem.* , ***485***, 211 (1931). ; ibid., ***515***, 185 (1935). b) H. C. Brown. *Chem. Ber.*, ***2***, 199 (1966). c) R. Huisgen, P. H. Ooms, M. Mingin and N. L. Allinger. *J. Am. Chem. Soc.*, ***102***, 3951 (1980). d) J. Spanget-Larsen and R. Gleiter. *Tetrahedron Lett.*, ***23***, 2435 (1982). R. Gleiter and J. Spanget-Larsen. *Tetrahedron*, ***39***, 3345 (1983). e) P. v. R. Schleyer. *J. Am. Chem. Soc.*, ***89***, 701 (1967).
6) a) S. Inagaki, H. Fujimoto and K. Fukui. *J. Am. Chem. Soc.*, ***98***, 4054 (1976). S. Inagaki and K. Fukui, *Chem. Lett.*, 509 (1974). b) W. N. Washburn and R. A. Hillson. *J. Am. Chem. Soc.*, ***106***, 4575 (1984).
7) M. J. S. Dewar and D. S. Urch. *J. Chem. Soc.*, 3079 (1958). K. Schofield, "*Aromatic Nitration*", Cambridge Univ. Press, chapter 13 (1980).
8) All the newly prepared compounds (**2** , **3**- **6**, and **10**- **11**) were fully characterized in terms of NMR spectroscopy and combustion analysis. The compound **2** was prepared by Dieckmann condensation of 9-ethoxycarbonyl-9-(3-ethoxycarbonylpropyl)fluorene, followed by decarbonylation in acidic methanol.
9) D. A. Stauffer and O. E. Fancher. *J. Org. Chem.*, ***25***, 935 (1960).
10) The structures of the alcohols were elucidated after isolation, on the basis of NOE detection and characteristic lower-field shift of H-1 or H-8 owing to the anisotoropic effect of the hydroxy group. The ratios were determined from NMR spectra before isolation.
11) The distance between the fluorine atom at C-2 and the carbonyl carbon atom is more than 5 Å on the basis of molecular models. The oxygen atoms of the nitro group at the 4-position are too far away to interact directly, or even in a coordinative manner, with the carbonyl group.
12) Molecular orbital calculations can estimate the ring charge of an aromatic compound (C_6H_5X) as the summation of charges of carbons and hydrogens except the C-X moiety. The calculations based on STO-3G basis sets showed that the rings of substituted benzenes (fluorobenzene, phenol, nitrobenzene) are positively charged (+0.13, +0.08 and +0.24, respectively), whereas the ring of the parent benzene is rather negatively charged (-0.06). The predominant alcohol, in all cases, can be regarded as the product arising from the addition of hydride to the face opposite the more electron-rich aromatic ring.
13) H. E. Simmons and T. Fukunaga, *J. Am. Chem. Soc.*, ***89***, 5208 (1967). R. Hoffmann, A. Imamura and G. D. Zeiss, *J. Am. Chem. Soc.*, ***89***, 5215 (1967). M. D. Gordon, T. Fukunaga and H. E. Simmons, *J. Am. Chem. Soc.*, ***98***, 8401 (1976).

(Received June 19, 1991)

DAVALLIN, A NEW TETRAMERIC PROANTHOCYANIDIN FROM THE RHIZOMES OF DAVALLIA MARIESII MOORE

Cheng-Bin CUI,[a] Yasuhiro TEZUKA,[a] Tohru KIKUCHI,*,[a] Hirofumi NAKANO,[b] Tatsuya TAMAOKI,[b] and Jong-Hee PARK[c]
Research Institute for Wakan-Yaku (Oriental Medicines),[a] Toyama Medical and Pharmaceutical University, 2630 Sugitani, Toyama 930-01, Japan, Tokyo Research Laboratories, Kyowa-Hakko Kogyo Co., Ltd.,[b] 3-6-6 Asahimachi, Machida-shi, Tokyo 194, Japan, and College of Pharmacy, Pusan National University,[c] Pusan 607, Korea

Davallin, a new tetrameric proanthocyanidin which inhibits protein kinase C, has been isolated from the rhizomes of Davallia mariesii MOORE (Davalliaceae), and its structure was determined to be epicatechin-(4β→6)-epiafzelechin-(4β→8)-epicatechin-(4β→6)-epicatechin by 2D NMR spectroscopy including HMQC and HMBC techniques.

KEYWORDS davallin; Davalliaceae; Davallia mariesii; epicatechin-(4β→6)-epiafzelechin-(4β→8)-epicatechin-(4β→6)-epicatechin; proanthocyanidin; NMR; HMBC; protein kinase C inhibitor

In previous papers,[1] we reported the isolation and structures of davallialactone, eriodictyol-7-O-β-D-glucuronide, davalliosides A and B from the rhizomes of a fern, Davallia mariesii MOORE. In a continued study, we have isolated a new tetrameric proanthocyanidin, named davallin (**1**), which inhibits protein kinase C. This paper describes the structure elucidation of **1** by the use of 2D NMR techniques.

The EtOAc-soluble fraction (106 g) of the aqueous acetone extract of the dried rhizomes (17.2 kg), obtained according to the procedure in a previous paper,[1a] was separated by repeated column chromatography on Sephadex LH-20 to give davallin (**1**, 997 mg) along with procyanidins B-2 (**2**, 1.3 g) and B-5 (**3**, 1.2 g),[2] epicatechin-(4β→8)-epicatechin-(4β→6)-epicatechin (**4**, 1.3 g),[3] and epicatechin-(4β→6)-epicatechin-(4β→8)-epicatechin-(4β→6)-epicatechin (**5**, 2.6 g).[4]

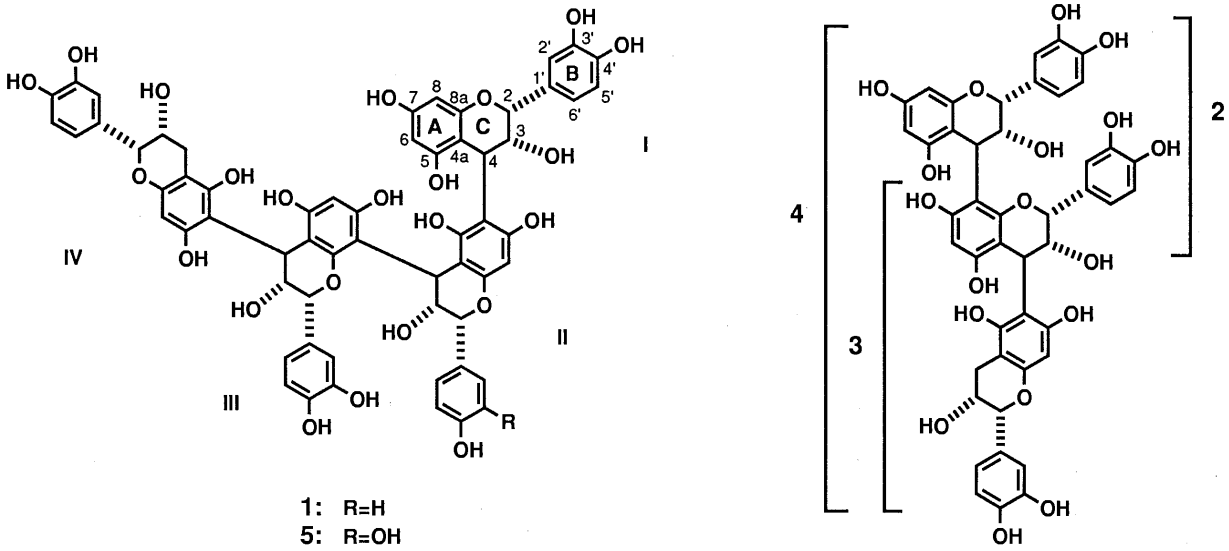

Davallin (**1**), a pale brown amorphous powder, $[\alpha]_D^{22}$ +185.8° (MeOH), showed positive color reactions with $FeCl_3$ (dark-blue) and anisaldehyde-sulfuric acid (orange-red) reagents.[5] The molecular formula of **1** was determined to be $C_{60}H_{50}O_{23}$ by elemental analysis and FAB-MS measurement (m/z: 1139 $[M+H]^+$). It showed UV absorptions at 223 and 281 nm (log ε: 4.84 and 4.18) and IR (KBr) absorptions at 3350 (br, OH), 1600, 1510, and 1440 cm^{-1} (aromatic ring). The ^1H- and ^{13}C-NMR spectra of **1** were almost superimposable on those of **5**, except for the appearance of signals due to a 1,4-disubstituted benzene ring and three 1,3,4-trisubstituted benzene rings instead of four 1,3,4-trisubstituted benzene rings in **5** (Table I). This indicates that **1** may be a tetrameric proanthocyanidin composed of an epiafzelechin and three epicatechin units.

Analysis of the ^1H-^1H COSY spectrum of **1** enabled us to correlate all protons in rings B/C in each flavanol unit with each other (Table I). For instance, correlation peaks between H-2 (δ 4.86), H-3 (δ 3.82), and

Table I. 400 MHz ^1H and 100 MHz ^{13}C NMR Data for **1** and **5** in CD_3OD-D_2O

Units	No	**1** δ_H (J in Hz)	**1** δ_C	**1** ^1H L. r. coupled ($^3J_{CH}$ $^2J_{CH}$)[b]	**5**[a] δ_H (J in Hz)	**5**[a] δ_C
I	2	4.86 br s	77.7 d		4.83 br s	77.78 d
	3	3.82 br s	73.2 d		3.79 br s	73.2 d
	4	4.37 br s	38.3 d		4.34 br s	38.3 d
	4a	----	99.9 s	I3,I6,I8 I4	----	100.0 s
	5	----	158.3 s	I4 I6	----	158.4 s
	6	6.11[c] d (2.1)	97.16 d	I8	6.10 d (2.4)	97.3 d
	7	----	159.4 s	I6,I8	----	159.5 s
	8	6.06[c] d (2.1)	97.6 d	I6	6.04 d (2.4)	97.7 d
	8a	----	159.6 s	I4 I8	----	159.7 s
	1'	----	133.2 s	I5' I2	----	133.3 s
	2'	7.08[d] d (1.8)	116.4 d	I2,I6'	7.06[d] d (1.5)	116.5 d
	3'	----	145.94 s	I5' I2'	----	145.9 s
	4'	----	145.82 s	I2',I6' I5'	----	145.8 s
	5'	6.41 d (8.2)	116.2 d	I6'	6.39 d (8.2)	116.3 d
	6'	6.18[d] dd (8.2, 1.8)	120.9 d	I2,I2'	6.14[d] dd (8.2, 1.5)	121.0 d
II	2	5.44 br s	77.4 d		5.36 br s	77.5 d
	3	4.00 br s	74.1 d		3.98 br s	74.2 d
	4	4.42 br s	38.6 d		4.38 br s	38.7 d
	4a	----	104.7 s	II3,II8 II4	----	104.9 s
	5	----	156.5 s	II4, I4	----	156.5 s
	6	----	106.8[e] s	II8, I3 I4	----	106.9 s
	7	----	155.1 s	I4 II8	----	155.1 s
	8	5.89[c] s	97.19 d		5.87 s	97.2 d
	8a	----	155.64 s	II4 II8	----	155.7 s
	1'	----	132.9 s	II3',II5' II2	----	133.6 s
	2'	7.42[d] d (8.9)	130.2 d	II2, II6' II3'	7.05[d] d (1.8)	116.6 d
	3'	6.86 d (8.9)	116.6 d	II5' II2'	----	145.9 s
	4'	----	157.5 s	II2',II6' II3',II5'	----	145.98 s
	5'	6.86 d (8.9)	116.6 d	II3' II6'	6.82 d (8.3)	117.1 d
	6'	7.42[d] d (8.9)	130.2 d	II2,II2' II5'	6.90[d] dd (8.3, 1.8)	121.0 d
III	2	4.64 br s	77.8 d		4.61 br s	77.84 d
	3	3.96 d (1.8)	72.4 d		3.93 d (1.8)	72.5 d
	4	4.51 br s	38.5 d		4.48 br s	38.6 d
	4a	----	99.9 s	III3,III6 III4	----	100.0 s
	5	----	157.3 s	III4, III6	----	157.4 s
	6	6.19[c] s	97.8 d		6.17 s	97.8 d
	7	----	157.5 s	II4 III6	----	157.6 s
	8	----	110.1[e] s	III6,II3 II4	----	110.2 s
	8a	----	156.6 s	III4,II4	----	156.7 s
	1'	----	132.2 s	III5' III2	----	132.3 s
	2'	6.66[d] d (1.8)	115.9 d	III2, III6'	6.63[d] d (1.8)	116.0 d
	3'	----	145.4 s	III5' III2'	----	145.44 s
	4'	----	145.3 s	III2',III6' III5'	----	145.41 s
	5'	6.63 d (8.2)	116.5 d		6.61 d (8.3)	116.6 d
	6'	6.27[d] dd (8.2, 1.8)	120.9 d	III2,III2'	6.24[d] dd (8.3, 1.8)	121.0 d
IV	2	4.27 br s	80.0 d		4.24 br s	80.1 d
	3	3.86 br s	68.3 d		3.84 br s	68.3 d
	4	2.29 br d (16.7)	29.8 t		2.26 br d (16.9)	29.9 t
		2.11 dd (16.7,4.4)			2.09 dd (16.9,4.6)	
	4a	----	102.5 s	IV3,IV8 IV4	----	102.6 s
	5	----	156.4 s	IV4,III4	----	156.5 s
	6	----	108.3[e] s	IV8,III3 III4	----	108.4 s
	7	----	155.2 s	III4 IV8	----	155.3 s
	8	6.07[c] s	96.9 d		6.05 s	96.9 d
	8a	----	155.57 s	IV4 IV8	----	155.6 s
	1'	----	133.0 s	IV5' IV2	----	133.1 s
	2'	7.01[d] d (1.5)	116.2 d	IV2, IV6'	6.99[d] d (1.5)	116.3 d
	3'	----	145.88 s	IV5' IV2'	----	146.04 s
	4'	----	145.7 s	IV2',IV6' IV5'	----	146.04 s
	5'	6.85 d (8.2)	117.1 d		6.83 d (8.2)	117.1 d
	6'	6.89[d] dd (8.2, 1.5)	120.7 d	IV2,IV2'	6.86[d] dd (8.2, 1.5)	120.8 d

Multiplicities of ^{13}C-signals were determined by the DEPT method and indicated as s (singlet), d (doublet), and t (triplet). a): Signals were assigned by 2D NMR spectroscopy including HMQC, HMBC, and long-range C-H J-resolved NMR methods. b): $^2J_{CH}$ and $^3J_{CH}$ indicate the protons coupled with the carbon through two and three bonds, respectively, which were observed in the HMBC spectrum. c) and e): Assignments are based on the comparison with the data of **5**. d): Long-range ^1H-^1H coupling was observed with 2-H of each unit in the ^1H-^1H COSY.

H-4 (δ 4.37) and between H-2' (δ 7.08), H-5' (δ 6.41), and H-6' (δ 6.18) in an epicatechin unit (unit I) were clearly recognized and long-range correlations between H-2 and H-2' and H-6' were also observed. Similarly, rings B/C protons in the epiafzelechin unit (unit II) were obviously discriminated from others (Table I). On the other hand, signals of the methine and methylene carbons in each flavanol unit were readily assigned by analysis of the HMQC spectrum (Table I).

Then, we measured the HMBC spectrum of **1** in order to clarify the connectivity of the flavanol units. As can be seen in Fig. 1, the quaternary carbons at δ 159.4 (C-I-7) and δ 99.9 (C-I-4a and C-III-4a) show long-range correlations with both the meta-coupled benzene protons at δ 6.06 and 6.11 (each d, 8-H and 6-H in unit I), and the carbons at δ 158.3 (C-I-5) and δ 159.6 (C-I-8a) show long-range correlations with the protons at δ 6.11 (I-6-H) and δ 6.06 (I-8-H), respectively. Thus, these carbons are assigned to C-7, C-4a, C-5, and C-8a of the upper terminal unit, respectively. And both C-I-5 (δ 158.3) and C-I-8a (δ 159.6) show long-range correlations with the proton at δ 4.37, indicating that this proton is H-4 of the upper terminal unit. Thus the upper terminal unit is determined to be epicatechin (unit I). On the other hand, both H-3 (δ 4.00) and H-4 (δ 4.42) in the epiafzelechin unit (unit II) show long-range correlations with the quaternary carbon at δ 104.7 (C-II-4a) which is correlated with the benzene proton at δ 5.89 (II-8-H), suggesting that these carbon and pro-

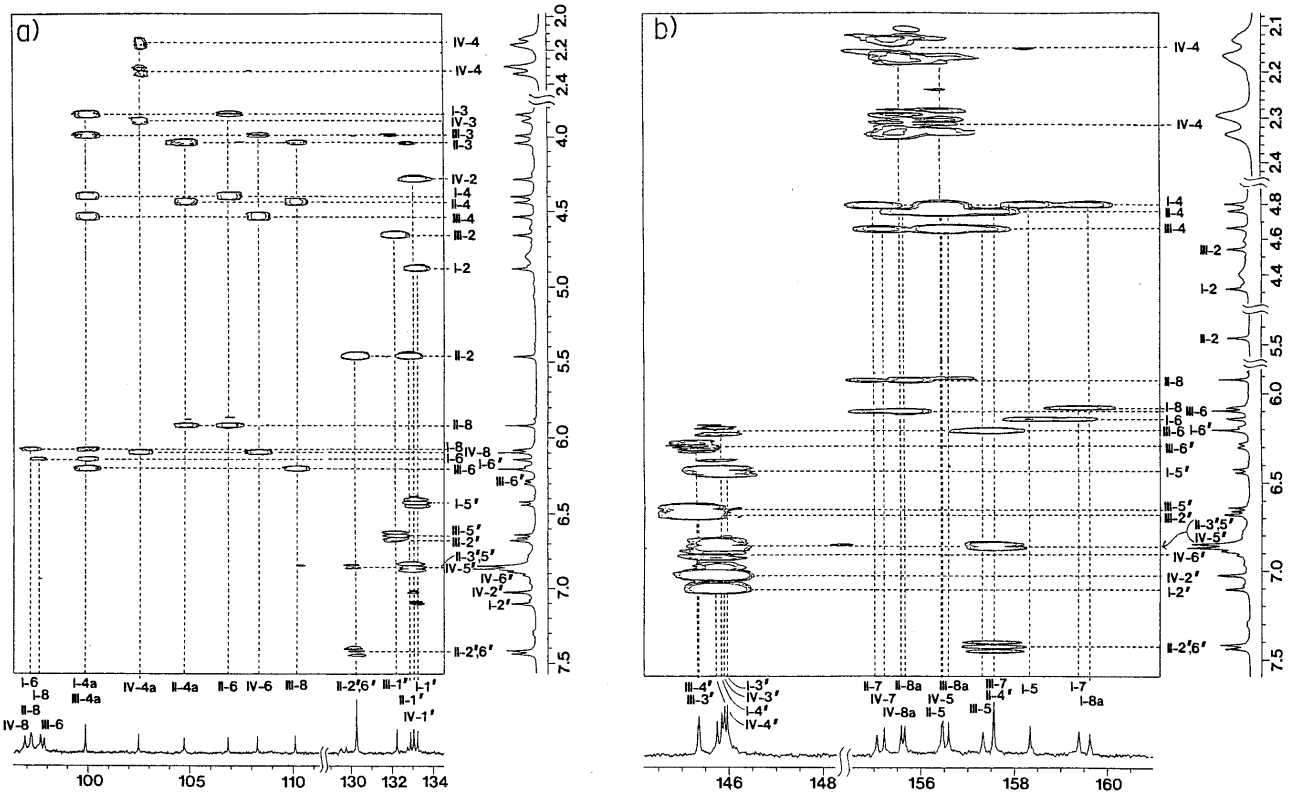

Fig. 1. HMBC Spectrum of **1** in CD_3OD-D_2O (2:1) (Sample: 123 mg, $^{lr}J_{CH}$=6 Hz, 108 h run)
a) High field region, b) Low field region.

ton are C-4a and the ring-A proton of the epiafzelechin unit, respectively (Fig. 1a). Because the latter proton (δ 5.89) is correlated with the quaternary carbon at δ 106.8 (C-II-6), which, in turn, shows long-range correlations with both H-3 and H-4 in the upper terminal epicatechin unit, epiafzelechin is concluded to form the second upper terminal unit in **1**. Thus the remaining two flavanol units must be epicatechins. The locations and relative stereochemistry of interflavonoid likages in **1** are believed to be the same as those of **5** in view of the apparent close similarity of the ^{1}H- and ^{13}C-NMR spectra (Table I).

Based on these findings and the comparison of the optical rotational value with that of **5** ($[\alpha]_D^{22}$ +168.5° (MeOH)), davallin was concluded to be epicatechin-(4β→6)-epiafzelechin-(4β→8)-epicatechin-(4β→6)-epicatechin (**1**). It showed an inhibitory activity against protein kinase C[6] with the IC_{50} value of 3.5 μM.

Even though many olygomeric proanthocyanidins have hitherto been reported, only a few kinds of dimeric proanthocyanidins which are composed of epicatechin and epiafzelechin have been known.[7] Our present result provides the first example of tetrameric proanthocyanidin of this novel class.

ACKNOWLEDGMENTS This work was supported in part by a Grant-in-Aid for Scientific Research (No. 63870090) from the Ministry of Education, Science and Culture of Japan. The authors are grateful to Prof. I. Nishioka and Assoc. Prof. G. Nonaka for a gift of an authentic sample of tetrameric tannin **5**.

REFERENCES

1) a) C.-B. Cui, Y. Tezuka, T. Kikuchi, H. Nakano, T. Tamaoki, and J.-H. Park, Chem. Pharm. Bull., **38**, 3218 (1990); b) C.-B. Cui, Y. Tezuka, T. Kikuchi, H. Nakano, and J.-H. Park, ibid., **38**, 2620(1990).
2) G. Nonaka, O. Kawahara, and I. Nishioka, Chem. Pharm. Bull., **30**, 4277 (1982).
3) E. Ezaki-Furuichi, G. Nonaka, I. Nishioka, and K. Hayashi, Agric. Biol. Chem., **50**, 2061 (1986).
4) T.-H. Hwang, Y. Kashiwada, G. Nonaka, and I. Nishioka, Phytochemistry, **29**, 297 (1990).
5) G. Nonaka, O. Kawahara, and I. Nishioka, Chem. Pharm. Bull., **31**, 3906 (1983).
6) T. Tamaoki, H. Nomoto, I. Takahashi, Y. Kato, M. Morimoto, and F. Tomita, Biochem. Biophys. Res. Commun., **135**, 397 (1986).
7) S. Morimoto, G. Nonaka, R.-F. Chen, and I. Nishioka, Chem. Pharm. Bull., **36**, 39 (1988).

(Received July 2, 1991)